COMMISSIONS 27 AND 42 OF THE I. A. U.

INFORMATION BULLETIN ON VARIABLE STARS

Nos. 6001 – 6100

2011 September – 2014 March

H–1121 BUDAPEST XII, Konkoly Thege str. 15-17., HUNGARY

URL http://www.konkoly.hu/IBVS/IBVS.html

HU ISSN 0374–0676

COPYRIGHT NOTICE

CONTENTS

2011

2012

2013

2014

AUTHOR INDEX

INDEX OF VARIABLES

COMMISSIONS 27 AND 42 OF THE IAU
INFORMATION BULLETIN ON VARIABLE STARS

Number 6001

Konkoly Observatory
Budapest
15 September 2011

HU ISSN 0374 – 0676

NEW LIGHT CURVES AND EPHEMERIS FOR THE CLOSE ECLIPSING BINARY V963 PERSEI

ODELL, ANDREW P.[1]; WILS, PATRICK[2]; DIRKS, CLARISSA[3]; GUVENEN, BLYTHE[4]; O'MALLEY, C. JO[4]; VILLARREAL, ANTONIO S.[4]; WEINZETTLE, RITA M.[4]

[1] NAU Department of Physics & Astronomy Box 6010, Flagstaff AZ 86011 USA; e-mail: WCorvi@yahoo.com

[2] Vereniging Voor Sterrenkunde, Belgium

[3] Evergreen State College, Olympia WA USA

[4] Steward Observatory, University of Arizona, Tucson AZ 85721 USA

V963 Per (GSC 3355 0394, $\alpha(2000)=04^{\rm h}45^{\rm m}35\overset{\rm s}{.}6$, $\delta(2000)=+52°22'35\overset{''}{.}4$) is a close eclipsing binary identified by Nicholson and Varley (Nicholson and Varley 2005) and was recently discussed extensively by Samec et al. (2010, hereafter referred to as RGS), who obtained and modeled BVRI light curves. This star is potentially interesting astrophysically because of its short period but large difference between eclipse depths, possibly similar to W Corvi (see Odell & Cushing 2004). RGS fit their light curves with a model having three spots on the secondary and one on the primary star. RGS also found a large mass ratio (q = $\sim$ 0.87), which gives the possibility of detecting the secondary star in spectral line profiles, thus revealing the spot characteristics. There are some inconsistencies in RGS, but, our new photometry confirms the basic shape of the light variation that RGS found, and the system remains an interesting one.

We have obtained new light curves in 2010–2011 at the 1.55 m Kuiper telescope of the Steward Observatory utilizing the Mont4KCCD camera binned 3×3 (described in detail by Randall et al. 2007) utilizing Bessell-*B*, -*V*, -*R* and Arizona-*I* filters. Data reduction was done in the following way: The two amplifier readouts were corrected for overscan and crosstalk on the fly using an IRAF script. Then the images were zero and flat field corrected using IRAF*, and magnitudes were extracted with qphot task with $4\overset{''}{.}2$ radius apertures.

The zero and flat field frames were the average of 200 images each, pointed at a dome screen such that $\sim$ 10K counts was reached for each flat. In order to minimize any flat-fielding problems, an autoguider kept all stars on the same pixels for the entire run, and focus was monitored carefully. To check for possible color terms in the extinction, the third comparison star (with very similar color to the eclipser) was treated as 'variable' and its (V−C) magnitude was plotted as a function of airmass. No significant effect was apparent (i.e. < 0.002 mag).

The comparison and check stars were treated in an unusual way, in that a 'combined comparison' was formed from the average of five bright stars surrounding the variable (see Table 1). This has two advantages: it improves the S/N of the comparison, and it better accounts for any variations in transparency over the field, as opposed to using only one

star. It also makes any anomalous reading immediately apparent. In order to compare our data to that of RGS, we then subtracted from each magnitude difference (Variable − Comparison) the filter-specific difference between RGS's comparison star and our average of five stars, averaged over each night, so our results are on the same scale as theirs.

Table 1. Comparison Stars

GSC number	Offset RA	Offset dec	comment
3355 0474	$-3^s.1$	$-3'07''$	
3355 0096	$-20^s.9$	$-2'06''$	
3355 0362	$15^s.3$	$+1'01''$	same color as variable
3355 0336	$-27^s.1$	$+3'04''$	
3355 0596	$7^s.4$	$+4'43''$	RGS comparison star

Our observations are given in Table 2, as HJD, orbital phase (based on Eq. 1) and delta magnitude: (Variable – Comparison star). (The table is available through the IBVS website as `6001-t2.txt`.)

Fig. 1 shows the complete dataset for our light curves. The number given in the key for each filter represents the magnitude difference required to correct to RGS's comparison star. It can be seen that the light curves do not reproduce perfectly - there is a small night-to-night scatter around phase 0.20, and a larger effect at phases between 0.40 and 0.90. The former could conceivably be due to a slightly incorrect period being used for the phasing (see the discussion of the ephemeris later in this paper); the latter must be caused by intrinsic variation of the star, as would general differences in level between RGS and our new data. The O'Connell effect is rather large; phase 0.75 is about 0.10 mag fainter than phase 0.25.

Five new times of primary minimum and two of secondary were obtained, which alter the ephemeris. The variations in the light curve near phase 0.5 must be real, as this is during secondary eclipse, which is obviously total. Fig. 2 shows the relevant part of the cycle in the B filter in detail; data from before January 1, 2011 is plotted as diamonds and after that date as triangles. The depth of secondary eclipse became fainter by about 0.04 mag somewhere around that date. The change extends from about phase 0.40 to about 0.80, which includes the time when the secondary star is completely eclipsed.

RGS present their data in Table 1 and Fig. 2 of that paper; although the figures seem to be correct, the magnitudes listed in the table for the R and I filters appear to be fluxes, since the value at maximum (phase 0.25) is exactly 1.0, and the light curves would be inverted if the numbers are correct. We also note that the HJD given for all filters is likely erroneous (see below). However, there seems to be a difference of about 0.1 mag at all phases between RGS's data and ours (in the sense they found the star to be fainter). The exact cause of this is not clear, since our images did not include RGS's check star.

We used the ephemeris of RGS to predict that a primary eclipse would be seen on our first night of observation, but in fact, secondary eclipse was observed, indicating a problem there. A new, preliminary ephemeris was determined from our five primary timings given in Table 3 to be HJD = 2455563.6833(2) + 0.462087(3) ×E (used to phase the data in our Fig. 1 and 2). We determined our times of minimum by folding our data to see where the ascending light best fell on the descending branch; our uncertainties come from this measure for the four different filters (standard deviation). The short time (200 cycles) over which the data were obtained makes this period rather uncertain, but definitely different from RGS's 0.46216 days.

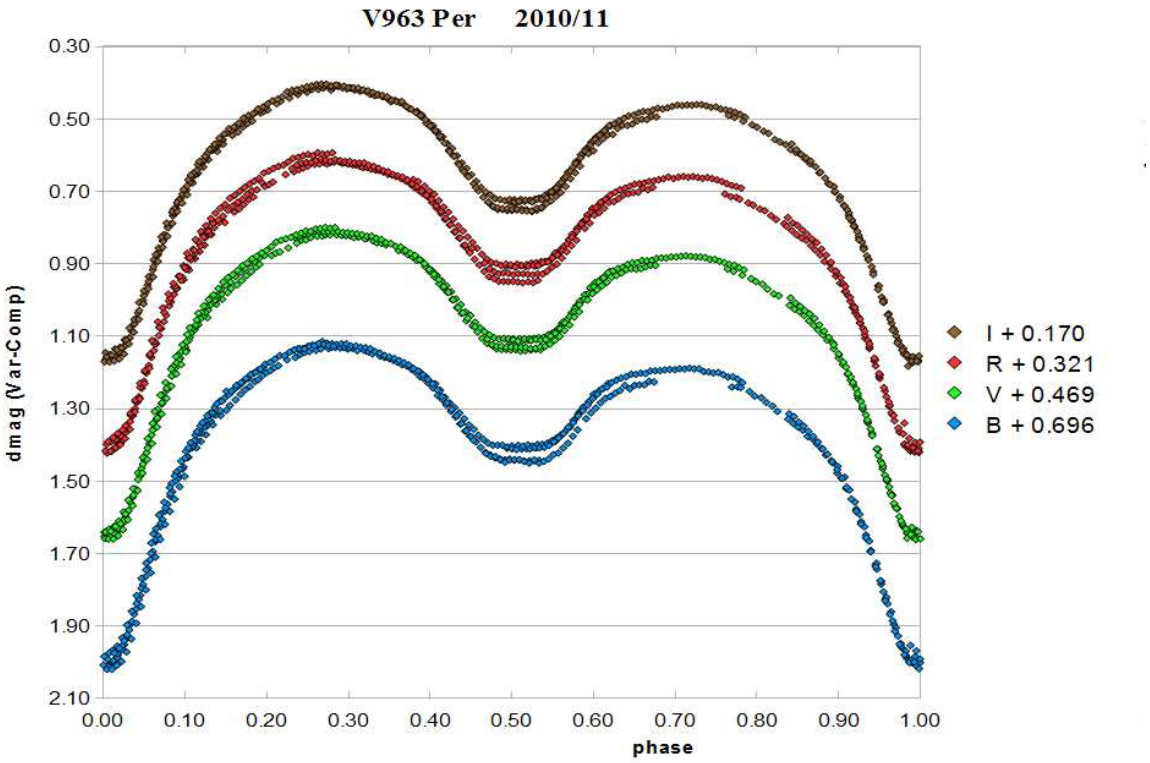

Figure 1. Light curves for V963 Per in 2010-11.

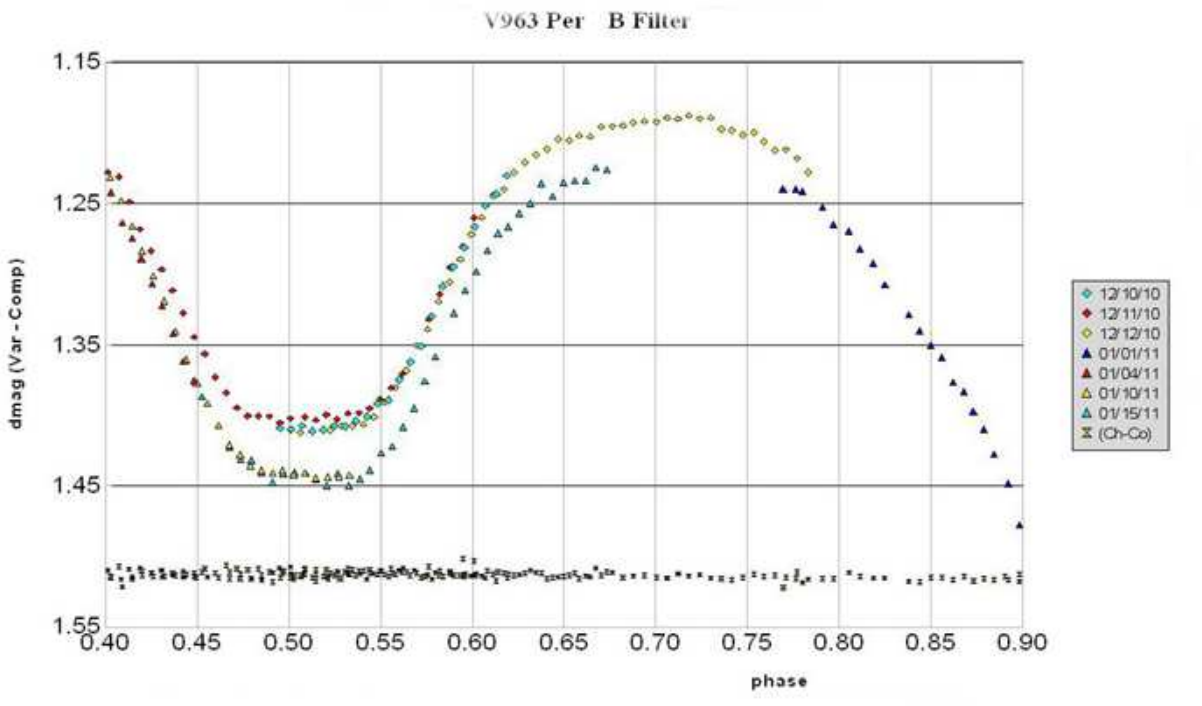

Figure 2. Variation of the light curve for V963 Per in B Filter. The points at dmag 1.51 are (Five-star-comp − Comp3) which would show any variability in the comparison stars.

Table 3. $O-C$ Linear Residuals, Eq. 1

No	Epoch HJD	Uncertainty days	Cycle	(Obs-Calc) minutes	Comment
1	2455542.6626	0.0005	-45.5	5.52	Secondary - not used
2	2455563.6835	0.0001	0.0	0.23	Primary
3	2455564.6077	0.0001	2.0	0.33	Primary
4	2455576.6212	0.0002	28.0	−0.47	Primary
5	2455577.7818	0.0006	30.5	7.32	Secondary - not used
6	2455601.5748	0.0013	82.0	1.46	Primary
7	2455618.6717	0.0002	507.0	1.55	Primary

When our new period was used to compute times of minimum to compare to RGS's timings, a problem developed. RGS tells of two nights' data acquisition, but gives timings on four nights, two in November 2007, one in December 2008, and one in January 2009. However, our current period yields residuals for the last four of RGS's timings of over two hours. The times of observation listed in RGS, Table 1, do not correspond to the nights they claimed to have observed this star. Thus we must hold off on using any of those timings in attempting to derive a better period or to test for period variation.

Instead, we use the data from the Northern Sky Variability Survey (NSVS, see Wozniak et al. 2004) taken in 2000 and 2001 and from the SuperWASP (see Butters et al. 2010) dataset taken in 2007 to improve the ephemeris. Each of these datasets contain only a few measurements on any one night, so the following strategy was adopted. We calculated phases for all unflagged measurements in the two datasets based on a chosen linear ephemeris and the predicted timings for all minima measured here and by RGS. The initial epoch was fixed on the value derived for our five primary minima. The period was varied so as to maintain small residuals for the most recent data (sensitive to the initial epoch but not the period), and to get a qualitatively good light curve for the NSVS and SuperWASP data sets (sensitive to the period, but not the initial epoch). This technique completely avoids any cycle count ambiguity, but precludes putting uncertainties on the results.

$$\mathrm{HJD\ T_{min}\ I} = 2455563.6833 + 0.462078\mathrm{d} \times \mathrm{E}. \quad (1)$$

The final ephemeris is given by Eq. 1. The residuals for our timings are given in Table 3, and the plots of the two earlier datasets are given in Fig. 3. Note that primary minimum in the NSVS data seems to be near phase 0.96, and in the SuperWASP data at phase 0.03. This constrains the period rather well; improving either of these datasets makes the other less compelling. The discrepancy of each at about 0.04 cycles could be due to inaccuracies in those datasets (there is large intrinsic scatter, for example), or could be indicating a quadratic ephemeris. Also note in Table 3 that the secondary eclipses have residuals of about six minutes, which indicates that they cannot be used (and were not used) to derive the ephemeris. This is also obvious from Fig. 2, where it can be seen that the change in secondary minimum is more prominent after phase 0.50 than before; time of secondary minimum is clearly affected by the variation of the light curve.

In order to better understand the ephemeris of RGS, we calculated the (O−C) residuals for the times of minimum they derived from their data; see Table 4. The fourth column gives the residuals for the timings given in RGS; for entries 3–6 we noticed a discrepancy of about two hours, and realized that, since the period is about 11 hours, changing the HJD to one day earlier (and the cycle count two cycles earlier), we could reduce the residuals to just a few minutes. We speculate that the JD for the UT-date was used as if it were for the calendar date. Since the calendar dates given in RGS do not correspond to

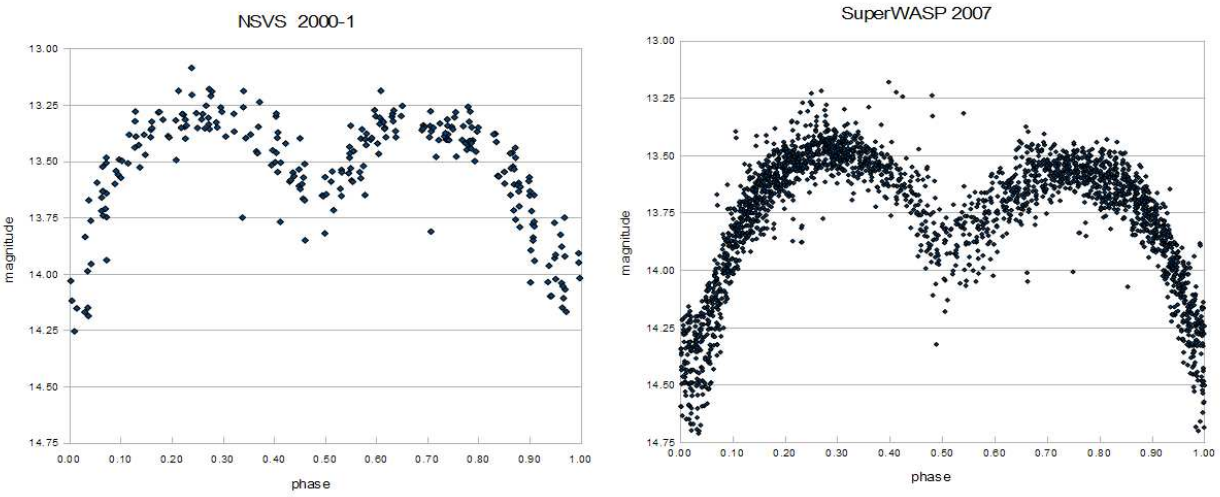

Figure 3. Light Curves from a) NSVS (left) and b) SuperWASP datasets.

these JD's, we cannot tell just what happened. Also, even though timings 1 and 2 seem to agree well with our ephemeris, no source data was cited in RGS, so we did not use these timings either.

Table 4. $O-C$ linear residuals for timings from RGS, based on our Eq. 1

No	Epoch (Obs) HJD	Cycle	$(O-C)$ minutes	$(O-C)$* minutes	Comment
1	2454408.9555	−2499.0	7.32	—	Primary
2	2454427.9001	−2458.0	6.46	—	Primary
3	2454829.7566	−1590.5	121.19	11.98	Secondary
4	2454829.9867	−1590.0	119.19	10.63	Primary
5	2454849.6213	−1547.5	114.49	5.28	Secondary
6	2454849.8522	−1547.0	114.29	5.08	Primary

* The residuals in col 5 result from increasing the cycle count by two and decreasing the HJD by 1 day.

A few comments about the first eight entries in Table 2 of RGS are in order; these come from the NSVS dataset we used in Fig. 3a here. The epochs given in RGS seem to have ignored the difference of 0.5 days for the MJD, in which those times are given. The times of minimum correspond to observations which were particularly faint, but not necessarily exact minima. However, many times of faint magnitude were ignored, and some were included in spite of the fact that the observation was flagged.

In conclusion, we find a new ephemeris for V963 Per, and caution that times of secondary minimum should not be included in calculating the ephemeris of this star. We would also caution that the formal errors of times of minimum, like the ones given in our Table 3, may be meaningless as well, since these times can be affected by starspots. We find that the star varies on a short timescale ($\sim$ one month) at the few percent level in brightness, and most of this variation is at a time in the cycle where the spots invoked by RGS are not visible, casting doubt on their interpretation of the spot characteristics. Given the nature of the star, its period is likely variable, but we cannot say at this point given the unresolved discrepancies in RGS's timings. Continued observations are

important to improve our understanding of this star's ephemeris and variability.

ACKNOWLEDGMENTS: We dedicate this paper to Hannah Varley (1978-2010). We thank Dr. Elizabeth M. Green of Steward Observatory for invaluable suggestions in obtaining and reducing the data from the Mont4K camera, and Steward Observatory for allocation of telescope time. We also thank Dr. Joel Eaton for comments on the manuscript. This publication makes use of the data from the Northern Sky Variability Survey created jointly by the Los Alamos National Laboratory and University of Michigan. We have used data from the SuperWASP public archive in this research. We thank the anonymous referee for careful reading and useful comments.

References:

Butters, O. W.; West, R. G.; Anderson, D. R.; Collier Cameron, A.; Clarkson, W. I.; Enoch, B.; Haswell, C. A.; Hellier, C.; Horne, K.; Joshi, Y.; Kane, S. R.; Lister, T. A.; Maxted, P. F. L.; Parley, N.; Pollacco, D.; Smalley, B.; Street, R. A.; Todd, I.; Wheatley, P. J.; & Wilson, D. M. 2010, *A&A*, **520**, L10 (SuperWASP)

Nicholson M.; Varley H. 2005, IBVS No. 5700

Odell A.P.; & Cushing G.E. 2004, IBVS No. 5514

Randall, S. K.; Green, E. M.; Van Grootel, V.; Fontaine, G.; Charpinet, S.; Lesser, M.; Brassard, P.; Sugimoto, T.; Chayer, P.; Fay, A.; Wroblewski, P.; Daniel, M.; Story, S.; & Fitzgerald, T. 2007, *A&A*, **476**, 1317

Samec, R. G.; Melton, R. A.; Figg, E. R.; Labadorf, C. M.; Martin, K. P.; Chamberlain, H. A.; Faulkner, D. R.; & Van Hamme, W. 2010, *Astron. J.*, **140**, 1150 (RGS)

Wozniak, P. R.; Vestrand, W. T.; Akerlof, C. W.; Balsano, R;, Bloch, J.; Casperson, D.; Fletcher, S.; Gisler, G.; Kehoe, R.; Kinemuchi, K.; Lee, B. C.; Marshall, S.; McGowan, K. E.; McKay, T. A.; Rykoff, E. S.; Smith, D. A.; Szymanski, J.; & Wren, J. 2004, *Astron. J.*, **127**, 2436 (NSVS)

* IRAF is distributed by the National Optical Astronomy Observatories, which are operated by the Association of Universities for Research in Astronomy, Inc., under cooperative agreement with the National Science Foundation.

COMMISSIONS 27 AND 42 OF THE IAU
INFORMATION BULLETIN ON VARIABLE STARS

Number 6002

Konkoly Observatory
Budapest
20 October 2011

HU ISSN 0374 – 0676

PHOTOMETRIC ANALYSIS OF V400 LYRAE

MARINO, GIUSEPPE [1,2]

[1] Gruppo Astrofili Catanesi - via Milo, 28 I-95125 Catania, ITALY, e-mail: giumar69@gmail.com

[2] Sezione Stelle Variabili – Unione Astrofili Italiani (UAI)

During 2010 I observed the EW-type eclipsing binary star V400 Lyrae with the aim of obtaining, for the first time, its physical parameters.

The data were acquired in five nights with a 0.20m Newtonian telescope equipped with a *SBIG ST-7XME* CCD camera provided with BVR_CI_C Johnson–Cousins *Custom Scientific* photometric filters.

At the beginning of each night, before starting the target's observing sequence, I observed standard stars in the open cluster IC 4665. For the target's images, the exposure times were 50–100 s (see the inset in Figure 2).

The CCD images were first corrected for dark and flat field frames; then, the following operations were performed:

- computation of the transformation coefficients to the Johnson–Cousins standard system through IC 4665 standards;
- determination of the magnitudes of four local comparison stars present in each image on the target;
- extraction and color-correction of the differential magnitudes of V400 Lyr;
- standard photometry of V400 Lyr with the help of the magnitudes of the local comparisons.

The dispersion of the magnitude data points was typically better than $0\overset{m}{.}02$–$0\overset{m}{.}03$. Some phase smearing was noted at the minima of the light curve for the 100 s exposures with the higher S/N ratio. However, the issue is generally indistinct in the noise.

I used atmospheric absorption coefficients computed, on each night, by means of the comparison stars observed in a suitable range of airmass. Zero points and color transformation coefficients were computed by analyzing the images of the standard stars in IC 4665 (Menzies & Marang 1996).

Differential and standard photometry were performed by using *MPO Canopus/PhotoRed* software. To evaluate the dependence on the specific procedure adopted, for one night I also performed the photometric reduction using *Iris* software, to extract the stellar fluxes subsequently converted into instrumental and standard magnitudes. These magnitudes are consistent with the results obtained with *MPO Canopus/PhotoRed*, with only a systematic shift within $0\overset{m}{.}01$, also using different photometric apertures.

The intrinsic precision of the procedure was also estimated applying the extraction of the magnitudes on the same standard stars of IC 4665, obtaining a standard deviation of $0\overset{\mathrm{m}}{.}01$ compared to the magnitudes tabulated by Menzies & Marang (1996).

The calibrated standard magnitudes of the comparison stars, obtained on three nights, are reported in Table 1; the RMSs of the comparison stars' magnitudes for corresponding stars are $\sim 0\overset{\mathrm{m}}{.}01$ and $\sim 0\overset{\mathrm{m}}{.}05$, respectively on those three nights and on all the five nights. The mean discrepancies of my magnitudes reported in Table 1 with respect to the values reported on MPOSC3 (the internal catalog of *MPO Canopus/PhotoRed* described in the user manual) are $0\overset{\mathrm{m}}{.}045$, $0\overset{\mathrm{m}}{.}023$, $0\overset{\mathrm{m}}{.}010$ and $0\overset{\mathrm{m}}{.}006$, respectively in the B, V, R_{C} and I_{C} bands.

To superimpose the data of different nights in a unique phased light curve, a revision of the ephemeris was necessary because of the period variation clearly evident in the O–C diagram present in the B.R.N.O. O–C *Gateway* web page (`http://var.astro.cz/ocgate`). No dependence of the O–C on the minimum type (primary or secondary) is evident, accounting for a half period difference between the two minima type, assuming phase 0.5 for secondary minima.

The linear best fit of the times of minimum spanning in the range 2009–2010 (Figure 1), leads to the following ephemeris:

$$\mathrm{T_{min}}\ (\mathrm{HJD}) = 2452500.084759(\pm 0.00164) + 0.25342419(\pm 0.00000015) \times \mathrm{E}$$

The first important step in my physical and geometrical analysis of V400 Lyr was to estimate its intrinsic colors.

As seen in Figure 2, the minimum at phase 0 (primary) is flatter (and slightly deeper) than the secondary one, so the star occulted at phase 0 should be smaller than its companion, and the orbital inclination should be near to 90° (total occultation).

The observed color indices at phase 0, quoted in the first line of Table 2, suggest a spectral classification in the ranges K1 V – K2 V (dwarfs), G9 IV – K1 IV (subgiants) and G5 III – G7 III (giants). We have to discard subgiant and giant stars, because they are incompatible with a period of $0\overset{\mathrm{d}}{.}25$. However, the observed color indices do not fit well a unique spectral type; this, coupled with the faint magnitude of the star (which indicates a distance larger than one hundred parsec), strongly suggests that this star is reddened by interstellar matter.

Thus, I computed all the possible dereddened colors, by letting the color excess $E(B-V)$ parameter free to vary from 0 to 0.60 in steps of 0.01. The color excesses $E(V-R)$ and $E(V-I)$ were deduced from $E(B-V)$ on the base of the relation represented in Figure 7 of Fitzpatrick (1999) assuming R=3.1. Comparing the dereddened colors at phase 0 with the expected ones for the various spectral types, I verified that the best fits is achieved for $E(B-V) \sim 0.11$ and spectral type between G8 V and K0 V.

The value of $E(B-V) = 0.11$ implies a distance of 0.43 kpc if we assume a standard reddening law $A(V) = 3.1 \times E(B-V)$ and an extinction value in V band of 0.8 mag/kpc typical of the Cygnus region (Mikolajewska & Mikolajewski 1980).

Table 1 Standard magnitudes and color indexes for the comparison stars

Star NOMAD1	$\alpha_{2000.0}$ hh:mm:ss	$\delta_{2000.0}$ ° ′ ″	V	$B-V$	$V-R_{\mathrm{C}}$	$V-I_{\mathrm{C}}$
1281-0377168	19:13:48.4	+38 07 57	11.777 ± 0.023	1.068 ± 0.019	0.575 ± 0.009	1.106 ± 0.009
1282-0369640	19:13:26.0	+38 16 12	12.158 ± 0.025	0.691 ± 0.021	0.412 ± 0.010	0.808 ± 0.011
1281-0377481	19:14:09.5	+38 07 19	11.584 ± 0.025	0.414 ± 0.014	0.246 ± 0.009	0.474 ± 0.011
1280-0380056	19:14:04.9	+38 00 13	11.632 ± 0.024	0.995 ± 0.019	0.535 ± 0.009	1.012 ± 0.009

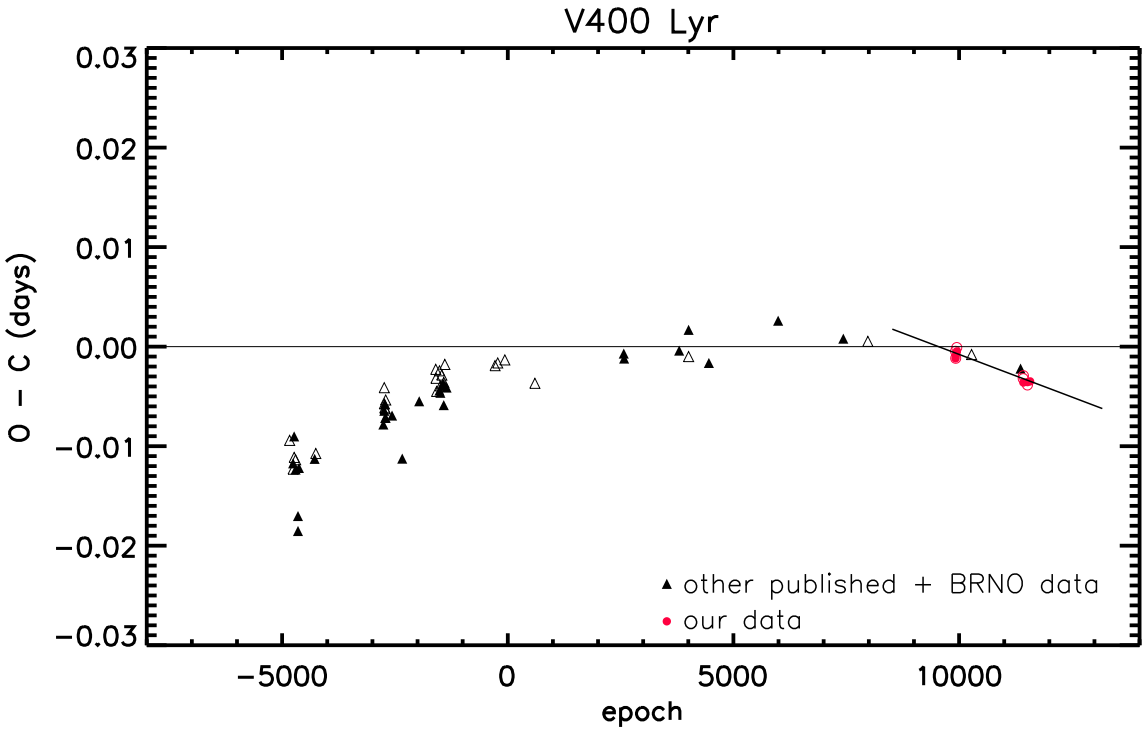

Figure 1. O−C diagram for V400 Lyr, assuming the ephemeris given in the web site of Kreiner (2004). Empty symbols are for secondary minima. The linear best fit for data spanning in the range 2009–2010 is shown. As "our data" are also considered the minima obtained by Marino et al. (2010).

Table 2 Observed and dereddened V magnitude and colors during the primary minimum of V400 Lyr

$E(B-V)$	V	$B-V$	$V-R_{\rm C}$	$V-I_{\rm C}$
0.00	13.32	0.859 ± 0.02	0.523 ± 0.01	0.998 ± 0.02
0.08	13.07	0.78	0.44	0.87
0.11	12.99	0.75	0.41	0.82

The comparison between dereddened V magnitude at the primary minimum and absolute magnitudes expected for G8 V – K0 V stars suggests $E(B-V) \sim 0.08$ and spectral type ∼K0 V.

Combining the previous considerations, it is reasonable to assume a temperature $T = 5300 \pm 100$ K for the "2" star visible at phase 0.

The following step of the analysis consisted in searching for the geometrical and surface model of the two eclipsing components to best reproduce the shape of each light curve. With this aim, I used PHOEBE software (Prsa & Zwitter 2005). A preliminary solution was found by using the v0.31a version for Windows, that is the latest stable publicly available version; after, the v0.32 subversion for Windows was used to find the final solution.

To give a relative weight to the different $BVR_{\rm C}I_{\rm C}$ light curves, for each photometric band I considered not only the photometric error in each individual point, but also the average of residuals with respect to the best fit solution. However, the resulting solution was found very similar to the fit of unweighted curves.

The shape of an eclipsing binary light curve essentially depends on *relative* quantities (star "2" with respect to star "1"); for instance, relative mass, relative size and relative effective temperature can be deduced. However, my estimation of distance and spectral type allows an absolute scaling of the system which is good enough to establish limb and gravity darkening coefficients, respectively x and g, typically tabulated as function of effective temperature and log g. The separation of the components, necessary to absolutely calibrate masses and sizes, was (approximately) obtained iteratively adjusting it up to obtain a bolometric magnitude consistent with the expected value for a G9 V spectral type, assumed for the component occulting visible at phase 0 (*secondary star* in the PHOEBE convention); distance and dereddened V observed magnitude were also taken into account. However, the best and more secure way to get an absolute scale for the system is to obtain the radial velocity curve of both components, which would require a telescope with a much larger aperture.

For each photometric band, linear limb darkening coefficients were assumed interpolating the values tabulated by van Hamme (1993) for solar abundances. Bolometric albedo was assumed to be 0.60. No third light was allowed and circular orbit and synchronous rotation were assumed. Gravity darkening was assumed as the average of the values recently given by Claret & Bloemen (2011) for different bands, which are considerably different from the value of $g = 0.32$, typically adopted in previous light curve modellings. By using $g = 0.32$, the temperature found is about 30 K higher, but similar values for the other fitted parameters and cost function were found. Negligible differences are obtained considering more complex expressions for the limb-darkening, such as quadratic or square-root laws.

The simultaneous fit of the $BVR_{\rm C}I_{\rm C}$ light curves was run using Differential correction method, stopping the iterations at the minimum value of the cost function. To avoid remaining trapped in local minima in the parameter space, several different starting pa-

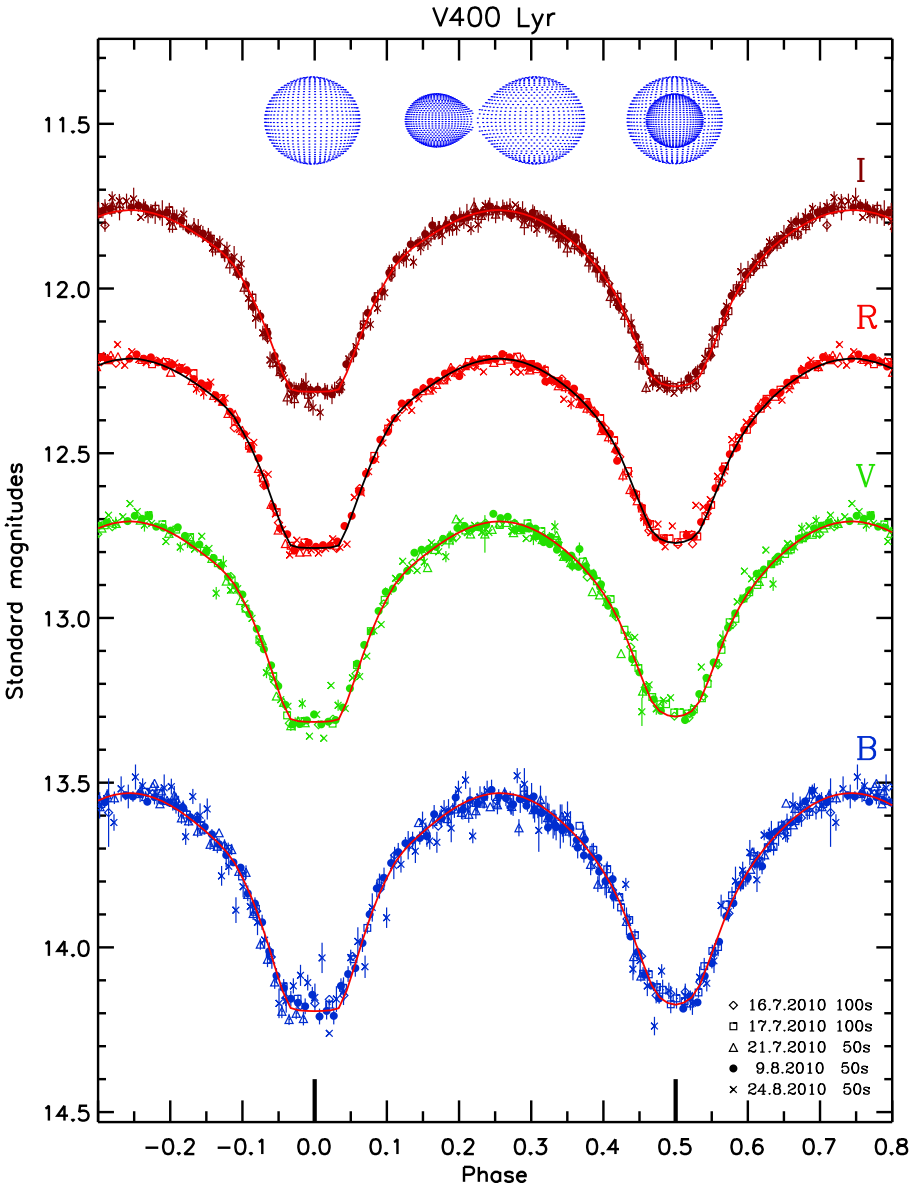

Figure 2. BVR_CI_C photometry of V400 Lyr. The synthetic light curves are shown as continuum line. The stellar configuration is represented at the phases 0.00, 0.25 ad 0.50. The (original not scaled) error bars are shown for errors larger than $0\overset{m}{.}015$.

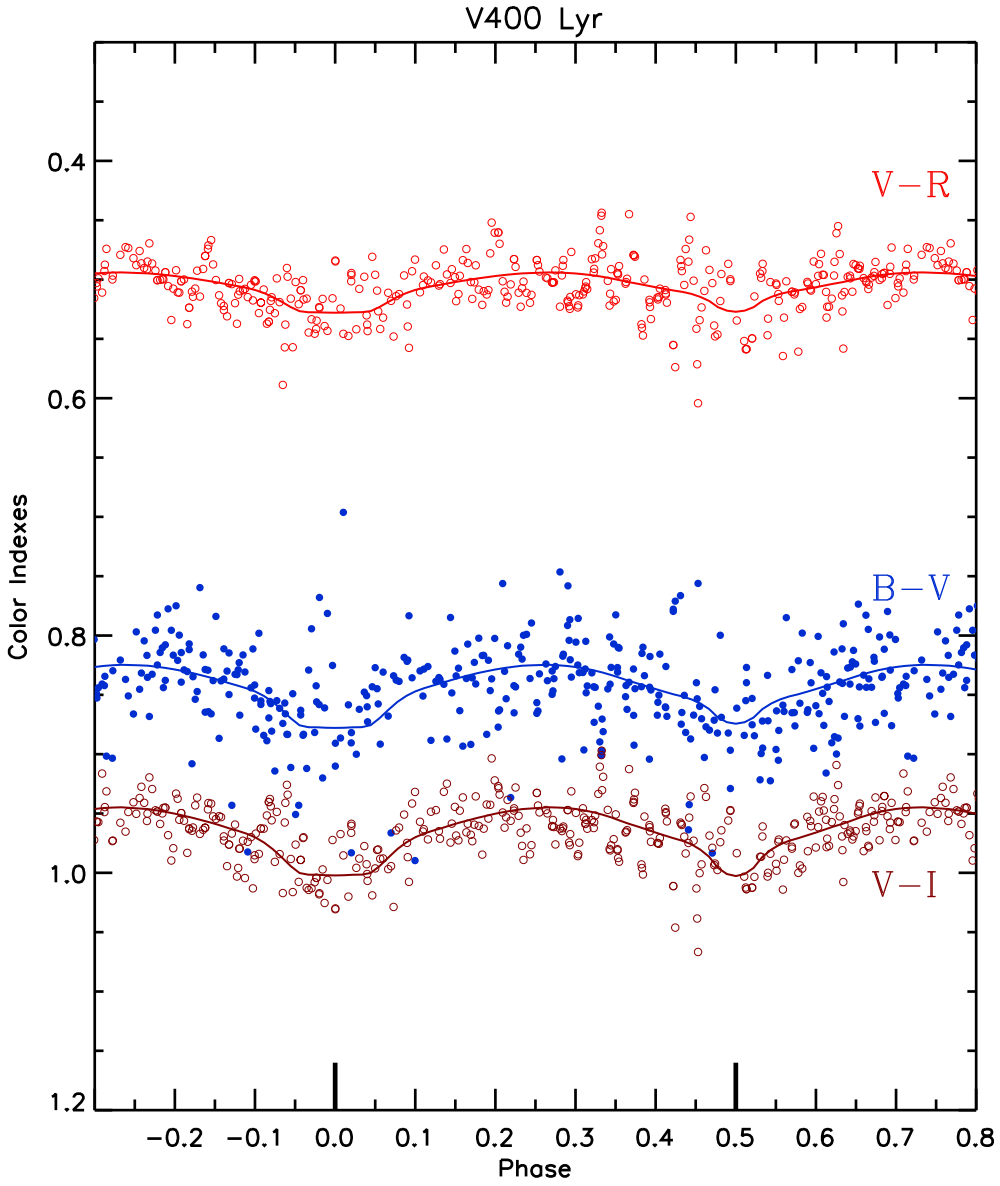

Figure 3. Color indices of V400 Lyr.

rameters were tried. Also running the Simplex method, the same region of the parameters' space was reached.

By adopting the "Overcontact binary of the W UMa type" Mode (that assumes thermal equilibrium between the two components) the solution found for mass ratio $q < 1$ is able to reproduce the different depths of the minima, but it shows a flatter minimum at phase 0.5, unlike the observed light curve. Instead, the solution obtained assuming $q > 1$ reproduces the flat minimum at phase 0, but it presents the deeper minimum at phase 0.5. Only by setting the "Overcontact binary not in thermal contact" Mode, is possible to correctly fit depth and shape of the minima (for $q > 1$).

As usual, the light curve modelling *does not* fit the relative shift between different photometric bands (i.e. the color indices), being the level of each synthetic curve optimized on the corresponding observed light curve, which is internally normalized by the fitting program. Thus, the light curve solutions are shifted to be superimposed on the observed light curves.

Figure 2 shows the best fit to the $BVR_{\rm C}I_{\rm C}$ light curves versus phase.

The geometrical representation of the system is given in the same Figure 2 for three different phases.

The color indices are shown in Figure 3; the continuum lines represent the synthetic curves obtained as the difference of the synthetic magnitudes.

The resulting fit indicates V400 Lyr is a W-type W UMa contact binary, being the larger secondary in front of the smaller primary component at the primary minimum.

It is useful to recall that radial velocity measures are strongly necessary to obtain an accurate absolute determination of masses and sizes. However, in the final rows of Table 3, possible absolute values are reported, deduced from the light curve model assuming that the secondary component is similar to a G9 V star. We note that the mass and the radius for the primary (hotter and smaller) star is much smaller than expected values typical of a main sequence star with effective temperature of ~ 5450 K. This is probably a consequence of stellar evolution strongly influenced by mass exchange and, eventually, by mass loss. In fact, stellar masses agree with the empirical relation given by Gazeas & Niarchos (2006) for contact binaries.

The asymmetry visible in B and V bands near the bottom of the secondary minimum is probably due to cool spots on the cooler star.

References:

Claret, A., Bloemen, S., 2011, *A&A*, **529**, A75
Fitzpatrick, E. L., 1999, *PASP*, **111**, 63
Gazeas, K. D., Niarchos, P. G., 2006, *MNRAS*, **370**, L29
Kreiner, J. M., 2004, *AcA*, **54**, 207, `http://www.as.up.krakow.pl/ephem`
Marino, G., *et al.*, 2010, *IBVS*, **5917**, 1
Menzies, J. W., Marang, F., 1996, *MNRAS*, **282**, 313
Mikolajewka, J., Mikolajewki, M., 1980, *AcA*, **30**, 347
Prsa, A., Zwitter, T., 2005, *ApJ*, **628**, 426
van Hamme, W., 1993, *AJ*, **106**, 2096

Table 3 Physics and geometrical elements of V400 Lyr

Parameter	Value	Error[1]
i	89.°6	0.°2 (1°)
T_1	5450 K	(110 K)[2]
T_2	5300 K	(assumed)
$q = M_2/M_1$	2.97	0.01 (0.1)
$\Omega_1 = \Omega_2$	6.47	0.01 (0.1)
g_1	0.48	(assumed)
g_2	0.51	(assumed)
$x_1(B)$	0.79	(assumed)
$x_1(V)$	0.65	(assumed)
$x_1(R_C)$	0.54	(assumed)
$x_1(I_C)$	0.44	(assumed)
$x_1(bol)$	0.52	(assumed)
$x_2(B)$	0.81	(assumed)
$x_2(V)$	0.68	(assumed)
$x_2(R_C)$	0.56	(assumed)
$x_2(I_C)$	0.46	(assumed)
$x_2(bol)$	0.53	(assumed)
A_1	0.6	(assumed)
A_2	0.6	(assumed)
$L_2/L_1(B)$	2.195	0.009 (0.04)
$L_2/L_1(V)$	2.295	0.007 (0.04)
$L_2/L_1(R_C)$	2.365	0.008 (0.04)
$L_2/L_1(I_C)$	2.414	0.008 (0.04)
(from q and Ω)		
R_1/a	0.301	(0.06)
R_2/a	0.488	(0.06)
(assuming $a = 1.80 R_\odot$)[3]		
M_1	$0.31 M_\odot$	($0.01 M_\odot$)
M_2	$0.91 M_\odot$	($0.01 M_\odot$)
R_1	$0.54 R_\odot$	($0.1 R_\odot$)
R_2	$0.88 R_\odot$	($0.1 R_\odot$)
M_{bol-1}	6.3	(0.4)
M_{bol-2}	5.4	(0.3)

[1] Formal errors from the differential corrections solution. In bracket, heuristic approximated errors based on the cost function's trend.

[2] Essentially derived from the uncertainty on T_2.

[3] Absolute values should be regarded as preliminary estimates, due to unavailability of radial velocities.

COMMISSIONS 27 AND 42 OF THE IAU
INFORMATION BULLETIN ON VARIABLE STARS

Number 6003

Konkoly Observatory
Budapest
10 November 2011

HU ISSN 0374 – 0676

IMPLICATIONS OF THE NON-DETECTION OF X-RAY EMISSION FROM HD 149427

STUTE, M.[1]; LUNA, G.J.M.[2,3]

[1] Institute for Astronomy and Astrophysics, Section Computational Physics, Eberhard Karls University Tübingen, Auf der Morgenstelle 10, 72076 Tübingen, Germany

[2] Instituto de Ciencias Astronomicas, de la Tierra y del Espacio (ICATE), Av. Espana Sur 1512, J5402DSP, San Juan, Argentina

[3] Harvard-Smithsonian Center for Astrophysics, 60 Garden St. MS 15, Cambridge, MA, 02138, USA

1 Introduction

HD 149427 (PC 11 = IRAS 16336-5536 = PN G 331.1-05.7) was first noticed to be a peculiar object by Webster (1966). Its exact nature is not known, several scenarios exist in the literature.

The object is listed in the Planetary Nebula (PN) catalogue of Peimbert & Costero (1961) as PC 11, in the catalogue of Southern PNe of Henize (1967) as Hen 2-172 and in the catalogue of Henize (1976) as Hen 3-1223 based on its Hα emission. Henize (1976) noted that the emission-line spectrum is that of a PN but with a continuum of an F star. Gutierrez-Moreno et al. (1987) systematically investigated HD 149427 using optical photographic, spectrophotometric and spectroscopic observations. They suggested that it is indeed a young peculiar PN. Gutierrez-Moreno et al. (1995) confirmed this with a diagram using the ratios of [OIII]λ4363/Hγ and [OIII]λ5007/Hβ. Parthasarathy et al. (2000) suggested that the central star is a close binary system with an early-F dwarf companion based on UV variations. Webster (1966) classified the object as a symbiotic star (SyS) based on its spectrum. Using NIR observations, Glass & Webster (1973) classified HD 149427 as SyS with a yellow supergiant as cool component, however, their NIR observations could not reliably identify its nature. Allen & Glass (1974) confirmed this result with new NIR observation, but pointed out the high density and high excitation in the nebulosity. Allen (1982) listed it as a D'-type SyS.

The distance is also very uncertain. Milne & Aller (1975) detected 5 GHz radio emission and estimated the distance > 6.7 kpc based on its radio flux. Milne (1979) revised the 5 GHz catalogue of PNe and listed a radio distance of > 10.5 kpc. However, it has been shown that a nearby radio source may be confused with HD 149427 (Wright & Allen 1978). Maciel (1984) used a relationship between nebular ionized mass and radius and estimated a distance of < 6.2 kpc. Gutierrez-Moreno et al. (1987) estimated a distance of about 3 kpc. Kenny (1995) used radio observations for determining the distance of about 5 kpc. Gutierrez-Moreno & Moreno (1998) measured the spectral type of the late component of

the central star and, using NIR colors of Glass & Webster (1973), determined a short distance of 420 pc assuming a luminosity class V. Assuming that the cool component is, however, a giant of luminosity class III, this estimated distance had to be increased to 850 pc (Gutierrez-Moreno & Moreno 1998). Tajitsu & Tamura (1998) derived a distance of 9 kpc using IRAS four-band fluxes. Phillips (2001) used the observed radial velocities of PNe and the galactic rotation curve for measuring the distance to 3.27 kpc. Pereira et al. (2010) analized high-resolution spectra of the late-type companion and found $\log g$ and T values implying a distance of 9.94 kpc. However, using the luminosity of the white dwarf in the system, the distance of about 10 kpc would result in a extremely large white dwarf radius of 0.14 $R_{\odot}$ (Pereira et al. 2010).

HD 149427 received our attention since it is a member of the list of symbiotic stars with possible jet detections compiled by Brocksopp et al. (2004). Brocksopp et al. (2003) found three peaks and extended emission in HST WFPC2 snapshot images taken in July 1999 with F502N and F656N filters corresponding to the central source and knots at distances of about 2″ and 12″. Radio observations show extended emission in the same direction as the peaks in the HST images (Brocksopp et al. 2003). Gutierrez-Moreno & Moreno (1998) found evidence for jet-like [OIII] emission moving away from the central nebula with a velocity of 120 km s^{-1}.

X-ray observations provide a direct probe of the two most important components of jet-driving systems: the bow and internal shocks of the jet emitting soft X-rays and the central parts of the jet engine, where gas is being accreted to power the jet, leading to hard X-ray emission. Currently R Aqr (Kellogg et al. 2001, 2007) and CH Cyg (Galloway & Sokoloski 2004; Karovska et al. 2007, 2010) are the only two jets from symbiotic stars that have been resolved in X-rays. All objects with jets, detected in other wavelength, when observed in X-rays, show soft components (< 2 keV; R Aqr, CH Cyg, MWC 560, RS Oph, AG Dra, Z And, V1329 Cyg). The three objects CH Cyg, R Aqr, MWC 560 also emit hard components (Mukai et al. 2007; Nichols et al. 2007; Stute & Sahai 2009). Z And showed hard emission in one of three observations only (Sokoloski et al. 2006).

2 Observation and analysis

We observed the field of HD 149427 with *XMM-Newton* in 2009 (Table 2) using the EPIC instrument operated in full window mode and with the medium thickness filter. Simultaneously, we used the Optical Monitor OM. All the data reduction was performed using the Science Analysis Software (SAS) software package version 8.0. We removed events at periods with high background levels from the pipeline products selecting events with pattern 0–4 (only single and double events) for the pn and pattern 0–12 for the MOS, respectively, and applying the filter FLAG=0. The resulting exposure time after these steps is 33.5 ks.

[†]http://xmm.esac.esa.int/

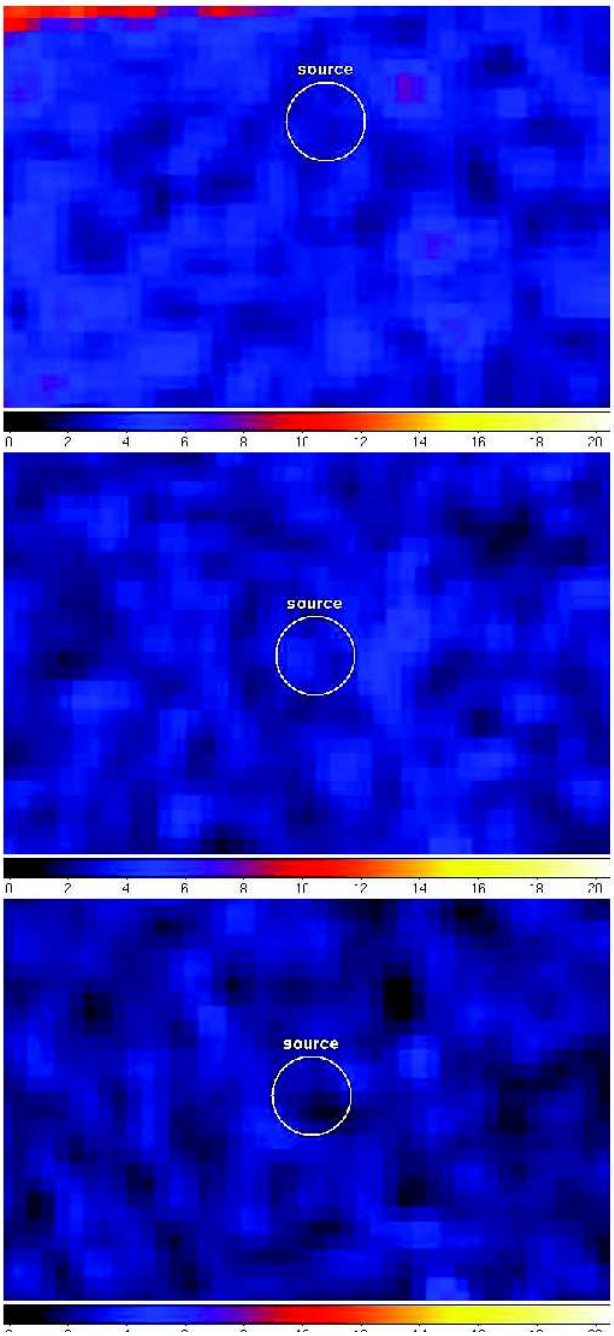

Figure 1. EPIC images of the region around HD 149427; top: pn, middle: MOS1, bottom: MOS2; colors show the number of counts.

Table 1. Observations on September 01/02, 2009 (ObsID: 0604920201)

Instrument	Filter	Duration	UT Start	UT Stop
pn	Medium	68430	19:05:32	14:06:02
MOS1	Medium	69504	18:43:12	14:01:36
MOS2	Medium	69515	18:43:11	14:01:46
OM	U	10× ∼1500	18:51:36	23:49:51
	UVW1	10× ∼1500	00:40:11	06:08:27
	UVM2	15× ∼1500	06:13:48	15:02:12

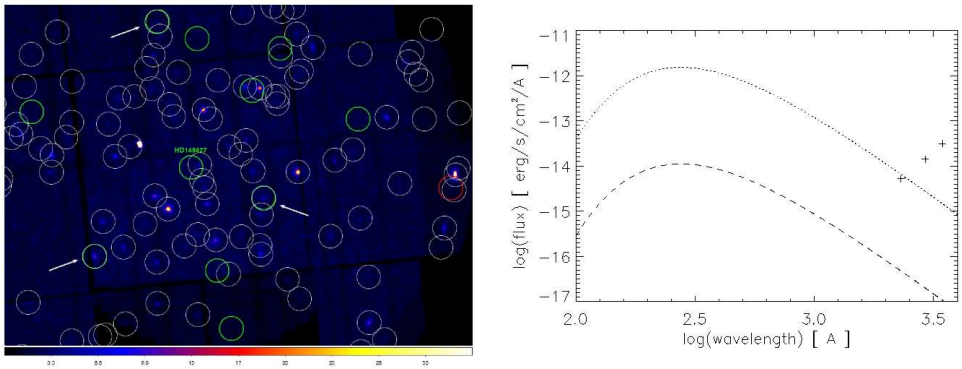

Figure 2. Left: Mosaic of EPIC images of the region around HD 149427 including our detected X-ray sources (white circles), the reference objects from SIMBAD (green circles) and also the closest source from the *ROSAT* faint source all-sky survey (red circle). We can clearly identify three objects, for which the SIMBAD position agrees perfectly with the position found in our source detection run (white arrows) and thus can exclude any pointing error and indeed report the non-detection of HD 149427 in X-rays. Right: Spectral energy distribution in the optical filters U, $UVW1$ and $UVM2$. Also plotted is blackbody emission representing a white dwarf with a temperature of 105000 K and radius of 8×10^8 cm at distances of 850 pc (dotted line) and 9.96 kpc (dashed line). The slope and flux level of the spectral energy distribution indicates that the optical flux is dominated by nebular emission.

3 Results

All three X-ray images with the EPIC pn, MOS1 and MOS2 cameras show no detection of emission above background levels centered on HD 149427 using the coordinates from SIMBAD (Fig. 1, white circles). In all bands, however, a faint source is visible, which is about 26″ away from the nominal position of HD 149427. According to Kerber et al. (2008), the proper motion of HD 149427 is of the order of a few mas in RA and about 20 mas in Dec, thus too small for explaining this discrepancy. In order to check, whether possible pointing errors arose during our *XMM* observations, we created images in the soft and hard band for all three cameras, ran a source detection with EDETECT and finally identified the closest 11 objects listed by SIMBAD in our mosaic. Fig. 2 shows the mosaic including our detected X-ray sources (white circles), the reference objects from SIMBAD (green circles) and also the closest source from the *ROSAT* faint source all-sky survey (red circle). While the pointing uncertainties in the *ROSAT* mission are obvious, we can clearly identify three objects, for which the SIMBAD position agrees perfectly with the position found in our source detection run (white arrows). Therefore we can exclude any pointing error and indeed report the non-detection of HD 149427 in X-rays.

Contrary to the X-ray band, HD 149427 has been detected in the three optical bands used. The average magnitudes in the optical filters U, $UVW1$ and $UVM2$ are $12\overset{\mathrm{m}}{.}7$, $13\overset{\mathrm{m}}{.}5$ and $14\overset{\mathrm{m}}{.}8$, respectively. The slope of the spectral energy distribution indicates that the optical flux is dominated by nebular emission (Fig. 2). The flux levels of blackbody emission corresponding to a white dwarf with a radius of 8×10^8 cm and with an effective temperature of 105000 K at a distance of 850 pc (Gutierrez-Moreno & Moreno 1998) are lower than the measured fluxes.

We examined the OM photometry (Fig. 3). The optical light curves are consistent with a constant flux. The measured rms variations, those expected from Poisson statistics, and the ratios of these two quantities are listed in Table 3. s and s_{exp} are given in percentage of the mean value. The optical light curves in filters UVW1 and UVM2 where the ratio of measured to expected rms s/s_{exp} is 1.27 and 1.21, respectively, may indicate weak variability, however, the presence of systematic and/or unknown errors is more likely. Since the optical flux is dominated by nebular emission, we do not expect variability in these bands.

Table 2. Measured and expected variations and their ratio

optical filter	measured variation s	expected variation s_{exp}	ratio s/s_{exp}
U	0.044 %	0.045 %	0.96
UVW1	0.045 %	0.046 %	1.27
UVM2	0.288 %	0.237 %	1.21

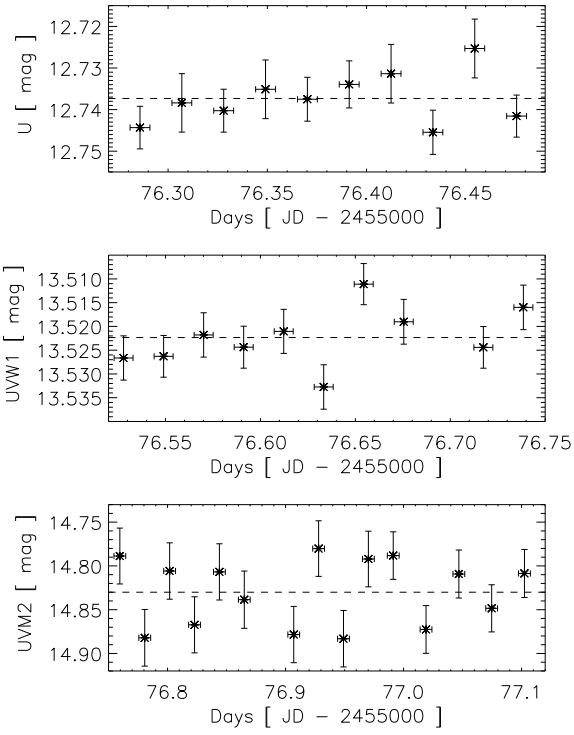

Figure 3. Light curves of the OM exposures for filters U (left, 3440 Å), $UVW1$ (middle, 2910 Å) and $UVM2$ (right, 2310 Å). The dotted lines show the average magnitude.

4 Discussion

Using the effective exposure time of 33.5 ks in all instruments, the sensitivity of *XMM-Newton* (Watson et al. 2001) gives an upper limit of about 10^{-15} erg s^{-1} cm^{-2} in the soft band (< 2 keV) and of about 10^{-14} erg s^{-1} cm^{-2} in the hard band (> 2 keV).

We can identify several different scenarios for the nature of HD 149427 in the literature: a planetary nebula or a symbiotic star, both either close to us or very distant.

Pereira et al. (2010) favor the idea of HD 149427 being a distant PN at about 10 kpc away from us. From the position of HD 149427 in the [OIII]λ5007/Hβ – [OIII]λ4363/Hγ diagram, they claim it is neither consistent with that of PNe nor that of symbiotic stars. They argue that the electron density observed in HD 149427 is higher than typical electron densities in PNe, but not as high as observed in D- and D'-type symbiotics. However, the closest object to HD 149427 in this diagram is another D'-type symbiotic. Or is HD 149427 a symbiotic star whose companion just turns into a PN?

In case of HD 149427 being a central star of a PN, we simply expect X-ray emission from a blackbody with a temperature of about 10^5 K (Gutierrez-Moreno & Moreno 1998) as given in Fig. 2. The emission at 0.2 keV (= 62 Å) would be fainter than our upper limits, so our non-detection would have no significant implications.

However, if HD 149427 were a symbiotic star and accretion was present in this object, we would be able to test the accretion rate with important implications (see below).

For deriving the distance to HD 149427, Pereira et al. (2010) used their fits to high resolution spectra, namely their derived values of $\log g$ and $\log T$. They estimated the luminosity of the star and calculated the distance to it using a measured V magnitude. They finally derived a distance of 9.94 ± 0.6 kpc. However, using the luminosity of the white dwarf in the system, the distance would result in a extremely large white dwarf radius of 0.14 $R_\odot$ (Pereira et al. 2010). Turning this argument around and using radius determinations of 0.01–0.02 $R_\odot$ (e.g. Gutierrez-Moreno & Moreno 1998), we would get a distance of about 0.7–1.5 kpc. A second point of criticism is that the error estimate mentioned above bases only on the error of $\log g$ and $\log T$, but not on the error of the V magnitude. The V magnitudes in the literature vary between $11\overset{\mathrm{m}}{.}2$ and $12\overset{\mathrm{m}}{.}7$ – the latter value has been used by Pereira et al. (2010). The former value, however, would imply a distance of only about 5 kpc, thus the distance based only on their own data is still highly uncertain. The smallest estimated distance to HD 149427 is only 850 pc (Gutierrez-Moreno & Moreno 1998), therefore we adopt two extremal distances of 850 pc and 10 kpc.

With a distance of 850 pc, the flux upper limits give an upper limit for the soft X-ray luminosity of about 8.6×10^{28} erg s^{-1} and for the hard X-ray luminosity of about 8.6×10^{29} erg s^{-1}; with the highest claimed distance of 9.96 kpc, these limits increase to 1.2×10^{31} erg s^{-1} and 1.2×10^{32} erg s^{-1}, respectively.

Since accretion should be the main source of hard X-ray emission in this objects, we can convert these upper limits of luminosities into upper limits for the accretion rates. From the definition

$$L_{\mathrm{acc}} \lesssim \frac{1}{2}\frac{G\,M\,\dot{M}}{R} = 3 \times 10^{32}\,\mathrm{erg\ s^{-1}} \left(\frac{M}{0.6\,\mathrm{M_\odot}}\right) \left(\frac{\dot{M}}{10^{-10}\,\mathrm{M_\odot\,yr^{-1}}}\right) \left(\frac{8 \times 10^8\,\mathrm{cm}}{R}\right) \quad (1)$$

follows that, after assuming the largest distance, the white dwarf accretes with a rate below 10^{-10} M$_\odot$ yr^{-1}. At these low accretion rates, a boundary layer between the accretion disk

and the surface of the white dwarf is optically thin (Pringle & Savonije 1979; Popham & Narayan 1995) and thus emitting hard X-rays with $L_{\rm acc}$. In case, the low distance of 850 pc is correct, the upper limit on the accretion rate reduces even to 10^{-13} $M_\odot$ yr^{-1}.

Gutierrez-Moreno & Moreno (1998) found an electron density of the potential jet knot of 10^5 cm^{-3}, an electron temperature of 20000 K and a velocity of this knot of 120 km s^{-1}. With a typical ionization fraction at this temperature and a typical compression factor – we assume that the observed values correspond to those of shocked jet material – we derive an (un-shocked) jet density in the same order of magnitude as the measured electron density.

The jet velocity is connected to the velocity of the contact discontinuity or knot via

$$v_{\rm knot} = v_{\rm jet} \frac{\sqrt{\eta}}{1+\sqrt{\eta}} \tag{2}$$

with η being the ratio of jet to ambient density. Therefore the jet velocity is always higher than the knot propagation velocity (e.g. a factor 4.2 for $\eta = 0.1$ or 1.3 for $\eta = 10$). The presence of a jet with a velocity of about 120 km s^{-1} naturally leads to shocks with temperatures of the order of 0.02 keV, which contribute only marginally to the bands observed with *XMM-Newton* or *Chandra*. Higher velocities above 300 km s^{-1}, however, should lead to soft X-ray emission. Assuming a cylindrical jet with a radius of about 1 AU, the mass-loss rate in the jet is

$$\dot{M}_{\rm jet} = \pi\, R_{\rm jet}^2\, n_{\rm jet}\, m_{\rm H}\, v_{\rm jet} > 2.3 \times 10^{-11}\, M_\odot\, {\rm yr}^{-1}\,. \tag{3}$$

Since the mass-loss rate through the jet is at most a few percent of the mass accretion rate (depending on the underlying jet formation model), the latter must have been of the order of 10^{-10} – 10^{-8} $M_\odot$ yr^{-1} at the time when the jet was formed.

The kinetic luminosity of the jet would be

$$L_{\rm kin} = \frac{1}{2}\, \dot{M}_{\rm jet}\, v_{\rm jet}^2 > 2 \times 10^{29}\, {\rm erg\ s}^{-1}\,. \tag{4}$$

Only a fraction of this kinetic luminosity ($\sim$ 1–20 %, Stute & Sahai 2007) would be radiated away in soft X-rays, thus the presence of an X-ray emitting jet cannot be ruled out by our non-detection, independent of adopting the small or large distance. Furthermore we can argue that if a larger fraction of the proposed observation time had not been affected by high background, we might have detected soft emission from the jet.

Another source of soft X-ray emission might be the presence of colliding winds as in β systems classified by Mürset et al. (1991, 1997). Their typical luminosity may also be of the order of 10^{31} erg s^{-1}.

5 Conclusion

We reported the non-detection of X-ray emission from the enigmatic object HD 149427. This result poses upper limits on the mass accretion rate of the white dwarf. Such low accretion rates are untypical of symbiotic stars and may favor the picture of HD 149427 being a young PN, even if we adopt the larger values of its distance. Unfortunately, the distance to HD 149427 is still highly uncertain.

We estimated the possible mass-loss rate and kinetic luminosity of the jet and found no contradiction with our upper limit of soft X-ray emission. If a larger fraction of the proposed observation time had not been affected by high background, we might have

detected soft emission from the jet. Therefore new X-ray observations might give new exciting results for this enigmatic object.

ACKNOWLEDGMENTS: This work is based on observations obtained with *XMM-Newton*, an ESA science mission with instruments and contributions directly funded by ESA Member States and the USA (NASA). GJML thanks NASA for funding this work by *XMM-Newton* AO-8 award NNX09AP88G.

References:

Allen, D.A., Glass, I.S. 1974, *MNRAS*, **167**, 337
Allen, D.A. 1982, *ASSL*, **95**, 27
Brocksopp, C., Bode, M. F., Eyres, S. P. S. 2003, *MNRAS*, **344**, 1264
Brocksopp, C., Sokoloski, J. L., Kaiser, C., et al. 2004, *MNRAS*, **347**, 430
Galloway, D. K., Sokoloski, J. L. 2004, *ApJ*, **613**, L61
Glass, I.S., Webster, B.L. 1973, *MNRAS*, **165**, 77
Gutierrez-Moreno, A., Moreno, H. 1998, *PASP*, **110**, 458
Gutierrez-Moreno, A., Moreno, H., Cortes, G. 1987, *Rev. Mex. A. A.*, **14**, 344
Gutierrez-Moreno, A., Moreno, H., Cortes, G. 1995, *PASP*, **107**, 462
Henize, K.G. 1967, *ApJS*, **14**, 125
Henize, K.G. 1976, *ApJS*, **30**, 491
Karovska, M., Carilli, C. L., Raymond, J. C., Mattei, J. A. 2007, *ApJ*, **661**, 1048
Karovska, M., Gaetz, T. J., Carilli, C. L., Hack, W., Raymond, J. C., Lee, N. P. 2010, *ApJ*, **710**, L132
Kellogg, E., Pedelty, J. A., Lyon, R. G. 2001, *ApJ*, **563**, L151
Kellogg, E., Anderson, C., Korreck, K., et al. 2007, *ApJ*, **664**, 1079
Kenny, H.T. 1995, PhD Thesis, University of Calgary
Kerber, F., Mignani, R. P., Smart, R. L., Wicenec, A. 2008, *A&A*, **479**, 155
Maciel, W. J. 1984, *A&AS*, **55**, 253
Milne, D.K. 1979, *A&AS*, **36**, 227
Milne, D.K., Aller, L.H. 1975, *A&A*, **38**, 183
Mukai, K., Ishida, M., Kilbourne, C., et al. 2007, *PASJ*, **59**, S177
Mürset, U., Nussbaumer, H., Schmid, H. M., Vogel, M. 1991, *A&A*, **248**, 458
Mürset, U., Wolff, B., Jordan, S. 1997, *A&A*, **319**, 201
Nichols, J. S., DePasquale, J., Kellogg, E., et al. 2007, *ApJ*, **660**, 651
Parthasarathy, M., Garcia-Lario, P., Pottasch, S. R., et al. 2000, *A&A*, **355**, 720
Peimbert, M., Costero, R. 1961, *BOTT*, **3**, 33
Pereira, C. B., Baella, N. O., Daflon, S., Miranda, L. F. 2010, *A&A*, **509**, A13
Phillips, J.P. 2001, *A&A*, **367**, 967
Popham, R., Narayan, R. 1995, *ApJ*, **442**, 337
Pringle, J. E., Savonije, G. J. 1979, *MNRAS*, **187**, 777
Sokoloski, J. L., Kenyon, S. J., Espey, B. R., et al. 2006, *ApJ*, **636**, 1002
Stute, M., Sahai, R. 2007, *ApJ*, **665**, 698
Stute, M., Sahai, R. 2009, *A&A*, **498**, 209
Tajitsu, A., Tamura, S. 1998, *AJ*, **115**, 1989
Watson, M. G., Augueres, J.-L., Ballet, J., et al. 2001, *A&A*, **365**, L51
Webster, L. B. 1966, *PASP*, **78**, 136
Wright, A.E., Allen, D.A. 1978, *MNRAS*, **184**, 893

COMMISSIONS 27 AND 42 OF THE IAU
INFORMATION BULLETIN ON VARIABLE STARS

Number 6004

Konkoly Observatory
Budapest
30 November 2011

HU ISSN 0374 – 0676

ANOTHER COMPONENT IN THE MULTIPLE SYSTEM η Mus

BUTLAND, R.J.[1]; BUDDING, E.[2,3,4]

[1] Royal Astronomical Society of New Zealand, Private Bag, Wellington, NZ email:roger.butland@gmail

[2] Carter Observatory, PO Box 2909, Wellington, NZ

[3] School of Chemical and Physical Sciences, Victoria University of Wellington (VUW), NZ

[4] Department of Physics and Astronomy, University of Canterbury (UC), NZ

The multiple star η Mus (HD 114911, HIP 64661, HR 4993) contains a bright ($V \sim$ 4.8-4.9, $B - V \approx -0.08$, $U - B \approx -0.34$) young B8V type eclipsing binary, about 58 arcsec from a 7.3 mag visual companion η Mus B (CD 67 1384B) and within ∼3 arcsec of a 10th mag (J) closer companion (η Mus C = DUN 131C). The sky location, HIPPARCOS distance 124 ± 9 pc and proper motions ($\mu_\alpha \cos\delta = -36.92$; $\mu_\delta = -10.63$ mas y^{-1}), make the system a likely member of the Lower Centaurus Crux concentration of the Sco-Cen OB2 Association (Nitschelm, 2004). This setting makes the system of interest for star formation studies and understanding gravitational binding within young associations.

Although included in several early programmes, the eclipsing binary nature only became clear after the HIPPARCOS light curve appeared (ESA, 1997). Buscombe and Morris (1961) had combined early spectroscopy with their own to produce a primary radial velocity curve and mass function, suggestive of a low secondary mass. The period used by Buscombe and Morris (1961) was apparently an alias of that found by HIPPARCOS, so promoting updated spectroscopic study, such as that published by Bakış et al. (2007).

Tokovinin's (1997) catalogue gave an estimate of the period for the wide pair at around 200000 y. But Bakış et al. (2007), noting the significant difference (∼ 12 km s^{-1}) in radial velocity between the A and B components then challenged the idea that the wide system is gravitationally bound. Hubrig et al. (2001), whilst examining η Mus for a possible X-ray source had discovered the additional pre-main sequence companion η Mus-C, separated by 2.71 arcsec at position angle 125 deg, with magnitude differences 5.25, 4.54 and 3.32 in the J, H and K-bands. If this star is bound to η Mus A it should have an orbital period in the order of 3000 y.

The classical EA light curve from HIPPARCOS suggests two fairly well separated stars at relatively low inclination, or perhaps third light. Curve-fitting experiments, that the present authors will present elsewhere, show an acceptable model for the HIPPARCOS data can be found without significant third light, however. This was also confirmed in fittings of the *uvby* photometry of the system by Hensberge et al. (2007).

New Component

Bakış et al. (2007) presented initial data taken with the HERCULES spectrograph of the Dept. Physics and Astronomy, UC (Hearnshaw et al. 2002). This has been added to our later data using essentially the same set-up. A slight difference between the γ velocity applying for May and September of 2006 was noticed and this prompted the present authors to further observations in 2010 and 2011. It has recently become apparent that the γ velocity of the main pair cycles in a rather eccentric orbit with the relatively short timescale shown in Fig. 1.

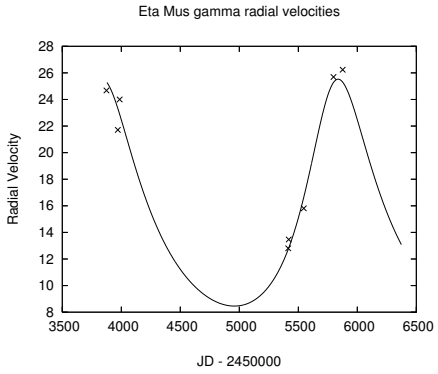

Figure 1. Preliminary model for the γ-velocity variation of η Mus

The $\sim$ y period orbit shown, which is plotted as y-velocity against time from the epoch JD 2453873 (2006 May 17), appears consistent with a small number of recent well-timed minima produced under the SBDSLR programme of the Variable Stars South (RASNZ); as well as photometry of the system, communicated privately by Dr H. Hensberge. Those data intermittently cover a timebase of $\sim$30y, although timing of the several minima they include is necessarily poor, relying only on model fitting to a small number of displaced points. The authors will provide more details of these analyses separately. More observations are clearly needed to substantiate this still very sketchily known inner system.

Acknowledgements We thank the Telescope Allocation Committee of the Mt John University Observatory, UC, for generous allocations of time for the Southern Binaries Programme (Budding, 2008), which has also been supported, in part, by the Turkish Science Research Council (TÜBİTAK), as well as the VSS Section of the RASNZ.

References:

Bakış, V., Bakış, H., Eker, Z., Demircan, O., 2007, *MNRAS*, **382**, 609
Budding, E., 2008, *Proc. 10th Asian-Pacific Regional IAU Meeting Kunming, China*, Eds. Shuang Nan Zhang, Yan Li & Qing Juan Yu, Nat. Obs. China Press, 33
Buscombe, W., Morris, P.M., 1961, *AJ*, **66**, 39
ESA, 1997, *The HIPPARCOS and Tycho Catalogues*, ESA SP-1200
Hearnshaw, J.B., et al., 2002, *Exp. Astron.*, **13**, 59
Hensberge, H., et al., 2007, *MNRAS*, **379**, 349
Hubrig, S., Le Mignant, D., North, P., Krautter, J., 2001, *A&A*, **372**, 152
Nitschelm, C., 2004, *ASPC*, **318**, 291
Tokovinin, A.A., 1997, *A&AS*, **124**, 75

COMMISSIONS 27 AND 42 OF THE IAU
INFORMATION BULLETIN ON VARIABLE STARS

Number 6005

Konkoly Observatory
Budapest
13 December 2011

HU ISSN 0374 – 0676

TIMES OF MINIMA OF ECLIPSING BINARIES AND TIMES OF MAXIMA OF PULSATING STARS

LIAKOS, A.; NIARCHOS, P.

Department of Astrophysics, Astronomy and Mechanics, National and Kapodistrian University of Athens, GR 157 84 Zografos, Athens, Hellas; e-mail: alliakos@phys.uoa.gr, pniarcho@phys.uoa.gr

Observatory and telescope:
T1: 40 cm Cassegrain telescope (f/8.1), **T2**: 25 cm Newtonian reflector telescope (f/4.7), **T3**: 8 cm Newtonian refractor telescope (f/7.5) at the University of Athens Observatory.

Detector:	**C1**: ST-10XME CCD camera, Peltier cooling, KAF-3200ME chip, $16' \times 11'$ and $25' \times 17'$ (using a focal reducer) FoV with T1, 2184 × 1472 pixels, **C2**: ST-8XMEI CCD camera, Peltier cooling, KAF-1603ME chip, $40' \times 27'$ with T2 and $79' \times 53'$ FoV with T3, 1530 × 1020 pixels. Both CCDs are equipped with the Bessell UBVRI filters.

Method of data reduction:
Differential photometry with the software Muniwin v.1.1.26 (Hroch 1998).

Method of minimum determination:
Kwee & van Woerden (1956).

Table 1: Times of maxima of pulsating stars

System	HJD	Error	Filters	Remark
BX Del	2455821.2972	0.0004	BV	C1+T1
	2455822.3886	0.0011	BV	C1+T1
	2455834.3970	0.0005	BV	C1+T1
	2455856.2340	0.0004	BV	C1+T1

Table 2: Times of minima of eclipsing binaries

System	HJD	Error	Type	Filters	Remark
AP And	2455837.4916	0.0001	II	BVI	C1+T1
	2455838.2851	0.0002	I	BVRI	C1+T1
	2455841.4597	0.0001	I	BVRI	C1+T1
	2455853.3646	0.0001	II	BVRI	C1+T1
QY Aql	2455794.4802	0.0020	I	BVI	C1+T1
BD+07 3142	2455695.4632	0.0002	II	BVRI	C1+T1
	2455696.4281	0.0002	I	BVRI	C1+T1
	2455697.3900	0.0002	II	BVRI	C1+T1
	2455697.5287	0.0002	I	BVRI	C1+T1
VW Boo	2455698.4256	0.0002	II	BVRI	C1+T1
	2455702.5323	0.0003	II	BVRI	C1+T1
	2455703.3886	0.0002	I	BVRI	C1+T1
	2455707.4961	0.0002	I	BVRI	C1+T1
EL Boo	2455696.3621	0.0005	I	BVRI	C2+T2
	2455697.3952	0.0004	II	BVRI	C2+T2
	2455698.4311	0.0006	I	BVRI	C2+T2
	2455699.4665	0.0007	II	BVRI	C2+T2
	2455702.3606	0.0004	II	BVRI	C2+T2
VZ Cep	2455804.3392	0.0004	II	BVRI	C2+T2
	2455807.2988	0.0002	I	BVRI	C2+T2
	2455814.3993	0.0002	I	BVRI	C2+T2
V1073 Cyg	2455774.3275	0.0007	I	BRI	C2+T2
	2455777.4684	0.0008	I	UBVRI	C1+T1
	2455779.4327	0.0002	II	UBVRI	C1+T1
	2455793.5788	0.0003	II	UBVRI	C1+T1
V1187 Cyg	2455848.2539	0.0002	II	BVRI	C1+T1
V1191 Cyg	2455833.3032	0.0002	I	BVRI	C1+T1
	2455835.3382	0.0007	II	BVRI	C1+T1
	2455847.2473	0.0002	II	BVRI	C1+T1
	2455848.3471	0.0003	I	BVRI	C1+T1
BW Del	2455813.3112	0.0003	I	BV	C1+T1
HI Dra	2455729.3917	0.0005	II	BVRI	C2+T2
	2455731.4815	0.0005	I	BVRI	C2+T2
	2455732.3786	0.0006	II	BVRI	C2+T2
GSC 3787-0502	2455569.3530	0.0006	I	B	C2+T2
	2455569.4813	0.0002	II	B	C2+T2
	2455569.6061	0.0007	I	B	C2+T2
	2455570.3820	0.0007	I	BV	C2+T2
	2455576.4544	0.0007	II	VI	C2+T2
	2455576.5799	0.0005	I	BVI	C2+T2
	2455577.2285	0.0007	II	BI	C2+T2
	2455580.5832	0.0008	II	BVI	C2+T2
	2455581.3580	0.0010	II	I	C2+T2
	2455581.4859	0.0007	I	BVI	C2+T2
	2455588.3333	0.0007	II	BVI	C2+T2
	2455588.5905	0.0011	II	BVI	C2+T2
	2455598.2753	0.0007	I	BVI	C2+T2

Table 2: cont.

System	HJD	Error	Type	Filters	Remark
	2455598.4099	0.0008	II	BVI	C1+T1
	2455598.5349	0.0004	I	BVI	C1+T1
	2455602.2830	0.0009	II	BVI	C1+T1
BO Her	2455711.4868	0.0001	I	BVI	C1+T1
	2455726.4452	0.0015	II	VI	C1+T1
V1010 Oph	2455750.4177	0.0008	I	B	C2+T3
	2455757.3644	0.0005	II	BVRI	C2+T3
	2455758.3547	0.0002	I	BVRI	C2+T3
V2388 Oph	2455746.4824	0.0005	I	BVRI	C2+T3
	2455748.4894	0.0005	II	BVRI	C2+T3
V2610 Oph	2455712.5283	0.0006	I	BVRI	C1+T1
	2455714.4490	0.0004	II	BVRI	C1+T1
	2455719.5665	0.0008	II	BVRI	C1+T1
	2455720.4206	0.0010	II	BVI	C1+T1
	2455722.5504	0.0006	II	BVRI	C1+T1
	2455723.4050	0.0007	II	BVRI	C1+T1
	2455727.4569	0.0012	I	BVRI	C1+T1
	2455741.5312	0.0011	I	BVRI	C1+T1
	2455744.5169	0.0008	I	BVRI	C1+T1
V2612 Oph	2455727.3963	0.0002	I	BVRI	C1+T1
	2455729.4632	0.0002	II	BVRI	C1+T1
V407 Peg	2455853.4082	0.0004	I	BVRI	C1+T1
	2455854.3718	0.0004	II	BVRI	C1+T1
	2455855.3207	0.0001	I	BVRI	C1+T1
V482 Per	2455847.6067	0.0003	II	BVRI	C1+T1
	2455852.4969	0.0002	II	BVRI	C1+T1
	2455868.3970	0.0003	I	BVRI	C1+T1
V881 Per	2455818.4056	0.0005	I	BVRI	C1+T1
	2455818.5984	0.0003	II	BVRI	C1+T1
	2455819.5681	0.0003	I	BVRI	C1+T1
	2455820.5353	0.0004	II	BVRI	C1+T1
	2455821.5049	0.0004	I	BVRI	C1+T1
	2455833.5136	0.0003	I	BVRI	C1+T1
	2455834.4814	0.0003	II	BVRI	C1+T1
	2455835.4501	0.0003	I	BVRI	C1+T1
AU Ser	2455730.4918	0.0001	II	BVRI	C1+T1
	2455731.4593	0.0001	I	BVRI	C1+T1
	2455739.3809	0.0001	II	BVRI	C1+T1
	2455740.3486	0.0001	I	BVRI	C1+T1
USNO-A2.0 0900-04405532	2455602.3200	0.0006	I	B	C1+T1
	2455603.4220	0.0018	I	I	C1+T1
	2455630.2951	0.0009	I	I	C1+T1
	2455632.2900	0.0011	II	VI	C1+T1
USNO-A2.0 0900-05986449	2455569.4588	0.0004	II	B	C1+T1
	2455576.3915	0.0006	I	VR	C1+T1
	2455576.5543	0.0006	II	VR	C1+T1
	2455580.5809	0.0004	I	VR	C1+T1

Table 2: cont.

System	HJD	Error	Type	Filters	Remark
	2455581.5516	0.0001	I	R	C1+T1
PY Vir	2455699.3574	0.0003	II	BVRI	C1+T1
	2455702.3154	0.0002	I	BVRI	C1+T1

Explanation of the remarks in the table:

T1, T2, T3, C1 and C2 refer to the instrumentation (telescope and CCD camera) used for the corresponding observations.

Remarks:

The systems GSC 3787-0502, USNO-A2.0 0900-04405532 and USNO-A2.0 0900-05986449 were recently discovered by Liakos & Niarchos (2011).

Acknowledgements:

This work has been financially supported by the Special Account for Research Grants No 70/4/11112 of the National & Kapodistrian University of Athens, Hellas.

References:

Hroch, F., 1998, *Proceedings of the 29th Conference on Variable Star Research*, editor J. Dusek and M. Zejda, Brno, p. 30

Kwee, K., van Woerden, H., 1956, *Bulletin of the Astronomical Institutes of the Netherlands*, **12**, 327

Liakos, A., Niarchos, P., 2011, *Peremennye Zvezdy Prilozhenie*, **11**, 26

COMMISSIONS 27 AND 42 OF THE IAU
INFORMATION BULLETIN ON VARIABLE STARS

Number 6006

Konkoly Observatory
Budapest
13 December 2011

HU ISSN 0374 – 0676

CCD MAXIMA OF PULSATING STARS AND TIMES OF MINIMA OF ECLIPSING BINARIES

MARTIGNONI, MASSIMILIANO

Stazione Astronomica Betelgeuse (SAB), Via Don Minzoni 26, I-20020 Magnago (Milano), Italy
massimiliano.martignoni@alice.it

Observatory and telescope:
0.2 m Schmidt-Cassegrain Telescope (f/10)

Detector:	765×510 pixels Kodak KAF401E CCD cooled to (typ.) -20°C; 1″.85 per pixel (2×2 binning); 12′×8′ field of view; equipped with BVR_CI_C photometric filters.

Method of data reduction:
Differential photometry on each CCD image using Prism 5.0 software. No reduction to standard photometric system was performed.

Method of minimum determination:
The times of maxima were calculated using parabolic fit; the minima times were calculated using Kwee & van Woerden's (1956) method.

Table 1: Times of maxima

Star name	Time of max. (HJD 2400000+)	Uncertainty	Filter
SW And	55498.3941	0.0029	CCD(R)
XX And	50769.3924	0.0021	CCD(V)
AT And	53331.2875	0.0016	CCD(V)
CI And	53325.4521	0.0008	CCD(V)
TZ Aur	53776.4290	0.0187	CCD(V)
ST Boo	55348.4811	0.0050	CCD(V)
CQ Boo	54979.4613	0.0013	CCD(V)
BL Cam	54419.4212	0.0003	CCD(V)
	54419.4596	0.0002	CCD(V)
AA CMi	53768.4206	0.0070	CCD(V)
TT Cnc	53446.3940	0.0018	CCD(V)
	54174.3927	0.0008	CCD(R)
EF Cnc	54171.4815	0.0082	CCD(V)
AW Cet	52989.4153	0.0033	CCD(V)
U Com	55698.3950	0.0003	CCD(V)
ROTSE1 J155733.60+283225.5	52080.4648	0.0074	CCD(V)
XZ Cyg	54307.4199	0.0013	CCD(V)
V2369 Cyg	53573.4608	0.0017	CCD(V)
	54306.4469	0.0013	CCD(V)
	54657.5026	0.0026	CCD(BVR_CI_C)
	54663.4490	0.0017	CCD(BVR_CI_C)
RW Dra	53566.4150	0.0008	CCD(V)
GI Gem	53773.3644	0.0004	CCD(V)
TW Her	54300.4447	0.0001	CCD(R)
VX Her	53557.4316	0.0004	CCD(V)
DL Her	53572.4564	0.0110	CCD(V)
RR Leo	54172.3756	0.0008	CCD(V)
ST Leo	54175.4313	0.0020	CCD(R)
SZ Leo	54173.4289	0.0016	CCD(V)
WW Leo	53443.4271	0.0004	CCD(V)
BM Lib	52822.4728	0.0004	CCD(V)
TT Lyn	53829.3530	0.0007	CCD(V)
CN Lyr	54299.4633	0.0004	CCD(R)
IO Lyr	53571.4257	0.0007	CCD(V)
	54656.4102	0.0003	CCD(V)
KX Lyr	54313.4277	0.0014	CCD(V)
DV Mon	52988.6319	0.0031	CCD(V)
ASAS 061518+0604.2	53045.3679	0.0012	CCD(V)
	53045.4300	0.0013	CCD(V)
	53045.4852	0.0013	CCD(V)
	53047.4050	0.0010	CCD(V)
	53047.4604	0.0011	CCD(V)
	53060.3573	0.0013	CCD(V)
	53060.4126	0.0013	CCD(V)
	53068.3705	0.0010	CCD(V)
	53068.4294	0.0012	CCD(V)

Table 1: cont.

Star name	Time of max. (HJD 2400000+)	Uncertainty	Filter
AV Peg	53613.4177	0.0009	CCD(V)
	54363.3365	0.0004	CCD(B)
	54411.3539	0.0001	CCD(V)
EV Psc	55498.3237	0.0014	CCD(R)
T Sex	53350.6887	0.0070	CCD(V)
	53839.3955	0.0008	CCD(V)
RU Sex	53081.3900	0.0017	CCD(V)
	53082.4438	0.0006	CCD(V)
SS Tau	53351.3765	0.0010	CCD(V)
BR Tau	53350.4787	0.0051	CCD(V)
U Tri	53333.3865	0.0035	CCD(V)
UX Tri	55496.4624	0.0009	CCD(R)
TU UMa	54175.3589	0.0021	CCD(R)
EX UMa	53447.4123	0.0010	CCD(V)
KT UMa	53838.4442	0.0028	CCD(V)
FU Vir	53487.3814	0.0030	CCD(V)
BN Vul	53612.3975	0.0020	CCD(V)

Table 2: Times of minima

Star name	Time of min. (HJD 2400000+)	Uncertainty	Type	Filter
BO Ari	54049.4078	0.0025	Min. I	CCD(V)
	54084.4127	0.0003	Min. I	CCD(V)
GN Boo	53509.4054	0.0003	Min. II	CCD(V)
	53510.4599	0.0003	Min. I	CCD(V)
	53514.3811	0.0002	Min. I	CCD(V)
	54231.4415	0.0002	Min. II	CCD(V)
	54238.3750	0.0004	Min. II	CCD(R_C)
	54572.3968	0.0003	Min. I	CCD(BVR_C)
NSV 3744	53404.3707	0.0002	Min. II	CCD(R_C)
	53405.4110	0.0004	Min. II	CCD(R_C)
	53411.3969	0.0004	Min. I	CCD(R_C)
V380 Gem	53408.4037	0.0003	Min. II	CCD(R_C)
	53419.3409	0.0002	Min. I	CCD(R_C)
GU Vul	51430.4182	0.0002	Min. II	CCD(V)

Reference:

Kwee, K.K., van Woerden, H., 1956, *B.A.N.*, **12**, 327

*This version of the paper contains corrections, and differs from the one appeared on-line originally. Date of last modification: Wed Apr 18 08:16:33 CEST 2012

COMMISSIONS 27 AND 42 OF THE IAU
INFORMATION BULLETIN ON VARIABLE STARS

Number 6007

Konkoly Observatory
Budapest
15 December 2011

HU ISSN 0374 – 0676

COLLECTION OF MINIMA

ZASCHE, P.[1]; UHLAŘ, R.[2]; KUČÁKOVÁ, H.[3]; SVOBODA, P.[4]

[1] Institute of Astronomy, Charles University, Prague, V Holešovičkách 2, Prague 8, CZ-18000 Czech Republic; e-mail: zasche@sirrah.troja.mff.cuni.cz

[2] Private Observatory, Pohoří 71, Jílové u Prahy, CZ-25401 Czech Republic

[3] Johann Palisa Observatory and Planetarium, Technical University Ostrava, 17. Listopadu 15, CZ-708 33 Ostrava, Czech Republic

[4] Private observatory, Výpustky 5, Brno, CZ-614 00 Czech Republic

Observatory and telescope:

CCD photometry with various ground-based and space telescopes as well as the data from the robotic/automatic photometric surveys were used for the times of minima determination.

Method of data reduction:

The CCD frames were reduced using the C-Munipack and IRAF routines.

Method of minimum determination:

The minima times were computed with the Kwee – van Woerden method (Kwee & van Woerden, 1956). Two remarkable minima observations are plotted in Figs. 1 and 2 below. The system V760 Oph shows one of the deepest primary minimum known among the eclipsing binaries, while V389 Cas was found to exhibit periodic pulsations of one of its components.

Explanation of the remarks in the table:

BVRI filters by the specification by Bessell (1990), *C* - unfiltered. Observers: PZ - Petr Zasche, RU - Robert Uhlař, HK - Hana Kučáková, PS - Petr Svoboda, MZ - Miloslav Zejda, MW - Marek Wolf. Instruments: OND - 65 cm telescope in Ondřejov Observatory, SPM - 84 cm telescope at San Pedro Mártir, Mexico, RF34/135 - 34 mm refractor, RF75/300 - 75 mm refractor, N254/1200 - 254 mm Newton reflector, N200/1000 - 200 mm Newton reflector, N200/2000 - 200 mm Newton reflector, M305/3050 - 30 cm Schmidt-Cassegrain reflector, Ath - 40 cm telescope at Athens University Observatory, OMC - Integral OMC camera. For V994 Her the following notation was used: period of pair A: 2.083268 day, period of pair B: 1.420025 day.

Table 1: Times of minima of eclipsing binaries

Star Name	HJD 24.....	Error	Type	Filter	Instrument/Source	Observer
UU And	55456.62189	0.00003	Pri	R	OND	PZ
WZ And	55873.50864	0.00010	Pri	R	N200/2000	HK
V372 And	55561.32461	0.00082	Sec	C	RF34/135	RU
V372 And	55877.48043	0.00059	Pri	C	RF34/135	RU
V392 And	55848.47851	0.00140	Pri	R	RF34/135	RU
SU Aqr	55052.91784	0.00013	Pri	V	SPM	PZ
CZ Aqr	52065.41858	0.00178	Pri	V	ASAS	PZ
CZ Aqr	52064.98507	0.00217	Sec	V	ASAS	PZ
CZ Aqr	52550.28425	0.00060	Pri	V	ASAS	PZ
CZ Aqr	52549.85580	0.00229	Sec	V	ASAS	PZ
CZ Aqr	52887.61885	0.00050	Pri	V	ASAS	PZ
CZ Aqr	52887.19110	0.00196	Sec	V	ASAS	PZ
CZ Aqr	53426.83663	0.00115	Pri	V	ASAS	PZ
CZ Aqr	53426.40785	0.00195	Sec	V	ASAS	PZ
CZ Aqr	54161.89728	0.00084	Pri	V	ASAS	PZ
CZ Aqr	54161.46574	0.00248	Sec	V	ASAS	PZ
CZ Aqr	54710.60306	0.00045	Pri	V	ASAS	PZ
CZ Aqr	54710.17341	0.00260	Sec	V	ASAS	PZ
CZ Aqr	55057.42720	0.00091	Pri	V	ASAS	PZ
CZ Aqr	55056.99203	0.00300	Sec	V	ASAS	PZ
DD Aqr	55866.39277	0.00020	Pri	R	M305/3050	HK
DD Aqr	55874.32299	0.00020	Pri	R	M305/3050	HK
V803 Aql	55053.67726	0.00002	Pri	R	SPM	PZ
V887 Aql	55456.32489	0.00252	Sec	R	OND	PZ
V887 Aql	55873.24259	0.00112	Pri	R	OND	PZ
V1470 Aql	55482.28020	0.00062	Pri	C	RF34/135	RU
sigma Aql	55053.37814	0.00220	Sec	C	RF34/135	RU
sigma Aql	55399.54892	0.00031	Pri	I	RF34/135	RU
sigma Aql	55754.50503	0.00028	Pri	I	RF34/135	RU
TX Ari	55161.23757	0.00168	Pri	R	OND	PZ
AL Ari	55868.32794	0.00025	Pri	R	M305/3050	HK
AL Ari	55836.51605	0.00045	Sec	C	RF34/135	RU
AL Ari	55879.57035	0.00060	Pri	C	RF34/135	RU
CL Aur	55868.69614	0.00030	Pri	R	N200/2000	HK
FO Aur	54405.54149	0.00106	Sec	R	OND	PZ
V417 Aur	55619.35468	0.00031	Pri	C	RF34/135	RU
V560 Aur	55878.49067	0.00121	Pri	C	RF34/135	RU
AC Boo	55602.55269	0.00019	Sec	C	RF34/135	RU
DV Boo	55644.56349	0.00098	Pri	C	RF34/135	RU
EL Boo	55643.60973	0.00083	Sec	R	RF34/135	RU
EM Boo	55651.45876	0.00121	Pri	R	RF34/135	RU
EM Boo	55673.46951	0.00042	Pri	R	RF34/135	RU
ET Boo	55602.65861	0.00019	Sec	C	RF34/135	RU
GU Boo	55700.34562	0.00007	Pri	R	OND	PZ
SZ Cam	54840.54681	0.0004	Sec	R	RF34/135	PS
SZ Cam	54534.27515	0.001	Pri	R	RF34/135	PS
SZ Cam	55257.45166	0.00041	Pri	R	RF34/135	PS
SZ Cam	55852.46557	0.00071	Sec	R	RF34/135	PS
SZ Cam	54809.50648	0.0006	Pri	R	RF34/135	RU
SZ Cam	55141.41783	0.00239	Pri	R	RF75/300	RU
SZ Cam	55141.42664	0.00430	Pri	V	RF75/300	RU
SZ Cam	55462.51935	0.00023	Pri	I	N254/1200	RU
SZ Cam	55593.40996	0.00235	Sec	V	RF34/135	RU

Table 1: (cont.)

Star Name	HJD 24.....	Error	Type	Filter	Instrument/Source	Observer
AT Cam	55500.37739	0.00049	Sec	R	N254/1200	RU
CV Cam	55496.47080	0.00052	Sec	C	RF34/135	RU
CV Cam	55879.44866	0.00052	Pri	C	RF34/135	RU
FZ CMa	55868.57263	0.00101	Pri	R	N200/2000	HK
BF CMi	55873.57009	0.00019	Pri	R	M305/3050	HK
RS CVn	55688.48534	0.00735	Sec	C	RF34/135	RU
DE CVn	54193.40825	0.00004	Pri	R	OND	PZ
TX Cas	55878.41211	0.00043	Pri	R	RF34/135	RU
CC Cas	55839.33773	0.00093	Sec	R	RF34/135	RU
CC Cas	55876.38437	0.00043	Sec	C	RF34/135	RU
CR Cas	55866.23094	0.00027	Pri	R	M305/3050	HK
CR Cas	55836.40797	0.00049	Sec	R	N200/1000	RU
DN Cas	55872.46075	0.00363	Sec	VRI	M305/3050	HK
V389 Cas	55851.56898	0.00239	Sec	R	M305/3050	HK
V389 Cas	55483.58449	0.00010	Pri	R	OND	PZ
V649 Cas	55461.50591	0.00061	Pri	R	RF34/135	PS
V772 Cas	55875.39469	0.00431	Pri	R	RF34/135	PS
V772 Cas	55880.41033	0.00228	Pri	R	RF34/135	RU
V785 Cas	55800.44136	0.00118	Pri	C	RF34/135	RU
V1018 Cas	55832.61170	0.00033	Pri	R	OND	PZ
AH Cep	55829.31526	0.00055	Sec	R	RF34/135	RU
CO Cep	54748.25653	0.00019	Sec	V	OND	PZ
CQ Cep	55811.54449	0.00073	Pri	C	RF34/135	RU
EM Cep	54995.45633	0.00295	Sec	BVRI	N254/1200	RU
EM Cep	55022.46170	0.00080	Pri	BVRI	N254/1200	RU
EM Cep	55819.37896	0.00160	Sec	I	N200/1000	RU
GT Cep	55834.40694	0.00128	Sec	C	RF34/135	RU
LP Cep	54364.35949	0.00007	Pri	R	OND	PZ
LP Cep	55357.51444	0.00004	Pri	R	OND	PZ
V338 Cep	55819.37283	0.00045	Pri	R	RF34/135	RU
V338 Cep	55839.36732	0.00058	Sec	C	RF34/135	RU
V383 Cep	55834.48375	0.00079	Pri	R	RF34/135	RU
TV Cet	55481.58714	0.00048	Pri	C	RF34/135	RU
WY Cet	55828.45940	0.00093	Sec	R	RF34/135	RU
KK Com	55623.47596	0.00052	Pri	C	RF34/135	RU
KR Com	55567.69969	0.00202	Sec	C	RF34/135	RU
KR Com	55584.62855	0.00142	Pri	C	RF34/135	RU
KR Com	55616.65167	0.00077	Sec	R	N200/1000	RU
KR Com	55619.50680	0.00087	Sec	C	RF34/135	RU
KR Com	55643.57679	0.00154	Sec	R	N200/1000	RU
KR Com	55662.34698	0.00069	Sec	R	RF34/135	RU
KR Com	55662.54314	0.00063	Sec	R	RF34/135	RU
VV Crt	54535.49078	0.00012	Pri	R	Ath	PZ+MZ
SW Cyg	55806.40772	0.00056	Pri	R	N200/1000	RU
GV Cyg	54748.37494	0.00003	Pri	V	OND	PZ
V382 Cyg	55811.43990	0.00030	Pri	C	RF34/135	RU
V442 Cyg	55700.45038	0.00007	Sec	B	OND	PZ
V1187 Cyg	55034.47375	0.00054	Sec	R	N254/1200	RU
V1187 Cyg	55413.48497	0.00053	Pri	R	N254/1200	RU
V1187 Cyg	55817.36114	0.00049	Pri	R	N200/1000	RU
V1191 Cyg	55028.51632	0.00041	Sec	R	N254/1200	RU
V1191 Cyg	55034.46897	0.00029	Sec	R	N254/1200	RU
V1191 Cyg	55413.51520	0.00041	Pri	R	N254/1200	RU

Table 1: (cont.)

Star Name	HJD 24.....	Error	Type	Filter	Instrument/Source	Observer
V1191 Cyg	55817.32750	0.00051	Sec	R	N200/1000	RU
V1191 Cyg	55054.68353	0.00012	Pri	R	SPM	PZ
V1191 Cyg	54219.49614	0.00023	Pri	R	OND	PZ
V1193 Cyg	54035.41966	0.00016	Sec	R	OND	PZ
V2154 Cyg	55799.55051	0.00010	Pri	I	N200/1000	RU
V2154 Cyg	55803.49189	0.00099	Sec	R	RF34/135	RU
TY Del	55049.43614	0.0053	Pri	BVRI	N254/1200	RU
TY Del	55068.49505	0.00007	Pri	VR	N254/1200	RU
TY Del	55071.47644	0.00198	Sec	VR	N254/1200	RU
TY Del	55054.79863	0.00034	Sec	I	SPM	PZ
DM Del	55836.43193	0.00045	Sec	R	RF34/135	PS
DM Del	55828.40298	0.00029	Pri	C	RF34/135	RU
DM Del	55831.36000	0.00040	Sec	C	RF34/135	RU
DM Del	55878.23688	0.00015	Pri	R	N200/1000	RU
MR Del	55083.45820	0.00025	Sec	R	N254/1200	RU
MR Del	55029.46271	0.0002	Pri	R	N254/1200	RU
MR Del	55045.37612	0.00087	Sec	R	N254/1200	RU
MR Del	55112.41118	0.00025	Pri	R	RF75/300	RU
MR Del	55141.36525	0.00014	Sec	R	N254/1200	RU
MR Del	55156.23370	0.00078	Pri	V	RF75/300	RU
MR Del	55355.52025	0.00032	Pri	R	N254/1200	RU
MR Del	55373.51796	0.00021	Sec	R	N254/1200	RU
MR Del	55378.47419	0.00019	Pri	R	N254/1200	RU
MR Del	55390.47109	0.00060	Pri	R	RF34/135	RU
MR Del	55455.42345	0.00035	Sec	R	RF75/300	RU
MR Del	55739.48259	0.00048	Pri	R	RF34/135	RU
MR Del	55770.52293	0.00017	Sec	R	N200/1000	RU
MR Del	55776.52223	0.00009	Pri	R	N200/1000	RU
MR Del	55791.39029	0.00014	Sec	R	N200/1000	RU
MR Del	55051.89565	0.00007	Pri	B	SPM	PZ
MR Del	55052.68010	0.00006	Sec	B	SPM	PZ
RX Dra	55862.37284	0.00044	Pri	R	M305/3050	HK
WW Dra	55076.41776	0.00008	Pri	R	N200/2000	HK
WX Dra	55456.49117	0.00005	Pri	R	OND	PZ
BE Dra	54193.48730	0.00012	Pri	R	OND	PZ
BE Dra	54763.27267	0.00012	Sec	R	OND	PZ
BV Dra	55323.43098	0.00041	Sec	I	RF34/135	RU
BV Dra	55329.55416	0.00017	Pri	I	RF34/135	RU
BV Dra	55664.39737	0.00112	Sec	R	RF34/135	RU
CM Dra	54252.36453	0.00003	Pri	R	OND	PZ
W Equ	54692.43944	0.00219	Sec	V	OND	PZ
QT Gem	55617.37801	0.00057	Pri	C	RF34/135	RU
QT Gem	55551.75812	0.00403	Sec	C	RF34/135	RU
GU Her	54223.54030	0.00019	Pri	R	OND	PZ
V338 Her	54035.26464	0.00033	Pri	R	OND	PZ
V501 Her	55648.59428	0.00087	Pri	R	RF34/135	RU
V624 Her	54950.55606	0.00460	Sec	RI	RF34/135	RU
V624 Her	54954.45122	0.00449	Sec	VRI	RF34/135	RU
V624 Her	55069.35237	0.00181	Pri	I	RF34/135	RU
V624 Her	55770.46916	0.01087	Pri	VRI	RF34/135	RU
V681 Her	53138.54781	0.00039	Sec	C	SWASP	PZ
V681 Her	53139.70576	0.00042	Sec	C	SWASP	PZ
V681 Her	53142.60272	0.00054	Pri	C	SWASP	PZ

Table 1: (cont.)

Star Name	HJD 24.....	Error	Type	Filter	Instrument/Source	Observer
V681 Her	53152.45100	0.00040	Sec	C	SWASP	PZ
V681 Her	53156.50777	0.00087	Pri	C	SWASP	PZ
V681 Her	53160.55879	0.00159	Sec	C	SWASP	PZ
V681 Her	53163.45872	0.00073	Pri	C	SWASP	PZ
V822 Her	55364.54469	0.00914	Pri	V	RF34/135	RU
V822 Her	55394.45839	0.00028	Sec	I	N254/1200	RU
V822 Her	55410.45443	0.00039	Pri	I	N254/1200	RU
V822 Her	55716.49916	0.00059	Pri	R	RF34/135	RU
V822 Her	55725.54637	0.00115	Sec	R	RF34/135	RU
V822 Her	55739.46812	0.00101	Sec	I	N200/1000	RU
V822 Her	55787.45865	0.00112	Pri	R	RF34/135	RU
V822 Her	55808.31573	0.00049	Pri	R	RF34/135	RU
V822 Her	53498.33531	0.00277	Sec	V	ASAS	PZ
V822 Her	53499.03693	0.00428	Pri	V	ASAS	PZ
V822 Her	54652.98276	0.00263	Sec	V	ASAS	PZ
V822 Her	54653.67866	0.00149	Pri	V	ASAS	PZ
V994 Her	55424.47871	0.00079	SecB	R	RF34/135	PS
V994 Her	55779.48535	0.00125	SecB	R	N200/1000	RU
V994 Her	55799.36956	0.00033	SecB	I	N200/1000	RU
V994 Her	55313.40261	0.00068	PriA	R	RF34/135	RU
V994 Her	55314.48274	0.00046	SecA	I	RF34/135	RU
V994 Her	55315.48964	0.00042	PriA	I	RF34/135	RU
V994 Her	55375.40806	0.00037	PriA	I	RF34/135	RU
V994 Her	55389.48381	0.00225	SecA	I	RF34/135	RU
V994 Her	55392.44779	0.00055	PriB	I	RF34/135	RU
V994 Her	55397.49810	0.00032	SecB	I	RF34/135	RU
V994 Her	55641.55985	0.00012	SecA	R	N200/1000	RU
V994 Her	55642.56748	0.00042	PriA	R	N200/1000	RU
V994 Her	55654.51845	0.00097	SecB	C	RF34/135	RU
V994 Her	55681.50533	0.00036	SecB	R	RF34/135	RU
V994 Her	55683.55108	0.00024	PriB	R	RF34/135	RU
V994 Her	55688.39802	0.00029	PriA	R	RF34/135	RU
V994 Her	55691.56016	0.00011	Sec	I	N200/1000	RU
V994 Her	55691.44530	0.00013	Sec	I	N200/1000	RU
KY Hya	52070.15039	0.01230	Sec	V	ASAS	PZ
KY Hya	52071.68718	0.00722	Pri	V	ASAS	PZ
KY Hya	52816.76765	0.00132	Sec	V	ASAS	PZ
KY Hya	52818.30357	0.00081	Pri	V	ASAS	PZ
KY Hya	53594.09677	0.00267	Sec	V	ASAS	PZ
KY Hya	53595.63795	0.00243	Pri	V	ASAS	PZ
KY Hya	54629.52233	0.00768	Sec	V	ASAS	PZ
KY Hya	54631.06000	0.00157	Pri	V	ASAS	PZ
RT Lac	55802.39433	0.00105	Pri	C	RF34/135	RU
AR Lac	55062.47453	0.00113	Sec	C	RF34/135	RU
AU Lac	54298.08919	0.00206	Pri	C	SWASP	PZ
AU Lac	54338.46793	0.00043	Pri	C	SWASP	PZ
ES Lac	55168.27112	0.00014	Pri	R	OND	PZ
V398 Lac	55837.46515	0.00082	Pri	R	RF34/135	PS
V401 Lac	55827.38073	0.00084	Sec	C	RF34/135	RU
V402 Lac	55500.29383	0.00052	Sec	V	RF34/135	PS
V402 Lac	55500.28830	0.00062	Sec	C	RF34/135	RU
V402 Lac	55815.48162	0.00033	Pri	R	RF34/135	RU
TX Leo	54974.39005	0.0031	Pri	R	RF34/135	PS

Table 1: (cont.)

Star Name	HJD 24.....	Error	Type	Filter	Instrument/Source	Observer
TX Leo	55304.49248	0.00136	Pri	R	RF34/135	PS
TX Leo	55287.37194	0.00635	Pri	I	RF34/135	RU
TX Leo	55590.54927	0.00069	Pri	R	RF34/135	RU
FK Leo	55636.33518	0.00052	Sec	R	RF34/135	RU
FK Leo	55642.41375	0.00031	Pri	C	RF34/135	RU
FM Leo	54534.58810	0.00077	Pri	I	Ath	PZ+MZ
FM Leo	54534.58768	0.00326	Pri	VR	Ath	PZ+MZ
FM Leo	55641.44522	0.00200	Sec	R	RF34/135	RU
FS Leo	55592.47240	0.00049	Pri	C	RF34/135	RU
FS Leo	55617.60629	0.00029	Pri	R	RF34/135	RU
T LMi	54535.44069	0.00050	Pri	VR	Ath	PZ+MZ
T LMi	55616.55458	0.00002	Pri	B	OND	PZ
VW LMi	55648.40821	0.00023	Sec	C	RF34/135	RU
VW LMi	55649.36211	0.00027	Sec	C	RF34/135	RU
IV Lib	55329.51713	0.00077	Pri	R	N254/1200	RU
DI Lyn	55303.39155	0.00044	Sec	R	RF34/135	PS
DI Lyn	55250.42199	0.00068	Pri	V	RF34/135	RU
DI Lyn	55255.46441	0.00087	Pri	VRI	N254/1200	RU
DI Lyn	55534.60115	0.00421	Pri	C	RF34/135	RU
DI Lyn	55561.50867	0.00048	Pri	C	RF34/135	RU
DI Lyn	55567.37941	0.00139	Sec	C	RF34/135	RU
DI Lyn	55599.33984	0.00058	Sec	C	RF34/135	RU
DI Lyn	55614.49151	0.00169	Sec	C	RF34/135	RU
DI Lyn	55872.59930	0.00100	Pri	R	RF75/300	RU
RV Lyr	55312.05371	0.00008	Pri	B	OND	PZ
V412 Lyr	55616.66689	0.00012	Pri	R	OND	PZ
AO Mon	55223.50760	0.00089	Pri	V	N254/1200	RU
IM Mon	55595.31194	0.00080	Pri	C	RF34/135	RU
V450 Mon	54531.26083	0.00020	Pri	R	Ath	PZ
V515 Mon	54138.17674	0.00102	Pri	C	COROT	PZ
V515 Mon	54138.61505	0.00057	Sec	C	COROT	PZ
V515 Mon	54139.05164	0.00119	Pri	C	COROT	PZ
V515 Mon	54139.48802	0.00021	Sec	C	COROT	PZ
V515 Mon	54146.04318	0.00022	Pri	C	COROT	PZ
V515 Mon	54146.48020	0.00012	Sec	C	COROT	PZ
V515 Mon	54149.54043	0.00050	Pri	C	COROT	PZ
V515 Mon	54149.97538	0.00078	Sec	C	COROT	PZ
V515 Mon	54156.53084	0.00094	Pri	C	COROT	PZ
V515 Mon	54156.96800	0.00057	Sec	C	COROT	PZ
V515 Mon	54157.84216	0.00083	Sec	C	COROT	PZ
V515 Mon	54158.27860	0.00145	Pri	C	COROT	PZ
V515 Mon	54160.02675	0.00125	Pri	C	COROT	PZ
KO Nor	52461.93059	0.02047	Sec	V	ASAS	PZ
KO Nor	53486.55317	0.00772	Pri	V	ASAS	PZ
KO Nor	53502.36514	0.02181	Sec	V	ASAS	PZ
KO Nor	54661.22432	0.01678	Pri	V	ASAS	PZ
KO Nor	54677.02581	0.00973	Sec	V	ASAS	PZ
V451 Oph	54535.63717	0.00049	Sec	BV	Ath	PZ+MZ
V760 Oph	55050.80621	0.00008	Pri	V	SPM	PZ
V2373 Oph	55461.30082	0.00234	Sec	I	N254/1200	RU
V2373 Oph	55641.60948	0.00138	Sec	R	RF34/135	RU
V2373 Oph	55697.56539	0.00245	Pri	C	RF34/135	RU
V2377 Oph	55698.49786	0.00048	Sec	C	RF34/135	RU

Table 1: (cont.)

Star Name	HJD 24.....	Error	Type	Filter	Instrument/Source	Observer
Z Ori	55640.34147	0.00074	Pri	R	N200/1000	RU
VV Ori	55515.52057	0.00138	Pri	I	RF34/135	RU
VV Ori	55553.40262	0.01020	Sec	I	RF34/135	RU
VV Ori	55544.48355	0.00158	Sec	I	RF34/135	RU
VV Ori	55591.27618	0.00425	Pri	I	RF34/135	RU
EF Ori	55168.43385	0.00022	Pri	R	OND	PZ
V643 Ori	52121.20335	0.04141	Pri	V	ASAS	PZ
V643 Ori	52697.78540	0.03827	Pri	V	ASAS	PZ
V643 Ori	52671.57191	0.03250	Sec	V	ASAS	PZ
V643 Ori	53064.70369	0.1898	Pri	V	ASAS	PZ
V643 Ori	53038.54694	0.08545	Sec	V	ASAS	PZ
V643 Ori	53431.67806	0.04141	Pri	V	ASAS	PZ
V643 Ori	53405.52748	0.07129	Sec	V	ASAS	PZ
V643 Ori	53798.59786	0.04299	Pri	V	ASAS	PZ
V643 Ori	53772.48842	0.02778	Sec	V	ASAS	PZ
V643 Ori	54427.67544	1.258	Pri	V	ASAS	PZ
V643 Ori	54401.49642	0.11847	Sec	V	ASAS	PZ
V643 Ori	55004.35238	0.04613	Pri	V	ASAS	PZ
V643 Ori	54978.10783	0.05033	Sec	V	ASAS	PZ
V1031 Ori	55255.35357	0.00379	Pri	BVR	RF75/300	RU
V1031 Ori	55599.34852	0.00093	Pri	R	RF34/135	RU
V1031 Ori	55616.39163	0.00256	Pri	C	RF34/135	RU
V1031 Ori	55645.32473	0.00202	Sec	R	RF34/135	RU
V1031 Ori	55878.60668	0.00064	Pri	VC	RF34/135	RU
V1804 Ori	55891.59140	0.00099	Pri	C	RF34/135	RU
V1834 Ori	55867.47221	0.00110	Pri	C	RF34/135	RU
V1834 Ori	55876.53932	0.00233	Pri	C	RF34/135	RU
V1834 Ori	55876.53888	0.00047	Pri	R	RF75/300	RU
delta Ori	55578.39624	0.00285	Pri	I	RF34/135	RU
AW Peg	55394.40088	0.00066	Pri	R	RF34/135	RU
AW Peg	54364.00387	0.00488	Pri	C	SWASP	PZ
AW Peg	54172.80122	0.00180	Pri	V	ASAS	PZ
KP Peg	55033.40866	0.0003	Pri	R	RF34/135	RU
KP Peg	55446.46482	0.00022	Pri	C	RF34/135	RU
KP Peg	55806.42826	0.00069	Pri	C	RF34/135	RU
KW Peg	54384.44946	0.00014	Pri	R	OND	PZ
PU Peg	55848.31676	0.00092	Sec	R	N200/1000	RU
V421 Peg	55829.45113	0.00019	Pri	C	RF34/135	RU
RW Per	54084.0680	0.0119	Pri	C	SWASP	PZ
RW Per	54387.6359	0.0035	Pri	C	SWASP	PZ
AG Per	55514.38896	0.00054	Sec	C	RF34/135	RU
AG Per	55515.41716	0.00068	Pri	C	RF34/135	RU
IQ Per	55834.52580	0.00027	Pri	R	RF34/135	PS
IZ Per	55830.51881	0.00094	Sec	R	RF34/135	RU
V511 Per	55831.58225	0.00073	Pri	C	RF34/135	RU
V572 Per	55096.60260	0.00079	Pri	RI	N254/1200	RU
V572 Per	55528.49141	0.00022	Pri	R	RF34/135	RU
V572 Per	55561.25110	0.00032	Pri	V	RF75/300	RU
V572 Per	55872.45001	0.00027	Sec	V	RF75/300	RU
V572 Per	55880.31685	0.00028	Pri	C	RF34/135	RU
V578 Per	55827.60450	0.00075	Pri	C	RF34/135	RU
V578 Per	55828.57453	0.00049	Pri	C	RF34/135	RU
V592 Per	55108.47238	0.00020	Pri	R	RF75/300	RU

Table 1: (cont.)

Star Name	HJD 24.....	Error	Type	Filter	Instrument/Source	Observer
V592 Per	55155.35195	0.00028	Sec	R	RF75/300	RU
V592 Per	55459.53447	0.00007	Sec	I	N254/1200	RU
V592 Per	55479.57125	0.00016	Sec	R	RF75/300	RU
V592 Per	55501.39909	0.00056	Pri	C	RF34/135	RU
V592 Per	55578.34227	0.00066	Sec	C	RF34/135	RU
V592 Per	55579.41526	0.00036	Pri	C	RF34/135	RU
V592 Per	55592.29655	0.00037	Pri	C	RF34/135	RU
V592 Per	55819.53848	0.00071	Sec	R	RF34/135	RU
V592 Per	55848.52375	0.00059	Pri	R	RF34/135	RU
V592 Per	54913.07857	0.00062	Pri	V	OMC	PZ
V592 Per	54083.56428	0.00049	Pri	C	SWASP	PZ
V592 Per	54084.63815	0.00086	Sec	C	SWASP	PZ
V592 Per	54092.51202	0.00063	Sec	C	SWASP	PZ
V592 Per	54111.48271	0.00088	Pri	C	SWASP	PZ
V592 Per	54115.41629	0.00078	Sec	C	SWASP	PZ
V592 Per	54121.49636	0.00151	Pri	C	SWASP	PZ
V592 Per	54135.45425	0.00085	Sec	C	SWASP	PZ
V592 Per	54140.46378	0.00090	Sec	C	SWASP	PZ
V592 Per	54396.69228	0.00034	Sec	C	SWASP	PZ
V592 Per	54406.71299	0.0015	Sec	C	SWASP	PZ
V592 Per	54410.64861	0.00196	Pri	C	SWASP	PZ
beta Per	55063.58012	0.00130	Pri	C	RF34/135	RU
beta Per	55565.36181	0.00029	Pri	C	RF34/135	RU
UV Psc	55483.56825	0.00082	Pri	R	N254/1200	RU
EU Psc	55879.49388	0.00068	Pri	R	RF34/135	RU
EU Psc	55885.41642	0.00027	Sec	R	RF34/135	RU
EY Psc	55837.42981	0.00062	Pri	C	RF34/135	RU
UZ Sge	54035.31348	0.00028	Pri	R	OND	PZ
UZ Sge	54252.45613	0.00019	Pri	R	OND	PZ
RS Sgr	52508.45123	0.0073	Pri	V	ASAS	PZ
RS Sgr	52507.23849	0.0041	Sec	V	ASAS	PZ
RS Sgr	52820.06436	0.00229	Pri	V	ASAS	PZ
RS Sgr	52818.86002	0.00698	Sec	V	ASAS	PZ
RS Sgr	53180.00925	0.00133	Pri	V	ASAS	PZ
RS Sgr	53178.79772	0.00263	Sec	V	ASAS	PZ
RS Sgr	53547.19518	0.00060	Pri	V	ASAS	PZ
RS Sgr	53545.98960	0.00698	Sec	V	ASAS	PZ
RS Sgr	53853.99261	0.00483	Pri	V	ASAS	PZ
RS Sgr	53852.75657	0.00768	Sec	V	ASAS	PZ
RS Sgr	54648.73918	0.00249	Pri	V	ASAS	PZ
RS Sgr	54647.54073	0.00464	Sec	V	ASAS	PZ
XY Sgr	55051.79217	0.00008	Sec	V	SPM	PZ
V505 Sgr	55376.47257	0.00345	Sec	BI	N254/1200	RU
V505 Sgr	55389.48432	0.00556	Sec	VI	N254/1200	RU
V505 Sgr	55392.44322	0.00052	Pri	VI	N254/1200	RU
V505 Sgr	55456.31537	0.00132	Pri	R	RF75/300	RU
V505 Sgr	55748.48040	0.00016	Pri	I	N200/1000	RU
V505 Sgr	55815.31167	0.00142	Sec	R	RF34/135	RU
V505 Sgr	55828.32514	0.00242	Sec	I	N200/1000	RU
V505 Sgr	55831.28028	0.00024	Pri	C	RF34/135	RU
BI Ser	54533.60975	0.00015	Pri	R	Ath	PZ+MZ
EQ Tau	54035.52240	0.00044	Pri	R	OND	PZ
V1121 Tau	55880.47701	0.00099	Pri	C	RF34/135	RU

Table 1: (cont.)

Star Name	HJD 24.....	Error	Type	Filter	Instrument/Source	Observer
V1121 Tau	55885.42210	0.00037	Pri	C	RF34/135	RU
V1268 Tau	55888.27374	0.00052	Pri	C	RF34/135	RU
lambda Tau	55579.31478	0.00189	Sec	I	RF34/135	RU
RS Tri	55055.86369	0.00003	Pri	B	SPM	PZ
AC UMa	55621.28361	0.00269	Pri	R	N200/1000	RU
AC UMa	55662.39936	0.00018	Pri	R	N200/1000	RU
HV UMa	55645.41050	0.00055	Pri	C	RF34/135	RU
LP UMa	55644.32685	0.00038	Sec	R	OND	PZ
AZ Vir	55672.46514	0.00036	Pri	R	RF34/135	RU
DL Vir	55258.57347	0.00012	Pri	R	RF75/300	RU
DL Vir	55308.55507	0.00036	Pri	I	N254/1200	RU
DL Vir	55600.59191	0.00028	Pri	R	RF34/135	RU
DL Vir	55621.63187	0.00125	Pri	C	RF34/135	RU
DL Vir	55650.57650	0.00008	Pri	R	RF75/300	RU
HT Vir	55578.58808	0.00024	Pri	R	RF34/135	RU
HT Vir	55599.58454	0.00021	Sec	R	RF34/135	RU
HT Vir	55672.35252	0.00018	Pri	R	RF34/135	RU
HT Vir	55672.55850	0.00018	Sec	R	RF34/135	RU
NY Vir	54195.41066	0.00006	Pri	R	OND	PZ
NY Vir	54195.46122	0.00021	Sec	R	OND	PZ
2MASS J19071662+4639532	55053.80435	0.00007	Sec	I	SPM	PZ
2MASS J22435517+2936475	55455.55597	0.00126	???	R	OND	PZ
BD-22 5866	55455.43138	0.00014	Pri	R	OND	PZ
GSC 00143-01246	55497.59070	0.00055	???	R	OND	PZ
GSC 01588-00632	55872.33165	0.00030	Sec	R	M305/3050	HK
GSC 01588-00632	55356.43822	0.00006	Pri	R	OND	PZ
GSC 02712-01201	55866.34828	0.00020	Pri	R	N200/2000	HK
GSC 04041-00673	52218.37777	0.00118	Pri	V	OND	MW
GSC 04041-00673	52219.70671	0.00207	Pri	R	OND	MW
GSC 04041-00673	51465.29835	0.00113	Pri	C	NSVS	PZ
GSC 04041-00673	51464.63045	0.00247	Sec	C	NSVS	PZ
GSC 04232-02830	54193.43729	0.00038	Sec	R	OND	PZ
GSC 04428-01574	54594.37573	0.00004	Pri	R	OND	PZ
GSC 04596-01254	54679.51034	0.00008	Sec	R	OND	PZ
HD 252984	54536.27139	0.00013	Pri	R	Ath	PZ+MZ
HD 252984	54536.27150	0.00012	Pri	V	Ath	PZ+MZ
HD 252984	54536.27145	0.00014	Pri	VR	Ath	PZ+MZ
HD 252984	55868.57561	0.00033	Pri	R	M305/3050	HK
HD 252984	55497.55228	0.00115	Sec	R	OND	PZ
LP 133-374	54600.32987	0.00033	Pri	R	OND	PZ
LP 133-374	55707.35836	0.00021	Sec	R	OND	PZ
NOMAD1 1322-0193464	55880.30762	0.00063	Pri	VRI	OND	PZ
NOMAD1 1322-0193464	55880.43012	0.00053	Sec	VRI	OND	PZ
NOMAD1 1322-0193464	55880.56146	0.00058	Pri	VRI	OND	PZ
NOMAD1 1322-0193464	55880.68394	0.00035	Sec	VRI	OND	PZ
NOMAD1 1322-0193464	55894.28031	0.00085	Sec	VRI	OND	PZ
NOMAD1 1322-0193464	55894.40461	0.00188	Pri	VRI	OND	PZ
NSVS 01286630	54384.28379	0.00007	Sec	R	OND	PZ
NSVS 2502726	54418.62531	0.00054	Pri	C	SWASP	PZ
NSVS 2502726	54437.65454	0.00093	Pri	C	SWASP	PZ
NSVS 2502726	54438.77370	0.00115	Pri	C	SWASP	PZ
NSVS 2502726	54439.61418	0.00163	Sec	C	SWASP	PZ
NSVS 2502726	54496.43210	0.00067	Pri	C	SWASP	PZ

Table 1: (cont.)

Star Name	HJD 24.....	Error	Type	Filter	Instrument/Source	Observer
NSVS 2502726	54501.46911	0.00016	Pri	C	SWASP	PZ
NSVS 2502726	54502.58799	0.00068	Pri	C	SWASP	PZ
NSVS 2502726	54524.41953	0.00019	Pri	C	SWASP	PZ
NSVS 2502726	54526.37965	0.00043	Sec	C	SWASP	PZ
NSVS 2502726	54527.49775	0.00027	Sec	C	SWASP	PZ
NSVS 2502726	54531.41661	0.00027	Sec	C	SWASP	PZ
NSVS 2502726	54532.53593	0.00114	Sec	C	SWASP	PZ
NSVS 2502726	54533.37699	0.00010	Pri	C	SWASP	PZ
NSVS 2502726	54534.49606	0.00046	Pri	C	SWASP	PZ
NSVS 2502726	54536.45305	0.00038	Sec	C	SWASP	PZ
NSVS 2502726	54539.53463	0.00109	Pri	C	SWASP	PZ
NSVS 2502726	54547.37041	0.00012	Pri	C	SWASP	PZ
NSVS 2502726	54554.36885	0.00045	Sec	C	SWASP	PZ
NSVS 2502726	54555.48444	0.00500	Sec	C	SWASP	PZ
NSVS 2502726	55280.40005	0.00012	Pri	R	OND	PZ
NSVS 2502726	55595.27551	0.00004	Pri	R	OND	PZ
NSVS 6507557	54763.37731	0.00007	Sec	R	OND	PZ
NSVS 6507557	54763.63632	0.00021	Pri	R	OND	PZ
NSVS 6507557	54763.37730	0.0008	Sec	V	OND	PZ
NSVS 7446320	54763.63620	0.00036	Sec	V	OND	PZ
NSVS 7446320	55280.50701	0.00013	Sec	V	OND	PZ
NSVS 10441882	54524.57292	0.00003	Pri	R	OND	PZ
NSVS 11868841	55054.97415	0.00006	Pri	R	SPM	PZ
NSVS 11868841	55154.26995	0.00026	Pri	R	OND	PZ

Notes on some systems:

V887 Aql – shows periodic pulsations with period about $0\overset{d}{.}045$

SU Aqr – shows periodic pulsations with period about $0\overset{d}{.}024$

V389 Cas – shows periodic pulsations with period about $0\overset{d}{.}041$

KO Nor – new eccentric binary with ephemerides:

$$\mathrm{HJD_{Pri}} = 2453486.551 + 33.562146 \times \mathrm{E} \ ,$$
$$\mathrm{HJD_{Sec}} = 2453502.355 + 33.562146 \times \mathrm{E} \ .$$

NOMAD1 1322-0193464 – newly discovered W UMa type binary with large O'Connell effect and asymmetric minima, following the ephemerides:

$$\mathrm{HJD_{Pri}} = 2455880.558 + 0.25407 \times \mathrm{E} \ .$$

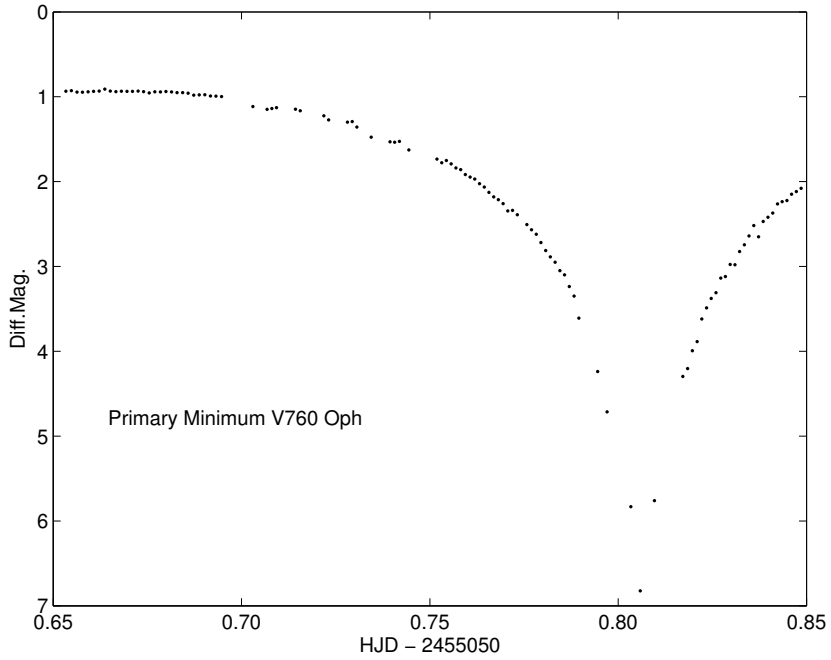

Figure 1. Primary minimum of V760 Oph, one of the deepest among known eclipsing binaries.

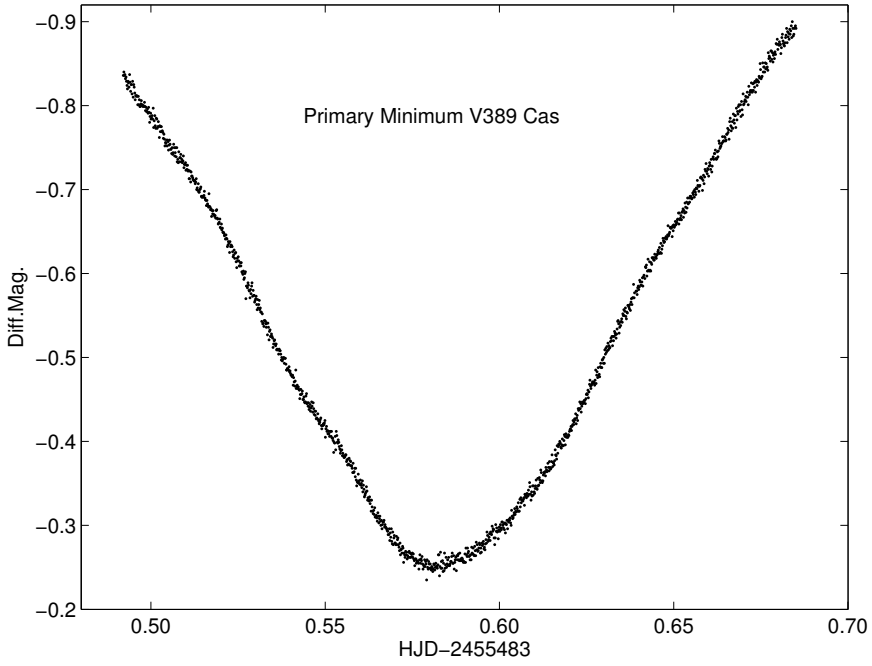

Figure 2. Primary minimum of V389 Cas, the periodic pulsations are clearly visible.

Acknowledgements:
Based on data from the OMC Archive at LAEFF, pre-processed by ISDC. We thank the ASAS, NSVS, SWASP, COROT and OMC teams for making all of the observations easily public available. We also thank M. Wolf and M. Zejda for their photometric data. This work was supported by the Czech Science Foundation grant no. P209/10/0715 and also by the Research Programme MSM0021620860 of the Czech Ministry of Education. The use of "O-C gateway" (Paschke & Brát 2006) is also acknowledged.

References:

Bessell, M. S. 1990, *PASP*, **102**, 1181
Kwee, K. K., van Woerden, H., 1956, *Bull. Astron. Inst. Neth.*, **12**, 327
Paschke, A., Brát, L., 2006, *Open European Journal on Variable Stars*, **23**, 13

COMMISSIONS 27 AND 42 OF THE IAU
INFORMATION BULLETIN ON VARIABLE STARS

Number 6008

Konkoly Observatory
Budapest
21 December 2011

HU ISSN 0374 – 0676

THE 80TH NAME-LIST OF VARIABLE STARS. PART II — RA 6^h TO 16^h

KAZAROVETS, E.V.[1]; SAMUS, N.N.[1,2]; DURLEVICH, O.V.[2]; KIREEVA, N.N.[1]; PASTUKHOVA, E.N.[1]

[1] Institute of Astronomy, Russian Academy of Sciences, 48, Pyatnitskaya Str., Moscow 119017, Russia
[helene@inasan.ru, samus@sai.msu.ru, kireeva@sai.msu.ru, pastukhova@sai.msu.ru]

[2] Sternberg Astronomical Institute, M.V. Lomonosov University of Moscow, 13, University Ave., Moscow 119992, Russia
[gcvs@sai.msu.ru]

Part I of the 80th Name-List of Variable Stars (Kazarovets et al., 2011b) contained information on 2036 stars recently named in the system of the General Catalogue of Variable Stars (GCVS; Samus et al. 2011), most of them in the range of right ascensions (J2000.0) between 0^h and 6^h. The present Part II of the 80th Name-List of Variable Stars contains data necessary for identifications of new variables finally designated in 2010–2011. Most stars in the Name-List are confined to right ascensions (J2000.0) between 6^h and 16^h. Exceptions are several Novae, named upon requests of the IAU Central Bureau of Astronomical Telegrams, and unusual variables, which are included no matter the right ascension. Besides, we have included 10 interesting young variable stars whose GCVS names were announced in Kazarovets et al. (2011a). With the 2159 stars of the current Name-List, the total number of named variable stars, not counting designated non-existing stars or stars subsequently identified with earlier-named variables, is now 45 678.

As it had been done in Part I, we separate the catalogue of newly designated variables (to be published elsewhere in the nearest future) from the Name-List proper. Table 1 of the current Name-List contains the new GCVS name, equatorial coordinates (rounded to an accuracy sufficient for identification), and variability type for each star. The order of stars in Table 1 corresponds to the order of stars in the GCVS. The remarks concerning the six unusual variables (type *), LT Cnc, V0484 Hya, V0488 Hya, BH Lep, AY Sex, and V0472 Vel, follow Table 1. The electronic version of the Name-List at http://www.sai.msu.su/gcvs/gcvs/nl80 additionally presents variability ranges, light elements, spectral types, identifications with astronomical catalogues, detailed remarks, bibliographic references for the newly named variable stars.

We continued naming Novae and other variables of astrophysical importance upon requests from the IAU Bureau of Astronomical Telegrams. Part II of the 80th Name-List contains six Novae. They are included in Table 1 and, besides, listed in Table 2 that contains, along with GCVS names, preliminary "constellation+year" designations for Novae.

Also, we named 10 interesting young variable stars upon well-prepared request from Dr. Bo Reipurth (Kazarovets et al., 2011a). They enter Table 1 and are listed in Table 3.

Acknowledgements: This study was supported in part by Russian Foundation for Basic Research and by the Programme "Origin and Evolution of Stars and Galaxies" of the Presidium of Russian Academy of Sciences.

References:

Kazarovets, E.V., Reipurth, Bo, Samus, N.N. 2011a, Perem. Zvezdy, **31**, 2

Kazarovets, E.V., Samus, N.N., Durlevich, O.V., Kireeva, N.N., Pastukhova, E.N. 2011b, *Inform. Bull. Var. Stars*, No. 5969

Samus, N.N., Durlevich, O.V., Kazarovets, E.V., Kireeva, N.N., Pastukhova, E.N., et al. 2011, *General Catalogue of Variable Stars* (GCVS database, version March 2011), CDS B/gcvs

Table 1

Name	R.A., Decl., 2000.0	Type	Name	R.A., Decl., 2000.0	Type
	h m s o ' "			h m s o ' "	
BW Ant	09 29 20.2 -31 23 03	XP	V0649 Aur	06 53 41.9 +42 42 19	BY
BX Ant	10 18 28.7 -31 50 03	IT	V0650 Aur	07 11 45.0 +40 32 07	ELL:
BY Ant	10 22 48.4 -33 36 58	EA	V0651 Aur	07 16 47.7 +43 18 17	RRAB
BZ Ant	10 29 34.8 -30 36 33	IT	V0652 Aur	07 21 35.7 +43 59 06	LB:
CC Ant	10 33 29.4 -36 03 58	EA	V0653 Aur	07 24 52.4 +35 31 27	RRAB
CD Ant	10 41 29.7 -34 12 52	EA	V0654 Aur	07 29 10.7 +36 58 39	XM
CE Ant	10 42 30.1 -33 40 17	IT	HW Boo	13 43 23.2 +15 09 17	UG
CF Ant	10 52 21.4 -36 18 11	EA	HX Boo	13 48 08.5 +07 49 13	SRB
QR Aps	13 57 35.8 -73 04 03	M	HY Boo	13 56 49.2 +24 29 27	RS
QS Aps	13 59 55.3 -78 52 51	M	HZ Boo	14 04 08.4 +12 10 34	RRAB
QT Aps	14 06 45.5 -81 06 16	SRB	II Boo	14 05 10.3 +14 04 51	RRAB
QU Aps	14 07 02.4 -72 11 30	M	IK Boo	14 08 46.2 +29 29 08	EW
QV Aps	14 08 00.8 -80 42 02	M	IL Boo	14 09 00.5 +45 18 37	EW
QW Aps	14 08 50.7 -72 52 48	SRB	IM Boo	14 09 05.6 +47 49 28	RRAB
QX Aps	14 09 56.3 -71 05 15	SRB	IN Boo	14 09 21.3 +31 10 08	EW:
QY Aps	14 13 19.2 -75 14 15	M	IO Boo	14 12 51.0 +24 32 02	EW
QZ Aps	14 13 55.9 -76 13 06	M	IP Boo	14 14 57.4 +39 19 24	RRC
V0335 Aps	14 14 51.7 -79 16 54	SRA	IQ Boo	14 15 25.5 +28 16 56	RRAB
V0336 Aps	14 15 03.0 -74 14 47	DSCT	IR Boo	14 15 46.6 +16 56 05	RRAB
V0337 Aps	14 19 51.1 -78 38 58	M	IS Boo	14 16 00.2 +49 14 16	EW
V0338 Aps	14 21 04.2 -75 45 20	RRAB	IT Boo	14 16 14.6 +48 39 22	SRD:
V0339 Aps	14 27 55.3 -72 52 31	EB	IU Boo	14 16 30.9 +26 55 25	BY
V0340 Aps	14 30 36.4 -73 29 46	EA	IV Boo	14 16 39.6 +30 17 03	EW:
V0341 Aps	14 36 24.2 -79 36 21	M	IW Boo	14 16 46.3 +43 08 45	EW
V0342 Aps	14 37 59.1 -72 52 45	DSCT:	IX Boo	14 16 53.6 +23 52 46	EW:
V0343 Aps	14 40 01.3 -72 43 07	DSCT	IY Boo	14 19 39.2 +25 47 24	RRAB
V0344 Aps	14 40 33.3 -78 19 15	RRC	IZ Boo	14 20 04.7 +39 03 01	BY:
V0345 Aps	14 49 20.1 -79 40 24	EW	KK Boo	14 20 14.7 +43 10 58	EW
V0346 Aps	14 52 39.5 -71 04 27	EA	KL Boo	14 20 19.6 +27 58 57	BY
V0347 Aps	14 59 38.0 -72 45 54	RRAB	KM Boo	14 20 53.8 +54 28 53	EW
V0348 Aps	15 07 53.2 -72 17 38	M	KN Boo	14 21 38.2 +07 53 20	RPHS
V0349 Aps	15 09 23.6 -76 16 48	SRB	KO Boo	14 21 57.5 +23 26 56	EW:
V0350 Aps	15 09 27.6 -82 26 43	M	KP Boo	14 23 35.3 +43 39 41	EB
V0351 Aps	15 09 51.9 -76 33 06	M	KQ Boo	14 25 10.3 +39 20 01	RS
V0352 Aps	15 11 31.9 -78 24 04	EW	KR Boo	14 25 29.4 +20 57 47	RRAB
V0353 Aps	15 13 37.3 -75 52 35	M	KS Boo	14 26 56.6 +23 36 53	BY
V0354 Aps	15 15 28.6 -77 46 42	EA	KT Boo	14 29 02.5 +33 50 39	BY
V0355 Aps	15 18 50.7 -73 16 01	M	KU Boo	14 30 30.8 +50 20 22	RRAB
V0356 Aps	15 27 45.1 -80 44 31	RRAB	KV Boo	14 30 33.5 +38 43 55	SRB
V0357 Aps	15 31 56.0 -78 23 05	EW	KW Boo	14 30 40.4 +27 13 29	EW:
V0358 Aps	15 37 54.4 -71 48 47	LB	KX Boo	14 31 00.9 +20 25 32	RRAB
V0359 Aps	15 38 47.0 -72 40 16	M	KY Boo	14 31 04.0 +44 04 22	RS
V0360 Aps	15 49 39.2 -76 25 18	DSCT	KZ Boo	14 32 34.4 +54 27 39	EW
V0361 Aps	15 53 03.9 -72 25 04	M	LL Boo	14 32 41.2 +46 11 40	RS
V1723 Aql	18 47 38.4 -03 47 14	NA	LM Boo	14 36 35.5 +24 00 37	EW
V0640 Aur	06 02 07.6 +52 31 44	EW	LN Boo	14 37 09.0 +25 44 47	RRAB
V0641 Aur	06 03 47.6 +42 19 07	EA	LO Boo	14 37 29.5 +41 28 35	BY
V0642 Aur	06 09 51.0 +32 29 48	BY	LP Boo	14 37 32.0 +35 28 19	SR
V0643 Aur	06 10 46.5 +52 46 43	RRAB	LQ Boo	14 37 53.7 +34 59 24	RRAB
V0644 Aur	06 18 25.7 +34 29 39	EA	LR Boo	14 38 06.8 +35 49 41	RS
V0645 Aur	06 19 15.5 +28 26 23	EA	LS Boo	14 38 21.8 +14 24 55	RRAB
V0646 Aur	06 35 40.5 +42 04 15	EW	LT Boo	14 38 45.1 +53 46 59	RRAB
V0647 Aur	06 36 32.5 +35 35 43	XM	LU Boo	14 38 54.6 +33 00 20	BY
V0648 Aur	06 41 16.9 +46 49 08	EW/RS	LV Boo	14 39 02.2 +53 57 44	RRAB

Table 1 (continued)

Name	R.A., Decl., 2000.0	Type	Name	R.A., Decl., 2000.0	Type
	h m s o ' "			h m s o ' "	
LW Boo	14 40 32.6 +17 35 57	RRAB	QQ Boo	15 32 04.8 +45 34 07	EW
LX Boo	14 41 45.3 +42 31 21	BY	QR Boo	15 33 20.4 +43 44 27	RRAB
LY Boo	14 41 53.8 +39 01 55	EW	QS Boo	15 34 42.3 +48 52 10	RR
LZ Boo	14 42 41.8 +50 06 24	RRAB	QT Boo	15 35 11.0 +49 47 44	EW
MM Boo	14 42 48.4 +42 31 30	RRAB	QU Boo	15 36 05.6 +42 00 23	SRD
MN Boo	14 43 51.2 +47 43 03	EW	QV Boo	15 36 29.5 +39 56 11	EW
MO Boo	14 44 21.2 +40 39 08	RRAB	QW Boo	15 36 34.6 +46 38 09	EW
MP Boo	14 44 38.3 +53 13 04	RS	QX Boo	15 36 49.3 +47 37 19	EW
MQ Boo	14 44 48.6 +44 39 00	EB	QY Boo	15 39 17.4 +43 45 45	EW
MR Boo	14 45 33.3 +51 10 45	EB	QZ Boo	15 39 20.9 +47 45 24	RS
MS Boo	14 45 41.0 +34 07 19	RS	V0335 Boo	15 40 58.9 +40 27 00	BY
MT Boo	14 47 06.7 +41 03 39	EW	V0336 Boo	15 44 36.6 +46 19 22	SXPHE
MU Boo	14 48 14.7 +19 20 19	RRC:	V0337 Boo	15 45 35.1 +42 05 07	BY
MV Boo	14 48 31.0 +35 03 18	EA/RS	V0338 Boo	15 46 26.1 +44 18 47	RR(B)
MW Boo	14 48 48.8 +47 40 42	EW	V0339 Boo	15 48 35.0 +43 28 45	EW
MX Boo	14 49 52.6 +42 06 27	RS	V0340 Boo	15 48 59.7 +40 14 08	RRAB
MY Boo	14 52 17.9 +54 15 51	EW	V0418 Cam	06 00 45.0 +71 36 26	EW
MZ Boo	14 52 40.2 +45 39 41	RRAB	V0419 Cam	06 01 00.4 +61 56 51	EW
NN Boo	14 53 39.9 +40 31 43	RR(B)	V0420 Cam	06 01 29.6 +71 08 19	EB
NO Boo	14 55 01.9 +14 42 03	EB:/RS	V0421 Cam	06 04 53.3 +79 53 42	EA
NP Boo	14 56 41.0 +27 30 25	M	V0422 Cam	06 07 38.2 +69 43 47	EA
NQ Boo	14 58 00.7 +13 11 49	RS	V0423 Cam	06 07 49.7 +72 46 37	EA/RS
NR Boo	14 58 28.4 +11 05 55	EW	V0424 Cam	06 08 44.4 +73 33 43	EW
NS Boo	15 00 18.9 +33 52 07	BY	V0425 Cam	06 09 27.4 +79 25 47	SRA
NT Boo	15 00 32.8 +49 55 03	EW	V0426 Cam	06 10 44.3 +68 00 15	EW
NU Boo	15 00 34.6 +54 10 54	EW	V0427 Cam	06 10 44.7 +70 34 15	SRA
NV Boo	15 00 47.6 +35 09 51	RRC	V0428 Cam	06 12 51.1 +77 10 51	EW
NW Boo	15 00 49.7 +35 08 35	EA	V0429 Cam	06 13 06.6 +76 29 49	EW
NX Boo	15 00 59.5 +34 11 41	EW	V0430 Cam	06 13 47.0 +63 35 10	RS
NY Boo	15 01 09.6 +48 48 16	EW	V0431 Cam	06 13 53.8 +67 21 00	SR
NZ Boo	15 02 41.0 +33 34 24	UGSU+E	V0432 Cam	06 14 13.8 +70 52 33	EW
OO Boo	15 02 47.4 +22 18 21	RS	V0433 Cam	06 15 18.1 +67 20 08	RRAB
OP Boo	15 03 12.1 +53 33 54	EW	V0434 Cam	06 15 19.6 +77 19 52	LB
OQ Boo	15 03 37.7 +28 03 34	EW	V0435 Cam	06 15 20.9 +82 08 13	SXPHE
OR Boo	15 04 27.4 +51 52 04	RRAB	V0436 Cam	06 15 55.8 +66 53 16	EA
OS Boo	15 04 37.6 +42 56 06	EW	V0437 Cam	06 18 43.6 +70 12 34	EB
OT Boo	15 06 50.4 +47 38 16	EA	V0438 Cam	06 20 00.8 +77 22 53	EW:
OU Boo	15 07 01.4 +41 22 53	RRAB	V0439 Cam	06 22 02.0 +72 18 47	EB
OV Boo	15 07 22.4 +52 30 39	EA	V0440 Cam	06 22 57.5 +73 30 43	EB
OW Boo	15 07 33.9 +10 02 49	RRAB	V0441 Cam	06 25 08.8 +69 48 52	LB
OX Boo	15 08 07.3 +33 00 39	RRAB	V0442 Cam	06 25 58.1 +73 31 15	EW:
OY Boo	15 11 13.3 +34 26 16	RRAB	V0443 Cam	06 28 02.5 +74 24 23	EW
OZ Boo	15 12 48.0 +28 40 14	EW	V0444 Cam	06 28 47.3 +79 22 12	EW
PP Boo	15 14 14.1 +45 49 13	NL	V0445 Cam	06 31 40.7 +78 39 52	EW
PQ Boo	15 17 03.2 +53 32 28	RRC	V0446 Cam	06 32 18.0 +70 08 16	SR
PR Boo	15 18 32.0 +44 57 12	EW	V0447 Cam	06 37 21.1 +68 04 41	EB
PS Boo	15 19 44.2 +50 20 57	EW	V0448 Cam	06 40 44.8 +73 22 01	SR
PT Boo	15 20 15.1 +43 23 49	EW	V0449 Cam	06 42 42.7 +63 20 16	EA
PU Boo	15 23 02.2 +45 39 20	EW	V0450 Cam	06 42 43.2 +72 00 03	EW
PV Boo	15 23 25.5 +33 51 58	EW	V0451 Cam	06 42 43.7 +64 21 52	EW
PW Boo	15 27 14.3 +34 14 52	RRAB	V0452 Cam	06 43 52.7 +70 21 50	EW
PX Boo	15 27 42.0 +49 48 17	RRAB	V0453 Cam	06 44 33.9 +71 37 02	ELL
PY Boo	15 28 22.1 +51 32 21	EW	V0454 Cam	06 45 11.3 +72 51 36	EA:
PZ Boo	15 30 07.9 +43 15 00	EW	V0455 Cam	06 47 25.0 +69 42 15	EA

Table 1 (continued)

Name	R.A., Decl., 2000.0	Type	Name	R.A., Decl., 2000.0	Type
	h m s o ' "			h m s o ' "	
V0456 Cam	06 47 52.2 +64 11 45	EW	V0510 Cam	09 24 14.8 +81 13 28	CWB
V0457 Cam	06 48 04.1 +70 45 34	EW	V0511 Cam	10 05 54.7 +81 59 00	EW
V0458 Cam	06 48 25.3 +64 29 47	LB:	V0512 Cam	10 16 41.7 +84 32 06	EW:
V0459 Cam	06 48 27.6 +65 20 57	EA	V0513 Cam	10 19 33.2 +83 36 13	RRAB
V0460 Cam	06 50 30.5 +64 46 25	EW	V0514 Cam	11 28 30.2 +79 38 56	EW
V0461 Cam	06 50 47.2 +73 21 33	EW	V0515 Cam	11 45 01.3 +76 24 20	EB
V0462 Cam	06 51 33.6 +74 23 34	EA	V0516 Cam	12 00 43.9 +77 05 00	EA
V0463 Cam	06 53 18.1 +72 45 42	RS	V0517 Cam	12 06 51.0 +77 18 57	EA
V0464 Cam	06 54 01.6 +80 21 26	EB	V0518 Cam	13 12 55.8 +83 41 43	EA
V0465 Cam	06 56 17.6 +67 04 49	EA	V0519 Cam	14 15 25.0 +84 03 33	EA
V0466 Cam	06 59 18.6 +71 49 52	EW	IV Cnc	08 01 59.8 +13 49 44	EW
V0467 Cam	07 02 18.1 +72 08 53	RRAB	IW Cnc	08 04 53.6 +19 45 11	RRAB
V0468 Cam	07 03 33.8 +63 08 09	EW	IX Cnc	08 05 40.0 +15 22 59	DSCT:
V0469 Cam	07 06 13.8 +67 18 13	EA	IY Cnc	08 06 29.2 +15 40 46	UV:
V0470 Cam	07 10 42.1 +66 55 44	EA	IZ Cnc	08 07 00.4 +15 11 00	SXPHE
V0471 Cam	07 13 17.1 +70 16 34	RS	KK Cnc	08 07 14.3 +11 38 11	UGSU
V0472 Cam	07 14 12.8 +76 49 51	SR	KL Cnc	08 07 50.6 +28 21 08	RS
V0473 Cam	07 17 04.9 +77 10 26	EW	KM Cnc	08 08 15.9 +23 04 10	EW
V0474 Cam	07 19 15.0 +69 03 16	EW	KN Cnc	08 10 35.2 +27 49 28	RS
V0475 Cam	07 22 48.0 +74 20 03	EW	KO Cnc	08 11 16.0 +11 56 58	RV
V0476 Cam	07 23 20.9 +75 28 21	EA	KP Cnc	08 14 27.0 +20 42 28	DSCTC
V0477 Cam	07 24 12.6 +75 35 03	EB	KQ Cnc	08 16 36.0 +18 20 58	RRAB
V0478 Cam	07 27 23.8 +77 22 23	EA	KR Cnc	08 26 22.6 +26 59 46	EA
V0479 Cam	07 27 24.5 +74 26 00	EW	KS Cnc	08 28 34.2 +32 04 04	RRAB
V0480 Cam	07 30 55.3 +63 43 50	RS:	KT Cnc	08 31 25.3 +11 48 13	EW
V0481 Cam	07 32 10.4 +84 33 52	EW	KU Cnc	08 35 26.9 +24 15 39	RS
V0482 Cam	07 33 41.4 +67 32 16	EA+NL	KV Cnc	08 40 02.4 +27 43 32	RRAB
V0483 Cam	07 35 40.2 +83 42 36	EW	KW Cnc	08 40 48.0 +15 24 52	RRAB
V0484 Cam	07 37 01.4 +70 45 50	EA	KX Cnc	08 42 46.2 +31 51 45	EA
V0485 Cam	07 37 08.8 +70 33 45	EA	KY Cnc	08 44 16.2 +25 04 33	EA
V0486 Cam	07 38 38.6 +69 20 48	RRAB	KZ Cnc	08 50 44.0 +11 42 49	EA
V0487 Cam	07 43 19.3 +78 07 00	EB	LL Cnc	08 50 51.2 +19 21 26	EB
V0488 Cam	07 47 39.0 +78 10 11	EW	LM Cnc	08 50 59.8 +13 57 45	EW
V0489 Cam	07 48 43.7 +76 28 09	EA/RS	LN Cnc	08 52 16.8 +11 48 32	EW:
V0490 Cam	07 51 52.2 +74 53 44	EW	LO Cnc	08 53 01.3 +12 08 21	EW
V0491 Cam	07 52 45.1 +81 19 52	RRC	LP Cnc	08 53 19.0 +12 10 02	EW
V0492 Cam	08 00 04.3 +67 22 45	RRAB	LQ Cnc	09 00 02.3 +27 39 29	RRC
V0493 Cam	08 00 52.2 +70 19 03	RRAB	LR Cnc	09 03 47.7 +12 18 26	RS
V0494 Cam	08 11 31.7 +74 16 26	EA	LS Cnc	09 04 04.8 +17 51 25	EW
V0495 Cam	08 19 25.6 +77 05 14	EW	LT Cnc	09 10 25.4 +12 08 27	*
V0496 Cam	08 19 52.4 +81 09 46	EW	LU Cnc	09 14 25.9 +18 53 54	EW
V0497 Cam	08 42 41.3 +83 47 14	EW	LV Cnc	09 19 45.3 +08 57 10	ZZ
V0498 Cam	08 51 58.1 +74 01 55	EA	EO CVn	12 22 24.7 +33 46 15	EW
V0499 Cam	08 54 24.3 +79 40 54	EA	EP CVn	12 23 08.7 +45 27 54	RS
V0500 Cam	08 55 59.1 +78 24 26	EW	EQ CVn	12 25 57.8 +33 46 51	EA/RS
V0501 Cam	08 57 10.7 +79 12 21	EW	ER CVn	12 27 51.2 +33 38 43	BY
V0502 Cam	08 59 18.4 +80 19 50	EA	ES CVn	12 37 04.0 +37 44 56	BY
V0503 Cam	09 00 46.9 +76 46 03	EA	ET CVn	12 43 28.0 +37 57 36	RS
V0504 Cam	09 04 00.0 +76 16 32	EA	EU CVn	12 43 52.3 +47 38 31	RRAB
V0505 Cam	09 08 49.1 +82 46 06	EW	EV CVn	12 44 05.2 +37 11 28	EW
V0506 Cam	09 10 27.5 +84 17 23	EW	EW CVn	12 44 08.5 +40 23 30	BY
V0507 Cam	09 11 13.8 +77 52 24	EA	EX CVn	12 44 27.6 +38 30 44	EW
V0508 Cam	09 21 18.1 +78 37 42	EW	EY CVn	13 06 25.4 +34 29 17	EW
V0509 Cam	09 24 13.3 +79 44 54	EW	EZ CVn	13 12 49.3 +46 28 29	LB

Table 1 (continued)

Name	R.A., Decl., 2000.0	Type	Name	R.A., Decl., 2000.0	Type
	h m s o ' "			h m s o ' "	
FF CVn	13 19 26.0 +36 04 07	BY	V0425 CMa	07 24 07.3 -23 30 46	M
FG CVn	13 24 26.4 +30 33 14	BY	V0426 CMa	07 24 35.3 -15 59 52	SR
FH CVn	13 27 12.1 +45 58 26	BY	V0427 CMa	07 24 38.5 -28 38 00	EA
FI CVn	13 28 37.3 +35 33 12	EW	DO CMi	07 12 19.4 +09 21 03	DSCT
FK CVn	13 29 31.2 +29 36 16	BY	DP CMi	07 18 14.9 +01 41 27	EA/RS
FL CVn	13 31 15.8 +40 56 57	RRAB	DQ CMi	07 20 38.5 +06 40 55	RRAB
FM CVn	13 32 40.5 +28 47 58	BY	DR CMi	07 24 31.4 +03 03 28	EA
FN CVn	13 36 09.3 +45 59 41	EW	DS CMi	07 25 19.0 -00 05 00	EW
FO CVn	13 37 22.1 +41 34 38	RRC	DT CMi	07 28 16.1 +09 49 26	RRAB
FP CVn	13 39 24.7 +40 09 05	BY	DU CMi	07 29 37.0 +01 01 41	SRB
FQ CVn	13 41 17.7 +31 54 30	EB	DV CMi	07 37 16.9 +11 39 54	SRB
FR CVn	13 43 28.2 +39 11 33	BY	DW CMi	07 40 33.1 +04 42 20	EW
FS CVn	13 43 30.7 +33 29 51	BY	DX CMi	07 46 53.2 +00 35 44	EA
FT CVn	13 48 42.5 +41 55 08	RRAB	DY CMi	07 47 27.6 +06 50 50	UGSU
FU CVn	13 52 09.7 +41 17 42	EW	DZ CMi	07 50 58.4 +06 59 34	RRAB
FV CVn	13 53 13.7 +32 22 47	EW	EE CMi	07 51 08.0 +00 56 35	SRB
FW CVn	13 54 18.8 +40 45 42	EW	EF CMi	07 52 50.4 +00 14 10	RRC:
FX CVn	13 55 52.0 +44 31 17	RRAB	EG CMi	07 53 30.4 +01 18 53	EW
FY CVn	13 56 42.5 +39 34 36	EW	EH CMi	07 55 01.1 +00 23 37	SRA
FZ CVn	13 58 12.2 +39 44 34	EW	EI CMi	07 57 06.3 +01 17 20	EW
GG CVn	13 58 43.3 +31 25 10	EW	EK CMi	07 57 17.5 -00 05 01	EB
GH CVn	13 59 20.3 +41 49 56	EW	EL CMi	07 59 46.8 +00 21 07	EA
GI CVn	13 59 51.0 +47 06 36	EW	EM CMi	08 02 22.0 -00 01 24	RRAB
GK CVn	14 00 48.2 +33 47 22	EB:	EN CMi	08 04 46.3 -00 18 18	RRAB
GL CVn	14 00 52.8 +34 00 57	EA	EO CMi	08 08 22.0 +00 00 39	RRAB
GM CVn	14 01 46.6 +32 08 48	EW	EP CMi	08 10 00.9 +00 10 22	EB
GN CVn	14 05 09.0 +38 54 19	EW	EQ CMi	08 10 44.7 +01 03 30	EW
GO CVn	14 06 45.5 +43 06 44	EB	ER CMi	08 11 05.3 +04 01 38	M
V0399 CMa	06 12 55.8 -14 40 06	RRC	V0680 Car	07 00 14.7 -60 51 55	BY:
V0400 CMa	06 15 23.4 -18 41 14	EW	V0681 Car	07 39 03.7 -60 37 09	EA+DSCT:
V0401 CMa	06 15 29.9 -18 40 40	EA	V0682 Car	08 21 22.3 -53 28 53	SR
V0402 CMa	06 15 33.9 -18 39 22	EA	V0683 Car	08 46 36.2 -58 07 26	LB
V0403 CMa	06 15 46.1 -18 37 07	ELL:	V0684 Car	08 57 29.6 -62 53 50	EA
V0404 CMa	06 15 55.4 -18 44 52	EA	V0685 Car	09 16 39.5 -74 36 45	LB
V0405 CMa	06 24 26.2 -20 44 54	EW	V0686 Car	09 33 38.8 -57 42 08	EA
V0406 CMa	06 29 27.1 -31 18 29	GDOR:	V0687 Car	09 44 16.5 -75 10 13	SRA
V0407 CMa	06 29 32.8 -31 17 46	BY:	V0688 Car	09 44 41.5 -62 47 32	M
V0408 CMa	06 29 33.0 -31 17 53	EW	V0689 Car	09 45 09.3 -63 27 26	RRAB
V0409 CMa	06 29 33.4 -31 16 24	DSCTC:	V0690 Car	09 48 26.8 -58 01 05	DCEP
V0410 CMa	06 29 34.3 -31 16 18	EA	V0691 Car	09 49 25.0 -72 45 02	RRAB
V0411 CMa	06 29 35.7 -31 17 04	EA	V0692 Car	09 49 49.4 -62 56 09	SR
V0412 CMa	06 29 41.1 -31 19 06	BY:	V0693 Car	09 52 29.9 -75 22 28	M
V0413 CMa	06 29 45.3 -31 17 19	EA	V0694 Car	09 54 39.5 -68 03 56	RRAB
V0414 CMa	06 34 42.6 -15 46 39	RRAB	V0695 Car	09 54 52.1 -60 35 26	M
V0415 CMa	06 36 41.1 -22 36 53	EA	V0696 Car	09 56 32.7 -67 26 42	RRAB
V0416 CMa	06 52 32.0 -25 33 30	EW	V0697 Car	10 00 08.5 -62 05 19	M
V0417 CMa	07 01 09.2 -29 06 25	ZAND	V0698 Car	10 03 57.6 -60 00 37	SRB
V0418 CMa	07 03 30.5 -15 32 36	CEP	V0699 Car	10 04 19.6 -59 04 00	M:
V0419 CMa	07 09 22.5 -16 20 31	EB	V0700 Car	10 06 57.2 -59 21 25	SR
V0420 CMa	07 15 56.7 -15 18 08	SR	V0701 Car	10 09 13.6 -57 14 33	CEP(B)
V0421 CMa	07 16 08.3 -23 27 02	I	V0702 Car	10 11 34.9 -57 57 53	M
V0422 CMa	07 18 21.9 -24 51 12	EA	V0703 Car	10 11 40.9 -63 21 06	SRB
V0423 CMa	07 23 15.2 -29 43 21	DCEP	V0704 Car	10 12 39.9 -60 13 30	SRA
V0424 CMa	07 24 03.5 -12 52 28	M:	V0705 Car	10 12 43.9 -61 17 24	M:

Table 1 (continued)

Name	R.A., Decl., 2000.0 h m s o ' "	Type	Name	R.A., Decl., 2000.0 h m s o ' "	Type
V0706 Car	10 14 53.2 -59 02 56	SRA	V0760 Car	10 53 26.9 -61 43 21	EA
V0707 Car	10 15 27.0 -57 58 11	LB	V0761 Car	10 53 29.5 -61 47 37	EA
V0708 Car	10 15 37.9 -59 33 05	DCEP	V0762 Car	10 53 33.5 -61 47 05	EA
V0709 Car	10 19 16.9 -57 19 26	LB	V0763 Car	10 53 40.6 -61 25 15	EP:
V0710 Car	10 21 44.0 -58 16 35	M	V0764 Car	10 53 51.1 -61 34 14	EA
V0711 Car	10 23 49.2 -59 13 54	M	V0765 Car	10 54 23.5 -61 37 21	EA
V0712 Car	10 23 58.0 -57 45 49	EB/WR	V0766 Car	10 54 27.4 -61 38 18	EA
V0713 Car	10 27 35.9 -58 23 26	EA	V0767 Car	10 55 10.1 -61 31 05	EA:
V0714 Car	10 28 15.8 -57 41 38	EA	V0768 Car	10 55 12.7 -61 54 55	EA
V0715 Car	10 29 44.3 -62 28 29	SR	V0769 Car	10 55 17.8 -61 54 36	EA
V0716 Car	10 31 10.7 -59 28 18	M	V0770 Car	10 55 19.3 -61 32 12	EA
V0717 Car	10 32 09.8 -59 05 42	EB+EB	V0771 Car	10 55 20.2 -61 25 00	EA
V0718 Car	10 33 08.1 -71 33 45	EW+EW	V0772 Car	10 55 44.1 -68 47 27	EB
V0719 Car	10 37 08.9 -60 59 34	SR	V0773 Car	10 55 48.8 -61 28 45	EA
V0720 Car	10 41 30.0 -59 56 58	ACV:	V0774 Car	10 56 11.1 -61 29 56	EA
V0721 Car	10 42 05.6 -59 33 27	SRB	V0775 Car	10 56 33.9 -61 37 11	EA
V0722 Car	10 42 32.1 -59 35 30	BE:	V0776 Car	10 56 36.5 -61 28 47	EA
V0723 Car	10 43 23.3 -59 33 57	FU:	V0777 Car	10 56 45.4 -60 03 37	M
V0724 Car	10 43 27.4 -60 05 55	BCEP	V0778 Car	10 56 51.6 -61 56 15	EA
V0725 Car	10 43 30.8 -59 29 24	EA	V0779 Car	10 57 23.3 -61 26 46	EA
V0726 Car	10 43 33.8 -59 18 28	SRB	V0780 Car	10 57 31.1 -61 27 22	EA
V0727 Car	10 44 10.2 -69 18 19	R	V0781 Car	10 57 42.4 -61 36 24	EA
V0728 Car	10 44 13.5 -59 36 40	SRB	V0782 Car	10 57 47.1 -62 19 16	M
V0729 Car	10 44 40.5 -60 03 33	SR:	V0783 Car	10 57 51.9 -61 43 59	EA
V0730 Car	10 44 57.3 -59 56 06	SRC:	V0784 Car	10 57 54.3 -61 42 03	EA
V0731 Car	10 45 12.7 -59 44 46	EA	V0785 Car	10 58 01.9 -61 49 51	EA
V0732 Car	10 46 16.0 -58 25 21	SR	V0786 Car	10 58 03.0 -61 34 26	EA
V0733 Car	10 46 38.8 -59 23 46	EA	V0787 Car	10 58 19.2 -61 29 28	EA
V0734 Car	10 47 27.8 -59 37 47	EA	V0788 Car	10 58 41.8 -61 53 13	EA
V0735 Car	10 47 30.5 -59 11 38	ACV	V0789 Car	10 58 59.9 -61 34 44	EA
V0736 Car	10 47 38.9 -60 37 04	EA	V0790 Car	10 59 00.1 -61 37 42	EA
V0737 Car	10 48 00.4 -59 41 21	SR	V0791 Car	10 59 05.5 -60 31 49	M
V0738 Car	10 48 46.5 -60 35 40	EB	V0792 Car	10 59 22.1 -61 25 22	EA
V0739 Car	10 50 04.8 -61 51 33	EP:	V0793 Car	10 59 26.4 -61 36 50	EA
V0740 Car	10 50 20.5 -61 28 35	EA	V0794 Car	10 59 35.4 -61 57 00	EA
V0741 Car	10 50 24.7 -61 26 12	EA	V0795 Car	10 59 39.2 -61 24 08	EA
V0742 Car	10 50 34.6 -61 57 26	EP	V0796 Car	10 59 41.5 -61 55 16	EA
V0743 Car	10 50 36.3 -61 40 37	EA	V0797 Car	10 59 41.9 -61 32 35	EA
V0744 Car	10 50 41.4 -59 12 46	EB	V0798 Car	10 59 49.5 -61 52 08	EA
V0745 Car	10 50 51.0 -61 34 56	EA	V0799 Car	11 00 34.7 -62 04 10	EA
V0746 Car	10 51 09.2 -61 43 12	EA	V0800 Car	11 01 13.8 -61 44 22	EP:
V0747 Car	10 51 23.4 -61 47 22	EA	V0801 Car	11 01 52.0 -61 58 02	EP:
V0748 Car	10 51 40.4 -61 34 16	EA	V0802 Car	11 02 04.3 -62 09 43	SRD
V0749 Car	10 51 58.6 -61 41 21	EA	V0803 Car	11 02 43.7 -61 37 47	EA
V0750 Car	10 52 20.7 -61 29 46	EA	V0804 Car	11 03 00.7 -61 33 27	M
V0751 Car	10 52 24.0 -61 31 09	EA	V0805 Car	11 04 23.7 -61 43 11	EP:
V0752 Car	10 52 24.4 -61 26 49	EP	V0806 Car	11 04 38.7 -74 01 09	E:
V0753 Car	10 52 28.3 -61 29 32	EA	V0807 Car	11 05 12.2 -61 14 01	EA
V0754 Car	10 52 46.4 -61 23 18	EA	V0808 Car	11 05 23.0 -73 18 57	SR
V0755 Car	10 52 55.4 -60 52 10	M	V0809 Car	11 05 33.5 -61 08 46	EA
V0756 Car	10 52 56.8 -61 50 55	EA	V0810 Car	11 05 48.8 -60 54 51	EA
V0757 Car	10 52 58.5 -61 51 44	EA	V0811 Car	11 05 58.9 -61 10 09	EA
V0758 Car	10 53 12.4 -61 30 19	EA	V0812 Car	11 06 06.3 -60 56 20	EA
V0759 Car	10 53 17.8 -61 24 21	EP	V0813 Car	11 06 10.6 -61 14 53	EA

Table 1 (continued)

Name	R.A., Decl., 2000.0 h m s o ' "	Type	Name	R.A., Decl., 2000.0 h m s o ' "	Type
V0814 Car	11 06 37.8 -61 19 16	EA	V1247 Cen	11 55 21.5 -62 03 56	EA
V0815 Car	11 06 49.6 -61 30 24	I:	V1248 Cen	11 55 29.4 -64 07 25	M:
V0816 Car	11 06 51.1 -61 11 10	EA	V1249 Cen	12 15 30.7 -39 48 43	BY
V0817 Car	11 06 51.9 -60 51 46	EA	V1250 Cen	12 34 20.5 -48 15 20	IT
V0818 Car	11 06 52.6 -61 14 17	EP:	V1251 Cen	12 34 20.6 -48 15 14	IT
V0819 Car	11 07 04.1 -60 54 21	EA	V1252 Cen	12 35 04.3 -41 36 39	IT
V0820 Car	11 07 50.8 -61 05 40	EA	V1253 Cen	12 38 03.8 -38 31 25	CEP
V0821 Car	11 07 53.4 -61 04 18	EA	V1254 Cen	12 44 52.7 -42 44 14	EW
V0822 Car	11 07 54.2 -73 57 57	E:	V1255 Cen	12 47 37.1 -39 32 42	RRAB
V0823 Car	11 08 29.5 -61 19 13	NC:	V1256 Cen	12 48 51.2 -48 17 08	M
V0824 Car	11 08 37.1 -61 20 17	EA	V1257 Cen	12 50 51.4 -51 56 35	RS
V0825 Car	11 08 37.2 -61 10 46	EA	V1258 Cen	13 00 29.0 -30 52 57	EA+UG
V0826 Car	11 08 41.0 -61 07 59	EA	V1259 Cen	13 02 20.3 -63 28 24	BCEP
V0827 Car	11 08 57.8 -60 52 59	EA	V1260 Cen	13 02 36.1 -59 56 01	EA
V0828 Car	11 08 57.9 -61 01 30	EP:	V1261 Cen	13 06 57.2 -49 54 27	BY:
V0829 Car	11 09 49.4 -60 28 10	EA	V1262 Cen	13 07 40.7 -37 29 34	EW
V0830 Car	11 12 36.4 -58 38 38	BCEP:	V1263 Cen	13 08 07.3 -32 54 13	EB
V0831 Car	11 15 14.5 -60 09 53	EA:	V1264 Cen	13 10 18.4 -45 09 14	EA+DSCT
V0832 Car	11 16 38.9 -65 50 56	M	V1265 Cen	13 10 55.2 -48 44 04	RS
V0833 Car	11 17 43.0 -57 59 30	ELL:	V1266 Cen	13 12 34.3 -60 33 39	EB
V1180 Cas	02 33 01.5 +72 43 27	INT	V1267 Cen	13 20 45.4 -46 11 38	IT
V1214 Cen	11 06 14.8 -42 24 32	EB+DSCTC	V1268 Cen	13 21 37.2 -44 21 52	IT
V1215 Cen	11 13 26.2 -45 23 43	IT	V1269 Cen	13 28 11.3 -33 23 47	EW
V1216 Cen	11 14 35.5 -55 30 08	EA	V1270 Cen	13 30 26.2 -64 10 10	EP:
V1217 Cen	11 21 05.5 -38 45 16	IT	V1271 Cen	13 30 28.2 -38 12 30	CWA:
V1218 Cen	11 22 17.5 -62 38 30	EA	V1272 Cen	13 30 42.9 -63 57 31	EA
V1219 Cen	11 23 25.9 -62 38 42	EA	V1273 Cen	13 30 55.7 -63 58 39	EA
V1220 Cen	11 30 45.0 -60 43 59	EA	V1274 Cen	13 30 58.5 -64 11 54	EA
V1221 Cen	11 31 04.5 -41 07 03	RRAB	V1275 Cen	13 31 01.0 -63 58 36	EP:
V1222 Cen	11 31 31.6 -60 36 53	EA	V1276 Cen	13 31 31.5 -64 10 52	EA
V1223 Cen	11 32 18.8 -61 20 34	M	V1277 Cen	13 31 54.4 -64 02 40	EA
V1224 Cen	11 32 21.8 -60 50 46	EP:	V1278 Cen	13 32 12.0 -64 32 57	EA
V1225 Cen	11 32 29.9 -60 58 26	EA	V1279 Cen	13 32 23.8 -64 10 35	EA
V1226 Cen	11 32 30.4 -60 38 42	EA	V1280 Cen	13 32 52.5 -63 57 45	EA
V1227 Cen	11 33 04.3 -60 34 05	EA	V1281 Cen	13 33 25.9 -64 16 39	EA
V1228 Cen	11 33 18.0 -63 06 16	BCEP	V1282 Cen	13 33 38.0 -64 05 24	EP:
V1229 Cen	11 33 33.9 -63 53 45	EB	V1283 Cen	13 33 54.7 -64 09 44	EA
V1230 Cen	11 34 03.8 -60 54 14	EA	V1284 Cen	13 33 56.9 -31 53 21	EW
V1231 Cen	11 34 05.5 -60 39 39	EP:	V1285 Cen	13 34 22.8 -64 07 18	EA
V1232 Cen	11 34 45.0 -38 25 49	SXPHE:	V1286 Cen	13 35 01.7 -42 19 43	EB
V1233 Cen	11 34 52.8 -60 52 36	EA	V1287 Cen	13 37 41.1 -58 23 10	M
V1234 Cen	11 35 40.4 -50 28 33	M	V1288 Cen	13 47 52.6 -31 04 01	RRAB
V1235 Cen	11 36 16.7 -60 29 18	M:	V1289 Cen	13 49 09.2 -47 46 34	EA
V1236 Cen	11 46 13.0 -57 04 05	LB	V1290 Cen	13 49 30.0 -31 14 30	SRB
V1237 Cen	11 46 33.6 -62 17 56	EW	V1291 Cen	13 51 53.6 -37 36 24	M
V1238 Cen	11 48 23.7 -37 28 49	IT	V1292 Cen	13 54 34.5 -64 03 23	M
V1239 Cen	11 48 24.2 -37 28 49	IT	V1293 Cen	13 54 52.2 -39 18 30	M
V1240 Cen	11 48 48.3 -63 37 27	M	V1294 Cen	13 55 41.8 -44 38 57	EA/RS
V1241 Cen	11 49 21.3 -60 07 05	M	V1295 Cen	13 55 54.8 -41 31 32	M
V1242 Cen	11 50 47.3 -55 55 06	EA	V1296 Cen	13 56 42.9 -42 24 17	EW
V1243 Cen	11 51 00.8 -49 06 09	M	V1297 Cen	13 56 45.5 -62 36 03	M
V1244 Cen	11 52 55.7 -62 16 54	EA	V1298 Cen	13 56 58.4 -63 13 57	EB
V1245 Cen	11 53 30.7 -61 03 33	M	V1299 Cen	13 57 09.7 -62 56 54	M
V1246 Cen	11 54 05.5 -62 04 39	EA	V1300 Cen	13 58 09.5 -63 13 15	M

Table 1 (continued)

Name	R.A., Decl., 2000.0	Type	Name	R.A., Decl., 2000.0	Type
	h m s o ' "			h m s o ' "	
V1301 Cen	13 58 11.0 -63 25 13	M	V1355 Cen	14 37 34.1 -34 49 27	M
V1302 Cen	13 58 17.1 -56 21 11	SRB	V1356 Cen	14 37 36.9 -61 08 48	EA
V1303 Cen	13 58 35.5 -63 24 56	M:	V1357 Cen	14 38 15.8 -64 07 52	M
V1304 Cen	13 58 56.8 -40 53 50	RRAB	V1358 Cen	14 38 22.3 -30 27 54	M
V1305 Cen	13 59 15.8 -63 09 45	M	V1359 Cen	14 39 04.9 -58 55 30	M
V1306 Cen	13 59 25.6 -62 54 24	M	V1360 Cen	14 39 29.8 -33 51 27	RRC
V1307 Cen	14 00 03.5 -59 37 45	SR:	V1361 Cen	14 40 39.4 -31 59 20	RRAB
V1308 Cen	14 00 09.6 -62 37 14	M	V1362 Cen	14 40 47.4 -37 25 17	EW
V1309 Cen	14 00 20.7 -59 31 08	M:	V1363 Cen	14 41 08.0 -61 18 54	M
V1310 Cen	14 00 27.7 -59 30 15	LB:	V1364 Cen	14 41 11.5 -62 48 33	M:
V1311 Cen	14 00 33.5 -38 41 07	SRB	V1365 Cen	14 48 21.4 -42 15 43	SRB
V1312 Cen	14 00 47.3 -59 36 39	EA	V1366 Cen	14 57 44.9 -30 26 39	RRAB
V1313 Cen	14 00 47.9 -59 38 24	EW	V1367 Cen	14 58 03.6 -35 49 05	RRAB:
V1314 Cen	14 00 48.7 -59 32 15	EA	GM Cha	11 09 28.6 -76 33 28	INT
V1315 Cen	14 00 53.5 -59 33 37	EW	GN Cha	09 30 06.1 -80 01 14	SRB
V1316 Cen	14 00 56.8 -59 33 23	EA	GO Cha	09 33 10.4 -80 28 34	EW
V1317 Cen	14 00 59.2 -59 35 42	EA	GP Cha	09 53 57.6 -76 36 52	RVB
V1318 Cen	14 01 03.7 -59 31 17	EW	GQ Cha	10 04 52.5 -79 28 05	EA
V1319 Cen	14 01 04.5 -59 32 56	EA	GR Cha	11 03 47.6 -77 19 56	INT
V1320 Cen	14 01 04.9 -59 30 54	EW	GS Cha	11 04 15.1 -76 06 38	INB
V1321 Cen	14 01 08.7 -59 28 02	EW	GT Cha	11 04 29.5 -76 56 19	E:
V1322 Cen	14 01 11.8 -59 27 30	EW	GU Cha	11 04 57.0 -77 15 57	INT
V1323 Cen	14 01 14.0 -59 39 09	SR:	GV Cha	11 05 19.4 -76 08 26	E:
V1324 Cen	14 01 20.7 -59 31 31	SR:	GW Cha	11 06 37.9 -79 10 11	E:
V1325 Cen	14 01 32.8 -59 37 37	EA	GX Cha	11 06 41.8 -76 35 49	INT
V1326 Cen	14 01 33.0 -59 32 46	EW	GY Cha	11 07 11.2 -76 19 47	E:
V1327 Cen	14 02 22.9 -60 37 37	SRB	GZ Cha	11 07 16.2 -77 23 07	INB
V1328 Cen	14 04 04.8 -61 01 50	M	HH Cha	11 07 29.9 -77 25 02	E:
V1329 Cen	14 04 32.8 -48 54 18	M	HI Cha	11 07 35.2 -77 34 49	INT
V1330 Cen	14 04 32.9 -59 41 22	M	HK Cha	11 07 42.5 -77 33 59	INT
V1331 Cen	14 04 33.9 -45 32 32	CWA	HL Cha	11 07 52.3 -77 36 57	INT
V1332 Cen	14 05 56.0 -52 05 29	SRB	HM Cha	11 07 57.3 -77 17 26	INT
V1333 Cen	14 05 59.9 -62 04 23	LB	HN Cha	11 07 58.1 -77 42 41	INT
V1334 Cen	14 06 37.1 -43 33 45	SRA	HO Cha	11 08 03.0 -77 38 43	INT
V1335 Cen	14 07 01.2 -42 33 01	RS	HP Cha	11 08 15.2 -77 33 53	INT
V1336 Cen	14 07 19.7 -48 10 20	M	HQ Cha	11 08 39.5 -77 34 17	INT
V1337 Cen	14 08 39.7 -49 35 13	M	HR Cha	11 08 54.2 -77 32 12	INT
V1338 Cen	14 08 58.5 -46 36 43	DSCT	HS Cha	11 08 55.0 -76 32 41	INT
V1339 Cen	14 10 08.5 -38 27 51	M	HT Cha	11 09 07.9 -76 49 11	ISB:
V1340 Cen	14 10 21.5 -61 52 07	SRB	HU Cha	11 09 18.1 -76 30 29	INT
V1341 Cen	14 19 09.8 -56 59 41	SRA	HV Cha	11 09 22.7 -76 34 32	INT
V1342 Cen	14 19 42.1 -30 28 05	RRAB	HW Cha	11 09 41.9 -76 34 58	INB
V1343 Cen	14 21 08.1 -37 04 16	RRC	HX Cha	11 09 54.1 -76 29 25	INT
V1344 Cen	14 23 30.4 -57 53 04	RRAB	HY Cha	11 09 54.4 -76 31 11	INT
V1345 Cen	14 23 45.7 -58 29 25	RRAB	HZ Cha	11 09 55.1 -76 32 41	INB
V1346 Cen	14 23 48.3 -57 44 01	M	II Cha	11 10 03.8 -75 53 40	E:
V1347 Cen	14 25 24.1 -30 13 16	EA	IK Cha	11 10 53.6 -77 25 00	INT
V1348 Cen	14 25 50.1 -32 24 28	RRAB	IL Cha	11 11 34.8 -76 36 21	INT
V1349 Cen	14 26 28.1 -60 02 11	SRB	IM Cha	11 12 03.5 -77 26 01	INT
V1350 Cen	14 27 05.3 -58 19 18	LB	IN Cha	11 12 09.8 -76 34 37	INT
V1351 Cen	14 28 33.6 -32 08 26	EW	IO Cha	11 13 33.6 -76 35 37	INT
V1352 Cen	14 29 02.8 -38 54 23	SRB	IP Cha	11 14 07.8 -76 36 09	E:
V1353 Cen	14 30 25.3 -36 04 35	RRAB	IQ Cha	11 15 08.0 -79 01 21	SR:
V1354 Cen	14 32 54.5 -31 13 10	RRC	IR Cha	12 32 15.9 -77 17 23	LB

Table 1 (continued)

Name	R.A., Decl., 2000.0	Type	Name	R.A., Decl., 2000.0	Type
	h m s o ' "			h m s o ' "	
IS Cha	12 43 38.3 -77 46 14	EA	OO Com	13 15 19.7 +19 30 24	RRAB
IT Cha	13 53 03.8 -80 01 09	EW	OP Com	13 18 12.5 +17 22 02	RRAB
DN Cir	13 51 29.2 -65 46 56	M	OQ Com	13 18 41.9 +17 45 24	RRAB
DO Cir	13 52 03.6 -67 30 56	M	OR Com	13 19 54.5 +19 53 57	RRAB
DP Cir	13 56 59.5 -70 35 17	M	OS Com	13 20 32.7 +19 09 22	RRC
DQ Cir	14 06 00.1 -68 44 12	M	OT Com	13 21 17.6 +21 01 25	BY
DR Cir	14 13 15.7 -65 12 57	M:	OU Com	13 21 18.4 +18 08 22	SXPHE
DS Cir	14 18 56.4 -69 14 27	SRB	OV Com	13 22 00.1 +18 27 09	RRAB
DT Cir	14 23 15.1 -65 33 31	M:	OW Com	13 24 12.8 +17 02 18	EW
DU Cir	14 24 36.7 -65 37 50	M	OX Com	13 24 48.6 +17 41 10	EW
DV Cir	14 38 48.7 -68 48 49	M	OY Com	13 28 10.4 +19 38 17	LB:
DW Cir	14 38 56.0 -69 22 32	M:	OZ Com	13 29 09.3 +18 00 17	RRAB
DX Cir	14 40 43.7 -64 53 07	M:	PP Com	13 31 00.9 +26 23 25	DSCTC
DY Cir	14 43 13.8 -57 08 45	M	PQ Com	13 31 53.6 +15 41 18	R
DZ Cir	14 44 26.3 -63 33 28	M	PR Com	13 32 04.6 +18 31 03	RRAB
EE Cir	14 45 48.6 -63 45 51	M	AX CrB	15 19 40.1 +31 50 33	BY
EF Cir	14 46 10.9 -56 52 09	M:	AY CrB	15 22 35.8 +31 08 03	EW
EG Cir	14 47 16.1 -64 14 02	M:	AZ CrB	15 25 02.7 +29 43 35	SRB
EH Cir	14 48 04.2 -57 20 37	M	BB CrB	15 25 54.3 +27 52 18	RRAB
EI Cir	14 49 16.9 -66 39 23	M	BC CrB	15 30 39.4 +30 12 25	RS
EK Cir	14 49 37.5 -67 06 19	M	BD CrB	15 31 22.4 +35 52 54	EW
EL Cir	14 49 41.0 -67 48 12	M	BE CrB	15 33 52.7 +31 18 01	BY
EM Cir	14 50 21.5 -67 38 24	M	BF CrB	15 34 06.0 +33 49 48	RRAB
EN Cir	14 51 52.0 -68 55 12	M	BG CrB	15 34 40.6 +26 54 43	RS
EO Cir	14 53 10.7 -64 00 34	M	BH CrB	15 35 11.3 +38 43 59	BY
EP Cir	14 54 16.2 -64 44 07	M	BI CrB	15 36 33.4 +27 10 29	RS:
EQ Cir	14 55 58.1 -65 55 52	SRA	BK CrB	15 36 50.3 +37 34 49	BY
ER Cir	14 59 02.2 -65 44 45	M	BL CrB	15 37 04.1 +37 48 28	BY
ES Cir	15 00 12.9 -62 54 03	DSCT	BM CrB	15 41 04.7 +36 02 53	XM
ET Cir	15 01 25.4 -65 44 24	M	BN CrB	15 43 11.0 +36 53 30	RRAB
EU Cir	15 03 56.6 -64 13 43	M	BO CrB	15 46 05.4 +37 49 46	UV
EV Cir	15 05 46.5 -58 22 55	DCEP	BP CrB	15 49 00.2 +35 15 59	RRAB
EW Cir	15 10 28.1 -63 54 23	RRAB	BQ CrB	15 52 22.7 +34 01 28	LB
EX Cir	15 12 14.6 -57 13 28	M	BR CrB	15 53 04.3 +36 18 45	EW
EY Cir	15 13 35.3 -63 53 34	SRB	BS CrB	15 54 31.4 +29 56 52	EW:
BE Col	06 04 02.4 -31 43 41	EA	BT CrB	15 56 57.0 +35 23 37	EA
MV Com	12 03 15.6 +16 06 38	BY	BU CrB	15 58 42.1 +32 30 46	BY
MW Com	12 19 11.6 +29 12 01	EA/RS	XX Crv	12 25 09.5 -21 39 52	RR(B)
MX Com	12 23 54.9 +22 45 46	EB	XY Crv	12 28 01.2 -23 28 27	RR(B)
MY Com	12 30 13.7 +21 58 11	BY	XZ Crv	12 31 21.9 -19 00 04	RRAB
MZ Com	12 32 40.7 +23 48 05	EA/RS	YY Crv	12 44 16.3 -12 03 07	RRAB
NN Com	12 35 31.9 +14 19 34	EW	AG Crt	11 03 30.1 -10 59 14	RRC
NO Com	12 41 07.8 +30 26 14	EA	AH Crt	11 25 01.4 -10 16 08	RRAB
NP Com	12 48 48.3 +14 45 30	RS	AI Crt	11 26 13.8 -14 04 08	RRAB
NQ Com	12 51 47.2 +22 32 39	BY	AK Crt	11 27 33.2 -24 50 08	EA+DSCTC
NR Com	12 55 32.9 +30 11 11	BY	AL Crt	11 29 37.2 -15 42 10	RRAB
NS Com	12 56 42.6 +23 09 07	EW	AM Crt	11 33 24.6 -10 36 59	M
NT Com	13 03 46.0 +28 37 21	RS	AN Crt	11 41 06.8 -10 37 07	RRAB
NU Com	13 10 08.4 +24 36 01	SRB	AO Crt	11 53 02.0 -23 12 59	CWA
NV Com	13 12 28.3 +25 14 27	EW:	AP Crt	11 56 05.0 -09 20 39	RRAB
NW Com	13 12 47.4 +26 52 52	DSCTC+GDOR	EU Cru	11 58 07.8 -64 14 44	M
NX Com	13 13 08.0 +29 40 52	BY	EV Cru	12 04 10.0 -62 42 26	SR
NY Com	13 14 34.5 +20 30 25	RRAB	EW Cru	12 10 35.8 -63 15 02	EA
NZ Com	13 15 04.5 +19 42 53	RRC	EX Cru	12 12 43.5 -61 39 01	LB

Table 1 (continued)

Name	R.A., Decl., 2000.0	Type	Name	R.A., Decl., 2000.0	Type
	h m s o ' "			h m s o ' "	
EY Cru	12 22 10.2 -60 24 15	M	V0335 Dra	15 40 40.7 +60 48 24	RRAB
EZ Cru	12 31 47.7 -56 09 40	SRB	V0336 Dra	15 45 10.3 +56 21 58	RRC
FF Cru	12 32 40.9 -58 11 29	M	V0337 Dra	15 47 18.5 +63 11 00	BY
FG Cru	12 37 47.7 -62 19 23	BCEP	V0338 Dra	15 49 11.1 +60 38 03	EW
FH Cru	12 38 22.0 -63 54 20	EA:	V0339 Dra	15 49 57.1 +55 21 42	EW
FI Cru	12 44 34.8 -63 31 46	RS	V0340 Dra	15 50 41.5 +62 26 50	SR
FK Cru	12 45 06.8 -62 33 38	M	V0341 Dra	15 52 57.7 +68 43 30	EA
FL Cru	12 53 18.7 -64 01 24	BCEP	V0342 Dra	15 53 02.4 +55 04 32	EW
V2492 Cyg	20 51 26.2 +44 05 24	INT	V0343 Dra	15 53 11.0 +54 09 07	EA
V2493 Cyg	20 58 17.0 +43 53 43	FU	V0344 Dra	15 57 09.1 +58 10 01	EW
V2494 Cyg	20 58 21.1 +52 29 28	FU	V0391 Gem	06 03 58.4 +22 28 33	BY
V2495 Cyg	21 00 25.2 +52 30 16	FU	V0392 Gem	06 08 13.2 +24 18 31	DSCT
BF Dor	06 05 54.5 -66 50 37	EW:	V0393 Gem	06 09 03.3 +24 23 15	E
NS Dra	09 42 54.7 +78 56 54	EA	V0394 Gem	06 14 19.7 +27 44 23	SR:
NT Dra	09 43 42.9 +77 26 50	EA	V0395 Gem	06 16 34.0 +25 17 41	SR:
NU Dra	10 15 36.6 +76 41 54	EA	V0396 Gem	06 20 00.7 +26 20 59	EA
NV Dra	10 41 01.5 +74 40 58	EA	V0397 Gem	06 22 44.3 +18 31 53	RRC
NW Dra	11 32 05.9 +69 57 42	EA	V0398 Gem	06 24 03.1 +22 53 36	BY
NX Dra	11 34 07.9 +75 16 43	EW	V0399 Gem	06 30 18.0 +25 43 43	EA
NY Dra	11 35 10.4 +75 05 47	SR	V0400 Gem	06 37 36.0 +17 47 33	EA
NZ Dra	11 38 50.4 +75 31 43	RRAB	V0401 Gem	06 40 16.1 +20 28 44	EA
OO Dra	11 40 01.4 +75 09 21	EA+DSCTC	V0402 Gem	06 42 17.4 +20 16 48	EW
OP Dra	11 40 42.7 +75 36 15	EB	V0403 Gem	06 44 01.1 +22 44 32	DSCT
OQ Dra	11 49 25.9 +72 34 01	EW	V0404 Gem	06 47 02.8 +15 37 23	EW
OR Dra	12 00 37.5 +69 11 08	DSCT	V0405 Gem	06 47 07.9 +15 38 37	EW
OS Dra	12 12 30.4 +65 30 23	RRAB	V0406 Gem	06 47 15.6 +14 34 39	RS
OT Dra	12 25 04.5 +66 38 40	RRAB	V0407 Gem	06 48 38.7 +16 24 47	RS:
OU Dra	12 47 19.5 +69 05 54	RRAB	V0408 Gem	06 50 07.3 +16 30 25	EA
OV Dra	12 50 23.9 +66 55 25	EA	V0409 Gem	06 53 23.5 +19 10 24	EB:
OW Dra	13 03 31.1 +71 06 44	RRC	V0410 Gem	06 54 08.1 +17 02 03	EA
OX Dra	13 07 27.5 +69 10 19	EA	V0411 Gem	06 54 32.6 +13 33 42	EW
OY Dra	13 08 41.8 +65 40 00	RRC	V0412 Gem	06 54 46.0 +13 35 31	EW
OZ Dra	13 27 23.4 +65 28 54	EA+NL	V0413 Gem	06 54 47.7 +13 36 49	EW
PP Dra	13 40 17.5 +65 00 48	RRAB	V0414 Gem	06 54 54.3 +18 12 50	EB
PQ Dra	14 30 33.9 +55 33 14	EB	V0415 Gem	06 55 57.5 +15 35 33	EW
PR Dra	14 35 10.6 +59 30 35	EW	V0416 Gem	06 59 47.3 +22 29 49	EW
PS Dra	14 48 03.4 +62 44 42	EW	V0417 Gem	06 59 48.4 +27 41 59	EW:
PT Dra	14 59 09.3 +55 08 48	EW	V0418 Gem	07 04 08.7 +26 25 10	XM
PU Dra	15 00 38.6 +57 46 30	EA	V0419 Gem	07 05 48.0 +15 38 32	SRB
PV Dra	15 06 27.7 +60 18 21	EA	V0420 Gem	07 08 18.6 +31 05 08	BY
PW Dra	15 07 28.6 +58 06 47	SRD	V0421 Gem	07 12 07.3 +25 57 50	EB:
PX Dra	15 07 50.2 +63 07 02	EA	V0422 Gem	07 12 41.7 +16 05 05	EA
PY Dra	15 11 49.3 +58 37 01	RRC	V0423 Gem	07 13 41.1 +27 31 04	BY
PZ Dra	15 12 12.5 +56 45 10	EB	V0424 Gem	07 16 50.4 +21 45 00	RS
QQ Dra	15 16 46.7 +61 44 56	RRAB	V0425 Gem	07 18 32.9 +14 59 44	EA
QR Dra	15 19 04.0 +62 30 48	SRA	V0426 Gem	07 19 25.5 +22 58 00	RRAB
QS Dra	15 21 34.7 +61 29 23	DSCT	V0427 Gem	07 21 34.4 +15 18 43	RRAB
QT Dra	15 24 15.1 +53 07 53	RS	V0428 Gem	07 23 25.7 +26 07 32	EB
QU Dra	15 25 23.4 +56 45 49	EW	V0429 Gem	07 23 43.6 +20 24 59	BY
QV Dra	15 26 11.7 +54 22 59	RRC	V0430 Gem	07 38 59.3 +23 50 38	E:
QW Dra	15 28 36.1 +64 42 45	RRAB	V0431 Gem	07 39 24.7 +23 56 25	EW:
QX Dra	15 36 04.5 +58 23 45	RRAB	V0432 Gem	07 40 16.7 +23 37 53	DSCT:
QY Dra	15 36 22.6 +57 50 54	BY:	V0433 Gem	07 40 17.1 +23 40 09	EP:
QZ Dra	15 39 43.4 +56 55 49	SR	V0434 Gem	07 48 13.4 +29 05 13	NL

Table 1 (continued)

Name	R.A., Decl., 2000.0	Type	Name	R.A., Decl., 2000.0	Type
	h m s o ' "			h m s o ' "	
V0435 Gem	07 54 57.7 +21 54 09	EW	V0508 Hya	08 54 40.1 -00 43 19	RRC:
V0436 Gem	07 56 24.6 +31 41 44	GDOR	V0509 Hya	08 58 42.4 -00 36 59	RRAB
V1137 Her	15 49 34.8 +49 50 12	EW	V0510 Hya	08 59 52.6 -00 06 01	RRAB
V1138 Her	15 50 09.3 +49 36 39	EW	V0511 Hya	09 00 47.0 -18 20 47	EA
V1139 Her	15 50 28.5 +45 57 52	SXPXE	V0512 Hya	09 01 15.4 -01 31 33	RRAB
V1140 Her	15 53 09.8 +46 52 06	EW	V0513 Hya	09 01 15.9 -00 58 01	RRAB
V1141 Her	15 54 58.5 +42 46 10	RRC	V0514 Hya	09 01 38.2 -02 11 58	EW
V1142 Her	15 56 00.6 +49 47 56	RRC	V0515 Hya	09 08 38.9 -00 38 49	RRC
V1143 Her	15 56 57.0 +50 54 06	EA	V0516 Hya	09 11 37.6 +04 02 30	RRAB:
V1144 Her	15 56 57.5 +42 13 37	EW	V0517 Hya	09 11 39.2 -00 39 05	RRAB
V1145 Her	15 57 49.6 +41 23 20	RS	V0518 Hya	09 11 47.5 -01 18 58	RRAB
V1146 Her	15 58 18.7 +48 14 48	EA	V0519 Hya	09 13 22.9 +04 32 36	EW
V0466 Hya	08 12 01.8 -00 33 00	EB	V0520 Hya	09 13 53.7 -01 20 02	RRC
V0467 Hya	08 12 52.1 -01 49 28	RRAB	V0521 Hya	09 16 05.5 -23 39 20	M
V0468 Hya	08 13 01.3 +01 19 41	RRC	V0522 Hya	09 18 15.3 -01 12 39	RRC
V0469 Hya	08 13 02.5 -02 14 21	RRC:	V0523 Hya	09 19 44.9 -00 01 57	RRAB
V0470 Hya	08 14 01.1 +00 22 56	EW	V0524 Hya	09 20 09.6 +00 42 46	EA
V0471 Hya	08 14 51.5 -00 04 50	RRAB	V0525 Hya	09 23 00.3 -00 40 31	RRAB
V0472 Hya	08 15 39.9 -00 56 41	EB	V0526 Hya	09 24 21.8 -02 11 55	RRAB
V0473 Hya	08 17 10.2 -00 38 45	RRC	V0527 Hya	09 24 55.9 -13 11 59	RRAB
V0474 Hya	08 18 43.5 +00 28 51	EB	V0528 Hya	09 26 44.4 -00 53 49	RRAB
V0475 Hya	08 19 20.2 +01 17 59	EW	V0529 Hya	09 27 01.7 -00 09 34	RRAB
V0476 Hya	08 20 59.9 +00 31 02	EW	V0530 Hya	09 29 07.3 +01 27 25	RRAB
V0477 Hya	08 22 02.5 -01 35 19	EW:	V0531 Hya	09 33 10.4 -00 06 13	RRAB
V0478 Hya	08 22 50.0 +01 51 34	BY	V0532 Hya	09 34 14.4 -01 34 48	RRAB
V0479 Hya	08 23 59.3 -00 05 26	RRAB	V0533 Hya	09 35 19.3 -01 30 42	RRC
V0480 Hya	08 25 13.8 -01 28 43	RRC	V0534 Hya	09 36 00.4 -01 28 27	RRAB
V0481 Hya	08 25 45.6 -01 54 34	RRAB	V0535 Hya	09 36 57.7 -13 37 12	RRAB
V0482 Hya	08 27 39.0 -02 00 34	RRC:	V0536 Hya	09 37 06.8 -00 04 25	RRAB
V0483 Hya	08 28 19.1 -10 42 28	EW	V0537 Hya	09 39 01.7 -01 00 35	RRAB
V0484 Hya	08 28 34.2 -13 09 20	*	V0538 Hya	09 39 26.0 -00 04 06	RRAB
V0485 Hya	08 29 41.9 -01 59 39	RRC	V0539 Hya	09 39 49.8 -01 22 37	RRAB
V0486 Hya	08 30 29.8 -02 42 37	RRAB	V0540 Hya	09 56 10.8 -17 00 08	RRAB
V0487 Hya	08 32 57.0 +02 59 03	RRAB	V0541 Hya	10 00 41.8 -11 51 35	RPHS
V0488 Hya	08 35 42.6 -08 19 24	*	V0542 Hya	10 20 13.6 -13 51 37	EW
V0489 Hya	08 36 11.0 -00 45 54	RRAB	V0543 Hya	10 26 08.4 -23 15 14	RRAB
V0490 Hya	08 39 23.5 -09 34 40	EA	V0544 Hya	10 33 21.0 -20 27 16	RRAB
V0491 Hya	08 39 55.4 -00 03 50	RRC:	V0545 Hya	10 35 12.8 -12 06 31	EW+EW
V0492 Hya	08 40 53.9 -05 09 36	SR	V0546 Hya	10 44 06.8 -18 52 39	RRAB
V0493 Hya	08 43 34.2 -17 27 12	RRAB	V0547 Hya	11 21 17.2 -34 46 46	IT
V0494 Hya	08 43 42.3 -01 20 17	RRC:	V0548 Hya	11 21 17.5 -34 46 50	IT
V0495 Hya	08 44 00.1 +02 39 20	UG	V0549 Hya	11 32 41.2 -26 52 09	IT
V0496 Hya	08 44 33.8 -00 13 03	RRAB	V0550 Hya	11 32 41.2 -26 51 56	IT
V0497 Hya	08 45 13.9 -00 15 33	RRC	V0551 Hya	12 00 54.6 -27 24 45	RPHS
V0498 Hya	08 45 55.1 +03 39 29	UGSU	V0552 Hya	12 12 06.1 -26 12 48	RRAB
V0499 Hya	08 47 23.8 -00 25 33	RRC	V0553 Hya	12 26 17.8 -25 46 20	EW
V0500 Hya	08 47 46.9 -03 39 00	RR(B)	V0554 Hya	13 28 01.7 -27 29 48	EW
V0501 Hya	08 48 06.6 -01 27 02	RRAB	V0555 Hya	13 29 06.0 -30 07 47	EB
V0502 Hya	08 49 03.6 -11 21 02	EA	V0556 Hya	13 39 51.7 -26 52 17	RRAB
V0503 Hya	08 49 19.8 +05 52 30	RS	V0557 Hya	13 53 32.8 -29 05 42	M
V0504 Hya	08 49 46.2 -00 00 15	RRC:	V0558 Hya	14 10 07.0 -26 09 40	LB
V0505 Hya	08 50 04.7 -01 30 09	RRC:	V0559 Hya	14 13 45.5 -22 54 42	RRAB
V0506 Hya	08 50 23.3 -01 31 43	RRAB	V0560 Hya	14 19 39.3 -25 44 12	RRAB
V0507 Hya	08 50 42.1 -01 33 15	RRAB	V0561 Hya	14 37 39.3 -29 58 54	RRC

Table 1 (continued)

Name	R.A., Decl., 2000.0	Type	Name	R.A., Decl., 2000.0	Type
	h m s o ' "			h m s o ' "	
V0562 Hya	14 46 44.7 -26 45 13	M	AE LMi	10 27 02.2 +33 16 59	EA
V0563 Hya	15 01 12.8 -25 39 25	M	AF LMi	10 37 45.9 +32 20 42	EW
HT Leo	09 22 05.1 +07 00 02	RS	AG LMi	10 44 48.8 +33 21 12	EA
HU Leo	09 24 44.5 +08 01 51	EA+AM:	AH LMi	10 45 56.7 +26 29 59	RS
HV Leo	09 25 17.0 +18 37 55	RRAB	AI LMi	10 46 46.9 +37 17 30	BY:
HW Leo	09 43 28.8 +29 27 14	RRAB	AK LMi	10 53 05.0 +38 13 33	RS
HX Leo	09 43 54.6 +27 46 59	EA	BH Lep	06 05 02.0 -23 42 27	*
HY Leo	09 46 34.5 +13 50 58	XM	LV Lib	14 24 04.7 -11 24 54	RRAB
HZ Leo	09 49 01.2 +11 44 01	RRAB	LW Lib	14 32 20.8 -12 22 48	ZZO
II Leo	10 14 34.2 +06 33 26	RRAB	LX Lib	14 35 49.0 -23 36 29	M
IK Leo	10 21 46.4 +23 49 28	UGSU	LY Lib	14 37 29.1 -20 19 42	M
IL Leo	10 31 00.6 +20 28 34	XM	LZ Lib	14 40 01.1 -19 59 33	EW
IM Leo	10 33 53.0 +19 15 35	RRAB	MM Lib	14 48 00.0 -01 49 43	RRAB
IN Leo	10 39 59.0 +13 27 22	RS	MN Lib	14 49 22.0 -01 52 46	RRAB
IO Leo	10 43 02.6 +06 34 46	RRAB	MO Lib	14 50 21.3 -09 05 50	RRAB
IP Leo	10 55 44.7 -01 30 22	RRAB	MP Lib	14 51 07.9 -24 53 53	LB
IQ Leo	10 56 03.0 +20 40 40	EW	MQ Lib	14 52 54.8 -01 20 48	RRAB
IR Leo	10 56 09.6 -05 40 22	BY	MR Lib	14 53 15.4 -14 35 57	RRAB
IS Leo	10 56 13.2 -01 56 57	RRAB	MS Lib	14 53 33.0 -02 06 52	RRAB
IT Leo	10 56 45.2 -00 47 27	RRAB	MT Lib	14 54 16.5 -15 37 20	RRAB
IU Leo	10 57 56.3 +09 23 15	UG	MU Lib	14 56 37.9 -00 56 23	RRAB
IV Leo	10 58 12.6 -00 05 40	RRAB	MV Lib	14 57 19.7 -00 53 28	RRAB
IW Leo	10 59 20.1 +04 53 17	RS	MW Lib	14 57 20.0 -01 53 55	RRAB
IX Leo	10 59 26.1 -00 59 28	RRAB	MX Lib	14 57 27.0 -01 58 12	RRAB
IY Leo	11 00 53.3 -01 57 57	RRAB	MY Lib	14 58 22.0 -01 02 03	RRAB
IZ Leo	11 05 35.6 +15 38 11	RRAB	MZ Lib	14 58 35.3 -19 43 34	SRB
KK Leo	11 08 38.3 -00 05 14	RRAB	NN Lib	14 59 08.3 -02 42 26	RRAB
KL Leo	11 09 24.2 -00 45 13	RRAB	NO Lib	14 59 22.8 -02 14 42	RRAB
KM Leo	11 10 13.0 +18 28 12	BY	NP Lib	15 00 00.2 -14 17 05	DSCT
KN Leo	11 13 42.3 -02 19 23	RRC	NQ Lib	15 01 29.3 -00 54 33	RRAB
KO Leo	11 18 30.0 -00 45 52	RRC	NR Lib	15 02 07.3 -12 01 52	RS
KP Leo	11 19 00.2 -00 13 29	RRAB	NS Lib	15 02 20.6 -01 00 50	RRAB
KQ Leo	11 19 59.7 -00 38 32	RRAB	NT Lib	15 02 33.5 -02 14 08	RRAB
KR Leo	11 20 19.5 -02 18 36	RRAB	NU Lib	15 02 37.7 -27 50 32	M
KS Leo	11 20 57.5 -02 03 27	RRC	NV Lib	15 03 39.6 -09 51 31	RRAB
KT Leo	11 23 12.5 -00 48 42	RRC:	NW Lib	15 04 00.5 -02 51 05	LB
KU Leo	11 24 25.4 -00 09 20	RRAB	NX Lib	15 05 41.7 -01 39 33	RRAB
KV Leo	11 25 50.1 +03 51 36	GDOR:	NY Lib	15 07 01.8 -01 12 58	RRC
KW Leo	11 25 57.0 -00 09 42	RRAB	NZ Lib	15 07 33.2 -26 38 48	SRA
KX Leo	11 27 59.4 +13 21 51	RRC	OO Lib	15 07 46.0 -01 36 14	RRC
KY Leo	11 28 37.7 -00 01 12	RRAB	OP Lib	15 08 08.7 -02 14 16	RRAB
KZ Leo	11 30 49.3 -00 59 18	RRAB	OQ Lib	15 08 36.6 -28 25 39	SRB
LL Leo	11 30 53.6 +13 19 28	RRAB	OR Lib	15 09 08.8 -24 33 30	SR
LM Leo	11 31 49.7 -02 14 26	RRAB	OS Lib	15 09 27.8 -01 32 27	RRAB
LN Leo	11 32 18.9 +03 17 13	RRAB	OT Lib	15 09 55.1 -01 32 58	RRAB
LO Leo	11 35 22.8 -00 53 43	RRAB	OU Lib	15 10 08.9 -00 58 29	RRAB
LP Leo	11 36 39.8 -01 25 17	RRAB	OV Lib	15 10 50.0 -01 26 21	RRC
LQ Leo	11 48 39.2 +23 11 39	BY	OW Lib	15 11 01.1 -01 37 55	RRAB
YZ LMi	09 26 38.7 +36 24 02	EA	OX Lib	15 11 08.7 -01 00 15	RRAB
ZZ LMi	09 31 12.7 +38 02 31	RS	OY Lib	15 11 27.6 -01 59 00	RRAB
AA LMi	09 47 53.0 +33 17 02	DSCTC	OZ Lib	15 13 40.7 -22 46 35	SR
AB LMi	10 04 36.4 +31 52 49	RRAB	PP Lib	15 14 53.1 -21 09 58	SRB
AC LMi	10 19 47.3 +33 57 54	UG	PQ Lib	15 15 06.0 -10 28 30	RRAB
AD LMi	10 26 22.8 +37 45 13	RS	PR Lib	15 16 10.5 -04 31 15	LB

Table 1 (continued)

Name	R.A., Decl., 2000.0	Type	Name	R.A., Decl., 2000.0	Type
	h m s o ' "			h m s o ' "	
PS Lib	15 17 21.2 -19 00 59	BY	QR Lup	14 42 52.6 -50 28 19	M
PT Lib	15 19 16.6 -22 09 44	EW	QS Lup	14 43 03.7 -47 46 53	M
PU Lib	15 20 15.8 -25 37 44	LB	QT Lup	14 45 42.4 -44 36 44	EW
PV Lib	15 21 19.1 -13 12 44	RRAB	QU Lup	14 49 10.0 -44 24 17	EW
PW Lib	15 21 53.1 -12 06 46	RRAB	QV Lup	14 49 56.6 -43 28 12	EW
PX Lib	15 22 16.3 -26 52 26	BY:	QW Lup	14 51 07.5 -54 46 19	M
PY Lib	15 25 40.4 -14 06 56	SRB	QX Lup	14 51 45.3 -50 04 55	M
PZ Lib	15 26 27.5 -05 25 18	RRAB	QY Lup	14 55 34.9 -48 45 41	M
QQ Lib	15 28 26.6 -04 47 36	RS	QZ Lup	14 56 21.8 -44 54 07	EB
QR Lib	15 29 01.9 -23 20 39	RRC	V0335 Lup	14 56 38.2 -45 07 19	LB
QS Lib	15 29 50.4 -17 34 05	LB	V0336 Lup	14 57 52.8 -47 28 40	M
QT Lib	15 32 44.1 -14 14 55	SRB	V0337 Lup	15 01 09.8 -42 44 51	M
QU Lib	15 33 12.0 -17 58 22	RRAB	V0338 Lup	15 03 07.7 -41 20 24	M
QV Lib	15 33 41.4 -29 14 41	SRB	V0339 Lup	15 03 27.4 -47 56 04	RRAB
QW Lib	15 33 52.4 -29 54 15	SRB	V0340 Lup	15 03 58.3 -46 20 18	SRA
QX Lib	15 35 03.8 -28 09 05	RRAB	V0341 Lup	15 04 04.4 -41 08 07	M
QY Lib	15 35 07.6 -08 49 50	RS	V0342 Lup	15 04 17.8 -41 44 27	M
QZ Lib	15 36 15.9 -08 39 07	UGSU	V0343 Lup	15 04 27.6 -30 52 46	M
V0335 Lib	15 36 45.0 -24 07 50	SRB	V0344 Lup	15 04 35.7 -37 08 31	M
V0336 Lib	15 37 40.6 -15 25 33	RRC	V0345 Lup	15 05 01.5 -45 03 22	SRB
V0337 Lib	15 37 57.9 -10 19 54	RRC	V0346 Lup	15 05 22.2 -36 15 33	LB
V0338 Lib	15 39 12.1 -19 48 46	RVA	V0347 Lup	15 06 06.7 -41 20 43	M
V0339 Lib	15 39 30.8 -19 42 51	EW	V0348 Lup	15 06 22.8 -52 57 33	M
V0340 Lib	15 40 53.4 -22 19 05	LB	V0349 Lup	15 08 44.7 -52 41 07	M
V0341 Lib	15 41 29.8 -13 32 55	RRC	V0350 Lup	15 08 50.4 -52 14 27	M
V0342 Lib	15 43 37.2 -21 49 31	SRB	V0351 Lup	15 08 54.2 -41 27 54	M
V0343 Lib	15 44 34.3 -14 16 06	LB:	V0352 Lup	15 08 54.8 -48 10 05	M
V0344 Lib	15 44 47.4 -19 01 26	SRB	V0353 Lup	15 09 22.8 -42 55 11	EW
V0345 Lib	15 45 24.3 -19 42 06	RRAB	V0354 Lup	15 09 25.2 -36 58 55	SRB
V0346 Lib	15 47 16.5 -28 17 36	RRAB	V0355 Lup	15 10 26.2 -48 47 59	LB
V0347 Lib	15 47 30.8 -17 22 30	LB	V0356 Lup	15 10 27.7 -43 39 24	LB
V0348 Lib	15 49 01.6 -18 19 42	RRAB:	V0357 Lup	15 11 01.5 -40 52 28	M
V0349 Lib	15 49 28.7 -17 33 54	RRC	V0358 Lup	15 11 41.5 -48 19 59	M
V0350 Lib	15 50 06.1 -17 11 25	SR:	V0359 Lup	15 12 15.1 -31 10 47	M
V0351 Lib	15 50 59.4 -11 39 08	EW	V0360 Lup	15 14 50.9 -50 17 51	M
V0352 Lib	15 52 33.2 -18 03 09	LB	V0361 Lup	15 14 56.2 -42 47 25	M
V0353 Lib	15 54 14.1 -13 31 40	RRAB	V0362 Lup	15 15 15.5 -40 32 25	M
V0354 Lib	15 54 44.9 -07 52 05	RS	V0363 Lup	15 16 43.4 -42 28 13	EW
V0355 Lib	15 54 46.5 -15 16 02	SRB	V0364 Lup	15 17 06.5 -43 56 38	RRAB
V0356 Lib	15 55 06.7 -19 46 31	BY	V0365 Lup	15 18 44.5 -36 33 58	M
V0357 Lib	15 55 34.7 -15 23 56	RRAB	V0366 Lup	15 18 45.3 -39 13 53	M
V0358 Lib	15 55 42.5 -16 09 43	LB:	V0367 Lup	15 20 15.7 -49 04 01	M
V0359 Lib	15 58 14.8 -13 12 12	SRB	V0368 Lup	15 23 12.9 -32 26 42	RRAB
V0360 Lib	15 58 30.6 -10 39 49	RRC	V0369 Lup	15 24 13.4 -42 56 30	SRA
PR Lup	14 54 23.1 -55 05 11	NA	V0370 Lup	15 24 20.8 -42 39 31	M:
PS Lup	14 20 08.4 -52 30 39	RRAB	V0371 Lup	15 24 54.6 -50 55 11	M
PT Lup	14 25 14.8 -48 02 48	M	V0372 Lup	15 25 47.6 -36 13 54	M
PU Lup	14 25 58.4 -48 46 47	M	V0373 Lup	15 27 23.2 -35 20 35	M
PV Lup	14 27 35.0 -47 37 09	M	V0374 Lup	15 27 56.8 -48 15 16	M
PW Lup	14 39 43.2 -49 39 51	RRAB	V0375 Lup	15 28 32.9 -30 51 50	CWB:
PX Lup	14 40 17.7 -48 32 37	M	V0376 Lup	15 28 55.7 -53 05 17	BCEP:
PY Lup	14 40 36.9 -46 53 35	M	V0377 Lup	15 29 00.0 -39 18 47	LB
PZ Lup	14 42 10.1 -43 20 06	EW	V0378 Lup	15 32 25.3 -40 30 46	EA
QQ Lup	14 42 26.4 -45 58 07	EW	V0379 Lup	15 34 27.5 -45 50 04	EA

Table 1 (continued)

Name	R.A., Decl., 2000.0	Type	Name	R.A., Decl., 2000.0	Type
	h m s o ' "			h m s o ' "	
V0380 Lup	15 34 56.1 -37 09 00	M	V0906 Mon	06 37 19.7 +07 26 24	EA
V0381 Lup	15 35 27.9 -30 36 54	RRAB	V0907 Mon	06 39 26.9 +07 13 45	EA
V0382 Lup	15 38 51.5 -39 21 20	M	V0908 Mon	06 40 05.7 +07 19 33	EA
V0383 Lup	15 42 24.7 -30 20 11	LB	V0909 Mon	06 40 06.8 +04 45 51	EA
V0384 Lup	15 43 44.7 -30 47 30	RRAB	V0910 Mon	06 40 13.7 +04 09 40	EA
V0385 Lup	15 44 47.8 -33 55 34	RRAB	V0911 Mon	06 40 37.6 +11 43 39	DCEP
V0386 Lup	15 45 18.2 -32 22 06	EW	V0912 Mon	06 40 59.3 +09 35 52	IN
V0387 Lup	15 50 14.6 -31 26 39	RRAB	V0913 Mon	06 45 33.7 +07 48 59	DCEP
V0388 Lup	15 50 38.7 -38 17 43	SRA	V0914 Mon	06 45 53.3 +10 03 41	DCEPS
V0389 Lup	15 51 00.4 -35 11 14	M	V0915 Mon	06 50 02.6 +06 28 25	EA
V0390 Lup	15 52 23.3 -39 59 56	SRB	V0916 Mon	06 51 24.3 +05 47 34	M:
V0391 Lup	15 52 53.6 -31 23 15	SRB	V0917 Mon	06 55 33.7 +07 44 44	EA
V0392 Lup	15 57 16.3 -36 10 15	M	V0918 Mon	06 55 40.3 -02 20 16	M:
V0393 Lup	15 57 37.8 -35 07 06	M	V0919 Mon	06 55 54.6 +08 01 23	EA
EO Lyn	07 09 01.2 +50 37 54	EB	V0920 Mon	06 57 57.8 +02 17 32	EA
EP Lyn	07 12 18.8 +47 19 32	RRAB	V0921 Mon	06 58 08.1 -07 17 46	DSCT
EQ Lyn	07 45 32.0 +45 38 32	ZZ+NL	V0922 Mon	06 58 29.9 +08 41 17	EA
ER Lyn	07 51 18.8 +36 29 57	RS	V0923 Mon	06 59 05.7 +03 37 56	M
ES Lyn	07 52 04.0 +53 56 54	LB	V0924 Mon	07 01 00.4 +10 03 46	RRAB:
ET Lyn	07 52 40.0 +39 32 18	DSCTC	V0925 Mon	07 01 05.1 -03 58 16	EA
EU Lyn	07 52 40.5 +36 28 23	E+AM	V0926 Mon	07 02 06.7 -03 45 17	SRC
EV Lyn	07 54 43.0 +50 07 29	EA+NL	V0927 Mon	07 02 23.7 +04 14 22	EW
EW Lyn	07 59 11.8 +45 19 37	RRAB	V0928 Mon	07 04 11.0 +00 03 52	RS:
EX Lyn	08 03 24.7 +38 18 36	UV	V0929 Mon	07 05 33.4 +00 30 31	EW
EY Lyn	08 04 21.5 +48 20 49	RRAB	V0930 Mon	07 07 20.7 -09 35 00	EB
EZ Lyn	08 04 34.3 +51 03 50	UGSU	V0931 Mon	07 08 07.7 -10 36 17	EA
FF Lyn	08 08 02.3 +53 39 31	RRAB	V0932 Mon	07 10 34.9 -01 11 26	M
FG Lyn	08 11 17.4 +52 52 35	EB	V0933 Mon	07 12 07.7 -10 16 39	SR
FH Lyn	08 13 21.9 +45 28 09	UGSS	V0934 Mon	07 14 55.6 -00 46 14	EW
FI Lyn	08 17 27.3 +51 51 47	EW	V0935 Mon	07 17 10.2 -01 32 14	EA
FK Lyn	08 17 44.5 +36 26 06	BY	V0936 Mon	07 19 10.4 -01 23 05	EW
FL Lyn	08 24 09.7 +49 31 25	UGSU	V0937 Mon	07 44 22.0 -06 41 49	EA+DSCT
FM Lyn	08 27 13.6 +41 28 33	RS	V0938 Mon	07 46 19.5 -04 32 41	EW
FN Lyn	08 37 16.6 +41 22 26	EA	V0939 Mon	07 46 21.4 -04 34 29	EA:
FO Lyn	08 37 26.4 +42 40 24	EW	V0940 Mon	07 46 38.3 -04 43 51	EA:
FP Lyn	08 41 46.8 +39 05 32	EW	V0941 Mon	07 46 49.2 -04 40 29	DSCTC:
FQ Lyn	08 46 26.4 +34 36 37	EW	V0942 Mon	07 46 52.6 -04 40 01	EA:
FR Lyn	08 54 14.0 +39 05 39	XM	V0943 Mon	08 00 08.2 -10 45 50	EA:
FS Lyn	08 54 44.3 +41 55 13	EB	V0944 Mon	08 00 32.8 -02 12 46	RRC:
FT Lyn	09 00 51.4 +34 22 36	EW	V0945 Mon	08 00 44.9 -02 10 43	RRAB
FU Lyn	09 01 44.2 +42 19 32	EW	V0946 Mon	08 01 18.1 -00 24 11	RRAB
FV Lyn	09 04 52.1 +44 02 57	NL	V0947 Mon	08 01 29.7 -00 23 08	RRAB
FW Lyn	09 19 51.5 +33 52 24	RRAB	V0948 Mon	08 01 51.2 -00 33 26	EW
FX Lyn	09 29 16.9 +39 40 11	RRAB	V0949 Mon	08 03 17.1 -02 06 04	RRAB
BB Men	06 22 54.3 -75 02 02	EW	V0950 Mon	08 03 29.1 -00 53 53	RRAB
BC Men	07 11 27.3 -84 28 13	BY	V0951 Mon	08 06 01.4 -01 16 43	RRC:
BD Men	07 33 38.3 -77 43 17	SR	V0952 Mon	08 07 23.5 -01 35 18	RRAB
V0899 Mon	06 09 19.2 -06 41 56	INT	V0953 Mon	08 07 37.2 -00 26 14	EW:
V0900 Mon	06 22 06.4 +04 28 17	EW	V0954 Mon	08 07 53.8 -01 27 00	RRAB
V0901 Mon	06 27 25.3 +01 11 32	CEP(B)	V0955 Mon	08 08 01.0 -01 39 32	RRAB
V0902 Mon	06 27 46.4 +01 48 11	E+NL	V0956 Mon	08 08 27.8 -00 48 26	RRAB
V0903 Mon	06 29 53.8 +06 03 19	EA	V0957 Mon	08 10 00.1 -02 11 56	RRAB
V0904 Mon	06 32 15.3 +08 54 20	EA	QZ Mus	11 33 57.9 -73 13 19	M
V0905 Mon	06 33 26.7 -00 04 30	L:	V0335 Mus	11 47 10.6 -70 12 58	LB

Table 1 (continued)

Name	R.A., Decl., 2000.0 h m s o ' "	Type	Name	R.A., Decl., 2000.0 h m s o ' "	Type
V0336 Mus	12 03 15.2 -66 14 50	SRA	V0437 Nor	15 52 19.5 -56 34 36	E:
V0337 Mus	12 25 44.6 -67 23 17	M	V0438 Nor	15 52 21.3 -56 31 47	EW
V0338 Mus	12 55 23.2 -73 22 12	RVA:	V0439 Nor	15 52 27.2 -56 28 52	M:
V0339 Mus	12 57 15.8 -69 01 51	M	V0440 Nor	15 52 39.2 -56 34 52	EB
V0340 Mus	13 06 32.4 -65 04 50	EA	V0441 Nor	15 52 40.0 -56 23 29	EW
V0341 Mus	13 13 12.7 -64 47 14	EP:	V0442 Nor	15 52 43.0 -56 34 59	EA
V0342 Mus	13 13 51.9 -64 41 30	EA	V0443 Nor	15 52 45.5 -56 24 55	EW:
V0343 Mus	13 14 56.0 -65 02 01	EP:	V0444 Nor	15 52 47.2 -56 26 06	EA
V0344 Mus	13 15 14.3 -64 49 29	EA	V0445 Nor	15 52 48.8 -56 35 07	EW:
V0345 Mus	13 17 23.3 -64 54 55	EA	V0446 Nor	15 52 49.5 -56 25 02	SR:
V0346 Mus	13 24 48.3 -64 51 38	EA	V0447 Nor	15 52 50.4 -56 27 28	EA
V0347 Mus	13 25 33.7 -64 55 35	EA	V0448 Nor	15 52 58.1 -56 23 56	EW
V0348 Mus	13 25 58.6 -65 14 51	EP:	V0449 Nor	15 52 58.4 -56 31 46	EW
V0349 Mus	13 27 47.2 -65 14 35	EA	V0450 Nor	15 53 00.3 -56 27 54	DSCT
V0350 Mus	13 32 25.3 -74 36 36	RRC	V0451 Nor	15 57 27.4 -59 20 15	EA
V0351 Mus	13 47 50.1 -66 56 43	M	V0452 Nor	15 57 59.7 -43 57 50	LB
V0352 Mus	13 48 47.7 -67 00 05	M	EW Oct	09 08 49.8 -84 29 12	RRAB
V0353 Mus	13 49 27.4 -72 11 41	M	EX Oct	15 17 08.7 -83 18 37	EB
V0401 Nor	15 25 38.5 -55 03 48	M	EY Oct	15 33 32.5 -86 24 59	M
V0402 Nor	15 30 01.9 -57 12 46	M	EZ Oct	15 43 13.6 -86 48 07	EW
V0403 Nor	15 32 10.7 -50 16 27	M	FF Oct	15 57 05.6 -87 30 05	RS
V0404 Nor	15 33 15.9 -48 56 20	RVA	V2675 Oph	16 26 36.8 -24 19 00	INT
V0405 Nor	15 33 51.0 -58 31 17	EA	V2775 Ori	05 42 48.5 -08 16 35	FU:
V0406 Nor	15 34 26.1 -57 14 39	M	V2776 Ori	06 00 34.9 -01 33 19	RRAB
V0407 Nor	15 35 08.8 -59 34 47	M	V2777 Ori	06 01 59.6 -01 25 13	RRAB
V0408 Nor	15 41 40.1 -50 56 38	LB	V2778 Ori	06 03 39.5 +03 38 27	EA
V0409 Nor	15 44 25.1 -50 45 01	RCB	V2779 Ori	06 03 52.4 -01 46 20	RRAB
V0410 Nor	15 51 23.0 -56 29 54	EW	V2780 Ori	06 04 23.7 +18 00 42	EA
V0411 Nor	15 51 25.4 -56 32 50	SR:	V2781 Ori	06 09 16.9 +20 25 07	EA
V0412 Nor	15 51 26.0 -56 30 12	EW	V2782 Ori	06 10 15.8 +21 19 56	BY
V0413 Nor	15 51 29.1 -56 33 09	EB	V2783 Ori	06 10 56.8 +06 21 04	EA
V0414 Nor	15 51 29.6 -56 31 30	EW:	V2784 Ori	06 11 07.0 +06 17 12	EA
V0415 Nor	15 51 39.7 -56 34 01	EW	V2785 Ori	06 11 28.8 +20 21 50	BY
V0416 Nor	15 51 40.2 -56 35 29	SR:	V2786 Ori	06 11 47.8 +19 08 20	M
V0417 Nor	15 51 42.8 -56 30 55	EW	V2787 Ori	06 12 17.1 +14 56 41	EB
V0418 Nor	15 51 44.0 -56 24 13	EW	V2788 Ori	06 13 48.5 +05 57 11	EW
V0419 Nor	15 51 45.1 -56 34 07	EB	V2789 Ori	06 14 34.5 +18 28 28	EB
V0420 Nor	15 51 47.1 -56 33 55	E:	V2790 Ori	06 15 31.4 +19 35 22	EW
V0421 Nor	15 51 47.8 -56 29 37	RRC	V2791 Ori	06 16 42.5 +01 15 18	RS
V0422 Nor	15 51 50.6 -56 28 10	EW	V2792 Ori	06 17 47.0 -00 14 39	SRB
V0423 Nor	15 51 54.6 -56 34 56	EA	V2793 Ori	06 18 10.7 +03 55 19	EA
V0424 Nor	15 51 55.0 -56 23 17	EB	AS Pic	06 05 56.8 -53 42 52	EW
V0425 Nor	15 51 55.3 -56 32 14	M:	AT Pic	06 23 39.5 -61 29 48	RRAB
V0426 Nor	15 51 57.3 -56 34 50	E:	AU Pic	06 34 47.2 -62 35 38	EW
V0427 Nor	15 52 00.7 -56 22 34	EW	V0646 Pup	07 50 35.6 -33 06 24	FU:
V0428 Nor	15 52 01.0 -56 36 17	EB	V0647 Pup	06 07 47.0 -44 43 46	DSCT
V0429 Nor	15 52 03.3 -56 32 10	LB	V0648 Pup	06 40 34.6 -37 50 11	SR
V0430 Nor	15 52 04.9 -56 33 38	EW	V0649 Pup	06 45 17.3 -46 42 06	EA:
V0431 Nor	15 52 09.3 -56 34 33	LB	V0650 Pup	07 05 06.3 -37 00 58	SRA
V0432 Nor	15 52 14.2 -56 34 19	EB	V0651 Pup	07 05 22.9 -35 53 20	EA
V0433 Nor	15 52 14.4 -56 34 24	SR:	V0652 Pup	07 09 58.8 -36 39 29	EW
V0434 Nor	15 52 14.8 -56 23 26	EW	V0653 Pup	07 21 14.7 -46 36 20	EW
V0435 Nor	15 52 16.9 -56 35 02	M:	V0654 Pup	07 21 20.6 -46 40 54	EW
V0436 Nor	15 52 19.0 -56 23 27	EW	V0655 Pup	07 26 08.0 -47 37 22	BY:

Table 1 (continued)

Name	R.A., Decl., 2000.0	Type	Name	R.A., Decl., 2000.0	Type
	h m s o ' "			h m s o ' "	
V0656 Pup	07 26 11.0 -47 43 03	EW	DS Pyx	09 11 39.1 -36 24 15	LB
V0657 Pup	07 26 16.4 -47 38 36	EA	DT Pyx	09 18 58.5 -29 42 37	UG
V0658 Pup	07 26 18.9 -47 41 47	EW	V5587 Sgr	17 47 46.2 -23 35 14	NA
V0659 Pup	07 26 23.7 -47 42 02	BY:	V5588 Sgr	18 10 21.4 -23 05 30	NA
V0660 Pup	07 26 26.7 -47 40 27	EA	V1312 Sco	16 55 09.5 -38 38 05	NA
V0661 Pup	07 26 32.9 -47 41 18	EA:	V1313 Sco	16 36 44.3 -41 32 38	NA
V0662 Pup	07 26 50.6 -47 45 27	EW	V1314 Sco	15 49 39.5 -25 12 53	SRB
V0663 Pup	07 26 53.7 -47 46 01	EW	V1315 Sco	15 52 44.8 -26 05 46	SRB
V0664 Pup	07 27 29.0 -50 56 30	EW	V1316 Sco	15 53 41.6 -25 17 12	M
V0665 Pup	07 28 11.9 -46 26 04	SRA	V1317 Sco	15 55 17.1 -29 24 37	RCB:
V0666 Pup	07 28 26.2 -36 45 51	SRB	V1318 Sco	15 55 26.1 -25 09 59	M
V0667 Pup	07 32 37.6 -13 31 09	XM	V1319 Sco	15 55 51.6 -21 48 33	RRC
V0668 Pup	07 33 21.5 -11 48 40	EA+BE	V1320 Sco	15 57 29.7 -23 45 10	SRB
V0669 Pup	07 37 02.1 -19 32 54	M	V1321 Sco	15 57 48.2 -29 18 11	SRB
V0670 Pup	07 38 21.5 -22 14 16	EA+BE:	V1322 Sco	15 58 15.6 -22 44 43	M
V0671 Pup	07 39 04.4 -40 28 47	M	V1323 Sco	15 58 56.3 -28 24 49	SRB
V0672 Pup	07 42 16.7 -29 51 04	SR	V0414 Ser	15 12 22.0 +11 54 35	RRAB
V0673 Pup	07 43 51.4 -37 05 55	LB	V0415 Ser	15 12 26.4 -00 35 37	RRAB
V0674 Pup	07 45 36.9 -31 09 32	EW	V0416 Ser	15 13 56.6 -01 15 29	RRAB
V0675 Pup	07 50 46.9 -30 22 12	EA	V0417 Ser	15 14 07.7 -01 26 07	RRAB
V0676 Pup	07 52 43.3 -28 26 52	M:	V0418 Ser	15 14 53.6 +02 09 35	UG
V0677 Pup	07 57 39.6 -45 51 41	M	V0419 Ser	15 16 09.5 -00 16 23	RRAB
V0678 Pup	07 57 47.4 -37 51 11	SR	V0420 Ser	15 16 49.1 -00 07 47	RRC
V0679 Pup	07 59 01.6 -39 51 26	SR	V0421 Ser	15 17 45.1 -00 38 44	RRAB
V0680 Pup	07 59 23.0 -50 30 49	SRB	V0422 Ser	15 18 13.6 -01 19 08	RRAB
V0681 Pup	07 59 24.3 -41 03 16	M	V0423 Ser	15 19 18.8 +07 53 06	RRAB
V0682 Pup	08 00 25.5 -19 42 11	M	V0424 Ser	15 19 27.8 -00 38 29	RRAB
V0683 Pup	08 01 12.0 -29 33 31	LPB	V0425 Ser	15 19 30.0 +19 15 58	EW
V0684 Pup	08 03 07.1 -26 34 31	M	V0426 Ser	15 19 51.9 +16 27 51	BY:
V0685 Pup	08 04 57.6 -29 51 26	SR	V0427 Ser	15 20 14.2 -00 26 03	RRAB
V0686 Pup	08 07 06.2 -28 47 40	M	V0428 Ser	15 20 39.6 -00 00 09	RRAB
V0687 Pup	08 07 25.4 -21 49 48	RRAB	V0429 Ser	15 21 13.8 -01 03 04	RRAB
V0688 Pup	08 09 20.3 -36 24 27	M	V0430 Ser	15 21 22.9 -00 05 31	RRAB
V0689 Pup	08 10 02.5 -33 08 29	M:	V0431 Ser	15 21 57.7 -02 10 33	RRAB
V0690 Pup	08 10 22.3 -35 46 23	EA	V0432 Ser	15 23 03.6 -01 41 21	RRAB
V0691 Pup	08 10 28.7 -12 53 01	EB	V0433 Ser	15 23 18.6 -00 55 21	RRAB
V0692 Pup	08 10 38.4 -12 50 17	EW	V0434 Ser	15 23 27.6 +02 33 30	EA
V0693 Pup	08 10 42.2 -12 49 39	DSCTC	V0435 Ser	15 23 29.3 +02 50 26	RRAB
V0694 Pup	08 10 44.7 -12 53 49	GDOR	V0436 Ser	15 23 46.1 -00 44 25	BY
V0695 Pup	08 10 46.1 -12 53 13	EW	V0437 Ser	15 24 30.7 +11 47 17	SR
V0696 Pup	08 10 46.3 -12 54 51	EA	V0438 Ser	15 25 29.9 -01 29 06	RRAB
V0697 Pup	08 10 48.8 -12 46 28	EB:	V0439 Ser	15 26 58.4 +05 38 15	RRAB
V0698 Pup	08 12 31.8 -36 32 28	EA	V0440 Ser	15 27 09.2 -00 20 45	RRAB
V0699 Pup	08 12 43.0 -35 44 36	SRB	V0441 Ser	15 27 55.2 -02 08 06	RRAB
V0700 Pup	08 19 08.2 -37 14 34	M:	V0442 Ser	15 28 20.9 -00 25 44	RRAB
V0701 Pup	08 19 32.9 -23 58 10	RRC	V0443 Ser	15 28 39.2 +05 00 50	RRAB
V0702 Pup	08 19 57.0 -20 27 20	RRAB	V0444 Ser	15 28 39.8 -01 19 16	RRAB
V0703 Pup	08 21 41.3 -34 57 24	M	V0445 Ser	15 29 51.1 +02 02 48	RS
V0704 Pup	08 25 09.6 -41 20 02	M	V0446 Ser	15 29 54.2 +12 41 10	RRC:
V0705 Pup	08 26 29.4 -19 27 04	SRB	V0447 Ser	15 31 20.4 -01 36 02	RRAB
DO Pyx	08 36 02.8 -34 07 34	M	V0448 Ser	15 31 38.9 -00 13 11	RRAB
DP Pyx	08 46 05.6 -27 45 49	M	V0449 Ser	15 32 09.9 -01 20 33	RRAB
DQ Pyx	08 54 20.9 -35 43 35	EB	V0450 Ser	15 33 06.7 +11 24 56	RRAB
DR Pyx	09 02 22.3 -37 09 35	SR	V0451 Ser	15 33 47.0 -01 53 08	RRAB

Table 1 (continued)

Name	R.A., Decl., 2000.0	Type	Name	R.A., Decl., 2000.0	Type
	h m s o ' "			h m s o ' "	
V0452 Ser	15 34 39.2 -00 26 15	RRAB	AG Sex	09 56 25.1 -00 44 00	RRAB
V0453 Ser	15 34 52.7 -01 40 17	RRAB	AH Sex	09 56 27.7 -01 17 25	RRC
V0454 Ser	15 36 34.4 +12 19 30	RS	AI Sex	10 03 46.3 +01 25 10	EB
V0455 Ser	15 37 01.9 -01 13 08	RRAB	AK Sex	10 08 37.7 -02 03 13	RRAB
V0456 Ser	15 37 32.8 -01 43 53	RRAB	AL Sex	10 10 14.2 -02 01 14	RRAB
V0457 Ser	15 38 08.0 +12 01 42	RRAB	AM Sex	10 11 23.1 -01 26 44	RRC
V0458 Ser	15 39 11.9 +03 55 25	RRAB	AN Sex	10 12 17.7 -03 44 44	RS
V0459 Ser	15 39 46.7 -00 37 46	RRAB	AO Sex	10 12 54.9 -00 24 57	RRC:
V0460 Ser	15 41 22.5 -00 29 29	RRAB	AP Sex	10 14 28.4 -01 41 11	RRAB
V0461 Ser	15 41 24.2 -00 22 26	RRAB	AQ Sex	10 14 52.5 -00 26 35	RRAB
V0462 Ser	15 41 52.3 -01 14 27	RRC	AR Sex	10 15 46.9 -00 12 37	RRAB
V0463 Ser	15 41 54.9 -00 45 54	RRC	AS Sex	10 16 52.5 -01 37 50	RRAB
V0464 Ser	15 43 29.6 -00 07 11	RRAB	AT Sex	10 17 50.0 -02 01 27	RRC
V0465 Ser	15 43 55.0 -01 28 52	RRAB	AU Sex	10 19 00.3 -02 13 29	RRAB
V0466 Ser	15 44 25.3 -00 13 13	RRC	AV Sex	10 19 35.9 -01 27 55	RRAB
V0467 Ser	15 44 35.2 +04 23 08	BY	AW Sex	10 19 45.1 -01 39 03	RRAB
V0468 Ser	15 46 05.1 -00 26 48	RRC	AX Sex	10 20 19.4 -01 01 31	RRAB
V0469 Ser	15 46 31.6 -00 15 59	RRC	AY Sex	10 23 47.7 +00 38 41	*
V0470 Ser	15 47 16.1 -00 44 39	RRAB	AZ Sex	10 24 24.3 -02 04 31	RRC
V0471 Ser	15 47 32.0 -00 16 37	RRAB	BB Sex	10 25 48.8 -00 37 31	RRAB
V0472 Ser	15 47 53.5 +00 41 18	LB	BC Sex	10 30 02.7 -00 47 32	RS
V0473 Ser	15 48 27.1 -01 18 57	RRAB	BD Sex	10 30 33.1 -01 18 20	RRAB
V0474 Ser	15 48 40.9 -03 10 44	RS	BE Sex	10 30 37.5 -00 47 13	RRC
V0475 Ser	15 49 46.6 +23 54 53	DSCT	BF Sex	10 30 58.3 -01 18 35	RRAB
V0476 Ser	15 50 21.4 -02 02 52	RRAB	BG Sex	10 31 40.1 -00 51 40	RRC
V0477 Ser	15 50 43.1 +02 27 52	RRAB	BH Sex	10 33 34.8 -01 17 54	RRAB
V0478 Ser	15 50 46.2 -01 19 35	RRAB	BI Sex	10 33 54.8 +01 49 30	RRAB
V0479 Ser	15 51 07.6 +11 16 19	RS	BK Sex	10 35 40.4 -00 58 19	RRAB
V0480 Ser	15 51 14.1 -00 58 28	RRAB	BL Sex	10 36 37.1 -00 41 12	RRAB
V0481 Ser	15 51 17.1 -01 37 06	RRAB	BM Sex	10 37 31.8 -00 39 52	RRAB
V0482 Ser	15 52 11.1 -00 56 22	RRAB	BN Sex	10 39 21.8 -01 13 53	RRAB
V0483 Ser	15 52 24.9 +19 36 32	RRAB	BO Sex	10 42 39.6 -01 16 28	RRAB
V0484 Ser	15 52 29.3 +10 08 34	RRAB	BP Sex	10 45 48.2 -10 42 49	ACV
V0485 Ser	15 52 43.8 -00 39 32	RRAB	BQ Sex	10 45 55.6 -07 21 36	RRAB
V0486 Ser	15 53 07.5 +20 28 39	RS	BR Sex	10 47 21.6 -01 57 27	RRC
V0487 Ser	15 53 15.7 +17 34 12	RRAB	BS Sex	10 48 00.5 -05 30 33	RRAB
V0488 Ser	15 54 28.1 +15 21 22	RRAB	BT Sex	10 48 42.0 -01 13 54	RRC
V0489 Ser	15 55 32.0 -00 10 55	EA	NW TrA	15 02 35.9 -68 16 36	M
V0490 Ser	15 56 21.1 -00 06 21	RRAB	NX TrA	15 04 31.1 -68 27 08	M
V0491 Ser	15 56 29.5 -00 59 22	RRAB	NY TrA	15 07 10.9 -65 09 40	M
V0492 Ser	15 56 36.3 -02 11 47	RRAB	NZ TrA	15 08 34.7 -65 44 09	M
V0493 Ser	15 56 44.2 -00 09 50	UGSU	OO TrA	15 12 35.0 -64 37 27	M:
V0494 Ser	15 56 57.6 -00 16 03	RRAB	OP TrA	15 13 00.6 -65 04 35	M
V0495 Ser	15 58 26.4 -01 50 42	RRAB	OQ TrA	15 13 11.1 -68 51 20	M
V0496 Ser	15 59 03.1 -00 47 32	RRAB	OR TrA	15 15 31.1 -66 32 32	M
V0497 Ser	15 59 07.9 -01 20 51	RRC	OS TrA	15 15 55.1 -64 52 51	M
V0498 Ser	15 59 36.0 +12 46 23	RRAB	OT TrA	15 18 21.9 -64 32 09	M
ZZ Sex	09 41 34.3 -00 35 43	RRC	OU TrA	15 19 28.8 -69 20 30	M
AA Sex	09 41 34.8 -05 53 06	RRAB	OV TrA	15 21 35.5 -64 12 13	M
AB Sex	09 43 04.9 -04 58 20	RRAB	OW TrA	15 22 44.8 -64 24 28	M
AC Sex	09 44 27.6 -03 41 48	RRAB	OX TrA	15 24 41.8 -65 16 05	M
AD Sex	09 48 54.7 -00 57 48	RRAB	OY TrA	15 25 12.3 -63 33 49	M
AE Sex	09 52 09.2 -01 44 04	RRAB	OZ TrA	15 25 16.4 -65 12 10	M
AF Sex	09 55 15.9 +03 45 32	RRAB	PP TrA	15 26 35.0 -62 53 04	M

Table 1 (continued)

Name	R.A., Decl., 2000.0	Type	Name	R.A., Decl., 2000.0	Type
	h m s o ' "			h m s o ' "	
PQ TrA	15 27 49.3 -70 16 41	RRAB	V0337 UMa	10 11 08.9 +50 35 21	EW
PR TrA	15 30 55.1 -67 07 54	M	V0338 UMa	10 26 37.3 +43 34 32	RRAB
PS TrA	15 31 29.2 -66 14 35	M	V0339 UMa	10 31 31.7 +50 15 00	RRAB
PT TrA	15 31 41.9 -65 36 10	M	V0340 UMa	10 34 39.6 +51 39 21	RS
PU TrA	15 31 51.7 -63 35 06	M	V0341 UMa	10 35 38.2 +58 15 49	RRAB
PV TrA	15 34 11.2 -64 36 22	M	V0342 UMa	10 45 14.7 +52 16 48	EW
PW TrA	15 34 40.3 -62 53 19	M	V0343 UMa	10 45 54.6 +52 16 26	EA:
PX TrA	15 35 28.3 -64 37 49	M	V0344 UMa	11 06 39.0 +70 18 26	RS
PY TrA	15 39 08.1 -65 25 14	M	V0345 UMa	11 17 49.4 +33 40 15	RRAB
PZ TrA	15 40 55.8 -68 26 12	M	V0346 UMa	11 48 23.6 +35 04 21	BY
QQ TrA	15 42 26.3 -67 07 54	M	V0347 UMa	11 49 03.6 +38 00 31	BY:
QR TrA	15 43 43.4 -63 39 53	M	V0348 UMa	11 53 59.3 +55 14 35	RRAB
QS TrA	15 44 29.9 -61 17 11	M	V0349 UMa	11 57 24.5 +38 25 34	RRAB
QT TrA	15 46 43.0 -63 41 35	M	V0350 UMa	12 00 26.5 +51 57 18	BY
QU TrA	15 47 54.6 -62 34 06	XR:	V0351 UMa	12 44 26.3 +61 35 15	NL
QV TrA	15 48 02.8 -63 57 55	M	V0352 UMa	12 55 39.0 +54 57 40	ELL:
QW TrA	15 49 45.4 -64 23 42	M:	V0353 UMa	13 19 22.4 +58 47 04	RRAB
QX TrA	15 52 30.1 -69 36 06	M	V0354 UMa	13 35 38.4 +49 14 06	EW
QY TrA	15 54 12.8 -67 05 33	NL:	V0355 UMa	13 39 41.2 +48 47 27	ZZ+NL
QZ TrA	15 56 22.7 -61 24 34	M	V0356 UMa	13 43 54.6 +50 28 37	EA
V0335 TrA	15 58 32.1 -65 22 20	M	V0357 UMa	13 45 42.3 +51 07 17	EA
V0336 TrA	15 59 06.4 -63 17 50	EW	V0358 UMa	13 47 39.5 +51 48 35	EA
OR UMa	08 13 29.5 +69 50 34	EA	V0359 UMa	13 51 20.2 +54 57 43	ZZA
OS UMa	08 19 17.2 +62 30 26	EA/RS	V0360 UMa	13 55 08.1 +48 26 01	EW
OT UMa	08 19 23.2 +66 12 36	EW	V0361 UMa	13 55 24.3 +60 08 45	RRAB
OU UMa	08 28 31.2 +67 29 47	RRAB	V0362 UMa	13 59 43.3 +49 49 42	EW
OV UMa	08 36 05.6 +71 10 22	EA	V0363 UMa	14 09 14.6 +55 39 24	EW
OW UMa	08 37 25.7 +49 16 08	RRC	V0364 UMa	14 09 54.2 +61 36 31	EW
OX UMa	08 39 18.2 +67 39 42	EA	V0365 UMa	14 11 27.4 +55 10 05	EW
OY UMa	08 50 31.6 +67 26 25	EA	V0366 UMa	14 13 44.4 +60 18 45	EW
OZ UMa	08 51 14.6 +56 21 20	RRC	V0367 UMa	14 22 15.4 +60 29 04	RRAB
PP UMa	08 52 15.1 +70 26 24	RRAB	V0368 UMa	14 26 05.1 +58 05 12	M
PQ UMa	08 55 39.6 +60 29 37	RRAB	VZ UMi	13 23 29.0 +74 54 09	EA
PR UMa	08 56 01.6 +62 14 45	RRAB	WW UMi	13 27 57.2 +72 56 23	EB:
PS UMa	08 56 46.5 +69 40 32	EA	WX UMi	13 43 13.8 +74 02 39	EW
PT UMa	08 58 19.8 +52 26 28	SR	WY UMi	13 44 58.3 +77 15 51	UV
PU UMa	09 01 03.9 +48 09 12	UG+EA	WZ UMi	13 51 17.0 +74 42 44	EW
PV UMa	09 03 32.3 +53 06 30	SRD:	XX UMi	14 13 20.4 +73 53 46	RRAB
PW UMa	09 15 31.2 +65 01 27	EW	XY UMi	14 17 55.7 +71 41 07	RRAB
PX UMa	09 15 44.9 +62 48 32	DSCTC:	XZ UMi	14 39 51.6 +74 45 02	RRAB
PY UMa	09 24 30.6 +42 18 17	RRAB	YY UMi	15 32 02.5 +71 27 15	RRAB
PZ UMa	09 29 07.1 +49 51 23	EW	YZ UMi	15 35 30.2 +85 37 39	DSCT
QQ UMa	09 29 09.7 +48 19 05	EW	ZZ UMi	15 36 36.6 +69 11 21	EA
QR UMa	09 30 38.3 +44 46 10	EA	AA UMi	15 46 42.7 +81 42 31	EA
QS UMa	09 32 14.8 +49 50 55	EA	V0446 Vel	08 12 45.4 -49 14 06	LB
QT UMa	09 36 29.2 +48 52 46	EW	V0447 Vel	08 14 18.6 -44 36 36	EB
QU UMa	09 39 11.6 +61 10 23	RRAB	V0448 Vel	08 24 55.5 -48 33 35	EW
QV UMa	09 44 23.5 +50 02 56	EW	V0449 Vel	08 30 41.4 -50 50 42	M
QW UMa	09 46 56.6 +63 41 44	RRC	V0450 Vel	08 30 56.7 -50 42 25	SRA
QX UMa	09 47 32.6 +51 27 24	RRC	V0451 Vel	08 34 08.1 -44 32 41	EB
QY UMa	09 49 54.8 +51 44 23	RRAB	V0452 Vel	08 37 43.4 -39 53 36	EW
QZ UMa	09 51 11.1 +47 09 13	RRAB	V0453 Vel	08 37 53.0 -38 42 18	LB
V0335 UMa	09 54 11.5 +42 39 01	SRD:	V0454 Vel	08 38 09.0 -40 04 52	EA
V0336 UMa	09 57 48.8 +60 44 28	RRAB	V0455 Vel	08 38 26.7 -52 45 07	BY:

Table 1 (continued)

Name	R.A., Decl., 2000.0	Type	Name	R.A., Decl., 2000.0	Type
	h m s o ' "			h m s o ' "	
V0456 Vel	08 42 15.6 -47 12 27	EW	V0510 Vel	10 18 03.9 -46 17 48	RRAB
V0457 Vel	08 42 33.3 -47 11 35	DSCTC	V0511 Vel	10 18 32.0 -46 37 33	EW
V0458 Vel	08 42 36.2 -47 11 29	DSCT	V0512 Vel	10 18 32.8 -46 30 42	EA
V0459 Vel	08 42 38.6 -47 12 07	DSCT	V0513 Vel	10 18 46.0 -46 30 13	EA
V0460 Vel	08 42 42.0 -47 12 09	DSCT	V0514 Vel	10 18 56.0 -46 36 10	EB:
V0461 Vel	08 42 43.7 -45 33 18	EA+BE	V0515 Vel	10 24 35.1 -52 44 20	M:
V0462 Vel	08 42 43.9 -47 12 32	GDOR	V0516 Vel	10 33 59.5 -47 31 50	EA
V0463 Vel	08 42 44.8 -47 13 01	DSCTC	V0517 Vel	10 43 09.3 -44 03 08	RVA
V0464 Vel	08 42 51.7 -47 11 43	EW	V0518 Vel	10 46 19.9 -45 58 00	EA
V0465 Vel	08 43 03.6 -52 56 13	EW	V0350 Vir	11 39 43.3 +09 08 09	RRAB
V0466 Vel	08 43 31.2 -52 55 02	E	V0351 Vir	11 39 54.6 -01 42 05	RRAB
V0467 Vel	08 43 49.8 -46 07 09	EA+BCEP:	V0352 Vir	11 41 54.6 -00 07 40	RRAB
V0468 Vel	08 44 12.3 -52 46 19	DSCT	V0353 Vir	11 42 51.4 -01 30 36	RRAB
V0469 Vel	08 45 15.6 -53 51 28	EA	V0354 Vir	11 43 32.2 +02 41 56	RRAB
V0470 Vel	08 45 33.3 -39 23 08	SRA	V0355 Vir	11 49 25.1 +05 29 46	BY:
V0471 Vel	08 47 16.8 -47 13 25	SR	V0356 Vir	11 51 57.7 -00 06 07	RRAB
V0472 Vel	08 48 45.5 -46 05 09	*	V0357 Vir	11 55 34.3 -00 36 02	RRAB
V0473 Vel	08 54 05.1 -45 39 45	LB:	V0358 Vir	11 56 51.6 +08 27 21	RS
V0474 Vel	08 55 01.5 -51 07 20	M	V0359 Vir	11 57 06.9 -00 55 08	RRAB
V0475 Vel	08 55 10.7 -47 35 55	M:	V0360 Vir	11 57 24.2 -00 53 58	RRAB
V0476 Vel	08 56 27.2 -47 27 39	LB	V0361 Vir	11 59 34.7 -01 51 35	RRAB
V0477 Vel	08 57 09.6 -39 54 06	SR	V0362 Vir	11 59 56.3 -00 00 04	RRAB
V0478 Vel	08 58 14.3 -41 28 49	SRB	V0363 Vir	12 00 16.0 +03 43 08	RRAB
V0479 Vel	09 04 51.3 -37 48 09	EA	V0364 Vir	12 00 44.4 -00 42 45	RRAB
V0480 Vel	09 05 45.0 -37 39 39	SRB	V0365 Vir	12 00 51.7 -01 52 30	RRAB
V0481 Vel	09 06 54.2 -43 33 54	LB	V0366 Vir	12 01 35.4 -00 14 05	RRC
V0482 Vel	09 10 58.2 -42 40 59	M	V0367 Vir	12 02 31.8 -01 53 45	RRAB
V0483 Vel	09 11 42.3 -46 53 10	EA	V0368 Vir	12 04 20.9 -02 10 42	RRC
V0484 Vel	09 12 24.9 -38 03 07	EA	V0369 Vir	12 04 51.0 -00 21 07	RRAB
V0485 Vel	09 14 50.1 -45 02 49	SR:	V0370 Vir	12 06 04.1 -02 12 57	RRAB
V0486 Vel	09 17 30.4 -49 57 30	LB	V0371 Vir	12 07 30.9 -00 04 12	RRAB
V0487 Vel	09 18 01.6 -54 02 27	RCB:	V0372 Vir	12 07 38.7 -00 45 10	RRC
V0488 Vel	09 19 17.2 -52 00 28	M	V0373 Vir	12 08 00.4 -01 12 34	RRC
V0489 Vel	09 26 18.7 -52 06 04	SR:	V0374 Vir	12 08 31.4 -00 47 18	RRAB
V0490 Vel	09 26 45.5 -49 22 25	M	V0375 Vir	12 09 10.4 -00 47 59	RRAB
V0491 Vel	09 34 41.3 -47 09 35	LB	V0376 Vir	12 09 15.7 -01 54 44	RRAB
V0492 Vel	09 34 50.7 -49 48 45	LB	V0377 Vir	12 09 19.8 -01 10 47	RRAB
V0493 Vel	09 34 57.0 -50 24 30	M	V0378 Vir	12 11 32.0 -01 52 36	RRC
V0494 Vel	09 41 51.9 -47 46 58	LB	V0379 Vir	12 12 09.3 +01 36 28	NL
V0495 Vel	09 45 53.6 -44 19 43	EA	V0380 Vir	12 12 15.5 -01 21 13	RRAB
V0496 Vel	09 50 47.6 -44 41 29	EA	V0381 Vir	12 15 27.8 -00 52 57	RRAB
V0497 Vel	09 51 31.9 -49 31 24	EA	V0382 Vir	12 15 51.7 -00 05 55	RRAB
V0498 Vel	09 52 49.7 -46 03 18	M:	V0383 Vir	12 16 53.0 +05 41 26	BY
V0499 Vel	09 53 06.7 -53 38 54	M	V0384 Vir	12 18 23.3 -01 54 49	RRAB
V0500 Vel	09 54 40.7 -55 20 16	M	V0385 Vir	12 18 43.0 -00 42 39	RRC
V0501 Vel	09 56 12.8 -48 10 29	EA	V0386 Vir	12 21 20.7 -01 24 14	RRAB
V0502 Vel	10 04 25.4 -50 05 30	LB	V0387 Vir	12 22 21.5 -01 24 37	RRC
V0503 Vel	10 06 53.7 -40 53 23	EA	V0388 Vir	12 22 52.8 +01 17 51	RRAB
V0504 Vel	10 16 36.9 -46 22 29	EW	V0389 Vir	12 23 10.9 -00 16 58	RRAB
V0505 Vel	10 17 07.7 -46 30 18	EW	V0390 Vir	12 24 15.7 -01 49 14	RRAB
V0506 Vel	10 17 13.7 -46 27 55	EW	V0391 Vir	12 24 18.5 +03 51 33	EW
V0507 Vel	10 17 17.2 -46 27 37	EW	V0392 Vir	12 24 19.9 -00 13 38	RRAB
V0508 Vel	10 17 25.7 -46 20 12	EA	V0393 Vir	12 25 41.6 -01 11 52	RRAB
V0509 Vel	10 17 52.8 -46 34 07	EW	V0394 Vir	12 25 49.8 +09 45 46	BY

Table 1 (continued)

Name	R.A., Decl., 2000.0	Type	Name	R.A., Decl., 2000.0	Type
	h m s o ' "			h m s o ' "	
V0395 Vir	12 26 27.4 -00 52 05	RRAB	V0449 Vir	13 09 21.7 -00 43 08	RRAB
V0396 Vir	12 27 43.3 -00 57 55	RRAB	V0450 Vir	13 10 20.9 -00 44 57	RRAB
V0397 Vir	12 27 48.2 -00 58 46	RRAB	V0451 Vir	13 10 50.3 -01 24 21	RRAB
V0398 Vir	12 28 03.9 -01 14 55	RRC	V0452 Vir	13 11 14.5 +11 09 29	RRAB
V0399 Vir	12 28 35.9 -00 38 40	RRAB	V0453 Vir	13 11 15.7 -00 29 00	RRAB
V0400 Vir	12 29 10.5 -01 34 00	RRC	V0454 Vir	13 11 17.1 -01 55 34	RRAB
V0401 Vir	12 30 18.0 -00 18 37	SXPHE:	V0455 Vir	13 11 50.9 -02 09 49	RRC
V0402 Vir	12 31 33.3 -00 20 10	RRAB	V0456 Vir	13 11 52.4 -00 22 33	RRAB
V0403 Vir	12 31 42.9 -01 31 14	RRC	V0457 Vir	13 12 53.6 +08 23 35	RS
V0404 Vir	12 31 47.2 -00 53 04	RRC	V0458 Vir	13 13 16.0 -00 40 11	RRAB
V0405 Vir	12 34 53.5 -00 18 00	RRAB	V0459 Vir	13 13 22.7 -02 05 29	SXPHE:
V0406 Vir	12 38 13.7 -03 39 33	NL	V0460 Vir	13 13 41.1 -00 01 10	RRAB
V0407 Vir	12 39 49.5 -00 00 06	RRAB	V0461 Vir	13 14 38.0 -00 20 39	SXPHE:
V0408 Vir	12 40 03.5 -00 04 10	RRAB	V0462 Vir	13 16 09.6 -00 44 17	RRAB
V0409 Vir	12 40 32.9 -00 03 13	SXPHE:	V0463 Vir	13 16 55.7 -00 49 15	RRAB
V0410 Vir	12 42 11.2 -01 33 40	RRC	V0464 Vir	13 17 17.8 -00 35 58	RRAB
V0411 Vir	12 42 24.9 -00 12 03	RRC	V0465 Vir	13 17 41.1 -00 15 25	RRAB
V0412 Vir	12 43 50.6 -01 28 21	RRAB	V0466 Vir	13 17 57.5 -00 08 19	RRAB
V0413 Vir	12 44 07.1 -00 56 49	RRC	V0467 Vir	13 22 44.8 -06 02 07	EW
V0414 Vir	12 44 50.1 -00 50 40	RRC	V0468 Vir	13 23 08.9 -01 49 16	RRAB
V0415 Vir	12 45 01.6 +07 57 05	EW	V0469 Vir	13 23 15.8 -01 20 16	RRAB
V0416 Vir	12 45 44.5 -01 53 27	RRAB	V0470 Vir	13 24 05.4 -02 05 27	RRAB
V0417 Vir	12 46 14.8 -01 03 12	RRAB	V0471 Vir	13 26 24.9 -00 26 12	RRAB
V0418 Vir	12 46 48.1 -02 07 19	RRAB	V0472 Vir	13 27 00.1 -00 54 57	RRAB
V0419 Vir	12 48 04.5 -08 20 47	RRAB	V0473 Vir	13 27 12.6 -01 16 30	RRAB
V0420 Vir	12 49 05.7 -02 16 58	RRAB	V0474 Vir	13 27 27.9 -00 49 59	RRAB
V0421 Vir	12 49 14.5 -00 49 26	RRC	V0475 Vir	13 27 52.5 -02 01 13	RRAB
V0422 Vir	12 51 02.3 -00 45 13	RRAB	V0476 Vir	13 29 22.5 -05 52 59	RRAB
V0423 Vir	12 52 05.4 -02 00 07	RRAB	V0477 Vir	13 31 02.4 -02 08 39	RRAB
V0424 Vir	12 52 08.7 -00 29 32	RRAB	V0478 Vir	13 33 23.5 -00 12 00	RRAB
V0425 Vir	12 52 41.7 -01 54 09	RRAB	V0479 Vir	13 33 30.5 -00 44 53	RRAB
V0426 Vir	12 52 44.6 -00 25 13	RRC	V0480 Vir	13 34 17.5 -01 58 28	RRC
V0427 Vir	12 53 32.5 -02 08 30	RRAB	V0481 Vir	13 35 51.9 -01 50 38	RRAB
V0428 Vir	12 55 02.0 -02 02 55	RRAB	V0482 Vir	13 35 52.2 -00 37 07	RRAB
V0429 Vir	12 55 06.0 -00 05 42	RRAB	V0483 Vir	13 36 10.6 -03 14 11	RRAB
V0430 Vir	12 55 58.8 +07 57 11	RS	V0484 Vir	13 37 19.2 -00 16 21	RRAB
V0431 Vir	12 56 00.9 -00 14 50	RRAB	V0485 Vir	13 37 48.9 -00 56 47	RRAB
V0432 Vir	12 56 10.6 -11 17 42	RRAB	V0486 Vir	13 38 48.9 -00 09 54	RRC
V0433 Vir	12 56 43.9 -01 01 50	RRAB	V0487 Vir	13 39 33.3 +00 01 55	RRAB
V0434 Vir	12 57 17.9 -01 12 58	RRAB	V0488 Vir	13 40 31.3 -00 41 12	RRAB
V0435 Vir	12 57 57.8 -00 58 57	RRAB	V0489 Vir	13 41 17.4 -01 21 40	RRAB
V0436 Vir	12 58 03.1 -02 00 34	RRAB	V0490 Vir	13 42 13.0 -02 09 27	RRAB
V0437 Vir	12 58 04.4 +09 50 44	RRAB	V0491 Vir	13 43 26.8 -00 40 13	RRAB
V0438 Vir	12 58 27.2 -03 36 06	RRAB	V0492 Vir	13 44 14.3 -00 40 07	RRC
V0439 Vir	13 01 10.5 +01 07 40	ZZA	V0493 Vir	13 44 31.3 -00 37 03	RRAB
V0440 Vir	13 01 40.6 -00 20 54	RRAB	V0494 Vir	13 45 21.3 -00 01 47	RRAB
V0441 Vir	13 02 45.9 -02 03 50	RRAB	V0495 Vir	13 45 40.8 -00 11 19	RRAB
V0442 Vir	13 02 52.2 -01 38 04	RRAB	V0496 Vir	13 45 46.9 -00 12 00	RRAB
V0443 Vir	13 03 13.6 -01 22 22	RRC	V0497 Vir	13 46 19.1 -01 37 11	RRAB
V0444 Vir	13 03 49.6 -00 44 20	RRAB	V0498 Vir	13 46 54.4 -03 07 35	RRAB
V0445 Vir	13 05 29.1 +12 49 36	RS	V0499 Vir	13 47 29.3 -12 12 40	RRAB
V0446 Vir	13 05 36.4 -00 48 25	RRAB	V0500 Vir	13 48 55.4 -01 36 56	RRAB
V0447 Vir	13 06 48.5 -01 17 53	RRAB	V0501 Vir	13 49 47.5 -02 06 49	RRC
V0448 Vir	13 08 55.3 -01 58 52	RRAB	V0502 Vir	13 50 07.5 -00 56 38	RRAB

Table 1 (continued)

Name	R.A., Decl., 2000.0						Type	Name	R.A., Decl., 2000.0						Type
	h	m	s	o	’	"			h	m	s	o	’	"	
V0503 Vir	13	50	48.7	+01	33	19	EW	V0557 Vir	14	26	41.8	-01	31	15	RRAB
V0504 Vir	13	51	56.2	-00	53	14	RRAB	V0558 Vir	14	27	01.6	-01	23	10	AM:
V0505 Vir	13	52	25.1	-00	17	26	RRAB	V0559 Vir	14	28	07.1	-00	03	42	RRAB
V0506 Vir	13	52	34.7	-01	15	14	RRAB	V0560 Vir	14	28	09.0	-00	11	48	RRAB
V0507 Vir	13	52	44.5	-02	18	29	RRAB	V0561 Vir	14	28	40.6	-01	27	59	RRAB
V0508 Vir	13	53	42.5	-00	17	09	RRAB	V0562 Vir	14	28	52.6	-00	05	21	SXPHE:
V0509 Vir	13	55	00.9	-00	59	54	RRAB	V0563 Vir	14	29	49.9	-01	15	48	RRAB
V0510 Vir	13	55	47.2	-02	00	41	RRAB	V0564 Vir	14	30	32.3	-00	03	29	RRAB
V0511 Vir	13	55	56.5	-00	48	36	RRAB	V0565 Vir	14	30	49.1	-01	22	16	RRAB
V0512 Vir	13	57	00.0	-01	34	26	RRAB	V0566 Vir	14	31	38.7	-01	29	59	RRAB
V0513 Vir	13	57	01.3	-02	05	23	RRAB	V0567 Vir	14	31	40.8	-00	53	24	RRAB
V0514 Vir	13	58	00.7	-02	08	31	RRAB	V0568 Vir	14	32	12.4	-02	11	45	RRAB
V0515 Vir	13	58	21.1	-01	36	49	RRAB	V0569 Vir	14	33	12.9	-00	07	33	RRAB
V0516 Vir	13	58	24.0	-00	28	19	RRAB	V0570 Vir	14	34	03.0	-00	12	52	RRAB
V0517 Vir	13	58	50.3	-02	24	23	RRAB	V0571 Vir	14	34	11.5	-01	54	48	RRAB
V0518 Vir	13	59	55.4	-00	26	27	RRAB	V0572 Vir	14	34	23.4	-00	58	16	RRAB
V0519 Vir	14	01	21.4	-01	24	21	RRAB	V0573 Vir	14	34	28.0	-00	39	37	RRAB
V0520 Vir	14	04	07.0	+02	24	15	RRAB	V0574 Vir	14	34	30.5	-08	18	33	RRAB
V0521 Vir	14	06	38.1	-01	50	32	RRAB	V0575 Vir	14	34	43.6	-01	13	09	RRAB
V0522 Vir	14	07	20.9	-01	31	16	RRAB	V0576 Vir	14	34	53.4	-00	39	01	RRAB
V0523 Vir	14	07	44.2	-01	57	54	RRC	V0577 Vir	14	35	17.0	-00	59	32	LB
V0524 Vir	14	08	30.0	-00	37	51	RRAB	V0578 Vir	14	35	17.6	-01	24	59	RRAB
V0525 Vir	14	08	47.8	-00	13	43	RRAB	V0579 Vir	14	36	04.5	-01	37	31	RRAB
V0526 Vir	14	08	49.8	-00	04	22	RRAB	V0580 Vir	14	37	00.9	-00	44	22	RRAB
V0527 Vir	14	09	44.1	-01	32	14	RRAB	V0581 Vir	14	37	01.0	-01	15	16	RRAB
V0528 Vir	14	10	06.8	-05	31	59	RRAB	V0582 Vir	14	37	13.9	+02	46	20	RRAB
V0529 Vir	14	10	30.5	-00	50	41	RRC	V0583 Vir	14	38	02.8	-01	28	23	RRAB
V0530 Vir	14	10	49.8	-02	14	06	RRAB	V0584 Vir	14	39	27.0	-01	23	42	RRAB
V0531 Vir	14	11	00.0	-00	29	16	RRAB	V0585 Vir	14	39	27.4	-03	27	37	RRAB
V0532 Vir	14	12	08.2	-01	52	10	RRC	V0586 Vir	14	39	47.5	-04	08	05	RRAB
V0533 Vir	14	12	38.6	-00	53	51	RRC:	V0587 Vir	14	40	27.9	-00	10	39	RRAB
V0534 Vir	14	12	59.4	-00	13	21	RRAB	V0588 Vir	14	40	52.8	-03	08	53	R
V0535 Vir	14	14	21.8	-01	15	26	RRAB	V0589 Vir	14	41	25.7	+03	39	00	EW
V0536 Vir	14	15	13.5	-00	53	03	RRAB	V0590 Vir	14	42	09.7	-00	10	33	RRAB
V0537 Vir	14	15	43.4	-00	06	13	RRAB	V0591 Vir	14	42	12.6	+03	24	14	EW
V0538 Vir	14	16	32.6	-01	29	00	RRAB	V0592 Vir	14	44	27.8	-00	58	06	RRAB
V0539 Vir	14	17	12.5	-01	53	28	RRAB	V0593 Vir	14	44	30.1	-01	28	26	RRC:
V0540 Vir	14	17	30.6	-10	18	06	RRAB	V0594 Vir	14	45	15.0	+00	02	49	RPHS
V0541 Vir	14	18	22.3	-00	15	06	RRAB	V0595 Vir	14	45	50.2	-02	13	50	RRAB
V0542 Vir	14	18	41.5	-00	17	56	RRAB	V0596 Vir	14	46	23.9	-00	06	57	RRC
V0543 Vir	14	18	58.1	-00	26	43	RRAB	V0597 Vir	14	47	20.4	-00	01	02	RRAB
V0544 Vir	14	19	09.5	-00	24	43	RRAB	V0598 Vir	14	49	39.6	-00	29	44	RRAB
V0545 Vir	14	19	34.1	-00	55	09	RRAB	V0599 Vir	14	53	27.5	-00	25	27	RRAB
V0546 Vir	14	19	40.6	+05	54	03	EW	V0600 Vir	14	55	27.3	+06	14	52	RRAB
V0547 Vir	14	19	52.3	-06	23	03	RRAB	V0601 Vir	15	00	13.9	+06	44	42	BY
V0548 Vir	14	20	06.5	-01	01	04	RRAB	V0602 Vir	15	04	10.0	+04	21	43	RRAB
V0549 Vir	14	22	00.0	-01	01	07	RRAB	V0603 Vir	15	05	42.9	+00	01	11	RRAB
V0550 Vir	14	22	57.4	-00	29	22	RRAB	V0604 Vir	15	06	12.7	+02	54	57	RRAB
V0551 Vir	14	23	05.6	+01	54	01	RRAB	V0605 Vir	15	08	17.3	+03	03	43	RRAB
V0552 Vir	14	24	10.7	-00	47	56	RRAB	AH Vol	07	10	01.1	-64	37	08	EA
V0553 Vir	14	24	33.5	-00	47	34	RRAB	AI Vol	07	45	02.4	-71	19	46	M
V0554 Vir	14	24	54.9	-00	19	50	RRAB	AK Vol	07	49	23.1	-65	49	27	RS
V0555 Vir	14	25	13.9	-02	00	38	RRAB	AL Vol	08	16	09.4	-66	44	48	RR(B)
V0556 Vir	14	26	05.7	-00	45	26	RRAB								

Remarks for unusual variable stars (type *).
LT Cnc. Cool sdB star pulsating with a rather long period.
V0484 Hya. Periodically variable brown dwarf.
V0488 Hya. Periodically variable brown dwarf.
BH Lep. Periodically variable brown dwarf.
AY Sex. Millisecond radio pulsar. Optical variations with the orbital period.
V0472 Vel. Atypical emission-line star with periodic brightness variations.

Table 2. Novae

GCVS	Nova name	GCVS	Nova name
V1723 Aql	Nova Aql 2010	V5588 Sgr	Nova Sgr 2011 No. 2
PR Lup	Nova Lup 2011	V1312 Sco	Nova Sco 2011 No. 1
V5587 Sgr	Nova Sgr 2011 No. 1	V1313 Sco	Nova Sco 2011 No. 2

Table 3. Young variables

GCVS	Type	GCVS	Type
V1180 Cas	INT	V2495 Cyg	FU
GM Cha	INT	V0899 Mon	INT
V2492 Cyg	INT	V2675 Oph	INT
V2493 Cyg	FU	V2775 Ori	FU:
V2494 Cyg	FU	V0646 Pup	FU:

ERRATUM FOR IBVS 6008

In the 80th Name-list of Variable Stars, Part II (IBVS No. 6008), it was overlooked by the authors that the name V0900 Mon had been reserved in Central Bureau Electronic Telegram (CBET) No. 2795, 2011 for another variable, and the name was used for a second time. To avoid further confusion, the GCVS team restores the name V0900 Mon for the star announced in CBET No. 2795:

V0900 Mon 06 57 22.2 -08 23 18 FU

The star erroneously named V0900 Mon should now be called V0958 Mon:

V0958 Mon 06 22 06.4 +04 28 17 EW

The authors are grateful to P. Wils and S. Otero for notifying them about the mistake.

COMMISSIONS 27 AND 42 OF THE IAU
INFORMATION BULLETIN ON VARIABLE STARS

Number 6009

Konkoly Observatory
Budapest
12 January 2012

HU ISSN 0374 – 0676

THE GEOS RR Lyr SURVEY

Fourteenth list of maxima of RR Lyr stars observed by the automated telescopes TAROT

(GEOS Circular RR 48)

LE BORGNE, J. F.[1,2,3]; KLOTZ, A.[2,3,4]; BOËR, M.[5]

[1] GEOS (Groupe Européen d'Observations Stellaires), 23 Parc de Levesville, 28300 Bailleau l'Evêque, France

[2] Université de Toulouse; UPS-OMP; IRAP; Toulouse, France

[3] CNRS; IRAP; 14, avenue Edouard Belin, F-31400 Toulouse, France

[4] Observatoire de Haute-Provence, Saint Michel l'Observatoire, France

[5] Artémis, CNRS, Observatoire de la Côte d'Azur, Université de Nice Sophia Antipolis, Nice, France

We present here the fourteenth list of light maxima of RR Lyrae stars from the GEOS RR Lyr Survey (Le Borgne et al. 2007), a GEOS program (`http://geos.webs.upv.es/`, Boninsegna et al., 2002) of observations of RR Lyr stars using the automatic telescopes TAROT (`http://tarot.obs-hp.fr`, Klotz et al., 2009). The present list contains 819 maxima (Table 1), 789 maxima observed between January and December 2011 and 30 older maxima recovered from Tarot image archive.
A description of the present list may be found in the former lists (for example Le Borgne et al. 2008). The data are also available in the GEOS RR Lyr web database (`http://rr-lyr.ast.obs-mip.fr/dbrr/dbrr-V1.0_0.php`). The $O-C$ residuals are computed with the most recent GCVS elements (Samus et al., 2011) when available. Otherwise, the reference of the elements, if exists, is given as a footnote to Table 1. All stars are of RRab type except NU And which is an RRc star.

References:

Agerer, F., Moschner, W., 1996, *IBVS*, **4391**
Baldwin, M.E., Samolyk, G., 2003, *AAVSO RR Lyrae Monographs*, **1**
Boninsegna, R., 1990, *JAAVSO*, **19**, 126
Boninsegna, R., Vandenbroere, J., Le Borgne, J. F., The GEOS Team, 2002, *ASP Conf. Ser.*, **259**, 166, IAU Colloq. 185
Samus N.N., Durlevich O.V., Kazarovets E V., Kireeva N.N., Pastukhova E.N., Zharova A.V., et al. 2011, General Catalog of Variable Stars (GCVS database, Version 2011Jan, http://www.sai.msu.su/gcvs/gcvs/index.htm)
Klotz, A., Boër, M., Atteia, J. L., Gendre, B., 2009, *AJ* **137**, 4100
Le Borgne, J. F., Klotz, A., Boër, 2008, *IBVS*, **5823**
Le Borgne, J. F., Paschke, A., Vandenbroere, J., Poretti, E., Klotz, A., Boër, M., Damerdji, Y., Martignoni, M., Acerbi, F., 2007, *A&A*, **476**, 307
Vandenbroere, J., 1995, *IBVS*, **4241**
Vandenbroere, J., Paris, B., Verrot, J.P., 1999, *IBVS*, **4815**

Table 1: Maxima of RR Lyrae stars

Variable star	Maximum HJD 24...	$O-C$ (days)	E	Obs	Variable star	Maximum HJD 24...	$O-C$ (days)	E	Obs.
SW And	55811.515±0.002	0.000	4694	C	VX Aps	55685.576±0.002	−0.238	44258	LS
SW And	55814.612±0.003	0.001	4701	C	VX Aps	55692.843±0.002	−0.240	44273	LS
SW And	55837.611±0.001	0.003	4753	C	VX Aps	55699.628±0.002	−0.239	44287	LS
SW And	55839.382±0.002	0.005	4757	C	VX Aps	55797.550±0.002	−0.201	44489	LS
SW And	55865.477±0.002	0.006	4816	C	VX Aps	55810.637±0.002	−0.199	44516	LS
SW And	55908.373±0.002	0.002	4913	C	XZ Aps	55668.544±0.003	−0.020	45883	LS
XX And	55782.424±0.002	0.003	2933	C	XZ Aps	55689.684±0.003	−0.028	45919	LS
XX And	55787.480±0.002	−0.001	2940	C	XZ Aps	55699.665±0.002	−0.033	45936	LS
XX And	55803.385±0.004	0.004	2962	C	XZ Aps	55729.617±0.002	−0.040	45987	LS
XX And	55805.552±0.005	0.002	2965	C	XZ Aps	55673.828±0.002	−0.023	45892	LS
XX And	55813.499±0.002	−0.001	2976	C	XZ Aps	55700.843±0.000	−0.030	45938	LS
XX And	55842.410±0.004	−0.000	3016	C	XZ Aps	55786.583±0.002	−0.056	46084	LS
XX And	55879.272±0.003	0.001	3067	C	BS Aps	55656.874±0.006	0.027	31305	LS
XX And	55889.392±0.003	0.003	3081	C	BS Aps	55669.691±0.003	0.028	31327	LS
XX And	55892.285±0.005	0.005	3085	C	BS Aps	55684.825±0.002	0.015	31353	LS
XX And	55910.351±0.002	0.002	3110	C	BS Aps	55708.716±0.002	0.022	31394	LS
AT And	55796.481±0.004	0.014	4067	C	BS Aps	55729.682±0.003	0.016	31430	LS
AT And	55801.415±0.003	0.013	4075	C	BS Aps	55785.614±0.002	0.022	31526	LS
AT And	55814.367±0.003	0.010	4096	C	BS Aps	55813.578±0.004	0.024	31574	LS
AT And	55815.605±0.003	0.014	4098	C	EX Aps	55683.850±0.002	0.017	58818	LS
AT And	55823.621±0.005	0.010	4111	C	EX Aps	55696.589±0.003	0.017	58845	LS
AT And	55888.398±0.004	0.011	4216	C	EX Aps	55724.895±0.002	0.016	58905	LS
AT And	55893.335±0.003	0.013	4224	C	EX Aps	55741.881±0.002	0.017	58941	LS
AT And	55904.436±0.002	0.009	4242	C	EX Aps	55764.528±0.002	0.017	58989	LS
AT And	55906.292±0.006	0.015	4245	C	EX Aps	55839.543±0.004	0.016	59148	LS
CI And	55782.526±0.002	−0.005	8955	C	SW Aqr	55765.507±0.001	0.020	6246	C
CI And	55784.463±0.002	−0.006	8959	C	SW Aqr	55770.561±0.001	0.021	6257	C
CI And	55785.432±0.001	−0.007	8961	C	SW Aqr	55783.422±0.002	0.022	6285	C
CI And	55811.603±0.002	−0.011	9015	C	SW Aqr	55799.497±0.001	0.022	6320	C
CI And	55813.543±0.002	−0.010	9019	C	SW Aqr	55804.550±0.002	0.022	6331	C
CI And	55836.323±0.002	−0.012	9066	C	SW Aqr	55834.403±0.001	0.020	6396	C
CI And	55842.627±0.002	−0.010	9079	C	SW Aqr	55846.348±0.002	0.023	6422	C
CI And	55843.594±0.002	−0.012	9081	C	SX Aqr	55753.521±0.002	−0.002	3492	C
DR And	55880.331±0.002	−0.067	5789	C	SX Aqr	55796.376±0.002	−0.003	3572	C
DR And	55916.348±0.003	−0.090	5853	C	SX Aqr	55799.590±0.002	−0.004	3578	C
NU And	55880.318±0.014	0.077	54950	C	SX Aqr	55804.411±0.002	−0.004	3587	C
NX And	55782.392±0.007	0.019	26450	C	TZ Aqr	55777.439±0.003	0.022	4998	C
NX And	55787.568±0.006	0.010	26458	C	WZ Aqr	55708.852±0.002	−0.022	4445	LS
NX And	55813.490±0.006	0.011	26498	C	WZ Aqr	55818.577±0.002	−0.024	4667	LS
BK Ant	55614.691±0.003	0.016	4799	LS	AA Aqr	55743.802±0.002	−0.021	3554	LS
TY Aps	54299.508±0.003	0.040	29048	LS	AA Aqr	55810.781±0.003	−0.020	3664	LS
TY Aps	55657.604±0.002	0.052	31755	LS	BO Aqr	55748.873±0.005	0.028	4072	LS
TY Aps	55665.632±0.002	0.053	31771	LS	BR Aqr	55796.596±0.001	0.003	7736	C
TY Aps	55670.643±0.002	0.047	31781	LS	BR Aqr	55797.559±0.002	0.002	7738	C
TY Aps	55685.691±0.002	0.044	31811	LS	BR Aqr	55862.613±0.002	0.003	7873	LS
TY Aps	55698.732±0.002	0.041	31837	LS	CP Aqr	55795.447±0.001	0.008	7986	C
TY Aps	55704.748±0.002	0.037	31849	LS	CP Aqr	55801.470±0.002	0.007	7999	C
TY Aps	55782.525±0.001	0.051	32004	LS	CP Aqr	55802.398±0.002	0.008	8001	C
TY Aps	55784.534±0.002	0.053	32008	LS	CP Aqr	55818.617±0.001	0.008	8036	LS
TY Aps	55785.535±0.002	0.051	32010	LS	CP Aqr	55828.347±0.002	0.006	8057	C
TY Aps	55786.538±0.003	0.051	32012	LS	DN Aqr	55783.843±0.004	−0.014	5917	LS
TY Aps	55791.551±0.003	0.047	32022	LS	OX Aqr	55771.831±0.003	0.094	5349	LS
VX Aps	54223.836±0.003	−0.006	41241	LS	AA Aql	55749.812±0.003	0.038	86798	LS
VX Aps	55667.649±0.002	−0.236	44221	LS	AA Aql	55754.516±0.002	0.038	86811	C
VX Aps	55668.616±0.003	−0.238	44223	LS	AA Aql	55763.561±0.002	0.039	86836	C
VX Aps	55684.605±0.003	−0.240	44256	LS	AA Aql	55766.455±0.001	0.038	86844	C

Table 1 (cont.): Maxima of RR Lyrae stars

Variable star	Maximum HJD 24...	$O-C$ (days)	E	Obs	Variable star	Maximum HJD 24...	$O-C$ (days)	E	Obs.
AA Aql	55768.624±0.001	0.036	86850	LS	CM Boo	55657.537±0.003	−0.005	2947	C
AA Aql	55771.520±0.002	0.039	86858	C	U Cae	55910.748±0.001	−0.145	51445	LS
AA Aql	55779.478±0.002	0.037	86880	C	AH Cam	55583.478±0.002	−0.470	45709	C
AA Aql	55791.415±0.002	0.035	86913	C	AH Cam	55803.585±0.001	−0.497	46306	C
AA Aql	55799.377±0.001	0.038	86935	C	AH Cam	55810.612±0.002	−0.476	46325	C
AA Aql	55804.442±0.001	0.038	86949	C	AH Cam	55813.547±0.001	−0.491	46333	C
AA Aql	55818.552±0.001	0.038	86988	LS	AH Cam	55817.601±0.003	−0.493	46344	C
AA Aql	55824.338±0.002	0.036	87004	C	AH Cam	55831.631±0.002	−0.475	46382	C
AA Aql	55828.319±0.002	0.037	87015	C	AH Cam	55838.607±0.002	−0.505	46401	C
V341 Aql	55713.854±0.002	0.039	25116	LS	AH Cam	55840.479±0.003	−0.477	46406	C
V341 Aql	55763.562±0.002	0.037	25202	C	AH Cam	55841.586±0.003	−0.476	46409	C
V341 Aql	55792.462±0.001	0.036	25252	C	RW Cnc	55875.643±0.002	0.213	29823	C
V341 Aql	55796.509±0.002	0.037	25259	C	RW Cnc	55904.641±0.001	0.210	29876	C
V341 Aql	55799.400±0.001	0.038	25264	C	RW Cnc	55915.597±0.002	0.222	29896	C
V341 Aql	55836.391±0.002	0.036	25328	C	SS Cnc	55888.536±0.001	0.059	89318	C
S Ara	55412.581±0.002	−0.049	5860	LS	SS Cnc	55893.678±0.001	0.058	89332	C
IN Ara	55710.872±0.003	0.025	4605	LS	TT Cnc	55577.379±0.002	0.108	27745	C
IN Ara	55786.633±0.003	0.007	4725	LS	TT Cnc	55586.392±0.003	0.106	27761	C
MS Ara	55748.767±0.003	−0.051	5391	LS	TT Cnc	55600.492±0.002	0.120	27786	C
X Ari	55587.395±0.002	0.033	4135	C	TT Cnc	55626.399±0.002	0.108	27832	C
X Ari	55589.351±0.003	0.035	4138	C	TT Cnc	55872.640±0.002	0.122	28269	C
X Ari	55816.613±0.003	0.042	4487	C	TT Cnc	55889.538±0.003	0.116	28299	C
X Ari	55844.607±0.004	0.036	4530	C	AN Cnc	55918.667±0.002	0.156	32197	C
X Ari	55893.448±0.002	0.039	4605	C	AS Cnc	55914.592±0.002	0.390	27066	C
X Ari	55914.286±0.003	0.040	4637	C	AS Cnc	55921.386±0.002	0.391	27077	C
TZ Aur	55613.378±0.002	0.000	4754	C	EZ Cnc [1]	55903.678±0.002	−0.041	16032	C
TZ Aur	55642.364±0.002	0.002	4828	C	EZ Cnc [1]	55915.686±0.001	−0.041	16054	C
TZ Aur	55838.592±0.001	0.001	5329	C	W CVn	55586.530±0.002	−0.144	61955	C
TZ Aur	55849.560±0.002	0.002	5357	C	W CVn	55598.672±0.002	−0.140	61977	C
TZ Aur	55863.659±0.003	0.001	5393	C	W CVn	55614.672±0.002	−0.141	62006	C
TZ Aur	55892.642±0.001	0.000	5467	C	W CVn	55661.571±0.002	−0.142	62091	C
TZ Aur	55903.611±0.001	0.002	5495	C	Z CVn	55577.465±0.002	0.516	25459	C
TZ Aur	55912.618±0.002	0.001	5518	C	Z CVn	55673.601±0.002	0.541	25606	C
TZ Aur	55915.360±0.001	0.001	5525	C	Z CVn	55677.526±0.002	0.543	25612	C
TZ Aur	55923.585±0.001	0.001	5546	C	Z CVn	55692.560±0.003	0.539	25635	C
BH Aur	55914.397±0.001	0.004	4734	C	Z CVn	55700.411±0.002	0.544	25647	C
RS Boo	53089.528±0.002	−0.006	12162	C	RU CVn	55575.665±0.002	0.225	36794	C
RS Boo	53418.574±0.003	0.000	13034	C	RU CVn	55726.431±0.002	0.228	37057	C
RS Boo	53886.466±0.002	−0.008	14274	C	RZ CVn	55599.681±0.002	−0.149	26887	C
RS Boo	55576.569±0.002	−0.007	18753	C	RZ CVn	55627.483±0.002	−0.151	26936	C
RS Boo	55585.627±0.002	−0.005	18777	C	RZ CVn	55643.372±0.002	−0.149	26964	C
RS Boo	55594.681±0.002	−0.007	18801	C	RZ CVn	55698.412±0.002	−0.148	27061	C
RS Boo	55645.624±0.002	−0.004	18936	C	SS CVn	53899.544±0.002	0.165	29835	C
RS Boo	55670.530±0.002	−0.003	19002	C	SS CVn	55577.701±0.001	0.149	33342	C
RS Boo	55733.542±0.002	−0.006	19169	C	SS CVn	55669.576±0.002	0.148	33534	C
ST Boo	53099.533±0.004	0.045	7391	C	SS CVn	55705.454±0.001	0.137	33609	C
ST Boo	53450.504±0.003	0.047	7955	C	UZ CVn	55642.407±0.002	0.252	41868	C
ST Boo	55613.579±0.002	0.056	11431	C	UZ CVn	55683.579±0.003	0.255	41927	C
ST Boo	55735.570±0.002	0.078	11627	C	UZ CVn	55697.536±0.003	0.256	41947	C
ST Boo	55740.546±0.002	0.076	11635	C	UZ CVn	55923.623±0.003	0.261	42271	C
TW Boo	55585.524±0.002	−0.025	7563	C	AA CMi	55586.564±0.003	0.074	39910	C
TW Boo	55587.646±0.003	−0.032	7567	C	AL CMi	55564.757±0.005	0.474	34454	LS
TW Boo	55660.567±0.002	−0.033	7704	C	AL CMi	55574.660±0.003	0.468	34472	LS
TW Boo	55684.518±0.003	−0.034	7749	C	AL CMi	55590.627±0.003	0.471	34501	LS
CM Boo	55596.627±0.003	−0.008	2847	C	AL CMi	55601.639±0.002	0.473	34521	LS
CM Boo	55646.574±0.002	−0.005	2929	C	AL CMi	55901.669±0.002	0.480	35066	C

Table 1 (cont.): Maxima of RR Lyrae stars

Variable star	Maximum HJD 24...	$O-C$ (days)	E	Obs	Variable star	Maximum HJD 24...	$O-C$ (days)	E	Obs.
RV Cap	55722.837±0.005	−0.035	48777	LS	RW Col	55909.777±0.005	−0.005	53098	LS
RV Cap	55765.826±0.003	−0.029	48873	LS	RX Col	55564.649±0.003	−0.050	45034	LS
TX Car	55570.763±0.002	0.131	51576	LS	RX Col	55583.641±0.002	−0.068	45066	LS
TX Car	55582.780±0.002	0.125	51596	LS	RX Col	55903.691±0.005	−0.207	45605	LS
TX Car	55585.784±0.002	0.123	51601	LS	RX Col	55906.659±0.005	−0.209	45610	LS
IU Car	55571.629±0.004	0.196	18824	LS	AV Col	55582.660±0.002	0.058	6225	LS
IU Car	55862.746±0.003	0.140	19219	LS	S Com	55646.623±0.003	−0.103	25558	C
IU Car	55899.594±0.004	0.130	19269	LS	S Com	55910.590±0.003	−0.102	26008	C
V363 Cas	53271.499±0.007	0.491	31340	C	ST Com	55662.424±0.005	−0.033	20767	C
V363 Cas	53323.411±0.009	0.482	31435	C	WW CrA	55679.764±0.002	−0.010	43599	LS
V363 Cas	54011.564±0.007	0.547	32694	C	WW CrA	55712.769±0.003	−0.014	43658	LS
V363 Cas	55753.512±0.004	0.687	35881	C	V413 CrA	55688.762±0.006	0.057	24075	LS
V363 Cas	55758.422±0.005	0.678	35890	C	V413 CrA	55744.752±0.008	0.059	24170	LS
V363 Cas	55764.447±0.006	0.691	35901	C	V413 CrA	55764.784±0.004	0.054	24204	LS
V363 Cas	55771.537±0.003	0.676	35914	C	TV CrB	55617.581±0.002	0.034	41051	C
V363 Cas	55776.451±0.004	0.671	35923	C	TV CrB	55641.544±0.002	0.028	41092	C
V363 Cas	55787.384±0.004	0.674	35943	C	TV CrB	55679.547±0.002	0.031	41157	C
V363 Cas	55789.572±0.004	0.676	35947	C	TV CrB	55741.511±0.002	0.026	41263	C
V363 Cas	55795.594±0.004	0.686	35958	C	TV CrB	55748.527±0.003	0.027	41275	C
V363 Cas	55805.428±0.006	0.682	35976	C	W Crt	55671.631±0.003	−0.026	38900	LS
V363 Cas	55812.554±0.005	0.703	35989	C	SW Cru	55586.758±0.002	0.064	90171	LS
V363 Cas	55818.534±0.004	0.671	36000	C	SW Cru	55607.738±0.003	0.066	90235	LS
V363 Cas	55836.589±0.005	0.691	36033	C	UY Cyg	55728.433±0.002	0.056	59380	C
V363 Cas	55842.589±0.004	0.679	36044	C	UY Cyg	55765.449±0.003	0.066	59446	C
V363 Cas	55845.328±0.005	0.685	36049	C	UY Cyg	55784.506±0.002	0.059	59480	C
V363 Cas	55854.634±0.006	0.700	36066	C	UY Cyg	55811.428±0.003	0.067	59528	C
V363 Cas	55892.354±0.004	0.709	36135	C	UY Cyg	55838.336±0.002	0.061	59576	C
BI Cen	54227.522±0.002	0.022	38698	LS	UY Cyg	55847.305±0.004	0.059	59592	C
BI Cen	55565.813±0.003	0.064	41651	LS	XZ Cyg [2]	55681.544±0.003	−0.010	15240	C
BI Cen	55570.793±0.003	0.059	41662	LS	XZ Cyg [2]	55688.550±0.002	−0.003	15255	C
BI Cen	55600.711±0.003	0.067	41728	LS	XZ Cyg [2]	55730.541±0.001	−0.006	15345	C
BI Cen	55668.683±0.002	0.061	41878	LS	XZ Cyg [2]	55744.529±0.003	−0.016	15375	C
BI Cen	55693.628±0.003	0.081	41933	LS	XZ Cyg [2]	55787.464±0.001	−0.008	15467	C
BI Cen	55694.534±0.003	0.081	41935	LS	XZ Cyg [2]	55795.391±0.002	−0.013	15484	C
BI Cen	55723.525±0.002	0.068	41999	LS	XZ Cyg [2]	55813.605±0.002	0.004	15523	C
BI Cen	55727.600±0.003	0.065	42008	LS	XZ Cyg [2]	55814.539±0.002	0.004	15525	C
V499 Cen	55611.751±0.002	0.034	27792	LS	DM Cyg	55776.579±0.003	0.072	31425	C
V499 Cen	55612.793±0.001	0.035	27794	LS	DM Cyg	55785.393±0.002	0.069	31446	C
AQ Cep	55912.669±0.002	0.070	42650	C	DM Cyg	55851.312±0.002	0.070	31603	C
FP Cep	55818.546±0.003	−0.042	39967	C	V939 Cyg [3]	55681.482±0.005	0.072	15206	C
RR Cet	55824.599±0.003	0.011	40944	C	V939 Cyg [3]	55795.424±0.005	0.079	15500	C
RR Cet	55840.640±0.003	0.014	40973	LS	V939 Cyg [3]	55813.638±0.004	0.079	15547	C
RR Cet	55841.744±0.003	0.012	40975	LS	BV Del	55743.495±0.005	0.023	71357	C
RR Cet	55889.308±0.003	0.016	41061	C	DU Del	55797.480±0.003	−0.180	46539	C
RR Cet	55920.275±0.003	0.013	41117	C	DX Del	55744.519±0.002	0.064	34652	C
RU Cet	55813.789±0.002	0.109	27269	LS	DX Del	55779.494±0.002	0.065	34726	C
RU Cet	55840.765±0.001	0.116	27315	LS	DX Del	55797.452±0.002	0.064	34764	C
RV Cet	55800.834±0.005	0.219	26768	LS	DX Del	55798.397±0.002	0.064	34766	C
RV Cet	55810.818±0.008	0.229	26784	LS	DX Del	55824.393±0.002	0.066	34821	C
RV Cet	55840.776±0.010	0.264	26832	LS	DX Del	55825.336±0.002	0.064	34823	C
RZ Cet	55851.732±0.003	−0.188	42978	LS	DX Del	55834.316±0.002	0.064	34842	C
RZ Cet	55852.761±0.002	−0.181	42980	LS	GV Del	55779.496±0.005	0.006	78516	C
UU Cet	55796.801±0.004	−0.145	24070	LS	GV Del	55797.369±0.006	0.044	78570	C
UU Cet	55810.742±0.004	−0.144	24093	LS	GV Del	55798.443±0.004	0.127	78573	C
RT Col	55903.742±0.003	−0.288	52413	LS	GV Del	55824.413±0.005	0.004	78652	C
RW Col	55908.686±0.002	−0.037	53096	LS	RT Dor	55844.793±0.003	−0.067	51938	LS

Table 1 (cont.): Maxima of RR Lyrae stars

Variable star	Maximum HJD 24...	$O-C$ (days)	E	Obs	Variable star	Maximum HJD 24...	$O-C$ (days)	E	Obs.
VW Dor	55563.801±0.003	−0.143	30116	LS	BD Dra	55784.482±0.002	0.617	23783	C
VW Dor	55578.640±0.002	−0.140	30142	LS	BD Dra	55787.425±0.002	0.615	23788	C
VW Dor	55846.804±0.002	−0.162	30612	LS	BD Dra	55807.457±0.003	0.619	23822	C
VW Dor	55850.804±0.002	−0.157	30619	LS	BD Dra	55817.424±0.005	0.572	23839	C
RW Dra	54256.453±0.002	0.151	33593	C	BD Dra	55821.585±0.003	0.610	23846	C
RW Dra	54904.496±0.005	0.207	35056	C	BD Dra	55831.607±0.002	0.618	23863	C
RW Dra	55628.648±0.002	0.189	36691	C	BD Dra	55840.412±0.004	0.587	23878	C
RW Dra	55669.394±0.002	0.187	36783	C	BD Dra	55841.584±0.005	0.581	23880	C
RW Dra	55726.563±0.001	0.220	36912	C	BD Dra	55903.465±0.002	0.612	23985	C
RW Dra	55757.554±0.002	0.207	36982	C	BK Dra	55739.432±0.002	−0.160	51034	C
RW Dra	55777.489±0.002	0.210	37027	C	BK Dra	55765.482±0.003	−0.162	51078	C
SU Dra	55576.347±0.003	0.056	17677	C	BK Dra	55784.433±0.002	−0.157	51110	C
SU Dra	55579.653±0.004	0.060	17682	C	BK Dra	55803.376±0.002	−0.161	51142	C
SU Dra	55583.612±0.004	0.056	17688	C	BT Dra	55641.416±0.002	−0.016	42310	C
SU Dra	55597.482±0.002	0.057	17709	C	BT Dra	55662.606±0.002	−0.018	42346	C
SU Dra	55626.543±0.003	0.060	17753	C	BT Dra	55741.489±0.003	−0.018	42480	C
SU Dra	55657.580±0.002	0.057	17800	C	RX Eri	55863.741±0.003	−0.008	58189	LS
SW Dra	55589.422±0.002	0.059	51547	C	RX Eri	55910.719±0.003	−0.010	58269	LS
SW Dra	55601.387±0.002	0.060	51568	C	XY Eri	54448.746±0.004	−0.230	53559	LS
SW Dra	55667.468±0.002	0.060	51684	C	RX For	55841.737±0.002	−0.054	26804	LS
SW Dra	55672.597±0.003	0.062	51693	C	SW For	55812.735±0.004	0.446	26711	LS
XZ Dra	55697.578±0.002	−0.130	28897	C	SW For	55824.795±0.005	0.450	26726	LS
XZ Dra	55728.548±0.002	−0.132	28962	C	SW For	55841.667±0.004	0.443	26747	LS
XZ Dra	55749.521±0.002	−0.125	29006	C	RR Gem	53375.528±0.002	−0.323	30250	C
XZ Dra	55758.572±0.002	−0.127	29025	C	RR Gem	55586.435±0.002	−0.449	35815	C
XZ Dra	55779.536±0.002	−0.129	29069	C	RR Gem	55602.325±0.001	−0.452	35855	C
XZ Dra	55790.492±0.002	−0.133	29092	C	RR Gem	55611.466±0.002	−0.449	35878	C
XZ Dra	55791.446±0.002	−0.132	29094	C	SZ Gem	55585.354±0.002	−0.060	56654	C
XZ Dra	55789.545±0.003	−0.127	29090	C	SZ Gem	55598.380±0.002	−0.063	56680	C
XZ Dra	55802.404±0.002	−0.133	29117	C	SZ Gem	55903.569±0.001	−0.067	57289	C
BC Dra	55583.499±0.007	0.096	18490	C	SZ Gem	55913.594±0.002	−0.065	57309	C
BC Dra	55601.489±0.005	0.096	18515	C	SZ Gem	55920.607±0.001	−0.067	57323	C
BC Dra	55611.562±0.005	0.095	18529	C	GI Gem	55597.410±0.001	0.070	58280	C
BC Dra	55627.397±0.004	0.100	18551	C	GI Gem	55865.599±0.001	0.069	58899	C
BC Dra	55657.614±0.006	0.094	18593	C	GI Gem	55912.393±0.002	0.069	59007	C
BC Dra	55683.519±0.005	0.095	18629	C	GI Gem	55913.691±0.001	0.068	59010	C
BC Dra	55691.433±0.004	0.093	18640	C	GI Gem	55922.356±0.002	0.067	59030	C
BC Dra	55760.514±0.003	0.095	18736	C	TW Her	55770.570±0.002	−0.013	85649	C
BC Dra	55765.551±0.003	0.095	18743	C	VX Her	55677.583±0.003	−0.452	74505	C
BC Dra	55778.503±0.003	0.095	18761	C	VX Her	55688.513±0.003	−0.451	74529	C
BC Dra	55791.457±0.004	0.096	18779	C	VZ Her	55656.579±0.001	0.071	42849	C
BC Dra	55834.626±0.005	0.091	18839	C	VZ Her	55753.452±0.002	0.072	43069	C
BC Dra	55840.389±0.006	0.097	18847	C	VZ Her	55779.430±0.002	0.071	43128	C
BC Dra	55845.429±0.004	0.100	18854	C	VZ Her	55801.447±0.001	0.071	43178	C
BC Dra	55879.249±0.005	0.100	18901	C	VZ Her	55812.455±0.002	0.071	43203	C
BD Dra	55589.521±0.002	0.632	23452	C	AR Her	55627.647±0.003	−1.334	30157	C
BD Dra	55595.376±0.003	0.597	23462	C	AR Her	55667.611±0.002	−1.323	30242	C
BD Dra	55613.681±0.004	0.641	23493	C	AR Her	55683.557±0.005	−1.358	30276	C
BD Dra	55625.442±0.003	0.621	23513	C	AR Her	55700.516±0.002	−1.320	30312	C
BD Dra	55672.554±0.004	0.609	23593	C	AR Her	55740.443±0.002	−1.345	30397	C
BD Dra	55691.420±0.005	0.625	23625	C	AR Her	55778.501±0.002	−1.359	30478	C
BD Dra	55728.536±0.002	0.631	23688	C	DL Her	55684.570±0.005	0.046	29539	C
BD Dra	55754.454±0.002	0.631	23732	C	DL Her	55687.524±0.003	0.042	29544	C
BD Dra	55764.429±0.003	0.592	23749	C	DL Her	55748.452±0.003	0.033	29647	C
BD Dra	55771.506±0.004	0.600	23761	C	DL Her	55764.445±0.003	0.052	29674	C
BD Dra	55778.594±0.003	0.620	23773	C	DL Her	55777.442±0.003	0.033	29696	C

Table 1 (cont.): Maxima of RR Lyrae stars

Variable star	Maximum HJD 24...	$O-C$ (days)	E	Obs	Variable star	Maximum HJD 24...	$O-C$ (days)	E	Obs.
V591 Her	55677.605±0.005	0.305	23952	C	AX Leo	55576.662±0.004	−0.027	41732	C
V593 Her	55704.495±0.003	−0.130	31999	C	AX Leo	55579.561±0.007	−0.035	41736	C
V650 Her	55739.518±0.002	0.036	31405	C	AX Leo	55662.417±0.005	−0.038	41850	C
V698 Her	55739.573±0.002	0.127	32092	C	V LMi	55576.411±0.003	0.034	66271	C
UU Hor	55842.805±0.002	0.179	48347	LS	V LMi	55669.422±0.002	0.035	66442	C
UU Hor	55844.740±0.002	0.183	48350	LS	V LMi	55670.508±0.002	0.033	66444	C
UU Hor	55904.599±0.002	0.180	48443	LS	V LMi	55888.619±0.002	0.032	66845	C
SZ Hya	55587.578±0.009	−0.250	27750	C	V LMi	55919.622±0.001	0.032	66902	C
SZ Hya	55627.366±0.002	−0.218	27824	C	U Lep	55563.672±0.005	0.048	24440	LS
UU Hya	55614.612±0.003	0.007	30801	LS	AO Lep	55575.631±0.005	−0.015	3228	LS
UU Hya	55921.624±0.002	0.033	31387	C	VY Lib	55722.531±0.002	−0.036	27303	LS
XX Hya	55591.616±0.002	0.035	31037	LS	VY Lib	55770.590±0.004	−0.031	27393	LS
BI Hya	55577.715±0.002	0.243	52570	LS	XX Lib	55730.644±0.005	0.126	39768	LS
BI Hya	55578.770±0.002	0.244	52572	LS	TT Lyn	55584.602±0.003	−0.046	31691	C
BI Hya	55597.721±0.001	0.243	52608	LS	TT Lyn	55589.387±0.002	−0.041	31699	C
BI Hya	55664.584±0.002	0.245	52735	LS	TT Lyn	55601.334±0.002	−0.042	31719	C
DD Hya	55586.501±0.002	−0.170	27684	C	TT Lyn	55917.376±0.002	−0.043	32248	C
DD Hya	55612.584±0.001	−0.179	27736	LS	TT Lyn	55920.365±0.004	−0.041	32253	C
DD Hya	55614.593±0.001	−0.177	27740	LS	TW Lyn	55584.405±0.003	0.058	21919	C
DD Hya	55622.629±0.001	−0.170	27756	LS	TW Lyn	55587.297±0.002	0.058	21925	C
DD Hya	55889.556±0.002	−0.187	28288	C	TW Lyn	55595.488±0.002	0.058	21942	C
DD Hya	55893.575±0.001	−0.183	28296	C	TW Lyn	55626.331±0.003	0.062	22006	C
DD Hya	55913.647±0.002	−0.182	28336	C	TW Lyn	55845.575±0.002	0.060	22461	C
DD Hya	55914.649±0.001	−0.183	28338	C	TW Lyn	55846.540±0.002	0.061	22463	C
DH Hya	55578.798±0.002	0.077	49903	LS	TW Lyn	55904.362±0.002	0.060	22583	C
ET Hya	55585.650±0.005	0.151	28685	LS	RZ Lyr	53897.517±0.003	0.006	24869	C
ET Hya	55587.711±0.004	0.156	28688	LS	RZ Lyr	53916.435±0.002	0.008	24906	C
FY Hya	55673.724±0.003	0.012	22908	LS	RZ Lyr	55078.462±0.002	−0.018	27179	C
FY Hya	55691.553±0.003	0.015	22936	LS	RZ Lyr	55672.513±0.002	−0.031	28341	C
GO Hya	55587.426±0.003	−0.077	47040	C	RZ Lyr	55673.532±0.002	−0.034	28343	C
GO Hya	55891.644±0.004	−0.076	47518	C	RZ Lyr	55741.543±0.002	−0.019	28476	C
IK Hya	55654.556±0.002	−0.104	26451	LS	RZ Lyr	55758.407±0.003	−0.026	28509	C
TW Hyi	55907.645±0.005	0.013	24345	LS	RZ Lyr	55763.514±0.002	−0.031	28519	C
PW Lac	55743.546±0.001	0.180	35570	C	RZ Lyr	55764.536±0.002	−0.031	28521	C
RR Leo	55576.633±0.003	0.110	27147	C	RZ Lyr	55785.495±0.002	−0.034	28562	C
RR Leo	55614.634±0.003	0.110	27231	C	RZ Lyr	55804.410±0.001	−0.035	28599	C
RR Leo	55643.586±0.001	0.109	27295	C	AW Lyr	55740.525±0.003	−0.046	61130	C
RR Leo	55890.602±0.002	0.118	27841	C	CN Lyr	55740.541±0.002	0.021	27357	C
RR Leo	55904.625±0.001	0.117	27872	C	CN Lyr	55743.421±0.002	0.021	27364	C
RX Leo	55577.572±0.004	0.103	29493	C	CN Lyr	55785.386±0.002	0.025	27466	C
RX Leo	55602.398±0.002	0.099	29531	C	CN Lyr	55792.377±0.002	0.023	27483	C
RX Leo	55658.593±0.003	0.101	29617	C	CN Lyr	55813.356±0.002	0.021	27534	C
RX Leo	55662.509±0.004	0.096	29623	C	CN Lyr	55815.412±0.004	0.020	27539	C
RX Leo	55901.666±0.005	0.105	29989	C	CN Lyr	55841.333±0.003	0.024	27602	C
SS Leo	55579.694±0.002	−0.076	22030	C	CR Lyr	55789.527±0.002	−0.015	52754	C
SS Leo	55598.486±0.002	−0.074	22060	C	CR Lyr	55841.322±0.005	−0.029	52859	C
SS Leo	55625.421±0.004	−0.072	22103	C	EZ Lyr	55402.384±0.003	−0.128	40909	C
SS Leo	55628.548±0.005	−0.076	22108	C	EZ Lyr	55777.421±0.003	−0.132	41623	C
SS Leo	55662.373±0.002	−0.074	22162	C	EZ Lyr	55798.432±0.004	−0.131	41663	C
ST Leo	55596.478±0.002	−0.019	57896	C	EZ Lyr	55807.362±0.003	−0.131	41680	C
ST Leo	55908.601±0.002	−0.020	58549	C	EZ Lyr	55818.394±0.003	−0.130	41701	C
ST Leo	55917.683±0.001	−0.020	58568	C	FN Lyr	55757.550±0.002	0.029	41578	C
TV Leo	55590.706±0.003	0.116	27568	LS	IK Lyr	55779.470±0.006	−0.132	64041	C
TV Leo	55592.725±0.002	0.116	27571	LS	IK Lyr	55831.385±0.003	−0.169	64167	C
AA Leo	55917.717±0.002	−0.088	27263	C	IO Lyr	55660.597±0.002	−0.039	27796	C
AE Leo	55917.599±0.002	0.073	57566	C	IO Lyr	55757.551±0.002	−0.042	27964	C

Table 1 (cont.): Maxima of RR Lyrae stars

Variable star	Maximum HJD 24...	$O-C$ (days)	E	Obs	Variable star	Maximum HJD 24...	$O-C$ (days)	E	Obs.
IO Lyr	55760.441±0.002	−0.038	27969	C	V455 Oph	55799.483±0.003	−0.281	30769	C
IO Lyr	55779.485±0.002	−0.039	28002	C	V784 Oph	55694.852±0.003	0.074	40757	LS
IO Lyr	55783.522±0.002	−0.041	28009	C	CM Ori	55564.651±0.004	−0.011	46143	LS
IO Lyr	55787.570±0.003	−0.033	28016	C	TY Pav	55668.783±0.003	0.190	19899	LS
IO Lyr	55797.376±0.002	−0.038	28033	C	TY Pav	55688.675±0.004	0.191	19927	LS
IO Lyr	55812.384±0.002	−0.036	28059	C	TY Pav	55843.533±0.003	0.182	20145	LS
IO Lyr	55827.387±0.002	−0.037	28085	C	WY Pav	55705.852±0.005	0.055	48995	LS
NQ Lyr	55757.576±0.003	0.001	64488	C	WY Pav	55725.868±0.003	0.059	49029	LS
V340 Lyr	55741.589±0.004	−0.029	44204	C	WY Pav	55787.668±0.005	0.058	49134	LS
AV Men	55901.671±0.003	−0.007	4988	LS	BN Pav	55749.521±0.002	−0.165	48333	LS
AV Men	55907.776±0.002	−0.007	4999	LS	BN Pav	55814.738±0.002	−0.173	48448	LS
Z Mic	55818.663±0.005	−0.124	24230	LS	BN Pav	55818.708±0.004	−0.173	48455	LS
DV Mon	55575.624±0.002	0.060	73366	LS	BP Pav	55696.679±0.002	−0.059	50916	LS
V895 Mon	55585.620±0.002	−0.027	5154	LS	BP Pav	55699.842±0.003	−0.121	50922	LS
TX Mus	55580.816±0.003	0.089	66185	LS	BP Pav	55724.616±0.002	−0.067	50968	LS
TX Mus	55581.764±0.002	0.091	66187	LS	DN Pav	55769.877±0.003	0.114	31138	LS
TX Mus	55670.729±0.002	0.089	66375	LS	DN Pav	55786.741±0.002	0.114	31174	LS
TX Mus	55672.622±0.003	0.089	66379	LS	DN Pav	55817.659±0.002	0.115	31240	LS
TX Mus	55698.649±0.003	0.089	66434	LS	DN Pav	55841.549±0.001	0.115	31291	LS
TX Mus	55725.621±0.002	0.087	66491	LS	VV Peg	55785.589±0.001	−0.017	33572	C
EM Mus	55667.577±0.002	−0.186	36661	LS	VV Peg	55793.401±0.001	−0.018	33588	C
EM Mus	55672.717±0.002	−0.186	36672	LS	VV Peg	55805.611±0.002	−0.019	33613	C
EM Mus	55677.856±0.002	−0.187	36683	LS	VV Peg	55828.564±0.003	−0.020	33660	C
EM Mus	55693.744±0.002	−0.187	36717	LS	VV Peg	55836.379±0.002	−0.019	33676	C
EM Mus	55694.681±0.002	−0.185	36719	LS	VV Peg	55904.267±0.002	−0.017	33815	C
EM Mus	55723.652±0.002	−0.186	36781	LS	AO Peg	55743.516±0.002	0.039	55239	C
Y Oct	55686.649±0.003	−0.310	42232	LS	AV Peg	55744.507±0.002	0.137	30622	C
Y Oct	55741.608±0.002	−0.314	42317	LS	AV Peg	55771.443±0.002	0.137	30691	C
Y Oct	55787.515±0.002	−0.318	42388	LS	AV Peg	55773.395±0.003	0.137	30696	C
RV Oct	55723.604±0.003	0.141	71095	LS	AV Peg	55792.523±0.001	0.137	30745	C
RY Oct	55813.858±0.003	0.052	49384	LS	AV Peg	55797.599±0.001	0.137	30758	C
SS Oct	55727.885±0.004	−0.000	44558	LS	AV Peg	55798.379±0.002	0.137	30760	C
SS Oct	55813.692±0.002	−0.005	44696	LS	AV Peg	55807.359±0.002	0.139	30783	C
SS Oct	55846.656±0.004	0.002	44749	LS	AV Peg	55832.344±0.003	0.140	30847	C
SS Oct	55849.763±0.005	−0.000	44754	LS	BH Peg	55783.532±0.002	−0.143	25614	C
UV Oct	54608.862±0.002	−0.143	37375	LS	BH Peg	55785.457±0.003	−0.141	25617	C
UV Oct	55670.703±0.004	−0.219	39332	LS	BH Peg	55799.557±0.002	−0.143	25639	C
UV Oct	55688.614±0.004	−0.215	39365	LS	BH Peg	55803.401±0.003	−0.144	25645	C
UV Oct	55701.637±0.003	−0.215	39389	LS	BH Peg	55837.380±0.003	−0.138	25698	C
UV Oct	55723.875±0.002	−0.225	39430	LS	BH Peg	55839.304±0.003	−0.137	25701	C
UV Oct	55726.589±0.002	−0.224	39435	LS	CG Peg	55773.570±0.002	−0.054	35688	C
UV Oct	55784.637±0.002	−0.237	39542	LS	CG Peg	55801.597±0.002	−0.056	35748	C
UW Oct	55713.808±0.003	−0.014	48092	LS	CG Peg	55848.310±0.002	−0.056	35848	C
UW Oct	55729.815±0.004	−0.009	48128	LS	CG Peg	55890.353±0.003	−0.056	35938	C
UW Oct	55779.591±0.003	−0.016	48240	LS	CG Peg	55891.288±0.001	−0.055	35940	C
UW Oct	55797.812±0.004	−0.019	48281	LS	CV Peg	55773.401±0.003	−0.059	55125	C
UW Oct	55850.708±0.003	−0.017	48400	LS	CV Peg	55778.468±0.004	−0.058	55134	C
UW Oct	55903.603±0.003	−0.016	48519	LS	DZ Peg	55779.548±0.003	0.166	36039	C
DY Oct	55563.825±0.003	0.002	3213	LS	DZ Peg	55796.555±0.002	0.167	36067	C
ST Oph	55767.539±0.002	−0.026	60710	LS	DZ Peg	55798.378±0.003	0.168	36070	C
V408 Oph	55797.415±0.002			C	DZ Peg	55804.452±0.002	0.169	36080	C
V445 Oph	55678.596±0.002	0.035	70865	C	DZ Peg	55812.348±0.002	0.169	36093	C
V455 Oph	55739.567±0.002	−0.281	30637	C	DZ Peg	55832.387±0.002	0.166	36126	C
V455 Oph	55749.559±0.003	−0.275	30659	C	DZ Peg	55849.397±0.004	0.170	36154	C
V455 Oph	55764.533±0.002	−0.280	30692	C	DZ Peg	55908.306±0.003	0.167	36251	C
V455 Oph	55795.395±0.002	−0.284	30760	C	AR Per	55596.408±0.002	0.059	66642	C

Table 1 (cont.): Maxima of RR Lyrae stars

Variable star	Maximum HJD 24...	$O-C$ (days)	E	Obs	Variable star	Maximum HJD 24...	$O-C$ (days)	E	Obs.
AR Per	55812.589±0.002	0.061	67150	C	CS Ser	55678.781±0.002	0.020	46512	LS
AR Per	55818.546±0.002	0.061	67164	C	RV Sex	55670.652±0.002	0.056	51707	LS
AR Per	55839.400±0.002	0.063	67213	C	SS Tau	55909.668±0.002	0.091	45622	LS
AR Per	55846.633±0.002	0.061	67230	C	GZ Tel	55788.704±0.003	0.007	8051	LS
AR Per	55865.357±0.002	0.061	67274	C	RW TrA	55675.842±0.002	−0.183	37928	LS
RV Phe	55817.833±0.004	−0.200	23310	LS	RW TrA	55697.535±0.002	−0.185	37986	LS
RV Phe	55844.668±0.005	−0.204	23355	LS	RW TrA	55706.887±0.001	−0.183	38011	LS
TZ Phe	55784.724±0.007			LS	RW TrA	55712.871±0.002	−0.185	38027	LS
TZ Phe	55811.806±0.006			LS	RW TrA	55730.827±0.004	−0.183	38075	LS
TZ Phe	55819.807±0.005			LS	RW TrA	55787.678±0.002	−0.186	38227	LS
TZ Phe	55840.729±0.004			LS	RW TrA	55817.603±0.003	−0.185	38307	LS
U Pic	55563.746±0.003	0.069	31558	LS	RW TrA	55844.533±0.002	−0.186	38379	LS
U Pic	55851.752±0.001	0.073	32212	LS	W Tuc	55563.644±0.005	0.177	29094	LS
RY Psc	55812.749±0.002	0.606	24789	LS	AE Tuc	55784.809±0.002	−0.078	51915	LS
XX Pup	55571.629±0.004	0.502	26679	LS	AE Tuc	55785.638±0.001	−0.078	51917	LS
XX Pup	55574.736±0.002	0.506	26685	LS	AE Tuc	55786.882±0.001	−0.077	51920	LS
XX Pup	55615.594±0.002	0.507	26764	LS	AE Tuc	55787.712±0.002	−0.076	51922	LS
XX Pup	55918.672±0.002	0.517	27350	LS	AE Tuc	55812.582±0.001	−0.068	51982	LS
CR Pup	55578.689±0.005	0.319	39323	LS	AE Tuc	55818.800±0.001	−0.065	51997	LS
HH Pup	55576.651±0.003	0.008	43702	LS	AE Tuc	55822.534±0.003	−0.060	52006	LS
HH Pup	55583.687±0.002	0.011	43720	LS	RV UMa	53101.428±0.005	0.092	17147	LS
HH Pup	55910.740±0.001	0.010	44557	LS	RV UMa	53107.512±0.003	0.091	17160	LS
HK Pup	55586.677±0.002	−0.295	25848	LS	RV UMa	53195.503±0.002	0.087	17348	LS
V440 Sgr	55798.583±0.002	0.107	29926	LS	RV UMa	53444.519±0.004	0.095	17880	LS
V440 Sgr	55799.542±0.002	0.111	29928	LS	RV UMa	53488.519±0.003	0.098	17974	LS
V440 Sgr	55819.595±0.003	0.109	29970	LS	RV UMa	55583.585±0.004	0.127	22450	C
V675 Sgr	55705.807±0.003	0.072	42533	LS	RV UMa	55598.559±0.003	0.123	22482	C
V675 Sgr	55723.796±0.002	0.077	42561	LS	RV UMa	55599.490±0.002	0.118	22484	C
V675 Sgr	55770.682±0.003	0.076	42634	LS	RV UMa	55613.539±0.002	0.125	22514	C
V675 Sgr	55788.665±0.002	0.075	42662	LS	RV UMa	55656.597±0.001	0.121	22606	C
V675 Sgr	55797.654±0.003	0.072	42676	LS	RV UMa	55660.343±0.002	0.123	22614	C
V756 Sgr	55669.763±0.002	0.100	50070	LS	RV UMa	55671.577±0.002	0.124	22638	C
V1130 Sgr	55807.622±0.003	0.042	50078	LS	TU UMa	55594.584±0.002	−0.045	22887	C
V1176 Sgr	55680.749±0.002	−0.158	96525	LS	TU UMa	55660.385±0.002	−0.048	23005	C
V1176 Sgr	55788.595±0.002	−0.175	96829	LS	TU UMa	55903.524±0.005	−0.048	23441	C
V1646 Sgr	55698.846±0.002	0.167	39259	LS	AB UMa	55575.501±0.010	0.111	32269	C
V494 Sco	55691.749±0.003	−0.271	34085	LS	AB UMa	55587.505±0.006	0.123	32289	C
V494 Sco	55798.571±0.003	−0.282	34335	LS	AB UMa	55671.445±0.005	0.122	32429	C
V690 Sco	55668.831±0.003	−0.017	28179	LS	AB UMa	55683.433±0.007	0.119	32449	C
V690 Sco	55705.745±0.002	−0.023	28254	LS	AB UMa	55919.684±0.006	0.137	32843	C
V690 Sco	55714.605±0.003	−0.023	28272	LS	AB UMa	55921.481±0.006	0.135	32846	C
V765 Sco	55675.800±0.002	0.145	55794	LS	EX UMa [4]	55578.570±0.003	0.032	12095	C
RU Scl	55820.815±0.003	0.450	50062	LS	EX UMa [4]	55614.383±0.004	0.018	12161	C
RU Scl	55822.787±0.002	0.449	50066	LS	EX UMa [4]	55642.622±0.005	0.030	12213	C
UZ Scl	55783.676±0.005	0.044	37120	LS	EX UMa [4]	55901.559±0.005	0.036	12690	C
VW Scl	55794.731±0.003	−0.003	54775	LS	KT UMa [5]	55575.470±0.010	0.068	10377	C
VW Scl	55843.779±0.002	−0.003	54871	LS	KT UMa [5]	55585.505±0.010	0.066	10393	C
VW Scl	55860.633±0.002	−0.009	54904	LS	KT UMa [5]	55602.423±0.004	0.047	10420	C
VX Scl	54777.746±0.003	−2.016	20657	LS	KT UMa [5]	55603.681±0.004	0.050	10422	C
VX Scl	55788.795±0.004	−1.779	22243	LS	AF Vel	55574.779±0.003	−0.203	26816	LS
AN Ser	55678.525±0.002	0.005	78475	C	AF Vel	55582.697±0.002	−0.196	26831	LS
AV Ser	53845.637±0.002	0.125	52306	LS	AF Vel	55583.751±0.002	−0.197	26833	LS
AV Ser	53892.452±0.002	0.134	52402	LS	AF Vel	55584.804±0.002	−0.199	26835	LS
AV Ser	55683.764±0.004	0.160	56076	LS	AF Vel	55592.721±0.002	−0.193	26850	LS
AV Ser	55691.550±0.002	0.145	56092	C	AF Vel	55610.636±0.002	−0.210	26884	LS
CS Ser	55667.719±0.002	0.021	46491	LS	AF Vel	55705.585±0.004	−0.192	27064	LS

Table 1 (cont.): Maxima of RR Lyrae stars

Variable star	Maximum HJD 24...	$O-C$ (days)	E	Obs	Variable star	Maximum HJD 24...	$O-C$ (days)	E	Obs.
CD Vel	55577.657±0.002	−0.087	46830	LS	AF Vir	55661.516±0.003	−0.191	31685	C
CD Vel	55608.616±0.002	−0.096	46884	LS	AF Vir	55701.664±0.002	−0.195	31768	LS
CD Vel	55663.676±0.002	−0.091	46980	LS	AV Vir	55630.634±0.002	0.021	21556	C
CD Vel	55682.598±0.002	−0.094	47013	LS	DO Vir	55701.742±0.002	0.226	54650	LS
FS Vel	55606.704±0.003	−0.074	33730	LS	V348 Vir	55676.843±0.005	0.143	3326	LS
FS Vel	55675.693±0.002	−0.066	33875	LS	V348 Vir	55744.654±0.005	0.128	3446	LS
FS Vel	55697.573±0.002	−0.070	33921	LS	SV Vol	55695.568±0.003	0.116	36864	LS
FS Vel	55698.525±0.002	−0.069	33923	LS	BN Vul	55733.454±0.003	0.073	17173	C
ST Vir	55662.551±0.002	−0.026	36332	C	BN Vul	55765.538±0.003	0.074	17227	C
UU Vir	55578.636±0.002	0.000	28976	C	BN Vul	55790.487±0.003	0.070	17269	C
UU Vir	55589.576±0.002	0.002	28999	C	BN Vul	55793.459±0.002	0.071	17274	C
UU Vir	55599.561±0.002	−0.001	29020	C	BN Vul	55802.371±0.002	0.071	17289	C
UU Vir	55617.637±0.002	0.002	29058	C	BN Vul	55815.439±0.002	0.068	17311	C
UU Vir	55658.536±0.003	−0.001	29144	C	BN Vul	55818.412±0.002	0.070	17316	C
UU Vir	55671.377±0.002	−0.002	29171	C	BN Vul	55827.324±0.001	0.071	17331	C
UV Vir	55601.492±0.002	0.012	26587	C	BN Vul	55843.364±0.004	0.069	17358	C
UV Vir	55602.666±0.002	0.012	26589	C	BN Vul	55849.306±0.001	0.070	17368	C
AF Vir	55656.677±0.003	−0.192	31675	LS					

* C = Calern, LS = La Silla
1 Boninsegna, 1990
2 Baldwin and Samolyk, 2003
3 Agerer and Moschner, 1996
4 Vandenbroere, 1995
5 Vandenbroere et al., 1999

COMMISSIONS 27 AND 42 OF THE IAU
INFORMATION BULLETIN ON VARIABLE STARS

Number 6010

Konkoly Observatory
Budapest
18 January 2012

HU ISSN 0374 – 0676

BAV-RESULTS OF OBSERVATIONS - PHOTOELECTRIC MINIMA OF SELECTED ECLIPSING BINARIES AND MAXIMA OF PULSATING STARS

(BAV MITTEILUNGEN NO. 220)

HÜBSCHER, JOACHIM; LEHMANN, PETER B.; WALTER, FRANK

Bundesdeutsche Arbeitsgemeinschaft für Veränderliche Sterne e.V. (BAV), Munsterdamm 90, 12169 Berlin, Germany, www.bav-astro.de, publikat@bav-astro.de

In this 71st compilation of BAV results, photoelectric observations obtained mostly in the year 2011 are presented on 641 variable stars giving 1,071 minima on eclipsing binaries and maxima on pulsating stars. All moments of minima and maxima are heliocentric UTC. The errors are tabulated in column '±'. The values in column '$O - C$' are determined without incorporation of nonlinear terms. The references are given in the section 'Remarks'. All information about photometers and filters are specified in the column 'Rem'. The observations were made at private observatories. The photoelectric measurements and all the lightcurves with evaluations can be obtained from the office of the BAV for inspection.

Please use the following link for an easy access to all the publications of the BAV including the "Lichtenknecker Database of the BAV": `http://www.bav-astro.de/sfs` .

Table 1: Times of minima of eclipsing binaries

Variable	HJD 24.....	±	Obs	$O-C$		Bibliography	Fil	n	Rem
RT And	55233.3594	.0035	PGL	−0.2714		GCVS 2009	V	331	17)
	55758.5155	.0012	AG	−0.2649		GCVS 2009	-Ir	32	11)
AB And	53674.2869	.0060	BO	−0.0041		GCVS 2009	o	145	18)
	53750.2929	.0003	BO	−0.0012		GCVS 2009	o	229	18)
	53752.2818	.0060	BO	−0.0036		GCVS 2009	o	248	18)
AS And	55482.3793	.0003	MS FR				o	675	5)
BD And	55480.5562	.0001	RAT RCR	−0.0180		GCVS 2009	-Ir	268	15)
DO And	55480.3515	.0001	MS FR	+0.0217		GCVS 2009	o	540	5)
KP And	55481.5462	.0002	RAT RCR	+0.0470		GCVS 2009	-Ir	298	15)
V422 And	55758.5142	.0021	AG	−0.0028		GCVS 2009	-Ir	32	11)
OO Aql	52915.3215	.0032	BO	+0.0216		GCVS 2009	o	145	18)
V640 Aql	55705.5011	.0002	MS FR	−0.0628	s	GCVS 2009	o	624	5)
V694 Aql	55673.5926	.0002	MS FR	+0.0243		IBVS 4481	o	470	5)
V1045 Aql	55727.4810	.0004	MS FR	−0.0135		GCVS 2009	o	624	5)
V1353 Aql	55369.4744	.0002	RAT RCR	+0.0226		BAVR 44,62	-Ir	159	15)
V1430 Aql	55479.3606	.0035	PGL	−0.0103	s	AJ 119,2391	V	392	17)
	55483.2911	.0035	PGL	−0.0115		AJ 119,2391	V	227	17)
	55689.4890	.0035	PGL	−0.0122		AJ 119,2391	V	227	17)
V1542 Aql	55784.3806	.0040	WTR	+0.0095		IBVS 5161	-Ir	77	8)
AH Aur	55623.3779	.0008	JU	−0.1045		BAVR 35,41	o	90	2)
DO Aur	55616.3336	.0021	FR	+0.0852	s	GCVS 2009	-Ir	40	11)
EM Aur	55616.2889	.0018	FR	−0.1994		GCVS 2009	-Ir	44	11)
GI Aur	55624.3047	.0022	JU	+0.0297		GCVS 2009	o	70	2)
V404 Aur	55480.5883	.0001	MS FR				o	540	5)

Table 1: (cont.)

Variable	HJD 24.....	±	Obs	$O-C$		Bibliography	Fil	n	Rem
V426 Aur	55640.2892	.0017	FR				-Ir	151	11)
SU Boo	55615.5842	.0019	SCI	+0.0140		GCVS 2009	o	90	2)
	55687.4067	.0022	AG	+0.0190		GCVS 2009	-Ir	71	11)
TU Boo	55661.4382	.0004	AG	+0.0271		GCVS 2009	-Ir	34	11)
	55661.6007	.0010	AG	+0.0275	s	GCVS 2009	-Ir	34	11)
TX Boo	55681.4483	.0115	AG	+0.8146	s	GCVS 2009	-Ir	95	11)
TY Boo	55642.3477	.0008	AG	−0.0370	s	BAVM 68	V	61	11)
	55642.5067	.0005	AG	−0.0366		BAVM 68	V	61	11)
	55648.3732	.0002	MS FR	−0.0374	s	BAVM 68	o	504	5)
TZ Boo	55622.6016	.0001	GB	−0.0322		BAVM 68	V	126	1)
	55623.4931	.0002	GB	−0.0321		BAVM 68	V	83	1)
	55624.5339	.0001	GB	−0.0314	s	BAVM 68	V	108	1)
	55625.5705	.0004	GB	−0.0348		BAVM 68	V	132	1)
	55626.4647	.0001	GB	−0.0321		BAVM 68	V	108	1)
	55626.6139	.0001	GB	−0.0315	s	BAVM 68	V	108	1)
	55627.5050	.0001	GB	−0.0318	s	BAVM 68	V	108	1)
	55627.6538	.0001	GB	−0.0316		BAVM 68	V	94	1)
	55628.5450	.0001	GB	−0.0319		BAVM 68	V	121	1)
	55629.4367	.0002	GB	−0.0317		BAVM 68	V	79	1)
	55629.5852	.0001	GB	−0.0317	s	BAVM 68	V	109	1)
	55632.5571	.0001	GB	−0.0314	s	BAVM 68	V	109	1)
	55635.5280	.0002	GB	−0.0321	s	BAVM 68	V	87	1)
	55640.5803	.0001	GB	−0.0314	s	BAVM 68	V	97	1)
	55642.3658	.0020	AG	−0.0289	s	BAVM 68	V	56	11)
	55642.5078	.0046	AG	−0.0355		BAVM 68	V	56	11)
	55642.5117	.0002	GB	−0.0316		BAVM 68	V	97	1)
	55642.6603	.0002	GB	−0.0315	s	BAVM 68	V	67	1)
	55643.5520	.0002	GB	−0.0313	s	BAVM 68	V	97	1)
	55650.3862	.0006	MS FR	−0.0317	s	BAVM 68	o	335	5)
	55662.4213	.0002	GB	−0.0314		BAVM 68	V	105	1)
	55689.4613	.0002	GB	−0.0327		BAVM 68	V	112	1)
	55690.5016	.0001	GB	−0.0325	s	BAVM 68	V	93	1)
	55691.3928	.0002	GB	−0.0327	s	BAVM 68	V	94	1)
	55695.4064	.0001	GB	−0.0307		BAVM 68	V	93	1)
	55700.4569	.0001	GB	−0.0319		BAVM 68	B	41	1)
	55700.4583	.0004	GB	−0.0305		BAVM 68	V	46	1)
	55702.3880	.0003	GB	−0.0323	s	BAVM 68	V	44	1)
	55702.3886	.0001	GB	−0.0317	s	BAVM 68	B	44	1)
	55706.5482	.0002	GB	−0.0323	s	BAVM 68	V	42	1)
	55706.5486	.0002	GB	−0.0319	s	BAVM 68	B	42	1)
	55707.4399	.0002	GB	−0.0321	s	BAVM 68	V	47	1)
	55707.4402	.0001	GB	−0.0318	s	BAVM 68	B	49	1)
	55711.4540	.0003	GB	−0.0296		BAVM 68	V	47	1)
	55711.4541	.0002	GB	−0.0295		BAVM 68	B	47	1)
	55712.4915	.0001	GB	−0.0321	s	BAVM 68	V	46	1)
	55712.4917	.0001	GB	−0.0319	s	BAVM 68	B	48	1)
	55739.5339	.0002	GB	−0.0310	s	BAVM 68	B	43	1)
	55739.5339	.0001	GB	−0.0310	s	BAVM 68	V	44	1)
	55740.4252	.0002	GB	−0.0312	s	BAVM 68	V	47	1)
	55740.4253	.0002	GB	−0.0311	s	BAVM 68	B	47	1)
	55741.4675	.0004	GB	−0.0289		BAVM 68	V	53	1)
	55741.4679	.0003	GB	−0.0285		BAVM 68	B	43	1)
	55743.3969	.0003	GB	−0.0310	s	BAVM 68	B	40	1)
	55743.3971	.0002	GB	−0.0308	s	BAVM 68	V	40	1)
UW Boo	55676.4331	.0013	MS FR	−0.0072	s	GCVS 2009	o	462	5)
VW Boo	55280.4598	.0004	MS FR	−0.0710	s	BAVR 32,122	o	351	5)
	55624.4853	.0003	MS FR	−0.0770	s	BAVR 32,122	o	396	5)
AC Boo	55619.4703	.0035	PGL	+0.0200		GCVS 2009	o	199	10)
	55621.4089	.0035	PGL	+0.0203	s	GCVS 2009	V	209	10)

Table 1: (cont.)

Variable	HJD 24.....	±	Obs	$O-C$		Bibliography	Fil	n	Rem
AC Boo	55624.5804	.0015	SCI	+0.0199	s	GCVS 2009	o	104	2)
	55625.4613	.0017	SCI	+0.0197		GCVS 2009	o	66	2)
	55625.6406	.0015	SCI	+0.0228	s	GCVS 2009	o	93	2)
	55628.4589	.0009	FR	+0.0217	s	GCVS 2009	-Ir	96	11)
	55628.6336	.0001	FR	+0.0202		GCVS 2009	-Ir	96	11)
	55640.4410	.0017	SCI	+0.0212	s	GCVS 2009	o	110	2)
	55640.6169	.0017	SCI	+0.0209		GCVS 2009	o	123	2)
	55641.323 :	.007	PGL	+0.022		GCVS 2009	V	171	10)
	55642.3793	.0001	FR	+0.0211		GCVS 2009	-Ir	81	11)
	55642.5573	.0003	FR	+0.0229	s	GCVS 2009	-Ir	81	11)
	55644.4939	.0001	MS FR	+0.0211		GCVS 2009	o	330	5)
AD Boo	55654.3923	.0019	SCI	+0.0283		GCVS 2009	o	183	2)
	55654.3941	.0011	AG	+0.0301		GCVS 2009	-Ir	65	11)
AQ Boo	55658.3588	.0003	MS FR				o	420	5)
AR Boo	55686.5190	.0022	AG	+0.0872		GCVS 2009	-Ir	48	11)
BG Boo	55648.6293	.0015	SCI	−0.0628	s	GCVS 2009	o	40	2)
	55649.6139	.0021	SCI	−0.0383		GCVS 2009	o	42	2)
CV Boo	55642.4851	.0007	AG	−0.0088	s	BAVR 49,117	V	61	11)
	55662.3878	.0005	SIR	−0.0104		BAVR 49,117	o	123	4)
DU Boo	55682.4886	.0150	AG				-Ir	81	11)
ET Boo	55628.4607	.0002	FR				-Ir	68	11)
	55642.3295	.0003	FR				-Ir	96	11)
	55642.6513	.0004	FR				-Ir	96	11)
	55758.4352	.0015	JU				o	60	2)
EW Boo	55642.5499	.0044	AG				V	61	11)
FI Boo	55627.5413	.0074	AG				V	61	11)
FY Boo	55686.4685	.0008	AG				-Ir	48	11)
	55686.5877	.0011	AG				-Ir	48	11)
GK Boo	55353.4489	.0001	RAT RCR				-Ir	230	15)
GL Boo	55654.4365	.0022	AG				-Ir	79	11)
GM Boo	55654.4777	.0021	AG				-Ir	66	11)
	55671.4512	.0007	MS FR				o	531	5)
GN Boo	55654.3994	.0012	FR				o	47	14)
	55654.5454	.0009	FR				o	47	14)
	55687.4214	.0012	AG				-Ir	71	11)
	55687.5750	.0014	AG				-Ir	71	11)
GQ Boo	55654.4942	.0025	AG				-Ir	66	11)
	55667.3784	.0003	MS FR				o	530	5)
GR Boo	55654.4247	.0022	AG				-Ir	66	11)
	55654.6138	.0016	AG				-Ir	66	11)
GV Boo	55624.4476	.0016	AG	−0.0704		GCVS 2009	-Ir	36	11)
	55624.6343	.0019	AG	−0.0676	s	GCVS 2009	-Ir	36	11)
	55661.6030	.0023	AG	−0.0708		GCVS 2009	-Ir	34	11)
GX Boo	55686.5466	.0107	AG	+0.0219		GCVS 2009	-Ir	48	11)
HR Boo	55654.4630	.0029	AG	−0.0407		GCVS 2009	-Ir	65	11)
	55654.6178	.0004	AG	−0.0439	s	GCVS 2009	-Ir	65	11)
Y Cam	55624.5320	.0270	AG	+0.4102	s	GCVS 2009	-Ir	94	11)
SV Cam	55589.4231	.0035	PGL	+0.0523		GCVS 2009	V	523	17)
UU Cam	55670.3962	.0035	AG	+0.0282		GCVS 2009	-Ir	86	11)
AK Cam	55624.4063	.0047	AG	+0.0364		BAVM 69	-Ir	94	11)
	55654.4705	.0262	AG	+0.0388	s	BAVM 69	-Ir	108	11)
AL Cam	55645.4510	.0037	AG	−0.0324		GCVS 2009	-Ir	342	11)
AN Cam	55627.6431	.0065	AG	−4.8515		GCVS 2009	-Ir	140	11)
AO Cam	55584.3608	.0002	JU	+0.0589	s	GCVS 2009	o	70	2)
AT Cam	55590.4187	.0035	PGL	−0.0226		BAVR 32,36	V	203	17)
AY Cam	55624.3796	.0053	AG	+0.0118	s	GCVS 2009	-Ir	94	11)
	55654.4649	.0061	AG	+0.0124	s	GCVS 2009	-Ir	108	11)
CD Cam	55644.4373	.0144	AG				-Ir	79	11)
FN Cam	55654.3513	.0028	AG				-Ir	108	11)

Table 1: (cont.)

Variable	HJD 24.....	±	Obs	$O-C$		Bibliography	Fil	n	Rem
HW Cam	55600.3101	.0004	JU				o	57	2)
NO Cam	55627.3569	.0047	AG	+0.0386		GCVS 2007	-Ir	131	11)
	55627.5705	.0042	AG	+0.0369	s	GCVS 2007	-Ir	131	11)
	55670.4308	.0037	AG	+0.0375		GCVS 2007	-Ir	86	11)
NQ Cam	55644.4862	.0011	AG	−0.0816		GCVS 2007	-Ir	78	11)
NR Cam	55624.3021	.0010	AG	+0.0063		GCVS 2009	-Ir	94	11)
	55624.4291	.0014	AG	+0.0054	s	GCVS 2009	-Ir	94	11)
	55624.5577	.0011	AG	+0.0060		GCVS 2009	-Ir	94	11)
NS Cam	55644.4303	.0076	AG	−0.0557		GCVS 2007	-Ir	67	11)
RY Cnc	55650.4399	.0001	FR	+0.0709		GCVS 2009	-Ir	69	11)
TU Cnc	55648.4197	.0021	SCI	−0.0624		GCVS 2009	o	145	2)
TX Cnc	55622.4497	.0048	AG	+0.0396		GCVS 2009	-Ir	88	11)
WW Cnc	55628.4586	.0009	AG	−0.0844		BAVR 32,36	V	50	11)
	55628.4588	.0010	AG	−0.0842		BAVR 32,36	B	45	11)
WX Cnc	55628.3258	.0038	AG	+0.0126	s	GCVS 2009	B	50	11)
	55628.3263	.0042	AG	+0.0131	s	GCVS 2009	V	50	11)
WY Cnc	55618.3763	.0037	DIE	−0.0355		GCVS 2009	o	30	14)
	55628.3289	.0005	DIE	−0.0353		GCVS 2009	o	36	14)
YY Cnc	55628.3580	.0033	AG				B	46	11)
	55628.3590	.0047	AG				V	49	11)
AC Cnc	55621.3118	.0008	AG	−0.0105		GCVS 2009	-Ir	40	11)
	55621.4598	.0009	AG	−0.0128	s	GCVS 2009	-Ir	40	11)
	55621.6139	.0009	AG	−0.0089		GCVS 2009	-Ir	40	11)
AD Cnc	55621.3014	.0006	AG	−0.0189		GCVS 2009	-Ir	39	11)
	55621.4443	.0022	AG	−0.0174	s	GCVS 2009	-Ir	39	11)
	55621.5826	.0017	AG	−0.0204		GCVS 2009	-Ir	39	11)
AE Cnc	55621.4657	.0025	AG	−0.1087		GCVS 2009	-Ir	38	11)
AH Cnc	55621.4321	.0025	AG	−0.0469	s	GCVS 2009	R	40	11)
	55621.4323	.0036	AG	−0.0467	s	GCVS 2009	B	40	11)
	55621.4325	.0030	AG	−0.0465	s	GCVS 2009	I	40	11)
	55621.4330	.0039	AG	−0.0460	s	GCVS 2009	V	41	11)
	55621.4331	.0025	AG	−0.0459	s	GCVS 2009	-Ir	41	11)
	55625.4152	.0021	SCI	−0.0286	s	GCVS 2009	o	40	2)
	55649.3804	.0011	SCI	−0.0327		GCVS 2009	o	39	2)
EH Cnc	55259.2970	.0001	RAT RCR				-Ir	72	15)
	55622.5675	.0029	AG				-Ir	89	11)
ES Cnc	55622.3679	.0020	SCI				o	94	2)
EV Cnc	55621.3991	.0095	AG				V	41	11)
	55621.4090	.0247	AG				B	40	11)
	55621.4146	.0108	AG				I	40	11)
FF Cnc	55621.4830	.0004	FR	−0.2038	s	IBVS 3859	-Ir	67	11)
HN Cnc	55622.4338	.0021	AG	−0.0251		IBVS 5260	-Ir	80	11)
HS Cnc	55621.3774	.0135	AG				R	40	11)
	55621.3778	.0070	AG				V	41	11)
IN Cnc	55625.5169	.0037	AG	−0.0013	s	GCVS 2009	-Ir	69	11)
IO Cnc	55625.4271	.0027	AG	+0.0732		GCVS 2007	-Ir	69	11)
	55625.6003	.0023	AG	+0.0725	s	GCVS 2007	-Ir	69	11)
IQ Cnc	55625.4424	.0020	AG	−0.1105		GCVS 2009	-Ir	72	11)
IT Cnc	55622.5429	.0053	AG	−0.0572		GCVS 2007	-Ir	77	11)
IU Cnc	55244.3755	.0010	RAT RCR	−0.0114	s	GCVS 2009	-Ir	118	15)
	55260.3969	.0002	RAT RCR	−0.0126	s	GCVS 2009	-Ir	97	15)
	55621.3208	.0024	AG	−0.0190	s	GCVS 2009	-Ir	39	11)
	55621.5365	.0030	AG	−0.0141		GCVS 2009	-Ir	39	11)
VZ CVn	55624.5011	.0020	AG	−0.0042		GCVS 2009	V	36	11)
YZ CVn	55661.4646	.0014	AG	−0.0151		GCVS 2009	-Ir	34	11)
BI CVn	55669.4261	.0016	AG	+0.0763	s	GCVS 2009	-Ir	38	11)
	55669.6163	.0001	AG	+0.0744		GCVS 2009	-Ir	38	11)
	55700.3526	.0011	AG	+0.0779		GCVS 2009	-Ir	47	11)
	55700.5462	.0038	AG	+0.0795	s	GCVS 2009	-Ir	47	11)

Table 1: (cont.)

Variable	HJD 24.....	±	Obs	$O-C$		Bibliography	Fil	n	Rem
BO CVn	55682.4753	.0031	AG				-Ir	81	11)
DF CVn	55669.4656	.0021	AG				-Ir	38	11)
	55700.3590	.0021	AG				-Ir	45	11)
	55700.5183	.0004	AG				-Ir	45	11)
DH CVn	55669.4614	.0016	AG				-Ir	38	11)
DI CVn	55669.3866	.0021	AG				-Ir	38	11)
	55669.5386	.0010	AG				-Ir	38	11)
	55700.4406	.0021	AG				-Ir	45	11)
DL CVn	55669.4800	.0063	AG				-Ir	31	11)
DR CVn	55310.5847	.0001	RAT RCR	+0.0449	s	GCVS 2009	-Ir	220	15)
	55669.4216	.0026	AG	+0.0496		GCVS 2009	-Ir	38	11)
	55669.5893	.0020	AG	+0.0527	s	GCVS 2009	-Ir	38	11)
	55700.3559	.0030	AG	+0.0529		GCVS 2009	-Ir	45	11)
	55700.5181	.0023	AG	+0.0506	s	GCVS 2009	-Ir	45	11)
DX CVn	55669.5329	.0029	AG	+0.0058	s	GCVS 2009	-Ir	38	11)
	55700.4445	.0023	AG	+0.0039		GCVS 2009	-Ir	46	11)
DY CVn	55669.3894	.0008	AG	−0.0045		GCVS 2007	-Ir	38	11)
	55669.5145	.0018	AG	−0.0024	s	GCVS 2007	-Ir	38	11)
	55700.3803	.0013	AG	−0.0032		GCVS 2007	-Ir	47	11)
	55700.5035	.0003	AG	−0.0030	s	GCVS 2007	-Ir	47	11)
EE CVn	55624.4284	.0013	AG	−0.0051		GCVS 2009	-Ir	36	11)
	55624.5670	.0011	AG	−0.0068	s	GCVS 2009	-Ir	36	11)
EF CVn	55624.4891	.0020	AG	−0.0083		GCVS 2009	-Ir	36	11)
	55624.6263	.0004	AG	−0.0072	s	GCVS 2009	-Ir	36	11)
	55661.4868	.0033	AG	−0.0094		GCVS 2009	-Ir	34	11)
	55661.6251	.0006	AG	−0.0071	s	GCVS 2009	-Ir	34	11)
EH CVn	55624.3719	.0012	AG	−0.0525		GCVS 2009	-Ir	36	11)
	55624.5039	.0016	AG	−0.0523	s	GCVS 2009	-Ir	36	11)
	55624.6342	.0013	AG	−0.0538		GCVS 2009	-Ir	36	11)
SX CMi	55621.3852	.0059	AG	−0.7116	s	GCVS 2009	-Ir	49	11)
TX CMi	55621.4197	.0010	AG	−0.0693		GCVS 2009	-Ir	49	11)
	55625.3126	.0016	AG	−0.0664		GCVS 2009	-Ir	39	11)
	55625.5047	.0012	AG	−0.0688	s	GCVS 2009	-Ir	39	11)
TY CMi	55625.3842	.0015	AG	+0.1550	s	GCVS 2009	-Ir	36	11)
TZ CMi	55621.5016	.0100	AG	+1.1376		GCVS 2007	-Ir	49	11)
UZ CMi	55621.4822	.0047	AG	−0.0114	s	GCVS 2009	-Ir	46	11)
	55625.3429	.0025	AG	+0.0396	s	GCVS 2009	-Ir	36	11)
XZ CMi	55625.3416	.0048	AG	+0.0006	s	GCVS 2009	-Ir	32	11)
BB CMi	55625.4851	.0152	AG	−0.0656		GCVS 2009	-Ir	39	11)
BF CMi	55244.2715	.0015	RAT RCR	−0.1398		GCVS 2009	-Ir	125	15)
TV Cas	55619.3853	.0035	PGL	−0.0242		GCVS 2009	V	554	10)
TW Cas	55590.3171	.0035	PGL	−0.0032		GCVS 2009	V	303	17)
	55600.3103	.0007	SIR	−0.0082		GCVS 2009	o	208	4)
AB Cas	55463.4821	.0035	PGL	+0.1875		GCVS 2009	V	150	17)
AX Cas	55473.3550	.0002	MS FR	−0.1006		GCVS 2009	o	610	5)
BH Cas	55776.4936	.0017	AG				-Ir	35	11)
EG Cas	55776.4741	.0019	AG	+0.0938	s	GCVS 2009	-Ir	35	11)
EY Cas	55776.4285	.0017	AG	+0.0434		GCVS 2009	-Ir	35	11)
GR Cas	55474.4499	.0001	MS FR	−0.0425		GCVS 2009	o	423	5)
GU Cas	55599.4015	.0011	JU	−0.3520		GCVS 2009	o	49	2)
IS Cas	55451.5573	.0005	RAT RCR	+0.0664	s	GCVS 2009	-Ir	198	15)
NN Cas	55776.5360	.0164	AG	+0.1076		GCVS 2009	-Ir	35	11)
QQ Cas	55776.5151	.0104	AG	+0.1182		BAVR 35,1	-Ir	35	11)
V336 Cas	55776.5318	.0024	AG	−0.0141		GCVS 2009	-Ir	35	11)
V345 Cas	55758.5318	.0025	AG	−0.0162	s	GCVS 2009	-Ir	32	11)
V359 Cas	55495.5532	.0004	RAT RCR	+0.0109	s	IBVS 5016	-Ir	244	15)
V385 Cas	53735.3504	.0011	AG	+0.5915	s	GCVS 2009	-Ir	40	1)
V523 Cas	53735.3238	.0004	AG	−0.0505		GCVS 2009	-Ir	40	1)
V651 Cas	55776.4043	.0020	AG	+0.0032		IBVS 3554	-Ir	35	11)

Table 1: (cont.)

Variable	HJD 24.....	±	Obs	$O-C$		Bibliography	Fil	n	Rem
V702 Cas	55759.4214	.0035	AG				-Ir	23	11)
V1004 Cas	55223.3990	.0005	RAT RCR	+0.0809		GCVS 2009	-Ir	264	15)
VZ Cep	55644.5836	.0055	AG	−0.0118	s	GCVS 2009	-Ir	54	11)
	55692.5121	.0018	AG	−0.0096		GCVS 2009	-Ir	40	11)
WW Cep	55482.5136	.0001	RAT RCR	+0.0004		IBVS 4131	-Ir	317	15)
ZZ Cep	55645.4727	.0054	AG	−0.0121		GCVS 2009	V	63	11)
AV Cep	55643.5478	.0039	AG	+0.3826	s	GCVS 2009	-Ir	212	11)
BU Cep	55645.5569	.0088	AG	−0.3433	s	GCVS 2009	-Ir	63	11)
CW Cep	55645.5235	.0169	AG	+0.0220		GCVS 2009	V	62	11)
DK Cep	55775.4660	.0009	AG	+0.0372		GCVS 2009	-Ir	49	11)
DL Cep	55669.5635	.0005	MS FR	+0.0040		IBVS 5016	o	585	5)
	55775.5447	.0029	AG	+0.0036		IBVS 5016	-Ir	49	11)
DV Cep	55644.3218	.0001	AG	+0.0054		BAVR 50,159	-Ir	55	11)
EO Cep	55483.5782	.0002	RAT RCR	+0.1178		GCVS 2009	-Ir	264	15)
GG Cep	55685.4470	.0015	AG	−0.0990		GCVS 2009	-Ir	38	11)
GI Cep	55644.3788	.0139	AG	−0.1055	s	GCVS 2009	-Ir	51	11)
GS Cep	55775.4693	.0082	AG	−0.1479	s	GCVS 2009	-Ir	43	11)
GT Cep	55645.4049	.0147	AG	+0.1120		GCVS 2009	V	58	11)
HI Cep	55495.3721	.0001	RAT RCR				-Ir	168	15)
IP Cep	55474.5094	.0002	RAT RCR	−0.0344		IBVS 5016	-Ir	334	15)
	55644.4018	.0043	AG	−0.0348		IBVS 5016	-Ir	54	11)
	55692.4995	.0041	AG	−0.0285	s	IBVS 5016	-Ir	39	11)
	55706.4263	.0009	MS FR	−0.0347		IBVS 5016	o	432	5)
KP Cep	55479.3889	.0007	MS FR	+0.0419		GCVS 2009	o	522	5)
	55775.4620	.0019	AG	+0.0438		GCVS 2009	-Ir	42	11)
LM Cep	55691.4802	.0042	AG	+0.1246		GCVS 2009	-Ir	48	11)
LP Cep	55691.5678	.0011	AG	−0.0681		GCVS 2009	-Ir	48	11)
	55775.4274	.0008	AG	−0.0693		GCVS 2009	-Ir	49	11)
NU Cep	55775.4868	.0015	AG	+0.0148		GCVS 2009	-Ir	49	11)
PX Cep	55685.5017	.0014	AG				-Ir	38	11)
V711 Cep	55645.4386	.0239	AG				V	62	11)
V737 Cep	55685.4877	.0006	AG	+0.0047	s	GCVS 2009	-Ir	38	11)
RW Com	55642.3780	.0007	SCI	−0.0093		GCVS 2009	o	116	2)
	55642.4947	.0007	SCI	−0.0113	s	GCVS 2009	o	59	2)
	55662.4333	.0009	AG	−0.0098	s	GCVS 2009	-Ir	56	11)
	55662.5526	.0012	AG	−0.0091		GCVS 2009	-Ir	56	11)
	55675.3704	.0016	AG	−0.0080		GCVS 2009	-Ir	38	11)
	55675.4870	.0006	AG	−0.0101	s	GCVS 2009	-Ir	38	11)
	55675.6067	.0004	AG	−0.0091		GCVS 2009	-Ir	38	11)
RZ Com	55675.3880	.0025	AG	+0.0441	s	GCVS 2009	-Ir	38	11)
	55675.5579	.0011	AG	+0.0448		GCVS 2009	-Ir	38	11)
UX Com	55662.4885	.0079	AG	−0.1322		BAVM 69	-Ir	56	11)
AQ Com	55628.5127	.0003	MS FR	+0.0526	s	GCVS 2009	o	405	5)
CC Com	55305.3560	.0001	RAT RCR	−0.0134		GCVS 2009	-Ir	132	15)
CM Com	55675.5613	.0017	AG	+0.1959		GCVS 2009	-Ir	38	11)
CN Com	55646.4118	.0023	SCI	+0.0610		GCVS 2009	o	25	2)
EK Com	55662.3620	.0002	AG				-Ir	56	11)
	55662.4941	.0013	AG				-Ir	56	11)
	55675.4300	.0020	AG				-Ir	38	11)
	55675.5625	.0012	AG				-Ir	38	11)
EQ Com	55643.3639	.0005	MS FR	+0.0327		GCVS 2009	o	390	5)
	55660.3743	.0008	MS FR	+0.0354		GCVS 2009	o	320	5)
LL Com	55624.4191	.0010	AG	+0.0408	s	IBVS 4386	-Ir	36	11)
	55624.6233	.0025	AG	+0.0415		IBVS 4386	-Ir	36	11)
LO Com	55662.4047	.0004	AG				-Ir	56	11)
	55662.5475	.0007	AG				-Ir	56	11)
	55675.4336	.0016	AG				-Ir	38	11)
	55675.5766	.0006	AG				-Ir	38	11)
LP Com	55646.5743	.0013	SCI				o	62	2)

Table 1: (cont.)

Variable	HJD 24.....	±	Obs	$O-C$		Bibliography	Fil	n	Rem
LP Com	55662.4597	.0018	AG				-Ir	56	11)
	55669.3850	.0029	SCI				o	36	2)
	55669.5580	.0028	SCI				o	51	2)
	55675.4728	.0021	AG				-Ir	38	11)
LQ Com	55662.4213	.0008	AG				-Ir	55	11)
	55662.6003	.0017	AG				-Ir	55	11)
	55675.4468	.0014	AG				-Ir	37	11)
LR Com	55667.3825	.0010	SIR				o	138	4)
LT Com	55662.3544	.0031	AG				-Ir	56	11)
	55662.6115	.0017	AG				-Ir	55	11)
	55675.4067	.0079	AG				-Ir	38	11)
MM Com	55624.3723	.0012	AG	−0.0186		GCVS 2009	-Ir	36	11)
	55624.5262	.0025	AG	−0.0157	s	GCVS 2009	-Ir	36	11)
MR Com	55624.4517	.0014	AG	−0.0426		GCVS 2009	-Ir	36	11)
U CrB	55654.3997	.0005	FR	+0.1189		GCVS 2009	-Ir	57	11)
RT CrB	55629.5479	.0076	AG	−0.0271		GCVS 2009	-Ir	54	11)
TU CrB	55705.4948	.0015	AG	+0.0725	s	GCVS 2009	-Ir	41	11)
TW CrB	55629.6819	.0008	AG	+0.0452	s	GCVS 2009	-Ir	54	11)
YY CrB	55351.4455	.0001	RAT RCR				-Ir	202	15)
	55705.4085	.0023	AG				-Ir	42	11)
AM CrB	55705.3806	.0009	AG				-Ir	42	11)
AR CrB	55629.5468	.0017	AG	−0.0056	s	GCVS 2009	-Ir	54	11)
AV CrB	55629.6122	.0016	AG	−0.0199	s	GCVS 2009	-Ir	54	11)
	55659.5075	.0024	AG	−0.0194	s	GCVS 2009	-Ir	31	11)
SW Cyg	55687.5096	.0033	AG	−0.3190		GCVS 2009	-Ir	25	11)
VV Cyg	55691.5271	.0008	AG	+0.0134		GCVS 2009	-Ir	23	11)
WZ Cyg	55373.4796	.0001	RAT RCR	+0.0639		GCVS 2009	-Ir	168	15)
BO Cyg	55461.5251	.0001	RAT RCR	+0.0884		GCVS 2009	-Ir	267	15)
DP Cyg	55775.4341	.0051	AG	+0.4291	s	GCVS 2009	-Ir	42	11)
EN Cyg	55707.5152	.0072	AG	+0.4636	s	GCVS 2009	-Ir	20	11)
GM Cyg	55686.4609	.0024	AG	−0.2199		GCVS 2009	-Ir	24	11)
KV Cyg	55686.5474	.0010	AG	+0.0525		GCVS 2009	-Ir	24	11)
	55740.4894	.0017	AG	+0.0536		GCVS 2009	-Ir	29	11)
NZ Cyg	55784.3916	.0026	AG	+0.0741		GCVS 2009	-Ir	34	11)
	55784.5894	.0015	AG	+0.0689	s	GCVS 2009	-Ir	34	11)
PV Cyg	55686.5169	.0018	AG	+0.2491		GCVS 2009	-Ir	24	11)
	55711.4995	.0049	AG	+0.2495		GCVS 2009	-Ir	28	11)
QU Cyg	55686.5124	.0004	AG	−0.0713		GCVS 2009	-Ir	24	11)
	55711.4898	.0006	AG	−0.0715		GCVS 2009	-Ir	28	11)
QW Cyg	55711.5177	.0019	AG	−0.0787		GCVS 2009	-Ir	28	11)
V401 Cyg	55483.3582	.0001	RAT RCR	+0.0691		GCVS 2009	-Ir	196	15)
	55741.5089	.0043	AG	+0.0740		GCVS 2009	-Ir	32	11)
	55776.4724	.0007	AG	+0.0742		GCVS 2009	-Ir	38	11)
V435 Cyg	55740.4562	.0047	AG	+0.2189		GCVS 2009	-Ir	29	11)
V443 Cyg	55376.4809	.0001	RAT RCR	+0.0321		GCVS 2009	-Ir	219	15)
	55740.5041	.0006	AG	+0.0327		GCVS 2009	-Ir	29	11)
V447 Cyg	55686.5160	.0044	AG	+0.1282		GCVS 2009	-Ir	24	11)
V454 Cyg	55711.4824	.0057	AG	−0.0060	s	GCVS 2009	-Ir	28	11)
	55740.4414	.0010	AG	−0.0081		GCVS 2009	-Ir	29	11)
V463 Cyg	55480.3911	.0035	PGL	+0.0469		GCVS 2009	V	171	10)
V484 Cyg	55645.6153	.0009	MS FR	+0.1174		GCVS 2009	o	510	5)
V490 Cyg	55690.5031	.0010	AG	+0.1640		GCVS 2009	-Ir	30	11)
V496 Cyg	55740.5130	.0017	AG	+0.0083		GCVS 2009	-Ir	29	11)
V499 Cyg	55690.4840	.0017	AG	+0.0297		GCVS 2007	-Ir	30	11)
V500 Cyg	55661.6084	.0001	MS FR	+0.1133		GCVS 2009	o	550	5)
V505 Cyg	55644.6050	.0003	MS FR	+0.0368	s	GCVS 2009	o	492	5)
V512 Cyg	55691.4400	.0010	AG	+0.1167		GCVS 2009	-Ir	22	11)
V534 Cyg	55691.5461	.0009	AG	+0.1872		GCVS 2009	-Ir	22	11)
V536 Cyg	55691.5511	.0007	AG	+0.4343		GCVS 2009	-Ir	23	11)

Table 1: (cont.)

Variable	HJD 24.....	±	Obs	$O-C$		Bibliography	Fil	n	Rem
V541 Cyg	55741.4299	.0064	AG	+0.0526		GCVS 2009	-Ir	32	11)
V635 Cyg	55691.4528	.0052	AG	−0.0493	s	GCVS 2009	-Ir	22	11)
V689 Cyg	55686.5243	.0095	AG	+0.1531	s	GCVS 2009	-Ir	24	11)
V704 Cyg	55691.4747	.0026	AG	+0.0324	s	GCVS 2009	-Ir	22	11)
V726 Cyg	55667.5437	.0002	MS FR	+0.0387		GCVS 2009	o	540	5)
	55686.4668	.0017	AG	+0.0389		GCVS 2009	-Ir	24	11)
V743 Cyg	55690.4869	.0106	AG	−0.2692		GCVS 2009	-Ir	30	11)
V753 Cyg	55674.3797	.0003	AG	+0.0040		BAVM 69	-Ir	29	11)
V796 Cyg	55687.5756	.0008	AG	−0.0054		GCVS 2009	-Ir	25	11)
V809 Cyg	55784.5494	.0018	AG	+0.0408		GCVS 2009	-Ir	34	11)
V822 Cyg	55643.6227	.0007	MS FR	−0.1515		GCVS 2009	o	434	5)
V824 Cyg	55711.4333	.0041	AG	+0.0156	s	GCVS 2009	-Ir	28	11)
V841 Cyg	55712.5228	.0088	AG	+0.0065	s	GCVS 2009	-Ir	26	11)
V842 Cyg	55712.5166	.0017	AG	+0.0324		GCVS 2009	-Ir	26	11)
V856 Cyg	55707.4948	.0030	AG	+0.0808		GCVS 2009	-Ir	20	11)
V865 Cyg	55712.5124	.0017	AG	+0.0531		GCVS 2009	-Ir	26	11)
V866 Cyg	55707.4431	.0003	AG	+0.1734	s	GCVS 2009	-Ir	19	11)
	55778.4821	.0073	AG	+0.1776	s	GCVS 2009	-Ir	42	11)
V869 Cyg	55676.5569	.0003	MS FR	+0.1218		GCVS 2009	o	400	5)
V874 Cyg	55712.4317	.0022	AG	+0.0746	s	GCVS 2009	-Ir	25	11)
V880 Cyg	55710.4821	.0019	AG	−0.0033	s	GCVS 2009	-Ir	25	11)
V885 Cyg	55370.4970	.0002	RAT RCR	−0.0956		GCVS 2009	-Ir	200	15)
V906 Cyg	55642.6120	.0004	MS FR	+0.0603		GCVS 2009	o	450	5)
V912 Cyg	55741.4938	.0011	AG	−0.1208		GCVS 2009	-Ir	32	11)
V957 Cyg	55690.4605	.0048	AG	+0.1346		GCVS 2009	-Ir	30	11)
V963 Cyg	55710.4984	.0009	AG	−0.0018		GCVS 2009	-Ir	25	11)
V970 Cyg	55372.4978	.0003	MS FR	−0.0041		GCVS 2007	o	480	5)
V1004 Cyg	55641.5876	.0004	MS FR	+0.1608	s	GCVS 2009	o	492	5)
	55685.4727	.0006	MS FR	+0.1611	s	GCVS 2009	o	315	5)
V1018 Cyg	55741.4626	.0043	AG	−0.0922	s	GCVS 2009	-Ir	32	11)
V1019 Cyg	55690.5400	.0023	AG	+0.1264		GCVS 2009	-Ir	25	11)
V1036 Cyg	55660.5273	.0003	MS FR	+0.0012		BAVM 141	o	500	5)
V1083 Cyg	55462.5284	.0006	RAT RCR	−0.0468	s	GCVS 2009	-Ir	261	15)
V1130 Cyg	55686.5052	.0006	AG	−0.0360		GCVS 2009	-Ir	24	11)
V1136 Cyg	55710.5024	.0009	AG	+0.0863		GCVS 2009	-Ir	25	11)
V1141 Cyg	55686.5030	.0025	AG	+0.1104		GCVS 2009	-Ir	24	11)
V1147 Cyg	55776.4108	.0017	AG	−0.1733	s	GCVS 2009	-Ir	38	11)
V1187 Cyg	55740.5046	.0022	AG	−0.0174		IBVS 4133	-Ir	29	11)
V1191 Cyg	55740.5386	.0014	AG	−0.0054		GCVS 2009	-Ir	29	11)
V1193 Cyg	55691.5553	.0045	AG	−0.1067		GCVS 2009	-Ir	48	11)
V1302 Cyg	55740.4097	.0035	AG	−0.0916		GCVS 2009	-Ir	29	11)
V1321 Cyg	55740.4211	.0012	AG	+0.0861		GCVS 2009	-Ir	29	11)
V1356 Cyg	55375.4963	.0002	RAT RCR	+0.1724		GCVS 2009	-Ir	200	15)
	55690.5430	.0045	AG	+0.1917		GCVS 2009	-Ir	30	11)
V2240 Cyg	55711.4554	.0010	AG				-Ir	27	11)
V2280 Cyg	55674.4255	.0014	AG				-Ir	29	11)
	55674.6015	.0001	AG				-Ir	29	11)
	55687.4995	.0019	AG				-Ir	25	11)
V2284 Cyg	55687.5063	.0001	AG				-Ir	25	11)
V2294 Cyg	55687.4421	.0029	AG				-Ir	24	11)
V2363 Cyg	55674.3887	.0015	AG	−0.0118		GCVS 2007	-Ir	29	11)
	55674.5707	.0035	AG	−0.0108	s	GCVS 2007	-Ir	29	11)
V2364 Cyg	55674.5767	.0024	AG	−0.0152		GCVS 2009	-Ir	29	11)
V2366 Cyg	55674.5151	.0015	AG	+0.0175		GCVS 2009	-Ir	28	11)
	55687.5268	.0019	AG	+0.0185	s	GCVS 2009	-Ir	24	11)
TT Del	55387.4761	.0002	RAT RCR	−0.0908		GCVS 2009	-Ir	12	15)
YY Del	55384.5027	.0003	RAT RCR	+0.0117	s	GCVS 2009	-Ir	197	15)
EQ Del	55739.4799	.0001	MS FR	−0.0611		GCVS 2009	o	616	5)
RZ Dra	55689.4938	.0063	AG	+0.0531	s	GCVS 2009	-Ir	64	11)

Table 1: (cont.)

Variable	HJD 24.....	±	Obs	$O-C$		Bibliography	Fil	n	Rem
TZ Dra	55682.4372	.0022	AG	−0.0323		GCVS 2009	-Ir	40	11)
WW Dra	55650.5224	.0035	SCI	+0.5590		GCVS 2009	o	185	2)
WX Dra	55674.5172	.0018	AG	+0.0209		GCVS 2009	-Ir	29	11)
XY Dra	55662.5619	.0015	AG	+0.2903		GCVS 2009	-Ir	45	11)
AI Dra	55645.4385	.0021	SCI	+0.0270		GCVS 2009	o	166	2)
AK Dra	55641.4636	.0015	SCI	+0.2532		GCVS 2009	o	47	2)
	55642.5739	.0031	SCI	+0.2544	s	GCVS 2009	o	76	2)
	55661.4271	.0018	SCI	+0.2526		GCVS 2009	o	80	2)
	55662.5394	.0161	AG	+0.2558	s	GCVS 2009	-Ir	45	11)
	55672.5242	.0010	AG	+0.2585		GCVS 2009	-Ir	39	11)
	55682.5042	.0075	AG	+0.2564	s	GCVS 2009	-Ir	39	11)
	55692.4893	.0021	AG	+0.2595		GCVS 2009	-Ir	32	11)
AR Dra	55314.4779	.0001	RAT RCR	+0.0189		GCVS 2009	-Ir	230	15)
BE Dra	55712.3864	.0019	AG	−0.1125	s	GCVS 2009	-Ir	24	11)
BS Dra	55674.3770	.0026	AG	+0.0021		GCVS 2009	-Ir	26	11)
BU Dra	55627.3450	.0134	AG	+0.0222		MVS 12,4	V	77	11)
	55667.5437	.0024	SCI	+0.0230	s	MVS 12,4	o	159	2)
CM Dra	55642.5207	.0006	AG	+0.0038		GCVS 2009	-Ir	77	11)
CV Dra	55662.4791	.0149	AG	+0.0025	s	BAVM 69	-Ir	42	11)
DW Dra	55628.4686	.0017	AG				-Ir	54	11)
EF Dra	55628.3942	.0042	AG	+0.0839		IBVS 3811	-Ir	46	11)
GQ Dra	55662.5155	.0052	AG				-Ir	45	11)
GV Dra	55626.6647	.0011	SCI	−0.0021		IBVS 4990	o	101	2)
	55662.5805	.0035	SCI	+0.1322	s	IBVS 4990	o	91	2)
IV Dra	55627.5160	.0013	AG				-Ir	61	11)
	55627.6477	.0015	AG				-Ir	61	11)
KK Dra	55689.3994	.0011	AG				-Ir	64	11)
LN Dra	55662.5558	.0024	AG				-Ir	45	11)
	55692.5525	.0040	AG				-Ir	32	11)
LZ Dra	55674.3757	.0011	AG				-Ir	23	11)
MU Dra	55674.4340	.0015	AG	−0.0465	s	GCVS 2009	-Ir	29	11)
TZ Gem	55629.4572	.0001	FR	+0.0985		GCVS 2009	-Ir	118	11)
YY Gem	55627.3045	.0035	PGL	−0.0060		GCVS 2009	V	165	17)
AL Gem	55623.3254	.0015	SCI	+0.0726		GCVS 2009	o	108	2)
AV Gem	55623.3950	.0042	AG	−0.0291	s	GCVS 2009	-Ir	49	11)
EN Gem	55627.3861	.0024	SCI	−0.0563		GCVS 2009	o	29	2)
FT Gem	55590.4231	.0017	FR	−0.0336	s	GCVS 2009	-Ir	45	11)
	55623.3323	.0055	AG	−0.0307	s	GCVS 2009	-Ir	49	11)
LO Gem	55629.3407	.0035	AG				-Ir	51	11)
MU Gem	55590.3097	.0029	FR	+0.0225		GCVS 2009	-Ir	57	11)
	55624.4375	.0007	FR	+0.0189		GCVS 2009	-Ir	46	11)
V339 Gem	55602.4084	.0007	SIR	+0.0039		IBVS 5557	o	136	4)
	55625.4475	.0006	FR	+0.0005		IBVS 5557	-Ir	51	11)
	55628.3316	.0008	SIR	+0.0042		IBVS 5557	o	132	4)
V388 Gem	55235.2896	.0002	RAT RCR	−0.0109		GCVS 2009	-Ir	93	15)
SZ Her	55396.4465	.0001	RAT RCR	−0.0223		GCVS 2009	-Ir	230	15)
	55670.5099	.0005	AG	−0.0218		GCVS 2009	V	35	11)
TU Her	55398.5239	.0002	RAT RCR	−0.2076		GCVS 2009	-Ir	250	15)
	55661.4905	.0012	AG	−0.2131		GCVS 2009	-Ir	41	11)
BO Her	55711.4884	.0024	AG	−0.0439		GCVS 2009	-Ir	43	11)
	55758.4881	.0038	AG	−0.0455		GCVS 2009	-Ir	35	11)
BV Her	55661.5599	.0013	SCI	−0.0571		GCVS 2009	o	22	2)
CT Her	55654.5786	.0014	SCI	+0.0054		GCVS 2009	o	70	2)
DD Her	55645.6362	.0028	SCI	+0.3862	s	GCVS 2009	o	43	2)
ES Her	55648.5246	.0003	MS FR	−0.0303		GCVS 2009	o	620	5)
	55670.4235	.0019	AG	−0.0282		GCVS 2009	-Ir	35	11)
	55673.5505	.0016	AG	−0.0293		GCVS 2009	-Ir	35	11)
IK Her	55671.5566	.0103	AG	+0.2649	s	GCVS 2009	-Ir	46	11)
IT Her	55711.4589	.0018	AG	−0.0383	s	GCVS 2009	-Ir	43	11)

Table 1: (cont.)

Variable	HJD 24.....	±	Obs	$O-C$		Bibliography	Fil	n	Rem
IT Her	55748.4518	.0017	JU	−0.0027		GCVS 2009	o	57	2)
	55758.4650	.0029	AG	−0.0481	s	GCVS 2009	-Ir	35	11)
MX Her	55741.3978	.0011	AG	+0.5823	s	GCVS 2009	-Ir	29	11)
PW Her	55705.2188	.0015	AG	−0.3551		BAVM 68	V	64	11)
V342 Her	55758.5173	.0053	AG	+0.0220		GCVS 2009	-Ir	35	11)
	55776.4026	.0004	WTR	+0.0209		GCVS 2009	-Ir	35	8)
V381 Her	55660.5641	.0008	AG	+0.1917		GCVS 2009	-Ir	54	11)
	55683.4500	.0001	MS FR	+0.1912		GCVS 2009	o	832	5)
	55689.5116	.0238	AG	+0.1947	s	GCVS 2009	-Ir	32	11)
V387 Her	55625.5973	.0001	MS FR	+0.0650	s	GCVS 2009	o	570	5)
	55689.5526	.0012	AG	+0.0626		GCVS 2009	-Ir	32	11)
V450 Her	55669.4507	.0090	AG	+0.1071	s	GCVS 2009	V	38	11)
V490 Her	55747.4839	.0010	JU	−0.3612	s	GCVS 2009	o	65	2)
V502 Her	55640.5493	.0002	MS FR	+0.0233		GCVS 2009	o	693	5)
	55661.5985	.0017	AG	+0.0237		GCVS 2009	-Ir	41	11)
	55670.4611	.0012	AG	+0.0237		GCVS 2009	-Ir	35	11)
V607 Her	55671.4793	.0464	AG	+0.1683		GCVS 2009	-Ir	46	11)
V607 Her	55707.4530	.0164	AG	+0.1774	s	GCVS 2009	-Ir	59	11)
V728 Her	55393.4819	.0002	RAT RCR	+0.0706		IBVS 3234	-Ir	201	15)
	55444.3817	.0001	RAT RCR	+0.0714		IBVS 3234	-Ir	171	15)
	55710.4278	.0031	AG	+0.0761	s	IBVS 3234	-Ir	27	11)
V732 Her	55685.5983	.0042	SCI	+0.0988		GCVS 2009	o	61	2)
V733 Her	55741.5505	.0004	AG	−0.0494	s	GCVS 2009	-Ir	29	11)
V829 Her	55659.4435	.0059	AG	+0.0405		IBVS 5496	V	29	11)
	55669.4722	.0027	AG	+0.0410		IBVS 5496	V	39	11)
V842 Her	55669.3690	.0002	MS FR	−0.0611		BAVR 49,180	o	430	5)
	55705.4057	.0008	JU	−0.0619		BAVR 49,180	o	30	2)
V856 Her	55669.4249	.0022	AG				-Ir	39	11)
V857 Her	55669.5466	.0045	AG				V	39	11)
	55749.4324	.0022	JU				o	76	2)
V861 Her	55669.3850	.0014	AG				-Ir	39	11)
	55669.5576	.0018	AG				-Ir	39	11)
	55710.3975	.0011	AG				-Ir	28	11)
V878 Her	55662.4798	.0119	AG				-Ir	45	11)
V883 Her	55670.4332	.0262	AG				-Ir	34	11)
V923 Her	55659.5074	.0039	AG				V	31	11)
V1032 Her	55659.4811	.0022	AG				-Ir	30	11)
	55669.4158	.0067	AG				-Ir	39	11)
V1033 Her	55671.4743	.0002	AG				-Ir	46	11)
	55707.3909	.0010	AG				-Ir	59	11)
	55707.5397	.0012	AG				-Ir	59	11)
V1036 Her	55707.5500	.0030	AG				-Ir	59	11)
V1038 Her	55659.4282	.0011	AG				-Ir	32	11)
	55659.5618	.0009	AG				-Ir	32	11)
	55661.4391	.0008	AG				-Ir	41	11)
	55661.5739	.0008	AG				-Ir	41	11)
V1042 Her	55689.5137	.0016	AG				-Ir	32	11)
V1044 Her	55669.4576	.0019	AG				-Ir	39	11)
	55669.5780	.0015	AG				-Ir	39	11)
V1047 Her	55661.4400	.0015	AG				-Ir	41	11)
	55661.6002	.0009	AG				-Ir	41	11)
	55746.4370	.0015	JU				o	48	2)
V1049 Her	55689.4449	.0135	AG				-Ir	32	11)
V1052 Her	55660.5256	.0023	AG				-Ir	54	11)
	55689.4502	.0019	AG				-Ir	32	11)
V1055 Her	55397.5008	.0001	RAT RCR				-Ir	225	15)
	55669.3797	.0022	AG				-Ir	39	11)
	55669.5406	.0016	AG				-Ir	39	11)
V1057 Her	55660.6150	.0022	AG				-Ir	54	11)

Table 1: (cont.)

Variable	HJD 24.....	±	Obs	$O-C$		Bibliography	Fil	n	Rem
V1057 Her	55689.3891	.0020	AG				-Ir	32	11)
V1065 Her	55670.4537	.0009	AG				-Ir	35	11)
V1066 Her	55461.3372	.0001	RAT RCR				-Ir	188	15)
	55741.4004	.0005	AG				-Ir	29	11)
V1068 Her	55461.3889	.0002	RAT RCR				-Ir	189	15)
	55672.3422	.0036	AG				-Ir	39	11)
	55672.5438	.0016	AG				-Ir	39	11)
	55692.4531	.0028	AG				-Ir	31	11)
	55741.5453	.0003	AG				-Ir	29	11)
V1069 Her	55672.4344	.0021	AG				-Ir	39	11)
V1071 Her	55662.3803	.0046	AG				-Ir	44	11)
	55672.5974	.0001	AG				-Ir	39	11)
	55682.5476	.0020	AG				-Ir	40	11)
	55692.4936	.0013	AG				-Ir	31	11)
	55741.4308	.0017	AG				-Ir	29	11)
V1073 Her	55670.4642	.0007	AG				-Ir	35	11)
	55670.6124	.0005	AG				-Ir	35	11)
	55673.4079	.0003	AG				V	35	11)
	55673.5556	.0016	AG				V	35	11)
	55705.4840	.0015	AG				-Ir	26	11)
V1088 Her	55659.4805	.0015	AG	+0.0150	s	GCVS 2009	-Ir	28	11)
	55661.4600	.0025	AG	+0.0187		GCVS 2009	-Ir	41	11)
	55671.5166	.0030	AG	+0.0169		GCVS 2009	-Ir	46	11)
V1091 Her	55669.5052	.0019	AG	+0.0383	s	GCVS 2009	-Ir	38	11)
V1092 Her	55661.5636	.0012	AG	+0.0412	s	GCVS 2009	-Ir	41	11)
V1095 Her	55405.4616	.0002	RAT RCR	−0.0235		GCVS 2009	-Ir	217	15)
V1096 Her	55405.4548	.0003	RAT RCR	+0.0209	s	GCVS 2009	-Ir	211	15)
V1098 Her	55662.3975	.0017	AG	+0.0525	s	GCVS 2009	-Ir	45	11)
	55662.5752	.0011	AG	+0.0541		GCVS 2009	-Ir	45	11)
	55672.4381	.0020	AG	+0.0536		GCVS 2009	-Ir	39	11)
	55692.5170	.0038	AG	+0.0534		GCVS 2009	-Ir	31	11)
	55741.4831	.0021	AG	+0.0548		GCVS 2009	-Ir	29	11)
V1101 Her	55445.3892	.0002	RAT RCR	+0.0193		GCVS 2009	-Ir	163	15)
	55672.5017	.0015	AG	+0.0260	s	GCVS 2009	-Ir	39	11)
	55682.4508	.0019	AG	+0.0261	s	GCVS 2009	-Ir	40	11)
V1102 Her	55672.4804	.0003	AG	+0.0068		GCVS 2009	-Ir	39	11)
	55682.3687	.0016	AG	+0.0069		GCVS 2009	-Ir	40	11)
	55682.5242	.0011	AG	+0.0079	s	GCVS 2009	-Ir	40	11)
	55741.5431	.0012	AG	+0.0069	s	GCVS 2009	-Ir	29	11)
V1103 Her	55670.3594	.0013	AG	−0.0012		GCVS 2009	-Ir	35	11)
	55670.5077	.0010	AG	+0.0014	s	GCVS 2009	-Ir	35	11)
	55673.4209	.0013	AG	+0.0011	s	GCVS 2009	-Ir	35	11)
	55673.5640	.0015	AG	−0.0015		GCVS 2009	-Ir	35	11)
	55705.4705	.0009	AG	+0.0018	s	GCVS 2009	-Ir	26	11)
V1104 Her	55672.3727	.0009	AG	−0.0049	s	GCVS 2009	-Ir	39	11)
	55672.4864	.0004	AG	−0.0052		GCVS 2009	-Ir	39	11)
	55672.5999	.0005	AG	−0.0056	s	GCVS 2009	-Ir	39	11)
	55682.4000	.0009	AG	−0.0042	s	GCVS 2009	-Ir	38	11)
	55682.5127	.0008	AG	−0.0054		GCVS 2009	-Ir	38	11)
	55692.4271	.0025	AG	−0.0037	s	GCVS 2009	-Ir	31	11)
	55692.5399	.0019	AG	−0.0048		GCVS 2009	-Ir	31	11)
	55741.4193	.0009	AG	−0.0049	s	GCVS 2009	-Ir	29	11)
	55741.5331	.0012	AG	−0.0050		GCVS 2009	-Ir	29	11)
V1105 Her	55670.4192	.0017	AG	−0.0133	s	GCVS 2009	-Ir	32	11)
	55670.5805	.0021	AG	−0.0129		GCVS 2009	-Ir	32	11)
	55673.4751	.0026	AG	−0.0136		GCVS 2009	-Ir	35	11)
	55705.4877	.0011	AG	−0.0106	s	GCVS 2009	-Ir	25	11)
CU Hya	55623.4632	.0027	AG	+0.1415	s	GCVS 2009	-Ir	61	11)
DF Hya	55621.3622	.0029	AG	+0.0499		GCVS 2009	-Ir	37	11)

Table 1: (cont.)

Variable	HJD 24.....	±	Obs	$O-C$		Bibliography	Fil	n	Rem
DF Hya	55621.5291	.0008	AG	+0.0515	s	GCVS 2009	-Ir	37	11)
FG Hya	55623.3952	.0037	AG	−0.0769		GCVS 2009	-Ir	46	11)
RW Lac	55758.4855	.0025	AG	−0.0237		GCVS 2009	-Ir	32	11)
	55784.3363	.0005	AG	+0.0130	s	GCVS 2009	-Ir	64	11)
TW Lac	55758.5375	.0018	AG	+0.3681		GCVS 2009	-Ir	32	11)
AG Lac	55775.3879	.0024	AG	−0.0159		GCVS 2009	-Ir	42	11)
AU Lac	55759.4458	.0001	AG	−0.0327	s	GCVS 2009	-Ir	23	11)
AW Lac	55754.5052	.0002	AG	+0.0497		BAVR 35,1	-Ir	23	11)
CN Lac	55672.5711	.0004	MS FR	−0.0698		GCVS 2009	o	450	5)
DG Lac	55784.5519	.0021	AG	−0.2238		GCVS 2009	-Ir	40	11)
EK Lac	55759.4671	.0041	AG	−0.0033		GCVS 2009	-Ir	23	11)
EM Lac	55754.4857	.0009	AG	+0.0864	s	GCVS 2009	-Ir	21	11)
EP Lac	55402.4688	.0004	MS FR	−0.3677		GCVS 2009	o	675	5)
EQ Lac	55707.4275	.0009	MS FR	+0.0192		GCVS 2009	o	510	5)
	55759.5037	.0002	AG	+0.0225		GCVS 2009	-Ir	20	11)
ER Lac	55784.5512	.0050	AG	−0.5458		GCVS 2009	-Ir	40	11)
EU Lac	55398.5201	.0002	MS FR	+0.2008		GCVS 2009	o	759	5)
EX Lac	55759.5208	.0090	AG	+0.2272	s	GCVS 2009	-Ir	22	11)
FI Lac	55393.4549	.0005	MS FR	+0.0179		GCVS 2009	o	690	5)
FL Lac	55759.5265	.0023	AG	−0.0513	s	GCVS 2009	-Ir	22	11)
	55784.4443	.0027	AG	−0.0483		GCVS 2009	-Ir	40	11)
HX Lac	55373.5619	.0001	MS FR	+0.0123		GCVS 2009	o	592	5)
IR Lac	55784.3898	.0030	AG	−0.0761	s	GCVS 2009	-Ir	40	11)
MZ Lac	55775.3749	.0019	AG	+0.2758	s	GCVS 2009	-Ir	43	11)
NR Lac	55397.4609	.0002	MS FR	+0.0653		GCVS 2009	o	710	5)
NS Lac	55396.4519	.0003	MS FR	−0.2270		GCVS 2009	o	520	5)
NW Lac	55759.5306	.0029	AG	−0.1476		GCVS 2009	-Ir	23	11)
V344 Lac	55445.4929	.0002	RAT RCR	−0.0929		GCVS 2009	-Ir	250	15)
V345 Lac	55775.4474	.0063	AG	+0.0784		GCVS 2009	-Ir	43	11)
UU Leo	55259.3833	.0002	MS FR	+0.1685		GCVS 2009	o	594	5)
	55625.5725	.0014	AG	+0.1742		GCVS 2009	-Ir	74	11)
UZ Leo	55259.3760	.0001	RAT RCR	−0.1016		GCVS 2009	-Ir	132	15)
	55632.3762	.0010	QU	−0.0902	s	GCVS 2009	V	75	3)
VZ Leo	55623.3839	.0008	FR	−0.0576	s	GCVS 2009	-Ir	43	11)
	55625.5694	.0195	AG	−0.0519	s	GCVS 2009	-Ir	72	11)
	55643.5406	.0004	FR	−0.0642		GCVS 2009	-Ir	45	11)
WZ Leo	55625.3079	.0017	AG	+0.2676		GCVS 2009	-Ir	74	11)
	55625.3132	.0008	DIE	+0.2729		GCVS 2009	o	31	14)
AM Leo	55626.4423	.0035	PGL	+0.0121	s	GCVS 2009	V	153	17)
BW Leo	55653.3907	.0021	SCI	+0.0625		GCVS 2009	o	28	2)
EX Leo	55671.4107	.0004	JU				o	65	2)
FM Leo	55668.3583	.0050	SIR	+0.0033	s	IBVS 5480	o	132	4)
GU Leo	55625.3181	.0004	AG	+0.0836	s	GCVS 2007	-Ir	61	11)
	55625.4951	.0012	AG	+0.0835		GCVS 2007	-Ir	61	11)
VW LMi	55659.3925	.0020	JU				o	65	2)
RZ Lyn	55629.3569	.0013	JU	−0.1242		GCVS 2009	o	67	2)
SW Lyn	55623.3364	.0011	DIE	+0.0598		GCVS 2009	o	33	14)
SX Lyn	55622.5802	.0048	AG	+0.0122		GCVS 2009	-Ir	152	11)
UV Lyn	55325.4219	.0001	RAT RCR	+0.0723		GCVS 2009	-Ir	143	15)
	55628.3615	.0011	JU	+0.0759		GCVS 2009	o	93	2)
AH Lyn	55624.2950	.0013	SCI				o	22	2)
	55628.3576	.0009	AG				-Ir	50	11)
DE Lyn	55622.3556	.0021	AG				-Ir	152	11)
	55622.5590	.0025	AG				-Ir	152	11)
EH Lyn	55628.3107	.0032	AG	+0.0016	s	GCVS 2009	-Ir	50	11)
	55628.4714	.0042	AG	−0.0011		GCVS 2009	-Ir	50	11)
	55628.6331	.0031	AG	−0.0028	s	GCVS 2009	-Ir	50	11)
AH Lyr	55372.4676	.0002	RAT RCR	−0.1430		GCVS 2009	-Ir	170	15)
	55707.4478	.0025	AG	−0.1436		GCVS 2009	-Ir	20	11)

Table 1: (cont.)

Variable	HJD 24.....	±	Obs	$O-C$		Bibliography	Fil	n	Rem
AH Lyr	55710.5406	.0015	AG	−0.1430		GCVS 2009	-Ir	25	11)
	55778.5669	.0006	AG	−0.1435		GCVS 2009	-Ir	42	11)
DF Lyr	55711.4958	.0031	AG	+0.0343	s	GCVS 2009	-Ir	43	11)
DU Lyr	55691.4597	.0001	MS FR	+0.1657		GCVS 2009	o	800	5)
EW Lyr	55480.3691	.0005	RAT RCR	+0.2380	s	GCVS 2009	-Ir	233	15)
	55481.3466	.0001	RAT RCR	+0.2411		GCVS 2009	-Ir	215	15)
	55705.4520	.0013	AG	+0.2434		GCVS 2009	-Ir	26	11)
FG Lyr	55740.4115	.0001	AG	−0.0820		GCVS 2009	-Ir	24	11)
FH Lyr	55412.4743	.0002	RAT RCR	+0.0186		GCVS 2009	-Ir	230	15)
GZ Lyr	55778.5719	.0016	AG	+0.0019		GCVS 2009	-Ir	42	11)
HY Lyr	55670.5209	.0016	AG				-Ir	35	11)
	55673.4733	.0015	AG				-Ir	35	11)
	55705.4000	.0008	AG				-Ir	27	11)
IP Lyr	55628.5992	.0001	MS FR	−0.0096		GCVS 2009	o	531	5)
	55673.5165	.0016	AG	−0.0089		GCVS 2009	-Ir	35	11)
	55705.4301	.0033	AG	−0.0097	s	GCVS 2009	-Ir	25	11)
LZ Lyr	55462.3152	.0002	RAT RCR	+0.3349		GCVS 2009	-Ir	132	15)
	55739.4471	.0010	JU	+0.3440		GCVS 2009	o	45	2)
NV Lyr	55740.5227	.0002	AG	−0.0817		GCVS 2009	-Ir	52	11)
PY Lyr	55624.6476	.0004	MS FR	+0.0694	s	GCVS 2009	o	522	5)
	55700.4516	.0010	AG	+0.0719		GCVS 2009	-Ir	36	11)
	55710.4814	.0008	AG	+0.0720		GCVS 2009	-Ir	25	11)
V400 Lyr	55784.4644	.0011	AG	+0.0551		GCVS 2009	-Ir	34	11)
V400 Lyr	55784.5902	.0003	AG	+0.0208	s	GCVS 2009	-Ir	34	11)
V401 Lyr	55784.5840	.0008	AG	+0.1125	s	GCVS 2009	-Ir	34	11)
V406 Lyr	55446.3681	.0001	RAT RCR	−0.0122		IBVS 4132	-Ir	130	15)
	55649.5135	.0002	MS FR	−0.0118		IBVS 4132	o	770	5)
V412 Lyr	55700.5013	.0030	AG	+0.2142		GCVS 2009	-Ir	33	11)
	55707.4870	.0048	AG	+0.2139	s	GCVS 2009	-Ir	20	11)
V574 Lyr	55673.3820	.0017	AG				-Ir	35	11)
	55673.5167	.0016	AG				-Ir	35	11)
V579 Lyr	55674.3741	.0004	AG				-Ir	29	11)
	55674.4950	.0009	AG				-Ir	29	11)
	55707.4079	.0007	JU				o	79	2)
	55707.5289	.0005	JU				o	79	2)
V582 Lyr	55739.3807	.0008	AG				-Ir	68	11)
	55739.5088	.0013	AG				-Ir	68	11)
V592 Lyr	55673.5112	.0003	AG	+0.0148		GCVS 2009	-Ir	35	11)
	55705.5241	.0003	AG	+0.0164		GCVS 2009	-Ir	25	11)
V594 Lyr	55674.4069	.0025	AG	−0.0282		GCVS 2009	-Ir	29	11)
	55674.5322	.0010	AG	−0.0309	s	GCVS 2009	-Ir	29	11)
	55682.4694	.0028	AG	−0.0298	s	GCVS 2009	-Ir	40	11)
V596 Lyr	55482.3152	.0002	RAT RCR	+0.0016		GCVS 2009	-Ir	199	15)
	55674.3766	.0005	AG	−0.0011		GCVS 2009	-Ir	29	11)
	55674.5252	.0008	AG	−0.0023	s	GCVS 2009	-Ir	29	11)
	55682.4658	.0007	AG	−0.0019		GCVS 2009	-Ir	40	11)
beta Lyr	55435.10	.02	VLM	+0.00		GCVS 2009	V	0	16)
	55441.26	.02	VLM	−0.30	s	GCVS 2009	V	0	16)
RW Mon	55623.3322	.0011	AG	−0.0714		GCVS 2009	V	47	11)
UX Mon	55618.3556	.0024	FR	−0.1758		GCVS 2009	-Ir	69	11)
AQ Mon	55622.2786	.0014	FR	−0.0085		BAVR 52,144	-Ir	67	11)
FS Mon	55629.3500	.0024	AG	−0.0133		GCVS 2009	V	33	11)
HP Mon	55629.3973	.0098	AG	+0.1139	s	GCVS 2009	-Ir	33	11)
IZ Mon	55236.3007	.0012	RAT RCR	−0.1351	s	GCVS 2009	-Ir	164	15)
	55623.4724	.0060	AG	−0.1385		GCVS 2009	-Ir	49	11)
V380 Mon	55627.3697	.0004	MS FR	−0.0715	s	GCVS 2007	o	472	5)
V453 Mon	55642.3550	.0002	MS FR	+0.0933		GCVS 2009	o	392	5)
V530 Mon	55625.3450	.0002	MS FR	+0.1319		GCVS 2009	o	408	5)
	55635.3309	.0050	SIR	+0.1327		GCVS 2009	o	65	4)

Table 1: (cont.)

Variable	HJD 24.....	±	Obs	$O-C$		Bibliography	Fil	n	Rem
V864 Mon	55629.4237	.0009	AG	−0.0084		GCVS 2009	V	33	11)
V735 Oph	55305.4953	.0001	RAT RCR	+0.0571		GCVS 2009	-Ir	250	15)
CQ Ori	55482.5594	.0005	MS FR	−0.0048		GCVS 2009	o	455	5)
FT Ori	55585.4255	.0010	SIR	+0.0169		GCVS 2009	o	86	4)
FZ Ori	55481.6185	.0002	MS FR	−0.0560		GCVS 2009	o	549	5)
BY Peg	55481.3292	.0003	MS FR	−0.0257		GCVS 2009	o	376	5)
GP Peg	55483.2783	.0004	MS FR	−0.0467		GCVS 2009	o	506	5)
V375 Peg	55408.5131	.0003	MS FR				o	816	5)
V404 Peg	55529.3916	.0004	RAT RCR	−0.0861	s	GCVS 2007	-Ir	222	15)
V427 Per	55481.4508	.0003	MS FR	+0.0128		GCVS 2009	o	539	5)
V449 Per	55462.5353	.0003	MS FR	+0.0498		GCVS 2009	o	588	5)
V450 Per	55446.5417	.0011	MS FR	+0.1057		GCVS 2009	o	444	5)
V482 Per	55599.252	.002	JU	+0.258		BAVM 68	o	30	2)
BR Sge	55782.4598	.0022	AG	+0.5968	s	GCVS 2009	-Ir	43	11)
CW Sge	55374.4705	.0002	RAT RCR	+0.0355		GCVS 2009	-Ir	198	15)
V384 Ser	55629.5769	.0016	AG	+0.0026	s	GCVS 2009	-Ir	54	11)
TY Tau	55473.5629	.0003	MS FR	+0.2546	s	GCVS 2009	o	510	5)
WY Tau	55629.4811	.0019	AG	+0.0568		GCVS 2009	-Ir	51	11)
EN Tau	55627.3727	.0010	JU	−0.0011		BAVR 52,49	o	88	2)
EO Tau	55591.5053	.0005	FR	−0.6268	s	GCVS 2009	-Ir	51	11)
EQ Tau	55480.4519	.0002	MS FR	−0.0252		GCVS 2009	o	322	5)
GW Tau	55622.3158	.0012	JU	−0.0826		GCVS 2009	o	59	2)
V781 Tau	55629.4407	.0061	AG	−0.0461		GCVS 2009	-Ir	49	11)
W UMa	55627.3272	.0021	PGL	−0.0119		BAVR 44,156	V	423	10)
	55629.3297	.0035	PGL	−0.0113		BAVR 44,156	V	333	10)
	55643.3424	.0035	PGL	−0.0112		BAVR 44,156	V	355	10)
RW UMa	55628.4317	.0013	SCI	−0.1627		GCVS 2009	o	278	2)
TW UMa	55635.5926	.0028	SCI	−0.3517		GCVS 2009	o	30	2)
	55659.4301	.0039	AG	−0.3492		GCVS 2009	-Ir	74	11)
	55685.4293	.0022	AG	−0.3519		GCVS 2009	-Ir	69	11)
TX UMa	55658.4103	.0024	SCI	+0.1939		GCVS 2009	o	138	2)
TY UMa	55311.5219	.0001	RAT RCR	−0.0699		GCVS 2009	-Ir	216	15)
XY UMa	55674.3998	.0004	JU	+0.0399		GCVS 2009	o	51	2)
AA UMa	55660.3981	.0017	SCI	+0.0404		GCVS 2009	o	72	2)
	55667.4179	.0005	JU	+0.0383		GCVS 2009	o	59	2)
AF UMa	55671.4511	.0017	AG	+0.5590		GCVS 2009	-Ir	260	11)
AW UMa	55669.3795	.0051	JU	−0.0819		GCVS 2009	-Ir	55	2)
BH UMa	55643.4067	.0024	SCI	−0.0606		GCVS 2009	o	83	2)
	55644.4630	.0024	SCI	−0.0524	s	GCVS 2009	o	83	2)
BQ UMa	55660.3853	.0035	AG	−0.1323		GCVS 2009	-Ir	53	11)
BS UMa	55660.4441	.0006	AG	−0.0169	s	GCVS 2009	-Ir	61	11)
	55660.6193	.0008	AG	−0.0602		GCVS 2009	-Ir	61	11)
DW UMa	55650.3492	.0004	JU				o	60	2)
	55662.3710	.0003	JU				o	31	2)
	55671.3874	.0018	SCI				o	78	2)
	55674.3928	.0018	SCI				o	30	2)
	55674.4566	.0030	SCI				o	23	2)
	55674.5291	.0012	SCI				o	42	2)
	55688.3865	.0028	SCI				o	31	2)
	55688.4623	.0012	SCI				o	27	2)
	55688.5117	.0005	SCI				o	20	2)
IW UMa	55235.4060	.0005	RAT RCR				-Ir	101	15)
LP UMa	55650.3681	.0007	JU				o	60	2)
	55674.3889	.0014	SCI				o	42	2)
	55688.4828	.0023	SCI				o	63	2)
MQ UMa	55660.5289	.0034	AG	+0.0779	s	GCVS 2009	-Ir	60	11)
MS UMa	55650.3854	.0022	AG	+0.0365	s	GCVS 2009	V	37	11)
OQ UMa	55659.4200	.0013	AG	+0.0005	s	GCVS 2009	-Ir	64	11)
	55685.4882	.0020	AG	+0.0000	s	GCVS 2009	-Ir	69	11)

Table 1: (cont.)

Variable	HJD 24.....	±	Obs	$O-C$		Bibliography	Fil	n	Rem
RT UMi	55408.4925	.0001	RAT RCR	+0.1412		GCVS 2009	-Ir	226	15)
RU UMi	55236.5289	.0001	RAT RCR	−0.0144		GCVS 2009	-Ir	326	15)
	55315.5306	.0002	RAT RCR	−0.0141	s	GCVS 2009	-Ir	227	15)
VW UMi	55244.5921	.0002	RAT RCR	+0.1038	s	GCVS 2009	-Ir	266	15)
VY UMi	55309.5649	.0001	RAT RCR				-Ir	275	15)
AG Vir	55672.4044	.0008	FR	−0.0073		GCVS 2009	o	70	14)
AH Vir	55672.3501	.0002	FR	+0.0321		GCVS 2009	o	70	14)
	55672.5508	.0010	FR	+0.0290	s	GCVS 2009	o	70	14)
AW Vir	55650.5433	.0020	AG	+0.0249	s	GCVS 2009	-Ir	95	11)
AX Vir	55650.4333	.0023	AG	+0.0171		BAVR 32,36	-Ir	95	11)
AZ Vir	55650.4368	.0021	AG	−0.0226		GCVS 2009	-Ir	95	11)
	55650.6120	.0017	AG	−0.0222	s	GCVS 2009	-Ir	95	11)
GR Vir	55632.5836	.0029	SCI	+0.0305		GCVS 2009	o	89	2)
XZ Vul	55776.4690	.0026	AG	+0.3546		GCVS 2009	-Ir	38	11)
AB Vul	55776.4629	.0007	AG	−0.0324		GCVS 2009	-Ir	38	11)
AT Vul	55787.3947	.0004	WTR	−0.0811		GCVS 2009	-Ir	84	8)
AZ Vul	55380.5002	.0002	RAT RCR	+0.0305		GCVS 2009	-Ir	151	15)
BU Vul	55378.4776	.0001	RAT RCR	+0.0153		GCVS 2009	-Ir	211	15)
FQ Vul	55712.5390	.0013	AG	+0.2693		GCVS 2009	-Ir	25	11)
FW Vul	55707.4975	.0043	AG	−0.0092		GCVS 2009	-Ir	20	11)
	55741.4251	.0101	AG	−0.0277	s	GCVS 2009	-Ir	32	11)
GO Vul	55776.4367	.0018	AG	−0.0374		GCVS 2007	-Ir	38	11)
GP Vul	55776.4924	.0027	AG	−0.0634	s	GCVS 2009	-Ir	38	11)
HI Vul	55741.4836	.0031	AG	−0.0617		GCVS 2009	-Ir	32	11)
	55776.4150	.0011	AG	−0.0608		GCVS 2009	-Ir	38	11)
HS Vul	55757.3970	.0005	GB	+0.0356		GCVS 2009	o	73	1)
	55775.4941	.0002	GB	+0.0350	s	GCVS 2009	o	110	1)
	55776.4903	.0001	GB	+0.0350	s	GCVS 2009	o	109	1)
	55778.4839	.0002	GB	+0.0362	s	GCVS 2009	o	100	1)
	55789.4428	.0003	GB	+0.0369	s	GCVS 2009	o	90	1)
	55790.4393	.0002	GB	+0.0372	s	GCVS 2009	o	110	1)
	55793.4280	.0002	GB	+0.0373	s	GCVS 2009	o	90	1)
	55794.4246	.0001	GB	+0.0377	s	GCVS 2009	o	112	1)
	55796.4165	.0001	GB	+0.0372	s	GCVS 2009	o	108	1)
KN Vul	55776.3912	.0016	AG	−0.0043	s	GCVS 2009	-Ir	38	11)
	55776.5722	.0012	AG	−0.0019		GCVS 2009	-Ir	38	11)
NO Vul	55682.5392	.0001	MS FR	+0.0920	s	GCVS 2009	o	424	5)
GSC 00124-00551	55600.4216	.0051	FR				-Ir	36	11)
GSC 00278-00814	55627.6472	.0025	FR				-Ir	48	11)
GSC 00279-00822	55280.4466	.0003	FR				-Ir	62	11)
	55627.5730	.0001	FR				-Ir	47	11)
GSC 00425-02297	55451.2996	.0007	FR				o	34	11)
GSC 00752-01971	51655.3177	.0007	FR				o	38	6)
GSC 00760-01355	55624.4345	.0007	FR				-Ir	45	11)
GSC 01330-00239	54910.3597	.0042	ATB				o	102	2)
GSC 01330-00287	54910.3696	.0014	ATB	−0.0003		BAVR 54.105	o	101	2)
GSC 01337-01137	55629.4073	.0003	FR				-Ir	43	11)
GSC 01383-01023	49029.361		FR					35	22)
GSC 01383-01601	55279.3090	.0005	FR				o	304	11)
	55279.4437	.0001	FR				o	76	11)
GSC 01403-00178	55643.4447	.0006	FR				-Ir	39	11)
GSC 01478-00244	55311.5097:	.0006	FR				-Ir	29	7)
GSC 01721-01591	55461.4040	.0015	MS FR				o	384	5)
	55474.3142	.0004	MS FR				o	315	5)
GSC 01864-01065	50839.3351	.0008	FR				o	34	6)
	55591.4098	.0001	FR				-Ir	82	11)
	55591.5904	.0003	FR				-Ir	82	11)
GSC 01921-00251	55625.3974	.0023	FR				-Ir	32	11)
GSC 01927-00862	55672.3950	.0020	QU				V	49	3)

Table 1: (cont.)

Variable	HJD 24.....	±	Obs	$O-C$	Bibliography	Fil	n	Rem
GSC 02038-00293	55662.5196	.0011	FR	+0.0040	BAVM 177	-Ir	48	11)
GSC 02133-02623	55483.3132	.0004	FR			o	25	11)
GSC 02134-00821	55385.5334	.0009	FR			-Ir	40	11)
	55387.5256	.0004	FR			-Ir	48	11)
	55409.4415	.0004	FR			o	48	11)
	55418.4074	.0006	FR			o	42	11)
	55429.3649	.0003	FR			o	49	11)
GSC 02157-00014	55473.4062	.0004	FR			o	53	11)
	55478.3598	.0005	FR			o	47	11)
GSC 02161-01573	55473.3601	.0007	FR			o	38	11)
	55478.4371	.0011	FR			o	41	11)
GSC 02411-01103	55632.5033	.0058	FR			-Ir	42	11)
GSC 02415-00286	55632.4150	.0007	FR			-Ir	53	11)
GSC 02423-00517	55599.2446	.0004	FR			-Ir	143	11)
	55599.4308	.0001	FR			-Ir	143	11)
	55599.6199	.0006	FR			-Ir	143	11)
GSC 02572-00373	55662.4238	.0038	FR			o	42	14)
	55662.5657	.0013	FR			o	42	14)
GSC 02606-00217	55033.5131	.0001	FR			-Ir	52	11)
GSC 02682-00817	54757.3134	.0003	FR			-Ir	17	11)
GSC 03137-03322	55686.5167	.0063	AG			-Ir	24	11)
GSC 03618-00307	55141.5643	.0008	FR			-Ir	51	11)
GSC 03619-00768	55141.4004	.0012	FR			-Ir	50	11)
GSC 03870-01172	55294.4344	.0001	FR			o	77	11)
	55294.5968	.0002	FR			o	77	11)
GSC 04030-02020	51430.4675	.0002	RAT RCR			o	127	2)
	51780.5733	.0003	RAT RCR			o	107	2)
GSC 04500-00730	55483.5563	.0001	RAT RCR			-Ir	239	15)
GSC 04828-00217	55622.3688	.0010	FR			-Ir	31	11)
GSC 04845-01474	55618.4517	.0007	FR			-Ir	40	11)
U-A2 0975-04179063	55590.2758	.0034	FR			-Ir	73	11)
	55590.5504	.0016	FR			-Ir	73	11)
U-A2 0975-04180434	55590.3028	.0005	FR			-Ir	67	11)
	55590.4884	.0004	FR			-Ir	67	11)
U-A2 1200-02901360	53764.3136	.0003	FR			o	34	7)
U-A2 1200-02929233	53764.3016	.0002	FR			o	36	7)
	53764.4272	.0022	FR			o	36	7)
	53764.5624	.0012	FR			o	36	7)
U-A2 1200-02953024	53764.3304	.0008	FR			o	34	7)
	53764.5555	.0007	FR			o	34	7)
U-A2 1200-02957976	53764.5016	.0002	FR			o	35	7)
U-A2 1275-00811770	54830.4914	.0015	FR			-Ir	37	11)
U-A2 1350-17859563	55480.5180	.0002	RAT RCR			-Ir	237	15)
U-A2 1425-13411870	54035.5187	.0019	AG			-Ir	35	1)
U-B1 1113-0494337	53934.4439	.0013	AG			-Ir	18	1)
	55042.5163	.0014	AG			-Ir	42	11)
	55393.4518	.0028	AG			-Ir	30	11)
U-B1 1416-0454010	55445.5928	.0005	RAT RCR			-Ir	244	15)
U-B1 1505-0372164	55451.6112	.0004	RAT RCR	+0.0062	PZP 10.13	-Ir	194	15)

Table 2: Times of maxima of pulsating stars

Variable	HJD 24.....	±	Obs	$O-C$	Bibliography	Fil	n	Rem
CY Aqr	53290.2660	.0007	BO	+0.0010	GCVS 2009	o	152	18)
	53290.3260	.0001	BO	+0.0000	GCVS 2009	o	152	18)
TZ Aur	55615.338 :	.007	PGL	+0.014	GCVS 2009	V	48	10)
V377 Aur	55645.3899	.0139	PGL			V	278	17)
V378 Aur	55650.52	.03	PGL			V	701	17) 20)
RS Boo	55644.4921	.0035	PGL	+0.0186	BAVR 36,157	V	124	10)
	55687.514	.001	AG	+0.024	BAVR 36,157	-Ir	71	11)
	55695.3554	.0006	RLF	−0.0588	BAVR 36,157	o	0	19)
TW Boo	55707.4059	.0021	RLF	−0.0098	A&A 476.307 (2007)	o	0	19)
UU Boo	55656.3803	.0035	PGL	−0.2193	GCVS 2009	V	133	10)
	55682.4200	.0011	RLF	−0.2241	GCVS 2009	o	0	19)
WW Boo	55688.4219	.0008	MZ	+0.1362	GCVS 2009	-Ir	120	2)
WZ Boo	55703.5169	.0013	MZ	−0.0152	GCVS 2009	-Ir	164	2)
	55714.4861	.0030	MZ	−0.1449	GCVS 2009	-Ir	133	2)
YZ Boo	55642.349	.001	AG	+0.003	GCVS 2009	V	61	11)
	55642.454	.001	AG	+0.004	GCVS 2009	V	61	11)
	55642.558	.001	AG	+0.004	GCVS 2009	V	61	11)
	55642.662	.001	AG	+0.004	GCVS 2009	V	61	11)
BU Boo	55686.5179	.0035	SCI			o	58	2)
CM Boo	55615.5098	.0035	PGL	−0.1226	GCVS 2009	V	127	17)
	55626.4698	.0035	PGL	−0.1260	GCVS 2009	V	222	10)
	55654.4908	.0035	PGL	−0.1227	GCVS 2009	V	177	10)
CS Boo	55705.5318	.0021	RLF	−0.0023	IBVS 2855	o	0	19)
CU Boo	55627.487	.001	AG			-Ir	61	11)
DD Boo	55649.433 :	.007	PGL			V	234	10)
	55683.3869	.0017	MZ			-Ir	136	2)
	55686.4487	.0020	MZ			-Ir	57	2)
	55704.4349	.0016	MZ			-Ir	113	2)
DG Boo	55706.3935	.0010	MZ			-Ir	98	2)
UY Cam	55644.594	.001	AG	+0.069	BAVR 49,41	-Ir	79	11)
CN Cam	55629.4775	.0030	MZ			-Ir	166	2) 21)
	55636.3228	.0020	MZ			-Ir	124	2)
	55645.643	.003	AG			-Ir	114	11)
SX Cnc	55641.3481	.0020	SB	+0.1700	GCVS 2007	V	38	13)
TT Cnc	55621.3337	.0035	PGL	−0.0044	A&A 476.307 (2007)	V	119	10)
AQ Cnc	55625.494	.001	AG	−0.077	GCVS 2009	-Ir	70	11)
EF Cnc	55622.595	.001	AG			-Ir	83	11)
	55628.4925:	.0030	MZ			-Ir	119	2)
	55661.3588	.0020	MZ			-Ir	114	2)
	55671.3942	.0030	MZ			-Ir	119	2)
Z CVn	55615.4073	.0026	SCI	−0.1169	GCVS 2009	o	68	2)
	55622.5978	.0023	SCI	−0.1185	GCVS 2009	o	86	2)
	55626.5241	.0021	SCI	−0.1151	GCVS 2009	o	46	2)
	55628.4774	.0035	PGL	−0.1232	GCVS 2009	V	395	10)
	55632.398 :	.004	PGL	−0.125	GCVS 2009	V	232	10)
	55636.3327	.0020	SCI	−0.1138	GCVS 2009	o	33	2)
	55645.475 :	.010	PGL	−0.125	GCVS 2009	V	211	10)
	55647.4418	.0035	PGL	−0.1196	GCVS 2009	V	327	10)
RX CVn	55682.519	.005	AG	−0.036	BAVM 75	-Ir	80	11)
SS CVn	55682.494	.001	AG	+0.146	GCVS 2009	-Ir	81	11)
ST CVn	55661.493	.002	AG	−0.089	BAVR 49,105	-Ir	34	11)
SZ CVn	55699.3877	.0024	MZ	−0.0145	GCVS 2009	-Ir	100	2)
TZ CVn	55624.515	.001	AG	+0.002	GCVS 2009	-Ir	36	11)
VW CVn	55661.476	.003	AG	+0.109	BAVR 49,105	-Ir	34	11)
AI CVn	55667.399 :	.014	PGL			V	443	10)
	55681.4811	.0069	PGL			V	999	10)
	55689.4363	.0035	PGL			V	965	10)
X CMi	55625.401	.001	AG	+0.022	BAVR 44,162	-Ir	35	11)
RV CMi	55625.302	.001	AG	+0.028	BAVR 49,41	-Ir	37	11)

Table 2: (cont.)

Variable	HJD 24.....	±	Obs	$O-C$	Bibliography	Fil	n	Rem
AL CMi	55625.318	.001	AG	−0.025	BAVR 49,41	-Ir	35	11)
BR Cas	55625.3077	.0007	MZ	+0.2880	GCVS 2007	-Ir	115	2)
QY Cas	55548.2725	.0030	MZ	−0.1815	GCVS 2007	-Ir	73	2)
V363 Cas	55776.453	.002	AG	+0.070	BAVR 49,41	-Ir	35	11)
V871 Cas	55495.5593	.0007	RAT RCR			-Ir	242	15)
EL Cep	55685.537	.001	AG	+0.115	GCVS 2009	-Ir	38	11)
FP Cep	55644.502	.001	AG	−0.040	GCVS 2009	-Ir	55	11)
S Com	55646.6270	.0009	SCI	+0.0173	A&A 476.307(2007)	o	58	2)
	55662.465	.001	AG	+0.018	A&A 476.307(2007)	-Ir	56	11)
	55669.5106	.0034	SCI	+0.0241	A&A 476.307(2007)	o	39	2)
	55675.368	.001	AG	+0.016	A&A 476.307(2007)	-Ir	38	11)
U Com	55662.383	.003	AG	+0.006	BAVR 49,41	-Ir	56	11)
AG Com	55675.391	.002	AG	−0.012	GCVS 2009	-Ir	38	11)
IS Com	55624.427	.001	AG			-Ir	36	11)
SU CrB	55705.438	.002	AG	+0.014	GCVS 2009	-Ir	41	11)
SZ CrB	55627.560	.003	MS FR	+0.014	BAVR 49,41	o	525	5)
AQ CrB	55690.390	.001	AG	+0.001	GCVS 2009	-Ir	21	11)
V759 Cyg	55687.590	.005	AG	+0.067	GCVS 2009	-Ir	25	11)
V2367 Cyg	55687.469	.001	AG	−0.022	GCVS 2009	-Ir	25	11)
V2470 Cyg	55740.4641	.0010	MZ			-Ir	249	2) 21)
	55746.4940	.0010	MZ			-Ir	115	2)
	55751.4250	.0010	MZ			-Ir	78	2)
BX Del	55740.512	.004	MS FR	+0.104	GCVS 2009	o	650	5)
RW Dra	55642.415	.001	AG	−0.217	GCVS 2009	-Ir	29	11)
SW Dra	55724.4359	.0035	PGL	+0.0036	BAVR 47,67	V	290	10)
VZ Dra	55620.3632	.0035	PGL	+0.0832	GCVS 2009	V	390	17)
	55627.4286	.0069	PGL	+0.0859	GCVS 2009	V	132	10)
	55641.5548	.0021	SCI	+0.0867	GCVS 2009	o	91	2)
	55642.517	.001	AG	+0.086	GCVS 2009	-Ir	66	11)
XZ Dra	55647.5469	.0069	PGL	−0.1287	GCVS 2009	V	204	10)
AV Dra	55672.426	.001	AG	+0.018	GCVS 2009	-Ir	39	11)
	55692.421	.003	AG	+0.012	GCVS 2009	-Ir	32	11)
BK Dra	55620.4218	.0035	PGL	+0.0740	BAVR 46,1	V	97	10)
RR Gem	55629.3401	.0035	PGL	−0.0240	BAVR 47,67	V	118	17)
SZ Gem	55589.3586	.0021	PGL	+0.0098	BAVR 48,65	V	243	10)
	55590.3614	.0035	PGL	+0.0104	BAVR 48,65	V	234	10)
	55623.4345	.0010	QU	+0.0087	BAVR 48,65	V	58	3)
	55629.4485	.0035	PGL	+0.0092	BAVR 48,65	V	98	17)
AK Gem	55590.422	.003	FR	−0.184	GCVS 2009	-Ir	124	11)
FV Gem	55601.4296	.0012	MZ	−0.0311	GCVS 2009	-Ir	110	2)
zeta Gem	55396.94	.02	VLM	−1.12	GCVS 2009	V	0	16)
TW Her	55647.4915	.0035	PGL	−0.0150	GCVS 2009	V	97	17)
	55723.4166	.0035	PGL	−0.0139	GCVS 2009	V	311	17)
AF Her	55710.393	.001	AG	−0.048	BAVR 49,105	-Ir	28	11)
AR Her	55615.4198	.0021	PGL	+0.0370	BAVR 52,3	V	253	17)
	55647.3832	.0035	PGL	+0.0414	BAVR 52,3	V	185	17)
	55662.4448	.0035	PGL	+0.0634	BAVR 52,3	V	187	17)
	55716.4512	.0035	PGL	+0.0217	BAVR 52,3	V	250	10)
	55723.5247	.0035	PGL	+0.0454	BAVR 52,3	V	198	10)
	55724.4808	.0035	PGL	+0.0616	BAVR 52,3	V	343	17)
CK Her	55758.414	.002	AG	−0.028	GCVS 2007	-Ir	35	11)
HP Her	55671.499	.006	AG	−0.122	GCVS 2007	-Ir	46	11)
V383 Her	55689.443	.002	AG	+0.036	GCVS 2009	-Ir	32	11)
V394 Her	55660.490	.001	AG	−0.155	GCVS 2009	-Ir	54	11)
V489 Her	55689.386	.001	AG	+0.025	GCVS 2009	-Ir	32	11)
V545 Her	55671.506	.001	AG	+0.133	GCVS 2009	-Ir	46	11)
	55707.391	.002	AG	+0.131	GCVS 2009	-Ir	59	11)
V633 Her	55729.4193	.0010	MZ	−0.0608	GCVS 2009	-Ir	135	2)
VX Hya	55674.3359	.0013	FLG			-Ir	58	9)

Table 2: (cont.)

Variable	HJD 24.....	±	Obs	$O-C$	Bibliography	Fil	n	Rem
CR Hya	55623.553	.002	AG	−0.188	GCVS 2009	-Ir	61	11)
CH Lac	55784.420	.002	AG	+0.013	GCVS 2009	-Ir	40	11)
BD Leo	55670.3552	.0013	MZ	+0.0759	GCVS 2009	-Ir	105	2)
	55674.3785	.0012	MZ	+0.0794	GCVS 2009	-Ir	73	2)
	55677.3940	.0015	MZ	+0.0800	GCVS 2009	-Ir	103	2)
	55682.4180	.0020	MZ	+0.0793	GCVS 2009	-Ir	88	2)
BO Leo	55664.4627	.0009	MZ	+0.1406	GCVS 2009	-Ir	133	2)
DI Leo	55658.4494	.0010	MZ	+0.2248	GCVS 2009	-Ir	64	2)
	55672.3859	.0010	MZ	−0.2590	GCVS 2009	-Ir	89	2)
WW Lyr	55710.403	.001	AG	+0.110	GCVS 2009	-Ir	25	11)
	55712.466	.001	AG	+0.110	GCVS 2009	-Ir	26	11)
BQ Lyr	55703.4123	.0069	PGL	+0.0972	GCVS 2009	V	134	10)
	55739.4639	.0040	MZ	+0.0405	GCVS 2009	-Ir	141	2)
EN Lyr	55747.4375	.0013	MZ	+0.1624	GCVS 2009	-Ir	106	2)
NR Lyr	55784.536	.002	AG	−0.029	GCVS 2009	-Ir	34	11)
V593 Lyr	55739.468	.001	AG	+0.027	GCVS 2009	-Ir	68	11)
UW Mon	55628.2973	.0010	MZ	−0.0282	GCVS 2009	-Ir	91	2)
GM Mon	55601.3110	.0013	MZ			-Ir	172	2) 21)
	55601.3172	.0020	SB			V	116	13)
V2509 Oph	55266.591	.001	MS FR			o	583	5)
V1640 Ori	55629.3764	.0020	MZ	−0.0586	BAVM 149	-Ir	105	2)
AR Per	55590.4501	.0035	PGL	+0.0588	GCVS 2009	V	208	10)
DF Ser	55716.4243	.0010	MZ	+0.0866	GCVS 2009	-Ir	119	2)
YZ Tau	55627.3463	.0020	MZ	+0.0597	GCVS 2009	-Ir	68	2)
BR Tau	53723.4906	.0010	MZ	+0.0105	GCVS 2009	Sy	45	12)
	55623.3380	.0008	MZ	+0.0145	GCVS 2009	-Ir	120	2)
RV UMa	55629.4553	.0035	PGL	+0.0137	BAVR 48,189	V	425	10)
SX UMa	55659.401	.001	AG	−0.043	GCVS 2009	-Ir	71	11)
	55685.505	.001	AG	−0.044	GCVS 2009	-Ir	69	11)
TU UMa	55617.4548	.0035	PGL	−0.0385	GCVS 2009	V	690	10)
	55621.3527	.0035	PGL	−0.0443	GCVS 2009	V	394	17)
	55624.6953	.0005	SCI	−0.0476	GCVS 2009	o	88	2)
	55626.3692	.0021	PGL	−0.0467	GCVS 2009	V	331	10)
	55632.5048	.0005	QU	−0.0454	GCVS 2009	V	99	3)
	55641.4279	.0006	QU	−0.0448	GCVS 2009	V	115	3)
	55645.3299	.0035	PGL	−0.0464	GCVS 2009	V	214	10)
	55660.3878	.0006	QU	−0.0453	GCVS 2009	V	80	3)
	55670.4246	.0006	QU	−0.0464	GCVS 2009	V	141	3)
AB UMa	55650.471	.005	AG	+0.245	BAVR 49,41	-Ir	37	11)
AE UMa	55620.3375	.0014	PGL	+0.0054	BAVR 48,189	V	371	10)
AV UMa	55660.537	.005	AG	−0.018	GCVS 2009	-Ir	61	11)
BB UMa	55650.506	.001	AG	+0.094	GCVS 2009	-Ir	38	11)
CD UMa	55672.550	.001	AG	+0.057	GCVS 2009	-Ir	188	11)
EX UMa	55622.539	.001	AG			-Ir	152	11)
ST Vir	55623.5150	.0010	SCI	−0.0332	GCVS 2009	o	46	2)
VZ Vir	55691.4055	.0013	MZ	−0.0335	GCVS 2009	-Ir	238	2) 21)
	55711.4343	.0009	MZ	−0.0418	GCVS 2009	-Ir	197	2) 21)
BC Vir	55650.612	.001	AG	+0.189	GCVS 2009	-Ir	94	11)
GSC 00472-02473	55444.3932	.0139	PGL			V	225	17)
	55445.353	.014	PGL			V	167	17)
	55479.4334	.0139	PGL			V	399	17)
	55481.2949	.0139	PGL			V	183	17)
	55482.286 :	.014	PGL			V	145	17)
GSC 01336-00829	55514.675	.010	FR			o	51	11)

Observers:

AG:	Agerer, F., Tiefenbach
ATB:	Achterberg, H., Norderstedt
BO:	Bode, H.-J., Hannover
DIE:	Dietrich, M., Radebeul
FLG:	Flechsig, Dr. G.-U., Teterow
FR:	Frank, P., Velden
GB:	Gröbel, R., Eckental
JU:	Jungbluth, Dr. H., Karlsruhe
MS:	Moschner, W., Lennestadt
MZ:	Maintz, Dr. G., Bonn
PGL:	Pagel, Dr. L., Klockenhagen
QU:	Quester, W., Esslingen
RAT:	Rätz, M., Herges-Hallenberg
RCR:	Rätz, K., Herges-Hallenberg
RLF:	Retzlaff, K., Gross Ammensleben
SB:	Steinbach, Dr. H., Neu-Anspach
SCI:	Schmidt, U., Karlsruhe
SIR:	Schirmer, J., Willisau (CH)
VLM:	Vollmann, W., Wien (A)
WTR:	Walter, F., München

Remarks:

:	uncertain
s	secondary minimum
	CCD-Cameras
1)	ccd-camera ST-6: chip 375*242 uncoated
2)	ccd-camera ST-7
3)	ccd-camera ST-7E
4)	ccd-camera ST-8XME
4)	ccd-camera ST-8XMEI: chip KAF1603ME
5)	ccd-camera ST-9XE
6)	ccd-camera OES-LcCCD11
7)	ccd-camera OES-LcCCD12
8)	ccd-camera Pictor 416XT
9)	ccd-camera Sigma 402: chip KAF0402ME
10)	ccd-camera Artemis 4021
11)	ccd-camera Sigma 1603
12)	ccd-camera Busca
13)	ccd-camera Sigma 402ME
14)	ccd-camera Canon EOS 450D
15)	ccd-camera Moravian G2-1600
16)	ccd-camera Canon powershot g3
17)	ccd-camera QHY8
18)	ccd-camera IOS (TI245)
19)	ccd-camera ATIK 314 L+
20)	normal maximum
21)	assembled from the observations of two nights
22)	evaluation: measurement with microphotometer
	Filter
o	without filter
B	B-filter
V	V-filter
R	R-filter
I	I-filter
-Ir	IR cut-off filter
Sy	Strömgren y (Calar Alto)

References:

A&A	Astronomy & Astrophysics
AJ vvv,ppp	Astronomical Journal volume, pages
BAVM nnn	BAV Mitteilungen No. nnn
BAVR vv,ppp	BAV Rundbrief volume, pages
GCVS 2009	General Catalogue of Variable Stars, version: iii.dat 20.11.2009
IBVS nnnn	Information Bulletin on Variable Stars No. nnnn
MVS vv,ppp	Mitteilungen für Veränderliche Sterne, volume, page
PZP vol.n	Peremennye Zvezdy Prilozhenie Vol, No.
	Star catalogues
GSC	The HST Guide Star Catalogue 1.2
U-A2	USNO A2.0 catalogue
U-B1	USNO B1.0 catalogue

ERRATUM FOR IBVS 5889 (BAVM 203)

BR Tau 54723.4862 MZ has to be deleted

ERRATUM FOR IBVS 5941 (BAVM 212)

KV Gem 54910.3597 ATB has to be deleted
KV Gem 54910.3696 ATB has to be deleted

ERRATUM FOR IBVS 6010 (BAVM 220)

DI Leo 55672.3859 MZ has to be deleted
BQ Lyr 55739.4639 MZ has to be deleted
GSC 01330-00239 54910.3597 ATB has to be deleted

ERRATUM FOR IBVS 6010 (BAVM 220)

AB Cas 55463.4821 PGL has to be deleted
WZ Boo 55703.5169 MZ has to be deleted
WZ Boo 55714.4861 MZ has to be deleted

COMMISSIONS 27 AND 42 OF THE IAU
INFORMATION BULLETIN ON VARIABLE STARS

Number 6011

Konkoly Observatory
Budapest
19 January 2012

HU ISSN 0374 – 0676

TIMINGS OF MINIMA OF ECLIPSING BINARIES

DIETHELM, ROGER

Bahnhofstrasse 3, CH–4118 Rodersdorf, Switzerland

The following Table lists timings of minima of eclipsing binaries secured by CCD photometry, obtained in the second half of 2011. The given O-C values generally refer to the linear elements of the newest electonic version of the GCVS (Samus et al., 2011), except for the cases stated in the remarks, where the determination of current elements made use of the up-to-date ASAS data (`http://www.astrouw.edu.pl/asas/`) and the Lafler-Kinman algorithm of the PERANSO software (`http://www.peranso.com/`). All times given are heliocentric UTC, JD 2450000 should be added. All data was obtained in the V band at the R. Szafraniec Observatory operated at Astrokolkhoz Obs., Cloudcroft, N.M., USA. The tremendous effort put in by T. Krajci at the site is acknowledged thankfully.

Table 1: Minima of eclipsing binaries

Variable	Type	HJD 24...	±	$O-C$	n	Remarks
WX And	p	55845.6912	0.0007	+0.0670	28	
AB And	p	55869.7476	0.0009	−0.0036	21	
DK And	s	55882.7202	0.0006	+0.0087	30	additional Delta Sct var.?
DO And	p	55845.8552	0.0006	+0.0258	35	
EP And	p	55893.7235	0.0004	−0.0134	36	el: IBVS 5184
FL And	p	55828.8737	0.0007	+0.0074	26	
GW And	p	55840.6385	0.0015	−0.4833	31	
GZ And	s	55843.8688	0.0005	−0.0001	22	
LM And	p	55903.6722	0.0007	−0.0104	36	
LY And	s	55844.8763	0.0008	+0.0043	20	
NZ And	p	55894.6853	0.0004	−0.0128	30	
QW And	p	55903.7220	0.0004	+0.0064	35	
QX And	p	55847.8904	0.0006	+0.0791	35	
V404 And	p	55894.6899	0.0005	+0.0132	24	
V444 And	p	55896.6603	0.0004	−0.0038	46	el: 52914.2861+0.4687794×E
V449 And	p	55843.8630	0.0007	−0.0109	24	
V452 And	p	55875.7839	0.0018	−0.0023	9	el: 52958.0826+0.9784385×E
V463 And	p?	55875.7023	0.0004	−0.0588	21	el: IBVS 5699; d=0.025 d
GSC 1739-1463	s	55894.6965	0.0006	−0.0026	21	el: IBVS 5960
GSC 2822-1558	s	55895.7078	0.0007	−0.0233	12	el: OEJV 104
GSC 2825-603	p	55894.6370	0.0010	+0.0102	35	el: OEJV 104
GSC 3234-1318	s	55881.7108	0.0007	+0.0498	22	el: PZP 10, 18
GSC 3243-336	s	55882.7059	0.0005	+0.0839	26	el: PZ 28, 2; d=0.03 d
GSC 3243-962	p	55883.776	0.004	+0.048	17	el: 51573.628+1.55768×E

Table 1: Minima of eclipsing binaries (continued)

Variable	Type	HJD 24...	±	$O-C$	n	Remarks
GSC 3627-1727	s	55881.7514	0.0005	+0.0464	20	el: IBVS 5920
GSC 3638-2422	p	55883.7319	0.0005	−0.0102	19	el: IBVS 5920
GSC 3644-1562	s	55881.7072	0.0005	+0.0436	27	el: IBVS 5960
ST Aqr	p	55862.7395	0.0006	−0.0106	42	
SU Aqr	p	55866.7360	0.0003	+0.0048	30	
CK Aqr	p	55846.6614	0.0009	+0.0148	13	
CR Aqr	p	55846.6647	0.0006	+0.0010	14	el: 54304.728+0.514491×E
CX Aqr	p	55864.7139	0.0002	−0.0072	40	
DD Aqr	s	55866.7468	0.0017	−0.0038	42	el: 54746.660+0.7210110×E
EF Aqr	p	55866.7125	0.0003	−0.0077	43	el: 55167.595+2.8535721×E
EX Aqr	s	55847.675	0.004	−0.002	37	el: 53912.821+0.8893845×E
FS Aqr	s	55854.6259	0.0001	+0.0376	14	
	p	55854.7582	0.0004	+0.0389	14	
GH Aqr	p	55862.5941	0.0016	+0.0023	16	
	s	55862.7473	0.0005	+0.0027	16	
GK Aqr	s	55862.7045	0.0002	+0.0190	21	
GM Aqr	s	55862.6792	0.0004	−0.0444	32	
GZ Aqr	s	55874.7448	0.0005	−0.1461	12	
HV Aqr	p	55855.7243	0.0004	−0.0128	20	
MO Aqr	s	55846.7195	0.0006	−0.0026	19	el: 55099.605+0.3981439×E
NN Aqr	p	55849.6291	0.0009	+0.0062	14	el: 54684.783+0.306779×E
	s	55849.7828	0.0022	+0.0066	9	
NW Aqr	p	55867.6697	0.0019	+0.0108	13	el: 54444.578+0.301628×E
GSC 529-281	p	55855.6411	0.0006	−0.0111	18	el: 53882.915+0.409027×E; asymmetric
GSC 567-602	p	55864.6070	0.0003	−0.0263	29	el: 54798.548+0.477316×E; d=0.04: d
GSC 568-1328	p	55866.7002	0.0005	−0.0020	26	el: IBVS 5920
GSC 5191-146	p	55846.6670	0.0002	−0.0095	25	el: 53470.900+0.274688×E
GSC 5197-695	s	55847.6921	0.0005	+0.0097	23	el: 53538.865+0.362936×E
GSC 5210-437	p	55854.6524	0.0003	−0.0061	30	el: IBVS 5960
GSC 5220-352	s	55850.6540	0.0003	+0.0039	17	el: 54738.702+0.294751×E; d=0.012 d
GSC 5233-327	p	55865.6651	0.0026	−0.0023	17	el: 54392.576+0.430351×E
GSC 5248-214	s	55868.7159	0.0003	+0.0024	13	el: 53702.570+0.323088×E
GSC 5777-383	p	55855.6520	0.0004	+0.0079	14	el: 53568.869+0.579077×E
GSC 5802-335	p	55854.7038	0.0002	+0.0324	32	el: IBVS 5960
GSC 5804-102	p	55854.7106	0.0004	−0.0344	39	el: IBVS 5920
GSC 5811-437	p	55864.7170	0.0004	−0.0068	19	el: 53270.617+0.297387×E
GSC 5817-92	s	55864.6813	0.0004	+0.0016	34	el. 2453583.779+0.369646×E
GSC 5817-435	s	55863.6485	0.0006	+0.0055	33	el: 55156.581+0.407646×E; d=0.04 d
GSC 5818-1148	p	55867.6744	0.0004	−0.0042	17	el: 54662.749+0.915600×E
GSC 5820-1011	p	55869.7249	0.0003	−0.0009	18	el. 2453912.879+0.394844×E
GSC 5821-87	p	55868.7239	0.0002	+0.0023	30	el: 54603.908+0.628635×E; d=0.026 d
GSC 5826-1082	p	55867.6564	0.0004	−0.0230	17	el: 52634.543+0.374119×E
GSC 5835-944	s	55883.7094	0.0003	−0.0098	17	el: 54658.879+0.280637×E
GSC 5836-40	s	55883.7335	0.0006	+0.0017	23	el: 53706.566+0.390488×E
GSC 6386-105	p	55874.7009	0.0015	−0.0170	12	el: 54703.754+0.256903×E
GSC 6403-431	p	55882.6838	0.0009	+0.0226	17	el: 54686.739+0.361415×E; d=0.026 d
V761 Aql	p	55828.6509	0.0014	+0.0953	28	
GSC 5160-500	s	55828.6836	0.0006	−0.0015	27	el: 53674.570+0.551136×E; d=0.04 d
GSC 5172-1240	p	55828.7051	0.0003	−0.0012	24	el: 54606.887+0.538721×E
GSC 5743-114	s	55828.6879	0.0006	−0.0051	20	el: 54253.815+0.434869×E
SS Ari	s	55840.9081	0.0002	−0.0074	23	
SZ Ari	p	55845.8704	0.0005	−0.0144	38	
TX Ari	p	55844.8377	0.0009	−0.0125	39	
AL Ari	p	55845.8522	0.0005	+0.0071	24	
BM Ari	p	55843.8969	0.0003	+0.0046	36	el: IBVS 5960
BN Ari	p	55843.8416	0.0005	−0.0009	13	el: IBVS 5960
	s	55843.9922	0.0016	0	8	
GSC 645-85	p	55851.9221	0.0008	+0.0083	22	el: IBVS 5960
GSC 1209-1201	s	55910.6473	0.0004	+0.0317	28	el: IBVS 5920
GSC 1210-442	s	55840.9023	0.0004	+0.0068	29	el: IBVS 5960; d=0.029 d
	p	55850.8731	0.0008	+0.0091	17	

Table 1: Minima of eclipsing binaries (continued)

Variable	Type	HJD 24...	±	$O-C$	n	Remarks
GSC 1213-1483	p	55905.6848	0.0008	+0.0341	19	el: IBVS 5960
GSC 1217-696	s	55855.8608	0.0002	−0.0021	24	el: IBVS 5920; d=0.035 d
GSC 1221-1118	p	55844.9231	0.0006	+0.0042	23	el: IBVS 5920; d=0.026 d
GSC 1240-657	p	55858.8497	0.0008	+0.0031	17	el: IBVS 5945
GSC 1749-393	s	55853.8075	0.0017		9	
	p	55853.9633	0.0003		21	
GSC 1772-674	p	55893.7121	0.0004	+0.0024	35	el: 54409.626+0.400887×E
GSC 3303-1583	p	55850.8921	0.0004	+0.0486	51	el: OEJV 104
RZ Aur	p	55892.8345	0.0004	−0.0352	47	
CI Aur	p	55883.9315	0.0003	+0.0035	35	
EU Aur	p	55863.8672	0.0007	+0.0621	35	
HW Aur	p	55883.8506	0.0007	−0.0039	30	
V410 Aur	p	55874.9056	0.0006	−0.0021	16	
V585 Aur	p	55881.9338	0.0006	+0.0330	43	
V591 Aur	p	55881.9203	0.0002	+0.0049	60	d=0.064 d
V594 Aur	p	55931.5945	0.0023	−0.0965	21	el: 51527.899+1.4368×E
V596 Aur	p	55934.6399	0.0007	+0.0117	28	
V599 Aur	p	55882.8905	0.0005	+0.0127	29	d=0.019 d
V603 Aur	p	55934.7653	0.0013	+0.1219	23	
UU Cam	p	55849.9057	0.0005	−0.0279	36	el: Contr. Sk. Pl. 33, 38; d=0.045 d
WW Cam	p	55933.6275	0.0005	−0.0280	45	
AO Cam	s	55874.8420	0.0003	−0.0515	20	el: PASP 97, 648
AQ Cam	p	55931.6529	0.0004	+0.0274	39	d=0.035 d
AS Cam	p	55866.8622	0.0004	−0.0359	33	non-circular
	s	55895.8519	0.0010	−0.2095	32	
AV Cam	p	55903.9269	0.0002	−0.0698	42	
CP Cam	p	55852.8737	0.0004	−0.0229	38	el: Hipparcos; d=0.033 d
MP Cam	p	55875.8709	0.0006	−0.1083	41	
MT Cam	p	55875.8871	0.0003	+0.0033	23	el: IBVS 5871; d=0.021 d
MX Cam	p	55866.8778	0.0001	−0.1494	39	
NO Cam	p	55863.8420	0.0004	+0.0116	28	el: IBVS 5894
OQ Cam	p	55932.6372	0.0003	−0.0609	22	el: 51475.66+0.437823×E
PS Cam	p	55933.7139	0.0005	+0.0541	43	el: 53709.9545+0.920027×E
QU Cam	p	55929.6670	0.0003	−0.0441	22	el: 51503.629+0.75184×E
V337 Cam	p	55931.6808	0.0002	−0.0287	41	el: 51523.466+0.75678×E
V362 Cam	s	55933.6530	0.0002	−0.0767	45	d=0.056 d
V368 Cam	s	55933.7679	0.0008	−0.0721	27	el: 51551.756+0.40891×E
V369 Cam	p	55931.590	0.003	+0.121	12	el: 51609.63+0.34525×E
V373 Cam	s	55934.5996	0.0006	−0.0583	22	el: 51553.706+0.3858×E
	p	55934.7850	0.0014	−0.0658	10	
V375 Cam	s	55931.6356	0.0006	−0.0098	21	el: 51497.087+0.32208×E
V381 Cam	p	55932.6820	0.0002	−0.0118	27	d=0.019 d
V395 Cam	p	55888.8754	0.0005	+0.0003	45	el: 51459.747+2.752721×E
V442 Cam	s	55895.9802	0.0006	−0.0002	27	el: 53062.177+0.4403735×E
V465 Cam	p	55895.9553	0.0008	−0.0092	42	el: OEJV 83
V497 Cam	p	55929.8856	0.0006	−0.0041	47	el: OEJV 83
V502 Cam	s	55932.9069	0.0005	+0.0281	40	el: 51577.76+3.785414×E
V503 Cam	p	55931.8562	0.0005	−0.0652	27	el: 51549.642+2.977092×E; d=0.021 d
IRAS 03530+5306	s	55929.6287	0.0013	+0.0392	42	el: PZP 10, 29; non-circular
	p	55888.8964	0.0004	+0.1060	69	el: PZP 10, 29; non-circular
TX Cnc	p	55929.9030	0.0002	+0.0391	38	
TY Cnc	p	55929.9466	0.0003	−0.2152	46	d=0.039 d
WX Cnc	p	55933.8624	0.0003	+0.0143	29	
WY Cnc	p	55931.8757	0.0006	−0.0384	19	
AC Cnc	p	55932.0033	0.0006	−0.0129	9	d=0.01 d
AD Cnc	s	55931.8936	0.0010	−0.0147	16	
AE Cnc	p	55934.8625	0.0008	−0.1163	37	d=0.041 d
GW Cnc	s	55932.9471	0.0005	−0.0021	16	el: IBVS 5992; marked O'Connell effect
LM Cnc	p	55932.8900	0.0007	−0.0466	26	
GSC 809-569	s	55929.8564	0.0003	+0.0135	31	el: IBVS 5992; d=0.019 d

Table 1: Minima of eclipsing binaries (continued)

Variable	Type	HJD 24...	±	$O-C$	n	Remarks
GSC 1395-877	p	55931.9085	0.0003	+0.0065	13	el: IBVS 5992
GSC 1397-1030	p	55932.8517	0.0002	−0.0276	21	el: IBVS 5945
	s	55932.9996	0.0004	−0.0252	13	
NSV 4188	p	55929.8603	0.0004	−0.0025	24	el: IBVS 5992
GSC 5375-1015	p	55896.9154	0.0005	+0.0119	14	el: IBVS 5992; d=0.020 d
GSC 5391-1821	p	55896.9402	0.0006	+0.0047	35	el: 54842.741+1.823866×E; non-circular
AV CMi	s	55905.9251	0.0004	+0.1556	37	el: IBVS 5945; non-circular
GSC 175-3820	p	55905.9102	0.0002	−0.0232	41	el: 53363.716+0.970312×E
WZ Cap	s	55855.6739	0.0006	−0.0010	21	el: 53541.798+0.313088×E
GSC 5793-556	s	55851.6854	0.0002	−0.0009	21	el: 55088.762+0.263032×E
GSC 5805-197	p	55852.7009	0.0002	−0.0035	25	el: 54768.591+0.266595×E
GSC 6363-550	p	55851.6837	0.0014	+0.0260	32	el: 54770.682+2.695700×E
AE Cas	p	55894.7510	0.0007	+0.0684	27	
AH Cas	p	55896.6807	0.0004	−0.2165	42	
AT Cas	p	55847.8021	0.0004	−0.0820	76	
AX Cas	p	55905.6282	0.0006	−0.0981	28	
BS Cas	p	55828.8977	0.0002	+0.0062	36	el: IBVS 5668; d=0.028 d
BW Cas	p	55910.6558	0.0005	+0.0189	34	el: IBVS 5960
BZ Cas	p	55903.6352	0.0006	+0.0675	37	el: Brno Contr. 28
DN Cas	p	55903.6532	0.0006	−0.0261	35	
DO Cas	s	55852.8886	0.0003	−0.0408	27	el: IBVS 5992; d=0.046 d
EY Cas	s	55883.6714	0.0003	+0.0466	26	
GR Cas	p	55845.8726	0.0003	−0.0427	28	
HQ Cas	p	55888.6501	0.0006	−0.5589	40	
IR Cas	p	55875.6679	0.0002	+0.0087	46	
IT Cas	s	55869.6607	0.0004	+0.1997	36	el: AJ 114, 1206; non-circular
LU Cas	p	55843.8746	0.0009	+0.2090	38	
LX Cas	p	55910.6502	0.0005	+0.0513	34	
LY Cas	p	55847.9375	0.0008	+0.1284	40	
MN Cas	p	55888.7419	0.0007	+0.0131	41	
MY Cas	p	55883.7166	0.0004	+0.0219	37	
OX Cas	p	55844.7696	0.0004	+0.0326	69	non-circular
	s	55875.8936	0.0012	+0.0398	26	
PV Cas	s	55847.7179	0.0005	−0.0043	36	non-circular
V345 Cas	s	55868.7314	0.0004	−0.0180	40	
V387 Cas	p	55840.8470	0.0010	+0.1129	52	
V419 Cas	p	55896.6741	0.0007	+0.0251	47	
V459 Cas	p	55855.9340	0.0005	−0.1074	41	non-circular
V471 Cas	s	55892.7426	0.0006	−0.0296	21	el: Krakow Catalogue
V473 Cas	p	55828.8868	0.0002	−0.0214	26	el: IBVS 4669; d=0.015 d
V541 Cas	s	55851.9077	0.0003	+0.0214	42	el: IBVS 2652
V608 Cas	p	55850.8534	0.0006	+0.0070	20	el: IBVS 5151; d=0.021 d
V775 Cas	s	55846.8490	0.0012	+0.8337	42	non-circular; el: IBVS 5557; d=0.08 d
	p	55875.6524	0.0012	−0.0089	43	
V821 Cas	s	55843.8610	0.0019	−0.1995	36	non-circular; el: IBVS 5386
	p	55844.9056	0.0006	−0.0399	31	
	s	55850.9355	0.0015	−0.2041	18	
V1011 Cas	p	55888.6865	0.0009	−0.0001	42	el: 55438.3845+0.677146×E
V1014 Cas	s	55892.6833	0.0008	+0.0023	38	el: IBVS 5871; d=0.070 d
V1018 Cas	s	55883.811	0.008	−0.421	35	el: IBVS 5894; non-circ.
	p	55931.6817	0.0011	−0.0202	42	
V1107 Cas	s	55905.6777	0.0006	+0.0584	17	
V1115 Cas	s	55892.6814	0.0002	−0.0535	11	d=0.036 d
V1137 Cas	s	55846.7747	0.0006	−0.0010	84	non-circular
	p	55869.6257	0.0006	−0.0248	35	d=0.033 d
GSC 3671-99	p	55868.9157	0.0010	+0.0012	35	el: 54158.301+4.30885×E; non-circular
	s	55874.6629	0.0015	−0.7148	29	

Table 1: Minima of eclipsing binaries (continued)

Variable	Type	HJD 24...	±	$O-C$	n	Remarks
GSC 4029-1087	p	55828.8165	0.0018	−0.0003	14	el: 51472.747+0.2707315×E
	s	55828.9579	0.0005	+0.0057	13	
	s	55895.6942	0.0005	+0.0067	19	
U2 1500-01070260	s	55895.7214	0.0005	−0.0762	20	el: 51467.746+0.31167×E; marked O'Connell e.
G2 N19M012679	s	55882.6145	0.0002	+0.0034	12	el: 54684.594+0.314234×E
	p	55882.7696	0.0010	+0.0014	11	
SU Cep	p	55852.6644	0.0005	+0.0036	38	
WZ Cep	s	55881.6584	0.0004	−0.1016	31	el: A&A Suppl. 131, 17; d=0.023 d
XX Cep	p	55883.6629	0.0002	−0.0075	39	
ZZ Cep	p	55874.6446	0.0005	−0.0128	37	
BE Cep	p	55875.6194	0.0002	−0.1079	33	
CM Cep	p	55881.7060	0.0002	−0.0354	41	
CO Cep	p	55850.7052	0.0004	−0.1974	47	non-circular
CW Cep	p	55844.7439	0.0009	+0.0151	32	non-circular
EF Cep	p	55929.7491	0.0006	+0.0672	21	el: IBVS 5960; d=0.031 d
GS Cep	s	55866.7147	0.0002	+0.0016	36	el: IBVS 3596
GW Cep	s	55895.6750	0.0005	+0.0007	23	el: IBVS 4293
IM Cep	p	55875.6825	0.0003	−0.1560	46	
KP Cep	p	55858.6706	0.0003	+0.0429	38	
LL Cep	s	55874.6827	0.0017	−0.0012	30	
MT Cep	s	55863.7424	0.0003	−0.0006	30	el: IBVS 5920
V698 Cep	p	55881.7029	0.0003	+0.0488	42	el: IBVS 4807
V699 Cep	p	55875.6424	0.0008	−0.0094	43	
V734 Cep	s	55845.6358	0.0021	+0.1936	37	el: IBVS 5630; non-circular
	p	55854.9424	0.0010	+0.0855	38	d=0.048 d
V744 Cep	p	55864.7150	0.0004	+0.0207	38	
V796 Cep	p	55896.7476	0.0006	+0.0001	22	el: 53433.636+0.3929661×E
V801 Cep	p	55903.6567	0.0011	−0.0225	36	
V804 Cep	s	55849.8828	0.0004	+0.0012	25	d=0.021 d
GSC 3965-1172	p	55846.617	0.007	−0.030	38	el: OEJV 83
GSC 3996-1098	p	55867.6607	0.0006	−0.0126	31	el: OEJV 104
GSC 4286-49	p	55849.8305	0.0021	−0.0008	26	el: IBVS 5570; non-circular
	s	55850.7091	0.0004	−0.0481	40	
GSC 4477-706	p	55866.6860	0.0003	+0.0037	43	el: OEJV 83
GSC 4481-1535	s	55869.6292	0.0008	−0.0187	22	el: OEJV 83
GSC 4482-7021	p	55882.7021	0.0004	−0.0055	26	el: OEJV 83
GSC 4482-1238	s	55869.7243	0.0011	+0.0186	23	el: OEJV 91
RW Cet	p	55855.8446	0.0006	−0.0259	31	
SS Cet	p	55866.980:	0.005	+0.045	36	
	p	55869.9531	0.0016	+0.0444	27	d=0.078:d
TT Cet	s	55896.7059	0.0005	−0.0628	42	
TV Cet	s	55863.9291	0.0005	−0.0526	33	non-circular
TX Cet	p	55903.624	0.005	−0.003	14	el: 53039.541+0.7408397×E
VV Cet	p	55896.6099	0.0004	−0.0049	45	el: 52945.606+0.5223949×E; d=0.029 d
XY Cet	s	55853.9074	0.0006	+0.0124	37	
DY Cet	p	55850.8857	0.0005	−0.109	28	el: IBVS 5806
HM Cet	s	55850.8967	0.0003	−0.0030	51	el: IBVS 5960
GSC 28-697	p	55892.6916	0.0006	+0.0043	18	el: IBVS 5960
GSC 44-1052	p	55840.8694	0.0005	−0.0341	16	el: IBVS 5920
GSC 44-1314	s	55893.6874	0.0003	+0.0030	34	el: IBVS 5960
GSC 49-120	p	55854.8959	0.0003	−0.0255	36	el: 54498.559+0.549357×E; d=0.034 d
GSC 54-373	s	55853.8778	0.0006	+0.0054	37	el: IBVS 5960; d=0.07:d
GSC 4684-99	p	55888.6759	0.0004	−0.0145	18	el: 53588.825+0.324748×E
GSC 4687-79	s	55905.6719	0.0004	−0.0112	33	el: IBVS 5960
GSC 4689-252	p	55893.6930	0.0003	+0.0094	46	el: IBVS 5960; d=0.036 d
GSC 4691-773	p	55854.9086	0.0004	+0.0057	42	el: IBVS 5960
GSC 4694-581	p	55843.8592	0.0006	+0.0150	20	el: 54435.602+0.914443×E

Table 1: Minima of eclipsing binaries (continued)

Variable	Type	HJD 24...	±	$O-C$	n	Remarks
GSC 4698-855	p	55844.9111	0.0005	+0.0114	38	el: 53712.613+0.516918×E
GSC 4708-841	p	55853.9175	0.0006	−0.0076	28	el: IBVS 5960
GSC 5276-366	p	55892.6804	0.0003	−0.0287	28	el: 53575.879+0.352877×E
GSC 5278-346	p	55903.6528	0.0005	−0.0054	35	el: 54128.548+0.448600×E
GSC 5281-1730	p	55840.9204	0.0002	+0.0062	38	el: 54681.884+0.509240×E
GSC 5284-2130	p	55851.8952	0.0004	−0.0022	23	el: 54438.741+1.353598×E
NSV 388	s	55888.7425	0.0002	+0.0460	20	el: IBVS 5871
VV Cyg	p	55840.7090	0.0010	+0.0135	35	
DK Cyg	p	55849.6735	0.0001	+0.0919	39	
LO Cyg	p	55852.6089	0.0022	−0.0380	38	
V387 Cyg	p	55845.6604	0.0002	+0.0213	36	
V519 Cyg	p	55844.7365	0.0005	+1.0126	44	d=0.036 d
V628 Cyg	p	55854.6719	0.0003	−0.0027	35	el: IBVS 4381
V664 Cyg	p	55852.6101	0.0003	+0.4424	23	
V679 Cyg	p	55853.6903	0.0013	−0.2530	37	
V704 Cyg	p	55844.7081	0.0004	+0.0318	27	
V706 Cyg	p	55849.7084	0.0008	−0.0604	17	
V836 Cyg	p	55855.6651	0.0003	+0.0202	25	
V1066 Cyg	p	55844.6987	0.0006	+0.0811	44	
V1074 Cyg	p	55845.6733	0.0007	−0.0845	32	
V1401 Cyg	p	55852.6292	0.0014	−0.3201	35	
V1414 Cyg	p	55853.7180	0.0013	+0.0500	39	
V1729 Cyg	p	55850.6855	0.0004	+0.0821	47	
V1815 Cyg	p	55853.6542	0.0003	+0.0037	39	el: BAV Rb. 55, 1
V1901 Cyg	s	55844.7006	0.0006	+0.0323	43	el: OEJV 72, 4; d=0.055 d
V1905 Cyg	p	55845.7599	0.0003	−0.0229	19	el: PZ 23, 329
V2021 Cyg	p	55844.6611	0.0005	+0.0126	43	el: IBVS 3815
G2 N2IU062855	p?	55828.7427	0.0008	−0.0487	19	el: PZP 10, No. 13
SV Equ	s	55844.6906	0.012	−0.0432	40	el: JAAVSO 26, 14
GSC 536-9	p	55847.7141	0.0008	−0.0058	27	el: 54962.908+0.430775×E; d=0.05 d
GSC 537-1462	p	55855.6602	0.0006	+0.0095	26	el: 54764.564+0.308478×E; d=0.020 d
GSC 540-68	s	55840.6918	0.0005	−0.0088	37	el: 54643.842+0.389539×E; d=0.024 d
GSC 1109-1267	s	55847.6994	0.0005	+0.0029	27	el: 54987.857+0.419741×E
RU Eri	p	55854.8782	0.0003	−0.0303	37	
TZ Eri	p	55874.895	0.006	−0.008	29	el. 2454183.516+2.606144×E
UX Eri	p	55852.8415	0.0005	+0.0147	29	el: IBVS 5960
VV Eri	p	55858.8670	0.0007	−0.0068	29	el: 53793.524+1.557579×E
YY Eri	s	55866.8783	0.0002	−0.0003	13	el: IBVS 5960
ZZ Eri	p	55869.9425	0.0001	−0.0122	24	
AM Eri	s	55869.9105	0.0004	−0.1022	17	
AS Eri	p	55866.9250	0.0003	−0.0122	32	
BC Eri	s	55854.8771	0.0004	+0.0036	37	el: IBVS 5960
BL Eri	s	55869.8564	0.0002	+0.0166	17	el: 53276.809+0.4169195×E
BV Eri	s	55874.8798	0.0012	−0.0192	21	el: IBVS 5960
BZ Eri	p	55849.9162	0.0005	+0.0013	16	
CD Eri	p	55855.8679	0.0005	+0.0017	43	el: 54336.892+2.876845×E
KZ Eri	p	55866.9188	0.0006	−0.0060	29	el: 54388.801+0.942681×E
LW Eri	p	55875.9475	0.0004	−0.0194	27	el: IBVS 5960
GSC 4700-802	p	55853.8561	0.0006	+0.0017	37	el: IBVS 5960
GSC 4725-661	s	55867.8566	0.0008	−0.0386	30	el: IBVS 5960
GSC 4732-1231	p	55868.8959	0.0006	−0.0035	33	el: IBVS 5960
GSC 5294-1116	p	55852.9126	0.0005	+0.0047	31	el: IBVS 5960
GSC 5303-939	p	55862.8754	0.0005	−0.0086	29	el: IBVS 5960
GSC 5314-2102	s	55881.8786	0.0002	+0.0049	35	el: IBVS 5960
GSC 5321-819	s	55875.8704	0.0005	−0.0011	16	el: IBVS 5960; d=0.03 d
GSC 5323-652	s	55883.9034	0.0007	+0.0041	20	el: IBVS 5992; pronounced O'Connell effect
GSC 5325-728	p	55883.8858	0.0010	+0.0063	26	el: IBVS 5960
GSC 5330-664	s	55934.6297	0.0006	+0.0038	19	el: 53090.536+0.229575×E

Table 1: Minima of eclipsing binaries (continued)

Variable	Type	HJD 24...	±	$O-C$	n	Remarks
GSC 5863-584	p	55850.8906	0.0003	+0.0062	31	el: IBVS 5960; d=0.024 d
SX Gem	p	55895.8912	0.0002	−0.0514	44	
AC Gem	p	55895.8546	0.0008	−0.3002	41	
AZ Gem	s	55894.8521	0.0002	+0.0881	43	
CX Gem	p	55893.8712	0.0001	−0.0355	42	
EL Gem	p	55895.8907	0.0003	−0.2308	42	
EN Gem	p	55903.9376	0.0008	−0.0515	39	
IM Gem	s	55893.9746	0.0011	+0.0588	43	
LO Gem	p	55888.9257	0.0001	+0.0167	46	
V401 Gem	p	55895.8575	0.0004	−0.0070	44	el: 52970.783+2.197657×E; add. δ Sct var.? (P=0.04 d)
GSC 1328-1420	s	55894.8778	0.0004	+0.0007	24	el: IBVS 5960
GSC 1336-717	p	55894.8714	0.0002	+0.0030	29	el: IBVS 5992
GSC 1337-1137	p	55895.9376	0.0004	+0.0120	31	el: IBVS 5992; d=0.035 d
GSC 1888-1148	p	55903.9190	0.0005	+0.0255	25	el: IBVS 5945
RX Hya	p	55932.9376	0.0004	+0.0762	37	2454164.659+2.281661×E; d=0.016 d
DI Hya	p	55933.8487	0.0005	−0.0297	25	
V409 Hya	p	55932.8884	0.0002	+0.0360	35	d=0.037 d
V412 Hya	p	55933.9039	0.0003	−0.0095	44	
V502 Hya	p	55929.9007	0.0007	+0.0118	45	el: 53834.534+2.4944701×E
GSC 213-980	p	55933.9176	0.0003	−0.0070	48	el: IBVS 5992
GSC 220-70	s	55933.8878	0.0005	+0.0052	17	el: IBVS 5992
GSC 221-871	s	55932.9431	0.0006	+0.0042	25	el: IBVS 5992
GSC 4867-982	s	55931.9044	0.0003	−0.0047	28	el: IBVS 5992
GSC 4894-2310	s	55934.8983	0.0007	−0.0090	24	el: IBVS 5992
GSC 5428-75	p	55934.9042	0.0007	+0.0173	37	el: IBVS 5992
GSC 5441-60	p	55929.9435	0.0006	−0.0397	42	el: IBVS 5992: d=0.035 d
GSC 5454-1746	p	55931.9012	0.0011	+0.0107	11	el: IBVS 5992
GSC 5467-1483	s	55931.9020	0.0004	−0.0021	38	el: IBVS 5894
GSC 6013-1086	s	55933.9183	0.0008	+0.0191	15	el: IBVS 5992
GSC 6014-855	s	55932.8743	0.0002	+0.0019	34	el: IBVS 5992
GSC 6027-137	p	55933.8289	0.0030	−0.0131	29	el: IBVS 5945
RW Lac	p	55851.8069	0.0004	+0.0582	44	el: IBVS 5682; non-circular
VV Lac	p	55863.6671	0.0006	−0.8336	40	d=0.078 d
VY Lac	s	55866.6856	0.0002	−0.0006	43	el: MVS 10, 55
ZZ Lac	p	55858.7077	0.0002	−0.0015	38	el: MVS 10, 169
CN Lac	p	55858.6788	0.0002	−0.0755	22	
CO Lac	s	55846.6859	0.0002	−0.0043	38	non-circular
	p	55853.6345	0.0009	+0.0043	29	min. asymmetric
ES Lac	s	55866.6982	0.0006	+0.2830	43	el: A&A 334, 840; non-circular
IL Lac	s	55862.7004	0.0007	−0.4679	42	non-circular
IP Lac	s	55862.6510	0.0003	+0.0849	27	
LU Lac	s?	55858.7034	0.0003	+0.0266	18	
LY Lac	p	55863.7430	0.0007	+0.2320	36	
MZ Lac	p	55852.6519	0.0005	−0.0053	24	el: JAAVSO 19, 12; non-circular
NS Lac	p	55865.6393	0.0006	−0.2313	17	
V339 Lac	p	55854.6936	0.0006	+0.1715	40	
V344 Lac	s	55858.7190	0.0004	+0.0257	27	el: BBSAG Bull. 127, 10
V364 Lac	p	55850.6923	0.0017	+0.0556	34	non-circular; d=0.08 d
GSC 3210-1456	p	55853.7566	0.0008	+0.0888	21	el: PZP 10, 13
GSC 3996-791	p	55867.6982	0.0005	−0.0139	40	el: OEJV 104
GSC 1429-560	p	55933.8351	0.0009	+0.0022	33	el: 54568.622+2.687423×E
GSC 5345-815	p	55893.9145	0.0005	+0.0110	20	el: IBVS 5960; d=0.022 d
GSC 5916-1668	s	55888.9366	0.0006	+0.0075	14	el: IBVS 5990
RY Lyn	p	55932.8843	0.0005	−0.0346	41	
DE Lyn	s	55934.8976	0.0006	+0.0137	33	el: IBVS 5871
FO Lyn	p	55929.9153	0.0001	+0.0177	47	el: 51498.85+0.634457×E
RW Mon	p	55895.9027	0.0002	−0.0724	44	d=0.055 d
VX Mon	p	55894.9613	0.0006	−0.8033	40	

Table 1: Minima of eclipsing binaries (continued)

Variable	Type	HJD 24...	±	$O-C$	n	Remarks
CK Mon	p	55903.8913	0.0005	+0.2000	40	
DN Mon	s	55905.9119	0.0009	−0.0426	41	el: 54969.485+1.201372×E
GU Mon	s	55894.8477	0.0008	−0.0934	43	
V395 Mon	p	55895.9028	0.0004	+0.0444	42	
V396 Mon	p	55894.9139	0.0004	−0.0873	25	d=0.024 d
V456 Mon	p	55905.8403	0.0005	−0.1361	38	
V714 Mon	p	55903.8908	0.0005	−0.0392	34	el: IBVS 4468
V874 Mon	s	55892.9054	0.0004	−0.0071	45	el: 53430.628+2.448816×E
GSC 4807-2393	s	55903.9963	0.0018	+0.0686	41	el: 54501.764+1.970715×E
GSC 4824-708	p	55905.9720	0.0010	+0.0346	41	el: 54433.776+3.228424×E
GSC 5364-356	p	55894.8605	0.0002	+0.0036	25	el: IBVS 5992; d=0.019 d
GSC 5382-452	p	55903.8460	0.0002	−0.0008	19	el: IBVS 5960
GSC 5384-975	s	55905.8913	0.0004	+0.0051	41	el: IBVS 5960
NSV 3180	p	55894.9239	0.0008	+0.0067	43	el: IBVS 5960
FH Ori	p	55882.8712	0.0004	−0.3839	45	
GG Ori	s	55867.8538	0.0004	−0.4342	47	non-circular
GU Ori	p	55896.8518	0.0004	+0.0042	30	el: ASAS
OS Ori	p	55892.9148	0.0002	−0.0124	47	
V1027 Ori	s	55874.9007	0.0021	+0.6122	24	el: 52906.916+10.393599; non-circular
V1353 Ori	p	55868.014	0.004	−0.004	17	el: IBVS 5313
V1633 Ori	s	55896.8687	0.0004	+0.0004	24	el: BAV Mitt. 125
V1637 Ori	p	55862.8894	0.0005	+0.0116	40	el: 53735.704+1.822771×E
V1638 Ori	p	55931.6971	0.0006	+0.0048	39	el: 54429.726+0.614050×E; d=0.031 d
V1848 Ori	p	55882.9303	0.0001	−0.0042	14	
V1865 Ori	p	55888.8871	0.0003	+0.0552	40	el: IBVS 5871
V2790 Ori	s	55896.8827	0.0003	+0.0018	26	el: IBVS 5960; d=0.020 d
GSC 85-1357	p	55883.804	0.003	+0.031	7	el: IBVS 5960
	s	55883.9485	0.0008	+0.0337	14	
GSC 89-1424	p	55883.8872	0.0007	+0.0151	28	el: IBVS 5960
GSC 93-668	p	55875.8722	0.0006	−0.0077	26	el: IBVS 5960
GSC 103-738	s	55882.8989	0.0004	+0.0004	21	el: IBVS 5960
GSC 103-894	s	55882.9072	0.0004	−0.0020	26	el: IBVS 5960
GSC 111-1902	p	55934.6716	0.0004	+0.0003	28	el: IBVS 5960
GSC 127-719	p	55893.8977	0.0002	+0.0164	44	el: IBVS 5894
GSC 128-980	p	55892.8764	0.0004	−0.0011	36	el: IBVS 5960
GSC 709-1047	p	55892.8398	0.0005	−0.0053	16	el: IBVS 5960
	s	55892.9731	0.0006	−0.0054	14	
GSC 1314-352	p	55896.9813	0.0013	−.0359	44	el: 54824.681+1.213050×E
GSC 1315-1104	p	55896.8506	0.0010	+0.0001	40	el: IBVS 5960
GSC 4753-984	s	55882.9111	0.0004	+0.0048	45	el: IBVS 5871
GSC 4754-44	p	55932.7182	0.0008	+0.0057	15	el: IBVS 5992
GSC 4766-69	s	55888.9339	0.0004	+0.0111	23	el: IBVS 5960
GSC 4772-934	p	55893.8896	0.0003	+0.0113	35	el: IBVS 5960
GSC 4780-344	p	55893.9118	0.0006	−0.0011	17	el: IBVS 5960; d=0.010 d
GSC 4783-467	p	55896.9211	0.0004	+0.0126	28	el: IBVS 5960
GSC 5337-337	p	55893.9020	0.0002	+0.0010	20	el: IBVS 5992
GSC 5346-275	p	55892.8664	0.0001	+0.0082	33	el: IBVS 5960
UX Peg	p	55854.6494	0.0003	−0.0088	40	
VW Peg	s	55855.7917	0.0003	−4.8159	58	el: IBVS 4916; non-circular
ZZ Peg	p	55866.6436	0.0004	+0.1458	40	
BB Peg	p	55862.7202	0.0006	−0.0036	21	el: 54632.894+0.361502×E
BX Peg	s	55849.7021	0.0004	−0.0061	21	el: IBVS 5668
	p	55850.6809	0.0003	−0.0088	19	d=0.020 d
BY Peg	p	55851.6460	0.0004	−0.0269	23	d=0.032 d
BZ Peg	p	55849.659	0.006	+0.001	37	el: Krakow Catalogue
CC Peg	p	55850.6679	0.0004	−0.0129	45	el: IBVS 5960; d=0.038 d
CE Peg	p	55849.7277	0.0004	+0.0049	26	el: 54694.718+0.642026×E

Table 1: Minima of eclipsing binaries (continued)

Variable	Type	HJD 24...	±	$O-C$	n	Remarks
CF Peg	p	55850.6853	0.0005	+0.1002	30	el: IBVS 5806; d=0.03 d
CU Peg	p	55853.7049	0.0002	+0.0148	39	
DV Peg	s	55855.7288	0.0004	−0.0061	39	el: 54376.501+0.642168×E; d=0.047 d
EU Peg	p	55875.7051	0.0003	+0.0380	37	
GP Peg	p	55867.6703	0.0002	−0.0481	37	
KW Peg	p	55850.7070	0.0003	+0.1694	18	el: IBVS 3579
MQ Peg	s	55867.7211	0.0008	+0.0449	29	el: IBVS 5547
V407 Peg	p	55882.7055	0.0005	−0.0253	37	
A 215503+2417.8	s	55851.6940	0.0004	+0.0271	39	el: 54296.736+0.601637×E; d=0.044 d
GSC 563-861	p	55863.7307	0.0003	−0.0033	20	el: IBVS 5920; d=0.028 d
GSC 566-150	p	55863.7056	0.0002	+0.0117	34	el: IBVS 5960; d=0.021 d
GSC 570-73	s	55864.6396	0.0013	+0.0017	21	el: 54764.589+0.354112×E
GSC 573-1241	p	55864.6636	0.0005	+0.0035	29	el: IBVS 5920
GSC 1127-2016	s	55845.6745	0.0007	−0.0073	25	el: 53672.524+0.347233×E
GSC 1141-480	p	55858.6587	0.0003	−0.0020	26	el: IBVS 5920
GSC 1166-399	p	55868.7192	0.0007	+0.0019	13	el: IBVS 5960
GSC 1654-575	p	55840.6772	0.0003	+0.0114	31	el: 55068.647+0.324514×E
GSC 1670-251	s	55851.6602	0.0003	+0.0030	22	el: IBVS 5960
GSC 1677-992	s	55851.6571	0.0004	+0.0109	43	el: 54595.925+0.557122×E; d=0.05 d
GSC 1686-1001	s	55858.6895	0.0005	−0.0011	26	el: IBVS 5920
GSC 1694-992	s	55858.6538	0.0005	−0.0025	14	el: IBVS 5920; pronounced O'Connell effect
GSC 1704-356	p	55864.7390	0.0006	+0.0056	40	el: 54292.768+0.477076×E
GSC 1709-614	s	55874.6984	0.0003	+0.0016	17	el: 53622.630+0.276412×E; pron. O'Connell e.
GSC 1715-1370	s	55869.6987	0.0010	+0.0077	13	el. IBVS 5920
GSC 1716-1457	p	55881.6571	0.0004	+0.0235	34	el: IBVS 5920
GSC 1718-1664	p	55868.7185	0.0005	−0.0016	12	el: IBVS 5920; pronounced O'Connell effect
GSC 2188-568	p	55849.6782	0.0004	−0.0259	26	el: IBVS 5960
GSC 2189-1101	s	55849.6908	0.0004	+0.0004	20	el: IBVS 5960
GSC 2203-1663	p	55854.6408	0.0007	−0.0033	28	el: IBVS 5960; d=0.035 d
GSC 2211-2152	p	55852.6839	0.0003	+0.0166	38	el: 52893.608+0.481853×E
GSC 2225-1482	p	55863.6621	0.0005	−0.0158	41	el: IBVS 5920
GSC 2226-2148	p	55862.6631	0.0005	+0.0224	24	el: IBVS 5920
GSC 2244-1064	s	55868.7286	0.0007	−0.0054	20	el: IBVS 5920; d=0.024 d
GSC 2740-1859	s	55874.6190	0.0009	+0.0080	13	el: 51447.718+0.248179×E
	p	55874.7432	0.0010	+0.0082	13	
GSC 2766-775	p	55883.6890	0.0003	+0.0762	31	el: IBVS 5920
ST Per	p	55847.8755	0.0006	+0.2203	40	d=0.043 d
WY Per	p	55853.8869	0.0004	−0.1983	36	
XZ Per	p	55867.9069	0.0001	−0.0595	47	
BE Per	p	55853.8672	0.0008	+0.0292	33	el: MVS 11, 38
BR Per	p	55862.9405	0.0001	−0.2171	24	el: PZ 23, 80
BY Per	p	55903.6518	0.0003	+0.0231	37	
CH Per	p	55910.6795	0.0006	−0.0761	29	
DK Per	p	55847.8848	0.0001	−0.0423	41	el: IBVS 3875
DZ Per	p	55854.8733	0.0008	+0.0411	42	
EQ Per	p	55851.9482	0.0008	+0.5908	28	
FQ Per	p	55869.867:	0.010	+0.742	43	
FW Per	p	55849.9086	0.0009	−0.0387	23	
HK Per	p	55883.9255	0.0004	+0.0945	36	d=0.05 d
HS Per	p	55847.8937	0.0002	−0.0848	41	el: IBVS 3754
HV Per	p	55867.8474	0.0004	−0.3241	46	
HW Per	p	55863.9364	0.0005	+0.0044	38	el: IBVS 4516
II Per	p	55869.9172	0.0007	−0.0038	41	el: IBVS 5741
IK Per	p	55863.8830	0.0004	−0.1928	38	d=0.043 d
IM Per	s	55854.8319	0.0011	+0.0853	36	non-circular
	p	55932.6164	0.0009	+0.0991	42	
IT Per	p	55845.8238	0.0026	−0.0266	40	
IU Per	p	55852.8924	0.0004	+0.0064	44	el: Krakow Catalogue; d=0.060 d

Table 1: Minima of eclipsing binaries (continued)

Variable	Type	HJD 24...	±	$O-C$	n	Remarks
KL Per	p	55854.8597	0.0005	+0.1334	41	d=0.044 d
KN Per	p	55863.8968	0.0004	+0.0068	38	
KW Per	p	55905.7370	0.0002	+0.0143	46	
MS Per	p	55866.8694	0.0007	+0.0019	39	el: IBVS 5960
PS Per	p	55852.8584	0.0002	+0.0657	29	
QT Per	p	55853.8928	0.0003	−0.0459	36	el: MVS 11, 65
QU Per	p	55851.8760	0.0004	−0.0130	41	d=0.088 d
QV Per	p	55933.6329	0.0008	−0.0578	25	
QW Per	p	55854.8647	0.0003	+0.0129	27	
V366 Per	p	55845.9137	0.0003	+0.1542	40	d=0.037 d
V432 Per	s	55846.9043	0.0003	−0.0152	25	el: BAV Mitt. 61; d=0.021 d
V434 Per	p	55858.9103	0.0010	−0.0054	29	el: Krakow Catalogue
V449 Per	s	55851.8987	0.0004	+0.0502	15	
V450 Per	p	55846.8893	0.0003	+0.1162	32	
V457 Per	p	55851.8889	0.0003	+0.0202	31	
V462 Per	p	55866.9365	0.0004	−0.3396	39	d=0.043 d
V680 Per	p	55847.8558	0.0010	−0.0384	18	el: IBVS 5960
V723 Per	p	55910.6380	0.0009	−0.0049	41	el: 51452.67+0.796351×E
V737 Per	p	55849.9422	0.0004	+0.1656	26	
V871 Per	s	55846.8248	0.0003	+0.1368	84	el: IBVS 5920
V873 Per	s	55845.8839	0.0002	−0.0103	26	
V877 Per	p	55840.8812	0.0007	−0.0099	28	
	p	55850.8792	0.0006	−0.0108	31	
V884 Per	p	55910.6974	0.0005	+0.0084	34	el: IBVS 5992; non-circular
V887 Per	p	55853.9283	0.0002	−0.0125	36	
V947 Per	p	55929.6086	0.0007	−0.0448	16	el: 53756.342+0.29768×E
	s	55929.7596	0.0005	−0.0426	13	
V951 Per	s	55929.6288	0.0002	−0.0190	21	el: 51439.815+0.27048×E
	p	55929.7609	0.0006	−0.0221	14	
V964 Per	p	55932.6038	0.0003	−0.0619	15	el: 51291.6775+0.41728×E
GSC 2344-92	p	55846.8517	0.0007	+0.0506	17	el: PZP 11, 1
	s	55846.9676	0.0008	+0.0494	14	
GSC 2344-527	s	55863.947	0.009	+0.013	38	el: 51492.57+0.797767×E
GSC 2361-2410	s	55862.8569	0.0008		14	el: 55866.8374+0.318232×E; close to BR Per
	p	55866.8378	0.0002	+0.0004	18	
	s	55866.9970	0.0002	+0.0005	6	
	s	55867.9513	0.0001	+0.0001	16	
	s	55875.9066	0.0004	−0.0004	13	
	s	55893.7278	0.0003	−0.0002	27	
	s	55929.6885	0.0008	+0.0003	15	
	p	55932.7134	0.0003	+0.0020	17	
RV Psc	p	55894.6762	0.0002	−0.0534	28	
SU Psc	p	55893.6968	0.0004	−0.3133	45	
VZ Psc	p	55881.5902	0.0018	+0.0096	13	el: ApJ Suppl. 58, 413
	s	55881.7179	0.0015	+0.0067	13	
AC Psc	p	55869.7318	0.0007	+0.0923	10	
CP Psc	p	55828.9306	0.0002	−0.0610	19	el: 55068.647+0.324514×E
DS Psc	p	55895.6851	0.0007	+0.0721	22	el: IBVS 4424
EM Psc	s	55888.7690	0.0020	+0.1425	18	d=0.05: d
ER Psc	p	55867.7397	0.0012	+0.2056	13	
GR Psc	s	55894.7021	0.0004	−0.0047	41	el: IBVS 5960; d=0.020 d
GW Psc	p	55888.6588	0.0003	+0.0003	16	el. 2454647.915+0.336336×E
HO Psc	p	55892.6666	0.0002	+0.0019	29	el: 54420.582+0.324748×E
GSC 24-466	s	55893.6992	0.0003	−0.0079	35	el: 54802.588+0.390732×E; d=0.029 d
GSC 575-429	p	55866.6691	0.0006	−0.0014	11	el: 5920; pronounced O'Connell effect
	s	55866.7852	0.0015	−0.0024	11	
GSC 610-198	s	55895.7407	0.0006	+0.0074	31	el: 54300.863+0.462885×E
GSC 611-249	s	55894.6678	0.0007	+0.0129	15	el: IBVS 5960; d=0.030 d

Table 1: Minima of eclipsing binaries (continued)

Variable	Type	HJD 24...	±	$O-C$	n	Remarks
GSC 611-829	s	55895.7256	0.0004	−0.0034	9	el: IBVS 5960; strong O'Connell effect (ΔV=0.24m)
GSC 619-1008	p	55828.8617	0.0005	−0.0002	20	el: 53651.668+0.293858×E
GSC 621-834	p	55892.7087	0.0003	+0.0096	18	el: IBVS 5920
GSC 1194-613	s	55896.7213	0.0006	+0.0011	29	el: IBVS 5960
GSC 1202-1038	s	55895.6914	0.0005	+0.0057	28	el: 53352.565+0.308089×E
GSC 1202-1193	s	55828.8641	0.0007	+0.0034	17	el: 53596.786+0.447893×E
GSC 1762-103	p	55892.6581	0.0010	−0.0196	12	el: IBVS 5960
GSC 5243-973	p	55869.7210	0.0012	+0.0137	14	el: 54705.703+0.332193×E; asymmetric
GSC 5254-59	p	55882.6277	0.0006	−0.0187	21	el: 54289.880+0.355687×E
GSC 5255-370	s	55883.7385	0.0007	+0.0078	22	el: 53704.564+0.463406×E
V595 Pup	p	55934.9087	0.0007	+0.0237	31	el: IBVS 5586
GSC 5998-968	s	55934.9202	0.0012	+0.0070	26	el: IBVS 5992
NSV 4095	p	55934.966	0.003	−0.023	29	el: 54107.768+7.308886×E; non-circular
CK Sge	p	55828.7051	0.0008	−0.0384	26	el: Hipparcos
GSC 1621-2192	s	55828.6892	0.0006	+0.0338	28	el: IBVS 5945
RZ Tau	p	55881.9376	0.0002	+0.0658	49	
TY Tau	p	55846.8702	0.0002	+0.2582	24	
AC Tau	p	55875.9319	0.0002	+0.0850	43	
AH Tau	s	55910.7312	0.0004	+0.0169	25	el: IBVS 5554
BN Tau	p	55867.8955	0.0003	−0.0843	46	
CF Tau	s	55868.8932	0.0006	−0.0133	39	el: IBVS 5992
CR Tau	p	55893.8452	0.0002	−0.0023	25	el: IBVS 4778
CU Tau	p	55862.9545	0.0006	+0.0427	23	el: AJ 130, 224
EQ Tau	s	55846.8886	0.0002	−0.0261	40	d=0.018 d
GR Tau	p	55867.8705	0.0004	−0.0409	25	
GW Tau	p	55934.6356	0.0009	−0.0901	39	d=0.046 d
IV Tau	p	55934.6555	0.0007	−0.0214	41	
V1022 Tau	p	55869.8583	0.0003	−0.0710	20	el: PASP 101, 177
V1094 Tau	p	55849.8700	0.0014	+0.0389	27	el: IBVS 4544; non-circular
V1112 Tau	p	55868.8482	0.0002	−0.0229	28	el: IBVS 5871
V1123 Tau	s	55868.8268	0.0004	+0.0003	23	el: IBVS 5688
V1220 Tau	p	55852.9822	0.0014	−0.0305	39	
V1222 Tau	p?	55858.8986	0.0013	+0.0035	16	el: IBVS 5960
V1223 Tau	p	55858.8740	0.0007	+0.0007	27	el: IBVS 5920
V1241 Tau	s	55855.9109	0.0005	+0.0181	43	
V1249 Tau	s	55855.9012	0.0004	−0.0093	33	non-circular
	p	55858.8755	0.0005	−0.0056	26	
V1250 Tau	s	55868.9184	0.0003	+0.0079	40	el: IBVS 5945
V1260 Tau	p	55883.9247	0.0002	+0.0311	37	non-circular
V1352 Tau	s	55929.6938	0.0019	−0.0220	39	el: 52692.497+6.909752×E; non-circular
V1356 Tau	s	55892.9832	0.0029	+0.7013	47	el: 54105.575+12.807935; non-circular
V1367 Tau	s	55888.9302	0.0006	+0.0086	16	el: IBVS 5699
GSC 67-348	p	55862.8656	0.0004	+0.0079	21	el: IBVS 5920
GSC 72-521	p	55862.9216	0.0005	+0.0093	19	el: IBVS 5945
GSC 74-465	p	55868.8378	0.0004	−0.0079	15	el: IBVS 5960
	s	55868.9926	0.0008	−0.0033	19	
GSC 76-527	p	55862.9047	0.0005	−0.0003	13	el: IBVS 5945
GSC 650-1226	p	55855.8896	0.0002	+0.0153	34	el: IBVS 5945
GSC 658-185	s	55863.8452	0.0007	+0.0082	20	el: IBVS 5920
GSC 659-262	s	55862.8719	0.0005	−0.0066	24	el: IBVS 5920
GSC 661-580	p	55867.8546	0.0003	−0.0016	26	el: IBVS 5945
GSC 663-23	s	55846.9344	0.0010	−0.0076	46	
GSC 664-423	p	55866.8773	0.0007	+0.0002	15	el: IBVS 5945
GSC 681-692	s	55868.8346	0.0003	−0.0037	18	el: IBVS 5945
	p	55868.9589	0.0005	−0.0031	13	
GSC 1235-663	p	55933.6960	0.0003	+0.0010	45	el: IBVS 5992
GSC 1256-188	s	55863.8866	0.0005	+0.0141	32	el: IBVS 5920; d=0.030 d
GSC 1273-661	p	55881.9122	0.0003	+0.0098	26	el: IBVS 5992

Table 1: Minima of eclipsing binaries (continued)

Variable	Type	HJD 24...	±	$O-C$	n	Remarks
GSC 1274-564	s	55881.9064	0.0002	+0.0151	47	el: IBVS 5960; d=0.026 d
GSC 1831-687	s	55929.6790	0.0003	+0.0062	15	el: IBVS 5960
GSC 1841-879	p	55881.9213	0.0002	+0.0039	48	el: 52623.651+0.935477×E
GSC 4709-1195	p	55858.8756	0.0010	+0.0025	34	el: 54160.557+1.579829×E
V Tri	p	55905.7014	0.0004	−0.0018	46	
RW Tri	p	55844.9040	0.0005	−0.0058	7	el: IBVS 5920
ST Tri	p	55847.8564	0.0011	−0.0013	17	el: IBVS 5609
VW Tri	s:	55840.9408	0.0006	−0.0333	23	el: MVS 11, 1
VZ Tri	p	55905.6766	0.0003	−0.0093	38	el: OEJV 107; d=0.031 d
AK Tri	p	55844.8792	0.0004	+0.1117	39	el: IBVS 4427
QY UMa	p	55934.8684	0.0002	−0.0014	37	el: OEJV 83
BI Vul	p	55855.6164	0.0002	+0.0062	11	el: 51483.4419+0.251824×E
	s	55855.7404	0.0002	+0.0043	21	
DZ Vul	s	55847.6881	0.0004	−0.0025	38	el: IBVS 5960
V384 Vul	p	55840.6234	0.0013	+0.0029	18	el: OJEV 137; might be pulsator
GSC 1660-1173	p	55845.7418	0.0003	+0.0133	24	el: 53857.909+0.433643×E
GSC 2175-940	s	55844.7137	0.0003	+0.0044	44	el: 53902.773+0.508560×E; d=0.026 d
GSC 2177-709	s	55840.7100	0.0007	+0.0032	31	el: 53632.527+0.377628×E
GSC 2190-1358	p	55840.6655	0.0007	−0.0012	37	el: 54295.714+0.521415×E

Abbreviations: U2: USNO-A2.0 ; G2: GSC 2.3 ; A: ASAS ; el: 24...

References:

Achterberg, H. et al., 2000, *IBVS*, No. 4916
Agerer, F., 1992, *BAV Mitt.* 61
Agerer, F., 1999, *IBVS*, No. 4778
Agerer, F., 2010, *PZP*, 10, 13
Agerer, F. et al., 1996, *IBVS*, No. 4381
Berdnikov, L. N., 1993, *PZ* 23, 80
Blättler, E., 2002, *BBSAG Bull.*, 127, 10
Blättler, E., Diethelm, R., 2001, *IBVS*, No. 5151
Borkovits, T. et al., 2002, *IBVS*, No. 5313
Bradstreet, D. H., 1985, *ApJ Suppl.*, 58, 413
Brat L. et al., 2009, *OEJV*, No. 107
Byboth, K. N. et al., 2004, *IBVS*, No. 5554
Cook, S.P., 1997, *JAAVSO*, 26, 14
Degirmenci, O.L. et al., 2003, *IBVS*, No. 5386
DeYoung, J.A., 1991, *IBVS*, No. 3579
Diethelm, R., 2009, *IBVS*, No. 5871
Diethelm, R., 2009, *IBVS*, No. 5894
Diethelm, R., 2010, *IBVS*, No. 5920
Diethelm, R., 2010, *IBVS*, No. 5945
Diethelm, R., 2011, *IBVS*, No. 5960
Diethelm, R., 2011, *IBVS*, No. 5992
Djurasevic, G. et al., 1998, *A&A Suppl.*, 131, 17
Evans III E. et al., 1985, *PASP*, 97, 648
Gessner, H., 1987, *MVS*, 11, 38
Gessner, H., 1987, *MVS*, 11, 65
Gomez-Forrellad, J.M., Garrigos Sanchez A., 1997, *IBVS*, No. 4427
Gushchin, I.A., 1994, *PZ*, 23, 329
Hanzl, D. et al., 1991, *IBVS*, No. 3596
Henden, A.A. et al., 1999, *IBVS*, No. 4807
Hoogeveen, G.J., 2005, *IBVS*, No. 5652
Kaiser, D.H., Baldwin, M.E., 1992, *IBVS*, No. 3815
Kaiser, D.H., Frey, G., 1998, *IBVS*, No. 4544
Krajci, T., 2007, *IBVS*, No. 5806

Khruslov, A. V., 2005, *IBVS*, No. 5699
Khruslov, A. V., 2010, *PZP*, 10, 18
Khruslov, A. V., 2011, *PZP*, 11, 1
Lacy, C. et al., 1997, *Astron. Journal*, 114, 1206
Lewandowski, M. et al., 2009, *OEJV*, No. 104
Meinunger, L., 1986, *MVS*, 11, 1
Moschner, W. et al., 1997, *IBVS*, No. 4468
Moschner, W. et al., 1999, *IBVS*, No. 4669
Otero, S.A., Dubovsky, P.A., 2004, *IBVS*, No. 5557
Otero, S. A. et al., 2004, *IBVS*, No. 5570
Otero, S. A. et al., 2005, *IBVS*, No. 5586
Otero, S. A., Wils, P., 2005, *IBVS*, No. 5630
Otero, S. A., 2007, *OEJV*, No. 72
Otero, S. A., 2008, *OEJV*, No. 83
Otero, S. A., 2008, *OEJV*, No. 91
Ozdarcan, O. et al., 2006, *IBVS*, No. 5688
Pensado, J., Lahulla, J.F., 1989, *PASP*, 101, 177
Pribulla, T. et al., 2001, *IBVS*, No. 5184
Pribulla, T. et al., 2003, *Contr. Astr. Obs. Skalnaté Pleso*, 33, 38
Pribulla, T. et al., 2005, *IBVS*, No. 5668
Qian, S. B. et al., 2005, *AJ*, 130, 224
Ragazzoni, R., Barbieri, C., 1996, *IBVS*, No. 4293
Samec, R.G. et al., 1997, *IBVS*, No. 4516
Samec, R.G. et al., 2005, *IBVS*, No. 5609
Silhan, J., 1990, *JAAVSO*, 19, 12
Vidal-Sainz, J, 1997, *IBVS*, No. 4424
Wetterer, C.J. et al., 2004, *IBVS*, No. 5547
Wolf, M. et al., 1998, *Astron. Astrophys.*, 334, 840
Wolf, M. et al., 2006, *IBVS*, No. 5682
Zakirov, M.M., Azimov, A.A., 1992, *IBVS*, No. 3754
Zakirov, M.M., Azimov, A.A., 1993, *IBVS*, No. 3875
Zejda, M. et al., 2006, *IBVS*, No. 5741
Zhang, J. et al., 1985, *IBVS*, No. 2652

ERRATA FOR IBVS 6011

The following errata were communicated by the author (6 February 2012):

GSC 1749-393 should read GSC 1794-393 .
Minimum time for V368 Cam should read 55937.7679 instead of 55933.7679 .
GSC 4482-7021 should be GSC 4482-981
The line on GSC5276-366 should read: GSC 5276-366 s 55892.6840 0.0003 -0.0090 28 ...
O-C for RX Hya is -0.0087 .
Instead of GSC 6027-137 it should read GSC 6027-134 .
Instead of QY UMa it should read OY UMa .

COMMISSIONS 27 AND 42 OF THE IAU
INFORMATION BULLETIN ON VARIABLE STARS

Number 6012

Konkoly Observatory
Budapest
7 February 2012

HU ISSN 0374 – 0676

LIGHT CURVE MODELING OF SHORT-PERIOD W UMa-TYPE STARS

PILECKI, B.[1,2]; STĘPIEŃ, K.[1]

[1] Warsaw University Observatory, Warsaw, Poland. e-mail: pilecki@astrouw.edu.pl; kst@astrouw.edu.pl

[2] Universidad de Concepción, Departamento de Astronomia, Casilla 160-C, Concepción, Chile. e-mail: bpilecki@astro-udec.cl

We report the results of the curve modeling of a selected set of W UMa-type variables. They all belong to the low mass contact binaries (LMCB) which have orbital periods shorter than about 0.3 d, the total mass lower than about 1.4 M$\odot$ mass, moderate mass ratios and radii indicating that both components are on the main sequence (Stępień and Gazeas 2012). As a rule, they belong to W-type variables, where the more massive component is cooler than its companion. According to Rucinski (2007) LMCBs make a majority of all W UMa-type stars existing in the solar neighbourhood, yet the knowledge of their properties is very limited. Accurate values of the binary parameters, based on the precise photometric and spectroscopic observations, are known for a mere dozen LMCBs (Gazeas and Stępień 2008). The reason for the shortage of good data is, of course, the intrinsic faintness of these stars.

Evolutionary models of cool contact binaries have been obtained by Stępień (2006, 2011) under the assumption that they originate from detached binaries with the initial periods close to 2 d and angular momentum loss (AML) by the magnetized winds occurs during the whole evolution. The results indicate that LMCB are old MS objects with a characteristic age of 8-9 Gyr, but their lifetime in contact takes only about 10% of their total age. The orbit evolution of a contact binary is determined by the mass transfer from the presently less massive component to its companion and AML by the wind. In LMCBs the AML dominates, so the orbit contracts quickly and the binary overflows its outer critical surface, which leads to coalescence of both components. The mass ratio never reaches the extreme value of 0.1 or less.

All the variables presented in this paper have been discovered during the ASAS survey (Pojmański 2002). They were selected for the further investigation because they were bright and there were high quality, two-color light curves available for them. The light curve modeling of our stars was a part of a larger project (Pilecki 2009) in which almost 3000 stars were modeled using Monte Carlo approach and the Wilson-Devinney code (Wilson and Devinney 1971, 1973) in order to better undestand the nature of contact binaries in particular and the evolution of compact binaries in general.

In this project light curves for systems that exhibit period change were cleared from this influence, we also subtracted all long-term brightness variation. Both actions were necessary because of the long time span of collected data. To make analysis of this amount of stars feasible we have varied the smallest possible subset of parameters including temperature ratio, modified potentials of both components and inclination. The temperature

Table 1: The data for the new, short-period W UMa-type variables

ASAS design.	Ephemeris HJD(T_0)=2450000+	$V_{\rm app}$ mag	ΔV mag	$V-I$ mag	T_2 K	T_1/T_2	i deg	q
033959+0314.5	1920.623+0.282709×E	11.33	0.87	0.99	4830	0.964 (12)	84.5 (1.4)	0.71
050837+0512.3	2496.963+0.266349×E	11.06	0.66	1.09	4550	0.955 (16)	73.8 (1.2)	0.71
050852+0249.3	1952.830+0.295706×E	11.25	0.7	0.95	4950	0.940 (12)	83.5 (4.3)	0.35
052452-2809.2	1868.922+0.275778×E	10.61	0.37	0.76	5510	0.964 (20)	68.5 (1.4)	0.25
061531+1935.4	2621.829+0.287842×E	11.06	0.59	0.83	5300	0.982 (16)	81.3 (4.7)	0.35
085710+1856.8	2622.863+0.291015×E	11.23	0.61	0.91	5060	0.957 (15)	78.2 (2.1)	0.35
095048-6723.3	1869.068+0.276944×E	11.13	0.74	1.12	4480	0.977 (09)	84.3 (3.0)	0.50
120036-3915.6	1871.020+0.292670×E	10.45	0.5	0.90	5100	0.974 (09)	80.8 (1.9)	0.25
143751-3850.8	1903.125+0.292395×E	11.35	0.79	1.14	4460	0.949 (12)	78.1 (1.5)	0.50
144243-7418.7	1903.86+0.294768×E	8.25	0.45	0.77	5460	0.951 (11)	72.1 (1.2)	0.25
155227-5500.6	1926.952+0.297646×E	11.45	0.33	0.93	5020	0.977 (35)	55.8 (5.4)	0.71
155906-6317.8	1920.924+0.266766×E	10.47	0.71	1.03	4710	0.949 (07)	78.4 (0.8)	0.50
174655+0249.9	2159.601+0.299953×E	9.57	0.25	0.95	4950	0.926 (30)	55.9 (1.8)	0.35
195350-5003.5	1874.706+0.286828×E	11.44	0.95	1.10	4520	0.935 (10)	83.9 (1.2)	0.71
212915+1604.9	2754.934+0.282956×E	11.33	0.61	1.03	4720	0.981 (12)	88.3 (3.6)	0.35

of the hotter component was based on the $V-I$ index and was set fixed. Keeping in mind that the photometric mass ratios are quite inaccurate (except for binaries with total eclipses) we have used a set of 12 predefined values spread logarithmically from 0.09 to 4.0 – the step in q-value roughly corresponding with the average accuracy that was expected for these data. The light curves were solved for this set and a best solution was then accepted.

Nevertheless we have crosschecked our values of q for about 50 stars with those already established in the literature and found that they seldom differ significantly for short-period compact systems presented here, which is rather expected as for such systems mass ratio manifests itself in the shapes of components and thus in the shapes of the light curves. This is not true for well resolved systems. Our results show also that the q-values are indeed concentrated around the value 0.5, the property noticed already by Rucinski (2010). Because of the performed Monte Carlo analysis we were able to determine values and their reliable errors for all the other parameters.

Table 1 presents the data for the investigated stars. The consecutive columns give ASAS designation (with the coordinates for 2000), ephemeris, apparent V magnitude, V-amplitude of the light curve, $V-I$ index, temperature of the hotter (but less massive) component, temperature ratio, orbit inclination i and mass ratio $q=M_1/M_2$. For the temperature ratio and the orbit inclination $1-\sigma$ errors in the last two digits are quoted in the parentheses.

Spectroscopic observations of these stars are urgently needed. They would permit calculations of the absolute parameters of the binaries and checking their values against model calculations. In particular, it will be possible to determine the progenitor binaries and evolutionary paths of LMCB.

Acknowledgements. This research was supported by the grant N203 304335 from the Polish Ministry of Science and Higher Education. Support from the BASAL Centro de Astrofisica y Tecnologias Afines (CATA) PFB-06/2007 and TEAM subsidies of the Foundation for Polish Science (FNP) is also acknowledged.

References:

Gazeas, K., and Stępień, K., 2008, *MNRAS*, **390**, 1577

Pilecki, B., 2009, PhD Thesis, Warsaw University
Pojmański G., 2002, *Acta Astr.*, **52**, 397
Rucinski, S.M., 2007, *MNRAS*, **382**, 393
Rucinski, S.M., 2010, ASP Conf. Ser. 435, 195
Stępień, K., 2006, *Acta Astr.*, **56**, 199
Stępień, K., 2011, *Acta Astr.*, **61**, 139
Stępień, K., and Gazeas, K., 2012, IAU Symp. 282, in press
Wilson, R.E., and Devinney, E.J., 1971, *ApJ*, **166**, 605
Wilson, R.E., and Devinney, E.J., 1973, *ApJ*, **182**, 539

COMMISSIONS 27 AND 42 OF THE IAU
INFORMATION BULLETIN ON VARIABLE STARS

Number 6013

Konkoly Observatory
Budapest
15 February 2012

HU ISSN 0374 – 0676

GSC 03949-00386 IS A DOUBLE-MODE HIGH-AMPLITUDE δ SCUTI STAR

BERNHARD, K.[1,4]; SRDOC, G.[2]; FRANK, P.[3,4]

[1] A–4030 Linz, Austria; e-mail: klaus.bernhard@liwest.at

[2] Sarsoni 90, Viskovo, Croatia; email: gregor@vip.hr

[3] D–84149 Velden; email: frank.velden@t-online.de

[4] Bundesdeutsche Arbeitsgemeinschaft für Veränderliche Sterne e.V. (BAV), Munsterdamm 90, D–12169 Berlin, Germany

GSC 03949-00386 (2MASS J20194496+5829200, 1SWASP J201944.95+582920.0) ($\alpha_{2000} = 20^{\rm h}19^{\rm m}44\overset{\rm s}{.}95$; $\delta_{2000} = +58°29'19\overset{''}{.}9$) was detected as a short period variable in the SuperWasp database (http://www.superwasp.org, Butters et al., 2010).

The star has $V = 10.82$ and $B - V = 0.553$ transformed from the Tycho-2 catalogue (Høg et al., 2000), the Tycho Input Catalogue, revised version gives $V = 11.00$ (Egret et al., 1992), the 2MASS catalogue gives $J - K = 0.167$ (Cutri et al., 2003). The average SuperWasp magnitude (~ 11.1 mag) differs from the V magnitude derived from Tycho-2 significantly. This can be explained by the different passbands, because SuperWasp uses a wide band V filter (CV).

GSC 03949-00386 was monitored by the authors from observatories in Germany (seven nights between JD 2 455 829 and JD 2 455 851) and Croatia (one night: JD 2 455 837).

The instruments used were a Teleview 509/5.0 telescope equipped with a Sigma 1603 CCD camera with −IR filter (PF), and a Meade 12" LX200 telescope with a CV filter and a SBIG ST-7XME CCD camera (GS).

For the decision, if the combination of these three data sets with somewhat different passbands is feasible, they were first analyzed separately (`Period04`, Lenz and Breger, 2005). The differences of the semiamplitudes of the fundamental period between the three sets were at most 0.003 mag. This is in the range of the calculated uncertainties (sigmas) of about 0.001 mag for the semiamplitudes of the single data sets. Therefore it is possible to combine these data sets applying a shift for different mean magnitudes.

The differential magnitudes of our telescopes were shifted to fit the SuperWasp magnitudes. The data are available electronically through the IBVS website as `6013-t1.txt`.

Our observations combined with the SuperWasp data showed that GSC 03949-00386 is a pulsating variable with a total amplitude of about 0.25 mag and two peaks in the periodogram, at 10.440179 c/d (period: 0.095783796 d) and 13.524850 c/d (period: 0.073937974 d) (Fig. 1).

Using the Fourier analysis program, other significant peaks at linear combinations of the main frequencies were found as well, see Table 1 for an overview.

The Fourier graph after prewhitening for the frequencies given in Table 1 is shown in Fig. 2.

Table 1. Frequencies detected in GSC 03949-00386

Mode	Frequency (c/d)	Semi-amplitude (mag)
f_0	10.440179 ± 0.000001	0.069
f_1	13.524850 ± 0.000002	0.035
$f_0 + f_1$	23.965029 ± 0.000006	0.010
$2f_0$	20.880358 ± 0.000007	0.009

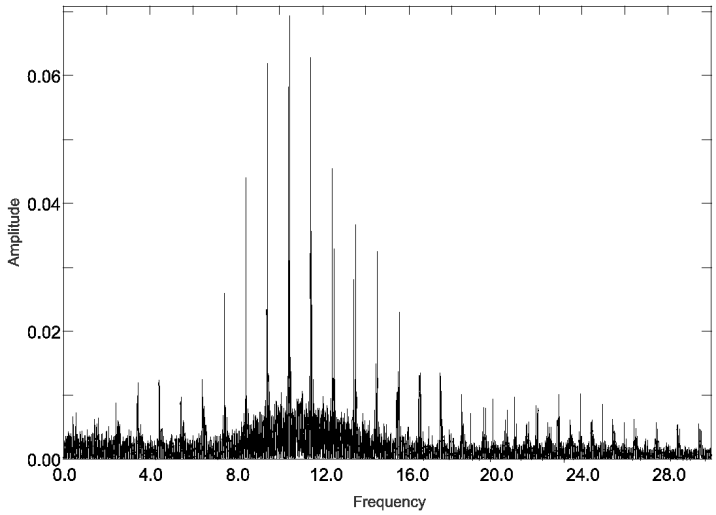

Figure 1. Fourier graph between 0 and 30 c/d

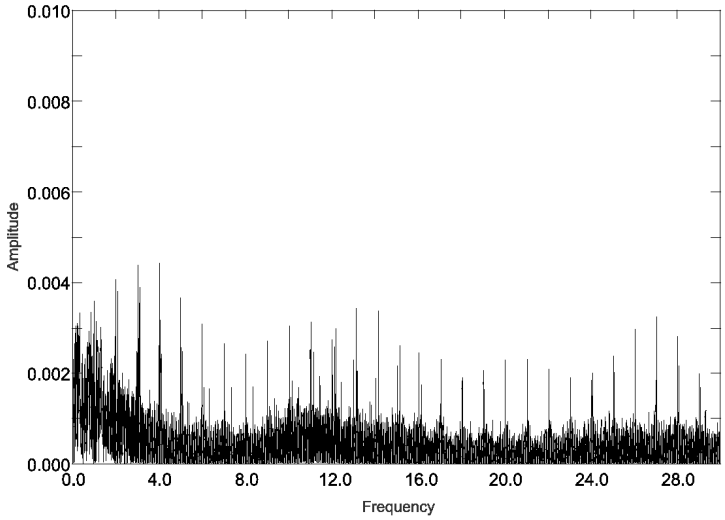

Figure 2. Fourier graph after prewhitening the detected frequencies of Table 1

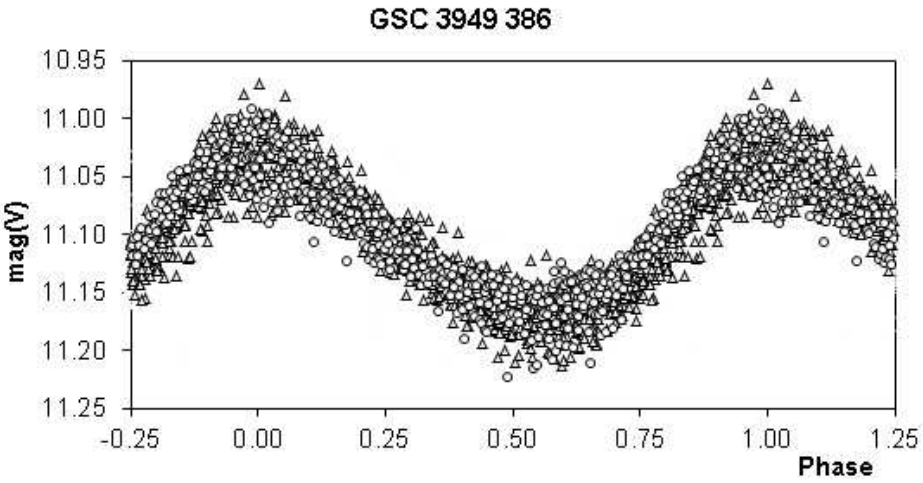

Figure 3. Phase plot for the fundamental period of 0.095783796 days, after prewhitening for the first overtone period.

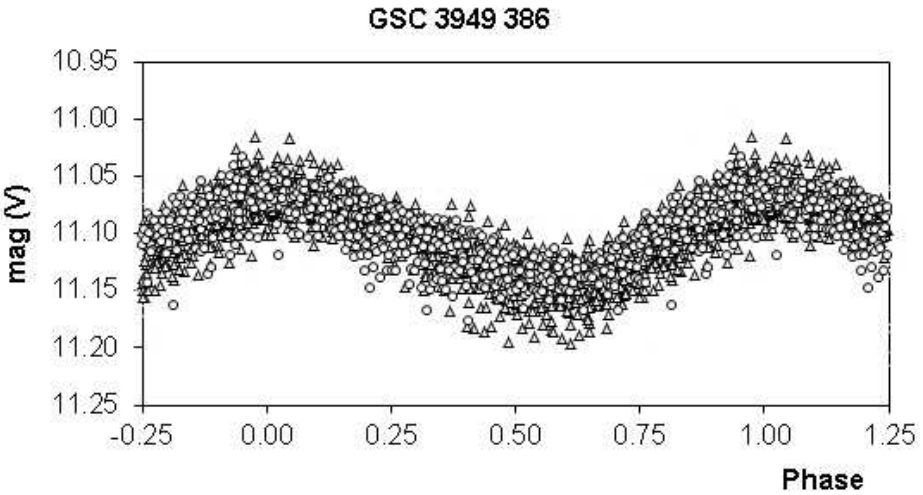

Figure 4. Phase plot for the first overtone period of 0.073937974 days, after prewhitening for the fundamental period and its first harmonic.

The remaining peaks emerge about integer frequency values, which is likely to originate from instrumental effects and atmospheric extinction.

Folded light curves for these periods, after prewhitening for the other, are given in Figs. 3 and 4.

CV filtered data are represented with open circles, −IR data with open triangles. The ratio between these periods is 0.7719257 ± 0.0000002, which makes this star a member of the rare group of radially pulsating double-mode HADS (e.g. Petersen and Christensen-Dalsgaard, 1996).

The proper motion of GSC 03949-00386 is small, −8.8 mas/y in RA and −9.9 mas/y in declination, according to the UCAC2 Bright Star Supplement catalog (Urban et al., 2006). Together with the relatively long period, this makes it an unlikely candidate to be an SX Phe star, but rather a Population I object. The classification HADS is also supported by the $B - V$ value derived from the Tycho-2 catalogue.

GSC 03949-00386 fits well to the period ratios clustering around 0.772 for $\log P_0 = -1.0$ found for other double mode HADS (Poretti et al., 2005).

Acknowledgements: It is a pleasure to thank John Greaves, UK, for helpful comments. This research has made use of the VizieR database operated at the *Centre de Données Astronomiques* (Strasbourg) in France and of the AAVSO-VSX data base.

References:

Butters, O. W., West, R. G., Anderson, D. R., Collier Cameron, A., Clarkson, W. I., Enoch, B., Haswell, C. A., Hellier, C., Horne, K., Joshi, Y., Kane, S. R., Lister, T. A., Maxted, P. F. L., Parley, N., Pollacco, D., Smalley, B., Street, R. A., Todd, I., Wheatley, P. J., Wilson, D. M., 2010, *A&A*, **520**, L10

Cutri, R.M., et al., 2003, 2MASS All-Sky Catalog of Point Sources, University of Massachusetts and IPAC/California, Institute of Technology

Egret, D., Didelon, P., McLean, B.J., Russell, J.L., Turon, C., 1992, *A&A*, **258**, 217

Høg, E., Fabricius, C., Makarov, V.V., Urban, S., Corbin, T., Wycoff, G., Bastian, U., Schwekendiek, P., Wicenec, A., 2000, *A&A*, **355**, L27

Lenz, P., Breger, M., 2005, *Comm. in Asteroseismology*, **146**, 53

Petersen, J.O, and Christensen-Dalsgaard, J., 1996, *A&A*, **312**, 463

Poretti, E., Suárez, J. C., Niarchos, P. G., Gazeas, K. D., Manimanis, V. N., van Cauteren, P., Lampens, P., Wils, P., Alonso, R., Amado, P. J., Belmonte, J. A., Butterworth, N. D., Martignoni, M., Martín-Ruiz, S., Moskalik, P., Robertson, C. W., 2005, *A&A*, **440**, 1097

Urban, S.E., Zacharias, N., Wycoff, G.L., 2004, The UCAC2 Bright Star Supplement, U.S. Naval Observatory, Washington D.C., 2004-2006

COMMISSIONS 27 AND 42 OF THE IAU
INFORMATION BULLETIN ON VARIABLE STARS

Number 6014

Konkoly Observatory
Budapest
16 February 2012

HU ISSN 0374 – 0676

NEW TIMES OF MINIMA OF SOME ECLIPSING VARIABLES

LACY, C. H. S.

Department of Physics, University of Arkansas, Fayetteville, Arkansas 72701, USA;
e-mail: clacy@uark.edu

Observatory and telescope:
URSA: URSA Observatory at the University of Arkansas; 10-inch Schmidt-Cassegrain reflector. NFO: NFO WebScope near Silver City, NM, USA (www.nfo.edu); 24-inch classical Cassegrain.

Detector:	URSA: 1020×1530 pixels SBIG ST8EN CCD cooled to (typ.) −20°C; 1.15 arcsec square pixels; 20'(N-S)×30'(E-W) field of view. NFO: 2102×2092 pixels Kodak KAF 4300E CCD cooled to (typ.) −20°C; 0.78 arcsec square pixels; 27' square field of view.

Method of data reduction:
Virtual measuring engine (Measure 2.0) writtem by C. H. S. Lacy in 2005.

Method of minimum determination:
Kwee & van Woerden (1956)

Remarks:
A sample of the observations has been published by Lacy, Hood & Straughn (2001). Mean deviations between independently timed eclipses by the two telescopes (URSA & NFO) are not significantly larger than expected based on the error estimates, implying that the estimated timing errors are realistic.

Times of minima:					
Star name	Time of min. HJD 2400000+	Error	Type	Filter	Rem.
AP And	55743.8409	0.0002	2	V	URSA
AP And	55758.9206	0.0003	1	V	URSA
AP And	55770.8254	0.0002	2	V	URSA
AP And	55801.7772	0.0002	1	V	URSA
AP And	55809.7138	0.0001	1	V	URSA
AP And	55816.8562	0.0003	2	V	URSA
AP And	55824.7931	0.0001	2	V	URSA
AP And	55835.9046	0.0003	2	V	URSA
AP And	55848.6023	0.0002	2	V	URSA
AP And	55848.6029	0.0002	2	V	NFO
AP And	55851.7772	0.0001	2	V	URSA
AP And	55851.7769	0.0002	2	V	NFO
AP And	55856.5392	0.0003	2	V	URSA
AP And	55866.8566	0.0001	1	V	NFO
AP And	55875.5867	0.0003	2	V	NFO
AP And	55890.6658	0.0002	1	V	URSA
AP And	55894.6339	0.0001	2	V	URSA
AP And	55925.5864	0.0002	1	V	NFO
V361 Cas	55762.8169	0.0006	2	V	URSA
V361 Cas	55799.6851	0.0004	2	V	URSA
V361 Cas	55805.8298	0.0005	1	V	URSA
V381 Cas	55825.9456	0.0004	2	V	NFO
V381 Cas	55862.6087	0.0004	2	V	NFO
V651 Cas	55775.9044	0.0002	2	V	URSA
V651 Cas	55776.9014	0.0003	2	V	URSA
V651 Cas	55779.8916	0.0004	2	V	URSA
V651 Cas	55787.8665	0.0002	2	V	URSA
V651 Cas	55800.8260	0.0002	2	V	URSA
V651 Cas	55806.8065	0.0003	2	V	URSA
V651 Cas	55807.8031	0.0002	2	V	URSA
V651 Cas	55811.7902	0.0003	2	V	URSA
V651 Cas	55817.7706	0.0001	2	V	URSA
V651 Cas	55825.7455	0.0002	2	V	URSA
V651 Cas	55830.7293	0.0002	2	V	URSA
V651 Cas	55832.7234	0.0002	2	V	URSA
V651 Cas	55833.7197	0.0003	2	V	URSA
V651 Cas	55834.7165	0.0002	2	V	URSA
V651 Cas	55835.7115	0.0004	2	V	URSA
V651 Cas	55838.7040	0.0002	2	V	URSA
V651 Cas	55839.6999	0.0003	2	V	URSA
V651 Cas	55841.6939	0.0002	2	V	URSA
V651 Cas	55842.6906	0.0002	2	V	URSA
V651 Cas	55851.6614	0.0002	2	V	URSA
V651 Cas	55853.6546	0.0002	2	V	URSA
V651 Cas	55854.6520	0.0003	2	V	URSA
V651 Cas	55855.6486	0.0003	2	V	URSA
V651 Cas	55863.6224	0.0002	2	V	URSA

Times of minima:					
Star name	Time of min. HJD 2400000+	Error	Type	Filter	Rem.
V651 Cas	55865.6165	0.0003	2	V	URSA
V651 Cas	55870.6002	0.0002	2	V	URSA
V651 Cas	55876.5811	0.0002	2	V	URSA
V651 Cas	55883.5588	0.0002	2	V	URSA
V651 Cas	55894.5238	0.0002	2	V	URSA
WW Cep	55760.8664	0.0003	2	V	URSA
WW Cep	55850.5829	0.0001	1	V	URSA
V1136 Cyg	55722.9106	0.0007	2	V	NFO
V1136 Cyg	55833.7128	0.0017	2	V	NFO
BF Dra	55695.8610	0.0002	1	V	NFO
BF Dra	55779.7569	0.0011	2	V	URSA
BF Dra	55824.6070	0.0005	2	V	URSA
V501 Her	55712.8993	0.0006	2	V	NFO
RW Lac	55742.8581	0.0004	2	V	NFO
AL Leo	55621.8084	0.0002	2	V	URSA
AL Leo	55622.6114	0.0002	1	V	URSA
AL Leo	55625.8225	0.0003	1	V	NFO
AL Leo	55626.6251	0.0003	2	V	NFO
AL Leo	55630.6391	0.0002	1	V	NFO
AL Leo	55634.6529	0.0002	2	V	NFO
AL Leo	55646.6939	0.0003	1	V	NFO
AL Leo	55893.9434	0.0002	1	V	NFO
AL Leo	55926.8563	0.0001	2	V	NFO
AL Leo	55930.8700	0.0002	1	V	NFO
AL Leo	55934.8841	0.0002	2	V	NFO
AL Leo	55946.9259	0.0002	1	V	URSA
AL Leo	55950.9395	0.0002	2	V	URSA
AL Leo	55955.7555	0.0002	2	V	URSA
AL Leo	55955.7557	0.0004	2	V	NFO
AL Leo	55967.7970	0.0002	1	V	NFO
V506 Oph	55737.7365	0.0002	1	V	URSA
V506 Oph	55762.6565	0.0001	2	V	URSA
V506 Oph	55763.7167	0.0002	2	V	URSA
V506 Oph	55788.6366	0.0002	1	V	URSA
V506 Oph	55805.6035	0.0003	1	V	URSA
V506 Oph	55806.6641	0.0004	1	V	URSA
IM Per	55853.7152	0.0008	1	V	NFO
IM Per	55854.8329	0.0006	2	V	NFO
IM Per	55855.9707	0.0006	1	V	URSA
IM Per	55855.9733	0.0004	1	V	NFO
IM Per	55862.7355	0.0003	1	V	NFO
IM Per	55932.6170	0.0003	1	V	URSA
IM Per	55933.7326	0.0005	2	V	NFO
IM Per	55941.6331	0.0003	1	V	URSA
IM Per	55950.6503	0.0002	1	V	URSA
NP Per	55884.9413	0.0002	1	V	NFO
V482 Per	55848.8258	0.0004	1	V	URSA

Times of minima:					
Star name	Time of min. HJD 2400000+	Error	Type	Filter	Rem.
V482 Per	55848.8265	0.0004	1	V	NFO
V482 Per	55865.9527	0.0004	1	V	URSA
V482 Per	55865.9522	0.0004	1	V	NFO
V482 Per	55875.7404	0.0005	1	V	URSA
V482 Per	55940.5796	0.0009	2	V	URSA
V482 Per	55946.6960	0.0004	1	V	URSA
V514 Per	55849.8523	0.0007	2	V	URSA
V514 Per	55850.7590	0.0009	1	V	URSA
V514 Per	55860.7655	0.0007	2	V	NFO
V514 Per	55869.8601	0.0011	2	V	NFO
AQ Ser	55760.6989	0.0005	1	V	URSA
V335 Ser	55630.9697	0.0002	1	V	NFO
V335 Ser	55694.9212	0.0005	2	V	NFO
TY Tau	55832.8640	0.0003	1	V	URSA
TY Tau	55853.8730	0.0008	2	V	URSA
TY Tau	55854.9496	0.0005	2	V	URSA
TY Tau	55859.7977	0.0003	1	V	URSA
TY Tau	55865.7230	0.0006	2	V	URSA
TY Tau	55875.9581	0.0004	1	V	URSA
TY Tau	55895.8895	0.0005	2	V	URSA
V1094 Tau	55813.9147	0.0004	1	V	URSA
V1094 Tau	55831.8918	0.0002	1	V	URSA
V1094 Tau	55855.7330	0.0002	2	V	URSA
V1094 Tau	55882.6987	0.0003	2	V	NFO
V1094 Tau	55894.8107	0.0002	1	V	URSA
V1094 Tau	55936.6296	0.0002	2	V	NFO
V1094 Tau	55945.6179	0.0003	2	V	NFO
HY Vir	55623.7767	0.0003	1	V	URSA
HY Vir	55716.6799	0.0003	1	V	URSA
BP Vul	55775.7640	0.0002	2	V	URSA
BT Vul	55693.8621	0.0003	1	V	NFO
BT Vul	55717.8267	0.0003	1	V	URSA
BT Vul	55733.8037	0.0002	1	V	NFO
BT Vul	55837.6522	0.0002	1	V	URSA
BT Vul	55849.6341	0.0003	2	V	URSA
BT Vul	55853.6290	0.0002	1	V	NFO
BT Vul	55865.6119	0.0002	2	V	NFO
BT Vul	55881.5898	0.0004	2	V	NFO

Acknowledgements:
Construction and operation of the URSA telescope were partially funded by the National Science Foundation and the University of Arkansas, Fayetteville. Construction and operation of the NFO telescope were partially funded by the National Science Foundation, the Arkansas Center for Space and Planetary Sciences, the NASA Arkansas Space Grant Consortium, the University of Arkansas, Fayetteville, the University of Arkansas at Little Rock, and the Harvard-Smithsonian Center for Astrophysics. We are grateful to Bill Neely for initial processing of the images and construction, maintenance, and operation of the NFO equipment and software.

References:

Kwee, K.K., van Woerden, H., 1956, *B.A.N.*, **12**, 327
Lacy, C. H. S., Hood, B. & Straughn, A., 2001, *IBVS*, **5067**

COMMISSIONS 27 AND 42 OF THE IAU
INFORMATION BULLETIN ON VARIABLE STARS

Number 6015

Konkoly Observatory
Budapest
1 March 2012

HU ISSN 0374 – 0676

PHOTOMETRY OF HIGH-AMPLITUDE DELTA SCUTI STARS

WILS, PATRICK[1]; PANAGIOTOPOULOS, KOSTAS[2,3]; VAN WASSENHOVE, JEROEN[1]; AYIOMAMITIS, ANTHONY[2,4]; NIEUWENHOUT, FRANS[5]; ROBERTSON, C.W.[6]; VANLEENHOVE, MAARTEN[1]; HAMBSCH, FRANZ-JOSEF[1,7]; HAUTECLER, HUBERT[1]; PICKARD, ROGER D.[8]; BAILLIEN, ANTOINE[1]; STAELS, BART[1,9]; KLEIDIS, STELIOS[2,10]; LAMPENS, PATRICIA[11]; VAN CAUTEREN, PAUL[1,11]

[1] Vereniging Voor Sterrenkunde, Belgium; e-mail: patrickwils@yahoo.com

[2] Helliniki Astronomiki Enosi, Greece

[3] Pouda Observatory, Diakopto, Greece

[4] Perseus Observatory, Athens, Greece

[5] Werkgroep Veranderlijke Sterren, The Netherlands

[6] SETEC Observatory, Goddard, Kansas, USA

[7] Bundesdeutsche Arbeitsgemeinschaft für Veränderliche Sterne e.V. Germany

[8] British Astronomical Association, UK

[9] Center for Backyard Astrophysics Flanders

[10] Zagori Observatory, Epirus, Greece

[11] Koninklijke Sterrenwacht van België (ROB), Brussel, Belgium

In this paper we report 432 further times of maxima for 64 High-Amplitude Delta Scuti Stars (HADS), following the reports of Wils et al. (2009, 2010, 2011). The majority of the data were obtained during 2011.

The observers and their instruments are listed in Table 1. The times of maxima obtained are given as an Appendix in Table 4. When the same maximum was observed in more than one filter, the table shows the average value of the times obtained in each band individually. The method used to calculate the times of maximum is described in Wils et al. (2009).

Elements for the previously unknown HADS GSC 3004-0870 (magnitude range 13.2-13.8V, J2000 position: $10^{\rm h}21^{\rm m}35\overset{\rm s}{.}33$ $+40°31'41\overset{''}{.}2$) are given in Table 2, together with elements for a number of other stars that have been observed in detail the past year, or for which the existing ephemeris deviates substantially from our recent observations. To get a better precision, use was made of data from the ASAS (Pojmański, 2002), NSVS (Woźniak et al., 2004) and SuperWASP surveys (Butters et al., 2010).

The star GSC 1924-1134 (= NSVS 7293918) discovered by Hoffman, Harrison and McNamara (2009) was found to be a double-mode HADS from observations by FN. It is pulsating in the fundamental and first overtone modes, with a period ratio of 0.7737, typical of other stars of the class and period (Poretti et al., 2005). The independent frequencies, and their amplitudes and phases, determined using Period04 (Lenz & Breger, 2005) are given in Table 3. The linear combinations $f_0 + f_1$ and $2f_0 + f_1$ of these independent frequencies were detected as well.

Table 1: List of instruments used for the observations.

Code	Observer(s)	Telescope	Observatory	CCD
AA	AA	Refractor 16 cm	Perseus Observatory	SBIG ST-10XME
AA30	AA	Refractor 30 cm	Perseus Observatory	SBIG ST-10XME
AB	AB	Refractor 10 cm	Carpe Noctem Observatory	SBIG ST-9E
BHO	PL+PVC	Newton 25 cm	Beersel Hills Observatory	SBIG ST-10XME
FN	FN	Catadioptric 40 cm	Alkmaar, Nederland	SBIG ST-7XME
FN25	FN	Catadioptric 25 cm	Alkmaar, Nederland	SBIG ST402XME
HHU	HH	Catadioptric 20 cm	Roosbeek Lake Observatory	SBIG ST-7XME
HMB4	FJH	Catadioptric 35 cm	Mol, Belgium	SBIG ST-8
HMB8	FJH	Ritchey-Chrétien 20 cm	Mol, Belgium	SBIG ST-8XME
HMBC	FJH	Catadioptric 28 cm	Mol, Belgium	SBIG ST-10XME
HMBH	FJH	Hypergraph 40 cm	Mol, Belgium	SBIG STL-11000XM
KP	KP	Modified Cassegrain 26 cm	Pouda Observatory	SBIG ST-10XME
MAV	MV	Newton 25 cm	Leest Observatory	SBIG ST-10XME
RP	RDP	Catadioptric 36 cm	Shobdon, UK	Starlight XPress SXV-H9
SBL	BS	Cassegrain 28 + 23.5 cm	Alan Guth Observatory	Starlight XPress MX-716
SK	SK	Catadioptric 30 cm	Zagori Observatory	SBIG ST-7XMEI
SO30	CWR	Catadioptric 30 cm	SETEC Observatory	SBIG ST-8XME
SO40	CWR	Catadioptric 40 cm	SETEC Observatory	SBIG ST-8XME
VWS	JVW	Refractor 15.2 cm	Hooglede, Belgium	SBIG ST-7XME

Some of the objects observed earlier turned out to be multiperiodic variables: V337 Ori (observations from MV, RDP and FN), GSC 1621-1643 (FJH), GSC 2847-0586 (FJH, KP and MV), GSC 3490-0814 = V1139 Her (KP, AA and MV) and GSC 4464-0924 (JVW and HH). The frequencies detected in these stars are also listed in Table 3. In all of these stars also the combination frequency $f_0 + f_1$ was detected. In V337 Ori the modes $2f_0+f_1$ and f_1-f_0 were detected as well. In GSC 2847-0586, a possible third independent frequency may have been detected at 6.373 c/d, but with a signal-to-noise ratio of 4.0 it is barely significant. For GSC 4464-0924 the influence of the secondary frequency on the time of maximum is negligible, so that its observed maxima are also included in Table 4. A sample light curve of V1139 Her is given in Fig. 1.

The period of GSC 4556-1113 seems to vary cyclically. Especially during the recent data when the star was followed closely by JVW, the $O-C$ varied with a period of 164 ± 3 days and an amplitude of 68 ± 6 seconds. The recent $O - C$ data, covering almost three of these cycles are given in Fig. 2. If the origin of this cyclical variation is the light-travel time effect caused by an unknown companion in a circular orbit, some further details can be calculated from the $O - C$ of the maxima or from the full light curve data as shown by Shibahashi & Kurtz (2012). Both methods give equivalent results. It follows that the projected radius $a\sin i$ of the orbit of the pulsating star equals 0.137(5) AU, its projected orbital velocity 9.1 ($\pm$ 0.4) km/s. Finally the mass function $f(m_1, m_2, \sin i) = 0.0126(13) M_\odot$, suggesting the companion is a red dwarf. Companions of HADS have been suggested before from $O - C$ data, but in many cases these are invalidated by further observations. Only in the case of SZ Lyn (Moffett et al., 1988) the presence of a companion is established without any doubt, as almost 16 cycles of the 1180 day orbital period have now been observed. Further observations are required to make sure the companion of GSC 4556-1113 is real as well.

GSC 4431-1487, one of the comparison stars used (for LW Dra), was found to be variable by one of us (JVW). It turns out to be a W UMa type variable with a period of 0.2548 days. The photometry for this object, together with those from Table 3, are

available from the IBVS website. GSC 1320-119 near V337 Ori is likely a new eclipsing variable with rare eclipses. It was found to have faded by about 0.4 magnitudes on JD 2455623 by one of us (MV).

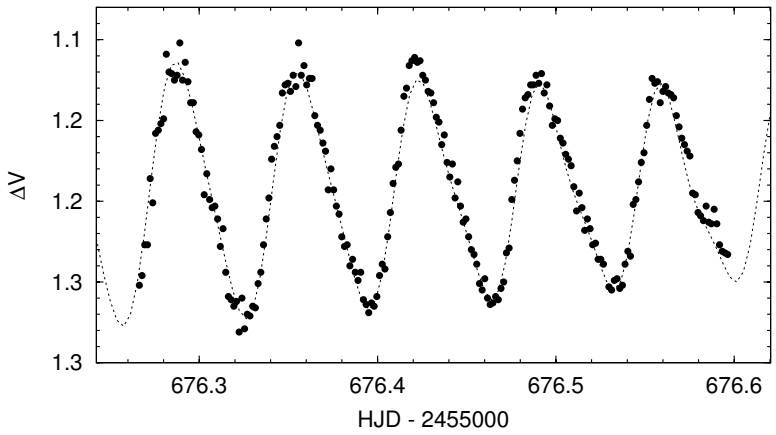

Figure 1. One night of data of V1139 Her plotted with the model light curve with all detected frequencies.

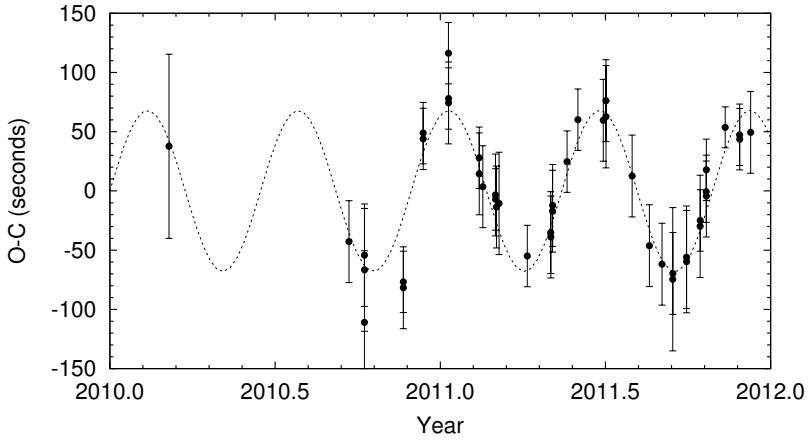

Figure 2. $O - C$ graph of GSC 4556-1113 with respect to a linear ephemeris. A proposed cyclical model with a period of 164 days and an amplitude of 68 seconds is added as a dotted line.

Table 2: Updated elements of known HADS. Uncertainties are given in units of the last decimal.

Star	Max (HJD)	Period (d)
V376 Cam	2454823.4142(1)	0.14032368(2)
GSC 2290-1195	2454410.548(3)	0.0779984(3)
GSC 3004-0870	2455601.4482(4)	0.08215879(2)
GSC 3428-1497	2455571.5826(3)	0.07484470(3)

Table 3: Independent frequencies detected in multiperiodic HADS. Uncertainties are given in units of the last decimal. The phase is given with respect to HJD = 0. Observations were obtained with a V filter.

Star		Frequency c/d	Semi-Amplitude Mag.	Phase
V1139 Her	f_0	14.57979(4)	0.0761(5)	0.497(1)
	f_1	13.7999(2)	0.0195(5)	0.993(4)
V337 Ori	f_0	4.968695(3)	0.182(2)	0.803(1)
	f_1	6.72403(3)	0.022(2)	0.383(9)
GSC 1621-1643	f_0	8.72095(8)	0.135(1)	0.235(1)
	f_1	12.1152(4)	0.022(1)	0.763(9)
GSC 1924-1134	f_0	11.29473(4)	0.1914(6)	0.0797(5)
	f_1	14.5982(5)	0.0169(7)	0.062(6)
GSC 2847-0586	f_0	7.077126(2)	0.1136(4)	0.0948(6)
	f_1	6.95255(1)	0.0171(4)	0.339(4)
GSC 4464-0924	f_0	12.402261(5)	0.1807(5)	0.0441(4)
	f_1	18.54333(7)	0.0113(5)	0.801(7)

Acknowledgements:
This work has made use of the SIMBAD database, operated at CDS, Strasbourg, France. FN is grateful to the University of Amsterdam for providing a CCD camera with filter wheel. Part of the equipment used at SETEC Observatory was purchased with a grant from the American Astronomical Society. PVC is grateful for support from Astrotechniek and Baader Planetarium. The BHO data were acquired with equipment purchased thanks to a research fund financed by the Belgian National Lottery (1999).

References:

Butters O.W., West R.G., Anderson D.R., et al., 2010, *A&A* **520**, L10
Hoffman D.I., Harrison T.E., McNamara B.J., 2009, *AJ* **138**, 466
Lenz P., Breger M., 2005, *Comm. in Asteroseismology* **146**, 53
Moffett T.J., Barnes III T.G., Fekel, Francis Jr. C., Jefferys W.H., Achtermann J.M., 1988, *AJ* **95**, 1534
Pojmański G., 2002, *Acta Astron.* **52**, 397
Poretti E., Suárez J.C., Niarchos P.G, et al., 2005, *A&A* **440**, 1097
Shibahashi H., Kurtz D.W., 2012, arXiv:1202.0105 [astro-ph.SR]
Wils P., Kleidis S., Hambsch F.-J., Vidal-Sáinz J., Vanleenhove M., Lampens P., Van Cauteren P., Robertson C.W., Staels B., Pickard R.D., Rozakis I., Dufoer S., Groenendaels R., Gómez-Forrellad J.M., García-Melendo E., Hautecler H., Van der Looy J., 2009, *IBVS* **5878**
Wils P., Hambsch F.-J., Lampens P., Van Cauteren P., Staels B., Pickard R.D., Kleidis S., Van Wassenhove J., Otero S.A., Bellocchio E., Thienpont E., Vanleenhove M., 2010, *IBVS* **5928**
Wils P., Hambsch F.-J., Robertson C.W., Lampens P., Van Cauteren P., Hautecler H., Panagiotopoulos K., Van Wassenhove J., Staels B., Vanleenhove M., Hoste S., Pickard R.D., Kleidis S., Ayiomamitis A., Nieuwenhout F., Strigachev A., Bernhard K., 2011, *IBVS* **5977**
Woźniak P.R., Vestrand W.T., Akerlof C.W., et al., 2004, *AJ* **127**, 2436

Appendix:

Table 4: Observed times of maximum (Epoch = HJD − 2400000).

Star	Epoch	Unc.	Obs.	Filter	Star	Epoch	Unc.	Obs.	Filter
GP And	55834.3764	0.0001	KP	BV	YZ Boo	55669.6213	0.0009	SBL	V
	55836.5010	0.0003	FN	V		55674.8256	0.0005	SO40	V
	55836.5797	0.0003	FN	V		55689.7107	0.0004	SO40	V
	55855.4635	0.0009	HMB4	V		55689.8148	0.0004	SO40	V
	55856.4078	0.0010	HMB4	V		55705.3246	0.0013	AA30	C
	55877.3372	0.0013	HMB4	V		55705.4286	0.0019	AA30	C
	55877.4153	0.0015	HMB4	V		55707.4067	0.0004	AA30	C
	55904.2470	0.0004	KP	V		55707.5102	0.0004	AA30	C
	55904.3257	0.0004	KP	V		55718.6480	0.0006	SO40	V
	55904.4042	0.0005	KP	V		55718.7523	0.0005	SO40	V
V460 And	55590.3099	0.0008	FN	V		55718.8562	0.0005	SO40	V
	55590.3844	0.0007	FN	V		55750.7084	0.0005	SO40	V
	55590.4591	0.0003	FN	V		55750.8125	0.0008	SO40	V
	55856.2666	0.0004	HHU	C	BL Cam	55893.4535	0.0004	AA30	C
	55856.3408	0.0002	HHU	C		55893.4924	0.0003	AA30	C
	55889.6329	0.0005	SO40	V		55893.5318	0.0003	AA30	C
	55889.7076	0.0007	SO40	V		55893.5710	0.0004	AA30	C
	55889.7826	0.0003	SO40	V	V367 Cam	55625.3385	0.0004	HMB4	VI
	55889.8579	0.0004	SO40	V		55626.4331	0.0008	HMB4	VI
	55889.9325	0.0006	SO40	V		55627.2837	0.0008	HMB4	V
	55890.0072	0.0005	SO40	V		55627.4063	0.0010	HMB4	V
	55893.6067	0.0004	SO40	V		55628.3786	0.0015	HMB4	V
	55893.6820	0.0004	SO40	V		55629.3516	0.0009	HMB4	V
	55893.7568	0.0005	SO40	V		55631.2980	0.0005	SK	BR
	55893.8316	0.0007	SO40	V		55861.3568	0.0009	MAV	V
	55893.9067	0.0006	SO40	V		55861.4784	0.0012	MAV	V
	55893.9823	0.0006	SO40	V	V376 Cam	55599.2639	0.0004	KP	V
	55894.5813	0.0006	SO40	V		55599.4041	0.0004	KP	V
	55894.6564	0.0003	SO40	V		55599.5444	0.0002	KP	V
	55894.7316	0.0003	SO40	V		55643.3253	0.0007	VWS	V
	55894.8064	0.0005	SO40	V		55643.4658	0.0003	VWS	V
	55894.8812	0.0004	SO40	V		55646.2723	0.0004	KP	V
	55894.9565	0.0005	SO40	V		55646.4127	0.0004	KP	V
	55897.2054	0.0005	AA30	C		55649.3594	0.0004	VWS	V
	55897.2808	0.0004	AA30	C		55715.4520	0.0003	VWS	V
	55897.3556	0.0003	AA30	C		55848.3387	0.0006	MAV	V
V524 And	55834.5624	0.0007	FN	V		55857.3194	0.0003	VWS	V
	55834.6567	0.0006	FN	V	AD CMi	55623.3957	0.0011	HHU	C
	55838.2473	0.0009	KP	V	V792 Cep	55839.3461	0.0009	KP	V
	55838.3417	0.0007	KP	V		55839.4790	0.0005	KP	V
	55838.4362	0.0004	KP	V		55839.6125	0.0005	KP	V
	55875.2877	0.0004	HHU	C	XX Cyg	55729.4472	0.0006	HHU	C
	55905.3365	0.0006	KP	V		55751.6988	0.0002	SO40	V
	55905.4308	0.0008	KP	V		55751.8337	0.0003	SO40	V
	55905.5250	0.0010	KP	V		55799.7108	0.0002	SO40	V
V544 And	55851.2895	0.0004	HHU	C		55804.7008	0.0002	SO40	V
	55870.2183	0.0006	KP	V		55804.8357	0.0002	SO40	V
	55870.3251	0.0004	KP	V		55809.6908	0.0002	SO40	V
	55870.4321	0.0004	KP	V		55809.8257	0.0002	SO40	V
	55870.5389	0.0005	KP	V		55866.3353	0.0006	HHU	C
CY Aqr	55833.3662	0.0004	HHU	C	V2455 Cyg	55820.3878	0.0011	HHU	C
	55848.3207	0.0004	KP	V		55855.3385	0.0004	HHU	C
	55905.2695	0.0001	HHU	C	LW Dra	55676.4152	0.0006	VWS	V
YZ Boo	55604.4597	0.0004	KP	B		55706.4260	0.0008	VWS	V
	55604.5637	0.0003	KP	B		55799.6521	0.0013	SO30	V
	55604.6675	0.0002	KP	B		55824.3433	0.0007	VWS	V
	55669.4122	0.0015	SBL	V		55829.4235	0.0007	VWS	V
	55669.5166	0.0012	SBL	V		55832.3773	0.0007	VWS	V

Table 4: Observed times of maximum (continued).

Star	Epoch	Unc.	Obs.	Filter	Star	Epoch	Unc.	Obs.	Filter
LW Dra	55833.3230	0.0006	VWS	V	DW Psc	55894.3975	0.0003	KP	C
	55833.4410	0.0006	VWS	V		55895.2326	0.0004	KP	C
	55834.3861	0.0009	VWS	V		55895.2921	0.0007	KP	C
	55836.3946	0.0009	VWS	V	GW UMa	55579.5936	0.0008	KP	V
	55849.3916	0.0009	VWS	V		55580.4056	0.0018	RP	V
	55878.4574	0.0009	VWS	V		55580.6099	0.0012	RP	V
DY Her	55718.7057	0.0006	SO30	V		55604.3831	0.0009	AA	C
	55718.8540	0.0005	SO30	V		55672.4532	0.0017	RP	V
	55750.8095	0.0006	SO30	V	QV Vir	55633.4015	0.0018	AA	C
	55751.7018	0.0008	SO30	V		55633.4680	0.0010	AA	C
	55751.8501	0.0003	SO30	V		55633.5352	0.0007	AA	C
KZ Hya	55601.4111	0.0003	AA	C		55633.6029	0.0014	AA	C
	55601.4705	0.0002	AA	C	GSC 0191-1282	55623.2787	0.0011	HMBC	V
	55601.5298	0.0002	AA	C		55623.3257	0.0005	HMBC	V
KZ Lac	55833.5293	0.0015	FN	V		55623.3739	0.0008	HMBC	V
	55833.6334	0.0019	FN	V		55623.4202	0.0007	HMBC	V
	55849.5041	0.0012	FN	V		55624.4171	0.0003	HMBC	V
	55849.6087	0.0020	FN	V		55628.3523	0.0005	FN25	V
	55854.4116	0.0007	KP	V		55628.3991	0.0003	FN25	V
	55854.5154	0.0010	KP	V		55635.2758	0.0006	AA	C
	55854.6197	0.0015	KP	V		55635.3226	0.0006	AA	C
	55869.2386	0.0013	KP	V		55635.3708	0.0007	AA	C
	55869.3433	0.0011	KP	V	GSC 0321-0314	55677.4380	0.0005	HHU	C
	55869.4467	0.0010	KP	V	GSC 0429-2098	55715.4915	0.0008	HHU	C
EH Lib	55675.4272	0.0002	AA	C	GSC 0612-0771	55849.5056	0.0007	HMB8	V
	55675.5156	0.0002	AA	C	GSC 0753-1489	55589.4289	0.0004	HHU	C
SZ Lyn	55583.5449	0.0008	RP	V		55627.3805	0.0005	MAV	V
	55583.6652	0.0007	RP	V	GSC 1076-0158	55775.4294	0.0007	HHU	C
	55587.6425	0.0008	SO30	V		55850.3085	0.0007	FN	V
	55587.7633	0.0005	SO30	V		55850.3955	0.0010	FN	V
	55587.8839	0.0006	SO30	V	GSC 1158-0921	55824.3442	0.0006	MAV	V
	55588.6074	0.0008	SO30	V		55824.4089	0.0007	MAV	V
	55588.7273	0.0015	SO30	V		55836.4205	0.0004	FN	V
	55588.8483	0.0007	SO30	V		55849.3368	0.0006	HMB8	V
	55588.9688	0.0008	SO30	V		55849.4013	0.0006	HMB8	V
	55629.3475	0.0004	HHU	C		55849.4656	0.0008	HMB8	V
V593 Lyr	55703.4063	0.0004	AA30	C		55850.3060	0.0005	HMB8	V
	55703.5085	0.0003	AA30	C		55850.3701	0.0005	HMB8	V
	55782.4717	0.0004	RP	V		55850.4344	0.0006	HMB8	V
	55834.3640	0.0006	AB	C		55853.2765	0.0005	KP	V
V1162 Ori	55590.6022	0.0010	SO30	V		55853.3410	0.0005	KP	V
	55590.6793	0.0011	SO30	V		55899.2570	0.0006	AA30	C
	55590.7584	0.0015	SO30	V	GSC 1220-1131	55578.2621	0.0007	HHU	C
	55591.3082	0.0018	BHO	V		55855.4001	0.0012	HHU	C
DY Peg	55806.3643	0.0004	MAV	V	GSC 1306-0466	55571.4641	0.0004	HHU	C
	55806.4374	0.0005	MAV	V		55601.4275	0.0021	AB	C
	55848.4427	0.0004	FN	V		55630.3555	0.0017	FN25	V
	55848.5157	0.0002	FN	V	GSC 1442-1358	55601.5056	0.0008	HMBC	V
	55854.2768	0.0003	KP	V		55601.5872	0.0005	HMBC	V
	55854.3501	0.0002	KP	V		55601.6691	0.0003	HMBC	V
	55903.2832	0.0012	RP	V		55660.3804	0.0004	HHU	C
	55903.3564	0.0004	RP	V		55674.3394	0.0007	AA	C
	55903.4292	0.0002	RP	V		55674.4213	0.0008	AA	C
DW Psc	55850.4960	0.0008	FN	V	GSC 1750-1237	55837.5423	0.0006	FN	V
	55850.5561	0.0005	FN	V		55877.3779	0.0008	HMB8	V
	55894.2197	0.0006	KP	C	GSC 2043-1201	55688.3253	0.0011	AA	C
	55894.2788	0.0002	KP	C		55688.4027	0.0008	AA	C
	55894.3379	0.0003	KP	C		55688.4805	0.0009	AA	C

Table 4: Observed times of maximum (continued).

Star	Epoch	Unc.	Obs.	Filter	Star	Epoch	Unc.	Obs.	Filter
GSC 2043-1201	55688.5584	0.0006	AA	C	GSC 3428-1497	55571.6567	0.0008	HMB8	V
GSC 2080-0986	55834.3094	0.0007	FN	V		55571.7318	0.0009	HMB8	V
	55834.4085	0.0007	FN	V		55625.3220	0.0009	HHU	C
GSC 2108-1564	55739.4349	0.0008	HMB8	V		55673.2974	0.0008	AA	C
	55739.5327	0.0010	HMB8	V		55673.3709	0.0007	AA	C
	55835.3969	0.0012	AB	C		55673.4463	0.0012	AA	C
GSC 2290-1195	55500.4988	0.0012	FN	V		55673.5202	0.0015	AA	C
	55500.5749	0.0009	FN	V		55880.4685	0.0010	MAV	V
	55838.3855	0.0013	HHU	C	GSC 3483-0746	55682.4568	0.0008	RP	V
GSC 2566-1398	55659.4801	0.0008	RP	V		55682.5691	0.0007	RP	V
	55659.5712	0.0006	RP	V	GSC 3489-0868	55713.3338	0.0008	AA30	C
	55714.3586	0.0006	AA30	C		55713.4204	0.0004	AA30	C
	55714.4492	0.0005	AA30	C		55729.3637	0.0005	AA30	C
	55714.5394	0.0005	AA30	C		55729.4504	0.0005	AA30	C
GSC 2696-1396	55829.3994	0.0005	HHU	C		55729.5369	0.0007	AA30	C
	55880.3186	0.0004	FN	V	GSC 3755-0845	55571.2812	0.0011	SBL	V
GSC 2843-1999	55572.3925	0.0028	HMB8	V		55629.3439	0.0007	FN	V
	55578.3535	0.0022	HMB8	V		55834.4275	0.0014	MAV	V
	55829.3389	0.0007	MAV	V		55834.5032	0.0009	MAV	V
	55829.4010	0.0008	MAV	V		55835.4178	0.0015	MAV	V
	55829.4625	0.0007	MAV	V		55835.4938	0.0015	MAV	V
	55856.2877	0.0006	MAV	V		55835.5686	0.0012	MAV	V
	55856.3499	0.0006	MAV	V		55893.2514	0.0007	MAV	V
	55856.4122	0.0005	MAV	V		55893.3274	0.0007	MAV	V
	55856.4741	0.0005	MAV	V		55893.4034	0.0008	MAV	V
	55880.2561	0.0008	MAV	V		55893.4037	0.0015	AB	C
	55880.3184	0.0007	MAV	V		55905.4261	0.0018	RP	V
	55880.3798	0.0007	MAV	V		55905.5040	0.0021	RP	V
	55887.2110	0.0005	AA30	C		55905.5797	0.0019	RP	V
	55887.2729	0.0006	AA30	C		55905.6554	0.0012	RP	V
	55887.3351	0.0007	AA30	C	GSC 3832-0152	55569.4240	0.0004	KP	V
	55887.3972	0.0006	AA30	C		55569.5153	0.0004	KP	V
	55887.4589	0.0004	AA30	C		55569.6065	0.0004	KP	V
GSC 2861-0970	55571.4510	0.0007	HMB8	V		55569.6979	0.0003	KP	V
	55594.3531	0.0005	RP	C		55641.3103	0.0016	HHU	C
	55641.3678	0.0005	FN	V		55641.4015	0.0008	HHU	C
	55859.2661	0.0006	MAV	V		55643.5027	0.0009	RP	V
	55859.3763	0.0007	MAV	V		55655.5595	0.0005	RP	V
	55882.2786	0.0006	MAV	V		55655.6509	0.0006	RP	V
	55882.3884	0.0006	MAV	V		55672.3665	0.0007	HHU	C
GSC 2977-0238	55570.3886	0.0002	KP	V		55672.4576	0.0005	HHU	C
	55570.4645	0.0003	KP	V		55684.4238	0.0004	FN25	V
	55592.4880	0.0013	RP	C		55684.5154	0.0004	FN25	V
	55592.5619	0.0007	RP	C		55684.6067	0.0003	FN25	V
	55592.6379	0.0007	RP	C	GSC 3863-0740	55576.5371	0.0022	KP	C
	55592.7138	0.0010	RP	C		55646.5217	0.0017	RP	V
	55629.3900	0.0004	FN25	V		55649.2944	0.0032	KP	V
	55644.2727	0.0004	KP	V		55676.5745	0.0023	RP	V
	55675.4058	0.0005	FN	V		55866.3658	0.0017	MAV	V
GSC 3004-0870	55601.4481	0.0003	HHU	C	GSC 3934-1904	55729.5173	0.0008	HMBH	C
	55627.4103	0.0006	HHU	C		55836.3808	0.0033	AB	C
	55641.3780	0.0012	AB	C	GSC 4417-0394	55603.5225	0.0008	KP	V
	55683.3606	0.0014	FN	V		55603.6546	0.0007	KP	V
	55683.4428	0.0008	FN	V		55730.3444	0.0008	AA30	C
GSC 3074-0114	55639.4398	0.0007	AA	C		55730.4767	0.0006	AA30	C
	55639.4911	0.0006	AA	C	GSC 4464-0924	55582.2948	0.0005	VWS	V
	55639.5423	0.0009	AA	C		55582.3750	0.0003	VWS	V
GSC 3428-1497	55571.5826	0.0007	HMB8	V		55591.3250	0.0017	VWS	V

Table 4: Observed times of maximum (continued).

Star	Epoch	Unc.	Obs.	Filter	Star	Epoch	Unc.	Obs.	Filter
GSC 4464-0924	55661.3921	0.0009	VWS	V	GSC 4556-1113	55684.4712	0.0004	VWS	V
	55661.4740	0.0006	VWS	V		55686.3710	0.0004	VWS	V
	55661.5532	0.0010	VWS	V		55686.4574	0.0004	VWS	V
	55670.3415	0.0006	VWS	V		55702.4313	0.0003	VWS	V
	55670.4239	0.0007	VWS	V		55714.4334	0.0003	VWS	V
	55670.5034	0.0010	VWS	V		55742.4949	0.0004	VWS	V
	55670.5855	0.0009	VWS	V		55745.4306	0.0005	VWS	V
	55716.4635	0.0004	VWS	V		55745.5171	0.0004	VWS	V
	55836.3616	0.0006	HHU	C		55774.4413	0.0004	VWS	V
	55866.2748	0.0004	VWS	V		55793.4361	0.0004	VWS	V
	55866.3554	0.0012	VWS	V		55807.4235	0.0004	VWS	V
	55906.2670	0.0015	VWS	V		55819.3387	0.0007	VWS	V
	55906.3483	0.0005	VWS	V		55819.4251	0.0004	VWS	V
GSC 4500-0083	55601.3466	0.0017	HHU	C		55834.5353	0.0005	VWS	V
	55818.3532	0.0018	MAV	V		55834.6216	0.0005	VWS	V
	55818.4399	0.0016	MAV	V		55849.5593	0.0005	VWS	V
	55836.3027	0.0019	KP	V		55849.6457	0.0003	VWS	V
	55836.3869	0.0010	KP	V		55856.2944	0.0003	VWS	V
GSC 4552-1498	55580.4278	0.0002	KP	C		55856.3807	0.0004	VWS	V
	55580.4838	0.0003	KP	C		55856.4673	0.0003	VWS	V
	55580.5394	0.0002	KP	C		55877.2764	0.0002	VWS	V
	55580.5952	0.0003	KP	C		55893.2498	0.0003	VWS	V
	55580.6512	0.0003	KP	C		55893.3361	0.0003	VWS	V
	55640.3689	0.0003	HHU	C		55905.4242	0.0004	VWS	V
	55640.3693	0.0003	FN	V	GSC 4638-0455	55605.4094	0.0005	KP	V
	55640.4251	0.0003	FN	V		55605.5059	0.0005	KP	V
	55646.2850	0.0003	AA	C		55605.6026	0.0004	KP	V
	55646.3407	0.0004	AA	C		55625.4078	0.0005	VWS	V
	55646.3967	0.0003	AA	C		55660.3807	0.0005	VWS	V
	55646.4523	0.0003	AA	C	GSC 4923-0693	55655.3007	0.0009	AA	C
	55683.3999	0.0003	FN25	V		55655.3663	0.0009	AA	C
GSC 4556-1113	55571.2772	0.0003	VWS	V		55655.4332	0.0009	AA	C
	55571.3631	0.0003	VWS	V		55661.4215	0.0007	AB	C
	55571.4494	0.0004	VWS	V		55663.4194	0.0006	RP	V
	55605.2952	0.0004	VWS	V		55663.4854	0.0008	RP	V
	55605.3817	0.0003	VWS	V	GSC 5018-1085	55676.3172	0.0008	AA	C
	55609.3532	0.0004	VWS	V		55676.3857	0.0004	AA	C
	55623.3407	0.0004	VWS	V		55676.4546	0.0004	AA	C
	55623.4270	0.0003	VWS	V		55676.5236	0.0004	AA	C
	55624.3767	0.0004	VWS	V	NSVS 11672463	55832.3697	0.0006	HHU	C
	55658.3954	0.0003	VWS	V		55866.3021	0.0008	FN	V
	55684.3849	0.0004	VWS	V	NSVS 14243430	55832.3942	0.0024	FN	V

COMMISSIONS 27 AND 42 OF THE IAU
INFORMATION BULLETIN ON VARIABLE STARS

Number 6016

Konkoly Observatory
Budapest
6 March 2012

HU ISSN 0374 – 0676

ZZ Cyg – FUNDAMENTAL PARAMETERS

NELSON, ROBERT H.[1,2]

[1] 1393 Garvin Street, Prince George, BC, Canada, V2M 3Z1; email: b-o-b.nelson@shaw.ca [remove dashes]

[2] Guest investigator, Dominion Astrophysical Observatory, Herzberg Institute of Astrophysics, National Research Council of Canada

Variability of ZZ Cyg (GSC 3576-0244, V∼11.0) was discovered by Williams (1907) using a 4″ portrait lens to obtain a large number of photographs. Two photographic minima, as well as 12 visual minima were reported. The data were sufficient to determine an accurate position, visual magnitudes, primary eclipse depth, and a period of 0.6286135 days. Although he plotted a visual light curve around a minimum, he did not furnish any other data but went on to classify the system as an Algol, presumably because of the apparent flatness of the light curve between eclipses. Shapley (1913) provided an early summary of the orbits of 87 eclipsing binaries – including ZZ Cyg – listing rough periods, magnitudes, amplitudes, spectral types and the results of various model fittings. Hall and Weedman (1971) performed UBV photometry on 19 eclipsing binaries with close companions – including ZZ Cyg. For ZZ Cyg, they listed the (AB-C) separation as 9″ in 1971. The V, $B-V$, and $U-B$ magnitudes of ZZ Cyg's close companion were provided (12.63 ± 2, 0.61 ± 1, and 0.15 ± 2, respectively), but alas, no infrared observations were possible at that time. They did list the spectral type of the Algol system as F7 + K5 IV. Hall and Cannon (1974) published their UBV data and performed an analysis based on the rectification method. They concluded that the visual companion (quoted as 5.″8 distant) was not physically connected. They also suggested that the primary, as observed between eclipses, underwent 0.05 magnitude fluctuations of period 0.1 days. Brancewicz & Dworak (1980) provided estimates of fundamental parameters of eclipsing binaries based on some simple equations. Following upon suggestions that ZZ Cyg had a δ Scuti variability in the primary component, Frolov et. al. (1982) undertook B and V photoelectric observations of ZZ Cyg obtained over 7 nights and saw no evidence of δ Sct varability in their published light curves. Shaw (1994) provided a list of 128 systems – including ZZ Cyg – that fell into his newly-defined class of near contact binaries (periods $<$ 1 day, evidence of tidal interaction, facing sides separated by $< 0.1 \times$ orbital radius, but not in contact like the EW-types). ZZ Cyg was listed as an Algol-type. However, he pointed out the difficulty in distinguishing between that class and that of contact binaries (and presumably also semi-detached).

From 1965 to the present, there have been many publications with times of minima and period studies (see Nelson, 2011), but surprisingly, there have been none with radial velocity data or modern light curve analysis.

Accordingly, photometric observations were undertaken by the author at his private observatory in Prince George, BC, Canada in June of 2003. Obtained were a total of

Table 1: Details of variable, comparison and check stars.

Type	GSC 3576-	R.A. J2000	Dec. J2000	V (Tycho) Mags	$B-V$ Mags
Variable	0244	$20^{\rm h}23^{\rm m}52\overset{\rm s}{.}944$	$46^\circ55'14\overset{''}{.}666$	10.98	0.582
Comparison	0964	$20^{\rm h}23^{\rm m}38\overset{\rm s}{.}139$	$46^\circ56'53\overset{''}{.}899$	11.11	0.100
Check	0702	$20^{\rm h}23^{\rm m}32\overset{\rm s}{.}522$	$46^\circ56'52\overset{''}{.}142$	11.31	0.437

Table 2: Log of DAO observations

DAO Image #	Mid Time (HJD−2400000)	Exposure (sec)	Phase at Mid-exp	V_1 (km/s)	V_2 (km/s)
13214	54000.7465	3600	0.847	82.5	−175.0
19121	55102.6356	3600	0.728	83.8	−213.3
19176	55104.8590	3600	0.265	−76.1	197.6
19178	55104.8989	3177	0.329	−73.9	194.1
17461	55476.6949	3600	0.780	87.4	−189.8

92 frames and 90 in the $I_{\rm C}$ (Cousins) band. Standard reductions were then applied. See Nelson (2004) for details. The comparison and check stars are listed in Table 1 (coordinates and magnitudes are from the GSC catalogue).

Examination of Digitized Sky Survey (DSS) images and also ST-7 images revealed an elongated shape to ZZ Cyg. As it was unresolvable into component images, apertures large enough to enclose the entire shape were used.

In September of the years 2006, 2009 and 2010 the author took five medium resolution (reciprocal dispersion = 10 Å/mm, resolving power = 10 000) spectra at the Dominion Astrophysical Observatory (DAO) in Victoria, British Columbia, Canada; he then used the Rucinski broadening functions (Rucinski, 2004) to obtain radial velocity (RV) curves (see Nelson, et al. (2006) and Nelson (2010b) for details). The spectral range was approximately 5000-5260Å. A log of DAO observations and RV results is presented in Table 2. The results were corrected (2.9% up in this case) to allow for the small phase smearing. (One simply divides by the factor $f = \frac{\sin(X)}{X}$, where $X = \frac{2\pi t}{P}$ and t=exposure time, P=period. For spherical stars, the correction is exact; in other cases, it can be shown to be close enough for any deviations to fall below observational errors.)

The author used the 2004 version of the Wilson-Devinney (WD) light curve and radial velocity analysis program with the Kurucz atmospheres (Wilson and Devinney, 1971, Wilson, 1990, Kallrath, et al., 1998) as implemented in the Windows software WDwint (Nelson, 2010a) to analyze the data. To get started, a spectral type F7 (Hall and Weedman, 1971) and a temperature $T_1 = 6381 \pm 66$ K were initially used; interpolated tables from Cox (2000) gave $\log g = 4.346$; an interpolation program by Terrell (1994, available from Nelson 2010b) gave the Van Hamme (1993) limb darkening values; and finally, a logarithmic (LD=2) law for the extinction coefficients was selected, appropriate for temperatures < 8500 K (ibid.). (The stated error in T_1 corresponds to one half spectral sub-class.) For some reason, the author started with mode 2 (detached). Convergence by the method of multiple subsets was reached in a small number of iterations. At first, a radiative envelope was chosen for star 1, (appropriate for hotter stars) and convective for the other, but shifting to convective envelopes for both stars gave a much better fit. The limb darkening coefficients are listed in Table 3.

Early on, it was discovered that $T_1 = 6381$ (F7) gave a poor fit. Higher values,

Table 3: Limb darkening values from Van Hamme (1993)

Quantity —	T_1=6650 Star 1	T_2=4307 Star 2	Error —	T_1=6514 Star 1	T_2=4264 Star 2
x (bol)	0.640	0.612	[fixed]	0.639	0.616
y (bol)	0.243	0.178	[fixed]	0.251	0.171
x (V)	0.705	0.795	[fixed]	0.710	0.797
y (V)	0.280	0.034	[fixed]	0.275	0.014
x (Ic)	0.548	0.680	[fixed]	0.553	0.682
y (Ic)	0.275	0.176	[fixed]	0.276	0.164

corresponding to earlier spectral types, gave a much better fit. F5 (T_1 = 6650 K) and F6 (T_1 = 6514 K) gave similar, better residuals; therefore, the results of both models are presented (as Models A & B, resp.). Since there was a known extra star, 3rd light was used. In any case, its inclusion improved the fit. A single spot on star 2 was required to account for the dip in light intensity from phase 0.6 to 0.9, approximately. Alternate configurations (dark spot on star 1, bright spots) were tried with no success. Next, non-zero eccentricity was tested for; a value of 0.0016 ± 0.0012 resulted. This is a very low value and is worth ignoring.

Mode 5 (Algol, where the secondary fills the Roche lobe) was then tried, resulting in marginally better residuals. The results are presented as Models C & D, respectively, in Table 4. Since the corresponding values are very close, an extra digit is included to show the tiny differences.

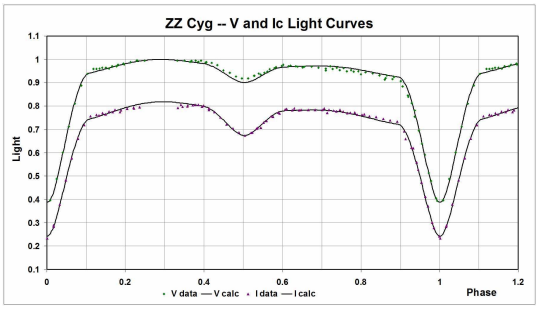

Figure 1. ZZ Cyg: V and I_C Light Curves – Data and WD Fit (all models)

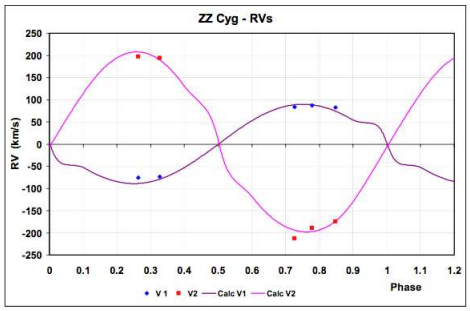

Figure 2. ZZ Cyg: Radial Velocity Curves – Data and WD Fit.

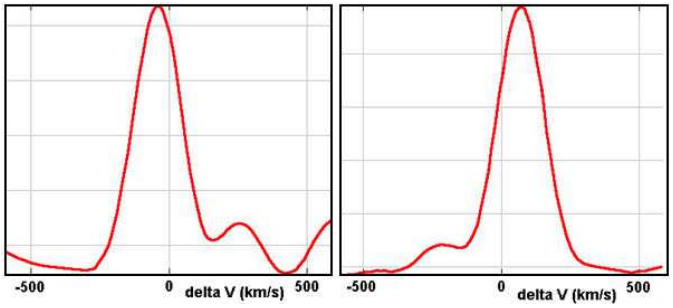

Figure 3. Representative broadening functions, at phases 0.265 and 0.728, resp.

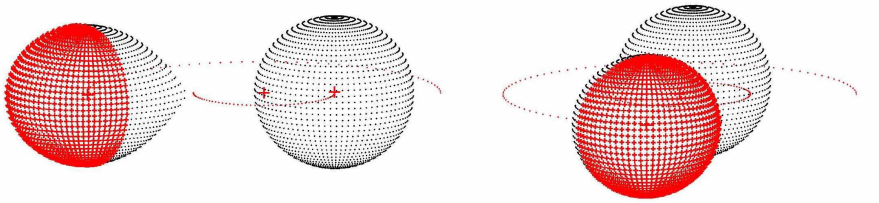

Figure 4. Binary Maker 3 representation of the system – at phases 0.75 and 0.97.

A plot of the V and I_C light curves, and WD fit are shown in Figure 1. Since the visual appearances of the four different models are virtually indistinguishable, only one plot is presented. The RVs are shown in Fig. 2 (again, for the same reason, only one plot is presented). Two representative examples of the broadening functions (Rucinski, 2004 and Nelson, 2010b) are depicted in Figure 3. These functions – in velocity space – represent the agents that would alter the sharp and unshifted lines from a non-rotating spherical star to those observed. In both of these cases, the peak of the large hump is at the primary RV and the weaker less distinct one, the secondary. The velocities, of course, need to be converted to heliocentric ones. A three dimensional representation from Binary Maker 3 (Bradstreet, 1993) is shown in Fig. 4.

The WD output fundamental parameters and errors are listed in Table 5 and – for comparison – the corresponding values of zero age main sequence stars (Cox, 2000). Most of the errors are output or derived estimates from the WD routines. The error in q was derived from the rms deviations of points from the best-fit double sine curves. In estimating the distance, galactic extinction was allowed for using the formula $A_V = 3E(B-V) = R \times [(B-V)_{data} - (B-V)_{tables}]$.

In conclusion, it is impossible to distinguish between the detached state where the secondary very nearly fills its Roche lobe and the Algol state (where the secondary star completely fills its Roche lobe), although the latter is favoured. In terms of the physical parameters, there is very little difference. More importantly, it was difficult to settle on the spectral type (and temperature T_1) of the primary. A re-determination of the primary spectral type from a high S/N classification is highly desirable for this interesting system. The main sequence values corresponding to single stars, but, since it is very likely

Table 4:

Wilson-Devinney Quantity	Model A Detached Value	Model B Detached Value	A.B Detached Error	Model C Algol Value	Model D Algol Value	C.D Algol Error
T_1 (K)	6650	6514	67	6650	6514	67
T_2 (K)	4362	4297	78	4333	4283	84
Ω_1	3.627	3.623	0.040	3.627	3.623	0.034
Ω_2	2.717	2.718	0.018	2.678	2.672	—
$q = M_2/M_1$	0.4143	0.4143	0.0047	0.3999	0.3972	0.0080
i (deg)	79.79	79.79	0.44	79.79	79.79	0.36
$L_1/(L_1+L_2)$ (V)	0.9134	0.9160	0.0013	0.9165	0.9169	0.0012
$L_1/(L_1+L_2)$ (I_C)	0.8414	0.8445	0.0022	0.8448	0.8492	0.0019
a (solar radii)	3.964	3.965	0.038	3.946	3.951	0.036
V_γ (km/s)	0.4	0.4	1.4	0.4	0.4	1.3
r_1 (pole)	0.3095	0.3099	0.0038	0.3082	0.3084	0.0037
r_1 (point)	0.3255	0.3260	0.0048	0.3235	0.3235	0.0046
r_1 (side)	0.3164	0.3168	0.0042	0.3149	0.3150	0.0041
r_1 (back)	0.3219	0.3223	0.0045	0.3201	0.3202	0.0044
r_2 (pole)	0.2834	0.2831	0.0039	0.2825	0.2820	0.0016
r_2 (point)	0.3817	0.3798	0.0317	0.4070	0.4064	0.0070
r_2 (side)	0.2952	0.2949	0.0046	0.2945	0.2940	0.0017
r_2 (back)	0.3267	0.3262	0.0074	0.3272	0.3266	0.0017
Spot co-latitude	90	90	[fixed]	90	90	[fixed]
Spot longitude	215.8	214.0	5.2	215.5	215.4	5.0
Spot radius	88.3	88.3	8.0	88.5	88.5	7.5
Spot temp factor	0.9090	0.9090	0.0082	0.9060	0.9075	0.0083
3^{rd} light (V)	0.0010	0.0010	0.016	0.0017	0.0010	0.016
3^{rd} light (I_C)	0.0397	0.0397	0.015	0.0414	0.0397	0.014
$\Sigma\omega^2_{res}$	0.00564	0.00563	—	0.00547	0.00541	—

Table 5: WD Output Values

Fundamental Quantity	Tabular value	Mdl A WD	Mdl C WD	Tabular value	Mdl B WD	Mdl D WD	Error WD
Eclipsing type	—	EB	Algol	—	EB	Algol	—
Sp. Type, star 1	F5	F5	F5	F6	F6	F6	—
Temperature (K), 1	6650	6650	6650	6514	6514	6514	67
Mass $(M_\odot)$, 1	1.40	1.500	1.495	1.32	1.501	1.504	0.15
Radius $(R_\odot)$, 1	1.30	1.25	1.24	1.26	1.26	1.24	0.006
$M_{\rm bol}$, 1	3.36	3.69	3.70	3.52	3.77	3.79	0.08
$\log g$ (cgs), 1	4.356	4.42	4.42	4.360	4.42	4.43	0.002
Luminosity $(L_\odot)$, 1	2.97	2.75	2.73	2.56	2.56	2.51	0.19
Sp. Type, star 2	K5	K5	K5	K6	K6	K6	—
Temperature (K), 2	4410	4362	4333	4290	4297	4283	59
Mass $(M_\odot)$, 2	0.67	0.622	0.598	0.63	0.622	0.597	0.036
Radius $(R_\odot)$, 2	(0.72)	1.20	1.19	(0.69)	1.20	1.19	0.006
M bol, 2	(6.63)	5.61	5.65	(6.788)	5.68	5.70	0.08
Log g (cgs), 2	(4.549)	4.07	4.06	(4.557)	4.07	4.06	0.002
Luminosity $(L_\odot)$, 2	(0.176)	0.47	0.45	(0.147)	0.44	0.43	0.03
Distance (pc)	—	90	90	—	87	86	10

that mass transfer occurred as some point, the comparison is mute (especially for the secondary).

No evidence of the 0.05-amplitude, 0.1-day delta Scuti variation was detected, confirming the conclusion of Frolov et al. (1982).

Reference to the $O-C$ relation (Nelson, 2011) reveals a more or less constant period decrease from 1965 to 2002; however, the large scatter in the data in that range prevents any definitive conclusions. Indeed, data since 2002 suggest that the period is constant. As is often the case, more accurate data and a longer time base are required. Also, a re-examination of the conclusion of Hall and Cannon (1974) – that the visual companion is not physically connected – might be worth re-examining.

Acknowledgements:
It is a pleasure to thank the staff members at the DAO (especially Dmitry Monin and Les Saddlemyer) for their usual splendid help and assistance.

References:

Bradstreet, D.H., 1993, "Binary Maker 2.0 - An Interactive Graphical Tool for Preliminary Light Curve Analysis", in Milone, E.F. (ed.) Light Curve Modelling of Eclipsing Binary Stars, pp 151-166 (Springer, New York)

Brancewicz, H.K., Dworak, T.Z., 1980, *Acta Astron.* **30**, 501.

Cox, A.N., ed, 2000, Allen's Astrophysical Quantities, 4th ed., (Springer-Verlag, New York, NY).

Frolov, M.S., Pastukhova, E.N., and Mironov, A.V., 1982, *IBVS* **2117**

Hall, D.S. and Weedman, S.L., 1971, *Publ. Astron. Soc. Pac.* **83**, 69

Hall, D.S. and Cannon, R.O., 1974, *Acta Astron.* **24**, 79

Kallrath, J., Milone, E.F., Terrell, D., and Young, A.T., 1998, *ApJ* **508**, 308.

Nelson, R.H., 2004, *IBVS* **5493**

Nelson, R.H., Terrell, D., and Gross, J., 2006, *IBVS* **5715**

Nelson, R.H., 2010a, Software, by Bob Nelson, http://members.shaw.ca/bob.nelson/software1.htm

Nelson, R.H., 2010b, "Spectroscopy for Eclipsing Binary Analysis" in The Alt-Az Initiative, Telescope Mirror & Instrument Developments (Collins Foundation Press, Santa Margarita, CA), R.M. Genet, J.M. Johnson and V. Wallen (eds)

Nelson, R.H., 2011, Bob Nelson's O-C Files, http://www.aavso.org/bob-nelsons-o-c-files

Rucinski, S.M., 2004, *IAU Symp.* **215**, 17

Shapley, H., 1913, *ApJ*, **38**, 158

Shaw, J.S., 1994, *Mem. Soc. Astron. Ital.* **65**, 95

Terrell, D., 1994, Van Hamme Limb Darkening Tables, vers. 1.1.

Van Hamme, W., 1993, *Astron. J.* **106**, 2096

Williams, A.S., 1907, *Astron. Nachr.* **174**, 9

Wilson, R.E., and Devinney, E.J., 1971, *Astrophys. J.* **166**, 605

Wilson, R.E., 1990, *Astrophys. J.* **356**, 613

COMMISSIONS 27 AND 42 OF THE IAU
INFORMATION BULLETIN ON VARIABLE STARS

Number 6017

Konkoly Observatory
Budapest
8 March 2012

HU ISSN 0374 – 0676

V881 PERSEI – A SPOTTED, DETACHED ECLIPSING BINARY

NELSON, ROBERT H.[1,2]

[1] 1393 Garvin Street, Prince George, BC, Canada, V2M 3Z1 email: b-o-b.nelson@shaw.ca [remove dashes]

[2] Guest investigator, Dominion Astrophysical Observatory, Herzberg Institute of Astrophysics, National Research Council of Canada

The optical variability of V881 Per [= GSC 2846-0404 = 1RXS J025952.4+380149, RA = $02^{\rm h}59^{\rm m}53\overset{\rm s}{.}12$, Dec = $+38°01'48\overset{''}{.}3$ (J2000)] was discovered as a by-product of the first Robotic Transient Search Experiment (ROTSE-1). The results were released in the Northern Sky Variability Survey (Wozniak, et al., 2004, available from SkyDOT – see reference below). The star was previously identified as a possible optical counterpart to an x-ray source (Li and Hu, 1998) but there seems to be no confirmation of that association since then. Follow-up observations of some 131 eclipsing systems – including V881 Per – by Otero et al. (2004) yielded improved light elements (HJD_0, Period) and V881 Per was designated as EW/KW. The system was then re-discovered as variable by Norton et al. (2007) from their SuperWASP photometric survey; they seem to have been unaware of the earlier discovery. They did, however, list the system as Pre-Main Sequence (PMS) and gave its V magnitude as 11.09.

Since the initial epoch, in 1999, by Otero et al. (2004), six times of minima have been determined by the author (4 have been previously published [Nelson, 2011a] and 2 are newly-reported here in Table 1).

Table 1: Newly determined times of minima for V881 Per

HJD−2400000	Error (days)	Type	Filter
55835.8376	0.0003	I	R
55848.8141	0.0002	II	R

The data are insufficient to conclude anything about possible period variation but do serve to refine the period (see Figure 1). The following elements were used:

$JD_{\rm hel}MinI = 2455848.6207 + 0.3873768(4)E$

See Nelson (2011b – updated annually) for the latest data and $O-C$ fit. Since the system has never had a full analysis, it was added to the author's observing programme.

A total of 118 frames in V, 116 in $R_{\rm C}$ (Cousins) and 126 in the $I_{\rm C}$ (Cousins) band were obtained by the author at his private observatory in Prince George, BC, Canada in July and September of 2010. (The telescope was a 33 cm f/4.5 Newtonian on a Paramount ME mount; the camera was an SBIG ST-7XME. See Nelson (2004) for more details.)

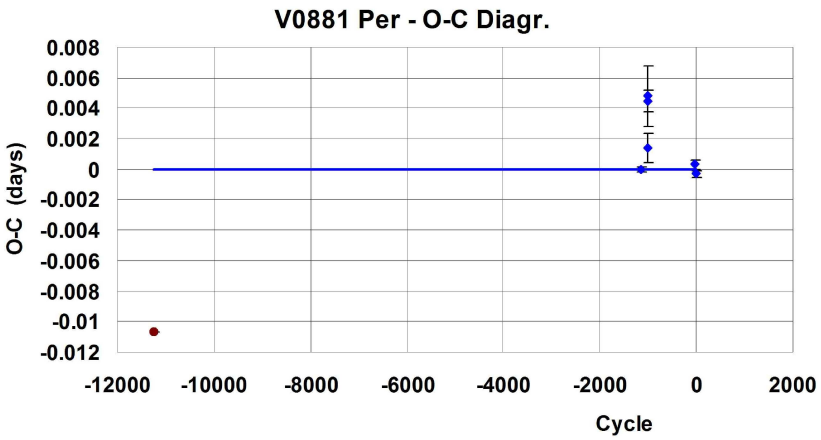

Figure 1. $O-C$ plot for V881 Per

Table 2: Details of variable, comparison and check stars.

Type of target	GSC 2846-	R.A. J2000	Dec. J2000	V (Tycho) Mags	$B-V$ Mags
Variable	0404	$2^{\rm h}59^{\rm m}53\overset{\rm s}{.}049$	$38°01'48\overset{''}{.}57$	10.69	1.398
Comparison	1254	$2^{\rm h}59^{\rm m}46\overset{\rm s}{.}874$	$38°00'48\overset{''}{.}67$	11.03	—
Check	0138	$2^{\rm h}59^{\rm m}54\overset{\rm s}{.}067$	$37°56'42\overset{''}{.}32$	11.33	—

Standard reductions were then applied. The comparison and check stars are listed in Table 2 (coordinates and V magnitudes are from the GSC catalogue, whereas the $B-V$ colour index is computed from the $V-R$ colour index taken from Norton et al., (2007) by the relation $(B-V) = 1.97(V-R) - 0.08$ due to Skiff (1998).

In September and October of 2010 the author took 10 medium resolution spectra at the Dominion Astrophysical Observatory (DAO) in Victoria, British Columbia, Canada using the Cassegrain spectrograph at the Plaskett 1.82 m telescope. The grating (#21181) was 1800 lines/mm, blazed at 5000 Å and used in first order, reciprocal linear dispersion = 10 Å/mm, resolving power = 10000. The camera was the SITe-2. The spectral range covered was from 5000 to 5260 Å, approximately.

The author then used the Rucinski broadening functions (Rucinski, 2004) to obtain radial velocity (RV) curves (see Nelson et al. (2006) and Nelson (2010b) for details). A log of DAO observations and RV results is presented in Table 3. The results were corrected 7.5% up in this case to allow for the small phase smearing in the following way: the RVs were divided by the factor $f = \frac{\sin X}{X}$ (where $X = \frac{2\pi t}{P}$ and t=exposure time, P=period). For spherical stars, the correction is exact; in other cases, it can be shown to be close enough for any deviations to fall below observational errors. This matter will be fully explored in a forthcoming paper.)

The author used the 2004 version of the Wilson-Devinney (WD) light curve and radial velocity analysis program with Kurucz atmospheres (Wilson and Devinney, 1971, Wilson, 1990, Kallrath et al., 1998) as implemented in the Windows front-end software WDwint (Nelson, 2010a) to analyze the data. To get started, a spectral type K0 (Li and Hu, 1998) and a temperature $T_1 = 5150 \pm 60$ K were used; interpolated tables from Cox (2000) gave $\log g = 4.476$; an interpolation program by Terrell (1994, available from Nelson 2010a)

Table 3: Log of DAO observations

DAO Image #	Mid Time (HJD−2400000)	Exposure (sec)	Phase at Mid-exp	V_1 (km/s)	V_2 (km/s)
17229	55466.9424	3600	0.702	143.6	−159.8
17252	55468.8752	3600	0.691	122.3	−178.8
17267	55469.0408	3600	0.118	−100.3	104.1
17283	55469.8306	3600	0.157	−132.1	148.1
17289	55469.9044	3600	0.347	−132.1	148.1
17318	55470.8482	3600	0.784	117.8	169.2
17330	55471.0065	3600	0.192	−142.7	171.4
17332	55471.0491	3600	0.302	−136.2	161.1
17371	55473.9191	1004	0.711	127.8	−166.6
17482−4	55475.8480	3102	0.690	131.7	−166.5

Table 4: Limb darkening values from Van Hamme (1993)

Band	x1	x2	y1	y2
Bol	0.646	0.628	0.170	0.151
V	0.794	0.797	0.140	0.016
Rc	0.729	0.753	0.187	0.104
Ic	0.642	0.667	0.1995	0.151

gave the Van Hamme (1993) limb darkening values; and finally, a logarithmic (LD=2) law for the extinction coefficients was selected, appropriate for temperatures < 8500 K (ibid.). (The stated error in T_1 corresponds to one half spectral sub-class.)

Mindful of the EW/KW designation (Otero, et al., 2004), the author started with mode 3 (overcontact). No fit was possible until he shifted to mode 5 (semi-detached – Algol) and mode 2 (detached). However, since an Algol system (containing as it does an evolved component) is unlikely to exist in the midst of a star-forming region, mode 2 was adopted. In any case, the latter gave better results.

Convergence by the method of multiple subsets was reached in a small number of iterations. Convective envelopes for both stars were used, appropriate for cooler stars (hence values gravity exponent, g = 0.32 and albedo, A = 0.500 were used for each). The limb darkening coefficients are listed in Table 4.

Early on, it was noted that the maxima between eclipses were unequal. This is the O'Connell effect (Davidge and Milone, 1984, and references therein) and is usually explained by the presence of one or more starspots. Accordingly, one was added first to star 1, but this gave a poor fit. Moving the spot to star 2 eventually gave a good agreement, calculated with observed.

The model is presented in Table 5. (Note that the uncertainty in temperature T_1 corresponds to one half a spectral sub-class, as noted before; this error in T_1 – when added statistically to the WD stated error in T_2 – yields a combined error of 65 K for T_2. In view of the uncertainty in spectra class, these errors are likely underestimated.) The light curve data and the fitted curves are depicted in Figure 2.

The presence of third light was tested for, but found not to be significant.

The RVs are shown in Fig. 3. A three dimensional representation from Binary Maker 3 (Bradstreet, 1993) is shown in Fig. 4.

Table 5: Wilson-Devinney parameters

WD Quantity	Value	error	Unit	W-D Quantity.	Value	error	Unit
Temperature T_1	5150	60	K	Potential Ω_1	3.675	0.017	—
Temperature T_2	4576	65	K	Potential Ω_2	3.412	0.019	—
$L_1/(L_1+L_2)$ (V)	0.6824	0.003	—	$q = M_2/M_1$	0.7928	0.0073	—
$L_1/(L_1+L_2)$ (R_C)	0.6513	0.003	—	Inclination, i	61.96	0.23	deg
$L_1/(L_1+L_2)$ (I_C)	0.6298	0.003	—	r_1 (pole)	0.3419	0.0021	orb. rad.
Semi-maj. axis a	2.793	0.017	Sol. rad.	r_1 (point)	0.3936	0.0054	orb. rad
V_γ	−4.0	0.75	km/s	r_1 (side)	0.3353	0.0025	orb. rad
Spot co-latitude	90	[fixed]	deg	r_1 (back)	0.3736	0.0033	orb. rad
Spot longitude	294	5	deg	r_2 (pole)	0.3359	0.0008	orb. rad
Spot radius	33.5	0.5	deg	r_2 (point)	0.4444	0.0027	orb. rad
Spot temp factor	0.8985	0.0077	—	r_2 (side)	0.3517	0.0008	orb. rad
Phase shift	0.0063	0.0005	—	r_2 (back)	0.3828	0.0008	orb. rad
$\Sigma\omega^2_{res}$	0.00616	—	—				

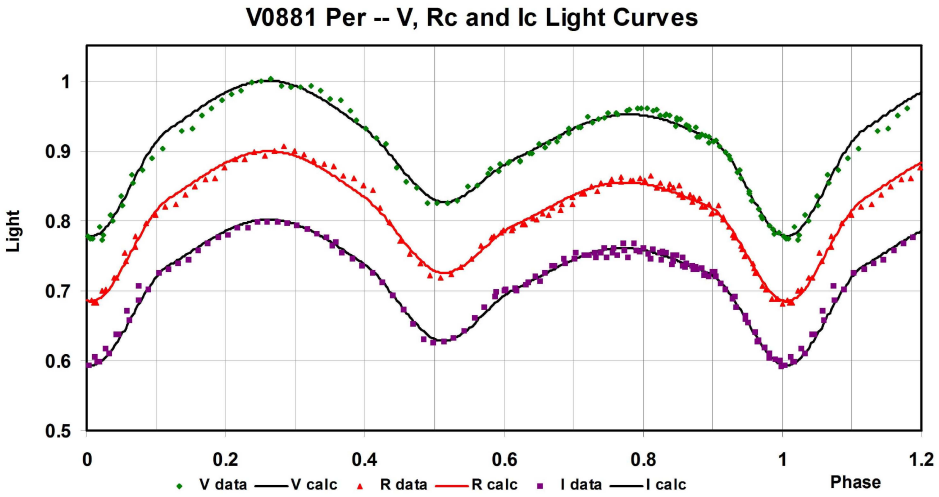

Figure 2. V881 Per: V, R_C, and I_C Light Curves – Data and WD Fit

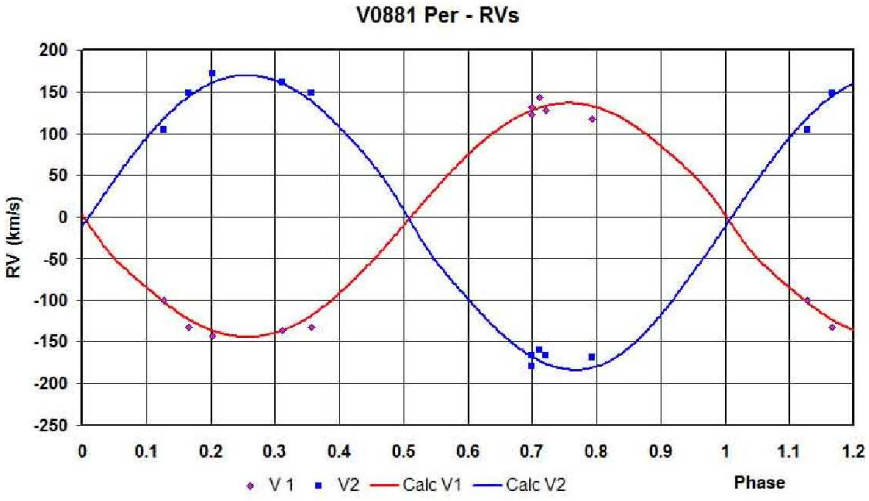

Figure 3. V881 Per: Radial Velocity Curves – Data and WD Fit.

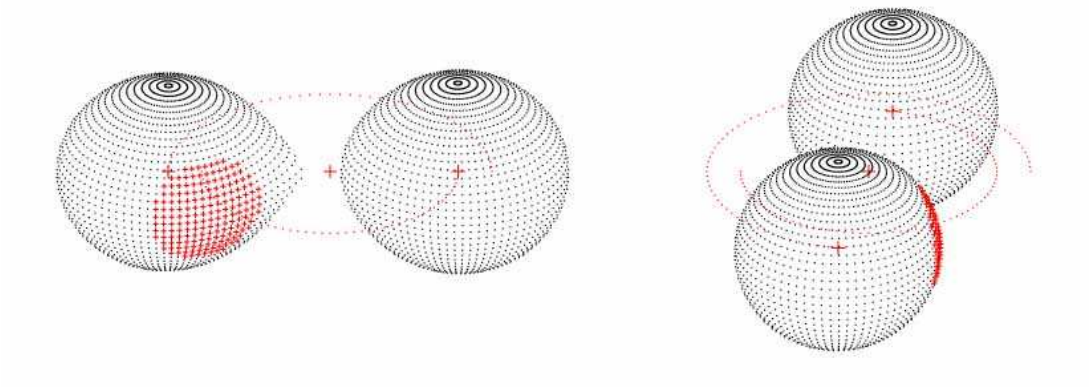

Figure 4. Binary Maker 3 representation of the system – at phases 0.75 and 0.97.

Table 6: Fundamental parameters

Quantity	Value	Error	unit
Temperature, T_1	5150	60	K
Temperature, T_2	4576	65	K
Mass, M_1	1.090	0.012	M_0
Mass, M_2	0.864	0.012	M_0
Radius, R_1	1.00	0.005	R_0
Radius, R_2	1.00	0.005	R_0
$M_{\rm bol}$, 1	5.29	0.11	mag
$M_{\rm bol}$, 2	5.80	0.11	mag
$\log g_1$	4.48	0.004	cgs
$\log g_2$	4.37	0.008	cgs
Luminosity, L_1	0.63	0.06	L_0
Luminosity, L_2	0.39	0.04	L_0
Distance, r	71	9	pc

The WD output fundamental parameters and errors are listed in Table 6. Most of the errors are output or derived estimates from the WD routines. In estimating the distance, galactic extinction was allowed for using the formula $A = 3E(B-V) = R[(B-V)_{\rm data} - (B-V)_{\rm tables}]$.

In conclusion, the fundamental parameters of this system have been determined. As to the suggestion that V881 Per might be a weak-lined T Tauri star (WTTS), there is little in the way of observables in this study that would either support or rule out the possibility (see Basri 2009, for a discussion of WTTS observable characteristics). The only things in favour would be the starspot, the late spectral type and the slight over-luminosity. Against that is the fact that erratic variations in brightness were not observed. Also, lithium (or any other) emission lines were not observed in the spectral range observed, although emission lines are more a characteristic of classical T Tauri behaviour and – while commonly seen for these stars – are not essential for the identification of the type.

Acknowledgements:
It is a pleasure to thank the staff members at the DAO (especially Dmitry Monin and Les Saddlemyer) for their usual splendid help and assistance. Thanks are also due to Dr. E.F. Milone for many useful comments.

References:

Basri, G., 2000, "T Tauri Stars' in Cox Allen's Astrophysical Quantities", 4th ed., page 408

Bradstreet, D.H., 1993, "Binary Maker 2.0 - An Interactive Graphical Tool for Preliminary Light Curve Analysis", in Milone, E.F. (ed.) Light Curve Modelling of Eclipsing Binary Stars, pp 151-166 (Springer, New York)

Cox, A.N., ed, 2000, Allen's Astrophysical Quantities, 4th ed., (Springer-Verlag, New York, NY).

Davidge, T.J., and Milone, E.F., 1984, *ApJS* **55**, 571

Kallrath, J., Milone, E.F., Terrell, D., and Young, A.T., 1998, *Astrophys. J.* **508**, 308

Li, J.Z. and Hu, J.Y., 1998, *A&AS* **132**, 173

Nelson, R.H., 2004, *IBVS* **5493**

Nelson, R.H., 2010a, Software, by Bob Nelson, http://members.shaw.ca/bob.nelson/software1.htm

Nelson, R.H., 2010b, "Spectroscopy for Eclipsing Binary Analysis" in The Alt-Az Initiative, Telescope Mirror & Instrument Developments (Collins Foundation Press, Santa Margarita, CA), R.M. Genet, J.M. Johnson and V. Wallen (eds)

Nelson, R.H., 2011a, *IBVS* **5466**

Nelson, R.H., 2011b, Bob Nelson's O-C Files, http://www.aavso.org/bob-nelsons-o-c-files

Nelson, R.H., Terrell, D., and Gross, J., 2006, *IBVS* **5715**

Norton, A.J., et al. (21 authors in all), 2007, *Astron. Astrophys.* **467**, 785

Otero, S.A., Wils, P., and Dubovsky, P. A., 2004, *IBVS* **5570**

Rucinski, S. M. 2004, *IAU Symp.*, **215**, 17

Skiff, B., 1998, VSNET Discussion Group post (1998 Oct 29)

SkyDOT (Sky Database for Objects in Time Domain), http://skydot.lanl.gov/nsvs/nsvs.php

Terrell, D., 1994, Van Hamme Limb Darkening Tables, vers. 1.1.

Van Hamme, W., 1993, *Astron. J.* **106**, 2096

Wilson, R.E., and Devinney, E.J., 1971, *Astrophys. J.* **166**, 605

Wilson, R.E., 1990, *Astrophys. J.* **356**, 613

Wozniak, P.R., et al., 2004, *Astron. J.* **127**, 2436

COMMISSIONS 27 AND 42 OF THE IAU
INFORMATION BULLETIN ON VARIABLE STARS

Number 6018

Konkoly Observatory
Budapest
19 March 2012

HU ISSN 0374 – 0676

CCD MINIMA FOR SELECTED ECLIPSING BINARIES IN 2011

NELSON, ROBERT H.

1393 Garvin Street, Prince George, BC, Canada, V2M 3Z1
e-mail: b-o-b.nelson@shaw.ca [remove dashes]

Observatory and telescope:
Sylvester Robotic Observatory (SyRO): 33 cm f/4.5 Newtonian on a Paramount ME

Detector:	SyRO: SBIG ST-7XME, 1.″25 pixels, 15.′8 × 10.′5 FOV, $-10 < T < -30$°C SyRO: SBIG ST-10XME, 6.″8 pixels, 34.′4 × 23.′2 FOV, $-10 < T < -30$°C

Method of data reduction:
Aperture photometry using MIRA, by Mirametrics. Bias and dark subtraction, flat-fielding using light-box flats; aperture photometry–all using MIRA, by Mirametrics. Check stars were used throughout.

Method of minimum determination:
Kwee & van Woerden (1956)

Remarks:
Digital tracing paper method, bisection of chords, curve fitting, and (occasionally) Kwee and van Woerden (1956)

Times of minima:						
Star name	Time of min. HJD 2400000+	Error	Type	Filter	$O-C$ [day]	Rem.
QX And	55842.742	0.002	I	R (2)	0.00176	
V0404 And	55848.7187	0.0003	I	C (2)	0.00308	
V0463 And	55847.6803	0.0002	II	C (2)	0.00000	
G0473-3466 Aql	55712.8756	0.0005	I	C (1)	0.00000	
G1045-1028 Aql	55700.92063	0.0001	!	C (1)	0.00000	
RX Ari	55850.799	0.001	I	C (2)	−0.00221	
BN Ari	55591.6207	0.0001	I	R (1)	−0.00057	
HL Aur	55836.903	0.0002	II	C (2)	−0.00249	
V0567 Aur	55592.9245	0.0003	II	C (1)	−0.00071	
G2374-0055 Aur	55904.6824	0.0005	II	C (2)	0.00044	
G2429-1010 Aur	55590.8436	0.0005	I	C (1)	0.00000	
G2933-1972 Aur	55849.8957	0.0001	I	C (2)	−0.00013	
SY Boo	55649.828	0.002	I	C (1)	−0.00268	(a)
TZ Boo	55927.0427	0.0002	I	R (2)	−0.00187	
DN Boo	55644.8241	0.0005	II	R (1)	−0.00034	
LR Cam	55840.9676	0.0002	II	R (2)	−0.00032	
NQ Cam	55847.9862	0.0002	II	C (2)	0.00235	
NR Cam	55926.75994	0.0002	I	C (2)	−0.00006	
G4327-2766 Cam	55847.779	0.001	I	C (2)	0.00000	
G4550-1548 Cam	55589.9006	0.0003	I	C (1)	0.00000	
BS Cas	55840.7898	0.0002	I	R (2)	0.00078	
CW Cas	55840.7047	0.0001	I	C (2)	−0.00073	
V0520 Cas	55798.7911	0.0001	II	C (1)	0.00194	
V0537 Cas	55838.7445	0.0002	I	R (1)	−0.00017	
V1060 Cas	55791.7579	0.0005	II	R (1)	−0.00010	
V0736 Cep	55705.882	0.001	I	R (1)	0.00000	
G4267-0682 Cep	55835.6839	0.0003	II	R (2)	−0.00067	
G4481-0080 Cep	55855.6247	0.0005	II	C (2)	0.00000	
G4484-1192 Cep	55839.6983	0.0002	II	C (2)	0.00000	
BB CMi	55916.862	0.001	II	C (2)	−0.00004	
HN CnC	55592.764	0.0002	I	C (1)	0.00345	
IU CnC	55909.937	0.0002	I	C (2)	−0.00056	
LP Com	55646.7451	0.0003	I	C (1)	0.00277	
UX CVn	55627.824	0.001	II	C (1)	0.00193	
BI CVn	55593.9265	0.0001	II	C (1)	0.00027	
DE CVn	55643.7487	0.005	I	C (1)	−0.02497	(b)
DL CVn	55653.742	0.0003	II	C (1)	−0.00061	
DQ CVn	55638.7056	0.0003	I	C (1)	0.00013	
DX CVn	55571.9634	0.0003	II	R (1)	−0.00105	
G2544-1007 CVn	55629.9079	0.0003	I	C (1)	−0.00271	
G2704-1999 Cyg	55714.883	0.001	I	R (1)	0.00000	
G2711-0645 Cyg	55710.89	0.001	II	C (1)	0.00000	
G3581-1856 Cyg	55701.8501	0.0002	!	R (1)	0.00000	
V2477 Cyg	55739.8398	0.0002	I	R (1)	−0.00169	
FU Dra	55626.8412	0.0002	I	C (1)	0.00029	
FU Dra	55626.9956	0.0002	II	C (1)	0.00133	
G4401-1126 Dra	55638.8295	0.0001	I	C (1)	0.00000	
G4420-1984 Dra	55591.9798	0.0002	I	C (1)	−0.00002	

Times of minima:						
Star name	Time of min. HJD 2400000+	Error	Type	Filter	$O-C$ [day]	Rem.
G4421-1217 Dra	55652.9379	0.0002	II	C (1)	0.00000	
G4421-1708 Dra	55685.802	0.002	I	C (1)	0.00000	(a)
G4439-1124 Dra	55659.9328	0.0003	II	C (1)	0.00000	
G4449-0995 Dra	55682.9286	0.0002	II	R (1)	0.00000	(c)
G4449-0995 Dra	55720.8416	0.0003	I	R (1)	0.00000	
QW Gem	55907.7418	0.0003	I	C (2)	−0.00412	
V0367 Gem	55835.9778	0.0002	I	C (2)	−0.00046	
G1335-1812 Gem	55592.657	0.002	I	C (1)	0.00000	
G1338-1984 Gem	55842.9759	0.0003	II	C (2)	0.00136	
G1883-1299 Gem	55833.013	0.003	II	R (2)	0.00000	
G1913-1513 Gem	55591.7373	0.0002	II	R (1)	0.00000	
V0728 Her	55695.8169	0.0003	II	R (1)	−0.00155	
V0829 Her	55658.9126	0.0002	II	R (1)	0.00097	
V1045 Her	55648.8726	0.0003	II	C (1)	−0.00001	(d)
V1071 Her	55590.0483	0.0003	I	C (1)	0.00077	
V1094 Her	55658.8186	0.0005	I	C (1)	−0.00533	
V1100 Her	55653.8851	0.0001	I	C (1)	0.00116	
V1101 Her	55643.9919	0.0001	I	C (1)	0.00166	
G2056-0117 Her	55643.8867	0.0001	I	C (1)	−0.00061	
G3532-0553 Her	55638.9668	0.0003	II	C (1)	−0.00094	
PP Lac	55711.9101	0.0005	I	C (1)	0.00143	
CE Leo	55917.0097	0.0001	II	C (2)	−0.00050	
XX LMi	55589.7767	0.0005	I	C (1)	0.00000	
G2515-0839 LMi	55902.9052	0.0001	I	C (2)	0.00000	
UU Lyn	55851.0346	0.0004	I	C (2)	0.00231	
G0140-0964 Mon	55907.8323	0.0003	II	C (2)	0.00000	
G0170-1717 Mon	55593.7021	0.0003	II	C (1)	0.00000	
G1322-0294 Ori	55902.785	0.0001	II	C (2)	−0.00001	
G1721-1141 Peg	55850.6855	0.0002	I	C (2)	0.00000	
V0578 Per	55798.9632	0.0009	I	R (1)	0.00011	
G2385-0341 Per	55571.6004	0.0001	I	R (1)	0.00001	
G0613-1099 Psc	55902.6186	0.0002	I	C (2)	0.00000	
V0366 Sge	55721.872	0.001	I	C (1)	0.00000	
CR Tau	55893.8458	0.0002	I	C (2)	0.00236	
EQ Tau	55901.675	0.002	I	C (2)	−0.00119	
V0781 Tau	55591.8441	0.0002	I	V (1)	0.00492	
G1305-1430 Tau	55842.85	0.0002	II	C (2)	0.00000	
TY UMa	55916.0343	0.0001	I	C (2)	−0.00228	
HH UMa	55907.97429	0.0003	II	C (2)	0.00472	
KM UMa	55659.75	0.01	II	R (1)	0.01664	
MT UMa	55926.9201	0.0003	II	C (2)	−0.00015	
G4375-0620 UMa	55628.7491	0.0005	I	C (1)	−0.00010	
VY UMi	55682.8051	0.0002	I	R (1)	0.03398	
G4408-0436 UMi	55654.79	0.003	II	C (1)	0.00000	(e)
G2166-0041 Vul	55702.848	0.001	II	C (1)	0.00000	

Remarks:
Star name: G denotes GSC (a) Rough minimum (b) Strange LC with transit (possibly planet?), see Fig. 1. (c) New variable (d) Period is very constant (e) Strange LC. Pair includes pulsating component? (See Fig. 2.) (1) ST-7XE (2) ST-10XE

Note: $O-C$ values were calculated using elements from the $O-C$ database mentioned in the references.

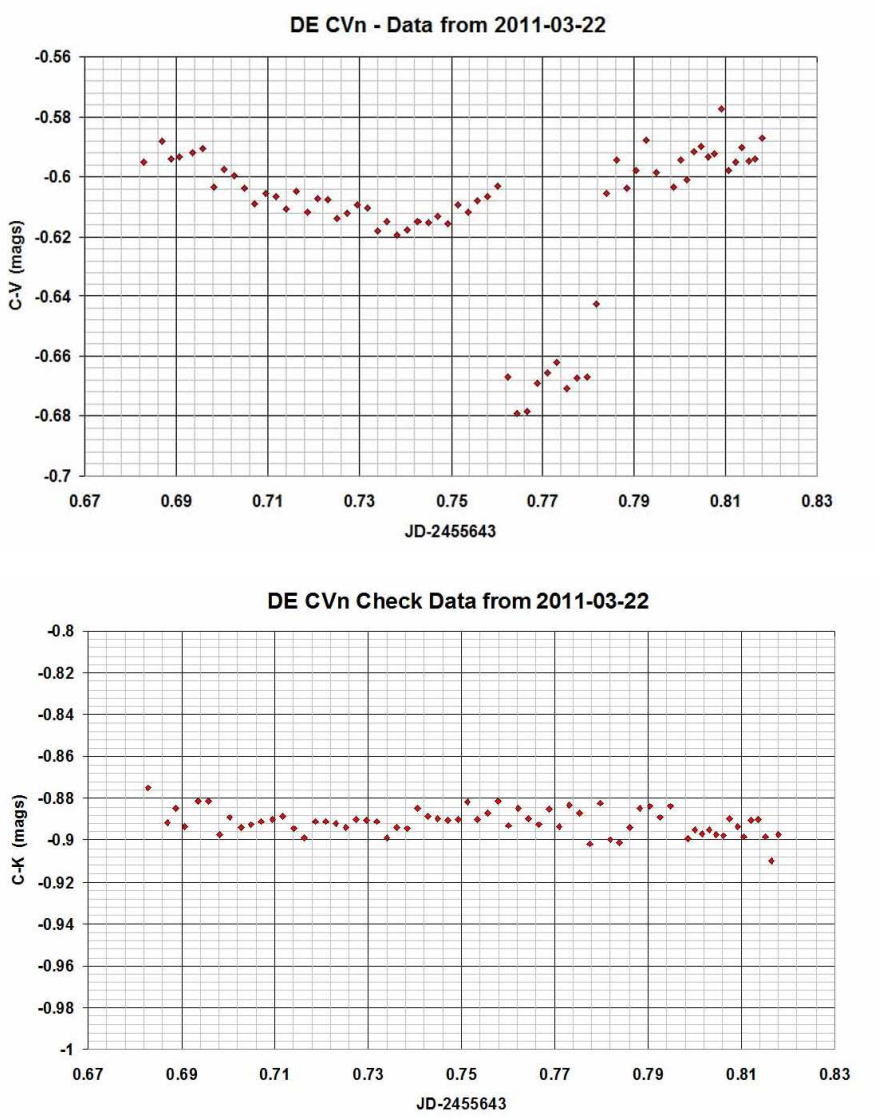

Figure 1. Upper panel: light curve of DE CVn during eclipse. A $0\overset{m}{.}07$ deep transit is visible at around JD 2455643.77. Lower panel: comparison minus check light curve.

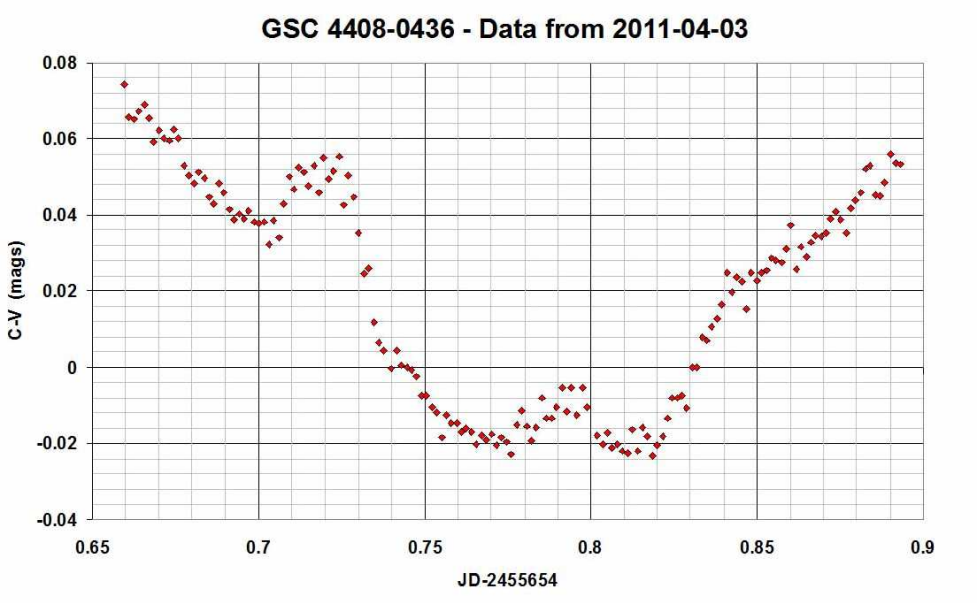

Figure 2. Light curve of G4408-0436 UMi during transit. The data suggest pulsating component.

Acknowledgements:

Thanks are due to Environment Canada for the website satellite views (see reference below) that were essential in predicting clear times for observing runs in this cloudy locale. Thanks are also due to Attilla Danko for his "Clear Sky Charts", (see below). This research has made use of the SIMBAD database, operated at CDS, Strasbourg, France.

References:

Danko, A., Clear Sky Charts, `http://cleardarksky.com/`
Kwee, K.K., & van Woerden, H., 1956, B.A.N. 12, (464), 327
Nelson, R.H., Bob Nelson's O-C Files,
`http://www.aavso.org/bob-nelsons-o-c-files`
Satellite Images for North America,
`http://www.weatheroffice.gc.ca/satellite/index_e.html`

COMMISSIONS 27 AND 42 OF THE IAU
INFORMATION BULLETIN ON VARIABLE STARS

Number 6019

Konkoly Observatory
Budapest
10 April 2012

HU ISSN 0374 – 0676

MAGNETIC FIELD AND SPECTRAL VARIABILITY OF THE Of?p STAR CPD–28 2561

HUBRIG, S.[1]; KHOLTYGIN, A.[2]; SCHÖLLER, M.[3]; LANGER, N.[4]; ILYIN, I.[1]; OSKINOVA, L.[5]

[1] Leibniz-Institut für Astrophysik Potsdam (AIP), An der Sternwarte 16, 14482 Potsdam, Germany

[2] Astronomical Institute, Saint-Petersburg State University, Saint-Petersburg, Russia

[3] European Southern Observatory, Karl-Schwarzschild-Str. 2, 85748 Garching, Germany

[4] Argelander-Institut für Astronomie, Universität Bonn, Auf dem Hügel 71, 53121 Bonn, Germany

[5] Institut für Physik und Astronomie, Universität Potsdam, 14476 Potsdam, Germany

Walborn (1973) introduced the Of?p category for massive O stars displaying recurrent spectral variations in certain spectral lines, sharp emission or P Cygni profiles in He I and the Balmer lines, and strong C III emission lines around 4650 Å. Only five Galactic Of?p stars are presently known: HD 108, NGC 1624-2, CPD−28 2561, HD 148937, and HD 191612 (Walborn et al. 2010). Using the high-resolution ESPaDOnS spectropolarimeter, installed on the 3.6-m Canada-France-Hawaii Telescope, and the NARVAL spectropolarimeter at the Bernard Lyot telescope, mean longitudinal magnetic fields of the order of a few hundred gauss were detected in two Galactic Of?p stars, HD 191612 (Donati et al. 2006) and HD 108 (Martins et al. 2010). The detection of a mean longitudinal magnetic field $\langle B_z \rangle = -254 \pm 81$ G in the third Of?p star HD 148937 using FORS 1 at the VLT was previously reported by Hubrig et al. (2008) and was later confirmed by additional observations by Hubrig et al. (2011) and Wade et al. (2012). Our observations of the fourth Of?p star, CPD−28 2561, in 2010 with FORS 2 (Hubrig et al. 2011) enabled us to detect a magnetic field at a significance level of more than 3σ in a single observation. A successful attempt has been made to measure the magnetic field in the fifth Of?p star, NGC 1624-2 (Wade et al., in preparation).

Due to the relative faintness of the Of?p star CPD−28 2561 with $m_V = 10.1$, it was only scarcely studied in the past. Levato et al. (1988) acquired radial velocities of 35 OB stars with carbon, nitrogen, and oxygen anomalies and found variability of a few emission lines with a probable period of 17 days. Walborn et al. (2010) mentioned that CPD−28 2561 undergoes extreme spectral transformations very similar to those of HD 191612, on a timescale of weeks, inferred from the variable emission intensity of the C III $\lambda\lambda$, 4647-4650-4652 triplet.

In this work we report on our new observations obtained in 2011 using FORS 2 at the VLT indicating the presence of a variable mean longitudinal magnetic field. Polarimetric spectra were obtained with the GRISM 600B and the narrowest slit width of 0.″4 to achieve a spectral resolving power of $R \sim 2000$. The use of the mosaic detector made of blue optimized E2V chips and a pixel size of 15 μm allowed us to cover a large spectral range, from 3250 to 6215 Å, which includes all hydrogen Balmer lines from Hβ to the Balmer jump. More details on the observing technique with FORS 1/2 and the data reduction can be found for example in Hubrig et al. (2004) and references therein. Using the method

Table 1: Longitudinal magnetic fields measured with FORS 2 in the Of?p star CPD−28 2561. All quoted errors are 1σ uncertainties.

MJD	$\langle B_z \rangle_{\rm all}$ [G]	$\langle B_z \rangle_{\rm hydr}$ [G]
55338.969	−381±122	−534±167
55685.982	99±82	65±108
55686.984	−44±80	6±102
55687.980	269±81	281±90

described in the same place, we obtained the mean longitudinal magnetic field $\langle B_z \rangle$, which is the component of the magnetic field parallel to the line of sight, averaged over the visible stellar hemisphere, weighted by the local emergent spectral line intensity. It is diagnosed from the slope of a linear regression of V/I versus the quantity $-\frac{g_{\rm eff} e}{4\pi m_e c^2} \lambda^2 \frac{1}{I} \frac{{\rm d}I}{{\rm d}\lambda} \langle B_z \rangle + V_0/I_0$, where V is the Stokes parameter that measures the circular polarization, I is the intensity observed in unpolarized light, $g_{\rm eff}$ is the effective Landé factor, e is the electron charge, λ is the wavelength, m_e is the electron mass, c is the speed of light, ${\rm d}I/{\rm d}\lambda$ is the derivative of Stokes I, V_0/I_0 is a constant, and $\langle B_z \rangle$ is the mean longitudinal magnetic field. The results of our measurements are presented in Table 1. Longitudinal magnetic fields were measured in two ways: using the entire spectrum including all available absorption lines (Column 2) and using only the absorption hydrogen Balmer lines (Column 3). The lines that show evidence of emission were not used to determine the magnetic field strength.

Our spectropolarimetric observations of this star indicate that the magnetic field is variable, but owing to the small number of measurements it is not possible to estimate the magnetic/rotation period. The new measurements obtained on May 5 and May 6 2011 are close to zero, while for the measurement carried out on May 7 2011 we achieve a 3 σ detection. This behaviour of the magnetic field can probably be explained by the strong geometric dependence of the longitudinal magnetic field, i.e. various orientation of the field at different rotation phases.

Spectropolarimetric observations on three consecutive nights in 2011 reveal strong variations in both the longitudinal magnetic field strength and several hydrogen and helium line profiles. The variation of He I λ4026, He I λ5876, and of Hβ on such a short time scale were not reported in the literature yet. A few examples of the detected spectral line profile variations are presented in Fig. 1. Apart from the He I λ4026 line, the contribution of a variable emission component is well visible in the other three lines. The profile of the He I λ4026 line appears only weakly variable. These variations have an amplitude of about 1–2% of the continuum level and can likely be explained by rotation modulation.

The line He II λ4686 exhibited strong emission during our observations in 2010, which transforms to a much weaker P Cygni line profile with a weak blue shifted absorption in 2011. A contribution of the emission component is clearly seen in the profile of the He I λ5876 line in 2010, but its presence can only be suspected in the variable line depth observed in 2011. A strong emission component is well visible in the line center of Hβ in 2010. The shape of the line profile of Hβ is similar to the behaviour of the Hα line profile in the spectra of 19 Cep presented in Fig. 13 of Kaper et al. (1997) and in Fig. 1 of Kholtygin et al. (2003).

Acknowledgments: Based on VLT observations in visitor mode (ESO programme 087.D-0049(A)).

References:

Babel, J., Montmerle, Th., 1997, *ApJ*, **485**, L29
Chlebowski, T. 1989, *ApJ*, **342**, 1091
Donati, J.-F., Howarth, I.D., Bouret, J.-C., et al., 2006, *MNRAS*, **365**, L6
Hubrig, S., Kurtz, D.W., Bagnulo, S., et al., 2004, *A&A*, **415**, 661
Hubrig, S., Schöller, M., Schnerr, R.S., et al., 2008, *A&A*, **490**, 793
Hubrig, S., Schöller, M, Kharchenko, N.V., et al., 2011, *A&A*, **528**, A151
Kaper, L., Henrichs, H.F., Fullerton, A.W., et al., 1997, *A&A*, **327**, 281
Kholtygin, A.F., Monin, D.N., Surkov, A.E., Fabrika, S.N., 2003, *Astronomy Letters*, **29**, 175
Levato, H., Morrell, N., Garcia, B., Malaroda, S., 1988, *ApJS*, **68**, 319
Martins, F., Donati, J., Marcolino, W.L.F., et al., 2010, *MNRAS*, **407**, 1423
Oskinova, L. M., 2005, *MNRAS*, **361**, 679
Wade, G.A., Grunhut, J., Gräfener, G., et al., 2012, *MNRAS*, **419**, 2459
Walborn, N.R., 1973, *AJ*, **78**, 1067
Walborn, N.R., Sota, A., Maíz Apellániz, J., et al., 2010, *ApJ*, **711**, L143

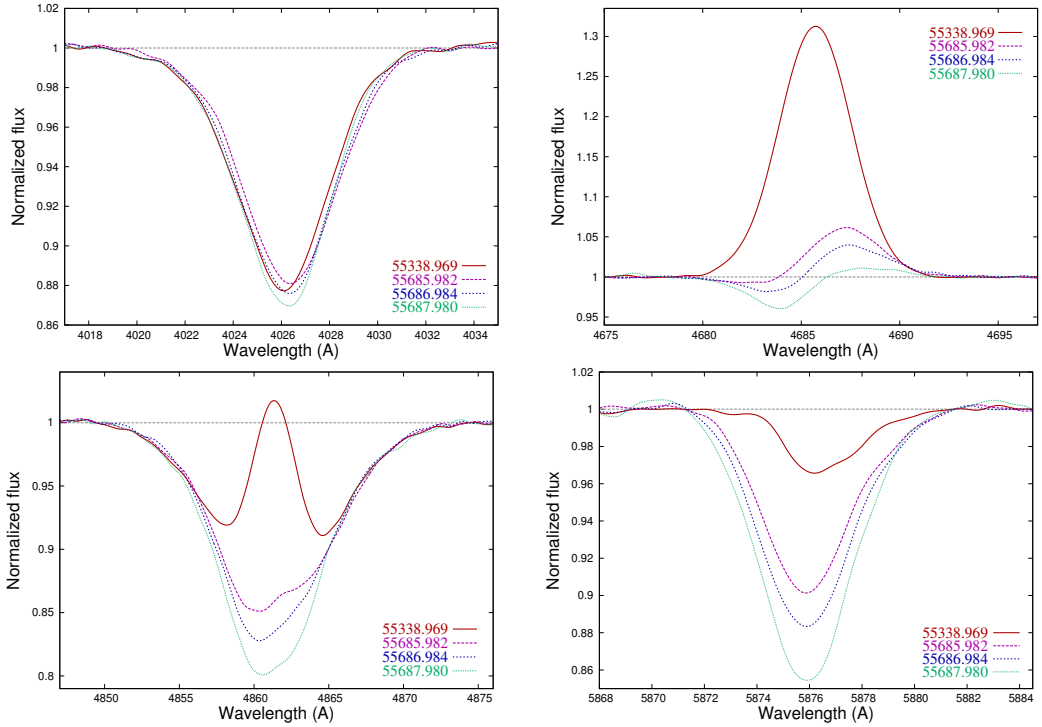

Figure 1. Distinct profile variability observed in the He I λ4026 (top left), He II λ4686 (top right), Hβ (bottom left), and He I λ5876 (bottom right) lines.

COMMISSIONS 27 AND 42 OF THE IAU
INFORMATION BULLETIN ON VARIABLE STARS

Number 6020

Konkoly Observatory
Budapest
10 April 2012

HU ISSN 0374 – 0676

APSIDAL MOTION OF THE ECCENTRIC ECLIPSING BINARY GSC 4487-0347

KOZYREVA, V.S.[1]; KUSAKIN, A.V.[2]; MENKE, J.[3]

[1] Sternberg Astronomical Institute, Moscow University, 13, Universitetsky Ave., Moscow 119899, Russia valq@sai.msu.ru

[2] National Space Agency, Republic of Kazakhstan JSCNCSRT Department, Fesenkov Astrophysical Institute, Almaty 050068, Kazakhstan un7gbd@gmail.com

[3] Starlight Farm Observatory, 22500 Old Hundred Rd, Barnesville, Washington, MD 20838, USA john@menkescientific.com

The recently discovered binary system (GSC 4487-0347, $\alpha_{2000}= 23^{\rm h}46^{\rm m}10\overset{\rm s}{.}45$, $\delta_{2000}= +71°29'55\overset{''}{.}3$, $P = 1\overset{\rm d}{.}98873$) belongs to the list of "50 new eccentric eclipsing binaries found in the ASAS, Hipparcos and NSVS databases" published by Otero et al. (2006).

We performed measurements in the B, V and R bands at the Tien Shan Astronomical Observatory using a Ritchey-Chrétien-350 telescope and an ST-402 CCD array in September-December 2009 and August-September 2011. We have only V light curve during minima.

The spectrophotometric observations were made in Barnesville near Washington using Newton-18-inch DSS-7 and ST-402 spectrophotometer.

At a distance of $3\overset{''}{.}5$ to the south of the binary star there is a neighbor fainter than the binary by $2\overset{\rm m}{.}5 \pm 0.2$. The image and the difference between stars were obtained by Menke on a clear January night. On the images obtain at the Tien Shan Observatory both stars appear as one.

The photometric elements of the system have been derived by minimizing functional depending on the measured and theoretical magnitude differences (Kozyreva & Zakharov, 2001). The model of spherical stars with linear laws of limb-darkening in eccentric orbits can be used for the analysis of the light curve.

The elements of the system are presented in Table 1. The luminosity of the nearby star is L_3. Since we did not have a sufficient phase coverage near quadratures, nor color indices throughout the whole orbit, a preliminary light curve analysis was made. We shall have more real system parameters only after measuring a better covered multicolour light curve and after more precise knowledge of the spectra of the system's stars.

Column 2 shows the solution for the 2009 light curve. All parameters except the coefficients of limb-darkening, u_1 and u_2, of the stars were free in the search. Column 3 corresponds to solution for the 2011 light curve. No reason to consider a significant change in the geometry of the binary system during the time between the two epochs of observations, the values of the parameter except ω were adopted in accordance with the results of our analysis of the most accurate 2009 light curve.

The light curve during minima is shown in Fig. 1 (2009) and in Fig. 2 (2011). The data of individual measurements are accessible on request (valq@sai.msu.ru). Given at the bottom are deviations $O-C$ of the individual measurements from the theoretical light curve as computed using the theoretical elements given in Table 1. They are shown shifted by $0\overset{m}{.}6$.

Table 1: The photometric elements of the star GSC 4487-0347, obtained from V light curve.

Element	2009-value	2011-value
r_1	0.199 ± 0.005	0.199 ± 0.005
r_2	0.151 ± 0.005	0.151 ± 0.005
i	$86\overset{\circ}{.}1 \pm 0\overset{\circ}{.}4$	$86\overset{\circ}{.}1 \pm 0\overset{\circ}{.}4$
e	0.131 ± 0.002	0.131 ± 0.002
ω	$336\overset{\circ}{.}0 \pm 0\overset{\circ}{.}3$	$340\overset{\circ}{.}5 \pm 0\overset{\circ}{.}5$
L_1	0.615 ± 0.020	0.615 ± 0.020
L_2	0.293 ± 0.020	0.293 ± 0.020
L_3	0.09 ± 0.020	0.09 ± 0.020
u_1	$0.38 \div 0.45$	$0.38 \div 0.45$
u_2	$0.38 \div 0.45$	$0.38 \div 0.45$
ϕ_{II}	$0\overset{p}{.}5762 \pm 0.0005$	$0\overset{p}{.}5786 \pm 0.0006$
J_2/J_1	0.827	0.827
L_2/L_1	0.476	0.476
σ_{O-C}	0.0082	0.0120

The B, V and R magnitudes of GSC 4487-0347 (including the optical component) with respect to the *WBVR* standard HD 222958 are given in Table 2. V magnitudes of each star are calculated using data of the luminosities (Table 1).

Table 2: The B, V and R magnitudes of GSC 4487-0347.

Stars	B	V	R
GSC 4487-0347	$11\overset{m}{.}50 \pm 0.02$	$11\overset{m}{.}19 \pm 0.01$	$11\overset{m}{.}01 \pm 0.02$
primary component	-	$11\overset{m}{.}72 \pm 0.02$	-
secondary component	-	$12\overset{m}{.}52 \pm 0.02$	-
optical component	-	$13\overset{m}{.}80 \pm 0.02$	-

In December 2010, Menke obtained spectra of GSC 4487-0347 including the optical component. SAO 10815 (A0V) was used as a comparison star. Unfortunately, the spectra have a low resolution ($\geq$ 7Å/pix) but we were able to estimate the spectral type for

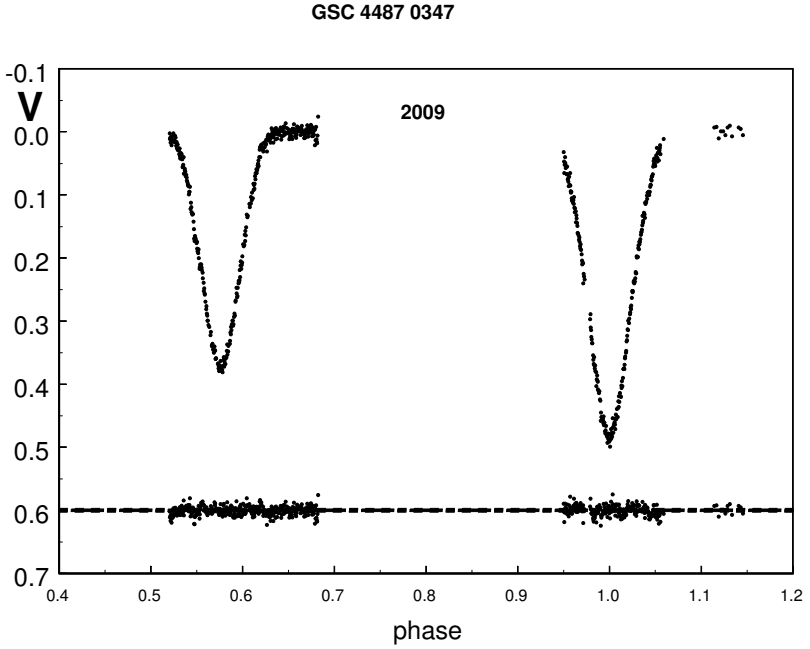

Figure 1. V light curve of GSC 4487-0347 obtained at the Tien Shan Observatory in 2009. The deviations $O - C$ are shifted by $0\overset{\text{m}}{.}6$.

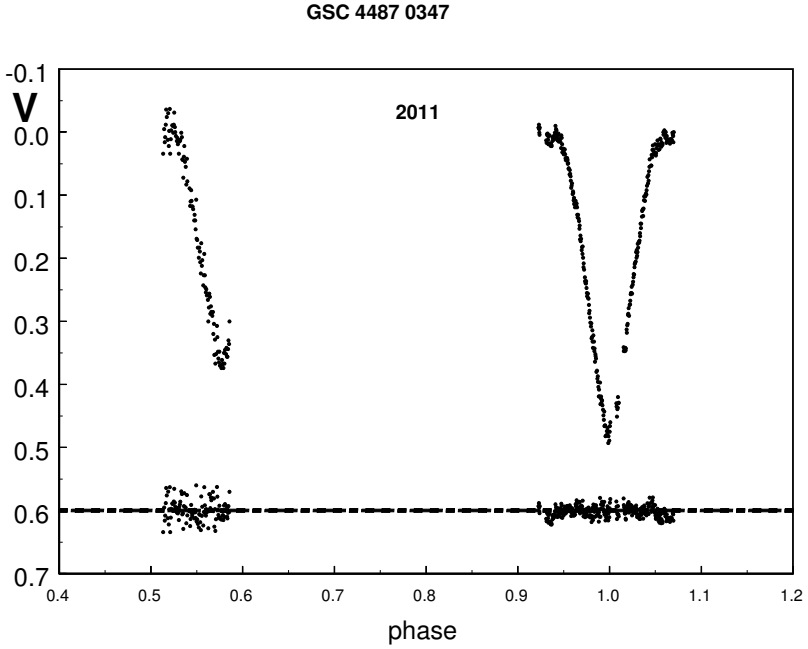

Figure 2. V light curve of GSC 4487-0347 obtained at the Tien Shan Observatory in 2011.

the components of the binary system. They are stars of B7÷A3. The coefficients of limb-darkening, u_1 and u_2, of the stars were chosen according to Van Hamme (1993) and remained constant during the calculation. We found a very weak dependence of the derived photometric elements on the coefficients of a selected range (u_1 and u_2).

The comparison of the longitude of periastron for two epochs of observation from Table 1 gives the apsidal motion:

$$\dot{\omega}_{obs} = 2.26 \pm 0.08^\circ/\text{year}; \quad U^{obs}_{apsid} = 160 \pm 6 \quad \text{years}.$$

The value of apsidal motion obtained using the data given by Otero et al. (2006) (the moment of primary minimum and the phase of the secondary minimum) does not contradict this value: $\dot{\omega}_{obs} = 2.0 \pm 0.3^\circ$/year. The same applies to the moments of minima obtained in 2008 by Kučákova and Kocián (Brát et al., 2008): $\dot{\omega}_{obs} = 2.8 \pm 1.5^\circ$/year. The moments of minima obtained in 2009 and 2011 are given in Table 3.

Table 3: The moments of minima of GSC 4487-0347.

$JD_\odot$ 2400000+	Min	2400000+	Min
55122.1578 ± 0.0005	I	55121.3150 ± 0.0005	II
55806.2827 ± 0.0005	I	55819.3656 ± 0.0008	II

The calculated ephemerides are:

$$\text{Min I} = \text{JD}_\odot\, 24\ 55122.1578(3) + 1\overset{\text{d}}{.}988731(1)\text{E}$$
$$\text{Min II} = \text{JD}_\odot\, 24\ 55121.3150(4) + 1\overset{\text{d}}{.}988751(1)\text{E}$$
$$\Delta P = P_{\text{II}} - P_{\text{I}} = 0\overset{\text{d}}{.}000020(2) = 1\overset{\text{s}}{.}73 \pm 0\overset{\text{s}}{.}20$$

The stars of the obtained spectral classes and parameters have such fast apsidal motion (2.26°/year) only on the stage of compression (Claret and Gimenez, 1993) and the theoretical apsidal motion in average is 1.5 times smaller on the later stage. We hope that the mass and accurate spectra of components will be derived, in the near future allowing us to compare the observational and theoretical values of apsidal motion.

Acknowledgements:
We wish to thank A.I. Zakharov, S.E. Leont'ev for the help on development of computer programs, V.B. Sekirov for the excellent Ritchey-Chrétien telescope, which he made with his own hands, M.A. Krugova for providing technical equipment and R.I. Kokumbaeva for the assistance in data processing.

References:

Brát, L., Šmelćer, L., Kučákova, H., Ehrenberger, R., Kocián, R., Lomoz, F., Urbančok, L., Svoboda, P., Trnka, J., Marek, P. and 5 coauthors, 2008, *OEJV*, **94**, 1
Claret, A., Gimenez, A., 1993, *Astron. & Astrophys.*, **277**, 487
Van Hamme, W., 1993, *Astron. J.*, **106**, 2096
Kozyreva, V.S., Zakharov, A.I., 2001, *Ast. Letters*, **27**, 712
Otero, S.A., Wils, R., Hoogeveen, G., Dubovsky, P.A., 2006, *IBVS*, **5681**

COMMISSIONS 27 AND 42 OF THE IAU
INFORMATION BULLETIN ON VARIABLE STARS

Number 6021

Konkoly Observatory
Budapest
16 April 2012

HU ISSN 0374 – 0676

PERIOD–AGE CORRELATIONS FOR ECLIPSING BINARIES IN STELLAR CLUSTERS

BUKOWIECKI, Ł.[1]; MACIEJEWSKI, G.[1]; KONORSKI, P.[2]; ERRMANN, R.[3]

[1] Centrum Astronomii Uniwersytetu Mikołaja Kopernika, Gagarina 11, Pl-87100 Toruń, Poland;
e-mail: gm@astri.uni.torun.pl

[2] Warsaw University Observatory, Al. Ujazdowskie 4, 00-478, Warsaw, Poland;
e-mail: piokon@astrouw.edu.pl

[3] Astrophysikalisches Institut und Universitäts-Sternwarte, Schillergässchen 2–3, D–07745 Jena, Germany;
e-mail: ronny.errmann@uni-jena.de

A stellar cluster is a group of stars born at the same place, roughly at the same time, and of the same chemically homogeneous cloud of gas and dust (Karttunen et al. 2003). Clusters offer useful observational tests to a variety of astrophysical and galactic studies. Their geometrical, physical, and chemical properties are directly related to processes and mechanisms of star formation and evolution. Binary star systems are very important in astrophysics because calculations of their orbits allow us to determine the masses of their components, that in turn allows other stellar parameters, such as radius and density, to be indirectly estimated. The orbital periods of binary stars are expected to become shorter during their evolution, e.g. as a result of magnetic braking mechanism. The theory and details of angular momentum loss has been described by Schatzman (1962), Huang (1966), Mestel (1968) and more recently Li et al. (2005), Eggleton (2006), Hussain (2011) and Stepien (2011). The observational data has been discussed by Mochnacki (1981) who estimated the time scale of this effect in W UMa stars is about $10^9 - 10^{10}$ years.

Our study on β Lyrae- (EB) and W UMa-type (EW) eclipsing binaries was focused on stars that belong to open and globular clusters only, i.e. probable members and concentrated on systems with relatively short orbital periods (less than few days). We searched the literature for variable stars discovered in the fields of open and globular clusters published after 1990 AD. From them we selected the EB and EW–type stars that, according to the authors, belong to the cluster. There were several different methods to establish the cluster membership probability in those publications, e.g. they used the position of the star on the HR–diagram, the apparent distance of the star from the cluster geometrical center; proper motion technique or the formula of Rucinski & Duerbeck (1997) to compare the system's distance to the cluster's distance modulus. We are aware that the membership of some stars may be more or less doubtful. Our goal was to gather information about periods and ages for as many as possible eclipsing binary stars (EB and EW–type) inside clusters to create a catalogue to investigate the period–age correlation. Taking this into consideration we think that the completeness of our catalog is high.

As a result, we collected 159 objects (35 EB and 124 EW type) from 34 open clusters, and 56 binary stars (6 EB and 50 EW type) from 13 globular clusters in the Galaxy. We considered only binary stars that, based on the literature data, belong to the cluster. If for a given star there is more than one paper, then the results of orbital periods were averaged. All binary systems from our list with main parameters (periods, ages) and references are listed in Tables 1 and 2. We refer to the catalogues that include eclipsing binary stars in open clusters: Popova & Kraicheva (1984) and Clausen & Gimenez (1987). Update of these catalogues was highly timely and necessary, consequently we performed this update.

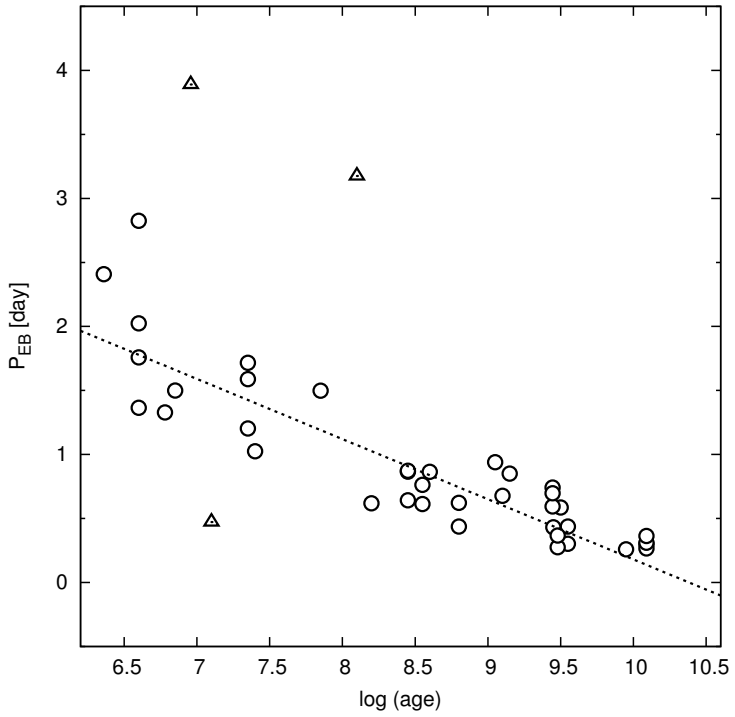

Figure 1. A relation between the orbital period of EB stars and open and globular cluster age.

In Fig. 1 we plotted the orbital period of EB stars (providing that age of binary stars is the same as the cluster age). Stars marked as triangles were rejected during fitting a linear relation. We fitted a linear trend that resulted in an equation:

$$P_{\rm EB}[\rm day] = (-0.47 \pm 0.05)\log(\rm age) + (4.88 \pm 0.35), \quad (1)$$

the correlation coefficient was found to be 0.89.

For contact systems (Fig. 2) we do not observe such a significant trend. We found only one open cluster with one EW-star. That suggest that stars of this type are rare in young open clusters. Since the membership of a young EW-star is disputable, we removed this system from the further analysis. We took an average orbital period for each star from cluster, errors are represented by a standard deviation (vertical bars). In a result we obtained the relation:

$$P_{\rm EW}[{\rm day}] = (-0.09 \pm 0.03)\log({\rm age}) + (1.17 \pm 0.25), \quad (2)$$

with the correlation coefficient 0.53. However, the maximum error obtained at the three sigma level suggests us to consider the age-dependence insignificant. It would be better to repeat the analysis if more EW–type stars would be discovered in less advanced age clusters. Lack of such systems in the younger clusters makes it difficult to draw general conclusions.

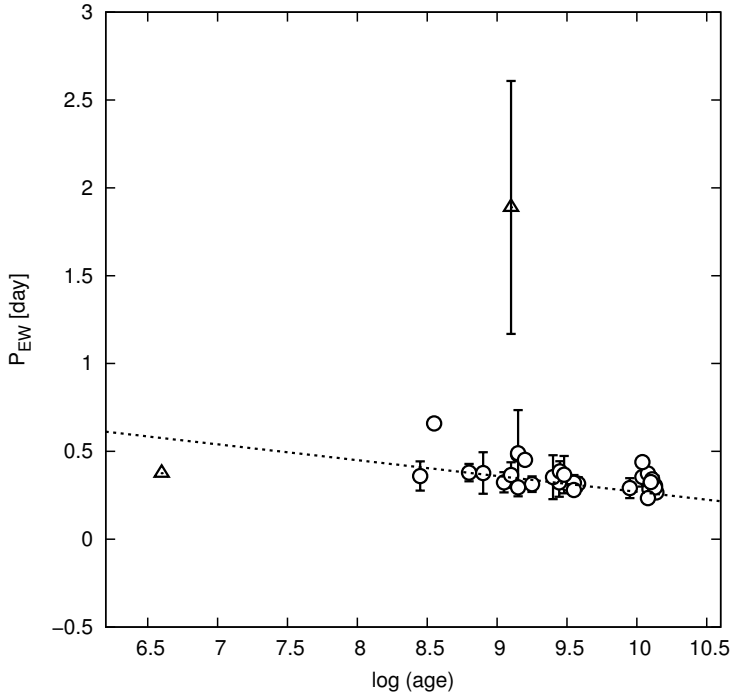

Figure 2. A relation between the orbital period of EW stars and open and globular cluster age.

The next step was to check the period-age relation for all eclipsing binaries together (Fig. 3). After empirical testing the best correlation was found for a non-linear function of the form $y = ax^{-1} + b$ with correlation coefficient equal 0.91. As a result, we obtained the relation:

$$P_{\rm EB+EW}[{\rm day}] = (31.19 \pm 1.78)[\log({\rm age})]^{-1} - (2.87 \pm 0.21). \quad (3)$$

The orbital periods of binary stars in clusters become shorter with time. This is a strong effect for binaries in open clusters younger than about 600 Myr. This suggests that the orbital period of binary systems in young star clusters decrease with time. Perhaps other stars in these clusters can receive a part of the orbital energy from the binary system

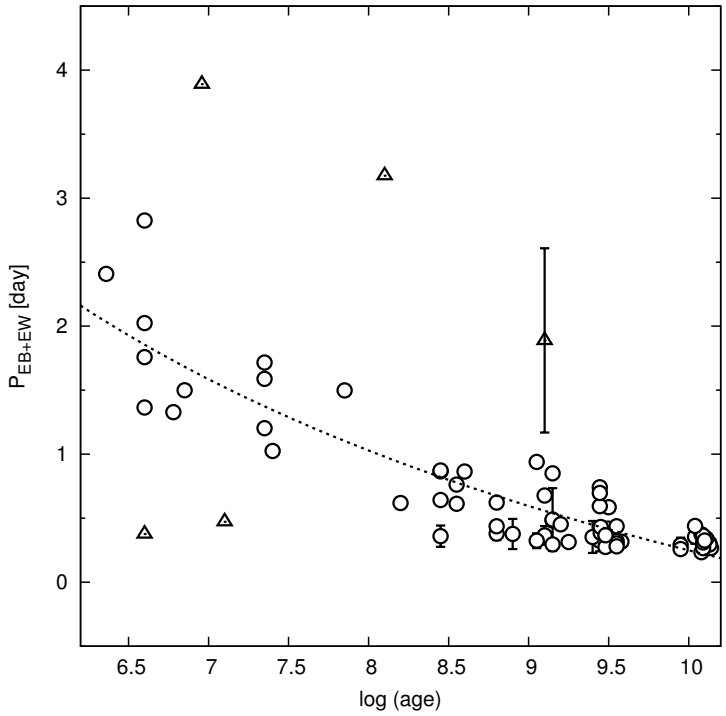

Figure 3. A relation between the orbital period of all eclipsing binaries and open and globular cluster age.

during close approach. But for the oldest systems with an age of several hundreds of Myrs orbital periods are almost constant.

A similar conclusion was obtained by Li et al. (2005) using Eggleton's code (Eggleton 1971, 1972, 1973). They noted a quasi-periodic behavior for orbital period around a constant value. So our results confirm their predictions. On the other hand Tylenda et al. (2011) observed a merger binary system. Maybe this is a result of the Darwin instability, where the tidal forces transport angular momentum from the orbit to the spin components (Chandrasekhar 1969) or it can also be caused by the aforementioned magnetic braking mechanism or a combination of both. In general the evolutionary paths of contact binaries are not exactly known and there is no unified theory in this subject, so probably this issue is more complicated (Webbink 2003, Csizmadia & Klagyivik 2004). Probably we need more well-studied binaries that belong to clusters to better understand their evolution outside and in clusters.

Acknowledgments: The research is supported by UMK grant 397-F and "Stypendium ze środków wspomagających młodych naukowców oraz uczestników studiów doktoranckich na Wydziale Fizyki, Astronomii i Informatyki Stosowanej UMK". RE would like to thank DFG for support in project NE 515 / 34-1.

Table 1. List of binary stars in open clusters, ID – identification number or the name of a star according to refereed papers, P – the period of variation, log(age) – decimal logarithm of the age (given in years). Type: EB and EW are β Lyrae and W UMa respectively.

Open cluster	log(age)	ID	Coordinates α δ J2000.0 for the binary system	Type	Period [day]
Berkeley 39[1]	9.95[2]	V3	07:46:46.9 −04:38:21.2	EW	0.38104
		V4	07:46:51.3 −04:36:07.4	EW	0.38132
		V5	07:46:52.9 −04:40:18.3	EW	0.30634
		V6	07:47:00.6 −04:38:44.4	EW	0.28444
		V7	07:46:46.2 −04:42:01.1	EW	0.27798
		V8	07:46:34.0 −04:42:27.9	EW	0.22876
		V9	07:46:47.2 −04:42:27.9	EB/EW	0.25863
Berkeley 39[3]	9.95[2]	V4	07:46:51.3 −04:35:07	EW	0.3813
		V5	07:46:52.9 −04:40:18	EW	0.2656
		V6	07:47:00.6 −04:38:44	EW	0.2844
		V7	07:46:46.2 −04:42:01	EW	0.278
		V8	07:46:33.9 −04:42:27	EW	0.2288
		V9	07:46:47.2 −04:42:28	EW	0.2598
		V11	07:46:32.7 −04:45:17	EW	0.2254
Collinder 228[4]	6.83[4]	DW Car	–	EB	1.3277493
Collinder 261[5]	9.45[2]	V2	12:37:13.6 −68:28:20	EW	0.355
		V4	12:37:57:9 −68:27:05	EW	0.3817
		V13	12:38:11.8 −68:24:10	EW	0.37494
		V15	12:38:18.5 −68.23:41	EW	0.31575
		V17	12:37:53.9 −68:23:22	EW	0.45709
		V19	12:37:47.3 −68.23.04	EW	0.34314
		V24	12:38:42.6 −68:22.04	EW	0.3543
		V25	12:38:16.5 −68:22:13	EW	0.40091
		V26	12:37:45.1 −68:22:17	EW	0.46133
		V28	12:38:10.0 −68:21:30	EW	0.38446
		V30	12:37:31.3 −68:21:28	EW	0.35132
		V31	12:37:57.5 −68:21:14	EW	0.38196
		V32	12:37:57.5 −68:20:02	EW	0.51901
		V33	12:38:12.1 −68:19:33	EW	0.28997
		V37	12:38:06.4 −68:17:39	EW	0.42947
		V39	12:39:07.3 −68:27:26	EB	0.4307
		V43	12:39:03.6 −68:16:25	EW	0.373
IC 4996[6]	6.85[2]	V2	20:14.42 +39:29:00	EB	1.499643
M11 (NGC 6705)[7]	8.45[2]	HV10	18:50:59.4 −06:13:43.3	EW	0.394555
		HV16	18:51:14.2 −06:17:42.1	EW	0.25532
M11 (NGC 6705)[8]	8.45[2]	243	18:51:14.8 −06:18:26.3	EB/EW	0.86577
		2740	18:50:59.4 −06:13:43.5	EW	0.39464
		8146	18:51:10.2 −06:12:50.1	EW	0.29357
		8641	18:51:09.3 −06:11:47.1	EW	0.4595
M37 (NGC 2099)[9]	8.9[2]	V3	05:52:33.03 +32:32:41.7	EW	0.4224
		V4	05:52:53.26 +32:33:01.2	EW	0.5585
		V5	05:53:00.63 +32:24:50.8	EW	0.3579
M37 (NGC 2099)[10]	8.9[2]	V3	05:51:33.12 +32:30:33.8	EW	0.422483
		V4	05:51:37.12 +32:40:23.4	EW	0.55819
		V7	05:51:45.62 +32:27:16.7	EW	0.357735
		V20	05:52:17.60 +32:30:12.6	EW	0.289456
		V24	05:52:40.10 +32:36:10.4	EW	0.252674
		V855	–	EW	0.564829
		V1160	–	EW	0.242092
		V1181	–	EW	0.25817
		V1194	–	EW	0.269735
		V1447	–	EW	0.296877

Table 1. – cont.

Open cluster	log(age)	ID	Coordinates α δ J2000.0 for the binary system	Type	Period [day]
M67 (NGC 2682)[11]	9.55[2]	5018	–	EW	0.28
Melotte 66[12]	9.445[13]	V4	111.57849 –47.69664	EW	0.402
		V5	111.56815 −47.64329	EB	0.7413
		V6	111.72366 −47.76692	EB	0.6974
		V7	111.56230 −47.72299	EB	0.5942
		V8	111.54562 −47.71756	EW	0.32903
		V9	111.71073 −47.75736	EW	0.2386
NGC 1245[14]	9.05[2]	20176	03:15:30 +47:14:37	EW	0.301
		20534	03:14:53 +47:16:32	EW	0.281
		60193	03:14:28 +47:11:07	EW	0.39
NGC 1647[15]	8.2[15]	M dwarf	04:46:32.86 +19:01:43.2	EB	0.61879
NGC 1850[16]	7.85[16]	39	05:08:42.8 −68:52:07	EB	1.4978
NGC 188[17]	9.5[2]	V1	0:46:54.15 +85:21:44.1	EW	0.289744
		V2	0:47:33.50 +85:16:24.8	EW	0.306905
		V3	0:50:27.77 +85:15:09.0	EW	0.285728
		V4	0:50:50.21 +85:16:12.4	EW	0.342457
		V5	0:48:22.65 +85:15:55.3	EB/EW	0.585984
		V6	0:47:16.51 +85:15:35.9	EW	0.3304345
		V7	0:46:12.23 +85:14:02.5	EW	0.3281916
NGC 188[18]	9.5[2]	V1	0:46:54.02 +85:21:43.58	EW	0.2897
		V2	0:47:33.37 +85:16:24.14	EW	0.3069
		V4	0:50:50.01 +85:16:11.66	EW	0.3425
		V5	0:48:22.53 +85:15:54.72	EB/EW	0.586
		V6	0:47:16.44 +85:15:35.31	EW	0.3304
		V13	0:51:14.99 +85:24:51.17	EW	0.3583
		V28	0:52:08.82 +85:19:05.97	EW	0.304
NGC 2099 (M37)[19]	8.6[2]	V4	05:52:53.272 +32:33:01.33	EW	0.4224
		KV12	05:51:29.340 +32:24:18.06	EB	0.864
NGC 2158[20]	9.1[2]	V12	06:07:18.7 +24:06:50.1	EW	1.0573
		V22	06:07:37.7 +24:07:40.2	EW	2.1311
		V24	06:07:43.4 +24:06:22.9	EW	2.3042
NGC 2204[21]	9.2[2]	892	06:15:55.42 -18:44:51.7	EW	0.45178
NGC 2243[22]	9.58[23]	V2	06:29:33.80 −31:17:02.8	EW	0.2853
		V3	06:29:44.87 −31:18:18.8	EW	0.356455
NGC 2243[24]	9.58[23]	V2	6:29:33.81 −31:17:03.4	EW	0.2853011
		V3	6:29:44.92 −31:18:19.4	EW	0.3564557
		V12	6:29:33.01 −31:17:53.6	EW	0.28598
NGC 2243[25]	9.58[23]	V2	06:29:33.81 −31:17:03.4	EW	0.285
		V3	06:29:44.92 −31:18:19.4	EW	0.356
NGC 2244[26]	6.36[26]	V578 Mon	06:32:00.61 +04:52:40.9	EB	2.40848
NGC 2301[27]	8.45[2]	V7	06:51:56.68 +00:25:49.2	EB	0.642
		V9	06:51:41:53 +00:23:45:5	EB	0.873
NGC 2506[28]	9.05[2]	V9	08:00:05.4 −10:43:39	EB	0.9392
NGC 2516[29]	8.1[2]	V392 Car	07:58:10.47 −60:51:57.5	EB	3.17499
NGC 457[30]	7.35[2]	V3	01:19:09 +58:17:25	EB	0.642
		V12	01:20:43 +58:28:21	EB	0.873
NGC 6253[31]	9.4[2]	41404	254.656188433 −52.616197780	EW	0.4968
		31606	254.800782797 −52.669356128	EW	0.2934
		30341	254.720919972 −52.690243537	EW	0.2692

Table 1. – cont.

Open cluster	log(age)	ID	Coordinates α δ J2000.0 for the binary system	Type	Period [day]
NGC 6259[32]	8.55[2]	V3	17:00:18.83 −44:38:02.7	EB/EW	0.763
		V15	17:01:13.97 −44:34:05.6	EW	0.6126
		V16	17:00:20.56 −44:44:02.2	EW	0.6588
NGC 633[33]	7.4[34]	V2	–	EB	1.025
NGC 6791[35]	9.55[2]	V3	19.354380 +37.769349	EW	0.31764
		V4	19.348396 +37.806652	EW	0.32568
		V5	19.346258 +37.813354	EW	0.31274
		V7	19.340271 +37.821892	EW	0.39174
		V8	19.341938 +37.865810	EW	0.33406
		V29	19.354796 +37.751386	EB	0.43662
		V117	19.343433 +37.665848	EW	0.36644
		V118	19.347500 +37.651222	EW	0.30623
		V119	19.351961 +37.916328	EB	0.30197
		01441_8	19.339422 +37.778118	EW	0.24544
NGC 6791[36]	9.55[2]	3	19:21:14.96 +37:46:09	EW	0.318
		5	19:20:53.62 +37:48:47	EW	0.2705
		7	19:20:25.30 +37:49:19	EW	0.3935
NGC 6791[37]	9.55[2]	V4	–	EB	0.325482
		V5	–	EB	0.270117
NGC 6819[38]	9.25[2]	52004	19:41:25.87 +40:12:22.2	EW	0.348687
		V2388	19:41:10.33 +40:15:18.3	EW	0.366025
		V2396	19:41:28.58 +40:16:24.8	EW	0.293151
		V2393	19:41:22.61 +40:11:07.1	EW	0.303209
		V2394	19:41:22.91 +40:14:39.5	EW	0.2561
NGC 6866[39]	8.8[40]	V5	20:03:34.93 +44:14:50.4	EW	0.321742
		V6	20:04:00.17 +44:14:03.5	EW	0.366528
		V7	20:03:49.82 +44:11:08.8	EW	0.41501
		V8	20:03:55.96 +44:10:46.5	EB	0.6222
		V9	20:03:38.79 +44:04:53.1	EW	0.43414
NGC 6866[40]	8.8[40]	0074	20:03:34.93 +44:14:50.1	EW	0.321750
		0248	20:03:38.79 +44:04:53.0	EB	0.437446
		0487	20:03:49.82 +44:11:08.5	EW	0.415110
NGC 6871[41]	6.958[42]	V453 Cyg	20:06:34.967 +35:44:26.28	EW	3.89
NGC 6939[43]	9.15[2]	V20	20:33:22 +60:37:14	EW	0.2951
NGC 7044[43]	9.15[2]	V3	21:13:16.97 +42:29:44.5	EW	0.46057
		V4	21:13:06.83 +42:29:18.7	EW	0.50262
NGC 7160[44]	7.35[2]	V497 Cep	21:52:00.4 +62:21:02	EB	1.2028351
NGC 7789[45]	9.15[2]	V2	23:57:33.51 +56:44:32.6	EW	0.72
		V3	23:57:39.49 +56:40:59.7	EW	0.5585
		V6	23:56:46.67 +56:43:23.7	EW	0.70
		V8	23:57:25.73 +56:43:32.8	EB	0.85
NGC 7789[46]	9.15[2]	V4	23:57:49.41 +56:46:59.91	EW	0.3375
		V7	23:57:24.45 +56:45:13.00	EW	0.4567
		V16	23:59:23.01 +56:35:51.05	EW	0.2317
		V20	23:57:10.65 +56:33:27.07	EW	0.279
		V22	23:56:38.70 +56:43:58.76	EW	0.3063
NGC 957[47]	7.1[2]	V2	23:30:8.17 +57:28:11.8	EB	0.47192
Tombaugh 2[48]	9.1[2]	V1	–	EB	0.6775
		V2	–	EW	0.3278
		V3	–	EW	0.4712
		V4	–	EW	0.3105
		V5	–	EW	0.3533

Table 1. – cont.

Open cluster	log(age)	ID	Coordinates α δ J2000.0 for the binary system	Type	Period [day]
Trumpler 37[49]	6.6[49]	3132	–	EW	0.3759
		3218	–	EB	1.3649
		6690	–	EB	2.0236
		7446	–	EB	2.8247
		9532	–	EB	1.7577

References – [1] Mazur et al. 1999; [2] Bukowiecki et al. 2011; [3] Kałużny et al. 1993b; [4] Southworth & Clausen 2007; [5] Mazur et al. 1995; [6] Pietrzyński 1996a; [7] Koo et al. 2007; [8] Hargis et al. 2005; [9] Kiss et al. 2001; [10] Hartman et al. 2008; [11] Sandquist 2006; [12] Zloczewski et al. 2007; [13] Mermilliod, J. C. 1996, http://www.univie.ac.at/webda/; [14] Pepper & Burke 2006; [15] Hebb et al. 2006; [16] Sebo & Wood 1995; [17] Zhang et al. 2002; [18] Mochejska et al. 2008; [19] Kang et al. 2007; [20] Koo et al. 2007; [21] Różyczka et al. 2007; [22] Kaluzny et al. 1996; [23] Anthony-Twarog et al. 2005; [24] Kałużny et al. 2006; [25] Kałużny et al. 1996b; [26] Hensberge et al. 2000; [27] Kim et al. 2001; [28] Arentoft et al. 2007; [29] Debernardi & North 2001; [30] Maciejewski et al. 2008a [31] De Marchi et al. 2010; [32] Chciechanowska et al. 2006; [33] Pietrzyński 1997; [34] Pietrzyński 1996b; [35] De Marchi et al. 2007; [36] Kałużny & Ruciński 1993a; [37] Ruciński et al. 1996; [38] Talamantes et al. 2010; [39] Molenda-Żakowicz et al. 2009; [40] Joshi et al. 2012; [41] Southworth et al. 2004; [42] Maciejewski et al. 2008b; [43] Kopacki et al. 2008; [44] Yakut et al. 2003; [45] Jahn et al. 1995; [46] Mochejska & Kałużny 1999; [47] Bukowiecki et al. 2009; [48] Kubiak & Kałużny 1992; [49] Errmann and the YETI team, in preparation

Table 2. List of binary stars in globular clusters, ID – identification number or the name of a star according to refereed papers, P – the period of variation, log (age) – the logarithm of age. Type: EB and EW are β Lyrae and W UMa respectively.

Open cluster	log(age)	ID	Coordinates α δ J2000.0 for a globular cluster	Type	Period [day]
NGC 104 (Tucanae 47)[1]	10.13[2]	V214	00:24:05.67 +72:04:52.6	EW	0.2737
		V221		EW	0.3135
		V225		EW	0.2346
		V227		EW	0.3788
		V238		EW	0.2506
		V244		EW	0.3837
		V245		EW	0.2789
		V249		EW	0.3226
NGC 288[3]	10.04[4]	V10	00:52:45.24 −26:34:57.4	EW	0.4388
NGC 3201[5]	10.11[6]	V1	10:17:36.82 −46:24:44.9	EW	0.303587
		V2		EW	0.345095
		V6		EW	0.37307
NGC 4372[7]	10.04[8]	V5	12:25:45.40 −72:39:32.4	EW	0.3403
		V16		EW	0.3084
		V22		EW	0.4150

Table 2. – cont.

Open cluster	log(age)	ID	Coordinates α δ J2000.0 for a globular cluster	Type	Period [day]
NGC 5139[9]	9.48[10]	V10	13:26:47.24 −7:28:46.5	EW	0.3687
(ω Centauri)		V11	–	EW	0.3073
		V12		EB	0.2759
		V13		EW	0.3055
		V19		EW	0.3982
		V20		EW	0.3418
		V21		EW	0.2493
		V44		EW	0.2963
		V49		EB	0.3663
		V54		EW	0.2838
		V56		EW	0.2812
		V58		EW	0.6309
		V61		EW	0.4158
		V64		EW	0.3851
		V65		EW	0.5122
NGC 5466[11]	10.10[12]	NH19	14:05:27.29 +28:32:04.0	EW	0.3421
		NH30		EW	0.2975
NGC 6121 (M4)[13]	10.09[14]	V44	16:23:35.22 −26:31:32.7	EW	0.2637
		V47		EW	0.2700
		V48		EW	0.2825
		V49		EB	0.2976
		V50		EB	0.2665
		V51		EW	0.3031
		V53		EW	0.3085
		V55		EB	0.3108
NGC 6362[15]	10.08[16]	V39	17:31:54.99 −67:02:54.0	EB	0.3633
NGC 6397[17]	10.14[18]	V7	17:40:42.09 −53:40:27.6	EW	0.2716
		V8		EW	0.2710
NGC 6397[19]	10.14[18]	V7	17:40:42.09 −53:40:27.6	EW	0.26992
		V19		EW	0.25382
NGC 6752[20]	10.13[21]	V4	19:10:52.11 −59:59:04.4	EW	0.2502
		V8		EW	0.3150
		V14		EW	0.3175
NGC 6838 (M71)[22]	10.08[23]	V1	19:53:46.49 +18:46:45.1	EW	0.3490
		V2		EW	0.3672
		V3		EW	0.3739
		V5		EW	0.4045
M22 (NGC 6656)[24]	10.08[25]	M22_03	18:36:23.94 −23:54:17.1	EW	0.220502
		M22_05		EW	0.242792
		M22_06		EW	0.239431
M55 (NGC 6809)[26]	10.10[27]	V53	19:39:59.71 −30:57:53.1	EW	0.32524682

References – [1] Kałużny et al. 1998; [2] Hesser et al. 1987; [3] Kałużny et al. 1997b; [4] Catelan et al. 2002; [5] von Braun & Mateo 2002; [6] Layden & Sarajedini 2003; [7] Kałużny & Krzemiński 1993c; [8] Alcaino et al. 1991; [9] Kałużny et al. 1997c; [10] Hilker et al. 2004; [11] Mateo et al. 1990; [12] Fakadu & Sandquist 2007; [13] Kałużny et al. 1997a; [14] Caputo 1985; [15] Mazur et al. 1999b; [16] Brocato et al. 1999; [17] Kałużny 1997d; [18] Gratton et al. 2003; [19] Kałużny & Thompson 2003; [20] Thompson et al. 1999; [21] Layden, et al. 1999; [22] Yan & Mateo 1994; [23] Grundahl et al. 2002; [24] Pietrukowiecz & Kałużny 2003; [25] Davidge & Harris 1996; [26] Kałużny et al. 2010; [27] Jimenez & Padoan 2008

References:

Alcaino, G., Liller, W., Alvarado, F., Wenderoth, E. 1991, *AJ*, **102**, 159

Anthony-Twarog, B. J., Atwell, J., Twarog, B. A. 2005, *AJ*, **129**, 872

Arentoft, T., De Ridder, J., Grundahl, F., Glowienka, L., Waelkens, C., Dupret, M.-A., Grigahcène, A., Lefever, K., Jensen, H. R., Reyniers, M., Frandsen, S., Kjeldsen, H. 2007, *A&A*, **465**, 965

von Braun, K. & Mateo, M. 2002, *AJ*, **123**, 279

Brocato, E., Castellani, V., Raimondo, G., Walker, A.R. 1999, *ApJ*, **527**, 230

Bukowiecki, Ł., Maciejewski, G., Konorski, P., Strobel, A. 2011, *AcA*, **61**, 231

Bukowiecki, Ł., Maciejewski, G., Bykowski, W., Georgiev, T., Boeva, S., Kacharov, N., Mihov, B., Latev, G., Ovcharov, E., Valcheva, A. 2009, *OEJV*, **112**, 1

Catelan, M., Bellazzini, M., Ferraro, F. R., Fusi Pecci, F., Galleti, S., Landsman, W. B 2002, *IAUS*, **207**, 116

Caputo, F., Castellani, V., Quarta, M. L. 1985, *A&A*, **143**, 8

Chandrasekhar, S. 1969, *ApJ*, **157**, 1419

Chciechanowska, A., Pietrzyński, G., Wyrzykowski, Ł., Szewczyk, O., Kubiak, M., Udalski, A., Szymański, M. K. 2006, *AcA*, **56**, 219

Csizmadia, Sz. & Klagyivik, P. 2004, *A&A*, **426**, 1001

Clausen, J. V., Gimenez, A. 1987, *PAICz*, **69**, 185

Davidge, T.J. & Harris, W.E. 1996, *ApJ*, **462**, 255

De Marchi, F., Poretti, E., Montalto, M., Desidera, S., Piotto, G. 2010, *A&A*, **509**, A17

De Marchi, F. Poretti, E., Montalto, M., Desidera, S., Piotto, G., Desidera, S., Bedin, R., Claudi, R., Arellano Ferro, A., Bruntt, H., Stetson, P.B. 2007, *A&A*, **471**, 515

Debernardi, Y. & North, P. 2001, *A&A*, **374**, 204

Eggleton, P.P. 1971, *MNRAS*, **151**, 351

Eggleton, P.P. 1972, *MNRAS*, **156**, 361

Eggleton, P.P. 1973, *MNRAS*, **163**, 279

Eggleton, P.P. 2006, Evolutionary Processes in Close Binary Stars, Cambridge Univ. Press

Errmann, R. and the YETI team, in preparation

Fakadu, N. & Sandquist, E. 2007, *ApJ*, **663**, 277

Gratton, R. G., Bragaglia, A., Carretta, E., Clementini, G., Desidera, S., Grundahl, F., Lucatello, S. 2003, *A&A*, **408**, 529

Grundahl, F., Stetson, P. B., Andersen, M. I. 2002, *A&A*, **395**, 481

Hargis, J. R., Sandquist, E. L., Bradstreet, David H. 2005, *AJ*, **130**, 2824

Hartman, J. D., Gaudi, B. S., Holman, M. J., McLeod, B. A., Stanek, K. Z., Barranco, J. A., Pinsonneault, M. H., Kalirai, J. S. 2008, *ApJ*, **675**, 1254

Hebb, L., Wyse, R. F. G., Gilmore, G., Holtzman, J. 2006, *AJ*, **131**, 555

Hensberge, H., Pavlovski, K., Verschueren, W. 2000, *A&A*, **358**, 553

Hesser, J. E., Harris, W. E., Vandenberg, D. A. 1987, *PASP*, **99**, 1148

Hilker, M., Kayser, A., Richtler, T., Willemsen, P. 2004, *A&A*, **422L**, 9

Huang S. S., 1966, *An.Ap*, **29**, 331

Hussain, G. A. J. 2011, *ASPC*, **447**, 143

Jahn, K. Kałużny, J., Ruciński, S. M. 1995, *A&A*, **295**, 101

Jimenez, R. & Padoan, P. 1998, *ApJ*, **498**, 704

Joshi, Y.C., Joshi, S., Kumar, B., Mondal, S., Balona, L.A. 2012, *MNRAS*, **419**, 2379

Kałużny, J. & Ruciński, S.M. 1993a, *MNRAS*, **265**, 34

Kałużny, J., Mazur, B., Krzemiński, W. 1993b, *MNRAS*, **262**, 49

Kałużny, J. & Krzemiński, W. 1993c, *MNRAS*, **264**, 785

Kałużny, J.; Krzemiński, W.; Thompson, I. B.; Stachowski, G. 2006, *AcA*, **56**, 51
Kałużny, J., Krzemiński, W., Mazur, B. 1996a, *A&AS*, **118**, 303
Kałużny, J., Krzemiński, W., Mazur, B. 1996b, *ASPC*, **90**, 152
Kałużny, J., Thompson, I. B., & Krzemiński, W. 1997a, *AJ*, **113**, 2219
Kałużny, J. 1997b, *A&AS*, **122**, 1
Kałużny, J., Kubiak, M., Szymanski, M., Udalski, A., Krzemiński, W., Mateo, M., Stanek, K. 1997c, *A&AS*, **122**, 471
Kałużny, J., Krzemiński, W., Nalezyty, M. 1997d, *A&AS*, **125**, 337
Kałużny, J., Kubiak, M., Szymanski, M., Udalski, A., Krzemiński, W., Mateo, M., & Stanek, K. Z. 1998, *A&AS*, **128**, 19
Kałużny, J. & Thompson I.B. 2003, *AJ*, **125**, 2534
Kałużny, J., Thompson, I.B., Krzemiński, W., Zloczewski, K. 2010, *AcA*, **60**, 245
Kang, Y. B., Kim, S.-L., Rey, S.-C., Lee, C.-U., Kim, Y. H., Koo, J.-R., Jeon, Y.-B. 2007, *PASP*, **119**, 239
Karttunen, H., Kröger, P., Oja, H., Poutanen, M., Donner, K.J. 2003, Fundamental astronomy, Fourth Edition, Berlin-Heidelberg-New York: Springer Verlag
Kim, S.-L., Chun, M.-Y., Park, B.-G., Lee, S. H., Sung, H., Ann, H. B., Lee, M. G., Jeon, Y.-B.,Yuk, I.-S. 2001, *A&A*, **371**, 571
Kiss, L. L. Szabó, Gy. M., Sziládi, K., Furész, G., Sárneczky, K., Csák, B. 2001, *A&A*, **376**, 561
Koo, J.-R., Kim, S.-L., Rey, S.-C., Lee, C.-U., Kim, Y. H., Kang, Y. B., Jeon, Y.-B. 2007, *PASP*, **119**, 1233
Kopacki, G., Drobek, D., Kołaczkowski, Z., Połubek, G. 2008, *AcA*, **58**, 373
Kubiak, M. & Kałużny, J. 1992, *AcA*, **42**, 155
Layden, A. C., Ritter, L. A., Welch, D. L., & Webb, T. M. A. 1999, *AJ*, **117**, 1313
Layden, A.C. & Sarajedini, A. 2003, *AJ*, **125**, 208
Li, L., Han, Z., Zhang, F. 2005, *MNRAS*, **360**, 272
Maciejewski, G., Bukowiecki, Ł., Brożek, T., Georgiev, TS., Boeva, S., Kacharov, N., Mihov, B., Latev, G., Ovcharov, E., Valcheva, A. 2008a, *IBVS*, **5864**
Maciejewski, G., Georgiev, Ts., Niedzielski, A. 2008b, *AN*, **329**, 387
Mateo, M., Harris, H.C., Nemec, J., & Olszewski, E. W. 1990, *AJ*, **100**, 469
Mazur, B., Krzemiński, W., Kałużny, J. 1999, *AcA*, **49**, 551
Mazur, B., Krzemiński, W., Kałużny, J. 1995, *MNRAS*, **273**, 59
Mazur, B., Kałużny, J., & Krzemiński, W. 1999b, *MNRAS*, **306**, 727
Mermilliod, J. C. 1996, *ASPC*, **90**, 475
Mestel, L. 1968, *MNRAS*, **140**, 177
Mochejska, B. J. Stanek, K. Z., Sasselov, D. D., Szentgyorgyi, A. H.,Cooper, R. L., Hickox, R. C., Hradecky, V., Marrone, D. P., Winn, J.N., Schwarzenberg-Czerny, A. 2008, *AcA*, **58**, 263
Mochejska, B.J. & Kałużny, J. 1999, *AcA*, **49**, 351
Mochnacki, S. W. 1981, *ApJ*, **245**, 650
Molenda-Żakowicz, J. Kopacki, G., Steślicki, M., Narwid, A. 2009, *AcA*, **59**, 193
Pepper, J. & Burke, Ch. 2006, *AJ*, **132**, 1177
Pietrukowiecz, P. & Kałużny, J. 2003, *AcA*, **53**, 371
Pietrzyński, G. 1996a, *AcA*, **46**, 417
Pietrzyński, G. 1996b, *AcA*, **46**, 357
Pietrzyński, G. 1997, *AcA*, **47**, 211
Popova, M., Kraicheva, Z., 1984, *AISAO*, **18**, 64
Różyczka, M., Kałużny, J., Krzemiński, W., Mazur, B. 2007, *AcA*, **57**, 323

Rucinski, S. M., Kałużny, J., Hilditch, R.W. 1996, *MNRAS*, **282**, 705
Rucinski, S. M. 2000, *AJ*, **120**, 319
Rucinski, S. M., Duerbeck, H. W. 1997, *PASP*, **109**, 1340
Sandquist, E. L. 2006, *IBVS*, **5679**
Schatzman, E. 1962, *AnAp*, **25**, 18
Sebo, K. M. & Wood, P. R. 1995, *ApJ*, **449**, 164
Southworth, J. & Clausen J. V. 2007, *A&A*, **461**, 1077
Southworth, J., Maxted, P.F.L., Smalley, B. 2004, *MNRAS*, **351**, 1277
Stepien, K. 2011, *AcA*, **61**, 139
Talamantes, A. Sandquist, E. L., Clem, J. L., Robb, R. M., Balam, D. D., Shetrone, M. 2010, *AJ*, **140**, 1268
Webbink, R. F. 2003, *ASPC*, **293**, 76
Thompson, I. B., Kałużny, J., Pych, W., & Krzemiński, W. 1999, *AJ*, **118**, 462
Tylenda, R., Hajduk, M., Kamiński, T., Udalski, A., Soszyński, I., Szymański, M. K., Kubiak, M., Pietrzyński, G., Poleski, R., Wyrzykowski, Ł., Ulaczyk, K. 2011, *A&A*, **528**, A114
Yakut, K., Tarasov, A.E., Ibanoglu, C., Harmanec, P., Kalomeni, B., Holmgren, D.E., Bozic, H., Eenens, P. 2003, *A&A*, **405**, 1087
Yan, L. & Mateo, M. 1994, *AJ*, **108**, 1810
Zhang, X. B., Deng, L., Tian, B., Zgou, X. 2002, *AJ*, **123**, 1548
Zloczewski, K., Kałużny, J., Krzemiński, W., Olech, A., Thompson I.B. 2007, *MNRAS*, **380**, 1191

COMMISSIONS 27 AND 42 OF THE IAU
INFORMATION BULLETIN ON VARIABLE STARS

Number 6022

Konkoly Observatory
Budapest
4 May 2012

HU ISSN 0374 – 0676

PHOTOMETRIC BEHAVIOUR OF V1343 AQUILAE (SS 433) IN 2011

VOLKOV, IGOR[1,2]

[1]Sternberg Astronomical Institute, M.V. Lomonosov Moscow University, Universitetsky Ave.,13, Moscow 119992, Russia

[2]Astronomical Institute of the Slovak Academy of Sciences, 059 60 Tatranská Lomnica, Slovak Republic; e-mail: volkov@ta3.sk

The X-ray orbital satellite *INTEGRAL* observed SS 433 in October 2011. In order to synchronize these observations with the optical light curve, I have observed the star during 34 nights at the Crimean Astrophysical Observatory (Simeiz site), Ukraine, with the 1-m telescope. Two CCD detectors: VersArray 512UV (Peltier cooling, –50°C) and VersArray 1340×1300 (liquid nitrogen cooling, –110°C) were used. The same filter set for both detectors provided the instrumental systems close to the standard Johnson $UBVRI$. The observations at JD=2 455 856 (last point in Fig. 1) were made at Stará Lesná Observatory of the Astronomical Institute of the Slovak Academy of Sciences (VersArray 512UV camera and a 60-cm Zeiss reflector). All the observations were corrected for atmospheric extinction by the method described in Moshkalev and Khaliullin (1985) and reduced to the standard Johnson $UBVRI$ system. These data are available in electronic table. The mean errors of the individual observations in U, B, V, R, I are 0.07, 0.03, 0.02, 0.015 and 0.018 magnitude, respectively.

During three nights with the most stable atmospheric transparency, I obtained magnitudes of stars in the frame with respect of the secondary photometric standard GSC 479.740 = 111.2009 from the Moffett and Barnes (1979) list. The results are presented in Table 1.

Table 1. Photoelectric magnitudes of neighboring stars

Star	V	$U-B$	$B-V$	$V-R$	$R-I$
1	11.422(5)	1.112(25)	1.483(9)	1.347(6)	1.056(9)
2	13.396(6)	0.443(20)	1.037(9)	0.912(7)	0.748(10)
3	13.005(6)	0.237(23)	0.770(9)	0.709(7)	0.543(9)
4	12.769(7)	0.243(19)	0.799(10)	0.730(8)	0.575(6)
5	15.488(24)	0.575(83)	0.995(27)	0.958(25)	0.655(28)
26	12.886(5)	−0.031(10)	0.750(9)	0.732(6)	0.548(16)

The numbers of the stars are those from Leibowitz and Mendelson (1982; hereafter, LM). My standardization in the V band coincides with LM better than to $0\overset{\mathrm{m}}{.}02$ for all

stars in common except No. 1 and No 2. Star No. 1 was supposed to be variable with an amplitude of $0\overset{m}{.}1$ by Kemp et al. (1986). It also shows irregular variations of brightness in present observations, with the full amplitude of $0\overset{m}{.}04$ in V. Its spectral type derived from the photometry is M2V if we assume $A_V = 0$, see Fig. 2. The star's high proper motion, $\mu = 0.123''$/year in the Tycho-2 catalogue, indicates the proximity of the star and agrees with such a possibility. Thus, it could be a BY Dra variable. Star No. 2 has a red companion at $6''$ distance that could influence measurements on nights with bad seeing. Therefore, star No. 4 was used as the main comparison star and star No. 3, as the check one. Their magnitudes match LM data well, and these stars did not show any significant variability in the present observations.

I have used all available V-band observations of SS 433 collected by Goranskij (2011) and the ephemeris from the same publication to obtain the mean curve of the star phased with the precession period: HJD Max $= 2449998.0 + 162.278 \cdot E$.

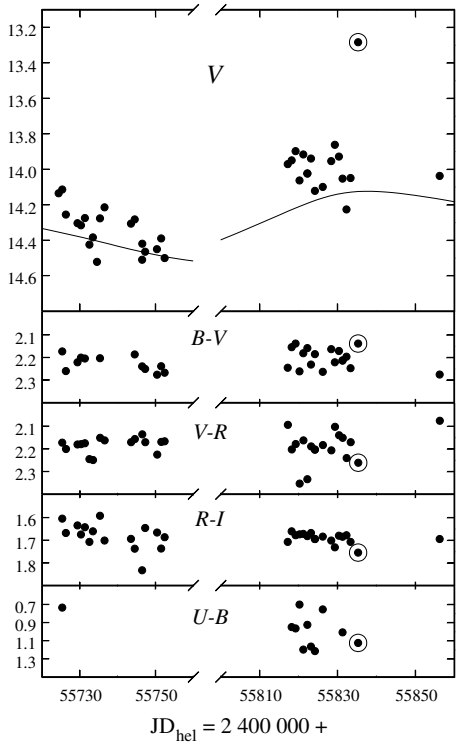

Figure 1. Nightly mean magnitudes of SS 433. The points corresponding to the flare are encircled. The solid curves in the upper panel denote the mean precession curve.

The comparison of this mean curve with the present data reveals that the object was in the active state during the autumn observations, see Fig. 1. A flare observed on JD 2455835 supports such an idea. It is interesting to note that the colours of the object did not change significantly during the flare (Fig. 1). Figure 2 displays the position of SS 433 in the two-colour $U-B, B-V$ diagram. Assuming that almost all the visible light comes from the thick disk (Leibowitz 1984, Antokhina and Cherepashchuk 1987, Hirai and Fukue 2001), one can find from this diagram that the spectrum of the object is B3 and $E(B-V) = 2.37 \pm 0.06$, so the lower limit of the temperature of the disk should be $T \approx 19000$ K. The interstellar extinction for SS 433 is $A_V = 7.35 \pm 0.18$, somewhat lower than the commonly accepted value from Perez and Blundell (2010): $A_V = 7.8$.

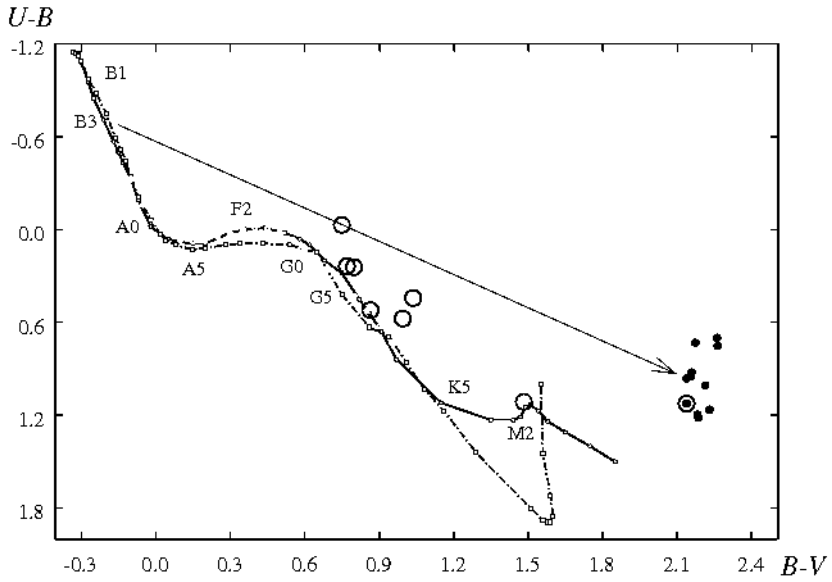

Figure 2. The position of SS 433 in the $U-B, B-V$ diagram - black points. Luminosity classes are plotted according to Straizys (1977): the dotted line stays for the luminosity class III and the solid line for V. The point in the flare is encircled. Big circles correspond to all measured stars in the sky region. The reddening vector is indicated by the arrow.

The analysis of the present data except for points in a flash for periodicity reveals another interesting fact. It is not the orbital period but the nutation period that dominates the periodogram, see Fig. 3. We present the nightly mean data folded with the best period found, $P_{nut} = 6\overset{\mathrm{d}}{.}109$, in Fig. 4 and the data folded with the orbital period, HJD Min $= 2450023.746 + 13.08223 \cdot E$ according to Goranskij (2011), in Fig. 5.

One can see that the present value of the nutation period is shorter than it follows from the equation: $1/P_{\mathrm{nut}} = 2/P_{\mathrm{orb}} + 1/P_{\mathrm{prec}}$, $P_{\mathrm{nut}} = 6\overset{\mathrm{d}}{.}2877$. This could be explained by the precession period variations found by Davydov, Esipov and Cherepashchuk (2008) spectroscopically. In this study, we may associate this effect with the active state of the object. It should be noted from Figs. 1 and 4 that the flare occurred at the brightness maxima of the nutation and precession curves, when the opening of the disk to the observer was maximal.

Acknowledgements. This study was supported by the SAIA (Slovakia) scholarship and the grant 11-02-01213a from the Russian Foundation for Basic Research. I would like to thank Dr. N. Samus for important discussions.

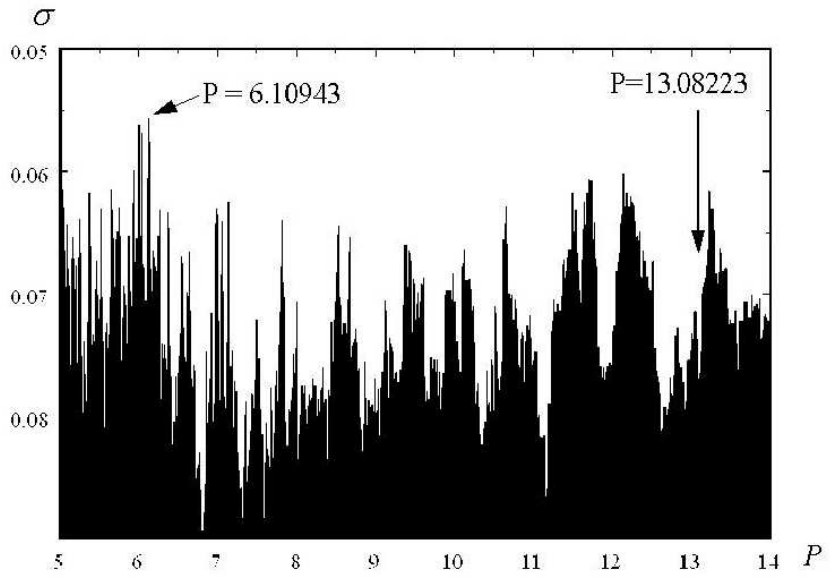

Figure 3. The periodogram of the V-band light variations in SS 433 based on 333 data points during 2011. The average precession curve was subtracted from the data. The double nutation period is also presented. Extra peaks are mainly due to the approximately three month gap between the observational sets.

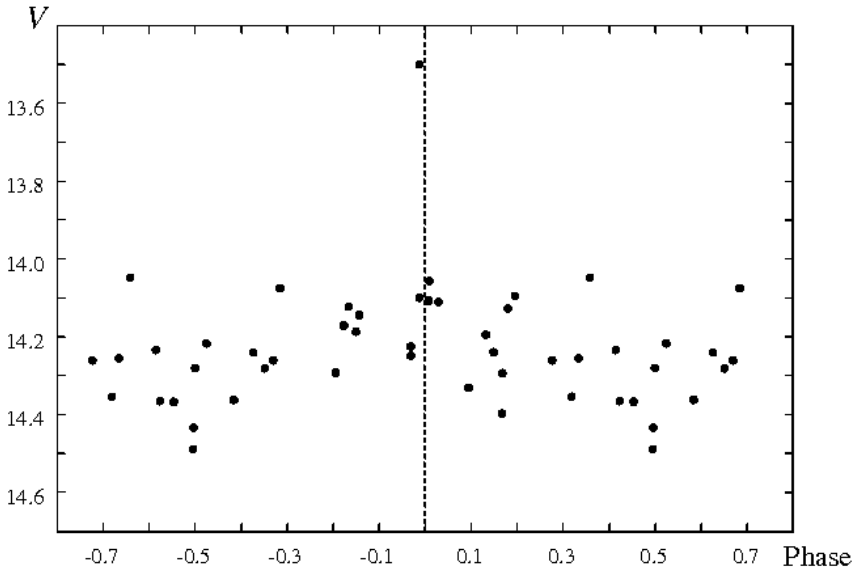

Figure 4. The V-band light curve phased with the nutation period, $6\overset{d}{.}109$. The average precession curve was subtracted from the data.

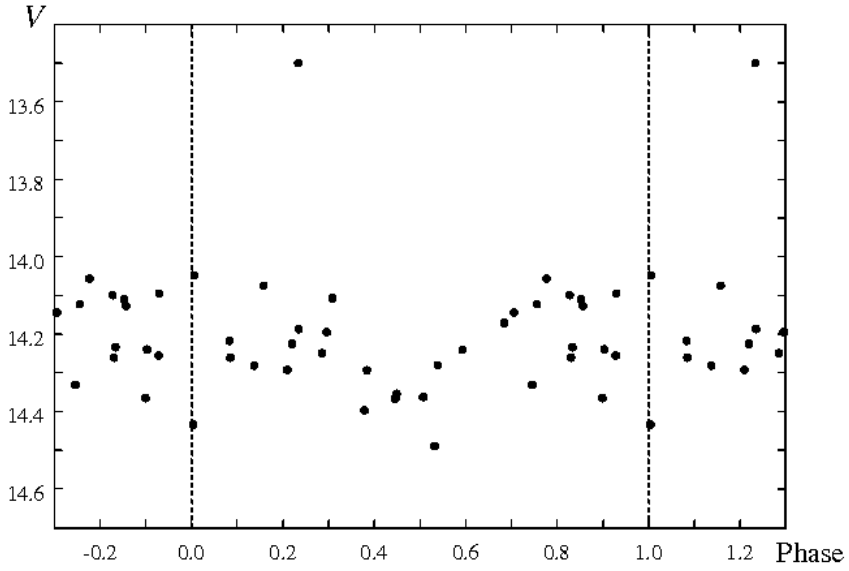

Figure 5. The V-band light curve phased with the orbital period, $13\overset{\mathrm{d}}{.}08223$. The average precession curve was subtracted from the data. The primary minimum is almost invisible.

References:

Antokhina, E. A. and Cherepashchuk, A. M., 1987, *SvA*, **31**, 295
Davydov, V. V., Esipov, V. F. and Cherepashchuk, A. M., 2008, *ARep*, **52**, 487
Goranskij, V, P., 2011, *Peremennye Zvezdy (Variable Stars)*, **31**, No. 5
Hirai, Y. and Fukue, J., 2001, *PASJ*, **53**, 679
Kemp, J. C., Henson, G. D., Kraus, D. J., Carroll, L. C., Beardsley, I. S., Takagishi, K., Jugaku, J., Matsuoka, M., Leibowitz, E. M., Mazeh, T. and Mendelson, H., 1986, *ApJ*, **305**, 805
Leibowitz, E. M., 1984, *MNRAS*, **210**, 279
Leibowitz, E. M. and Mendelson, H., 1982, *PASP*, **94**, 977
Moffett, T. J. and Barnes, T. G., 1979, *AJ*, **84**, 627
Moshkalev, V. G. and Khaliullin, K. F., 1985, *SvA*, **29**, 227
Perez, S. M. and Blundell, K. M., 2010, *MNRAS*, **408**, 2
Straizys, V. L., 1977, *Multicolor Stellar Photometry*, Mosklas, Vilnyus, (in Russian); 1992, Pachart Publ., Tucson, (in English)

COMMISSIONS 27 AND 42 OF THE IAU
INFORMATION BULLETIN ON VARIABLE STARS

Number 6023

Konkoly Observatory
Budapest
4 May 2012

HU ISSN 0374 – 0676

PERIOD ANALYSIS OF THE Hα LINE PROFILE VARIATION OF THE Be BINARY STAR π Aqr

POLLMANN, ERNST

Spektroskopische Arbeitsgemeinschaft ASPA, 51375 Leverkusen, Germany

The spectrum of the classical, rapidly rotating ($v \sin i \sim 300$ km/s) Be binary star π Aqr (HR 8539) has been already investigated photographically since 1911 (Merill, 1913, Lockyer, 1924, 1928).

The star is now well-known for its transition from a Be- to a normal B-star phase and for strong long-term and short-term V/R variations of the hydrogen Balmer line profiles. In many Be-stars, the emission line profiles occasionally have the shape of asymmetrically double peaks. For characterizing the asymmetry, the maximum intensity of the short-wave (violet) peak of the line is marked with V (in intensities of the continuum), and the long-wave (red) peak is marked with R. As quantitative dimension for the asymmetry of line profiles, the intensity ratio is indicated as V/R.

The V/R measurements in the Hα spectra of the binary star π Aqr obtained between October 2004 and August 2011, together with the available spectra of the data base BeSS (http://basebe.obspm.fr/basebe) were subjected to an analysis of a possible periodic behavior using the program AVE (http://www.astrogea.org/soft/ave/aveint.htm).

Figure 1 shows the V/R time behaviour in eight visibility phases, Figure 2 shows a dominant frequency with a period of 83.8 ± 0.8 day in the power spectrum, and Figure 3 shows the phase diagram based on ephemeris: $\mathrm{JD}\,2\,453\,280.0 + 83.8(\pm 0.8) \cdot T$.

This period falls suspiciously near to the orbital period of 84.1 ± 0.004 day of the binary system (Bjorkman et al., 2002). Thomas Rivinius (ESO) confirms this period in his spectra, from phases almost without emissions (private communication, Nov. 2010). The cause for the found periodicity is the "traveling emission component", as it was found and examined in the paper of Bjorkman et al. (2002) in B-phase of the star.

Since π Aqr is still well visible at present, it would be desirable, if potential observers could dedicate themselves to this star. In addition, spectra, which have not been deposited in data base BeSS so far, would contribute for completion of this analysis.

References:

Bjorkman K. S., Miroshnichenko A. S., McDavid D. & Pogrosheva T., 2002, *ApJ*, **573**, 812

Lockyer W.J.S., 1924, *MNRAS*, **84**, 409

Lockyer W.J.S., 1928, *MNRAS*, **88**, 683

Merrill, P.W., 1913, *Lick Observatory Bulletin*, **7**, 162

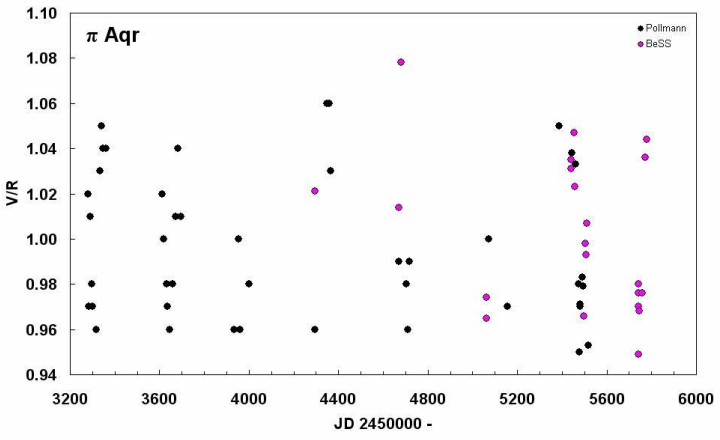

Figure 1. The V/R time behaviour in eight visibility phases.

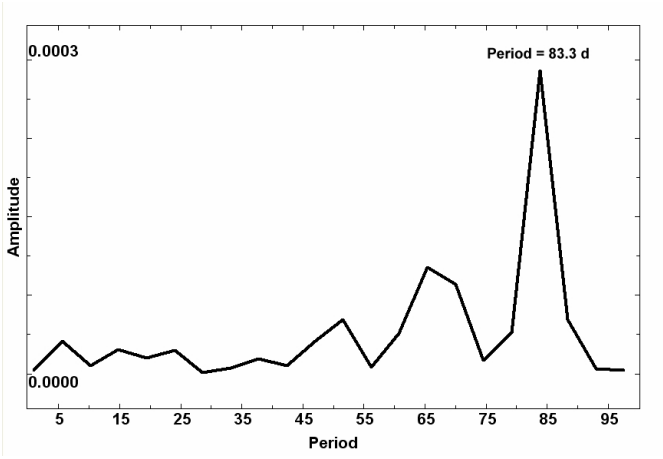

Figure 2. Power spectrum of the V/R data.

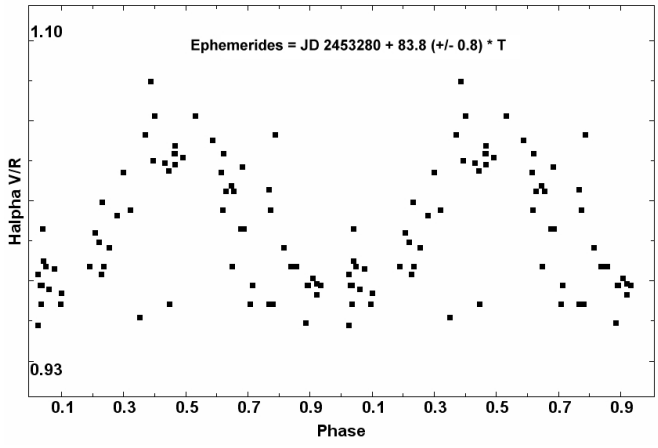

Figure 3. Phase diagram of the V/R data.

COMMISSIONS 27 AND 42 OF THE IAU
INFORMATION BULLETIN ON VARIABLE STARS

Number 6024

Konkoly Observatory
Budapest
15 May 2012

HU ISSN 0374 – 0676

PHOTOMETRIC SEQUENCES AND ASTROMETRIC POSITIONS OF SN 2011fe IN M101 AND SN 2012aw IN M95

HENDEN, ARNE;[1] KRAJCI, TOM;[1] MUNARI, ULISSE[2]

[1] AAVSO, American Association of Variable Star Observers, 49 Bay State Road, Cambridge, MA 02138, USA

[2] INAF Osservatorio Astronomico di Padova, Sede di Asiago, I-36032 Asiago (VI), Italy

SN 2011fe was discovered in M101 by the Palomar Transient Factory (Nugent et al. 2011a) on Aug. 24 with the Palomar 1.2m Schmidt telescope when the object was at $g = 17.2$ magnitude, and within a few hours from discovery it was classified as a type Ia with the Liverpool Telescope (La Palma, Canary Islands). Comparison with explosion models suggests that SN 2011fe was discovered only about 11 hours after its actual explosion (Nugent et al. 2011b). The supernova peaked at $V \approx 9.9$ mag, making it the fifth-brightest supernova in the past century. A flurry of papers have been already published, mainly triggered by the absence of early radio emission, the lack of an optical counterpart for the progenitor in archival HST images, and negative detection in early X-ray observations. Analysis of archival HST images of the location of SN 2011fe by Li et al. (2011) shows that the luminosity of the progenitor system (especially the companion star) is 10−100 times fainter than previous limits on other type Ia supernova progenitor systems, which rules out luminous red giants and almost all helium stars as the mass-donating companion to the exploding white dwarf, and the Bloom et al. (2012) analysis also rules out main sequence stars. The absence of early radio and X-ray emission, induced by the SN ejecta slamming onto or expanding through pre-existing, slowly moving circumstellar material was used by Horesh et al. (2012) and Chomiuk et al. (2012), to put stringent limits on the density of any circumstellar material, the mass loss rate and therefore on the nature of the SN progenitor.

SN 2012aw was discovered by Paolo Fagotti (Bastia Umbra, Italy) in M95 on CCD images taken on Mar. 16.86 UT with a 0.5-m reflector (cf. CBET 3054). It was classified by Itoh et al. (2012) as a type-IIP supernova from spectra obtained on March 19.5 UT, and confirmed by Siviero et al. (2012) on Asiago spectra obtained on Mar. 17.77 and 19.85 UT as a very young type-II supernova, resembling the type-IIP supernova 1999gi about 4–5 days after the core-collapse.

For both SNe, the amount of published multi-band photometry is minimal with respect to the vast amount being continuously collected world-wide. One possible reason is the absence of accurate local photometric sequences. This IBVS aims to remedy the situation.

In this note we present a $BVR_{\rm C}I_{\rm C}$ photometric sequence around both SNe, optimized for CCD observations and their color corrections. To calibrate the sequences, we obtained CCD photometry with a 0.35-m telescope located at Astrokolkhoz Observatory in Cloudcroft (New Mexico, USA), during a large number of photometric nights, using $BVR_{\rm C}I_{\rm C}$

filters and an SBIG STL-1001E CCD camera. Pixel size is 1.″25/pix and the field of view is 20×20′. Observations on each photometric night included BVR_CI_C exposures of Landolt standard fields (Landolt 1983, 1992) taken at high and low airmasses. The photometric sequences are presented in Figures 1 and 2. Astrometry was performed using SLALIB (Wallace 1994) linear plate transformation routines in conjunction with the UCAC2 reference catalog. Errors in coordinates were less than 0.1 arcsec in both coordinates, referred to the mean coordinate zero point of the reference stars in each field.

The position we derived for SN 2011fe in M101 is: $\alpha_{J2000} = 14^h03^m05^s.711$ (±0.″27), $\delta_{J2000} = +54°16'25.''22$ (±0.″23). The end figures of the supernova position derived by Li et al. (2012) are $05^s.733$ and 25.″18 (J2000.0), who observed with the Near-Infrared Camera 2 (NIRC2) mounted behind the adaptive optics (AO) system on the Keck II telescope. Other positions as appeared on CBET 2792 are: $05^s.81$ and 25.″4 (Palomar 1.2m Schmidt), $05^s.75$ and 25.″2 (R.A. Koff, 0.25m), 05.″74 and 25.″3 (J. Brimacombe, 0.5m), $05^s.74$ and 25.″7 (G. Masi, 0.43m).

Our position for SN 2012aw in M95 is: $\alpha_{J2000} = 10^h43^m53^s.735$ (±0.″091), $\delta_{J2000} = +11°40'17.''63$ (±0.″084). It is within 0.11 arcsec of the unweighted mean of the other determinations of the supernova position so far published. Ending figure given at the time of discovery and summarized in CBET 3054 are: $53^s.76$ and 17.″9 (P. Fagotti, 0.5m), $53^s.78$ and 17.″0 (A. Dimai, 0.28m), $53^s.72$ and 17.″7 (J. Skvarc, 0.6m), $53^s.73$ and 17.″8 (G. Masi, 0.43m); a radio observation by Yadav et al. (2012) provides $53^s.72$ and 17.″5. Positive searches for the progenitor on archival HST images of M95 are mentioned by Elias-Rosa et al. (2012) and Fraser et al. (2012a,b), but no explicit astrometric position is given for the SN.

References:

Bloom, J.S. et al. 2012, *ApJ*, **744**, L17
Chomiuk, L. et al. 2012, *ApJ*, **750**, 164
Elias-Rosa, N. et al. 2012, *ATel*, **3991**
Fraser, M. et al. 2012a, *ATel*, **3994**
Fraser, M. et al. 2012b, arXiv:1204.1523 [astro-ph.CO]
Horesh, A. et al. 2012, *ApJ*, **746**, 21
Itoh, R. et al. 2012, *CBET*, **3054**
Landolt, A.U. 1983, *AJ*, **88**, 439
Landolt, A.U. 1992, *AJ*, **104**, 340
Li, W. et al. 2011, *Nature*, **480**, 348
Nugent, P.E. et al. 2011a, *CBET*, **2792**
Nugent, P.E. et al. 2011b, *Nature*, **480**, 344
Siviero, A. et al. 2012, *CBET*, **3054**
Wallace, P. 1994, *ASPC*, **61**, 481
Yadav, N. et al. 2012, *ATel*, **4010**

SN 2011fe in M101 $\alpha_{\rm J2000} = 14\ 03\ 05.711$ $\delta_{\rm J2000} = +54\ 16\ 25.22$

	α_{J2000} (±")		δ_{J2000} (±")		N	V (±)		B–V (±)		V–$R_{\rm C}$ (±)		$R_{\rm C}$–$I_{\rm C}$ (±)		V–$I_{\rm C}$ (±)	
a	210.957751	0.100	54.151578	0.127	16	11.756	0.005	0.611	0.015	0.318	0.007	0.342	0.005	0.662	0.005
b	211.175550	0.113	54.351805	0.059	16	12.356	0.005	0.744	0.015	0.409	0.004	0.352	0.005	0.760	0.005
c	210.810842	0.060	54.370365	0.059	14	12.927	0.008	0.501	0.014	0.308	0.004	0.294	0.006	0.601	0.005
d	211.018410	0.095	54.225612	0.078	16	13.343	0.006	0.940	0.012	0.510	0.004	0.441	0.004	0.951	0.005
e	211.011509	0.081	54.305018	0.035	15	13.509	0.005	0.617	0.011	0.363	0.003	0.350	0.004	0.713	0.005
f	210.710320	0.054	54.369486	0.065	16	13.646	0.009	0.789	0.015	0.444	0.004	0.402	0.007	0.846	0.007
g	210.806928	0.074	54.262027	0.043	15	13.860	0.010	0.944	0.010	0.556	0.005	0.547	0.004	1.105	0.005
h	210.725528	0.052	54.274797	0.063	13	13.999	0.009	0.618	0.012	0.360	0.003	0.355	0.005	0.715	0.005
i	210.623308	0.080	54.282115	0.084	10	14.150	0.009	0.891	0.013	0.518	0.004	0.432	0.006	0.950	0.007
j	211.067646	0.047	54.428807	0.093	16	14.309	0.005	0.816	0.014	0.464	0.003	0.400	0.007	0.864	0.007
k	210.692101	0.079	54.150685	0.089	13	14.727	0.010	0.583	0.015	0.336	0.005	0.334	0.006	0.670	0.009
l	210.843222	0.090	54.260075	0.045	14	14.827	0.011	1.346	0.017	0.821	0.005	0.751	0.006	1.576	0.005
m	210.898393	0.104	54.341882	0.260	8	15.387	0.047	1.031	0.056	0.572	0.033	0.522	0.012	1.133	0.010
n	210.651256	0.086	54.315059	0.061	11	15.617	0.025	1.310	0.026	0.859	0.011	0.768	0.010	1.630	0.004
p	210.942033	0.160	54.446751	0.236	8	15.694	0.010	0.500	0.012	0.324	0.005	0.303	0.016	0.631	0.016

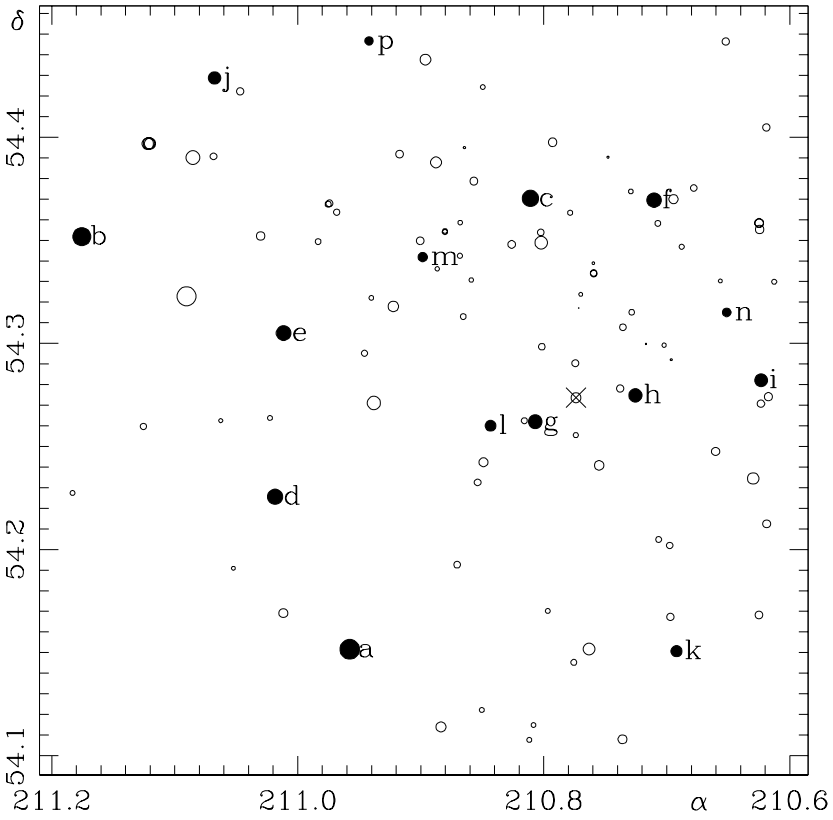

Figure 1. $BVR_{\rm C}I_{\rm C}$ photometric comparison sequence around SN 2011fe in M101. The cross indicates the SN. N is the number of nights in which the given star has been measured, the photometric uncertainties are errors of the mean. The errors in α and δ are expressed in arcsec. The panel covers a $20' \times 6'$ area.

SN 2012aw in M95 $\alpha_{\rm J2000} = 10\ 43\ 53.735$ $\delta_{\rm J2000} = +11\ 40\ 17.63$

	α_{J2000} (±")		δ_{J2000} (±")		N	V (±)		B–V (±)		V–$R_{\rm C}$ (±)		$R_{\rm C}$–$I_{\rm C}$ (±)		V–$I_{\rm C}$ (±)	
a	160.885499	0.075	11.709246	0.032	7	10.329	0.020	0.554	0.020	0.331	0.008	0.363	0.014	0.696	0.016
b	160.878388	0.054	11.830937	0.064	6	11.171	0.011	0.412	0.008	0.259	0.002	0.264	0.007	0.522	0.006
c	160.913578	0.072	11.738825	0.031	4	11.943	0.017	1.033	0.013	0.560	0.007	0.471	0.006	1.035	0.011
d	161.043388	0.114	11.515533	0.094	6	12.082	0.010	0.907	0.008	0.506	0.004	0.430	0.009	0.936	0.010
e	161.096381	0.165	11.712065	0.065	7	12.696	0.007	0.601	0.005	0.347	0.004	0.327	0.005	0.673	0.006
f	160.891623	0.048	11.824786	0.058	6	13.435	0.012	0.650	0.007	0.385	0.002	0.360	0.004	0.745	0.005
g	161.112808	0.168	11.571551	0.167	6	13.487	0.009	0.740	0.007	0.424	0.003	0.370	0.008	0.793	0.008
h	160.879769	0.089	11.504159	0.096	6	13.835	0.007	0.685	0.012	0.418	0.003	0.373	0.007	0.790	0.007
i	160.880875	0.054	11.621125	0.088	7	13.894	0.008	1.085	0.005	0.657	0.005	0.531	0.005	1.187	0.006
j	161.043249	0.132	11.530116	0.097	7	14.440	0.012	0.730	0.007	0.413	0.006	0.356	0.006	0.767	0.003
k	160.910322	0.073	11.583798	0.044	5	14.649	0.008	0.885	0.013	0.503	0.005	0.474	0.005	0.977	0.007
l	160.908136	0.055	11.538903	0.091	7	14.675	0.006	1.215	0.016	0.737	0.014	0.567	0.013	1.303	0.007
m	161.067779	0.241	11.576674	0.123	6	14.839	0.015	0.859	0.020	0.486	0.008	0.408	0.010	0.894	0.003
n	160.936673	0.099	11.684353	0.130	7	14.954	0.010	0.414	0.019	0.256	0.005	0.260	0.010	0.516	0.013

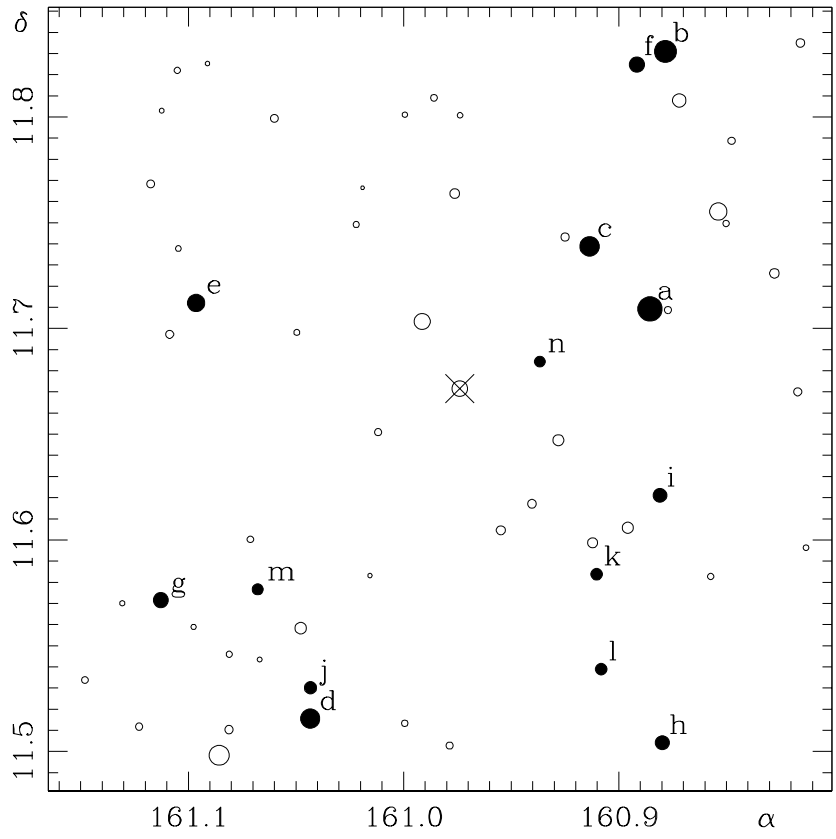

Figure 2. $BVR_{\rm C}I_{\rm C}$ photometric comparison sequence around SN 2012aw in M95. The cross indicates the SN. N is the number of nights in which the given star has been measured, the photometric uncertainties are errors of the mean. The errors in α and δ are expressed in arcsec. The panel covers a $20' \times 20'$ area.

COMMISSIONS 27 AND 42 OF THE IAU
INFORMATION BULLETIN ON VARIABLE STARS

Number 6025

Konkoly Observatory
Budapest
25 June 2012

HU ISSN 0374 – 0676

VR_CI_C OPTICAL LIGHT CURVES OF V1647 Ori DURING THE CONTINUING SECOND OUTBURST

SEMKOV, E. H.; PENEVA, S. P.

Institute of Astronomy and National Astronomical Observatory, Bulgarian Academy of Sciences, 72 Tsarigradsko Shose blvd., BG-1784 Sofia, Bulgaria, e-mail: esemkov@astro.bas.bg, speneva@astro.bas.bg

The outburst of the pre-main sequence (PMS) star V1647 Ori was discovered by the amateur astronomer Jay McNeil in January 2004 (McNeil 2004). The star showed an increase of its optical brightness by around 5 mag beginning from November 2003 till February-March 2004 (Briceño et al. 2004). V1647 Ori remained in a state of maximum light about two years, then its brightness declined to the pre-outburst level (Kóspál et al. 2005). The optical and infrared light curves of V1647 Ori during the outburst are well studied and documented (Acosta-Pulido et al. 2007, Fedele et al. 2007, Aspin & Reipurth 2009, García-Alvarez et al. 2011). During the outburst V1647 Ori exhibited a strong emission spectrum in the optical and near-IR, typical for eruptive PMS stars of EXor type (Herbig 2008). However, the spectral structure in the infrared and the relatively long outburst give some reasons to classify the star as a FUor (Aspin et al. 2008).

A second outburst of the star was registered in 2008, when its brightness increased again to the level of the first eruption (Itagaki et al. 2008, Kun 2008). The optical and infrared follow-up observations show that the star and the surrounding nebula appear photometrically and morphologically similar to the first outburst (Aspin et al. 2009). Only a few papers publishing data from optical and infrared photometric observations during the second outburst have appeared until now (Kaurav et al. 2010, García-Alvarez et al. 2011, Aspin 2011). During both outbursts V1647 Ori showed a strong emission Hα line with blueshifted absorption (P Cygni profile) while in the time between the outburst the Hα line weakened and the blueshifted component disappeared (Aspin & Reipurth 2009, Aspin 2011). A correlation between the X-ray luminosity and I_C magnitude during the two outbursts were found by Teets et al. (2011).

The present paper is a continuation of our photometric study of the star during the first outburst (Semkov 2004, 2006). We present new VR_CI_C photometric data of V1647 Ori in the period November 2008 – April 2012. A part of our data (from 2008 Nov 20 till 2010 Aug 20) are presented in Fig. 1 of García-Alvarez et al. (2011). Our data were obtained in two observatories with three telescopes: the 2-m RCC and the 50/70-cm Schmidt telescopes of the National Astronomical Observatory Rozhen (Bulgaria) and the 1.3-m RC telescope of the Skinakas Observatory of the Institute of Astronomy, University of Crete (Greece). The technical parameters and chip specifications of the CCD cameras

Table 1. CCD cameras and chip specifications

Telescope	CCD type	Size	Pixel size [μm]	Field	RON [ADU/rms]
2-m RCC	VersArray 1300B	1340×1300	20	5′.6×5′.6	2.8
1.3-m RC	ANDOR DZ436-BV	2048×2048	13.5	9′.6×9′.6	5.3
50/70-cm Schmidt	STL-11000M	4008×2672	9	72′×48′	13
50/70-cm Schmidt	FLI PL16803	4096×4096	9	74′×74′	9

used are summarized in Table 1. All frames were taken through a standard Johnson–Cousins set of filters. Aperture photometry was performed using DAOPHOT routines.

The VR_CI_C comparison sequence reported in Semkov (2006) was used as a reference. In order to minimize the light from the surrounding nebula, all frames were reduced using the same aperture of 2″.5 radius and the background was taken between radii 20″ and 25″. The typical errors in the reported magnitudes are in the range $0^m.01$-$0^m.03$ (I and R) and $0^m.02$-$0^m.05$ (V) for observations made with 2-m RCC and 1.3-m RC telescopes and in the range $0^m.02$-$0^m.04$ (I) and $0^m.02$-$0^m.06$ (R) for observations made with the Schmidt telescope. The results from our CCD photometric observations are given in Table 2. The table contains date, the Julian date, the I_C, R_C and V magnitudes. Fig. 1 shows the V, R_C and I_C light curves of V1647 Ori for the period of our photometric observations. Typical error bars for each filter are shown at the left.

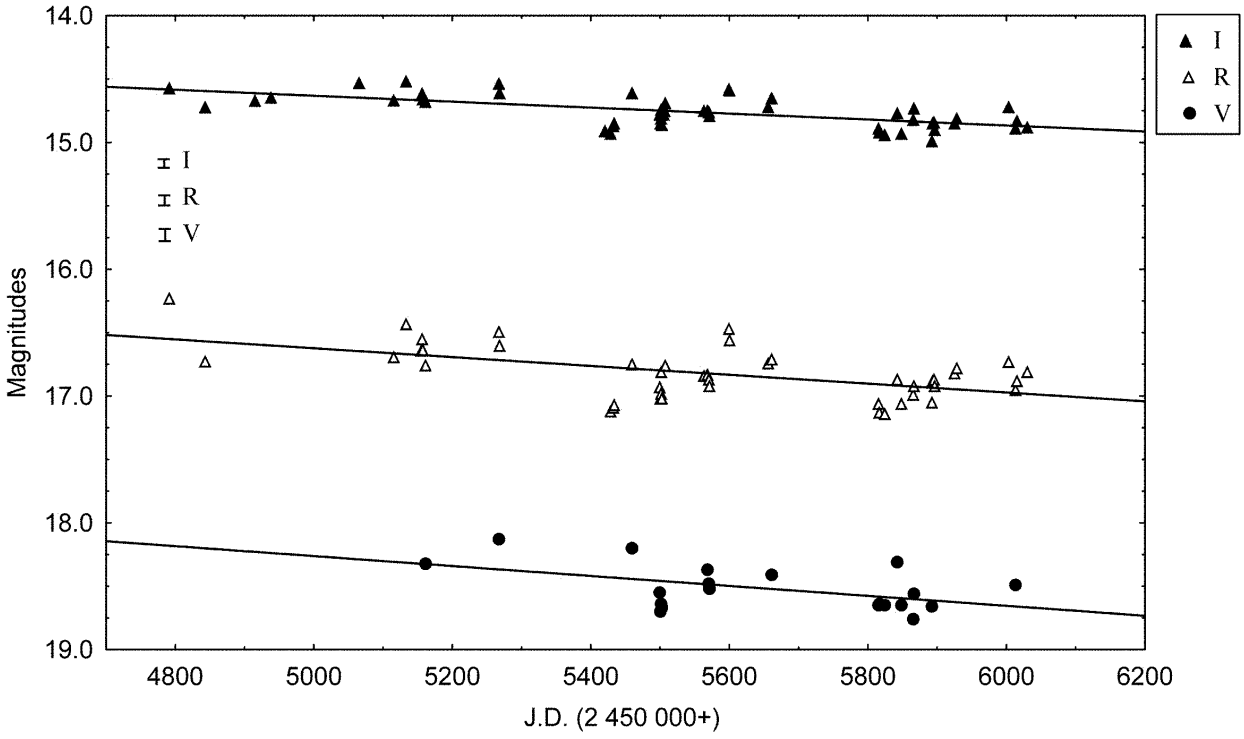

Figure 1. V, R_C and I_C light curves of V1647 Ori

Table 2. Photometric observations of V1647 Ori

Date	J.D.(245...)	I_C	R_C	V	Tel.	CCD
2008 Nov 20	4791.387	14.57	16.23	–	Schmidt	STL11000
2009 Jan 11	4843.263	14.72	16.73	–	Schmidt	STL11000
2009 Mar 24	4915.262	14.67	–	–	Schmidt	STL11000
2009 Apr 16	4938.277	14.65	–	–	Schmidt	STL11000
2009 Aug 21	5065.562	14.53	–	–	Schmidt	FLI
2009 Oct 09	5115.453	14.67	16.69	–	Schmidt	FLI
2009 Oct 28	5133.419	14.52	16.43	–	Schmidt	FLI
2009 Nov 19	5155.411	14.63	16.64	–	Schmidt	FLI
2009 Nov 20	5156.473	14.61	16.55	–	Schmidt	FLI
2009 Nov 21	5157.474	14.66	16.64	–	Schmidt	FLI
2009 Nov 25	5161.497	14.68	16.76	18.32	2m RCC	VA
2010 Mar 11	5267.277	14.54	16.49	18.13	2m RCC	VA
2010 Mar 12	5268.324	14.61	16.60	–	2m RCC	VA
2010 Aug 12	5420.616	14.91	–	–	1.3m RC	ANDOR
2010 Aug 20	5428.613	14.93	17.12	–	1.3m RC	ANDOR
2010 Aug 24	5432.588	14.87	17.09	–	1.3m RC	ANDOR
2010 Aug 25	5433.598	14.85	17.07	–	1.3m RC	ANDOR
2010 Sep 20	5459.639	14.61	16.75	18.20	1.3m RC	ANDOR
2010 Oct 30	5499.526	14.78	16.93	18.55	2m RCC	VA
2010 Oct 31	5500.506	14.85	17.02	18.70	2m RCC	VA
2010 Nov 01	5501.501	14.81	16.98	18.64	2m RCC	VA
2010 Nov 02	5502.571	14.86	17.02	18.67	2m RCC	VA
2010 Nov 04	5505.475	14.78	–	–	Schmidt	FLI
2010 Nov 06	5506.504	14.75	–	–	Schmidt	FLI
2010 Nov 07	5507.514	14.69	16.76	–	Schmidt	FLI
2011 Jan 01	5563.423	14.75	16.84	–	Schmidt	FLI
2011 Jan 06	5568.391	14.75	16.83	18.37	2m RCC	VA
2011 Jan 08	5570.277	14.76	16.87	18.48	2m RCC	VA
2011 Jan 09	5571.381	14.79	16.92	18.52	2m RCC	VA
2011 Feb 06	5599.324	14.58	16.47	–	Schmidt	FLI
2011 Feb 07	5600.302	14.59	16.56	–	Schmidt	FLI
2011 Apr 04	5656.256	14.72	16.74	–	Schmidt	FLI
2011 Apr 09	5661.263	14.65	16.71	18.41	2m RCC	VA
2011 Sep 11	5815.567	14.89	17.06	18.65	1.3m RC	ANDOR
2011 Sep 12	5816.594	14.92	17.13	18.64	1.3m RC	ANDOR
2011 Sep 20	5824.540	14.94	17.14	18.65	1.3m RC	ANDOR
2011 Oct 08	5842.513	14.77	16.87	18.31	1.3m RC	ANDOR
2011 Oct 14	5848.502	14.93	17.06	18.65	1.3m RC	ANDOR
2011 Oct 30	5865.486	14.82	16.99	18.76	2m RCC	VA
2011 Nov 01	5866.530	14.73	16.92	18.56	2m RCC	VA
2011 Nov 26	5892.477	14.99	17.05	18.66	2m RCC	VA
2011 Nov 27	5893.420	14.85	16.88	–	Schmidt	FLI
2011 Nov 29	5895.489	14.84	16.87	–	Schmidt	FLI
2011 Nov 30	5896.445	14.90	16.92	–	Schmidt	FLI
2011 Dec 29	5925.475	14.85	16.82	–	Schmidt	FLI
2012 Jan 01	5928.383	14.81	16.78	–	Schmidt	FLI
2012 Mar 16	6003.261	14.72	16.73	–	Schmidt	FLI
2012 Mar 26	6013.262	14.89	16.95	18.49	2m RCC	VA
2012 Mar 28	6015.312	14.83	16.88	–	2m RCC	VA
2012 Apr 12	6030.270	14.88	16.85	–	Schmidt	FLI

The long-term photometric study of V1647 Ori can be very useful to determine the type of the eruption: FUor or EXor. Our observations suggest that the second outburst of V1647 Ori persists for approximately four years. The photometric data show a continuous slight decrease in brightness during the period of observations. In the meantime the star becomes redder with decreasing of its brightness. Using a linear approximation for our data, we calculated the following values for the rates of decline: $\sim$0.07 mag yr^{-1} for I, $\sim$0.11 mag yr^{-1} for R and $\sim$0.15 mag yr^{-1} for V. Random fluctuations in brightness with amplitudes of few tenths of magnitude and timescales of some days were recorded during the first outburst (see Aspin & Reipurth 2009 and references therein). Such a short time scale variability in brightness is observed during the second outburst.

According to Aspin et al. (2009) the decrease in brightness of V1647 Ori over the period 2006–2008 was caused by reduction of the accretion rate and reformation of dust in the circumstellar environment of the star. Therefore, we observe the same outburst that has slowed down temporarily. Such interpretation of the observational results leads Aspin et al. (2009) to the hypothesis that V1647 Ori is a FUor object. Our data show similar photometric behavior of the star during both outbursts and also support the hypothesis of the FUor nature of V1647 Ori. On the other hand the spectrum of the star during the second outburst remains similar to the spectra of EXor objects (Aspin 2011). Therefore, during the second outburst V1647 Ori continues to show the photometric properties of a FUor and the spectral properties of an EXor.

Acknowledgements: This work was partly supported by grants DO 02-85 and DO 02-273 of the National Science Fund of the Ministry of Education, Youth and Science, Bulgaria. The authors thank the Director of Skinakas Observatory Prof. I. Papamastorakis and Prof. I. Papadakis for the telescope time. This research has made use of NASA's Astrophysics Data System.

References:

Acosta-Pulido, J. A., Kun, M., Ábrahám, P. et al. 2007, *AJ*, **133**, 2020
Aspin, C. 2011, *AJ*, **142**, 135
Aspin, C., Beck, T. L., Reipurth, B. 2008, *AJ*, **135**, 423
Aspin, C., Reipurth, B., Beck, T. L. et al. 2009, *ApJ*, **692**, L67
Aspin, C., Reipurth, B. 2009, *AJ*, **138**, 1137
Briceño, C., Vivas, A. K., Hernandez, J. et al. 2004, *ApJ*, **606**, L123
Fedele, D., van den Ancker, M. E., Petr-Gotzens, M. G., et al. 2007, *A&A*, **472**, 207
García-Alvarez, D., Wright, N. J., Drake, J. J. et al. 2011, *ASP Conference Series*, **448**, 609 (arXiv:1108.0828)
Herbig, G. H. 2008, *AJ*, **135**, 637
Itagaki, K., Nakano, S., Yamaoka, H. 2008, *IAUC*, **8968**
Kaurav, S. S., Ojha, D. K., Ninan, J. P., et al. 2010, *ASI Conference Series*, **1**, 237
Kóspál, A., Ábrahám, P., Acosta-Pulido, J., et al. 2005, *IBVS*, 5661
Kun, M. 2008, *IBVS*, **5850**
McNeil, J. W. 2004, *IAU Circ.*, **8284**
Semkov, E. H. 2004, *IBVS*, **5578**
Semkov, E. H., 2006, *IBVS*, **5683**
Teets, W. K., Weintraub, D. A., Grosso, N., et al. 2011, *ApJ*, **741**, 83

COMMISSIONS 27 AND 42 OF THE IAU
INFORMATION BULLETIN ON VARIABLE STARS

Number 6026

Konkoly Observatory
Budapest
27 June 2012

HU ISSN 0374 – 0676

BAV-RESULTS OF OBSERVATIONS - PHOTOELECTRIC MINIMA OF SELECTED ECLIPSING BINARIES AND MAXIMA OF PULSATING STARS

(BAV MITTEILUNGEN NO. 225)

HÜBSCHER, JOACHIM; LEHMANN, PETER B.

Bundesdeutsche Arbeitsgemeinschaft für Veränderliche Sterne e.V. (BAV), Munsterdamm 90, 12169 Berlin, Germany, www.bav-astro.de, publikat@bav-astro.de

In this 72th compilation of BAV results, photoelectric observations obtained mostly in the years 2011 and 2012 are presented on more than 600 variable stars giving over 1,200 minima on eclipsing binaries and maxima on pulsating stars. All moments of minima and maxima are heliocentric UTC. The errors are tabulated in column '±'. The values in column '$O-C$' are determined without incorporating nonlinear terms. The references are given in the section 'Remarks'. All information about photometers and filters are specified in the column 'Rem'. The observations were made at private observatories. The photoelectric measurements and all the light curves with evaluations can be obtained from the office of the BAV for inspection.

Please use the following link for an easy access to all the publications of the BAV including the "Lichtenknecker Database of the BAV": `http://www.bav-astro.de/sfs` .

Table 1: Times of minima of eclipsing binaries

Variable	HJD 24.....	±	Obs	$O-C$		Bibliography	Fil	n	Rem
TT And	55758.4051	.0009	MS FR	+0.0021		GCVS 2012	o	351	6)
UU And	55850.4181	.0001	RAT RCR	−0.0325		GCVS 2012	-U-I	283	15)
WZ And	55807.4200	.0004	MS FR	+0.0020		GCVS 2012	o	340	6)
AA And	55839.5130	.0123	AG	+0.0195	s	GCVS 2012	-Ir	40	13)
	55849.3087	.0020	AG	−0.0033		GCVS 2012	-Ir	50	13)
AB And	55851.3250	.0018	AG	−0.0063	s	GCVS 2012	V	63	13)
	55851.4919	.0007	AG	−0.0053		GCVS 2012	V	63	13)
AD And	55829.3556	.0008	JU	−0.0487	s	GCVS 2012	o	118	3)
	55849.5734	.0011	AG	−0.0033		GCVS 2012	-Ir	49	13)
BD And	55832.3609	.0004	JU	−0.0216		GCVS 2012	o	80	3)
	55839.3033	.0021	AG	−0.0228		GCVS 2012	-Ir	43	13)
	55873.5574	.0025	AG	−0.0237		GCVS 2012	-Ir	54	13)
	55877.2615	.0004	MS FR	−0.0229		GCVS 2012	o	276	6)
BL And	55815.3623	.0025	AG	−0.0020		GCVS 2012	-Ir	44	13)
	55839.5706	.0043	AG	+0.0067	s	GCVS 2012	-Ir	41	13)
	55849.3133	.0014	AG	−0.0026		GCVS 2012	-Ir	49	13)
	55873.5212	.0090	AG	+0.0057	s	GCVS 2012	-Ir	54	13)
BX And	55850.4604	.0017	AG	−0.0094		GCVS 2012	-Ir	54	13)
CP And	55850.4863	.0012	AG				-Ir	54	13)
CZ And	55833.5371	.0003	RAT RCR				-U-I	348	15)
DK And	55839.4269	.0017	AG	+0.0026		BAVR 55,106	-Ir	41	13)
	55849.4556	.0017	AG	+0.0022	s	BAVR 55,106	-Ir	49	13)
DS And	55828.3301	.0008	DIE	+0.0083		GCVS 2012	o	37	19)
	55829.3360	.0028	DIE	+0.0037		GCVS 2012	o	36	19)
EP And	55889.2774	.0009	BHE	+0.0688		GCVS 2012	-Ir	84	17)
GZ And	55850.2730	.0012	AG	−0.0012	s	GCVS 2012	-Ir	52	13)
	55850.4258	.0016	AG	−0.0009		GCVS 2012	-Ir	52	13)
	55850.5776	.0021	AG	−0.0016	s	GCVS 2012	-Ir	52	13)
	55872.3868	.0019	JU	−0.0011		GCVS 2012	o	45	3)
	55880.3170	.0013	BHE	−0.0014		GCVS 2012	-Ir	195	17)
KN And	55859.3359	.0011	AG	+0.0979		BAVR 39,19	-Ir	45	13)
KP And	55838.5170	.0002	RAT RCR	+0.0512		GCVS 2012	-U-I	280	15)
LM And	55850.3890	.0005	AG	−0.0108		GCVS 2012	-Ir	53	13)
MO And	55858.3170	.0002	MS FR	+0.0074		GCVS 2012	o	567	6)
QR And	55857.4089	.0015	AG				-Ir	82	13)
QX And	55861.2883	.0013	MS FR	+0.0929	s	GCVS 2012	o	320	6)
V404 And	55849.3946	.0010	JU	+0.0121		GCVS 2012	o	57	3)
V412 And	55887.3202	.0012	JU	+0.0651	s	GCVS 2012	o	79	3)
V422 And	55873.2735	.0030	AG	−0.0046		GCVS 2012	-Ir	52	13)
V425 And	55839.5153	.0030	AG	−0.0349		GCVS 2012	-Ir	42	13)
	55849.4612	.0026	AG	−0.0342		GCVS 2012	-Ir	49	13)
V441 And	55866.3051	.0005	MS FR	+0.1101	s	GCVS 2012	o	440	6)
V449 And	55850.2920	.0009	AG				-Ir	54	13)
	55850.4611	.0006	AG				-Ir	54	13)
	55850.6304	.0002	AG				-Ir	54	13)
V452 And	55849.3681	.0026	AG	+0.1135		GCVS 2012	-Ir	49	13)
	55873.3397	.0074	AG	+0.1143	s	GCVS 2012	-Ir	54	13)
V463 And	55830.6260	.0003	RAT RCR	−0.0585		GCVS 2012	-U-I	336	15)
	55832.4509	.0002	RAT RCR	−0.0611	s	GCVS 2012	-U-I	340	15)
	55832.6554	.0007	RAT RCR	−0.0596		GCVS 2012	-U-I	340	15)
CX Aqr	55855.2662	.0003	DIE	−0.0032		GCVS 2012	o	32	19)
HS Aqr	48830.440	.001	WU	−0.005		GCVS 2012	V	41	1)
HV Aqr	55805.3636	.0002	RAT RCR				-U-I	123	15)
V343 Aql	55828.3377	.0024	FR	−0.0554		GCVS 2012	o	38	14)
V417 Aql	55795.5348	.0027	AG	−0.0580		BAVR 33,152	-Ir	39	13)
V418 Aql	55795.4758	.0035	AG	−0.0005		GCVS 2012	-Ir	38	13)
V420 Aql	55795.5330	.0025	AG	+0.3125		GCVS 2012	-Ir	34	13)
V1713 Aql	55795.4037	.0013	AG				-Ir	34	13)
RX Ari	55856.4602	.0139	AG	+0.0669	s	GCVS 2012	V	57	13)
	55901.249 :	.003	BHE	+0.067		GCVS 2012	-Ir	80	17)

Table 1: (cont.)

Variable	HJD 24.....	±	Obs	$O-C$		Bibliography	Fil	n	Rem
SS Ari	55856.3359	.0023	AG	−0.0069	s	GCVS 2012	V	57	13)
	55856.5367	.0016	AG	−0.0091		GCVS 2012	V	57	13)
XZ Ari	55856.3202	.0042	AG				-Ir	57	13)
	55856.4482	.0039	AG				-Ir	57	13)
	55856.5839	.0017	AG				-Ir	57	13)
BQ Ari	55866.378	.000	RAT RCR	−0.020		GCVS 2012	-U-I	110	15)
ZZ Aur	55851.4580	.0002	MS FR	+0.0185		GCVS 2012	o	576	6)
CI Aur	55861.4918	.0005	MS FR	+0.1354		GCVS 2012	o	555	6)
IY Aur	55957.5053	.0035	PGL	−0.1305		GCVS 2012	V	104	12)
MO Aur	55856.4259	.0017	MS FR	+0.0912		BAVM 68	o	494	6)
NN Aur	55887.3193	.0004	FR				-Ir	77	13)
V523 Aur	55820.6211	.0008	MS FR				o	390	6)
V585 Aur	55615.3521	.0001	RAT RCR	+0.0292		GCVS 2012	-U-I	198	15)
V596 Aur	55619.3130	.0002	RAT RCR	+0.0086	s	GCVS 2012	-U-I	94	15)
V607 Aur	55866.5805	.0001	RAT RCR	+0.5029		GCVS 2012	-U-I	232	15)
V623 Aur	55621.4724	.0005	RAT RCR	+0.1050		GCVS 2012	-U-I	213	15)
V627 Aur	55621.3658	.0007	RAT RCR	−0.0962		GCVS 2012	-U-I	210	15)
SU Boo	55601.5353	.0002	MS FR	+0.0163		GCVS 2012	o	550	6)
TU Boo	55592.5267	.0001	MS FR	+0.0266	s	GCVS 2012	o	371	6)
	55602.5803	.0002	MS FR	+0.0273	s	GCVS 2012	o	329	6)
TZ Boo	55716.5058	.0001	RAT RCR	−0.0295		BAVM 68	-U-I	185	15)
UW Boo	55676.4280	.0007	RAT RCR	−0.0123	s	GCVS 2012	-U-I	220	15)
XY Boo	55682.4033	.0001	RAT RCR	+0.0337	s	GCVS 2012	-U-I	141	15)
GH Boo	55628.4586	.0006	RAT RCR				-U-I	238	15)
GR Boo	55614.4970	.0005	MS FR				o	780	6)
	55677.4013	.0002	MS FR				o	336	6)
HH Boo	55676.4812	.0002	RAT RCR	−0.0377	s	GCVS 2012	-U-I	220	15)
UU Cam	55942.3979	.0023	JU	+0.0427		GCVS 2012	o	71	3)
	55969.3566	.0014	JU	+0.0416		GCVS 2012	o	55	3)
XZ Cam	55643.3345	.0010	RAT RCR	+0.1131		GCVS 2012	-U-I	243	15)
AO Cam	55896.2846	.0002	JU	+0.0462		GCVS 2012	o	42	3)
AT Cam	55648.3443	.0002	RAT RCR	−0.0267	s	BAVR 32,36	-U-I	124	15)
	55879.3600	.0069	PGL	−0.0317		BAVR 32,36	V	251	16)
AZ Cam	55648.5040	.0001	RAT RCR	+0.0213		GCVS 2012	-U-I	301	15)
CD Cam	55887.4455	.0067	AG				-Ir	74	13)
FN Cam	55622.5246	.0001	RAT RCR				-U-I	350	15)
HW Cam	55615.5941	.0001	RAT RCR				-U-I	334	15)
LR Cam	55625.4144	.0001	RAT RCR				-U-I	175	15)
NQ Cam	55887.2744	.0009	AG	−0.0748	s	GCVS 2012	-Ir	74	13)
	55887.4567	.0016	AG	−0.0735		GCVS 2012	-Ir	74	13)
	55887.6366	.0009	AG	−0.0747	s	GCVS 2012	-Ir	74	13)
NS Cam	55614.4872	.0004	RAT RCR	−0.0569		GCVS 2012	-U-I	326	15)
	55887.5897	.0040	AG	−0.0608		GCVS 2012	-Ir	74	13)
NU Cam	55621.6503	.0002	RAT RCR	+0.0618		GCVS 2012	-U-I	266	15)
OQ Cam	55609.2946	.0002	RAT RCR	−0.0154	s	GCVS 2012	-U-I	142	15)
PP Cam	55960.3175	.0014	JU	−0.0447	s	GCVS 2012	o	94	3)
	55978.3862	.0013	JU	−0.0446		GCVS 2012	o	73	3)
V335 Cam	55642.3161	.0003	RAT RCR	−0.0070		GCVS 2012	-U-I	180	15)
V382 Cam	55645.3523	.0001	RAT RCR	+0.0196		GCVS 2012	-U-I	224	15)
V395 Cam	55616.3496	.0004	RAT RCR	+0.0256		GCVS 2012	-U-I	211	15)
	55649.3836	.0004	RAT RCR	+0.0272		GCVS 2012	-U-I	178	15)
V514 Cam	55645.5666	.0002	RAT RCR				-U-I	277	15)
EH Cnc	55887.5995	.0002	MS FR				o	590	6)
IL Cnc	55627.3762	.0002	RAT RCR	+0.0635	s	GCVS 2012	-U-I	182	15)
IU Cnc	55626.3803	.0002	RAT RCR	−0.0192	s	GCVS 2012	-U-I	189	15)
RS CVn	55700.5012	.0006	FR	−0.7137		GCVS 2012	-Ir	82	13)
TU CMi	55615.3947	.0014	MS FR	−0.0498		GCVS 2012	o	440	6)
BH CMi	48683.480	.001	WU				B	37	1)
TY Cap	55775.4426	.0002	RAT RCR				-U-I	187	15)
TW Cas	55807.4191	.0001	WLH	−0.0064		GCVS 2012	-Ir	299	4)

Table 1: (cont.)

Variable	HJD 24.....	±	Obs	$O-C$		Bibliography	Fil	n	Rem
XX Cas	55858.5329	.0231	AG	+0.0290	s	GCVS 2012	-Ir	61	13)
AB Cas	55804.4452	.0174	AG	+0.1156	s	GCVS 2012	-Ir	55	13)
AE Cas	55804.4133	.0013	AG	+0.0659		GCVS 2012	-Ir	55	13)
AH Cas	55944.3596	.0005	JU				o	92	3)
AL Cas	55804.4364	.0010	AG	+0.0070		GCVS 2012	-Ir	55	13)
AQ Cas	55808.0400	.0100	AG	−0.0369		GCVS 2012	-Ir	72	13)
AT Cas	55857.3723	.0097	AG	−0.0851		GCVS 2012	-Ir	81	13)
AX Cas	55820.3715	.0005	MS FR	−0.1014		GCVS 2012	o	750	6)
	55835.3807	.0009	JU	−0.1016		GCVS 2012	o	80	3)
	55858.5025	.0040	AG	−0.0943	s	GCVS 2012	-Ir	52	13)
BG Cas	55857.5738	.0064	AG	+0.4368		GCVS 2012	-Ir	81	13)
BH Cas	55838.3941	.0029	AG				-Ir	57	13)
	55838.5950	.0017	AG				-Ir	57	13)
	55857.2667	.0028	AG				-Ir	80	13)
	55857.4710	.0059	AG				-Ir	80	13)
BN Cas	55858.5343	.0078	AG	+0.5114		GCVS 2012	-Ir	61	13)
BS Cas	55858.4093	.0025	AG	−0.0187		IBVS 4778	-Ir	61	13)
	55858.6300	.0018	AG	−0.0182	s	IBVS 4778	-Ir	61	13)
	55859.2905	.0020	AG	−0.0184		IBVS 4778	-Ir	54	13)
	55859.5104	.0024	AG	−0.0188	s	IBVS 4778	-Ir	54	13)
BU Cas	55808.4239	.0024	AG	−0.0227		GCVS 2012	-Ir	26	13)
CR Cas	55836.4147	.0015	JU	+0.1482	s	GCVS 2012	o	61	3)
CW Cas	55884.2307	.0006	FR	−0.0031		GCVS 2012	o	43	14)
	55884.3893	.0007	FR	−0.0039	s	GCVS 2012	o	43	14)
DN Cas	55879.3873	.0123	AG	−0.0270	s	GCVS 2012	-Ir	64	13)
	55880.5433	.0002	RAT RCR	−0.0265		GCVS 2012	-U-I	358	15)
	55953.3388	.0035	PGL	−0.0261	s	GCVS 2012	V	208	12)
DP Cas	55807.4850	.0083	AG	+0.0071		GCVS 2012	-Ir	56	13)
DZ Cas	55787.4647	.0003	AG	−0.1711	s	GCVS 2012	-Ir	30	13)
EG Cas	55838.5382	.0038	AG	+0.0952		GCVS 2012	-Ir	56	13)
	55874.3050	.0022	AG	+0.0918	s	GCVS 2012	-Ir	56	13)
EN Cas	55856.6264	.0088	AG	+0.2601		GCVS 2012	-Ir	54	13)
	55874.3730	.0076	AG	+0.2558		GCVS 2012	-Ir	58	13)
EP Cas	55797.4460	.0012	AG	−0.0372	s	GCVS 2012	-Ir	30	13)
	55829.5771	.0001	RAT RCR	−0.0370		GCVS 2012	-U-I	274	15)
	55838.5258	.0020	AG	−0.0361		GCVS 2012	-Ir	66	13)
	55856.4211	.0024	AG	−0.0365		GCVS 2012	-Ir	54	13)
	55874.3166	.0013	AG	−0.0367		GCVS 2012	-Ir	56	13)
ES Cas	55874.3783	.0080	AG	−0.4700		GCVS 2012	-Ir	55	13)
EY Cas	55787.5147	.0006	AG	+0.0442		GCVS 2012	-Ir	31	13)
	55838.3641	.0018	AG	+0.0450	s	GCVS 2012	-Ir	56	13)
	55838.6043	.0004	AG	+0.0443		GCVS 2012	-Ir	56	13)
	55856.4374	.0020	AG	+0.0442		GCVS 2012	-Ir	54	13)
	55874.2698	.0018	AG	+0.0435		GCVS 2012	-Ir	61	13)
	55874.5118	.0019	AG	+0.0445	s	GCVS 2012	-Ir	61	13)
GG Cas	55879.2557	.0010	FR	−0.0655		GCVS 2012	-Ir	95	13)
	55894.2859	.0082	AG	−0.0702		GCVS 2012	-Ir	44	13)
GK Cas	55879.3925	.0028	AG	−0.3367		GCVS 2012	-Ir	65	13)
IL Cas	55884.4362	.0009	FR	+0.0003		BAVR 51,1	-Ir	38	13)
IQ Cas	55859.4361	.0097	AG	−0.2571		GCVS 2012	-Ir	55	13)
IR Cas	55815.4271	.0011	AG	+0.0086	s	GCVS 2012	-Ir	44	13)
	55839.5926	.0016	AG	+0.0097		GCVS 2012	-Ir	40	13)
	55873.2867	.0017	AG	+0.0099	s	GCVS 2012	-Ir	53	13)
IS Cas	55835.5128	.0001	RAT RCR	+0.0666		GCVS 2012	-U-I	328	15)
IT Cas	55828.5451	.0001	RAT RCR	+0.0636		GCVS 2012	-U-I	282	15)
	55836.3389	.0028	PGL	+0.0641		GCVS 2012	V	151	16)
	55873.5567	.0039	AG	+0.0573	s	GCVS 2012	-Ir	57	13)

Table 1: (cont.)

Variable	HJD 24.....	±	Obs	$O-C$		Bibliography	Fil	n	Rem
IV Cas	55775.4590	.0001	MS FR	−0.0896		GCVS 2012	o	825	6)
	55808.4092	.0002	MS FR	−0.0907		GCVS 2012	o	530	6)
	55851.3448	.0004	QU	−0.0917		GCVS 2012	V	77	4)
	55873.3127	.0010	AG	−0.0913		GCVS 2012	-Ir	53	13)
KR Cas	55797.5313	.0040	AG	−0.1522		GCVS 2012	-Ir	25	13)
MN Cas	55806.31 :	.00	MS FR	+0.01		GCVS 2012	o	992	6)
MS Cas	55857.6211	.0033	AG	+0.0421		GCVS 2012	-Ir	81	13)
MT Cas	55797.5418	.0087	AG	+0.0189	s	GCVS 2012	-Ir	23	13)
MV Cas	55857.6031	.0054	AG	−0.0991	s	GCVS 2012	-Ir	80	13)
NN Cas	55856.4737	.0086	AG	+0.1084	s	GCVS 2012	-Ir	54	13)
NU Cas	55787.6010	.0003	AG	−0.1366	s	GCVS 2012	-Ir	31	13)
	55797.5675	.0013	AG	−0.1369	s	GCVS 2012	-Ir	28	13)
	55856.6013	.0024	AG	−0.1376	s	GCVS 2012	-Ir	54	13)
	55874.2355	.0007	AG	−0.1371	s	GCVS 2012	-Ir	35	13)
OX Cas	55858.4661	.0057	AG	+0.0078	s	GCVS 2012	-Ir	61	13)
V344 Cas	55874.4168	.0021	AG	−0.1158	s	GCVS 2012	-Ir	48	13)
V345 Cas	55808.4653	.0008	AG	−0.0177		GCVS 2012	-Ir	26	13)
	55815.3537	.0010	AG	−0.0169		GCVS 2012	-Ir	44	13)
	55839.4607	.0003	AG	−0.0165		GCVS 2012	-Ir	40	13)
	55873.5566	.0064	AG	−0.0142	s	GCVS 2012	-Ir	52	13)
V350 Cas	55815.4763	.0020	AG	−0.0572		GCVS 2012	-Ir	44	13)
V357 Cas	55856.3299	.0030	AG	−0.0049	s	GCVS 2012	-Ir	54	13)
	55874.5936	.0047	AG	+0.0009	s	GCVS 2012	-Ir	47	13)
V359 Cas	55838.4792	.0068	AG	+0.0175	s	IBVS 5016	-Ir	56	13)
	55849.5615	.0002	RAT RCR	+0.0169		IBVS 5016	-U-I	295	15)
	55874.3362	.0007	MS FR	+0.0180		IBVS 5016	o	531	6)
	55874.3363	.0030	AG	+0.0181		IBVS 5016	-Ir	56	13)
V360 Cas	55873.4646	.0044	AG	−0.1029		GCVS 2012	-Ir	54	13)
	55882.4666	.0017	SCI	−0.1045		GCVS 2012	o	35	3)
V361 Cas	55787.3956	.0029	AG	−0.2046		GCVS 2012	-Ir	32	13)
	55905.3777	.0007	RAT RCR	−0.2050		GCVS 2012	-U-I	127	15)
V366 Cas	55858.3228	.0030	AG	−0.0205		IBVS 4798	-Ir	61	13)
V368 Cas	55883.3271	.0034	FR	−0.0298		GCVS 2012	-Ir	31	13)
V374 Cas	55797.5505	.0022	AG	+0.0206		GCVS 2012	-Ir	31	13)
	55856.5821	.0033	AG	+0.0204	s	GCVS 2012	-Ir	54	13)
	55874.3431	.0041	AG	+0.0197	s	GCVS 2012	-Ir	55	13)
V375 Cas	55878.3180	.0005	FR	+0.2515		BAVR 32,36	-Ir	79	13)
	55942.4127	.0007	QU	+0.2542	s	BAVR 32,36	V	97	4)
V381 Cas	55794.5174	.0032	AG	−0.0019	s	BAVR 32,36	-Ir	64	13)
V387 Cas	55858.5333	.0027	AG	+0.1089		GCVS 2012	-Ir	61	13)
V411 Cas	55797.4914	.0009	AG	+0.1740		GCVS 2012	-Ir	22	13)
V419 Cas	55879.2275	.0012	FR				-Ir	82	13)
V427 Cas	55874.3044	.0021	AG	−0.2274	s	GCVS 2012	-Ir	48	13)
V471 Cas	55817.3650	.0009	AG	−0.0713	s	GCVS 2012	-Ir	35	13)
	55817.5647	.0022	AG	−0.0396		GCVS 2012	-Ir	35	13)
	55894.3439	.0014	AG	−0.0359	s	GCVS 2012	-Ir	43	13)
	55894.5450	.0003	AG	−0.0028		GCVS 2012	-Ir	43	13)
V473 Cas	55817.4635	.0024	AG	−0.0195	s	IBVS 4669	-Ir	34	13)
	55856.3069	.0004	MS FR	−0.0217		IBVS 4669	o	426	6)
	55859.4233	.0033	AG	−0.0212	s	IBVS 4669	-Ir	54	13)
	55894.3234	.0024	AG	−0.0198	s	IBVS 4669	-Ir	44	13)
	55894.5285	.0014	AG	−0.0224		IBVS 4669	-Ir	44	13)
V520 Cas	55839.4508	.0027	AG	−0.1021	s	GCVS 2012	-Ir	43	13)
	55856.3509	.0027	AG	−0.0929		GCVS 2012	-Ir	54	13)
	55856.5946	.0022	AG	−0.0940	s	GCVS 2012	-Ir	54	13)
	55905.3308	.0002	RAT RCR	−0.0720		GCVS 2012	-U-I	136	15)
	55943.2919	.0015	JU	−0.0541	s	GCVS 2012	o	88	3)

Table 1: (cont.)

Variable	HJD 24.....	±	Obs	$O-C$		Bibliography	Fil	n	Rem
V523 Cas	55794.3984	.0008	AG	−0.0245		GCVS 2012	-Ir	64	13)
	55794.5140	.0005	AG	−0.0257	s	GCVS 2012	-Ir	64	13)
	55850.3669	.0002	JU	−0.0249	s	GCVS 2012	o	104	3)
	55850.4836	.0003	JU	−0.0250		GCVS 2012	o	104	3)
V544 Cas	55794.6022	.0029	AG				-Ir	64	13)
V546 Cas	55857.6239	.0043	AG	−0.0057		GCVS 2012	-Ir	81	13)
V608 Cas	55804.4469	.0006	AG				-Ir	55	13)
V651 Cas	55874.5883	.0018	AG	+0.0014	s	IBVS 3554	-Ir	56	13)
V765 Cas	55859.5542	.0093	AG				-Ir	54	13)
V776 Cas	55804.3990	.0163	AG				-Ir	55	13)
V860 Cas	55794.4123	.0173	AG				-Ir	64	13)
V952 Cas	55804.5716	.0024	AG	−0.0061		BAVM 148	-Ir	55	13)
V969 Cas	55858.2634	.0074	AG				-Ir	61	13)
V1001 Cas	55873.3517	.0010	AG	+0.0582	s	GCVS 2012	-Ir	53	13)
	55873.5637	.0017	AG	+0.0558		GCVS 2012	-Ir	53	13)
V1004 Cas	55851.5674	.0002	RAT RCR	+0.0961	s	GCVS 2012	-U-I	344	15)
V1011 Cas	55808.4448	.0025	AG	+0.0743	s	GCVS 2012	-Ir	33	13)
	55858.5540	.0035	AG	+0.0796	s	GCVS 2012	-Ir	61	13)
V1063 Cas	55873.5517	.0001	RAT RCR	+0.0595		GCVS 2012	-U-I	366	15)
V1094 Cas	55858.3200	.0015	AG	+0.0617		GCVS 2012	-Ir	61	13)
	55858.5773	.0035	AG	+0.0618	s	GCVS 2012	-Ir	61	13)
V1107 Cas	55858.2432	.0008	AG			GCVS 2012	-Ir	52	13)
	55858.3804	.0013	AG			GCVS 2012	-Ir	52	13)
	55858.5156	.0010	AG			GCVS 2012	-Ir	52	13)
	55893.2382	.0009	AG			GCVS 2012	-Ir	19	13)
V1115 Cas	55817.3613	.0029	AG	−0.0471	s	GCVS 2012	-Ir	34	13)
	55817.5199	.0015	AG	−0.0502		GCVS 2012	-Ir	34	13)
	55894.2998	.0007	AG	−0.0516	s	GCVS 2012	-Ir	43	13)
	55894.4585	.0015	AG	−0.0546		GCVS 2012	-Ir	43	13)
V1138 Cas	55817.4101	.0183	AG	+0.0061	s	GCVS 2012	-Ir	34	13)
	55859.3173	.0010	AG	+0.0043		GCVS 2012	-Ir	54	13)
	55894.4398	.0021	AG	+0.0030		GCVS 2012	-Ir	44	13)
V1139 Cas	55817.4526	.0012	AG	+0.0115	s	GCVS 2012	-Ir	34	13)
	55894.2537	.0021	AG	+0.0123		GCVS 2012	-Ir	43	13)
	55894.4005	.0013	AG	+0.0105	s	GCVS 2012	-Ir	43	13)
XX Cep	55867.3026	.0006	JU	−0.0065		GCVS 2012	o	60	3)
BE Cep	55874.3478	.0014	AG	−0.1064		GCVS 2012	-Ir	48	13)
	55874.5606	.0021	AG	+0.1064		GCVS 2012	-Ir	48	13)
BU Cep	55807.4984	.0014	AG	−0.3493		GCVS 2012	-Ir	56	13)
CM Cep	55831.5141	.0001	RAT RCR	−0.0362		GCVS 2012	-U-I	287	15)
CW Cep	55858.3854	.0026	JU	+0.0110		GCVS 2012	o	55	3)
	55873.3583	.0010	FR	−0.0336	s	GCVS 2012	-Ir	36	13)
DL Cep	55802.4455	.0055	AG	+0.0014	s	IBVS 5016	-Ir	33	13)
DP Cep	55874.5702	.0019	AG	−0.0581		GCVS 2012	-Ir	48	13)
DW Cep	55874.3117	.0002	RAT RCR	+0.4619		GCVS 2012	-U-I	220	15)
EF Cep	55796.4009	.0009	JU	−0.0496	s	GCVS 2012	o	48	3)
HI Cep	55879.2615	.0002	RAT RCR				-U-I	137	15)
IM Cep	55807.4845	.0025	AG	−0.1564		GCVS 2012	-Ir	56	13)
IW Cep	55801.5429	.0102	AG	+0.0408	s	GCVS 2012	-Ir	41	13)
KP Cep	55802.5508	.0018	AG	+0.0411		GCVS 2012	-Ir	34	13)
	55808.3606	.0034	AG	+0.0456		GCVS 2012	-Ir	26	13)
KV Cep	55801.3448	.0017	AG	+0.1068		GCVS 2012	-Ir	41	13)
	55806.4978	.0049	AG	+0.1104		GCVS 2012	-Ir	47	13)
	55873.4865	.0027	AG	+0.1572		GCVS 2012	-Ir	48	13)
LM Cep	55787.5582	.0074	AG	+0.1312		GCVS 2012	-Ir	35	13)
	55807.4078	.0015	JU	+0.1040		GCVS 2012	o	45	3)
LP Cep	55787.5551	.0033	AG	−0.0702	s	GCVS 2012	-Ir	41	13)
NN Cep	55807.5071	.0103	AG	+0.0093		GCVS 2012	-Ir	56	13)
	55873.3692	.0001	FR	+0.0057		GCVS 2012	-Ir	23	13)
NW Cep	55805.3846	.0033	AG	−0.4724		GCVS 2012	-Ir	30	13)

Table 1: (cont.)

Variable	HJD 24.....	±	Obs	$O-C$		Bibliography	Fil	n	Rem
V737 Cep	55787.3664	.0007	AG	+0.0079	s	GCVS 2012	-Ir	32	13)
V743 Cep	55806.3265	.0024	AG				-Ir	81	13)
V744 Cep	55837.5519	.0006	RAT RCR				-U-I	278	15)
RZ Com	55662.3559	.0002	RAT RCR	+0.0445		GCVS 2012	-U-I	135	15)
SS Com	55663.3683	.0005	RAT RCR	−0.0199		BAVR 33,152	-U-I	110	15)
EQ Com	55615.4990	.0004	MS FR	+0.0316		GCVS 2012	o	371	6)
LL Com	55683.4223	.0003	RAT RCR	+0.0439	s	IBVS 4386	-U-I	131	15)
LO Com	55650.3766	.0003	RAT RCR				-U-I	124	15)
MR Com	55673.3606	.0003	RAT RCR	−0.0444	s	GCVS 2012	-U-I	142	15)
RT CrB	55775.3971	.0014	FR	−0.0169	s	GCVS 2012	V	30	14)
RW CrB	55662.41	.01	FR	+0.00	s	GCVS 2012	V	20	14)
	55775.3713	.0001	FR	+0.0005		GCVS 2012	V	60	14)
	55776.4636	.0017	FR	+0.0032	s	GCVS 2012	V	43	14)
TW CrB	55775.427	.001	FR	+0.044		GCVS 2012	V	63	14)
AR CrB	55775.3756	.0006	FR	−0.0050	s	GCVS 2012	V	53	14)
SY Cyg	55707.584 :	.005	FR	+0.278	s	GCVS 2012	-Ir	23	13)
VW Cyg	55836.4577	.0004	FR	+0.2683		GCVS 2012	-Ir	82	13) 21)
WZ Cyg	55882.2587	.0002	RAT RCR	+0.0654	s	GCVS 2012	-U-I	99	15)
CG Cyg	55837.3774	.0014	DIE	+0.0648		GCVS 2012	o	32	19)
	55856.3151	.0011	DIE	+0.0682		GCVS 2012	o	31	19)
CV Cyg	55873.2695	.0004	RAT RCR	+0.2063		GCVS 2012	-U-I	253	15)
DO Cyg	55802.4831	.0031	AG	−0.0241		GCVS 2012	-Ir	34	13)
	55850.3645	.0013	AG	−0.0230		GCVS 2012	-Ir	50	13)
	55879.4344	.0009	AG	−0.0232		GCVS 2012	-Ir	34	13)
DP Cyg	55795.3838	.0021	AG	−0.3662		GCVS 2012	-Ir	39	13)
	55802.4253	.0026	AG	−0.2397	s	GCVS 2012	-Ir	34	13)
	55815.3323	.0019	AG	+1.1423		GCVS 2012	-Ir	49	13)
	55849.3621	.0049	AG	+0.5971	s	GCVS 2012	-Ir	55	13)
	55850.5339	.0137	AG	−0.5361		GCVS 2012	-Ir	49	13)
EM Cyg	55405.413	.001	PGL				V	116	12)
	55824.3905	.0056	PGL				V	293	12)
	55836.4061	.0035	PGL				V	304	12)
GG Cyg	55801.3626	.0018	AG	+0.1428		GCVS 2012	-Ir	44	13)
GV Cyg	55858.4211	.0037	AG	+0.1541		GCVS 2012	-Ir	42	13)
KR Cyg	55801.3912	.0014	AG	+0.0166		GCVS 2012	-Ir	44	13)
MR Cyg	55858.5951	.0027	AG	−0.0001		GCVS 2012	V	42	13)
PQ Cyg	55799.3886	.0008	AG	+0.0270		GCVS 2012	-Ir	35	13)
V370 Cyg	55707.4842	.0012	FR	−0.0277	s	GCVS 2012	-Ir	36	13)
	55885.2416	.0002	RAT RCR	−0.0281		GCVS 2012	-U-I	134	15)
V401 Cyg	55778.5087	.0019	FR	+0.0709	s	GCVS 2012	V	32	14)
	55794.5369	.0061	FR	+0.0743		GCVS 2012	o	38	14)
	55804.4421	.0021	AG	+0.0732		GCVS 2012	-Ir	34	13)
	55849.3117	.0002	RAT RCR	+0.0732		GCVS 2012	-U-I	213	15)
V442 Cyg	55799.4673	.0016	AG	−0.0415		GCVS 2012	-Ir	35	13)
V443 Cyg	55799.5126	.0020	AG	+0.0330		GCVS 2012	-Ir	35	13)
V447 Cyg	55804.5007	.0096	AG	+0.1140	s	GCVS 2012	-Ir	34	13)
	55856.3337	.0011	FR	+0.1157		GCVS 2012	-Ir	51	13)
V453 Cyg	54718.5100	.0046	FR	+0.0363	s	GCVS 2012	-Ir	50	8)
	55856.3105	.0006	FR	+0.0666		GCVS 2012	-Ir	71	13)
V454 Cyg	55799.5210	.0091	AG	−0.0093	s	GCVS 2012	-Ir	35	13)
V463 Cyg	55857.3263	.0002	RAT RCR	+0.0560		GCVS 2012	-U-I	241	15)
V466 Cyg	55794.4381	.0004	AG	+0.0064		GCVS 2012	-Ir	37	13)
	55794.4396	.0013	FR	+0.0079		GCVS 2012	o	36	14)
V469 Cyg	55836.3391	.0001	FR	−0.1363		GCVS 2012	-Ir	95	13)
	55874.4014	.0004	FR	−0.1370		GCVS 2012	-Ir	37	13)
V484 Cyg	55790.5278	.0060	AG	+0.1215		GCVS 2012	-Ir	37	13)
	55799.5832	.0010	AG	+0.1201		GCVS 2012	-Ir	33	13)

Table 1: (cont.)

Variable	HJD 24.....	±	Obs	$O-C$		Bibliography	Fil	n	Rem
V488 Cyg	55801.3385	.0040	AG	+0.0569		GCVS 2012	-Ir	44	13)
	55801.6116	.0004	AG	+0.0498	s	GCVS 2012	-Ir	44	13)
	55829.3614	.0012	FR	+0.0542		GCVS 2012	o	45	14)
	55838.3274	.0034	AG	+0.0520		GCVS 2012	-Ir	40	13)
V494 Cyg	55836.5552	.0011	FR				-Ir	88	13)
V496 Cyg	55799.5089	.0031	AG	+0.0076		GCVS 2012	-Ir	35	13)
V502 Cyg	55851.3197	.0012	SCI	+0.1249		GCVS 2012	o	33	3)
V505 Cyg	55799.5023	.0022	AG	+0.0342	s	GCVS 2012	-Ir	35	13)
V512 Cyg	55851.4710	.0040	FR	+0.1221		GCVS 2012	o	41	14)
V541 Cyg	55794.4734	.0017	AG	+0.1347	s	GCVS 2012	V	38	13)
V616 Cyg	55815.3787	.0028	AG	−0.3260		GCVS 2012	-Ir	37	13)
V635 Cyg	55815.3887	.0041	AG	−0.0521	s	GCVS 2012	-Ir	37	13)
V675 Cyg	55815.3947	.0053	AG	+0.6178		GCVS 2012	-Ir	38	13)
V680 Cyg	55815.3907	.0046	AG	+0.0175		BAVR 32,36	-Ir	37	13)
V700 Cyg	55799.3959	.0007	AG	−0.0622		GCVS 2012	-Ir	35	13)
	55799.5409	.0011	AG	−0.0872	s	GCVS 2012	-Ir	35	13)
V711 Cyg	55799.4485	.0146	AG	−0.0712		GCVS 2012	-Ir	28	13)
	55815.5668	.0009	AG	−0.0747	s	GCVS 2012	-Ir	37	13)
V725 Cyg	55801.5481	.0049	AG	+0.2364	s	GCVS 2012	-Ir	44	13)
	55829.3734	.0038	FR	+0.2601	s	GCVS 2012	o	22	14)
V728 Cyg	55832.3689	.0001	FR	+0.0482		GCVS 2012	-Ir	82	13)
	55835.4599	.0013	FR	+0.0490	s	GCVS 2012	-Ir	46	13)
V753 Cyg	55671.5208	.0012	FR	+0.0022		BAVM 69	o	29	14)
V789 Cyg	54639.4796	.0003	AG	+0.0594		GCVS 2012	-Ir	42	13)
	55478.2920	.0003	AG	+0.0501		GCVS 2012	-Ir	33	13)
	55794.4722	.0014	AG	−0.0230		GCVS 2012	-Ir	37	13)
V796 Cyg	55776.4318	.0002	RAT RCR	−0.0014		GCVS 2012	-U-I	163	15)
V859 Cyg	55791.5635	.0019	AG	+0.0204		GCVS 2012	-Ir	30	13)
V869 Cyg	55826.4872	.0005	FR	+0.1238	s	GCVS 2012	-Ir	40	13)
V873 Cyg	55838.3076	.0017	FR	−0.0395	s	GCVS 2012	-Ir	47	13)
V877 Cyg	55794.4754	.0017	AG	+0.0246		GCVS 2012	-Ir	37	13)
	55804.5522	.0011	FR	+0.0242		GCVS 2012	-Ir	46	13)
V889 Cyg	55794.5221	.0036	AG	−0.1853	s	GCVS 2012	V	37	13)
	55794.5287	.0074	FR	−0.1787	s	GCVS 2012	o	18	14)
V891 Cyg	55802.4346	.0005	FR	+0.0461		GCVS 2012	-Ir	53	13)
V907 Cyg	55802.5293	.0008	FR	+0.1067		GCVS 2012	-Ir	29	13)
V931 Cyg	55801.3831	.0008	AG	−0.0715		GCVS 2012	-Ir	44	13)
	55801.5526	.0008	AG	−0.0728	s	GCVS 2012	-Ir	44	13)
V934 Cyg	55801.4370	.0028	AG	−0.0748		GCVS 2012	-Ir	44	13)
V941 Cyg	55791.5031	.0036	AG	−0.0721		GCVS 2012	-Ir	34	13)
V947 Cyg	55837.2973	.0002	FR	−0.0027	s	GCVS 2012	-Ir	103	13)
	55837.5129	.0007	FR	−0.0017		GCVS 2012	-Ir	103	13)
V959 Cyg	55801.5003	.0025	AG	−0.0535		GCVS 2012	-Ir	44	13)
V961 Cyg	55804.4471	.0016	AG	−0.0822	s	GCVS 2012	-Ir	34	13)
V962 Cyg	55790.4844	.0134	AG	−0.2060		GCVS 2012	-Ir	34	13)
V963 Cyg	55837.4140	.0001	FR	−0.0010		GCVS 2012	-Ir	77	13)
V965 Cyg	55791.4779	.0050	AG	−0.1199		GCVS 2012	-Ir	30	13)
	55837.2704	.0027	FR	−0.1283	s	GCVS 2012	-Ir	112	13)
V974 Cyg	55790.4192	.0037	AG	−0.1604		GCVS 2012	-Ir	36	13)
	55801.5472	.0018	AG	−0.1802	s	GCVS 2012	-Ir	44	13)
V975 Cyg	55804.4923	.0010	AG	−0.1264		GCVS 2012	-Ir	33	13)
V1004 Cyg	55790.3825	.0011	AG	+0.1588	s	GCVS 2012	-Ir	37	13)
	55794.4978	.0016	AG	+0.1599	s	GCVS 2012	-Ir	37	13)
	55804.4432	.0022	AG	+0.1626		GCVS 2012	-Ir	32	13)
V1011 Cyg	55794.6075	.0018	AG	+0.0442		GCVS 2012	-Ir	63	13)
	55833.4810	.0009	FR	+0.0453		GCVS 2012	-Ir	39	13)
V1013 Cyg	55833.4748	.0008	FR	+0.1637		GCVS 2012	-Ir	33	13)
V1034 Cyg	55838.3506	.0095	AG	+0.0062	s	GCVS 2012	-Ir	36	13)
V1061 Cyg	55851.5121	.0134	FR	−0.0135	s	GCVS 2012	o	21	14)
V1083 Cyg	55806.3751	.0002	RAT RCR	−0.0674		GCVS 2012	-U-I	138	15)

Table 1: (cont.)

Variable	HJD 24.....	±	Obs	$O-C$		Bibliography	Fil	n	Rem
V1141 Cyg	55833.3018	.0002	RAT RCR	+0.0155		GCVS 2012	-U-I	161	15)
V1147 Cyg	55837.4174	.0003	FR	+0.2291	s	GCVS 2012	-Ir	61	13)
V1171 Cyg	55790.5487	.0036	AG	−0.0553	s	GCVS 2012	-Ir	36	13)
	55889.2390	.0002	RAT RCR	−0.0584		GCVS 2012	-U-I	115	15)
V1256 Cyg	55802.5041	.0008	FR	−0.0229		GCVS 2012	-Ir	61	13)
V1305 Cyg	55799.4956	.0046	AG	−0.0076		GCVS 2012	-Ir	35	13)
V1401 Cyg	55858.5427	.0064	AG	+0.2700		GCVS 2012	-Ir	41	13)
V1411 Cyg	55805.4293	.0080	AG	−0.1546	s	GCVS 2012	-Ir	31	13)
	55839.6062	.0021	AG	−0.1542	s	GCVS 2012	-Ir	46	13)
V1414 Cyg	55799.5736	.0022	AG	+0.0463		GCVS 2012	-Ir	28	13)
V1417 Cyg	55799.5292	.0098	AG	+0.1565		GCVS 2012	-Ir	28	13)
	55839.5037	.0115	AG	+0.1584		GCVS 2012	-Ir	42	13)
V1437 Cyg	55804.4208	.0009	FR				-Ir	47	13)
	55838.2826	.0010	FR				-Ir	44	13)
V1481 Cyg	55795.4198	.0050	AG				-Ir	38	13)
	55806.4689	.0112	AG				-Ir	43	13)
V1763 Cyg	55820.3807	.0002	RAT RCR				-U-I	161	15)
	55851.3688	.0002	RAT RCR				-U-I	217	15)
V1815 Cyg	55848.330 :	.001	FR	+0.003		BAVR 55,1	-Ir	32	13)
V1823 Cyg	55836.5287	.0002	FR				-Ir	54	13)
V1908 Cyg	55825.5540	.0005	RAT RCR				-U-I	228	15)
V1918 Cyg	55671.5979	.0010	FR				o	29	14)
	55830.4699	.0035	PGL				V	200	12)
V2080 Cyg	55671.5356	.0015	FR				o	29	14)
V2181 Cyg	55801.5666	.0119	AG	+0.0093	s	BAVR 50,45	-Ir	44	13)
	55829.3826	.0004	FR	+0.0115		BAVR 50,45	o	45	14)
V2240 Cyg	55799.5628	.0037	AG				-Ir	35	13)
V2261 Cyg	55795.5499	.0032	AG				-Ir	38	13)
V2263 Cyg	55795.4239	.0049	AG				-Ir	38	13)
	55806.4223	.0041	AG				-Ir	43	13)
V2277 Cyg	55834.4488	.0002	RAT RCR				-U-I	216	15)
V2364 Cyg	55838.3043	.0003	RAT RCR	−0.0136	s	GCVS 2012	-U-I	171	15)
	55848.3708	.0003	RAT RCR	−0.0135	s	GCVS 2012	-U-I	125	15)
V2456 Cyg	55825.5819	.0005	RAT RCR	+0.1023	s	GCVS 2012	-U-I	228	15)
Z Dra	55685.4249	.0001	RAT RCR	−0.1936		GCVS 2012	-U-I	264	15)
RR Dra	55831.3486	.0002	RAT RCR	+0.0210		GCVS 2012	-U-I	167	15)
TZ Dra	55825.3342	.0009	JU	−0.0310		GCVS 2012	o	74	3)
WX Dra	55867.3164	.0015	SCI	+0.0205		GCVS 2012	o	19	3)
AU Dra	55710.4184	.0018	SCI	+0.0156		GCVS 2012	o	32	3)
AX Dra	55602.5275	.0001	RAT RCR	−0.0031		BAVR 32,36	-U-I	255	15)
MU Dra	55832.3045	.0004	RAT RCR	−0.0511		GCVS 2012	-U-I	142	15)
MY Dra	55672.5395	.0002	RAT RCR				-U-I	303	15)
AV Gem	55907.4267	.0030	BHE	−0.0322		GCVS 2012	-Ir	85	17)
FT Gem	55624.4982	.0005	FR	−0.0400	s	GCVS 2012	-Ir	125	13)
GQ Gem	54513.3919	.0030	SB	+0.0173	s	GCVS 2012	V	44	11)
GZ Gem	54506.3515	.0030	SB	−0.0743	s	GCVS 2012	V	35	11)
AK Her	55751.4745	.0035	PGL	+0.0147		GCVS 2012	V	806	12)
	55774.4446	.0035	PGL	+0.0097	s	GCVS 2012	V	182	12)
V342 Her	55689.5248	.0003	RAT RCR	+0.0196		GCVS 2012	-U-I	173	15)
V490 Her	55699.5882	.0014	SCI	+0.3831		GCVS 2012	o	20	3)
V857 Her	55673.3859	.0003	MS FR				o	344	6)
V1054 Her	55682.5241	.0003	RAT RCR				-U-I	186	15)
V1055 Her	55705.4968	.0001	RAT RCR				-U-I	226	15)
V1062 Her	54937.5694	.0009	AG				-Ir	40	13)
V1066 Her	55711.4536	.0003	RAT RCR				-U-I	173	15)
V1073 Her	55829.3747	.0001	RAT RCR				-U-I	213	15)
V1092 Her	55675.6014	.0004	RAT RCR	+0.0443		GCVS 2012	-U-I	197	15)
	55707.5176	.0003	RAT RCR	+0.0460		GCVS 2012	-U-I	207	15)
V1100 Her	55683.5486	.0001	RAT RCR	+0.0627	s	GCVS 2012	-U-I	213	15)
V1101 Her	55828.4344	.0002	RAT RCR	+0.0268		GCVS 2012	-U-I	222	15)

Table 1: (cont.)

Variable	HJD 24.....	±	Obs	$O-C$		Bibliography	Fil	n	Rem
V1103 Her	55691.4854	.0002	RAT RCR	+0.0017	s	GCVS 2012	-U-I	233	15)
WY Hya	55629.3380	.0001	RAT RCR	+0.0298		GCVS 2012	-U-I	108	15)
V470 Hya	55629.3279	.0007	RAT RCR				-U-I	108	15)
SW Lac	55740.5287	.0001	FR	+0.0580		GCVS 2012	-Ir	71	13)
	55741.4916	.0035	PGL	+0.0587		GCVS 2012	V	187	16)
	55825.3561	.0005	DIE	+0.0548	s	GCVS 2012	o	37	19)
	55834.3409	.0056	PGL	+0.0594	s	GCVS 2012	V	339	12)
	55851.3393	.0014	AG	+0.0596	s	GCVS 2012	V	63	13)
	55851.4977	.0033	AG	+0.0576		GCVS 2012	V	63	13)
UY Lac	55887.2452	.0010	AG				-Ir	69	13)
VV Lac	55801.4879	.0034	AG	−0.8282		GCVS 2012	-Ir	41	13)
	55839.4833	.0039	AG	−0.8345		GCVS 2012	-Ir	43	13)
VY Lac	55849.5890	.0011	AG	−0.1692		GCVS 2012	-Ir	50	13)
	55858.3951	.0039	AG	−0.1713	s	GCVS 2012	V	41	13)
ZZ Lac	55815.3652	.0029	AG	−0.1653	s	GCVS 2012	-Ir	44	13)
AG Lac	55801.3359	.0011	AG	−0.0181	s	GCVS 2012	-Ir	41	13)
	55851.3574	.0040	AG	−0.0166		GCVS 2012	-Ir	44	13)
AU Lac	55839.5143	.0029	AG	−0.0296		GCVS 2012	-Ir	48	13)
	55881.2866	.0013	JU	−0.0305		GCVS 2012	o	24	3)
AW Lac	55849.3619	.0052	AG	+0.0494		BAVR 35,1	-Ir	55	13)
BB Lac	55799.5116	.0016	AG	−0.5971		GCVS 2012	-Ir	28	13)
CG Lac	55839.5061	.0016	AG	−0.1566		GCVS 2012	-Ir	41	13)
	55849.3386	.0027	AG	−0.1568		GCVS 2012	-Ir	50	13)
	55858.3525	.0015	AG	−0.1562		GCVS 2012	-Ir	41	13)
CN Lac	55858.3599	.0022	AG	−0.0757	s	GCVS 2012	-Ir	42	13)
	55879.3943	.0062	AG	−0.0746	s	GCVS 2012	-Ir	34	13)
	55887.3587	.0012	AG	−0.0774		GCVS 2012	-Ir	35	13)
CO Lac	55861.3380	.0011	JU	−0.0022		GCVS 2012	o	80	3)
	55874.4475	.0016	AG	−0.0014	s	GCVS 2012	-Ir	48	13)
CY Lac	55795.5436	.0047	AG	+0.6784	s	GCVS 2012	-Ir	39	13)
	55887.5117	.0017	AG	+0.6775	s	GCVS 2012	-Ir	51	13)
DG Lac	55848.5406	.0001	RAT RCR	−0.2246		GCVS 2012	-U-I	249	15)
EK Lac	55796.3628	.0004	RAT RCR	−0.0032		GCVS 2012	-U-I	86	15)
	55799.4379	.0020	AG	−0.0027		GCVS 2012	-Ir	28	13)
	55839.4076	.0011	AG	−0.0032		GCVS 2012	-Ir	45	13)
	55879.3777	.0027	AG	−0.0034		GCVS 2012	-Ir	34	13)
EM Lac	55801.3767	.0006	AG	+0.0869		GCVS 2012	-Ir	41	13)
	55801.5709	.0016	AG	+0.0865	s	GCVS 2012	-Ir	41	13)
	55806.4354	.0015	AG	+0.0868		GCVS 2012	-Ir	47	13)
	55850.4078	.0023	AG	+0.0871		GCVS 2012	-Ir	52	13)
	55850.6014	.0010	AG	+0.0862	s	GCVS 2012	-Ir	52	13)
EO Lac	55802.5535	.0012	AG	+0.2804		GCVS 2012	-Ir	34	13)
EP Lac	55805.4152	.0050	AG	−0.3632		GCVS 2012	-Ir	29	13)
	55879.4212	.0017	AG	−0.3669		GCVS 2012	-Ir	33	13)
EQ Lac	55858.4399	.0023	AG	+0.0201		GCVS 2012	-Ir	41	13)
ER Lac	55849.3418	.0091	AG	−0.5551		GCVS 2012	-Ir	55	13)
ES Lac	55801.5074	.0100	AG	+0.1390		GCVS 2012	-Ir	41	13)
	55850.5652	.0068	AG	+0.1439		GCVS 2012	-Ir	49	13)
EU Lac	55839.3657	.0036	AG	+0.2061		GCVS 2012	-Ir	43	13)
EX Lac	55806.4877	.0138	AG	+0.2332	s	GCVS 2012	-Ir	46	13)
	55873.4508	.0055	AG	+0.2335		GCVS 2012	-Ir	51	13)
	55887.3634	.0017	AG	+0.2317		GCVS 2012	-Ir	35	13)
EY Lac	55851.3309	.0030	AG	−0.3725	s	GCVS 2012	-Ir	43	13)
FI Lac	55874.6043	.0045	AG	+0.0195		GCVS 2012	-Ir	48	13)
FL Lac	55815.4513	.0024	AG	−0.0463		GCVS 2012	-Ir	44	13)
	55851.4387	.0193	AG	−0.0469	s	GCVS 2012	-Ir	43	13)
	55887.4266	.0028	AG	−0.0470		GCVS 2012	-Ir	35	13)
GH Lac	55799.3887	.0007	AG	−0.0627	s	GCVS 2012	-Ir	28	13)
	55808.4437	.0006	AG	−0.0626	s	GCVS 2012	-Ir	28	13)
	55879.2817	.0014	AG	−0.0664	s	GCVS 2012	-Ir	34	13)

Table 1: (cont.)

Variable	HJD 24.....	±	Obs	$O-C$		Bibliography	Fil	n	Rem
GX Lac	55834.5156	.0002	RAT RCR	−0.0354		GCVS 2012	-U-I	287	15)
HR Lac	55799.4061	.0025	AG	−0.1066		GCVS 2012	-Ir	28	13)
	55802.4095	.0023	AG	−0.1067		GCVS 2012	-Ir	34	13)
IM Lac	55801.5575	.0023	AG	−0.1894	s	GCVS 2012	-Ir	41	13)
	55850.3900	.0021	AG	−0.1883		GCVS 2012	-Ir	51	13)
IP Lac	55802.5816	.0022	AG	+0.0822		GCVS 2012	-Ir	34	13)
IU Lac	55839.5433	.0027	AG	+0.0131		GCVS 2012	-Ir	42	13)
	55873.4638	.0082	AG	+0.0166		GCVS 2012	-Ir	51	13)
IZ Lac	55815.4039	.0148	AG	+0.0575		GCVS 2012	-Ir	36	13)
	55849.3554	.0055	AG	+0.0567	s	GCVS 2012	-Ir	55	13)
	55851.3580	.0131	AG	+0.0621		GCVS 2012	-Ir	43	13)
KU Lac	55873.4426	.0020	AG				-Ir	47	13)
LY Lac	55851.3819	.0042	AG	+0.2321		GCVS 2012	-Ir	43	13)
LZ Lac	55849.4313	.0042	AG	−0.2854	s	GCVS 2012	-Ir	55	13)
MZ Lac	55849.4955	.0008	AG	+0.1647		GCVS 2012	-Ir	60	13)
	55887.4017	.0008	AG	+0.1653		GCVS 2012	-Ir	35	13)
NR Lac	55808.4287	.0183	AG	+0.0689	s	GCVS 2012	-Ir	28	13)
	55887.3543	.0024	AG	+0.0676		GCVS 2012	-Ir	35	13)
OO Lac	55850.4865	.0001	AG	+0.1559		GCVS 2012	-Ir	49	13)
OS Lac	55849.5567	.0062	AG	+0.3110	s	GCVS 2012	-Ir	55	13)
OX Lac	55808.3933	.0006	AG	+0.1521		GCVS 2012	-Ir	26	13)
PP Lac	55801.3708	.0013	AG	−0.0551		GCVS 2012	-Ir	41	13)
	55801.5708	.0010	AG	−0.0557	s	GCVS 2012	-Ir	41	13)
	55815.4110	.0012	AG	−0.0556		GCVS 2012	-Ir	44	13)
	55815.6116	.0013	AG	−0.0556	s	GCVS 2012	-Ir	44	13)
	55851.3146	.0015	AG	−0.0561	s	GCVS 2012	-Ir	43	13)
	55851.5153	.0005	AG	−0.0560		GCVS 2012	-Ir	43	13)
	55882.4046	.0007	JU	−0.0562		GCVS 2012	o	66	3)
V339 Lac	55873.4128	.0117	AG	+0.1439		GCVS 2012	-Ir	51	13)
V342 Lac	55808.4198	.0018	AG	−0.0795		GCVS 2012	-Ir	26	13)
	55849.4021	.0052	AG	−0.0810	s	GCVS 2012	-Ir	55	13)
	55851.5033	.0033	AG	−0.0815	s	GCVS 2012	-Ir	43	13)
V344 Lac	55839.3042	.0023	AG	−0.0781		GCVS 2012	-Ir	44	13)
	55839.4988	.0033	AG	−0.0797	s	GCVS 2012	-Ir	44	13)
	55849.3067	.0012	AG	−0.0774	s	GCVS 2012	-Ir	58	13)
	55849.5019	.0019	AG	−0.0784		GCVS 2012	-Ir	58	13)
V345 Lac	55805.4147	.0029	AG	+0.0783		GCVS 2012	-Ir	29	13)
	55815.5456	.0015	AG	+0.1701	s	GCVS 2012	-Ir	37	13)
	55850.3632	.0047	AG	+0.0756		GCVS 2012	-Ir	49	13)
V364 Lac	55740.4345	.0003	FR	−0.0097		BAVR 47,33	-Ir	51	13)
	55832.4147	.0083	PGL	+0.0160	s	BAVR 47,33	V	613	12)
V441 Lac	55806.4070	.0027	AG	−0.0452	s	IBVS 5024	-Ir	47	13)
	55806.5648	.0021	AG	−0.0418		IBVS 5024	-Ir	47	13)
V441 Lac	55808.4186	.0021	AG	−0.0414		IBVS 5024	-Ir	28	13)
	55839.3121	.0020	AG	−0.0373		IBVS 5024	-Ir	42	13)
	55839.4642	.0039	AG	−0.0396	s	IBVS 5024	-Ir	42	13)
	55873.2928	.0021	AG	−0.0349		IBVS 5024	-Ir	51	13)
V459 Lac	55805.4860	.0025	AG	−0.6494		GCVS 2012	-Ir	29	13)
	55858.5276	.0022	AG	+0.2392	s	GCVS 2012	-Ir	41	13)
RW Leo	55654.3816	.0003	RAT RCR	−0.1233		GCVS 2012	-U-I	127	15)
WZ Leo	55601.3679	.0002	RAT RCR	+0.2223		GCVS 2012	-U-I	123	15)
XX LMi	55625.5702	.0006	RAT RCR	+0.0043	s	GCVS 2012	-U-I	228	15)
XY LMi	55625.6233	.0002	RAT RCR	−0.0210		GCVS 2012	-U-I	228	15)
	55641.3516	.0002	RAT RCR	−0.0207		GCVS 2012	-U-I	150	15)
SW Lyn	55670.3553	.0001	RAT RCR	+0.0621		GCVS 2012	-U-I	88	15)
SX Lyn	55618.5343	.0001	RAT RCR	+0.0112		GCVS 2012	-U-I	300	15)
UU Lyn	55857.5883	.0003	MS FR	−0.0092		GCVS 2012	o	512	6)
TZ Lyr	55850.374 :	.005	FR	−0.002	s	GCVS 2012	o	28	14)
ET Lyr	55790.4155	.0084	AG				-Ir	35	13)

Table 1: (cont.)

Variable	HJD 24.....	±	Obs	$O-C$		Bibliography	Fil	n	Rem
IP Lyr	55592.6665	.0002	MS FR	−0.0091		GCVS 2012	o	544	6)
	55833.3234	.0007	JU	−0.0103		GCVS 2012	o	57	3)
NY Lyr	55857.3958	.0002	FR	−0.0788		GCVS 2012	-Ir	53	13)
PV Lyr	55791.4517	.0074	AG	+0.0073		GCVS 2012	-Ir	30	13)
QT Lyr	55794.4924	.0028	AG				-Ir	37	13)
QU Lyr	55794.4247	.0013	AG	+0.0001	s	GCVS 2012	-Ir	37	13)
V417 Lyr	55615.6343	.0012	MS FR				o	380	6)
V563 Lyr	55850.3094	.0029	FR				o	29	14)
V580 Lyr	55794.4092	.0006	JU				o	48	3)
GU Mon	55866.6060	.0005	MS FR	−0.0896		GCVS 2012	o	520	6)
IX Mon	55592.3297	.0001	MS FR	−0.0364		GCVS 2012	o	737	6)
V453 Mon	55593.3001	.0003	MS FR	+0.1607	s	GCVS 2012	o	396	6)
V515 Mon	55600.3340	.0002	RAT RCR	−0.0407		GCVS 2012	-U-I	120	15)
V527 Mon	55593.3998	.0004	MS FR	−0.0280		GCVS 2012	o	222	6)
V530 Mon	55941.4532	.0069	PGL	−0.1286		GCVS 2012	V	236	16)
V634 Mon	55851.6314	.0010	MS FR	+0.1125		GCVS 2012	o	540	6)
V456 Oph	55676.5346	.0001	RAT RCR	+0.0160		GCVS 2012	-U-I	160	15)
V913 Oph	55674.5605	.0002	RAT RCR	+0.3055		GCVS 2012	-U-I	190	15)
V2388 Oph	55754.4974	.0014	FR				V	25	14)
V2640 Oph	55706.5133	.0003	RAT RCR				-U-I	188	15)
FT Ori	55941.4222	.0001	PGL	+0.0167		GCVS 2012	V	165	12)
V1633 Ori	55856.6377	.0004	MS FR	+0.2106	s	BAVM 125	o	484	6)
V1865 Ori	55943.4082	.0015	QU				V	105	4)
U Peg	55857.3681	.0012	AG	−0.0210		BAVR 45,3	V	75	13)
	55857.5549	.0026	AG	−0.0216	s	BAVR 45,3	V	75	13)
BB Peg	55831.2683	.0015	BHE	−0.0052		GCVS 2012	-Ir	87	17)
	55857.2983	.0005	DIE	−0.0034		GCVS 2012	o	42	19)
BK Peg	55817.5771	.0056	AG	+0.0084		GCVS 2012	V	70	13)
BN Peg	55830.2833	.0010	BHE	+0.0038		GCVS 2012	-Ir	110	17)
BY Peg	55807.5392	.0014	AG	−0.0238		GCVS 2012	-Ir	31	13)
	55850.292 :	.003	BHE	−0.013		GCVS 2012	-Ir	33	17)
BZ Peg	55807.5213	.0009	AG	+0.2666	s	GCVS 2012	-Ir	31	13)
CE Peg	55806.3898	.0026	AG	+0.1616		GCVS 2012	-Ir	29	13)
DI Peg	55820.3461	.0006	DIE	−0.0076		GCVS 2012	o	31	19)
	55887.2592	.0011	BHE	−0.0053		GCVS 2012	-Ir	65	17)
DM Peg	55857.3615	.0028	AG	+0.0748		GCVS 2012	V	75	13)
DP Peg	55849.2523	.0062	BHE				-Ir	82	17)
DV Peg	55806.5998	.0051	AG	+0.1050		GCVS 2012	-Ir	33	13)
	55807.5674	.0021	AG	+0.1264		GCVS 2012	-Ir	31	13)
	55855.4080	.0012	SCI	+0.1818	s	GCVS 2012	o	55	3)
	55857.3354	.0019	SCI	+0.2168	s	GCVS 2012	o	45	3)
EE Peg	55832.3270	.0031	BHE	+0.0024		GCVS 2012	-Ir	270	17)
ER Peg	55826.4021	.0064	BHE	+0.1423		GCVS 2012	-Ir	505	17)
	55851.4239	.0112	AG	+0.1428		GCVS 2012	V	62	13)
GH Peg	55874.2126	.0033	BHE	+0.0072		GCVS 2012	-Ir	137	17)
GH Peg	55879.3153	.0016	SCI	−0.0024		GCVS 2012	o	101	3)
GP Peg	55817.4263	.0018	AG	−0.0478	s	GCVS 2012	-Ir	69	13)
	55851.5757	.0030	AG	−0.0450	s	GCVS 2012	V	63	13)
HI Peg	55835.3399	.0017	BHE				-Ir	129	17)
IP Peg	55835.3722	.0001	PGL				V	286	16)
	55850.3988	.0005	SCI				o	34	3)
	55850.4730	.0019	SCI				o	30	3)
	55850.5581	.0005	SCI				o	14	3)
	55858.3980	.0012	SCI				o	26	3)
	55858.4687	.0004	SCI				o	30	3)
	55861.3219	.0008	SCI				o	22	3)
	55878.2460	.0007	SCI				o	19	3)
	55887.2627	.0004	SCI				o	23	3)
KV Peg	55877.3851	.0104	PGL				V	296	16)
KW Peg	55857.2382	.0021	BHE				-Ir	74	17)

Table 1: (cont.)

Variable	HJD 24.....	±	Obs	$O-C$		Bibliography	Fil	n	Rem
V357 Peg	55817.4295	.0022	AG				V	70	13)
V404 Peg	55851.3295	.0027	AG	−0.0900	s	GCVS 2012	V	63	13)
	55851.5345	.0025	AG	−0.0946		GCVS 2012	V	63	13)
V411 Peg	55806.4966	.0016	AG	−0.0103	s	GCVS 2012	-Ir	29	13)
ST Per	55980.2937	.0007	JU	+0.2228		GCVS 2012	o	59	3)
BO Per	55877.3362	.0015	MS FR	−0.0422		GCVS 2012	o	550	6)
BR Per	55598.481	.001	AG				-Ir	59	13)
BY Per	55894.4317	.0008	AG	+0.0241		GCVS 2012	-Ir	44	13)
DK Per	55859.5707	.0014	AG	+0.0127		GCVS 2012	-Ir	54	13)
	55879.3455	.0012	AG	+0.0122		GCVS 2012	-Ir	65	13)
IQ Per	55964.3487	.0050	JU	−0.0710	s	GCVS 2012	o	93	3)
IT Per	55850.4336	.0024	AG	−0.0180		GCVS 2012	-Ir	53	13)
IU Per	55850.3212	.0007	DIE	+0.0063		GCVS 2012	o	41	19)
KL Per	55850.4131	.0043	AG	+0.1330		GCVS 2012	-Ir	53	13)
	55859.3066	.0006	MS FR	+0.1342		GCVS 2012	o	468	6)
KN Per	55794.5770	.0003	MS FR	+0.0075		BAVR 52,93	o	429	6)
	55951.4037	.0097	PGL	+0.0040		BAVR 52,93	V	178	12)
KQ Per	55807.5186	.0010	FR				-Ir	29	13)
KW Per	55879.2817	.0019	BHE	+0.0999	s	GCVS 2012	-Ir	98	17)
PS Per	55850.4039	.0026	AG	+0.0689	s	GCVS 2012	-Ir	53	13)
QT Per	55807.4869	.0005	MS FR	+0.2199		GCVS 2012	o	645	6)
V366 Per	55859.4239	.0051	AG	+0.1555	s	GCVS 2012	-Ir	44	13)
	55894.2637	.0011	AG	+0.1567		GCVS 2012	-Ir	37	13)
V432 Per	55894.2424	.0006	AG	−0.0327		IBVS 3797	-Ir	33	13)
	55894.4322	.0020	AG	−0.0345	s	IBVS 3797	-Ir	33	13)
V449 Per	55859.4689	.0017	AG	+0.0508	s	GCVS 2012	-Ir	44	13)
	55894.4778	.0014	AG	+0.0502	s	GCVS 2012	-Ir	34	13)
V450 Per	55894.3200	.0010	AG	+0.1136		GCVS 2012	-Ir	35	13)
V680 Per	55859.2671	.0015	AG				-Ir	44	13)
	55859.4552	.0010	AG				-Ir	44	13)
	55894.2583	.0007	AG				-Ir	36	13)
	55894.4451	.0012	AG				-Ir	36	13)
SU Psc	55888.3355	.0012	BHE	−0.3118		GCVS 2012	-Ir	150	17)
UV Psc	55850.3760	.0008	BHE	−0.0151		GCVS 2012	-Ir	474	17)
AQ Psc	47804.431	.001	WU				o	52	1)
	47985.360	.001	WU				o	43	1)
	48983.221	.001	WU				V	56	1)
	48987.260	.001	WU				V	34	1)
	48992.254	.001	WU				V	35	1)
DZ Psc	55857.3370	.0037	AG				V	84	13)
	55857.5184	.0016	AG				V	84	13)
U Sge	55828.3559	.0032	FR	−0.0050		GCVS 2012	-Ir	56	13)
	55850.342 :	.003	FR	+0.007	s	GCVS 2012	-Ir	21	13)
V Sge	55805.4400	.0097	AG	−0.0576		GCVS 2012	-Ir	36	13)
	55831.3985	.0014	JU	−0.0659	s	GCVS 2012	o	80	3)
	55837.3096	.0035	JU	−0.0681		GCVS 2012	o	44	3)
V Sge	55838.3525	.0030	JU	−0.0536		GCVS 2012	o	72	3)
TU Sge	55790.7055	.0009	AG	+0.5954		GCVS 2012	-Ir	60	13)
	55805.4329	.0068	AG	+0.5960		GCVS 2012	-Ir	35	13)
CU Sge	55828.3394	.0007	FR	+0.0208		GCVS 2012	o	49	14)
CW Sge	55805.3576	.0040	AG	+0.0455	s	GCVS 2012	-Ir	34	13)
DK Sge	55790.5471	.0019	AG	+0.1598		GCVS 2012	-Ir	32	13)
	55797.3881	.0006	AG	+0.1608		GCVS 2012	-Ir	25	13)
	55802.3617	.0020	AG	+0.1598		GCVS 2012	-Ir	36	13)
	55805.4716	.0021	AG	+0.1606		GCVS 2012	-Ir	36	13)
DL Sge	55859.2706	.0002	WN	+0.1387		GCVS 2012	V	139	10)
	55862.2764	.0101	WN	+0.1441	s	GCVS 2012	V	115	10)
	55877.2773	.0002	WN	+0.1428		GCVS 2012	V	148	10)
FF Sge	55797.4616	.0033	AG	+0.0376		GCVS 2012	-Ir	25	13)
	55805.4241	.0042	AG	+0.0385		GCVS 2012	-Ir	35	13)

Table 1: (cont.)

Variable	HJD 24.....	±	Obs	$O-C$		Bibliography	Fil	n	Rem
FH Sge	55790.5493	.0086	AG				-Ir	31	13)
V384 Ser	55662.4937	.0003	FR	+0.0001		GCVS 2012	-Ir	79	13)
	55689.5043	.0004	FR	+0.0034	s	GCVS 2012	-Ir	36	13)
	55754.4014	.0002	FR	+0.0025		GCVS 2012	-Ir	60	13)
	55754.5363	.0005	FR	+0.0030	s	GCVS 2012	-Ir	60	13)
	55775.3623	.0009	FR	+0.0025		GCVS 2012	-Ir	22	13)
RW Tau	55859.4280	.0001	FR	+0.0094		BAVR 45,124	-Ir	81	13)
TY Tau	55896.4306	.0013	SCI	+0.2602		GCVS 2012	o	67	3)
AP Tau	55887.4591	.0002	MS FR	+0.0261		GCVS 2012	o	350	6)
CU Tau	55887.2915	.0002	MS FR	+0.0230	s	GCVS 2012	o	550	6)
GR Tau	55880.3413	.0033	DIE	−0.0358		BAVR 35,1	o	30	19)
V1022 Tau	55859.4439	.0004	FR				-Ir	209	13)
	55859.6164	.0001	FR				-Ir	209	13)
V1121 Tau	55890.3804	.0039	BHE				-Ir	227	17)
V Tri	55889.2774	.0011	BHE	−0.0400		GCVS 2012	-Ir	192	17)
	55896.3357	.0010	BHE	−0.0042		GCVS 2012	-Ir	136	17)
RV Tri	55859.5774	.0007	AG	−0.0342		GCVS 2012	-Ir	44	13)
RW Tri	55828.4413	.0005	BHE	−0.0047		GCVS 2012	-Ir	162	17)
ST Tri	55859.3540	.0021	AG	−0.0575		GCVS 2012	-Ir	44	13)
	55859.5955	.0010	AG	−0.0555	s	GCVS 2012	-Ir	44	13)
	55894.3244	.0012	AG	−0.0580		GCVS 2012	-Ir	36	13)
VZ Tri	55849.3248	.0036	BHE				-Ir	123	17)
WW Tri	55859.3632	.0102	AG				-Ir	45	13)
BU Tri	55859.2659	.0026	AG	+0.0727		GCVS 2012	-Ir	44	13)
	55859.4072	.0019	AG	+0.0662	s	GCVS 2012	-Ir	44	13)
	55859.5566	.0027	AG	+0.0678		GCVS 2012	-Ir	44	13)
BV Tri	55859.3246	.0030	AG	+0.0120	s	GCVS 2012	-Ir	44	13)
	55859.5627	.0002	AG	+0.0030		GCVS 2012	-Ir	44	13)
W UMa	55953.2873	.0035	PGL	−0.0138		BAVR 44,156	V	310	16)
NT UMa	55887.3035	.0020	AG				-Ir	74	13)
W UMi	55887.3619	.0003	QU	−0.1713		GCVS 2012	V	119	4)
AG Vir	55674.3274	.0002	FR	−0.0122		GCVS 2012	-Ir	297	13)
LU Vir	55674.3536	.0023	FR				o	53	14)
AW Vul	55791.4992	.0007	FR	−0.0118	s	GCVS 2012	-Ir	34	13)
	55819.3192	.0011	DIE	−0.0143		GCVS 2012	o	31	19)
AX Vul	55791.5372	.0002	FR	−0.0309		GCVS 2012	-Ir	34	13)
AZ Vul	55838.5333	.0014	AG	+0.0324		GCVS 2012	-Ir	40	13)
BG Vul	55791.5440	.0037	AG	+0.0546		GCVS 2012	-Ir	35	13)
	55806.4628	.0016	AG	+0.0531		GCVS 2012	-Ir	29	13)
	55807.4707	.0012	AG	+0.0529	s	GCVS 2012	-Ir	31	13)
BK Vul	55807.4919	.0021	AG	−0.0029	s	GCVS 2012	-Ir	31	13)
BO Vul	55790.5588	.0017	AG	−0.0351		GCVS 2012	-Ir	29	13)
	55835.3122	.0003	FR	−0.0367		GCVS 2012	o	22	14)
BQ Vul	55830.4433	.0017	FR	+0.7786	s	GCVS 2012	-Ir	22	13)
BS Vul	55790.5521	.0008	AG	−0.0275		GCVS 2012	-Ir	31	13)
	55797.4537	.0034	AG	−0.0275	s	GCVS 2012	-Ir	24	13)
CD Vul	55838.4575	.0032	AG	+0.0004	s	GCVS 2012	-Ir	39	13)
EO Vul	55838.4991	.0026	AG				-Ir	40	13)
EQ Vul	55801.4955	.0072	AG	−1.6769	s	GCVS 2012	-Ir	44	13)
EU Vul	55797.3801	.0002	AG	+0.0443	s	GCVS 2012	-Ir	28	13)
	55805.3268	.0012	AG	+0.0436	s	GCVS 2012	-Ir	36	13)
EV Vul	55790.4531	.0092	AG	+0.5131	s	GCVS 2012	-Ir	30	13)
EY Vul	55802.3963	.0021	AG	+0.0584		GCVS 2012	-Ir	35	13)
	55802.3972	.0003	WTR	+0.0593		GCVS 2012	-Ir	98	9)
FF Vul	55838.4475	.0034	AG	−0.0835		GCVS 2012	-Ir	40	13)
FM Vul	55791.4371	.0053	AG	+0.0321	s	GCVS 2012	-Ir	30	13)
FR Vul	55797.4092	.0013	AG	−0.0070		GCVS 2012	-Ir	26	13)
GI Vul	55797.4717	.0033	AG	−0.0134		GCVS 2012	-Ir	27	13)
	55801.3233	.0001	AG	−0.0137		GCVS 2012	-Ir	44	13)
	55801.5670	.0039	AG	−0.0107	s	GCVS 2012	-Ir	44	13)

Table 1: (cont.)

Variable	HJD 24.....	±	Obs	$O-C$		Bibliography	Fil	n	Rem
GP Vul	55778.556 :	.001	FR	−0.044	s	GCVS 2012	V	36	14)
	55835.3460	.0018	FR	−0.0419	s	GCVS 2012	o	19	14)
GU Vul	55797.4504	.0018	AG	+0.0303		GCVS 2012	-Ir	24	13)
	55835.3885	.0045	FR	+0.0313		GCVS 2012	o	22	14)
HS Vul	55790.4400	.0014	AG	+0.0379	s	GCVS 2012	-Ir	31	13)
	55797.4132	.0013	AG	+0.0377	s	GCVS 2012	-Ir	26	13)
	55799.4058	.0002	GB	+0.0379	s	GCVS 2012	o	85	2)
	55802.3952	.0024	AG	+0.0387	s	GCVS 2012	-Ir	34	13)
	55802.5625	.0020	AG	+0.0400		GCVS 2012	-Ir	34	13)
	55804.3870	.0003	GB	+0.0381	s	GCVS 2012	o	108	2)
	55805.3834	.0002	GB	+0.0383	s	GCVS 2012	o	109	2)
	55806.3800	.0001	GB	+0.0387	s	GCVS 2012	o	100	2)
	55806.5467	.0005	GB	+0.0394		GCVS 2012	o	86	2)
	55808.3722	.0001	GB	+0.0385	s	GCVS 2012	o	75	2)
KN Vul	55801.4051	.0021	AG	−0.0036	s	GCVS 2012	-Ir	44	13)
	55801.5870	.0026	AG	−0.0004		GCVS 2012	-Ir	44	13)
	55835.3535	.0017	FR	−0.0018	s	GCVS 2012	o	15	14)
NO Vul	55790.4319	.0022	AG	+0.0911	s	GCVS 2012	-Ir	32	13)
V467 Vul	55791.5332	.0079	AG	−0.0415	s	GCVS 2012	-Ir	35	13)
	55806.4902	.0037	AG	−0.0441	s	GCVS 2012	-Ir	29	13)
	55807.5557	.0021	AG	−0.0472		GCVS 2012	-Ir	31	13)
GSC 00871-00486	55672.5278	.0014	FR				o	69	14)
GSC 01100-01182	55396.5292	.0015	AG				-Ir	25	13)
GSC 01127-01808	55867.3481	.0006	QU				V	101	4)
GSC 01383-00181	55621.3707	.0002	FR				-Ir	97	13)
	55621.5034	.0003	FR				-Ir	97	13)
GSC 01383-01023	55621.4382	.0018	FR				-Ir	40	13)
GSC 01643-01880	55802.3625	.0039	AG				-Ir	36	13)
	55838.4136	.0016	JU				o	78	3)
GSC 02038-00293	55689.4590	.0007	FR	−0.0565	s	BAVM 177	-Ir	32	13)
	55784.3952	.0022	FR	+0.0087		BAVM 177	-Ir	18	13)
GSC 02040-00212	55662.4878	.0030	FR				o	21	14)
GSC 02140-01485	55802.4368	.0008	AG	−0.0337		BAV unpb	-Ir	33	13)
	55802.5864	.0007	AG	−0.0347	s	BAV unpb	-Ir	33	13)
GSC 02157-00014	55830.4388	.0004	FR				-Ir	51	13)
GSC 02161-01310	55791.4917	.0012	FR	+0.0813		BAVRb 59,3	-Ir	47	13)
GSC 02192-01283	55791.4506	.0014	AG	+0.0263		IBVS 5500-22	-Ir	35	13)
	55806.5328	.0011	AG	+0.0292	s	IBVS 5500-22	-Ir	29	13)
GSC 02484-00139	55628.3682	.0023	AG				-Ir	50	13)
	55628.5046	.0012	AG				-Ir	50	13)
	55628.6442	.0013	AG				-Ir	50	13)
GSC 02537-00520	55624.4746	.0018	AG				-Ir	36	13)
GSC 02569-00553	55642.3715	.0098	AG	−0.0239	s	PZP 10.4	-Ir	61	13)
	55642.5185	.0081	AG	−0.0246		PZP 10.4	-Ir	61	13)
GSC 02610-00088	55640.5405	.0018	MS FR				o	690	6)
	55661.5774	.0048	AG				-Ir	41	13)
	55670.4678	.0058	AG				-Ir	35	13)
GSC 02656-04286	55791.5641	.0046	AG	−0.0116	s	IBVS 5900-4	-Ir	34	13)
GSC 02656-04286	55804.5063	.0022	AG	−0.0163		IBVS 5900-4	-Ir	34	13)
GSC 02660-04155	55707.4537	.0012	FR				-Ir	37	13)
GSC 02673-02495	55741.4453	.0010	AG	+0.0539	s	PZP 10.4	-Ir	32	13)
	55790.4948	.0257	AG	+0.0393		PZP 10.4	-Ir	35	13)
	55794.5402	.0155	AG	+0.0441	s	PZP 10.4	-Ir	37	13)
GSC 02677-00988	55833.4133	.0014	FR				-Ir	32	13)
GSC 03547-02135	55671.6031	.0010	FR				o	19	14)
GSC 03575-06239	55691.4271	.0029	AG	+0.0869	s	PZP 10.4	-Ir	23	13)
GSC 03612-00014	55839.3787	.0213	AG	+0.0110	s	PZP 10.4	-Ir	50	13)
GSC 03618-00448	55815.4250	.0150	AG	−0.0090		PZP 10.4	-Ir	36	13)
GSC 03619-00047	55784.3678	.0039	AG	+0.0030		PZP 10.4	-Ir	40	13)
	55849.3456	.0115	AG	+0.0045		PZP 10.4	-Ir	55	13)

Table 1: (cont.)

Variable	HJD 24.....	±	Obs	$O-C$		Bibliography	Fil	n	Rem
GSC 03619-00715	55815.5678	.0092	AG				-Ir	44	13)
GSC 03679-02129	55817.4563	.0120	AG				-Ir	35	13)
	55859.4320	.0076	AG				-Ir	54	13)
	55894.4146	.0034	AG				-Ir	43	13)
GSC 03688-01184	55817.4624	.0030	AG	−0.0020		PZP 10.4	-Ir	34	13)
	55894.3670	.0041	AG	+0.0036		PZP 10.4	-Ir	44	13)
GSC 03949-01072	55829.5325	.0005	FR				-Ir	64	13)
	55831.3351	.0004	FR				-Ir	78	13)
	55831.5602	.0003	FR				-Ir	78	13)
	55834.4897	.0002	FR				-Ir	81	13)
	55839.4468	.0002	FR				-Ir	77	13)
	55851.3911	.0004	FR				-Ir	91	13)
	55851.6137	.0008	FR				-Ir	91	13)
GSC 04009-00670	55838.3957	.0108	AG	−0.0018		PZP 10.4	-Ir	66	13)
	55856.3101	.0064	AG	−0.0047		PZP 10.4	-Ir	54	13)
	55856.5837	.0114	AG	−0.0110	s	PZP 10.4	-Ir	54	13)
	55874.5045	.0096	AG	−0.0075	s	PZP 10.4	-Ir	56	13)
GSC 04285-00122	55857.3166	.0028	AG	+0.0040		PZP 10.4	-Ir	81	13)
	55857.4957	.0040	AG	−0.0042	s	PZP 10.4	-Ir	81	13)
GSC 04339-01166	55627.5533	.0141	AG	−0.0074	s	PZP 10.13	-Ir	120	13)
	55670.5409	.0001	AG	−0.0054	s	PZP 10.13	-Ir	86	13)
	55888.6709	.0007	RAT RCR	+0.0858		PZP 10.13	-U-I	352	15)
GSC 04827-02862	55622.3413	.0003	FR				-Ir	121	13)
	55622.4735	.0003	FR				-Ir	121	13)
GSC 04827-02889	55622.3597	.0008	FR				-Ir	35	13)
GSC 04965-00293	55674.3657	.0023	FR				o	53	14)
GSC 06281-00246	55799.4295	.0008	FR	+0.0035		BAVR 59,2	-Ir	33	13)
NSV 2146	55887.4076	.0009	FR				-Ir	40	13)
NSV 24737	55850.2381	.0001	FR				-Ir	167	13)
NSV 5501	55590.4919	.0105	RAT RCR				-U-I	217	15)
	55592.5546	.0004	RAT RCR				-U-I	252	15)
	55601.4967	.0003	RAT RCR				-U-I	222	15)
NSVS 10105062	55621.3449	.0005	FR				-Ir	87	13)
	55621.4655	.0002	FR				-Ir	87	13)
NSVS 10123419	55622.5038	.0114	AG				-Ir	77	13)
NSVS 103152	55578.3813	.0210	AG				-Ir	107	13)
	55578.6463	.0041	AG				-Ir	107	13)
NSVS 1701206	55884.4597	.0013	FR				-Ir	36	13)
NSVS 1810013	55878.6637	.0017	FR				o	64	14)
	55879.4687	.0016	FR				o	87	14)
NSVS 1857770	55879.2456	.0026	FR				o	41	14)
NSVS 4307145	55859.3821	.0002	FR				o	50	14)
NSVS 4319623	55859.3239	.0039	FR				o	50	14)
	55859.5362	.0044	FR				o	50	14)
NSVS 5811775	55851.3548	.0021	FR				o	49	14)
U-A2 1200-07442402	55642.5912	.0069	AG				V	61	13)
U-A2 1200-11760524	55707.4877	.0025	AG				-Ir	20	13)
U-A2 1200-12680286	55791.5824	.0015	AG	−0.0184		IBVS 5700-73	-Ir	34	13)
	55804.4784	.0026	AG	−0.0187	s	IBVS 5700-73	-Ir	34	13)
U-A2 1275-16067829	55372.4595	.0074	AG				-Ir	33	13)
U-A2 1500-01208912	55808.4125	.0023	AG	+0.0188		IBVS 5900-6	-Ir	34	13)
U-B1 1092-0472807	55805.4634	.0077	AG				-Ir	35	13)
U-B1 1108-0490540	55042.4918	.0006	AG				-Ir	42	13)
	55393.4034	.0047	AG				-Ir	30	13)
	55802.5274	.0031	AG				-Ir	37	13)
	55805.4052	.0049	AG				-Ir	36	13)
U-B1 1135-0102876	55629.3283	.0032	AG				-Ir	50	13)
U-B1 1166-0562907	55481.3536	.0072	AG				-Ir	40	13)
U-B1 1316-0383362	55711.3882	.0003	AG	+0.0317		BAV unpb	-Ir	28	13)
	55711.5531	.0007	AG	+0.0313	s	BAV unpb	-Ir	28	13)

Table 1: (cont.)

Variable	HJD 24.....	±	Obs	$O-C$		Bibliography	Fil	n	Rem
U-B1 1332-0399848	55687.4809	.0024	AG	−0.0060	s	BAV unpb	-Ir	25	13)
U-B1 1398-0469064	55784.4185	.0022	AG	−0.0835		PZP 10.4	-Ir	40	13)
	55784.5762	.0014	AG	+0.0742		PZP 10.4	-Ir	40	13)
	55799.4984	.0027	AG	+0.0367		PZP 10.4	-Ir	28	13)
	55849.2907	.0027	AG	+0.0717		PZP 10.4	-Ir	50	13)
	55849.4581	.0043	AG	+0.0765	s	PZP 10.4	-Ir	50	13)
	55849.6179	.0012	AG	+0.0737		PZP 10.4	-Ir	50	13)
U-B1 1400-0455467	55799.4702	.0269	AG	+0.1584		PZP 10.13	-Ir	28	13)
U-B1 1416-0454010	55784.3858	.0029	AG				-Ir	40	13)
	55784.5468	.0026	AG				-Ir	40	13)
	55849.2661	.0020	AG				-Ir	55	13)
	55849.5826	.0076	AG				-Ir	55	13)
U-B1 1440-0411990	55801.5131	.0033	AG	−0.0711		IBVS 5700-54	-Ir	41	13)
	55850.4522	.0122	AG	−0.0723		IBVS 5700-54	-Ir	49	13)
U-B1 1441-0441871	55808.4442	.0059	AG	+0.0079		PZP 10.13	-Ir	26	13)
	55839.4475	.0016	AG	+0.0099		PZP 10.13	-Ir	40	13)
	55873.3142	.0035	AG	+0.0111	s	PZP 10.13	-Ir	52	13)
U-B1 1492-0009970	55776.4611	.0044	AG	−0.0073	s	PZP 10.13	-Ir	35	13)
	55838.3596	.0115	AG	−0.0595	s	PZP 10.13	-Ir	57	13)
U-B1 1500-0005759	55857.3168	.0085	AG	+0.1172	s	AJ 133.1470	-Ir	81	13)
	55857.6288	.0062	AG	+0.1080		AJ 133.1470	-Ir	81	13)
U-B1 1503-0282065	55691.5213	.0022	AG				-Ir	48	13)
	55787.3717	.0014	AG				-Ir	35	13)
	55787.5531	.0012	AG				-Ir	35	13)
U-B1 1505-0372164	55776.3721	.0016	AG	+0.0207	s	PZP 10.13	-Ir	35	13)
	55776.5293	.0012	AG	+0.0208		PZP 10.13	-Ir	35	13)
	55835.5169	.0003	RAT RCR	−0.0650		PZP 10.13	-U-I	317	15)
	55835.6755	.0020	RAT RCR	−0.0635	s	PZP 10.13	-U-I	317	15)
U-B1 1508-0029126	55808.4194	.0036	AG	+0.0027	s	IBVS 5900-5	-Ir	34	13)
U-B1 1514-0040346	55858.6204	.0095	AG	+0.0101		PZP 10.13	-Ir	61	13)

Table 2: Times of maxima of pulsating stars

Variable	HJD 24.....	±	Obs	$O-C$	Bibliography	Fil	n	Rem	
SW And	55796.4804	.0035	PGL	−0.0037	A	A 476.307 2007	V	299	16)
XX And	55446.3386	.0035	PGL	+0.0219	BAVR 48,189	V	202	16)	
CC And	55878.3887	.0028	WN	+0.0086	GCVS 2012	V	74	10)	
	55887.3968	.0019	WN	+0.0233	GCVS 2012	V	131	10)	
DM And	55851.495	.002	AG	+0.134	GCVS 2012	-Ir	63	13)	
DU And	55850.334	.002	AG	−0.127	GCVS 2012	-Ir	53	13)	
	55859.436	.001	AG	−0.127	GCVS 2012	-Ir	45	13)	
GP And	55858.5320	.0010	WN	+0.0052	GCVS 2012	V	112	10)	
	55878.4388	.0008	WN	+0.0052	GCVS 2012	V	180	10)	
	55878.5172	.0010	WN	+0.0049	GCVS 2012	V	180	10)	
	55879.4614	.0012	WN	+0.0049	GCVS 2012	V	52	10)	
	55879.5392	.0007	WN	+0.0041	GCVS 2012	V	36	10)	
	55886.3862	.0008	WN	+0.0057	GCVS 2012	V	161	10)	
	55886.4642	.0008	WN	+0.0050	GCVS 2012	V	161	10)	
	55893.3889	.0007	WN	+0.0056	GCVS 2012	V	43	10)	
	55893.4669	.0007	WN	+0.0049	GCVS 2012	V	44	10)	
	55894.4108	.0006	WN	+0.0046	GCVS 2012	V	49	10)	
	55895.3551	.0007	WN	+0.0047	GCVS 2012	V	51	10)	
	55896.3780	.0006	WN	+0.0047	GCVS 2012	V	114	10)	
	55908.3381	.0007	WN	+0.0051	GCVS 2012	V	147	10)	
	55908.4169	.0008	WN	+0.0052	GCVS 2012	V	147	10)	
	55958.2232	.0007	WN	+0.0053	GCVS 2012	V	48	10)	
MV And	55859.456	.003	AG			-Ir	45	13)	
V460 And	55850.343	.001	AG			-Ir	24	13)	
	55850.569	.001	AG			-Ir	29	13)	
	55894.283	.001	AG			-Ir	35	13)	
	55894.358	.001	AG			-Ir	35	13)	
	55894.433	.001	AG			-Ir	35	13)	
CY Aqr	55793.4464	.0010	TMG	−0.0037	GCVS 2012	o	160	5)	
	55793.5077	.0004	TMG	−0.0034	GCVS 2012	o	160	5)	
	55793.5685	.0003	TMG	−0.0036	GCVS 2012	o	160	5)	
	55878.2906	.0004	WN	−0.0028	GCVS 2012	V	56	10)	
	55879.3887	.0004	WN	−0.0034	GCVS 2012	V	47	10)	
	55886.3477	.0007	WN	−0.0028	GCVS 2012	V	69	10)	
	55887.2642	.0009	WN	−0.0019	GCVS 2012	V	136	10)	
	55887.3242	.0007	WN	−0.0029	GCVS 2012	V	136	10)	
	55893.2453	.0006	WN	−0.0025	GCVS 2012	V	68	10)	
	55893.3065	.0006	WN	−0.0024	GCVS 2012	V	32	10)	
	55894.2222	.0009	WN	−0.0023	GCVS 2012	V	135	10)	
	55894.2829	.0005	WN	−0.0026	GCVS 2012	V	135	10)	
	55895.1984	.0008	WN	−0.0027	GCVS 2012	V	201	10)	
	55895.2593	.0007	WN	−0.0028	GCVS 2012	V	201	10)	
	55895.3202	.0003	WN	−0.0030	GCVS 2012	V	201	10)	
	55896.2362	.0005	WN	−0.0025	GCVS 2012	V	94	10)	
FY Aqr	55807.4812	.0015	MZ	+0.0225	GCVS 2012	o	91	3)	
GW Aqr	55877.2592	.0015	MZ			-Ir	60	3)	
X Ari	55940.3312	.0028	PGL	+0.0769	BAVR 48,189	V	631	12)	
RV Ari	55857.4789	.0005	WLH	+0.0030	GCVS 2012	-Ir	129	4)	
SY Ari	55856.404	.003	AG	−0.010	GCVS 2012	-Ir	56	13)	
TU Ari	55856.413	.001	AG	−0.169	GCVS 2012	-Ir	56	13)	
TV Ari	55856.379	.002	AG			-Ir	57	13)	
TY Ari	55856.565	.001	AG	+0.005	GCVS 2012	-Ir	57	13)	
TZ Aur	55951.3947	.0021	PGL	+0.0141	GCVS 2012	V	144	16)	
V378 Aur	55650.271	.001	PGL			V	701	16) 20)	
BG Boo	54924.547	.003	AG	+0.144	GCVS 2012	-Ir	38	13)	
	55686.529	.005	AG	+0.111	GCVS 2012	-Ir	47	13)	
BU Boo	55711.4670	.0031	SCI			o	26	3)	
CG Boo	55628.5386	.0004	RAT RCR			-U-I	234	15)	
CM Boo	55640.4812	.0008	QU	−0.1234	GCVS 2012	V	35	4)	
CS Boo	55704.4231	.0013	SCI	−0.0042	IBVS 2855	o	109	3)	

Table 2: (cont.)

Variable	HJD 24.....	±	Obs	$O-C$	Bibliography	Fil	n	Rem	
DD Boo	55662.345	.007	MS FR			o	531	6)	
UY Cam	55887.336	.002	AG	+0.072	BAVR 49,41	-Ir	74	13)	
	55887.601	.002	AG	+0.070	BAVR 49,41	-Ir	74	13)	
EW Cam	55887.471	.002	AG			-Ir	74	13)	
NT Cam	55887.241	.001	AG			-Ir	74	13)	
	55887.329	.001	AG			-Ir	74	13)	
	55887.410	.001	AG			-Ir	74	13)	
	55887.487	.001	AG			-Ir	74	13)	
	55887.570	.001	AG			-Ir	74	13)	
	55887.659	.001	AG			-Ir	74	13)	
SY CMi	55943.5163	.0026	WU	+0.0843	GCVS 2012	V	275	17)	
HU Cas	55894.489	.001	AG	−0.040	GCVS 2012	-Ir	44	13)	
PS Cas	55817.526	.002	AG	−0.177	GCVS 2012	-Ir	34	13)	
	55894.280	.002	AG	−0.174	GCVS 2012	-Ir	43	13)	
V470 Cas	55859.555	.003	AG	+0.251	IBVS 4332	-Ir	54	13)	
V823 Cas	55878.310	.002	FR			-Ir	119	13)	
V871 Cas	55849.5109	.0005	RAT RCR			-U-I	269	15)	
	55849.6341	.0020	RAT RCR			-U-I	269	15)	
V1040 Cas	55856.335	.001	AG	−0.013	GCVS 2012	-Ir	26	13)	
	55856.554	.002	AG	−0.014	GCVS 2012	-Ir	28	13)	
	55874.368	.001	AG	−0.012	GCVS 2012	-Ir	35	13)	
RZ Cep	50463.617	.001	SCG	−0.017	GCVS 2012	V	100	1)	
	55807.461	.003	AG	−0.132	GCVS 2012	-Ir	56	13)	
SZ CrB	55662.554	.010	FR	+0.014	BAVR 49,41	o	37	14)	
UY Cyg	48085.448	.001	WU	+0.038	GCVS 2012	V	40	1)	
	48893.425	.001	WU	+0.040	GCVS 2012	V	29	1)	
XX Cyg	55830.3257	.0005	WN	+0.0030	GCVS 2012	V	56	10)	
	55835.3151	.0008	WN	+0.0024	GCVS 2012	V	60	10)	
	55837.3383	.0006	WN	+0.0026	GCVS 2012	V	67	10)	
	55848.2625	.0009	WN	+0.0027	GCVS 2012	V	75	10)	
	55850.2861	.0001	WN	+0.0033	GCVS 2012	V	89	10)	
	55858.3776	.0006	WN	+0.0029	GCVS 2012	V	55	10)	
	55879.2815	.0007	WN	+0.0027	GCVS 2012	V	66	10)	
	55880.2275	.0004	WNI	+0.0047	GCVS 2012	V	100	10)	
XZ Cyg	55461.3129	.0022	WN	+0.0355	BAVR 48,189	V	130	10)	
	55830.4013	.0014	WN	+0.0472	BAVR 48,189	V	105	10)	
DM Cyg	48106.526	.001	WU	+0.014	A	A 476.307	V	30	1)
	48484.407	.001	WU	+0.018	A	A 476.307	V	56	1)
	48893.345	.001	WU	+0.008	A	A 476.307	V	32	1)
	55835.3553	.0012	WN	−0.0068	A	A 476.307	V	65	10)
IV Cyg	55833.477	.004	FR			-Ir	64	13)	
KP Cyg	54317.391	.002	MZ	−0.084	GCVS 2012	-Ir	75	3)	
	55820.393	.002	MZ	−0.106	GCVS 2012	-Ir	115	3)	
V791 Cyg	55804.474	.004	FR	−0.113	GCVS 2012	-Ir	46	13)	
	55826.454	.004	FR	−0.106	GCVS 2012	-Ir	47	13)	
	55838.292	.004	FR	−0.100	GCVS 2012	-Ir	44	13)	
V794 Cyg	55790.503	.002	AG			-Ir	34	13)	
V798 Cyg	55791.519	.001	AG	−0.063	GCVS 2012	-Ir	31	13)	
V881 Cyg	55802.562	.005	FR	+0.088	GCVS 2012	-Ir	61	13)	
V1719 Cyg	55834.518	.003	FR	−0.055	GCVS 2012	o	394	14)	
	55851.361	.003	FR	−0.052	GCVS 2012	o	40	14)	
V1821 Cyg	53662.355	.004	FR			o	60	7)	
	55856.293	.004	FR			-Ir	39	13)	
V2088 Cyg	55835.351	.002	FR			o	19	14)	
V2109 Cyg	55671.586	.004	FR			o	58	14)	
	55778.378	.001	FR			-Ir	39	13)	
	55801.448	.002	FR			-Ir	37	13)	
V2238 Cyg	53662.414	.005	FR			o	60	7)	
	55856.341	.003	FR			-Ir	33	13)	
V2455 Cyg	55834.519	.002	FR			o	97	14)	

Table 2: (cont.)

Variable	HJD 24.....	±	Obs	$O-C$	Bibliography	Fil	n	Rem	
V2470 Cyg	55774.4695	.0015	MZ			-Ir	119	3)	
	55807.3839	.0015	MZ			-Ir	90	3)	
DX Del	55806.4347	.0250	MOO	+0.0670	GCVS 2012	V	42	16)	
	55806.4349	.0017	WLH	+0.0672	GCVS 2012	o	285	4)	
	55833.3708	.0030	WN	+0.0639	GCVS 2012	V	147	10)	
	55879.2153	.0023	WN	+0.0646	GCVS 2012	V	73	10)	
	55905.2089	.0020	WNI	+0.0643	GCVS 2012	V	82	10)	
EF Del	55829.3427	.0008	MZ	+0.1104	GCVS 2012	-Ir	96	3)	
	55855.3045	.0015	MZ	+0.1127	GCVS 2012	-Ir	108	3)	
FF Del	55836.3773	.0010	SB			V	40	11)	
SU Dra	50200.496	.001	WU	+0.024	GCVS 2012	V	30	1)	
BK Dra	55852.5230	.0017	SCI	+0.0829	BAVR 46,1	o	75	3)	
RR Gem	55952.3371	.0021	PGL	−0.0256	BAVR 47,67	V	202	16)	
V397 Gem	55263.470	.002	FR			-Ir	50	13)	
VX Her	55776.3958	.0021	PGL	+0.0006	GCVS 2012	V	143	12)	
AR Her	55739.5068	.0035	PGL	+0.0480	BAVR 52,3	V	204	12)	
	55748.4135	.0035	PGL	+0.0250	BAVR 52,3	V	204	12)	
	55787.4497	.0035	PGL	+0.0525	BAVR 52,3	V	247	12)	
	55810.4569	.0035	PGL	+0.0305	BAVR 52,3	V	142	12)	
	55834.4560	.0049	PGL	+0.0603	BAVR 52,3	V	267	16)	
	55836.3272	.0014	WN	+0.0516	BAVR 52,3	V	106	10)	
DY Her	55836.2707	.0012	WN	−0.0065	BAVR 48,189	V	47	10)	
V392 Her	55797.4037	.0012	MZ	−0.1369	GCVS 2012	-Ir	136	3)	
	55849.3196	.0018	MZ	−0.1360	GCVS 2012	-Ir	74	3)	
V633 Her	55805.3758:	.0020	MZ	+0.0039	BAVR 61.83	-Ir	60	3)	
V929 Her	55670.538 :	.005	FR			o	79	14)	
V1131 Her	55861.3743	.0015	MZ			-Ir	119	3)	
XZ Lac	55799.396	.001	AG			-Ir	28	13)	
CH Lac	55849.463	.005	AG	+0.011	GCVS 2012	-Ir	50	13)	
CZ Lac	55833.4323	.0062	PGL	−0.2126	BAVR 53,12	V	107	16)	
ST Leo	55672.477	.003	FR	−0.020	GCVS 2012	-Ir	106	13)	
SZ Lyn	55262.4417	.0022	WS	+0.0269	GCVS 2012	o	0	18)	
RZ Lyr	55867.3043	.0035	PGL	−0.0240	BAVR 48,189	V	98	16)	
WW Lyr	54339.488	.014	FR	+0.098	GCVS 2012	-Ir	17	8)	
	55857.397	.003	FR	+0.111	GCVS 2012	-Ir	55	13)	
ZZ Lyr	55832.3476	.0005	MZ			-Ir	100	3)	
	55836.3691	.0005	MZ			-Ir	119	3)	
CN Lyr	55834.3342	.0032	WN	−0.0015	A	A 476.307	V	171	10)
	55848.3203	.0032	WN	−0.0024	A	A 476.307	V	83	10)
EN Lyr	55806.4841	.0013	MZ	+0.1595	GCVS 2012	-Ir	81	3)	
	55835.3034	.0014	MZ	+0.1570	GCVS 2012	-Ir	79	3)	
EX Lyr	55748.4633	.0020	MZ	−0.0872	GCVS 2012	-Ir	86	3)	
	55805.4907	.0010	MZ	−0.0823	GCVS 2012	-Ir	118	3)	
QV Lyr	55794.409	.001	AG	+0.117	GCVS 2012	-Ir	37	13)	
VZ Peg	55817.571	.002	AG	−0.010	BAVR 49,41	-Ir	63	13)	
AO Peg	55806.450	.002	AG	−0.015	BAVR 49,41	-Ir	29	13)	
AV Peg	55806.578	.001	AG	+0.012	A	A 476.307	-Ir	29	13)
BH Peg	55835.4566	.0049	PGL	−0.0214	BAVR 47,67	V	378	12)	
	55896.3953	.0035	PGL	+0.0235	BAVR 47,67	V	296	12)	
	55941.2217	.0035	PGL	−0.0192	BAVR 47,67	V	299	12)	
	55957.2423	.0035	PGL	−0.0233	BAVR 47,67	V	184	12)	
BP Peg	55791.437	.001	AG	−0.026	BAVR 48,189	-Ir	16	13)	
	55791.543	.001	AG	−0.029	BAVR 48,189	-Ir	19	13)	
	55806.444	.001	AG	−0.026	BAVR 48,189	-Ir	32	13)	
	55806.555	.001	AG	−0.025	BAVR 48,189	-Ir	32	13)	
	55807.426	.001	AG	−0.030	BAVR 48,189	-Ir	31	13)	
	55807.537	.001	AG	−0.029	BAVR 48,189	-Ir	31	13)	
	55839.298	.005	FR	−0.036	BAVR 48,189	o	45	14)	
CS Peg	55798.3949	.0006	MZ	+0.2375	GCVS 2012	-Ir	118	3)	
	55828.3174	.0012	MZ	+0.2394	GCVS 2012	-Ir	90	3)	

Table 2: (cont.)

Variable	HJD 24.....	±	Obs	$O-C$	Bibliography	Fil	n	Rem
DY Peg	55796.5192	.0028	PGL	−0.0115	GCVS 2012	V	213	12)
	55833.4192	.0021	PGL	−0.0122	GCVS 2012	V	225	12)
	55835.4623	.0004	WN	−0.0110	GCVS 2012	V	130	10)
	55836.4099	.0006	WN	−0.0115	GCVS 2012	V	155	10)
	55836.4831	.0006	WN	−0.0112	GCVS 2012	V	155	10)
	55837.4307	.0005	WN	−0.0116	GCVS 2012	V	250	10)
	55837.5046	.0008	WN	−0.0107	GCVS 2012	V	250	10)
	55848.3705	.0009	WN	−0.0108	GCVS 2012	V	136	10)
	55848.4420	.0005	WN	−0.0122	GCVS 2012	V	136	10)
	55849.3909	.0007	WN	−0.0114	GCVS 2012	V	277	10)
	55849.4641	.0007	WN	−0.0111	GCVS 2012	V	277	10)
	55849.5366	.0008	WN	−0.0115	GCVS 2012	V	277	10)
	55856.3923	.0004	WN	−0.0109	GCVS 2012	V	203	10)
	55856.4648	.0005	WN	−0.0113	GCVS 2012	V	203	10)
	55857.3400	.0006	WN	−0.0112	GCVS 2012	V	256	10)
	55857.4130	.0010	WN	−0.0111	GCVS 2012	V	256	10)
	55857.4853	.0007	WN	−0.0118	GCVS 2012	V	256	10)
	55858.4334	.0006	WN	−0.0117	GCVS 2012	V	93	10)
	55859.3820	.0009	WN	−0.0112	GCVS 2012	V	95	10)
	55867.3309	.0006	WN	−0.0112	GCVS 2012	V	177	10)
	55867.4040	.0006	WN	−0.0110	GCVS 2012	V	177	10)
	55877.3217	.0008	WN	−0.0113	GCVS 2012	V	54	10)
	55878.3419	.0006	WN	−0.0121	GCVS 2012	V	61	10)
	55879.3634	.0014	WN	−0.0116	GCVS 2012	V	72	10)
	55879.4366	.0019	WN	−0.0113	GCVS 2012	V	43	10)
	55879.5106	.0009	WN	−0.0102	GCVS 2012	V	41	10)
	55886.2915	.0006	WN	−0.0115	GCVS 2012	V	58	10)
	55893.2923	.0008	WN	−0.0116	GCVS 2012	V	50	10)
	55893.3654	.0014	WN	−0.0114	GCVS 2012	V	51	10)
	55893.4377	.0008	WN	−0.0120	GCVS 2012	V	51	10)
	55894.3133	.0007	WN	−0.0116	GCVS 2012	V	141	10)
	55894.3872	.0009	WN	−0.0106	GCVS 2012	V	141	10)
	55896.2829	.0001	WN	−0.0110	GCVS 2012	V	141	10)
	55896.3552	.0008	WN	−0.0116	GCVS 2012	V	141	10)
	55908.2422	.0009	WN	−0.0116	GCVS 2012	V	158	10)
	55908.3145	.0003	WN	−0.0122	GCVS 2012	V	158	10)
ET Per	55817.4490	.0010	AG	−0.0274	BAVR 49,41	-Ir	35	13)
KV Per	55859.306	.002	AG	−0.001	GCVS 2012	-Ir	53	13)
	55859.553	.002	AG	−0.003	GCVS 2012	-Ir	53	13)
	55878.2389	.0035	PGL	−0.0012	GCVS 2012	V	555	16)
	55879.486	.001	AG	+0.000	GCVS 2012	-Ir	63	13)
	55894.432	.002	AG	−0.001	GCVS 2012	-Ir	44	13)
V447 Per	55894.467	.002	AG			-Ir	37	13)
DP Sge	55790.467	.002	AG	−0.159	GCVS 2012	-Ir	30	13)
EH Sge	55802.428	.001	AG			-Ir	34	13)
GW Sge	55805.444	.008	AG	+0.182	GCVS 2012	-Ir	23	13)
V1025 Sgr	55799.439	.004	FR	−0.023	GCVS 2012	-Ir	39	13)
SX Tri	55886.3338	.0018	MZ			-Ir	156	3) 20)
TU UMa	55984.3792	.0035	PGL	−0.0536	GCVS 2012	V	219	12)
UZ UMa	55887.633	.001	AG	−0.005	GCVS 2012	-Ir	74	13)
AE UMa	55984.4472	.0014	PGL	+0.0049	BAVR 48,189	V	227	16)
KT UMa	55879.701	.000	MS FR			o	550	6)
BN Vul	55752.4651	.0028	PGL	+0.0721	GCVS 2012	V	96	16)
HR Vul	55802.423	.001	AG	+0.084	GCVS 2012	-Ir	34	13)
GSC 00612-00771	55959.2511	.0010	WN			V	79	10)
	55960.2551	.0009	WNI			V	73	10)
	55963.2684	.0011	WNI			V	92	10)

Table 2: (cont.)

Variable	HJD 24.....	±	Obs	$O-C$	Bibliography	Fil	n	Rem
GSC 01220-01131	55959.3557	.0010	WN			V	129	10)
	55964.2385	.0016	WN			V	160	10)
	55964.3180	.0013	WN			V	160	10)
	55966.2712	.0015	WN			V	123	10)
	55968.3045	.0019	WN			V	135	10)
	55969.2803	.0011	WN			V	111	10)
GSC 01594-02234	55837.2877	.0014	WN			V	77	10)
	55849.3176	.0018	WN			V	142	10)
	55856.2891	.0014	WN			V	97	10)
	55857.2445	.0015	WN			V	140	10)
	55858.3392	.0023	WN			V	196	10)
	55859.2980	.0020	WN			V	139	10)
	55861.3477	.0033	WN			V	206	10)
	55867.2240	.0022	WN			V	120	10)
	55870.2302	.0016	WN			V	120	10)
	55877.2005	.0014	WN			V	148	10)
	55886.2231	.0016	WN			V	103	10)
GSC 02108-01564	55830.2922	.0015	WN			V	56	10)
GSC 02670-04008	55829.431	.002	FR	−0.022	PZP 10.13	o	64	14)
	55838.335	.002	AG	+0.001	PZP 10.13	-Ir	36	13)
	55838.436	.002	AG	+0.006	PZP 10.13	-Ir	36	13)
GSC 02671-02149	55801.428	.003	AG	−0.013	BAV unpb	-Ir	44	13)
GSC 02671-02149	55829.480	.004	FR	−0.045	BAV unpb	o	64	14)
GSC 03650-01998	55877.285	.001	FR			-Ir	36	13)
GSC 03755-00845	55958.3910	.0010	WN			V	77	10)
	55959.3795	.0009	WN			V	123	10)
	55959.4562	.0013	WN			V	123	10)
	55963.3365	.0147	WN			V	135	10)
	55964.4031	.0013	WN			V	202	10)
	55964.4776	.0010	WN			V	202	10)
	55966.3812	.0012	WN			V	216	10)
	55966.4574	.0014	WN			V	216	10)
	55968.3598	.0006	WN			V	77	10)
	55969.3490	.0011	WN			V	190	10)
	55969.4248	.0019	WN			V	190	10)
GSC 03949-00386	55832.329	.003	FR			-Ir	142	13)
	55834.335	.001	FR			-Ir	140	13)
	55834.625	.001	FR			-Ir	140	13)
	55835.295	.001	FR			-Ir	125	13)
	55835.585	.001	FR			-Ir	125	13)
	55839.509	.001	FR			-Ir	136	13)
	55851.483	.001	FR			-Ir	163	13)
GSC 03986-01266	52148.548	.003	AG	−0.029	IBVS 5700-47	o	18	2)
	52858.466	.003	AG	−0.051	IBVS 5700-47	-Ir	35	2)
	52928.454	.003	AG	−0.023	IBVS 5700-47	o	35	2)
	52928.600	.003	AG	−0.097	IBVS 5700-47	o	35	2)
	53303.483	.003	AG	−0.094	IBVS 5700-47	-Ir	22	2)
	54035.414	.004	AG	−0.103	IBVS 5700-47	-Ir	35	2)
	54035.562	.004	AG	+0.045	IBVS 5700-47	-Ir	35	2)
	54222.460	.003	AG	−0.057	IBVS 5700-47	-Ir	18	2)
	54244.456	.005	AG	−0.061	IBVS 5700-47	-Ir	38	2)
	54357.381	.005	AG	+0.004	IBVS 5700-47	-Ir	39	2)
	55805.339	.003	AG	−0.078	IBVS 5700-47	-Ir	30	13)
	55805.488	.003	AG	+0.071	IBVS 5700-47	-Ir	30	13)
NSVS 1637092	55878.678	.005	FR			o	128	14)
NSVS 3660070	55878.417	.004	FR			o	117	14)
	55879.292	.004	FR			o	84	14)
TYC 1698-01052-1	55941.2429	.0021	PGL			V	192	12)
	55951.3047	.0021	PGL			V	119	12)
	55952.2813	.0021	PGL			V	138	12)

Table 2: (cont.)

Variable	HJD 24.....	±	Obs	$O-C$	Bibliography	Fil	n	Rem
U-A2 1200-07442272	55642.532	.003	AG	+0.079	IBVS 5700-69	V	61	13)
U-B1 1422-0506537	55775.413	.001	AG	−0.012	PZP 10.13	-Ir	42	13)
	55775.527	.001	AG	−0.011	PZP 10.13	-Ir	42	13)
U-B1 1424-0504416	55775.417	.001	AG	−0.002	PZP 10.13	-Ir	42	13)
	55775.563	.001	AG	−0.009	PZP 10.13	-Ir	42	13)
	55801.437	.003	AG	+0.009	PZP 10.13	-Ir	41	13)
	55801.583	.003	AG	+0.002	PZP 10.13	-Ir	41	13)
U-B1 1646-0035146	55627.375	.001	AG	−0.021	PZP 10.13	-Ir	120	13)

Observers:

AG:	Agerer, F., Tiefenbach
BHE:	Böhme, D., Nessa
DIE:	Dietrich, M., Radebeul
FR:	Frank, P., Velden
GB:	Gröbel, R., Eckental
JU:	Jungbluth, Dr. H., Karlsruhe
MOO:	Moos, C., Netphen
MS:	Moschner, W., Lennestadt
MZ:	Maintz, Dr. G., Bonn
PGL:	Pagel, Dr. L., Klockenhagen
QU:	Quester, W., Esslingen
RAT:	Rätz, M., Herges-Hallenberg
RCR:	Rätz, K., Herges-Hallenberg
SB:	Steinbach, Dr. H., Neu-Anspach
SCG:	Schurig, S., Nürnberg
SCI:	Schmidt, U., Karlsruhe
TMG:	Team Marinus Gymnasium, Linz
WLH:	Wollenhaupt, G., Oberwiesenthal
WN:	Wischnewski, M., Springe
WNI:	Wischnewski, N., Springe
WS:	Wischnewski, E., Kaltenkirchen
WTR:	Walter, F., München
WU:	Wunder, E., Edingen

Remarks:

:	uncertain
s	secondary minimum
	Photometer
1)	photometer 1P21
2)	ccd-camera ST-6: chip 375*242 uncoated
3)	ccd-camera ST-7
4)	ccd-camera ST-7E
5)	ccd-camera ST-9: chip 512*512
6)	ccd-camera ST-9XE: chip 512*512
7)	ccd-camera OES-LcCCD11
8)	ccd-camera OES-LcCCD12
9)	ccd-camera Pictor 416XT
10)	ccd-camera Meade DSI Pro 2
11)	ccd-camera Sigma 402: chip KAF0402ME
12)	ccd-camera Artemis 4021
13)	ccd-camera Sigma 1603
14)	ccd-camera Canon EOS 450D
15)	ccd-camera Moravian G2-1600
16)	ccd-camera QHY8
17)	ccd-camera Meade DSI Pro 3
18)	ccd-camera Canon EOS 40D
19)	ccd-camera Canon EOS 450D
20)	normal maximum
21)	normal minimum
	Filter
o	without filter
B	B-filter
V	V-filter
-Ir	IR cut-off filter
-U-I	U and IR cut-off filter
n	Number of measurements

References:

A&A	Astronomy & Astrophysics
AJ vvv,ppp	Astronomical Journal volume, pages
BAV unpb	unpublished preliminary elements of the BAV
BAVM nnn	BAV Mitteilungen No. nnn
BAVR vv,ppp	BAV Rundbrief volume, pages
GCVS 2009	General Catalogue of Variable Stars, version: iii.dat 15.05.2012
IBVS nnnn	Information Bulletin on Variable Stars No. nnnn
PZP vol.n	Peremennye Zvezdy Prilozhenie Vol, No.
	Star catalogues
GSC	The HST Guide Star Catalogue 1.2
TYC	Tycho Catalogue
U-A2	USNO A2.0 catalogue
U-B1	USNO B1.0 catalogue

COMMISSIONS 27 AND 42 OF THE IAU
INFORMATION BULLETIN ON VARIABLE STARS

Number 6027

Konkoly Observatory
Budapest
28 June 2012

HU ISSN 0374 – 0676

CALL FOR OBSERVATIONS OF THE AZ Cas ECLIPSE AND PERIASTRON PASSAGE OF 2012-2014

GAŁAN, C.[1]; TOMOV, T.[1]; MIKOŁAJEWSKI, M.[1]; ŚWIERCZYŃSKI, E.[1]; WYCHUDZKI, P.[2]; BONDAR, A.[3]; KOLEV, D.[4]; BROŻEK, T.[1]; DROZD, K.[1]; IŁKIEWICZ, K.[1]

[1] Toruń Centre for Astronomy, Nicolaus Copernicus University, ul. Gagarina 11, 87-100 Toruń, Poland, e-mail: cgalan@astri.uni.torun.pl

[2] Olsztyn Planetarium and Astronomical Observatory, Al. Marszałka J. Piłsudskiego 38, 10-450 Olsztyn, Poland

[3] International Centre for Astronomical and Medico-Ecological Research, Terskol, Russia

[4] Institute of Astronomy and National Astronomical Observatory, Bulgarian Academy of Sciences, 72 Tsarigradsko Shose blvd., BG-1784 Sofia, Bulgaria

AZ Cas ($m_{\rm V}$=9.3) was discovered as a variable star by Beljawsky (1931). Ashbrook (1956) has found it to be an eclipsing binary of Algol type with very long orbital period ($P_{\rm orb}$≈9.3yr). There are yet only a few eclipsing binary systems known to contain giant/supergiant stars, which have very long orbital periods, lasting decades. Eclipses in these systems are rare but if they occur they are very long and accompanied by interesting phenomena. A good example is VV Cep ($P_{\rm orb}$ ≈ 20.3 yr), in which the eclipses last for nearly 2 years. Its most recent eclipse in 1997 was delayed by 1% of the orbital period relative to the predictions (Graczyk et al. 1999). This system is the prototype of the group of variables consisting of an M or late K type supergiant and an early B type star, in whose spectra strong Balmer and [Fe] emission lines are present (Cowley 1969). AZ Cas belongs to this group. Among dozens of known VV Cep type binaries, only these two show eclipses.

The next spectacular event is about to begin in the AZ Cas system, which consists of two components with masses as high as about 30 $M_{\odot}$. The more massive component of the system is a supergiant of late K or early M spectral type ($T_{\rm eff}$ ∼ 4000 K), of which linear diameter may reach up to 1000 $R_{\odot}$. Its companion is a hot B star ($T_{\rm eff}$ ∼ 21000 K) with a diameter several tens of times smaller (D ∼ 30 $R_{\odot}$). Its total amount of emitted radiation equals to the supergiant and exceeds it many times in the ultraviolet. Due to the great difference in size and surface brightness between the components, photometrically only the primary eclipses can be observed, when the hot component is obscured. The depth of the eclipses differ strongly in different bands: reaches up to ∼ $2\overset{\rm m}{.}1$ in U and decreases rapidly towards the red, being only ∼ $0\overset{\rm m}{.}23$ in V (Fig. 1 a). The most interesting light variations appear during and near to the eclipses. In the $BV(RI)_{\rm C}$ photometric bands a gradual increase in the brightness of the system happens, reaching a maximum around phase 0.09, and then follows a relatively rapid decline. This is best seen in the V light curve (where the most numerous and accurate photometric data is available). There we can see the brightness drift starting already a bit before phase −0.05 (about half a year before the

photometric eclipse) and the eclipse appears to be imposed on this (Fig. 1 b). The totality in the whole observed range has a convex bottom with an increasing maximum towards the shorter wavelengths (Fig. 1 b & c). A slow increase in brightness by about $0\overset{m}{.}4$ over about 7-8 month after the egress in U band has been observed, for the first time with the 60 cm telescope at Piwnice Observatory (Fig. 1 c).

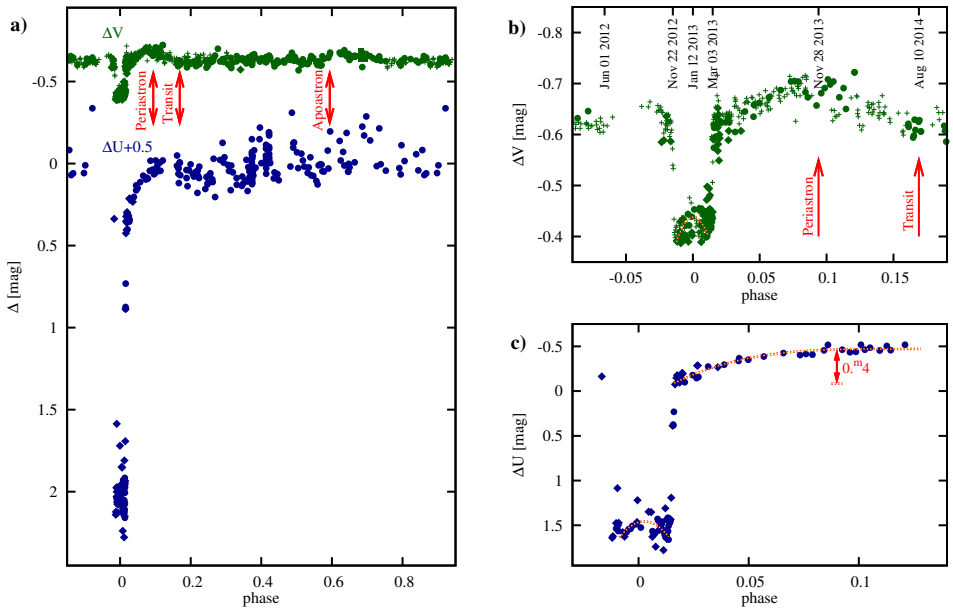

Figure 1. Left (panel a): U and V light curves obtained with the 0.6 m telescope at Piwnice Observatory since the last eclipse during 0.9 of orbital phase (points) are shown together with data obtained during the previous eclipses: Suhora and Kraków measurements (Mikolajewski et al. 2004) (diamonds) and older Larsson-Leander (1960) and Tempesti (1980) data (crosses). An expanded view of the curves around the eclipse and the periastron are shown on the right (panels: b & c): the V light curve with some dates of characteristic stages, predicted according to the ephemeris (Eq. 1) (top - panel b) and U light curve (bottom - panel c). The convex bottom and the long atmospheric eclipse are highlighted with dashed lines.

The unusual photometric behavior shown above is caused by the specificity of the orbit and the characteristics of the components. The orbit is highly eccentric ($e = 0.55$) and has a very special (close to zero) value of periastron longitude ($\omega = 4°$) (Cowley et al. 1977), so that the phase of occultation (primary eclipse) and transit are very close to the periastron (see Fig. 2). The supergiant has a huge diameter and furthermore it is surrounded by a very extended gaseous envelope formed as a result of an efficient mass loss process. When the components approach each other during the periastron passage then the equipotential surface is shrinking and the tidal forces lead to great deformation of the supergiant from the spherical symmetry. This phenomenon is responsible for the increase in brightness with maximum around the periastron. The maximum observed during the totality phase, seen as a convex bottom, could indicate the appearance of some additional, third light in the system. The increasing amplitude of this phenomenon towards the short wavelengths suggests that scattering effect could be responsible for that. In AZ Cas we observe probably for the first time such a strong scattering of the bright B stars radiation off particles in the extended envelope. More detailed studies of the brightening in the bottom shows that its maximum is shifted somewhat towards the end of the eclipse in agreement with

the change in brightness profile generated by orbiting scattering particles (Galan 2009). The effect connected with scattering is strong during the occultation, while it seems absent or very weak during the transit, which suggests that the Mie scattering dominates on particles of significant size in proportion to the wavelength of radiation. Additional support for the scattering nature of the phenomenon is the behavior of the color changes during the eclipses. The supergiant is significantly less reddened during the eclipse than its companion what indicates the existence of radiation excess in the short wavelengths (Galan et al. 2011).

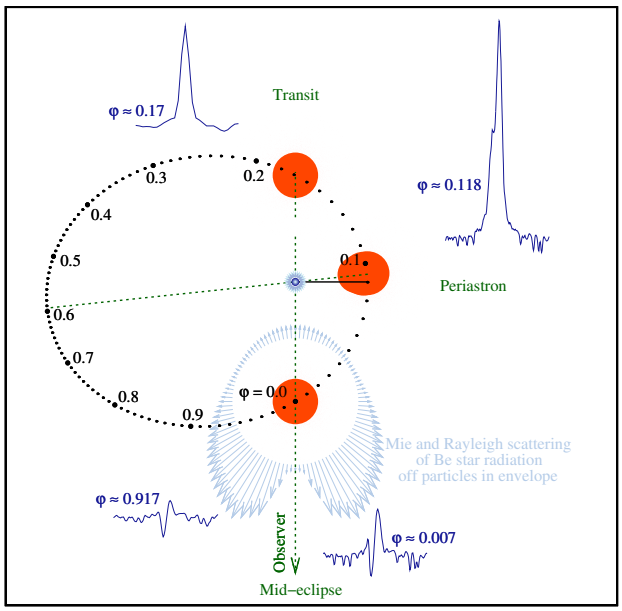

Figure 2. Schematic representation the supergiant and its extended envelope orbiting the B star. The special cases of mid-eclipse, periastron phase and transit are denoted. At the mid-eclipse position the scattering effect of the B star radiation off particles in the envelope is shown with blue arrows. During the periastron phase the supergiant is strongly distorted from the spherical symmetry as a result of ellipsoidal effect. The changes in the Hα profile ($FWZI \approx 13$Å) observed in the selected spectra obtained at Rozhen, Asiago, Piwnice and Terskol observatories at orbital phases: 0.007, 0.118, 0.17 and 0.917, respectively are shown.

The envelope causing the scattering can be responsible for the brightness increase after the egress in the U band. We interpret this as a result of the absorption by the envelope (extensive atmosphere) of the supergiant - a phenomenon analogous to that occurring in ζ Aurigae type eclipsing binaries - a class related to the VV Cep stars. If the proposed interpretation is correct, we should expect a similar "wing" caused by absorption which precedes the eclipse, and it should start in a short time. The last spectrum obtained in April 2012 at phase 0.917 shows a strong absorption component in the Hα line profile (Fig 2). This could indicate that the spectroscopic eclipse is already in progress.

An opportunity to observe and study in details the phenomena in AZ Cas system happens once in every 10 years. To exploit this opportunity, a dense coverage with photometric and spectroscopic observations is needed. The long time scales of changes in AZ Cas - the whole phenomenon will take more than 2 years - demands the involvement of a large number of observatories at different locations to reduce the dependency on the weather conditions and guarantee success during the important phases of the eclipse, which will be

relatively short (e.g. ingress and egress). In addition an engagement of a large number of instruments in the observations should increase the accuracy of the obtained light curves. This is very important when some changes have an amplitude as small as few hundredths of a magnitude. To achieve these goals we organize an international campaign for observations of the 2012/13 AZ Cas eclipse similar to the very fruitful observational campaigns for another, unique eclipsing binary EE Cep (Mikolajewski et al. 2005 a & b, Galan et al. 2010, Galan et al. 2012 a). To support the campaign coordination and to help the observers, we have prepared a special webpage: `http://www.astri.uni.torun.pl/~cgalan/AZCas`. All willing to participate in the observational campaign please contact the authors at `cgalan@astri.uni.torun.pl`. We invite both professional and amateur astronomers around the world. Multicolor photometry is especially desirable obtained in bands close to the standard Johnson or Johnson-Cousins $UBV(RI)_{\rm C}$ and spectra with low and high resolution covering the whole wavelength ranges from UV to IR. Nevertheless, photometric observations obtained with photographic filters RGB (owned by many amateurs) could also be very valuable. Although they differ from the standard Johnson BVR filters, it is possible to transform them to standard bands. Unfiltered CCD observations should be useful as well for timing purposes, i.e. to determine the precise moments of minimum. However, because of the strong supergiant domination in the infrared, it will be better to use at least an UV-IR blocking filter.

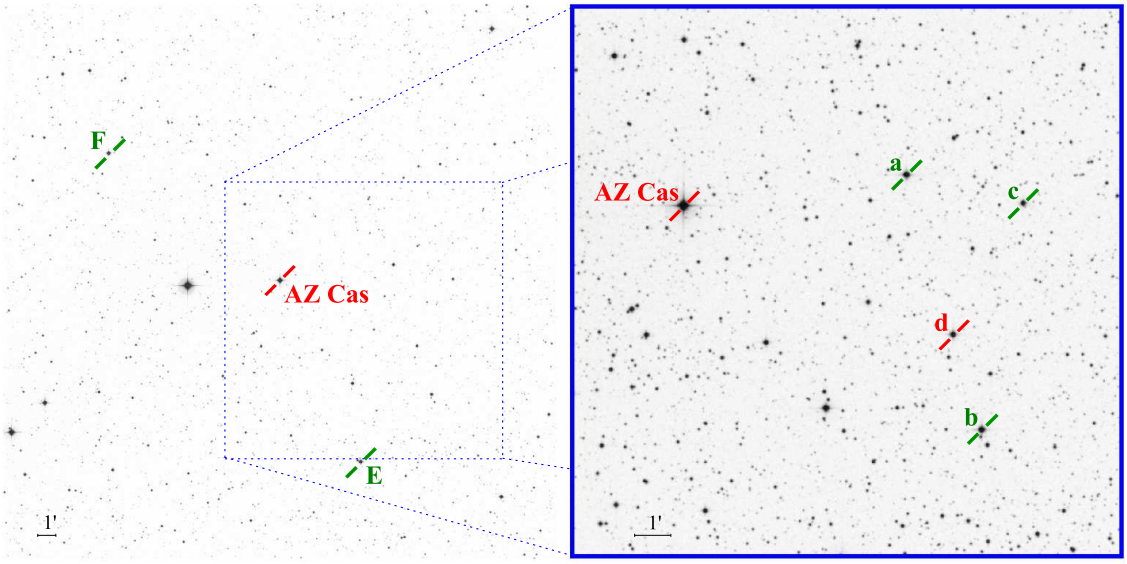

Figure 3. The sky area ($30' \times 30'$) around AZ Cas ($\alpha_{2000} = 1^{\rm h}\,42^{\rm m}\,17^{\rm s}$, $\delta_{2000} = +61^\circ\,25\farcm3$) (left) with expanded view of closer area ($15' \times 15'$) shown on the right. The comparison stars recommended for the CCD photometry are marked with green color (see Table 1 for details). Star "d" (TYC 4031-791-1) is variable (see the text).

BD+60°306 and BD+60°317 could be used as comparison stars. Both checked to be constant in V band within $0\fm01$ (Tempesti 1980). We have used these objects for multicolor $UBV(RI)_{\rm C}$ photometry of AZ Cas carried out by a single-channel diaphragm photometer with cooled Burle C31034 photomultiplier attached to the 60 cm Cassegrain telescope at Piwnice Observatory (53.0943 °N, 18.5532 °E) during the period August 2003 – November 2004. We have found these stars to be constant within $< 0\fm01$ in $V(RI)_{\rm C}$ bands and within $< 0\fm02$ in UB. However the angular distance between AZ Cas and

these stars (see Table 1) is too large. For the purpose of our CCD observations of AZ Cas carried out during the last 7 years using the SBIG-STL 11000 and SBIG-STL 1001 CCD cameras we established a new sequence of comparison stars: BD+60° 303, TYC 4031-437-1 and TYC 4031-125-1 (see Fig 3 and Table 1). We discovered that one of the brightest stars in our photometric field - TYC 4031-791-1 - is a previously unknown eclipsing binary of Algol type (Galan et al. 2012b). Using photometric Johnsons magnitudes published for BD+60°317 by Bern & Virdefors (1972), we have obtained UBV magnitudes for the stars mentioned above. They are shown in Table 1 together with the coordinates. We suggest to use star "a" (BD+60° 303) as main comparison star for the photometric measurements during the campaign. The simultaneous use of other comparisons (stars: "b", "c", "E", "F" in Table 1) is recommended. The variable star "d" is not suitable to be used as comparison, but campaign will provide a unique opportunity to obtain an accurate multicolor light curves for this object.

Table 1. The list of stars selected among those observed at Piwnice Observatory to establish the sequence of comparison stars.

Des.	Identifier	α_{2000}	δ_{2000}	Dist.*	Brightness [mag]		
		[h m s]	[° ’]	[’]	U ($3\sigma_U$)	B ($3\sigma_B$)	V ($3\sigma_V$)
a	BD+60° 303	1 41 24.9	61 25.76	6.2	11.30 (0.05)	11.09 (0.04)	10.60 (0.03)
b	TYC 4031-437-1	1 41 11.2	61 18.65	10.2	12.39 (0.05)	11.75 (0.04)	10.93 (0.03)
c	TYC 4031-125-1	1 40 58.5	61 24.79	9.3	12.67 (0.05)	12.41 (0.04)	11.80 (0.03)
d**	TYC 4031-791-1	1 41 16.4	61 21.31	8.2	11.66 (0.06)	11.71 (0.04)	11.16 (0.03)
E	BD+60° 306	1 41 44.8	61 15.25	10.7	11.68 (0.04)	10.95 (0.03)	9.90 (0.02)
F***	BD+60° 317	1 43 31.0	61 32.62	12.0	10.24 (0.03)	10.02 (0.02)	9.59 (0.01)

$\star$ The angular distance from AZ Cas in arcminutes.
$\star\star$ The eclipsing variable of Algol type discovered at Piwnice Observatory. The UBV magnitudes mean the average brightness outside eclipses in this case.
$\star\star\star$ UBV magnitudes by Bern & Virdefors (1972)

The most important moments during the campaign are marked in Fig. 1 b. To cover with observations the time interval in which we are interested, it is necessary to observe from June 2012 to August 2014. The complete lack of multicolor observations is particularly unfortunate in orbital phases preceding the eclipse. We emphasize the particular importance of filling this gap. It can contain the initial phase of the drift in brightness mentioned above and the atmospheric eclipse in U. The mid-eclipse, according to the ephemeris (Galan et al. 2011):

$$JD_{\mathrm{mid-ecl}} = 2432477.8 + 3403.85 \times E, \tag{1}$$

should occur on Jan 12, 2013. It will be important to intensify the observations by about one month around mid-eclipse because of the expected maximum in the convex bottom as well as during and around the rapid brightness changes occurring in ingress and egress. The mid-ingress is expected on Nov. 22, 2012 and mid-egress on Mar. 3, 2013. Because of the disparities in the components sizes, both of these stages are amazingly short. The expected duration of the ingress is 11 days while the egress should be about 4 days shorter due to the increasing orbital velocity of the system components when they approach the periastron. It would be also valuable to intensify observations around the periastron passage in November and December 2013 due to the presence of the ellipsoidal effect maximum, and the intriguing local minimum visible in the V light curve.

References:

Ashbrook, J., 1956, *Harvard Obs. Announcement Card*, No. 1340
Beljawsky, S., 1931, *AN*, **243**, 115
Bern, K., & Virdefors, B., 1972, *A&AS*, **6**, 117
Cowley, A. P., 1969, *PASP*, **81**, 297
Cowley, A. P., Hutchings, J. B., Popper, D. M., 1977, *PASP*, **89**, 882
Galan, C., 2009, *Doctoral Thesis (in Polish)*, UMK (Library of the Centre for Astronomy), Torun
Galan, C., Mikolajewski, M., Tomov, T., et al., 2010, *ASPC*, **435**, 423
Galan, C., Mikolajewski, M., Tomov, T., et al., 2011, *arXiv:1102.5198*
Galan, C., Mikolajewski, M., Tomov, T., et al. 2012 a, *A&A*, (in press) arXiv:1205.0028
Galan, C., Tomov, T., Świerczyński, E., et al., 2012 b, *IBVS*, No. 6028
Graczyk, D., Mikolajewski, M., Janowski, J. L, 1999, *IBVS*, No. 4679
Larsson-Leander, G. 1960, *Arkiv för Astron.*, **2**, 347
Mikolajewski, M., Zola, S., Kurpinska-Winiarska, M., et al., 2004, *ASPC*, **318**, 378
Mikolajewski, M., Galan, C., Gazeas, K., et al., 2005 a, *Ap&SS*, **296**, 445
Mikolajewski, M., Tomov, T., Hajduk, M., et al., 2005 b, *Ap&SS*, **296**, 451
Tempesti, P. 1980, A&AS, **39**, 115

COMMISSIONS 27 AND 42 OF THE IAU
INFORMATION BULLETIN ON VARIABLE STARS

Number 6028

Konkoly Observatory
Budapest
28 June 2012

HU ISSN 0374 – 0676

TYC 4031-791-1 - A NEW ECLIPSING BINARY OF ALGOL TYPE

GAŁAN, C.[1]; TOMOV, T.[1]; ŚWIERCZYŃSKI, E.[1]; WYCHUDZKI, P.[2]; BROŻEK, T.[1]; IŁKIEWICZ, K.[1]; MIKOŁAJEWSKI, M.[1]; DROZD, K.[1]

[1] Toruń Centre for Astronomy, Nicolaus Copernicus University, ul. Gagarina 11, 87-100 Toruń, Poland, e-mail: cgalan@astri.uni.torun.pl

[2] Olsztyn Planetarium and Astronomical Observatory, Al. Marszałka J. Piłsudskiego 38, 10-450 Olsztyn, Poland

TYC 4031-791-1 is an 11th magnitude star located in the constellation Cassiopeia in close proximity (8.2 arcmin) to the long-period eclipsing binary AZ Cas ($P_{\rm orb} \approx 9.3\,{\rm yr}$). We have monitored the photometric variability of AZ Cas since August 2003 with the 60-cm Cassegrain telescope at Piwnice Observatory (53.0943 °N, 18.5532 °E). In 2005 we switched from photomultiplier to CCD (SBIG-STL-1001) and we needed new comparison stars for photometry. TYC 4031-791-1 was one among many in the group of stars that have been tested to establish the sequence of comparison stars for AZ Cas (Galan et al. 2012), suitable for the narrow field of view of our CCD camera ($11.4' \times 11.4'$). We collected differential light curves for TYC 4031-791-1 with respect to all comparison stars during the last 7 years. We have observed deviations with similar amplitudes in all $(UBV(RI)_{\rm C})$ photometric bands (the V light curve is shown in Fig. 1).

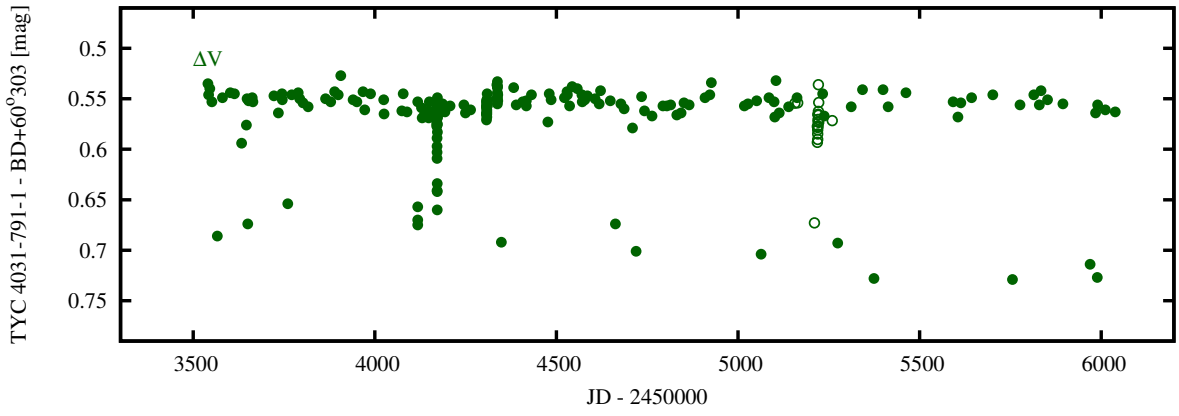

Figure 1. The V band differential light curve of TYC 4031-791-1 obtained with respect to BD+60°303. The data collected at Piwnice Observatory are shown with filled circles. Some of the data, presented with open circles, have been obtained with the 25/250 cm Schmidt-Cassegrain telescope and a SBIG-ST-8XME CCD camera at the Olsztyn Planetarium and Astronomical Observatory.

We checked that this star has not been reported variable in the GCVS catalogue (Samus et al. 2012) or in any other electronically available database. Assuming that the observed phenomenon is caused by eclipses, we searched for the orbital period using the `PerSea 2.6` tool (a program written by Gracjan Maciejewski: `http://www.astri.uni.torun.pl/~gm/software.html`), in which the ANOVA method for optimal period search by Schwarzenberg-Czerny (1996) is implemented. We have obtained the orbital period of 6.6827 ± 0.0002 days. Using the method of Kwee & van Woerden (1956) we have determined the time of primary minimum and obtained the ephemeris:

$$JD_{\mathrm{mid-ecl}} = 2453650.327(\pm 0.015) + 6.6827(\pm 0.0002) \times E \qquad (1)$$

The BVR_{C} light curves phased with the orbital period are shown in Figure 2. The secondary minimum occurs at phase 0.445 ± 0.003 indicating that the orbit is slightly eccentric. The minima are quite shallow - the primary minimum is not deeper than $0\overset{\mathrm{m}}{.}2$. The second eclipse is shallower by about only $0\overset{\mathrm{m}}{.}02$. The depths of the eclipses seem to be independent or depend very weakly on the photometric band. This suggests that the photospheres of the system components may have similar effective temperatures.

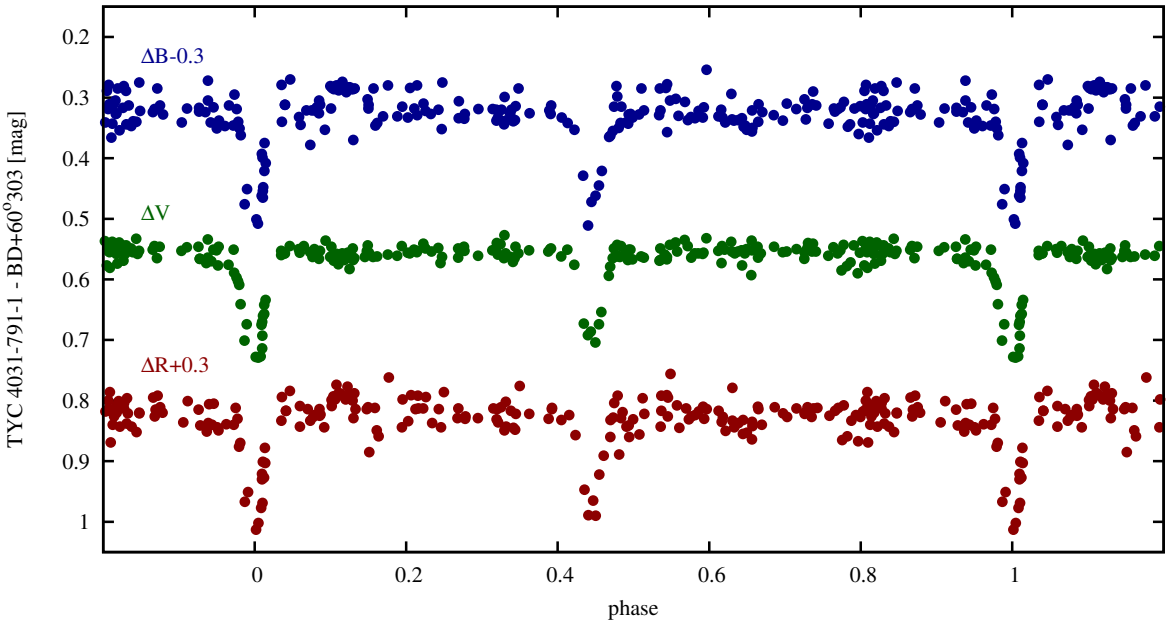

Figure 2. BVR_{C} light curves of TYC 4031-791-1 phased with the orbital period.

Fransworth (1956) has reported B1 spectral type for TYC 4031-791-1. In the spectrum obtained on Mar 10, 2003 (Fig. 3), the strongest features are the Hα, HeI 5876Å and HeI 6677Å absorption lines which confirms that star is of type B. However, the position of TYC 4031-791-1 on the $U-B$, $B-V$ two-color diagram (Fig. 4) indicates a somewhat later spectral type: B5 with an accuracy of about 3 subtypes. TYC 4031-791-1 is strongly reddened by interstellar matter – the color excess is large: $E(B-V) = 0.72 \pm 0.12$. This explains the very strong DIBs (5780 Å , 5797 Å , 6284 Å , 6614Å) and NaI interstellar doublet in the spectrum (Fig. 3).

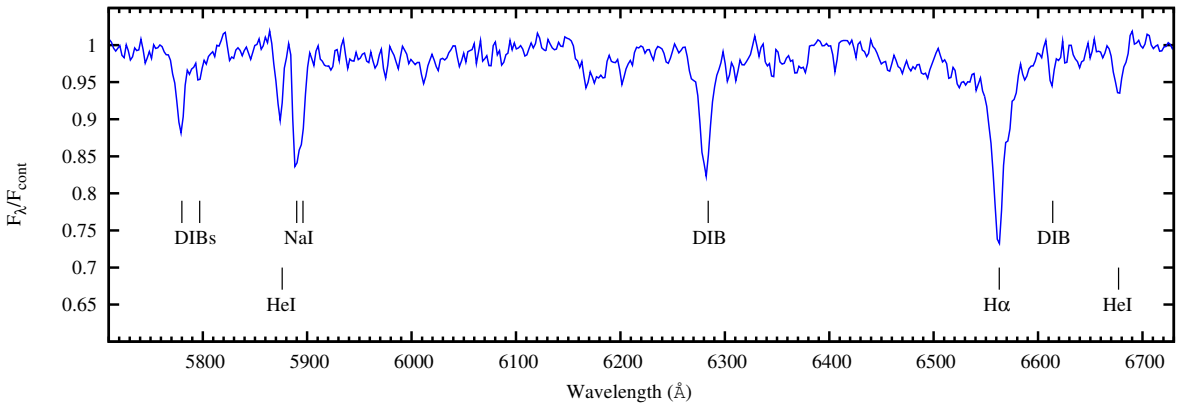

Figure 3. A medium resolution spectrum ($R \sim 2000$) of TYC 4031-791-1, obtained on Mar 10, 2007 with the CCS spectrograph on the 60/90-cm Schmidt-Cassegrain telescope at Piwnice Observatory.

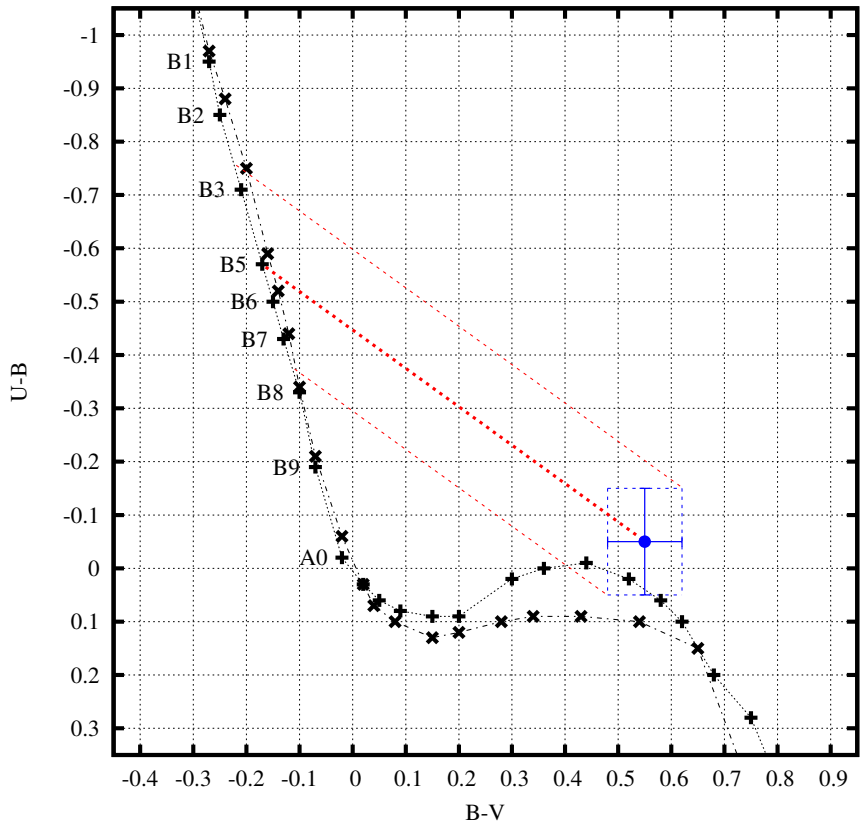

Figure 4. Location of TYC 4031-791-1 on the $U-B$, $B-V$ color-color diagram (blue point with errorbars), constructed with average out-of-eclipse magnitudes of the star: $m_{\rm U} = 11.66 \pm 0.06$, $m_{\rm B} = 11.71 \pm 0.04$, $m_{\rm V} = 11.16 \pm 0.03$ (Galan et al. 2012). The calibrations of Straižys (1977) for dwarfs (+) and giants (×) are shown as well. The red-dashed lines indicate the direction of the interstellar reddening.

Additional photometric and spectroscopic observations are needed to constrain the system parameters further. We intend to obtain accurate multicolor photometry of eclipses using our ephemeris and radial velocities with high-resolution spectra for further analysis.

Acknowledgements: We thank K. Czart, B. Deka, S. Frąckowiak, A. Karska, D. Kubicki, D. Puchalski, M. Radecki, P. Różański, W. Tyrkin, M. Więcek, P. Wirkus, M. Starszak, O. Ziołowska and one unidentified student for their occasional contribution to the collection of photometric data.

References:

Fransworth, A. H., 1955, *ApJS*, **2**, 123
Galan, C., Tomov, T., Mikolajewski, M., et al., 2012, *IBVS*, No. 6027
Kwee, K. K. & van Woerden, H., 1956, *BAN*, **12**, 327
Samus, N. N., Durlevich O. V., Kazarovets E. V., 2012, *General Catalog of Variable Stars (GCVS database, Version 2012 Jan)*, VizieR On-line Data Catalog B/gcvs
Schwarzenberg-Czerny, A., 1996, *ApJL*, **460**, 107
Straižys, V., 1977, "Multicolor Stellar Photometry" (in Russian), MOKSLAS Publ., Vilnius

COMMISSIONS 27 AND 42 OF THE IAU
INFORMATION BULLETIN ON VARIABLE STARS

Number 6029

Konkoly Observatory
Budapest
6 July 2012

HU ISSN 0374 – 0676

TIMINGS OF MINIMA OF ECLIPSING BINARIES

DIETHELM, ROGER

Bahnhofstrasse 3, CH–4118 Rodersdorf, Switzerland

The following Table lists timings of minima of eclipsing binaries secured by CCD photometry, obtained in the first half of 2012. The given O-C values generally refer to the linear elements of the newest electronic version of the GCVS (Samus et al., 2011), except for the cases stated in the remarks, where the determination of current elements made use of the up-to-date ASAS data (http://www.astrouw.edu.pl/asas/) and the Lafler-Kinman algorithm of the PERANSO software (http://www.peranso.com/). All times given are heliocentric UTC. All data were obtained at the R. Szafraniec Observatory operated at Astrokolkhoz Obs., Cloudcroft, N.M., USA. The tireless support by T. Krajci at the site is acknowledged thankfully.

Table 1: Minima of eclipsing binaries

Variable	Type	HJD 24...	±	$O-C$	n	Remarks
KP Aql	s	56046.8321	0.0009	−0.0205	33	V
V802 Aql	s	56089.8711	0.0004	+0.0017	30	V; el: IBVS 5527
V803 Aql	p	56089.8499	0.0001	−0.0005	30	V; el: 53806.895 + 0.263423 * E
						GSC 5140-253
V889 Aql	s	56072.8587	0.0008	−1.8072	29	V; el: Sov. Astr. 33, 41; non-circular
V962 Aql	s	56093.8969	0.0011	+0.0055	28	V; el: 54358.588 + 1.1650241 * E
UCAC3 178-203153	p	56089.8898	0.0010	+0.0468	30	V; el: 53806.895 + 2.291935 * E
ZZ Aur	p	55956.6728	0.0004	−0.0017	45	V
AP Aur	p	55980.6722	0.0004	+0.0837	41	V
DO Aur	p	55952.6895	0.0006	−0.0014	39	V
EI Aur	s	55947.7309	0.0007	+0.0070	38	V
EP Aur	p	55959.6743	0.0003	+0.0232	36	V; el: IBVS 4099
FO Aur	p	55957.6857	0.0005	−0.0227	34	V; d=0.025d
FP Aur	p	55956.7327	0.0004	+0.0014	45	V
HP Aur	s	55946.5998	0.0005	+0.0061	61	V
HU Aur	p	55937.6254	0.0003	−0.0004	37	V
IZ Aur	p	55953.7127	0.0004	−0.0004	36	V
MU Aur	p	55956.6420	0.0004	+0.0031	45	V
V523 Aur	s	55982.6984	0.0008	−0.0012	16	V
V618 Aur	p	55953.7628	0.0010	+0.0664	36	V
V636 Aur	s	55955.7311	0.0005	+0.0005	31	V
V639 Aur	p:	55957.6874	0.0004	+0.0509	37	V
SU Boo	p	56030.8842	0.0003	−0.0151	37	V
SY Boo	p	56014.9270	0.0007	−0.0018	31	V
TU Boo	s	56003.8809	0.0002	+0.0052	36	V; d=0.016d
	p	56075.7098	0.0003	+0.0054	27	V; d=0.015d
TX Boo	p	56015.9111	0.0011	+0.0498	34	V

Table 1: Minima of eclipsing binaries (continued)

Variable	Type	HJD 24...	±	$O-C$	n	Remarks
TY Boo	s	56023.8779	0.0003	−0.0015	37	V
	s	56085.7218	0.0005	−0.0016	26	V
TZ Boo	s	56021.8417	0.0009	−0.0014	10	V
	s	56077.7008	0.0007	−0.0087	22	V
VW Boo	p	56011.8126	0.0035	−0.0055	12	V; el: 53903.606 + 0.3423153 * E
	s	56076.6812	0.0005	−0.0057	29	V
XY Boo	s	55998.8716	0.0004	−0.0131	39	V; el: IBVS 5945
	p	56051.6795	0.0007	−0.0120	39	V
AC Boo	s	56023.9063	0.0005	+0.0004	20	V; d=0.020d
	s	56093.6968	0.0004	+0.0061	37	V; d=0.023d
AD Boo	s	56029.8810	0.0004	−0.0006	26	V
AR Boo	p	56000.8701	0.0004	−0.0094	34	V
CK Boo	p	56013.9024	0.0005	+0.0187	31	V; el: 53898.896 + 0.3551524 * E
	p	56086.7062	0.0006	+0.0162	25	V
CV Boo	p	56035.9128	0.0002	−0.0002	30	V
	p	56075.7212	0.0002	−0.0004	27	V
EF Boo	s	56013.8511	0.0006	+0.0080	35	V; el: IBVS 5992
EW Boo	p	56035.9060	0.0007	+0.0087	32	V
FY Boo	s	55991.8976	0.0004	+0.0085	34	V
	s	56051.7029	0.0005	+0.0064	39	V; asymmetric
GH Boo	s	56015.9187	0.0004	−0.0027	34	V; d=0.054d
GI Boo	p	56008.9288	0.0002	+0.0086	36	V; el: 51567.835 + 1.0335336 * E
	p	56093.6788	0.0004	+0.0089	37	V; d=0.037d
GK Boo	s	56010.8659	0.0004	+0.0025	34	V
	s	56078.7095	0.0005	+0.0024	27	V
GL Boo	p	56034.9083	0.0010	−0.0828	44	V; el: 55008.582 + 3.197536 * E
GN Boo	p	56018.8849	0.0001	+0.0177	40	V
GO Boo	p	56046.7757	0.0005	+0.0081	62	V; el: IBVS 5992
GQ Boo	p	56023.9431	0.0008	+0.0036	37	V
	p	56089.7139	0.0004	+0.0010	32	V
GR Boo	s	56018.8509	0.0002	−0.0082	40	V
GS Boo	p	56075.6681	0.0008	+0.0290	27	V; el: IBVS 5992
GU Boo	p	56023.8864	0.0006	+0.0002	36	V
	s	56086.6872	0.0009	−0.0009	15	V; D=0.04d!
GW Boo	s	56001.8846	0.0004	+0.0047	37	V; el: IBVS 5945; d=0.043d
	s	56074.7055	0.0006	+0.0038	38	V
HH Boo	s	56011.8778	0.0004	−0.0040	35	V
	p	56076.7261	0.0004	−0.0043	28	V
HR Boo	s	56016.8750	0.0004	+0.0012	32	V; el: 54203.696 + 0.3159672 * E
	p	56077.6962	0.0004	−0.0012	33	V
IL Boo	s	56003.8396	0.0003	+0.0029	36	V; el: 51438.735 + 0.347407 * E
	p	56078.7045	0.0007	+0.0016	28	V
IN Boo	p	56003.8617	0.0005	+0.0143	36	V
	s	56077.7333	0.0003	+0.0151	33	V
IO Boo	p	56008.9071	0.0005	+0.0024	31	V; el: 52395.7197 + 0.271138 * E
	p	56011.8924	0.0004	+0.0052	36	V
	s	56078.7247	0.0005	+0.0020	28	V
IS Boo	s:	56013.9565	0.0002	+0.0024	25	V
	p	56078.7064	0.0003	+0.0039	28	V
KM Boo	p	56009.8504	0.0010	−0.0011	17	V
	p	56078.7157	0.0005	+0.0015	28	V; asymmetric light curve
KW Boo	s	56013.8938	0.0006	+0.0084	37	V
	p	56016.8567	0.0012	+0.0059	32	V; pulsator?
KZ Boo	s:	56014.8622	0.0007	−0.0215	32	V; d=0.032d
	p:	56085.7441	0.0005	−0.0193	26	V
LM Boo	p	56013.9204	0.0003	−0.0077	37	V
	s	56077.6998	0.0004	−0.0098	33	V
MT Boo	s	56017.9557	0.0008	+0.0027	33	V; el: 51415.847 + 0.365377 * E; d=0.036:d
	p	56077.6955	0.0019	+0.0034	32	V
MY Boo	p	56018.9495	0.0003	+0.0023	40	V; el: 51387.9 + 0.473377 * E; d=0.021d
	p	56076.7020	0.0006	+0.0028	28	V

Table 1: Minima of eclipsing binaries (continued)

Variable	Type	HJD 24...	±	$O-C$	n	Remarks
NR Boo	s	56018.8648	0.0003	+0.0326	40	V; el: IBVS 5894
	p	56089.6769	0.0004	+0.0345	32	V; d=0.019d
NU Boo	p:	56023.9524	0.0012	−0.0815	22	V; pulsator?
NX Boo	p	56016.8937	0.0003	+0.0022	32	V; el: 51578.8373 + 0.2511348 * E
	p	56086.7081	0.0003	+0.0011	29	V
NY Boo	p:	56021.9009	0.0014	+0.0107	19	V
PY Boo	p:	56029.8606	0.0005	+0.0335	31	V; d=0.014d
PZ Boo	p	56033.8442	0.0003	+0.0038	29	V; el: 51400.538 + 0.622672 * E
	p	56073.6929	0.0004	+0.0016	29	V
QQ Boo	p	56023.8138	0.0009	−0.0544	18	V
	s	56023.9493	0.0005	−0.0571	19	V
QX Boo	s:	56033.9347	0.0005	+0.0418	31	V; d=0.021d
GSC 900-421	p	56001.8446	0.0004	+0.0120	37	V; el: IBVS 5992
GSC 902-318	s	56011.9300	0.0005	−0.0035	36	V; el: IBVS 5992
	s	56089.7265	0.0003	−0.0001	32	V
GSC 912-792	p	56009.8852	0.0016	+0.0026	17	V; el: IBVS 5894
	s	56089.6711	0.0001	+0.0033	32	V
GSC 1467-1309	p	56010.9285	0.0007	−0.0004	35	V; el: IBVS 5945
GSC 1470-582	s	56002.8436	0.0007	+0.0074	13	V; el: IBVS 5945
	p	56075.7346	0.0004	+0.0043	28	V
GSC 1477-516	p	56017.8284	0.0002	+0.0031	33	V; el: IBVS 5992
	p	56074.7477	0.0005	+0.038	36	V; d=0.016d
GSC 1478-669	s	56018.8401	0.0008	−0.0005	40	V; el: IBVS 5894; d=0.041d
	p	56086.6771	0.0005	+0.0007	31	V; d=0.032d
GSC 1484-525	p	56016.8527	0.0003	−0.0095	32	V; el: IBVS 5894
	s	56093.7433	0.0003	−0.0116	34	V
GSC 1999-404	p	56000.8639	0.0003	−0.0015	35	V; el: IBVS 5992; d=0.018d
GSC 3039-709	s	56015.9249	0.0004	−0.0257	34	V; el: PZP 11, 1
	p	56087.7430	0.0008	−0.0288	26	V
GSC 3475-348	s	56011.9131	0.0007	−0.0087	34	V; el: 51421.637 + 0.253698 * E
	p	56076.7370	0.0005	−0.0046	20	V
AK Cam	p	56009.6457	0.0018	+0.0393	28	V; el: BAV Mitt. 69
AL Cam	p	55978.8606	0.0004	−0.0344	24	V
AZ Cam	p	56008.662	0.003	+0.031	25	V
HW Cam	p	55940.9309	0.0007	+0.0925	22	V; el: IBVS 4526
LR Cam	p	55959.7033	0.0002	−0.0713	36	V; el: IBVS 5132
QZ Cam	p	55944.6853	0.0004	+0.0689	45	V; el: 51513.91 + 3.371922 * E; d=0.051d
V343 Cam	p	55937.7529	0.0015	+0.0022	36	V; el: IBVS 5992
V368 Cam	p	55937.6494	0.0012	−0.0753	24	V
V372 Cam	p	55937.6617	0.0010	+0.0002	34	V
V379 Cam	p	55937.7401	0.0005	−0.0043	37	V; el: 54481.2279 + 1.1670805 * E
V392 Cam	s	55957.773	0.005	+0.116	25	V
V401 Cam	p:	55963.7858	0.0020	+0.0278	16	V
V420 Cam	p	55960.773	0.004	+0.026	12	V
V424 Cam	s:	55960.6247	0.0009	−0.0527	21	V
V426 Cam	p:	55963.7647	0.0010	+0.0787	16	V
V451 Cam	s:	55971.6343	0.0008	−0.0703	26	V; el: 51553.64 + 0.401478 * E
V457 Cam	p:	55971.6959	0.0004	−0.0051	23	V
V468 Cam	p	55973.6530	0.0002	−0.0119	40	V; el: 51623.76 + 0.347492 * E
V470 Cam	p	55976.6647	0.0008	−0.0289	28	V
V473 Cam	s	55991.6706	0.0006	+0.0140	33	V
V474 Cam	p	55979.6598	0.0002	−0.0026	27	V
V479 Cam	s	55982.7317	0.0007	+0.0199	21	V; d=0.020d
V483 Cam	p	55991.7020	0.0007	−0.0076	32	V; el: 51460.74 + 0.382554 * E
V496 Cam	p	55998.6665	0.0005	−0.0829	27	V; d=0.05d
V497 Cam	s	56021.6811	0.0018	−0.0024	19	V
V500 Cam	p	56000.7137	0.0003	+0.0089	39	V; d=0.012d
	s	56021.6993	0.0011	+0.0089	19	V
V505 Cam	p	55937.810	0.003	+0.019	14	V
	s	56021.7320	0.0007	+0.0192	17	V

Table 1: Minima of eclipsing binaries (continued)

Variable	Type	HJD 24...	±	$O-C$	n	Remarks
V506 Cam	p	55937.9074	0.0005	+0.0131	27	V; el: 51525.790 + 0.340099 * E
V507 Cam	p	56002.6934	0.0005	−0.0330	31	V
V509 Cam	s	55937.8301	0.0003	−0.0863	23	V; d=0.016d
	s	56017.7080	0.0004	−0.0860	38	V
V514 Cam	p	55976.9312	0.0003	+0.0547	42	V; el: 51577.59 + 0.362738 * E; d=0.026d
	p	56035.6943	0.0004	+0.0543	31	V; d=0.024d
V515 Cam	p	55973.799	0.010	−0.047	33	V
	s	55937.9814	0.0004	+0.0223	15	V
	p	55983.973	0.006	−0.034	35	V
	p	56035.7715	0.0009	−0.0443	22	V; flare at 0.7115d
V517 Cam	p	56048.6666	0.0010	−0.0075	29	V
V518 Cam	p	55983.8406	0.0020	+0.0386	34	V
V519 Cam	p	56015.8711	0.0003	−0.0046	32	V
NSV 4638	p	55963.9239	0.0006	+0.0606	37	V; el: IBVS 5945; d=0.06d
	s	56009.786	0.004	+0.0975	27	V
WW Cnc	p	56015.6963	0.0003	−0.5524	40	V
YY Cnc	p	56002.7244	0.0004	−0.0084	33	V; el: IBVS 5591
AB Cnc	p	55998.7181	0.0004	+0.0728	32	V; el: IBVS 5337
AH Cnc	p	56001.7214	0.0005	+0.1574	29	V; d=0.029d
AO Cnc	p	56000.7039	0.0003	−0.0704	35	V
EH Cnc	p	56000.6766	0.0002	−0.0071	40	V; el: IBVS 5992
GQ Cnc	p	56002.6490	0.0006	+0.0025	32	V; el. Krakow Catalog
GW Cnc	p	56021.7252	0.0012	−0.0096	11	V; el: IBVS 5992
IL Cnc	p	56000.619	0.004	+0.069	11	V
	s	56000.7575	0.0007	+0.0730	21	V
IM Cnc	s	56014.6911	0.0004	−0.0256	33	V
IO Cnc	p	56003.7142	0.0004	−0.0009	37	V; el: IBVS 5992; d=0.024d
IR Cnc	p	55998.6716	0.0002	+0.0034	32	V; el: IBVS 5871
IU Cnc	p	56002.7006	0.0003	−0.0193	32	V
KT Cnc	s	55940.9382	0.0006	−0.0057	21	V
KY Cnc	s	56003.6513	0.0004	−0.0054	37	V; el: 54428.816 + 2.3807116 * E
LU Cnc	p	56001.6870	0.0002	−0.0220	36	V
GSC 795-590	s	55998.6819	0.0004	+0.0044	32	V; el: IBVS 5992
GSC 800-1379	s	55940.8353	0.0005	+0.0176	18	V; el: IBVS 5992
GSC 808-1106	s	56009.650	0.005	0	26	V; el: IBVS 5992; d=0.033d
GSC 815-1932	s	56003.7155	0.0005	+0.0087	35	V; el: IBVS 5992; d=0.052d
GSC 817-322	p	56001.7262	0.0004	−0.0145	36	V; el: IBVS 5992
GSC 817-411	s	56002.6746	0.0007	+0.0027	21	V; el: IBVS 5992
GSC 819-48	s	55945.9150	0.0004	+0.0056	46	V; el: IBVS 5992
GSC 819-595	p	56014.6375	0.0017	+0.0203	33	V; el: IBVS 5945
GSC 1383-181	s	55998.6939	0.0006	+0.0048	18	V; el: IBVS 5992
GSC 1407-222	s	56010.7502	0.0004	−0.0141	36	V; el: 54888.723 + 0.923871 * E
GSC 1927-1182	p	55998.6333	0.0013	−0.0226	33	V; el: 54435.81 + 2.2199516 * E
GSC 1950-1942	p	56003.618	0.003	+0.006	18	V; el: IBVS 5992
	s	56003.7721	0.0010	+0.0314	18	V; d=0.017d
GSC 2484-139	p	55940.8922	0.0005	−0.0002	22	V; PZP 10, 13
NSV 4158	p	55940.9437	0.0005	+0.0001	26	V; el: IBVS 5992
RV CVn	p	56001.8955	0.0002	+0.0235	38	V
VV CVn	p	56021.9451	0.0017	+0.0428	22	V; el: IBVS 5894
VZ CVn	s	55998.971	0.005	−0.008	39	V; el: MNRAS 376, 573
	p	56072.6944	0.0004	+0.0001	39	V
YZ CVn	p	55998.8486	0.0002	−0.0163	39	V
BI CVn	p	55989.8547	0.0003	+0.0555	37	V; el: IBVS 4554
	p	56051.7145	0.0004	+0.0582	39	V
BO CVn	p	55990.8849	0.0005	+0.0035	31	V; el: Krakow Catalog
	p	56074.7115	0.0002	+0.0014	37	V; d=0.037d
CI CVn	s	55989.8392	0.0006	−0.0217	19	V; el: Hipparcos
	p	56054.7029	0.0009	−0.0202	20	V
DF CVn	p	55986.8780	0.0003	−0.0037	38	V; el: IBVS 5894
	s	56052.7504	0.0003	−0.0008	37	V

Table 1: Minima of eclipsing binaries (continued)

Variable	Type	HJD 24...	±	$O-C$	n	Remarks
DH CVn	s	55968.8739	0.0006	−0.0262	28	V; el: IBVS 5149; d=0.033d
	s	56045.6913	0.0002	−0.0285	27	V; d=0.030d
DI CVn	s	55982.8469	0.0027	−0.0064	15	V; el: IBVS 5224
	s	56047.7125	0.0006	−0.0058	30	V
DK CVn	p	55982.9341	0.0011	+0.0010	9	V; el: IBVS 5642
	p	56049.7519	0.0026	−0.0012	7	V; very distorted light curve
DQ CVn	s	55983.9351	0.0005	+0.0085	32	V; el: IBVS 5541
	s	56052.7333	0.0005	+0.0078	26	V
DR CVn	p	55989.9224	0.0003	+0.0528	38	V
	p	56054.7544	0.0005	+0.0615	18	V
DX CVn	p	55989.9251	0.0008	+0.0050	37	V
	s	56048.7131	0.0003	+0.0037	26	V
DY CVn	p	55987.8966	0.0002	−0.0019	33	V
	s	56049.7524	0.0003	−0.0024	35	V
EE CVn	s	55998.8407	0.0006	−0.0041	25	V; d=0.014d
	p	56051.7246	0.0003	−0.0064	39	V; d=0.019d
EF CVn	s	55991.8936	0.0004	−0.0065	19	V
	p	56049.7002	0.0005	−0.0104	35	V
EI CVn	s	56003.8957	0.0003	−0.0210	36	V
	s	56077.6921	0.0002	−0.0219	33	V
EN CVn	p	56051.6867	0.0003	+0.1086	39	V; el: IBVS 5992; non-circular
EX CVn	s	55983.8236	0.0006	−0.0741	15	V
	p	55983.9603	0.0006	−0.0759	18	V
	p	56050.7542	0.0016	−0.0780	21	V
FQ CVn	p	55998.8488	0.0003	−0.0185	39	V
FU CVn	s	55990.959	0.003	−0.031	31	V
	s	56072.7394	0.0011	−0.0318	38	V
	s	56073.705	0.003	−0.029	31	V
FV CVn	s	56001.8793	0.0006	−0.0064	24	V
	s	56074.7247	0.0003	−0.0109	38	V
FZ CVn	s:	56002.8541	0.0004	−0.0416	30	V
GG CVn	s	56002.9185	0.0004	+0.0214	33	V
	p	56085.7061	0.0002	+0.0236	27	V
GI CVn	s:	56003.8986	0.0004	−0.0020	37	V
	s:	56089.6951	0.0004	+0.0002	32	V
GN CVn	s	56008.9064	0.0003	+0.0105	36	V; el: 53382.6919 + 0.395007; d=0.021d
	s	56073.6878	0.0005	+0.0107	22	V; d=0.022d
GO CVn	s	56001.970	0.005	−0.001	13	V; el: 51389.637 + 0.537662 * E
	s	56076.7055	0.0014	+0.0000	28	V
RR CMa	p	55982.7358	0.0006	−0.0028	28	V; el: IBVS 5992
GSC 5391-1821	s	55952.6229	0.0013	+0.0594	43	V; el: IBVS 5960; non-circular
GSC 5404-2421	s	55944.6857	0.0006	+0.9883	58	V; el: IBVS 5992; non-circular
GSC 5406-2659	p	55981.7274	0.0013	+0.0041	16	V; el: IBVS 5992
GSC 5934-2133	s	55960.6444	0.0005	+0.0038	23	V; el: IBVS 5992
GSC 5948-2942	p	55971.6372	0.0009	−0.0127	17	V; el: IBVS 5960; d=0.02d
TX CMi	s	55987.6717	0.0005	+0.0063	38	V; el: BBSAG Bull. 106, 7
TY CMi	p	55982.6390	0.0022	−0.0212	30	V; el: 50904.3817 + 1.2991247 * E
UZ CMi	p	55980.6971	0.0002	+0.0203	40	V; el: IBVS 5894; d=0.026d
AC CMi	p	55982.6947	0.0005	+0.0373	30	V; el: PASP 98, 690
AG CMi	p	55984.7025	0.0003	−0.1616	38	V
AK CMi	p	55987.7000	0.0004	−0.0239	38	V; d=0.020d
AO CMi	p	55979.7148	0.0005	−0.1183	40	V
AV CMi	p	55986.6445	0.0006	+0.0148	37	V; el: IBVS 5945; non-circular
CX CMi	s	55978.6719	0.0006	+0.0072	33	V; d=0.06d
DW CMi	p	55987.6523	0.0009	+0.0069	25	V
EL CMi	p	55989.7018	0.0003	−0.0016	35	V; d=0.018d
EQ CMi	s	55989.6890	0.0009	−0.0285	35	V
GSC 167-251	s	55979.7210	0.0003	−0.0048	40	V; el: IBVS 5945
GSC 199-2035	p	55983.7167	0.0006	+0.0039	21	V; el: 54473.760 + 1.0127115 * E
GSC 762-958	s	55978.6850	0.0004	+0.0032	43	V

Table 1: Minima of eclipsing binaries (continued)

Variable	Type	HJD 24...	±	$O-C$	n	Remarks
GSC 763-1042	p	55979.6453	0.0005	−0.0156	39	V; el: IBVS 5992
GSC 764-235	p	55987.7031	0.0001	+0.0034	39	V; el: IBVS 5992
GSC 772-425	s	55979.6360	0.0005	−0.0025	16	V; el: 53759.638 + 0.2868403 * E
GSC 5407-2794	s	55980.6632	0.0003	−0.0058	27	V; el: IBVS 5992; d=0.018d
GSC 4286-49	p	56086.8825	0.0017	−0.0009	28	V; el: IBVS 5570; non-circular
RW Com	s	55981.9020	0.0003	−0.0087	41	V
	p	56046.6987	0.0004	−0.0073	28	V
RZ Com	p	55982.9226	0.0002	+0.0073	44	V; el: IBVS 5992
	s	56042.6697	0.0005	+0.0081	31	V; d=0.018d
SS Com	s	55987.8490	0.0005	+0.0140	33	V; el: IBVS 5992
	s	56047.7080	0.0001	+0.0139	31	V; d=0.032d
UX Com	p	56015.8038	0.0004	−0.1317	71	V; el: BAV Mitt. 69; d=0.064d
AQ Com	s	55981.8645	0.0004	−0.0086	22	V; el: IBVS 5684
	p	56048.6829	0.0013	−0.0063	14	V
CC Com	p	55980.8725	0.0003	−0.0176	18	V
	s	55980.9838	0.0003	−0.0166	12	V
	s	56039.6847	0.0006	−0.0183	27	V
CM Com	p	55981.9302	0.0005	−0.0162	41	V; el: IBVS 5894
	p	56045.6964	0.0009	−0.0192	18	V; asymmetric
CN Com	p	55986.9213	0.0002	+0.0618	19	V; d=0.024d
	p	56034.7230	0.0007	+0.0599	20	V
DD Com	p	55981.8703	0.0005	+0.0899	41	V; el: IBVS 4167; d=0.020d
	s	56047.6890	0.0006	+0.0877	31	V
DG Com	p	56052.7572	0.0003	−0.0534	37	V
EK Com	p	55986.9185	0.0003	−0.0591	38	V; el: IBVS 4167
	s	56049.7199	0.0004	−0.0626	35	V
EQ Com	s	55987.8814	0.0006	+0.0054	14	V; Krakow Catalog
	p	56050.6711	0.0012	+0.0082	13	V
LL Com	p	55990.8474	0.0011	+0.0580	29	V; el: IBVS 4386
	s	56051.6833	0.0008	+0.0627	39	V
LO Com	s	55982.8406	0.0004	+0.0082	17	V; el: IBVS 5052
	p	55982.9856	0.0007	+0.0010	12	V
	p	56046.6982	0.0003	+0.0075	29	V
LP Com	p	55984.8448	0.0005	−0.0238	26	V; el: IBVS 5052
	p	56047.7010	0.0006	−0.0236	31	V
LR Com	p	55973.9181	0.0002	−0.0190	27	V; el: IBVS 5894
	p	55982.8804	0.0002	−0.0197	39	V
MM Com	s	55989.9338	0.0007	−0.0159	37	V
	S	56049.7302	0.0006	−0.0135	33	V; strong O'Connell effect
NN Com	s	55982.9150	0.0005	+0.0071	23	V; el: IBVS 5894
	p	56042.6503	0.0022	+0.0007	16	V
GSC 871-248	p	55980.8378	0.0007	+0.0295	18	V; el: IBVS 5945
	s	55980.9661	0.0003	+0.0315	18	V; d=0.021d
	p	56038.7220	0.0006	+0.0349	26	V
GSC 881-218	p	55986.9313	0.0004	+0.0047	37	V; el: IBVS 5894
	s	56048.7335	0.0007	+0.0015	27	V
GSC 1445-866	s	55983.8932	0.0006	+0.0078	28	V; el: IBVS 5992
	s	56047.6833	0.0004	+0.0116	31	V; d=0.018d
GSC 1446-1499	s	55983.9096	0.0006	+0.0029	14	V; el: IBVS 5894
	s	56050.7183	0.0021	+0.0049	14	V
GSC 1446-2377	s	55981.8251	0.0003	−0.0050	19	V; el: IBVS 5894
	p	55981.9730	0.0007	−0.0061	16	V
	s	56047.6609	0.0019	−0.0049	13	V
GSC 1994-465	s	55991.9154	0.0003	+0.0107	35	V; el: IBVS 5992; d=0.027d
	s	56052.7322	0.0005	+0.0108	38	V
GSC 1994-935	s	55998.9415	0.0005	+0.0223	39	V; el: IBVS 5894
	s	56050.6885	0.0002	+0.0203	16	V
RT CrB	p	56038.9262	0.0018	−0.0216	31	V
RW CrB	p	56036.8767	0.0002	−0.0022	35	V
TU CrB	p	56029.8280	0.0003	+0.0002	32	V; el: 51343.887 + 1.613616 * E

Table 1: Minima of eclipsing binaries (continued)

Variable	Type	HJD 24...	±	$O-C$	n	Remarks
TW CrB	p	56036.8896	0.0002	+0.0470	36	V
YY CrB	p	56034.8912	0.0005	−0.0009	42	V; el: Krakow Catalog
AR CrB	p	56052.9262	0.0024	−0.0048	30	V
AS CrB	s	56038.8460	0.0003	+0.0156	31	V; d=0.030d
AV CrB	s	56042.8932	0.0003	−0.0258	33	V
AY CrB	p	56029.8695	0.0005	+0.0013	32	V; el: 51462.65 + 0.4604979 * E
	p	56089.7329	0.0004	−0.0000	32	V
BD CrB	p:	56029.9165	0.0007	+0.0734	30	V
W Crv	p	55980.9384	0.0008	+0.0145	17	V
	p	56045.7491	0.0005	+0.0157	28	V
GSC 5532-1333	p	55980.8511	0.0002	+0.0113	37	V; el: IBVS 5992
	p	56048.7064	0.0004	+0.0127	29	V
GSC 6094-1317	p	55956.8731	0.0005	+0.0101	39	V; el: IBVS 5992
	p	56048.7384	0.0006	+0.0105	29	V
GSC 6095-294	s	55979.9382	0.0002	−0.0019	14	V; el: IBVS 5992
	s	56042.6895	0.0003	−0.0017	31	V
V Crt	p	55956.8582	0.0004	+0.0020	41	V; el: IBVS 5992
	p	56039.6979	0.0004	+0.0013	30	V
AC Crt	p	55960.8408	0.0006	+0.0033	43	V; el: IBVS 5945
	s	56016.7005	0.0005	+0.0009	32	V
GSC 5500-260	s	55960.9490	0.0004	−0.0076	20	V; el: IBVS 5992
	s	56033.6935	0.0007	−0.0051	26	V; d=0.021d
GSC 5507-705	p	55960.9140	0.0002	+0.0107	45	V; el: IBVS 5992
	s	56017.7158	0.0007	+0.0147	18	V
GSC 5509-447	p	55980.8495	0.0003	−0.0095	37	V; el: IBVS 5992
	p	56041.6684	0.0007	−0.0057	20	V
GSC 5509-1073	p	55980.8374	0.0005	+0.0035	37	V; el: IBVS 5992
	p	56035.6652	0.0006	+0.0018	31	V
GSC 5509-1347	p	55979.8693	0.0005	+0.0014	25	V; el: IBVS 5992; d=0.031d
	p	56046.7118	0.0003	+0.0040	30	V: d=0.033d
GSC 5516-355	s	55976.8847	0.0005	+0.0011	41	V; el: IBVS 5992
	p	56036.6629	0.0006	+0.0023	14	V
GSC 5524-817	p	55979.8614	0.0002	+0.0042	26	V; el: 53476.605 + 0.296313 * E
	s	56038.6822	0.0008	+0.0068	18	V
GSC 6077-1825	p	55963.8735	0.0005	−0.0065	35	V; el: IBVS 5992
	p	56041.6719	0.0009	−0.0072	19	V
GSC 6085-670	p	55978.9525	0.0006	+0.0241	30	V; el: IBVS 5992
V477 Cyg	s	56086.883	0.008	−0.450	32	V; non-circular
V498 Cyg	s	56072.849	0.005	+0.175	29	V; non-circular
V974 Cyg	s	56073.9218	0.0004	−0.2505	37	V; non-circular
	p	56078.8164	0.0012	−0.1625	29	V; non-circular
V1136 Cyg	p	56049.8564	0.0006	+0.0892	27	V; non-circular
	s	56051.8743	0.0011	+0.3757	32	V; non-circular
GSC 3152-1202	p	56086.9107	0.0016	+0.0132	31	V; el: IBVS 5909; non-circular
Z Dra	p	55971.848	0.003	−0.194	16	V
	p	56039.7220	0.0007	−0.1926	18	V
RX Dra	p	56047.9050	0.0005	+0.0581	27	V; d=0.036d
AR Dra	p	55980.8543	0.0007	+0.0196	37	V
	p	56045.7398	0.0006	+0.0247	27	V
AU Dra	p	56072.9076	0.0005	−0.0135	29	V; el: IBVS 4587
AX Dra	p	55984.8995	0.0004	−0.0616	27	V
	p	56049.6708	0.0002	−0.0610	35	V
BF Dra	s	56048.828	0.008	−0.236	31	V; el: IBVS 3867; non-circular
BU Dra	p	56017.8384	0.0002	+0.1624	33	V; d=0.024d
BX Dra	p	56047.8895	0.0002	+0.0342	28	V; el: IBVS 4266; d=0.030d
CM Dra	p	56087.7239	0.0003	+0.0023	26	V
CV Dra	p	56072.8749	0.0006	+0.0040	29	V; el: BAV Mitt. 69
FU Dra	p	56029.8695	0.0004	+0.0022	30	V; el: Krakow Catalog
IV Dra	s	56030.8836	0.0006	+0.0060	37	V; el: IBVS 5894
LN Dra	p	56077.8912	0.0007	+0.0013	28	V; el: 51306.863 + 0.612141 * E; d=0.041d

Table 1: Minima of eclipsing binaries (continued)

Variable	Type	HJD 24...	±	$O-C$	n	Remarks
MU Dra	s	56089.8348	0.0009	−0.0005	31	V; el: 52146.5052 + 0.3496635 * E
MY Dra	p	56035.7523	0.0008	+0.0314	31	V
NT Dra	p	56016.7281	0.0005	+0.0059	37	V
NV Dra	s	55982.8273	0.0005	+0.0533	45	V
	s	56035.6866	0.0005	+0.0551	31	V; d=0.024d
NW Dra	p	55973.9046	0.0007	+0.0002	14	V
	s	56034.7040	0.0007	+0.0040	18	V; asymmetric
OO Dra	p	55944.9791	0.0006	−0.0041	25	V
	p	56036.630	0.005	+0.006	15	V
OQ Dra	s	55978.8218	0.0011	+0.0535	18	V
	p	55978.9957	0.0016	+0.0575	10	V
	s	56041.6672	0.0008	+0.0600	18	V
PQ Dra	p	56017.9010	0.0004	−0.0030	33	V; el: 51363.779 + 0.320952 * E
QU Dra	p	56029.8462	0.0002	−0.0367	32	V
V338 Dra	p	56033.8434	0.0006	−0.0258	17	V
	s	56033.9595	0.0018	−0.0273	10	V
V339 Dra	p:	56034.9328	0.0004	+0.0392	43	V; d=0.034d
V341 Dra	p	56030.9135	0.0010	+0.0068	37	V
V342 Dra	p	56035.9362	0.0003	+0.0558	31	V; el: 51286.67 + 0.392205 * E
V344 Dra	p:	56045.9308	0.0015	−0.0233	28	V
GSC 4190-894	p	56042.8379	0.0005	−0.0010	31	V; el: 51427.83 + 0.334882 * E
GSC 4193-44	p	56047.8557	0.0004	+0.1394	28	V; el: PZP 11, 1
GSC 4194-2180	p	56049.8921	0.0006	−0.0006	14	V; el: 51400.699 + 0.2682124; d=0.023d
WW Eri	p	55940.7222	0.0005	+0.0648	44	V; d=0.067d
BQ Eri	p	55945.7587	0.0010	−0.0045	48	V; el: 53453.544 + 0.821972 * E
GSC 4739-480	p	55944.6055	0.0007	+0.0042	45	V; el: 55072.919 + 0.671041 * E
GSC 5322-2251	p	55945.7538	0.0002	+0.0121	48	V; el: IBVS 5960
GSC 5330-664	p	55944.6158	0.0005	+0.0034	19	V; el: 53090.536 + 0.229575 * E
	s	55944.7273	0.0005	+0.0001	18	V
TZ Gem	p	55971.7099	0.0014	−0.0069	25	V; el: IBVS 5960
WW Gem	s	55959.7291	0.0006	+0.0220	35	V
CK Gem	p	55968.6970	0.0005	−0.0692	18	V
DP Gem	p	55957.6453	0.0006	+0.0026	37	V; el: 53005.676 + 0.558450 * E
EY Gem	p	55968.7146	0.0003	−0.2279	29	V
FT Gem	s	55984.7061	0.0013	−0.0383	37	V
HR Gem	p	55956.6411	0.0005	+0.0134	43	V
KQ Gem	p	55971.6647	0.0006	−0.0867	23	V; d=0.029d
V404 Gem	p	55968.6914	0.0005	+0.0034	20	V; el: IBVS 5992
V410 Gem	p	55945.7172	0.0004	+0.0023	47	V; el: 52676.633 + 3.470363 * E; non-circular
	s	55978.7095	0.0011	+0.0261	42	V
V415 Gem	s	55978.6749	0.0005	+0.0051	39	V
V425 Gem	s	55987.62	0.02	−0.07	39	V; el: 54532.623 + 8.484334 * E; d>.1d
GSC 753-1431	s	55976.7211	0.0003	−0.0029	35	V; el: 54849.650 + 0.367664 * E
GSC 758-823	p	55971.6534	0.0007	−0.0034	23	V; el: 54548.573 + 0.466891 * E
GSC 774-58	s	55973.7234	0.0008	+0.0473	35	V; el: IBVS 5945; d=0.025d
GSC 1351-225	p	55980.6873	0.0001	+0.0210	38	V; el: IBVS 5992
GSC 1351-383	p	55980.7336	0.0004	+0.0106	37	V; el: 54464.710 + 0.652610 * E
GSC 1360-49	p	55984.6721	0.0009	+0.0075	35	V; el: IBVS 5992
GSC 1368-1192	s	55987.6893	0.0003	+0.0123	39	V; el: 53339.751 + 1.445769 * E; d=0.027d
GSC 1368-1411	s	55983.6944	0.0003	+0.0010	27	V; el: IBVS 5871; d=0.04d
GSC 1368-1825	s	55986.6840	0.0005	+0.0112	39	V; el: IBVS 5945; d=0.013d
GSC 1369-98	S	55987.7252	0.0006	+0.0131	37	V; el: IBVS 5960; D=0.028d
GSC 1864-1065	s	55958.6694	0.0006	−0.0045	15	V; el: IBVS 5960
GSC 1909-2392	s	55980.6298	0.0006	+0.0014	19	V; el: IBVS 5992
TT Her	p	56054.8566	0.0007	+0.0360	24	V
CT Her	p	56036.8652	0.0007	+0.0078	36	V
DI Her	p	56085.7177	0.0013	−0.0005	26	V; non-circular
FW Her	p	56076.8430	0.0004	+0.0783	32	V; d=0.024d

Table 1: Minima of eclipsing binaries (continued)

Variable	Type	HJD 24...	±	$O-C$	n	Remarks
HS Her	s	56046.912	0.005	−0.008	29	V; non-circular
	p	56073.914	0.005	−0.025	38	V
LV Her	p	56048.8649	0.0004	+0.0335	30	V; el: IBVS 5201; non-circular
MM Her	s	56086.890	0.004	−0.017	26	V
V338 Her	p	56074.8591	0.0002	+0.1046	32	V
V359 Her	p	56049.8261	0.0007	+0.2271	29	V; d=0.026d
V450 Her	s	56041.8460	0.0021	+0.0020	32	V; el: IBVS 3852
V477 Her	p	56074.8628	0.0003	−0.0049	31	V; el: Krakow Catalog
V502 Her	s	56073.8983	0.0004	+0.0260	38	V; d=0.015d
V681 Her	p	56047.8392	0.0005	−0.0011	28	V; el: IBVS 5992
V687 Her	p	56041.8969	0.0004	−0.1778	32	V
V733 Her	p	56074.9186	0.0007	+0.0147	32	V
V789 Her	s	56054.9124	0.0007	+0.0346	26	V; el: IBVS 5741
V842 Her	p	56041.8882	0.0003	+0.0793	33	V; el: IBVS 3946
V848 Her	p	56046.8997	0.0006	+0.0552	34	V; el: Krakow Catalog
V856 Her	p	56038.8642	0.0002	−0.0563	30	V; el: IBVS 4342
V857 Her	s	56049.8621	0.0008	+0.0079	23	V; el: IBVS 4364; d=0.054d
V1005 Her	s	56047.8993	0.0005	−0.0101	25	V; el: Krakow Catalog
V1024 Her	s	56089.6740	0.0004	+0.0326	32	V; el: IBVS 5894
V1025 Her	p	56048.9143	0.0002	−0.0286	15	V; el: IBVS 5894; D=0.066d!
V1026 Her	p	56034.8529	0.0007	+0.0005	42	V; el: IBVS 5992
V1031 Her	p	56073.8407	0.0005	+0.0071	38	V; el: IBVS 5894
V1033 Her	p	56050.889	0.004	−0.019	11	V; el: IBVS 5146
V1034 Her	p	56052.8317	0.0016	+0.0045	18	V; el: IBVS 5231
V1036 Her	s	56051.8374	0.0013	+0.0124	12	V; el: IBVS 5146
V1037 Her	s	56045.8657	0.0006	+0.0005	28	V; el: IBVS 5997
V1038 Her	s	56051.9046	0.0006	+0.0065	30	V; el: IBVS 5146
V1040 Her	s	56054.8709	0.0005	+0.0160	26	V; el: IBVS 5992
V1042 Her	s	56073.8981	0.0002	−0.0303	38	V; el: IBVS 4998
V1044 Her	p	56054.8407	0.0007	−0.0063	14	V; el: IBVS 5192
V1067 Her	s	56077.8631	0.0003	−0.0137	29	V; el: IBVS 4966
V1073 Her	s	56085.8404	0.0005	+0.0206	32	V; el: IBVS 4975
V1094 Her	p	56074.8496	0.0005	−0.0282	32	V
V1095 Her	s	56074.8446	0.0005	−0.0269	32	V
V1102 Her	s	56075.8891	0.0004	+0.0095	29	V
V1119 Her	p	56048.9001	0.0003	+0.0042	31	V; el: IBVS 5945
V1133 Her	s	56033.9093	0.0007	−0.0636	25	V
	p	56054.8828	0.0006	−0.0642	26	V
V1134 Her	p	56086.8513	0.0012	−0.0248	32	V
V1143 Her	p	56086.7161	0.0006	−0.0014	30	V; el: 51604.75 + 1.686218; d=0.016d
GSC 381-743	p	56042.8517	0.0004	−0.0183	32	V; el: IBVS 5992; d=0.023d
GSC 394-1770	p	56049.8432	0.0004	+0.0080	28	V; el: IBVS 5992; d=0.04:d
GSC 950-560	p	56049.9286	0.0005	−0.0047	29	V; el: IBVS 5894; d=0.020d
GSC 954-418	s	56042.8661	0.0001	−0.0074	33	V; el: IBVS 5992
GSC 960-163	s	56046.9033	0.0005	+0.0036	32	V; el: IBVS 5945
GSC 960-1531	p	56045.8427	0.0004	+0.0037	28	V; el: IBVS 5945
GSC 965-581	s	56048.9047	0.0005	+0.0051	32	V; el: IBVS 5894; d=0.030d
GSC 967-1277	p	56042.8696	0.0003	+0.0066	33	V; el: IBVS 5945; d=0.031d
GSC 971-933	p	56036.9360	0.0007	+0.0032	13	V; el: IBVS 5992
GSC 973-1212	s	56046.8827	0.0003	+0.0010	34	V; el: IBVS 5894
GSC 987-1582	s	56073.8295	0.0004	−0.0043	38	V; el: IBVS 5945
GSC 1505-565	s	56039.8883	0.0006	+0.0193	30	V; el: IBVS 5945
GSC 1528-936	p	56042.9081	0.0004	−0.0025	32	V; el: IBVS 5894
GSC 1538-342	s	56072.8575	0.0006	−0.0088	29	V; el: 54527.891 + 0.516110 * E
GSC 1539-326	s	56054.8499	0.0005	+0.0137	24	V; el: IBVS 5894
GSC 1546-1276	p	56072.8666	0.0003	−0.0022	29	V; el: IBVS 5992
GSC 1552-839	p	56077.8344	0.0003	−0.0098	28	V; el: 53902.772 + 0.674023 * E
GSC 1553-1964	p	56076.9004	0.0007	−0.0114	30	V; el: 53496.877 + 0.458836 * E
GSC 1577-974	p	56051.941	0.004	−0.010	32	V; el: IBVS 5992; non-circular
GSC 1580-1606	s	56075.9075	0.0006	−0.0017	29	V; el: 54187.891 + 0.401066 * E

Table 1: Minima of eclipsing binaries (continued)

Variable	Type	HJD 24...	±	$O-C$	n	Remarks
GSC 1581-2444	p	56087.9058	0.0006	+0.0353	28	V; el: 53591.536 + 0.809447 * E
GSC 2043-227	s	56046.9241	0.0002	+0.0132	34	V; el: IBVS 5894; d=0.017d
GSC 2090-1621	p	56085.8293	0.0004	−0.0017	33	V; el: 54952.827 + 0.316747 * E
GSC 2093-1834	p	56078.8616	0.0002	−0.0125	32	V; el: 53476.823 + 0.763961 * E
GSC 2094-2056	s	56085.8491	0.0005	−0.0132	33	V; el: IBVS 5992
GSC 3080-1410	s	56052.9357	0.0013	−0.0088	30	V; el: AJ 133, 255
SY Hya	p	56002.639	0.003	−0.014	33	V; el: IBVS 5992
UW Hya	p	55940.8718	0.0006	+0.0268	36	V; el: MVS 12, 48; d=0.037d
VW Hya	p	55990.6598	0.0002	+0.0295	34	V; el: IBVS 5992
AV Hya	p	56013.6734	0.0006	+0.0049	22	V; el: 54493.788 + 0.6833995 * E
CQ Hya	p	56009.6616	0.0011	+0.2021	27	V
CU Hya	p	56001.6945	0.0004	−0.2215	36	V; d=0.026d
DE Hya	p	56003.6659	0.0009	−0.0040	37	V; d=0.101d
DF Hya	p	55989.6593	0.0002	+0.0031	34	V; el: IBVS 5992; d=0.018d
EZ Hya	s	56011.6844	0.0003	+0.0179	31	V; el: IBVS 5992; d=0.025d
FG Hya	p	56000.7286	0.0004	+0.0133	40	V; el: IBVS 5992; d=0.03:d
V358 Hya	p	55944.9088	0.0004	+0.0555	44	V; el: IBVS 4432
V410 Hya	p	56015.6938	0.0009	−0.0472	35	V; el: 54468.747 + 3.1507005 * E; d=0.06d
V475 Hya	s	55998.6767	0.0007	−0.0087	25	V
V476 Hya	p	55990.6811	0.0005	+0.0169	34	V; el: IBVS 5920
V514 Hya	p	56001.6884	0.0006	+0.0107	35	V; el: IBVS 5945
V519 Hya	s	56011.6830	0.0004	+0.0258	33	V
GSC 201-1119	s	56000.7412	0.0002	+0.0073	38	V; el: IBVS 5992
GSC 217-849	s	55998.6621	0.0003	+0.0061	21	V; el: IBVS 5945
GSC 230-1627	s	56014.7490	0.0007	+0.0341	34	V; el: IBVS 5894
GSC 235-461	p	56015.6551	0.0009	+0.0496	36	V; el: IBVS 5894
GSC 238-2372	s	55946.8734	0.0003	+0.0008	31	V; el: IBVS 5992
	s	56029.7130	0.0003	+0.0015	35	V; d=0.021d
GSC 4861-1380	s	56001.7100	0.0005	−0.0101	36	V; el: IBVS 5992
GSC 4870-779	p	56000.7122	0.0006	+0.0121	33	V; el: IBVS 5992
GSC 4878-113	p	56001.6976	0.0003	−0.0069	35	V; el: IBVS 5992
GSC 4879-1416	p	56011.6880	0.0005	+0.0069	33	V; el: IBVS 5992; d=0.019d
GSC 4881-888	s	55945.9020	0.0003	+0.0321	14	V; el: IBVS 5945; d=0.014d
	p	56016.6767	0.0006	+0.0302	15	V
GSC 4882-117	p	56009.7062	0.0001	−0.0001	28	V; el: IBVS 5992
GSC 4884-1351	p	55945.8999	0.0004	+0.0002	45	V; el: IBVS 5992; d=0.054d
GSC 4887-1149	s	56008.6752	0.0015	−0.0104	11	V; el: IBVS 5945
	s	56010.6924	0.0002	−0.0097	21	V; d=0.016d
GSC 4893-1294	p	56003.6352	0.0027	−0.0035	36	V; el: IBVS 5992; d=0.04:d
GSC 4897-1114	p	55944.9091	0.0004	+0.0033	41	V; el: IBVS 5992
GSC 4897-1250	p	55944.8460	0.0007	+0.0113	25	V; el: IBVS 5992
GSC 5426-1920	p	55990.6467	0.0005	−0.0114	33	V; el: IBVS 5992
GSC 5427-2330	p	55990.7158	0.0002	+0.0075	33	V; el: IBVS 5992
GSC 5428-504	s	55940.9077	0.0004	−0.0009	34	V; el: 54541.616 + 1.774626 * E
GSC 5429-1473	p	55940.9172	0.0009	−0.0007	17	V; el: IBVS 5992
GSC 5447-940	p	55991.636	0.005	+0.013	31	V; el: IBVS 5894
GSC 5447-1531	p	55990.7039	0.0006	+0.0129	34	V; el: 54490.747 + 3.164439 * E
GSC 5449-1194	s	56000.6812	0.0007	+0.0364	39	V; el: IBVS 5992
GSC 5457-59	s	56002.7157	0.0004	+0.0120	33	V; el: IBVS 5945
GSC 5458-351	s	56002.7241	0.0004	−0.0024	32	V; el: IBVS 5945
GSC 5463-45	s	56010.7003	0.0004	−0.0252	38	V; el: IBVS 5945
GSC 5472-602	s	55947.9250	0.0005	+0.0196	24	V; el: IBVS 5992
	p	56018.7300	0.0002	+0.0223	43	V
GSC 5472-966	p	55945.9406	0.0006	+0.0001	30	V; el: IBVS 5945
GSC 5472-1583	s	56010.6515	0.0001	+0.0088	37	V; el: IBVS 5992
GSC 5487-197	s	55944.8847	0.0004	−0.0007	41	V; el: IBVS 5992; d=0.041d
	p	56030.683	0.003	+0.004	13	V
GSC 5487-801	p	55957.8351	0.0009	−0.0190	32	V; el: IBVS 5992
	p	56017.7036	0.0002	−0.0217	38	V; d=0.020d
GSC 5489-511	s	55953.9343	0.0004	+0.0072	38	V; el: IBVS 5992; d=0.038d
	p	56018.6366	0.0026	+0.0049	42	V; d=0.027d

Table 1: Minima of eclipsing binaries (continued)

Variable	Type	HJD 24...	±	$O-C$	n	Remarks
GSC 5489-963	s	55955.8808	0.0003	−0.0057	38	V; el: IBVS 5992; d=0.032d
	s	56013.6668	0.0005	−0.0063	32	V; d=0.030d
GSC 5495-765	p	55958.8543	0.0005	+0.0066	19	V; el: IBVS 5992
	p	56030.707	0.004	+0.012	15	V
GSC 5497-221	s	55958.8751	0.0007	+0.0017	14	V; el: IBVS 5992
	p	56015.6912	0.0002	+0.0026	39	V
GSC 6011-1986	p	56001.6518	0.0005	−0.0055	35	V; el: IBVS 5992
GSC 6013-1086	p	55991.6839	0.0003	+0.0209	22	V; el: IBVS 5992
GSC 6027-1009	p	56010.7043	0.0002	−0.0051	35	V; el: IBVS 5992
GSC 6029-311	p	56003,6458	0,0008	−0, 0005	36	V; el: IBVS 5945; d=0,035d
GSC 6046-312	s	55953.9324	0.0002	−0.0053	22	V; el: IBVS 5992
	p	56013.6764	0.0003	−0.0058	32	V
ES Lac	p	56086.9133	0.0007	−0.2419	31	V; el: A&A 334, 840; non-circular
Y Leo	p	55945.9020	0.0002	−0.0228	43	V
RW Leo	p	55953.8725	0.0003	−0.1274	40	V; d=0.018d
UU Leo	p	56018.6344	0.0016	+0.1767	38	V
UZ Leo	p	55959.9478	0.0006	+0.0013	36	V; el: IBVS 5992; d=0.042d
	p	56018.6659	0.0011	+0.0038	42	V
VZ Leo	p	56021.7423	0.0005	−0.0599	17	V
XX Leo	p	55946.9434	0.0005	−0.0143	46	V; el: IBVS 5945; d=0.07d
XY Leo	p	55953.9161	0.0005	+0.0329	41	V; el: IBVS 5945
	s	56013.7212	0.0005	+0.0349	19	V
XZ Leo	s	55952.8778	0.0004	+0.0588	42	V
	s	56018.7197	0.0017	+0.0564	41	V; d=0.017d
AG Leo	p	56003,6716	0,0008	+0, 0278	36	V; el: IBVS 5945; d=0,070d
AL Leo	p	55946.9253	0.0004	+0.0140	40	V; el: IBVS 3401
AM Leo	s	55958.9527	0.0003	+0.0127	35	V; d=0.018d
	s	56034.6719	0.0003	+0.0119	38	V; d=0.015d
AP Leo	s	55960.9007	0.0003	−0.0239	45	V; d=0.024d
	p	56034.7053	0.0005	−0.0257	36	V
BG Leo	p	55971.905	0.013	+0.021	8	V; el: OEJV 137
BL Leo	p	55973.8831	0.0006	−0.0251	12	V
	p	56038.7232	0.0005	−0.0300	31	V
BW Leo	s	55956.8610	0.0004	−0.0013	27	V; el: Krakow Catalog
	p	56041.7126	0.0015	+0.0010	17	V
CE Leo	s	55968.8958	0.0008	−0.0084	19	V
	p	56036.7116	0.0002	−0.0090	29	V
DU Leo	p	55947.8993	0.0002	+0.0008	41	V; el: IBVS 3999
GV Leo	p	55953.9083	0.0001	−0.0109	28	V; el: 54531.701 + 0.2667326 * E; d=0.026d
	p	56017.6556	0.0002	−0.0127	22	V; d=0.025d
HI Leo	p	55956.9040	0.0002	+0.0042	41	V
	p	56035.7362	0.0002	+0.0044	31	V
HS Leo	p	55963.9429	0.0003	−0.0017	21	V; el: 51286.7082 + 0.3377066 * E
	s	56034.6956	0.0009	+0.0014	19	V
GSC 234-960	s	56014.7047	0.0004	−0.0078	33	V; el: IBVS 5992
GSC 262-948	p	56014.7225	0.0007	+0.0511	33	V; el: IBVS 5894; d=0.032d
GSC 263-585	p	56030.635	0.004	−0.021	23	V; el: IBVS 5894
GSC 265-617	s	55963.9349	0.0008	+0.0005	21	V; el: IBVS 5945
	s	56029.6820	0.0004	+0.0020	34	V
GSC 267-162	p	55984.853	0.008	+0.030	28	V; el: IBVS 5945
	p	56036.7304	0.0010	+0.0269	28	V; d=0.072d
GSC 267-253	s	55976.8487	0.0006	−0.0050	42	V; el: OEJV 137
	p	56017.6980	0.0005	−0.0066	37	V; d=0.023:d
GSC 270-9	s	55973.8969	0.0007	−0.0001	24	V; el: IBVS 5992
	s	56018.7053	0.0004	+0.0153	40	V; d=0.032d
GSC 270-593	s	55963.8852	0.0002	+0.0020	13	V; el: IBVS 5945
	p	56017.6971	0.0007	+0.0014	15	V
GSC 270-777	s	55956.8754	0.0003	−0.0159	41	V; el: IBVS 5945
	p	56034.6704	0.0005	−0.0225	36	V; d=0.014d
GSC 827-1011	p	55946.9362	0.0004	+0.0023	45	V; el: IBVS 5992
	p	56016.6724	0.0009	+0.0031	38	V

Table 1: Minima of eclipsing binaries (continued)

Variable	Type	HJD 24...	±	$O-C$	n	Remarks
GSC 828-1721	p	55944.8611	0.0006	+0.0215	40	V; el: IBVS 5945
GSC 829-1040	p	56010.7073	0.0003	+0.0070	36	V; el: IBVS 5992
GSC 832-1401	p	56009.6772	0.0010	−0.0067	27	V; el: IBVS 5992
GSC 835-652	p	56009.7280	0.0008	+0.0181	24	V; el: IBVS 5945
GSC 840-216	p	55955.8608	0.0005	+0.0032	30	V; el: IBVS 5945
	p	56016.6949	0.0005	+0.0081	29	V
GSC 847-367	p	55958.8780	0.0002	+0.0171	29	V; el: IBVS 5945
	p	56034.7264	0.0004	+0.0142	37	V
GSC 851-768	p	55989.8579	0.0003	+0.0030	38	V; el: IBVS 5945; d=0.026d
	p	56045.7225	0.0003	+0.0044	28	V
GSC 859-1106	s	55956.8789	0.0002	+0.0111	39	V; el: IBVS 5945
	p	56039.6543	0.0006	+0.0076	30	V
GSC 870-349	s	55978.9004	0.0008	−0.0210	17	V; el: IBVS 5894
	s	56041.7184	0.0017	−0.0227	19	V; d=0.018:d
GSC 1410-439	p	55944.9348	0.0005	−0.0052	43	V; el: IBVS 5945
GSC 1417-401	s	55957.8674	0.0008	+0.0064	13	V; el: IBVS 5945
	p	55957.9819	0.0005	+0.0032	10	V
	s	56023.7364	0.0006	+0.0059	18	V
GSC 1419-666	p	55957.8908	0.0004	+0.0063	39	V; el: IBVS 5945; d=0.024d
	p	56033.6582	0.0009	+0.0090	27	V
GSC 1422-142	p	55957.9233	0.0002	+0.0067	38	V; el: IBVS 5945
	s	56018.6747	0.0003	+0.0068	38	V
GSC 1429-137	p	55960.9358	0.0003	+0.0072	46	V; el: IBVS 5945
	p	56036.6524	0.0029	+0.0069	12	V
GSC 1429-560	s	56042.6751	0.0003	+0.0016	32	V; el: IBVS 6011
GSC 1434-1034	p	55984.8506	0.0003	−0.0042	24	V; el: IBVS 5945
	p	56018.6872	0.0004	−0.0010	42	V
GSC 1441-914	p	55976.8709	0.0002	−0.0023	41	V; el: IBVS 5945
	s	56038.7179	0.0007	−0.0000	23	V
GSC 1443-87	p	55973.8650	0.0007	−0.0289	15	V; el: IBVS 5945
	s	56041.7390	0.0021	−0.0399	10	V
GSC 1963-488	s	55947.9096	0.0003	−0.0011	41	V; el: IBVS 5992; d=0.033d
	p	56029.6877	0.0003	+0.0007	35	V
GSC 1969-579	p	56010.6733	0.0007	+0.0273	15	V; el: IBVS 5945
GSC 1971-916	p	55957.8560	0.0003	+0.0211	19	V; el: IBVS 5945
	p	56016.7083	0.0003	+0.0222	25	V; d=0.021d
GSC 1981-237	p	55956.8767	0.0001	+0.0011	37	V; el: IBVS 5945
	p	56038.7154	0.0002	+0.0093	31	V
GSC 4920-943	p	55976.8848	0.0002	+0.0073	41	V; el: IBVS 5992
GSC 4921-819	p	55976.8533	0.0006	−0.0083	42	V; el: IBVS 5992
	p	56047.7078	0.0003	−0.0064	32	V
GSC 4936-907	s	55956.8302	0.0003	+0.0003	14	V; el: 54566.531 + 0.267134 * E; d=0.015d; O'Connell effect
	s	56036.7040	0.0006	+0.0010	28	V
RT LMi	s	56008.6851	0.0010	−0.0098	24	V
	s	56014.6862	0.0004	−0.0075	34	V
XY LMi	p	55955.9084	0.0004	−0.0245	34	V
	p	56033.6778	0.0003	−0.0215	27	V
AE LMi	p	55955.8827	0.0009	+0.0034	17	V; el: 51518.88 + 0.52834 * E
	p	56017.6994	0.0004	+0.0043	37	V
AF LMi	s	55958.8674	0.0006	−0.0489	35	V; d=0.022d
	s	56011.7308	0.0006	−0.0432	33	V
AG LMi	p	55987.8430	0.0004	+0.0046	33	V
	p	56015.7058	0.0004	+0.0076	39	V
Z Lep	p	55946.7347	0.0001	+0.0618	62	V; el: JAAVSO 21, 111
GSC 5337-1744	p	55952.7042	0.0003	−0.0130	40	V; el: IBVS 5894
GSC 5351-457	p	55955.6746	0.0004	+0.0093	45	V; el: 53415.622 + 0.902004 * E; d=0.019d
GSC 5352-540	s	55959.6624	0.0015	+0.0062	26	V; el: IBVS 5960
GSC 5358-917	p	55953.7105	0.0004	−0.0102	37	V; el: IBVS 5871
GSC 5361-545	s	55959.6516	0.0002	+0.0071	16	V; el: IBVS 5894
NSV 2698	p	55958.6515	0.0007	+0.0038	19	v; el: IBVS 5894

Table 1: Minima of eclipsing binaries (continued)

Variable	Type	HJD 24...	±	$O-C$	n	Remarks
SS Lib	p	56093.7274	0.0004	−0.0063	36	V; el: IBVS 5992; d=0.032d
TY Lib	p	56035.9082	0.0004	−0.0292	31	V; d=0.044d
VZ Lib	s	56016.9007	0.0001	+0.0023	31	V; el: IBVS 5992; d=0.024d
	p	56093.7440	0.0004	−0.0001	35	V
FU Lib	p	56036.8852	0.0002	−0.0056	32	V; el: IBVS 5992; d=0.030d
GK Lib	p	56036.9137	0.0006	−0.0221	33	V; el: IBVS 5992
	p	56087.7112	0.0012	−0.0186	13	V
V351 Lib	s	56039.8861	0.0008	−0.0065	14	V; el: 54938.751 + 0.3497353 * E; d=0.019 strong O'Connell effect
GSC 4987-740	p	56014.8807	0.0006	−0.0034	27	V; el: IBVS 5992
	p	56085.6917	0.0004	−0.0011	25	V
GSC 5028-828	s	56035.8686	0.0013	+0.0191	31	V; el: IBVS 5992
	s	56093.7038	0.0013	+0.0247	37	V
GSC 5569-173	p	56093.6658	0.0005	+0.0100	37	V; el: IBVS 5992
GSC 5572-705	p	56014.8716	0.0004	−0.0047	31	V; el: 54917.791 + 0.3585246 * E; d=0.021d
GSC 5600-923	p	56039.8313	0.0002	+0.0025	31	V; el: IBVS 5992; d=0.018d
GSC 5605-700	s	56033.9045	0.0004	+0.0015	29	V; el: IBVS 5992
GSC 6155-352	p	56073.7047	0.0009	−0.0117	31	V; el: IBVS 5992
GSC 6171-209	p	56045.8694	0.0007	−0.0059	26	V; el: IBVS 5992; d=0.046d
RY Lyn	p	55991.7228	0.0003	−0.0306	27	V
RZ Lyn	p	55945.9005	0.0005	−0.1300	37	V
SX Lyn	p	55990.6742	0.0002	+0.0164	33	V
UU Lyn	p	56011.7108	0.0003	−0.0101	33	V
UV Lyn	s	55991.6787	0.0005	+0.0773	32	V
AH Lyn	p	56021.7065	0.0004	−0.0117	17	V; el: AJ 87, 314
DE Lyn	s	55989.6762	0.0003	+0.0108	33	V; el: IBVS 5871; d=0.021d
EK Lyn	p	55990.639	0.003	−0.053	33	V; el: 51497.84 + 2.23525 * E
FI Lyn	p	55990.7600	0.0005	+0.0148	34	V; el: OEJV 83
FU Lyn	p	55937.8980	0.0005	−0.0434	37	V
	s	56021.668	0.003	−0.025	20	V
TZ Lyr	p	56075.9285	0.0017	+0.0072	18	V
NY Lyr	p	56093.8863	0.0004	+0.0046	27	V; Krakow Catalog
V361 Lyr	p	56093.8825	0.0003	−0.0178	28	V; el: IBVS 4177
V571 Lyr	p	56086.8572	0.0005	+0.0216	32	V; el: JAAVSO 39, 102
V574 Lyr	s	56078.8397	0.0004	−0.0033	30	V; el: IBVS 4976
V582 Lyr	p	56089.8415	0.0004	−0.0002	30	V; el: 51766.5843 + 0.2559049 * E
V592 Lyr	p	56087.8856	0.0005	+0.0198	29	V; d=0.024d
GSC 2115-1000	s	56075.8459	0.0006	−0.0005	29	V; el: IBVS 5945
RU Mon	p	55956.6313	0.0002	−0.0932	44	V; non-circular
	s	55968.6907	0.0003	−0.5804	37	V
AS Mon	p	55986.7247	0.0005	+0.0151	39	V; el: 53830.607 + 3.6730880 * E
AT Mon	p	55987.7218	0.0005	+0.0122	39	V; d=0.030d
EZ Mon	p	55978.7344	0.0003	+0.0324	38	V; el: 54462.751 + 0.752333 * E; d=0.024d
FH Mon	p	55976.6356	0.0012	−0.1047	34	V
FS Mon	p	55987.6542	0.0003	−0.0123	39	V
GG Mon	p	55981.7191	0.0024	−0.0561	16	V
GH Mon	p	55973.6417	0.0005	−0.0781	38	V
HM Mon	s	55978.6288	0.0008	+0.0065	26	V; el: IBVS 5506
HT Mon	p	55984.769	0.005	+0.011	38	V
KR Mon	p	55989.6959	0.0004	+0.0102	33	V; el: IBVS 5894; d=0.040d
MX Mon	p	55983.6853	0.0002	−0.1183	36	V
NN Mon	p	55986.6790	0.0004	−0.0065	38	V; el: 55162.824 + 0.9123605 * E
V383 Mon	p	55973.6606	0.0021	−0.0255	39	V
V384 Mon	p	55973.6826	0.0008	−0.0436	32	V
V452 Mon	p	55971.6669	0.0006	+0.0254	20	V; el: 53725.749 + 3.076565 * E
V457 Mon	s	55978.6620	0.0007	−0.0052	28	V
V463 Mon	p	55976.6984	0.0007	−0.0945	35	V
V524 Mon	p	55973.6771	0.0004	+0.1229	40	V
V528 Mon	p	55984.6944	0.0006	−0.2320	31	V
V530 Mon	p	55976.6601	0.0004	+0.0100	33	V; el: IBVS 5992
V532 Mon	p	55973.6913	0.0005	−0.0297	39	V

Table 1: Minima of eclipsing binaries (continued)

Variable	Type	HJD 24...	±	$O-C$	n	Remarks
V843 Mon	s	55973.6616	0.0006	+0.0107	38	V; el: Krakow Catalog
V925 Mon	p	55990.76	0.02	0	33	V; el: 54537.582 + 5.955660 * E; non-circular
V929 Mon	s	55984.6674	0.0010	−0.0191	31	V
V934 Mon	s	55979.7367	0.0002	+0.0044	38	V; el: 54807.761 + 0.509442 * E
V948 Mon	s	55989.6866	0.0005	−0.0030	35	V; el: IBVS 5992; d=0.033d
V953 Mon	p	55990.6559	0.0009	−0.0310	34	V
GSC 163-1374	s	55979.7163	0.0003	−0.0083	18	V; el: IBVS 5992
GSC 4815-2034	p	55983.6446	0.0005	+0.0056	41	V; el: 54427.804 + 1.201417 * E
GSC 4824-2990	s	55976.6667	0.0005	−0.0020	34	V; el: 55158.796 + 1.406488 * E
GSC 4827-2862	s	55976.6660	0.0002	−0.0024	34	V; el: IBVS 5992
GSC 4828-2284	p	55980.6648	0.0004	−0.0029	42	V; el: 54512.585 + 0.477736 * E
GSC 4834-3265	s	55986.6733	0.0004	+0.0060	37	V; el: IBVS 5992; d=0.029d
GSC 4835-106	p	55991.6631	0.0005	+0.0101	33	V; el: 54857.628 + 1.467044 * E
GSC 4835-1947	p	55986.6519	0.0009	+0.0162	38	V; el: 54433.824 + 0.637705 * E
GSC 4839-280	s	55982.6627	0.0011	+0.0116	29	V; el: IBVS 5894
GSC 4840-528	p	55983.6641	0.0006	−0.0086	39	V; el: IBVS 5945
GSC 4854-2084	p	55991.6867	0.0008	−0.0085	21	V; el: IBVS 5992; d=0.024d
GSC 4855-2438	s	55986.6887	0.0005	−0.0036	35	V; el: 54593.504 + 4.067703 * E; d=0.031d
GSC 4858-2028	s	55989.7277	0.0005	−0.0045	34	V; el: IBVS 5992
GSC 5385-870	s	55976.6810	0.0004	−0.0066	35	V; el: 53388.675 + 1.259680 * E
GSC 5398-2032	s	55983.6439	0.0006	+0.0038	40	V; el: IBVS 5992
GSC 5399-2407	p	55980.6273	0.0004	+0.0018	39	V; el: IBVS 5894
V391 Oph	p	56072.8760	0.0005	+0.0503	29	V
V456 Oph	p	56078.8733	0.0003	+0.0189	32	V
V508 Oph	p	56076.9082	0.0004	−0.0215	32	V
V511 Oph	p	56085.8839	0.0003	−0.0345	32	V; el: BAV Rb. 54, 8
V586 Oph	p	56087.8659	0.0003	−0.0213	28	V
V839 Oph	s	56078.8426	0.0004	−0.0050	32	V; el: 54282.692 + 0.4090073 * E
V983 Oph	p	56018.8707	0.0005	+0.0002	36	V; el: 54292.63 + 23.01654 * E; non-circular
V1016 Oph	s	56045.8721	0.0003	+0.0031	28	V; el: IBVS 5992
V1120 Oph	s	56045.8584	0.0011	−0.0126	28	V
V2425 Oph	s	56073.8310	0.0004	−0.1537	38	V; el: IBVS 4407
V2563 Oph	p	56085.8834	0.0002	+0.0103	32	V; el: IBVS 5992
V2612 Oph	s	56078.8687	0.0003	−0.0003	32	V; el: 54234.797 + 0.3753072 * E
V2650 Oph	s	56077.8673	0.0004	−0.0036	28	V; el: 54644.785 + 0.3840509 * E
GSC 419-1667	s	56072.8918	0.0005	+0.0220	28	V; el: 54748.511 + 0.321876 * E
GSC 429-1488	s	56085.8685	0.0008	+0.0171	32	V; el: IBVS 5945
GSC 436-1066	p	56078.8494	0.0003	+0.0075	32	V; el: IBVS 5945
GSC 440-1798	s	56087.8287	0.0004	−0.0117	30	V; el: 54934.855 + 0.322018 * E
GSC 978-768	s	56074.8301	0.0005	+0.0042	33	V; el: IBVS 5992
GSC 978-1292	p	56052.9077	0.0006	+0.0024	30	V; el: IBVS 5894
GSC 979-1273	p	56051.8897	0.0003	+0.0109	33	V; el: IBVS 5894
GSC 1006-1687	p	56077.8361	0.0004	−0.0394	28	V; el: 54229.847 + 0.545624 * E
GSC 1010-1632	s	56075.9297	0.0012	+0.0054	12	V; el: IBVS 5945
GSC 5044-460	p	56038.9248	0.0007	+0.0071	31	V; el: IBVS 5992; d=0.036d
GSC 5054-1417	p	56048.9008	0.0006	+0.0226	31	V; el: IBVS 5992
GSC 5059-477	p	56048.8507	0.0005	+0.0045	31	V; el; 54968.778 + 1.457582 * E
GSC 5059-1258	p	56051.8865	0.0003	+0.0022	32	V; el: IBVS 5992; d=0.021d
GSC 5076-483	p	56052.8927	0.0007	+0.0102	31	V; el: IBVS 5992
GSC 5080-1864	s	56072.8368	0.0003	+0.0036	29	V; el: 53798.878 + 0.273921 * E
GSC 5085-331	p	56077.8515	0.0005	+0.0035	28	V; el: 53822.850 + 0.942331 * E
GSC 5629-912	p	56049.8705	0.0005	−0.0023	29	V; el: IBVS 5992
GSC 5636-400	p	56047.9272	0.0013	+0.0125	27	V; el: IBVS 5992
GSC 5640-366	p	56052.8690	0.0013	+0.0151	27	V; el: IBVS 5992
NSV 7727	p	56042.8615	0.0002	+0.0190	32	V; el: IBVS 5945
NSV 7838	p	56051.8725	0.0003	−0.0108	31	V; el: IBVS 5945; d=0.042d
NSV 9555	p	56077.8808	0.0007	+0.0371	27	V; el: OEJV 91
UW Ori	s	55955.628	0.006	+0.042	44	V; el: Chin. AA, 14, 298
DZ Ori	p	55956.6991	0.0001	+0.0080	45	V; el: Krakow Catalog, d=0.051d
EF Ori	p	55958.7239	0.0011	+0.0031	34	V; el: IBVS 5699

Table 1: Minima of eclipsing binaries (continued)

Variable	Type	HJD 24...	±	$O-C$	n	Remarks
EG Ori	p	55958.7265	0.0009	−0.0817	35	V; d=0.05d
EH Ori	p	55960.6960	0.0004	+0.0342	36	V; el: 53414.657 + 1.513677 * E
EQ Ori	p	55937.6290	0.0007	−0.0398	37	V
ER Ori	p	55946.7085	0.0003	+0.1027	41	V; d=0.013d
EW Ori	p	55956.6631	0.0004	−0.0121	41	V; el: 52668.607 + 6.936829 * E; d=0.012d; non-circular
FT Ori	s	55946.7136	0.0002	+0.5824	55	V; non-circular
	p	55947.7244	0.0003	+0.0180	36	V
GG Ori	p	55944.6390	0.0004	+0.0891	43	V; non-circular
V519 Ori	p	55958.6882	0.0008	+0.0135	38	v; el: IBVS 5960; D=0.05:d
V641 Ori	p	55957.6857	0.0003	−0.0040	36	V; el: IBVS 5920
V1353 Ori	s	55944.6238	0.0008	−0.0055	43	V; el: IBVS 5313
V1626 Ori	p	55956.6755	0.0003	−0.0057	45	V; el: IBVS 5339
V1799 Ori	s	55937.590	0.003	+0.005	6	V; el: IBVS 5960
	p	55937.7353	0.0008	+0.0057	21	V
V1851 Ori	s	55946.6664	0.0002	+0.0030	36	V; el: IBVS 5493
V1853 Ori	s	55947.6845	0.0003	−0.0174	40	V; d=0.028d
V2685 Ori	p	55955.6676	0.0003	+0.0216	44	V; el: 54165.634 + 0.409989 * E
V2735 Ori	p	55955.6553	0.0010	−0.0089	22	V
V2759 Ori	p	55952.6414	0.0004	−0.0194	36	V
V2783 Ori	s	55946.8232	0.0004	+0.2267	83	V; el: IBVS 5992; non-circular
V2793 Ori	s	55958.6874	0.0006	−0.0358	35	V; el: 53716.744 + 1.4506498 * E; d=0.03d
GSC 108-1146	s	55947.6688	0.0005	+0.0094	40	V; el: IBVS 5992
GSC 122-419	p	55953.6807	0.0004	+0.0021	37	V; el: IBVS 5945
GSC 706-845	p	55952.7217	0.0005	−0.0141	33	V; el: IBVS 5799
GSC 730-243	p	55959.6829	0.0006	+0.0185	32	V; el: IBVS 5960
GSC 4754-17	p	55940.6353	0.0003	+0.0065	44	V; el: IBVS 5960
GSC 4783-266	s	55959.7343	0.0008	+0.0179	36	V; el: IBVS 5960; asymmetric light curve
GSC 4783-2332	p	55958.6871	0.0003	−0.0018	33	V; el: IBVS 5960
GSC 4784-830	p	55960.6572	0.0005	−0.0060	26	V; el: IBVS 5992
NSV 1864	p	55946.7374	0.0003	+0.0061	60	V; el: 53009.584 + 0.5944439 * E; d= 0.053d
NO Per	p	55944.761	0.009	+0.003	45	V; el: 51504.78 + 5.69228 * E; non-circular
	s	55946.762	0.010	−0.679	59	V
NP Per	s	55940.6570	0.0002	−0.0559	44	V
OX Per	p	55944.6151	0.0007	−0.1124	42	V
V963 Per	p	55947.6703	0.0005	+0.0002	41	V; el: IBVS 6001; d=0.025d
VY Pup	s	55987.7281	0.0002	−0.0054	38	V; el: 53750.699 + 1.633468 * E
GV Pup	p	55980.7469	0.0011	+0.0153	40	V; el: 54207.621 + 0.988356 * E; d=0.074d
KW Pup	p	55984.6595	0.0005	+0.0278	37	V; d=0.030d
MO Pup	s	55982.6360	0.0019	+0.0098	30	V; el: 53465.621 + 3.671780 * E
GSC 5404-4206	p	55986.6750	0.0004	−0.0091	38	V; el: IBVS 5894
GSC 5405-3070	p	55987.6559	0.0006	+0.0020	38	V; el: 54509.740 + 1.9891169 * E; d=0.037d
GSC 5421-76	p	55989.7091	0.0002	−0.0019	35	V; el: IBVS 5992
GSC 5422-1430	p	55982.7082	0.0002	+0.0117	30	V; el: IBVS 5992
GSC 5998-1918	p	56000.7072	0.0005	+0.0019	22	V; el: IBVS 5992
NSV 4095	s	55945.8074	0.0009	−0.1454	50	V; el: IBVS 6011
V1109 Sgr	p	56093.8882	0.0017	−0.0198	27	V; el: 54373.579 + 0.6111293 * E
GSC 6265-1357	p	56086.885	0.004	+0.089	20	V; el: 54282.713 + 1.0350448 * E
V784 Sco	p	56035.8768	0.0005	+0.0195	31	V; el: IBVS 5992
GSC 5623-1173	p	56051.8799	0.0002	−0.0013	33	V; el: IBVS 5992
NSV 7481	s	56039.8112	0.0021	+0.0157	8	V; el: 51926.362 + 0.293408 * E
	p	56039.9558	0.0012	+0.0136	16	V
U Sct	p	56089.8769	0.0004	−0.0105	31	V
VZ Sct	p	56076.8520	0.0006	+0.1460	31	V; d=0.040d
EZ Sct	p	56078.895	0.003	−0.008	30	V; el: 53524.795 + 1.134655 * E
GSC 5124-377	p	56077.8821	0.0005	+0.0029	23	V; el: 53822.845 + 1.638833 * E; d=0.05:d
AO Ser	p	56023.9255	0.0002	−0.0139	37	V
AQ Ser	p	56018.8745	0.0002	−0.0017	39	V; el: IBVS 5992
AS Ser	p	56030.9211	0.0003	+0.0025	37	V; el: IBVS 5945; d=0.025d
AU Ser	p	56034.8573	0.0001	+0.0022	43	V; el: IBVS 5992
BI Ser	p	56034.8544	0.0001	+0.0522	42	V

Table 1: Minima of eclipsing binaries (continued)

Variable	Type	HJD 24...	±	$O-C$	n	Remarks
CC Ser	p	56029.8851	0.0002	+0.0077	32	V; el: BBSAG Bull. 128, 10
CQ Ser	p	56075.8392	0.0002	−0.0018	29	V; el: 54529.879 + 0.7600600 * E
V384 Ser	s	56035.889	0.003	−0.003	22	V; strong O'Connell effect
V385 Ser	p	56038.8724	0.0004	+0.0605	30	V; d=0.025d
V425 Ser	p	56010.9475	0.0003	+0.0113	34	V; el: 54885.888 + 0.5442904 * E
	p	56093.6790	0.0007	+0.0106	37	V
V434 Ser	p	56033.8984	0.0001	−0.0076	16	V
GSC 355-983	s	56030.9020	0.0004	+0.0216	37	V; el: IBVS 5945; d=0.021d
GSC 357-162	p	56030.9114	0.0004	+0.0046	36	V; el: IBVS 5894; d=0.027d
GSC 361-795	p	56041.8794	0.0003	+0.0016	32	V; el: IBVS 5992
GSC 362-302	p	56034.8311	0.0003	−0.0065	44	V; el: IBVS 5992
GSC 366-196	s	56038.9295	0.0002	+0.0051	29	V; el: IBVS 5945
GSC 368-118	s	56041.9220	0.0004	−0.0034	30	V; el: IBVS 5945
GSC 370-468	s	56041.8939	0.0005	+0.0162	29	V; el: IBVS 5945
GSC 378-1212	s	56039.9030	0.0004	+0.0006	21	V; el: IBVS 5894
GSC 930-267	p	56034.8810	0.0003	+0.0198	44	V; el: IBVS 5894
GSC 945-626	p	56039.8983	0.0008	−0.0184	16	V; el: IBVS 5992; d=0.014d
GSC 949-1089	s	56039.8596	0.0003	+0.0049	30	V; el: IBVS 5894
GSC 1499-834	p	56036.8925	0.0003	+0.0110	34	V; el: IBVS 5894
GSC 2034-1670	s	56036.8387	0.0006	−0.0015	23	V; el: IBVS 5894
GSC 5017-129	p	56038.8345	0.0009	−0.0128	28	V; el: IBVS 5894
GSC 5037-866	s	56041.9071	0.0005	+0.0040	18	V; el: IBVS 5894
GSC 5108-617	p	56076.8460	0.0012	−0.0007	32	V; el: IBVS 5992
GSC 5681-848	s	56075.8561	0.0004	−0.0016	23	V; el: IBVS 5992
NSV 10497	p	56086.8409	0.0012	−0.0048	32	V; el: 53466.866 + 4.112998 * E
Y Sex	s	55952.9331	0.0003	+0.0016	43	V; el: IBVS 5945; d=0.034d
	s	56035.643	0.002	+0.007	20	V
WW Sex	p	56015.7739	0.0001	−0.0037	39	V; el: 54429.831 + 1.4391530 * E
WX Sex	s	55952.8933	0.0003	+0.0164	39	V; el: IBVS 5992; d=0.035d
	s	56035.6670	0.0005	+0.0184	32	V
WZ Sex	p	55947.9443	0.0012	−0.0085	35	V; el: IBVS 5894
AI Sex	p	56011.7432	0.0005	+0.0010	33	V; el: IBVS 5945; d=0.029d
GSC 242-2191	p	56030.715	0.002	+0.027	19	V; el: IBVS 5992
	p	55946.8650	0.0002	+0.0234	35	V; el: IBVS 5992; d=0.019d
GSC 243-397	s	56008.7133	0.0001	−0.0009	24	V; el: IBVS 5992
GSC 246-90	s	55959.8423	0.0009	+0.0027	15	V; el: IBVS 5945
	p	56014.6728	0.0008	+0.0018	33	V
GSC 250-668	s	55953.8568	0.0006	+0.0073	25	V; el: IBVS 5945
	p	56030.652	0.003	+0.001	17	V
GSC 253-870	s	55959.9224	0.0005	−0.0001	20	V; el: IBVS 5945
	p	56015.7154	0.0002	+0.0024	39	V
GSC 256-41	s	55960.9104	0.0003	−0.0024	20	V; el: IBVS 5945
	s	56030.7120	0.0011	−0.0024	22	V
GSC 4895-1885	s	55946.8878	0.0004	+0.0152	36	V; el: IBVS 5992
	p	56018.6883	0.0002	+0.0169	43	V
GSC 4896-33	p	55952.9489	0.0005	+0.0210	31	V; el: IBVS 5992
	p	56013.6456	0.0004	+0.0198	32	V; d=0.020d
GSC 4896-135	s	56014.6610	0.0009	+0.0073	34	V; el: IBVS 5992
GSC 4906-447	s	55952.8917	0.0004	−0.0018	23	V; el: IBVS 5992
	s	56013.6812	0.0008	−0.0038	14	V
GSC 4907-992	p	55953.8859	0.0007	+0.0104	39	V; el: IBVS 5992
GSC 4907-1262	s	55955.8896	0.0003	+0.0094	40	V; el: IBVS 5992; d=0.020d
GSC 4908-1303	p	55958.8696	0.0003	−0.0038	38	V; el: IBVS 5894
GSC 4909-1434	s	55957.8723	0.0004	−0.0008	40	V; el: IBVS 5992; d=0.017d
GSC 4911-1235	p	55955.8450	0.0001	+0.0043	17	V; el: IBVS 5894
	p	56029.6753	0.0004	+0.0060	34	V
GSC 4913-1090	p	55959.9140	0.0004	−0.0033	31	V; el. IBVS 5992
	p	56030.720	0.006	−0.003	20	V
GSC 4916-292	p	55955.9166	0.0005	−0.0026	39	V; el: IBVS 5894

Table 1: Minima of eclipsing binaries (continued)

Variable	Type	HJD 24...	±	$O-C$	n	Remarks
GSC 4916-492	p	55959.8589	0.0005	−0.0009	21	V; el: IBVS 5992
	s	56033.7037	0.0007	−0.0017	27	V
GSC 4918-1155	p	55958.9262	0.0005	−0.0016	37	V; el: IBVS 5894
GSC 5477-108	p	55959.8705	0.0006	+0.0025	25	V; el: IBVS 5992
	s	56011.6837	0.0006	+0.0074	32	V
GSC 5478-562	s:	55947.8513	0.0002	+0.0029	25	V; el: IBVS 5992
GSC 5481-1160	p	55957.8865	0.0003	−0.0093	38	V; el: IBVS 5992; d=0.038d
	p	56030.713	0.002	−0.020	16	V
GSC 5499-1020	s	55955.9053	0.0006	+0.0389	16	V; el: IBVS 5992; d=0.014d
	p	56029.6865	0.0005	+0.0353	34	V
AL Tau	p	55957.6504	0.0004	+0.0532	35	V
AN Tau	p	55940.7078	0.0002	−0.0015	44	V; el: Krakow Catalog
AP Tau	p	55947.7200	0.0003	+0.0247	40	V
AQ Tau	p	55940.7312	0.0005	−0.1032	44	V
AS Tau	p	55947.7019	0.0004	+0.5534	40	V
CC Tau	p	55940.6439	0.0004	−0.0069	43	V; el: ASAS; d=0.034d
EN Tau	p	55955.7185	0.0007	−0.0036	44	V
V781 Tau	p	55955.7210	0.0004	−0.0034	45	V; el: IBVS 5960
V1094 Tau	s	55945.6205	0.0006	+1.4104	50	V; el: IBVS 4544; non-circular
V1260 Tau	s	55946.6788	0.0003	+0.3314	61	V; non-circular
V1305 Tau	p	55947.6187	0.0003	+0.0100	41	V; el: 51910.2865 + 0.59077 * E
V1355 Tau	s	55940.5787	0.0013	−0.0319	12	V
	p	55940.7012	0.0006	−0.0318	23	V
V1369 Tau	p	55953.7310	0.0007	+0.0731	37	V
V1370 Tau	s	55953.6685	0.0004	−0.0563	23	V
V1374 Tau	s	55955.6190	0.0008	+0.0134	16	V; el: IBVS 5849
	p	55955.7474	0.0007	+0.0164	17	V
A054432+1305.7	p	55955.6874	0.0003	−0.0047	45	V; el: IBVS 5945
GSC 727-47	p	55957.6870	0.0004	−0.0160	37	V; el: IBVS 5992
GSC 1293-1162	p	55940.6798	0.0004	+0.0287	44	V; el: IBVS 5960; d=0.015d
GSC 1304-227	s	55952.7149	0.0003	+0.0043	34	V; el: IBVS 5960
TY UMa	s	55968.8654	0.0007	+0.1658	15	V; el: MNRAS 317, 111; d=0.017d
	p	56046.6880	0.0004	+0.1672	30	V
UX UMa	p	55991.9013	0.0006	−0.0012	35	V
UY UMa	s	55998.9224	0.0007	+0.1234	39	V; d=0.028d
VV UMa	p	55945.8946	0.0004	−0.0483	44	V
	p	56016.6904	0.0003	−0.0527	38	V
XY UMa	p	55937.8468	0.0006	+0.0399	16	V
	p	56021.6725	0.0017	+0.0415	21	V
XZ UMa	p	55946.8753	0.0001	−0.1107	47	V
ZZ UMa	p	55968.8402	0.0005	−0.0014	28	V; d=0.026d
AA UMa	p	55946.8926	0.0004	+0.0420	47	V
BE UMa	p	55979.8559	0.0014	+0.0140	10	V
	p	56041.709	0.005	+0.005	7	V
BH UMa	p	55959.9257	0.0010	−0.0119	32	V; el: IBVS 5992
	p	56034.6826	0.0006	−0.0216	38	V
BM UMa	s	55963.9355	0.0007	+0.0091	23	V
	p	56033.7769	0.0019	+0.0112	10	V
BQ UMa	p	55952.8966	0.0001	−0.1359	43	V; d=0.065d
	p	56045.758	0.008	−0.136	25	V
BS UMa	p	55968.8859	0.0008	+0.0010	12	V; el: IBVS 5894
	p	56036.6896	0.0006	−0.0002	31	V
ES UMa	p	55963.8235	0.0024	−0.0015	38	V; el: Krakow Catalog
	s	56029.6708	0.0006	+0.0038	34	V
IW UMa	p	55945.8267	0.0005	+0.0191	43	V; el: IBVS 4402
KM UMa	p	55968.8436	0.0002	−0.0210	14	V; el: IBVS 4810
	p	56029.7174	0.0005	−0.0193	34	V
LO UMa	p	55953.9111	0.0005	−0.0217	41	V; el: IBVS 5084; d=0.04d
	p	56038.7184	0.0003	−0.0182	27	V; d=0.040d

Table 1: Minima of eclipsing binaries (continued)

Variable	Type	HJD 24...	±	$O-C$	n	Remarks
MS UMa	p	55971.9181	0.0019	+0.0333	11	V
	p	56034.7099	0.0004	+0.0364	37	V; d=0.037d
MT UMa	s	55982.9616	0.0005	+0.1479	45	V
PW UMa	s	55937.8422	0.0007	−0.0024	37	V; el: 51559.940 + 0.555325 * E
	s	56016.6974	0.0004	−0.0033	26	V
PZ UMa	s	55937.809	0.004	−0.001	8	V; el: 51337.714 + 0.262660 * E
	p	55937.9390	0.0006	−0.0023	14	V
	s	56017.6618	0.0003	+0.0032	14	V
OQ UMa	s	56000.8628	0.0006	−0.0007	14	V
	p	56074.6804	0.0004	+0.0027	38	V
QT UMa	s	55944.8923	0.0004	−0.0203	42	V
	s	56029.6547	0.0002	−0.0217	35	V
QV UMa	p	55947.8592	0.0002	+0.0010	20	V
	s	55948.0146	0.0023	+0.0006	11	V
	s	56009.6808	0.0003	−0.0115	28	V
V337 UMa	s	55952.9244	0.0004	+0.0671	37	V
	p	56013.6929	0.0007	+0.0730	23	V; d=0.017d
V342 UMa	s	55958.8411	0.0005	−0.0149	17	V
	p	56013.6833	0.0002	−0.0175	32	V
	s	56042.7440	0.0006	−0.0124	32	V
V343 UMa	p	55960.8430	0.0005	−0.0098	24	V
	p	56042.6979	0.0005	−0.0089	32	V
V356 UMa	p	56011.8988	0.0004	−0.0021	35	V
V357 UMa	p	56050.6422	0.0024	+0.0238	20	V
V358 UMa	p	56017.798	0.003	−0.013	34	V; el: 51553.87 + 4.669394 * E
V360 UMa	p	55998.8230	0.0013	−0.0017	39	V; el: 51422.539 + 0.360224 * E
	s	56075.7308	0.0004	−0.0017	28	V; d=0.019d
V362 UMa	p	56003.8572	0.0006	−0.0002	37	V; el: 51419.762 + 0.342813 * E; d=0.017d
	s	56075.6761	0.0005	−00007	26	V
V364 UMa	p:	56000.9007	0.0003	+0.0224	23	V; d=0.028d
	s:	56076.6819	0.0003	+0.0222	29	V; d=0.026d
V366 UMa	p	56016.962	0.003	+0.004	6	V; el: 51403.675 + 0.457304 * E
	p	56078.6967	0.0007	+0.0029	27	V
GSC 3011-1150	p	55963.8427	0.0007	−0.0088	37	V; el: 53818.286 + 0.57692 * E
	p	56033.6535	0.0029	−0.0053	27	V
RU UMi	p	55990.8466	0.0007	−0.0156	31	V
	p	56051.7421	0.0004	−0.0116	39	V
RZ UMi	p	56023.8672	0.0007	+0.0342	38	V
VZ UMi	p	55987.9648	0.0015	−0.0006	10	V; el: 51613.87 + 0.628101 * E
	p	56016.8578	0.0007	−0.0003	32	V
GSC 4407-351	s:	55990.8620	0.0008	+0.0401	31	V; el: PZP 10, 18
	s:	56050.7168	0.0010	+0.0376	17	V; close double
GSC 4418-800	p	56039.8363	0.0006	+0.0058	25	V; el: PZP 11, 1
GSC 4579-1005	s	56047.8832	0.0011	−0.0032	16	V; el: 51453.603 + 0.643412 * E
GSC 4647-555	p	56052.8546	0.0016	+0.0041	31	V; el: OEJV 83
VV Vir	p	56008.9261	0.0005	−0.0414	19	V
	s	56074.7326	0.0009	−0.0400	38	V; asymmetric
AG Vir	s	55979.9189	0.0009	−0.0011	32	V
	s	56039.657:	0.003	−0.029	29	V
AH Vir	s	55981.8687	0.0004	+0.0385	40	V; d=0.032d
	s	56046.6697	0.0009	+0.0437	30	V; d=0.029d
AW Vir	p	55990.9141	0.0006	+0.0276	31	V
	p	56072.6842	0.0005	+0.0244	39	V
AX Vir	p	55991.8638	0.0004	+0.0199	35	V
AZ Vir	p	56001.8493	0.0001	−0.0235	38	V
	s	56073.7060	0.0002	−0.0230	31	V
BF Vir	p	56000.9030	0.0004	−0.0042	34	V; el: IBVS 5992
BH Vir	p	56008.9221	0.0001	−0.0095	37	V
	p	56085.7085	0.0003	−0.0090	27	V
CG Vir	p	56030.8783	0.0003	+0.0098	33	V; el: IBVS 5992

Table 1: Minima of eclipsing binaries (continued)

Variable	Type	HJD 24...	±	$O-C$	n	Remarks
CX Vir	p	56010.9016	0.0003	+0.0056	35	V; el: IBVS 5992
DM Vir	s	56013.9123	0.0003	+0.0065	38	V; el: IBVS 5992
DY Vir	p	55979.9102	0.0003	−0.1392	36	V
	p	56039.7015	0.0002	−0.1418	28	V
FQ Vir	p	56074.6980	0.0004	+0.0091	38	V; el: IBVS 5992
IR Vir	s	55984.9162	0.0002	+0.0077	15	V; el: IBVS 5894
	s	56047.7132	0.0006	+0.0106	31	V
PS Vir	s	55978.8938	0.0005	−0.0139	11	V; strong O'Connell effect
	p	56036.7153	0.0006	−0.0089	15	V; d=0.018d
PY Vir	s	55987.8922	0.0004	−0.0296	24	V
QX Vir	s	56014.9001	0.0008	+0.0127	15	V
	p	56085.7062	0.0002	+0.0121	27	V
V337 Vir	p	55983.8905	0.0005	−0.0478	35	V
V340 Vir	s	55991.8715	0.0007	+0.0112	19	V; el: IBVS 5992
V342 Vir	p	56001.9021	0.0003	+0.0025	38	V; el: IBVS 5992; d=0.044d
V391 Vir	p	55980.8743	0.0005	+0.0056	37	V; el: 54588.591 + 0.354316 * E
	p	56045.7158	0.0007	+0.0073	27	V
V467 Vir	s	55987.8350	0.0014	−0.0023	31	V; el: IBVS 5992; d=0.05d
V589 Vir	p	56015.8500	0.0006	−0.0129	34	V; el: 55364.825 + 0.2718321 * E
	s	56087.7623	0.0009	−0.0002	27	V
V591 Vir	p	56015.8947	0.0008	+0.0107	33	V; el: 53802.811 + 0.3509472 * E
GSC 272-94	s	55978.8695	0.0007	+0.0033	36	V; el: IBVS 5945
	s	56038.6879	0.0008	+0.0037	27	V
GSC 272-630	p	55973.8755	0.0006	−0.0086	20	V; el: IBVS 5945
	p	56042.7293	0.0003	−0.0157	30	V
GSC 274-437	p	55973.8683	0.0008	+0.0179	20	V; el: IBVS 5945
	p	56038.6692	0.0006	+0.0138	30	V
GSC 279-35	p	55976.9215	0.0004	−0.0009	41	V; el: IBVS 5945
GSC 279-822	s	55979.8845	0.0006	+0.0014	32	V; el: IBVS 5945; d=0.035d
	p	56039.7188	0.0002	+0.0056	20	V
GSC 286-631	p	55979.9131	0.0003	+0.0075	24	V; el: IBVS 5894
	p	56042.6636	0.0004	+0.0079	31	V
GSC 291-860	p	55986.8580	0.0005	−0.0030	24	V; el: IBVS 5945
	p	56048.6707	0.0005	−0.0046	27	V
GSC 296-9	s	55983.8750	0.0004	+0.0035	33	V; el: IBVS 5894; d=0.026d
	p	56054.6746	0.0002	+0.0023	20	V
GSC 303-36	p	56001.9117	0.0001	−0.0104	38	V; el: IBVS 5894
	p	56072.7015	0.0004	−0.0131	39	V
GSC 303-65	p	55991.9056	0.0001	+0.0099	35	V; el: IBVS 5894
	p	56072.7020	0.0002	+0.0109	40	V
GSC 303-735	s	55990.8596	0.0004	+0.0011	13	V; el: IBVS 5894
GSC 304-73	s	55989.8367	0.0005	−0.0088	35	V; el: IBVS 5945
	s	56054.725	0.010	−0.004	23	V
GSC 314-388	s	56000.8888	0.0002	+0.0024	35	V; el: IBVS 5894
GSC 314-1184	p	56015.9356	0.0003	+0.0065	33	V; el: IBVS 5992
GSC 316-99	p	56008.8587	0.0007	−0.0013	35	V; el: IBVS 5894
	p	56085.6729	0.0003	+0.0004	20	V
GSC 317-161	s	56013.9057	0.0003	+0.0046	37	V; el: IBVS 5992; d=0.036d
	p	56014.8390	0.0010	+0.0058	32	V
	p	56085.6818	0.0009	+0.0063	27	V
GSC 317-1142	p	56009.8335	0.0005	−0.0005	17	V; el: 53583.514 + 0.301333 * E
	p	56011.9415	0.0007	−0.0018	13	V
	s	56014.8036	0.0014	−0.0024	7	V
	p	56014.9558	0.0005	−0.0009	17	V
	s	56017.8214	0.0010	+0.0021	17	V
	p	56017.9711	0.0018	+0.0011	16	V
GSC 318-1169	s	56010.8828	0.0004	−0.0058	34	V; el: IBVS 5894
	s	56077.7002	0.0011	−0.0086	33	V
GSC 322-760	s	56002.8530	0.0007	+0.0134	32	V; el: IBVS 5945; d=0.016d
	p	56075.7212	0.0004	+0.0136	27	V; d=0.025d

Table 1: Minima of eclipsing binaries (continued)

Variable	Type	HJD 24...	±	$O-C$	n	Remarks
GSC 323-602	p	56008.8825	0.0004	+0.0083	36	V; el: IBVS 5945; d=0.023d
GSC 330-1394	s	56018.9157	0.0003	+0.0180	40	V; el: IBVS 5894; d=0.029d
	p	56087.7259	0.0004	+0.0209	27	V; d=0.035d
GSC 332-302	p	56002.8873	0.0003	+0.0106	32	V; el: IBVS 5992
GSC 873-411	s	55984.8322	0.0003	−0.0020	20	V; el: IBVS 5945
	p	56046.6602	0.0003	−0.0012	29	V
GSC 873-420	p	55976.8414	0.0004	+0.0035	41	V; el: IBVS 5992
GSC 878-260	p	56038.6726	0.0006	+0.0047	30	V; el: IBVS 5894
	p	56039.6418	0.0013	+0.0092	29	V
GSC 881-920	s	55984.9155	0.0007	−0.0035	20	V; el: IBVS 5945
	s	56052.6962	0.0002	−0.0082	38	V
GSC 883-1116	p	55986.8822	0.0002	−0.0045	36	V; el: IBVS 5894; d=0.031d
	s	56046.6950	0.0003	−0.0056	29	V; d=0.028d
GSC 886-340	p	55998.8503	0.0005	+0.0101	39	V; el: IBVS 5992
	p	56052.7109	0.0005	+0.0137	22	V
GSC 887-564	s	55990.9077	0.0007	−0.0046	31	V; el: IBVS 5992
	p	56072.6850	0.0010	−0.0060	40	V
GSC 891-117	p	55978.9115	0.0008	+0.0035	22	V; el: IBVS 5992
	p	56048.7720	0.0009	+0.0087	28	V; d=0.025d
GSC 892-892	s	55991.8874	0.0003	−0.0028	34	V; el: IBVS 5894
	s	56049.7097	0.0002	−0.0038	35	V
GSC 897-470	p	56009.8467	0.0003	+0.0135	16	V; el: IBVS 5894
GSC 898-3	p	56000.8827	0.0002	−0.0019	13	V; el: IBVS 5894
	p	56073.7288	0.0005	−0.0025	31	V
GSC 4955-767	p	55986.8674	0.0004	+0.0037	38	V; el: IBVS 5894
	p	56045.6822	0.0006	+0.0041	27	V
GSC 4956-1196	s	55989.8934	0.0004	+0.0054	38	V; el: IBVS 5992
	p	56054.7076	0.0009	+0.0071	24	V
GSC 4958-415	p	55990.9284	0.0003	−0.0022	32	V; el: IBVS 5894
GSC 4958-697	s	55989.8963	0.0004	+0.0070	37	V; el: IBVS 5992; d=0.018d
	p	56054.6558	0.0018	+0.0084	23	V
GSC 4968-751	s	56000.9065	0.0003	−0.0022	35	V; el: IBVS 5992
GSC 4969-725	p	56011.9342	0.0007	+0.0144	36	V; el: IBVS 5992
GSC 4977-1397	p	56010.8648	0.0003	+0.0146	34	V; el: IBVS 5992
	s	56086.7342	0.0006	+0.0123	31	V; d=0.020d
GSC 4980-656	s	56003.9122	0.0004	+0.0114	35	V; el: IBVS 5992
	p	56074.7140	0.0004	+0.0131	38	V
GSC 5519-1371	p	55978.8433	0.0003	+0.0035	16	V; el: IBVS 5992
	s	55978.9838	0.0006	+0.0031	11	V
	p	56039.7175	0.0005	+0.0058	14	V
GSC 5529-1490	s	55981.8625	0.0003	+0.0028	40	V; el: IBVS 5992
	s	56046.6486	0.0022	+0.0001	17	V
GSC 5539-45	p	55984.8409	0.0016	+0.0176	28	V; el: IBVS 5992
GSC 5542-599	s	55987.8559	0.0003	−0.0040	33	V; el: IBVS 5992
	p	56054.7486	0.0007	−0.0028	18	V
GSC 5543-1042	p	55990.9085	0.0003	+0.0156	31	V; el: IBVS 5992
	s	56072.7402	0.0002	+0.0196	37	V; d=0.026:d
GSC 5548-1080	p	56054.6979	0.0018	+0.0064	24	V; el: IBVS 5992
GSC 5553-1474	s	56002.8491	0.0003	+0.0026	21	V; el: IBVS 5992
	p	56075.6979	0.0004	+0.0015	28	V
GSC 6136-609	s	56002.8512	0.0006	+0.0002	33	V; el: IBVS 5992
DR Vul	s	56073.813	0.004	+0.212	25	V; non-circular
	p	56074.810	0.004	+0.084	31	V
GSC 1624-493	s	56074.9244	0.0032	+0.0791	32	V; el: IBVS 5860; non-circular

Remarks:
n: number of measurements incorporated in the determination of the timing of minimum
d: Time spent by star in totality at minimum
D: total duration of the eclipse

References:

Agerer, F., 2010, *PZP*, 10, 13
Agerer, F. et al., 1994, *BAV Mitt.*, 69, 1
Agerer, F., Dahm, M., 1995, *IBVS*, No. 4266
Agerer, F., Lichtenknecker, D., 1989, *IBVS*, No. 3401
Antipin, S.V., 1996, *IBVS*, No. 4342
Arena, C. et al., 2011, *IBVS*, No. 5997
Berthold, T., Agerer, F., 1997, *IBVS*, No. 4432
Biro, I.B. et al., 2006, *IBVS*, No. 5684
Blättler, E., 1998, *IBVS*, No. 4587
Blättler, E., Diethelm, R., 2000, *IBVS*, No. 4966
Blättler, E., Diethelm, R., 2000, *IBVS*, No. 4975
Blättler, E., Diethelm, R., 2000, *IBVS*, No. 4976
Blättler, E., Diethelm, R., 2001, *IBVS*, No. 5052
Blättler, E., Diethelm, R., 2001, *IBVS*, No. 5146
Blättler, E., Diethelm, R., 2001, *IBVS*, No. 5192
Blättler, E., Diethelm, R., 2002, *BBSAG Bull.*, 128, 10
Blättler, E., Diethelm, R., 2004, *IBVS*, No. 5541
Blättler, E., Diethelm, R., 2007, *IBVS*, No. 5799
Bloomer, R. et al., 2001, *IBVS*, No. 5149
Borkovits, T. et al., 2002, *IBVS*, No. 5313
Borovicka, J., Sarounova, L., 1996, *IBVS*, No. 4402
Brat, L. et al., 2011, *OEJV*, No. 137
Diethelm, R., Wolf, M., Agerer, F., 1993, *IBVS*, No. 3867
Diethelm, R., 2009, *IBVS*, No. 5871
Diethelm, R., 2009, *IBVS*, No. 5894
Diethelm, R., 2010, *IBVS*, No. 5920
Diethelm, R., 2010, *IBVS*, No. 5945
Diethelm, R., 2011, *IBVS*, No. 5960
Diethelm, R., 2011, *IBVS*, No. 5992
Diethelm, R., 2012, *IBVS*, No. 6011
Escola Sirisi, E., Garcia-Melendo, E., 1999, *IBVS*, No. 4810
Faulkner, D.R., 1986, *Publ. Astron. Soc. Pac.*, **98**, 690
Frank, P. et al., 1996, *IBVS*, No. 4386
Fuhrmeister, T., 1990, *MVS*, **12**, 48
Gomez-Forrellad, J.M., Garcia-Melendo, E., 1996, *IBVS*, No. 4364
Gray, J.D. et al., 1995, *IBVS*, No. 4177
Grobel, R., 1993, *IBVS*, No. 3852
Hajek, P. et al., 2002, *IBVS*, No. 5337
Häussler, K., 2005, *BAV Rb.*, **54**, 8
Ibanoglu, C. et al., 2007, *MNRAS*, **376**, 573
Kaiser, D.H., Frey, G., 1998, *IBVS*, No. 4544
Kaiser, D.H. et al., 2002, *IBVS*, No. 5231
Khaliullin, K.F., Khaliullina, A.I., 1989, *Soviet Astr.*, **33**, 41
Khruslov, A.V., 2010, *PZP*, **10**, 18
Khruslov, A.V., 2011, *PZP*, **11**, 1
Kinman, T.D. et al., 1982, *AJ*, **87**, 314
Kleidis, S. et al., 2008, *IBVS*, No. 5860
Kozyreva, V.S. et al., 2009, *IBVS*, No. 5909
Kreiner, J.M., 2004, *Acta Astr.*, **54**, 207, Krakow Catalog
Lasala-Garcia, A., 1996, *IBVS*, No. 4407
Lister, T.A., McDermid, R.M., Hilditch, R.W., 2000, *MNRAS*, **317**, 111
Lloyd, C. et al., 2002, *IBVS*, No. 5339
Lu, W., Hrivnak, B. J., Rush, B. W., 2007, *AJ*, **133**, 255
Lubcke, G.C. et al., 2000, *IBVS*, No. 4998
Marchini, A. et al., 2011, *JAAVSO*, **39**, 102
Nelson, R.H., 2002, *IBVS*, No. 5224
Nelson, R.H., 2004, *IBVS*, No. 5493
Nelson, R.H., 2006, *IBVS*, No. 5699
Odell, A.P. et al., 2011, *IBVS*, No. 6001
Otero, S.A. et al., 2004, *IBVS*, No. 5570
Otero, S.A., 2008, *OEJV*, No. 83

Otero, S.A., 2008, *OEJV*, No. 91
Paschke, A., 1994, *BBSAG Bull.*, **106**, 7
Pejcha, O. et al., 2001, *IBVS*, No. 5132
Samec, R.G. et al., 1995, *IBVS*, No. 4167
Samec, R.G. et al., 2004, *IBVS*, No. 5506
Samec, R.G. et al., 2004, *IBVS*, No. 5527
Samec, R.G. et al., 2008, *IBVS*, No. 5849
Samolyk, G., 1992, *JAAVSO*, **21**, 111
Terrell, D. et al., 2005, *IBVS*, No. 5642
Torres, G. et al., 2001, *IBVS*, No. 5201
Vandenbroere, J., 1993, *IBVS*, No. 3946
Vandenbroere, J., 1998, *IBVS*, No. 4554
Vidal-Sainz, J., 1997, *IBVS*, No. 4526
Williams, D.B., 1994, *IBVS*, No. 3999
Williams, D.B., 2001, *IBVS*, No. 5084
Wolf, M. et al., 1998, *Astron. Astrophys.*, **334**, 840
Zejda, M. et al., 2006, *IBVS*, No. 5741
Zhang, R. et al., 1990, *Chin. AA* , **14**, 298
Zhang, R. et al., 1994, *IBVS*, No. 4099
Zola, S. et al., 2005, *IBVS*, No. 5591

*This version of the paper contains corrections, and differs from the one appeared on-line originally. Date of last modification: Wed Jul 11 09:33:26 CEST 2012

COMMISSIONS 27 AND 42 OF THE IAU
INFORMATION BULLETIN ON VARIABLE STARS

Number 6030

Konkoly Observatory
Budapest
10 July 2012

HU ISSN 0374 – 0676

PHOTOMETRIC BEHAVIOR OF EIGHT Be/X-RAY BINARIES IN THE SMC

SARRAJ, I.[1]; SANDERS, R.J.[1]; SCHMIDTKE, P.C.[1]

[1] School of Earth and Space Exploration, Arizona State University, Box 871404, Tempe, Arizona 85287 USA

E-mail: Ibrahim.Sarraj@asu.edu, Raymond.J.Sanders@asu.edu, Paul.Schmidtke@asu.edu

We have examined the photometric behavior of eight Be/X-ray binaries in the SMC. Systems like these contain a mass-accreting neutron star in orbit with a Be star and show a variety of optical signatures (see Schmidtke & Cowley 2006; Coe et al. 2005). For binaries in which the neutron star pierces the Be star's envelope, recurring outbursts are observed that mark the orbital period. Non-radial pulsations of the Be star itself are apparent in some systems (see Balona 2010). Our sample is listed in Table 1 and consists of eight systems from the surveys of Antoniou et al. (2009b), Haberl & Pietsch (2004), and Laycock et al. (2010). None of the X-ray sources is known to be a pulsar. The magnitudes of all optical counterparts are consistent with B-type stars in the SMC. Except for object 2 (CXOU J005047.9−731817), the spectrum of each source was discussed by Antoniou et al. (2009a). They classified the stars as type B1.5e or earlier, with strong Hα emission. Hence, the observed $B-V$ colors (between −0.10 and 0.00) imply large contributions to the light from cooler circumstellar disks surrounding the primary stars.

Table 1. Source Identifications, Magnitudes, Colors, and Spectral Types

Object	X-ray Source	OGLE-II	MACHO	[M2002][a]	V^a	$B-V^a$	Sp.Typ.[b]
1	XMMU J004834.5−730230	smc_sc5_43566[c]	212.15851.9	11182	14.84	−0.05	B1.5e
2	CXOU J005047.9−731817	smc_sc5_180008	...	17703	14.50	−0.03	...
3	CXOU J005057.2−731008	smc_sc5_271074	...	18200	14.33	0.00	B0.5e
4	CXOU J005245.0−722844	...	207.16145.12[d]	24501	14.65	−0.10	O9-B0e
5	CXOU J005252.2−724830	smc_sc6_147662	208.16140.14[e]	24914	14.19	0.00	O2((f))+OBe
6	CXOU J005446.2−722523	smc_sc7_70843	207.16259.37	31155	15.25	−0.10	B1e
7	XMMU J010030.2−722035	smc_sc8_204456[f]	207.16603.13	49014	14.60	−0.07	B1.5e
8	XMMU J010435.7−722143	smc_sc10_61612	206.16887.12	59680	15.15	−0.03	B1.5e

[a]From Massey (2002) [b]From Antoniou et al. (2009a)
[c]Also smc_sc4_178950 [d]Also 208.16145.10 [e]Also 207.16140.17 [f]Also smc_sc9_35989

Photometric data for all objects were obtained from the MACHO and OGLE web sites. Long-term trends in the observations were removed by subtracting low-order polynomial fits from segments of data. The flattened values were then searched for periodicities in the frequency range $0-3$ day^{-1}, using the Period04 analysis package (Lenz & Breger 2005).

For sources in this study, significant one-day aliasing is present in the Fourier spectra due to the character of the data sampling. This problem can be further complicated for short-period signals if the fundamental frequency is itself changing, as discussed by Schmidtke & Cowley (2012). They find that small variations in a pulsation period have

the effect of reducing the significance of a short-period signal while artificially increasing the apparent significance of a long-period alias. Hence, the highest peak in a Fourier plot might not be the proper choice. In selecting the most likely period for each object studied here, we considered not only the relative strengths of peaks in the Fourier spectrum of the entire data set but also the Fourier spectrum from each individual season, the shape of the resulting (folded) light curve, and the agreement of data taken in different bandpasses.

Periodic signals were found in four systems. We did not identify a meaningful signal for objects 3, 5, 7, and 8. The maximum amplitude in each of these stars was <0.01 mag. The results are summarized in Table 2, and individual systems are discussed below.

Table 2. Photometric Periods and Amplitudes

	OGLE-II *I*		MACHO Blue		MACHO Red	
Object	Period (days)	Amplitude (mag)	Period (days)	Amplitude (mag)	Period (days)	Amplitude (mag)
1	1.053	0.037	1.025	0.022	...	...
2	1.050	0.017	...	...	...	...
4	...	...	...	...	17.541	0.042
6	0.731	0.015	0.730	0.008	0.730	0.010

Object 1 (XMMU J004834.5−730230): A periodic signal with P=1.053 days was found in season 1 of the OGLE-II *I* data. The folded light curve, shown in Figure 1, is sinusoidal in shape with a full amplitude of 0.037 mag. This behavior is consistent with non-radial pulsations of the Be star. Similar variations, with a period of 1.025 days and an amplitude of 0.022 mag, are present in MACHO blue-bandpass data.

Object 2 (CXOU J005047.9−731817): The high-precision position of the *Chandra* X-ray source is coincident with OGLE-II star smc_sc5_180008, but not with emission-line object [MA93]396 (Meyssonnier & Azzopardi 1993), which lies $\sim 5''$ to the north. Although the X-ray spectral parameters are consistent with a Be/X-ray binary (Antoniou et al. 2009b), Hα emission has not yet been confirmed in smc_sc5_180008. A weak optical periodicity, however, is present in season 4 of the OGLE-II *I* data for this star, as shown in Figure 2. These variations, with P=1.050 days and an amplitude of 0.017 mag, are approximately sinusoidal and might be due to non-radial pulsations of the primary star.

Object 4 (CXOU J005245.0−722844): A signal with a period of 17.541 days and an amplitude of 0.042 mag is clearly present in all seasons of the MACHO red-bandpass data. The folded light curve, shown in Figure 3, has a non-sinusoidal shape. The distinct brightening might represent an orbital outburst lasting $\sim$0.4P.

Object 6 (CXOU J005446.2−722523): Periodic variations, with P=0.731 days and an amplitude of 0.015 mag, are present in season 4 of the OGLE-II *I* data. Although the amplitude is small, see Figure 4, the folded light curve is roughly sinusoidal and might be caused by non-radial pulsations. Similar signals were found in both red and blue MACHO data, reinforcing this interpretation.

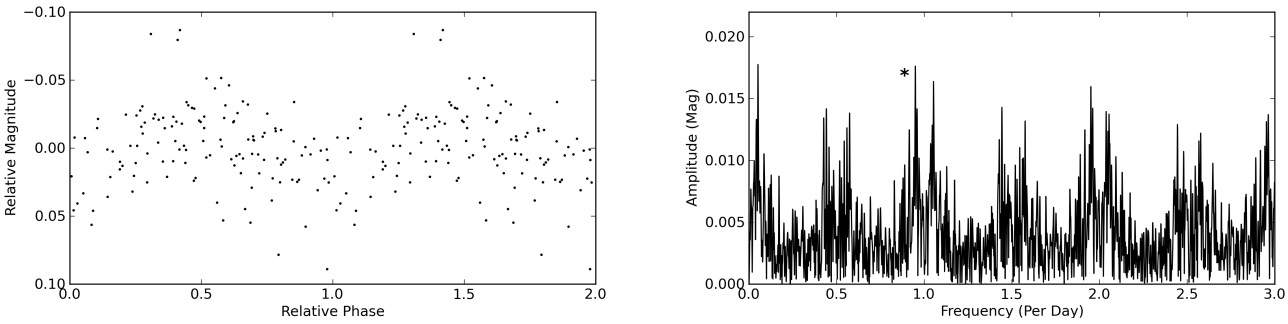

Figure 1. Light curve of detrended OGLE-II data and Fourier spectrum for object 1. The data are folded with P=1.053 days, which is the period marked by $*$ in the Fourier spectrum.

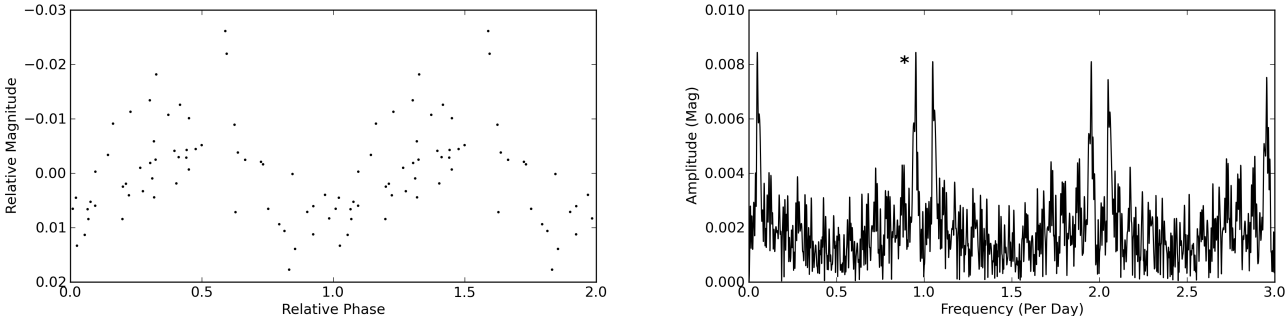

Figure 2. Light curve of detrended OGLE-II data and Fourier spectrum for object 2. The data are folded with P=1.050 days, which is the period marked by $*$ in the Fourier spectrum.

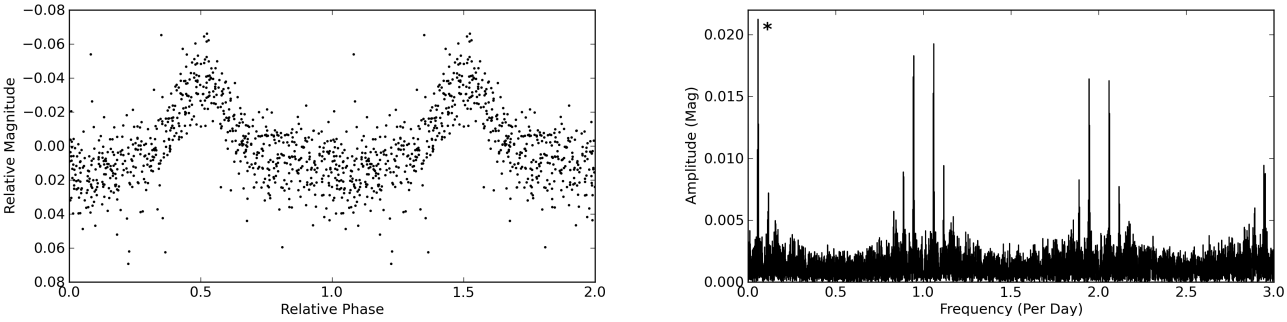

Figure 3. Light curve of detrended MACHO data and Fourier spectrum for object 4. The data are folded with P=17.541 days, which is the period marked by $*$ in the Fourier spectrum.

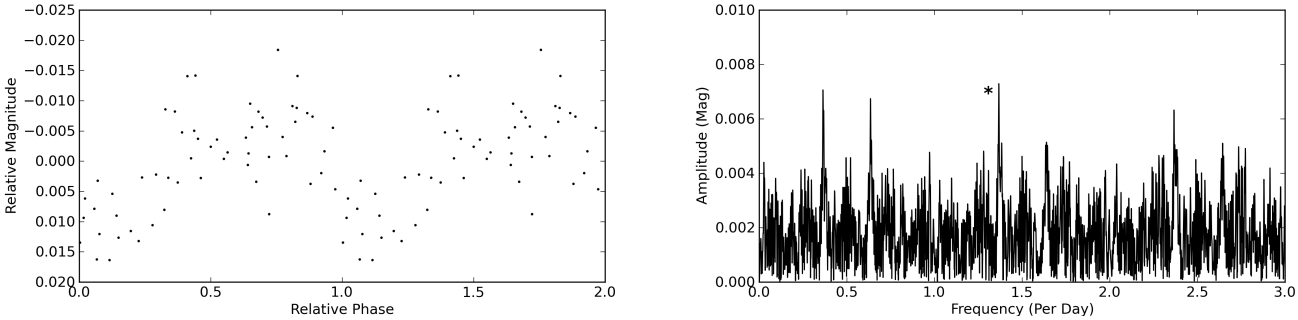

Figure 4. Light curve of detrended OGLE-II data and Fourier spectrum for object 6. The data are folded with P=0.731 days, which is the period marked by $*$ in the Fourier spectrum.

Acknowledgments: This paper utilizes public domain data obtained by the MACHO Project, jointly funded by the US Department of Energy through the University of California, Lawrence Livermore National Laboratory under contract No. W-7405-Eng-48, by the National Science Foundation through the Center for Particle Astrophysics of the University of California under cooperative agreement AST-8809616, and by the Mount Stromlo and Siding Spring Observatory, part of the Australian National University.

The OGLE-II database, as described by Udalski et al. (1997), Zebrun et al. (2001), and Szymanski (2005), was also used in this investigation.

References:

Antoniou, V., Hatzidimitriou, D., Zezas, A., Reig, P. 2009a, *ApJ*, **707**, 1080
Antoniou, V., Zezas, A., Hatzidimitriou, A., McDowell, J.C. 2009b, *ApJ*, **697**, 1695
Balona, L.A. 2010, in *Challenges in Stellar Pulsation*, Bentham Science Publishers
Coe, M.J., Edge, W.R.T., Galache, J.L., McBride, V.A. 2005, *MNRAS*, **356**, 502
Haberl, F., Pietsch, W. 2004, *A&A*, **414**, 667
Lacock, S., Zezas, A., Hong, J., Drake, J.J., Antoniou, V. 2010, *ApJ*, **716**, 1217
Lenz, P, Breger, M. 2005, *CoAst*, **146**, 53
Massey, P. 2002, *ApJS*, **141**, 81 ([M2002])
Meyssonnier, N., Azzopardi, M. 1993, *A&AS*, **102**, 451 ([MA93])
Schmidtke, P.C., Cowley, A.P. 2006, *AJ*, **132**, 919
Schmidtke, P.C., Cowley, A.P. 2012, submitted
Szymanski, M. 2005, *Acta Astron.*, **55**, 43
Udalski, A., Kubiak, M., Szymanski, M. 1997, *Acta Astron.*, **47**, 319
Zebrun, K., et al. 2001, *Acta Astron.*, **51**, 317

COMMISSIONS 27 AND 42 OF THE IAU
INFORMATION BULLETIN ON VARIABLE STARS

Number 6031

Konkoly Observatory
Budapest
16 July 2012

HU ISSN 0374 – 0676

SPECTRAL DETECTION OF A VERY STRONG FLARE ON WX UMa

MELIKIAN, N. D.[1]; NATSVLISHVILI, R. Sh.[2]; TAMAZIAN, V. S.[3]; KARAPETIAN, A. A.[1]

[1] Byurakan Astrophysical Observatory, Armenia

[2] Abastumani Astrophysical Observatory, Georgia

[3] Astronomical Observatory R. M. Aller, University of Santiago de Compostela, Spain

WX UMa (= Gliese 412B) is a relatively faint ($m_V = 14\overset{\mathrm{m}}{.}41$) M6V flare star located at a distance of 4.8 pc (Gould & Chaname, 2004; Pettersen, 1991). Being the secondary component B in the double system WDS 11055+4332, it exhibits a well studied large scale magnetic field (Morin et al. 2010) and has been identified as an X-ray source, while no significant X-ray emission was detected from the primary component A (Schmitt et al. 1995). The first flare with an amplitude of $1\overset{\mathrm{m}}{.}5$ on this star was probably detected by A. van Maanen on photographic plates obtained with the Mount Wilson 100″ telescope in 1939 (Joy, 1967).

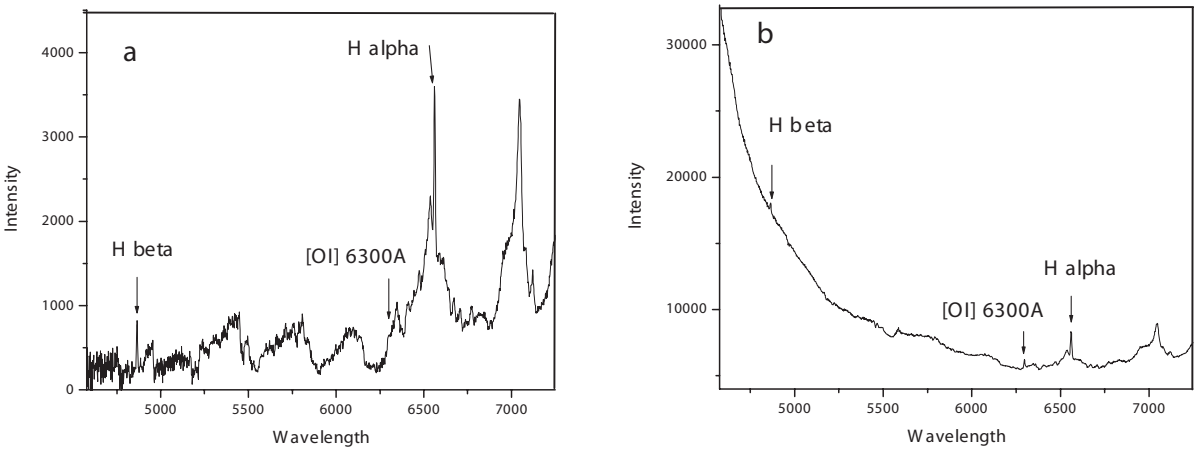

Figure 1. Spectra of WX UMa before (a) and during (b) the flare event.

In the framework of our study of binary flare stars in the solar vicinity, spectral monitoring of HU Del, CM Dra, WX UMa and VW Com is being carried out with the 2.6m telescope of Byurakan Astrophysical Observatory. The observations were performed with

the SCORPIO spectral camera providing the spectral resolution of 1.7Å/pix. (Afanasiev et al. 2005). For data reduction, we have made use of the SCORPIO dedicated software packages (Moiseev, 2002; Moiseev & Afanasiev 2005) for background sky subtraction, extraction, wavelength calibration (using a Neon lamp in our observations), and flux calibration.

During four nights within a period from May 18 to June 1, 2012, 70 spectra were obtained for these stars. Their preliminary processing allowed us to detect a very strong flare on the secondary component of WX UMa on May 18. In this report, some observational characteristics of this event are reported, while more detailed results of the monitoring will be presented later.

Spectra were obtained with equal exposures of 300 s and time interval between them about 80 s. As a standard, BD+28 4211 (m_V =10.$^{\rm m}$56) was used. In 33 minutes five spectra were obtained, and a very strong flare was detected on the last spectrum. In Fig. 1, the spectra before (a) and during (b) the flare are presented. An unusually strong brightening in the blue part is clearly seen in Fig. 1b, which in terms of energy distribution transforms the M6 spectrum to an early B type. Apart from this, the appearance of the [OI] 6300Å emission line during the flare event (see Fig. 2a,b) should be noticed. The equivalent widths of emission lines Hα and Hβ measured on all spectra are presented in Table 1.

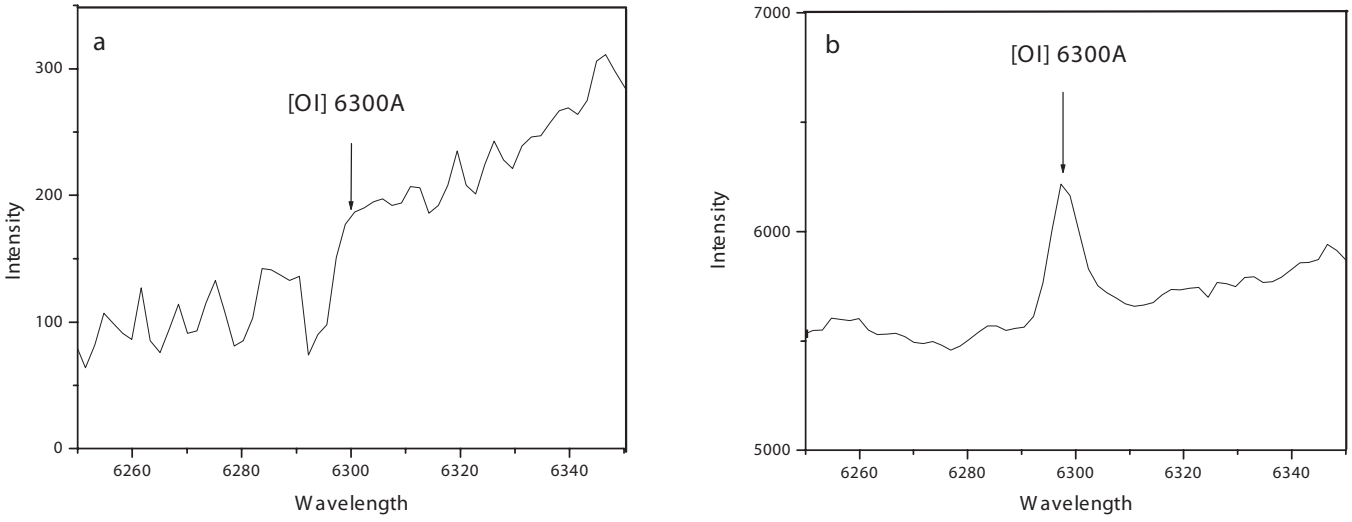

Figure 2. The emission line [OI] 6300Å before (a) and during (b) the flare event.

The data overview shows that the equivalent widths of Hα and Hβ on the first four spectra increase while on the last spectrum they clearly decrease. This fact along with the disappearance of some absorption lines on the last spectrum is probably a result of veiling by the strong continuous emission formed during the flare. Brightness in the quiescent state (spectral region 4500−7250Å) varies in the range $\Delta m = 0.^{\rm m}0 - 0.^{\rm m}5$, while a simultaneous increase of Hα and Hβ EWs is clearly detected. The very strong lowering of the EWs during the flare is probably caused by the brightening of continuum. It is worth noting that the existence of two phases during a flare event has been suggested on the basis of high time-resolution observations of UV Ceti type stars (Moffett & Bopp, 1976). These are the spike phase dominated by continuum emission, and the slow phase showing strong emission-line radiation along with decreasing continuum.

Table 1. Equivalent widths of the Hα and Hβ emission lines

Sp. No.	Start exp. (UT) [h m s]	EW Hβ (Å)	EW Hα (Å)
1	21 22 15	11.9	11.9
2	21 28 14	14.7	12.1
3	21 36 33	16.9	12.4
4	21 43 29	19.2	13.6
5	21 50 58	0.9	3.1

The estimated amplitudes of brightening (Δm) in the spectral ranges 4600−7250Å and 4600−5000Å are $2\overset{\mathrm{m}}{.}8$ and $4\overset{\mathrm{m}}{.}5$ respectively. In reality, the amplitude of this flare is much higher since detected relatively "low" amplitude is a result of the low time-resolution of our observations. Notice that the decrease of the flare amplitude from the blue to the red part of the spectrum is typical of UV Ceti stars.

References:

Afanasiev, V.L., Gazhur, E.B., Zhelenkov, S.R., Moiseev, A.V., 2005, *Bull. Special Astrophys. Obs.*, **58**, 90 http://unipaq.sao.ru/hq/lsfvo/devices/scorpio/BSAO_eng.pdf

Afanasiev, V.L., Moiseev, A. V., 2005, *Astron. Lett.*, **31**, 194

Joy, A.H., 1967, *ASPL*, **10**, 41

Gould, A., Chaname, J., 2004, *ApJS*, **150**, 455

Moffett, T.J., Bopp, B. W., 1976, *ApJS*, **31**, 61

Moiseev, A.V., 2002, *Bull. Special Astrophys. Obs.*, **54**, 74

Morin, J., Donati, J.-F., Petit, P., Delfosse, X., Forveille, T., Jardine, M.M. 2010, *MNRAS*, **407**, 2269

Pettersen, B. R. 1991, *MmSAI*, **62**, 217

Schmitt, J.H.M.M., Fleming, T.A., Giampapa, M.S., 1995, *ApJ*, **450**, 392

COMMISSIONS 27 AND 42 OF THE IAU
INFORMATION BULLETIN ON VARIABLE STARS
Number 6032

Konkoly Observatory
Budapest
8 August 2012
HU ISSN 0374 – 0676

SPECTRAL AND PHOTOMETRIC OBSERVATIONS OF MWC 560 IN 2009 – 2012

KONDRATYEVA, L.; RSPAEV, F.

Fessenkov Astrophysical Institute, Almaty, Kazakhstan. e-mail: kondr.lud@gmail.com; lu_kondr@mail.ru

The peculiar object MWC 560 was discovered as an emission star by Merrill & Burwell (1943). It consists of a red giant and a white dwarf. Its orbital period, as estimated by Gromadzki et al. (2007), equals to $P_{\rm orb} = 1931 \pm 162$ days. Photometry of this object has been obtained by Doroshenko et al. (1993), Tomov et al. (1996), Zamanov et al. (2011) and Goranskij et al. (2011). The spectrum of MWC 560 contains several emission lines of H I, FeII, superimposed on the late-type continuum. The most spectacular feature of the spectrum is the highly blue-shifted broad absorption components of the hydrogen lines. During a stable state the absorption components show a maximum outflow speed of $\sim 1580 - 2140$ km s^{-1} and widths of $500 - 1400$ km s^{-1}.

The first large outburst took place in 1989 – 1990, when the brightness of the object reached V=9.$^{\rm m}$2, and the absorption components were shifted with up to -6500 km s^{-1}. Then, in 1993 and 1998, blue-ward velocities of the absorption components of more than 3000 km s^{-1} were observed (Iijima, 2002). These authors proposed a classification of the absorption profiles and defined four types: A, B - for a stable state and C, D - for an active state.

The faint stable stage of the object, which continued between January 2008 and December 2009, was followed by the flash, registered on December 24, 2010 by Goranskij et al. (2011).

Our observations in Fessenkov Astrophysical Institute have been made before and after the last flash. B, V, $R_{\rm C}$ magnitudes were measured using the 1-meter Carl Zeiss Jena and the 70-cm AZT-8 reflectors equipped with CCD ST-8 (1530×1020, 9 μ) and of B, V, $R_{\rm C}$ filters. All frames were dark subtracted and flat field corrected. The stars HD 62834, HD 163355 and HD 58457 were adopted as standards. The obtained B, V, $R_{\rm C}$ magnitudes are listed in Table 1. They supplement the data of Goranskij et al. (2011). Photometric phases were computed according to the ephemeris:
JD$_{\rm max}$=2 448 080 + 1931×E (Gromadzki et al., 2007).

Spectral observations have been carried out with the slit spectrograph for faint emission objects, attached to the AZT-8 telescope and with the UAGS spectrograph, attached to the 1-m telescope. Both spectrographs were equipped with ST–8 CCD cameras. The slit width was between $3' - 4'$. Wavelength calibration was done using a laboratory source of HeI, NeI and ArI emission lines. Spectra of standard stars obtained just before or after

Table 1: Photometric results

Date	HJD	Phase	B	V	R
	2400000+		mag	mag	mag
10.02.2010	55238.234	0.707	10.76±0.05	10.46±0.06	8.94±0.05
10.11.2010	55511.444	0.848	10.26±0.05	9.90±0.04	9.20±0.05
13.11.2010	55514.410	0.850	10.25±0.04	9.89±0.04	9.12±0.04
13.02.2012	55971.151	0.087	10.39±0.05	10.13±0.05	8.96±0.04
03.03.2012	55990.130	0.096	10.90±0.05	10.22±0.04	9.22±0.06

the target were used for flux calibration. All spectrograms were corrected for atmospheric extinction.

All Balmer lines from Hβ to Hδ produce the strong and deep jet absorptions. For Hα the absorption is less deep due to the significant contribution of the red giant spectrum to the total continuum. Table 2 presents the spectral parameters of the Hβ and Hα lines: equivalent widths (EW) and the absolute fluxes ($F_{\rm abs}$) of the absorption and emission components and the spectral resolution of observations. $F_{\rm abs}$ values are expressed in erg cm^{-2}s^{-1} with the multiplier 10^{-12}. Observations on 13.02.2012 were carried out only in the red wavelength range. For some dates only equivalent widths of the lines are presented, because the absolute spectral calibration was absent. Figure 1 shows the normalized profiles of Hα and Hβ.

The radial velocities of the Hα and Hβ absorption components are listed in Table 3. The errors of the presented values depend on the spectral resolution and the structure of the measured profiles. As it was mentioned above, the period in 2008 – 2009 appeared to be rather stable for MWC 560. However the profiles of Hα and Hβ, registered on 21.12.2008 and 04.01.2009, appeared to be quite unusual. There was flat continuum (up to -800 km s^{-1}) between the emission and an absorption components. Such features have been registered earlier during the active stage (profiles of C-type by Iijima, 2002), but simultaneously they have been followed by a blue shift of absorption component up to -4000 km s^{-1}. On the contrary, the blue sides of our profiles are at about -2100 km s^{-1} the typical value for a stable stage (in accordance with the classification of Iijima, 2002). This feature (the flat continuum between the emission and absorption components) has disappeared from the profiles obtained on 10.02.2010: the blue-ward velocity has not changed, but the velocity of the red wing has shifted to about -500 km s^{-1}. The highly blue-shifted components with RVs up to -3500 km s^{-1} appeared in the profiles of Hα and Hβ on November, 10 – 13 2010, just before the last flash (24.12.2010). On February, 2012 the blue-shifted components returned to $V_r \sim -2000$ km s^{-1}, but the emission flux of Hα remained as high as before the flash.

Table 2: Spectral results

HJD 2400000+	Hβ absorption EW Å	Hβ absorption F_{abs} 10^{-12}	Hβ emission EW Å	Hβ emission F_{abs} 10^{-12}	Hα absorption EW Å	Hα absorption F_{abs} 10^{-12}	Hα emission EW Å	Hα emission F_{abs} 10^{-12}	R=λ/Δλ for Hβ – Hα
54822.34	12.5		21.6		6.7		121.9		10000 – 13000
54836.32	12.1	1.91	16.2	3.31	7.6	0.995	121.2	11.0	3000 – 4500
55238.21	18.2	3.86	17.3	3.74	9.8	2.24	120.6	24.1	7000 – 9000
55511.42	21.0		18.6		22.9		122.5		10000 – 13000
55514.35	23.4	11.92	17.5	9.04	27.1	1.11	127.8	45.1	10000 – 13000
55971.16					14.2	4.44	165.8	54.4	7000 – 9000
55990.12	11.3		30.5		7.7		188.0		7000 – 9000

Table 3: Radial velocities of absorption components of Hβ and Hα

Date	HJD	Hβ absorption			Hα absorption		
	2400000+	blue wing	red wing	centre	blue wing	red wing	centre
21.12.2008	54822.34	−1970	−670	−1320	−2100	−700	−1400
		±40	±40	±40	±30	±30	±30
04.01.2009	54836.32	−2250	−860	−1555	−2200	−740	−1470
		±80	±80	±80	±60	±60	±60
10.02.2010	55238.21	−2260	−420	−1390	−2220	−540	−1380
		±45	±45	±45	±30	±30	±30
10.11.2010	55511.42	−3490	−1590	−2540	−3780	−1100	−2440
		±30	±30	±30	±20	±20	±20
13.11.2010	55514.35	−3370	−780	−2075	−3410	−920	−2165
		±40	±40	±40	±30	±30	±30
13.02.2012	55971.16				−2060	−570	−1315
					±40	±40	±40
03.03.2012	55990.12	−2270	−430	−1350	−1600	−600	−1100
		±45	±45	±45	±40	±40	±40

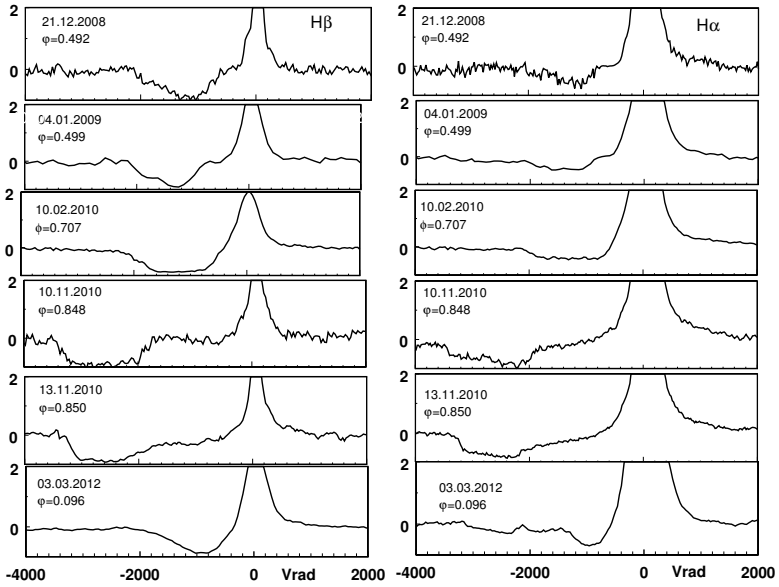

Figure 1. The absorption components of Hβ and Hα profiles. The horizontal axis corresponds to the heliocentric radial velocities.

References:

Doroshenko, V.T., Goranskij, V.P., Efimov, Y.S., 1993, *IBVS*, No. 3824
Goranskij, V., Doroshenko, V., et al., 2011, *ATel* No. 3149
Gromadzki, M., J. Mikolajewska, J., Whitelock, P.A., et al., 2007, *A&A*, **463**, 703
Iijima, T., 2002, *A&A*, **391**, 617
Merrill, P., Burwell, C., 1943, *ApJ*, **98**, 153
Tomov, T., et al., 1996, *A&AS*, **116**, 1
Zamanov, R., Boeva, S., et al., 2011, *IBVS*, No. 5995

COMMISSIONS 27 AND 42 OF THE IAU
INFORMATION BULLETIN ON VARIABLE STARS

Number 6033

Konkoly Observatory
Budapest
7 September 2012

HU ISSN 0374 – 0676

MINIMA OF ECLIPSING BINARIES AND NEW EPHEMERIDES FOR GSC 03881-00579 AND EZ LACERTAE

BANFI, M.[1]; ACETI, P.[1,2]; ARENA, C.[1,3]; BIANCIARDI, G.[1,4]; BONAVENTURA, G.[1,3]; CHIAPPINI, M.[5]; CORFINI, G.[1]; DE PONTI, J.M.[2]; LO SAVIO, E.[3]; LUCIDI, F.[1]; MARCHINI, A.[1,5]; MARINO, G.[1,3]; MARTINENGO, M.[1]; NASIMI, H.[5]; PESENTI, L.[2]; PRANDONI, F. [2]; RUOCCO, N.[1,6]; SALVAGGIO, F.[1,3]; VINCENZI, M.[1]; ZAMBELLI, R.[1]

[1] Sezione Stelle Variabili – Unione Astrofili Italiani (UAI), e-mail: `stellevariabili@uai.it`

[2] Liceo Scientifico *Iris Versari*, Cesano Maderno (MI), ITALY

[3] Gruppo Astrofili Catanesi - via Milo, 28 I-95125 Catania, ITALY

[4] Skylive/Telescopio remoto UAI - ITALY

[5] University of Siena Astronomical Observatory - Via Roma, 56 I-53100 Siena, ITALY

[6] Astrocampania, Sez. Stabia – Penisola Sorrentina - ITALY

The list below contains 163 times of minimum for 79 eclipsing binary stars (including the cataclysmic AM Her) calculated from CCD observations made by participants in the SSV-UAI Eclipsing Binaries Program. All the observatories are located in Italy; one is managed by the Physics Department of the University of Siena, while the others are privately operated. Some light curves were remotely obtained (via Internet) using the Italian and Australian telescopes of the Skylive-UAI Project, that are publicly available on the web site `http://www.skylive.it`.
The observations were reduced following standard procedures (see next section) and the light curves were analyzed using the Kwee−van Woerden algorithm (Kwee & van Woerden, 1956) to determine the times of minimum. All the times of minimum listed in this paper are heliocentric.
It is worth noting that most of the observed stars are neglected objects.

Observatory and telescope:
University of Siena Astron. Observatory: 32-cm Maksutov–Cassegrain (MC32)
Australian Skylive remote telescope: 36-cm Schmidt–Cassegrain (SC36)
Other private astronomical stations:
30-cm Schmidt–Cassegrain (SC30)
23-cm Schmidt–Cassegrain (SC23)
25-cm Newton (NW25)
25-cm Schmidt–Cassegrain (SC25)
20-cm Newton (NW20)
20-cm Schmidt–Cassegrain (SC20)
13-cm Maksutov–Cassegrain (MK13)
8-cm ED Refractor (ED8)

Detector:	Meade DSI Pro II Monochromatic CCD camera (DSI) QSI 516wsg CCD Camera SBIG ST-7 CCD Camera (ST7) SBIG ST-8XME CCD Camera (ST8) SBIG ST-9 CCD Camera (ST9) Sony ICX429ALL based CCD camera (CCD-UAI) Canon Eos 1100D DSLR(Eos)

Method of data reduction:

Frame calibration (dark subtraction and flat field correction) and photometric analysis (differential photometry on each image) were performed using MaxIm DL or Mira Pro software packages.

Method of minimum determination:

Times of minima, expressed as Heliocentric Julian Day (see the attached Table), were computed adopting the KW method (Kwee & van Woerden, 1956) using AVE (Barberá, 1996). This algorithm also provides an error estimate, that is the formal internal error of the KW method, which can be considered as a lower limit of the actual uncertainty on times of minimum. Together with that error, we provide an alternative estimate error according to the Arlot's (modified) method (Arlot et al., 2009) by adopting the formula $\sigma_{ToM} = \frac{1}{\sqrt{2}}\frac{\sigma_m}{\Delta m}\Delta t$, where σ_m is the error in magnitude and Δm is the magnitude drop during a time range Δt delimiting the part of the light curve where the speed of decrease in magnitude is the highest.
The types of minimum quoted in the Table were deduced according to the ephemeris provided by Kreiner's (2004) web site (`http://www.as.up.krakow.pl/ephem`), by B.R.N.O. – *O−C Gateway* web site (`http://var.astro.cz/ocgate`) or by our updated elements. In the latter case we are sure that the primary minimum (conventionally at zero phase) is the deepest one.

Times of minima:

Star name	Time of min. HJD 2400000+	Error	Type	Filter	Rem.
V473 And	55836.3902	0.0006[a] 0.0004[b]	I	*V*	Martinengo/SC20/QSI 516
V473 And	55837.3928	0.0010 0.0005	II	*V*	Martinengo/SC20/QSI 516
V473 And	55837.5932	0.0013 0.0003	I	*V*	Martinengo/SC20/QSI 516
V473 And	55843.4114	0.0008 0.0005	II	*V*	Banfi/SC25/ST7
V473 And	55843.6124	0.0008 0.0005	I	*V*	Banfi/SC25/ST7
V473 And	55846.4217	0.0012 0.0004	I	*V*	Banfi/SC25/ST7
V473 And	55878.5260	0.0011 0.0003	I	*V*	Vincenzi/SC30/ST9
V480 And	55836.3021	0.0007 0.0004	I	*V*	Zambelli/SC25/ST8
V487 And	55830.5409	0.0029 0.0007	I	*V*	Banfi/SC25/ST7
V502 And	55804.4732	0.0015 0.0005	I	*V*	Banfi/SC25/ST7
V502 And	55836.3609	0.0007 0.0003	I	–	Corfini/NW20/CCD-UAI
V502 And	55879.4120	0.0009 0.0004	I	*V*	Corfini/NW20/CCD-UAI
XX Ant	55916.2133	0.0007 0.0009	II	*r*	Marino/SC36/ST8
CK Aqr	55791.4012	0.0006 0.0002	I	*V*	Vincenzi/SC30/ST9
GS Aqr	55838.3281	0.0003 0.0002	II	–	Corfini/NW20/CCD-UAI
AL Ari	55898.3071	0.0003 0.0001	I	*R*	Marino/NW25/ST7
EM Aur	55954.2639	0.0022 0.0005	II	*R*	Marino/NW25/ST7
MM Aur	55945.3071	0.0037 0.0011	I	–	Ruocco/SC25/ST7
MR Aur	55938.4642	0.0061 0.0019	I	–	Ruocco/SC25/ST7
V562 Aur	55915.3709	0.0017 0.0003	I	*Y*495	Corfini/NW20/CCD-UAI
V594 Aur	55904.2955:	0.0023 0.0020	I	–	Ruocco/SC25/ST7
TU Boo	55924.5934	0.0005 0.0001	I	*V*	Vincenzi/SC30/ST9

Times of minima:					
Star name	Time of min. HJD 2400000+	Error	Type	Filter	Rem.
EF Boo	56036.3468	0.0006 0.0001	I	*R*	Marino et al./NW20/ST7
XZ CMi	55863.5173	0.0006 0.0001	I	*V*	Vincenzi/SC30/ST9
AE Cas	55940.2959	0.0002 0.0001	I	*R*	Marino/NW25/ST7
DO Cas	55919.3001	0.0005 0.0001	I	*R*	Marino/NW20/ST7
V541 Cas	55928.3368	0.0001 0.0001	II	*R*	Marino/NW25/ST7
DM CVn	56046.3212	0.0008 0.0004	I	–	Ruocco/SC25/ST7
EL CVn	56076.4101	0.0004 0.0001	I	*V*	Martinengo/SC20/QSI 516
EV CVn	56043.4320	0.0007 0.0004	II	–	Ruocco/SC25/ST7
EV CVn	56043.5978	0.0007 0.0003	I	–	Ruocco/SC25/ST7
UX CrB	56058.4798	0.0004 0.0001	I	–	Ruocco/SC25/ST7
V997 Cyg	55764.5449	0.0005 0.0003	II	*V*	Banfi/SC25/ST7
V1187 Cyg	55826.4039	0.0007 0.0002	I	*V*	Banfi/SC25/ST7
V1187 Cyg	55835.4441	0.0005 0.0002	I	*V*	Zambelli/SC25/ST8
V1191 Cyg	55826.4072	0.0007 0.0001	II	*V*	Banfi/SC25/ST7
V1905 Cyg	55765.4700	0.0001 0.0002	I	–	Ruocco/SC25/ST7
V1763 Cyg	55802.3573	0.0008 0.0006	I	*V*	Banfi/SC25/ST7
V2287 Cyg	55832.3206	0.0016 0.0009	I	*V*	Banfi/SC25/ST7
V2486 Cyg	55806.3740	0.0037 0.0012	I	–	Ruocco/SC25/ST7
CR Del	55820.3994	0.0027 0.0008	II	*V*	Banfi/SC25/ST7
KO Del	55834.3197	0.0003 0.0001	I	–	Corfini/NW20/CCD-UAI
HL Dra	55852.3251	0.0004 0.0002	I	–	Corfini/NW20/CCD-UAI
G3881.0579 Dra	55773.3453	0.0002 0.0001	I	–	Corfini/NW20/CCD-UAI
G3881.0579 Dra	56014.4160	0.0004 0.0002	I	*V*	Marchini et al./MC32/ST7
G3881.0579 Dra	56014.5801	0.0002 0.0001	II	*V*	Marchini et al./MC32/ST7
G3881.0579 Dra	56015.4038	0.0002 0.0001	I	*V*	Marchini et al./MC32/ST7
G3881.0579 Dra	56015.5680	0.0002 0.0001	II	*V*	Marchini et al./MC32/ST7
G3881.0579 Dra	56016.3917	0.0002 0.0002	I	*V*	Marchini et al./MC32/ST7
G3881.0579 Dra	56016.5560	0.0003 0.0001	II	*V*	Marchini et al./MC32/ST7
G3881.0579 Dra	56025.4483	0.0013 0.0002	II	–	Arena/NW20/DSI
G3881.0579 Dra	56025.6136	0.0013 0.0002	I	–	Arena/NW20/DSI
G3881.0579 Dra	56039.6080	0.0005 0.0002	II	–	Arena/NW20/DSI
G3881.0579 Dra	56042.4066	0.0006 0.0001	I	*R*	Arena/NW20/ST7
G3881.0579 Dra	56059.3676	0.0005 0.0001	II	*V*	Aceti et al./SC20/ST8
VV Eri	55877.5609	0.0016 0.0002	I	*V*	Vincenzi/SC30/ST9
VV Eri	55891.5794	0.0006 0.0002	I	*V*	Vincenzi/SC30/ST9
VV Eri	55895.4695	0.0034 0.0007	II	*V*	Vincenzi/SC30/ST9
VV Eri	55952.3246	0.0003 0.0001	I	*V*	Zambelli/SC25/ST8
VV Eri	55952.3248	0.0004 0.0001	I	*r*	Corfini/NW20/CCD-UAI
AM Her[c]	55834.3195	0.0006 0.0013	I	*V*	Banfi/SC25/ST7
V1072 Her	56036.4881	0.0054 0.0003	II	–	Arena/NW20/DSI
V1088 Her	56060.3817	0.0008 0.0009	II	–	Ruocco/SC25/ST7
V1088 Her	56060.5613	0.0008 0.0007	I	–	Ruocco/SC25/ST7
V1088 Her	56063.4342	0.0008 0.0003	I	–	Ruocco/SC25/ST7
V1088 Her	56075.4689	0.0009 0.0004	II	–	Ruocco/SC25/ST7
V1106 Her	55776.3528	0.0003 0.0002	I	–	Corfini/NW20/CCD-UAI
V1106 Her	55778.3904	0.0006 0.0002	I	–	Corfini/NW20/CCD-UAI
V1106 Her	55831.3476	0.0019 0.0004	I	*V*	Banfi/SC25/ST7
V1106 Her	55839.3658	0.0010 0.0002	II	*V*	Marchini/MC32/ST7
V1106 Her	55843.3139	0.0009 0.0003	I	–	Corfini/NW20/CCD-UAI
V1106 Her	55844.3320	0.0007 0.0003	I	–	Corfini/NW20/CCD-UAI
V1106 Her	55844.3323	0.0005 0.0003	I	*V*	Marchini/MC32/ST7
V1106 Her	55851.3321	0.0008 0.0002	II	–	Corfini/NW20/CCD-UAI
V1106 Her	56004.6007	0.0025 0.0006	II	–	Bonaventura/MK13/Eos

Times of minima:					
Star name	Time of min. HJD 2400000+	Error	Type	Filter	Rem.
G1518.0913 Her	56038.4225	0.0021 0.0002	I	–	Arena/NW20/DSI
G1518.0913 Her	56038.5845	0.0013 0.0001	II	–	Arena/NW20/DSI
G1518.0913 Her	56051.4334	0.0013 0.0011	II	*V*	Aceti et al./SC25/ST8
EZ Lac	55881.3430	0.0006 0.0003	I	–	Ruocco/SC25/ST7
EZ Lac	55892.5071	0.0013 0.0002	I	–	Vincenzi/SC30/ST9
EZ Lac	55895.2961	0.0011 0.0003	I	–	Ruocco/SC25/ST7
EZ Lac	55948.3194	0.0010 0.0021	I	*V*	Marchini/MC32/ST7
EZ Lac	56118.5614	0.0016 0.0005	I	–	Marchini/MC32/ST7
EZ Lac	56121.3466	0.0072 0.0003	I	–	Marchini/MC32/ST7
EZ Lac	56125.5141	0.0056 0.0014	II	*I*	Zambelli/SC25/ST8
EZ Lac	56125.5326	0.0079 0.0017	II	–	Corfini/NW20/CCD-UAI
EZ Lac	56125.5384	0.0091 0.0012	II	–	Banfi/SC25/ST7
EZ Lac	56125.5631	0.0031 0.0012	II	–	Marchini/MC32/ST7
EZ Lac	56139.4754	0.0143 0.0022	II	*V*	Martinengo/SC20/QSI 516
EZ Lac	56139.4956	0.0169 0.0036	II	–	Marchini/MC32/ST7
FU Lac	55818.5718	0.0070 0.0081	I	–	Ruocco/SC25/ST7
FU Lac	55840.3395	0.0122 0.0024	II	–	Ruocco/SC20/ST7
FU Lac	55864.3560	0.0035 0.0011	I	–	Ruocco/SC25/ST7
XX Leo	56019.3106	0.0047 0.0005	II	*V*	Salvaggio,Lo Savio/SC23/ST7
VW LMi	55983.4129	0.0016 0.0005	I	–	Bonav., Marino/MK13/Eos
WZ LMi	56004.3405	0.0031 0.0008	II	–	Ruocco/SC25/ST7
AA Lyn	56001.3162	0.0003 0.0002	I	–	Ruocco/SC25/ST7
CW Lyn	56014.3550	0.0011 0.0003	I	*V*	Martinengo/SC20/QSI 516
DI Lyn	55942.3894	0.0044 0.0014	II	*H*	Corfini/NW20/CCD-UAI
EH Lyn	55974.4884	0.0014 0.0006	I	–	Corfini/NW20/CCD-UAI
EH Lyn	55979.3903	0.0005 0.0004	I	–	Zambelli/SC25/ST8
EH Lyn	55980.3702	0.0003 0.0003	I	–	Zambelli/SC25/ST8
EH Lyn	55984.4597	0.0011 0.0003	II	–	Corfini/NW20/CCD-UAI
EH Lyn	55988.3799	0.0015 0.0007	II	–	Corfini/NW20/CCD-UAI
HY Lyr	55825.3577	0.0008 0.0004	II	*V*	Banfi/SC25/ST7
PV Lyr	55803.4355	0.0017 0.0004	I	*V*	Banfi/SC25/ST7
QQ Lyr	55769.5520	0.0012 0.0008	I	–	Ruocco/SC25/ST7
V574 Lyr	55791.5070	0.0003 0.0002	II	*BVRI*	Arena/NW20/ST7
V574 Lyr	55795.4688	0.0003 0.0002	I	*BVRI*	Arena/NW20/ST7
V574 Lyr	55798.3359	0.0003 0.0003	II	*BVRI*	Arena/NW20/ST7
V574 Lyr	55798.4728	0.0003 0.0004	I	*BVRI*	Arena/NW20/ST7
V574 Lyr	55799.4278	0.0010 0.0003	II	*BVRI*	Arena/NW20/ST7
V574 Lyr	55800.3850	0.0007 0.0003	I	*BVRI*	Arena/NW20/ST7
V574 Lyr	55800.5196	0.0007 0.0010	II	*BVRI*	Arena/NW20/ST7
V574 Lyr	55801.3399	0.0003 0.0003	II	*BVRI*	Arena/NW20/ST7
V574 Lyr	55801.4776	0.0003 0.0004	I	*BVRI*	Arena/NW20/ST7
V574 Lyr	55802.4325	0.0005 0.0003	II	*BVRI*	Arena/NW20/ST7
G3108.0057 Lyr	55775.5515	0.0004 0.0002	I	–	Arena/NW20/DSI
DD Mon	55975.3123	0.0002 0.0001	I	*R*	Marino/NW25/ST7
V383 Mon	55985.4022	0.0019 0.0007	I	–	Ruocco/SC25/ST7
V383 Mon	55999.3652	0.0014 0.0009	I	–	Ruocco/SC25/ST7
V383 Mon	56007.3029	0.0024 0.0022	II	–	Ruocco/SC25/ST7
V464 Mon	55911.2019	0.0006 0.0002	I	–	Marino/SC36/ST8
V527 Mon	55909.2121	0.0009 0.0004	I	–	Marino/SC36/ST8
ET Ori	55876.1011	0.0002 0.0001	I	–	Bianciardi, Ruocco/SC36/ST8
BW Peg	55838.4471	0.0015 0.0004	I	–	Ruocco/SC20/ST7
BW Peg	55846.3719	0.0004 0.0005	I	–	Corfini/NW20/CCD-UAI
V365 Peg	55840.3521	0.0060 0.0005	II	*V*	Banfi/SC25/ST7
V963 Per	55922.2549	0.0002 0.0001	I	–	Ruocco/SC25/ST7
V963 Per	55923.4136	0.0009 0.0003	II	–	Ruocco/SC25/ST7
V963 Per	55923.6407	0.0005 0.0003	I	–	Ruocco/SC25/ST7
GR Psc	55818.5789	0.0010 0.0001	II	*V*	Banfi/SC25/ST7
CP Sge	55805.3585	0.0022 0.0008	I	*V*	Banfi/SC25/ST7

Times of minima:					
Star name	Time of min. HJD 2400000+	Error	Type	Filter	Rem.
V423 Tau	55948.3316	0.0061 0.0017	II	–	Ruocco/SC25/ST7
V423 Tau	55952.4212	0.0048 0.0008	II	–	Ruocco/SC25/ST7
V423 Tau	55953.4434:	– 0.0100	I	–	Ruocco/SC25/ST7
V423 Tau	55956.5144	0.0041 0.0022	II	–	Ruocco/SC25/ST7
V1374 Tau	55919.3776	0.0002 0.0003	I	$Y495$	Corfini/NW20/CCD-UAI
V1374 Tau	55937.4361	0.0003 0.0002	I	r	Corfini/NW20/CCD-UAI
BE Tri	55819.6384	0.0014 0.0004	I	V	Banfi/SC20/ST7
BE Tri	55835.3955	0.0006 0.0003	I	–	Corfini/NW20/CCD-UAI
BM Tri	55850.4697	0.0007 0.0002	I	V	Banfi/SC25/ST7
BX Tri	55838.4592	0.0010 0.0008	II	V	Banfi/SC25/ST7
BX Tri	55839.4206	0.0031 0.0009	II	V	Banfi/SC25/ST7
BX Tri	55839.5158	0.0009 0.0005	I	V	Banfi/SC25/ST7
BX Tri	55839.6150	0.0018 0.0004	II	V	Banfi/SC25/ST7
CM Tri	55825.6310	0.0015 0.0007	I	V	Banfi/SC25/ST7
CN Tri	55803.5678	0.0007 0.0003	I	V	Banfi/SC25/ST7
CS Tri	55924.4591	0.0018 0.0005	I	V	Banfi/SC25/ST7
XY UMa	56004.4285	0.0003 0.0001	I	–	Bonaventura/MK13/Eos
GZ UMa	55933.4127:	0.0044 0.0002	I	V	Lucidi/ED8/DSI
LL UMa	56013.4238	0.0012 0.0006	I	–	Ruocco/SC25/ST7
LL UMa	56013.5882	0.0016 0.0006	II	–	Ruocco/SC25/ST7
MS UMa	55983.4140	0.0007 0.0003	I	V	Aceti et al./SC25/ST7
EY Vul	55839.3213	0.0024 0.0007	I	V	Banfi/SC25/ST7
V384 Vul	55706.5493	0.0009 0.0003	II	V	Banfi/SC25/ST7
V384 Vul	55750.4349	0.0020 0.0004	II	V	Banfi/SC25/ST7
V384 Vul	55790.3715	0.0011 0.0001	II	V	Vincenzi/SC30/ST9
V384 Vul	55803.5366	0.0015 0.0001	II	V	Vincenzi/SC30/ST9
V384 Vul	55805.5119	0.0018 0.0003	I	V	Vincenzi/SC30/ST9
V384 Vul	55819.3355	0.0007 0.0003	II	V	Marchini/MC32/ST7
V467 Vul	55442.3386	0.0004 0.0003	II	V	Corfini/NW20/CCD-UAI
V467 Vul	55827.4316	0.0007 0.0002	II	–	Corfini/NW20/CCD-UAI

Explanation of the remarks in the table:

Rem.: Observer[s]/Telescope/Detector
[a] Arlot's modified method
[b] as given by KW method
[c] cataclysmic variable
: uncertain

Remarks:

GSC 03881-0579 − We found relevant discrepancies between our observed times of the minima and the computed times of the minima based on the period of $0^{\rm d}.3293363$ given by Devor et al. (2008). Our data better fit to the $0^{\rm d}.329333$ value given by Gettel et al. (2006). The best linear fit of the O−C vs. the epoch, leaving the initial epoch and period free to vary, including the time of minimum given by the VSX catalogue (deduced from Devor et al., 2008 data), leads to the following updated ephemeris:

$$T_{min}\ (\mathrm{HJD}) = 2453128.48509(\pm 0.00091) + 0^{\rm d}.3293313(\pm 0.0000001) \times E$$

EZ Lac − Considering our data together with those found in literature, the best linear fit of the O−C leads to the following average ephemeris:

$$T_{min}\ (\mathrm{HJD}) = 2429231.3909(\pm 0.0263) + 2^{\rm d}.7908638(\pm 0.0000035) \times E$$

Figure 1 shows the O−C diagram computed using the above mentioned average ephemeris. The high dispersion of the old data (photographic) does not allow to establish with certainty a variation of O−C or period in the range from the first observations (1938) up to our observations. However, the average ephemeris leads to a discrepancy of about half an hour with respect to the recent times of minimum. Our minima better fit to the following updated ephemeris:

$$T_{min}\ (\mathrm{HJD}) = 2455881.34265(\pm 0.0013) + 2^{\rm d}.790773(\pm 0.000025) \times E$$

obtained taking into account only our primary minima, whose depth allows a more precise timing of the minima.

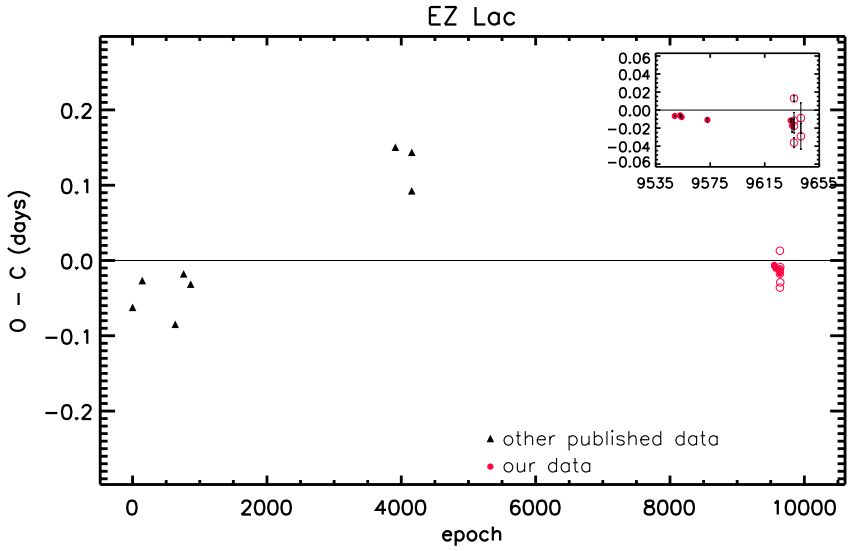

Figure 1. O−C diagram for EZ Lac. Empty symbols for secondary minima.

References:

Arlot, J.-E. et al., 2009, *A&A*, **493**, 1171
Devor, J., Charbonneau, D., O'Donovan, F. T., Mandushev, G., Torres, G., 2008, *AJ*, **135**, 850
Gettel, S.J., Geske, M.T., McKay, T.A., 2006, *AJ*, **131**, 621
Kreiner, J. M., 2004, *AcA*, **54**, 207, `http://www.as.up.krakow.pl/ephem`
Kwee, K. K., van Woerden, H., 1956, *Bull. Astr. Inst. Neth.*, **12**, 327, (No. 464)

COMMISSIONS 27 AND 42 OF THE IAU
INFORMATION BULLETIN ON VARIABLE STARS

Number 6034

Konkoly Observatory
Budapest
7 September 2012

HU ISSN 0374 – 0676

NON-RADIAL PULSATIONS OF ζ Oph

POLLMANN, E.

Spektroskopische Arbeitsgemeinschaft ASPA, 51375 Leverkusen, Germany

Fast line profile variations in the spectra of Be stars are now attributed to non-radial pulsations of these stars, assiciated with the equivalent width variations. Strictly speaking this is true only for the periodic variations. There are transient ones as well. Whether this mechanism produces the disk around a Be star, is still the subject of debate. Spectra of the HeI λ 6678 line of the Be star zeta Oph (O9V) show distortions which propagate uniformly across the absorption line profile. Vogt and Penrod (1983) concluded from their observations, that the line profile distortions are caused by high-order non-radial pulsation and an l=8, m=8 mode provides a good fit to many of the line profiles. The observed amplitude of the pulsation correlates apparently with episodes of emission outburst of ζ Oph from season to season.

The author's first measurements with the LHIRES III slit-grating spectrograph (0.11 Å/pix, spectral resolution R = 14000) in Fig. 1. were made during 1.5 hours (JD 2456061.418-2456061.492) with the 40-cm SC telescope of the Vereinigung der Sternfreunde Köln (Germany). The individual spectra were taken with 15 minute exposure time in a cadence of 30 minutes. A comparison with Vogt & Penrod-spectra taken on 29 June 1980 and 1 July 1980 (see Fig. 1 in Vogt & Penrod, 1983) shows a high similarity, and encouraged further observations.

HeI λ6678 equivalent width measurements of the author's 2012/05/16 observation (Fig. 2) are compared with the August 1981 series of Vogt and Penrod's spectra in Fig. 3 [planimetering by P. Harmanec of the line-profile plots in Vogt and Penrod's paper (Harmanec, 1989, table 4)]. Harmanec (1989, p. 231) concludes that "no clear correlation of the equivalent width changes with the 0.643 day period is apparent". Contrary to that conclusion, the observations presented here show a very clear increase with time during JD 2456064.371 to JD 2456064.598.

Follow-up observation runs during 2012/05/24-27 were dedicated to figure out whether the equivalent width is suitable for determination of the period behaviour (Figs. 4 and 5).

The HeI λ6678 absorption line profiles of these observations in Fig. 4 are strongly shaped by the appearance and disappearance of an absorption bump at 6575-6580 Å, which usually moves uniformly across the line. This bump often shows a noticeable asymmetry in the way in which it traverses the profile.

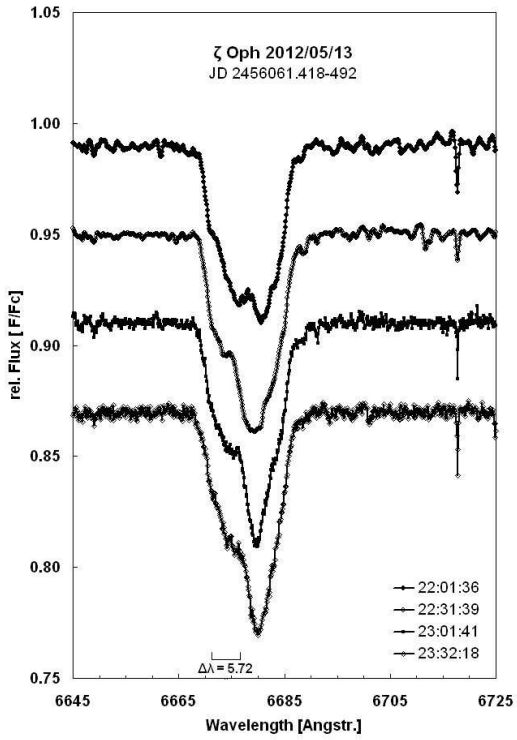

Figure 1. The first 40-cm SC telescope measurements (JD 2456061.418-2456061.492)

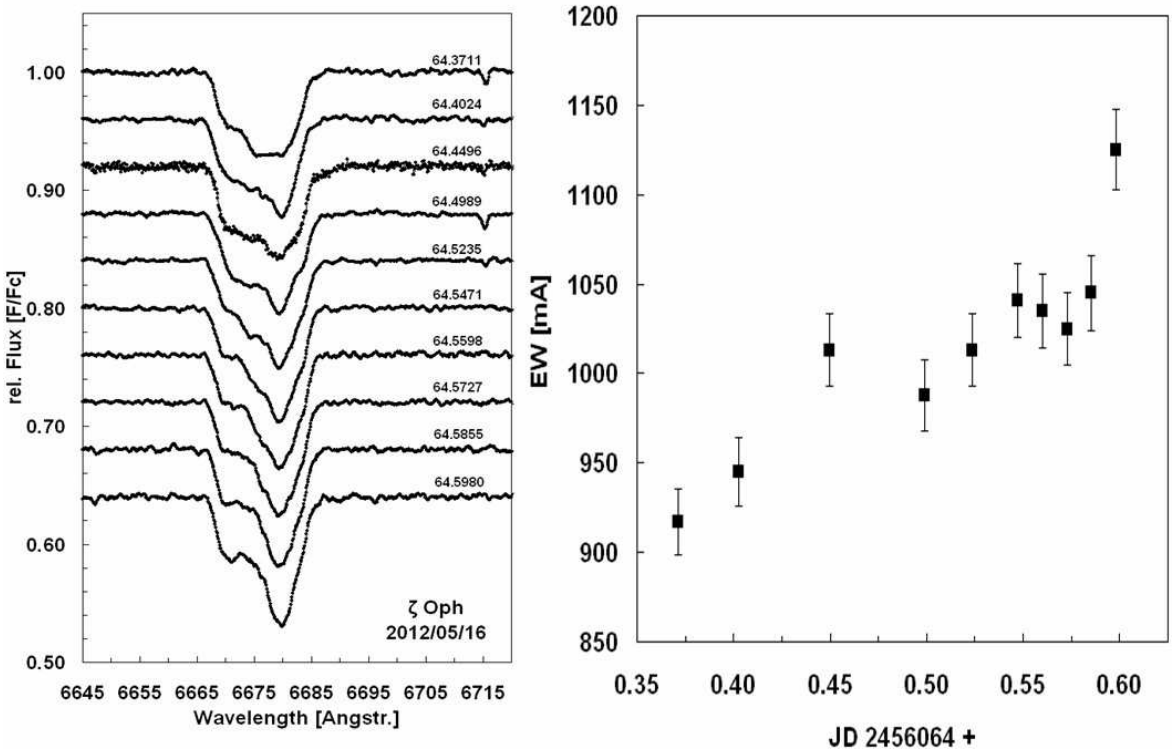

Figure 2. Observations of 2012/05/16; individual spectra (left), equivalent width vs. time (right)

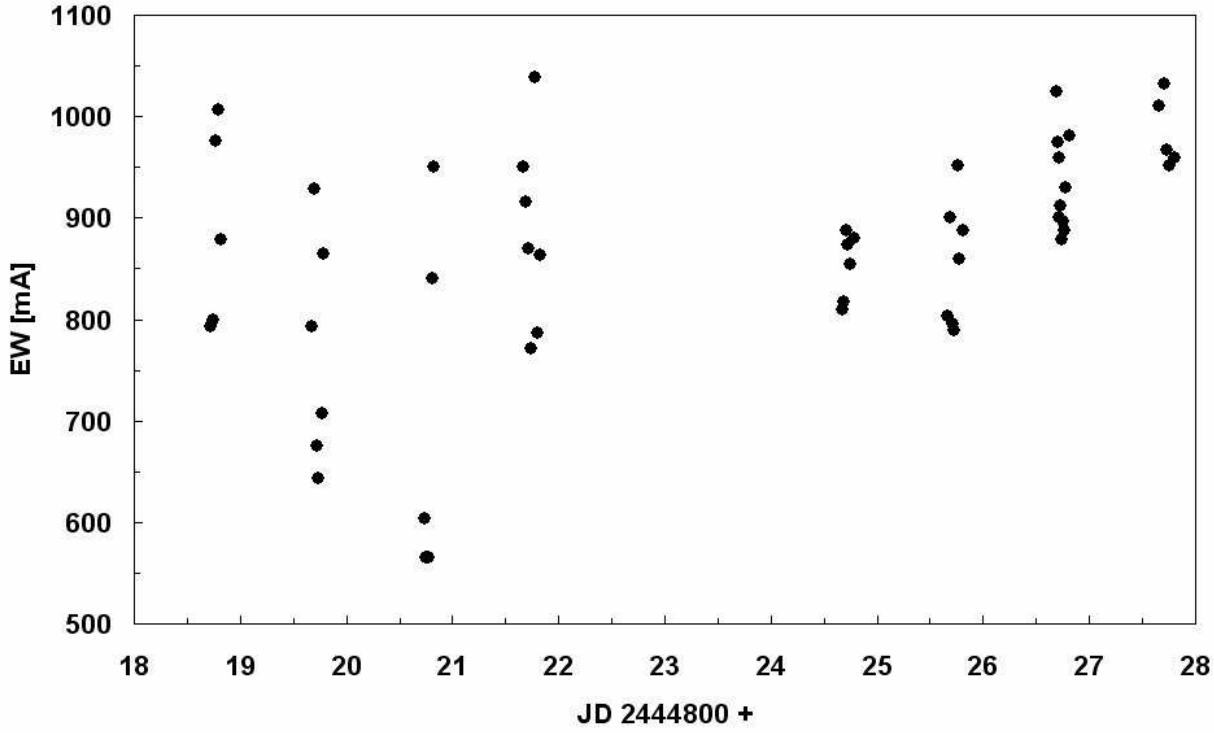

Figure 3. Planimetric measurements of HeI λ 6678 equivalent width (no error bars were indicated) in August 1981 spectra of Vogt & Penrod

Fig. 5 shows the period and phase analysis of the 2012/05/24-27 observations. The upper plot shows the time behaviour of the HeI λ6678 equivalent width, the middle plot shows the dominant period at 0.643 d and the lower plot shows the phase representation of this period. I used the AVE program (http://www.astrogea.org/soft/ave/aveint.htm) to search for periodicities and found a period of 0.643 days, whereas Harmanec (1989) found no variation in EW in August 1981 spectra of Vogt & Penrod.

The importance of these observations should be seen in the context of the many publications in the past, particularly the highly precise MOST (Microvariability and Oscillations of Stars) photometric and ground-based spectroscopic data of Walker et al. (2005). They conclude that the 0.643 d period might be the signature of very fast equatorial rotation.

Acknowledgements:
I am grateful to Prof. Dr. Gordon A. H. Walker (referee of this observation report) for his positive evaluation and encouragement, to continue my observations during coming visibility periods of the star.

References:

Harmanec, P., 1989, *Bull. Astron. Inst. Czechosl.*, **40**, 201
Vogt, S. S. & Penrod G. D., 1983, *ApJ*, **275**, 661
Walker, G. A. H. et al., 2005, *ApJ*, **623**, L145

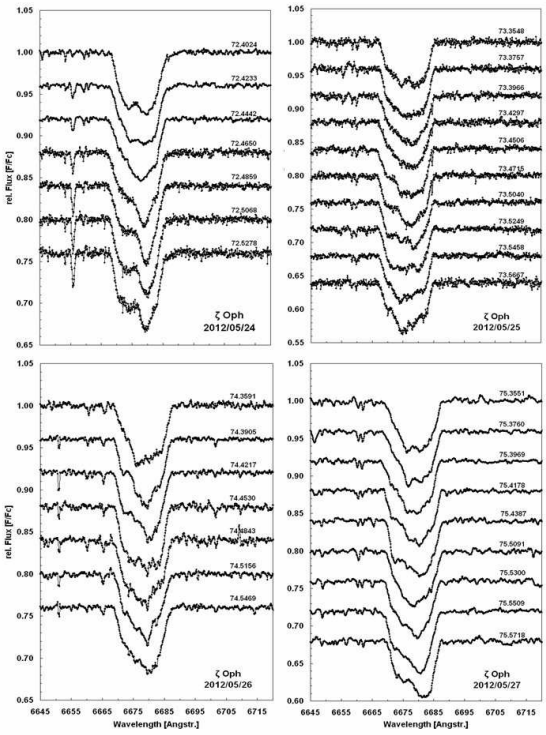

Figure 4. Individual spectra of the 2012/05/24-27 observations

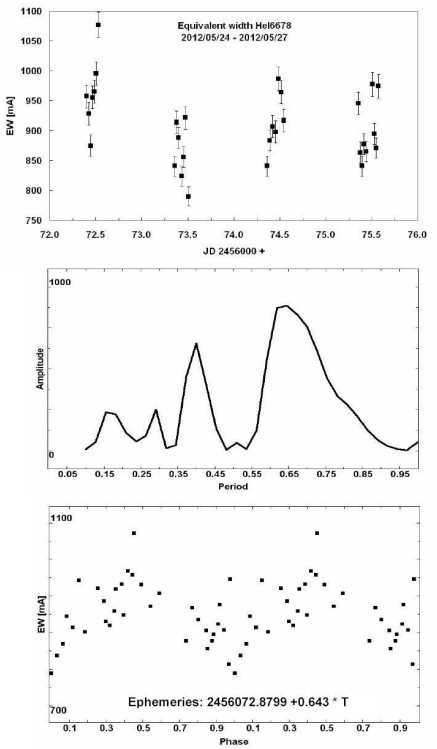

Figure 5. Equivalent width versus time (top), periodogram (middle), phase curve (below)

COMMISSIONS 27 AND 42 OF THE IAU
INFORMATION BULLETIN ON VARIABLE STARS

Number 6035

Konkoly Observatory
Budapest
7 September 2012

HU ISSN 0374 – 0676

UBVR$_C$I$_C$ PHOTOMETRIC STUDY OF THE NEAR CONTACT ECLIPSING BINARY Mis V1287

SAMEC, RONALD G.[1]; DIGNAN, JAMES G.[1]; SMITH, PAUL M.[1]; REHN, TRAVIS[1]; OLIVER, BRUCE M.[1]; FAULKNER, DANNY R.[2]; VAN HAMME, WALTER[3]

[1] Astronomy program, Department of Physics, Bob Jones University, Greenville, SC 29614, USA

[2] University of South Carolina, Lancaster, USA

[3] Florida International University, Miami, FL 33199, USA

Mis V1287 (Lacerta) [GSC 3992 2510, 2MASS J22455869+5628318, $\alpha(2000) = 22^h45^m58^s.68$, $\delta(2000) = +56°28'31''.87$] was recently discovered by Seiichi Yoshida of the MISAO Project (Nakajima, et al. 2006), and identified as an EB type variable with a period of 0.7655d. The magnitude range is 12.25 - 12.78 (V). The discovery ephemeris is:

$$\text{HJD T}_{\text{min}}\text{I} = 2453294.9863 + 0.7655\text{d} \times \text{E} \quad (1)$$

Monochromatic but phased photometric data is available at http://www.aerith.net/misao/data/misv.cgi?1287. Parabola fits were performed on all eclipse data, and 4 new times of minimum light were determined. These were used in our period study.

Our U, B, V, R_C, I_C light curves were taken with the Lowell 31 inch reflector in Flagstaff with a CRYOTIGER cooled (−100°C) NASACAM and a 2K×2K chip and standard $UBVR_CI_C$ filters. They were taken on 22-24 September, 2009. We undertook the observing run under the auspices of the National Undergraduate Observatory (NURO) and were granted observing time by the Lowell TAC. We used the Lowell program LOIS to take our observations.

Our modeled light curves included 39 U, 298 B, 294 V, 296 R_C and 285 I_C individual CCD observations. Our U light curve is incomplete, but it was included in the analysis. These were taken by Samec and Faulkner as well as several students: Adam Jaso, Travis Rehn, Bruce Oliver. The photometric precision was ±0.005 in U and ±0.0065 in B, ±0.0045 in V, and ±0.006 in R_C and ±0.0075 in I_C. Figure 1 shows sample observations of B, V and $B-V$ color curves on the night of September 22, 2009. The complete observations are given in Tables 1-5 (available electronically), in delta magnitudes, variable minus comparison star.

The variable star Mis V1287 was observed along with a comparison star (GSC 3992 2679) [$\alpha(2000) = 22^h46^m18^s.069$, $\delta(2000) = +56°30'57''.77$], B−V = 0.501, and a check star (GSC 3992 2099) [$\alpha(2000) = 22^h45^m59^s.812$, $\delta(2000) = +56°29'45''.09$], B−V = 0.568. The field including these stars is given in Figure 2 as a convenience for future observers.

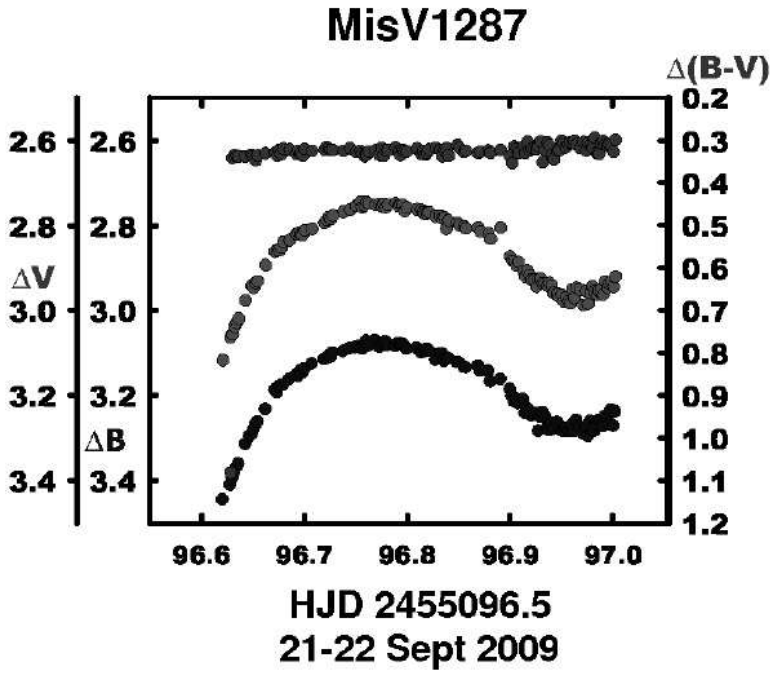

Figure 1. B, V and $B-V$ color curves of Mis V1287 on 2009 September 22.

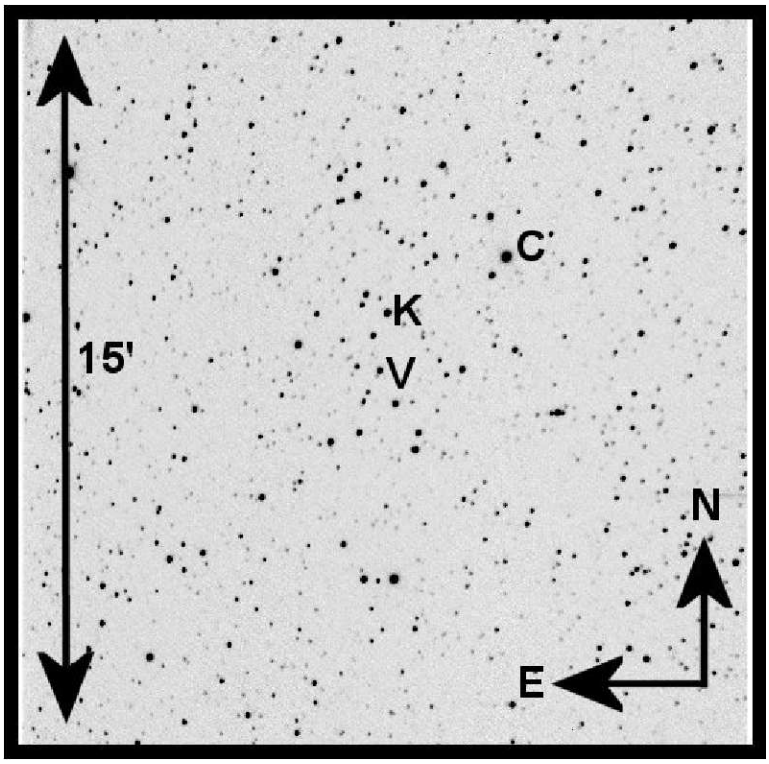

Figure 2. Finding Chart, Mis V1287 Variable (V), Comparison (C) and Check (K).

Three times of minimum light were determined from our present observations. The minima were calculated using parabola fits in each band and averaged by Samec and Dignan. With their standard errors in parentheses, they include: Min I = HJD 2455098.8780 (±0.0004) and Min II = HJD 2455097.7316 (±0.0002), 2455096.964 (±0.001). Other timings were calculated from fits to the CCD data of Nakajima (Nakajima, et al. 2006): Min I = HJD 2453299.9623, 2453293.0726, Min II = HJD 2453294.9832, 2453294.2179. The following ephemeris was calculated from all the available timings:

$$T_{min}I = \text{HJD } 2455098.8786 \pm 0.0007 + (0.7654970 \pm 0.0000004)\text{d} \times \text{E} \quad (2)$$

The well-iterated ephemeris from our Wilson-Devinney program used to phase our data was:

$$T_{min}I = \text{HJD } 2455098.8785 \pm 0.0002 + (0.7644 \pm 0.0001)\text{d} \times \text{E} \quad (3)$$

The linear O−C residuals, calculated from Eq. 2, are given in Table 6. The resulting O−C diagram is given in Figure 3.

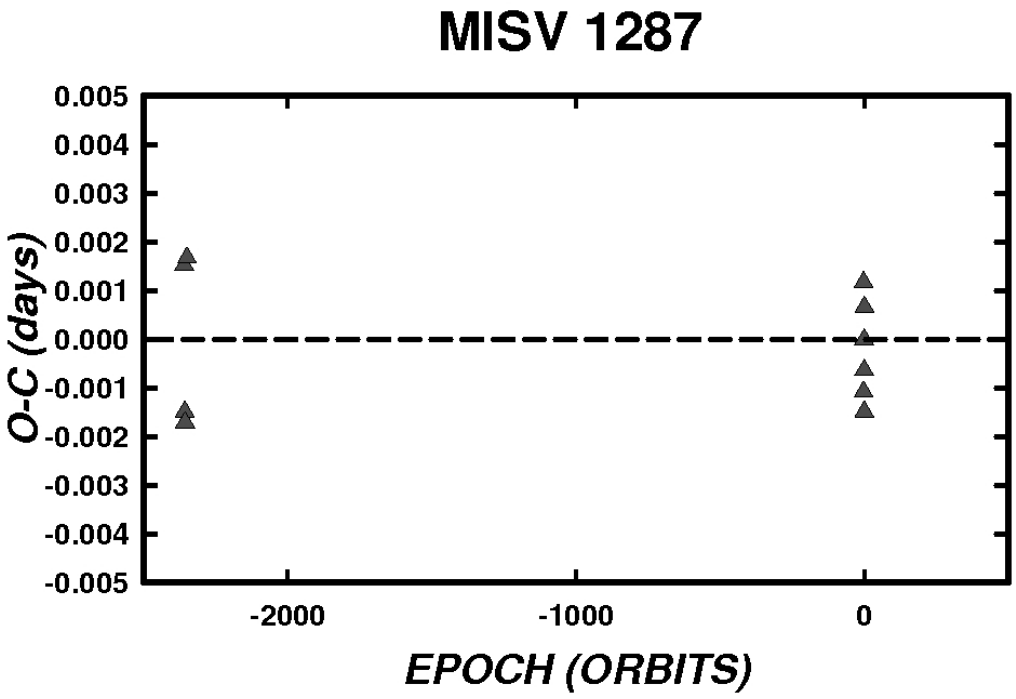

Figure 3. O−C residuals from period study calculated from Equation 2.

It is noted that the period is shorter in Eq. 3 with respect to Eq. 2. This may mean that the period is decreasing as we would expect in the scenario developed later in this paper. But further timings are needed to establish this trend.

Table 6. O−C linear residuals, Eq. [2]

No.	Epochs	Cycles	Weight	O−C
1	2453293.0726	−2359.0	0.5	0.0015
2	2453294.2179	−2357.5	0.5	−0.0015
3	2453294.9832	−2356.5	0.5	−0.0017
4	2453299.9623	−2350.0	0.5	0.0017
5	2455096.9638	−2.5	0.5	−0.0011
6	2455097.7316	−1.5	1.0	0.0012
7	2455098.8780	0.0	1.0	−0.0006

The $BVR_{\rm C}I_{\rm C}$ phased light curves, phase versus delta magnitudes, in the sense of V−C, are given as Figures 4 and 5. The $UBVR_{\rm C}I_{\rm C}$ curves are of an EB type. The light curves show effects of night to night variability which is seen in the high scatter in the secondary minima. Light curve characteristics at quadratures are given in Table 7. The $UBVR_{\rm C}I_{\rm C}$ curves are typical of a semi-detached binary with a primary amplitude of 0.56 to 0.43 mags in U to $I_{\rm C}$, respectively, and a secondary of only 0.19 to 0.25 mags in U to $I_{\rm C}$, respectively. The difference in maxima light curves is about 2% in each filter. Thus, magnetic activity is strong in the system with dark spots and/or hot spots present. The difference of eclipse depths are 0.4 to 0.2 mags, U to $I_{\rm C}$, respectively, indicate EB light curves and that the components are not in contact.

Table 7. Light curve characteristics of Mis V1287

Filter	Phase	Mag MaxI	Phase	Mag MaxII
U	0.25	3.426±0.020	0.75	3.442±0.020
B		3.078±0.006		3.098±0.004
V		2.751±0.002		2.773±0.005
$R_{\rm C}$		2.554±0.006		2.576±0.003
$I_{\rm C}$		2.317±0.007		2.333±0.006
Filter	Phase	Mag MinII	Phase	Mag MinI
U	0.50	3.629±0.020	0.00	4.000±0.020
B		3.289±0.016		3.571±0.010
V		2.975±0.021		3.249±0.005
$R_{\rm C}$		2.806±0.021		3.019±0.008
$I_{\rm C}$		2.588±0.006		2.764±0.008
Filter	MinI−MaxII	MinII−MaxII	MinII−MinI	
U	0.558±0.040	0.187±0.040	0.371±0.040	
B	0.473±0.015	0.190±0.010	0.283±0.026	
V	0.478±0.026	0.204±0.026	0.274±0.026	
$R_{\rm C}$	0.443±0.014	0.230±0.010	0.213±0.029	
$I_{\rm C}$	0.431±0.015	0.254±0.013	0.177±0.014	
Filter	MaxII−MaxI			
U	0.0162±0.040			
B	0.0205±0.010			
V	0.0220±0.007			
$R_{\rm C}$	0.0213±0.010			
$I_{\rm C}$	0.0169±0.013			

Dips in the color curves at phase 0.0 and rises at 0.5 indicate the system is semidetached with the primary filling its Roche-lobe(s) and the sceondary underfilling (as we view the cooler back parts of the Roche-lobe(s)).

The U, B, V, $R_{\rm C}$, $I_{\rm C}$ light curves were hand modeled with Binary Maker 3.0 (Bradstreet et Steelman 2002). Averaged values of parameters were then entered into the Wilson-Devinney program; Wilson, 1990, 1994; Van Hamme and Wilson, 1998). From these we ran a full $UBVR_{\rm C}I_{\rm C}$ simultaneous solution. A mass ratio search covering regions from 0.25 to 1.9 was performed which indicated the value minimizes near ∼0.7, however there is a fairly broad area of low residual values from 0.5 to about 1.3, so the minimized q value is somewhat in doubt (see Figure 6). The full synthetic light curve solution is given in Tables 8 and 9. The temperature of the primary component (6250±500K, F8±6V spectral type, Cox 2000) which we used to model our light curves, was taken from recent 2MASS B−V, J−H color indices. The light curve solutions are shown in Figure 7 and 8. where the solution is overlying the normalized flux light curves. The Roche lobe surfaces arising from the calculation are displayed by quadratures in Figures 9-12.

Table 8. Synthetic curve parameters for Mis V1287

Parameters	Values
l_U, l_B, l_V, l_R, l_I (nm)	360, 440, 550, 640, 790
$xbol_{1,2}$, $ybol_{1,2}$	0.644, 0.643, 0.231, 0.160
$x_{1I,2I}$, $y_{1I,2I}$	0.572, 0.647, 0.267, 0.183
$x_{1R,2R}$, $y_{1R,2R}$	0.655, 0.735, 0.278, 0.165
$x_{1V,2V}$, $y_{1V,2V}$	0.728, 0.797, 0.269, 0.108
$x_{1B,2B}$, $y_{1B,2B}$	0.817, 0.853, 0.215, −0.018
$x_{1U,2U}$, $y_{1U,2U}$	0.859, 0.855, 0.208, −0.209
g_1 =g_2	0.32
A_1 =A_2	0.5
Inclination (°)	69.18±0.03
T_1, T_2 (K)	6250±500, 4982±1
Ω_1, Ω_2	3.267, 3.273±0.001
$q(m_2/m_1)$	0.7133±0.0005
Fill-outs: F_1, F_2	100%, 99.8%
$L1/(L1+L2)_I$	0.752±0.001
$L1/(L1+L2)_R$	0.7845±0.0005
$L1/(L1+L2)_V$	0.8112±0.0005
$L1/(L1+L2)_B$	0.8521±0.0006
$L1/(L1+L2)_U$	0.9092±0.0004
JD_0 (days)	2 455 098.8785±0.0001
Period (days)	0.7644±0.0001
r_1, r_2(pole)	0.384±0.002, 0.327±0.003
r_1, r_2(point)	0.534±0.002, 0.443±0.023
r_1, r_2(side)	0.406±0.002, 0.342±0.003
r_1, r_2(back)	0.435±0.003, 0.374±0.005

$\sum(W \times Res^2) = 2.713610$

All errors are formal, here the error in T2 is in relation to T1. We expect errors to T_1 to be on the order of ∼500K.

Table 9. Spot Parameters

STAR 1 (Cool Spot)	
Colatitude (°)	88.3±0.2
Longitude (°)	87.5±0.6
Spot radius (°)	15.6±0.01
Spot T-factor	0.673±0.009
STAR 1 (Cool Spot)	
Colatitude (°)	29.7±0.6
Longitude (°)	255.1±0.5
Spot radius (°)	15.44±0.06
Spot T-factor	0.50±0.05
STAR 2 (Hot Spot)	
Colatitude (°)	107.8±0.6
Longitude (°)	8.3±1.0
Spot radius (°)	16.2±0.2
Spot T-factor	1.286±0.007

Our model shows Mis V1287 is a semidetached, near contact binary with a mass ratio of ∼0.7. The system parameters from our model include a temperature difference of ∼1250 K, Roche lobe fill-outs of 100% and 99.8% (ratio of actual to the critical potential) for the primary and secondary components, respectively calculated by potentials. This means that the binary is very near contact. Three spots were needed to model the light curve asymmetries. Two are due to solar type activity and one is probably a stream spot since it modeled near colatitude 90°. (The presence of other spots would change the light center of the modeled hot spot.) Our photometry reveals that the secondary component is early main sequence K-type. Since it is of solar type, we expect this system will eventually become a W UMa contact binary. Thus, this is a coming-into-contact W UMa system, a rare V1010 Oph binary. The process of coalescence is believed to be magnetic braking due to stellar winds leaving the system via stiff dipole magnetic field lines. It is noted that this precess may undergo some oscillations in and out of contact until permanent contact is achieved (Csizmadia and Klagyivik 2004).

Finally, spectral identification and radial velocities are needed to confirm the mass ratios and absolute parameters of the system and to confirm the spectral type of the components.

We wish to thank Lowell Observatory for their allocation of observing time, and the American Astronomical Society and the Arizona Space Grant for travel support for this observing run.

References:

Bradstreet, D. H., Steelman, D. P., 2002, *AAS*, **201** 7502
Csizmadia, Sz., Klagyivik, P., 2004, *A&A*, **426**, 1001
Cox, A. N., ed. 2000, Allen's Astrophysical Quantities (4th ed.; New York: Springer).
Nakajima, K. Yoshida, S., Ohkura, N., 2006, *IBVS*, **5700**
Van Hamme, W. V., Wilson, R.E 1998, *BAAS*, **30**, 1402
Wilson, R. E. & Devinney, E. J. 1971, *ApJ*, **166**, 605
Wilson, R. E. 1990, *ApJ*, **356**, 613
Wilson, R. E. 1994, *PASP*, **106**, 921

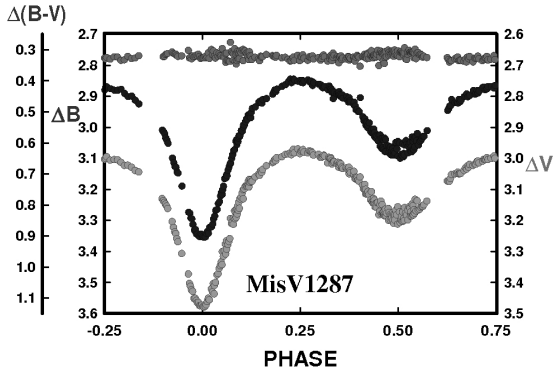

Figure 4. B, V delta magnitude and color magnitudes vs. phase plots in the sense of V−C.

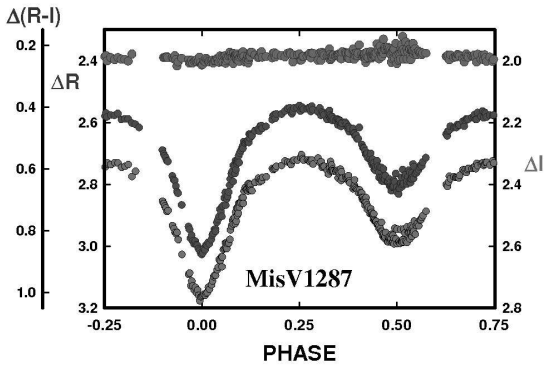

Figure 5. R, I delta magnitude and color magnitudes vs. phase plots in the sense of V−C.

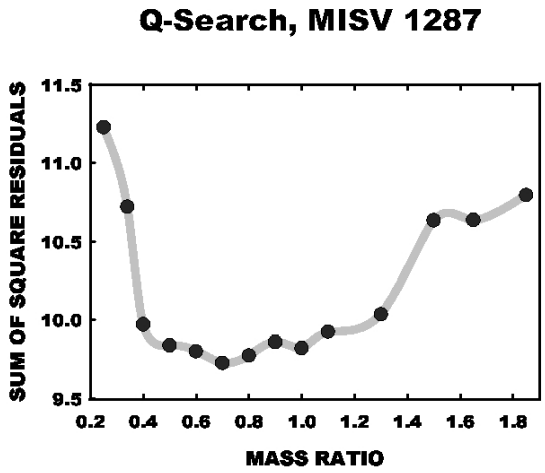

Figure 6. Mass ratio (q) search to determine the lowest residual value.

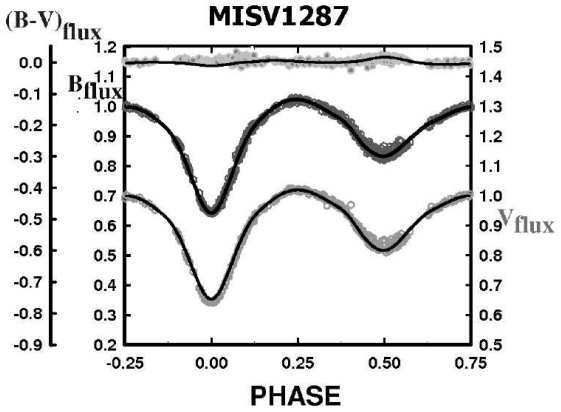

Figure 7. B,V normalized flux curves and the synthetic light curve solutions.

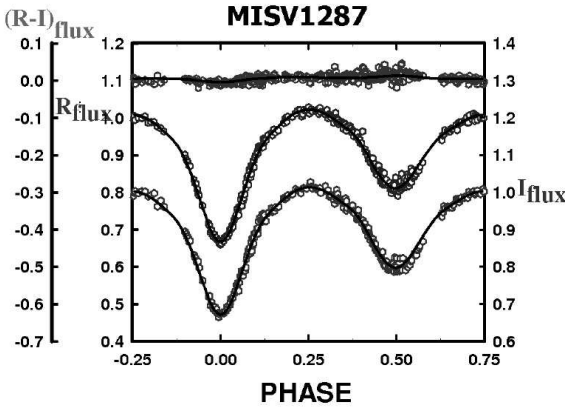

Figure 8. R,I normalized flux curves and the synthetic light curve solutions.

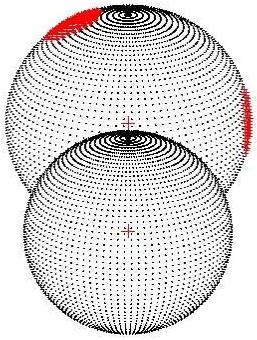

Figure 9. Roche lobe surfaces from our BVRI solution, phase 0.00 (the primary eclipse).

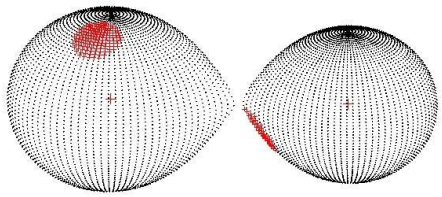

Figure 10. Roche lobe surfaces from our BVRI solution, phase 0.24.

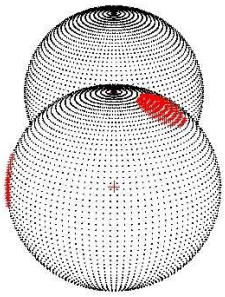

Figure 11. Roche lobe surfaces from our BVRI solution, phase 0.50 (the secondary eclipse).

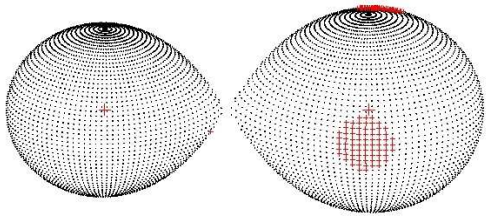

Figure 12. Roche lobe surfaces from our BVRI solution, phase 0.75.

ERRATUM FOR IBVS 6035

n the article appeared originally, author Smith, Paul M. was erroneously given as Samec, Paul M.

The Author

*This version of the paper contains corrections, and differs from the one appeared on-line originally. Date of last modification: Wed Sep 19 09:22:55 CEST 2012

COMMISSIONS 27 AND 42 OF THE IAU
INFORMATION BULLETIN ON VARIABLE STARS

Number 6036

Konkoly Observatory
Budapest
17 September 2012

HU ISSN 0374 – 0676

FIRST SOLUTION OF THE LIGHT CURVE OF THE NEW VARIABLE STAR 3UC 281-203711

GORDA, S.YU.; SOBOLEV, A.M.

Astronomical Observatory, Ural Federal University, 19 Mira st., Ekaterinburg, 620002, Russia
E-mail: stanislav.gorda@usu.ru

A new variable star 3UC 281-203711 $V = 12\overset{m}{.}4$ was discovered during monitoring of the young irregular variable V645 Cyg at the Astronomical Observatory of the Ural Federal University (Gorda & Sobolev, 2011: GS2011). The first brightness decrease of 3UC 281-203711 by $0\overset{m}{.}08$ was registered on JD 2454966.30. The finding chart and the data table are presented in GS2011. Coordinates of the target, comparison and check stars are given in Table 1 of the current paper.

The AZT-3 reflector (D = 0.45m, F_{Newton} = 2.0 m) with an Alta-U6 CCD camera (Kodak KAF-1001E, 1048x1048, 24-micron chip) was used. The photometry was carried out using the V and R Cousins/Bessell filters. The uncertainty of our brightness measurements during individual nights was within $\pm 0\overset{m}{.}003$ – $\pm 0\overset{m}{.}007$, as estimated by the brightness difference between the comparison star 3UC 281-203713 and the check star 3UC 281-203646. The reduction of the CCD frames was carried out using *Muniwin* software.

Time of minimum $HJDI_{min}$ = 2455543.1338 was calculated from observations of one completely covered primary minimum, namely part of the light curve prior to the eclipse, descending branch, whole bottom plateau and a considerable part of the ascending branch. Preliminary estimate of the period given in GS2011 was based on the observational data covering parts of the primary minimum: four descending branches complemented with small parts of the bottom plateau (brightness decrease by $0\overset{m}{.}08$) and two parts of the bottom plateau complemented with ascending branches (brightness increase by the same amount).

3UC 281-203711 is an eclipsing system. The light curve is of Algol type and manifests pronounced ellipsoidal effects. The primary minimum is not so deep but is much deeper than the secondary minimum. The mean depths of the minima are about the same in both colours and equal to $0\overset{m}{.}103$ and $0\overset{m}{.}030$ for the primary and secondary minima, respectively. A plateau is observed in the bottom of the primary minimum, indicating that one of the eclipses is total GS2011, Fig. 1, bottom panel).

Photometric reduction of CCD frames using *Muniwin* package was carried out prior to the solution of the lights curves. The results differ within observational uncertainties from the ones given in GS2011, which were obtained using the *MaxIM DL* package. For the majority of observational points the difference between the values computed using the two packages did not exceed $0\overset{m}{.}003$. But for the data obtained in filter V during the nights

JD 2454965 and JD 2455127 these differences were systematic and reached the values about $0\overset{m}{.}01 - 0\overset{m}{.}02$. For solutions of the light curves we used almost the same data as provided in GS2011. Data on the two nights mentioned above were an exception because they have shown better correspondence with the data for the same photometric phases obtained during other nights. Altered data points are provided in (electronic) Tables 4 and 5.

A solution of the light curve was carried out with the *PHOEBE* package with a graphic interface for Windows. Realizations of the Wilson-Devinney light curve analysis method and of the Nelder-Mead simplex method for search of the optimum solution from this package were used.

Nothing was known about the physical nature of components of this eclipsing binary system. Hence, the initial values of physical parameters were chosen on the basis of values of the period, surface brightness ratio, ratio of the radii of components and their relative sizes. These values were defined from the form, depth and duration of the primary minimum under the hypothesis of a total eclipse. Initial values of the temperatures corresponding to spectral class F0 were chosen. Estimate of the spectral class is based on the values of 3UC 281-203711 brightness in the optical and infrared ranges taken from the *NOMAD* catalog. Initial values of the mass ratio of the components and the semi-major axis of the orbit were chosen by assuming that both components belong to the main sequence.

Determination of the orbital elements and the physical parameters of the components were carried out with simultaneous use of the data in both V and R filters. As a result of the preliminary solution it was established that the total eclipse occurs in the secondary minimum which is not deep. During the primary minimum the smaller and cooler star passes in front of the bigger and hotter component, being completely projected on its surface at the moments of time close to the middle of the eclipse.

Calculation of the physical parameters of the system with the *PHOEBE* package requires knowledge of the value of semi-major axis of the mutual orbit, a. This value does not influence the light curve and, hence, cannot be estimated from our data. For the current analysis we adopted the value $a = 9R_{\odot}$ (see consideration of the physical meaning of this value below).

Further, the calculation of the physical parameters of the system requires the knowledge of the value of another parameter - the mass ratio of the components, q. This parameter only weakly influences the form of the light curve and requires special efforts for its determination. A number of solutions were obtained for a set of given values of $q = 0.2, 0.3, ..., 0.8$. The other parameters remained free. It was found that the theoretical light curves do not show considerable (i.e. exceeding observational uncertainties) systematic deviations from the observational points by changing only the values of q within the interval $0.3 - 0.6$. Calculations with released parameter of q showed that the values $q \sim 0.5$ provide the best fit.

A criterion of proximity of the values of effective temperatures, masses and radii of components to the values of corresponding parameters of the main sequence stars was applied in order to choose the admissible values for the semi-major axis of the eclipsing system, a.

It was found that the values of a in the range $8R_{\odot} - 10R_{\odot}$ bring the parameters of the secondary component (mass, radius, effective temperature) into close agreement with a main sequence star of spectral class K0 – K3. Therefore we assume that the value of the semi-major axis for the 3UC 281-203711 eclipsing binary is $a \sim 9R_{\odot}$.

At the same time, there are no values of a leading to overall agreement between the

physical parameters of the primary component. Estimates of the spectral class vary in the range A0 − F0, depending on the physical parameter (mass or temperature) used for the estimate. The values of the radius for the given mass and temperature are too high in all cases. Most likely, this reflects that the star does not belong to the main sequence: it is possibly a subgiant or starts its transformation to become a subgiant.

Values of the photometric parameters and absolute values of the parameters for 3UC 281-203646 components with adopted value of $a = 9R_{\odot}$ are given in Tables 2 and 3, respectively. Accuracy of the parameter estimates for light curve solutions reflects scatter for a and q in the ranges $8 - 10$ and $0.4 - 0.6$, respectively.

More accurate value of the period for this eclipsing system was obtained in the course of solution of the light curve. The new ephemeris is the following:

$$\begin{array}{rcccc} HJDI_{min} & = & 2454966.4565 & + & 1\overset{\mathrm{d}}{.}948234 \cdot E. \\ & & \pm 8 & & \pm 11 \end{array}$$

In Figure 1 light curves (observational points and theoretical curves) are shown for V and R filters, respectively. In Figure 2 residual values versus photometric phases are shown.

Observational light curves are fitted by the theoretical curves quite well. This is seen in the residual plots which do not show significant systematic deviations in either passbands. The brighter and more massive component has a considerable tidal deformation. This follows from the well pronounced maxima of brightness in phases 0.25 and 0.75. It can be caused by rather high values of the radius and of the component mass ratio, $q \sim 0.5$.

Figure 2 (the bottom curve) shows that the color index of the system does not vary with phase within observational accuracy. It finds natural explanation in the fact that both ratios of the sizes and the surface brightness of the primary and the secondary components are high ($r_1/r_2 \sim 4$ and $j_1/j_2 \sim 16$, see Table 1) and the luminosity of the primary component exceeds that of the secondary component more than 200 times.

Quality of the observational data and existence of the total eclipse in the system allowed obtaining estimates of the relative photometric elements with small uncertainties. At the same time absolute parameters were found with relatively high uncertainties. This comes from the low accuracy of the value of semi-major axis of the orbit which can be improved only by spectroscopic observations.

Figure 3 shows the configuration of the system corresponding to our solution. It is seen that neither components of the 3UC 281-203711 fills its Roche lobe. Hence, this system is a completely detached eclipsing binary. The primary component is probably a subgiant, hence, it is likely to fill in its Roche lobe in the future. In this case, after the start of the mass exchange phase the value of q will increase and the system can become a reverse Algol.

Authors would like to thank the referee Dr. T. Borkovits for useful suggestions and comments which improved this paper. The study was partly supported by the Russian federal task program “Research and operations on priority directions of development of the science and technology complex of Russia for 2007-2012” (state contract No. 16.518.11.7074).

Reference:

Gorda, S.Yu., Sobolev, A.M., 2011, *Peremennye Zvezdy Prilozhenie*, **11**, 19 (GS2011)

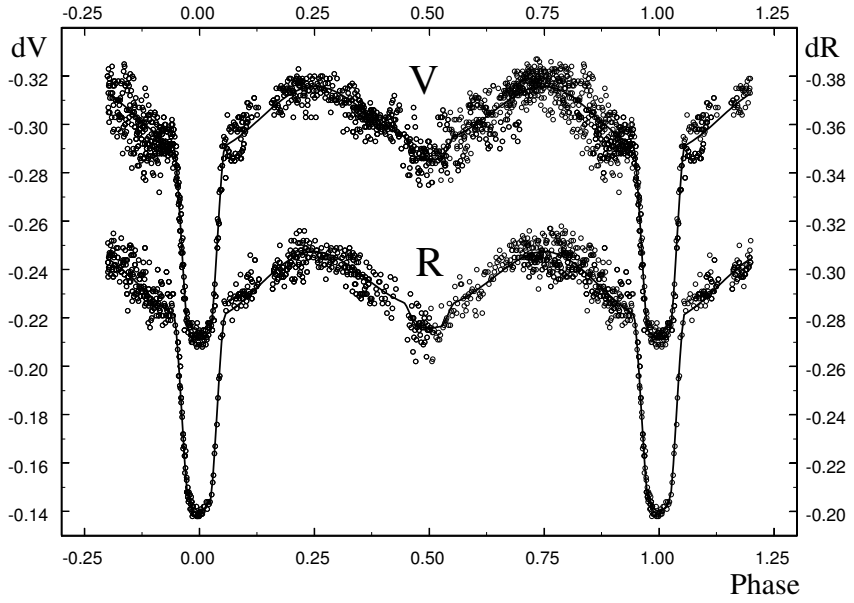

Figure 1. Theoretical (solid line) and observational (open circles) light curves of 3UC 281-203711

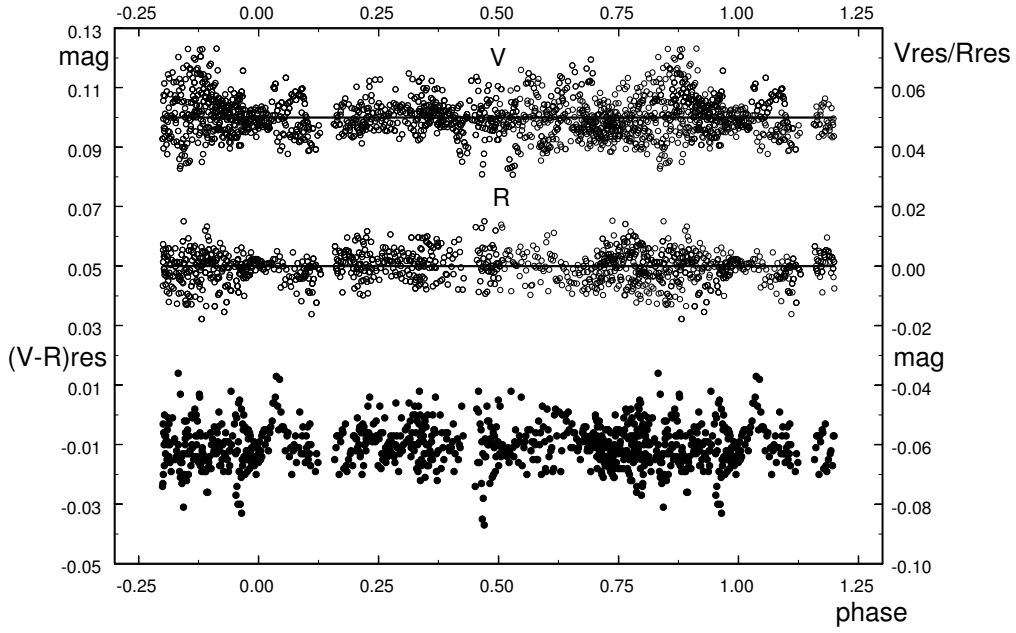

Figure 2. Model fitting residuals for the light curves and color index curve of 3UC 281-203711. The residuals for filter V are shifted up by $0\overset{\mathrm{m}}{.}05$.

Table 1. Designations and coordinates of the stars

Name	$\alpha(2000)$	$\delta(2000)$	m_V
3UC 281-203711 (variable)	$21^{\rm h}39^{\rm m}52\overset{\rm s}{.}4$	$+50°18'27''$	$12\overset{\rm m}{.}40$
3UC 281-203713 (comparison)	$21^{\rm h}39^{\rm m}52\overset{\rm s}{.}4$	$+50°15'55''$	$12\overset{\rm m}{.}60$
3UC 281-203646 (check)	$21^{\rm h}39^{\rm m}47\overset{\rm s}{.}6$	$+50°17'03''$	$12\overset{\rm m}{.}22$

Table 2. Photometric parameters of the eclipsing variable star 3UC 281-203711.

k	0.257 ± 0.010	i	$81\overset{\circ}{.}2 \pm 0\overset{\circ}{.}5$
r_1	0.294 ± 0.008	q	0.49 ± 0.11
$r_{1(pole)}$	0.289	j_1/j_2	15.8 ± 1.4
$r_{1(point)}$	0.302	L_1	0.996 ± 0.001
$r_{1(side)}$	0.294	L_2	0.004 ± 0.001
$r_{1(back)}$	0.299		
r_2	0.076 ± 0.002		

Table 3. Estimates of absolute parameters of the eclipsing variable star 3UC 281-203711

$a\,(R_\odot)$	9.0 ± 1.0	$R_1\,(R_\odot)$	2.65 ± 0.30
$T_{eff1}\,(K)$	9800 ± 100	$R_2\,(R_\odot)$	0.68 ± 0.08
$T_{eff2}\,(K)$	4900 ± 80	$L_1\,(L_\odot)$	21.85 ± 0.08
$M_1\,(M_\odot)$	1.74 ± 0.57	$L_2\,(L_\odot)$	0.09 ± 0.02
$M_2\,(M_\odot)$	0.85 ± 0.28		

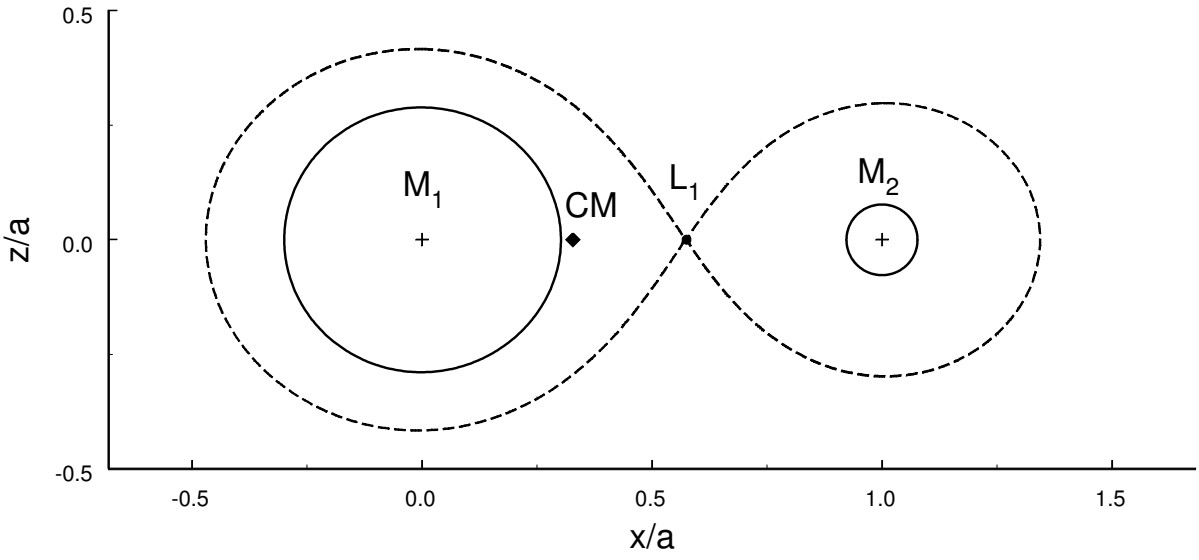

Figure 3. Configuration of the system 3UC 281-203711 in the polar plane corresponding to the light curve solution. Plus signs mark centers of mass of the stars; solid lines show surfaces of the stars; dashed line shows Roche lobes; dot shows L_1 point; filled diamond shows center of mass of the system

COMMISSIONS 27 AND 42 OF THE IAU
INFORMATION BULLETIN ON VARIABLE STARS

Number 6037

Konkoly Observatory
Budapest
26 September 2012

HU ISSN 0374 – 0676

NEW VARIABLE STARS IN THE GLOBULAR CLUSTER NGC 5694

RODRIGUES DE ANDRADE, L.[1,2,3]; CATELAN, M.[1,3]; SMITH, H. A.[4]

[1] Departamento de Astronomía y Astrofísica, Facultad de Física, Pontifícia Universidad Católica de Chile, Av. Vicuña Mackenna 4860, 782-0436 Macul, Santiago, Chile; e-mail: mcatelan@astro.puc.cl

[2] Departamento de Astronomía, Universidad de Chile. Santiago, Chile; e-mail: lrodrigu@das.uchile.cl

[3] The Milky Way Millennium Nucleus, Av. Vicuña Mackenna 4860, 782-0436 Macul, Santiago, Chile

[4] Dept. of Physics and Astronomy, Michigan State University, East Lansing, MI 48824, USA; e-mail: smith@pa.msu.edu

NGC 5694 (RA 14h39m36s, DEC $-26\,^{\circ}32'18''$, J2000) is a metal-poor ([Fe/H] $= -1.98$) globular cluster in the outer Galactic halo, at a Galactocentric distance of 29.4 kpc and a distance of 35.0 kpc from the Sun (quantities from Harris 1996, Dec. 2010 update). Ortolani & Gratton (1990) presented deep ($V \simeq 24$) CCD photometry for NGC 5694 and a (V, $B-V$) color-magnitude diagram (CMD) that shows an almost nonexistent red horizontal branch (HB) and a well-populated blue HB, which does not extend redward very far into the instability strip. This CMD morphology is confirmed in the *Hubble Space Telescope* snapshot study of Piotto et al. (2002). Hazen (1996) presented a search for variable stars in NGC 5694, using photographic plates, and found no candidates.

Lee et al. (2006) performed a chemical abundance analysis of one RGB star in NGC 5694, and found that the cluster has a very distinctive elemental abundance pattern, similar in some respects to those of nearby dwarf spheroidal (Sph) galaxies. This could mean that NGC 5694 has once been associated with a (currently unidentified) dwarf galaxy. Recent work by Correnti et al. (2011) reported the discovery of an extended stellar halo surrounding NGC 5694, based on deep ($V \simeq 24.5$) wide-field photometry with VIMOS-VLT. They were unable to draw a firm conclusion about the origin of this stellar halo, but suggested that NGC 5694 may indeed be the remnant of a disrupted dwarf satellite.

Given all the evidence for a possible extragalactic origin for NGC 5694, the analysis of this cluster in terms of the Oosterhoff (1939, 1944) argument is potentially relevant (Catelan 2009): is it an Oosterhoff-intermediate cluster, as commonly found in globulars that belong to the Milky Way's dSph satellites? Or can it instead be classified into an Oosterhoff type I or II, as is typically the case among bona-fide Galactic globulars?

In this note, we present the results of a search for variable stars in NGC 5694, and report on the discovery of 15 variable stars candidates in the cluster, including 3 RR Lyrae stars.

Our work is based on three sets of BVI observations, obtained with the SMARTS Consortium telescopes at Cerro Tololo Interamerican Observatory (CTIO). The first dataset was obtained in 44 service mode observations, between June 30 and August 3, 2007, with

the 1.3m telescope, comprising a total of 41, 43, and 44 images in B, V, and I, respectively. The second dataset was obtained in the course of 4 nights, between June 30 and July 23, 2007, with the 0.9m telescope, comprising a total of 5 images per filter. The third dataset was again obtained in the course of 4 nights, between January 10 and 14, 2010, with the 1.0m telescope, comprising a total of 6 images per filter.

To search for variability in our data, we used the image subtraction technique with the package ISIS v2.2 (Alard & Lupton 1998; Alard 2000), only on the 1.3m images, since there were not enough images from the other telescopes.

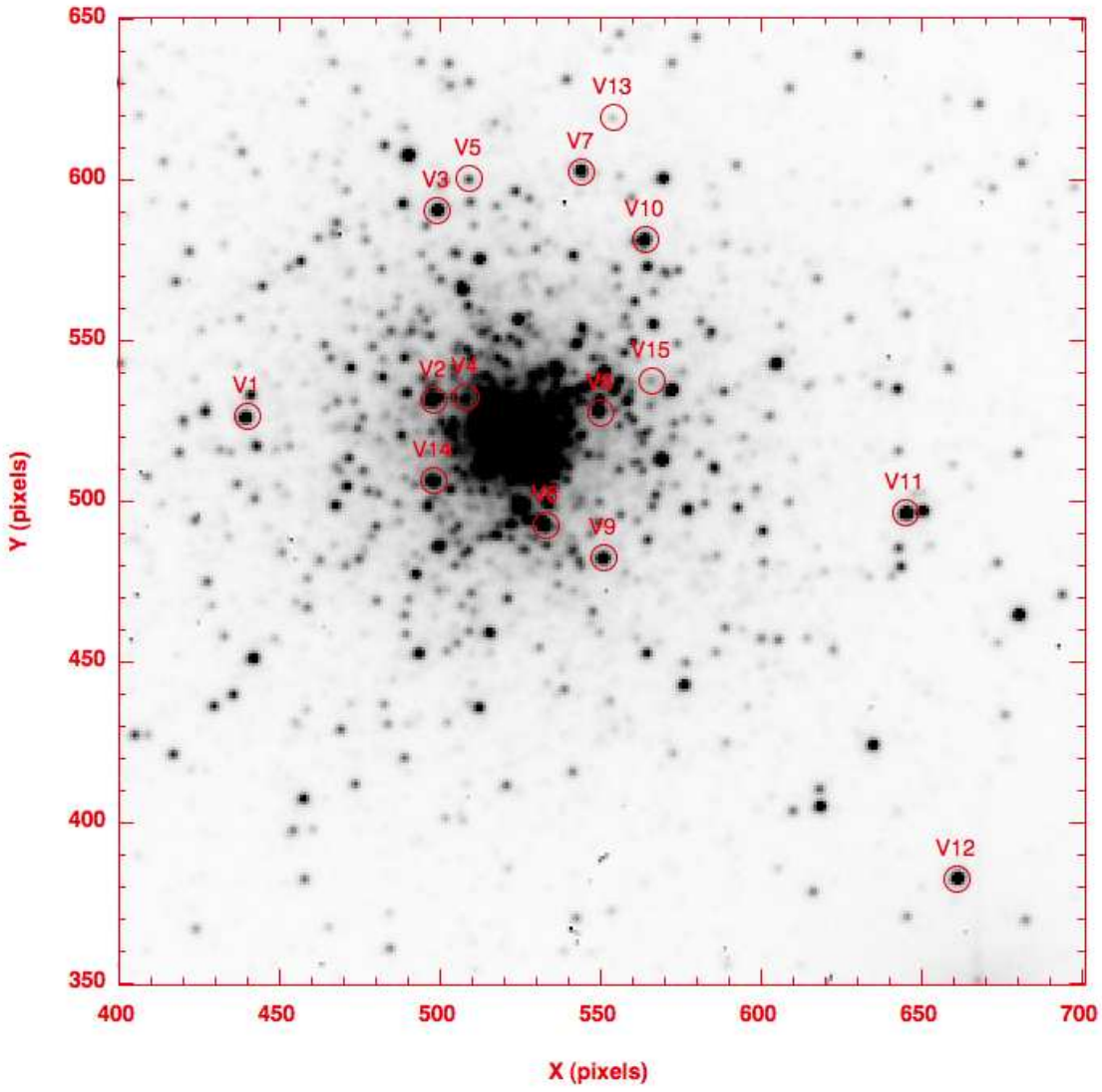

Figure 1. Finding chart for the variable star candidates in NGC 5694. North is up and East is to the right. The plate scale is 0.371 arcsec/pixel.

We also performed PSF photometry on these data, using the DAOPHOT package (Stetson 1987) in IRAF.[1] This photometry was used to construct a CMD, generate independent light curves (using the coordinates of the variable stars generated by ISIS),

[1]IRAF is distributed by the National Optical Astronomy Observatories, which are operated by the Association of Universities for Research in Astronomy, Inc., under cooperative agreement with the National Science Foundation.

and calibrate the ISIS light curves into standard magnitudes. DAOPHOT also enabled us to incorporate the images obtained with the 0.9m and 1.0m telescopes into our final light curves. We used the Stetson (2000) photometric standard field to perform the photometric calibration of the B and V data. Since there is no standard field available for NGC 5694 in the I filter, we could not calibrate the I-band data. The astrometry of our images was also done using the Stetson standards.

In our work, we found 15 variable star candidates, listed in Table 1 with their coordinates, intensity-weighted mean B and V magnitudes and possible period and variability type. Their positions in the cluster are shown in Figure 1, and our preliminary CMD with the variable candidates highlighted is given in Figure 2. B- or V-band light curves for all candidates are shown in Figure 3. For V15, the second faintest star in our sample, we were not able to calibrate the ISIS light curves. The star was detected with DAOPHOT on only 3 images, and ISIS only detected its variability in the V-band. For the same reason, the magnitudes and colors of V15 listed in Table 1 are not an average over the whole curve, and its position in the CMD is not very precise.

Table 1. Variable star candidates in NGC 5694.

Name	RA	DEC (J2000)	$\langle B \rangle$	$\langle V \rangle$	$\langle B \rangle - \langle V \rangle$	Period (d)	Type
V1	14:39:38.68	-26:32:19.14	17.118	15.781	1.338	21.3	LPV
V2	14:39:37.08	-26:32:16.50	16.528	15.365	1.163		SR
V3	14:39:37.08	-26:31:54.51	17.074	15.730	1.343		SR
V4	14:39:36.79	-26:32:16.25	17.775	17.393	0.382	0.393	RRc
V5	14:39:36.82	-26:31:50.89	18.899	18.570	0.329	0.6342?	RRab?
						0.3878?	RRc?
						0.2792?	RRc?
						0.2182?	RRe?
V6	14:39:36.09	-26:32:30.53	16.490	15.282	1.208		SR/LPV
V7	14:39:35.86	-26:31:49.46	17.249	16.163	1.085		LPV
V8	14:39:35.65	-26:32:17.18	16.858	15.755	1.104		SR/LPV
V9	14:39:35.58	-26:32:34.19	16.977	15.670	1.306		SR/LPV
V10	14:39:35.30	-26:31:57.20	16.929	15.516	1.413		SR/LPV
V11	14:39:32.98	-26:32:27.92	16.597	15.724	0.873	4.153	BL Her
V12	14:39:32.45	-26:33:09.89	17.002	15.589	1.413		SR
V13	14:39:35.61	-26:31:43.30	20.031	19.284	0.747	0.37	EB?
V14	14:39:37.05	-26:32:25.87	16.810	15.771	1.039		SR
V15	14:39:35.22	-26:32:13.50	19.256	19.133	0.122	0.265	RRc?

V5 is a particularly interesting star, as we have found at least four periods which may phase the available data, as shown in Table 1. Irrespective of the adopted period, the shape of the light curve seems nearly sinusoidal, which would be more consistent with a c-type RR Lyrae. However, the least noisy light curve is obtained with a period around 0.634 d, which is more typical of ab-type RR Lyrae. The light curve amplitudes can help with the classification. However, while for most of our stars the amplitudes obtained on the basis of DAOPHOT and ISIS are consistent, this is not so in the case of V5, for which we find a smaller amplitude in the B band with ISIS than with DAOPHOT. This may be due to a calibration problem. If the amplitude is really close to 1 mag in B, as ISIS suggests, that might be more consistent with an RRab than an RRc. On the other hand, the smaller DAOPHOT amplitudes in this filter (and also in the V data) suggest an RRc (or even an RRe) instead. Clearly, the photometry and calibration of this star must be revisited in future work, but meanwhile it seems almost certain that the star is indeed an RR Lyrae. The period used to plot its light curve in Figure 3 is 0.3876 d.

As for V1, although the data suggest low-amplitude variability with a 21.3 d period,

this needs confirming because it would be unusually short for a variable near the tip of the red giant branch (RGB).

The presence of a candidate short-period type II Cepheid, V11, is also worth noting. Type II Cepheids are typically found in systems with blue HB morphologies (see §4.2 in Catelan 2009 for a recent review). It is unclear why this star was not detected in previous studies, especially in view of the fact that it is not located near the cluster core (Fig. 1). In this sense, it should be noted that the light curves for the star in the other passbands are significantly noisier than the one in the B band that is shown in Figure 3.

As for V13, it is a possible eclipsing binary (EB) with a 0.37 d period. However, its location in the CMD indicates a star starting to ascend the RGB, and a period of 0.37 d may be a problem for an eclipsing star where at least the brighter member is a red giant. Since the eclipser classification mainly depends on two low points, more and better data will be needed in order to properly classify this star.

Unfortunately, NGC 5694 turns out to be an intrinsically very RR Lyrae-poor cluster, and so it is impossible to properly classify the cluster in terms of an Oosterhoff status.

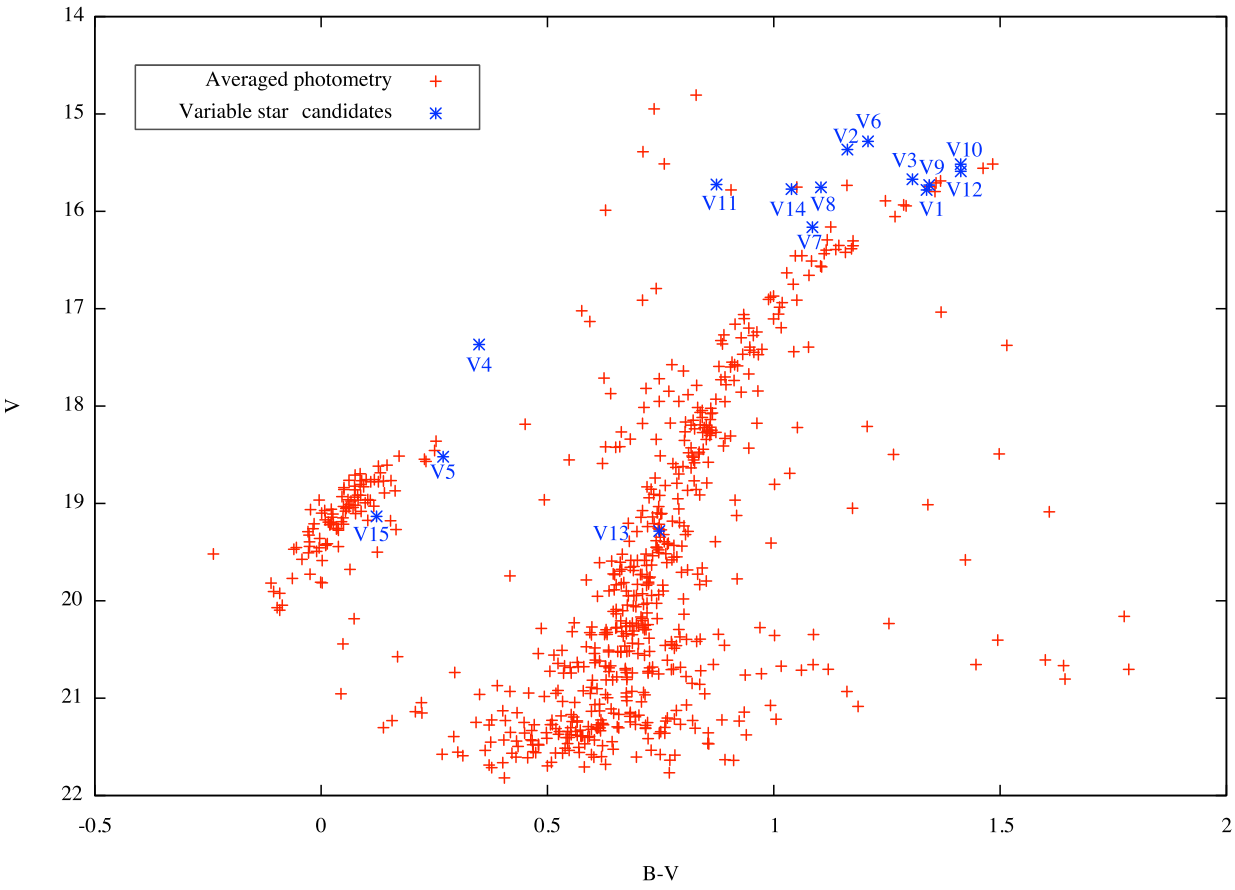

Figure 2. The NGC 5694 CMD, with the positions of the variable star candidates shown as asterisks.

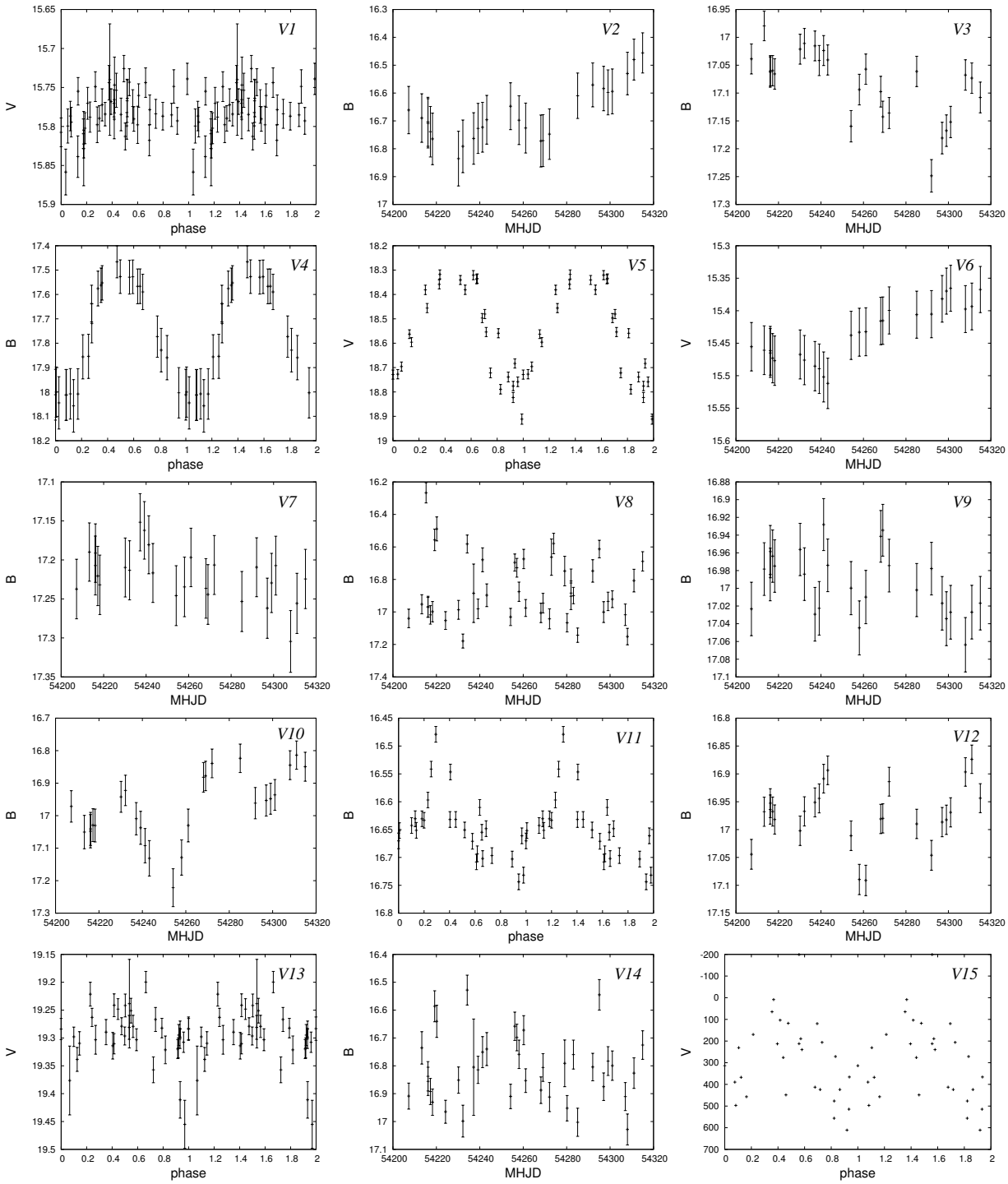

Figure 3. *B*- or *V*-band light curves of the NGC 5694 variable star candidates V1–V15. For V15, for which magnitudes could not be obtained, the y-axis scale corresponds to relative ISIS fluxes.

Acknowledgments: We thank P. Arriagada, C. Contreras, and P. Amigo for some useful discussions. Support for L.R. and M.C. is provided by the Ministry for the Economy, Development, and Tourism's Programa Inicativa Científica Milenio through grant P07-021-F, awarded to The Milky Way Millennium Nucleus; by Proyecto Basal PFB-06/2007; by Proyecto FONDECYT Regular #1110326; and by Proyecto Anillo ACT-86.

References:

Alard, C. 2000, *A&AS*, **144**, 363
Alard, C., & Lupton, R. H. 1998, *ApJ*, **503**, 325
Catelan, M. 2009, *Ap&SS*, **320**, 261
Correnti, M., Bellazzini, M., Dalessandro, E., Mucciarelli, A., Monaco, L., & Catelan, M. 2011, *MNRAS*, **417**, 2411
Harris, W. E. 1996, *AJ*, **112**, 1487
Hazen, M. L. 1996, *AJ*, **111**, 1184
Lee, J.-W., López-Morales, M., & Carney, B. W. 2006, *ApJ*, **646**, L119
Oosterhoff, P. T. 1939, *Observatory*, **62**, 104
Oosterhoff, P. T. 1944, *Bull. Astron. Inst. Neth.*, **10**, 55
Ortolani, S., & Gratton, R. 1990, *A&AS*, **82**, 71
Piotto, G., et al. 2002, *A&A*, **391**, 945
Stetson, P. B. 1987, *PASP*, **99**, 191
Stetson, P. B. 2000, *PASP*, **112**, 925

COMMISSIONS 27 AND 42 OF THE IAU
INFORMATION BULLETIN ON VARIABLE STARS

Number 6038

Konkoly Observatory
Budapest
29 October 2012

HU ISSN 0374 – 0676

FINAL CLASSIFICATION OF THE BRIGHT VARIABLE STAR WW CMa

SZABADOS, L.

Konkoly Observatory, Research Centre for Astronomy and Earth Sciences, Hungarian Academy of Sciences, H-1121 Budapest, Konkoly Thege M. str. 15-17. Hungary
email: szabados@konkoly.hu

The brightness variability of the star BD -21° 1424 was discovered by Hoffmeister (1933). This star preliminarily designated as 176.1932 was characterised with a short period in the discovery note. Florja (1937a) observed the star visually but his 42 brightness estimates obtained on 21 nights (in 1933 and 1935) were inconclusive: in Florja (1937b) he remarked 'that confirmation of variability is still required'. Parenago (1939), however, determined a period of 5.7660 days based on the analysis of Florja's visual data, and without explicitly stating that 176.1932 CMa is a Cepheid, the English translation of the Russian title of this communication (On the period of 15 Cepheids) implies this classification. Interestingly enough, Joy (1937) already included this variable among his sample in his seminal study of radial velocity of Cepheids in spite of the fact, that no hint at the Cepheid nature of this star was available in the literature at that time. Soon after, a new suggestion emerged: Kanda (1938) classified this star as an RR Lyrae type variable with a period of 0.499355 day.

The photographic magnitudes based on the Dushanbe (Stalinabad) plate archive, however, contradicted both period values (Erleksova, unpublished). Therefore, though the compilers of the first edition of the General Catalogue of Variable Stars classified this star (designated as WW Canis Maioris in the meantime) as a Cepheid variable characterised with Parenago's (1939) elements (Kukarkin & Parenago 1948), in the subsequent editions of the GCVS no definite type of variability has been assigned to this rather bright star, though the editors mention rapid variations in its brightness.

While it was classified among classical Cepheids, several studies involved WW CMa in the Cepheid sample investigated from statistical point of view. The first reliable photoelectric data published by Irwin (1961) were decisive: neither the shape, nor the amplitude resembled typical Cepheids, in addition, the $B-V$ colour index remains practically constant. The classification of this variable star as a Cepheid became untenable.

Decades later, new reliable photometric data became available thanks to the ASAS project (Pojmanski & Maciejewski 2004). The long and homogeneous observational series covering the interval 2000-2009 clearly indicated that WW CMa was originally misclassified. In fact, it is an eclipsing binary, as is correctly referred to in the ASAS on-line catalogue quoting an orbital period of 2.5163 days. This value was refined by Sebastian Otero who determined a period of 2.51636 days from the same data (VSX, 2010).

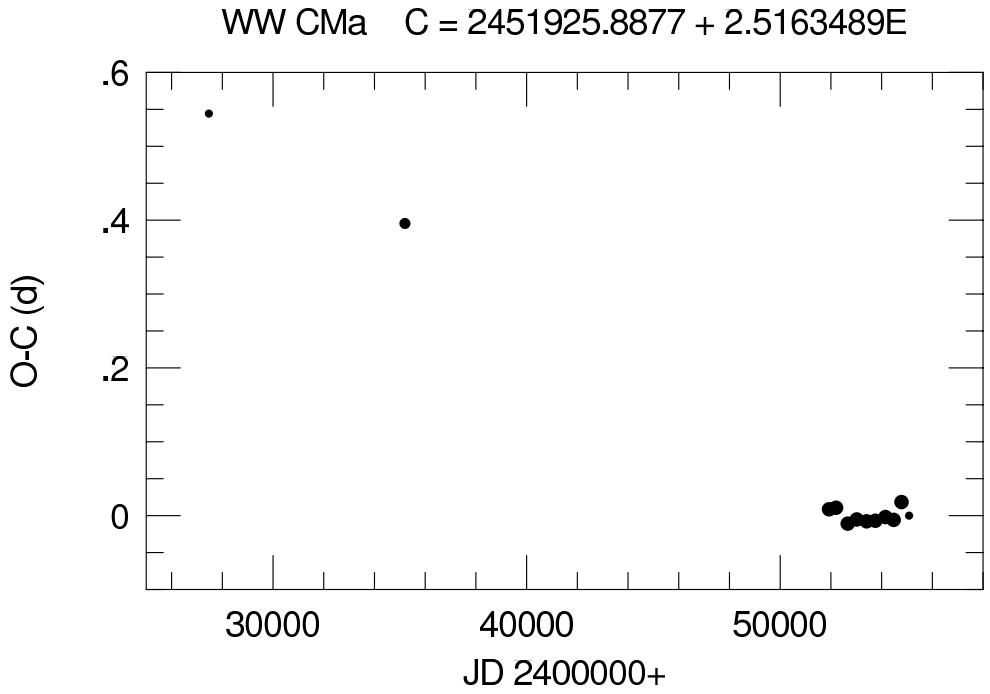

Figure 1. $O-C$ diagram of WW CMa

To facilitate the correct classification of this bright variable star, here I revise and improve the orbital period and discuss the available information on WW CMa. The early and the modern photometric data have been subjected to an $O-C$ analysis. The ASAS data provide a reliable normal light curve so the normal maxima for earlier data have been determined by fitting Florja's (1937a) and Irwin's (1961) observations to this normal curve. Moreover, the ASAS data have been divided into annual segments. The resulting moments of normal maxima, the epoch, the $O-C$ value and its weight in the least squares fit, as well as the source of the observations are listed in Table 1. The tabulated $O-C$ values have been calculated by using the ephemeris:

$$C = 2451925^{\rm d}.8877 + 2^{\rm d}.5163489E.$$

This period has been obtained by a least squares fit to the ASAS normal maxima. The $O-C$ diagram in Figure 1 clearly indicates that the orbital period of WW CMa is not stable on the time scale of decades: between JD 2430000 - JD 2450000 it was 2.5163 days, i.e., shorter than in the last decade. The pattern of the $O-C$ values cannot be approximated with a parabola implying a continuous period change, so the underlying physical mechanism causing the instability of the orbital period can be the episodic mass loss/exchange.

WW CMa was a target in the sample of ASAS eclipsing variables with the aim at searching for chromospheric activity (Parihar et al. 2009). They observed this binary star on JD 2 453 267 and did not find any chromospheric emission. In addition, Parihar et al. (2009) determined the spectral types of the components from the 2MASS colour indices of WW CMa ($J-H = 0.31$, $H-K = 0.08$, $V-J = 1.15$; Cutri et al. 2003). The resulting spectral types are: G0V+G6V, i.e., both components are nearly solar type stars.

Table 1: $O-C$ residuals of WW CMa

$JD_\odot$ 2 400 000 +	E	$O-C$ d	W	Data source
27470.0369	−9719	0.0603	1	Florja (1937a)
35200.1131	−6647	0.0629	2	Irwin (1961)
51925.8963	0	0.0000	3	ASAS
52205.2131	111	0.0075	3	ASAS
52663.1671	293	−0.0051	3	ASAS
53020.4943	435	0.0075	3	ASAS
53408.0095	589	0.0125	3	ASAS
53755.2665	727	0.0201	3	ASAS
54150.3382	884	0.0327	3	ASAS
54474.9434	1013	0.0352	3	ASAS
54784.4785	1136	0.0654	3	ASAS
55083.9056	1255	0.0528	1	ASAS

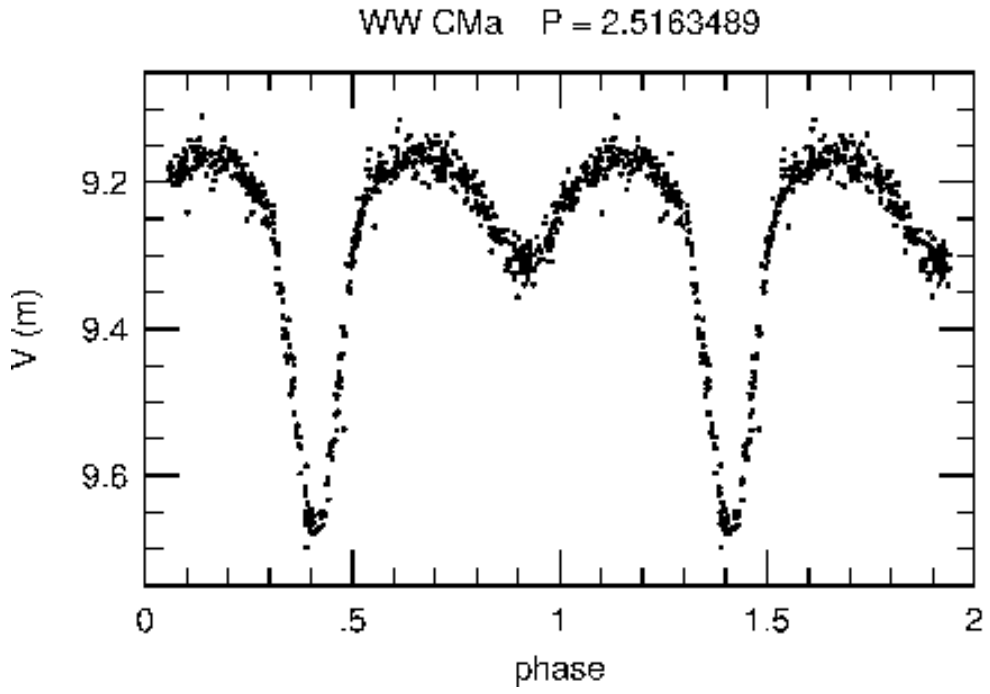

Figure 2. Photometric phase curve based on the ASAS data

The eclipsing light curve folded on the accurate period of 2.5163489 days is plotted in Fig. 2 based on the ASAS photometry (the outlying points have been omitted).

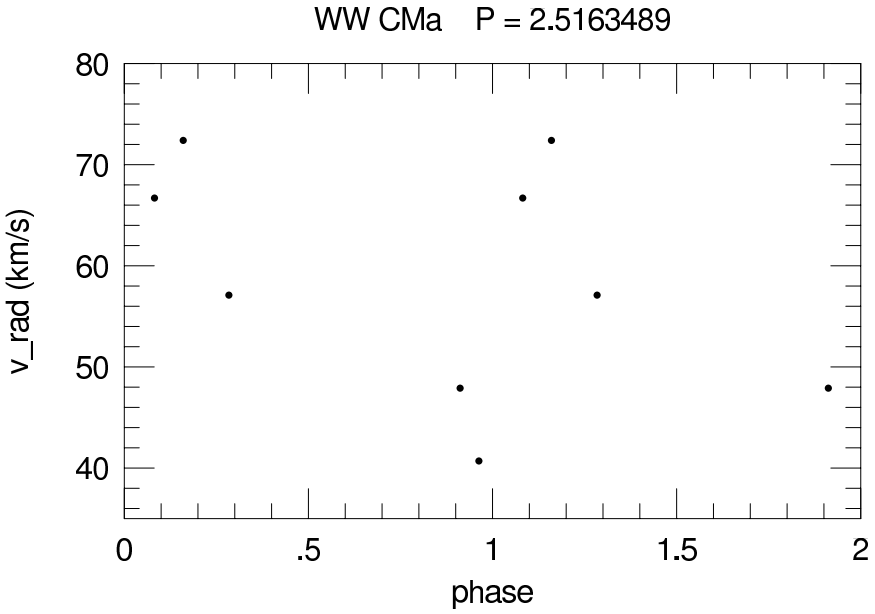

Figure 3. Radial velocity phase curve based on Joy's (1937) data

The radial velocity data published by Joy (1937) are plotted in Fig. 3. When plotting these data, the proper phase shift deduced from Fig. 1 has been taken into account but the same period was used for folding the data as for the photometric phase curve. The radial velocity phase curve is compatible with the orbital effect. However, a new series of accurate radial velocities is necessary to determine the orbital elements of this binary system formed by solar type stars.

This work has been supported by the ESTEC Contract No. 4000106398/12/NL/KML.

References:

Cutri R. M. et al. 2003, VizieR On-line Data Catalog: II/246
Florja N. F. 1937a, *Sternberg Publ.*, **8**, No. 2, 106
Florja N. F. 1937b, *Perem. Zvezdy*, **5**, 104
Hoffmeister C. 1933, *Astr. Nachr.*, **247**, 281
Irwin J. B. 1961, *ApJS*, **6**, 253
Joy A. H. 1937, *ApJ*, **86**, 363
Kanda S. 1938, *Tokyo Bull.*, **284**
Kukarkin B. V. & Parenago P. P. (eds.) 1948, General Catalogue of Variable Stars, 1st Edition, Moscow
Parenago P. P. 1939, *Perem. Zvezdy*, **5**, 280
Parihar P., Messina S., Bama P., Medhi B. J., Muneer S., Velu C., Ahmad A. 2009, *MNRAS*, **395**, 593
Pojmanski G. & Maciejewski G. 2004, *AcA*, **54**, 153
VSX 2010, http://www.aavso.org/vsx/index.php?view=detail.top&oid=5198

COMMISSIONS 27 AND 42 OF THE IAU
INFORMATION BULLETIN ON VARIABLE STARS

Number 6039

Konkoly Observatory
Budapest
15 November 2012

HU ISSN 0374 – 0676

MINIMA TIMES OF SOME ECLIPSING BINARY STARS

GÖKAY, G.; DEMİRCAN, Y.; GÜRSOYTRAK, H.; TERZİOĞLU, Z.; OKAN, A.; DOĞRUEL, M.B.; SARAL, G.; CERİT, S.; ŞEMUNİ, M.; KILIÇ, Y.; ÇOKER, D.; DERMAN, E.; GÜROL, B.

Ankara University Observatory, Faculty of Science, Astronomy and Space Sciences Department
06100, Tandoğan, Ankara, TÜRKİYE; e-mail: ggokay@science.ankara.edu.tr

Observatory and telescope:
16″ Schmidt/Cassegrain telescope at Ankara University Observatory

Detector:	Apogee ALTA U47+ back illuminated CCD camera, Peltier cooling, E2V CCD47−10 chip, 1024 × 1024 pixels.

Method of data reduction:
Reduction of the CCD frames was made with the IRAF[1] CCDRED and DAOPHOT packages.

Method of minimum determination:
The minima times were computed with several methods in Minima25b (Nelson, 2006): parabolic fit, tracing paper, bisectors of chords, Kwee and van Woerden method (Kwee & van Woerden, 1956), Fourier fit and sliding integrations technique. Then weighted mean minimum-time values were calculated for all filters used.

[1]IRAF is distributed by the National Optical Astronomical Observatories, operated by the Association of the Universities for Research in Astronomy, inc., under cooperative agreement with the National Science Foundation

Times of minima:					
Star name	Time of min. HJD 2400000+	Error	Type	Filter	Rem.
V546 And	55456.3647	0.0004	I	BVRI	GS
	55456.5558	0.0003	II	BVRI	GS
	55467.4721	0.0002	I	BVRI	YD−TO
BO Ari	55487.3294	0.0002	II	BVRI	GS−SS−GV
	55487.4889	0.0001	I	BVR	GS−SS−GV
	55509.4440	0.0008	I	BVRI	AO−SC−YŞ
	55528.3768	0.0000	II	BVRI	YD
	55551.2872	0.0001	II	BVRI	AO−YŞ−ND
	55553.1962	0.0001	II	BVRI	GS
AP Aur	55603.4537	0.0004	II	BVRI	GS−AY−CY
GS Boo	55328.5045	0.0031	II	BVRI	GS
	55330.3878	0.0003	I	BVRI	YD
HH Boo	55602.5508	0.0006	I	BVRI	BG−AO
	55609.4030	0.0010	II	BVRI	GG
	55637.4459	0.0006	II	BVRI	AY−MMK
	55645.4128	0.0002	II	BVRI	AY−GS
	55645.5708	0.0003	I	BVRI	AY−GS
	55647.4830	0.0005	I	BVRI	YD−TO−AK
	55648.4386	0.0012	I	BVRI	MSH−ZT−MAk
CD Cam	55372.3935	0.0022	I	VRI	GS
ASAS J013630+0150.3	55450.5883	0.0002	I	BVRI	GG−MSH−YK
GW Cnc	55502.5278	0.0000	I	BVRI	AO−SC−YŞ
	55508.5771	0.0001	II	BVRI	ZT−GV−MSH
	55515.6124	0.0002	II	BVRI	HG−GV−MSH
	55635.3537	0.0003	I	BVRI	AO−YŞ−ND
	55636.3383	0.0007	II	BVRI	GG−YK−MÖ
V1073 Cyg	55447.4114	0.0001	I	BVRI	GG−MD
V1918 Cyg	55468.5269	0.0007	I	BVRI	GG−YK−MSH
ASAS J202521+0425.5	55458.3026	0.0005	I	BVRI	YD
	55463.3044	0.0007	II	BVRI	GS
	55464.3567	0.0004	II	BVRI	AO−SC
GSC 4428−1574	55604.3181	0.0012	II	BVRI	GS−AY−CY
	55604.5627	0.0005	I	BVRI	GS−AY−CY
	55649.4931	0.0001	II	BVRI	AO−YŞ−ND
GV Leo	55599.5559	0.0005	II	BVRI	ZT−MSH−ZSŞ
GSC 3526−2369	55416.3474	0.0003	I	BVRI	YD
	55418.3287	0.0004	I	BVRI	UD
V566 Oph	55036.4336	0.0003	I	BVRI	ED
V407 Peg	55443.5811	0.0014	II	BVRI	AO−MD
	55459.5026	0.0005	II	BVRI	ZT−GV−MSH
GSC 2751−1007	55445.4778	0.0007	I	BVRI	UD−MD
	55448.4001	0.0004	I	BVRI	HG
	55449.4447	0.0007	II	BVRI	GS−MD
ASAS J225956+1418.2	55501.3022	0.0002	II	BVRI	ZT−MSH−SS
V1367 Tau	55528.5606	0.0003	I	VRI	YD
	55595.3150	0.0002	I	BVRI	EA
V Tri	55207.2586	0.0006	II	VRI	UD

Explanation of the remarks in the table:
Observers: AK: Altuğ KARADAĞ, AO: Abdullah OKAN, AY: Arzu YOLKOLU, BG: Birol GÜROL, CY: Ceren YILDIRIM, EA: Emre AYDIN, ED: Ethem DERMAN, GG: Gökhan GÖKAY, GS: Gözde SARAL, GV: Gamze VAROL, HG: Hande GÜRSOYTRAK, MAk : Mihriban AKI, MD: Mehtap DO˘ANAY, MMK: Metehan Metin KEKLİK, MÖ: Maksude ÖZTÜRK, MSH: Muhammed ŞEMUNİ, ND: Nermin DEMİRCİOĞLU, SC: Sonay CERİT, SS: Sümeyye SURİ, TO: Tahsin OZUN, UD: Utku DERMİRHAN, YD: Yahya DEMİRCAN, YK: Yücel KILIÇ, YŞ: Yunus ŞENDAĞ, ZSŞ: Zeynep Sinem ŞAHİN, ZT: Zahide TERZİOĞLU

Remarks:
The times of minima are weighted averages from all filters observed.

Acknowledgements:
We are grateful to Ankara University Observatory for use of the telescope time allocation and other facilities.

References:

Kwee, K. K., van Woerden, H., 1956, *Bull. Astron. Inst. Neth.*, **12**, 327.
Nelson, B., 2006, Minima v2.3,
`http://www.members.shaw.ca/bob.nelson/software1.htm`

COMMISSIONS 27 AND 42 OF THE IAU
INFORMATION BULLETIN ON VARIABLE STARS

Number 6040

Konkoly Observatory
Budapest
24 November 2012

HU ISSN 0374 – 0676

A NEW VARIABLE STAR: GSC 02936-00267

ZHANG, Y.P.[1]; YAN, K.Z.[1]; FU, J.N.[1]; BAI, Y.[1]; ZHANG, C.[2]; ZHA, Q.[1]

[1] Department of Astronomy, Beijing Normal University, Beijing 100875, China. e-mail: zhangyp@bnu.edu.cn

[2] National Astronomical Observatories, Chinese Academy of Sciences, Beijing 100012, China

During the observations of the eclipsing binary GSC 2936-0478 (Yang et al. 2005) with the 85-cm telescope at Xinglong Station of National Astronomical Observatories of China on January 15, 2008, a new variable star was discovered in the field of view. The new variable star was identified to be GSC 02936-00267 according to the GSC 1 catalog (Morrison et al. 2001), which was named as GSC N8QG000518 in GSC 2.3 (Lasker et al. 2008) and 06361162+4200575 in 2MASS Point Source Catalog. The coordinates of the star is R.A. = $06^{\rm h}36^{\rm m}11\overset{\rm s}{.}61$, DEC=$+42°00'58\overset{''}{.}7$ (epoch=J2000), $V = 13\overset{\rm m}{.}58$.

Time-series photometric observations were made for the field of GSC 02936-00267 with the 85-cm reflecting telescope at Xinglong station. A PI 1024×1024 BFT CCD camera was mounted at the primary focus of the telescope (Zhou et al. 2009). Each pixel of the CCD camera scales $0.96''$ on the sky, leading to a field of view of $16.5' \times 16.5'$. The CCD camera was equipped with a set of standard Johnson-Cousins-Bessell $UBVRI$ filters. Observation dates, available frames and exposure time in the different filters are listed in Table 1.

Table 1. Observation dates, available frames and exposure time in the different filters

Observation date	Filter /available frames	Filter /exposure time
Jan. 15, 2008	$B/225$, $V/225$	$B/80$ s, $V/45$ s
Dec. 08, 2010	$R/112$, $V/112$	$V/80$ s, $R/60$ s
Dec. 11, 2010	$R/155$, $V/148$	$V/80$ s, $R/60$ s
Dec. 13, 2010	$R/66$, $V/71$	$V/80$ s, $R/60$ s
Jan. 21, 2011	$R/140$, $V/140$	$V/90$ s, $R/50$ s
Jan. 22, 2011	$R/136$, $V/138$	$V/90$ s, $R/50$ s
Jan. 26, 2011	$R/158$, $V/158$	$V/90$ s, $R/50$ s

Four reference stars and one check star, as shown in Figure 1, were chosen to obtain differential photometry for the target star. Names, coordinates and magnitudes of these stars are listed in Table 2.

We used the software package IRAF[1] for data reduction and aperture photometry. The same apertures were used for the 6 stars and light curves of $m_{Chk}-(m_{Ref1}+m_{Ref2}+m_{Ref3}+m_{Ref4})/4$ and $m_{Obj}-(m_{Ref1}+m_{Ref2}+m_{Ref3}+m_{Ref4})/4$ were calculated, where m denotes

[1]IRAF is distributed by the National Optical Astronomy Observatories, which are operated by the Association of Universities for Research in Astronomy, Inc., under cooperative agreement with the National Science Foundation.

magnitude. By choosing the light curves of $m_{Chk} - (m_{Ref1} + m_{Ref2} + m_{Ref3} + m_{Ref4})/4$ which have the smallest value of dispersion, we could determine the best aperture for photometry and obtain light curves of the target star and the check star relative to the reference stars. Light curves of the target star in V are shown in Figure 2.

Table 2. Names, coordinates and magnitudes of the reference stars and check star

Number	Name	$\alpha_{2000.0}$ hh:mm:ss	$\delta_{2000.0}$ ° ′ ″	Magnitude (V)
Ref1	GSC 02936-00201	06 36 05.62	+41 59 59.1	13.86
Ref2	GSC 02936-00284	06 35 45.11	+42 01 26.4	13.56
Ref3	GSC 02936-00466	06 35 21.54	+42 04 09.8	12.85
Ref4	GSC 02936-00460	06 36 23.30	+42 04 00.1	12.67
Chk1	GSC 02936-00417	06 35 56.05	+42 05 41.9	13.24

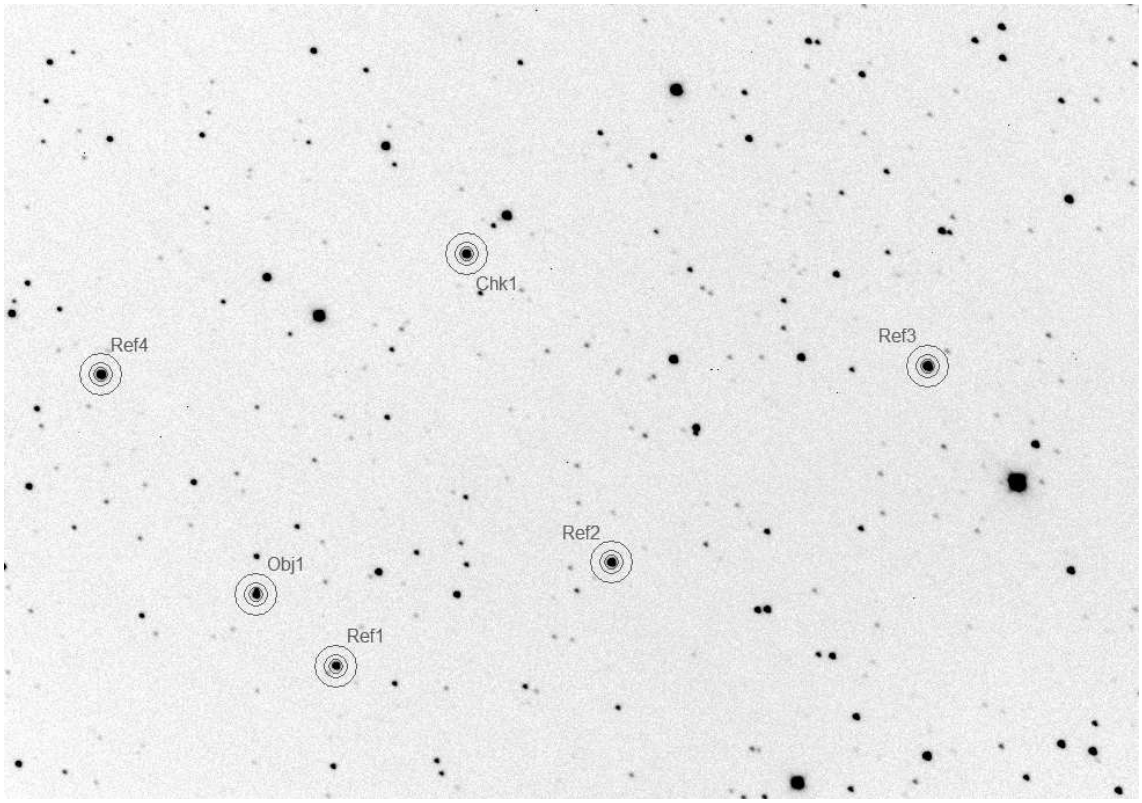

Figure 1. Observed field of GSC 02936-00267 (Obj). The reference stars (Ref) and check star (Chk) are also marked. The size of the FOV is $16.5' \times 12'$.

On 20 November 2011, the OMR low-dispersion spectrograph mounted on the 2.16-m telescope at Xinglong station was used to take a spectrum of GSC 02936-00267. The slit width was $2''.2$. The reciprocal linear dispersion of the grating is 200 Å/mm or 9.36 Å/pixel. The spectral range is 400 nm — 800 nm. The central wavelength is 600 nm. The spectrum is shown in Figure 3.

From the spectrum of the star GSC 02936-00267, we identified the spectral lines of $H_\alpha, H_\beta, H_\gamma, H_\delta$ and the spectral line of sodium at 589 nm. According to the reference of

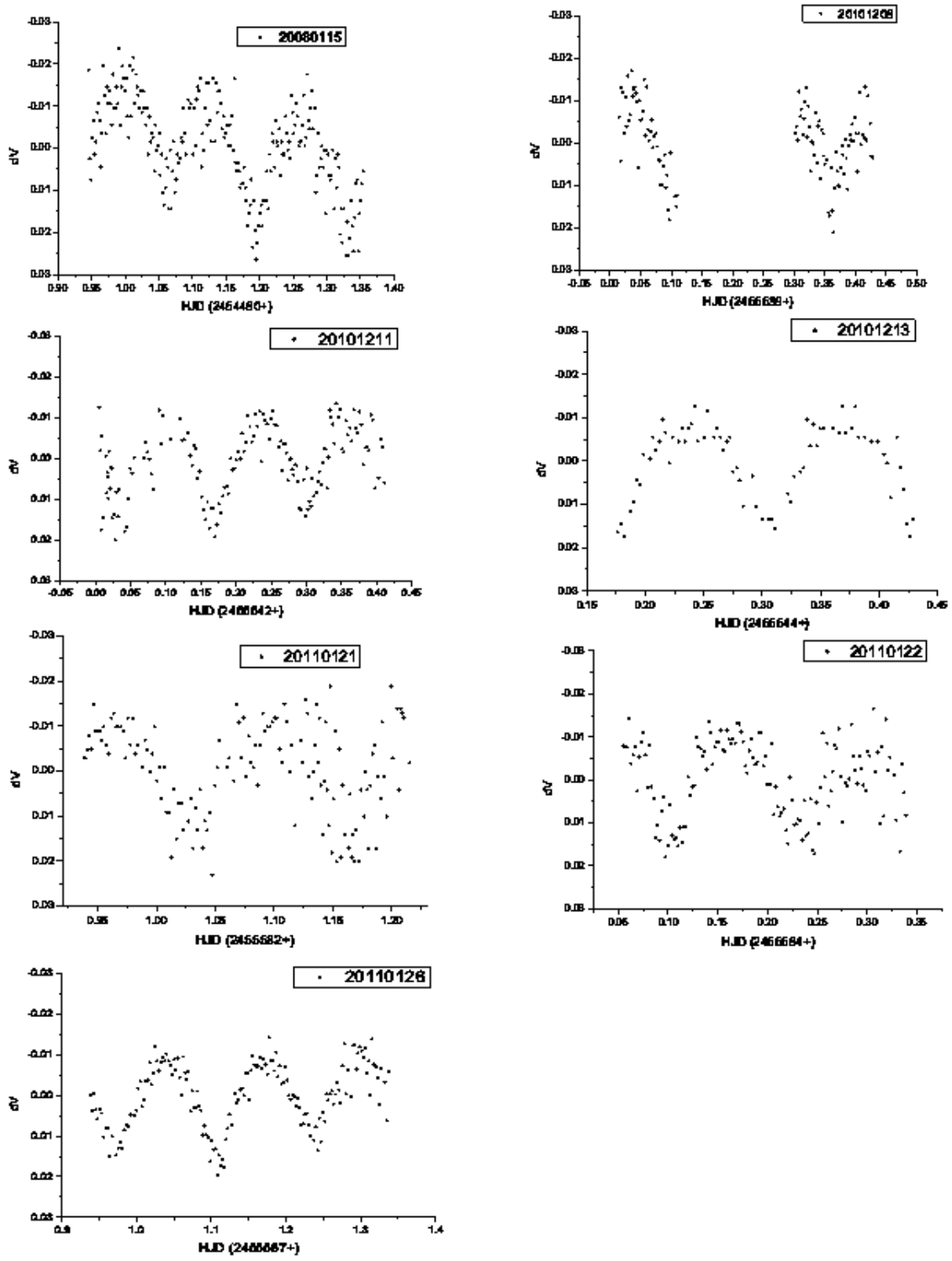

Figure 2. Light curves of GSC 02936-00267 in V

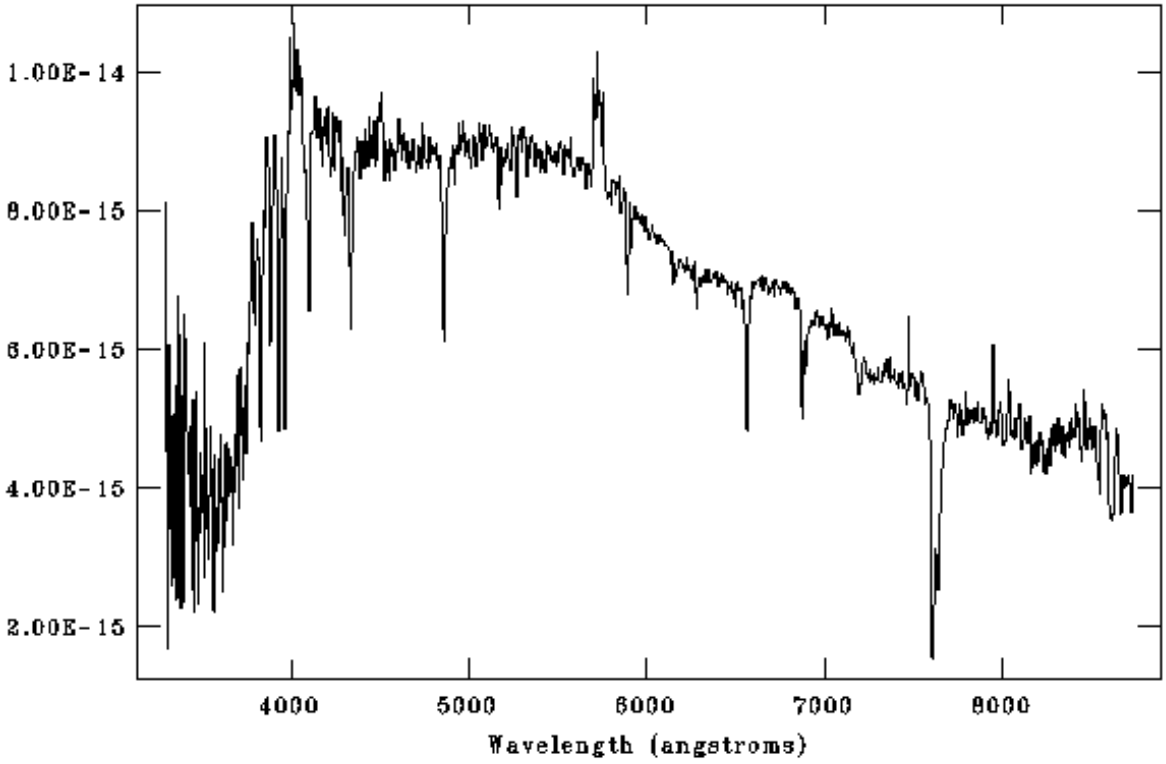

Figure 3. Low-dispersion spectrum of GSC 02936-00267. The y axis is the flux in erg $s^{-1}cm^{-2}Å^{-1}$.

Pickles Atlas (Pickles 1998), we identified the spectral type of GSC 02936-00267 as F2V based on the ratio of depths of the spectral lines of H_α and of sodium at 589 nm. We note that there is a strong emission line with a central wavelength of 572.5 nm and full width at half maxium of around 6.5 nm. Since there was a fainter star very close to GSC 02936-00267 in the slit during the observations, we suspect that the emmission line was created by the fainter star whose spectral type is unknown. This needs to be confirmed with spectroscopic observations for the two stars respectively with larger-aperture telescopes.

The software package Period04 (Lenz & Breger 2005) was used to analyze pulsation periods of GSC 02936-00267. The results ot the analysis are as follows:

Main frequency $(f_1) = 7.488423\ \mathrm{d}^{-1}$

Amplitude of the main frequency $(A) = 0\overset{\mathrm{m}}{.}010 \pm 0.001$ mag

$T_{\mathrm{Max}} = \mathrm{HJD}\ 2454480.99916 + 0\overset{\mathrm{d}}{.}133539(5) \times E$.

According to the pulsation frequency and the spectrum of GSC 02936-00267, we classify it as a δ Scuti type variable.

Since there is a faint neighboring star ($V = 13\overset{\mathrm{m}}{.}58$) very close to GSC 02936-00267, and because the amplitude of pulsation is small ($A \sim 0\overset{\mathrm{m}}{.}01$), more time-series photometric data and spectroscopic observations are needed to confirm the spectral type classification and check the pulsation period.

Acknowledgments: We acknowledge the support from National Natural Science Foundation of China (NSFC), through the Grants 10778601 and U1231202. The research is partially supported by National Basic Research Program of China (973 Program 2013CB834900) and the fundamental Research Funds for the Central Universities.

References:

Lasker, B.M., Lattanzi, M.G., McLean, B.J. et al. 2008, *AJ*, **136**, 735
Lenz, P., and Breger, M. 2005, *Commun. Asteroseismol.*, **146**, 53
Morrison, J.E., Roeser, S., McLean B., Bucciarelli, B., Lasker, B. 2001, *AJ*, **121**, 1752
Pickles, A.J. 1998, *PASP*, **110**, 863
Yang, Y.G., Qian, S.B., Gonzalez-Rojas, D.J. and Yuan, J.Z. 2005, *ApSS*, **300**, 337
Zhou, A.Y., Jiang, X.J., Zhang, Y.P., Wei, J.Y. 2009, *Res. Astron. Astrophys.*, **9**, 349

COMMISSIONS 27 AND 42 OF THE IAU
INFORMATION BULLETIN ON VARIABLE STARS

Number 6041

Konkoly Observatory
Budapest
29 December 2012

HU ISSN 0374 – 0676

TIMES OF MINIMA OF SOME ECLIPSING BINARY STARS

DEMİRCAN, Y.; GÖKAY, G.; OKAN, A.; GÜRSOYTRAK, H.; TERZİOĞLU, Z.; SARAL, G.; KILIÇ, Y.; CERİT, S.; ŞEMUNİ, M.; AYDIN, E.; DEMİRHAN, U.; GÜROL, B.

Ankara University Observatory, Faculty of Science, Astronomy and Space Sciences Department 06100, Tandoğan, Ankara, TÜRKİYE; e-mail: demircan@ankara.edu.tr

Observatory and telescope:
16" Schmidt/Cassegrain telescope at Ankara University Observatory

Detector:	Apogee ALTA U47+ back illuminated CCD camera, Peltier cooling, E2V CCD47-10 chip, 1024 × 1024 pixels.

Method of data reduction:
Reduction of the CCD frames was made with the IRAF[1], CCDRED and DAOPHOT packages.

Method of minimum determination:
The minimum times were computed with several methods in Minima25b (Nelson, 2006): parabolic fit, tracing paper, bisectors of chords, Kwee and van Woerden method (Kwee & van Woerden, 1956), Fourier fit and sliding integrations technique. Then weighted mean minimum-time values were calculated for all filters were used.

[1]IRAF is distributed by the National Optical Astronomical Observatories, operated by the Association of the Universities for Research in Astronomy, inc., under cooperative agreement with the National Science Foundation

Times of minima:					
Star name	Time of min. HJD 2400000+	Error	Type	Filter	Rem.
TZ Boo	55705.5096	0.0002	I	BVRI	AO
	55732.4022	0.0001	II	BVRI	MMK
	55733.4450	0.0004	I	BVRI	AO-YŞ
	55738.3456	0.0002	II	BVRI	YD-TO-AK
	55742.3592	0.0004	I	BVRI	ZT-MSH-MA
	55743.3972	0.0003	II	BVRI	GS-MD
GK Boo	55735.4284	0.0002	I	BVRI	MSH-MA-CY
	55736.3838	0.0001	I	BVRI	CY-AY-MA
	55737.3393	0.0001	I	BVRI	UD-CY
	55741.3997	0.0002	II	BVRI	YK
GS Boo	55663.4409	0.0015	I	BVRI	AO-YŞ
HH Boo	55678.3929	0.0002	I	BVRI	YK-MSH
	55678.5538	0.0004	II	BVRI	YK-MSH
	55682.3781	0.0004	II	BVRI	YD-SI
	55682.5356	0.0003	I	BVRI	YD-SI
EG Cep	55761.4450	0.0007	II	BVRI	AO-YŞ
	55784.3194	0.0008	II	BVRI	ZT-SC
	55809.3717	0.0003	II	BVRI	AY
	55818.3583	0.0002	I	BVRI	GS
EF Cep	55803.3699	0.0001	II	BVRI	AO
TYC 4589-2999-1	55809.3530	0.0004	I	BVRI	AY
DY CVn	55691.5255	0.0004	I	VRI	AO-YŞ
V1191 Cyg	55753.3880	0.0003	I	BVRI	MMK
	55754.3298	0.0009	I	BVRI	MA-YŞ
	55754.4851	0.0004	II	BVRI	MA-YŞ
V1918 Cyg	55815.3895	0.0002	II	BVRI	AO-TO-AK
ASAS 202521+0425.5	55771.5033	0.0004	I	BVRI	MBD-YK-MA
	55793.3487	0.0004	II	BVRI	CY-MA
HI Dra	55820.5036	0.0014	I	BVRI	AO-GS
V1033 Her	55755.3770	0.0006	II	BVRI	GS-CY
	55755.5253	0.0002	I	BVRI	GS-CY
	55758.3571	0.0002	II	BVRI	CY-MA
	55758.5054	0.0002	I	BVRI	CY-MA
	55770.4272	0.0004	I	BVRI	MSH-MA
	55771.3221	0.0004	I	BVRI	MBD-YK-MA
GSC 2751-1007	55764.4106	0.0010	I	BVRI	YK-TO-MD
	55778.3963	0.0006	II	BVRI	YK-AK-TO
	55781.5255	0.0003	I	BVRI	MMK
	55783.4059	0.0009	II	BVRI	GS
	55790.5024	0.0006	II	BVRI	YK-MBD-AK
	55799.2681	0.0004	II	BVRI	YK-MBD-TO
	55799.4769	0.0007	I	BVRI	YK-MBD-TO

Times of minima:					
Star name	Time of min. HJD 2400000+	Error	Type	Filter	Rem.
ASAS 231700+1944.9	55795.3673	0.0007	II	BVRI	CY-MBD
	55795.5467	0.0003	I	BVRI	CY-MBD
	55805.3737	0.0004	II	BVRI	MSH
	55805.5521	0.0005	I	BVRI	MSH
CD Tri	55814.4427	0.0004	II	VRI	CY-MBD
	55816.4709	0.0011	I	BVRI	MBD-MNB
	55817.3930	0.0004	II	I	AO
	55817.5764	0.0007	I	VRI	AO

Explanation of the remarks in the table:

Observers: AK: Altuğ KARADAĞ, AO: Abdullah OKAN, AY: Arzu YOLKOLU, CY: Ceren YILDIRIM, GS: Gözde SARAL, MA: Mehmet ALPSOY, MBD: Mustafa Burak DOĞRUEL, MD: Mehtap DOĞANAY, MMK: Metehan Metin KEKLİK, MNB: Mehmet Naim BAĞIRAN, MSH: Muhammed ŞEMUNİ, SC: Sonay CERİT, SI: Süleyman IŞILDAK, TO: Tahsin OZUN, UD: Utku DERMİRHAN, YD: Yahya DEMİRCAN, YK: Yücel KILIÇ, YŞ: Yunus ŞENDAĞ, ZT: Zahide TERZİOĞLU

Remarks:

The times of minima are weighted averages from all filters observed.

Acknowledgements:

We are grateful to Ankara University Observatory for use of the telescope time allocation and other facilities.

References:

Kwee, K. K., van Woerden, H., 1956, *Bull. Astron. Inst. Neth.*, **12**, 327.
Nelson, B., 2006, `http://www.members.shaw.ca/bob.nelson/software1.htm`

COMMISSIONS 27 AND 42 OF THE IAU
INFORMATION BULLETIN ON VARIABLE STARS

Number 6042

Konkoly Observatory
Budapest
11 January 2013

HU ISSN 0374 – 0676

TIMINGS OF MINIMA OF ECLIPSING BINARIES

DIETHELM, ROGER

Bahnhofstrasse 3, CH–4118 Rodersdorf, Switzerland

The following Table lists timings of minima of eclipsing binaries secured by CCD photometry, obtained in the second half of 2012. The given O−C values generally refer to the linear elements of the newest electronic version of the GCVS (Samus et al., 2012), except for the cases stated in the remarks, where the determination of current elements made use of the up-to-date ASAS data (`http://www.astrouw.edu.pl/asas/`) and the Lafler-Kinman algorithm of the PERANSO software (`http://www.peranso.com/`). All times given are heliocentric UTC. All data were obtained at the R. Szafraniec Observatory operated at Astrokolkhoz Obs., Cloudcroft, N.M., USA. The untiring support by T. Krajci at the site is acknowledged thankfully.

Table 1: Minima of eclipsing binaries

Variable	Type	HJD 24...	$O-C$	n	Remarks
RT And	p	56226.7518(3)	+0.0537	42	V
XZ And	p	56265.6514(1)	−0.0369	48	V
AA And	p	56232.6993(5)	−0.0024	38	V; d=0.054d
AB And	s	56226.6913(3)	−0.0089	44	V
AD And	s	56237.6501(2)	−0.0478	45	V
BD And	p	56233.6979(2)	−0.0239	49	V
BL And	p	56238.6738(2)	−0.0028	38	V; d=0.038d
BX And	p	56261.6736(2)	−0.0117	48	V
CN And	s	56245.7135(8)	−0.0117	24	V
CU And	p	56226.6989(3)	−0.1054	44	V
DK And	s	56226.6455(4)	+0.0106	43	V
EP And	p	56202.8681(2)	−0.0134	48	V; d=0.025d
EX And	p	56238.6878(4)	−0.0006	38	V
GZ And	s	56273.6354(2)	−0.0023	30	V
	p	56273.7868(15)	−0.0034	12	V
HR And	p	56258.7026(5)	+0.0446	39	V; el: Krakow Catalog
HS And	p	56255.7393(2)	−0.0002	43	V
KP And	p	56237.645(3)	+0.051	34	V; el: IBVS 5674
LM And	p	56205.8626(5)	−0.0099	39	V; d=0.038d
LO And	p	56226.6783(2)	−0.0084	40	V
LY And	s	56261.6786(3)	−0.0138	48	V; d=0.024d
MO And	p	56265.6489(3)	+0.0123	47	V
QX And	p	56273.6643(3)	+0.0007	53	V; el: 46785.8003+0.4121753×E
V372 And	p	56203.9367(6)	+0.0703	51	V; d=0.07d
V382 And	p	56237.7508(15)	+0.0844	34	V
V422 And	p	56225.6767(3)	−0.0093	35	V

Table 1: Minima of eclipsing binaries (continued)

Variable	Type	HJD 24...	$O-C$	n	Remarks
V440 And	p	56245.6533(2)	−0.0041	47	V; el: IBVS 5871; D=0.11d
V449 And	s	56202.8563(4)	−0.0287	47	V
V473 And	?	56254.7403(6)	+0.0833	41	V; d=0.031d
V489 And	p	56258.7405(5)	+0.0011	40	V; el: IBVS 5960
V502 And	p:	56256.6562(6)	+0.0013	44	V; pulsator?
V506 And	s:	56258.6505(4)	−0.0104	36	V
V546 And	s:	56262.6190(3)	+0.0009	36	V; el: 51475.6132+0.383037×E; d=0.032d
V563 And	s	56205.8131(6)	−0.0021	18	V; el: 51478.76+0.303201×E
	p	56205.9641(2)	−0.0026	19	V
V566 And	s	56265.7532(3)	−0.0050	47	V; el: 51478.78+0.389708×E
	p	56273.7423(5)	−0.0049	51	V
V568 And	p	56279.6244(4)	+0.0046	47	V; el: 51509.93+0.394287×E; d=0.036d
V571 And	p:	56214.8637(6)	+0.0166	37	V
GSC 1734-408 And	s	56256.6788(3)	−0.0010	44	V; el: IBVS 5960; d=0.014d
GSC 1739-1463 And	s	56259.6686(5)	−0.0112	23	V; el. IBVS 5960
GSC 3234-1318 And	s	56237.6898(5)	+0.0508	33	V; el: PZP 10, 18
GSC 3243-962 And	s	56232.6355(4)	+0.0005	39	V; el: 51573.628+1.557415×E
GSC 3303-1583 And	p	56210.9291(3)	+0.0583	49	V; el: OEJV 104
GSC 3627-1727 And	s	56232.7149(4)	−0.0027	39	V; el: 51400.783+0.396792×E
GSC 3638-2422 And	p	56238.6504(2)	−0.0142	38	V; el: IBVS 5920
GSC 3641-587 And	p	56226.7457(6)	−0.0158	43	V; el: IBVS 5920
BW Aqr	s	56227.6129(10)	−0.1851	27	V; non-circular
EF Aqr	p	56237.6776(1)	−0.0069	34	V; el: IBVS 6011
EL Aqr	p	56239.7331(5)	+0.0205	36	V; el: 53541.891+0.4814100×E
GN Aqr	s	56228.6388(15)	−0.0320	28	V; el: 53116.924+4.404454×E
GS Aqr	p	56227.7316(5)	+0.0033	38	V; el: 54383.578+0.374067×E
NN Aqr	p	56218.6831(6)	+0.0051	16	V; el: IBVS 6011
GSC 529-285 Aqr	p	56205.7195(3)	−0.0001	46	V; el: 54333.645+0.412988×E
GSC 5210-437 Aqr	p	56219.7229(3)	−0.0056	45	V; el: IBVS 5960
GSC 5220-352 Aqr	s	56214.6728(4)	+0.0051	43	V; el: IBVS 6011
GSC 5248-214 Aqr	p	56231.7048(5)	+0.0019	45	V; el: IBVS 6011
GSC 5777-383 Aqr	s	56205.7046(3)	+0.0085	19	V; el: IBVS 6011
GSC 5811-437 Aqr	s	56227.6767(7)	−0.0079	31	V; el: IBVS 6011
GSC 5817-92 Aqr	s	56227.6723(7)	+0.0003	30	V; el: IBVS 6011
GSC 5817-435 Aqr	s	56227.6820(4)	+0.0112	30	V; el: IBVS 6011; d=0.035d
GSC 5826-1082 Aqr	p	56231.6635(3)	−0.0337	41	V; el: IBVS 6011
GSC 5835-944 Aqr	s	56231.7014(3)	−0.0077	45	V; el: IBVS 6011
RX Ari	p	56262.6536(5)	+0.0728	36	V; d=0.046d
SS Ari	s	56262.7230(5)	−0.0084	36	V
SZ Ari	p	56290.7143(2)	+0.0084	42	V; el: Krakow Catalog
TX Ari	p	56210.8569(3)	−0.0171	44	V
BO Ari	p	56279.6322(1)	−0.0224	30	V; d=0.027d
GSC 645-85 Ari	s	56210.8677(2)	+0.0040	49	V; el: IBVS 5960
GSC 1213-1483 Ari	s	56265.6434(1)	+0.0326	47	V; el: IBVS 5960
GSC 1217-696 Ari	p	56214.9015(4)	+0.0015	37	V; el: IBVS 5920; d=0.034d
GSC 1240-657 Ari	s	56282.6595(4)	−0.0016	30	V; el: IBVS 5945; d=0.041d
GSC 1794-393 Ari	p:	56226.8980(7)	−0.0119	38	V; el: PZ 10, 18; strong O'Connell effect
GSC 1794-1525 Ari		56226.8823(6)		38	V; new variable
DO Aur	p	56246.8586(6)	−0.0007	42	V; d=0.027d
KO Aur	p	56257.8623(3)	−0.0026	47	V
KU Aur	p	56256.9315(3)	+0.0190	49	V
QT Aur	p	56255.9495(5)	−0.0061	38	V
V365 Aur	p	56246.8892(5)	−0.0168	42	V
V379 Aur	p	56258.8964(5)	−0.0109	40	V
V585 Aur	p	56245.9387(5)	+0.0360	43	V; d=0.029d
V599 Aur	p	56246.9026(5)	+0.0096	42	V
V608 Aur	p	56239.8784(3)	−0.0162	52	V; D=0.072d; d=0.014d
V612 Aur	p	56258.8677(5)	+0.0457	41	V; el: OEJV 83
V641 Aur	p	56255.8185(6)	−0.0186	38	V
GSC 3751-178 Aur	p	56256.9238(5)	+0.0046	17	V; el: 53285.2664+0.327997; l.c. asymmetric

Table 1: Minima of eclipsing binaries (continued)

Variable	Type	HJD 24...	$O-C$	n	Remarks
AO Cam	s	56230.8016(3)	−0.0599	12	V; el: PASP 97, 648
AS Cam	s	56238.9423(6)	−0.2162	46	V; d=0.046d; non-circular
LR Cam	p	56261.8668(1)	+0.0015	46	V; el: 51975.6040+0.4341399×E
NO Cam	p	56230.8428(19)	+0.0108	12	V; el: IBVS 5894
NR Cam	p	56290.8875(4)	+0.0064	38	V; el: Krakow Catalog
NX Cam	s	56279.7330(6)	−0.0079	47	V; el: 51447.79+0.605318×E
	s	56290.6348(9)	−0.0019	41	V
OQ Cam	s:	56227.9635(5)	−0.0463	38	V; el: IBVS 6011; d=0.024d
QV Cam	p	56232.8763(6)	+0.0112	50	V; el: IBVS 5960
QZ Cam	p	56227.9250(7)	+0.0681	33	V; el: IBVS 6029
PP Cam	s	56220.8376(23)	−0.0029	8	V: el: 51421.782+0.840392×E
	p	56233.8648(2)	−0.0018	44	V
V337 Cam	p	56232.8761(3)	−0.0318	50	V; el: IBVS 6011
V387 Cam	p	56258.9061(5)	0	40	V; 51520.553+0.651141×E
V389 Cam	s:	56238.8259(4)	−0.0390	46	V
V392 Cam	p	56258.8871(7)	−0.0012	40	V; el: 51508.525+0.664015×E
V393 Cam	p	56258.8581(3)	+0.0229	40	V
V401 Cam	s	56258.9114(4)	+0.0196	39	V
V418 Cam	s:	56261.8714(2)	−0.0100	46	V
V424 Cam	s	56261.8763(4)	+0.0006	46	V; el: 51523.877+0.3258484×E
V426 Cam	p	56261.8552(3)	−0.0001	45	V; el: 51521.549+0.3478358×E
V437 Cam	p:	56261.8954(7)	−0.0374	45	V
V442 Cam	p:	56261.8339(3)		45	V
V443 Cam	s:	56261.8349(7)		45	V
V466 Cam	s:	56273.8334(5)	−0.0318	38	V
GSC 3715-43 Cam	p	56232.8335(4)	+0.0035	51	V; new variable in the field of NX Cam;
	p	56279.7683(3)	+0.0035	47	V; el: 56232.83+0.464701×E
	s	56290.6896(3)	+0.0043	42	V
KM Cnc	p	56282.8608(5)	−0.0005	40	V; el: IBVS 5871; d=0.030d
GSC 1388-132 Cnc	p	56282.8654(4)	+0.0020	40	V; el: IBVS 5992
GSC 5388-967 CMa	p	56273.9314(6)	+0.0026	38	V; el: 54761.822+1.724181×E
GSC 5404-2421 CMa	s	56246.841(4)	+0.974	32	V; el: IBVS 5992; non-circular
GSC 5406-2659 CMa	p	56273.8538(6)	+0.0024	37	V; el: IBVS 5992
GSC 5407-430 CMa	p	56273.8755(4)	+0.0003	36	V; el: 54597.533+1.011673×E
AH Cas	p	56262.6723(1)	+0.0005	37	V; el: Krakow Catalog
AL Cas	p	56203.8792(2)	+0.0062	50	V
BH Cas	p	56245.7090(5)	+0.0380	47	V; el: IBVS 4482
BS Cas	p	56202.8523(3)	+0.0037	48	V; d=0.026d
BU Cas	p	56261.7177(2)	−0.0239	49	V
BW Cas	p	56261.7230(3)	+0.0193	48	V; el: IBVS 5960
BZ Cas	p	56273.6427(4)	−0.0024	53	V; el: Krakow Catalog
CW Cas	p	56259.6856(11)	−0.0711	23	V
DP Cas	p	56238.7058(3)	−0.0048	38	V
EG Cas	p	56246.6712(4)	−0.0037	48	V; el: Krakow Catalog; d=0.036d
EI Cas	p	56239.6419(5)	+0.1100	36	V
EY Cas	p	56251.6576(3)	−0.0105	40	V; el: Krakow Catalog
IR Cas	p	56233.7098(2)	+0.0101	49	V
IT Cas	p	56237.6919(4)	−0.0024	33	V; el: AJ 114, 1206; non-circular
LQ Cas	p	56246.6776(4)	−0.0065	48	V; el: Krakow Catalog; d=0.044d
LX Cas	p	56290.6728(5)	+0.0504	42	V
MR Cas	s	56251.6599(3)	+0.0026	40	V; el: Krakow Catalog
MS Cas	p	56251.6606(2)	+0.0422	40	V
MT Cas	p	56254.7090(2)	+0.0233	41	V; d=0.017d
MU Cas	s	56245.6904(6)	+1.1432	47	V; el: Krakow Catalog; non-circular
NN Cas	s	56254.6716(4)	−0.0213	41	V; el: Krakow Catalog; d=0.040d
NT Cas	p	56255.6852(3)	+0.0172	43	V; d=0.024d
OX Cas	p	56215.6890(5)	+0.0400	47	V; non-circular
	s	56261.7344(5)	+0.0325	49	V

Table 1: Minima of eclipsing binaries (continued)

Variable	Type	HJD 24...	$O-C$	n	Remarks
PV Cas	p	56203.9091(5)	−0.0337	44	V; non-circular
QQ Cas	s	56246.7019(5)	+0.0028	48	V; el: Krakow Catalog
V344 Cas	s	56225.6843(3)	−0.1115	34	V
	s	56233.6898(3)	−0.1121	49	V
V336 Cas	p	56256.7510(3)	−0.0142	45	V
V361 Cas	p	56239.6513(7)	−0.0066	36	V; el: Krakow Catalog
V375 Cas	p	56246.6770(2)	+0.0153	48	V; el: Krakow Catalog
V380 Cas	p	56254.6574(3)	−0.0683	40	V
V411 Cas	p	56254.6978(4)	+0.1634	41	V; d=0.039d
V427 Cas	s	56225.6153(9)	−0.0003	36	V; el: 54366.5402+1.305989×E
V445 Cas	s	56255.6322(6)	−0.0210	44	V; el: BAVM 69, 1
V459 Cas	s	56257.6390(2)	−0.1713	39	V; non-circular
V520 Cas	p	56246.7444(2)	+0.0014	48	V; el: Krakow Catalog
V523 Cas	s	56255.7069(3)	+0.0419	36	V; el: MNRAS 317, 111
V537 Cas	p	56256.6474(2)	−0.0056	44	V; el: Krakow Catalog
V541 Cas	s	56205.8428(7)	+0.0260	38	V; el: IBVS 2652
V608 Cas	p	56203.8719(3)	+0.0134	50	V; el: IBVS 5151; d=0.018d
V775 Cas	s	56245.7195(6)	+0.8317	47	V; el: IBVS 5557; non-circular
	p	56290.6914(4)	−0.0130	42	V
V821 Cas	p	56230.7058(3)	−0.0481	51	V; el: IBVS 5386; non-circular
V851 Cas	s	56238.7552(14)	+0.0019	38	V; el: Krakow Catalog
V860 Cas	p	56256.6727(3)	−0.0091	45	V; el: IBVS 5111
V959 Cas	s	56245.7027(4)	+0.0174	47	V; el: IBVS 5960
V1001 Cas	s	56238.6941(7)	+0.0630	14	V; D=0.068d!
V1007 Cas	s	56251.6848(6)	−0.0004	32	V; el: 51415.83+0.3320075×E; d=0.022d
V1030 Cas	s:	56254.6904(4)	−0.0394	41	V
V1031 Cas	p	56245.7488(4)	+0.0486	47	V; d=0.027d
V1043 Cas	p	56255.6059(7)	+0.0005	43	V; el: 53300.9578+0.661587×E
V1060 Cas	p	56257.6634(6)	+0.0013	39	V; el: 51339.88+1.816020×E
V1107 Cas	s	56202.8746(6)	+0.0629	48	V
V1137 Cas	s	56262.6625(5)	−0.0201	37	V; non-circular
V1138 Cas	p	56261.6452(5)	+0.0023	48	V; el: Krakow Catalog
GSC 3671-99 Cas	p	56256.7136(4)	+0.0027	44	V; non-circular
	s	56279.7064(3)	−0.7033	48	V; d=0.040d
GSC 4029-1087 Cas	p	56257.6794(4)	+0.0238	40	V; el: PZP 11, 1
U J232931+6031.6 Cas	s:	56237.6617(11)	+0.0353	34	V; el: PZP 10, 13; d=0.019d
VZ Cep	p	56203.7246(4)	−0.0106	50	V
WZ Cep	p	56226.6716(2)	−0.1081	43	V; el: AAS 131, 17
XY Cep	p	56251.6668(2)	−0.0499	40	V
CO Cep	p	56214.8111(3)	−0.1995	78	V; non-circular
	s	56233.6425(4)	+0.0128	48	V
DL Cep	p	56220.6692(3)	+0.0057	40	V; el: IBVS 5016; d=0.035d
DP Cep	s	56225.7137(6)	−0.0606	36	V
DY Cep	p	56237.647(4)	−0.027	33	V; Krakow Catalog
GW Cep	p	56202.8701(2)	+0.0023	47	V; el: IBVS 4293
IP Cep	p	56219.6983(4)	−0.0357	45	V; el: IBVS 5016; d=0.067d
LL Cep	p	56232.6514(3)	+0.0024	39	V
NN Cep	p	56237.6811(22)	−0.0024	32	V
OT Cep	s	56259.6547(12)	−0.0028	24	V; el: IBVS 5212
V358 Cep	p	56214.8991(2)	+0.0150	36	V; el: BBSAG Bull. 96, 10; d=0.028d
V699 Cep	p	56230.6795(2)	−0.0099	50	V; d=0.042d
V731 Cep	p	56256.6194(4)	−0.0153	45	V; el: IBVS 5616; non-circular
V734 Cep	s	56214.6998(4)	+0.1054	76	V; el: Krakow Catalog; d=0.053d; non-circular
	p	56261.6641(3)	−0.0049	49	V
V744 Cep	p	56230.7047(4)	+0.0241	52	V
V756 Cep	p	56255.6161(8)	+0.0009	44	V; el: 51454.597+1.722648×E
V757 Cep	p	56254.6091(4)	−0.0333	22	V
	s	56254.7828(22)	−0.0316	20	V

Table 1: Minima of eclipsing binaries (continued)

Variable	Type	HJD 24...	$O-C$	n	Remarks
V790 Cep	s	56257.6999(11)	+0.0190	40	V
V796 Cep	p	56202.8658(4)	−0.0033	29	V; el: IBVS 6011
V804 Cep	p	56203.9039(3)	−0.0003	50	V
V805 Cep	p	56232.8985(2)	+0.0159	51	V
GSC 3965-1172 Cep	p	56215.7601(9)	−0.0439	48	V; el: OEJV 83
GSC 3996-1098 Cep	p	56225.6628(5)	−0.0083	37	V; el: 53965.3635+0.352018×E
GSC 4286-49 Cep	s	56226.6597(6)	−0.0474	44	V; el: IBVS 5570
GSC 4477-706 Cep	p	56232.7471(9)	+0.0039	40	V; el: OEJV 83
GSC 4481-1535 Cep	p	56226.6656(6)	−0.0228	44	V; el: OEJV 83
GSC 4482-1238 Cep	s	56232.6397(4)	+0.0219	33	V; el: OEJV 91
GSC 4487-347 Cep	p	56251.7536(6)	−0.0034	40	V; el: IBVS 6020; non-circular
GSC 4488-376 Cep	p	56228.6183(4)	−0.0182	26	V; el: OEJV 83
GSC 4490-777 Cep	s	56233.7203(4)	−0.0005	48	V; el: 51532.589+1.698079×E
SS Cet	p	56226.833(5)	+0.047	38	V
TV Cet	s	56282.6777(7)	−0.0552	42	V; d=0.034d; non-circular
HM Cet	p	56205.9229(4)	−0.0058	39	V; el: IBVS 5960
HS Cet	p	56215.9058(4)	+0.0043	44	V; el: 54292.901+3.69098×E
GSC 44-1314 Cet	p	56205.8863(3)	+0.0023	39	V; el: IBVS 5960
GSC 49-120 Cet	p	56210.8716(2)	−0.0332	49	V; el: IBVS 6011; d=0.036d
GSC 54-373 Cet	s	56214.8777(7)	+0.0065	36	V; el: IBVS 5960; d=0.073d
GSC 4698-855 Cet	p	56210.8904(3)	+0.0127	48	V; el: IBVS 6011
GSC 4708-841 Cet	s	56226.8893(5)	−0.0140	38	V; el: IBVS 5960
GSC 5268-1013 Cet	s	56258.6955(7)	−0.0087	29	V; el: IBVS 5960
GSC 5270-645 Cet	p	56258.6677(6)	−0.0035	39	V; el: OEJV 116
GSC 5284-2130 Cet	s	56205.8612(4)	−0.0020	36	V; el: IBVS 6011
DK Cyg	p	56218.6994(3)	+0.0965	18	V
LO Cyg	p	56203.7214(12)	−0.0370	50	V
V387 Cyg	p	56205.6746(3)	+0.0203	47	V
V525 Cyg	p	56205.6783(2)	−0.0304	47	V; d=0.032d
V616 Cyg	p	56214.6951(3)	−0.3328	43	V; d=0.030d
V628 Cyg	s	56214.7247(3)	−0.0050	43	V; el: IBVS 4381
V680 Cyg	p	56220.7049(4)	+0.0676	40	V
V704 Cyg	p	56203.6814(4)	+0.0323	50	V
V706 Cyg	s	56219.6872(5)	−0.0557	46	V
V711 Cyg	p	56220.6533(6)	−0.0355	40	V; el: IBVS 5741
V836 Cyg	p	56215.6944(4)	+0.0194	48	V
V1815 Cyg	s	56223.6539(4)	+0.0037	27	V; el: BAV Rb. 55, 1
GSC 536-9 Equ	p	56205.6894(3)	−0.0045	47	V; el: IBVS 6011
GSC 537-1462 Equ	p	56215.6555(4)	+0.0109	48	V; el: IBVS 6011; d=0.022d
RU Eri	p	56227.8738(5)	−0.0324	32	V
TZ Eri	p	56231.9311(3)	−0.0141	49	V; el: IBVS 6011; d=0.048d
UX Eri	p	56226.8886(5)	+0.0215	38	V; el: IBVS 5960
YY Eri	p	56231.9373(5)	−0.0033	19	V; el: IBVS 5960
AM Eri	p	56231.9102(3)	−0.0040	49	V; el: Krakow Catalog
BC Eri	p	56237.9268(4)	+0.0054	43	V; el: IBVS 5960; d=0.026d
BL Eri	p	56231.9565(2)	+0.0221	47	V; el: IBVS 6011; d=0.018d
KZ Eri	p	56282.6398(4)	−0.0073	28	V; el: IBVS 6011: d=0.025d
GSC 4703-84 Eri	p	56215.8764(4)	+0.0083	41	V; el: 54866.544+2.570141×E; d=0.035d
GSC 4732-1231 Eri	p	56231.9265(2)	−0.0014	49	V; el: IBVS 5960
GSC 4739-480 Eri	p	56237.8511(3)	+0.0049	47	V; el: IBVS 6029
GSC 5294-1116 Eri	s	56226.8841(2)	+0.0019	37	V; el: IBVS 5960
GSC 5303-939 Eri	s	56227.8773(3)	−0.0051	38	V; el: IBVS 5960
GSC 5322-2251 Eri	p	56245.9000(2)	+0.0133	43	V; el: IBVS 5960; d=0.019d
GSC 5323-652 Eri	s	56239.8918(5)	+0.0098	52	V; el: IBVS 5992
GSC 5330-664 Eri	s	56238.8162(6)	+0.0034	17	V; el: IBVS 6029
	p	56238.9278(5)	+0.0002	30	V
LO Gem	p	56255.9201(4)	+0.0148	38	V; el: IBVS 5020
MU Gem	s	56279.837(3)	+0.020	37	V
V410 Gem	s	56245.9220(8)	+0.0207	42	V; el: IBVS 6029; non-circular
GSC 1351-383 Gem	p	56282.8892(3)	+0.0078	40	V; el: IBVS 6029; d=0.037d

Table 1: Minima of eclipsing binaries (continued)

Variable	Type	HJD 24...	$O-C$	n	Remarks
GSC 1368-1411 Gem	p	56282.8734(2)	−0.0008	33	V; el: IBVS 5871; d=0.023d
GSC 1864-1065 Gem	s	56265.8572(4)	−0.0103	23	V; el: IBVS 5960
A J065830+1311.5 Gem	p	56279.8742(3)	−0.0492	38	V; el: 54856.3476+0.330296×E
RW Lac	p	56214.7328(3)	+0.0618	42	V; el: IBVS 5682; non-circular
TZ Lac	p	56223.6518(6)	+0.3701	26	V
VY Lac	p	56225.7451(3)	+0.0005	37	V; el: MitVS 10, 55
CO Lac	p	56203.7095(2)	−0.0018	50	V; non-circular
	s	56230.6957(2)	−0.0043	52	V
EM Lac	s	56227.6794(2)	+0.0939	38	V
FL Lac	p	56230.7007(5)	−0.0430	51	V; d=0.033d
GX Lac	s	56231.7110(10)	−0.0436	46	V
MZ Lac	p	56231.7105(4)	−0.0052	46	V; el: JAAVSO 19, 12; non-circular
V364 Lac	s	56214.6902(4)	+0.1532	42	V; non-circular
GSC 3208-2644 Lac	p	56228.6896(10)	+0.0223	22	V; el: IBVS 5998
GSC 3210-1456 Lac	s	56223.6278(4)	−0.0030	27	V; el: 55095.3968+0.372293×E
Z Lep	p	56238.8836(3)	+0.0617	45	V; el: JAAVSO 21, 111
RR Lep	p	56238.8796(3)	−0.0388	46	V
GSC 5916-1668 Lep	s	56254.8596(5)	+0.0096	36	V; el: IBVS 5992
NSV 2698 Lep	p	56265.8354(5)	+0.0038	23	V; el. IBVS 5894
CL Lyn	p	56290.8795(13)	+0.0022	20	V; el: 48500.18+1.586054×E
DY Lyn	p	56282.8914(16)	+0.0069	18	V; el: IBVS 5894
RU Mon	s	56251.8685(31)	−0.5977	23	V; non-circular
	p	56282.8397(4)	−0.0970	38	V
UV Mon	s	56279.946(4)	+0.010	37	V; el: Krakow Catalog; unique light curve
BP Mon	p	56279.8541(3)	−0.0823	36	V; el: 54111.772+2.057082×E
GG Mon	p	56279.8908(2)	+0.0068	37	V; el: Krajau Catalog
V383 Mon	p	56273.8634(6)	−0.0302	37	V
V464 Mon	p	56273.9068(5)	+0.0101	37	V; el: Krakow Catalog
V530 Mon	s	56273.8469(5)	+0.0112	38	V; el: IBVS 5992
V843 Mon	s	56279.8642(3)	+0.0123	38	V; el: Krakow Catalog
V873 Mon	s	56257.8802(2)	+0.0428	50	V; el: 54761.825+3.1966076×E
V900 Mon	p	56257.8920(2)	+0.0088	50	V; el: IBVS 5992
V925 Mon	p	56246.8787(19)	+0.0223	37	V; el: IBVS 6029; non-circular
GSC 174-675 Mon	s	56279.8521(5)	+0.0038	37	V; el: 53818.583+0.262409×E
GSC 4785-147 Mon	p	56257.9289(2)	+0.0265	49	V; el: IBVS 5992
GSC 4827-2862 Mon	p	56273.9018(3)	−0.0056	37	V; el: IBVS 5992
DZ Ori	p	56257.8432(4)	+0.0066	50	V; el: Krakow Catalog
EF Ori	s	56255.8945(9)	+0.0051	38	V; el: IBVS 5699
EH Ori	p	56255.8685(3)	+0.0135	38	V; el: 53414.658+1.5136905×E; d=0.019d
EQ Ori	p	56237.9499(2)	−0.0406	47	V
ER Ori	s	56239.9165(4)	+0.1071	52	V
EW Ori	p	56254.9519(5)	−0.0081	45	V; el: IBVS 6029; non-circular
FK Ori	p	56245.8087(16)	−0.0482	42	V
GG Ori	s	56245.8479(1)	−0.4339	26	V; non-circular
GU Ori	p	56256.9186(3)	+0.0024	49	V; el: ASAS; d=0.025d
V392 Ori	p	56256.9435(2)	+0.0312	49	V; el: PAS Japan 54, 139
V645 Ori	p	56255.9328(4)	+0.0115	38	V; el: 54140.693+1.0404468×E
V1027 Ori	p	56232.9108(3)	+0.0431	50	V; el: IBVS 6011; non-circular
V1353 Ori	s	56245.8835(4)	−0.0044	42	V; el: IBVS 5313
V1626 Ori	p	56255.9151(3)	−0.0057	38	V; el: IBVS 5339
V1642 Ori	p	56254.9031(2)	−0.0061	44	V; el: 53268.857+3.037693×E
V1799 Ori	p	56237.9093(2)	+0.0064	47	V; el: IBVS 5960
V1848 Ori	s	56238.9099(2)	−0.0008	47	V
V1851 Ori	s	56246.8793(4)	+0.0154	38	V
GSC 85-1357 Ori	p	56245.8774(4)	+0.0269	43	V; el: 53804.538+0.2839726×E
GSC 89-1424 Ori	p	56239.9112(4)	+0.0199	52	V; el: IBVS 5960; d=0.037d
GSC 93-668 Ori	s	56237.8965(2)	−0.0058	47	V; el: IBVS 5960
GSC 103-738 Ori	p	56238.8603(2)	+0.0006	47	V; el: IBVS 5960
GSC 103-894 Ori	s	56246.9167(4)	−0.0067	42	V; el: IBVS 5960
GSC 111-1902 Ori	p	56239.8877(4)	+0.0020	46	V; el: IBVS 5960

Table 1: Minima of eclipsing binaries (continued)

Variable	Type	HJD 24...	$O-C$	n	Remarks
GSC 122-419 Ori	p	56254.9137(3)	−0.0031	44	V; el: IBVS 5945
GSC 128-980 Ori	p	56265.8509(4)	−0.0041	24	V; el: IBVS 5960
GSC 4780-344 Ori	p	56265.8630(6)	−0.0019	23	V; el: IBVS 5960; d=0.016d
GSC 709-1047 Ori	s	56254.9233(4)	−0.0037	44	V; el: IBVS 5960
GSC 730-243 Ori	p	56256.9089(4)	+0.0029	49	V; el: IBVS 5960
GSC 730-2307 Ori	p	56256.8691(2)	−0.0378	49	V; el: IBVS 5960
GSC 1315-1104 Ori	p	56257.8596(4)	+0.0003	50	V; el: IBVS 5960
GSC 4741-1062 Ori	p	56237.9417(5)	−0.0025	44	V; el: 53806.546+2.448538×E
GSC 4754-44 Ori	p	56239.8962(2)	+0.0092	52	V; el: IBVS 5992; d=0.012d
GSC 4754-339 Ori	p	56246.8914(3)	+0.0016	42	V; el: IBVS 5992
GSC 4766-69 Ori	p	56254.8717(4)	+0.0070	44	V; el: IBVS 5960
GSC 4783-2332 Ori	p	56256.8764(4)	−0.0022	49	V; el: IBVS 5960
NSV 1864 Ori	s	56238.9063(3)	+0.0058	46	V; el: IBVS 6029; d=0.052d
ZZ Peg	p	56231.6857(3)	+0.1419	45	V; d=0.041d
BQ Peg	p	56220.7091(4)	+0.2528	42	V; d=0.030d
BX Peg	p	56214.6638(4)	−0.0083	43	V; el: IBVS 5668; d=0.020d
	p	56219.7116(3)	−0.0080	46	V
BY Peg	s	56203.6711(4)	−0.0261	50	V; d=0.025d
CC Peg	p	56220.6898(3)	−0.0133	42	V; el: IBVS 5960; d=0.045:d
CF Peg	s	56218.6962(5)	−0.0005	17	V; el: Krakow Catalog
DK Peg	p	56246.7005(3)	+0.1271	48	V; d=0.048d
DM Peg	p	56245.7068(4)	+0.0715	47	V
DV Peg	p	56215.6612(4)	−0.0090	48	V; el: IBVS 6011
EU Peg	p	56232.6571(3)	+0.0386	40	V
FL Peg	s	56203.6520(6)	−0.0187	22	V
GP Peg	p	56226.6952(3)	−0.0506	44	V
KW Peg	p	56219.7187(4)	−0.0018	42	V; el: Krakow Catalog
V407 Peg	p	56238.7230(6)	−0.0288	35	V
V411 Peg	p	56203.7118(5)	−0.0194	47	V; formerly BM Vul
V421 Peg	s	56258.6253(14)	−0.0079	22	V
A212654+1912.6 Peg	p	56215.6181(4)		25	V
	s	56215.789(4)		20	V
A215503+2417.8 Peg	s	56218.6936(7)	+0.0282	17	V; el: IBVS 6011
GSC 570-73 Peg	s	56228.6662(4)	+0.0012	24	V; el: IBVS 6011
GSC 573-1241 Peg	s	56228.6471(3)	−0.0034	27	V; el: IBVS 5920
GSC 1158-201 Peg	p	56230.6586(2)	+0.0044	49	V; el: 52910.692+1.242966×E; d=0.033d
GSC 1174-344 Peg	s	56239.6954(5)	+0.0142	35	V; el: IBVS 5920; d=0.036d
GSC 1178-1208 Peg	p	56251.7340(5)	+0.0064	33	V; el: IBVS 5920
GSC 1664-110 Peg	p	56203.6702(2)	+0.0111	49	V; el: 55079.738+0.282961×E
GSC 1677-992 Peg	s	56220.7042(4)	+0.0153	40	V; el: IBVS 6011; d=0.058:d
GSC 1686-1001 Peg	p	56228.7223(2)	+0.0002	27	V; el: IBVS 5920
GSC 1704-356 Peg	p	56230.6573(3)	+0.0066	52	V; el: IBVS 6011
GSC 1709-614 Peg	s	56230.719382)	+0.0038	43	V; el: IBVS 6011
GSC 1715-1370 Peg	p	56233.6504(3)	+0.0045	49	V; el: IBVS 5920
GSC 1716-1457 Peg	p	56233.6879(3)	+0.0195	49	V; el: IBVS 5920; d=0.022d
GSC 1718-1664 Peg	s	56233.6416(3)	−0.0089	28	V; el: IBVS 5920
	p	56233.7695(5)	−0.0100	21	V; d=0.011d
GSC 1721-1591 Peg	p	56238.7047(3)	−0.0186	38	V; el: 54307.796+0.318898×E
GSC 2188-568 Peg	p	56219.6773(2)	−0.0303	33	V; el: IBVS 5960
GSC 2189-1101 Peg	s	56218.7262(13)	+0.0021	17	V; el: IBVS 5960
	s	56219.6833(2)	+0.0000	12	V
GSC 2223-87 Peg	p	56228.6789(2)	−0.0109	27	V; el: IBVS 5920
GSC 2740-1859 Peg	p	56225.6626(3)	+0.0025	37	V; el: IBVS 6011
GSC 2744-1229 Peg	s	56227.7171(4)	+0.0254	34	V; el: PZP 11, 1
GSC 2749-2238 Peg	p	56227.7475(6)	+0.0541	37	V; el: OEJV 83
GSC 2755-2136 Peg	p	56225.7059(3)	+0.0231	36	V; el: IBVS 83
GSC 2766-775 Peg	s	56239.7130(4)	+0.0030	31	V; el: 53254.588+0.375747×E; d=0.035:d
BE Per	p	56233.9018(5)	+0.0363	44	V; el: MVS 11, 38
BY Per	p	56273.6476(3)	+0.0231	53	V
CH Per	p	56261.6898(3)	−0.0772	48	V

Table 1: Minima of eclipsing binaries (continued)

Variable	Type	HJD 24...	$O-C$	n	Remarks
DK Per	p	56203.8404(4)	−0.0430	50	V; el: IBVS 3875
FW Per	p	56232.8612(4)	−0.0373	50	V
IM Per	p	56227.9232(6)	+0.1032	27	V; non-circular
IT Per	p	56210.8556(5)	−0.0216	48	V
IU Per	p	56279.6932(3)	+0.0088	47	V
KL Per	p	56203.8859(2)	+0.1361	50	V; d=0.037d
KN Per	p	56233.8798(3)	+0.0088	44	V; el: Krakow Catalog, d=0.054d
NO Per	s	56202.960:(10)	−0.624	46	V; d>= 0.12d; non-circular
	p	56257.8376(8)	+0.1792	49	V; el: IBVS 6029
QT Per	p	56226.8816(4)	−0.0441	38	V; MVS 11, 65
QW Per	p	56233.8496(5)	+0.0078	45	V
V434 Per	p	56233.9215(5)	−0.0590	44	V
V450 Per	p	56215.9226(5)	+0.1184	45	V
V482 Per	p	56232.9677(6)	+0.2610	50	V; el: BAV Mit. 68, 21
V680 Per	s	56214.9626(3)	+0.0073	36	V; el: IBVS 5960
V723 Per	p	56202.9342(14)	+0.0305	47	V; el: IBVS 6011
V737 Per	p	56233.9545(4)	−0.0005	43	V; el: Krakow Catalog
V761 Per	p	56205.978(3)	+0.129	38	V; GSC 3698-3021
V789 Per	p	56214.8494(2)	+0.0931	36	V
V871 Per	s	56233.8950(3)	+0.1912	45	V; el: IBVS 5920; non-circular
V873 Per	p	56215.8368(4)	−0.0144	28	V
	s	56215.9849(12)	−0.013	12	V
V876 Per	s:	56226.8638(4)	+0.0137	38	V
V877 Per	p	56220.8373(19)	+0.0000	8	V; el: 53341.17+1.11098275×E
	p	56279.7233(4)	+0.0039	47	V
GSC 2344-92 Per	s	56227.9086(6)	+0.0446	38	V; el: PZP 11, 1
GSC 2361-2410 Per	s	56273.7191(2)	−0.0002	52	V; el: 55866.838+0.318249×E
GSC 2854-125 Per	p	56215.9328(25)		44	V
Y Psc	p	56239.6278(3)	−0.0130	35	V
VZ Psc	p	56231.6784(3)	+0.0107	45	V; el: ApJS 58, 413
EX Psc	p	56257.6600(2)	−0.0220	40	V; d=0.021d
GSC 14-479 Psc	s	56258.6587(4)	+0.0270	40	V; el: 54103.545+0.394091×E
GSC 24-466 Psc	s	56265.6660(3)	−0.0180	48	V; el: IBVS 6011; d=0.026d
GSC 575-429 Psc	p	56231.6721(8)	−0.0004	15	V; el: IBVS 5920
	s	56231.7870(10)	−0.0027	11	V
GSC 621-834 Psc	s	56265.6886(3)	+0.0118	48	V; el: IBVS 5920
GSC 1179-501 Psc	p	56257.6724(5)	+0.0242	40	V; el: IBVS 5960
GSC 1183-1110 Psc	p	56259.6614(7)	−0.0061	24	V; el: 54760.697+0.649186×E
GSC 1762-103 Psc	s	56265.6853(2)	−0.0241	48	V; el: IBVS 5960
GSC 5253-982 Psc	s	56239.7227(5)	+0.0065	35	V; el: 53615.898+0.521582×E; d=0.043d
GSC 5255-370 Psc	s	56239.6355(2)	+0.0089	36	V; el: IBVS 6011
UZ Pup	p	56282.8974(5)	−0.0113	36	V
AV Pup	p	56290.8767(15)	+0.0043	18	V; el: IBVS 5992
GSC 5404-4206 Pup	p	56282.8568(4)	−0.0086	33	V; el: IBVS 5894
GSC 5424-55 Pup	p	56282.9049(6)	−0.0029	32	V; el: IBVS 5992
AH Tau	s	56282.6621(4)	+0.0207	50	V; el: IBVS 5554; d=0.016d
AQ Tau	p	56245.9207(10)	−0.1055	43	V
EQ Tau	s	56290.6423(3)	−0.0254	41	V; d=0.017d
V1249 Tau	s	56215.9410(4)	−0.0078	44	V; non-circular
	p	56237.9234(2)	−0.0079	36	V
V1260 Tau	s	56239.9422(9)	+0.3332	52	V; non-circular
V1352 Tau	p	56257.9032(11)	−0.0258	50	V; el: IBVS 6011; d=0.115d; non-circular
V1355 Tau	s	56245.9238(6)	−0.0350	22	V
V1356 Tau	s	56238.799(4)	+0.785	47	V; el: Krakow Catalog; non-circular
GSC 67-348 Tau	p	56282.6899(3)	+0.0093	48	V; el: IBVS 5920
GSC 74-465 Tau	s	56231.8923(4)	−0.0073	49	V; el: IBVS 5960; d=0.020d
GSC 76-527 Tau	s	56231.8865(3)	+0.0027	50	V; el: IBVS 5945
GSC 650-1226 Tau	s	56227.9428(3)	+0.0195	38	V; el: IBVS 5945
GSC 658-185 Tau	p	56290.7072(3)	+0.0089	41	V; el: IBVS 5920; asymmetric light curve
GSC 661-580 Tau	s	56282.6371(5)	−0.0022	27	V; el: IBVS 5945

Table 1: Minima of eclipsing binaries (continued)

Variable	Type	HJD 24...	$O-C$	n	Remarks
GSC 663-23 Tau	s	56282.6782(9)	−0.0035	50	V; el: IBVS 5920; d=0.047d
GSC 1235-663 Tau	p	56290.6815(4)	−0.0026	41	V; el: IBVS 5992; d=0.022d
GSC 1256-188 Tau	p	56227.8921(5)	+0.0136	36	V; el: IBVS 5920; d=0.025d
GSC 1291-1139 Tau	p	56239.8626(3)	−0.0161	53	V; el: IBVS 5992; d=0.039d
GSC 1304-227 Tau	s	56254.9299(1)	+0.0021	45	V; el: IBVS 5960
GSC 2258-1489 Tau	s:	56243.6613(12)		18	V
RW Tri	p	56279.6872(2)	−0.0037	47	V
VW Tri	p	56205.8516(5)	−0.0345	39	V; el: MVS 11, 1
VZ Tri	p	56273.7018(1)	−0.0111	52	V; el: OEJV 107; d=0.022d
BF Tri	s:	56265.6859(4)	−0.0527	48	V
CC Tri	s	56279.7398(6)	−0.0933	47	V
CM Tri	p:	56210.8790(3)	−0.0610	49	V
CR Tri	p:	56210.8999(4)	−0.0116	41	V
BG Vul	s	56205.6710(5)	−0.1598	19	V; asymmetric; d=0.034d
BI Vul	p	56205.6532(6)	+0.0077	13	V; el: IBVS 6011
	s	56205.7826(5)	+0.0112	8	V
V384 Vul	s	56215.6261(5)	+0.0022	48	V
GSC 2177-709 Vul	p	56205.6873(5)	+0.0032	47	V; el: IBVS 6011

n: number of measurements incorporated in the determination of the minimum time.
d: Time spent by star in totality at minimum.
D: total duration of the eclipse.
A: ASAS ; U: UCAC3

References:

Agerer, F., 2001, *IBVS*, No. 5212
Agerer, F., 2010, *PZP*, **10**, 13
Agerer, F. et al., 1988, *IBVS*, No. 3234
Agerer, F. et al., 1994, *BAV Mitt.*, **69**, 1
Agerer, F. et al., 1996, *IBVS*, No. 4381
Agerer, F., Hübscher, J., 2001, *IBVS*, No. 5016
Bakis, V. et al., 2005, *IBVS*, No. 5616
Blättler, E., Diethelm, R., 2001, *IBVS*, No. 5151
Borkovits, T. et al., 2002, *IBVS*, No. 5313
Bradstreet, D. H., 1985, *ApJ Suppl.*, **58**, 413
Brat, L. et al., 2009, *OEJV*, No. 107
Byboth, K. N. et al., 2004, *IBVS*, No. 5554
Degirmenci, O.L. et al., 2003, *IBVS*, No. 5386
Diethelm, R., 1990, *BBSAG Bull.*, **96**, 10
Diethelm, R., 2009, *IBVS*, No. 5871
Diethelm, R., 2009, *IBVS*, No. 5894
Diethelm, R., 2010, *IBVS*, No. 5920
Diethelm, R., 2010, *IBVS*, No. 5945
Diethelm, R., 2011, *IBVS*, No. 5960
Diethelm, R., 2011, *IBVS*, No. 5992
Diethelm, R., 2012, *IBVS*, No. 6011
Diethelm, R., 2012, *IBVS*, No. 6029
Djurasevic, G. et al., 1998, *A&A Suppl.*, **131**, 17
Evans III E. et al., 1985, *PASP*, 97, 648
Gessner, H., 1987, *MVS*, **11**, 38
Gessner, H., 1987, *MVS*, **11**, 65

Hübscher, J., Agerer, F., Frank, P., Wunder, E., 1994, *BAV Mitt.*, **68**, 1
Khruslov, A.V., 2010, *PZP*, **10**, 18
Khruslov, A.V., 2010, *PZP*, **10**, 29
Khruslov, A.V., 2011, *PZP*, **11**, 1
Kozyreva, V.S. et al., 2012, *IBVS*, No. 6020
Kreiner, J.M., 2004, *AcA*, **54**, 207 Krakow Catalog
Lacy, C. et al., 1997, *AJ*, **114**, 1206
Lewandowski, M. et al., 2009, *OEJV*, No. 104
Liakos, A., Niarchos, P., 2010, *IBVS*, No. 5998
Lister, T.A., McDermid, R.M., Hilditch, R.W., 2000, *MNRAS*, **317**, 111
Lloyd, C. et al., 2001, *IBVS*, No. 5111
Lloyd, C. et al., 2002, *IBVS*, No. 5339
Meinunger, L., 1984, *MitVS*, **10**, 56
Meinunger, L., 1986, *MitVS*, **11**, 1
Metcalfe, T., 1997, *IBVS*, No. 4482
Narusawa, S. et al., 2002, *PASJ*, **54**, 139
Nelson, R.H., 2006, *IBVS*, No. 5699
Otero, S.A., Dubovsky, P.A., 2004, *IBVS*, No. 5557
Otero, S.A. et al., 2004, *IBVS*, No. 5570
Otero, S.A., Wils, P., 2005, *IBVS*, No. 5630
Otero, S.A. et al., 2006, *IBVS*, No. 5674
Otero, S.A., 2008, *OEJV*, No. 83
Otero, S.A., 2008, *OEJV*, No. 91
Paschke, A., 2009, *OEJV*, No. 116
Pribulla, T. et al., 2005, *IBVS*, No. 5668
Ragazzoni, R., Barbieri, C., 1996, *IBVS*, No. 4293
Samolyk, G., 1992, *JAAVSO*, **21**, 111
Samus, N.N. et al., 2012, General catalogue of Variable Stars
Silhan, J., 1990, *JAAVSO*, 19, 12
Siviero, A. et al., 2010, *IBVS*, No. 5936
Vandenbroere, J. et al., 2001, *IBVS*, No. 5020
Von Poschinger, K. et al., 2006, *BAV Rb.*, **55**, 1
Wolf, M. et al., 2006, *IBVS*, No. 5682
Zakirov, M.M., Azimov, A.A., 1993, *IBVS*, No. 3875
Zhang, J. et al., 1985, *IBVS*, No. 2652

*This version of the paper contains corrections, and differs from the one appeared on-line originally. Date of last modification: Thu Jan 17 13:19:11 CET 2013

COMMISSIONS 27 AND 42 OF THE IAU
INFORMATION BULLETIN ON VARIABLE STARS

Number 6043

Konkoly Observatory
Budapest
15 January 2013

HU ISSN 0374 – 0676

THE GEOS RR Lyr SURVEY

Fifteenth list of maxima of RR Lyr stars observed by the automated telescopes TAROT

(GEOS Circular RR 51)

LE BORGNE, J. F.[1,2,3]; KLOTZ, A.[2,3,4]; BOËR, M.[5]

[1] GEOS (Groupe Européen d'Observations Stellaires), 23 Parc de Levesville, 28300 Bailleau l'Evêque, France

[2] Université de Toulouse; UPS-OMP; IRAP; Toulouse, France

[3] CNRS; IRAP; 14, avenue Edouard Belin, F-31400 Toulouse, France

[4] Observatoire de Haute-Provence, Saint Michel l'Observatoire, France

[5] Artémis, CNRS, Observatoire de la Côte d'Azur, Université de Nice Sophia Antipolis, Nice, France

We present here the fifteenth list of light maxima of RR Lyrae stars from the GEOS RR Lyr Survey (Le Borgne et al. 2007), a GEOS program (`http://geos.webs.upv.es/`, Boninsegna et al., 2002) of observations of RR Lyr stars using the automatic telescopes TAROT (`http://tarot.obs-hp.fr`, Klotz et al., 2009). The present list contains 2157 maxima (Table 1) observed between January and December 2012 and 2 older maxima recovered from Tarot image archive. A description of the present list may be found in the former lists (for example Le Borgne et al. 2008). The data are also available in the GEOS RR Lyr web database (`http://rr-lyr.ast.obs-mip.fr/dbrr/dbrr-V1.0_0.php`). The $O-C$'s are computed with recent GCVS elements (Samus et al., 2011) when available. Otherwise, the reference of the elements, if exists, is given as a footnote of Table 1. It concerns 281 stars of RRab type and 2 of RRc type (NU And and V1028 Oph). Large $O-C$ values are observed for some stars for which there is a need to update elements.

References:

Agerer, F., Moschner, W., 1996, *IBVS*, **4391**

Baldwin, M.E., Samolyk, G., 2003, *AAVSO RR Lyrae Monographs*, **1**

Boninsegna, R., 1990, *JAAVSO*, **19**, 126

Boninsegna, R., Vandenbroere, J., Le Borgne, J. F., The GEOS Team, 2002, IAU Colloq. 185, *ASP Conf. Ser.*, **259**, 166

Klotz, A., Boër, M., Atteia, J. L., Gendre, B., 2009, AJ, 137, 4100

Le Borgne, J. F., Klotz, A., Boër, 2008, *IBVS*, **5823**

Le Borgne, J. F., Paschke, A., Vandenbroere, J., Poretti, E., Klotz, A., Boër, M., Damerdji, Y., Martignoni, M., Acerbi, F., 2007, *A&A*, **476**, 307

Samus N.N., Durlevich O.V., Kazarovets E V., Kireeva N.N., Pastukhova E.N., Zharova A.V., et al. General Catalog of Variable Stars (GCVS database, Version 2011Jan, http://www.sai.msu.su/gcvs/gcvs/index.htm)

Vandenbroere, J., 1995, *IBVS*, **4241**

Vandenbroere, J., Paris, B., Verrot, J.P., 1999, *IBVS*, **4815**

Table 1: maxima of RR Lyrae stars

Variable star	Maximum HJD 24...	$O-C$ (days)	E	Obs.	Variable star	Maximum HJD 24...	$O-C$ (days)	E	Obs.
SW And	56137.465±0.002	0.003	5431	C	DM And	56204.524±0.004	0.146	4575	C
SW And	56140.560±0.001	0.003	5438	C	DR And	56136.544±0.002	−0.078	6244	C
SW And	56141.445±0.002	0.003	5440	C	DR And	56140.482±0.003	−0.082	6251	C
SW And	56160.462±0.002	0.002	5483	C	DR And	56153.410±0.003	−0.106	6274	C
SW And	56164.442±0.001	0.003	5492	C	DR And	56154.545±0.003	−0.097	6276	C
SW And	56167.539±0.001	0.003	5499	C	DR And	56163.569±0.002	−0.084	6292	C
SW And	56168.421±0.002	0.001	5501	C	DR And	56198.482±0.005	−0.085	6354	C
SW And	56178.599±0.003	0.007	5524	C	DR And	56210.293±0.004	−0.099	6375	C
SW And	56182.572±0.002	−0.001	5533	C	DR And	56219.314±0.004	−0.088	6391	C
SW And	56186.555±0.002	0.002	5542	C	DR And	56239.600±0.002	−0.075	6427	C
SW And	56195.400±0.003	0.002	5562	C	DR And	56247.482±0.001	−0.077	6441	C
SW And	56205.572±0.002	0.002	5585	C	DR And	56250.295±0.002	−0.079	6446	C
SW And	56210.437±0.001	0.002	5596	C	DR And	56264.356±0.005	−0.097	6471	C
SW And	56216.629±0.002	0.002	5610	C	DR And	56265.474±0.004	−0.105	6473	C
SW And	56264.393±0.002	0.002	5718	C	NU And	56247.475±0.010	0.085	56121	C
SW And	56265.277±0.002	0.002	5720	C	NU And	56250.307±0.011	0.096	56130	C
XX And	56139.468±0.005	0.005	3427	C	NU And	56264.394±0.010	0.073	56175	C
XX And	56152.474±0.002	0.001	3445	C	NX And	56139.456±0.005	0.009	27001	C
XX And	56160.427±0.003	0.004	3456	C	NX And	56152.417±0.003	0.009	27021	C
XX And	56162.592±0.002	0.001	3459	C	NX And	56214.622±0.003	0.002	27117	C
XX And	56168.381±0.003	0.007	3467	C	WY Ant	55991.670±0.003	0.006	13043	LS
XX And	56170.546±0.003	0.004	3470	C	WY Ant	56018.668±0.002	0.010	13090	LS
XX And	56181.387±0.004	0.004	3485	C	WY Ant	56026.713±0.004	0.015	13104	LS
XX And	56188.611±0.002	0.000	3495	C	WY Ant	56056.575±0.005	0.011	13156	LS
XX And	56214.630±0.003	0.000	3531	C	BK Ant	55972.673±0.003	0.015	5492	LS
XX And	56244.264±0.002	0.001	3572	C	BK Ant	55973.710±0.005	0.019	5494	LS
XX And	56288.354±0.002	0.003	3633	C	BK Ant	55974.739±0.003	0.015	5496	LS
XX And	56293.414±0.002	0.004	3640	C	BK Ant	55991.792±0.005	0.021	5529	LS
AT And	56123.445±0.005	0.015	4597	C	BK Ant	56001.598±0.002	0.012	5548	LS
AT And	56126.530±0.004	0.015	4602	C	BK Ant	56002.638±0.003	0.019	5550	LS
AT And	56134.550±0.004	0.015	4615	C	BK Ant	56047.580±0.003	0.019	5637	LS
AT And	56142.569±0.004	0.014	4628	C	BK Ant	56286.750±0.004	0.017	6100	LS
AT And	56168.477±0.003	0.012	4670	C	BN Ant	55934.776±0.002	0.090	5772	LS
AT And	56178.357±0.006	0.021	4686	C	BN Ant	55964.788±0.002	0.092	5828	LS
AT And	56179.580±0.007	0.011	4688	C	BN Ant	55992.655±0.002	0.092	5880	LS
AT And	56195.617±0.003	0.008	4714	C	BN Ant	56291.704±0.002	0.108	6438	LS
AT And	56197.471±0.003	0.011	4717	C	BN Ant	56292.775±0.002	0.108	6440	LS
AT And	56234.489±0.003	0.014	4777	C	TY Aps	55979.695±0.005	0.056	32397	LS
AT And	56247.435±0.003	0.005	4798	C	TY Aps	55981.700±0.002	0.054	32401	LS
AT And	56249.298±0.005	0.017	4801	C	TY Aps	55982.706±0.002	0.057	32403	LS
AT And	56252.376±0.004	0.011	4806	C	TY Aps	55990.732±0.002	0.056	32419	LS
AT And	56263.483±0.005	0.013	4824	C	TY Aps	55994.742±0.002	0.052	32427	LS
AT And	56265.333±0.005	0.013	4827	C	TY Aps	55996.754±0.002	0.057	32431	LS
CI And	56161.575±0.001	−0.011	9737	C	TY Aps	56000.768±0.002	0.058	32439	LS
CI And	56162.546±0.002	−0.011	9739	C	TY Aps	56022.833±0.002	0.048	32483	LS
CI And	56163.514±0.001	−0.012	9741	C	TY Aps	56024.836±0.001	0.044	32487	LS
CI And	56167.392±0.002	−0.011	9749	C	TY Aps	56029.853±0.002	0.044	32497	LS
CI And	56182.418±0.002	−0.012	9780	C	TY Aps	56078.527±0.002	0.054	32594	LS
CI And	56193.568±0.002	−0.011	9803	C	TY Aps	56079.532±0.002	0.056	32596	LS
CI And	56208.593±0.002	−0.012	9834	C	TY Aps	56108.632±0.002	0.057	32654	LS
CI And	56234.293±0.005	−0.003	9887	C	VX Aps	55997.715±0.002	−0.167	44902	LS
CI And	56263.380±0.002	0.001	9947	C	VX Aps	55998.685±0.002	−0.167	44904	LS
CI And	56264.349±0.002	0.000	9949	C	VX Aps	56008.859±0.002	−0.169	44925	LS
CI And	56280.340±0.002	−0.005	9982	C	VX Aps	56023.880±0.002	−0.170	44956	LS
CI And	56291.491±0.002	−0.003	10005	C	VX Aps	56025.816±0.002	−0.172	44960	LS
CI And	56293.428±0.001	−0.004	10009	C	VX Aps	56026.782±0.005	−0.175	44962	LS

Table 1 (cont.): maxima of RR Lyrae stars

Variable star	Maximum HJD 24...	$O-C$ (days)	E	Obs	Variable star	Maximum HJD 24...	$O-C$ (days)	E	Obs.
VX Aps	56039.868±0.001	−0.173	44989	LS	EX Aps	56172.635±0.002	0.017	59854	LS
VX Aps	56055.863±0.002	−0.169	45022	LS	EX Aps	56182.543±0.001	0.018	59875	LS
VX Aps	56056.833±0.001	−0.168	45024	LS	EX Aps	56198.583±0.001	0.017	59909	LS
VX Aps	56057.803±0.001	−0.167	45026	LS	EX Aps	56199.527±0.002	0.018	59911	LS
VX Aps	56070.893±0.002	−0.161	45053	LS	SW Aqr	56120.550±0.001	0.023	7019	C
VX Aps	56082.528±0.002	−0.156	45077	LS	SW Aqr	56121.468±0.002	0.023	7021	C
VX Aps	56105.798±0.002	−0.145	45125	LS	SW Aqr	56148.567±0.002	0.023	7080	C
VX Aps	56110.646±0.002	−0.143	45135	LS	SW Aqr	56160.510±0.002	0.024	7106	C
VX Aps	56129.549±0.002	−0.138	45174	LS	SW Aqr	56161.428±0.002	0.024	7108	C
VX Aps	56160.567±0.002	−0.134	45238	LS	SW Aqr	56177.503±0.002	0.023	7143	C
VX Aps	56161.534±0.002	−0.136	45240	LS	SW Aqr	56181.636±0.001	0.022	7152	LS
XZ Aps	55982.731±0.002	−0.110	46418	LS	SW Aqr	56206.439±0.001	0.023	7206	C
XZ Aps	55986.842±0.002	−0.111	46425	LS	SW Aqr	56219.299±0.002	0.023	7234	C
XZ Aps	55989.779±0.002	−0.112	46430	LS	SX Aqr	56109.766±0.002	−0.003	4157	LS
XZ Aps	55996.824±0.001	−0.116	46442	LS	SX Aqr	56120.478±0.001	−0.006	4177	C
XZ Aps	55999.764±0.002	−0.113	46447	LS	SX Aqr	56124.763±0.002	−0.006	4185	LS
XZ Aps	56013.857±0.002	−0.118	46471	LS	SX Aqr	56128.514±0.001	−0.005	4192	C
XZ Aps	56022.669±0.002	−0.118	46486	LS	SX Aqr	56131.728±0.002	−0.005	4198	LS
XZ Aps	56023.841±0.002	−0.121	46488	LS	SX Aqr	56135.479±0.002	−0.004	4205	C
XZ Aps	56038.525±0.002	−0.123	46513	LS	SX Aqr	56138.695±0.002	−0.003	4211	LS
XZ Aps	56048.505±0.002	−0.129	46530	LS	SX Aqr	56146.729±0.002	−0.004	4226	LS
XZ Aps	56049.681±0.002	−0.128	46532	LS	SX Aqr	56149.408±0.001	−0.003	4231	C
XZ Aps	56050.853±0.002	−0.130	46534	LS	SX Aqr	56150.478±0.002	−0.005	4233	C
XZ Aps	56055.553±0.002	−0.130	46542	LS	SX Aqr	56160.657±0.002	−0.004	4252	LS
XZ Aps	56109.583±0.002	−0.144	46634	LS	SX Aqr	56175.656±0.002	−0.005	4280	LS
XZ Aps	56110.757±0.002	−0.145	46636	LS	SX Aqr	56186.372±0.002	−0.003	4300	C
XZ Aps	56113.692±0.001	−0.147	46641	LS	SX Aqr	56187.443±0.003	−0.004	4302	C
XZ Aps	56146.580±0.002	−0.156	46697	LS	SX Aqr	56189.586±0.001	−0.004	4306	LS
BS Aps	55998.834±0.003	0.027	31892	LS	SX Aqr	56230.299±0.002	−0.005	4382	C
BS Aps	56011.639±0.003	0.016	31914	LS	TZ Aqr	56120.723±0.002	0.021	5599	LS
BS Aps	56022.710±0.003	0.018	31933	LS	TZ Aqr	56129.864±0.002	0.023	5615	LS
BS Aps	56026.795±0.006	0.025	31940	LS	TZ Aqr	56147.569±0.003	0.021	5646	C
BS Aps	56053.590±0.003	0.023	31986	LS	TZ Aqr	56148.715±0.003	0.024	5648	LS
BS Aps	56054.751±0.004	0.019	31988	LS	TZ Aqr	56150.428±0.002	0.024	5651	C
BS Aps	56082.715±0.005	0.020	32036	LS	TZ Aqr	56159.568±0.002	0.025	5667	C
BS Aps	56083.878±0.002	0.018	32038	LS	TZ Aqr	56160.708±0.003	0.022	5669	LS
BS Aps	56086.791±0.003	0.018	32043	LS	TZ Aqr	56182.413±0.003	0.022	5707	C
BS Aps	56110.676±0.002	0.018	32084	LS	TZ Aqr	56192.694±0.003	0.022	5725	LS
BS Aps	56120.573±0.002	0.012	32101	LS	WZ Aqr	56103.767±0.002	−0.027	5244	LS
BS Aps	56135.730±0.004	0.022	32127	LS	WZ Aqr	56109.695±0.002	−0.030	5256	LS
BS Aps	56138.645±0.004	0.025	32132	LS	WZ Aqr	56149.737±0.003	−0.024	5337	LS
BS Aps	56169.504±0.003	0.008	32185	LS	YZ Aqr	56102.783±0.002	0.004	5827	LS
EX Aps	56009.867±0.001	0.020	59509	LS	YZ Aqr	56108.850±0.002	−0.000	5838	LS
EX Aps	56020.714±0.002	0.017	59532	LS	YZ Aqr	56124.864±0.002	0.008	5867	LS
EX Aps	56054.686±0.003	0.019	59604	LS	YZ Aqr	56164.598±0.002	0.002	5939	LS
EX Aps	56059.874±0.002	0.017	59615	LS	YZ Aqr	56165.699±0.003	−0.000	5941	LS
EX Aps	56084.881±0.002	0.018	59668	LS	AA Aqr	56101.826±0.002	−0.022	4142	LS
EX Aps	56099.506±0.002	0.018	59699	LS	AA Aqr	56126.792±0.002	−0.021	4183	LS
EX Aps	56101.864±0.002	0.017	59704	LS	AA Aqr	56134.706±0.002	−0.023	4196	LS
EX Aps	56109.886±0.002	0.018	59721	LS	AA Aqr	56162.713±0.002	−0.024	4242	LS
EX Aps	56113.659±0.001	0.017	59729	LS	AA Aqr	56165.758±0.002	−0.023	4247	LS
EX Aps	56124.511±0.002	0.017	59752	LS	BN Aqr	56103.818±0.001	0.411	6819	LS
EX Aps	56139.614±0.004	0.023	59784	LS	BN Aqr	56110.865±0.002	0.413	6834	LS
EX Aps	56148.573±0.001	0.017	59803	LS	BN Aqr	56136.694±0.002	0.410	6889	LS
EX Aps	56149.515±0.003	0.016	59805	LS	BN Aqr	56147.498±0.002	0.411	6912	C
EX Aps	56171.691±0.002	0.017	59852	LS	BN Aqr	56149.848±0.002	0.412	6917	LS

Table 1 (cont.): maxima of RR Lyrae stars

Variable star	Maximum HJD 24...	$O-C$ (days)	E	Obs	Variable star	Maximum HJD 24...	$O-C$ (days)	E	Obs.
BN Aqr	56154.544±0.003	0.411	6927	C	AA Aql	56183.596±0.001	0.039	87997	LS
BN Aqr	56158.771±0.001	0.412	6936	LS	AA Aql	56191.554±0.001	0.038	88019	LS
BN Aqr	56175.676±0.002	0.408	6972	LS	AA Aql	56206.389±0.001	0.039	88060	C
BN Aqr	56182.724±0.001	0.410	6987	LS	V341 Aql	56102.864±0.002	0.041	25789	LS
BN Aqr	56204.333±0.002	0.414	7033	C	V341 Aql	56129.452±0.002	0.040	25835	C
BN Aqr	56206.677±0.004	0.410	7038	LS	V341 Aql	56137.542±0.002	0.038	25849	C
BN Aqr	56219.359±0.002	0.410	7065	C	V341 Aql	56151.419±0.003	0.043	25873	C
BO Aqr	56102.824±0.002	0.024	4582	LS	V341 Aql	56159.509±0.002	0.041	25887	C
BO Aqr	56166.675±0.002	0.024	4674	LS	V341 Aql	56160.662±0.002	0.038	25889	LS
BO Aqr	56184.723±0.002	0.028	4700	LS	V341 Aql	56164.711±0.003	0.040	25896	LS
BR Aqr	56121.860±0.002	0.003	8411	LS	V341 Aql	56192.455±0.002	0.039	25944	C
BR Aqr	56135.833±0.002	0.002	8440	LS	S Ara	55384.566±0.005	−0.049	5798	LS
BR Aqr	56137.758±0.001	−0.000	8444	LS	S Ara	55412.581±0.002	−0.049	5860	LS
BR Aqr	56138.723±0.002	0.001	8446	LS	S Ara	56105.776±0.002	−0.005	7394	LS
BR Aqr	56155.588±0.002	0.001	8481	C	S Ara	56114.813±0.002	−0.005	7414	LS
BR Aqr	56157.518±0.002	0.003	8485	C	S Ara	56115.718±0.002	−0.004	7416	LS
BR Aqr	56163.780±0.001	0.001	8498	LS	S Ara	56147.799±0.002	−0.005	7487	LS
BR Aqr	56178.721±0.002	0.003	8529	LS	IN Ara	56053.789±0.004	0.044	5148	LS
BR Aqr	56181.608±0.002	−0.000	8535	LS	IN Ara	56079.668±0.002	0.032	5189	LS
BR Aqr	56191.729±0.002	0.001	8556	LS	IN Ara	56086.620±0.002	0.037	5200	LS
BR Aqr	56204.741±0.002	0.003	8583	LS	IN Ara	56105.532±0.002	0.005	5230	LS
BR Aqr	56219.679±0.003	0.003	8614	LS	MS Ara	56062.708±0.003	−0.052	5989	LS
BR Aqr	56220.642±0.002	0.002	8616	LS	MS Ara	56086.858±0.003	−0.052	6035	LS
BT Aqr	56183.414±0.003	0.003	8115	C	MS Ara	56101.556±0.004	−0.053	6063	LS
BT Aqr	56192.352±0.001	0.001	8137	C	MS Ara	56116.781±0.002	−0.053	6092	LS
BT Aqr	56205.356±0.002	0.001	8169	C	MS Ara	56145.656±0.003	−0.052	6147	LS
CP Aqr	56100.831±0.002	0.011	8645	LS	MS Ara	56175.583±0.002	−0.049	6204	LS
CP Aqr	56123.535±0.001	0.008	8694	C	X Ari	55951.400±0.002	0.038	4694	C
CP Aqr	56129.558±0.002	0.007	8707	C	X Ari	56182.564±0.003	0.039	5049	C
CP Aqr	56162.461±0.002	0.008	8778	C	X Ari	56193.638±0.003	0.043	5066	C
CP Aqr	56176.362±0.002	0.007	8808	C	X Ari	56195.589±0.001	0.041	5069	C
CP Aqr	56188.410±0.002	0.007	8834	C	X Ari	56197.545±0.002	0.043	5072	C
DN Aqr	56105.802±0.004	−0.005	6425	LS	X Ari	56208.615±0.002	0.044	5089	C
DN Aqr	56131.794±0.005	0.003	6466	LS	X Ari	56210.570±0.002	0.045	5092	C
DN Aqr	56138.762±0.005	−0.001	6477	LS	X Ari	56225.547±0.002	0.045	5115	C
DN Aqr	56192.629±0.004	−0.003	6562	LS	X Ari	56236.613±0.002	0.042	5132	C
DN Aqr	56204.667±0.005	−0.007	6581	LS	X Ari	56246.382±0.002	0.043	5147	C
DN Aqr	56216.704±0.003	−0.011	6600	LS	X Ari	56263.309±0.003	0.040	5173	C
DN Aqr	56230.648±0.006	−0.010	6622	LS	X Ari	56278.287±0.003	0.041	5196	C
OX Aqr	56137.823±0.004	0.081	6041	LS	SY Ari	56226.439±0.003	−0.018	4658	C
OX Aqr	56164.798±0.003	0.081	6092	LS	TZ Aur	55929.462±0.001	0.003	5561	C
OX Aqr	56189.659±0.004	0.084	6139	LS	TZ Aur	55982.336±0.001	0.001	5696	C
OX Aqr	56216.631±0.004	0.081	6190	LS	TZ Aur	56203.634±0.002	0.002	6261	C
OX Aqr	56234.613±0.004	0.080	6224	LS	TZ Aur	56225.568±0.001	0.003	6317	C
AA Aql	56075.784±0.002	0.040	87699	LS	TZ Aur	56230.660±0.001	0.003	6330	C
AA Aql	56104.725±0.002	0.038	87779	LS	TZ Aur	56250.634±0.002	0.001	6381	C
AA Aql	56118.474±0.001	0.039	87817	C	BH Aur	56188.508±0.002	0.005	5335	C
AA Aql	56118.835±0.001	0.038	87818	LS	BH Aur	56192.612±0.001	0.004	5344	C
AA Aql	56122.454±0.001	0.039	87828	C	BH Aur	56197.629±0.002	0.005	5355	C
AA Aql	56126.433±0.001	0.039	87839	C	BH Aur	56198.537±0.003	−0.000	5357	C
AA Aql	56136.564±0.002	0.040	87867	C	BH Aur	56214.504±0.002	0.004	5392	C
AA Aql	56137.647±0.002	0.037	87870	LS	BH Aur	56225.451±0.002	0.005	5416	C
AA Aql	56148.502±0.002	0.039	87900	C	BH Aur	56239.589±0.002	0.003	5447	C
AA Aql	56155.377±0.003	0.040	87919	C	BH Aur	56256.464±0.002	0.004	5484	C
AA Aql	56158.631±0.001	0.038	87928	LS	BH Aur	56278.357±0.002	0.004	5532	C
AA Aql	56161.525±0.002	0.037	87936	C	BH Aur	56279.266±0.002	0.001	5534	C

Table 1 (cont.): maxima of RR Lyrae stars

Variable star	Maximum HJD 24...	$O-C$ (days)	E	Obs	Variable star	Maximum HJD 24...	$O-C$ (days)	E	Obs.
BH Aur	56292.497±0.002	0.005	5563	C	AH Cam	56195.524±0.002	−0.523	47369	C
RS Boo	55937.679±0.002	−0.010	19710	C	AH Cam	56219.526±0.002	−0.489	47434	C
RS Boo	55945.600±0.002	−0.013	19731	C	AH Cam	56228.341±0.003	−0.524	47458	C
RS Boo	55971.634±0.002	−0.015	19800	C	AH Cam	56229.468±0.004	−0.503	47461	C
RS Boo	55979.559±0.002	−0.014	19821	C	AH Cam	56237.559±0.003	−0.524	47483	C
RS Boo	55987.487±0.002	−0.010	19842	C	AH Cam	56240.527±0.003	−0.506	47491	C
RS Boo	55994.652±0.002	−0.014	19861	C	AH Cam	56249.352±0.003	−0.531	47515	C
RS Boo	55995.408±0.002	−0.014	19863	C	AH Cam	56252.338±0.002	−0.494	47523	C
RS Boo	56016.537±0.002	−0.016	19919	C	AH Cam	56263.403±0.003	−0.491	47553	C
RS Boo	56053.520±0.002	−0.012	20017	C	AH Cam	56292.493±0.002	−0.531	47632	C
RS Boo	56070.499±0.002	−0.013	20062	C	RW Cnc	55996.572±0.001	0.211	30044	C
ST Boo	55995.696±0.004	0.089	12045	C	RW Cnc	56011.354±0.002	0.219	30071	C
ST Boo	56010.626±0.001	0.084	12069	C	RW Cnc	56013.539±0.003	0.215	30075	C
ST Boo	56025.561±0.002	0.084	12093	C	RW Cnc	56252.667±0.002	0.217	30512	C
ST Boo	56038.625±0.002	0.080	12114	C	SS Cnc	55996.536±0.001	0.061	89612	C
ST Boo	56050.444±0.002	0.076	12133	C	SS Cnc	56230.528±0.001	0.059	90249	C
ST Boo	56081.545±0.003	0.062	12183	C	SS Cnc	56248.529±0.001	0.060	90298	C
ST Boo	56101.454±0.002	0.058	12215	C	SS Cnc	56284.529±0.002	0.061	90396	C
SW Boo	56001.437±0.002	0.009	4792	C	TT Cnc	55930.659±0.004	0.106	28372	C
SW Boo	56005.545±0.001	0.008	4800	C	TT Cnc	55950.388±0.002	0.114	28407	C
SW Boo	56017.357±0.002	0.009	4823	C	TT Cnc	55973.495±0.002	0.120	28448	C
SW Boo	56019.413±0.003	0.010	4827	C	TT Cnc	56003.340±0.003	0.102	28501	C
SW Boo	56037.386±0.002	0.009	4862	C	TT Cnc	56279.435±0.005	0.106	28991	C
SW Boo	56058.443±0.002	0.010	4903	C	AN Cnc	55996.336±0.003	0.153	32340	C
SW Boo	56081.551±0.002	0.009	4948	C	AN Cnc	56010.456±0.002	0.151	32366	C
SW Boo	56100.552±0.002	0.008	4985	C	AN Cnc	56245.644±0.004	0.151	32799	C
TW Boo	55966.622±0.003	−0.034	8279	C	AN Cnc	56250.530±0.003	0.149	32808	C
TW Boo	55975.669±0.001	−0.035	8296	C	AQ Cnc	55960.638±0.002	−0.079	41857	C
TW Boo	56054.446±0.002	−0.035	8444	C	AQ Cnc	55969.418±0.002	−0.075	41873	C
TW Boo	56064.558±0.001	−0.036	8463	C	AQ Cnc	55981.480±0.002	−0.080	41895	C
UU Boo	55989.486±0.001	0.004	3278	C	AQ Cnc	55986.419±0.003	−0.078	41904	C
UU Boo	56011.420±0.002	0.005	3326	C	AQ Cnc	55998.486±0.002	−0.079	41926	C
UU Boo	56025.584±0.002	0.003	3357	C	AQ Cnc	56014.391±0.003	−0.081	41955	C
UU Boo	56038.378±0.001	0.004	3385	C	AQ Cnc	56243.675±0.002	−0.078	42373	C
UU Boo	56084.528±0.001	0.003	3486	C	AS Cnc	55995.487±0.001	0.390	27197	C
UU Boo	56100.522±0.002	0.005	3521	C	AS Cnc	56013.395±0.002	0.390	27226	C
XX Boo	55989.616±0.003	−0.111	4307	C	AS Cnc	56026.367±0.002	0.394	27247	C
XX Boo	56014.624±0.003	−0.104	4350	C	AS Cnc	56224.593±0.002	0.396	27568	C
XX Boo	56088.453±0.003	−0.113	4477	C	AS Cnc	56229.534±0.002	0.396	27576	C
CM Boo	55948.668±0.002	−0.009	3425	C	AS Cnc	56245.591±0.003	0.398	27602	C
CM Boo	55981.560±0.002	−0.007	3479	C	EZ Cnc [1]	55996.470±0.007	−0.033	16202	C
CM Boo	56006.529±0.003	−0.010	3520	C	EZ Cnc [1]	56014.474±0.002	−0.040	16235	C
CM Boo	56034.546±0.004	−0.010	3566	C	EZ Cnc [1]	56230.603±0.002	−0.041	16631	C
CM Boo	56036.372±0.002	−0.011	3569	C	EZ Cnc [1]	56248.615±0.002	−0.041	16664	C
CM Boo	56037.593±0.002	−0.008	3571	C	EZ Cnc [1]	56288.461±0.002	−0.037	16737	C
CM Boo	56056.473±0.002	−0.010	3602	C	W CVn	55939.657±0.001	−0.142	62595	C
CM Boo	56059.518±0.002	−0.010	3607	C	W CVn	55949.587±0.002	−0.144	62613	C
U Cae	56266.721±0.003	−0.157	52293	LS	W CVn	55964.489±0.005	−0.140	62640	C
U Cae	56282.679±0.002	−0.151	52331	LS	W CVn	55980.485±0.002	−0.144	62669	C
U Cae	56284.777±0.001	−0.152	52336	LS	W CVn	55985.450±0.001	−0.145	62678	C
U Cae	56285.615±0.002	−0.153	52338	LS	W CVn	55990.418±0.003	−0.143	62687	C
AH Cam	55937.449±0.003	−0.484	46669	C	W CVn	56006.419±0.002	−0.143	62716	C
AH Cam	55947.384±0.003	−0.505	46696	C	W CVn	56070.423±0.004	−0.143	62832	C
AH Cam	56167.528±0.002	−0.496	47293	C	Z CVn	55941.734±0.004	0.608	26016	C
AH Cam	56181.521±0.002	−0.514	47331	C	Z CVn	55960.691±0.002	0.604	26045	C
AH Cam	56188.557±0.003	−0.484	47350	C	Z CVn	55993.404±0.005	0.626	26095	C

Table 1 (cont.): maxima of RR Lyrae stars

Variable star	Maximum HJD 24...	$O-C$ (days)	E	Obs	Variable star	Maximum HJD 24...	$O-C$ (days)	E	Obs.
Z CVn	56023.486±0.004	0.633	26141	C	AL CMi	55997.456±0.003	0.480	35240	C
Z CVn	56053.561±0.003	0.632	26187	C	AL CMi	56243.538±0.003	0.489	35687	C
Z CVn	56072.529±0.003	0.639	26216	C	AL CMi	56244.638±0.002	0.487	35689	C
Z CVn	56089.533±0.005	0.644	26242	C	AL CMi	56280.424±0.003	0.491	35754	C
Z CVn	56289.639±0.005	0.681	26548	C	RV Cap	56082.844±0.002	−0.014	49581	LS
Z CVn	56291.600±0.003	0.681	26551	C	RV Cap	56100.750±0.002	−0.018	49621	LS
RU CVn	55931.658±0.002	0.233	37415	C	RV Cap	56104.781±0.002	−0.016	49630	LS
RU CVn	55935.669±0.002	0.231	37422	C	RV Cap	56121.798±0.002	−0.013	49668	LS
RU CVn	55974.650±0.002	0.231	37490	C	RV Cap	56130.751±0.002	−0.015	49688	LS
RU CVn	55978.665±0.004	0.234	37497	C	RV Cap	56135.675±0.002	−0.017	49699	LS
RU CVn	55988.409±0.002	0.233	37514	C	RV Cap	56147.759±0.002	−0.022	49726	LS
RU CVn	56035.415±0.002	0.233	37596	C	RV Cap	56165.667±0.002	−0.023	49766	LS
RU CVn	56036.565±0.004	0.236	37598	C	RV Cap	56200.578±0.004	−0.036	49844	LS
RU CVn	56040.572±0.002	0.231	37605	C	IU Car	55938.649±0.003	0.116	19322	LS
RU CVn	56059.494±0.002	0.235	37638	C	IU Car	55994.659±0.003	0.103	19398	LS
RX CVn	56024.345±0.006	−0.059	30477	C	IU Car	55997.605±0.002	0.101	19402	LS
RX CVn	56059.452±0.003	−0.053	30542	C	IU Car	56000.557±0.002	0.104	19406	LS
RZ CVn	55960.560±0.002	−0.144	27523	C	IU Car	56014.556±0.002	0.097	19425	LS
RZ CVn	55972.475±0.002	−0.145	27544	C	IU Car	56025.613±0.003	0.097	19440	LS
RZ CVn	55986.660±0.002	−0.145	27569	C	IU Car	56212.813±0.002	0.061	19694	LS
RZ CVn	56001.414±0.002	−0.144	27595	C	IU Car	56226.814±0.004	0.056	19713	LS
RZ CVn	56036.592±0.002	−0.145	27657	C	IU Car	56232.711±0.004	0.056	19721	LS
RZ CVn	56060.425±0.002	−0.143	27699	C	IU Car	56235.665±0.003	0.062	19725	LS
RZ CVn	56293.637±0.003	−0.137	28110	C	IU Car	56246.714±0.003	0.053	19740	LS
SS CVn	55936.585±0.002	0.142	34092	C	IU Car	56249.663±0.004	0.054	19744	LS
SS CVn	55947.589±0.002	0.140	34115	C	IU Car	56254.818±0.002	0.049	19751	LS
SS CVn	55961.469±0.002	0.143	34144	C	IU Car	56257.770±0.003	0.052	19755	LS
SS CVn	55969.596±0.002	0.135	34161	C	IU Car	56263.667±0.004	0.052	19763	LS
SS CVn	55971.514±0.002	0.139	34165	C	IU Car	56274.720±0.004	0.048	19778	LS
SS CVn	56002.574±0.003	0.095	34230	C	IU Car	56280.614±0.004	0.045	19786	LS
SS CVn	56013.581±0.005	0.096	34253	C	IU Car	56288.723±0.004	0.045	19797	LS
SS CVn	56048.556±0.002	0.139	34326	C	HU Cas	56129.510±0.005	−0.040	59997	C
SS CVn	56059.563±0.001	0.140	34349	C	HU Cas	56139.388±0.002	−0.041	60021	C
SS CVn	56083.472±0.002	0.123	34399	C	HU Cas	56155.441±0.002	−0.040	60060	C
SV CVn	55998.397±0.005	0.124	24018	C	HU Cas	56159.556±0.001	−0.040	60070	C
SV CVn	56018.441±0.002	0.126	24048	C	HU Cas	56166.555±0.002	−0.039	60087	C
SV CVn	56026.456±0.004	0.124	24060	C	HU Cas	56180.546±0.002	−0.042	60121	C
SV CVn	56054.529±0.005	0.139	24102	C	HU Cas	56193.308±0.001	−0.039	60152	C
UZ CVn	55930.601±0.003	0.262	42281	C	HU Cas	56206.476±0.002	−0.042	60184	C
UZ CVn	55949.436±0.003	0.256	42308	C	HU Cas	56210.597±0.002	−0.037	60194	C
UZ CVn	55997.583±0.002	0.256	42377	C	HU Cas	56237.348±0.002	−0.040	60259	C
UZ CVn	56071.549±0.003	0.257	42483	C	HU Cas	56251.341±0.001	−0.041	60293	C
UZ CVn	56288.562±0.004	0.260	42794	C	HU Cas	56252.577±0.001	−0.041	60296	C
AA CMi	55951.430±0.001	0.076	40676	C	HU Cas	56277.273±0.002	−0.040	60356	C
AA CMi	55957.624±0.003	0.078	40689	LS	IU Cas	56107.468±0.003	−0.003	42131	C
AA CMi	55971.438±0.003	0.079	40718	C	IU Cas	56116.557±0.002	−0.006	42145	C
AA CMi	55973.342±0.002	0.078	40722	C	IU Cas	56131.500±0.003	0.001	42168	C
AA CMi	55976.676±0.002	0.077	40729	LS	IU Cas	56133.446±0.003	−0.001	42171	C
AA CMi	55982.392±0.001	0.078	40741	C	IU Cas	56142.534±0.002	−0.004	42185	C
AA CMi	56229.602±0.001	0.076	41260	C	IU Cas	56153.570±0.003	−0.008	42202	C
AA CMi	56240.560±0.002	0.079	41283	C	IU Cas	56157.470±0.003	−0.004	42208	C
AA CMi	56251.517±0.002	0.080	41306	C	IU Cas	56166.559±0.003	−0.006	42222	C
AA CMi	56276.764±0.003	0.082	41359	LS	IU Cas	56179.553±0.006	0.000	42242	C
AA CMi	56279.619±0.002	0.079	41365	C	IU Cas	56181.503±0.003	0.002	42245	C
AA CMi	56286.768±0.004	0.083	41380	LS	IU Cas	56205.524±0.003	−0.004	42282	C
AL CMi	55972.683±0.002	0.480	35195	LS	IU Cas	56209.433±0.005	0.008	42288	C

Table 1 (cont.): maxima of RR Lyrae stars

Variable star	Maximum HJD 24...	$O-C$ (days)	E	Obs	Variable star	Maximum HJD 24...	$O-C$ (days)	E	Obs.
IU Cas	56224.361±0.002	0.001	42311	C	RU Cet	56190.777±0.007	0.119	27912	LS
IU Cas	56237.346±0.003	−0.002	42331	C	RU Cet	56196.632±0.003	0.111	27922	LS
IU Cas	56244.493±0.002	0.002	42342	C	RU Cet	56210.714±0.002	0.122	27946	LS
IU Cas	56252.286±0.003	0.002	42354	C	RU Cet	56213.649±0.002	0.126	27951	LS
BI Cen	55934.727±0.002	0.087	42465	LS	RU Cet	56216.577±0.003	0.122	27956	LS
BI Cen	55938.803±0.002	0.084	42474	LS	RU Cet	56223.608±0.001	0.118	27968	LS
BI Cen	55939.710±0.002	0.085	42476	LS	RU Cet	56237.693±0.003	0.132	27992	LS
BI Cen	55958.737±0.003	0.078	42518	LS	RV Cet	56161.807±0.005	0.242	27347	LS
BI Cen	55959.641±0.002	0.076	42520	LS	RV Cet	56181.768±0.005	0.254	27379	LS
BI Cen	55964.620±0.002	0.070	42531	LS	RV Cet	56186.744±0.005	0.243	27387	LS
BI Cen	55972.776±0.002	0.069	42549	LS	RV Cet	56196.708±0.004	0.233	27403	LS
BI Cen	55977.762±0.002	0.070	42560	LS	RV Cet	56221.633±0.003	0.221	27443	LS
BI Cen	55979.575±0.002	0.070	42564	LS	RV Cet	56234.726±0.007	0.223	27464	LS
BI Cen	55981.840±0.002	0.069	42569	LS	RV Cet	56239.713±0.006	0.223	27472	LS
BI Cen	55984.559±0.002	0.069	42575	LS	RV Cet	56244.708±0.005	0.231	27480	LS
BI Cen	55989.548±0.002	0.073	42586	LS	RV Cet	56249.699±0.006	0.234	27488	LS
BI Cen	56002.699±0.002	0.081	42615	LS	RV Cet	56264.668±0.005	0.242	27512	LS
BI Cen	56023.554±0.002	0.090	42661	LS	RX Cet	56136.720±0.002	0.330	27908	LS
BI Cen	56033.515±0.002	0.081	42683	LS	RX Cet	56167.699±0.003	0.330	27962	LS
BI Cen	56055.711±0.001	0.071	42732	LS	RX Cet	56186.639±0.006	0.338	27995	LS
BI Cen	56062.509±0.002	0.072	42747	LS	RX Cet	56194.667±0.003	0.334	28009	LS
BI Cen	56067.495±0.002	0.072	42758	LS	RZ Cet	56166.777±0.003	−0.190	43595	LS
BI Cen	56085.637±0.002	0.086	42798	LS	RZ Cet	56167.799±0.002	−0.189	43597	LS
BI Cen	56105.583±0.003	0.093	42842	LS	RZ Cet	56168.820±0.002	−0.190	43599	LS
V499 Cen	55992.763±0.002	0.042	28523	LS	RZ Cet	56189.746±0.002	−0.199	43640	LS
V499 Cen	55993.799±0.002	0.036	28525	LS	RZ Cet	56191.798±0.002	−0.189	43644	LS
V499 Cen	56039.666±0.001	0.036	28613	LS	RZ Cet	56212.728±0.002	−0.194	43685	LS
V499 Cen	56065.726±0.002	0.036	28663	LS	RZ Cet	56215.788±0.002	−0.198	43691	LS
V499 Cen	56085.533±0.002	0.037	28701	LS	RZ Cet	56224.484±0.004	−0.182	43708	C
V671 Cen	55994.722±0.004	0.027	49341	LS	RZ Cet	56225.492±0.004	−0.195	43710	C
V671 Cen	56019.648±0.004	0.005	49398	LS	RZ Cet	56234.683±0.003	−0.195	43728	LS
V671 Cen	56061.718±0.003	0.059	49494	LS	RZ Cet	56235.710±0.002	−0.190	43730	LS
V671 Cen	56083.528±0.003	−0.014	49544	LS	RZ Cet	56244.385±0.002	−0.195	43747	C
V674 Cen	56065.550±0.002	−0.198	43799	LS	RZ Cet	56288.293±0.003	−0.200	43833	C
AQ Cep	55950.456±0.002	0.073	42708	C	RZ Cet	56292.379±0.004	−0.198	43841	C
AQ Cep	56204.520±0.001	0.074	43098	C	UU Cet	56130.748±0.004	−0.148	24621	LS
RR Cet	56165.818±0.002	0.011	41561	LS	UU Cet	56159.837±0.002	−0.151	24669	LS
RR Cet	56168.585±0.002	0.013	41566	C	UU Cet	56187.717±0.004	−0.151	24715	LS
RR Cet	56183.517±0.003	0.014	41593	C	UU Cet	56195.592±0.004	−0.155	24728	LS
RR Cet	56185.726±0.002	0.010	41597	LS	UU Cet	56204.685±0.003	−0.153	24743	LS
RR Cet	56186.836±0.002	0.014	41599	LS	UU Cet	56210.748±0.003	−0.151	24753	LS
RR Cet	56191.810±0.002	0.011	41608	LS	UU Cet	56215.599±0.003	−0.149	24761	LS
RR Cet	56193.469±0.002	0.011	41611	C	UU Cet	56221.654±0.003	−0.154	24771	LS
RR Cet	56195.681±0.002	0.011	41615	LS	UU Cet	56235.596±0.003	−0.152	24794	LS
RR Cet	56206.732±0.007	0.001	41635	LS	RT Col	56268.614±0.002	−0.300	53093	LS
RR Cet	56208.401±0.002	0.011	41638	C	RT Col	56284.711±0.002	−0.301	53123	LS
RR Cet	56211.721±0.003	0.013	41644	LS	RW Col	55961.609±0.003	−0.038	53196	LS
RR Cet	56216.698±0.002	0.013	41653	LS	RW Col	55967.611±0.003	0.143	53207	LS
RR Cet	56237.712±0.002	0.012	41691	LS	RW Col	56232.781±0.004	0.166	53708	LS
RR Cet	56239.370±0.003	0.011	41694	C	RW Col	56238.779±0.003	−0.186	53720	LS
RR Cet	56250.433±0.002	0.013	41714	C	RW Col	56243.693±0.003	−0.036	53729	LS
RR Cet	56291.356±0.003	0.012	41788	C	RW Col	56244.785±0.003	−0.002	53731	LS
RU Cet	56136.848±0.002	0.127	27820	LS	RW Col	56261.701±0.006	−0.022	53763	LS
RU Cet	56139.784±0.004	0.132	27825	LS	RW Col	56272.612±0.003	−0.224	53784	LS
RU Cet	56163.811±0.003	0.122	27866	LS	RW Col	56284.613±0.003	0.133	53806	LS
RU Cet	56180.803±0.002	0.112	27895	LS	RW Col	56285.704±0.004	0.166	53808	LS

Table 1 (cont.): maxima of RR Lyrae stars

Variable star	Maximum HJD 24...	$O-C$ (days)	E	Obs	Variable star	Maximum HJD 24...	$O-C$ (days)	E	Obs.
RW Col	56290.616±0.003	−0.214	53818	LS	WW CrA	56171.533±0.002	−0.020	44478	LS
RX Col	55966.606±0.002	−0.261	45711	LS	V413 CrA	56038.842±0.004	0.069	24669	LS
RX Col	56242.687±0.002	0.184	46175	LS	V413 CrA	56064.779±0.003	0.075	24713	LS
RX Col	56255.750±0.004	0.179	46197	LS	V413 CrA	56067.712±0.005	0.062	24718	LS
RX Col	56258.713±0.004	0.171	46202	LS	V413 CrA	56103.653±0.003	0.053	24779	LS
RX Col	56261.687±0.005	0.175	46207	LS	V413 CrA	56104.835±0.002	0.056	24781	LS
RX Col	56267.627±0.005	0.175	46217	LS	V413 CrA	56129.585±0.004	0.054	24823	LS
RX Col	56286.635±0.004	0.173	46249	LS	V413 CrA	56132.536±0.003	0.058	24828	LS
RX Col	56293.765±0.005	0.175	46261	LS	V413 CrA	56182.636±0.004	0.064	24913	LS
RY Col	56258.743±0.002	−0.237	45835	LS	TV CrB	55966.589±0.002	0.027	41648	C
RY Col	56261.622±0.006	−0.231	45841	LS	TV CrB	55983.542±0.003	0.026	41677	C
RY Col	56291.806±0.004	−0.215	45904	LS	TV CrB	55993.486±0.002	0.032	41694	C
RY Col	56292.762±0.004	−0.217	45906	LS	TV CrB	56014.531±0.002	0.031	41730	C
AV Col	55935.626±0.002	0.060	6978	LS	TV CrB	56018.620±0.002	0.028	41737	C
AV Col	55964.690±0.002	0.062	7040	LS	TV CrB	56045.522±0.003	0.037	41783	C
AV Col	55965.627±0.001	0.062	7042	LS	W Crt	55961.689±0.002	−0.026	39604	LS
AV Col	56233.752±0.002	0.066	7614	LS	W Crt	55963.748±0.001	−0.026	39609	LS
AV Col	56256.721±0.002	0.066	7663	LS	W Crt	55999.594±0.003	−0.026	39696	LS
AV Col	56264.689±0.001	0.066	7680	LS	W Crt	56029.671±0.002	−0.026	39769	LS
AV Col	56278.752±0.002	0.066	7710	LS	W Crt	56055.627±0.002	−0.027	39832	LS
AV Col	56286.718±0.002	0.064	7727	LS	X Crt	55964.822±0.008	0.084	19331	LS
AV Col	56287.657±0.002	0.065	7729	LS	X Crt	55989.738±0.003	0.083	19365	LS
S Com	55934.641±0.003	−0.101	26049	C	X Crt	56017.575±0.005	0.073	19403	LS
S Com	55937.571±0.002	−0.104	26054	C	X Crt	56058.608±0.003	0.067	19459	LS
S Com	55964.555±0.002	−0.103	26100	C	SW Cru	55938.794±0.003	0.064	91245	LS
S Com	55974.528±0.002	−0.103	26117	C	SW Cru	55939.777±0.002	0.064	91248	LS
S Com	55984.502±0.001	−0.101	26134	C	SW Cru	55965.674±0.003	0.066	91327	LS
S Com	55998.577±0.002	−0.104	26158	C	SW Cru	55966.658±0.003	0.067	91330	LS
S Com	56005.616±0.002	−0.103	26170	C	SW Cru	55971.571±0.002	0.063	91345	LS
S Com	56011.483±0.002	−0.103	26180	C	SW Cru	55976.815±0.003	0.063	91361	LS
S Com	56042.572±0.003	−0.103	26233	C	SW Cru	55989.599±0.003	0.063	91400	LS
S Com	56055.477±0.003	−0.103	26255	C	SW Cru	55994.845±0.004	0.065	91416	LS
S Com	56290.701±0.002	−0.102	26656	C	SW Cru	55995.830±0.003	0.066	91419	LS
RY Com	55973.601±0.002	−0.109	34918	C	SW Cru	55998.776±0.002	0.062	91428	LS
RY Com	55974.537±0.002	−0.111	34920	C	SW Cru	56005.661±0.002	0.063	91449	LS
RY Com	55982.501±0.002	−0.119	34937	C	SW Cru	56012.544±0.003	0.064	91470	LS
RY Com	55983.442±0.002	−0.116	34939	C	SW Cru	56021.721±0.003	0.063	91498	LS
RY Com	56011.581±0.003	−0.115	34999	C	SW Cru	56023.690±0.002	0.065	91504	LS
RY Com	56015.331±0.002	−0.116	35007	C	SW Cru	56032.537±0.002	0.062	91531	LS
RY Com	56045.341±0.002	−0.119	35071	C	SW Cru	56047.615±0.002	0.063	91577	LS
RY Com	56057.525±0.001	−0.128	35097	C	SW Cru	56048.602±0.002	0.066	91580	LS
RY Com	56066.434±0.002	−0.129	35116	C	SW Cru	56049.582±0.002	0.062	91583	LS
RY Com	56290.577±0.003	−0.146	35594	C	SW Cru	56050.566±0.002	0.063	91586	LS
ST Com	55947.513±0.003	−0.034	21243	C	SW Cru	56052.535±0.003	0.065	91592	LS
ST Com	55963.684±0.004	−0.034	21270	C	SW Cru	56053.519±0.003	0.066	91595	LS
ST Com	55972.668±0.003	−0.034	21285	C	SW Cru	56057.777±0.002	0.063	91608	LS
ST Com	55974.466±0.003	−0.033	21288	C	SW Cru	56083.671±0.003	0.062	91687	LS
ST Com	55999.618±0.003	−0.036	21330	C	UY Cyg	56148.415±0.004	0.070	60129	C
ST Com	56014.592±0.003	−0.035	21355	C	UY Cyg	56149.527±0.004	0.061	60131	C
ST Com	56056.519±0.002	−0.033	21425	C	UY Cyg	56185.409±0.002	0.058	60195	C
ST Com	56293.690±0.003	−0.038	21821	C	UY Cyg	56204.481±0.005	0.066	60229	C
WW CrA	56046.774±0.002	−0.016	44255	LS	XZ Cyg [2]	56038.496±0.003	−0.006	16005	C
WW CrA	56115.583±0.003	−0.022	44378	LS	XZ Cyg [2]	56051.565±0.001	−0.002	16033	C
WW CrA	56134.611±0.002	−0.016	44412	LS	XZ Cyg [2]	56116.421±0.003	−0.004	16172	C
WW CrA	56148.599±0.002	−0.015	44437	LS	XZ Cyg [2]	56129.484±0.003	−0.005	16200	C
WW CrA	56162.591±0.003	−0.010	44462	LS	XZ Cyg [2]	56130.418±0.002	−0.005	16202	C

Table 1 (cont.): maxima of RR Lyrae stars

Variable star	Maximum HJD 24...	$O-C$ (days)	E	Obs	Variable star	Maximum HJD 24...	$O-C$ (days)	E	Obs.
XZ Cyg [2]	56136.484±0.002	−0.004	16215	C	VW Dor	56018.562±0.002	−0.158	30913	LS
XZ Cyg [2]	56142.543±0.001	−0.011	16228	C	VW Dor	56022.551±0.002	−0.163	30920	LS
XZ Cyg [2]	56143.478±0.001	−0.009	16230	C	VW Dor	56205.711±0.002	−0.169	31241	LS
XZ Cyg [2]	56144.411±0.002	−0.009	16232	C	VW Dor	56222.826±0.001	−0.172	31271	LS
XZ Cyg [2]	56164.485±0.003	0.001	16275	C	VW Dor	56225.682±0.002	−0.170	31276	LS
XZ Cyg [2]	56172.415±0.003	−0.001	16292	C	VW Dor	56226.825±0.002	−0.168	31278	LS
XZ Cyg [2]	56176.610±0.002	−0.006	16301	C	VW Dor	56233.665±0.002	−0.175	31290	LS
XZ Cyg [2]	56184.544±0.002	−0.004	16318	C	VW Dor	56234.807±0.003	−0.174	31292	LS
DM Cyg	56099.450±0.001	0.072	32194	C	VW Dor	56237.656±0.002	−0.178	31297	LS
DM Cyg	56112.467±0.001	0.072	32225	C	VW Dor	56253.639±0.002	−0.172	31325	LS
DM Cyg	56135.560±0.001	0.073	32280	C	VW Dor	56258.770±0.003	−0.177	31334	LS
DM Cyg	56146.478±0.002	0.075	32306	C	VW Dor	56261.619±0.002	−0.181	31339	LS
DM Cyg	56148.577±0.001	0.075	32311	C	VW Dor	56262.760±0.003	−0.181	31341	LS
DM Cyg	56157.394±0.001	0.075	32332	C	VW Dor	56266.760±0.005	−0.175	31348	LS
DM Cyg	56161.592±0.001	0.074	32342	C	VW Dor	56269.614±0.002	−0.174	31353	LS
DM Cyg	56188.464±0.002	0.075	32406	C	VW Dor	56286.729±0.003	−0.178	31383	LS
DM Cyg	56191.403±0.003	0.075	32413	C	VW Dor	56290.718±0.002	−0.183	31390	LS
DM Cyg	56228.348±0.002	0.072	32501	C	RW Dra	55993.613±0.003	0.191	37515	C
V939 Cyg [3]	56051.588±0.005	0.083	16161	C	RW Dra	56002.480±0.002	0.199	37535	C
V939 Cyg [3]	56115.538±0.004	0.090	16326	C	RW Dra	56018.451±0.002	−0.217	37572	C
V939 Cyg [3]	56129.480±0.006	0.080	16362	C	RW Dra	56099.507±0.002	−0.215	37755	C
V939 Cyg [3]	56136.467±0.004	0.092	16380	C	RW Dra	56114.537±0.003	0.198	37788	C
V939 Cyg [3]	56143.448±0.004	0.097	16398	C	RW Dra	56118.518±0.002	0.193	37797	C
V939 Cyg [3]	56164.373±0.004	0.095	16452	C	RW Dra	56122.505±0.002	0.194	37806	C
V939 Cyg [3]	56184.532±0.005	0.102	16504	C	RW Dra	56134.499±0.002	−0.214	37834	C
DU Del	56124.536±0.003	−0.167	47041	C	RW Dra	56145.574±0.002	−0.212	37859	C
DX Del	56107.492±0.002	0.067	35420	C	SU Dra	55937.600±0.002	0.059	18224	C
DX Del	56108.437±0.003	0.067	35422	C	SU Dra	55939.581±0.002	0.059	18227	C
DX Del	56123.558±0.002	0.064	35454	C	SU Dra	55941.563±0.002	0.060	18230	C
DX Del	56124.506±0.002	0.067	35456	C	SU Dra	55961.380±0.004	0.064	18260	C
DX Del	56151.443±0.002	0.065	35513	C	SU Dra	55964.680±0.003	0.062	18265	C
DX Del	56157.587±0.002	0.065	35526	C	SU Dra	55996.381±0.003	0.063	18313	C
DX Del	56158.532±0.002	0.065	35528	C	SU Dra	56050.535±0.003	0.062	18395	C
DX Del	56161.365±0.001	0.062	35534	C	SU Dra	56054.495±0.002	0.059	18401	C
DX Del	56184.525±0.003	0.064	35583	C	SW Dra	55966.545±0.002	0.060	52209	C
DX Del	56193.504±0.002	0.063	35602	C	SW Dra	55983.636±0.003	0.061	52239	C
DX Del	56203.429±0.002	0.063	35623	C	SW Dra	55989.334±0.002	0.062	52249	C
DX Del	56230.370±0.002	0.065	35680	C	SW Dra	55993.322±0.004	0.063	52256	C
GV Del	56193.516±0.004	−0.157	79770	C	SW Dra	55995.596±0.003	0.058	52260	C
RT Dor	55964.549±0.004	−0.055	52186	LS	SW Dra	56035.477±0.002	0.062	52330	C
RT Dor	55992.551±0.002	−0.057	52244	LS	SW Dra	56048.576±0.004	0.059	52353	C
RT Dor	56019.586±0.002	−0.061	52300	LS	SW Dra	56051.427±0.003	0.061	52358	C
RT Dor	56196.782±0.001	−0.066	52667	LS	XZ Dra	56045.423±0.002	−0.128	29627	C
RT Dor	56198.713±0.002	−0.066	52671	LS	XZ Dra	56064.493±0.002	−0.117	29667	C
RT Dor	56199.681±0.003	−0.064	52673	LS	XZ Dra	56084.502±0.003	−0.121	29709	C
RT Dor	56226.718±0.001	−0.066	52729	LS	XZ Dra	56093.552±0.002	−0.124	29728	C
RT Dor	56229.615±0.001	−0.066	52735	LS	XZ Dra	56115.473±0.001	−0.123	29774	C
RT Dor	56230.583±0.003	−0.064	52737	LS	XZ Dra	56124.531±0.001	−0.118	29793	C
RT Dor	56256.656±0.003	−0.064	52791	LS	XZ Dra	56143.591±0.002	−0.118	29833	C
RT Dor	56257.623±0.002	−0.063	52793	LS	XZ Dra	56154.545±0.002	−0.123	29856	C
RT Dor	56285.630±0.002	−0.060	52851	LS	XZ Dra	56167.421±0.002	−0.113	29883	C
VW Dor	55934.678±0.002	−0.162	30766	LS	XZ Dra	56176.468±0.006	−0.119	29902	C
VW Dor	55939.821±0.002	−0.155	30775	LS	BC Dra	55934.652±0.005	0.096	18978	C
VW Dor	55963.785±0.002	−0.156	30817	LS	BC Dra	55937.541±0.006	0.106	18982	C
VW Dor	55967.779±0.001	−0.156	30824	LS	BC Dra	55950.478±0.005	0.091	19000	C
VW Dor	56002.575±0.002	−0.168	30885	LS	BC Dra	55970.631±0.005	0.096	19028	C

Table 1 (cont.): maxima of RR Lyrae stars

Variable star	Maximum HJD 24...	$O-C$ (days)	E	Obs	Variable star	Maximum HJD 24...	$O-C$ (days)	E	Obs.
BC Dra	55986.461±0.004	0.095	19050	C	BD Dra	56234.485±0.005	0.585	24547	C
BC Dra	55988.629±0.005	0.104	19053	C	BD Dra	56243.331±0.002	0.595	24562	C
BC Dra	56017.408±0.005	0.100	19093	C	BD Dra	56250.374±0.005	0.569	24574	C
BC Dra	56019.564±0.004	0.098	19096	C	BD Dra	56263.360±0.003	0.596	24596	C
BC Dra	56035.396±0.005	0.099	19118	C	BD Dra	56288.682±0.003	0.589	24639	C
BC Dra	56050.506±0.003	0.098	19139	C	BD Dra	56291.628±0.002	0.590	24644	C
BC Dra	56091.523±0.005	0.099	19196	C	BK Dra	56051.457±0.002	−0.162	51561	C
BC Dra	56099.441±0.005	0.102	19207	C	BK Dra	56070.406±0.003	−0.160	51593	C
BC Dra	56117.430±0.005	0.101	19232	C	BK Dra	56083.431±0.002	−0.161	51615	C
BC Dra	56140.456±0.004	0.101	19264	C	BK Dra	56096.458±0.002	−0.159	51637	C
BC Dra	56145.489±0.003	0.097	19271	C	BK Dra	56119.547±0.001	−0.161	51676	C
BC Dra	56150.525±0.003	0.096	19278	C	BK Dra	56122.508±0.002	−0.161	51681	C
BC Dra	56155.566±0.003	0.100	19285	C	BK Dra	56135.533±0.002	−0.162	51703	C
BC Dra	56158.445±0.004	0.101	19289	C	BK Dra	56144.414±0.002	−0.162	51718	C
BC Dra	56166.360±0.004	0.100	19300	C	BK Dra	56151.521±0.002	−0.160	51730	C
BC Dra	56176.427±0.010	0.093	19314	C	BK Dra	56154.481±0.003	−0.160	51735	C
BC Dra	56178.599±0.006	0.106	19317	C	BK Dra	56164.546±0.002	−0.161	51752	C
BC Dra	56181.472±0.010	0.101	19321	C	BT Dra	55970.494±0.005	−0.007	42869	C
BC Dra	56191.538±0.006	0.093	19335	C	BT Dra	55971.665±0.002	−0.013	42871	C
BC Dra	56204.497±0.004	0.100	19353	C	BT Dra	55974.608±0.002	−0.013	42876	C
BC Dra	56232.559±0.005	0.098	19392	C	BT Dra	55981.674±0.002	−0.012	42888	C
BC Dra	56243.354±0.005	0.100	19407	C	BT Dra	55999.330±0.004	−0.016	42918	C
BC Dra	56248.396±0.006	0.105	19414	C	BT Dra	56033.469±0.002	−0.020	42976	C
BC Dra	56250.549±0.005	0.099	19417	C	BT Dra	56050.548±0.001	−0.013	43005	C
BC Dra	56251.268±0.004	0.098	19418	C	BT Dra	56119.415±0.003	−0.020	43122	C
BC Dra	56263.509±0.005	0.106	19435	C	RX Eri	56220.785±0.002	−0.010	58797	LS
BD Dra	55930.558±0.003	0.608	24031	C	RX Eri	56223.721±0.003	−0.010	58802	LS
BD Dra	55934.648±0.004	0.575	24038	C	RX Eri	56253.674±0.003	−0.007	58853	LS
BD Dra	55937.579±0.004	0.561	24043	C	RX Eri	56256.608±0.003	−0.009	58858	LS
BD Dra	55950.589±0.002	0.612	24065	C	RX Eri	56267.766±0.003	−0.009	58877	LS
BD Dra	55966.468±0.003	0.586	24092	C	RX Eri	56277.750±0.004	−0.008	58894	LS
BD Dra	55970.616±0.003	0.611	24099	C	RX Eri	56280.684±0.003	−0.010	58899	LS
BD Dra	55986.471±0.006	0.561	24126	C	SV Eri	56216.686±0.006	0.885	28949	LS
BD Dra	55990.620±0.004	0.587	24133	C	SV Eri	56221.691±0.007	0.893	28956	LS
BD Dra	56013.572±0.004	0.566	24172	C	SV Eri	56236.681±0.007	0.894	28977	LS
BD Dra	56035.358±0.004	0.557	24209	C	SV Eri	56246.673±0.005	0.893	28991	LS
BD Dra	56042.473±0.004	0.604	24221	C	SV Eri	56251.674±0.005	0.897	28998	LS
BD Dra	56072.510±0.003	0.599	24272	C	SV Eri	56266.660±0.007	0.893	29019	LS
BD Dra	56095.485±0.002	0.601	24311	C	SV Eri	56276.655±0.008	0.895	29033	LS
BD Dra	56102.532±0.003	0.579	24323	C	XY Eri	56291.642±0.006	−0.215	56884	LS
BD Dra	56128.440±0.003	0.569	24367	C	BB Eri	56226.795±0.002	0.267	29246	LS
BD Dra	56138.470±0.002	0.585	24384	C	BB Eri	56230.789±0.005	0.272	29253	LS
BD Dra	56141.421±0.002	0.591	24389	C	BB Eri	56254.727±0.003	0.274	29295	LS
BD Dra	56145.548±0.002	0.594	24396	C	BB Eri	56266.698±0.003	0.277	29316	LS
BD Dra	56155.523±0.005	0.556	24413	C	BB Eri	56282.648±0.002	0.270	29344	LS
BD Dra	56158.454±0.004	0.541	24418	C	BB Eri	56290.626±0.003	0.270	29358	LS
BD Dra	56168.520±0.002	0.593	24435	C	RX For	56182.828±0.002	−0.030	27375	LS
BD Dra	56178.489±0.005	0.548	24452	C	RX For	56185.804±0.002	−0.040	27380	LS
BD Dra	56181.430±0.004	0.544	24457	C	RX For	56200.724±0.003	−0.053	27405	LS
BD Dra	56184.382±0.005	0.551	24462	C	RX For	56206.713±0.007	−0.037	27415	LS
BD Dra	56185.576±0.003	0.567	24464	C	RX For	56212.698±0.002	−0.025	27425	LS
BD Dra	56191.488±0.002	0.588	24474	C	RX For	56234.778±0.002	−0.046	27462	LS
BD Dra	56198.553±0.003	0.585	24486	C	RX For	56237.775±0.003	−0.036	27467	LS
BD Dra	56204.406±0.003	0.547	24496	C	RX For	56243.760±0.002	−0.024	27477	LS
BD Dra	56205.583±0.003	0.546	24498	C	RX For	56261.644±0.006	−0.059	27507	LS
BD Dra	56224.462±0.003	0.575	24530	C	RX For	56267.632±0.002	−0.044	27517	LS

Table 1 (cont.): maxima of RR Lyrae stars

Variable star	Maximum HJD 24...	$O-C$ (days)	E	Obs	Variable star	Maximum HJD 24...	$O-C$ (days)	E	Obs.
SS For	56262.593±0.002	−0.139	35512	LS	RW Gru	56172.719±0.002	−0.148	39637	LS
SW For	56164.787±0.005	0.460	27149	LS	RW Gru	56173.815±0.002	−0.153	39639	LS
SW For	56168.806±0.005	0.460	27154	LS	TW Her	56003.537±0.001	−0.013	86232	C
SW For	56172.825±0.003	0.460	27159	LS	TW Her	56033.507±0.001	−0.013	86307	C
SW For	56226.679±0.005	0.464	27226	LS	TW Her	56089.449±0.002	−0.015	86447	C
SW For	56230.695±0.005	0.461	27231	LS	TW Her	56117.422±0.002	−0.014	86517	C
SW For	56234.712±0.004	0.459	27236	LS	TW Her	56127.413±0.002	−0.013	86542	C
SW For	56238.731±0.004	0.460	27241	LS	TW Her	56135.404±0.001	−0.014	86562	C
SW For	56255.614±0.005	0.464	27262	LS	TW Her	56137.402±0.001	−0.014	86567	C
SW For	56259.626±0.005	0.457	27267	LS	TW Her	56139.400±0.001	−0.014	86572	C
SW For	56263.642±0.004	0.455	27272	LS	TW Her	56141.398±0.002	−0.014	86577	C
SW For	56275.705±0.005	0.462	27287	LS	TW Her	56143.397±0.001	−0.013	86582	C
SX For	56173.777±0.003	0.052	28109	LS	TW Her	56149.390±0.001	−0.014	86597	C
SX For	56196.775±0.004	0.047	28147	LS	TW Her	56153.386±0.002	−0.015	86607	C
SX For	56199.808±0.003	0.054	28152	LS	TW Her	56159.380±0.001	−0.014	86622	C
SX For	56207.669±0.003	0.045	28165	LS	TW Her	56169.370±0.002	−0.014	86647	C
SX For	56230.677±0.004	0.050	28203	LS	TW Her	56175.362±0.002	−0.016	86662	C
SX For	56233.703±0.003	0.050	28208	LS	TW Her	56185.352±0.001	−0.017	86687	C
SX For	56244.601±0.004	0.052	28226	LS	VX Her	55983.583±0.001	−0.462	75177	C
SX For	56256.711±0.006	0.055	28246	LS	VX Her	56003.621±0.001	−0.461	75221	C
SX For	56262.761±0.003	0.051	28256	LS	VX Her	56008.629±0.001	−0.461	75232	C
SX For	56290.611±0.005	0.056	28302	LS	VX Her	56050.522±0.002	−0.463	75324	C
SX For	56293.635±0.003	0.053	28307	LS	VX Her	56065.546±0.001	−0.466	75357	C
RR Gem	55943.598±0.001	−0.469	36714	C	VX Her	56101.524±0.001	−0.463	75436	C
RR Gem	55946.379±0.002	−0.469	36721	C	VX Her	56102.434±0.002	−0.463	75438	C
RR Gem	55969.418±0.001	−0.474	36779	C	VX Her	56112.452±0.002	−0.464	75460	C
RR Gem	55971.407±0.002	−0.471	36784	C	VX Her	56117.460±0.002	−0.465	75471	C
RR Gem	55973.397±0.001	−0.468	36789	C	VZ Her	55980.662±0.001	0.073	43585	C
RR Gem	56000.412±0.001	−0.470	36857	C	VZ Her	55984.625±0.003	0.073	43594	C
RR Gem	56012.325±0.002	−0.476	36887	C	VZ Her	56006.640±0.001	0.072	43644	C
RR Gem	56214.543±0.001	−0.489	37396	C	VZ Her	56055.519±0.002	0.074	43755	C
RR Gem	56216.537±0.002	−0.482	37401	C	VZ Her	56092.506±0.001	0.073	43839	C
RR Gem	56229.642±0.002	−0.488	37434	C	VZ Her	56100.431±0.002	0.073	43857	C
RR Gem	56247.524±0.002	−0.485	37479	C	VZ Her	56140.500±0.002	0.072	43948	C
RR Gem	56249.509±0.004	−0.487	37484	C	VZ Her	56144.463±0.001	0.072	43957	C
SZ Gem	55932.635±0.001	−0.067	57347	C	VZ Her	56152.390±0.001	0.073	43975	C
SZ Gem	55945.665±0.002	−0.066	57373	C	VZ Her	56166.479±0.003	0.072	44007	C
SZ Gem	56273.406±0.002	−0.068	58027	C	VZ Her	56178.371±0.002	0.075	44034	C
SZ Gem	56285.432±0.002	−0.070	58051	C	AR Her	55972.593±0.002	−1.389	30891	C
GI Gem	55940.555±0.002	0.069	59072	C	AR Her	55979.675±0.002	−1.357	30906	C
GI Gem	55947.487±0.001	0.069	59088	C	AR Her	55980.616±0.003	−1.356	30908	C
GI Gem	55948.354±0.002	0.069	59090	C	AR Her	56011.625±0.003	−1.369	30974	C
GI Gem	55971.316±0.002	0.068	59143	C	AR Her	56043.573±0.006	−1.383	31042	C
GI Gem	55980.414±0.001	0.068	59164	C	AR Her	56060.513±0.001	−1.364	31078	C
GI Gem	55984.314±0.001	0.069	59173	C	AR Her	56139.466±0.006	−1.376	31246	C
GI Gem	56003.377±0.001	0.068	59217	C	AR Her	56146.550±0.003	−1.342	31261	C
GI Gem	56219.577±0.002	0.068	59716	C	BD Her	56149.559±0.005	0.148	49633	C
GI Gem	56225.642±0.001	0.068	59730	C	DL Her	56045.463±0.002	0.047	30149	C
GI Gem	56251.638±0.001	0.068	59790	C	DL Her	56116.459±0.002	0.047	30269	C
GI Gem	56278.503±0.003	0.070	59852	C	DL Her	56142.498±0.003	0.054	30313	C
RR Gru	56138.799±0.003	0.032	39370	LS	GY Her	55993.561±0.005	0.178	37388	C
RR Gru	56199.570±0.004	0.025	39480	LS	GY Her	56023.448±0.002	0.175	37445	C
RR Gru	56200.675±0.003	0.025	39482	LS	GY Her	56036.558±0.002	0.176	37470	C
RW Gru	56129.798±0.005	−0.145	39559	LS	GY Her	56100.482±0.004	0.125	37592	C
RW Gru	56146.861±0.002	−0.142	39590	LS	GY Her	56152.386±0.003	0.116	37691	C
RW Gru	56166.681±0.002	−0.133	39626	LS	V542 Her	56008.673±0.002	0.131	27061	C

Table 1 (cont.): maxima of RR Lyrae stars

Variable star	Maximum HJD 24...	$O-C$ (days)	E	Obs	Variable star	Maximum HJD 24...	$O-C$ (days)	E	Obs.
V591 Her	56050.526±0.005	0.320	24483	C	XX Hya	55982.580±0.002	0.018	31807	LS
V593 Her	56050.551±0.004	−0.126	32669	C	XX Hya	55984.613±0.002	0.020	31811	LS
V593 Her	56065.526±0.002	−0.129	32698	C	XX Hya	56013.551±0.002	0.016	31868	LS
V593 Her	56096.516±0.005	−0.129	32758	C	XX Hya	56015.582±0.001	0.016	31872	LS
V593 Her	56127.507±0.004	−0.128	32818	C	XX Hya	56016.599±0.001	0.017	31874	LS
V650 Her	56003.624±0.003	0.039	31914	C	XX Hya	56287.742±0.002	0.012	32408	LS
V698 Her	56050.537±0.002	0.126	32672	C	XX Hya	56288.759±0.002	0.013	32410	LS
UU Hor	56169.800±0.002	0.184	48855	LS	BI Hya	55974.678±0.002	0.251	53324	LS
UU Hor	56171.735±0.003	0.188	48858	LS	BI Hya	55984.680±0.001	0.251	53343	LS
UU Hor	56178.811±0.001	0.183	48869	LS	BI Hya	55986.784±0.001	0.249	53347	LS
UU Hor	56187.825±0.002	0.186	48883	LS	BI Hya	56032.589±0.002	0.252	53434	LS
UU Hor	56198.768±0.002	0.187	48900	LS	BI Hya	56053.648±0.002	0.252	53474	LS
UU Hor	56200.698±0.002	0.185	48903	LS	BI Hya	56062.599±0.002	0.253	53491	LS
UU Hor	56216.792±0.002	0.187	48928	LS	DD Hya	55960.306±0.001	−0.188	28429	C
UU Hor	56220.653±0.002	0.186	48934	LS	DD Hya	55983.391±0.001	−0.184	28475	C
UU Hor	56229.666±0.002	0.188	48948	LS	DD Hya	55985.396±0.002	−0.187	28479	C
UU Hor	56236.746±0.002	0.187	48959	LS	DD Hya	55999.449±0.002	−0.184	28507	C
UU Hor	56247.690±0.003	0.189	48976	LS	DG Hya	55986.644±0.003	−0.093	44120	LS
UU Hor	56249.621±0.002	0.189	48979	LS	DH Hya	55958.755±0.002	0.082	50680	LS
UU Hor	56258.632±0.003	0.188	48993	LS	DH Hya	55981.739±0.001	0.083	50727	LS
UU Hor	56265.712±0.002	0.187	49004	LS	DH Hya	55983.695±0.001	0.083	50731	LS
UU Hor	56274.727±0.002	0.191	49018	LS	DH Hya	56007.656±0.001	0.083	50780	LS
UU Hor	56276.657±0.004	0.190	49021	LS	DH Hya	56008.632±0.001	0.082	50782	LS
UU Hor	56285.667±0.003	0.188	49035	LS	DH Hya	56011.568±0.001	0.083	50788	LS
UW Hor	56263.685±0.002	0.228	39361	LS	ET Hya	55941.436±0.003	0.153	29204	C
UW Hor	56265.671±0.003	0.227	39364	LS	ET Hya	55945.549±0.003	0.153	29210	C
UW Hor	56269.638±0.003	0.221	39370	LS	ET Hya	55960.634±0.003	0.157	29232	LS
SV Hya	55992.834±0.002	0.130	34844	LS	ET Hya	55974.344±0.002	0.156	29252	C
SV Hya	56019.619±0.002	0.116	34900	LS	ET Hya	55985.311±0.003	0.155	29268	C
SV Hya	56020.579±0.002	0.119	34902	LS	ET Hya	55997.649±0.002	0.154	29286	LS
SZ Hya	55933.577±0.002	−0.234	28394	C	ET Hya	55998.332±0.002	0.151	29287	C
SZ Hya	55957.746±0.002	−0.241	28439	LS	ET Hya	56006.562±0.002	0.155	29299	LS
SZ Hya	55961.512±0.002	−0.236	28446	C	FX Hya	56018.626±0.002	−0.050	52177	LS
SZ Hya	55969.572±0.003	−0.234	28461	C	FX Hya	56028.640±0.002	−0.053	52201	LS
SZ Hya	55970.647±0.002	−0.233	28463	LS	FX Hya	56033.648±0.002	−0.053	52213	LS
SZ Hya	55972.792±0.002	−0.237	28467	LS	FX Hya	56068.706±0.001	−0.053	52297	LS
SZ Hya	55979.722±0.003	−0.291	28480	LS	FX Hya	56084.565±0.002	−0.053	52335	LS
SZ Hya	55982.454±0.002	−0.246	28485	C	FY Hya	56029.613±0.003	0.013	23467	LS
SZ Hya	55996.431±0.002	−0.237	28511	C	FY Hya	56048.713±0.002	0.013	23497	LS
SZ Hya	55999.650±0.002	−0.241	28517	LS	FY Hya	56064.630±0.002	0.014	23522	LS
SZ Hya	56002.319±0.003	−0.259	28522	C	FY Hya	56066.543±0.003	0.017	23525	LS
SZ Hya	56013.623±0.001	−0.237	28543	LS	GO Hya	55933.646±0.004	−0.079	47584	C
UU Hya	55957.771±0.005	0.033	31456	LS	GO Hya	55947.641±0.007	−0.086	47606	C
UU Hya	55976.609±0.002	0.011	31492	LS	GO Hya	55968.651±0.005	−0.078	47639	LS
UU Hya	55977.652±0.002	0.007	31494	LS	GO Hya	55979.467±0.003	−0.082	47656	C
UU Hya	55987.615±0.002	0.016	31513	LS	GO Hya	55996.649±0.004	−0.083	47683	LS
UU Hya	55997.583±0.002	0.031	31532	LS	GO Hya	56002.384±0.004	−0.076	47692	C
UU Hya	55999.681±0.002	0.033	31536	LS	GO Hya	56273.505±0.004	−0.078	48118	C
UU Hya	56004.378±0.002	0.015	31545	C	GO Hya	56285.596±0.004	−0.079	48137	C
UU Hya	56006.477±0.002	0.019	31549	C	IK Hya	56009.598±0.004	0.038	26997	LS
UU Hya	56014.323±0.003	0.007	31564	C	IK Hya	56011.540±0.004	0.030	27000	LS
WZ Hya	55970.677±0.003	0.004	30394	LS	IK Hya	56020.648±0.005	0.038	27014	LS
WZ Hya	55971.741±0.002	−0.007	30396	LS	TW Hyi	56290.590±0.003	0.017	24912	LS
WZ Hya	55998.624±0.002	−0.010	30446	LS	TW Hyi	56292.616±0.003	0.017	24915	LS
WZ Hya	56012.609±0.002	−0.005	30472	LS	V Ind	56119.850±0.002	0.383	33364	LS
WZ Hya	56026.591±0.002	−0.004	30498	LS	V Ind	56137.592±0.003	0.380	33401	LS

Table 1 (cont.): maxima of RR Lyrae stars

Variable star	Maximum HJD 24...	$O-C$ (days)	E	Obs	Variable star	Maximum HJD 24...	$O-C$ (days)	E	Obs.
V Ind	56171.646±0.002	0.383	33472	LS	SZ Leo	56015.471±0.003	0.470	19750	C
V Ind	56172.604±0.002	0.382	33474	LS	SZ Leo	56025.618±0.003	0.470	19769	LS
V Ind	56181.717±0.002	0.383	33493	LS	SZ Leo	56283.582±0.003	0.483	20252	C
CQ Lac	56123.491±0.002	0.165	34009	C	TV Leo	55958.759±0.002	0.118	28115	LS
CQ Lac	56128.452±0.002	0.165	34017	C	TV Leo	55981.633±0.002	0.115	28149	LS
CQ Lac	56141.476±0.002	0.168	34038	C	TV Leo	55983.656±0.003	0.120	28152	LS
CQ Lac	56159.452±0.001	0.164	34067	C	TV Leo	55987.691±0.002	0.117	28158	LS
CQ Lac	56169.372±0.002	0.163	34083	C	TV Leo	56000.474±0.003	0.116	28177	C
CQ Lac	56185.499±0.003	0.169	34109	C	TV Leo	56010.567±0.002	0.117	28192	LS
CQ Lac	56195.416±0.002	0.165	34125	C	WW Leo	55979.610±0.002	0.043	34996	LS
CQ Lac	56203.477±0.002	0.165	34138	C	WW Leo	55999.503±0.003	0.042	35029	C
CQ Lac	56206.576±0.002	0.164	34143	C	WW Leo	56014.576±0.003	0.044	35054	LS
CQ Lac	56208.436±0.002	0.164	34146	C	WW Leo	56278.621±0.003	0.043	35492	C
CQ Lac	56239.440±0.002	0.166	34196	C	AA Leo	55998.533±0.002	−0.091	27398	C
RR Leo	55946.699±0.003	0.118	27965	C	AA Leo	56010.510±0.002	−0.087	27418	C
RR Leo	55951.674±0.001	0.117	27976	C	AA Leo	56290.675±0.002	−0.093	27886	C
RR Leo	55961.627±0.001	0.117	27998	C	AE Leo	56001.569±0.002	0.062	57700	C
RR Leo	55980.628±0.001	0.118	28040	C	AE Leo	56006.582±0.002	0.061	57708	C
RR Leo	55987.415±0.001	0.119	28055	C	AE Leo	56288.611±0.004	0.065	58158	C
RR Leo	55988.319±0.001	0.118	28057	C	AX Leo	55933.523±0.004	−0.039	42223	C
RR Leo	56000.532±0.003	0.117	28084	C	AX Leo	55949.512±0.004	−0.040	42245	C
RR Leo	56035.369±0.001	0.119	28161	C	AX Leo	55981.494±0.004	−0.038	42289	C
RR Leo	56251.619±0.001	0.125	28639	C	AX Leo	55984.399±0.004	−0.041	42293	C
RR Leo	56285.548±0.001	0.125	28714	C	AX Leo	56013.475±0.004	−0.038	42333	C
RX Leo	55935.644±0.003	0.105	30041	C	AX Leo	56273.681±0.006	−0.036	42691	C
RX Leo	55960.470±0.005	0.101	30079	C	AX Leo	56289.664±0.005	−0.043	42713	C
RX Leo	55962.437±0.005	0.108	30082	C	V LMi	55932.675±0.001	0.032	66926	C
RX Leo	55983.345±0.005	0.107	30114	C	V LMi	55948.452±0.002	0.034	66955	C
RX Leo	55990.532±0.005	0.106	30125	C	V LMi	55969.662±0.002	0.032	66994	C
RX Leo	56037.574±0.004	0.103	30197	C	V LMi	55972.382±0.001	0.032	66999	C
RX Leo	56043.460±0.005	0.108	30206	C	V LMi	55980.541±0.002	0.033	67014	C
RX Leo	56058.478±0.004	0.098	30229	C	V LMi	55997.406±0.004	0.036	67045	C
RX Leo	56263.660±0.004	0.108	30543	C	V LMi	56040.374±0.002	0.034	67124	C
SS Leo	55961.760±0.002	−0.079	22640	LS	V LMi	56247.604±0.002	0.031	67505	C
SS Leo	55963.639±0.005	−0.079	22643	C	V LMi	56285.678±0.001	0.031	67575	C
SS Leo	55973.656±0.004	−0.084	22659	C	X LMi	55997.552±0.003	0.243	24546	C
SS Leo	55985.555±0.002	−0.085	22678	C	X LMi	55999.603±0.002	0.242	24549	C
SS Leo	55986.811±0.002	−0.082	22680	LS	X LMi	56034.506±0.006	0.244	24600	C
SS Leo	55998.715±0.003	−0.079	22699	LS	X LMi	56244.595±0.003	0.247	24907	C
SS Leo	56000.592±0.003	−0.081	22702	C	X LMi	56279.496±0.003	0.248	24958	C
SS Leo	56027.525±0.004	−0.081	22745	C	X LMi	56283.603±0.002	0.249	24964	C
SS Leo	56057.588±0.002	−0.082	22793	LS	U Lep	56291.679±0.003	0.046	25692	LS
ST Leo	55929.632±0.002	−0.020	58593	C	AO Lep	56242.714±0.002	0.006	4419	LS
ST Leo	55961.658±0.002	−0.019	58660	C	AO Lep	56247.752±0.002	0.003	4428	LS
ST Leo	55975.518±0.002	−0.021	58689	C	AO Lep	56265.672±0.002	0.000	4460	LS
ST Leo	55998.462±0.002	−0.020	58737	C	AO Lep	56284.709±0.002	−0.005	4494	LS
ST Leo	55999.418±0.001	−0.020	58739	C	AO Lep	56293.664±0.003	−0.012	4510	LS
ST Leo	56001.330±0.002	−0.020	58743	C	TV Lib	56003.746±0.003	−0.005	133469	LS
ST Leo	56029.531±0.002	−0.020	58802	C	TV Lib	56010.755±0.002	−0.007	133495	LS
ST Leo	56040.525±0.003	−0.019	58825	C	TV Lib	56067.646±0.001	−0.006	133706	LS
ST Leo	56054.388±0.001	−0.018	58854	C	TV Lib	56084.634±0.001	−0.005	133769	LS
ST Leo	56289.556±0.004	−0.018	59346	C	TV Lib	56114.562±0.002	−0.005	133880	LS
SZ Leo	55957.772±0.005	0.450	19642	LS	VY Lib	56032.750±0.001	−0.037	27884	LS
SZ Leo	55972.721±0.005	0.445	19670	LS	VY Lib	56047.700±0.002	−0.036	27912	LS
SZ Leo	55973.799±0.003	0.455	19672	LS	VY Lib	56070.660±0.002	−0.036	27955	LS
SZ Leo	55990.359±0.005	0.459	19703	C	VY Lib	56085.611±0.002	−0.035	27983	LS

Table 1 (cont.): maxima of RR Lyrae stars

Variable star	Maximum HJD 24...	$O-C$ (days)	E	Obs	Variable star	Maximum HJD 24...	$O-C$ (days)	E	Obs.
XX Lib	56049.861±0.002	0.160	40225	LS	EZ Lyr	56143.530±0.003	−0.134	42320	C
AZ Lib	56062.785±0.003	0.201	43106	LS	EZ Lyr	56161.388±0.002	−0.135	42354	C
AZ Lib	56085.588±0.002	0.205	43141	LS	EZ Lyr	56182.404±0.004	−0.130	42394	C
AZ Lib	56113.596±0.002	0.204	43184	LS	IK Lyr	56186.415±0.010	−0.142	65028	C
LQ Lib	56011.732±0.003	0.002	3725	LS	IO Lyr	56015.530±0.002	−0.037	28411	C
LQ Lib	56058.684±0.003	0.030	3806	LS	IO Lyr	56045.538±0.002	−0.039	28463	C
TT Lyn	55960.388±0.002	−0.046	32320	C	IO Lyr	56101.518±0.002	−0.040	28560	C
TT Lyn	55972.340±0.002	−0.043	32340	C	IO Lyr	56116.527±0.002	−0.036	28586	C
TT Lyn	55975.328±0.002	−0.042	32345	C	IO Lyr	56131.527±0.002	−0.041	28612	C
TT Lyn	55988.467±0.002	−0.047	32367	C	IO Lyr	56138.456±0.002	−0.038	28624	C
TT Lyn	55998.627±0.004	−0.043	32384	C	IO Lyr	56142.494±0.002	−0.040	28631	C
TT Lyn	56013.559±0.003	−0.047	32409	C	IO Lyr	56146.533±0.002	−0.041	28638	C
TT Lyn	56243.572±0.002	−0.046	32794	C	IO Lyr	56164.422±0.002	−0.042	28669	C
TT Lyn	56246.563±0.003	−0.042	32799	C	IO Lyr	56168.464±0.002	−0.040	28676	C
TT Lyn	56252.536±0.003	−0.044	32809	C	IO Lyr	56175.385±0.002	−0.045	28688	C
TT Lyn	56285.393±0.002	−0.046	32864	C	IO Lyr	56186.354±0.002	−0.041	28707	C
TW Lyn	55950.621±0.002	0.060	22679	C	V340 Lyr	56055.440±0.005	−0.031	44741	C
TW Lyn	55966.524±0.003	0.062	22712	C	V392 Lyr	56142.546±0.010	0.123	44267	C
TW Lyn	55970.376±0.002	0.059	22720	C	V392 Lyr	56164.380±0.007	0.112	44306	C
TW Lyn	55995.433±0.002	0.059	22772	C	AV Men	56279.601±0.003	−0.005	5669	LS
TW Lyn	56216.608±0.002	0.060	23231	C	AV Men	56289.587±0.003	−0.009	5687	LS
TW Lyn	56229.619±0.002	0.061	23258	C	Z Mic	56203.669±0.002	−0.147	24886	LS
TW Lyn	56246.486±0.003	0.063	23293	C	DV Mon	56281.703±0.002	0.062	75074	LS
TW Lyn	56280.695±0.001	0.060	23364	C	DV Mon	56286.667±0.003	0.065	75086	LS
RZ Lyr	56055.428±0.002	−0.037	29090	C	TX Mus	55961.760±0.002	0.086	66990	LS
RZ Lyr	56058.497±0.002	−0.035	29096	C	TX Mus	55978.799±0.002	0.089	67026	LS
RZ Lyr	56101.448±0.002	−0.028	29180	C	TX Mus	55990.627±0.002	0.086	67051	LS
RZ Lyr	56102.471±0.002	−0.028	29182	C	TX Mus	55991.575±0.002	0.088	67053	LS
RZ Lyr	56124.440±0.002	−0.042	29225	C	TX Mus	55995.833±0.002	0.087	67062	LS
RZ Lyr	56126.483±0.003	−0.044	29229	C	TX Mus	55996.780±0.002	0.088	67064	LS
RZ Lyr	56127.506±0.001	−0.044	29231	C	TX Mus	56009.558±0.002	0.088	67091	LS
RZ Lyr	56146.421±0.001	−0.045	29268	C	TX Mus	56023.755±0.002	0.089	67121	LS
RZ Lyr	56152.551±0.002	−0.050	29280	C	TX Mus	56024.699±0.002	0.086	67123	LS
RZ Lyr	56169.423±0.002	−0.049	29313	C	TX Mus	56049.782±0.002	0.088	67176	LS
RZ Lyr	56187.322±0.002	−0.043	29348	C	TX Mus	56054.517±0.004	0.091	67186	LS
AW Lyr	56042.470±0.003	−0.051	61737	C	TX Mus	56060.664±0.002	0.086	67199	LS
AW Lyr	56128.519±0.002	−0.061	61910	C	TX Mus	56079.595±0.002	0.088	67239	LS
AW Lyr	56142.445±0.002	−0.063	61938	C	EM Mus	55963.835±0.001	−0.193	37295	LS
CN Lyr	56042.493±0.003	0.018	28091	C	EM Mus	55965.705±0.002	−0.193	37299	LS
CN Lyr	56051.551±0.003	0.026	28113	C	EM Mus	55970.844±0.001	−0.194	37310	LS
CN Lyr	56091.449±0.003	0.020	28210	C	EM Mus	55977.855±0.002	−0.193	37325	LS
CN Lyr	56119.424±0.002	0.021	28278	C	EM Mus	55978.788±0.001	−0.194	37327	LS
CN Lyr	56126.417±0.002	0.020	28295	C	EM Mus	55987.668±0.002	−0.193	37346	LS
CN Lyr	56128.477±0.002	0.024	28300	C	EM Mus	55994.677±0.002	−0.193	37361	LS
CN Lyr	56133.414±0.003	0.024	28312	C	EM Mus	55999.817±0.002	−0.193	37372	LS
CN Lyr	56142.462±0.002	0.022	28334	C	EM Mus	56010.565±0.002	−0.193	37395	LS
CN Lyr	56144.517±0.003	0.020	28339	C	EM Mus	56023.648±0.002	−0.194	37423	LS
CN Lyr	56146.577±0.004	0.023	28344	C	EM Mus	56024.584±0.002	−0.193	37425	LS
CN Lyr	56158.506±0.004	0.022	28373	C	EM Mus	56029.724±0.002	−0.193	37436	LS
CN Lyr	56184.421±0.004	0.020	28436	C	EM Mus	56039.536±0.001	−0.194	37457	LS
CR Lyr	56051.539±0.005	−0.011	53285	C	EM Mus	56051.689±0.003	−0.191	37483	LS
CR Lyr	56091.499±0.005	−0.018	53366	C	EM Mus	56068.507±0.002	−0.196	37519	LS
CR Lyr	56128.513±0.003	−0.011	53441	C	EM Mus	56075.516±0.002	−0.197	37534	LS
CR Lyr	56133.439±0.003	−0.019	53451	C	EM Mus	56109.626±0.003	−0.199	37607	LS
CX Lyr	56169.497±0.005	−0.004	37461	C	EM Mus	56110.562±0.002	−0.198	37609	LS
EZ Lyr	56120.417±0.003	−0.136	42276	C	EM Mus	56118.508±0.002	−0.196	37626	LS

Table 1 (cont.): maxima of RR Lyrae stars

Variable star	Maximum HJD 24...	$O-C$ (days)	E	Obs	Variable star	Maximum HJD 24...	$O-C$ (days)	E	Obs.
VY Nor	56003.886±0.008	−0.124	81184	LS	SS Oct	56226.605±0.002	0.016	45360	LS
VY Nor	56050.802±0.007	−0.121	81309	LS	SS Oct	56229.712±0.004	0.014	45365	LS
VY Nor	56118.738±0.006	−0.115	81490	LS	SS Oct	56239.665±0.003	0.018	45381	LS
VY Nor	56133.750±0.005	−0.116	81530	LS	SS Oct	56244.635±0.003	0.013	45389	LS
Y Oct	55960.797±0.002	0.315	42655	LS	SS Oct	56249.614±0.005	0.017	45397	LS
Y Oct	55971.789±0.002	0.314	42672	LS	SS Oct	56254.586±0.004	0.015	45405	LS
Y Oct	55991.837±0.003	0.317	42703	LS	SS Oct	56277.598±0.004	0.019	45442	LS
Y Oct	55993.774±0.003	0.314	42706	LS	UV Oct	56002.771±0.003	−0.238	39944	LS
Y Oct	56002.828±0.003	0.315	42720	LS	UV Oct	56003.856±0.003	−0.238	39946	LS
Y Oct	56019.638±0.002	0.313	42746	LS	UV Oct	56015.787±0.003	−0.245	39968	LS
Y Oct	56022.871±0.002	0.313	42751	LS	UV Oct	56020.672±0.002	−0.244	39977	LS
Y Oct	56026.748±0.003	0.310	42757	LS	UV Oct	56048.878±0.001	−0.255	40029	LS
Y Oct	56033.860±0.002	0.309	42768	LS	UV Oct	56051.591±0.002	−0.254	40034	LS
Y Oct	56054.555±0.003	0.312	42800	LS	UV Oct	56054.848±0.002	−0.253	40040	LS
Y Oct	56081.710±0.003	0.309	42842	LS	UV Oct	56063.535±0.005	−0.248	40056	LS
Y Oct	56083.648±0.002	0.307	42845	LS	UV Oct	56067.867±0.002	−0.257	40064	LS
Y Oct	56109.511±0.002	0.305	42885	LS	UV Oct	56069.500±0.005	−0.252	40067	LS
Y Oct	56120.501±0.002	0.302	42902	LS	UV Oct	56083.602±0.003	−0.258	40093	LS
Y Oct	56162.529±0.002	0.300	42967	LS	UV Oct	56084.689±0.002	−0.256	40095	LS
RV Oct	55965.784±0.003	0.148	71519	LS	UV Oct	56101.514±0.003	−0.253	40126	LS
RV Oct	55969.780±0.003	0.146	71526	LS	UV Oct	56110.738±0.002	−0.253	40143	LS
RV Oct	55992.625±0.002	0.145	71566	LS	UV Oct	56135.706±0.002	−0.246	40189	LS
RV Oct	55993.765±0.003	0.142	71568	LS	UV Oct	56165.548±0.003	−0.249	40244	LS
RV Oct	55996.623±0.002	0.144	71573	LS	UV Oct	56166.628±0.003	−0.254	40246	LS
RV Oct	56024.610±0.003	0.144	71622	LS	UW Oct	56069.840±0.003	−0.019	48893	LS
RV Oct	56025.753±0.003	0.145	71624	LS	UW Oct	56077.838±0.002	−0.021	48911	LS
RV Oct	56048.606±0.002	0.152	71664	LS	UW Oct	56081.836±0.002	−0.024	48920	LS
RV Oct	56056.594±0.002	0.143	71678	LS	UW Oct	56085.841±0.002	−0.019	48929	LS
RV Oct	56057.742±0.002	0.149	71680	LS	UW Oct	56118.733±0.002	−0.019	49003	LS
RV Oct	56100.578±0.002	0.148	71755	LS	UW Oct	56138.735±0.002	−0.020	49048	LS
RV Oct	56108.570±0.002	0.144	71769	LS	UW Oct	56158.737±0.003	−0.020	49093	LS
RV Oct	56136.559±0.002	0.146	71818	LS	UW Oct	56159.623±0.002	−0.023	49095	LS
RY Oct	56070.784±0.003	0.036	49840	LS	UW Oct	56160.517±0.003	−0.018	49097	LS
RY Oct	56110.773±0.002	0.019	49911	LS	UW Oct	56165.849±0.002	−0.019	49109	LS
RY Oct	56115.838±0.002	0.013	49920	LS	UW Oct	56175.628±0.003	−0.019	49131	LS
RY Oct	56124.859±0.002	0.018	49936	LS	UW Oct	56181.848±0.002	−0.023	49145	LS
RY Oct	56166.565±0.003	0.027	50010	LS	UW Oct	56185.847±0.002	−0.023	49154	LS
RY Oct	56172.773±0.003	0.037	50021	LS	UW Oct	56199.631±0.003	−0.019	49185	LS
RY Oct	56197.549±0.002	0.021	50065	LS	UW Oct	56203.633±0.002	−0.017	49194	LS
RY Oct	56203.755±0.002	0.028	50076	LS	UW Oct	56210.742±0.002	−0.020	49210	LS
RY Oct	56219.528±0.004	0.024	50104	LS	UW Oct	56214.745±0.003	−0.017	49219	LS
RY Oct	56224.599±0.005	0.024	50113	LS	UW Oct	56219.635±0.003	−0.017	49230	LS
RY Oct	56229.677±0.004	0.031	50122	LS	UW Oct	56223.633±0.003	−0.019	49239	LS
RY Oct	56264.614±0.002	0.033	50184	LS	UW Oct	56243.633±0.002	−0.021	49284	LS
SS Oct	56084.821±0.002	0.008	45132	LS	UW Oct	56255.634±0.003	−0.021	49311	LS
SS Oct	56120.881±0.002	0.002	45190	LS	UW Oct	56259.639±0.003	−0.017	49320	LS
SS Oct	56158.822±0.004	0.012	45251	LS	UW Oct	56263.634±0.003	−0.022	49329	LS
SS Oct	56167.531±0.003	0.015	45265	LS	AR Oct	56278.617±0.002	0.061	49383	LS
SS Oct	56168.772±0.002	0.013	45267	LS	AR Oct	56291.617±0.002	0.071	49416	LS
SS Oct	56175.613±0.002	0.014	45278	LS	DY Oct	56264.797±0.002	0.009	4469	LS
SS Oct	56190.544±0.003	0.021	45302	LS	DY Oct	56274.842±0.002	0.008	4487	LS
SS Oct	56196.762±0.004	0.021	45312	LS	DY Oct	56293.817±0.002	0.008	4521	LS
SS Oct	56198.623±0.003	0.016	45315	LS	ST Oph	56060.723±0.002	−0.024	61361	LS
SS Oct	56213.547±0.003	0.016	45339	LS	ST Oph	56071.531±0.002	−0.024	61385	C
SS Oct	56219.764±0.003	0.015	45349	LS	ST Oph	56072.434±0.005	−0.022	61387	C
SS Oct	56221.630±0.002	0.016	45352	LS	ST Oph	56078.736±0.001	−0.025	61401	LS

Table 1 (cont.): maxima of RR Lyrae stars

Variable star	Maximum HJD 24...	$O-C$ (days)	E	Obs	Variable star	Maximum HJD 24...	$O-C$ (days)	E	Obs.
ST Oph	56089.546±0.002	−0.023	61425	C	BP Pav	56069.887±0.002	0.193	51610	LS
ST Oph	56117.468±0.001	−0.023	61487	C	BP Pav	56086.754±0.002	−0.137	51642	LS
ST Oph	56134.581±0.002	−0.024	61525	LS	BP Pav	56108.894±0.002	−0.030	51683	LS
ST Oph	56148.543±0.001	−0.023	61556	LS	BP Pav	56114.692±0.001	−0.144	51694	LS
V408 Oph	56072.459±0.002			C	BP Pav	56127.870±0.002	0.137	51718	LS
V408 Oph	56089.458±0.002			C	BP Pav	56137.887±0.002	−0.057	51737	LS
V408 Oph	56096.433±0.002			C	BP Pav	56164.771±0.002	−0.043	51787	LS
V408 Oph	56119.532±0.002			C	BP Pav	56172.678±0.002	−0.197	51802	LS
V408 Oph	56120.406±0.002			C	BP Pav	56189.546±0.002	0.012	51833	LS
V408 Oph	56143.507±0.002			C	BP Pav	56199.561±0.002	−0.184	51852	LS
V408 Oph	56147.431±0.002			C	BP Pav	56210.630±0.002	0.137	51872	LS
V408 Oph	56154.403±0.001			C	BP Pav	56229.607±0.002	−0.232	51908	LS
V445 Oph	56022.822±0.002	0.043	71732	LS	DN Pav	56066.873±0.002	0.117	31772	LS
V445 Oph	56058.557±0.002	0.046	71822	C	DN Pav	56081.863±0.004	0.118	31804	LS
V445 Oph	56064.509±0.002	0.042	71837	C	DN Pav	56082.798±0.003	0.116	31806	LS
V445 Oph	56086.739±0.002	0.039	71893	LS	DN Pav	56114.654±0.002	0.118	31874	LS
V452 Oph	56023.529±0.004	0.007	34758	C	DN Pav	56118.871±0.002	0.119	31883	LS
V452 Oph	56033.556±0.001	0.005	34776	C	DN Pav	56119.808±0.002	0.119	31885	LS
V452 Oph	56066.429±0.003	0.005	34835	C	DN Pav	56125.898±0.001	0.119	31898	LS
V452 Oph	56101.528±0.003	0.003	34898	C	DN Pav	56172.742±0.001	0.119	31998	LS
V452 Oph	56115.460±0.002	0.006	34923	C	DN Pav	56173.678±0.002	0.118	32000	LS
V452 Oph	56125.491±0.003	0.008	34941	C	DN Pav	56187.733±0.002	0.120	32030	LS
V455 Oph	56089.532±0.003	−0.281	31408	C	DN Pav	56203.659±0.002	0.119	32064	LS
V455 Oph	56094.528±0.003	−0.278	31419	C	DN Pav	56205.532±0.002	0.118	32068	LS
V455 Oph	56118.586±0.003	−0.277	31472	C	DN Pav	56226.613±0.002	0.119	32113	LS
V455 Oph	56144.455±0.002	−0.281	31529	C	VV Peg	56124.530±0.002	−0.017	34266	C
V455 Oph	56163.518±0.002	−0.283	31571	C	VV Peg	56127.460±0.001	−0.016	34272	C
V706 Oph	56058.538±0.006	−0.160	54857	C	VV Peg	56148.462±0.002	−0.016	34315	C
V784 Oph	56043.577±0.003	−0.007	41684	C	VV Peg	56163.601±0.002	−0.016	34346	C
V784 Oph	56047.794±0.002	0.071	41695	LS	VV Peg	56166.533±0.001	−0.015	34352	C
V784 Oph	56059.842±0.005	0.078	41727	LS	VV Peg	56184.601±0.002	−0.017	34389	C
V784 Oph	56133.472±0.005	−0.042	41923	C+LS	VV Peg	56185.581±0.002	−0.014	34391	C
V788 Oph	56040.614±0.006	−0.064	34758	C	VV Peg	56191.440±0.002	−0.015	34403	C
V788 Oph	56092.590±0.004	−0.065	34853	C	VV Peg	56208.534±0.002	−0.015	34438	C
V1028 Oph	56091.524±0.007	0.063	34193	C	VV Peg	56209.513±0.004	−0.013	34440	C
CM Ori	56275.676±0.003	−0.006	47227	LS	AV Peg	56125.519±0.001	0.143	31598	C
V964 Ori	55937.658±0.002	−0.452	48425	LS	AV Peg	56139.573±0.001	0.144	31634	C
V964 Ori	56265.672±0.002	−0.464	49075	LS	AV Peg	56150.504±0.001	0.144	31662	C
V964 Ori	56268.699±0.003	−0.465	49081	LS	AV Peg	56152.455±0.001	0.143	31667	C
TY Pav	56009.759±0.003	0.174	20379	LS	AV Peg	56155.580±0.002	0.145	31675	C
WY Pav	56047.816±0.002	0.054	49576	LS	AV Peg	56181.345±0.003	0.146	31741	C
WY Pav	56053.704±0.004	0.056	49586	LS	AV Peg	56186.420±0.002	0.146	31754	C
WY Pav	56066.655±0.002	0.058	49608	LS	AV Peg	56204.376±0.002	0.145	31800	C
WY Pav	56086.657±0.003	0.049	49642	LS	AV Peg	56216.478±0.002	0.145	31831	C
WY Pav	56100.787±0.003	0.053	49666	LS	AV Peg	56229.360±0.002	0.144	31864	C
WY Pav	56116.677±0.002	0.051	49693	LS	BH Peg	56126.463±0.003	−0.143	26149	C
WY Pav	56159.643±0.002	0.051	49766	LS	BH Peg	56133.514±0.003	−0.143	26160	C
WY Pav	56169.649±0.004	0.051	49783	LS	BH Peg	56149.536±0.003	−0.146	26185	C
BN Pav	56060.872±0.004	−0.192	48882	LS	BH Peg	56158.506±0.002	−0.150	26199	C
BN Pav	56130.624±0.002	−0.202	49005	LS	BH Peg	56160.431±0.003	−0.148	26202	C
BN Pav	56173.725±0.001	−0.206	49081	LS	BH Peg	56181.598±0.005	−0.133	26235	C
BN Pav	56197.544±0.002	−0.208	49123	LS	BH Peg	56190.563±0.005	−0.142	26249	C
BN Pav	56223.631±0.002	−0.211	49169	LS	BH Peg	56203.394±0.003	−0.131	26269	C
BP Pav	56047.745±0.001	0.085	51569	LS	BH Peg	56205.328±0.008	−0.120	26272	C
BP Pav	56049.855±0.001	0.045	51573	LS	BH Peg	56244.443±0.003	−0.106	26333	C
BP Pav	56058.817±0.002	−0.129	51590	LS	CG Peg	56108.505±0.002	−0.058	36405	C

Table 1 (cont.): maxima of RR Lyrae stars

Variable star	Maximum HJD 24...	$O-C$ (days)	E	Obs	Variable star	Maximum HJD 24...	$O-C$ (days)	E	Obs.
CG Peg	56109.442±0.002	−0.054	36407	C	TZ Phe	56207.638±0.003			LS
CG Peg	56122.519±0.002	−0.057	36435	C	TZ Phe	56210.712±0.005			LS
CG Peg	56130.460±0.003	−0.058	36452	C	TZ Phe	56213.788±0.004			LS
CG Peg	56138.404±0.002	−0.055	36469	C	TZ Phe	56215.631±0.005			LS
CG Peg	56150.546±0.002	−0.059	36495	C	TZ Phe	56223.640±0.005			LS
CG Peg	56157.555±0.001	−0.057	36510	C	TZ Phe	56231.646±0.007			LS
CG Peg	56164.563±0.002	−0.056	36525	C	TZ Phe	56239.647±0.006			LS
CG Peg	56186.518±0.002	−0.057	36572	C	TZ Phe	56242.727±0.005			LS
CG Peg	56230.427±0.002	−0.059	36666	C	TZ Phe	56247.648±0.005			LS
CG Peg	56237.433±0.002	−0.059	36681	C	TZ Phe	56252.569±0.004			LS
CG Peg	56239.302±0.002	−0.059	36685	C	U Pic	55936.742±0.002	0.071	32405	LS
CV Peg	56136.455±0.003	−0.063	55770	C	U Pic	56194.806±0.002	0.077	32991	LS
CV Peg	56150.526±0.002	−0.064	55795	C	U Pic	56198.767±0.002	0.075	33000	LS
CV Peg	56155.589±0.002	−0.067	55804	C	U Pic	56221.670±0.003	0.079	33052	LS
CV Peg	56229.327±0.002	−0.066	55935	C	U Pic	56232.677±0.002	0.076	33077	LS
DZ Peg	56135.455±0.002	0.169	36625	C	U Pic	56246.771±0.002	0.079	33109	LS
DZ Peg	56138.491±0.002	0.169	36630	C	U Pic	56247.651±0.003	0.078	33111	LS
DZ Peg	56141.528±0.004	0.169	36635	C	U Pic	56262.624±0.002	0.078	33145	LS
DZ Peg	56166.429±0.003	0.169	36676	C	U Pic	56265.706±0.002	0.077	33152	LS
DZ Peg	56177.362±0.004	0.170	36694	C	U Pic	56284.642±0.002	0.077	33195	LS
DZ Peg	56186.471±0.002	0.168	36709	C	RY Psc	56133.767±0.002	0.620	25395	LS
DZ Peg	56189.507±0.003	0.168	36714	C	RY Psc	56168.739±0.005	0.630	25461	LS
DZ Peg	56195.581±0.002	0.168	36724	C	RY Psc	56177.730±0.003	0.616	25478	LS
DZ Peg	56208.338±0.005	0.171	36745	C	RY Psc	56182.503±0.005	0.622	25487	C
DZ Peg	56234.453±0.004	0.170	36788	C	RY Psc	56194.687±0.003	0.623	25510	LS
DZ Peg	56237.482±0.003	0.163	36793	C	RY Psc	56209.520±0.004	0.624	25538	C
DZ Peg	56265.429±0.005	0.172	36839	C	RY Psc	56210.581±0.005	0.625	25540	LS
AR Per	55951.317±0.002	0.060	67476	C	RY Psc	56216.404±0.003	0.621	25551	C
AR Per	56164.522±0.002	0.065	67977	C	RY Psc	56219.584±0.004	0.623	25557	LS
AR Per	56167.499±0.002	0.063	67984	C	RY Psc	56220.641±0.003	0.621	25559	LS
AR Per	56187.501±0.003	0.065	68031	C	RY Psc	56243.434±0.004	0.636	25602	C
AR Per	56192.606±0.002	0.063	68043	C	RY Psc	56277.332±0.002	0.633	25666	C
AR Per	56209.627±0.002	0.062	68083	C	XX Pup	55932.637±0.002	0.518	27377	LS
AR Per	56210.479±0.002	0.063	68085	C	XX Pup	55933.672±0.002	0.518	27379	LS
AR Per	56228.353±0.002	0.064	68127	C	XX Pup	55977.633±0.001	0.519	27464	LS
AR Per	56237.292±0.002	0.066	68148	C	XX Pup	55978.669±0.002	0.521	27466	LS
AR Per	56239.416±0.002	0.063	68153	C	XX Pup	56006.597±0.002	0.521	27520	LS
AR Per	56247.501±0.002	0.062	68172	C	XX Pup	56007.630±0.002	0.520	27522	LS
AR Per	56265.374±0.002	0.062	68214	C	BB Pup	55969.690±0.001	0.130	35707	LS
AR Per	56280.269±0.001	0.062	68249	C	BB Pup	55996.601±0.001	0.130	35763	LS
AR Per	56291.333±0.002	0.062	68275	C	BB Pup	56288.778±0.003	0.136	36371	LS
AR Per	56292.610±0.002	0.063	68278	C	BB Pup	56289.737±0.002	0.134	36373	LS
AR Per	56293.462±0.002	0.064	68280	C	HH Pup	55960.754±0.001	0.008	44685	LS
RV Phe	56160.766±0.003	−0.208	23885	LS	HH Pup	55966.617±0.002	0.010	44700	LS
RV Phe	56166.727±0.003	−0.211	23895	LS	HH Pup	55969.743±0.001	0.010	44708	LS
RV Phe	56194.756±0.003	−0.214	23942	LS	HH Pup	55982.637±0.001	0.009	44741	LS
RV Phe	56203.707±0.003	−0.209	23957	LS	HH Pup	55991.625±0.001	0.010	44764	LS
RV Phe	56221.598±0.004	−0.210	23987	LS	HH Pup	56257.726±0.003	0.013	45445	LS
RV Phe	56237.699±0.004	−0.213	24014	LS	HH Pup	56264.757±0.002	0.011	45463	LS
RV Phe	56243.668±0.005	−0.208	24024	LS	HH Pup	56266.712±0.003	0.012	45468	LS
TZ Phe	56128.837±0.004			LS	HH Pup	56282.732±0.002	0.011	45509	LS
TZ Phe	56149.763±0.004			LS	HH Pup	56284.686±0.002	0.011	45514	LS
TZ Phe	56173.774±0.005			LS	HH Pup	56286.639±0.001	0.010	45519	LS
TZ Phe	56181.777±0.004			LS	HH Pup	56291.720±0.002	0.012	45532	LS
TZ Phe	56186.704±0.005			LS	HK Pup	55967.731±0.004	−0.311	26367	LS
TZ Phe	56194.707±0.003			LS	HK Pup	55973.603±0.003	−0.313	26375	LS

Table 1 (cont.): maxima of RR Lyrae stars

Variable star	Maximum HJD 24...	$O-C$ (days)	E	Obs	Variable star	Maximum HJD 24...	$O-C$ (days)	E	Obs.
HK Pup	56279.771±0.005	−0.322	26792	LS	RU Scl	56238.692±0.002	0.469	50909	LS
HK Pup	56282.697±0.004	−0.333	26796	LS	RU Scl	56239.677±0.003	0.467	50911	LS
V440 Sgr	56068.843±0.002	0.114	30492	LS	RU Scl	56243.623±0.003	0.467	50919	LS
V440 Sgr	56081.736±0.005	0.115	30519	LS	RU Scl	56244.610±0.002	0.467	50921	LS
V440 Sgr	56124.711±0.002	0.116	30609	LS	RU Scl	56245.594±0.002	0.464	50923	LS
V440 Sgr	56134.737±0.002	0.115	30630	LS	UZ Scl	56167.668±0.002	0.039	37975	LS
V440 Sgr	56136.648±0.002	0.117	30634	LS	UZ Scl	56175.751±0.002	0.038	37993	LS
V440 Sgr	56190.603±0.002	0.116	30747	LS	UZ Scl	56194.614±0.001	0.038	38035	LS
V675 Sgr	56039.813±0.005	0.088	43053	LS	UZ Scl	56203.598±0.002	0.039	38055	LS
V675 Sgr	56064.850±0.001	0.076	43092	LS	UZ Scl	56229.648±0.002	0.041	38113	LS
V675 Sgr	56066.775±0.002	0.073	43095	LS	VW Scl	56127.849±0.002	−0.001	55427	LS
V675 Sgr	56129.721±0.005	0.075	43193	LS	VW Scl	56147.775±0.002	−0.001	55466	LS
V675 Sgr	56149.639±0.004	0.082	43224	LS	VW Scl	56167.701±0.002	−0.000	55505	LS
V756 Sgr	56052.790±0.002	0.106	50801	LS	VW Scl	56168.724±0.003	0.001	55507	LS
V756 Sgr	56064.843±0.002	0.108	50824	LS	VW Scl	56190.692±0.002	−0.001	55550	LS
V756 Sgr	56115.667±0.002	0.107	50921	LS	VW Scl	56192.734±0.002	−0.002	55554	LS
V756 Sgr	56126.670±0.003	0.106	50942	LS	VW Scl	56194.781±0.002	0.001	55558	LS
V1130 Sgr	56067.794±0.002	0.043	50536	LS	VW Scl	56196.825±0.002	0.001	55562	LS
V1130 Sgr	56108.693±0.002	0.041	50608	LS	VW Scl	56214.703±0.002	−0.003	55597	LS
V1130 Sgr	56124.598±0.002	0.041	50636	LS	VW Scl	56232.588±0.002	0.000	55632	LS
V1130 Sgr	56149.594±0.002	0.042	50680	LS	VW Scl	56238.719±0.002	0.000	55644	LS
V1130 Sgr	56158.682±0.002	0.041	50696	LS	VW Scl	56257.623±0.002	0.001	55681	LS
V1130 Sgr	56162.658±0.002	0.041	50703	LS	VW Scl	56258.644±0.002	−0.000	55683	LS
V1176 Sgr	56039.779±0.002	0.155	97536	LS	VW Scl	56259.665±0.002	−0.001	55685	LS
V1176 Sgr	56050.779±0.004	0.155	97567	LS	VX Scl	56139.820±0.002	−1.925	22794	LS
V1176 Sgr	56099.731±0.002	0.143	97705	LS	VX Scl	56169.760±0.003	−1.940	22841	LS
V1176 Sgr	56119.598±0.003	0.140	97761	LS	VX Scl	56204.803±0.002	−1.950	22896	LS
V1176 Sgr	56130.596±0.002	0.139	97792	LS	VX Scl	56257.674±0.003	−1.978	22979	LS
V1646 Sgr	56121.871±0.003	0.160	40036	LS	AE Scl	56129.859±0.002	−0.261	27109	LS
V1646 Sgr	56131.672±0.003	0.161	40054	LS	AE Scl	56167.812±0.002	−0.264	27178	LS
V494 Sco	56061.777±0.003	−0.313	34951	LS	AE Scl	56220.632±0.002	−0.253	27274	LS
V494 Sco	56067.756±0.004	−0.316	34965	LS	AE Scl	56221.730±0.001	−0.254	27276	LS
V494 Sco	56118.605±0.003	−0.320	35084	LS	AE Scl	56231.629±0.002	−0.257	27294	LS
V494 Sco	56126.730±0.004	−0.314	35103	LS	AE Scl	56232.728±0.003	−0.259	27296	LS
V494 Sco	56159.626±0.002	−0.323	35180	LS	AE Scl	56242.628±0.002	−0.260	27314	LS
V690 Sco	56048.846±0.002	−0.024	28951	LS	AE Scl	56247.580±0.003	−0.259	27323	LS
V690 Sco	56050.815±0.002	−0.023	28955	LS	AE Scl	56259.686±0.003	−0.255	27345	LS
V690 Sco	56079.860±0.003	−0.021	29014	LS	VY Ser	56016.590±0.003	0.053	34717	C
V690 Sco	56117.760±0.002	−0.025	29091	LS	VY Ser	56033.734±0.006	0.059	34741	LS
V690 Sco	56161.570±0.002	−0.026	29180	LS	VY Ser	56058.719±0.006	0.051	34776	LS
V765 Sco	56032.819±0.002	0.145	56564	LS	VY Ser	56059.432±0.005	0.050	34777	C
V765 Sco	56046.731±0.004	0.148	56594	LS	AN Ser	55986.550±0.002	0.007	79065	C
V765 Sco	56047.654±0.002	0.143	56596	LS	AN Ser	56042.412±0.004	0.008	79172	C
V765 Sco	56058.784±0.002	0.145	56620	LS	AN Ser	56057.547±0.002	0.003	79201	C
V765 Sco	56059.711±0.002	0.145	56622	LS	AN Ser	56092.529±0.002	0.006	79268	C
V765 Sco	56085.677±0.002	0.146	56678	LS	AT Ser	56058.448±0.005	0.084	19101	C
V765 Sco	56098.661±0.002	0.148	56706	LS	AT Ser	56064.420±0.003	0.084	19109	C
V765 Sco	56117.669±0.002	0.146	56747	LS	AT Ser	56066.663±0.003	0.087	19112	LS
V765 Sco	56130.653±0.002	0.147	56775	LS	AT Ser	56075.624±0.003	0.090	19124	LS
RU Scl	56113.865±0.002	0.457	50656	LS	AT Ser	56093.534±0.003	0.083	19148	C
RU Scl	56161.728±0.003	0.466	50753	LS	AT Ser	56096.525±0.003	0.087	19152	C
RU Scl	56167.644±0.002	0.462	50765	LS	AT Ser	56099.512±0.004	0.088	19156	C
RU Scl	56191.819±0.002	0.463	50814	LS	AV Ser	56005.561±0.001	0.169	56736	C
RU Scl	56192.804±0.002	0.462	50816	LS	AV Ser	56033.839±0.002	0.169	56794	LS
RU Scl	56193.793±0.002	0.464	50818	LS	AV Ser	56059.681±0.002	0.171	56847	LS
RU Scl	56195.768±0.002	0.466	50822	LS	AV Ser	56064.549±0.002	0.163	56857	C

Table 1 (cont.): maxima of RR Lyrae stars

Variable star	Maximum HJD 24...	$O-C$ (days)	E	Obs	Variable star	Maximum HJD 24...	$O-C$ (days)	E	Obs.
AV Ser	56102.572±0.002	0.157	56935	LS	AE Tuc	56265.663±0.003	0.115	53075	LS
AV Ser	56119.644±0.002	0.164	56970	LS	AE Tuc	56287.633±0.002	0.124	53128	LS
CS Ser	55990.648±0.003	0.024	47104	C	AG Tuc	56264.649±0.003	0.056	27336	LS
CS Ser	56017.516±0.002	0.025	47155	C	BK Tuc	56266.599±0.002	−0.005	35498	LS
CS Ser	56019.621±0.002	0.023	47159	C	BK Tuc	56288.599±0.002	−0.014	35538	LS
CS Ser	56022.782±0.002	0.023	47165	LS	RV UMa	55963.647±0.003	0.124	23262	C
CS Ser	56036.480±0.003	0.025	47191	C	RV UMa	55997.354±0.003	0.131	23334	C
CS Ser	56049.645±0.002	0.020	47216	LS	RV UMa	56054.448±0.002	0.122	23456	C
CS Ser	56064.388±0.002	0.013	47244	C	TU UMa	55951.478±0.002	−0.053	23527	C
DF Ser	55990.492±0.003	0.095	60038	C	TU UMa	55961.517±0.002	−0.052	23545	C
DF Ser	56010.629±0.001	0.093	60084	C	TU UMa	55979.363±0.002	−0.051	23577	C
DF Ser	56042.588±0.001	0.093	60157	C	TU UMa	55989.399±0.002	−0.053	23595	C
DF Ser	56050.471±0.002	0.096	60175	C	TU UMa	56008.360±0.002	−0.052	23629	C
DF Ser	56074.549±0.002	0.095	60230	C	TU UMa	56015.608±0.002	−0.054	23642	C
DF Ser	56089.432±0.002	0.093	60264	C	TU UMa	56029.549±0.002	−0.055	23667	C
DF Ser	56099.504±0.002	0.096	60287	C	TU UMa	56038.474±0.003	−0.052	23683	C
GZ Tel	56061.916±0.005	0.007	8651	LS	TU UMa	56285.513±0.003	−0.055	24126	C
GZ Tel	56171.659±0.002	0.010	8892	LS	TU UMa	56290.533±0.004	−0.054	24135	C
HH Tel	56100.635±0.002	−0.006	5949	LS	AB UMa	55934.660±0.005	0.123	32868	C
HH Tel	56115.584±0.003	−0.002	5980	LS	AB UMa	55963.451±0.008	0.134	32916	C
HY Tel	56115.777±0.002	0.005	8095	LS	AB UMa	55970.638±0.005	0.127	32928	C
HY Tel	56146.788±0.003	0.006	8172	LS	AB UMa	55984.421±0.003	0.119	32951	C
RW TrA	56005.745±0.002	−0.187	38810	LS	AB UMa	55997.617±0.005	0.125	32973	C
RW TrA	56008.736±0.003	−0.188	38818	LS	AB UMa	56006.621±0.006	0.135	32988	C
RW TrA	56012.851±0.002	−0.188	38829	LS	AB UMa	56280.622±0.007	0.129	33445	C
RW TrA	56018.836±0.002	−0.187	38845	LS	AB UMa	56283.626±0.005	0.135	33450	C
RW TrA	56024.819±0.001	−0.189	38861	LS	AB UMa	56292.627±0.008	0.143	33465	C
RW TrA	56071.575±0.002	−0.189	38986	LS	EX UMa [4]	55949.327±0.005	0.035	12778	C
RW TrA	56085.788±0.001	−0.190	39024	LS	EX UMa [4]	55975.374±0.005	0.026	12826	C
RW TrA	56123.564±0.002	−0.191	39125	LS	EX UMa [4]	55987.324±0.005	0.034	12848	C
RW TrA	56126.560±0.003	−0.188	39133	LS	EX UMa [4]	56003.602±0.004	0.027	12878	C
W Tuc	56168.633±0.001	0.186	30036	LS	EX UMa [4]	56026.409±0.005	0.035	12920	C
W Tuc	56171.848±0.002	0.189	30041	LS	EX UMa [4]	56248.424±0.004	0.032	13329	C
W Tuc	56193.681±0.003	0.186	30075	LS	EX UMa [4]	56279.361±0.006	0.028	13386	C
W Tuc	56195.611±0.003	0.190	30078	LS	KT UMa [5]	55947.445±0.006	0.054	10970	C
W Tuc	56207.816±0.004	0.192	30097	LS	KT UMa [5]	55962.514±0.006	0.068	10994	C
W Tuc	56225.800±0.003	0.194	30125	LS	KT UMa [5]	55964.383±0.006	0.055	10997	C
W Tuc	56243.778±0.003	0.189	30153	LS	KT UMa [5]	56002.650±0.005	0.057	11058	C
W Tuc	56254.696±0.003	0.190	30170	LS	KT UMa [5]	56023.347±0.006	0.053	11091	C
W Tuc	56256.623±0.004	0.190	30173	LS	KT UMa [5]	56043.422±0.005	0.054	11123	C
W Tuc	56290.664±0.003	0.193	30226	LS	KT UMa [5]	56051.584±0.004	0.061	11136	C
YY Tuc	56113.811±0.002	−0.076	22392	LS	KT UMa [5]	56273.651±0.005	0.064	11490	C
YY Tuc	56169.684±0.003	−0.085	22480	LS	KT UMa [5]	56280.558±0.007	0.071	11501	C
YY Tuc	56171.587±0.002	−0.087	22483	LS	KT UMa [5]	56290.584±0.006	0.060	11517	C
YY Tuc	56195.722±0.004	−0.083	22521	LS	KT UMa [5]	56292.475±0.006	0.069	11520	C
YY Tuc	56223.652±0.005	−0.094	22565	LS	AF Vel	55938.705±0.003	−0.182	27506	LS
YY Tuc	56230.638±0.003	−0.093	22576	LS	AF Vel	55939.757±0.002	−0.185	27508	LS
AE Tuc	56114.774±0.001	0.054	52711	LS	AF Vel	55957.677±0.002	−0.197	27542	LS
AE Tuc	56116.846±0.001	0.054	52716	LS	AF Vel	55966.639±0.002	−0.201	27559	LS
AE Tuc	56138.817±0.001	0.064	52769	LS	AF Vel	55967.694±0.002	−0.200	27561	LS
AE Tuc	56179.854±0.002	0.079	52868	LS	AF Vel	55994.605±0.003	−0.187	27612	LS
AE Tuc	56199.752±0.002	0.088	52916	LS	AF Vel	55997.776±0.003	−0.180	27618	LS
AE Tuc	56206.801±0.002	0.092	52933	LS	AF Vel	56015.693±0.002	−0.194	27652	LS
AE Tuc	56231.672±0.002	0.102	52993	LS	AF Vel	56025.711±0.002	−0.197	27671	LS
AE Tuc	56235.817±0.002	0.103	53003	LS	AF Vel	56053.678±0.002	−0.182	27724	LS
AE Tuc	56258.616±0.001	0.112	53058	LS	CD Vel	55936.669±0.003	−0.079	47456	LS

Table 1 (cont.): maxima of RR Lyrae stars

Variable star	Maximum HJD 24...	$O-C$ (days)	E	Obs	Variable star	Maximum HJD 24...	$O-C$ (days)	E	Obs.
CD Vel	55967.635±0.002	−0.081	47510	LS	AM Vir	56071.599±0.005	−0.043	47493	LS
CD Vel	55968.783±0.002	−0.080	47512	LS	AM Vir	56084.529±0.005	−0.030	47514	LS
CD Vel	55971.653±0.003	−0.078	47517	LS	AS Vir	56056.614±0.002	0.132	30540	LS
CD Vel	55972.800±0.003	−0.078	47519	LS	AT Vir	55948.607±0.002	−0.322	30945	C
CD Vel	55991.726±0.002	−0.077	47552	LS	AT Vir	55979.626±0.002	−0.325	31004	C
CD Vel	56025.561±0.002	−0.078	47611	LS	AT Vir	55987.509±0.001	−0.329	31019	C
FS Vel	55971.612±0.001	−0.052	34497	LS	AT Vir	55989.614±0.001	−0.327	31023	C
FS Vel	55978.749±0.002	−0.052	34512	LS	AT Vir	56000.655±0.002	−0.328	31044	LS
FS Vel	55989.690±0.001	−0.052	34535	LS	AT Vir	56001.705±0.002	−0.330	31046	LS
FS Vel	56009.672±0.001	−0.051	34577	LS	AT Vir	56008.542±0.002	−0.327	31059	C
FS Vel	56020.616±0.002	−0.049	34600	LS	AT Vir	56018.530±0.002	−0.330	31078	C
FS Vel	56059.626±0.002	−0.049	34682	LS	AT Vir	56039.562±0.002	−0.330	31118	LS
FS Vel	56071.522±0.002	−0.046	34707	LS	AT Vir	56069.532±0.002	−0.330	31175	LS
ST Vir	55975.579±0.001	−0.049	37094	C	AT Vir	56070.583±0.001	−0.331	31177	LS
ST Vir	55982.561±0.001	−0.051	37111	C	AV Vir	55988.650±0.003	0.021	22101	C
ST Vir	55993.661±0.002	−0.044	37138	C	AV Vir	56001.789±0.001	0.022	22121	LS
ST Vir	56004.747±0.001	−0.050	37165	LS	AV Vir	56032.665±0.003	0.023	22168	LS
ST Vir	56017.487±0.002	−0.045	37196	C	AV Vir	56038.572±0.002	0.018	22177	C
ST Vir	56020.773±0.001	−0.046	37204	LS	AV Vir	56063.536±0.004	0.020	22215	LS
ST Vir	56029.805±0.001	−0.052	37226	LS	AV Vir	56082.585±0.004	0.018	22244	LS
ST Vir	56045.422±0.001	−0.047	37264	C	AV Vir	56086.528±0.003	0.020	22250	LS
ST Vir	56056.508±0.002	−0.053	37291	C	BB Vir	55985.616±0.002	0.295	34752	C
ST Vir	56058.558±0.001	−0.057	37296	C	BB Vir	56001.634±0.001	0.295	34786	C
ST Vir	56060.618±0.003	−0.051	37301	LS	BB Vir	56011.528±0.002	0.296	34807	C
ST Vir	56064.725±0.001	−0.052	37311	LS	BB Vir	56018.594±0.002	0.296	34822	C
ST Vir	56072.532±0.002	−0.052	37330	C	BB Vir	56019.535±0.002	0.294	34824	C
ST Vir	56083.619±0.001	−0.057	37357	LS	BB Vir	56059.579±0.002	0.295	34909	LS
UU Vir	55950.559±0.001	−0.001	29758	C	BB Vir	56060.523±0.002	0.297	34911	C
UU Vir	56026.661±0.002	0.004	29918	LS	BB Vir	56067.589±0.001	0.297	34926	LS
UU Vir	56040.451±0.002	0.002	29947	C	BB Vir	56084.546±0.002	0.294	34962	LS
UU Vir	56056.623±0.001	0.003	29981	LS	BC Vir	56000.622±0.001	0.200	63910	C
UV Vir	55929.685±0.004	0.026	27146	C	BC Vir	56012.479±0.002	0.202	63931	C
UV Vir	55972.532±0.003	0.016	27219	C	BC Vir	56060.465±0.002	0.204	64016	C
UV Vir	55975.470±0.004	0.019	27224	C	BC Vir	56061.592±0.002	0.202	64018	LS
UV Vir	55977.816±0.003	0.016	27228	LS	BQ Vir	56001.599±0.006	−0.116	56837	C
UV Vir	55987.799±0.003	0.019	27245	LS	BQ Vir	56017.496±0.006	−0.117	56862	C
UV Vir	55989.559±0.003	0.018	27248	C	BQ Vir	56064.644±0.007	−0.026	56936	LS
UV Vir	56000.712±0.002	0.016	27267	LS	DO Vir	56002.738±0.003	0.234	55215	LS
UV Vir	56010.692±0.003	0.016	27284	LS	DO Vir	56008.596±0.002	0.232	55226	C
UV Vir	56015.392±0.005	0.019	27292	C	DO Vir	56011.792±0.002	0.232	55232	LS
UV Vir	56016.562±0.003	0.015	27294	C	DO Vir	56019.783±0.005	0.232	55247	LS
UV Vir	56033.600±0.003	0.028	27323	LS	DO Vir	56038.429±0.002	0.233	55282	C
UV Vir	56057.665±0.002	0.022	27364	LS	DO Vir	56056.540±0.003	0.231	55316	C
UV Vir	56060.597±0.005	0.019	27369	LS	DO Vir	56059.738±0.002	0.233	55322	LS
AF Vir	55985.611±0.002	−0.215	32355	C	DO Vir	56065.597±0.003	0.232	55333	LS
AF Vir	55986.578±0.002	−0.216	32357	C	EG Vir	55989.668±0.006	−0.030	30046	C
AF Vir	55988.510±0.002	−0.219	32361	C	EG Vir	56015.359±0.003	−0.044	30090	C
AF Vir	56009.804±0.002	−0.210	32405	LS	EG Vir	56016.529±0.003	−0.042	30092	C
AF Vir	56012.711±0.002	−0.205	32411	LS	EG Vir	56040.484±0.006	−0.040	30133	C
AF Vir	56017.544±0.002	−0.210	32421	C	V348 Vir	55983.773±0.003	0.164	3869	LS
AF Vir	56057.695±0.003	−0.211	32504	LS	V348 Vir	56004.721±0.005	0.199	3906	LS
AM Vir	56005.777±0.003	−0.050	47386	LS	V348 Vir	56017.705±0.007	0.183	3929	LS
AM Vir	56007.626±0.005	−0.047	47389	LS	V348 Vir	56038.600±0.003	0.165	3966	LS
AM Vir	56029.770±0.004	−0.046	47425	LS	V348 Vir	56056.662±0.005	0.140	3998	LS
AM Vir	56031.620±0.004	−0.041	47428	LS	V348 Vir	56099.647±0.006	0.169	4074	LS
AM Vir	56055.619±0.004	−0.031	47467	LS	SV Vol	55934.654±0.003	−0.010	37496	LS

Table 1 (cont.): maxima of RR Lyrae stars

Variable star	Maximum HJD 24...	$O-C$ (days)	E	Obs	Variable star	Maximum HJD 24...	$O-C$ (days)	E	Obs.
SV Vol	55937.706±0.003	0.014	37504	LS	SV Vol	56276.804±0.003	−0.024	38400	LS
SV Vol	55957.818±0.003	0.065	37557	LS	SV Vol	56278.642±0.003	−0.079	38405	LS
SV Vol	55959.653±0.002	0.008	37562	LS	SV Vol	56289.612±0.003	−0.085	38434	LS
SV Vol	55965.749±0.002	0.048	37578	LS	SV Vol	56292.659±0.004	−0.066	38442	LS
SV Vol	55967.581±0.002	−0.013	37583	LS	BN Vul	56071.513±0.001	0.072	17742	C
SV Vol	55970.627±0.002	0.006	37591	LS	BN Vul	56096.467±0.002	0.073	17784	C
SV Vol	55978.557±0.002	−0.013	37612	LS	BN Vul	56121.420±0.002	0.073	17826	C
SV Vol	55990.754±0.002	0.072	37644	LS	BN Vul	56128.551±0.001	0.074	17838	C
SV Vol	55992.586±0.002	0.012	37649	LS	BN Vul	56137.462±0.002	0.073	17853	C
SV Vol	55998.688±0.002	0.057	37665	LS	BN Vul	56143.403±0.003	0.073	17863	C
SV Vol	56004.788±0.002	0.101	37681	LS	BN Vul	56147.560±0.002	0.071	17870	C
SV Vol	56025.528±0.003	0.024	37736	LS	BN Vul	56162.416±0.002	0.074	17895	C
SV Vol	56050.525±0.001	0.040	37802	LS	BN Vul	56178.458±0.002	0.074	17922	C
SV Vol	56061.505±0.002	0.043	37831	LS	BN Vul	56209.351±0.002	0.072	17974	C
SV Vol	56259.724±0.003	−0.072	38355	LS	BN Vul	56225.392±0.003	0.072	18001	C
SV Vol	56262.775±0.002	−0.049	38363	LS					

* C = Calern, LS = La Silla
1 Boninsegna, 1990
2 Baldwin and Samolyk, 2003
3 Agerer and Moschner, 1996
4 Vandenbroere, 1995
5 Vandenbroere et al., 1999

COMMISSIONS 27 AND 42 OF THE IAU
INFORMATION BULLETIN ON VARIABLE STARS

Number 6044

Konkoly Observatory
Budapest
19 January 2013

HU ISSN 0374 – 0676

MINIMA TIMES OF SELECTED ECLIPSING BINARIES

PARIMUCHA, Š.[1]; DUBOVSKÝ, P.[2]; VAŇKO, M.[3]

[1] Institute of Physics, Faculty of Natural Sciences, University of P.J. Šafárik, Košice, The Slovak Republic; e-mail: stefan.parimucha@upjs.sk

[2] Kolonica Observatory, The Slovak Republic; e-mail: var@kozmos.sk

[3] Astronomical Institute of the Slovak Academy of Sciences, Tatranská Lomnica, Slovakia; e-mail: vanko@ta3.sk

Observatory and telescope:
K1 - 5.6/400 mm photolense, K2 - 1000/9000 Cassegrain, K3 - pointer-300/2400

Detector:	K1-G, Moravian Instruments G2-1600, K1-M - Meade DSI Pro, K2-F - FLI PL1001E, K3-F - FLI PL1001E

Method of data reduction:
All observations were reduced and photometry were performed using C-Munipack package (http://c-munipack.sourceforge.net/)

Method of minimum determination:
The minima times were computed by Kwee & van Woerden (1956) method.

Times of minima:					
Star name	Time of min. HJD 2400000+	Error	Type	Filter	Rem.
RT And	56167.3140	0.0005	II	R	K1-G
	56180.5270	0.0002	II	R	K1-G
AB And	55777.4791	0.0001	I	V	K1-M
	56079.4993	0.0001	I	V	K1-G
	56148.3660	0.0002	II	R	K1-G
BX And	55792.5015	0.0002	I	V	K1-M
	56162.5334	0.0007	II	V	K1-G
	56167.4121	0.0005	II	R	K1-G
	56197.3101	0.0008	II	R	K1-G
EP And	55795.5269	0.0004	I	V	K1-M
	56183.4696	0.0005	I	R	K1-G
	56222.4654	0.0004	II	V	K1-G
	56222.4656	0.0003	II	R	K1-G
LO And	55784.4147	0.0004	II	V	K1-M
	56160.4783	0.0008	I	V	K1-G
	56181.4067	0.0003	I	R	K1-G
	56187.3034	0.0004	II	V	K1-G
V376 And	56220.3286	0.0006	II	V	K1-G
SS Ari	55799.4976	0.0003	II	V	K1-M
	56167.5183	0.0002	I	R	K1-G
	56168.5349	0.0002	II	R	K1-G
V402 Aur	56220.5318	0.0009	II	V	K1-G
TY Boo	55681.5158	0.0003	I	V	K1-M
	56078.4252	0.0005	II	R	K1-G
TZ Boo	55629.4369	0.0002	I	V	K1-M
	55652.4671	0.0002	II	V	K1-M
	55680.5487	0.0003	I	V	K1-M
	55980.5324	0.0009	II	R	K1-G
AC Boo	55643.4363	0.0002	II	V	K1-M
	56009.4576	0.0003	I	R	K1-G
FI Boo	55644.5159	0.0003	I	V	K1-M
	55662.4535	0.0004	I	V	K1-M
	56006.4224	0.0007	I	V	K1-G
	56045.4175	0.0013	I	R	K1-G
	56046.4016	0.0008	II	R	K1-G
SV Cam	55784.5464	0.0003	I	V	K1-M
	55990.3397	0.0004	I	R	K1-G
	56003.3883	0.0003	I	V	K1-G
	56219.5592	0.0005	II	V	K1-G
AO Cam	56181.4839	0.0001	II	R	K1-G
DN Cam	55794.4968	0.0002	II	V	K1-M
	56150.5401	0.0003	I	R	K1-G
	56199.3753	0.0002	I	R	K1-G
FN Cam	55995.2896	0.0003	II	R	K1-G
V442 Cam	55960.3929	0.0001	II	R	K2-F
	55960.6151	0.0001	I	R	K2-F

Times of minima:					
Star name	Time of min. HJD 2400000+	Error	Type	Filter	Rem.
V442 Cam	55991.3762	0.0002	II	R	K2-F
TX Cnc	55674.3301	0.0002	II	V	K1-M
EH Cnc	55629.2576	0.0008	I	V	K1-M
BI CVn	55643.2990	0.0005	I	V	K1-M
	55672.4987	0.0003	I	V	K1-M
CW Cas	55765.4553	0.0005	I	V	K1-M
	55776.4570	0.0003	II	V	K1-M
	56181.5638	0.0002	I	R	K1-G
	56182.3621	0.0007	II	R	K1-G
V523 Cas	55778.3891	0.0001	I	V	K1-M
	55778.5058	0.0002	II	V	K1-M
	56183.3786	0.0002	I	R	K1-G
	56189.4547	0.0006	I	R	K1-G
V651 Cas	55751.4831	0.0001	I	V	K1-M
	55752.4795	0.0002	I	V	K1-M
	55801.3236	0.0002	I	V	K1-M
	56192.5706	0.0002	I	R	K1-G
V776 Cas	55779.5150	0.0006	II	V	K1-M
	56156.5120	0.0008	II	V	K1-G
	56221.2511	0.0007	II	V	K1-G
	56221.4725	0.0003	I	V	K1-G
VW Cep	56047.5062	0.0003	II	V	K1-G
	56050.4266	0.0004	I	V	K1-G
	56222.2839	0.0003	II	R	K1-G
RW Com	55624.5767	0.0003	I	V	K1-M
RZ Com	55624.4438	0.0003	I	V	K1-M
	55650.3390	0.0004	II	V	K1-M
SS Com	55618.5706	0.0009	I	V	K1-M
	55628.4837	0.0004	I	V	K1-M
CC Com	55622.5926	0.0002	II	V	K1-M
	55657.3499	0.0003	I	V	K1-M
YY CrB	55665.4931	0.0002	I	V	K1-M
	55987.6363	0.0002	II	V	K1-G
	55992.5311	0.0002	II	V	K1-G
	56005.5229	0.0004	I	V	K1-G
	56011.5475	0.0001	I	V	K1-G
	56149.3672	0.0002	I	V	K1-G
	56199.2609	0.0002	II	V	K1-G
V1191 Cyg	55739.4416	0.0003	I	V	K1-M
	56187.4335	0.0004	II	V	K1-G
V1918 Cyg	55628.6347	0.0006	II	V	K1-M
	56188.2828	0.0003	I	V	K1-G
	56189.3145	0.0002	I	R	K1-G
	56219.2699	0.0002	I	R	K1-G
LS Del	55735.4497	0.0003	I	V	K1-M

Times of minima:					
Star name	Time of min. HJD 2400000+	Error	Type	Filter	Rem.
LS Del	56105.4773	0.0006	I	R	K1-G
	56105.4772	0.0012	I	R	K1-G
	56180.4321	0.0004	I	R	K1-G
FU Dra	55650.4580	0.0003	I	V	K1-M
	55655.3656	0.0002	I	V	K1-M
	55795.3851	0.0003	II	V	K1-M
TX Her	56159.3251	0.0002	I	R	K1-G
V728 Her	55629.6014	0.0003	I	V	K1-M
	56159.3360	0.0004	I	R	K1-G
V829 Her	55655.5047	0.0004	I	V	K1-M
	56177.3396	0.0006	I	R	K1-G
V857 Her	55657.5051	0.0006	I	V	K1-M
	56132.4272	0.0007	II	R	K1-G
	56150.3923	0.0006	II	V	K1-G
SW Lac	55798.4196	0.0002	I	V	K1-M
	56159.5534	0.0001	I	R	K1-G
	56162.4397	0.0003	I	R	K1-G
PP Lac	55798.5621	0.0003	I	V	K1-M
	56219.3799	0.0004	I	V	K1-G
AM Leo	55651.3162	0.0002	II	V	K1-M
	56027.3572	0.0002	II	V	K1-G
CE Leo	55623.4385	0.0004	I	V	K1-M
EX Leo	56011.3759	0.0005	I	V	K1-G
UV Leo	56007.3447	0.0002	II	V	K1-G
RT LMi	55622.3333	0.0005	I	V	K1-M
VW LMi	55630.5019	0.0003	I	V	K1-M
	55644.3502	0.0002	I	V	K1-M
	56004.4254	0.0003	I	V	K1-G
	56047.4058	0.0003	I	V	K1-G
UV Lyn	55992.3026	0.0003	I	V	K1-G
	55995.4149	0.0004	II	R	K1-G
V508 Oph	55650.5739	0.0002	II	V	K1-M
	55693.5000	0.0002	I	V	K1-M
	56160.3469	0.0002	I	V	K1-G
V2610 Oph	56075.4947	0.0008	I	V	K1-G
	56097.4559	0.0005	I	V	K1-G
V2612 Oph	55651.5852	0.0005	I	V	K1-M
	55686.4890	0.0003	I	V	K1-M
	56073.4293	0.0011	I	V	K1-G
U Peg	56159.4378	0.0002	I	V	K1-G
AT Peg	56168.3363	0.0002	I	V	K1-G
BB Peg	55779.3937	0.0002	II	V	K1-M
	56222.2304	0.0002	II	V	K1-G
BX Peg	55777.3539	0.0004	I	V	K1-M
	56180.3142	0.0004	I	R	K1-G

Times of minima:					
Star name	Time of min. HJD 2400000+	Error	Type	Filter	Rem.
BX Peg	56181.2950	0.0002	II	R	K1-G
DI Peg	56163.4447	0.0002	I	V	K1-G
V351 Peg	56164.4041	0.0004	II	V	K1-G
V357 Peg	55791.3990	0.0003	II	V	K1-M
	56165.3672	0.0003	I	V	K1-G
V432 Per	55477.3971	0.0001	II	V	K1-M
	55800.5236	0.0002	II	V	K1-M
	56182.4883	0.0003	I	R	K1-G
	56222.5454	0.0005	II	V	K1-G
DV Psc	55801.4633	0.0003	I	V	K1-M
	55838.3350	0.0003	II	V	K2-F
	55838.4878	0.0003	I	V	K2-F
GSC 00008-00901	56183.4042	0.0002	I	V	K2-F
AU Ser	55651.4545	0.0002	I	V	K1-M
	55693.3885	0.0002	II	V	K1-M
OU Ser	55989.6151	0.0005	II	V	K1-G
	56048.5211	0.0004	I	R	K1-G
	56048.3773	0.0004	II	R	K1-G
Y Sex	55648.3509	0.0003	I	V	K1-M
AH Tau	55624.3006	0.0003	II	V	K1-M
	56222.6137	0.0003	I	V	K1-G
EQ Tau	56222.3719	0.0002	I	V	K1-G
V781 Tau	55994.3528	0.0002	I	R	K1-G
	56199.5748	0.0002	I	R	K1-G
W UMa	56049.3739	0.0002	I	R	K1-G
XY UMa	55630.3319	0.0003	I	V	K1-M
	56028.3765	0.0002	I	V	K1-G
AA UMa	55622.4783	0.0005	I	V	K1-M
	55628.3317	0.0005	I	V	K1-M
AW UMa	55629.4563	0.0002	I	R	K3-F
	55644.3729	0.0003	I	V	K3-F
	55644.5939	0.0004	II	V	K3-F
HH UMa	55684.3666	0.0006	I	V	K1-M
HV UMa	56070.4467	0.0007	I	V	K1-G
TV UMi	55686.3779	0.0003	I	V	K1-M
	55792.3430	0.0002	I	V	K1-M
	55991.3931	0.0010	I	V	K1-G
	55991.5914	0.0008	II	V	K1-G
	56010.5063	0.0010	I	V	K1-G
AH Vir	56014.4730	0.0004	I	V	K1-G
AZ Vir	55677.3605	0.0003	I	V	K1-M
PY Vir	56012.4809	0.0004	II	V	K1-G

Explanation of the remarks in the table:
Remarks give an observatory and used instrument.

Remarks:

Minima types are calculated according to O-C gateway of Czech Astronomical Society (http://var.astro.cz/ocgate). The elements for GSC 00008-00901 are taken from Parimucha et al. (2008).

Acknowledgements:

This paper was supported by the realisation of the project ITMS No. 26220120029, based on the supporting operational Research and development program financed from the European Regional Development Fund.

References:

Kwee, K. K., van Woerden, H., 1956, *Bull. Astron. Inst. Netherlands*, 12, 327

Parimucha, Š., Pribulla, T., Vaňko, M., Dubovský, P., Hambálek, Ľ., 2008, *Ap&SS* **313**, 419

COMMISSIONS 27 AND 42 OF THE IAU
INFORMATION BULLETIN ON VARIABLE STARS

Number 6045

Konkoly Observatory
Budapest
30 January 2013

HU ISSN 0374 – 0676

THE DETECTION OF A 3.486 HOUR PHOTOMETRIC PERIOD IN THE CLASSICAL NOVA V2468 CYGNI

CHOCHOL, D.[1]; SHUGAROV, S.Y.[1,2]; VOLKOV, I.M.[1,2]; GORANSKIJ, V.P.[2]; METLOVA, N.V.[2]; BARSUKOVA, E.A.[3]; GABDEEV, M.M.[3]

[1] Astronomical Institute of the Slovak Academy of Sciences, 059 60 Tatranská Lomnica, Slovakia, e-mail: chochol@ta3.sk

[2] Sternberg Astronomical Institute, Universitetski prospect 13, Moscow, 119992 Russia

[3] Special Astrophysical Observatory of the Russian Academy of Sciences, Nizhniy Arkhyz, Karachai-Cherkesia, 369167 Russia

Classical nova V2468 Cyg (Nova Cygni 2008) was discovered by H. Kaneda on March 7.801 UT (JD 2454534.301) at $8\overset{m}{.}2$ at the coordinates α_{2000} =$19^h58^m33\overset{s}{.}39$, $\delta_{2000} = +29°52'06\overset{''}{.}5$, measured by K. Kadota on the CCD image taken on March 8.716 UT (Nakano, 2008). It was classified as a Williams Fe II class nova (Beaky, 2008); Henden and Munari (2008) found a faint star USNO-B1 1198-0459968 ($R = 18$ mag) close to the position, visible only on POSS-II red plates, not on the blue ones. The amplitude of the outburst was larger than 12 mag in the B band. The nova entered to a nebular stage 122 days after the outburst (Iijima & Naito, 2011). The supersoft X-ray source (SSS) stage of the nova started in June 2009 (∼460 days after outburst) when the object was detected by Swift with the XRT and UVOT instruments. The X-ray light curve was variable with a large amplitude on time scale of 500 seconds, UV observations showed large amplitude variations of the order 0.3 mag (Schwarz et al., 2009). In July 2012 (1602 days after outburst) the X-ray flux of the nova strongly increased (Page et al., 2012). At that time, the duration of the SSS stage already exceeded 3 years.

Chochol et al. (2012) used the B and V photometric light curves to find the rates of decline $t_{2,V} = 9$, $t_{2,B} = 10$, $t_{3,V} = 20$ and $t_{3,B} = 22$ days of this fast nova. They determined its basic parameters: $M_{V,\max}$ = -8.70± 0.07, interstellar extinction $E(B-V) = 0.79\pm0.01$ and distance $d = 5.4\pm0.6$ kpc.

In 2011 and 2012 we monitored V2468 Cyg in the V passband, with the time resolution from one to two minutes, using the 0.5 m and 0.6 m telescopes of the Stará Lesná observatory (Slovakia), 0.6 m and 1.25 m telescopes at the Crimean Laboratory of the Sternberg Institute in Nauchnyj (Ukraine), 0.6 m and 1 m Zeiss telescopes at Simeiz Observatory at Mt. Koshka (Ukraine), and 1 m Zeiss SAO RAS telescope of the Special Astrophysical Observatory in Nizhniy Arkhyz (Karachai-Cherkesia, Russia).

Our V light curve, presented in Fig. 1, shows a large variability due to the presence of quasi-periodic oscillations (QPO) with periods in the range 21 - 50 minutes and amplitudes up to 0.5 mag (for details see Chochol et al., 2012), combined with strictly periodic light variations with the amplitude (0.08 - 0.15) mag and the stable period of 3.486 hours. The QPO either disappeared or their amplitudes were very small after the increase of X-ray brightness in July 2012.

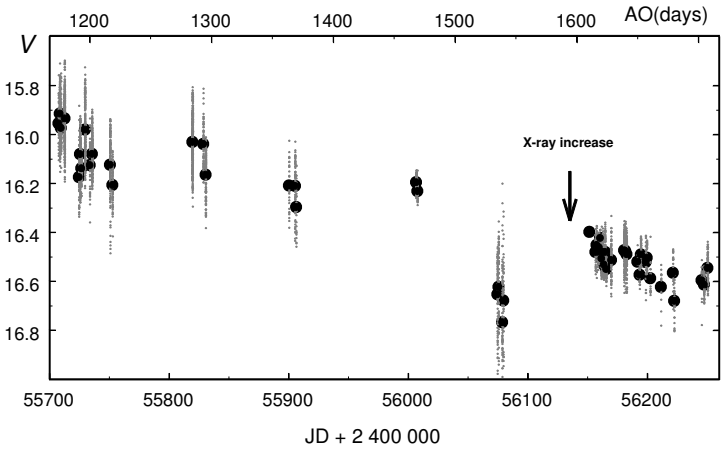

Figure 1. *V* light curve of V2468 Cyg in 2011-12 during the decline from the outburst.

The long night runs with the QPO and without QPO are shown in Fig. 2 and Fig. 3, respectively. Due to the fact that different telescopes and CCD cameras were used, we were forced to use different check stars, to demonstrate their brightness stability.

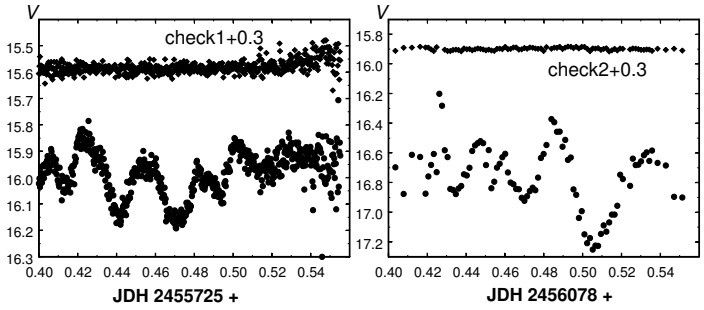

Figure 2. The nightly runs with QPO.

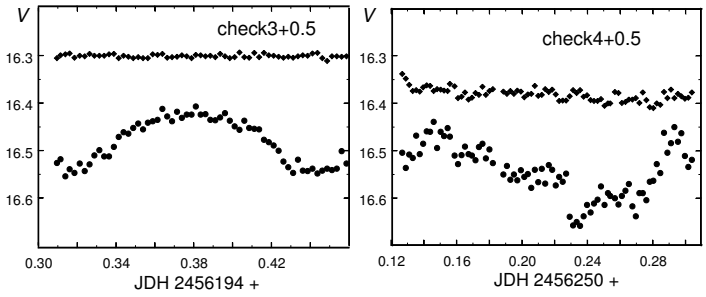

Figure 3. The nightly runs without QPO.

The best period was found by Fourier analysis of the data in nights JD 2456006-007, JD 2456156-250 (see Fig. 4). We determined the following ephemeris for the minima of brightness:

$$\text{Min} = JD2456006.355 + 0\overset{d}{.}145250(5) \times E.$$

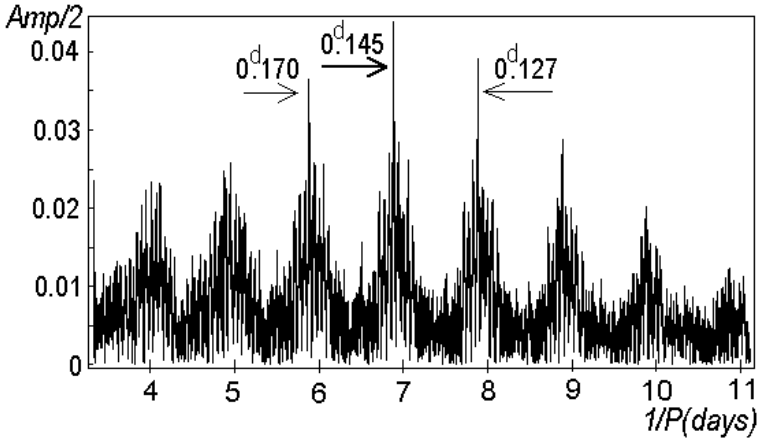

Figure 4. The best period $0^d.145250$ ($3^h.486$) and its one day aliases found by the Fourier analysis.

The phase light curve corresponding to these data is presented in Fig. 5.

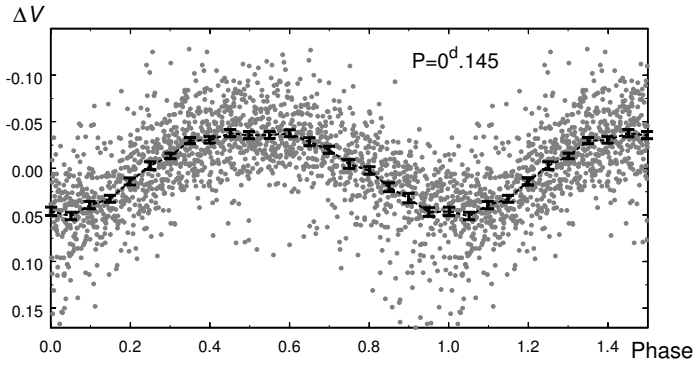

Figure 5. The V phase light curve of V2468 Cyg in 2012, corresponding to our ephemeris.

The nature of SSSs in classical novae is explained with the steady thermonuclear burning on the surface of a white dwarf with high accretion rate (Kahabka & van den Heuvel, 1997). The light variations are most probably caused by orbital motion in the binary system and irradiation of the secondary star by the hot white dwarf. The rotation of the magnetic white dwarf with the magnetic axis inclined to the rotational axis can explain the periodic variations, too. In such a case a thermonuclear burning runs nearby the magnetic pole of the white dwarf.

Acknowledgements This work has been supported by the Slovak Academy of Sciences VEGA Grant No. 2/0002/13, SAIA scholarship, RFBR grant 11-02-01213a, 11-02-00258a, NSh 2374.2012.5 and by the Ministry of Education and Science of the Russian Federation, Project No. 8406. This article was supported by the realization of the Project ITMS No. 26220120029, based on the supporting operational Research and development program financed from the European Regional Development Fund.

References:

Beaky, M.M. 2008, *IAUC*, No. 8928
Chochol, D., Shugarov, S.Y., Pribulla, T. & Volkov, I. 2012, *Mem. Soc. Astron. It.*, **83**, 767
Henden, A., & Munari, U. 2008, *IBVS*, No. 5822
Iijima, T., & Naito, H. 2011, *A&A*, **526**, A73
Kahabka, P., & van den Heuvel, E.P.G. 1997, *Annual Review of Astron. Astrophys.*, **35**, 69
Nakano, S. 2008, *IAUC*, No. 8927
Page, K.L. et al. 2012, *The Astronomer's Telegram*, No. 4286
Schwarz, G.J. et al. 2009, *The Astronomer's Telegram*, No. 2157

COMMISSIONS 27 AND 42 OF THE IAU
INFORMATION BULLETIN ON VARIABLE STARS

Number 6046

Konkoly Observatory
Budapest
14 February 2013

HU ISSN 0374 – 0676

NEW TIMES OF MINIMA OF SOME ECLIPSING VARIABLES

LACY, C.H.S.

Department of Physics, University of Arkansas, Fayetteville, Arkansas 72701, USA; e-mail: clacy@uark.edu

Observatory and telescope:
URSA: URSA Observatory at the University of Arkansas; 10-inch Schmidt-Cassegrain reflector. NFO: NFO WebScope near Silver City, NM, USA (http://www.nfo.edu); 24-inch classical Cassegrain.

Detector:	URSA: 1020×1530 pixels SBIG ST8EN CCD cooled to (typ.) -20 °C; 1.15 arcsec square pixels; $20'(\mathrm{N}-\mathrm{S}) \times 30'(\mathrm{E}-\mathrm{W})$ field of view. NFO: 2102×2092 pixels Kodak KAF 4300E CCD cooled to (typ.) -20 °C; 0.78 arcsec square pixels; $27'$ square field of view.

Method of data reduction:
Virtual measuring engine (Measure 2.0) written by C.H.S. Lacy (2005).

Method of minimum determination:
Kwee & van Woerden (1956).

Times of minima:					
Star name	Time of min. HJD 2400000+	Error	Type	Filter	Rem.
AP And	56085.9022	0.0003	1	V	NFO
	56120.8227	0.0002	1	V	URSA
	56186.6957	0.0002	2	V	NFO
	56190.6635	0.0003	1	V	NFO
	56225.5845	0.0003	1	V	NFO
	56298.5993	0.0002	1	V	NFO
V361 Cas	56196.6404	0.0006	1	V	NFO
V651 Cas	56087.9058	0.0004	2	V	URSA
	56088.9028	0.0003	2	V	URSA
	56126.7793	0.0003	2	V	URSA
V1136 Cyg	56042.9316	0.0011	1	V	NFO
	56049.8544	0.0009	1	V	NFO
V501 Her	56069.8817	0.0011	1	V	URSA
	56099.7924	0.0003	2	V	NFO
AL Leo	55987.8671	0.0002	2	V	URSA
	55995.8932	0.0004	2	V	NFO
	56000.7102	0.0002	2	V	NFO
	56041.6510	0.0002	1	V	URSA
	56045.6646	0.0003	2	V	NFO
	56049.6784	0.0003	1	V	URSA
V506 Oph	56053.7434	0.0007	1	V	URSA
	56063.8175	0.0002	2	V	URSA
	56063.8176	0.0002	2	V	NFO
	56064.8781	0.0002	2	V	URSA
	56070.7101	0.0002	1	V	URSA
	56071.7712	0.0002	1	V	URSA
	56074.9519	0.0003	1	V	NFO
	56087.6774	0.0002	1	V	URSA
	56088.7374	0.0003	1	V	URSA
	56088.7375	0.0002	1	V	NFO
	56089.7979	0.0002	1	V	NFO
	56090.8583	0.0003	1	V	NFO
	56097.7511	0.0002	2	V	URSA
	56106.7647	0.0002	1	V	NFO
IM Per	56217.7647	0.0005	2	V	NFO
	56269.6109	0.0006	2	V	NFO
	56314.6955	0.0004	2	V	NFO
NP Per	56186.9104	0.0010	2	V	NFO
	56195.8284	0.0010	2	V	NFO
	56196.9427	0.0002	1	V	NFO
	56216.9989	0.0005	1	V	NFO
	56235.9476	0.0010	2	V	NFO
	56263.8011	0.0003	1	V	NFO
	56264.9188	0.0018	2	V	NFO
	56310.6001	0.0004	1	V	NFO
V482 Per	56221.9605	0.0006	2	V	NFO
	56324.7231	0.0006	2	V	NFO

Times of minima:					
Star name	Time of min. HJD 2400000+	Error	Type	Filter	Rem.
V514 Per	56230.9645	0.0017	1	V	NFO
TY Tau	55996.6219	0.0003	1	V	URSA
BT Vul	56041.9265	0.0003	1	V	URSA
	56120.6694	0.0003	1	V	URSA
	56121.8113	0.0002	1	V	URSA
	56189.7140	0.0004	2	V	NFO

Remarks:

A sample of the observations has been published by Lacy, Hood & Straughn (2001). Mean deviations between independently timed eclipses by the two telescopes (URSA & NFO) are not significantly larger than expected based on the error estimates, implying that the estimated timing errors are realistic.

Acknowledgements:

Construction and operation of the URSA telescope were partially funded by the National Science Foundation and the University of Arkansas, Fayetteville. Construction and operation of the NFO telescope were partially funded by the National Science Foundation, the Arkansas Center for Space and Planetary Sciences, the NASA Arkansas Space Grant Consortium, the University of Arkansas, Fayetteville, the University of Arkansas at Little Rock, and the Harvard-Smithsonian Center for Astrophysics. We are grateful to Bill Neely for initial processing of the images and construction, maintenance, and operation of the NFO equipment and software.

References:

Kwee, K. K. & van Woerden, H. 1956, BAN, 12, 327
Lacy, C. H. S., Hood, B. & Straughn, A., 2001, IBVS, No. 5067

COMMISSIONS 27 AND 42 OF THE IAU
INFORMATION BULLETIN ON VARIABLE STARS

Number 6047

Konkoly Observatory
Budapest
20 February 2013

HU ISSN 0374 – 0676

VARIABILITY TYPE OF BD+46°2731

SEREBRYANSKIY, A.V.; GAYNULLINA, E.R.; STREL'NIKOV, D.V.; KHALIKOVA, A.V.

Ulugh Beg Astronomical Institute, Astronomicheskaya str., 33, 100072 Tashkent, Uzbekistan
email: alex@astrin.uz, evelina@astrin.uz

BD+46°2731 (R.A.=$19^h35^m17\overset{s}{.}87$; DEC.=+46°25′08″.35 [2000.0]) is a relatively bright star with V≈ 9 mags and spectral type F0 and included in many star catalogs. It was also mentioned as an unconfirmed variable star in the "New Catalogue of Suspected Variable Stars" (Kukarkin et al., 1982) with number NSV 12196. The premise for placing the star in the catalog was the study by Seliwanow, Henroteau and Fredette (1923). It was that paper where the photographic magnitudes obtained by Fredette during 27 nights of observation from Aug to Dec 1920 (see Figure 1) were presented. Those observations appeared to confirm the variability with a period of approximately 28.5 days. The authors proposed to classify this star as an ellipsoidal variable.

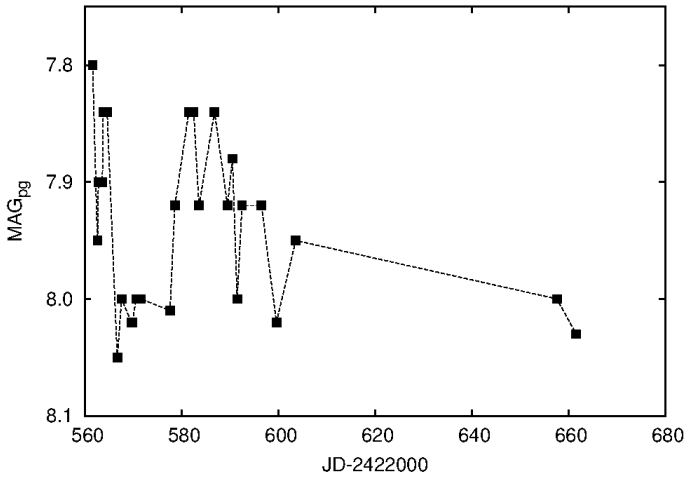

Figure 1. Photographic magnitudes obtained for BD+46°2731 by J.F. Fredette in Aug–Sep 1920.

We observed the field of the open cluster NGC 6811 in the Maidanak Observatory (Uzbekistan) during several nights in 2010 with Taiwan Automated Telescope (TAT, Chou et al., 2010). The TAT uses a 9-cm Maksutov-type telescope with f=25, manufactured by "Questar". The CCD camera is Apogee Alta U6 16-bit 1024 × 1024, the CCD chip is a Kodak KAF-1101E, its scale is 2″.18 per pixel which gives a field of view of $0\overset{\circ}{.}62\times0\overset{\circ}{.}62$. Because the telescope was not originally equipped with standard color filters, observations

were made in integrated light, exposure times were either 280 or 320 sec. The main goal of the observations was a search for new variables as well as asteroseismic analysis of known δ Sct stars. Among all nights of observations we had four nights (Aug 26, 27 and Sep 7, 10) when the star BD+46°2731 was found in the field of view close to the edge of the frames. Basic reduction of the frames was done using standard IRAF† software.

To obtain light curve of the BD+46°2731 we used the method of differential photometry. For this goal we extract photometry of a set of stars across the field of NGC 6811. During the photometric analyses we encountered two main problems: (i) strong coma distortions of the stellar profiles due to a quite wide field of view of the telescope, and (ii) moderate star crowding on the field.

To avoid these problems we performed only aperture photometry with an aperture radius is being approximately equal to FWHM. Having had the instrumental magnitudes we computed the light curve and subtracted low-frequency trends (due to possible effects of differential absorption) by fitting low-order polynomial. Then we used the method of ensemble photometry (Honeycutt, 1992) realized in "Ensemble-0.7" software by Michael Richmond (http://spiff.rit.edu/ensemble). Due to the proximity of BD+46°2731 to the edge of the frames some pixels have poor count statistics for sky background estimation. These pixels were removed from our data analyses. The final light curve contains 225 data points and is shown in Figure 2.

For the power spectral analysis of the light curve the FAMIAS software package (Zima, 2008) was used. The width of the smoothing window for noise level estimation was set to 5 c/d, the Nyquist frequency (approximated by the inverse mean of the time-difference of consecutive measurements by neglecting large gaps) was set to 121.561 c/d and frequency resolution was set to 0.003289 c/d. Only those modes were selected whose amplitudes in power spectra exceeded 4σ. These modes have frequencies of 18.95 c/d, 13.66 c/d, 16.70 c/d and 8.23 c/d. Parameters of the modes are presented in Table 1. The power spectra after subsequent pre-whitening procedures are shown in Figure 3. The observed and fitted light curve is plotted in Figure 4.

Table 1. Mode parameters of BD+46°2731

Mode	P (c/d)	σ(P) (c/d)	A (mmag)	σ(A) (mmag)	S/N
f1	18.9510	0.00137	11.925	0.697	9.30
f2	13.6533	0.00240	6.480	0.690	7.61
f3	16.7796	0.00332	5.097	0.690	6.95
f4	8.2332	0.00323	4.745	0.680	4.91

Considering the amplitudes and periods of oscillations, as well as the spectral type of the star we conclude that BD+46°2731 could be a variable of δ Sct type. Taking into account its brightness it will be a convenient target for a future asteroseismic campaign even with small telescopes. It should be mentioned that BD+46°2731 is located in the Kepler field (KIC 9715035) but unfortunately it was not observed.

†IRAF is distributed by the NOAO, which are operated by the AURA, Inc., under cooperative agreement with the NSF

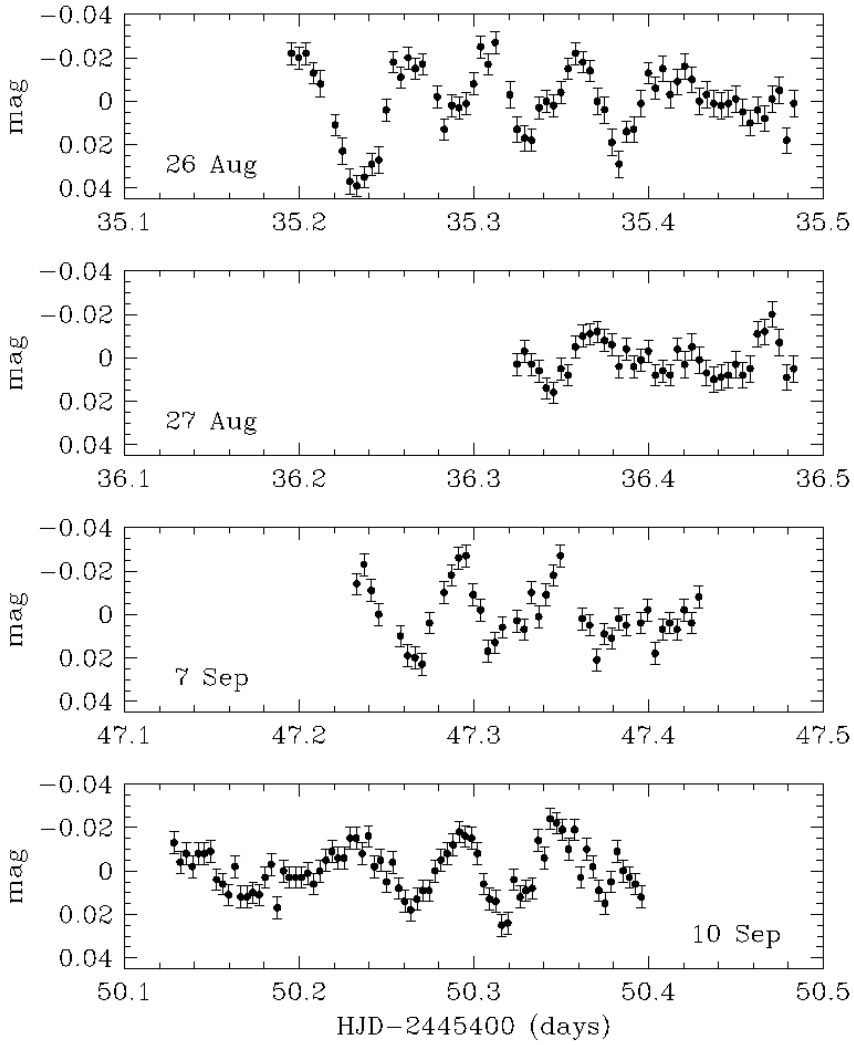

Figure 2. Light curves of the star BD+46°2731 observed in the Maidanak Observatory in 2010.

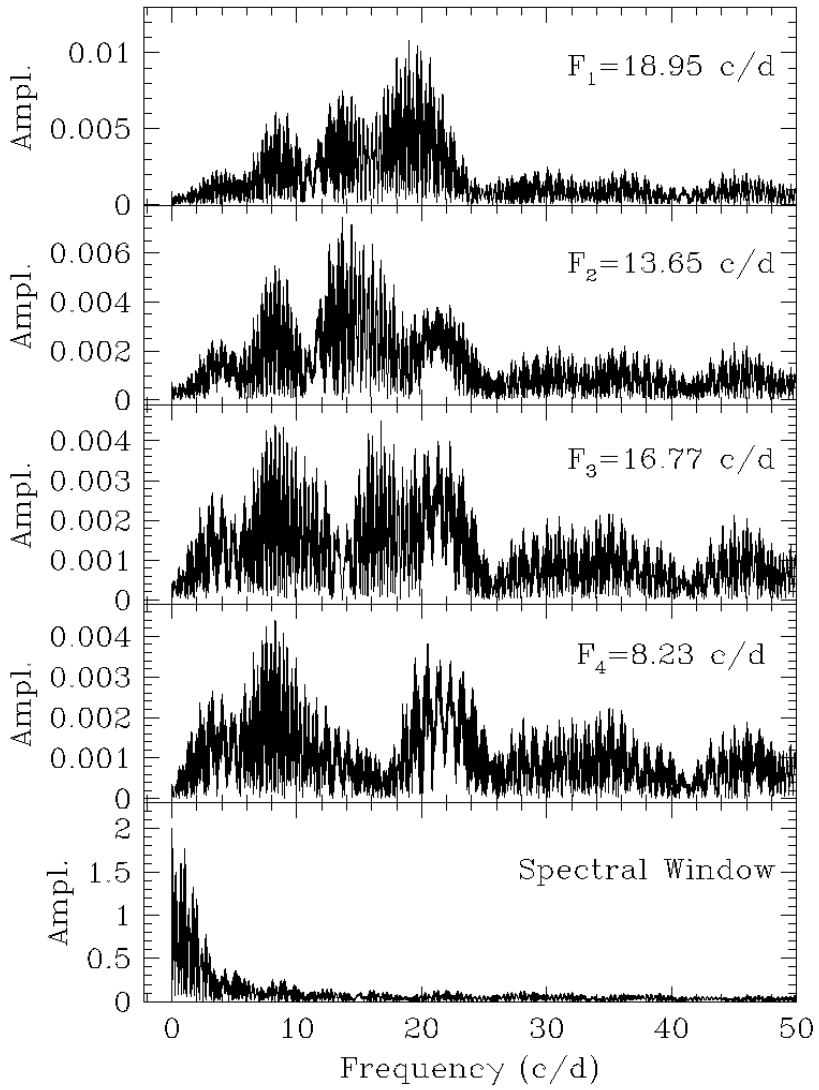

Figure 3. Four panels from the top: amplitude spectra for different identified modes which satisfied the 4σ rejection criteria. The last panel: amplitude spectrum of window function.

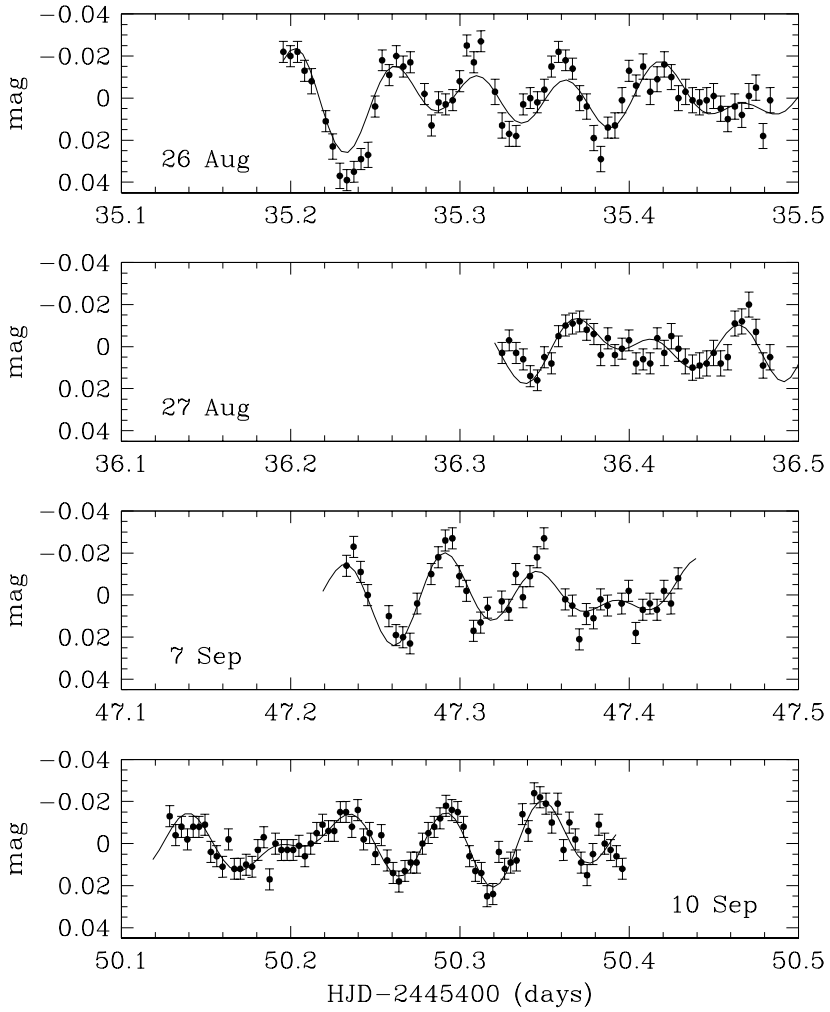

Figure 4. Light curves and fitting results for BD+46°2731.

Acknowledgements:
The authors are supported by Fundamental Research Grant FA-F02-F028 of the Uzbek Academy of Sciences. We thanks the anonymous referee for important suggestions and comments.

References:

Chou, D.-Y., Sun, M.-T., Fernandez, F.J. et al., 2010, *Advances in Astronomy*, **2010**, 13
Honeycutt, R.K., 1992, *PASP*, **104**, 435
Kukarkin, B.V., Kholopov P.N., Artiukhina N.M. et al., 1982, *New Catalogue of Suspected Variable Stars*, Moscow: Nauka Publishing House
Seliwanow, S., Henroteau, F. and Fredette, J.F., 1923, *AN*, **219**, 351
Zima, W., 2008, *Communications in Asteroseismology*, 155, 17

COMMISSIONS 27 AND 42 OF THE IAU
INFORMATION BULLETIN ON VARIABLE STARS

Number 6048

Konkoly Observatory
Budapest
25 February 2013

HU ISSN 0374 – 0676

BAV-RESULTS OF OBSERVATIONS - PHOTOELECTRIC MINIMA OF SELECTED ECLIPSING BINARIES AND MAXIMA OF PULSATING STARS

(BAV MITTEILUNGEN NO. 228)

HÜBSCHER, JOACHIM; BRAUNE, WERNER; LEHMANN, PETER B.

Bundesdeutsche Arbeitsgemeinschaft für Veränderliche Sterne e.V. (BAV), Munsterdamm 90, 12169 Berlin, Germany, www.bav-astro.de, publikat@bav-astro.de

In this 74th compilation of BAV results, photoelectric observations obtained mostly in the years 2011 and 2012 are presented on 386 variable stars giving over 700 minima on eclipsing binaries and maxima on pulsating stars. All moments of minima and maxima are heliocentric UTC. The errors are tabulated in column '±'. The values in column '$O-C$' are determined without incorporating nonlinear terms. The references are given in the section 'Remarks'. All information about photometers and filters are specified in the column 'Rem'. The observations were made at private observatories. The photoelectric measurements and all the light curves with evaluations can be obtained from the office of the BAV for inspection.

Please use the following link for an easy access to all the publications of the BAV including the "Lichtenknecker Database of the BAV": `http://www.bav-astro.de/sfs` .

Table 1: Times of minima of eclipsing binaries

Variable	HJD 24.....	±	Obs	$O-C$		Ref	Fil	n	Rem
BD And	55851.3404	0.0040	WTR	−0.0213		⟨59⟩	-Ir	75	(21)
LM And	55978.2678	0.0016	SCI	−0.0108		⟨59⟩	o	68	(12)
V346 Aql	56158.3718	0.0001	WTR	−0.0104		⟨59⟩	o	80	(11)
V1426 Aql	56159.3769	0.0002	WTR	+0.8669		⟨65⟩	o	75	(11)
V1542 Aql	56151.3954	0.0040	WTR	+0.0101		⟨72⟩	o	90	(11)
SS Ari	55894.3004	0.0012	DIE	−0.0018		⟨59⟩	o	22	(20)
SX Aur	55953.2903	0.0018	FR	+0.0132	s	⟨59⟩	V	31	(30)
TT Aur	55953.3289	0.0004	FR	−0.0106		⟨59⟩	V	35	(30)
ZZ Aur	55885.4331	0.0006	MS FR	+0.0249	s	⟨59⟩	o	252	(17)
AH Aur	56001.3662	0.0004	AG	+0.0972	s	⟨45⟩	V	23	(26)
AP Aur	55980.3890	0.0020	WTR	+0.1269	s	⟨64⟩	-Ir	79	(21)
	55980.3830	0.0039	FR	+0.1209	s	⟨64⟩	V	13	(30)
CQ Aur	56003.4062	0.0074	FR	+1.1387	s	⟨59⟩	-Ir	22	(26)
EM Aur	55882.2999	0.0006	MS FR	−0.1980		⟨59⟩	o	559	(17)
EP Aur	56001.3437	0.0010	AG	+0.0153	s	⟨59⟩	V	21	(26)
FN Aur	55295.2963	0.0002	FR	+3.3790		⟨59⟩	-Ir	19	(26) (2)
	55979.4341	0.0067	FR	+3.3608		⟨59⟩	-Ir	18	(26)

Table 1: (cont.)

Variable	HJD 24.....	±	Obs	$O-C$		Ref	Fil	n	Rem
FZ Aur	56001.3342	0.0110	AG	+0.2772	s	⟨59⟩	-Ir	20	(26)
HL Aur	55961.4025	0.0033	AG	−0.0162	s	⟨59⟩	-Ir	95	(26)
HW Aur	55953.3208	0.0027	FR	+0.0242		⟨71⟩	V	40	(30)
KL Aur	55961.5337	0.0078	AG	−0.7313		⟨59⟩	-Ir	94	(26)
KO Aur	55961.3282	0.0014	AG	+0.0500		⟨59⟩	-Ir	87	(26)
MN Aur	55979.4024	0.0065	AG	−0.0338		⟨59⟩	I	96	(26)
	55979.4017	0.0110	AG	−0.0345		⟨59⟩	V	96	(26)
	55979.4016	0.0087	AG	−0.0347		⟨59⟩	R	97	(26)
	55979.4005	0.0047	AG	−0.0358		⟨59⟩	B	95	(26)
MT Aur	55881.4808	0.0009	MS FR	+0.0092		⟨59⟩	o	405	(17)
NN Aur	55961.3047	0.0004	FR	+0.0012		⟨42⟩	-Ir	75	(26)
V426 Aur	56009.2949	0.0005	FR				-Ir	124	(26)
V596 Aur	55953.3366	0.0023	FR	+0.0078		⟨59⟩	V	35	(30)
V640 Aur	56013.3885	0.0003	FR	−0.0179	s	⟨59⟩	-Ir	98	(26)
	56013.5521	0.0002	FR	−0.0183		⟨59⟩	-Ir	98	(26)
V644 Aur	56001.3635	0.0027	AG	+0.0016		⟨59⟩	V	23	(26)
SS Boo	56007.4719	0.0239	AG	+0.0396		⟨59⟩	V	42	(26)
TZ Boo	56061.5029	0.0003	GB	−0.0312		⟨43⟩	B;V	50	(16)
	56062.3981	0.0003	GB	−0.0275		⟨43⟩	B;V	52	(16)
	56061.3585	0.0003	GB	−0.0270	s	⟨43⟩	B;V	40	(16)
	56060.4672	0.0004	GB	−0.0269	s	⟨43⟩	B;V	28	(16)
	56003.5624	0.0002	GB	−0.0262		⟨43⟩	B;V	62	(16)
	56019.4611	0.0002	GB	−0.0254	s	⟨43⟩	B;V	67	(16)
	55993.6068	0.0002	GB	−0.0270	s	⟨43⟩	B	69	(16)
	55978.5997	0.0001	GB	−0.0277		⟨43⟩	V	190	(16)
	56002.5219	0.0002	GB	−0.0266	s	⟨43⟩	B;V	63	(16)
	56055.4168	0.0003	GB	−0.0256	s	⟨43⟩	B;V	45	(16)
	55993.6071	0.0002	GB	−0.0267	s	⟨43⟩	V	69	(16)
	56008.6141	0.0002	GB	−0.0261		⟨43⟩	B;V	67	(16)
	56048.4324	0.0002	GB	−0.0268		⟨43⟩	B;V	46	(16)
	56006.5340	0.0002	GB	−0.0261		⟨43⟩	B;V	61	(16)
	56007.5740	0.0002	GB	−0.0262	s	⟨43⟩	B;V	61	(16)
UW Boo	56013.5148	0.0014	AG	−0.0060		⟨59⟩	-Ir	38	(26)
AD Boo	56015.4018	0.0013	AG	+0.0317		⟨59⟩	V	34	(26)
AQ Boo	56009.4855	0.0001	MS FR	−0.0044		⟨42⟩	o	360	(17)
BG Boo	56002.5908	0.0027	SCI	−0.0274		⟨59⟩	o	25	(12)
EF Boo	56013.6385	0.0003	AG	+0.0034		⟨42⟩	V	38	(26)
	56013.4273	0.0027	AG	+0.0024	s	⟨42⟩	V	38	(26)
ET Boo	56061.6081	0.0010	SCI	+0.0064		⟨42⟩	o	130	(12)
	56062.5716	0.0015	SCI	+0.0023	s	⟨42⟩	o	113	(12)
GH Boo	56015.5905	0.0021	AG				-Ir	34	(26)
GM Boo	56015.4167	0.0021	AG	+0.0028	s	⟨42⟩	-Ir	34	(26)
	56009.4585	0.0027	AG	+0.0030		⟨42⟩	-Ir	49	(26)
	56015.5986	0.0015	AG	+0.0041		⟨42⟩	-Ir	34	(26)
	56009.6398	0.0019	AG	+0.0038	s	⟨42⟩	-Ir	49	(26)
GN Boo	56009.3847	0.0027	AG	+0.0112	s	⟨42⟩	-Ir	48	(26)
	56009.5366	0.0010	AG	+0.0123		⟨42⟩	-Ir	48	(26)
GQ Boo	56009.5149	0.0028	AG	−0.0006	s	⟨42⟩	-Ir	49	(26)
GR Boo	56009.4346	0.0012	AG	−0.0040	s	⟨42⟩	-Ir	49	(26)
	56009.6239	0.0009	AG	−0.0031		⟨42⟩	-Ir	49	(26)
GT Boo	56012.4765	0.0002	MS FR	−0.0016		⟨42⟩	o	396	(17)
GX Boo	56006.5113	0.0010	MS FR	+0.0434		⟨59⟩	o	0	(17)
HH Boo	56013.4735	0.0005	AG	+0.0161		⟨59⟩	-Ir	38	(26)
	55384.4248	0.0042	AG	+0.0786	s	⟨59⟩	-Ir	39	(26)
	56012.3570	0.0001	MS FR	+0.0148	s	⟨59⟩	o	378	(17)
	56013.6323	0.0011	AG	+0.0156	s	⟨59⟩	-Ir	38	(26)
HR Boo	56015.6119	0.0010	AG	−0.0455		⟨59⟩	-Ir	34	(26)
	56009.4493	0.0030	AG	−0.0467	s	⟨59⟩	-Ir	49	(26)
	56015.4520	0.0023	AG	−0.0474	s	⟨59⟩	-Ir	34	(26)

Table 1: (cont.)

Variable	HJD 24.....	±	Obs	$O-C$		Ref	Fil	n	Rem
HR Boo	56008.5003	0.0002	MS FR	−0.0478	s	⟨59⟩	o	357	(17)
	56009.6077	0.0008	AG	−0.0463		⟨59⟩	-Ir	49	(26)
IL Boo	56013.3922	0.0009	AG	−0.0377		⟨59⟩	-Ir	38	(26)
	56013.5672	0.0013	AG	−0.0364	s	⟨59⟩	-Ir	38	(26)
IW Boo	56013.6215	0.0009	AG	−0.0531	s	⟨59⟩	-Ir	38	(26)
	56013.3573	0.0031	AG	+0.0404	s	⟨59⟩	-Ir	38	(26)
	56013.4962	0.0023	AG	+0.0004		⟨59⟩	-Ir	38	(26)
IX Boo	56015.5488	0.0031	AG	+0.0764	s	⟨59⟩	-Ir	34	(26)
KO Boo	56015.5774	0.0057	AG	−0.0533	s	⟨59⟩	-Ir	34	(26)
KP Boo	56013.4191	0.0029	AG	−0.0890		⟨59⟩	-Ir	38	(26)
KW Boo	56015.4619	0.0030	AG	+0.0066		⟨59⟩	-Ir	34	(26)
	56009.5321	0.0019	AG	+0.0075		⟨59⟩	-Ir	50	(26)
	56009.3617	0.0048	AG	+0.0116	s	⟨59⟩	-Ir	50	(26)
LM Boo	56015.3956	0.0003	AG	−0.0082	s	⟨59⟩	-Ir	34	(26)
	56015.5604	0.0010	AG	−0.0074		⟨59⟩	-Ir	34	(26)
LY Boo	56007.4594	0.0050	AG	+0.0281		⟨59⟩	-Ir	42	(26)
MN Boo	56013.4828	0.0041	AG	+0.0884		⟨59⟩	V	38	(26)
MQ Boo	56013.5003	0.0023	AG	+0.0789		⟨59⟩	-Ir	38	(26)
	56007.5791	0.0007	AG	+0.0785		⟨59⟩	-Ir	42	(26)
MT Boo	56007.5482	0.0007	AG	+0.0893		⟨59⟩	-Ir	42	(26)
	56007.3636	0.0014	AG	+0.0874	s	⟨59⟩	-Ir	42	(26)
OQ Boo	56009.5128	0.0085	AG	+0.0697		⟨59⟩	-Ir	48	(26)
	56012.4909	0.0032	FR	+0.0629	s	⟨59⟩	o	39	(30)
PT Boo	56007.5317	0.0082	AG	−0.0750	s	⟨59⟩	V	42	(26)
PU Boo	56007.4728	0.0040	AG	−0.0143		⟨59⟩	V	42	(26)
AV Cam	55970.3922	0.0015	AG	−0.0707		⟨59⟩	-Ir	50	(26)
HW Cam	56043.5527	0.0018	AG	+0.0012		⟨42⟩	-Ir	28	(26)
NR Cam	55970.5149	0.0026	AG	+0.0067		⟨59⟩	-Ir	48	(26)
	55970.3866	0.0024	AG	+0.0063	s	⟨59⟩	-Ir	48	(26)
V375 Cam	56015.5437	0.0020	AG	−0.0036		⟨59⟩	-Ir	35	(26)
V428 Cam	55970.5196	0.0028	AG	−0.0607	s	⟨59⟩	-Ir	49	(26)
	55970.3772	0.0021	AG	−0.0578		⟨59⟩	-Ir	49	(26)
V429 Cam	55970.4826	0.0017	AG	+0.0316		⟨59⟩	-Ir	50	(26)
V438 Cam	55970.4451	0.0060	AG	−0.0337	s	⟨59⟩	-Ir	49	(26)
V473 Cam	55970.3299	0.0014	AG	+0.0116		⟨59⟩	-Ir	50	(26)
	55970.4778	0.0005	AG	+0.0103	s	⟨59⟩	-Ir	50	(26)
V476 Cam	56002.4958	0.0032	AG	−0.1729		⟨59⟩	-Ir	38	(26)
V478 Cam	55996.4404	0.0166	AG	−0.0065	s	⟨59⟩	-Ir	30	(26)
V479 Cam	55993.3046	0.0002	AG	+0.0176		⟨59⟩	-Ir	11	(26)
V483 Cam	56043.4996	0.0020	AG	−0.0369		⟨59⟩	-Ir	28	(26)
V488 Cam	55970.4531	0.0025	AG	+0.0625		⟨59⟩	-Ir	47	(26)
	55970.3172	0.0029	AG	+0.0603	s	⟨59⟩	-Ir	47	(26)
	55970.5848	0.0026	AG	+0.0605	s	⟨59⟩	-Ir	47	(26)
V489 Cam	56002.6001	0.0021	AG	+0.0213	s	⟨59⟩	-Ir	38	(26)
	55970.3703	0.0028	AG	+0.0187	s	⟨59⟩	-Ir	48	(26)
V496 Cam	56043.4597	0.0017	AG	−0.0792		⟨59⟩	-Ir	29	(26)
V497 Cam	56043.5868	0.0008	AG	−0.0053		⟨59⟩	-Ir	28	(26)
V500 Cam	55996.3679	0.0007	AG	+0.0092	s	⟨59⟩	-Ir	42	(26)
	55996.4941	0.0007	AG	+0.0113		⟨59⟩	-Ir	42	(26)
V501 Cam	55996.4177	0.0035	AG	+0.0788	s	⟨59⟩	-Ir	47	(26)
V505 Cam	56043.4303	0.0021	AG	+0.0223		⟨59⟩	-Ir	30	(26)
V506 Cam	56043.5089	0.0017	AG	+0.0079		⟨59⟩	-Ir	28	(26)
V509 Cam	55996.3387	0.0005	AG	−0.0845	s	⟨59⟩	-Ir	42	(26)
	55996.5138	0.0013	AG	−0.0846		⟨59⟩	-Ir	42	(26)
V511 Cam	56043.5097	0.0030	AG	+0.0833	s	⟨59⟩	-Ir	28	(26)
V512 Cam	56043.5387	0.0058	AG	+0.0439		⟨59⟩	-Ir	28	(26)
S Cnc	55963.5030	0.0004	FR	−0.1138		⟨59⟩	o	50	(30)
SW Cnc	55880.6365	0.0003	MS FR	−0.0825		⟨59⟩	o	468	(17)
TX Cnc	55963.5982	0.0017	FR	+0.0407		⟨59⟩	o	95	(30)

Table 1: (cont.)

Variable	HJD 24.....	±	Obs	$O-C$		Ref	Fil	n	Rem
TX Cnc	55963.4119	0.0012	FR	+0.0458	s	⟨59⟩	o	95	(30)
KM Cnc	55996.3963	0.0015	QU				V	67	(13)
RS CVn	56012.3569	0.0009	AG	−0.7206		⟨59⟩	-Ir	74	(26)
	56012.3525	0.0003	FR	−0.7250		⟨59⟩	-Ir	109	(26) (2)
BI CVn	56012.5240	0.0011	AG	−0.0727		⟨59⟩	-Ir	49	(26)
CI CVn	56008.6090	0.0013	FR				o	29	(30)
DF CVn	56012.5440	0.0021	AG	+0.0020	s	⟨42⟩	-Ir	49	(26)
	56012.3759	0.0027	AG	−0.0027		⟨42⟩	-Ir	49	(26)
DI CVn	56012.3754	0.0004	AG	+0.0001		⟨42⟩	-Ir	49	(26)
	56012.5278	0.0005	AG	−0.0005	s	⟨42⟩	-Ir	49	(26)
DL CVn	56012.5476	0.0028	AG	+0.0040		⟨42⟩	-Ir	49	(26)
DM CVn	56011.3484	0.0002	MS FR				o	312	(17)
DR CVn	56012.4680	0.0015	AG	+0.0583	s	⟨59⟩	-Ir	49	(26)
	56012.6294	0.0018	AG	+0.0552		⟨59⟩	-Ir	49	(26)
DX CVn	56012.6201	0.0015	AG	+0.0063	s	⟨59⟩	-Ir	49	(26)
	56012.4395	0.0006	AG	+0.0044		⟨59⟩	-Ir	49	(26)
EE CVn	56010.4819	0.0001	MS FR	−0.0063		⟨59⟩	o	385	(17)
EX CVn	56012.5111	0.0013	AG	+0.0658	s	⟨59⟩	-Ir	49	(26)
	56012.6453	0.0001	AG	+0.0614		⟨59⟩	-Ir	49	(26)
	56012.3698	0.0009	AG	+0.0631		⟨59⟩	-Ir	49	(26)
GO CVn	56013.5414	0.0039	AG	+0.0821	s	⟨59⟩	-Ir	38	(26)
R CMa	55970.3387	0.0008	FR	+0.1015		⟨59⟩	V	34	(30)
AM CMi	55980.4415	0.0010	QU	+0.1963		⟨59⟩	V	87	(13)
TV Cas	54778.3426	0.0013	MON	−0.0225		⟨59⟩	-Ir	531	(15)
	54778.3424	0.0005	MON	−0.0227		⟨59⟩	V	359	(11)
BS Cas	55885.2773	0.0004	MS FR	−0.0194		⟨67⟩	o	450	(17)
IT Cas	54751.3203	0.0005	MON	+0.0526	s	⟨59⟩	V	82	(11)
MR Cas	56007.5038	0.0014	SCI	−0.0841		⟨59⟩	o	32	(12)
	56010.5470	0.0030	SCI	−0.0409	s	⟨59⟩	o	26	(12)
	56010.3398	0.0031	SCI	−0.0716		⟨59⟩	o	39	(12)
	56007.288	0.001	SCI	+0.053		⟨59⟩	o	34	(12)
OX Cas	55802.4482	0.0002	FLG	+0.0301		⟨59⟩	V	151	(24)
XX Cep	54995.4695	0.0001	MON	−0.0168		⟨59⟩	V	200	(11)
	54995.4699	0.0005	MON	−0.0164		⟨59⟩	V	55	(15)
EF Cep	56015.5131	0.0037	AG	−0.0325		⟨59⟩	-Ir	35	(26)
V790 Cep	56055.4926	0.0018	AG	+0.0359	s	⟨59⟩	-Ir	17	(26)
V803 Cep	56055.5391	0.0003	AG	+0.0508		⟨59⟩	-Ir	15	(26)
V804 Cep	56055.4820	0.0007	AG	−0.0004		⟨59⟩	-Ir	18	(26)
UX Com	56008.5221	0.0056	AG	−0.1286		⟨44⟩	V	40	(26)
CM Com	56014.3643	0.0001	MS FR	−0.8973	s	⟨59⟩	o	648	(17)
EK Com	56012.3834	0.0011	SCI	+0.0034	s	⟨42⟩	o	97	(12)
	56012.5195	0.0020	SCI	+0.0062		⟨42⟩	o	100	(12)
	56012.6513	0.0014	SCI	+0.0046	s	⟨42⟩	o	50	(12)
	56072.5232	0.0016	SCI	+0.0060		⟨42⟩	o	46	(12)
	56008.5185	0.0022	AG	+0.0054		⟨42⟩	-Ir	40	(26)
	56072.3875	0.0015	SCI	+0.0037	s	⟨42⟩	o	60	(12)
	56008.3846	0.0013	AG	+0.0049	s	⟨42⟩	-Ir	40	(26)
	56008.6520	0.0005	AG	+0.0056	s	⟨42⟩	-Ir	40	(26)
LL Com	56008.5509	0.0018	AG	+0.0615	s	⟨66⟩	-Ir	40	(26)
LQ Com	56008.3722	0.0018	AG	+0.0001	s	⟨42⟩	-Ir	40	(26)
	56008.5497	0.0004	AG	−0.0008		⟨42⟩	-Ir	40	(26)
LT Com	56008.5039	0.0025	AG	+0.0029	s	⟨42⟩	V	40	(26)
MM Com	56008.3538	0.0010	AG	−0.0173	s	⟨59⟩	-Ir	40	(26)
	56008.5006	0.0016	AG	−0.0215		⟨59⟩	-Ir	40	(26)
	56008.6550	0.0004	AG	−0.0181	s	⟨59⟩	-Ir	40	(26)
MR Com	56008.5083	0.0017	AG	−0.0489	s	⟨59⟩	-Ir	40	(26)
	56010.3655	0.0002	MS FR	−0.0491		⟨59⟩	o	450	(17)
RW CrB	56012.5446	0.0059	FR	+0.0005	s	⟨59⟩	o	19	(30)
TU CrB	56073.4059	0.0008	SCI	+0.0617	s	⟨59⟩	o	55	(12)

Table 1: (cont.)

Variable	HJD 24.....	±	Obs	$O-C$		Ref	Fil	n	Rem
Y Cyg	55833.5244	0.0017	FR	−0.1302		⟨59⟩	o	42	(30)
WZ Cyg	55833.4556	0.0002	FR	+0.0652		⟨59⟩	o	82	(30)
ZZ Cyg	55851.4754	0.0007	FR	−0.0586		⟨59⟩	o	45	(30)
BO Cyg	54757.2776	0.0013	MON	+0.0879		⟨59⟩	V	123	(11)
CV Cyg	55836.3959	0.0042	FR	+0.2114	s	⟨59⟩	o	42	(30)
DO Cyg	55850.3640	0.0020	WTR	−0.0235		⟨59⟩	-Ir	90	(21)
GO Cyg	55833.3929	0.0014	FR	+0.0655	s	⟨59⟩	o	39	(30)
PV Cyg	56008.6581	0.0008	MS FR	+0.2508		⟨59⟩	o	448	(17)
V444 Cyg	55836.4109	0.0034	FR	+0.2061		⟨59⟩	o	22	(30)
V501 Cyg	56132.4424	0.0035	SCI	−0.2858		⟨59⟩	o	66	(12)
V502 Cyg	56010.6365	0.0002	MS FR	+0.1265		⟨59⟩	o	440	(17)
V700 Cyg	56006.6127	0.0001	MS FR	+0.0665		⟨59⟩	o	450	(17)
V711 Cyg	54222.5011	0.0004	MS FR	+0.0204	s	⟨59⟩	o	424	(17)
V743 Cyg	56135.4481	0.0023	SCI	−0.2612		⟨59⟩	o	106	(12)
V842 Cyg	56133.5030	0.0017	SCI	+0.0416		⟨59⟩	o	39	(12)
V907 Cyg	56009.5979	0.0004	MS FR	−0.1010	s	⟨59⟩	o	387	(17)
V1305 Cyg	55836.4364	0.0026	FR	−0.0037		⟨59⟩	o	42	(30)
V1792 Cyg	55833.5013	0.0052	FR				o	42	(30)
V1918 Cyg	56154.3998	0.0030	WTR	+0.0038		⟨42⟩	o	60	(11)
V2154 Cyg	55857.4266	0.0010	FR				o	51	(30)
V2197 Cyg	55833.3278	0.0020	FR				o	42	(30)
V2239 Cyg	55836.5253	0.0019	FR	+0.0008		⟨42⟩	o	43	(30)
V2247 Cyg	55833.4098	0.0011	FR				o	40	(30)
UZ Dra	56001.5486	0.0029	AG	+0.0025		⟨59⟩	-Ir	89	(26)
WW Dra	56002.3948	0.0021	SCI	+0.5800		⟨59⟩	o	127	(12)
WX Dra	56075.4308	0.0028	SCI	+0.0196	s	⟨59⟩	o	33	(12)
BE Dra	56001.5923	0.0042	AG	−0.1054		⟨59⟩	-Ir	89	(26)
	56001.3260	0.0033	AG	−0.1105	s	⟨59⟩	-Ir	89	(26)
BV Dra	56001.5108	0.0013	SCI	−0.0007	s	⟨59⟩	o	68	(12)
	56001.3312	0.0017	SCI	−0.0053		⟨59⟩	o	83	(12)
	56007.4620	0.0013	AG	−0.0006	s	⟨59⟩	-Ir	55	(26)
	56007.6363	0.0003	AG	−0.0014		⟨59⟩	-Ir	55	(26)
BW Dra	56007.4486	0.0016	AG	+0.0448	s	⟨59⟩	-Ir	55	(26)
	56007.5937	0.0009	AG	+0.0438		⟨59⟩	-Ir	55	(26)
EF Dra	56001.5469	0.0040	AG	+0.0956		⟨63⟩	-Ir	87	(26)
	56001.3329	0.0056	AG	+0.0936	s	⟨63⟩	-Ir	87	(26)
FU Dra	56007.6346	0.0007	AG	+0.0043	s	⟨42⟩	-Ir	55	(26)
	56007.4786	0.0002	AG	+0.0017		⟨42⟩	-Ir	55	(26)
	56007.3281	0.0057	AG	+0.0045	s	⟨42⟩	-Ir	55	(26)
GV Dra	56008.3421	0.0024	SCI	+0.0060		⟨70⟩	o	95	(12)
PV Dra	56007.4306	0.0046	AG	+0.0295	s	⟨59⟩	-Ir	55	(26)
V338 Dra	56007.6219	0.0002	AG	−0.0281	s	⟨59⟩	-Ir	55	(26)
	56007.5056	0.0012	AG	−0.0268		⟨59⟩	-Ir	55	(26)
	56007.3877	0.0004	AG	−0.0271	s	⟨59⟩	-Ir	55	(26)
RU Gem	56014.4252	0.0078	AG	+0.1512		⟨59⟩	-Ir	50	(26)
RY Gem	55943.3217	0.0002	FR	−0.1994		⟨59⟩	-Ir	113	(26) (2)
WW Gem	56015.4323	0.0015	QU	+0.0237	s	⟨59⟩	V	84	(13)
	56007.3858	0.0007	QU	+0.0230		⟨59⟩	V	126	(13)
EN Gem	55970.3605	0.0080	AG	−0.0481		⟨59⟩	-Ir	116	(26)
EY Gem	55943.3038	0.0002	MS FR	−0.2278		⟨59⟩	o	550	(17)
IV Gem	53813.30	0.000	FR				-Ir	45	(19)
	56003.5147	0.0012	FR				o	14	(30)
KV Gem	56001.3213	0.0006	QU	−0.0293		⟨53⟩	Ic	76	(13)
	56002.3974	0.0007	QU	−0.0288		⟨53⟩	V	78	(13)
KY Gem	55966.266	0.020	AG	−0.444		⟨59⟩	-Ir	239	(26)
OW Gem	56053.	0.0	VLM	−0.4		⟨73⟩	o	29	(30)
V345 Gem	56003.5134	0.0028	FR	+0.0103	s	⟨42⟩	V	45	(30)
	53446.3120	0.0028	SCI				o	140	(12)
	56003.3805	0.0013	FR	+0.0147		⟨42⟩	V	45	(30)

Table 1: (cont.)

Variable	HJD 24.....	±	Obs	$O-C$		Ref	Fil	n	Rem
V345 Gem	56014.5182	0.0029	SCI	+0.0241	s	⟨42⟩	o	104	(12)
	56014.3743	0.0021	SCI	+0.0176		⟨42⟩	o	133	(12)
V390 Gem	56014.3604	0.0024	AG	−0.0345	s	⟨59⟩	-Ir	50	(26)
V405 Gem	54910.3597	0.0042	ATB	−0.0022		⟨54⟩	o	102	(11)
KL Her	55705.5505	0.0035	SCI	−0.0736	s	⟨59⟩	o	37	(12)
V338 Her	56094.4443	0.0017	FR	+0.1037		⟨59⟩	o	20	(30)
V728 Her	56055.4165	0.0016	AG	+0.0829	s	⟨62⟩	V	25	(26)
V731 Her	56006.5255	0.0019	SCI	+0.1275		⟨59⟩	o	65	(12)
	56055.5548	0.0014	AG	+0.1058	s	⟨59⟩	-Ir	25	(26)
	56001.6202	0.0016	SCI	+0.1002		⟨59⟩	o	46	(12)
V732 Her	56055.5117	0.0069	AG	+0.0523		⟨59⟩	-Ir	25	(26)
V857 Her	56055.4104	0.0003	AG	+0.0056		⟨42⟩	V	24	(26)
V861 Her	56055.5421	0.0017	AG	−0.0074		⟨42⟩	-Ir	25	(26)
V1055 Her	56055.4441	0.0023	AG	+0.0055		⟨42⟩	V	24	(26)
WY Hya	56003.4528	0.0010	AG	+0.0312	s	⟨59⟩	-Ir	33	(26)
AI Hya	55963.4102	0.0011	FR	−0.0184	s	⟨59⟩	-Ir	36	(26)
DE Hya	55961.3896	0.0086	AG	−0.0036		⟨59⟩	-Ir	470	(26)
DK Hya	56013.3512	0.0002	WTR	−0.0763	s	⟨59⟩	V	73	(32)
FG Hya	55979.5835	0.0026	AG	−0.0780	s	⟨59⟩	-Ir	32	(26)
	56003.3548	0.0024	AG	−0.0746		⟨59⟩	-Ir	34	(26)
V470 Hya	56003.3689	0.0063	AG				-Ir	33	(26)
V474 Hya	55963.5672	0.0009	FR	−0.1057	s	⟨59⟩	-Ir	52	(26)
	56003.4547	0.0017	AG	−0.1052		⟨59⟩	-Ir	34	(26)
V475 Hya	55979.4966	0.0022	AG	−0.0039		⟨59⟩	-Ir	29	(26)
	56003.4371	0.0031	AG	−0.0049	s	⟨59⟩	-Ir	32	(26)
V476 Hya	55963.5221	0.0021	FR	−0.0145		⟨59⟩	-Ir	44	(26)
	55979.4862	0.0019	AG	−0.0120	s	⟨59⟩	-Ir	26	(26)
SW Lac	56159.3956	0.0010	FR	+0.0634		⟨59⟩	o	75	(30)
	56159.5532	0.0002	FR	+0.0607	s	⟨59⟩	o	75	(30)
V339 Lac	55815.4692	0.0044	AG	+0.1447		⟨59⟩	-Ir	44	(26) (6)
	55815.4680	0.2100	AG	+0.1435		⟨59⟩	-Ir	37	(26)
	55815.4692	0.2100	AG	+0.1447		⟨59⟩	-Ir	44	(26) (5)
	55815.4680	0.0021	AG	+0.1435		⟨59⟩	-Ir	37	(26)
V345 Lac	55156.2602	0.0008	MON	−1.0302	s	⟨59⟩	V	354	(15)
V364 Lac	56159.4748	0.0010	FR	−0.0084		⟨47⟩	o	37	(30)
AM Leo	56010.3486	0.0014	PGL	+0.0141		⟨59⟩	V	323	(28)
AP Leo	56010.3915	0.0005	QU	−0.0242	s	⟨59⟩	V	74	(13)
	55988.4418	0.0005	QU	−0.0257	s	⟨59⟩	V	90	(13)
ET Leo	56008.3665	0.0010	MS FR	−0.0223		⟨42⟩	o	235	(17)
FM Leo	56001.4257	0.0050	SIR	+0.0035		⟨74⟩	o	283	(16)
	56001.4253	0.0002	FR	+0.0031		⟨74⟩	-Ir	49	(26)
FS Leo	56001.4582	0.0016	FR				V	55	(30)
FZ Leo	56002.4341	0.0002	FR				V	37	(30)
WZ LMi	55996.3593	0.0073	AG	+0.0743		⟨59⟩	-Ir	93	(26)
XX LMi	55996.3689	0.0072	AG	+0.0097		⟨59⟩	-Ir	79	(26)
	56014.5427	0.0114	AG	+0.0056		⟨59⟩	-Ir	52	(26)
XY LMi	55996.3266	0.0023	AG	−0.0186	s	⟨59⟩	-Ir	88	(26)
	55996.5409	0.0040	AG	−0.0227		⟨59⟩	-Ir	88	(26)
AE LMi	55996.2983	0.0001	AG	+0.0009	s	⟨59⟩	-Ir	96	(26)
	55996.5617	0.0013	AG	+0.0001		⟨59⟩	-Ir	96	(26)
	56014.5290	0.0019	AG	+0.0038		⟨59⟩	-Ir	56	(26)
AF LMi	55996.4842	0.0085	AG	−0.0426		⟨59⟩	-Ir	75	(26)
	56014.5747	0.0073	AG	−0.0458	s	⟨59⟩	-Ir	56	(26)
RY Lyn	55944.3668	0.0001	MS FR	−0.0320		⟨59⟩	o	650	(17)
SW Lyn	56008.4817	0.0024	AG	+0.0552		⟨59⟩	-Ir	84	(26)
	56012.3465	0.0012	AG	+0.0556		⟨59⟩	V	42	(26)
TY Lyn	56012.4326	0.0044	AG	+0.0600		⟨59⟩	V	45	(26)
UU Lyn	56013.3567	0.0017	SCI	−0.0038	s	⟨59⟩	o	99	(12)
	54765.6094	0.0006	MON	−0.0075		⟨59⟩	-Ir	114	(15)

Table 1: (cont.)

Variable	HJD 24.....	±	Obs	$O-C$		Ref	Fil	n	Rem
UU Lyn	55644.4397	0.0001	MON	−0.0084		⟨59⟩	V	421	(15)
	56046.3787	0.2100	PGL	−0.0082		⟨59⟩	V	295	(25)
	56002.3429:	0.0056	PGL	−0.0088		⟨59⟩	V	205	(25)
	56013.5866	0.0024	SCI	−0.0081		⟨59⟩	o	115	(12)
	56009.3714	0.0021	PGL	−0.0072		⟨59⟩	V	197	(25)
BG Lyn	56006.3772	0.0019	SCI	−0.0043		⟨42⟩	o	142	(12)
	56012.3796	0.0017	AG	−0.0011		⟨42⟩	V	42	(26)
CD Lyn	54736.5408	0.0006	MON	−0.0135		⟨69⟩	V	144	(11)
DY Lyn	56008.4321	0.0033	AG	−0.1681		⟨59⟩	-Ir	81	(26)
	56012.3720	0.0025	AG	−0.1680		⟨59⟩	V	43	(26)
DZ Lyn	56008.5715	0.0047	AG	−0.0124		⟨59⟩	-Ir	83	(26)
	56012.3502	0.0035	AG	−0.0139		⟨59⟩	V	41	(26)
	56008.3821	0.0091	AG	−0.0128	s	⟨59⟩	-Ir	83	(26)
	56012.5408	0.0026	AG	−0.0123	s	⟨59⟩	V	41	(26)
EL Lyn	56008.5920	0.0125	AG	+0.0606	s	⟨59⟩	-Ir	72	(26)
FN Lyn	56008.4916	0.0064	AG	+0.0667		⟨59⟩	-Ir	86	(26)
FO Lyn	56008.5900	0.0070	AG	+0.0196		⟨59⟩	-Ir	85	(26)
TZ Lyr	56132.5157	0.0022	FR	+0.0100		⟨59⟩	o	29	(30)
TZ Lyr	56094.4365	0.0005	FR	+0.0063		⟨59⟩	o	28	(30)
UZ Lyr	56153.3996	0.0003	WTR	−0.0290		⟨59⟩	o	74	(11)
AA Lyr	56136.5454	0.0003	FR	+0.1423		⟨59⟩	-Ir	21	(26)
NV Lyr	55384.4527	0.0007	AG	−0.0822		⟨59⟩	-Ir	16	(26)
NY Lyr	55384.4114	0.0017	AG	−0.0898		⟨59⟩	-Ir	16	(26)
V563 Lyr	56132.4897	0.0029	FR	+0.0028		⟨42⟩	o	32	(30)
V574 Lyr	56134.5591	0.0016	SCI	+0.0043	s	⟨42⟩	o	57	(12)
	56134.4219	0.0010	SCI	+0.0036		⟨42⟩	o	53	(12)
V576 Lyr	56094.4093	0.0002	FR				o	23	(30)
beta Lyr	55823.19	0.000	VLM	+0.68		⟨59⟩	o	84	(30)
	55816.76	0.000	VLM	+0.70	s	⟨59⟩	o	54	(30)
UV Mon	55980.4438	0.0020	AG	−0.0721	s	⟨59⟩	-Ir	29	(26)
CF Mon	55980.3692	0.0092	AG	+0.0217	s	⟨59⟩	-Ir	28	(26)
DD Mon	55980.4267	0.0014	AG	−0.1132	s	⟨59⟩	-Ir	28	(26)
EZ Mon	55970.4609	0.0010	FR	+0.0441	s	⟨59⟩	-Ir	38	(26)
GU Mon	55980.4791	0.0020	AG	−0.0950		⟨59⟩	-Ir	30	(26)
V380 Mon	55980.4276	0.0054	AG	−0.0364		⟨59⟩	-Ir	30	(26)
V384 Mon	55980.3973	0.0052	AG	−0.0397		⟨59⟩	-Ir	31	(26)
V450 Mon	55980.4014	0.0064	AG	+0.0715		⟨59⟩	-Ir	28	(26)
V514 Mon	55980.4254	0.0017	AG	+0.0833		⟨59⟩	-Ir	30	(26)
V521 Mon	55980.4407	0.0064	AG	−0.1096		⟨59⟩	-Ir	28	(26)
V532 Mon	55861.6144	0.0009	MS FR	−0.0302		⟨59⟩	o	260	(17)
EW Ori	55953.4105	0.0001	FR	−0.0160	s	⟨59⟩	-Ir	55	(26)
FT Ori	54750.5629	0.0003	MON	+0.0142		⟨59⟩	V	179	(11)
GG Ori	54757.5989	0.0009	MON	+0.0821		⟨59⟩	V	93	(11)
V648 Ori	55880.4726	0.0002	MS FR	+0.0660		⟨59⟩	o	728	(17)
V1633 Ori	55882.4990	0.0002	MS FR	+0.2055		⟨68⟩	o	420	(17)
RV Per	54364.457	0.006	AG	+0.969		⟨59⟩	-Ir	62	(11) (2)
IK Per	55953.4503	0.0019	FR	+0.1376		⟨59⟩	V	37	(30)
IQ Per	54816.2831	0.0011	MON	+0.0043		⟨59⟩	V	375	(11)
KN Per	55834.4380	0.0069	PGL	+0.0111		⟨53⟩	V	308	(25)
KR Per	55953.3117	0.0010	FR	−0.0199	s	⟨59⟩	V	31	(30)
LX Per	55978.6486	0.0007	FR	−0.0548		⟨59⟩	-Ir	48	(26) (2)
V570 Per	55978.4546	0.0017	FR	−0.0003		⟨42⟩	-Ir	31	(26)
V592 Per	55953.3761	0.0009	FR				V	35	(30)
PV Pup	55970.4448	0.0018	FR	−0.0019		⟨59⟩	V	37	(30)
CW Sge	56152.3775	0.0070	WTR	+0.0525		⟨59⟩	o	80	(11)
V384 Ser	56045.4316	0.0002	FR	−0.0008		⟨59⟩	-Ir	69	(26)
	56132.4991	0.0004	FR	−0.0015		⟨59⟩	-Ir	45	(26)
	56132.3628	0.0011	FR	−0.0035	s	⟨59⟩	-Ir	45	(26)
	56045.5651	0.0001	FR	−0.0017	s	⟨59⟩	-Ir	69	(26)

Table 1: (cont.)

Variable	HJD 24.....	±	Obs	$O-C$		Ref	Fil	n	Rem
V384 Ser	56065.4508	0.0002	FR	−0.0019	s	⟨59⟩	-Ir	45	(26)
	56008.4824	0.0003	FR	+0.0002	s	⟨59⟩	-Ir	63	(26)
	56094.4726	0.0003	FR	−0.0029	s	⟨59⟩	-Ir	36	(26)
	56008.6162	0.0001	FR	−0.0004		⟨59⟩	-Ir	63	(26)
CR Tau	55942.3179	0.0001	MS FR	−0.0015		⟨67⟩	o	624	(17)
V1128 Tau	55942.2954	0.0012	SCI	+0.0011		⟨42⟩	o	100	(12)
	55942.4478	0.0010	SCI	+0.0008	s	⟨42⟩	o	89	(12)
X Tri	54765.3663	0.0001	MON	−0.0720		⟨59⟩	V	245	(11)
	54765.3663	0.0002	MON	−0.0720		⟨59⟩	-Ir	244	(15)
RW UMa	56009.4979	0.0085	AG	−0.1649		⟨59⟩	-Ir	112	(26)
	56009.4934	0.0005	SCI	−0.1694		⟨59⟩	o	256	(12)
AN UMa	56002.3990	0.0004	AG	+0.0195	s	⟨59⟩	-Ir	119	(26)
	56002.6089	0.0002	AG	−0.0099	s	⟨59⟩	-Ir	130	(26)
	56002.6366	0.0002	AG	+0.0178	s	⟨59⟩	-Ir	130	(26)
	56002.3709	0.0001	AG	−0.0086	s	⟨59⟩	-Ir	119	(26)
AW UMa	55590.6314	0.0001	MON	−0.0780	s	⟨59⟩	V	244	(15)
	55578.5648	0.0001	MON	−0.0795		⟨59⟩	V	364	(15)
KM UMa	55942.4530	0.0001	MS FR	+0.0003		⟨42⟩	o	567	(17)
MS UMa	56009.4749	0.0029	AG	+0.0400	s	⟨59⟩	-Ir	112	(26)
V342 UMa	56009.5583	0.0039	AG	−0.0162		⟨59⟩	-Ir	112	(26)
V342 UMa	56009.3875	0.0046	AG	−0.0151	s	⟨59⟩	-Ir	112	(26)
V343 UMa	56009.3413	0.0169	AG	−0.0072	s	⟨59⟩	-Ir	112	(26)
	56009.6175	0.0033	AG	−0.0113		⟨59⟩	-Ir	112	(26)
V354 UMa	56019.4003	0.0024	FR	+0.0452		⟨59⟩	o	49	(30)
	56019.5476	0.0018	FR	+0.0456	s	⟨59⟩	o	49	(30)
	56008.5255	0.0015	FR	+0.0419		⟨59⟩	o	32	(30)
V356 UMa	56008.6280	0.0008	FR	−0.0044		⟨59⟩	o	29	(30)
V360 UMa	56013.5926	0.0015	AG	−0.0777		⟨59⟩	-Ir	38	(26)
	56013.4154	0.0017	AG	−0.0748	s	⟨59⟩	-Ir	38	(26)
AG Vir	56002.4223	0.0015	FR	+0.0018	s	⟨59⟩	V	47	(30)
AH Vir	56002.6558	0.0030	FR	+0.0420	s	⟨59⟩	V	45	(30)
	56002.4514	0.0015	FR	+0.0414		⟨59⟩	V	45	(30)
V355 Vir	56002.5960	0.0060	FR				-ir	69	(26)
BK Vul	55481.4556	0.0026	AG	+0.0058	s	⟨59⟩	-Ir	40	(26)
FASTT 390	56003.3959	0.0025	AG				-Ir	33	(26)
GSC 00279-00822	56002.4870	0.0003	FR				-Ir	69	(26)
GSC 02016-00444	56015.4875	0.0039	AG				-Ir	34	(26)
	55654.4134	0.0073	AG				-Ir	66	(26)
	55654.5671	0.0088	AG				-Ir	66	(26)
	56009.4721	0.0060	AG				-Ir	49	(26)
GSC 02038-00293	56045.4786	0.0015	FR	+0.0110		⟨76⟩	-Ir	48	(26)
	56132.4165	0.0031	FR	+0.0045	s	⟨76⟩	-Ir	36	(26)
	56008.5739	0.0021	FR	+0.0144	s	⟨76⟩	-Ir	32	(26)
	56094.5265	0.0024	FR	+0.0133		⟨76⟩	-Ir	31	(26)
	56065.5288	0.0003	FR	−0.0029	s	⟨76⟩	-Ir	36	(26)
GSC 02411-00613	56009.3889	0.0001	FR				-Ir	32	(26)
GSC 02415-00286	56009.3979	0.0004	FR				-Ir	50	(26)
GSC 02423-00517	54829.4881	0.0030	FR				-Ir	96	(19)
	54829.6696	0.0020	FR				-Ir	96	(19)
	56003.4357	0.0001	FR				-Ir	41	(26)
	54829.3005	0.0017	FR				-Ir	96	(19)
GSC 02761-01817	56159.5022	0.0014	FR				o	36	(30)
GSC 02898-02901	55953.3665	0.0009	FR				V	36	(30)
GSC 03097-01297	56094.4816	0.0011	FR				o	23	(30)
GSC 03109-00859	56094.4336	0.0053	FR				o	24	(30)
	56132.4178	0.0021	FR				o	28	(30)
GSC 03208-01986	56159.5065	0.0010	FR				o	36	(30)
GSC 03575-06239	56152.4543	0.0031	FR	+0.1627	s	⟨77⟩	V	27	(30)
GSC 03578-00263	55851.4750	0.0018	FR				o	46	(30)

Table 1: (cont.)

Variable	HJD 24.....	±	Obs	$O-C$		Fil	n	Rem
GSC 03578-00263	56152.5008:	0.0009	FR			V	58	(30)
	55851.2846	0.0015	FR			o	46	(30)
GSC 03581-01856	55851.5496	0.0079	FR			o	51	(30)
	55851.4101	0.0019	FR			o	51	(30)
	55851.2735	0.0042	FR			o	51	(30)
GSC 04190-01948	56002.3141	0.0024	SCI			o	127	(12)
	56046.5129	0.0028	SCI			o	132	(12)
	55944.4295	0.0021	SCI			o	115	(12)
GSC 04922-00116	56001.2957	0.0021	FR			-Ir	98	(26)
	56001.6120	0.0010	FR			-Ir	98	(26)
NSV 12079	55451.4446	0.0032	AG			-Ir	36	(26)
NSVS 5071111	56019.3358	0.0018	FR			o	33	(30)
NSVS 5149208	56013.4579	0.0020	AG			-Ir	38	(26)
NSVS 710419	55996.3670	0.0029	AG			-Ir	47	(26)
	55996.5394	0.0011	AG			-Ir	47	(26)
U-A2 0975-04356998	55624.4539	0.0023	FR			-Ir	38	(26)
U-A2 1425-14529683	55874.4815	0.0023	AG			-Ir	48	(26)
U-A2 1425-15156364	55874.4272	0.0121	AG			-Ir	47	(26)
U-B1 0903-0102370	55980.3892	0.0019	AG			-Ir	30	(26)
U-B1 1447-0060874	55894.4804	0.0030	AG	-0.0042	$\langle 77 \rangle$	-Ir	44	(26)

Table 2: Times of maxima of pulsating stars

Variable	HJD 24.....	±	Obs	$O-C$	Ref	Fil	n	Rem
AC And	55071.603	0.001	FR	−0.298	⟨59⟩	-Ir	69	(26)
FI And	55849.4645	0.0010	MZ	+0.0045	⟨57⟩	-Ir	95	(13)
	55896.3442	0.0010	MZ	+0.0042	⟨57⟩	-Ir	138	(13)
GP And	55075.6374	0.0007	MON	+0.0040	⟨59⟩	o	36	(31)
	54788.3675	0.0006	MON	+0.0049	⟨59⟩	-Ir	98	(15)
	54737.5373	0.0005	MON	+0.0038	⟨59⟩	V	70	(11)
	54750.4422	0.0008	MON	+0.0047	⟨59⟩	V	60	(11)
	54750.3629	0.0007	MON	+0.0041	⟨59⟩	V	60	(11)
	54737.4587	0.0007	MON	+0.0038	⟨59⟩	V	70	(11)
	55075.6377	0.0004	MON	+0.0043	⟨59⟩	V	191	(15)
	54788.2889	0.0004	MON	+0.0050	⟨59⟩	-Ir	98	(15)
	55807.6245	0.0005	MON	+0.0054	⟨59⟩	V	57	(15)
	54750.2851	0.0009	MON	+0.0050	⟨59⟩	V	60	(11)
SW Aqr	55806.3873	0.0012	FLG	+0.0218	⟨59⟩	V	117	(24)
RV Ari	55890.3556	0.0008	MON	+0.0054	⟨59⟩	V	94	(15)
	55894.2582	0.0004	MON	−0.0034	⟨59⟩	V	94	(15)
	55831.5865	0.0006	MON	+0.0002	⟨59⟩	V	58	(15)
	55831.6742	0.0006	MON	−0.0052	⟨59⟩	V	58	(15)
	55894.3508	0.0006	MON	−0.0039	⟨59⟩	V	94	(15)
	55887.3653	0.0005	MON	−0.0048	⟨59⟩	V	136	(15)
MV Aur	55943.4388	0.0012	MZ	−0.1295	⟨59⟩	-Ir	85	(13)
V574 Aur	56013.443	0.003	FR	−0.059	⟨59⟩	-Ir	64	(26)
RS Boo	56009.3602	0.0014	PGL	+0.0003	⟨46⟩	V	193	(28)
VY Boo	56015.501	0.001	AG	+0.005	⟨55⟩	-Ir	34	(26)
	56009.547	0.001	AG	+0.006	⟨55⟩	-Ir	49	(26)
WW Boo	56070.3952	0.0010	MZ	+0.1340	⟨59⟩	-Ir	114	(13)
YZ Boo	55640.5793	0.0007	MON	+0.0030	⟨59⟩	V	233	(15)
	55644.5350	0.0007	MON	+0.0033	⟨59⟩	V	225	(15)
	55640.6834	0.0008	MON	+0.0031	⟨59⟩	V	233	(15)
	55644.6392	0.0007	MON	+0.0034	⟨59⟩	V	225	(15)
CS Boo	54841.6972	0.0012	MON	−0.0014	⟨61⟩	o	62	(31)
	54841.6970	0.0012	MON	−0.0016	⟨61⟩	V	101	(31)
DD Boo	56009.487	0.001	AG			-Ir	48	(26)
	56015.619	0.002	AG			-Ir	34	(26)
DG Boo	56061.3936	0.0007	MZ			-Ir	84	(13)
NN Boo	56007.423	0.001	AG	−0.054	⟨59⟩	-Ir	42	(26)
UY Cam	55672.3695	0.0002	RAT RCR	+0.0728	⟨50⟩	-U-I	104	(27)
CN Cam	55877.4359	0.0015	MZ	−0.0081	⟨57⟩	-Ir	235	(13)
	55882.4167	0.0015	MZ	+0.0011	⟨57⟩	-Ir	136	(13)
	54219.4109	0.0080	MZ	−0.0139	⟨57⟩	-Ir	78	(13)
	55961.3441	0.0020	MZ	+0.0048	⟨57⟩	-Ir	133	(13)
	55854.4496	0.0018	MZ	−0.0009	⟨57⟩	-Ir	102	(13)
V390 Cam	56015.522	0.001	AG	−0.022	⟨59⟩	-Ir	35	(26)
	56015.586	0.001	AG	−0.021	⟨59⟩	-Ir	35	(26)
	56015.460	0.001	AG	−0.020	⟨59⟩	-Ir	35	(26)
	56015.397	0.001	AG	−0.020	⟨59⟩	-Ir	35	(26)
Y Cnc	56002.3863	0.0013	MZ			-Ir	173	(13)
AM Cnc	56012.4156	0.0011	MZ	+0.0370	⟨59⟩	-Ir	179	(13) (1)
	56026.378	0.001	GB	+0.059	⟨59⟩	o	119	(16)
	56031.3915	0.0005	GB	+0.0540	⟨59⟩	o	74	(16)
	56036.4107	0.0005	GB	+0.0547	⟨59⟩	o	68	(16)
	56003.4968	0.0013	MZ	+0.0401	⟨59⟩	-Ir	59	(13)
Z CVn	55600.3768	0.0006	SCI	−0.1096	⟨59⟩	o	33	(12)
	55592.5135	0.0017	SCI	−0.1271	⟨59⟩	o	61	(12)
RZ CVn	54842.7414	0.0011	MON	+0.1282	⟨49⟩	V	99	(15)
SV CVn	56012.427	0.001	AG	+0.125	⟨59⟩	-Ir	49	(26)
SW CVn	56012.403	0.001	AG	−0.112	⟨59⟩	-Ir	49	(26)
SY CMi	55959.3555	0.0052	WU	+0.0755	⟨59⟩	V	78	(29)
	52285.4986	0.0067	PS	+0.1246	⟨59⟩	o	114	(22)

Table 2: (cont.)

Variable	HJD 24.....	±	Obs	$O-C$	Ref	Fil	n	Rem
SY CMi	55964.4478	0.0064	WU	+0.0738	⟨59⟩	V	104	(29)
V845 Cas	55858.2908	0.0013	MZ			-Ir	58	(12)
V845 Cas	55894.2476	0.0014	MZ			-Ir	81	(12)
V1040 Cas	54491.305	0.001	AG	+0.023	⟨75⟩	o	84	(26)
RZ Cep	55879.365	0.001	MZ	−0.152	⟨59⟩	-Ir	176	(13)
	55879.3988	0.0015	MZ	−0.1180	⟨59⟩	-Ir	176	(13) (4)
ET Cep	56055.478	0.001	AG			-Ir	17	(26)
KM Cep	55855.4316	0.0008	MZ	−0.2431	⟨59⟩	-Ir	119	(12)
	55838.3946	0.0007	MZ	−0.2407	⟨59⟩	-Ir	234	(12)
	55854.2925	0.0015	MZ	−0.2462	⟨59⟩	-Ir	110	(12)
	55880.4130	0.0013	MZ	−0.2528	⟨59⟩	-Ir	130	(12)
U Com	56008.398	0.001	AG	+0.006	⟨50⟩	-Ir	40	(26)
ST Com	54861.6592	0.0011	MON	−0.0020	⟨48⟩	V	212	(15)
FV Com	56008.565	0.001	AG	+0.020	⟨59⟩	-Ir	40	(26)
UY Cyg	56116.4451	0.0014	PGL	+0.0606	⟨59⟩	V	99	(28)
V1369 Cyg	55848.3814	0.0014	MZ	−0.0988	⟨59⟩	-Ir	96	(12)
	55856.2946	0.0015	MZ	−0.1022	⟨59⟩	-Ir	77	(12)
BT Dra	56007.572	0.001	AG	−0.015	⟨59⟩	-Ir	55	(26)
QS Dra	56007.507	0.001	AG			-Ir	55	(26)
	56007.591	0.001	AG			-Ir	55	(26)
	56007.429	0.001	AG			-Ir	55	(26)
V335 Dra	56007.414	0.002	AG	−0.094	⟨59⟩	-Ir	55	(26)
RR Gem	55563.3938	0.0021	PGL	−0.0197	⟨48⟩	V	238	(28)
	56006.3666	0.0014	PGL	−0.0279	⟨48⟩	V	69	(28)
EW Gem	56008.3521	0.0016	MZ	+0.1846	⟨59⟩	-Ir	75	(13)
AR Her	56132.4022	0.0014	PGL	+0.0362	⟨52⟩	V	174	(25)
	56075.5419	0.0139	PGL	+0.0441	⟨52⟩	V	133	(25)
	56116.4621	0.0035	PGL	+0.0756	⟨52⟩	V	213	(25)
DY Her	55264.6365	0.0010	MON	−0.0052	⟨49⟩	V	80	(11)
	55352.4777	0.0012	MON	−0.0050	⟨49⟩	V	146	(11)
	55621.6488	0.0007	MON	−0.0050	⟨49⟩	V	215	(15)
	54999.4796	0.0007	MON	−0.0040	⟨49⟩	V	147	(11)
	55964.6892	0.0009	MON	−0.0053	⟨49⟩	V	145	(15)
V448 Her	56055.506	0.001	AG	+0.163	⟨59⟩	-Ir	22	(26)
V759 Her	55058.443	0.005	FR	−0.176	⟨59⟩	-Ir	61	(26)
V487 Hya	55979.481	0.002	AG	−0.034	⟨59⟩	-Ir	27	(26)
V491 Hya	56003.448	0.002	AG	+0.104	⟨59⟩	-Ir	28	(26)
CQ Lac	56159.465	0.005	FR	+0.176	⟨59⟩	o	36	(30)
RR Leo	56006.4214	0.0010	WLH	+0.0143	⟨41⟩	-U-I	155	(18)
SS Leo	56002.4710	0.0021	PGL	−0.0808	⟨59⟩	V	145	(28)
AN Leo	56014.500	0.001	GB	+0.147	⟨59⟩	o	155	(16)
	56045.376 :	0.002	GB	+0.133	⟨59⟩	o	122	(16)
BO Leo	56006.4665	0.0014	MZ	−0.0058	⟨56⟩	-Ir	73	(13)
BU Leo	56055.4573	0.0020	MZ	−0.1088	⟨59⟩	-Ir	120	(13)
BX Leo	56064.4126	0.0019	MZ	−0.1636	⟨59⟩	-Ir	91	(13)
DL Leo	55672.3859	0.0010	MZ	+0.0330	⟨60⟩	-Ir	89	(12)
HO Leo	56009.433	0.001	GB	+0.088	⟨59⟩	o	93	(16)
	56015.435	0.001	GB	+0.092	⟨59⟩	o	104	(16)
	56046.380	0.001	GB	+0.123	⟨59⟩	o	115	(16)
Y LMi	53068.5178	0.0086	PC	+0.0066	⟨50⟩	-Ir	58	(14)
EH Lib	55310.5450	0.0006	MON	+0.0031	⟨59⟩	V	99	(15)
	55310.4566	0.0005	MON	+0.0031	⟨59⟩	V	165	(11)
	55653.5002	0.0007	MON	+0.0034	⟨59⟩	V	74	(11)
	55653.5886	0.0006	MON	+0.0033	⟨59⟩	V	74	(11)
	55310.4571	0.0007	MON	+0.0036	⟨59⟩	V	99	(15)
	55646.5155	0.0005	MON	+0.0033	⟨59⟩	V	143	(15)
	55310.5453	0.0006	MON	+0.0034	⟨59⟩	V	165	(11)
SZ Lyn	56012.407	0.001	AG	+0.024	⟨59⟩	V	43	(26)
	56002.5231	0.0021	PGL	+0.0239	⟨59⟩	V	253	(25)

Table 2: (cont.)

Variable	HJD 24.....	±	Obs	$O-C$	Ref	Fil	n	Rem
SZ Lyn	56008.433	0.001	AG	+0.028	⟨59⟩	-Ir	82	(26)
	56008.551	0.001	AG	+0.025	⟨59⟩	-Ir	82	(26)
	56012.532	0.001	AG	+0.028	⟨59⟩	V	43	(26)
	54758.5988	0.0011	MON	+0.0200	⟨59⟩	V	234	(11)
TV Lyn	56012.337	0.002	AG	+0.020	⟨59⟩	V	45	(26)
	56012.579	0.002	AG	+0.021	⟨59⟩	V	45	(26)
TW Lyn	56012.301	0.001	AG	+0.062	⟨59⟩	V	43	(26)
AN Lyn	56050.3713	0.0014	PGL			V	136	(25)
	56014.4033	0.0014	PGL			V	243	(25)
	56035.4350	0.0014	PGL			V	173	(28)
	56010.3768	0.0007	PGL			V	198	(25)
	56075.4335	0.0035	PGL			V	187	(25)
	56012.3398	0.0007	PGL			V	108	(25)
	55642.4279	0.0025	MON			V	100	(15)
	55964.5794	0.0016	MON			V	179	(15)
	54765.6156	0.0019	MON			V	145	(11)
	55644.3925	0.0014	MON			V	388	(15)
	56035.4347	0.0014	PGL			V	220	(25)
	56032.3885	0.0007	PGL			V	114	(25)
	55964.3817	0.0015	MON			V	179	(15)
	55964.4798	0.0018	MON			V	179	(15)
	56071.4031	0.0007	PGL			V	323	(25)
	55642.3308	0.0016	MON			V	131	(11)
	55642.4286	0.0022	MON			V	131	(11)
	56002.4136	0.0021	PGL			V	202	(25)
	56009.3932	0.0007	PGL			V	224	(25)
	56013.3234	0.0007	PGL			V	131	(25)
BE Lyn	55646.3023	0.0006	MON			V	260	(15)
	56002.3621	0.0021	PGL			V	168	(28)
	55968.3289	0.0007	MON			V	240	(15)
	55646.3984	0.0005	MON			V	260	(15)
	56050.3923	0.0035	PGL			V	156	(28)
BE Lyn	56046.4638	0.0021	PGL			V	383	(28)
BO Lyn	55654.4061	0.0018	MON			V	191	(15)
EY Lyn	56012.390	0.001	AG	+0.058	⟨59⟩	-Ir	45	(26)
Y Lyr	56094.519	0.005	FR	−0.010	⟨59⟩	o	22	(30)
ZZ Lyr	55879.2675	0.0008	MZ	−0.0298	⟨59⟩	-Ir	72	(12)
BQ Lyr	55739.5143	0.0010	MZ	+0.0909	⟨59⟩	-Ir	141	(12)
CG Lyr	55838.3231	0.0010	MZ	+0.0027	⟨57⟩	-Ir	75	(12)
LX Lyr	56094.402	0.006	FR	+0.015	⟨51⟩	o	28	(30)
V593 Lyr	56132.546	0.005	FR	−0.036	⟨59⟩	o	32	(30)
	56132.443	0.005	FR	−0.037	⟨59⟩	o	32	(30)
V567 Oph	55353.5507	0.0024	MON	−0.0052	⟨49⟩	V	162	(11)
	56096.5253	0.0035	PGL	−0.0132	⟨49⟩	V	128	(28)
V1640 Ori	55958.4399	0.0014	MZ	+0.0089	⟨56⟩	-Ir	100	(13)
AV Peg	55796.4274	0.0010	FLG	+0.0109	⟨41⟩	V	183	(24)
BP Peg	55817.2891	0.0008	MON	−0.0263	⟨49⟩	V	66	(15)
	55852.3450	0.0010	MON	−0.0245	⟨49⟩	V	235	(15)
CI Peg	55851.2982	0.0014	MZ	+0.1400	⟨59⟩	-Ir	262	(12)
DY Peg	55155.2802	0.0007	MON	−0.0096	⟨59⟩	o	135	(31)
	55814.3864	0.0004	MON	−0.0112	⟨59⟩	V	192	(15)
	55478.4163	0.0005	MON	−0.0099	⟨59⟩	V	290	(15)
	54736.3201	0.0004	MON	−0.0081	⟨59⟩	V	55	(11)
	55852.4536	0.0004	MON	−0.0116	⟨59⟩	V	323	(15)
	55371.5791	0.0008	MON	−0.0101	⟨59⟩	V	30	(15)
	55074.6241	0.0006	MON	−0.0092	⟨59⟩	V	49	(11)
	54737.3409	0.0005	MON	−0.0083	⟨59⟩	V	49	(11)
	55814.4597	0.0004	MON	−0.0109	⟨59⟩	V	192	(15)
	54736.4660	0.0005	MON	−0.0080	⟨59⟩	V	55	(11)

Table 2: (cont.)

Variable	HJD 24.....	±	Obs	$O-C$	Ref	Fil	n	Rem
DY Peg	55074.4778	0.0006	MON	−0.0096	⟨59⟩	V	49	(11)
	55478.3428	0.0005	MON	−0.0105	⟨59⟩	V	290	(15)
	55371.5791	0.0005	MON	−0.0101	⟨59⟩	V	43	(11)
	54736.3926	0.0005	MON	−0.0085	⟨59⟩	V	55	(11)
	55074.5511	0.0004	MON	−0.0092	⟨59⟩	V	49	(11)
	54737.4136	0.0004	MON	−0.0085	⟨59⟩	V	49	(11)
	55155.2806	0.0005	MON	−0.0092	⟨59⟩	V	394	(15)
	54737.2680	0.0006	MON	−0.0082	⟨59⟩	V	49	(11)
	55814.5323	0.0004	MON	−0.0112	⟨59⟩	V	192	(15)
KV Per	55960.4454	0.0046	MZ	−0.0046	⟨59⟩	-Ir	85	(13)
CW Ser	55632.6013	0.0012	MON	−0.0083	⟨49⟩	V	57	(15)
	55628.6282	0.0014	MON	−0.0092	⟨49⟩	V	115	(15)
	55629.5736	0.0014	MON	−0.0095	⟨49⟩	V	78	(15)
	55625.6019	0.0011	MON	−0.0091	⟨49⟩	V	110	(15)
YZ Tau	55964.3102	0.0020	MZ	+0.0251	⟨59⟩	-Ir	170	(13)
RV UMa	56019.349	0.004	FR	+0.009	⟨49⟩	o	99	(30)
TU UMa	56003.3405	0.0008	QU	−0.0527	⟨59⟩	V	202	(13) (3)
	56013.3735	0.0007	PGL	−0.0576	⟨59⟩	V	251	(28)
	56013.3776	0.0006	QU	−0.0535	⟨59⟩	V	142	(13) (3)
	56019.5119	0.0012	SCI	−0.0534	⟨59⟩	o	150	(12)
	55942.5529	0.0010	SCI	−0.0555	⟨59⟩	o	154	(12)
	56008.3591	0.0006	QU	−0.0530	⟨59⟩	V	141	(13) (3)
AE UMa	56008.4479	0.0012	WN	+0.0068	⟨49⟩	V	83	(23)
	56008.3552	0.0008	WN	+0.0001	⟨49⟩	V	82	(23)
	56002.4207	0.0006	WN	+0.0008	⟨49⟩	V	62	(23)
	56014.4243	0.0014	PGL	−0.0380	⟨49⟩	V	127	(28)
	56006.4676	0.0001	WN	+0.0049	⟨49⟩	V	44	(23)
	56009.4738	0.0007	WN	+0.0005	⟨49⟩	V	61	(23)
BH UMa	56009.687	0.005	AG	+0.110	⟨59⟩	-Ir	112	(26)
BN Vul	55799.3999	0.0018	FLG	+0.0707	⟨59⟩	V	75	(24)
GSC 00472-02473	56132.5124	0.0028	PGL			V	248	(28)
GSC 01442-01358	56073.4062	0.0014	WU			V	194	(29)
GSC 01442-01358	56072.4203	0.0016	WU			V	234	(29)
	56076.4441	0.0015	WU			V	133	(29)
	56075.4602	0.0012	WU			V	201	(29)
	56075.3756	0.0015	WU			V	201	(29)
GSC 01566-02802	56157.3792	0.0007	WU			V	308	(29)
	56158.3459	0.0007	WU			V	183	(29)
	56157.4399	0.0007	WU			V	308	(29)
GSC 01566-02802	56158.4069	0.0007	WU			V	183	(29)
GSC 01773-01319	55993.3102	0.0048	WU			V	98	(29)
	55964.2878	0.0014	WU			V	96	(29)
GSC 03428-01497	56009.4247	0.0016	WN			V	73	(23)
	56009.3509	0.0012	WN			V	73	(23)
	56012.4192	0.0016	WN			V	103	(23)
	56003.5130	0.0009	WN			V	98	(23)
	56006.4302	0.0001	WN			V	125	(23)
	56003.4382	0.0008	WN			V	98	(23)
GSC 03682-00018	55499.632	0.001	AG			-Ir	48	(26)
GSC 03755-00845	56006.3322	0.0009	WN			V	115	(23)
	56003.3643	0.0007	WN			V	83	(23)
	56002.3761	0.0008	WN			V	79	(23)
	55993.3206	0.0017	WN			V	154	(23)
	56003.2891	0.0012	WN			V	83	(23)
	56009.3002	0.0007	WN			V	92	(23)
	56008.3111	0.0011	WN			V	96	(23)
	56002.3008	0.0009	WN			V	79	(23)
	56012.3444	0.0007	WN			V	123	(23)
GSC 03851-00240	55686.5565	0.0009	MON			V	50	(15)

Table 2: (cont.)

Variable	HJD 24.....	±	Obs	$O-C$	Ref	Fil	n	Rem
GSC 03851-00240	55688.4611	0.0007	MON			V	40	(15)
	55688.3932	0.0005	MON			V	40	(15)
	55661.5562	0.0006	MON			V	37	(15)
	55661.4876	0.0008	MON			V	37	(15)
	55686.3546	0.0009	MON			V	50	(15)
	55688.5981	0.0007	MON			V	40	(15)
	55688.5305	0.0009	MON			V	40	(15)
	55661.4185	0.0007	MON			V	37	(15)

Observers:

AG:	Agerer, F., Tiefenbach
ATB:	Achterberg, H., Norderstedt
DIE:	Dietrich, M., Radebeul
FLG:	Flechsig, Dr. G., Teterow
FR:	Frank, P., Velden
GB:	Gröbel, R., Eckental
MON:	Monninger, Dr. G., Gemmingen
MS:	Moschner, W., Lennestadt
MZ:	Maintz, Dr. G., Bonn
PC:	Poschinger, K., Hamburg
PGL:	Pagel, Dr. L., Klockenhagen
PS:	Paschke, A., Rüti
QU:	Quester, W., Esslingen
RAT:	Rätz, M., Herges-Hallenberg
RCR:	Rätz, K., Herges-Hallenberg
SCI:	Schmidt, U., Karlsruhe
SIR:	Schirmer, J., Willisau
VLM:	Vollmann, W., Wien
WLH:	Wollenhaupt, G., Oberwiesenthal
WN:	Wischnewski, M., Springe
WTR:	Walter, F., München
WU:	Wunder, E., Edingen

Remarks:

n	number of measurements
:	uncertain
s	secondary minimum
(1)	normal maximum
(2)	normal minimum
(3)	maximum determination as described in 1999AJ....118.2442W (Wade et. Al.)
(4)	double maximum: time of the second maximum
(5)	telescope Celestron 8
(6)	telescope Celestron 14
	Photometer
(11)	CCD camera ST-6: chip 375*242 uncoated
(12)	CCD camera ST-7
(13)	CCD camera ST-7E
(14)	CCD camera ST-10
(15)	CCD camera ST-10 XMR/XME
(16)	CCD camera ST-8 XME
(17)	CCD camera ST-9 XE
(18)	CCD camera ST-7 XE
(19)	CCD camera OES-LcCCD12
(20)	CCD camera Pictor 1616XT
(21)	CCD camera Pictor 416XT
(22)	CCD camera hisis 22
(23)	CCD camera Meade DSI Pro 2
(24)	CCD camera Sigma 402: chip KAF0402ME
(25)	CCD camera Artemis 4021
(26)	CCD camera Sigma 1603
(27)	CCD camera Moravian G2-1600
(28)	CCD camera QHY8
(29)	CCD camera Meade DSI Pro 3
(30)	CCD camera Canon EOS 450D
(31)	CCD camera MX516
(32)	CCD camera Canon EOS1000D
	Filter
o	without filter
B	B-filter
V	V-filter
R	R-filter
I	I-filter
Ic	I-filter cousins
-Ir	IR cut-off filter
-U-I	U and IR cut-off filter

References:

Lichtenknecker Database of the BAV `http://www.bav-astro.de/LkDB/index.php?lang=en&sprache_dial=de`
BAV Services for Scientists, 2013, `http://www.bav-astro.de/sfs/index.php?sprache=en&sprache_dial=de`
Achterberg, H., 2003, *BAV Rb.*, **52**, 93. ⟨53⟩

Agerer, F. et al., 1988, *IBVS*, No. 3234 (*BAV Mitt.*, **51**) ⟨62⟩
Agerer, F. Splittgerber, E., 1993, *IBVS*, No. 3942 (*BAV Mitt.*, **67**) ⟨64⟩
Agerer, F. et al., 1994, *BAV Mitt.*, **69**, http://www.bav-astro.de/sfs/mitteilungen/BAVM069.pdf ⟨44⟩
Agerer, F., 1999, *IBVS*, No. 4778 (*BAV Mitt.*, **123**) ⟨67⟩
Agerer, F., Hübscher, J., 2001, *IBVS*, No. 5016 (*BAV Mitt.*, **132**) ⟨71⟩
Agerer, F., Berthold, T., 2006, *IBVS*, No. 5700, Obj. 80 ⟨75⟩
Agerer, F., Quester, W., 2008, *BAV Rb.*, **57**, 232. ⟨54⟩
Agerer, F., 2010, *PZP*, **10**, 4. ⟨77⟩
Baldwin, M.E., 2000, *IBVS*, No. 4911 ⟨69⟩
Bernhard, K. Frank, P., 2006, *IBVS*, No. 5719 (*BAV Mitt.*, **177**) ⟨76⟩
Berthold, T., Busch, H., 1998, *BAV Rb.*, **47**, 33, http://www.bavdata-astro.de/rb/RB1998-2/seite33.html ⟨47⟩
Dahm, M., Kleikamp, W., 1998, *BAV Rb.*, **47**, 67, http://www.bavdata-astro.de/rb/RB1998-3/seite67.html ⟨48⟩
Dahm, M., Kleikamp, W., 1999, *BAV Rb.*, **48**, 189, http://www.bavdata-astro.de/rb/RB1999-4/seite189.html ⟨49⟩
Dahm, M., 2000, *BAV Rb.*, **49**, 41, http://www.bavdata-astro.de/rb/RB2000-2/seite41.html ⟨50⟩
Dahm, M., Paschke, A., 2000, *BAV Rb.*, **49**, 105, http://www.bavdata-astro.de/rb/RB2000-3/seite105.html ⟨51⟩
Dallaportas, S., et. al., 2000, *IBVS*, No. 4990 ⟨70⟩
Frank, P. et al., 1996, *IBVS*, No. 4386 (*BAV Mitt.*, **88**) ⟨66⟩
Hübscher, J., et al., 1992, *IBVS*, No. 3811 (*BAV Mitt.*, **63**) ⟨63⟩
Hübscher, J., et al., 1994, *BAV Mitt.*, **68**, http://www.bav-astro.de/sfs/mitteilungen/BAVM068.pdf ⟨43⟩
Huisong, T., 1984, *IBVS*, No. 2533 ⟨60⟩
Husar, D., 2003, *BAV Rb.*, **52**, 1. ⟨52⟩
Kaiser, D. H., et. al., 2002, *IBVS*, No. 5347 ⟨73⟩
Kreiner, J. M., 2004, *Acta Astr.*, **54**, 207. ⟨42⟩
Le Borgne, J. F., et. al., 2007, *Astron. Astrophys.*, **476**, 307. ⟨41⟩
Lichtenknecker, D., 1986, *BAV Rb.*, **35**, 41, http://www.bavdata-astro.de/rb/RB1986-2/seite41.html ⟨45⟩
Lloyd, C. et al., 1999, *IBVS*, No. 4797 (*BAV Mitt.*, **125**) ⟨68⟩
Maintz, G., 2010, *BAV Rb.*, **59**, 170. ⟨55⟩
Maintz, G., 2011, *BAV Rb.*, **60**, 164. ⟨56⟩
Maintz, G., 2012, *BAV Rb.*, **61**, 83. ⟨57⟩
Otero, S. A., 2003, *IBVS*, No. 5480 ⟨74⟩
Quester, W., Bernhard, K., 2001, *IBVS*, No. 5161 (*BAV Mitt.*, **138**) ⟨72⟩
Roizman, G. S., et. al., 1995, *IBVS*, No. 4267 ⟨65⟩
Rossiger, S., 1986, *IBVS*, No. 2855 ⟨61⟩
Samus, N .N., et. al., 2011, http://www.sai.msu.su/gcvs/gcvs/index.htm ⟨59⟩
Wunder, E., 1987, *BAV Rb.*, **36**, 157, http://www.bavdata-astro.de/rb/RB1987-4/seite157.html ⟨46⟩
Wunder, E., 2012, *BAV Rb.*, **61**, 93. ⟨58⟩

ERRATUM FOR IBVS 4472 (BAVM 99)

TY UMa	50192.5267 FR	has to be deleted
TY UMa	50193.5905 FR	has to be deleted
TY UMa	50194.4775 FR	has to be deleted
TY UMa	50195.3645 FR	has to be deleted
TY UMa	50195.5409 FR	has to be deleted

ERRATUM FOR IBVS 5643 (BAVM 172)

SY CMi	52285.538 PS	has to be deleted

ERRATUM FOR IBVS 5959 (BAVM 214)

GW Boo	55310.4066 AG	has to be deleted
	55310.5829 AG	has to be deleted

ERRATUM FOR IBVS 6010 (BAVM 220)

DI Leo	55672.3859 MZ	has to be deleted
BQ Lyr	55739.4639 MZ	has to be deleted
GSC 01330-00239	54910.3597 ATB	has to be deleted

COMMISSIONS 27 AND 42 OF THE IAU
INFORMATION BULLETIN ON VARIABLE STARS

Number 6049

Konkoly Observatory
Budapest
28 February 2013

HU ISSN 0374 – 0676

PHOTOMETRY OF HIGH-AMPLITUDE DELTA SCUTI STARS IN 2012

WILS, PATRICK[1]; AYIOMAMITIS, ANTHONY[2,3]; VANLEENHOVE, MAARTEN[1]; HAMBSCH, FRANZ-JOSEF[1,4]; PANAGIOTOPOULOS, KOSTAS[2,5]; LAMPENS, PATRICIA[6]; VAN CAUTEREN, PAUL[1,6]; VAN WASSENHOVE, JEROEN[1]; VAN DE STADT, INGE[7]; STAELS, BART[1,8]; HAUTECLER, HUBERT[1]; ROBERTSON, C.W.[9]; BAILLIEN, ANTOINE[1]; PICKARD, ROGER D.[10]; CARREÑO GARCERÁN, ALFONSO[11]; NIEUWENHOUT, FRANS[7]; WOLLENHAUPT, GUIDO[4]

[1] Vereniging Voor Sterrenkunde, Belgium; e-mail: patrickwils@yahoo.com

[2] Helliniki Astronomiki Enosi, Greece

[3] Perseus Observatory, Athens, Greece

[4] Bundesdeutsche Arbeitsgemeinschaft für Veränderliche Sterne e.V. Germany

[5] Pouda Observatory, Diakopto, Greece

[6] Koninklijke Sterrenwacht van België (ROB), Brussel, Belgium

[7] Werkgroep Veranderlijke Sterren, The Netherlands

[8] Center for Backyard Astrophysics Flanders

[9] SETEC Observatory, Goddard, Kansas, USA

[10] British Astronomical Association, UK

[11] Zonalunar Observatory, València, Spain

This paper is the fifth in a series reporting on photometry of High-Amplitude Delta Scuti (HADS) Stars (see Wils et al., 2012 for references to the earlier papers). This report presents details on 385 times of maximum for 79 HADS, obtained during 2012. A description of the method used to calculate the times of maximum is given in the first paper of the series (Wils et al., 2009).

The code used for the observers and the instruments are given in Table 1. In Table 2 we list the star name (Col. 1), the epoch (Col. 2), the uncertainty of the epoch (Col. 3), the observer's code (Col. 4) and the filter used (Col. 5). When a maxima was observed in more than one filter by the same observer, the table shows the average value of the times obtained in each filter individually (note that there may be a significant delay between the maximum times when observed in different filters).

For some stars the times of maximum were deviating considerably from their ephemeris, mostly because of insufficient precision in the original determination of the period. For these stars new elements are given in Table 3. To obtain the highest possible precision, data from the ASAS (Pojmański, 2002), NSVS (Woźniak et al., 2004) and SuperWASP surveys (Butters et al., 2010) were used in conjunction with our own data.

Two stars observed by FJH, GSC 8740-0359 (= ASAS J172915-5939.9) and GSC 9049-0905 (= ASAS J162330-6720.7) were found to be multiperiodic pulsators. Details about the independent frequencies f_0, probably the fundamental radial mode, and f_1, likely a non-radial mode, are given in Table 4. The frequencies, amplitudes and phases, and their

Table 1: List of instruments used for the observations.

Code	Observer(s)	Telescope	Observatory	CCD
AA	AA	Refractor 16 cm	Perseus Observatory	SBIG ST-10XME
AA30	AA	Refractor 30 cm	Perseus Observatory	SBIG ST-10XME
AB	AB	Refractor 10 cm	Carpe Noctem Observatory	SBIG ST-9E
ABC	AB	Catadioptric 35 cm	Carpe Noctem Observatory	SBIG ST-9E
AC	AC	Refractor 10 cm	Zonalunar Observatory	ATIK 383L+
FN	FN	Catadioptric 40 cm	Alkmaar, Nederland	SBIG ST-7XME
GW	GW	Newton 20 cm	Farm Tivoli, Namibia	SBIG ST-7
HH11	HH	Catadioptric 28 cm	Roosbeek Lake Observatory	SBIG ST7ME
HH8	HH	Catadioptric 20 cm	Roosbeek Lake Observatory	SBIG ST-7
HMB4	FJH	Catadioptric 35 cm	Mol, Belgium	SBIG ST-8
HMBC	FJH	Catadioptric 28 cm	Mol, Belgium	SBIG ST-10XME
HMBK	FJH	Catadioptric 28 cm	Astrokolkhoz, New Mexico	SBIG ST-8
HMBN	FJH	Catadioptric 28 cm	Farm Hakos, Namibia	SBIG ST-8XME
HO18	PL+PVC	Refractor 18 cm	R.O.B.-Humain	SBIG ST-10XME, STL6303
HO40	PL+PVC	Newton 40 cm	R.O.B.-Humain	SBIG ST-10XME
IS	IS	Catadioptric 25 cm	ABT Metius	SBIG ST402XME
KP	KP	Modified Cassegrain 26 cm	Pouda Observatory	SBIG ST-10XME
MAV	MV	Maksutov 26 cm	Leest Observatory	SBIG ST-10XME
MAVN	MV	Newton 35 cm	Leest Observatory	QSI583 WSG
RP	RDP	Catadioptric 36 cm	Shobdon, UK	Starlight XPress SXV-H9
SBL	BS	Cassegrain 28 + 23.5 cm	Alan Guth Observatory	Starlight XPress MX-716
SO30	CWR	Catadioptric 30 cm	SETEC Observatory	SBIG ST-8XME
SO40	CWR	Catadioptric 40 cm	SETEC Observatory	SBIG ST-8XME
VWS	JVW	Refractor 15.2 cm	Hooglede, Belgium	SBIG ST-7XME

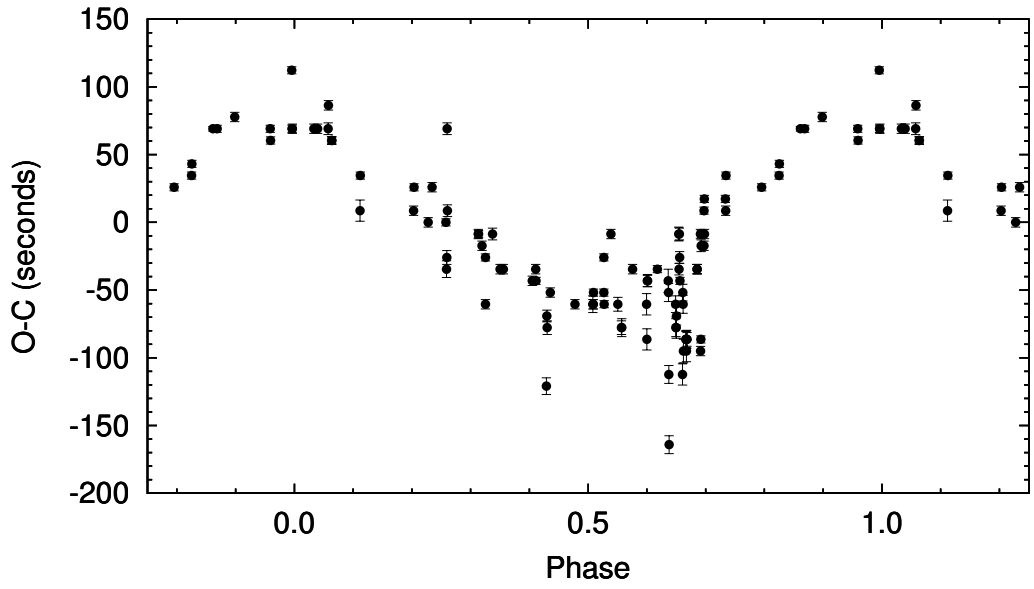

Figure 1. Phase plot of the $O-C$ values of GSC 4556-1113 with respect to a binary orbit with a period of 164 days (phase zero corresponds to JD 2455572).

uncertainties were determined using Period04 (Lenz & Breger, 2005). The uncertainties were derived using Monte Carlo simulations. A number of linear combinations of the independent frequencies could be detected as well in both stars. The data for GSC 8740-0359 and GSC 9049-0905 are available from the IBVS website. GSC 3043-0463 was also found to be a multiperiodic variable, but there are not enough data to accurately determine additional frequencies at this moment.

The cyclical period change of GSC 4556-1113 first reported in Wils et al. (2012) is confirmed, with two more binary cycles observed. A plot of the $O - C$ data calculated from a linear ephemeris and phased with the probable binary period of 164 ± 3 days is given in Fig. 1. There are no indications at this moment that the orbit deviates from a circle.

Acknowledgements:
This work has made use of the SIMBAD database, operated at CDS, Strasbourg, France. PL acknowledges support from the Royal Observatory of Belgium (ROB) for operating a small optical telescope at the radio-astronomy station of Humain under the project HOACS (HOACS stands for the Humain Optical Observatory for Astrophysics of Coeval Stars). The HOACS data were also acquired thanks to equipment financed by the Belgian National Lottery (1999). PVC is grateful for support from Astrotechniek and Baader Planetarium. Part of the equipment used at SETEC Observatory was purchased with a grant from the American Astronomical Society. FN is grateful to the University of Amsterdam for providing a CCD camera with filter wheel.

References:

Butters O.W., West R.G., Anderson D.R., et al., 2010, *A&A* **520**, L10
Lenz P., Breger M., 2005, *Comm. in Asteroseismology* **146**, 53
Pojmański G., 2002, *Acta Astron.* **52**, 397
Wils P., Kleidis S., Hambsch F.-J., Vidal-Sáinz J., Vanleenhove M., Lampens P., Van Cauteren P., Robertson C.W., Staels B., Pickard R.D., Rozakis I., Dufoer S., Groenendaels R., Gómez-Forrellad J.M., García-Melendo E., Hautecler H., Van der Looy J., 2009, *IBVS* **5878**
Wils P., Panagiotopoulos K., Van Wassenhove J., Ayiomamitis A., Nieuwenhout F., Robertson C.W., Vanleenhove M., Hambsch F.-J., Hautecler H., Pickard R.D., Baillien A., Staels B., Kleidis S., Lampens P., Van Cauteren P., 2012, *IBVS* **6015**
Woźniak P.R., Vestrand W.T., Akerlof C.W., et al., 2004, *AJ* **127**, 2436

Table 2: Observed times of maximum (Epoch = HJD − 2400000).

Star	Epoch	Unc.	Obs.	Filter	Star	Epoch	Unc.	Obs.	Filter
GP And	55940.2845	0.0030	RP	V	LW Dra	55968.6079	0.0009	IS	V
	55940.3638	0.0010	RP	V		55968.7264	0.0007	IS	V
	55942.2505	0.0001	HH8	C		56010.5525	0.0011	IS	V
	56176.4112	0.0007	HO40	V		56012.5602	0.0009	IS	V
	56241.2453	0.0002	KP	BV		56100.3492	0.0008	AA30	C
	56241.3240	0.0003	KP	BV		56100.4673	0.0005	AA30	C
	56241.4026	0.0002	KP	BV	DY Her	56117.3341	0.0011	AA30	C
	56241.4814	0.0003	KP	BV	V1086 Her	56108.3661	0.0013	AA30	C
	56241.5600	0.0004	KP	BV		56108.4964	0.0008	AA30	C
	56263.1978	0.0003	AA	C	V1116 Her	56081.4256	0.0007	AA30	C
	56263.2764	0.0003	AA	C	KZ Lac	56132.4682	0.0018	MAV	V
	56263.3550	0.0003	AA	C		56174.4433	0.0015	HO40	C
V460 And	56176.5845	0.0004	RP	V		56197.3096	0.0011	AA	C
	56176.6597	0.0007	RP	V		56197.4148	0.0010	AA	C
	56254.2645	0.0010	ABC	C		56197.5197	0.0013	AA	C
V524 And	56131.4553	0.0006	MAVN	V	SZ Lyn	56001.3182	0.0004	HH8	C
	56131.5491	0.0015	MAVN	V	V593 Lyr	56073.3973	0.0005	MAV	C
	56202.2294	0.0008	AA	C		56073.4998	0.0005	MAV	C
	56202.3236	0.0006	AA	C	V1162 Ori	55942.3267	0.0030	HO18	V
	56202.4180	0.0005	AA	C		55942.4066	0.0017	HO18	V
	56202.5127	0.0006	AA	C		55942.4854	0.0033	HO18	V
V544 And	56228.3511	0.0007	MAV	V		55943.3507	0.0027	HO18	V
	56235.3026	0.0014	ABC	C		55943.4276	0.0024	HO18	V
CY Aqr	56134.4084	0.0005	MAV	V		55944.3715	0.0021	HO18	V
	56134.4694	0.0003	MAV	V		55944.4519	0.0032	HO18	V
	56168.5285	0.0003	IS	V		55958.3796	0.0028	HO18	V
	56168.5896	0.0004	IS	V	DY Peg	56133.4374	0.0008	MAVN	V
	56233.3507	0.0007	ABC	C		56175.5164	0.0003	RP	V
YZ Boo	56033.4210	0.0006	SBL	V		56175.5891	0.0007	RP	V
	56033.5250	0.0005	SBL	V		56198.2694	0.0003	AA	C
	56033.6290	0.0007	SBL	V		56198.3420	0.0004	AA	C
	56034.4624	0.0006	HMB4	V		56198.4153	0.0004	AA	C
	56034.5659	0.0009	HMB4	V		56198.4880	0.0004	AA	C
	56074.4331	0.0005	SBL	V		56223.3549	0.0007	SBL	V
	56074.5372	0.0007	SBL	V		56223.4277	0.0006	SBL	V
V336 Boo	56090.3333	0.0005	AA30	C		56223.5011	0.0006	SBL	V
	56090.4461	0.0003	AA30	C		56266.3809	0.0003	AC	C
V367 Cam	55967.3883	0.0024	FN	V		56266.4536	0.0005	AC	C
V376 Cam	55943.4782	0.0007	IS	V	DW Psc	56179.5212	0.0002	HO40	C
	55943.6184	0.0007	IS	V		56179.5813	0.0002	HO40	C
	55943.7589	0.0004	IS	V		56180.4763	0.0002	HO40	C
	55968.3155	0.0005	VWS	V		56180.5355	0.0002	HO40	C
	55968.4558	0.0002	VWS	V		56222.3496	0.0004	HO40	C
AD CMi	55968.4618	0.0009	FN	V		56223.3036	0.0006	HO40	C
V1040 Cas	56179.3031	0.0012	AA	C		56223.3632	0.0004	HO40	C
	56179.3763	0.0009	AA	C		56223.4235	0.0004	HO40	C
	56179.4498	0.0008	AA	C		56245.1949	0.0004	AA	C
	56179.5229	0.0006	AA	C		56245.2550	0.0004	AA	C
V792 Cep	56131.5161	0.0012	MAV	V		56245.3146	0.0002	AA	C
XX Cyg	56132.5579	0.0002	IS	V		56245.3738	0.0002	AA	C
	56236.2693	0.0002	KP	V		56245.4338	0.0003	AA	C
	56236.4041	0.0003	KP	V		56269.2924	0.0010	AC	C
	56240.3152	0.0002	KP	BV		56269.3519	0.0009	AC	C
	56240.4500	0.0001	KP	BV		56269.4119	0.0006	AC	C
V2455 Cyg	56107.3405	0.0005	AA30	B		56269.4715	0.0007	AC	C
	56107.4348	0.0005	AA30	B		56269.5307	0.0011	AC	C
	56107.5286	0.0005	AA30	B		56270.5463	0.0003	HMBK	r

Table 2: Observed times of maximum (continued).

Star	Epoch	Unc.	Obs.	Filter	Star	Epoch	Unc.	Obs.	Filter
DW Psc	56270.6053	0.0004	HMBK	r	GSC 1306-0466	55929.3910	0.0012	AB	C
	56270.6652	0.0003	HMBK	r	GSC 1442-1358	56008.2908	0.0008	KP	V
	56270.7253	0.0004	HMBK	r		56008.3729	0.0006	KP	V
V1307 Sco	56093.5035	0.0004	HMBN	V		56008.4548	0.0006	KP	V
	56093.6204	0.0004	HMBN	V		56008.5368	0.0004	KP	V
CW Ser	56074.4583	0.0024	IS	V		56008.6189	0.0010	KP	V
GW UMa	55968.3014	0.0009	MAV	C	GSC 1594-2234	56077.4436	0.0014	MAVN	V
	55991.4664	0.0018	RP	V	GSC 1716-1598	56208.2505	0.0008	AA	C
	56001.4223	0.0006	MAV	C		56208.3496	0.0009	AA	C
	56005.2831	0.0006	KP	V		56208.4478	0.0009	AA	C
	56005.4860	0.0007	KP	V	GSC 1750-1237	56199.2812	0.0009	AA	C
	56010.3633	0.0008	KP	V		56199.3678	0.0007	AA	C
	56010.5660	0.0008	KP	V		56199.4547	0.0007	AA	C
	56040.6387	0.0006	SO30	V		56199.5416	0.0007	AA	C
	56041.6549	0.0006	SO30	V	GSC 2080-0986	56077.4385	0.0008	MAV	V
	56041.8589	0.0010	SO30	V		56077.5381	0.0009	MAV	V
	56052.8300	0.0011	SO30	V		56089.3425	0.0006	AA30	C
YZ UMi	55958.4266	0.0005	VWS	V		56089.4414	0.0004	AA30	C
	55959.2956	0.0008	VWS	V	GSC 2108-1564	56076.4677	0.0016	MAVN	V
	56002.3849	0.0004	VWS	V		56088.3411	0.0009	AA30	C
	56015.3304	0.0005	VWS	V		56088.4384	0.0005	AA30	C
	56047.5015	0.0010	HMBC	V	GSC 2290-1195	56206.2250	0.0015	AA	C
	56092.3302	0.0005	AA30	C		56206.3056	0.0019	AA	C
	56092.4265	0.0004	AA30	C		56206.3839	0.0014	AA	C
	56158.5086	0.0005	VWS	V		56206.4597	0.0013	AA	C
GSC 0191-1282	55943.3531	0.0004	HH8	C		56206.5377	0.0014	AA	C
	55943.4002	0.0002	HH8	C		56229.3140	0.0026	ABC	C
	56010.3062	0.0006	HH8	C	GSC 2566-1398	56019.3238	0.0006	SBL	V
	56010.3534	0.0007	HH8	C		56019.4134	0.0005	SBL	V
	56012.3450	0.0003	HH8	C		56019.5040	0.0011	SBL	V
	56014.3355	0.0005	HO18	V		56019.5957	0.0009	SBL	V
	56015.3325	0.0004	HH8	C	GSC 2696-1396	56105.3342	0.0020	AA30	C
	56015.3800	0.0004	HH8	C		56105.4369	0.0005	AA30	C
	56015.4274	0.0005	HH8	C		56254.2788	0.0006	HH11	C
GSC 0321-0314	56009.4265	0.0011	HO18	V	GSC 2843-1999	55967.3751	0.0019	IS	V
	56009.5042	0.0005	HO18	V		55967.4369	0.0021	IS	V
GSC 0429-2098	56076.4702	0.0017	MAV	C		56243.3216	0.0010	AB	C
GSC 0513-0624	56172.3269	0.0005	AA	C	GSC 2861-0970	55944.3783	0.0003	FN	V
	56172.3992	0.0004	AA	C		56211.2730	0.0010	MAV	V
GSC 0612-0771	55943.3064	0.0014	AB	C		56211.3836	0.0005	MAV	V
	55943.3661	0.0013	AB	C		56211.4936	0.0005	MAV	V
	55943.4315	0.0010	AB	C		56257.2985	0.0019	ABC	C
	56200.2794	0.0009	AA	C	GSC 2977-0238	55941.4762	0.0005	HO18	V
	56200.3416	0.0007	AA	C		55942.5388	0.0028	RP	V
	56200.4047	0.0007	AA	C		56002.3746	0.0002	HH8	C
	56200.4671	0.0004	AA	C		56003.3618	0.0005	KP	BV
	56200.5296	0.0004	AA	C		56003.4376	0.0007	KP	BV
GSC 0753-1489	55958.4130	0.0033	AB	C		56003.5135	0.0008	KP	BV
GSC 0933-0651	56074.4930	0.0009	FN	V		56228.5047	0.0005	MAV	V
GSC 1076-0158	56145.2935	0.0007	AA30	C		56228.5805	0.0005	MAV	V
	56145.3805	0.0006	AA30	C	GSC 3031-0307	56008.4150	0.0012	MAV	C
	56145.4676	0.0005	AA30	C	GSC 3043-0463	56014.4659	0.0029	HO18	V
GSC 1158-0921	56133.4262	0.0006	MAV	V		56015.5055	0.0020	HO18	V
	56133.4908	0.0006	MAV	V	GSC 3074-0114	56077.5105	0.0004	IS	V
	56133.5554	0.0006	MAV	V		56077.5617	0.0004	IS	V
	56223.3858	0.0004	ABC	C	GSC 3428-1497	55943.3385	0.0007	MAV	V
GSC 1220-1131	55943.2519	0.0012	HH8	C		55943.4139	0.0008	MAV	V

Table 2: Observed times of maximum (continued).

Star	Epoch	Unc.	Obs.	Filter	Star	Epoch	Unc.	Obs.	Filter
GSC 3428-1497	55943.4884	0.0006	MAV	V	GSC 4464-0924	56144.2903	0.0008	AA30	C
	56002.2401	0.0003	KP	BV		56144.3693	0.0010	AA30	C
	56002.3156	0.0001	KP	BV		56144.4516	0.0006	AA30	C
	56002.3895	0.0001	KP	BV		56144.5305	0.0008	AA30	C
	56002.4649	0.0003	KP	BV	GSC 4500-0083	56110.4734	0.0017	MAV	V
	56002.5390	0.0001	KP	BV		56110.5602	0.0016	MAV	V
	56002.6135	0.0002	KP	BV		56134.4619	0.0012	MAVN	V
GSC 3489-0868	56075.4428	0.0008	FN	V		56134.5487	0.0014	MAVN	V
	56075.5293	0.0009	FN	V		56135.3980	0.0019	MAVN	V
GSC 3755-0845	55930.2353	0.0011	AA	C		56135.4824	0.0023	MAVN	V
	55930.3108	0.0005	AA	C		56146.2889	0.0017	AA30	C
	55942.2583	0.0011	SBL	V		56146.3731	0.0020	AA30	C
	55942.3342	0.0017	SBL	V		56146.4587	0.0017	AA30	C
	55942.4106	0.0017	SBL	V		56146.5427	0.0014	AA30	C
	55942.4860	0.0016	SBL	V		56223.3583	0.0016	MAV	V
	55942.5623	0.0010	SBL	V		56224.2954	0.0010	HO40	C
	56003.3646	0.0009	HH8	C	GSC 4552-1498	55941.4134	0.0004	MAV	C
	56223.5166	0.0007	MAV	V		55941.4694	0.0003	MAV	C
	56223.5924	0.0004	MAV	V		55941.5249	0.0004	MAV	C
GSC 3810-1553	56009.3647	0.0004	HO18	V		55962.2868	0.0004	MAV	C
	56013.3954	0.0008	RP	V		55962.3425	0.0006	MAV	C
	56245.4709	0.0004	AA	C		55962.3984	0.0005	MAV	C
	56245.5415	0.0004	AA	C		56001.2993	0.0003	KP	V
	56245.6121	0.0002	AA	C		56001.3546	0.0003	KP	V
GSC 3832-0152	55961.4652	0.0009	RP	V		56001.4108	0.0004	KP	V
	55964.2963	0.0004	MAV	C		56001.4665	0.0004	KP	V
	55964.3870	0.0004	MAV	C		56001.5222	0.0004	KP	V
	55964.4787	0.0004	MAV	C		56001.5783	0.0003	KP	V
	56006.3130	0.0006	MAV	C		56001.6338	0.0004	KP	V
	56006.3130	0.0004	KP	V		56002.3033	0.0003	MAV	C
	56006.4042	0.0005	MAV	C		56002.3588	0.0004	MAV	C
	56006.4042	0.0003	KP	V		56002.4150	0.0004	MAV	C
	56006.4955	0.0004	KP	V		56064.4772	0.0005	IS	V
	56006.5869	0.0004	KP	V		56064.5328	0.0005	IS	V
	56040.6578	0.0003	SO40	V		56075.5281	0.0004	IS	V
	56040.7491	0.0004	SO40	V		56075.5831	0.0005	IS	V
	56040.8406	0.0005	SO40	V	GSC 4556-1113	55942.2919	0.0003	VWS	V
	56040.9314	0.0004	SO40	V		55942.4641	0.0007	IS	V
	56041.6623	0.0003	SO40	V		55942.5506	0.0006	IS	V
	56041.7538	0.0003	SO40	V		55942.6380	0.0005	IS	V
	56041.8451	0.0004	SO40	V		55942.7237	0.0005	IS	V
	56041.9365	0.0004	SO40	V		55953.3435	0.0003	VWS	V
	56052.6234	0.0005	SO40	V		55958.3504	0.0003	VWS	V
	56052.7147	0.0004	SO40	V		55966.3811	0.0004	VWS	V
	56082.3098	0.0004	AA30	C		55983.3904	0.0004	VWS	V
	56082.4009	0.0004	AA30	C		55983.4769	0.0003	VWS	V
GSC 3863-0740	55994.4789	0.0014	RP	V		56001.3501	0.0003	VWS	V
GSC 3934-1904	56013.6154	0.0006	IS	V		56007.3080	0.0006	KP	V
	56014.5987	0.0007	IS	V		56007.3941	0.0005	KP	V
	56101.3577	0.0008	AA30	C		56007.4807	0.0005	KP	V
	56101.4666	0.0007	AA30	C		56007.5669	0.0005	KP	V
	56168.4482	0.0013	IS	I		56007.6530	0.0003	KP	V
	56180.3585	0.0007	IS	V		56008.3442	0.0004	VWS	V
	56180.4682	0.0008	IS	V		56013.3521	0.0004	VWS	V
GSC 3986-1266	56174.2778	0.0022	AA	C		56074.3974	0.0003	VWS	V
	56174.4243	0.0023	AA	C		56074.4837	0.0003	VWS	V
GSC 4464-0924	56034.3902	0.0010	VWS	V		56131.3827	0.0004	VWS	V

Table 2: Observed times of maximum (continued).

Star	Epoch	Unc.	Obs.	Filter	Star	Epoch	Unc.	Obs.	Filter
GSC 4556-1113	56131.4689	0.0003	VWS	V	GSC 7737-0184	56097.2476	0.0006	HMBN	V
	56150.3782	0.0003	VWS	V		56097.3502	0.0005	HMBN	V
	56150.4642	0.0003	VWS	V	GSC 8459-0201	56089.5293	0.0008	HMBN	V
	56158.4080	0.0004	VWS	V		56089.6403	0.0006	HMBN	V
	56178.3538	0.0003	VWS	V		56156.3815	0.0005	GW	V
	56178.4402	0.0003	VWS	V		56156.4928	0.0004	GW	V
	56211.3376	0.0004	VWS	V	GSC 8729-0957	56096.5257	0.0004	HMBN	V
	56246.3924	0.0003	VWS	V		56096.6394	0.0005	HMBN	V
GSC 4923-0693	56004.2822	0.0009	KP	V	GSC 8814-0245	56092.4559	0.0006	HMBN	V
	56004.3487	0.0006	KP	V		56092.5477	0.0009	HMBN	V
	56004.4153	0.0004	KP	V	GSC 9238-0506	56096.2389	0.0012	HMBN	V
	56004.4820	0.0005	KP	V		56096.3609	0.0009	HMBN	V
	56004.5485	0.0004	KP	V	NSVS 11672463	56178.2632	0.0006	AA	C
	56004.6146	0.0006	KP	V		56178.3703	0.0007	AA	C
GSC 5752-1767	56091.4728	0.0005	HMBN	V		56178.4783	0.0005	AA	C
GSC 6640-0450	56095.3277	0.0004	HMBN	V		56179.3404	0.0006	HO40	C
GSC 7269-0239	56100.2988	0.0007	HMBN	V		56179.4478	0.0004	HO40	C
	56100.4118	0.0007	HMBN	V		56180.4176	0.0008	HO40	C
GSC 7438-1045	56100.5015	0.0003	HMBN	V	NSVS 14243430	56115.3235	0.0008	AA30	C
	56100.5649	0.0003	HMBN	V		56115.4100	0.0005	AA30	C
	56100.6281	0.0002	HMBN	V		56115.4956	0.0004	AA30	C
GSC 7519-0109	56091.6819	0.0005	HMBN	V					

Table 3: Updated elements of known HADS. Uncertainties are given in units of the last decimal.

Star	Max (HJD)	Period (d)
V792 Cep	2455839.3456(3)	0.13341129(6)
V1086 Her	2452451.0716(2)	0.13059901(2)
V593 Lyr	2452084.4969(2)	0.102151174(5)
GSC 0191-1282	2452396.5461(9)	0.047418463(13)
GSC 0612-0771	2451921.7513(5)	0.062783796(8)
GSC 4500-0083	2455108.9778(5)	0.08506724(6)
GSC 8459-0201	2451869.7022(4)	0.111420450(15)

Table 4: Independent frequencies detected in two multiperiodic HADS observed with a V filter. Uncertainties are given in units of the last decimal. The phase is given with respect to HJD = 0.

Star		Frequency c/d	Semi-Amplitude Mag.	Phase
GSC 8740-0359	f_0	9.69946(2)	0.187(1)	0.2636(8)
	f_1	11.4105(2)	0.0169(9)	0.849(9)
GSC 9049-0905	f_0	7.21672(2)	0.213(2)	0.323(1)
	f_1	11.1079(3)	0.019(2)	0.176(12)

COMMISSIONS 27 AND 42 OF THE IAU
INFORMATION BULLETIN ON VARIABLE STARS

Number 6050

Konkoly Observatory
Budapest
8 March 2013

HU ISSN 0374 – 0676

CCD MINIMA FOR SELECTED ECLIPSING BINARIES IN 2012

NELSON, ROBERT H.

1393 Garvin Street, Prince George, BC, Canada, V2M 3Z1, e-mail: bob.nelson@shaw.ca

Observatory and telescope:
Sylvester Robotic Observatory (SyRO): 33 cm f/4.5 Newtonian on a Paramount ME

Detector:	Wright CCD camera, Peltier cooling, EEV ZYa7 chip, $5' \times 7'$ FOV, 758×1061 pixels.

Method of data reduction:
Bias and dark subtraction, flat-fielding using light-box flats; aperture photometry– all using MIRA, by Mirametrics. Check stars were used throughout.

Method of minimum determination:
Digital tracing paper method, bisection of chords, curve fitting, and (occasionally) Kwee and van Woerden (1956)

Times of minima:					
Star name	Time of min. HJD 2400000+	Error	Type	Filter	Rem.
BX And	56206.7650	0.0001	I	R	
LO And	56114.8274	0.0002	I	VRI	
LO And	56117.8716	0.0005	I	VRI	
LO And	56118.8233	0.0002	II	VRI	
BO Ari	56167.946	0.002	II	VRI	
V0599 Aur	56221.8936	0.0003	I	c	
V0644 Aur	56266.7145	0.0005	I	c	
AC Boo	55928.0411	0.0002	II	c	
DN Boo	56022.7913	0.0003	I	R	
GR Boo	55938.0573	0.0002	II	c	
GT Boo	55937.94459	0.0004	I	c	
IK Boo	55937.0004	0.0002	I	c	
CD Cam	55939.7940	0.0002	II	c	
NR Cam	55937.6349	0.0005	II	R	
OQ Cam	56205.8503	0.0001	I	R	
PQ Cam	55942.5967	0.0001	II	c	
V0447 Cam	56280.8158	0.0005	I	c	
V0517 Cam	55981.7173	0.0004	I	c	
WZ Cep	56121.8942	0.0003	I	c	
G4475-0618 Cep	56122.7914	0.0003	I	c	
G4267-0588 Cep	56210.6422	0.0002	I	R	(a)
G4267-0682 Cep	56210.6605	0.0001	I	R	
G4481-0080 Cep	56215.6783	0.0005	I	c	
TX Cnc	55944.8369	0.0002	I	c	
IR Cnc	56249.8917	0.0005	I	c	
RW Com	55932.8908	0.0002	I	c	
CC Com	55939.9368	0.0001	II	c	
LT Com	55992.8843	0.0003	I	R	
MM Com	56023.7542	0.0004	II	c	
TW CrB	56026.8778	0.0002	I	VRI	
AR CrB	55940.0777	0.0001	I	c	
BO CVn	56012.8749	0.0002	II	R	
DQ CVn	56011.6998	0.0003	I	c	
EY CVn	56015.7324	0.0004	II	c	
FV CVn	56010.8612	0.0004	I	c	
GM CVn	56014.7339	0.0003	II	R	
GN CVn	55945.9039	0.0002	I	c	
V0700 Cyg	56013.0066	0.0001	II	c	
V1187 Cyg	56011.0094	0.0005	II	c	
V1191 Cyg	56010.9962	0.0003	II	c	
V2197 Cyg	56143.7546	0.0003	I	VRI	
V2197 Cyg	56146.7823	0.0002	II	VRI	
V2197 Cyg	56149.8858	0.0002	I	VRI	
BL Dra	56119.7962	0.0004	I	R	
BX Dra	56019.8048	0.0002	II	c	
DD Dra	56058.957	0.002	I	c	
FX Dra	56017.9214	0.0003	II	R	
GZ Dra	56021.936	0.001	I	c	

Times of minima:					
Star name	Time of min. HJD 2400000+	Error	Type	Filter	Rem.
G3888-0464 Dra	56008.8950	0.0003	I	c	
G4428-1574 Dra	56017.8201	0.0001	I	c	
G3900-0615 Dra	56022.8906	0.0003	II	c	
AC Gem	55945.7102	0.0003	I	c	
V0450 Her	55946.0039	0.0001	I	c	
V0731 Her	56024.8529	0.0003	I	c	
V0829 Her	56009.9040	0.0002	II	R	
V0829 Her	56023.872	0.001	II	c	
V0857 Her	55984.886	0.004	II	c	
V1066 Her	55980.9925	0.0005	I	c	
V1073 Her	55992.9961	0.0001	I	c	
V1091 Her	56019.9692	0.0004	I	c	
V1097 Her	56024.9749	0.0002	I	c	
V1097 Her	56061.7807	0.0002	I	VRI	
V1097 Her	56072.7903	0.0015	II	VRI	
V1100 Her	56059.8007	0.0002	II	VRI	
V1100 Her	56060.8415	0.0002	II	VRI	
V1100 Her	56071.769	0.001	I	VRI	
V1100 Her	56073.8503	0.0004	I	VRI	
V1100 Her	56089.8106	0.0002	I	VRI	
G2587-1888 Her	56011.7973	0.0003	I	c	
G2587-1888 Her	56011.9532	0.0003	II	c	
G3621-0711 Lac	56122.855	0.001	I	R	
XZ Leo	55945.8032	0.0001	I	c	
AM Leo	56025.712	0.0003	I	R	
ET Leo	56013.735	0.001	II	c	
GU Leo	55984.7157	0.0001	II	c	
HI Leo	55941.9466	0.0001	I	c	
G1965-0735 Leo	56006.6928	0.0003	II	R	
XY LMi	56280.9573	0.0005	I	c	
AG LMi	55936.8803	0.0002	I	c	
FG Lyn	56275.8813	0.0005	II	R	
V1363 Ori	55944.6503	0.0002	II	c	(b)
U Peg	56209.6587	0.0001	I	R	
BN Peg	56124.8728	0.0001	I	R	
BN Peg	56128.7993	0.0005	II	VRI	
V0404 Peg	56120.8570	0.0002	II	R	
G1684-0522 Peg	56207.6524	0.0003	II	c	
RZ Tau	55938.6772	0.0001	II	R	
CU Tau	56207.8158	0.0007	II	VRI	
CU Tau	56209.879	0.001	II	VRI	
CU Tau	56210.9095	0.0005	I	VRI	
V0781 Tau	56217.8548	0.0005	I	c	
ES UMa	56012.7443	0.0003	II	R	
KM UMa	56010.7147	0.0003	I	c	
MQ UMa	55937.8357	0.0004	I	c	
MS UMa	55938.885	0.001	II	c	
QT UMa	55932.8144	0.0002	II	c	

Times of minima:					
Star name	Time of min. HJD 2400000+	Error	Type	Filter	Rem.
RU UMi	55927.8576	0.0001	I	c	
WW UMi	56275.9918	0.0005	II	c	
AZ Vir	56021.7800	0.0003	I	c	
PS Vir	56026.7135	0.0002	II	c	
PY Vir	56024.775	0.002	I	c	
G2157-0387 Vul	56121.8229	0.0005	I	c	

Explanation of the remarks in the table:
Star name G denotes GSC (a) New variable - field of G4267-0682 P = 2.632979 days (b) New period: P = 0.6629525 days

Acknowledgements:
Thanks are due to Environment Canada for the website satellite views (see reference below) that were essential in predicting clear times for observing runs in this cloudy locale. Thanks are also due to Attilla Danko for his Clear Sky Charts, (see below). This research has made use of the SIMBAD database, operated at CDS, Strasbourg, France

References:

Danko, A., Clear Sky Charts, `http://cleardarksky.com/`
Kwee, K.K., & van Woerden, H., 1956, B.A.N. 12, (464), 327-330
Satellite Images for North America, `http://www.weatheroffice.gc.ca/`

ERRATUM FOR IBVS 6050

The detector given in the article is incorrect. It should be

Detector:	SBIG ST-10XME, 6.″8 pixels, 34.′4 × 23.′2 FOV, $-10 <$ T < -30°C

The Author

*This version of the paper contains corrections, and differs from the one appeared on-line originally. Date of last modification: Mar 9 20:29:50 CET 2013

COMMISSIONS 27 AND 42 OF THE IAU
INFORMATION BULLETIN ON VARIABLE STARS

Number 6051

Konkoly Observatory
Budapest
26 March 2013

HU ISSN 0374 – 0676

FIRST RESULT OF THE CZECH RR LYRAE STARS OBSERVATION PROJECT - A NEW BLAZHKO STAR CN Cam

SKARKA, M.[1]; HOŇKOVÁ, K.[2]; JURYŠEK, J.[2]

[1] Department of Theoretical Physics and Astrophysics, Faculty of Science, Masaryk University, Kotlářská 2, Brno, Czech Republic, e-mail: maska@physics.muni.cz

[2] Observatory and Planetarium of Johann Palisa, VŠB Technical University of Ostrava, 17. listopadu 15, Ostrava-Poruba, Czech Republic

We introduce a new project which attempts to provide precise, filtered measurements of RR Lyraes, which were not observed by automatic surveys (or the survey data were of bad quality), and which were not studied in detail, or are somehow interesting. The basic goal is to obtain well-covered light curves to determine ephemerides, periods, light curve characteristics (amplitude, rising time) and finally to obtain Fourier parameters to estimate the basic physical parameters.

We founded a project now called *The Czech RR Lyrae Stars Observation Project* (hereafter CRRLSOP), which cooperates with amateur observers from the Variable Star and Exoplanet Section of Czech Astronomical Society.[1] In 2012 our group comprised five members and we hope that this number will increase in years to come. A similar, but professional survey, dealing with RR Lyraes is under way in Hungary – *The Konkoly Blazhko Survey* (Sódor 2007). They use only one telescope contrary to our project that using many telescopes. Another project focused on RR Lyraes cooperating with amateurs is *GEOS RR Lyr database* (Boninsegna et al. 2002). The GEOS database deals with maxima timings of RR Lyraes.

To be able to get data of high quality, CRRLSOP focuses on bright RR Lyraes with V$<$ 12 mag at maximum light. This value is chosen to suit the telescopes that amateurs use, which are typically of the diameter between 20 and 30 cm. Another restriction is imposed by the location of the Czech Republic. We choose targets with a declination of typically more than 20°, which are easily observable for a long time during the year.

Each target is carefully selected to suit an observer's equipment and taking the observer's time constrains into account. Observers are briefed in detail about exposure times and about field of view selection. All the observations are subsequently discussed. Each star is monitored by only one observer to avoid merging data from different devices. We also put emphasis on the comparison star selection.

All the measurements gathered by observers are processed in the same way using aperture photometry software CMunipack.[2] The structure of the observations is as follows: stars which are expected to have a stable light curve are observed two nights in a row

[1] http://var2.astro.cz/EN/
[2] http://c-munipack.sourceforge.net/

followed by observations taken after one week, a few weeks and finally after a few months to verify the stability of the stellar pulsation. In the case of Blazhko stars, the objects are monitored as often as possible to cover all Blazhko phases. The time schedule of observations is not strictly given, because of weather or other unpredictable reasons.

CN Cam (= NSV 5256 = SAO1900 = BD+82 338 = GSC 04556-00251, J2000 $11^{\rm h}36^{\rm m}11\overset{\rm s}{.}8$, $+81°17'37\overset{''}{.}1$), found to be a variable by Strohmeier & Knigge (1961), was first proposed to be an eclipsing binary. Based on a 12-night study, Campos-Cucarella et al. (1996) (hereafter CC96) classified CN Cam as an RRab star and established its period as 0.6214(1) d. Kinman et al. (2007) (hereafter K07) improved the period to 0.621445(2) d and determined the amplitude of the light changes to be 0.36 mag in V and 0.49 mag in B, CC96 gives 0.350(5) mag in V and 0.474(4) mag in B. K07 also estimated the metallicity of CN Cam using Fourier coefficients, amplitude in V and rise-time (methods listed in Sandage (2004)). The values of metallicity that K07 obtained were around [Fe/H] = −1.1. K07 found the distance of CN Cam as 594 pc.

One of the most recent observations was performed by Maintz (2012). Between the years 2006 and 2012 she obtained seven maxima timings and improved the value of the period to 0.6214465(3) d. The Blazhko effect was not noted in any of these works.

We observed CN Cam in BVR_cI_c passbands during 20 nights from the end of January till the end of June 2012. We obtained between 1340 and 1630 points in each filter. Observations were carried out using the 20-cm Newtonian telescope of the Observatory and Planetarium of Johann Palisa in Ostrava equipped with an SBIG-ST8 XME camera. The data were reduced in the classic way and were transformed into the standard Johnson-Cousins magnitudes using stars in Landolt fields (Landolt 1992).

Similarly as CC96 and K07, we used GSC 04556-00278 (= SAO1899 = BD+82 337) as a comparison star and GSC 04556-00278 as a check star. According to the $J = 9.453(23)$ and $K = 9.248(22)$ magnitudes of the comparison taken from 2MASS All-Sky Catalog of Point Sources (Cutri et al. 2003) we got Johnson-Cousins magnitudes of the comparison via the relations in Warner (2007) (see Table 1). Our $V = 10.24(5)$ magnitude of the comparison fall between the magnitudes given by CC96 and K07 (10.3 and 10.201(3) mag, respectively).

Table 1. Observation log and magnitude of the comparison star in different passbands.

Nights	Time-span [d]	B	V	R_c	I_c
20	186	1341	1498	1495	1629
brightness of the comparison star [mag]		10.62(9)	10.24(5)	10.01(5)	9.77(5)

After performing the period analysis with Period04 (Lenz & Breger 2005) we found the following ephemeris:

$$\text{HJD } \mathrm{T_{max}} = 2455959.4707(36) + 0.621446(3)\mathrm{E_{puls}}. \quad (1)$$

The time of the extremum is based on the V data and it was determined using lesvephotometry software (de Ponthire 2010) by fitting the light curve with a smoothing spline function (Reinsch 1967). The value of the period is within the error bars in agreement with the period determined by Maintz (2012).

Frequency analysis with Period04 revealed additional frequency peaks on the right-hand side of the basic pulsation frequency ($f_0 = 1.6091504(73)$ c/d) and its harmonics (kf_0, where $k = 1, 2, 3...$). Such a frequency structure is one of the most noticeable

manifestations of the Blazhko effect. In total we identified peaks related to the basic pulsation frequency up to $k = 8$ and four peaks corresponding to the modulation frequency ($kf_0 + f_B$ up to $k = 4$). The spacings of the side peaks were not equidistant, but they were slightly decreasing with rising k. The side peak with the highest amplitude was $f_0 + f_B = 1.629877(61)$ c/d. Therefore we give the first rough estimation of the Blazhko period of CN Cam $P_{\rm BL} = 48.25(14)$ d.[3]

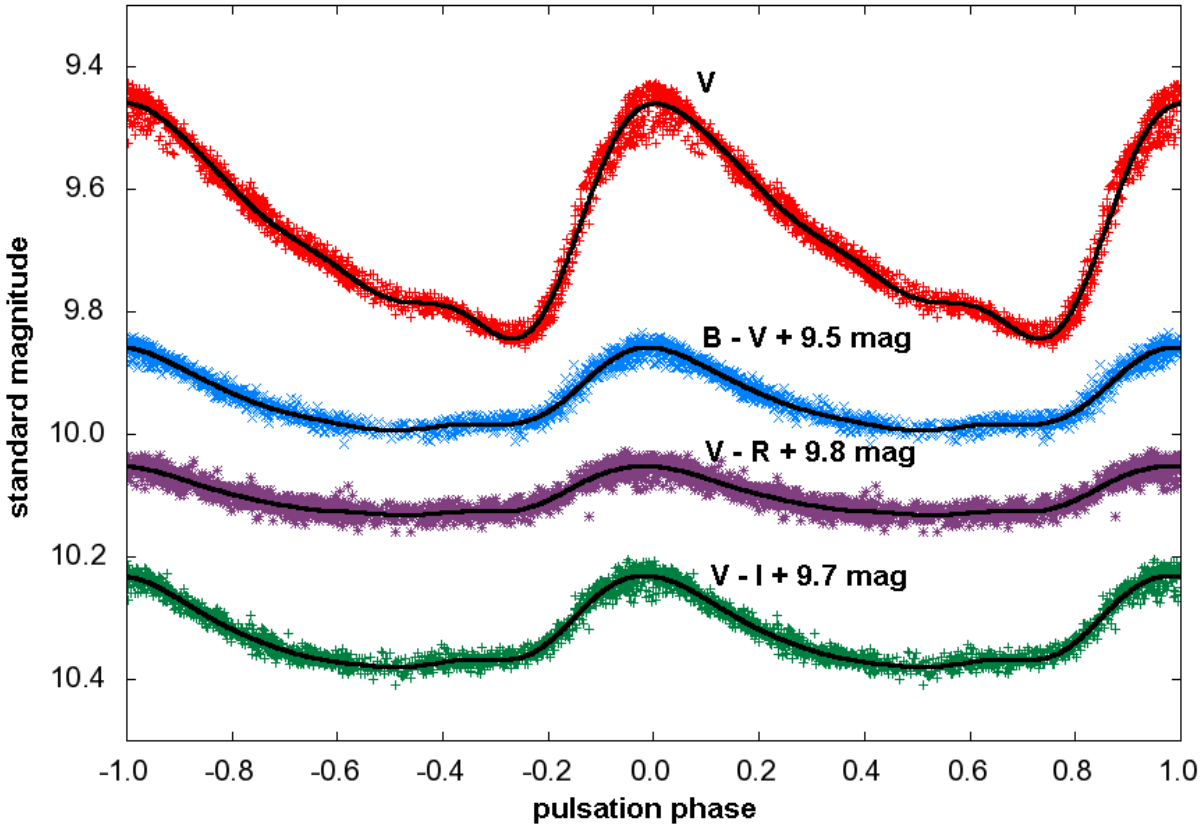

Figure 1. Calibrated data of CN Cam folded according to equation 1. The solid lines are the light curve fit with the sum of sines.

Although the coverage of the light curves was not ideal, we fitted V, $B - V$, $V - R$ and $V - I$ data with the sum of sines and we got the approximations of the mean light curves (Figure 1). The degree of the fit was chosen based on visual inspection. Analysing the mean light curves allowed us to determine Fourier coefficients based on the sine-term decomposition of the V light curve, and it also allowed us to estimate mean color indices, mean magnitudes (zero points), mean amplitudes and mean rise-time (duration from minimum to maximum in phase) during the Blazhko cycle (see Table 2). The times and the values of the extrema for rise-time and amplitude estimation were determined using LESVEPHOTOMETRY as mentioned above.

We could estimate metallicity of CN Cam using Fourier coefficients and pulsation period. Formula (3) from Jurcsik & Kovács (1996) gives $[\mathrm{Fe/H}]_{\rm JK} = -0.90$ dex. Transforming this value to the more common Zinn & West (1984) scale using the $[\mathrm{Fe/H}]_{\rm ZW} =$

[3] All values of frequencies and periods in this paragraph are based on V data analysis

$1.05[\mathrm{Fe/H}]_{\mathrm{JK}} - 0.20$ relation, adopted from Sandage (2004), we obtained $[\mathrm{Fe/H}]_{\mathrm{ZW}} = -1.15$ dex, which agrees well with the spectroscopic value [Fe/H] = −1.2 dex given in K07.

Following the analysis in K07, our parameters gave: [Fe/H] = −1.15 with Sandage's equation (3),[4] [Fe/H] = −1.05 with Sandage's relation (6) and [Fe/H] = −1.00 with Sandage's equation (7) (with rise-time 0.272). If we fix our metallicity at [Fe/H] = −1.15 dex and consider the calibration

$$M_V = 0.214[\mathrm{Fe/H}] + 0.86 \tag{2}$$

of Clementini et al. (2003) we obtain $M_V = 0.61$ mag. The distance of CN Cam is therefore 608 pc.[5]

Table 2. Characteristics of the light curves and sine-term Fourier coefficients based on the V light curve fit. N is the degree of the fit, A_0 denotes the mean magnitude. Phases ϕ_{ij} are in radians, Fourier combinations R_{ij} in mag.

	N	A_0 [mag]	max [mag]	amplitude [mag]	rise-time
B	4	10.1168(7)	9.817(3)	0.510(4)	0.268(4)
V	4	9.6751(4)	9.460(2)	0.384(3)	0.272(4)
R_c	4	9.3703(4)	9.207(2)	0.313(3)	0.272(4)
I_c	4	9.0460(3)	8.925(2)	0.253(3)	0.282(4)
$B-V$	4	0.4456(4)	0.358(2)	0.130(4)	
$V-R$	5	0.3022(3)	0.252(4)	0.079(4)	
$V-I$	5	0.6262(9)	0.531(3)	0.149(4)	
ϕ_{21}	ϕ_{31}	ϕ_{41}	R_{21}	R_{31}	R_{41}
2.578(13)	5.567(28)	2.984(74)	0.365(5)	0.155(4)	0.054(4)

Amplitudes and zero points of our mean light curves differ from the values given by CC96 and K07. Our range in $(B-V)$ (0.358(2)-0.488(3)) is significantly higher than $0.26 - 0.38$ mag (CC96) and $0.325 - 0.454$ mag (K07). According to our $(B-V)$ range CN Cam varies between spectral types F2 to F6. Our amplitude in $B = 0.510(4)$ mag is also larger than 0.474(4) mag (CC96) and 0.49 mag (K07). Our metallicity estimation is slightly lower than K07 derived, but close to the value based on spectroscopy.

All the discrepancies are probably caused by changing characteristics during the Blazhko cycle, which were not caught in CC96 and K07 (visual estimates of the amplitude of the modulation in V is about 0.09 mag and about 0.11 in B). The slightly different magnitude of the comparison star that we used can also play a minor role. Our mean light curves could also differ from the 'true' mean light curves due to non-uniform coverage of our light curves ('true' mean amplitudes of BVR_cI_c are probably slightly lower than ours). For more reliable analysis more extended observations will be needed.

In the future we plan to focus on the observations of other interesting or poorly observed stars with stable and also with modulated light curves. We will also try to complete missing parts of the light curves of already observed stars. Any new observer interested in RR Lyraes is warmly welcome to join CRRLSOP.

The financial support of MU MUNI/A/0735/2012 is acknowledged. The International Variable Star Index (VSX) database, operated at AAVSO, Cambridge, Massachusetts, USA has been used. This research also has also used the VizieR catalogue access tool, CDS, Strasbourg, France. We would like to thank S. N. de Villiers and our referee for

[4] to use Sandage's (2004) equation (3), ϕ_{31} from the Table 2 has to be decreased by the parameter π

[5] taking into account the extinction $\mathrm{E}(B-V) = 0.047$ from Schlegel et al. (1998)

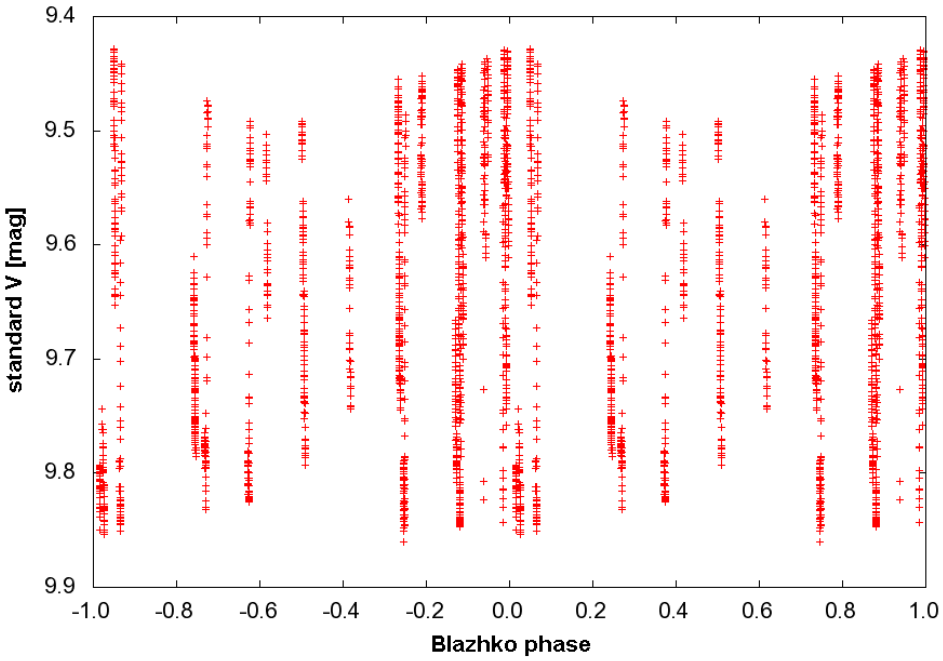

Figure 2. Standard V data phased with the period 47.25 d according to the epoch given in equation 1.

useful comments and suggestions. We would also like to thank the director of Observatory and Planetarium of Johann Palisa in Ostrava, Tomáš Gráf.

References:

Boninsegna, R., Vandenbroere, J., Le Borgne, J. F., & Geos Team 2002, *IAU Colloq. 185*, **259**, 166

Campos-Cucarella, F., Nomen-Torres, J., Gomez-Forrellad, J. M., & Garcia-Melendo, E. 1996, *IBVS*, **4323**, 1

Clementini, G., Gratton, R., Bragaglia, A., et al. 2003, *AJ*, **125**, 1309

Cutri, R. M., Skrutskie, M. F., van Dyk, S., et al. 2003, *VizieR Online Data Catalog*, **2246**, 0

de Ponthiére, P. 2010, LESVEPHOTOMETRY automatic photometry software, http://www.dppobservatory.net

Jurcsik, J., & Kovács, G. 1996, *A&A*, **312**, 111

Kinman, T. D., Harmer, D. L., Saha, A., & Willmarth, D. W. 2007, *IBVS*, **5805**, 1

Landolt A.U., 1992, *AJ*, **104**, 340

Lenz P., Breger M., 2005, *Comm. Asteroseismology*, **146**, 53

Maintz, G. 2012, *BAV Rundbrief - Mitteilungsblatt der Berliner Arbeits-gemeinschaft für Veränderliche Sterne*, **61**, 83
Reinsch, C. H. 1967, *Numer. Math.*, **10**, 177
Sandage, A. 2004, *AJ*, **128**, 858
Schlegel, D. J., Finkbeiner, D. P., & Davis, M. 1998, *ApJ*, **500**, 525
Schwarzenberg-Czerny, A., 1996, *ApJ*, **460**, L107
Sódor Á., 2007, *AN*, **328**, 829
Strohmeier, W., & Knigge, R. 1961, *AN*, **286**, 133
Warner, B. D. 2007, *Minor Planet Bulletin*, **34**, 113
Zinn, R., & West, M. J. 1984, *ApJS*, **55**, 45

*This version of the paper contains corrections, and differs from the one appeared on-line originally. Date of last modification: Apr 3 13:40:03 CEST 2013

COMMISSIONS 27 AND 42 OF THE IAU
INFORMATION BULLETIN ON VARIABLE STARS

Number 6052

Konkoly Observatory
Budapest
5 April 2013

HU ISSN 0374 – 0676

THE 80TH NAME-LIST OF VARIABLE STARS. PART III — RA 16^h TO 24^h

KAZAROVETS, E.V.[1]; SAMUS, N.N.[1,2]; DURLEVICH, O.V.[2]; KIREEVA, N.N.[1]; PASTUKHOVA, E.N.[1]

[1] Institute of Astronomy, Russian Academy of Sciences, 48, Pyatnitskaya Str., Moscow 119017, Russia [helene@inasan.ru, samus@sai.msu.ru, kireeva@sai.msu.ru, pastukhova@sai.msu.ru]

[2] Sternberg Astronomical Institute, M.V. Lomonosov University of Moscow, 13, University Ave., Moscow 119992, Russia [gcvs@sai.msu.ru]

Parts I and II of the 80th Name-List of Variable Stars (Kazarovets et al., 2011ab) contained information on 4195 stars recently named in the system of the General Catalogue of Variable Stars (GCVS; Samus et al., 2012), most of them in the range of right ascensions (J2000.0) between 0^h and 16^h. The present Part III of the 80th Name-List of Variable Stars contains data necessary for identifications of 2133 new variables finally designated in 2010–2013. Most stars in the Name-List are confined to right ascensions (J2000.0) between 16^h and 24^h. Exceptions are several Novae, named upon requests of the IAU Central Bureau of Astronomical Telegrams or after announcements in the Bureau's publications. With the 6328 stars in the three parts of the current Name-List, the total number of named variable stars, not counting designated non-existing stars or stars subsequently identified with earlier-named variables, is now 47 811.

As it had been done in Parts I and II, we separate the catalogue of newly designated variables (to be published elsewhere in the nearest future) from the Name-List proper. Table 1 of the current Name-List contains the new GCVS name, equatorial coordinates (rounded to an accuracy sufficient for identification), and variability type for each star. The order of stars in Table 1 corresponds to the order of stars in the GCVS. The remarks concerning the four unusual variables (type *): V1801 Aql, V1815 Aql, V0354 Dra, and V0722 Lyr, follow Table 1. The electronic version of the Name-List at `http://www.sai.msu.su/gcvs/gcvs/nl80` additionally presents variability ranges, light elements, spectral types, identifications with astronomical catalogues, detailed remarks, bibliographic references for the newly named variable stars.

We continued naming Novae upon requests from the IAU Bureau of Astronomical Telegrams (BAT). In 2012, there were cases of delays of such requests, and we extracted information on stars requiring quick designation from the BAT Internet pages. Part III of the 80th Name-List contains fourteen Novae. They are included in Table 1 and, besides, listed in Table 2 that contains, along with GCVS names, preliminary "constellation+year" designations for Novae (one of them, V5590 Sgr, was actually later identified as a possible symbiotic star). The GCVS names for these fourteen stars, with additional information concerning variability types, variation ranges, and references, were announced in Kazarovets and Samus (2013).

This study was supported in part by Russian Foundation for Basic Research and by the Programme "Non-stationary Phenomena of Objects in the Universe" of the Presidium of Russian Academy of Sciences.

References:

Kazarovets, E.V. and Samus, N.N. 2013, Perem. Zvezdy, 33, 3

Kazarovets, E.V., Samus, N.N., Durlevich, O.V., Kireeva, N.N., Pastukhova, E.N. 2011a, *Inform. Bull. Var. Stars*, No. 5969

Kazarovets, E.V., Samus, N.N., Durlevich, O.V., Kireeva, N.N., Pastukhova, E.N. 2011b, *Inform. Bull. Var. Stars*, No. 6008

Samus, N.N., Durlevich, O.V., Kazarovets, E.V., Kireeva, N.N., Pastukhova, E.N., et al. 2012, *General Catalogue of Variable Stars* (GCVS database, version April 2012), VizieR On-line Data Catalog: B/gcvs

Table 1

Name	R.A., Decl., 2000.0 h m s o ' "	Type	Name	R.A., Decl., 2000.0 h m s o ' "	Type
V0578 And	22 58 50.0 +40 56 11	BY	V0632 And	23 18 58.4 +44 05 49	RV:
V0579 And	22 59 11.1 +36 21 18	EW	V0633 And	23 19 18.7 +39 47 35	EW
V0580 And	23 00 04.7 +48 47 37	SR	V0634 And	23 19 22.3 +36 49 09	EB
V0581 And	23 00 23.9 +48 18 10	EA	V0635 And	23 19 31.4 +46 52 26	SR
V0582 And	23 01 02.1 +47 53 44	SR	V0636 And	23 19 31.9 +49 27 25	LB
V0583 And	23 01 35.5 +48 39 11	EB	V0637 And	23 19 45.4 +44 49 30	LB
V0584 And	23 01 47.8 +35 28 48	BY	V0638 And	23 19 50.5 +44 07 33	EW
V0585 And	23 01 48.6 +44 48 29	EB	V0639 And	23 21 00.9 +48 46 10	SR:
V0586 And	23 02 09.3 +35 15 39	BY	V0640 And	23 21 17.4 +49 28 47	LB
V0587 And	23 02 22.4 +47 21 29	LB	V0641 And	23 21 24.0 +40 21 59	EB
V0588 And	23 02 33.1 +46 49 48	M	V0642 And	23 21 27.2 +49 25 39	LB
V0589 And	23 02 52.1 +48 06 10	SR	V0643 And	23 21 45.3 +45 52 09	EA
V0590 And	23 03 25.7 +44 12 14	EA	V0644 And	23 22 32.4 +47 15 41	SR:
V0591 And	23 03 42.6 +53 00 14	EA	V0645 And	23 23 00.6 +49 14 34	EW
V0592 And	23 03 43.7 +46 29 16	SR	V0646 And	23 23 04.9 +44 37 06	LB
V0593 And	23 03 44.1 +36 15 23	EW	V0647 And	23 23 05.8 +47 06 52	SR
V0594 And	23 04 15.6 +47 19 52	SR:	V0648 And	23 23 51.9 +39 32 34	EB
V0595 And	23 04 18.6 +48 19 48	RRC	V0649 And	23 24 29.1 +47 43 50	EA
V0596 And	23 04 22.8 +47 03 18	SR	V0650 And	23 24 41.3 +46 38 26	LB
V0597 And	23 06 04.1 +48 35 25	EW:	V0651 And	23 24 48.9 +48 30 07	EA
V0598 And	23 06 06.4 +48 15 55	SR	V0652 And	23 24 50.7 +43 34 53	BY:
V0599 And	23 06 21.6 +44 12 18	EA	V0653 And	23 25 07.6 +48 25 03	SRB
V0600 And	23 06 36.2 +47 15 31	EW	V0654 And	23 25 10.6 +48 44 44	SR:
V0601 And	23 06 38.1 +49 23 28	EA	V0655 And	23 25 12.6 +47 14 49	SR
V0602 And	23 06 54.9 +47 16 36	SR	V0656 And	23 25 19.3 +48 07 46	LB
V0603 And	23 07 15.1 +48 28 41	LB	V0657 And	23 25 44.8 +47 05 14	SR
V0604 And	23 07 18.0 +48 05 22	SR	V0658 And	23 26 11.5 +49 13 15	SRD:
V0605 And	23 07 29.2 +44 29 50	SR	V0659 And	23 27 37.9 +47 48 02	SR
V0606 And	23 07 37.3 +44 31 18	LB	V0660 And	23 27 52.1 +44 54 15	RRC
V0607 And	23 07 41.9 +45 09 31	LB	V0661 And	23 28 08.1 +44 56 21	LB
V0608 And	23 08 07.8 +44 10 45	LB	V0662 And	23 28 27.5 +45 22 40	EA/RS
V0609 And	23 08 19.8 +44 00 48	SR:	V0663 And	23 28 56.9 +45 38 29	LB
V0610 And	23 09 15.4 +49 01 33	M:	V0664 And	23 28 59.5 +35 24 44	EW
V0611 And	23 09 19.9 +48 14 47	EB	V0665 And	23 29 33.5 +45 26 23	EA
V0612 And	23 09 35.3 +45 16 45	CEP:	V0666 And	23 29 33.6 +45 59 09	EW
V0613 And	23 10 12.4 +47 34 14	EA	V0667 And	23 29 43.2 +48 36 58	EB
V0614 And	23 10 50.3 +48 15 49	LB	V0668 And	23 29 53.8 +46 58 08	LB
V0615 And	23 11 30.1 +47 02 52	M	V0669 And	23 30 34.3 +43 30 42	LB
V0616 And	23 11 47.2 +48 03 18	LB	V0670 And	23 30 37.3 +46 24 04	DSCT
V0617 And	23 12 23.5 +44 05 34	LB	V0671 And	23 30 50.0 +48 11 32	SR
V0618 And	23 12 33.6 +45 11 59	LB	V0672 And	23 30 55.3 +45 16 24	CEP:
V0619 And	23 12 53.2 +45 29 13	SRB	V0673 And	23 31 03.8 +35 55 47	EB
V0620 And	23 12 53.3 +45 06 03	SR	V0674 And	23 32 41.3 +46 47 58	EA
V0621 And	23 13 20.0 +48 39 27	SR:	V0675 And	23 33 24.1 +48 45 38	DSCTC:
V0622 And	23 13 26.3 +44 01 26	DSCT	V0676 And	23 34 13.9 +36 39 58	EW
V0623 And	23 13 52.4 +44 20 09	LB	V0677 And	23 34 23.1 +39 14 23	UGSU:
V0624 And	23 15 31.5 +44 11 25	LB	V0678 And	23 35 12.3 +44 39 34	EW
V0625 And	23 15 40.3 +36 08 53	EW	V0679 And	23 35 28.5 +47 28 25	SR
V0626 And	23 16 03.2 +48 46 36	LB	V0680 And	23 35 33.3 +43 46 57	EW
V0627 And	23 16 09.8 +48 01 30	EB	V0681 And	23 35 42.5 +39 44 27	R
V0628 And	23 16 22.1 +47 29 10	LB	V0682 And	23 36 03.7 +46 55 46	LB
V0629 And	23 16 53.0 +44 29 18	EA	V0683 And	23 36 27.8 +44 07 24	EA
V0630 And	23 17 03.9 +53 02 19	EA	V0684 And	23 37 38.1 +48 53 26	SR
V0631 And	23 18 20.9 +46 53 36	SRB	V0685 And	23 37 45.7 +48 13 23	LB

Table 1 (continued)

Name	R.A., Decl., 2000.0	Type	Name	R.A., Decl., 2000.0	Type
	h m s o ' "			h m s o ' "	
V0686 And	23 37 55.4 +43 36 37	LB	QW Aqr	21 07 26.1 +01 10 18	RR(B)
V0687 And	23 38 27.9 +36 34 51	EW	QX Aqr	21 14 06.0 +00 19 12	CWA
V0688 And	23 38 40.2 +49 12 23	SR	QY Aqr	21 29 55.0 +01 00 24	RRAB
V0689 And	23 38 54.6 +35 12 17	SR	QZ Aqr	21 31 22.4 -00 39 37	UGSU
V0690 And	23 39 06.3 +44 03 06	LB	V0335 Aqr	21 34 18.6 -03 39 55	EA
V0691 And	23 39 06.4 +42 05 54	BY	V0336 Aqr	21 40 12.7 -01 22 49	RRAB
V0692 And	23 39 12.4 +45 27 52	EW	V0337 Aqr	21 41 05.8 +02 22 15	RS
V0693 And	23 40 40.7 +44 48 56	LB	V0338 Aqr	21 46 10.0 -01 06 48	EW
V0694 And	23 40 42.2 +34 02 41	BY:	V0339 Aqr	21 46 48.0 -01 32 45	EA
V0695 And	23 40 42.3 +47 14 26	LB	V0340 Aqr	21 48 42.5 -00 07 23	UGSU:
V0696 And	23 41 14.2 +35 24 39	EB	V0341 Aqr	21 51 41.3 -03 08 29	RRAB
V0697 And	23 42 09.1 +46 24 34	SR	V0342 Aqr	21 53 56.7 -02 34 31	BY
V0698 And	23 42 29.5 +43 46 02	LB	V0343 Aqr	22 00 18.9 -10 02 48	BY
V0699 And	23 42 57.3 +47 49 20	LB	V0344 Aqr	22 15 19.8 -00 32 57	UG:
V0700 And	23 42 58.3 +48 27 16	LB	V0345 Aqr	22 23 00.5 -03 22 56	BY
V0701 And	23 43 47.3 +45 40 45	LB	V0346 Aqr	22 31 52.9 +02 37 25	RRAB
V0702 And	23 43 50.9 +35 49 21	EW	V0347 Aqr	22 33 03.2 -11 16 50	RRAB
V0703 And	23 44 18.9 +48 08 50	LB	V0348 Aqr	22 36 48.1 -08 01 08	RRC
V0704 And	23 44 57.5 +43 31 22	NL:	V0349 Aqr	22 38 43.8 +01 08 21	XM:
V0705 And	23 45 21.6 +34 08 21	EW	V0350 Aqr	22 39 27.3 -01 36 57	EW
V0706 And	23 48 19.8 +34 48 34	EA	V0351 Aqr	22 44 10.1 +00 58 54	EW
V0707 And	23 48 23.6 +36 18 40	EA	V0352 Aqr	22 46 24.4 -12 54 48	RRAB
V0708 And	23 50 46.2 +33 21 04	RRAB	V0353 Aqr	22 46 46.1 -20 58 38	BY
V0709 And	23 51 11.8 +34 24 48	SR	V0354 Aqr	22 52 47.5 -24 42 14	RRAB
V0710 And	23 51 19.5 +33 33 50	RRC:	V0355 Aqr	23 08 40.2 -16 23 00	BY
V0711 And	23 51 32.0 +35 18 54	SR	V0356 Aqr	23 15 49.9 -23 00 13	RRAB
V0712 And	23 54 39.2 +36 45 16	EW	V0357 Aqr	23 16 03.1 -15 53 31	EW
V0713 And	23 55 08.3 +33 22 29	RRC:	V0358 Aqr	23 16 03.6 -05 27 09	XM
V0714 And	23 56 30.5 +36 28 54	EA	V0359 Aqr	23 17 07.0 -12 38 13	RRAB
V0715 And	23 57 50.2 +33 43 49	BY	V0360 Aqr	23 20 30.7 -14 47 57	RRAB
V0362 Aps	16 01 24.5 -77 03 44	RRC	V0361 Aqr	23 23 34.0 -08 00 45	RRAB
V0363 Aps	16 03 32.3 -70 53 25	RRAB	V0362 Aqr	23 25 47.8 -11 36 36	EA+DSCTC
V0364 Aps	16 10 19.3 -76 52 04	EW	V0363 Aqr	23 54 27.8 -12 36 34	EA
V0365 Aps	16 19 26.1 -71 41 15	EA	V1724 Aql	18 52 35.0 -00 18 43	NA:
V0366 Aps	17 50 33.3 -69 16 18	GDOR	V1725 Aql	18 49 11.4 +00 23 59	EA
OY Aqr	20 38 50.6 -09 45 56	RRAB	V1726 Aql	18 49 53.4 +11 00 10	LB
OZ Aqr	20 39 17.3 -05 30 26	RRAB	V1727 Aql	18 50 09.5 +10 59 36	LB
PP Aqr	20 42 43.8 -09 05 45	DSCT	V1728 Aql	18 51 05.4 -03 15 40	DSCTC
PQ Aqr	20 43 15.8 -09 09 29	RRAB	V1729 Aql	18 51 22.2 -03 19 04	DSCTC
PR Aqr	20 43 34.7 -07 36 48	LB	V1730 Aql	18 53 54.9 -00 48 12	BE:
PS Aqr	20 44 03.7 -03 23 12	RRAB	V1731 Aql	18 55 20.6 -01 05 31	SR
PT Aqr	20 44 29.6 -00 28 39	RS	V1732 Aql	18 56 59.1 +00 28 12	EB
PU Aqr	20 47 39.4 +00 08 40	UG	V1733 Aql	18 57 50.4 +01 31 15	SRB
PV Aqr	20 48 59.6 -06 44 55	RS	V1734 Aql	18 58 50.4 +17 42 09	LB
PW Aqr	20 50 17.9 -05 36 27	E+XM	V1735 Aql	18 59 19.2 +17 44 32	M
PX Aqr	20 52 53.7 -00 38 00	RRAB	V1736 Aql	18 59 41.3 +18 09 37	SR
PY Aqr	20 53 56.0 -06 32 02	EW	V1737 Aql	19 00 47.6 -08 57 21	M
PZ Aqr	20 54 13.3 -08 18 38	EW	V1738 Aql	19 01 15.5 -11 48 40	LB
QQ Aqr	20 54 38.1 -07 38 57	EW	V1739 Aql	19 01 56.3 -01 15 06	EA
QR Aqr	20 55 01.3 -06 57 55	EW	V1740 Aql	19 02 07.0 +02 07 27	EW
QS Aqr	20 58 35.6 -13 22 07	EA	V1741 Aql	19 02 39.6 +01 29 14	SR
QT Aqr	20 59 14.9 -06 12 20	UG	V1742 Aql	19 03 32.0 +10 43 53	M
QU Aqr	21 00 14.1 +00 44 46	UGSU	V1743 Aql	19 07 19.7 +04 15 39	EB+EA
QV Aqr	21 04 49.9 +01 05 46	UG	V1744 Aql	19 07 20.8 +04 20 47	EW

Table 1 (continued)

Name	R.A., Decl., 2000.0	Type	Name	R.A., Decl., 2000.0	Type
	h m s o ' "			h m s o ' "	
V1745 Aql	19 07 21.9 +04 16 14	EW	V1799 Aql	19 13 50.5 +11 09 44	EW
V1746 Aql	19 07 22.4 +04 14 43	CWA:	V1800 Aql	19 15 24.8 +10 30 22	EA
V1747 Aql	19 07 23.4 +08 43 32	EA	V1801 Aql	19 18 22.7 -02 42 11	*
V1748 Aql	19 07 23.8 +04 19 07	CWA:	V1802 Aql	19 18 38.0 +12 43 25	SR
V1749 Aql	19 07 24.3 +04 08 11	BY:	V1803 Aql	19 20 07.0 +12 47 43	DCEP
V1750 Aql	19 07 27.9 +04 15 09	GDOR	V1804 Aql	19 20 36.2 +12 47 37	DCEP
V1751 Aql	19 07 28.6 +04 11 07	EW	V1805 Aql	19 22 19.3 +12 15 48	EA
V1752 Aql	19 07 28.7 +04 18 54	GDOR:	V1806 Aql	19 22 30.8 +11 57 34	BE
V1753 Aql	19 07 30.2 +04 20 47	EW	V1807 Aql	19 23 33.5 +04 37 25	EA
V1754 Aql	19 07 31.9 +04 14 41	BY	V1808 Aql	19 23 49.1 +08 18 26	EW
V1755 Aql	19 07 32.3 +04 19 05	SR:	V1809 Aql	19 29 44.9 +03 25 54	SR:
V1756 Aql	19 07 37.1 +04 20 02	SR	V1810 Aql	19 30 19.6 +13 29 19	SR
V1757 Aql	19 07 38.3 +04 18 23	EA	V1811 Aql	19 40 42.4 +01 41 06	EA
V1758 Aql	19 07 39.7 +04 12 40	EW	V1812 Aql	19 51 10.6 -01 01 26	EW
V1759 Aql	19 07 40.7 +04 11 58	EB	V1813 Aql	19 53 30.1 +02 01 25	EW
V1760 Aql	19 07 41.1 +04 15 55	GDOR:	V1814 Aql	19 54 55.1 +06 54 56	EA
V1761 Aql	19 07 43.8 +04 19 03	SR:	V1815 Aql	19 56 29.2 -01 02 32	*
V1762 Aql	19 07 44.7 +04 17 34	EA	V1816 Aql	19 57 42.9 -01 45 40	SRB:
V1763 Aql	19 07 44.9 +04 10 32	EA	V1817 Aql	20 01 11.9 +07 58 53	EA
V1764 Aql	19 07 46.1 +04 09 55	EW	V1818 Aql	20 01 34.8 +04 59 25	SR
V1765 Aql	19 07 46.6 +04 19 41	EW	V1819 Aql	20 04 42.0 -01 14 46	EW
V1766 Aql	19 07 47.2 +04 19 30	CWB:	V1820 Aql	20 04 55.8 +01 21 57	EA
V1767 Aql	19 07 47.4 +04 19 58	LB	V1821 Aql	20 06 36.7 +09 29 53	RRC
V1768 Aql	19 07 48.2 +04 20 09	EA	V1822 Aql	20 07 11.6 +08 54 41	LB
V1769 Aql	19 07 48.6 +04 18 20	EW	V1823 Aql	20 08 30.6 -02 45 58	SR
V1770 Aql	19 07 49.0 +04 12 52	SR:	V1824 Aql	20 10 01.8 +02 38 13	SRB
V1771 Aql	19 07 50.8 +04 15 12	EW	V1825 Aql	20 13 09.8 +10 20 39	EA
V1772 Aql	19 07 52.1 +04 10 16	EW	V1826 Aql	20 13 42.6 +13 56 25	EA
V1773 Aql	19 07 53.5 +04 17 49	SR	V1827 Aql	20 19 47.7 +04 34 02	EA
V1774 Aql	19 07 53.6 +04 19 01	EW	V1828 Aql	20 20 00.5 +04 37 57	EA
V1775 Aql	19 07 57.8 +04 10 43	SR	V1829 Aql	20 27 37.8 -01 39 59	RRAB
V1776 Aql	19 07 59.1 +04 16 46	EW:	V0897 Ara	16 35 31.0 -50 32 10	M
V1777 Aql	19 07 59.1 +04 17 46	EA	V0898 Ara	16 44 08.9 -47 19 04	BCEP
V1778 Aql	19 08 00.3 +04 08 47	GDOR	V0899 Ara	16 45 54.9 -53 57 31	M
V1779 Aql	19 08 00.3 +04 09 02	LB:	V0900 Ara	16 46 30.2 -47 01 10	BCEP
V1780 Aql	19 08 00.7 +04 10 19	EW	V0901 Ara	16 55 53.6 -48 08 52	BCEP
V1781 Aql	19 08 01.3 +04 13 23	EA	V0902 Ara	16 57 32.4 -46 37 47	SR
V1782 Aql	19 08 02.2 +04 09 01	DSCT	V0903 Ara	17 03 29.0 -56 57 57	EW
V1783 Aql	19 08 03.6 +04 11 30	EB	V0904 Ara	17 11 45.1 -60 26 14	RR:
V1784 Aql	19 08 04.4 +04 16 12	EW	V0905 Ara	17 13 01.2 -61 09 50	EW
V1785 Aql	19 08 05.7 +04 12 06	LB	V0906 Ara	17 13 17.8 -61 10 35	EA
V1786 Aql	19 08 06.9 +04 08 53	BY:	V0907 Ara	17 20 22.6 -58 43 51	EW
V1787 Aql	19 08 07.7 +04 19 28	EA	V0908 Ara	17 29 56.8 -55 43 46	RRAB
V1788 Aql	19 08 10.1 +04 13 26	EB	V0909 Ara	17 40 28.4 -47 44 15	M
V1789 Aql	19 08 10.8 +04 10 20	EW	V0910 Ara	17 43 23.3 -47 33 53	EA
V1790 Aql	19 08 11.3 +04 16 34	EB	V0911 Ara	17 48 35.1 -46 00 36	EB
V1791 Aql	19 08 12.3 +04 08 19	BY:	V0912 Ara	17 50 31.7 -49 31 54	DSCT
V1792 Aql	19 08 13.1 +04 21 54	M:	V0913 Ara	17 57 37.8 -51 42 48	RRAB
V1793 Aql	19 08 13.4 -06 12 47	SR:	V0914 Ara	17 58 24.0 -49 25 39	EA
V1794 Aql	19 08 14.4 +04 14 52	EW	V0915 Ara	18 00 02.5 -50 11 44	RRC
V1795 Aql	19 09 31.2 +11 48 54	DCEP	CT Cap	20 11 59.5 -15 54 02	RRAB
V1796 Aql	19 10 14.1 +05 01 38	EW	CU Cap	20 19 03.0 -14 02 04	RS
V1797 Aql	19 12 32.7 +10 56 35	LB:	CV Cap	20 19 08.4 -16 48 00	EW
V1798 Aql	19 12 48.7 +14 57 22	EW	CW Cap	20 19 11.3 -16 39 59	EW

Table 1 (continued)

Name	R.A., Decl., 2000.0 h m s o ' "	Type	Name	R.A., Decl., 2000.0 h m s o ' "	Type
CX Cap	20 24 11.7 -24 57 01	RVA:	V1222 Cas	23 57 30.0 +56 57 34	EA/RS
CY Cap	20 28 42.3 -09 43 17	RS	V1223 Cas	23 57 34.7 +56 33 20	EW
CZ Cap	20 32 24.4 -11 25 17	RRAB	V1224 Cas	23 57 38.6 +56 35 58	E
DD Cap	20 34 25.0 -10 40 58	EA/RS	V1225 Cas	23 57 44.9 +56 33 56	ELL:
DE Cap	20 35 10.3 -19 14 11	EW	V1226 Cas	23 57 45.1 +56 55 37	EA:
DF Cap	20 36 41.3 -19 15 00	RPHS	V1227 Cas	23 57 51.2 +56 42 03	EA
DG Cap	20 41 42.2 -22 19 20	BY	V1228 Cas	23 58 10.6 +56 29 33	EW
DH Cap	21 11 55.5 -21 09 41	RRAB	V1229 Cas	23 58 12.1 +56 38 06	EW
DI Cap	21 13 05.3 -17 29 13	BY	V1230 Cas	23 58 13.4 +56 45 36	EA
DK Cap	21 35 13.3 -13 33 23	RPHS	V1231 Cas	23 58 13.5 +56 47 26	EB
DL Cap	21 39 02.0 -21 12 46	RRAB	V1232 Cas	23 58 27.3 +56 46 36	E
DM Cap	21 54 11.1 -09 01 22	NL	V1233 Cas	23 58 29.2 +56 32 42	EA/RS
V0834 Car	10 50 19.7 -64 06 47	NA	V1234 Cas	23 58 33.9 +56 37 05	EA
V1181 Cas	22 57 14.8 +57 28 45	BE	V1235 Cas	23 58 36.7 +56 26 55	EA
V1182 Cas	22 58 35.0 +57 09 19	BY:	V1236 Cas	23 58 37.7 +56 39 54	EA
V1183 Cas	23 02 37.4 +59 36 18	DSCTC	V1237 Cas	23 58 39.4 +56 36 45	EA/RS
V1184 Cas	23 03 49.5 +59 30 04	EW	V1238 Cas	23 58 46.4 +56 46 02	EW
V1185 Cas	23 26 05.4 +52 18 12	EA	V1239 Cas	23 59 03.8 +56 39 17	E
V1186 Cas	23 27 02.4 +52 14 47	EW:	V1240 Cas	23 59 21.5 +56 29 48	EA
V1187 Cas	23 27 05.4 +57 25 35	SR	V1241 Cas	23 59 23.0 +56 35 51	EW
V1188 Cas	23 29 42.2 +55 03 47	EW:	V1242 Cas	23 59 33.5 +56 43 24	EA
V1189 Cas	23 29 47.2 +59 43 53	EW	V1243 Cas	23 59 40.9 +56 43 08	EW
V1190 Cas	23 29 53.6 +56 50 22	SR	V1244 Cas	23 59 50.8 +56 44 55	EW
V1191 Cas	23 32 22.7 +60 05 14	EA	V1368 Cen	13 41 09.3 -58 15 17	NA
V1192 Cas	23 36 30.5 +63 27 29	SRA	V0809 Cep	23 08 04.7 +60 46 52	N
V1193 Cas	23 41 30.8 +51 32 59	LB	V0810 Cep	20 02 04.1 +61 33 12	EB
V1194 Cas	23 42 33.8 +56 11 20	DSCTC	V0811 Cep	20 04 16.8 +61 05 32	EW
V1195 Cas	23 53 54.4 +59 09 01	LB	V0812 Cep	20 05 23.6 +61 34 45	EA
V1196 Cas	23 55 18.4 +56 43 14	EA/RS	V0813 Cep	20 08 29.8 +60 57 35	EW
V1197 Cas	23 55 43.0 +56 39 15	EA	V0814 Cep	20 11 38.6 +61 33 49	EA
V1198 Cas	23 55 58.9 +56 40 30	EA	V0815 Cep	20 13 57.9 +61 24 19	SRB
V1199 Cas	23 55 59.2 +56 45 14	EA	V0816 Cep	20 26 12.0 +75 56 01	EW
V1200 Cas	23 56 01.7 +56 43 08	EA/RS	V0817 Cep	20 29 24.7 +60 29 44	EW
V1201 Cas	23 56 08.3 +56 41 34	UV	V0818 Cep	20 29 35.2 +60 38 34	RRAB
V1202 Cas	23 56 09.0 +56 33 43	EA	V0819 Cep	20 30 01.3 +60 46 03	EW
V1203 Cas	23 56 11.8 +56 45 56	EA/RS	V0820 Cep	20 30 04.4 +60 34 33	EW
V1204 Cas	23 56 15.3 +56 35 36	EW	V0821 Cep	20 30 16.2 +60 36 32	EW
V1205 Cas	23 56 18.3 +56 34 15	EW	V0822 Cep	20 32 40.4 +60 45 41	DSCT:
V1206 Cas	23 56 26.7 +58 01 37	DCEP	V0823 Cep	20 32 45.7 +60 35 55	SR:
V1207 Cas	23 56 35.9 +56 44 30	EW	V0824 Cep	20 33 02.1 +60 43 23	EA:
V1208 Cas	23 56 36.7 +56 52 43	EA	V0825 Cep	20 33 16.0 +60 44 24	BY:
V1209 Cas	23 56 44.6 +56 49 44	EB	V0826 Cep	20 33 22.8 +60 37 14	EW
V1210 Cas	23 56 46.8 +56 36 14	EA	V0827 Cep	20 37 07.7 +63 39 15	UG
V1211 Cas	23 56 47.1 +56 51 10	EA	V0828 Cep	20 46 05.7 +55 42 01	SR
V1212 Cas	23 56 47.7 +56 36 28	EA/RS	V0829 Cep	20 49 05.1 +70 19 20	EW
V1213 Cas	23 56 50.8 +56 38 26	E	V0830 Cep	20 54 43.7 +69 59 58	EW
V1214 Cas	23 56 56.4 +56 48 35	EA	V0831 Cep	20 55 15.8 +60 52 02	LB:
V1215 Cas	23 56 57.2 +56 34 03	EA	V0832 Cep	20 55 26.1 +61 35 28	RS
V1216 Cas	23 57 10.7 +56 33 27	EW	V0833 Cep	20 55 41.6 +62 44 35	EB
V1217 Cas	23 57 11.9 +56 31 25	E	V0834 Cep	20 57 21.5 +55 30 04	EB
V1218 Cas	23 57 12.9 +56 31 26	EA	V0835 Cep	21 01 37.6 +62 00 41	EW:
V1219 Cas	23 57 18.0 +56 51 12	EA	V0836 Cep	21 01 45.4 +61 40 09	EW
V1220 Cas	23 57 24.5 +56 55 17	EP:	V0837 Cep	21 02 11.4 +59 53 19	EW
V1221 Cas	23 57 25.2 +56 34 37	EW	V0838 Cep	21 02 37.4 +62 50 55	EB

Table 1 (continued)

Name	R.A., Decl., 2000.0 h m s o ' "	Type	Name	R.A., Decl., 2000.0 h m s o ' "	Type
V0839 Cep	21 03 31.7 +59 25 50	EA	V0893 Cep	22 35 26.9 +64 07 55	SR
V0840 Cep	21 07 14.7 +64 17 15	SR	V0894 Cep	22 36 30.3 +63 25 59	LB
V0841 Cep	21 11 32.0 +59 27 24	EA	V0895 Cep	22 36 37.3 +64 32 53	EA
V0842 Cep	21 11 40.7 +76 40 10	EW	V0896 Cep	22 37 15.6 +82 10 27	ELL
V0843 Cep	21 13 47.6 +78 05 46	EW	V0897 Cep	22 37 18.8 +70 54 29	EA
V0844 Cep	21 14 22.8 +82 18 31	RS	V0898 Cep	22 38 02.4 +67 27 59	EA
V0845 Cep	21 15 31.2 +78 00 55	EW:	V0899 Cep	22 39 15.5 +64 06 36	SRA
V0846 Cep	21 18 16.0 +64 25 08	SR	V0900 Cep	22 39 49.5 +58 32 55	EA
V0847 Cep	21 19 12.1 +73 55 57	SRB	V0901 Cep	22 40 10.4 +60 33 50	DCEP
V0848 Cep	21 20 50.2 +57 13 35	SR	V0902 Cep	22 41 07.8 +82 42 25	EW
V0849 Cep	21 25 27.2 +70 40 02	EA	V0903 Cep	22 42 02.9 +58 04 06	LB
V0850 Cep	21 29 52.1 +64 55 17	EA	V0904 Cep	22 42 15.4 +63 18 53	SR
V0851 Cep	21 30 22.7 +70 19 29	LB	V0905 Cep	22 43 27.4 +74 22 21	RRAB
V0852 Cep	21 32 53.9 +70 37 43	RS	V0906 Cep	22 44 00.8 +67 12 59	SRA
V0853 Cep	21 33 17.1 +70 18 56	EW	V0907 Cep	22 45 43.4 +73 21 59	EB
V0854 Cep	21 34 52.4 +73 36 47	EA	V0908 Cep	22 46 21.7 +59 57 31	DCEPS
V0855 Cep	21 35 01.0 +70 31 04	EW	V0909 Cep	22 47 12.2 +59 58 34	EW
V0856 Cep	21 39 22.8 +79 42 08	EW	V0910 Cep	22 48 05.4 +61 45 02	EA
V0857 Cep	21 45 41.7 +77 56 34	RRAB	V0911 Cep	22 48 23.1 +60 24 17	DCEP
V0858 Cep	21 47 45.0 +72 57 46	LB	V0912 Cep	22 49 02.3 +72 35 54	SR
V0859 Cep	21 47 59.7 +57 12 24	DCEP	V0913 Cep	22 49 46.2 +68 24 12	LB
V0860 Cep	21 48 20.7 +55 39 01	DCEP	V0914 Cep	22 51 07.6 +78 27 22	EW
V0861 Cep	21 49 02.8 +83 03 21	RRAB	V0915 Cep	22 51 28.0 +71 43 21	EA
V0862 Cep	21 50 44.2 +80 08 16	EA	V0916 Cep	22 53 40.5 +60 23 23	SR
V0863 Cep	21 52 33.0 +65 47 34	EB	V0917 Cep	22 57 58.9 +68 53 53	EW
V0864 Cep	21 53 09.7 +70 49 24	EB	V0918 Cep	22 58 44.1 +81 49 52	EW
V0865 Cep	21 55 46.9 +56 12 37	M	V0919 Cep	22 59 40.8 +65 12 40	EA
V0866 Cep	21 57 04.3 +68 15 31	EW	V0920 Cep	23 01 09.6 +59 56 41	BE
V0867 Cep	21 57 35.0 +71 18 29	LB:	V0921 Cep	23 01 14.0 +62 34 05	EA
V0868 Cep	22 02 02.8 +56 44 43	EA	V0922 Cep	23 01 39.2 +69 42 45	EA
V0869 Cep	22 03 36.1 +55 14 14	SR	V0923 Cep	23 02 24.9 +72 48 42	EA
V0870 Cep	22 04 26.6 +61 54 01	EW	V0924 Cep	23 03 07.9 +77 59 30	EA
V0871 Cep	22 06 34.3 +56 50 58	SR	V0925 Cep	23 05 42.2 +75 18 39	EA
V0872 Cep	22 12 30.4 +57 17 33	EW	V0926 Cep	23 05 59.0 +81 10 42	CWA
V0873 Cep	22 12 33.6 +57 15 58	ACYG	V0927 Cep	23 06 41.7 +70 44 59	EA
V0874 Cep	22 12 34.0 +57 15 29	BCEP	V0928 Cep	23 07 30.1 +62 40 42	LB
V0875 Cep	22 13 01.2 +83 20 05	EW	V0929 Cep	23 07 54.5 +60 10 28	EA
V0876 Cep	22 13 37.0 +55 44 28	DSCT	V0930 Cep	23 10 27.1 +69 54 48	EW
V0877 Cep	22 13 45.8 +75 43 48	EA	V0931 Cep	23 10 53.1 +64 55 47	CEP
V0878 Cep	22 14 44.8 +68 04 45	BY	V0932 Cep	23 17 52.0 +75 43 54	RRAB
V0879 Cep	22 18 01.3 +72 41 14	LB	V0933 Cep	23 18 35.1 +80 43 35	EB
V0880 Cep	22 24 59.6 +70 18 54	EA	V0934 Cep	23 19 06.7 +69 45 14	EW
V0881 Cep	22 25 15.9 +70 14 34	EA	V0935 Cep	23 22 24.0 +74 38 44	EB
V0882 Cep	22 25 31.1 +62 45 27	BY	V0936 Cep	23 22 43.2 +75 12 40	EW
V0883 Cep	22 26 16.0 +74 06 29	EA	V0937 Cep	23 23 50.4 +78 14 17	EA
V0884 Cep	22 28 51.3 +73 17 58	SR	V0938 Cep	23 24 25.2 +68 38 29	EA
V0885 Cep	22 29 03.1 +71 48 43	EW	V0939 Cep	23 24 39.8 +71 13 10	EA
V0886 Cep	22 30 57.1 +65 53 06	EA	V0940 Cep	23 25 59.0 +64 34 56	EB
V0887 Cep	22 31 00.2 +69 52 21	EA	V0941 Cep	23 27 11.3 +70 08 08	EA
V0888 Cep	22 31 37.7 +71 53 59	EA	V0942 Cep	23 28 52.5 +74 26 00	EA
V0889 Cep	22 34 16.8 +66 46 33	EW	V0943 Cep	23 29 19.6 +76 12 53	EW
V0890 Cep	22 34 46.0 +58 18 05	EA	V0944 Cep	23 30 34.9 +66 33 46	EA
V0891 Cep	22 35 00.9 +59 52 46	EA	V0945 Cep	23 32 54.6 +65 44 17	EB
V0892 Cep	22 35 09.4 +74 27 17	EW	V0946 Cep	23 34 34.3 +67 42 35	EB

Table 1 (continued)

Name	R.A., Decl., 2000.0	Type	Name	R.A., Decl., 2000.0	Type
	h m s o ' "			h m s o ' "	
V0947 Cep	23 35 54.5 +81 15 34	EW	CT CrB	16 18 34.3 +27 28 13	RRAB
V0948 Cep	23 36 57.6 +74 20 30	EA	CU CrB	16 21 57.2 +38 17 34	RS
V0949 Cep	23 38 26.9 +77 24 34	EA	V2496 Cyg	19 23 45.0 +51 16 12	RS
V0950 Cep	23 38 27.1 +64 54 39	SR	V2497 Cyg	19 23 57.4 +29 37 13	EW
V0951 Cep	23 39 15.4 +78 06 51	EB	V2498 Cyg	19 24 03.7 +29 40 32	DSCTC
V0952 Cep	23 39 41.5 +66 07 25	LB	V2499 Cyg	19 26 46.7 +54 27 10	LB
V0953 Cep	23 41 42.9 +81 03 35	EA/RS	V2500 Cyg	19 27 53.1 +33 22 26	DSCTC
V0954 Cep	23 42 12.1 +67 49 01	EB	V2501 Cyg	19 36 58.2 +46 20 24	DSCTC:
V0955 Cep	23 43 43.6 +81 27 52	EA	V2502 Cyg	19 37 03.2 +46 19 26	DSCTC:
V0956 Cep	23 45 17.8 +80 04 12	EA	V2503 Cyg	19 37 21.5 +46 24 34	DSCTC:
V0957 Cep	23 46 10.5 +71 29 55	EA	V2504 Cyg	19 37 24.1 +46 23 52	DSCTC:
V0958 Cep	23 49 50.0 +82 22 26	EW	V2505 Cyg	19 37 32.1 +46 19 15	DSCTC:
V0959 Cep	23 50 12.9 +68 33 25	EW	V2506 Cyg	19 37 58.8 +46 14 20	DSCT
V0960 Cep	23 51 13.1 +68 55 26	EW	V2507 Cyg	19 38 02.9 +46 17 23	DSCT
V0961 Cep	23 58 06.0 +67 36 11	EA	V2508 Cyg	19 39 10.0 +40 52 15	BY
V0736 CrA	18 01 10.3 -43 55 04	SRB	V2509 Cyg	19 41 22.3 +30 52 23	EW
V0737 CrA	18 02 32.9 -40 05 16	BCEP	V2510 Cyg	19 43 40.5 +46 40 03	RS
V0738 CrA	18 07 01.4 -44 00 45	RRC	V2511 Cyg	19 45 43.5 +32 10 02	EW
V0739 CrA	18 07 19.3 -43 27 47	RRAB	V2512 Cyg	19 45 53.3 +32 13 35	SR
V0740 CrA	18 07 46.0 -44 02 25	RRAB	V2513 Cyg	19 49 29.6 +31 27 16	SRD:
V0741 CrA	18 07 56.3 -43 52 48	RRAB	V2514 Cyg	19 51 24.8 +40 44 07	RS
V0742 CrA	18 08 10.7 -43 43 05	RRAB	V2515 Cyg	19 55 41.3 +52 52 58	SR
V0743 CrA	18 08 34.8 -43 54 43	RRAB	V2516 Cyg	19 57 35.0 +55 39 32	SR
V0744 CrA	18 08 40.0 -39 30 23	RRAB	V2517 Cyg	19 59 16.3 +36 32 08	EA
V0745 CrA	18 09 08.5 -43 30 21	RRAB	V2518 Cyg	19 59 37.1 +48 34 07	SR
V0746 CrA	18 10 57.8 -40 01 50	RRC	V2519 Cyg	20 00 50.8 +55 41 22	EA:
V0747 CrA	18 21 58.5 -44 51 17	LB	V2520 Cyg	20 06 53.7 +32 46 59	EA
V0748 CrA	18 28 28.6 -42 51 25	M	V2521 Cyg	20 07 07.3 +50 34 01	EW:
V0749 CrA	18 39 15.0 -44 43 10	RRAB	V2522 Cyg	20 08 07.9 +58 59 23	LB
V0750 CrA	18 44 27.4 -37 17 28	EW	V2523 Cyg	20 09 28.6 +35 44 01	SXARI:
V0751 CrA	18 48 40.1 -39 33 19	SRA	V2524 Cyg	20 13 33.4 +58 36 25	EW
V0752 CrA	19 03 02.4 -39 42 55	M	V2525 Cyg	20 16 03.0 +35 42 07	BY
V0753 CrA	19 17 43.8 -44 00 17	RS	V2526 Cyg	20 17 23.8 +36 07 36	EA:
BV CrB	16 01 27.2 +30 02 41	RRAB	V2527 Cyg	20 19 20.6 +55 12 19	SR
BW CrB	16 01 50.7 +33 30 35	LB	V2528 Cyg	20 20 27.3 +37 09 57	GCAS:
BX CrB	16 02 29.6 +37 33 30	EW	V2529 Cyg	20 21 00.7 +49 12 19	EA
BY CrB	16 03 06.2 +26 14 23	DSCT	V2530 Cyg	20 21 15.4 +37 24 31	BE
BZ CrB	16 04 41.7 +29 16 26	RRAB	V2531 Cyg	20 21 56.8 +36 39 50	BE
CC CrB	16 05 18.1 +37 26 24	RS	V2532 Cyg	20 22 51.7 +54 17 56	SR
CD CrB	16 05 33.4 +29 12 40	SRB	V2533 Cyg	20 22 58.9 +40 45 39	BCEP
CE CrB	16 05 47.9 +39 33 26	RRAB	V2534 Cyg	20 23 07.3 +40 46 55	BCEP
CF CrB	16 06 00.1 +29 49 54	EW	V2535 Cyg	20 23 07.6 +40 46 09	BCEP
CG CrB	16 07 14.0 +34 01 36	BY	V2536 Cyg	20 23 09.8 +40 45 52	BE
CH CrB	16 07 45.0 +36 23 21	EA+NL	V2537 Cyg	20 23 14.5 +40 45 19	EB
CI CrB	16 08 20.8 +28 12 30	EW:	V2538 Cyg	20 23 33.5 +37 25 45	EB
CK CrB	16 09 58.3 +36 59 52	RRAB	V2539 Cyg	20 23 33.7 +40 45 20	BCEP
CL CrB	16 10 09.3 +35 57 31	EW	V2540 Cyg	20 23 37.9 +46 55 52	EW
CM CrB	16 10 43.4 +34 37 14	DSCT:	V2541 Cyg	20 24 11.9 +48 55 26	EA
CN CrB	16 12 13.0 +34 14 16	BY	V2542 Cyg	20 24 44.8 +54 54 17	SR
CO CrB	16 13 03.6 +35 26 20	LB	V2543 Cyg	20 25 31.9 +44 54 16	GCAS:
CP CrB	16 13 24.1 +34 25 51	RRAB	V2544 Cyg	20 27 17.3 +37 56 27	EA
CQ CrB	16 14 26.2 +34 47 14	RRAB	V2545 Cyg	20 27 26.5 +31 05 38	EW
CR CrB	16 14 28.0 +30 31 45	DSCT:	V2546 Cyg	20 28 04.9 +31 17 10	EW
CS CrB	16 18 26.9 +27 33 15	EW	V2547 Cyg	20 28 22.7 +38 37 19	WR

Table 1 (continued)

Name	R.A., Decl., 2000.0 h m s o ' "	Type	Name	R.A., Decl., 2000.0 h m s o ' "	Type
V2548 Cyg	20 30 01.9 +53 26 47	SR	V2602 Cyg	21 13 13.0 +42 25 36	EW
V2549 Cyg	20 31 22.0 +30 58 38	EA	V2603 Cyg	21 13 15.3 +42 33 21	LB
V2550 Cyg	20 34 58.8 +41 36 17	EA	V2604 Cyg	21 13 17.0 +42 29 44	EW
V2551 Cyg	20 35 36.5 +52 45 45	EW	V2605 Cyg	21 13 17.6 +42 25 48	LB
V2552 Cyg	20 35 57.2 +49 00 42	EW	V2606 Cyg	21 13 17.7 +48 06 44	EA
V2553 Cyg	20 37 13.1 +44 54 54	EA	V2607 Cyg	21 13 18.4 +54 31 58	SR:
V2554 Cyg	20 38 42.1 +48 41 18	EA	V2608 Cyg	21 13 19.7 +42 25 27	DSCTC
V2555 Cyg	20 39 01.6 +45 12 28	EB	V2609 Cyg	21 13 24.1 +48 29 50	EW
V2556 Cyg	20 43 14.4 +54 02 31	SR	V2610 Cyg	21 13 25.6 +42 32 57	EW
V2557 Cyg	20 43 43.7 +51 36 31	EA	V2611 Cyg	21 13 29.2 +42 27 44	LB
V2558 Cyg	20 49 13.5 +35 03 14	EA	V2612 Cyg	21 13 33.4 +42 29 49	EA
V2559 Cyg	20 50 50.8 +41 09 47	EB	V2613 Cyg	21 13 35.3 +48 15 19	EP:
V2560 Cyg	20 52 13.8 +46 35 27	EB	V2614 Cyg	21 13 37.2 +48 10 38	EP:
V2561 Cyg	20 52 58.3 +44 07 20	BY	V2615 Cyg	21 13 40.1 +42 24 52	LB
V2562 Cyg	20 55 19.4 +42 43 32	EB	V2616 Cyg	21 15 10.0 +43 27 30	EA
V2563 Cyg	20 55 44.8 +43 28 28	EW	V2617 Cyg	21 15 23.8 +43 32 10	EB
V2564 Cyg	20 56 33.8 +46 04 27	SR	V2618 Cyg	21 19 04.0 +43 45 49	EA
V2565 Cyg	20 56 40.5 +41 18 28	RRAB	V2619 Cyg	21 19 26.8 +34 52 50	EW
V2566 Cyg	20 58 47.5 +41 46 37	BE+BCEP:	V2620 Cyg	21 21 03.3 +36 26 14	EW
V2567 Cyg	20 59 16.3 +53 50 42	SR	V2621 Cyg	21 21 09.4 +36 41 36	CEP:
V2568 Cyg	21 01 48.8 +50 47 10	DCEPS:	V2622 Cyg	21 21 27.8 +37 08 11	LB
V2569 Cyg	21 01 55.9 +31 59 13	LB	V2623 Cyg	21 21 32.8 +36 49 31	RRAB
V2570 Cyg	21 05 51.7 +35 14 32	EA	V2624 Cyg	21 23 03.3 +37 03 08	EA
V2571 Cyg	21 08 00.1 +37 34 18	SR	V2625 Cyg	21 23 11.1 +35 52 08	RRAB
V2572 Cyg	21 10 21.2 +48 22 19	EW	V2626 Cyg	21 23 18.2 +35 41 10	EW
V2573 Cyg	21 10 27.8 +48 14 31	EW	V2627 Cyg	21 23 37.9 +37 05 28	EA
V2574 Cyg	21 10 31.9 +48 08 19	EW	V2628 Cyg	21 23 42.7 +35 44 22	EW
V2575 Cyg	21 10 33.1 +48 15 21	EW	V2629 Cyg	21 24 16.4 +36 35 48	EA
V2576 Cyg	21 10 50.9 +48 32 19	EW	V2630 Cyg	21 24 17.6 +32 03 30	RRAB
V2577 Cyg	21 11 04.9 +48 08 04	EW	V2631 Cyg	21 24 20.5 +37 08 44	EA
V2578 Cyg	21 11 08.6 +47 10 06	CWB:	V2632 Cyg	21 24 26.7 +36 51 01	EW
V2579 Cyg	21 11 12.5 +48 09 31	EW	V2633 Cyg	21 25 00.6 +36 03 28	EW
V2580 Cyg	21 11 23.9 +48 11 44	EW	V2634 Cyg	21 25 02.4 +36 19 56	EW
V2581 Cyg	21 11 34.4 +44 12 00	DSCT	V2635 Cyg	21 25 09.9 +36 12 04	IN:
V2582 Cyg	21 11 37.4 +48 21 46	EW	V2636 Cyg	21 26 10.2 +36 59 49	EW
V2583 Cyg	21 11 42.5 +48 09 46	EP:	V2637 Cyg	21 26 41.2 +35 46 40	LB
V2584 Cyg	21 11 45.0 +44 45 30	GDOR:	V2638 Cyg	21 26 42.1 +35 59 51	SRB:
V2585 Cyg	21 12 01.0 +48 17 29	EW	V2639 Cyg	21 27 43.7 +35 40 25	EW
V2586 Cyg	21 12 29.2 +48 07 32	EW	V2640 Cyg	21 28 06.1 +36 54 15	RS
V2587 Cyg	21 12 39.1 +42 25 51	LB	V2641 Cyg	21 28 45.6 +37 04 34	EW
V2588 Cyg	21 12 40.5 +42 30 39	EW	V2642 Cyg	21 30 18.5 +47 10 07	EA+UV:
V2589 Cyg	21 12 45.2 +42 25 17	LB	V2643 Cyg	21 30 29.9 +31 14 30	EB
V2590 Cyg	21 12 47.1 +41 30 46	SR	V2644 Cyg	21 37 45.2 +34 37 13	RRAB
V2591 Cyg	21 12 48.9 +42 27 38	LB	V2645 Cyg	21 43 29.1 +53 08 43	EA
V2592 Cyg	21 12 51.0 +42 28 11	EA	V2646 Cyg	21 44 34.5 +54 22 01	EW
V2593 Cyg	21 12 56.3 +42 24 00	EB	V2647 Cyg	21 47 03.3 +50 03 18	EA
V2594 Cyg	21 13 01.7 +42 24 53	LB	V2648 Cyg	21 47 35.2 +51 37 25	EA
V2595 Cyg	21 13 03.9 +42 29 47	EA	V2649 Cyg	21 47 42.2 +30 42 11	BY
V2596 Cyg	21 13 04.5 +42 26 00	EA	V2650 Cyg	21 47 55.8 +54 20 58	DCEP
V2597 Cyg	21 13 05.6 +42 29 07	EA	V2651 Cyg	21 48 06.7 +51 15 30	DCEP
V2598 Cyg	21 13 06.7 +42 25 14	LB	V2652 Cyg	21 48 25.2 +38 47 20	EA
V2599 Cyg	21 13 06.8 +42 29 18	EW	V2653 Cyg	21 49 16.1 +31 25 03	BY
V2600 Cyg	21 13 08.5 +42 29 07	EA	V2654 Cyg	21 50 11.2 +40 46 50	RS
V2601 Cyg	21 13 12.0 +48 18 01	EA	V2655 Cyg	21 51 35.5 +51 54 09	EA

Table 1 (continued)

Name	R.A., Decl., 2000.0	Type	Name	R.A., Decl., 2000.0	Type
	h m s o ' "			h m s o ' "	
V2656 Cyg	21 52 27.0 +42 08 13	EB	V0369 Dra	17 21 13.6 +51 09 50	EW
V2657 Cyg	21 53 38.1 +48 24 13	EW	V0370 Dra	17 21 58.3 +57 49 22	BY
V2658 Cyg	21 56 18.2 +41 02 45	R	V0371 Dra	17 25 24.3 +50 42 12	BY
OY Del	20 17 49.9 +10 16 30	SR	V0372 Dra	17 25 40.8 +59 15 31	EB/RS
OZ Del	20 23 11.1 +18 54 46	EW	V0373 Dra	17 26 23.0 +53 50 33	EW
PP Del	20 28 23.9 +11 31 11	E+RS	V0374 Dra	17 27 20.3 +56 22 30	EW
PQ Del	20 29 32.8 +12 27 31	BY	V0375 Dra	17 32 23.7 +51 40 47	RRAB
PR Del	20 31 06.4 +09 09 04	SRB	V0376 Dra	17 35 00.1 +68 59 25	EA
PS Del	20 31 35.0 +12 54 20	EA	V0377 Dra	17 37 31.6 +65 20 25	EW
PT Del	20 32 38.6 +20 01 43	EA	V0378 Dra	17 41 26.8 +71 59 58	RRAB
PU Del	20 33 27.7 +04 39 09	RRAB	V0379 Dra	17 42 12.4 +63 34 02	RRC
PV Del	20 35 53.0 +10 06 12	BY	V0380 Dra	17 45 24.5 +69 18 22	EA
PW Del	20 36 22.0 +12 15 39	BY	V0381 Dra	17 46 30.5 +53 11 58	EA+DSCTC
PX Del	20 37 47.8 +19 51 15	EB	V0382 Dra	17 47 19.6 +51 33 19	RS
PY Del	20 37 56.5 +13 37 53	EA:	V0383 Dra	17 47 46.9 +52 13 41	BY
PZ Del	20 39 39.0 +03 52 28	RRAB	V0384 Dra	17 52 01.4 +53 56 14	RRAB
QQ Del	20 40 17.1 +14 30 36	BY	V0385 Dra	17 52 53.4 +67 37 20	EA
QR Del	20 44 04.8 +13 14 12	BY	V0386 Dra	17 53 04.3 +51 29 20	EW
QS Del	20 47 51.7 +13 50 28	RS	V0387 Dra	17 54 12.9 +51 01 22	RRAB
QT Del	20 48 53.4 +12 22 30	BY	V0388 Dra	17 56 09.6 +71 26 40	EB
QU Del	20 49 22.9 +06 47 39	RS	V0389 Dra	17 57 34.1 +58 44 14	BY
QV Del	20 54 28.0 +09 06 07	BY	V0390 Dra	17 57 58.9 +55 06 08	BY
QW Del	20 54 36.7 +12 22 11	SR	V0391 Dra	17 59 10.4 +58 42 59	EA/RS
QX Del	20 55 50.9 +10 23 41	RS	V0392 Dra	17 59 46.3 +77 41 46	RRAB
QY Del	20 59 02.5 +18 47 02	RS	V0393 Dra	18 00 29.4 +51 00 09	BY
QZ Del	21 00 21.3 +15 48 35	RRAB	V0394 Dra	18 01 52.5 +60 06 43	RRAB
V0335 Del	21 00 44.1 +15 19 55	EB	V0395 Dra	18 02 39.5 +62 43 08	DSCT
V0336 Del	21 00 47.5 +14 52 46	EW	V0396 Dra	18 05 20.1 +65 30 24	LB
V0337 Del	21 01 27.7 +15 28 11	EW	V0397 Dra	18 06 19.1 +65 41 37	EW
V0338 Del	21 01 34.6 +15 23 16	EW	V0398 Dra	18 07 11.0 +53 15 45	RRAB
V0345 Dra	16 00 48.0 +51 16 48	EW	V0399 Dra	18 12 12.7 +68 42 12	EA
V0346 Dra	16 08 21.2 +62 29 55	RRAB	V0400 Dra	18 16 57.8 +69 26 46	EW
V0347 Dra	16 08 32.6 +63 18 39	EA/RS	V0401 Dra	18 17 25.1 +48 22 02	BY
V0348 Dra	16 10 33.7 +51 44 01	EW	V0402 Dra	18 21 13.9 +65 15 10	EW
V0349 Dra	16 13 22.0 +51 55 23	EW	V0403 Dra	18 23 52.1 +57 29 49	EA
V0350 Dra	16 17 36.6 +56 14 20	DSCTC	V0404 Dra	18 30 53.1 +48 58 49	EW
V0351 Dra	16 18 01.1 +51 11 52	RRAB	V0405 Dra	18 31 13.4 +52 47 07	EW
V0352 Dra	16 25 59.2 +65 14 13	RRAB	V0406 Dra	18 34 05.9 +58 55 57	LB
V0353 Dra	16 27 49.1 +58 50 23	EB	V0407 Dra	18 35 46.0 +73 25 29	EA
V0354 Dra	16 40 57.2 +53 41 09	*	V0408 Dra	18 37 56.3 +56 49 45	RRAB
V0355 Dra	16 54 59.7 +54 42 31	RRAB	V0409 Dra	18 39 38.0 +58 06 00	RRAB
V0356 Dra	16 55 36.9 +52 22 44	DSCT	V0410 Dra	18 39 56.3 +51 05 34	BY
V0357 Dra	16 55 57.2 +68 12 00	EW	V0411 Dra	18 44 12.0 +57 12 41	DSCTC
V0358 Dra	16 57 01.8 +66 35 11	RRAB	V0412 Dra	18 46 33.1 +48 54 45	BY
V0359 Dra	17 02 43.9 +55 55 43	RRAB	V0413 Dra	18 47 29.6 +49 25 55	EA
V0360 Dra	17 03 34.0 +57 29 59	ELL:	V0414 Dra	18 53 30.2 +63 55 04	RRC:
V0361 Dra	17 07 18.3 +64 39 33	UV+BY	V0415 Dra	18 55 50.5 +51 00 08	EW
V0362 Dra	17 11 12.1 +68 33 24	EW	V0416 Dra	18 57 20.4 +71 31 19	UG+E
V0363 Dra	17 13 20.0 +69 07 55	RR(B)	V0417 Dra	19 00 58.8 +48 44 42	RRAB
V0364 Dra	17 15 20.2 +52 54 39	RRAB	V0418 Dra	19 05 23.1 +73 46 26	EA
V0365 Dra	17 16 48.3 +54 46 15	EW	V0419 Dra	19 07 17.2 +55 22 15	RRAB
V0366 Dra	17 17 22.0 +58 05 59	RPHS	V0420 Dra	19 18 09.3 +65 35 18	RRC
V0367 Dra	17 18 21.9 +51 17 32	RRAB	V0421 Dra	19 19 31.5 +81 55 35	EW
V0368 Dra	17 19 06.2 +57 41 21	E	V0422 Dra	19 21 36.5 +56 50 35	EB

Table 1 (continued)

Name	R.A., Decl., 2000.0	Type	Name	R.A., Decl., 2000.0	Type
	h m s o ' "			h m s o ' "	
V0423 Dra	19 23 04.0 +56 08 05	EA	V1151 Her	16 03 55.3 +48 57 13	EW
V0424 Dra	19 25 09.4 +75 32 58	RRC	V1152 Her	16 04 18.9 +18 08 34	RRAB
V0425 Dra	19 44 18.4 +81 47 32	EA	V1153 Her	16 04 34.8 +50 45 13	EW
V0426 Dra	19 51 10.0 +71 26 59	RRAB	V1154 Her	16 06 50.6 +41 17 35	RS
V0427 Dra	19 54 43.0 +83 15 51	EW	V1155 Her	16 08 59.6 +42 01 41	EW
V0428 Dra	19 55 28.6 +65 17 33	LB	V1156 Her	16 09 13.6 +41 36 42	RRAB
V0429 Dra	19 59 32.2 +61 31 21	RRAB	V1157 Her	16 10 59.6 +39 52 54	EW
V0430 Dra	19 59 54.5 +61 35 59	EW	V1158 Her	16 11 23.2 +44 06 21	EW:
V0431 Dra	20 00 39.0 +71 03 37	RRAB	V1159 Her	16 11 34.4 +47 16 12	EW
V0432 Dra	20 01 28.4 +61 10 18	EA	V1160 Her	16 12 16.2 +43 16 31	EW
V0433 Dra	20 01 54.5 +70 12 30	RRC	V1161 Her	16 15 28.7 +26 11 02	RRAB
V0434 Dra	20 04 14.3 +74 25 36	RS	V1162 Her	16 17 00.5 +10 17 28	RRAB
V0435 Dra	20 04 46.8 +68 29 57	EW	V1163 Her	16 17 44.8 +08 54 59	RS
V0436 Dra	20 05 29.4 +71 10 21	EW	V1164 Her	16 18 58.3 +49 54 33	RRAB
V0437 Dra	20 06 46.2 +63 18 38	EW	V1165 Her	16 20 00.0 +04 36 46	RS
V0438 Dra	20 07 04.6 +75 14 26	EW	V1166 Her	16 20 01.8 +04 28 41	DSCT
V0439 Dra	20 09 28.1 +65 45 43	EW	V1167 Her	16 20 03.2 +07 07 29	EW
V0440 Dra	20 09 32.7 +69 55 22	LB	V1168 Her	16 20 44.5 +09 44 27	RRAB
V0441 Dra	20 12 39.6 +82 38 21	EA	V1169 Her	16 22 01.2 +22 50 22	BY
V0442 Dra	20 13 27.8 +67 52 26	SRD	V1170 Her	16 22 40.8 +43 01 08	EW
V0443 Dra	20 17 42.0 +72 31 57	EB	V1171 Her	16 22 55.3 +22 46 04	BY
V0444 Dra	20 18 53.8 +70 17 32	EW	V1172 Her	16 23 37.2 +15 57 20	EW
V0445 Dra	20 22 26.0 +74 04 33	EW	V1173 Her	16 24 10.4 +45 55 27	EW
V0446 Dra	20 29 32.1 +83 12 18	RRC	V1174 Her	16 24 23.4 +04 45 22	RS
V0447 Dra	20 32 33.5 +82 15 22	RRC	V1175 Her	16 24 46.2 +21 39 03	EW
V0448 Dra	20 33 02.6 +68 06 53	SR	V1176 Her	16 25 06.6 +30 02 26	BY
V0449 Dra	20 34 02.6 +81 31 00	EW	V1177 Her	16 25 10.0 +05 14 54	RS:
TY Equ	21 01 24.6 +05 42 13	BY	V1178 Her	16 26 41.3 +33 50 42	BY
TZ Equ	21 01 44.8 +10 08 41	BY	V1179 Her	16 27 44.9 +11 03 38	EW
UU Equ	21 02 36.1 +06 35 01	RRC	V1180 Her	16 28 15.4 +33 01 08	EW:
UV Equ	21 07 07.1 +06 32 32	BY	V1181 Her	16 28 17.3 +37 11 24	EW
UW Equ	21 07 14.3 +09 53 24	RRAB	V1182 Her	16 28 23.0 +36 56 02	EA
UX Equ	21 09 01.2 +09 30 21	BY	V1183 Her	16 28 29.6 +34 31 49	EW
UY Equ	21 10 54.2 +08 58 16	RS	V1184 Her	16 28 35.2 +36 02 35	RS
UZ Equ	21 14 40.5 +12 50 52	EB	V1185 Her	16 28 36.1 +47 17 58	EW
VV Equ	21 16 05.4 +11 34 07	UG	V1186 Her	16 29 14.8 +24 59 39	RRAB
VW Equ	21 18 39.3 +06 12 16	RRC	V1187 Her	16 29 19.9 +35 40 03	EW
VX Equ	21 21 35.9 +09 48 35	BY	V1188 Her	16 29 29.9 +04 29 17	RRAB
DZ Gru	21 33 32.5 -49 18 38	RRAB	V1189 Her	16 29 36.6 +26 35 20	NL:
EE Gru	21 38 29.7 -49 00 53	RRAB	V1190 Her	16 29 43.0 +48 22 24	RS
EF Gru	21 43 17.6 -39 52 11	RRAB	V1191 Her	16 29 46.6 +28 10 38	BY
EG Gru	21 46 19.4 -42 50 49	RRAB	V1192 Her	16 30 19.3 +48 13 44	EW
EH Gru	21 47 30.6 -37 15 51	EW	V1193 Her	16 30 49.9 +04 52 11	RRAB
EI Gru	21 56 16.9 -40 08 27	RS	V1194 Her	16 30 52.9 +24 12 24	BY
EK Gru	22 20 07.5 -48 37 38	BY	V1195 Her	16 31 35.7 +48 43 36	RRAB
EL Gru	22 23 26.1 -47 10 09	EB	V1196 Her	16 32 07.3 +28 47 16	RRAB
EM Gru	22 56 58.6 -45 13 20	BY:	V1197 Her	16 33 22.9 +28 18 20	EW
EN Gru	23 15 23.7 -50 18 28	EW	V1198 Her	16 34 20.9 +42 44 33	EW
EO Gru	23 17 33.4 -52 48 10	BY	V1199 Her	16 35 15.4 +26 55 41	EW
EP Gru	23 23 57.4 -53 18 11	RRC	V1200 Her	16 35 27.4 +35 00 57	BY
V1147 Her	16 00 44.2 +43 08 42	EW	V1201 Her	16 35 41.3 +28 24 48	RRAB
V1148 Her	16 01 22.0 +48 29 38	EW	V1202 Her	16 35 47.4 +45 24 58	EW
V1149 Her	16 03 43.4 +50 13 33	CWB	V1203 Her	16 36 17.0 +50 09 37	RRC
V1150 Her	16 03 51.7 +42 36 54	BY	V1204 Her	16 37 37.3 +06 48 12	RRAB

Table 1 (continued)

Name	R.A., Decl., 2000.0	Type	Name	R.A., Decl., 2000.0	Type
	h m s o ' "			h m s o ' "	
V1205 Her	16 37 39.5 +22 11 13	BY	V1259 Her	17 23 39.8 +35 27 57	EA/RS
V1206 Her	16 37 41.4 +29 19 50	BY	V1260 Her	17 23 41.5 +37 19 31	RRAB
V1207 Her	16 38 45.5 +25 06 43	EW	V1261 Her	17 23 47.4 +20 54 43	EW
V1208 Her	16 38 50.6 +40 57 58	EW	V1262 Her	17 24 05.0 +18 29 37	RS
V1209 Her	16 41 06.8 +40 42 26	SXPHE	V1263 Her	17 24 13.7 +40 26 17	BY
V1210 Her	16 41 53.1 +11 40 21	RS	V1264 Her	17 27 15.6 +33 30 06	EB
V1211 Her	16 42 14.2 +42 52 34	RPHS	V1265 Her	17 28 31.9 +38 22 42	RRAB
V1212 Her	16 43 28.8 +45 23 34	RRAB	V1266 Her	17 28 52.7 +19 13 12	BY
V1213 Her	16 43 50.9 +09 53 26	RRAB	V1267 Her	17 29 07.0 +27 49 21	RRAB
V1214 Her	16 47 03.5 +09 45 58	RS	V1268 Her	17 29 27.2 +35 24 05	BY
V1215 Her	16 47 18.1 +49 37 19	EW	V1269 Her	17 30 05.0 +18 43 39	BY
V1216 Her	16 48 15.5 +44 44 29	EW	V1270 Her	17 31 03.3 +28 15 07	BY
V1217 Her	16 48 42.8 +09 56 22	RRAB	V1271 Her	17 31 09.4 +40 41 18	EW
V1218 Her	16 49 29.4 +04 52 46	RRAB	V1272 Her	17 31 48.4 +36 32 14	BY
V1219 Her	16 49 42.9 +22 20 04	EB	V1273 Her	17 32 16.1 +48 47 50	BY
V1220 Her	16 49 56.8 +32 52 36	BY	V1274 Her	17 33 53.1 +16 55 13	BY
V1221 Her	16 50 00.0 +41 22 26	BY	V1275 Her	17 36 01.7 +47 02 18	EW
V1222 Her	16 50 25.8 +27 28 17	BY	V1276 Her	17 36 36.8 +15 15 08	BY
V1223 Her	16 50 34.1 +45 46 37	EW	V1277 Her	17 36 37.5 +46 05 13	EB
V1224 Her	16 51 23.1 +23 55 42	BY	V1278 Her	17 36 58.2 +30 09 48	BY
V1225 Her	16 52 11.9 +20 21 46	BY	V1279 Her	17 36 59.3 +48 59 46	BY
V1226 Her	16 53 08.7 +25 58 35	CWA	V1280 Her	17 37 33.4 +41 46 20	BY
V1227 Her	16 53 59.1 +20 10 11	UGSU	V1281 Her	17 38 29.9 +19 48 05	RRAB
V1228 Her	16 54 45.0 +42 32 27	BY	V1282 Her	17 38 34.2 +45 27 19	EW
V1229 Her	16 56 58.1 +21 21 40	NL	V1283 Her	17 38 37.4 +37 53 57	RRC
V1230 Her	16 57 26.6 +14 40 46	EW	V1284 Her	17 39 25.3 +36 46 59	EW
V1231 Her	16 58 20.7 +33 33 53	BY	V1285 Her	17 41 07.3 +48 43 14	RR(B)
V1232 Her	16 58 40.6 +37 46 19	EW	V1286 Her	17 41 43.8 +34 12 09	EW
V1233 Her	16 58 52.5 +39 14 23	EW	V1287 Her	17 42 52.8 +14 18 05	RRAB
V1234 Her	16 59 09.6 +20 58 16	BY	V1288 Her	17 43 11.1 +33 49 49	BY
V1235 Her	16 59 21.9 +34 28 23	BY	V1289 Her	17 43 57.2 +34 18 03	EW
V1236 Her	17 00 33.8 +20 01 34	BY	V1290 Her	17 44 07.6 +44 04 52	RS
V1237 Her	17 00 53.3 +40 03 58	XM	V1291 Her	17 46 05.2 +31 21 05	BY
V1238 Her	17 01 21.8 +42 09 50	EW	V1292 Her	17 46 25.3 +22 29 00	BY
V1239 Her	17 02 13.3 +32 29 54	UGSU+EA	V1293 Her	17 46 47.2 +48 34 36	LB
V1240 Her	17 02 44.1 +22 35 48	NL:	V1294 Her	17 47 05.0 +33 21 29	BY
V1241 Her	17 03 03.1 +32 03 26	BY	V1295 Her	17 47 37.0 +45 02 15	EW
V1242 Her	17 03 13.5 +24 53 21	BY	V1296 Her	17 49 03.2 +23 07 46	BY
V1243 Her	17 04 20.2 +39 28 59	BY	V1297 Her	17 49 47.0 +33 50 59	BY
V1244 Her	17 05 38.1 +33 51 00	RS	V1298 Her	17 49 51.7 +23 28 07	EA
V1245 Her	17 07 06.3 +20 29 22	RS	V1299 Her	17 50 41.6 +48 27 17	LB
V1246 Her	17 07 58.0 +29 19 15	BY	V1300 Her	17 51 23.4 +37 43 05	EW
V1247 Her	17 11 45.1 +30 13 20	NL	V1301 Her	17 51 34.0 +41 41 27	BY
V1248 Her	17 12 45.6 +32 25 40	RRAB	V1302 Her	17 52 39.1 +43 49 29	EW
V1249 Her	17 13 31.0 +23 20 26	BY	V1303 Her	17 52 39.9 +48 37 02	RRAB
V1250 Her	17 14 52.3 +30 19 41	UV	V1304 Her	17 52 42.7 +23 27 29	BY:
V1251 Her	17 17 33.6 +49 55 16	BY	V1305 Her	17 52 49.1 +24 45 16	RRC
V1252 Her	17 17 52.1 +40 53 10	EW	V1306 Her	17 53 08.1 +42 34 39	EW
V1253 Her	17 18 00.3 +21 28 09	BY	V1307 Her	17 53 19.2 +21 30 30	BY
V1254 Her	17 18 08.6 +25 06 12	BY	V1308 Her	17 54 47.0 +32 13 35	BY
V1255 Her	17 19 21.1 +48 03 43	BY	V1309 Her	17 55 35.8 +43 48 20	EW
V1256 Her	17 20 21.5 +16 30 53	EW	V1310 Her	17 55 40.6 +37 25 16	EA/RS
V1257 Her	17 22 28.6 +36 58 42	BY	V1311 Her	17 56 59.6 +29 47 15	SRB
V1258 Her	17 23 14.2 +28 36 50	BY	V1312 Her	17 57 11.4 +22 47 06	BY

Table 1 (continued)

Name	R.A., Decl., 2000.0	Type	Name	R.A., Decl., 2000.0	Type
	h m s o ' "			h m s o ' "	
V1313 Her	17 57 18.9 +31 33 16	BY:	DG Ind	22 18 42.4 -69 53 01	RRAB
V1314 Her	17 59 00.4 +39 49 33	RRAB	DH Ind	22 32 11.6 -68 18 56	RRAB
V1315 Her	18 00 25.6 +40 11 04	EW	V0460 Lac	22 02 27.8 +42 18 03	EW
V1316 Her	18 00 57.1 +47 38 22	RRC	V0461 Lac	22 03 15.0 +42 23 30	EW
V1317 Her	18 01 00.5 +23 39 45	BY	V0462 Lac	22 04 10.9 +46 24 31	DSCTC:
V1318 Her	18 01 21.2 +22 50 38	RRAB	V0463 Lac	22 04 50.8 +46 23 00	DSCTC:
V1319 Her	18 01 47.3 +27 39 10	BY	V0464 Lac	22 04 52.5 +46 27 01	DSCTC
V1320 Her	18 02 07.5 +18 30 44	EA/RS	V0465 Lac	22 05 59.2 +46 27 17	LB:
V1321 Her	18 02 13.9 +47 01 12	EW	V0466 Lac	22 11 54.8 +47 39 18	EA
V1322 Her	18 02 38.8 +33 56 35	BY	V0467 Lac	22 22 48.0 +52 58 49	EA
V1323 Her	18 03 39.7 +40 12 20	XM	V0468 Lac	22 31 05.8 +50 21 53	LPB
V1324 Her	18 04 26.6 +39 30 47	BY	V0469 Lac	22 31 53.3 +36 35 06	BY
V1325 Her	18 05 00.8 +41 56 47	GDOR	V0470 Lac	22 36 44.8 +37 24 43	RRAB
V1326 Her	18 05 25.0 +17 57 30	BY	V0471 Lac	22 36 55.2 +40 10 28	BY
V1327 Her	18 06 15.7 +28 01 08	EW	V0472 Lac	22 37 09.3 +42 15 02	EB
V1328 Her	18 08 53.5 +37 07 07	BY	V0473 Lac	22 41 45.2 +37 07 16	RRAB
V1329 Her	18 08 59.3 +45 49 10	BY	V0474 Lac	22 45 58.7 +56 28 32	EB
V1330 Her	18 09 21.7 +36 45 16	RRC	V0475 Lac	22 48 24.6 +39 31 26	LB
V1331 Her	18 09 21.8 +38 17 06	EA	V0476 Lac	22 49 18.1 +52 26 36	EA
V1332 Her	18 10 48.8 +17 12 30	RRAB	V0477 Lac	22 49 35.7 +52 55 05	SR
V1333 Her	18 10 58.2 +49 10 53	EW	V0478 Lac	22 50 47.7 +35 40 56	EW
V1334 Her	18 13 06.6 +26 01 52	BY	V0479 Lac	22 52 50.7 +35 58 57	EW
V1335 Her	18 14 43.1 +30 09 42	EW	V0480 Lac	22 55 51.4 +39 45 46	EW
V1336 Her	18 21 31.6 +23 34 31	BY	V0361 Lib	16 00 57.8 -18 48 06	SRB
V1337 Her	18 23 19.1 +24 16 16	BY	V0394 Lup	16 01 04.6 -40 40 03	M
V1338 Her	18 24 39.1 +12 11 43	EW	V0395 Lup	16 01 57.3 -38 46 48	M
V1339 Her	18 24 44.5 +12 05 37	RRAB	V0396 Lup	16 03 02.1 -37 49 21	EW
V1340 Her	18 24 47.9 +12 11 16	EW	V0397 Lup	16 03 26.2 -30 47 00	LB
V1341 Her	18 25 18.0 +12 28 34	EW	V0398 Lup	16 04 09.9 -35 08 25	M
V1342 Her	18 25 37.0 +12 25 52	LB	V0399 Lup	16 04 39.7 -40 24 32	M
V1343 Her	18 25 55.2 +14 57 58	LPB:	V0400 Lup	16 07 22.8 -29 57 12	CWA
V1344 Her	18 27 18.4 +19 08 33	EA	V0637 Lyr	18 14 14.3 +46 14 11	RS
V1345 Her	18 27 36.7 +12 32 07	EA	V0638 Lyr	18 14 37.5 +42 30 37	RRAB
V1346 Her	18 28 27.1 +12 30 14	EB	V0639 Lyr	18 15 49.5 +32 18 38	EB
V1347 Her	18 28 42.4 +12 34 29	EB	V0640 Lyr	18 17 05.2 +43 49 59	BY
V1348 Her	18 29 13.7 +21 04 18	RRAB	V0641 Lyr	18 17 35.0 +33 45 19	EW
V1349 Her	18 29 45.3 +21 58 26	LB	V0642 Lyr	18 18 40.1 +31 57 39	EW
V1350 Her	18 33 44.7 +22 55 21	BY	V0643 Lyr	18 18 48.0 +34 22 35	BY
V1351 Her	18 35 12.8 +18 55 02	EA	V0644 Lyr	18 19 28.2 +36 52 47	E:/RS
V1352 Her	18 36 47.0 +17 18 47	RV:	V0645 Lyr	18 19 38.1 +36 40 59	BY
V1353 Her	18 38 12.2 +22 24 30	EA	V0646 Lyr	18 21 22.3 +31 41 17	SRB
V1354 Her	18 38 25.3 +18 58 38	LB	V0647 Lyr	18 22 47.1 +44 34 43	BY
V1355 Her	18 38 49.8 +24 44 16	EW	V0648 Lyr	18 23 45.5 +41 05 48	EW
V1356 Her	18 43 02.3 +13 56 36	LB	V0649 Lyr	18 24 26.9 +45 39 01	EW
V1357 Her	18 43 30.1 +22 44 47	SRD	V0650 Lyr	18 27 14.3 +30 22 10	BY
V1358 Her	18 43 37.3 +22 43 44	SRB	V0651 Lyr	18 28 50.3 +35 06 34	BY
V1359 Her	18 52 17.4 +17 00 32	EA:	V0652 Lyr	18 29 34.9 +29 58 05	BY:
V1360 Her	18 55 09.2 +18 08 58	EA	V0653 Lyr	18 30 16.5 +41 05 08	EW
CX Ind	21 01 21.2 -49 33 07	BY	V0654 Lyr	18 30 16.8 +27 08 19	SR:
CY Ind	21 20 44.1 -54 37 59	RS	V0655 Lyr	18 30 18.9 +34 46 56	BY:
CZ Ind	21 24 33.2 -57 12 04	RRAB	V0656 Lyr	18 30 31.5 +33 55 29	EW
DD Ind	21 24 47.1 -47 10 50	EW	V0657 Lyr	18 30 37.3 +43 35 53	BY
DE Ind	21 40 57.0 -57 34 43	RRAB	V0658 Lyr	18 33 36.1 +46 35 42	EW
DF Ind	21 57 51.5 -68 12 50	RS	V0659 Lyr	18 33 40.2 +36 13 20	BY

Table 1 (continued)

Name	R.A., Decl., 2000.0 h m s o ' "	Type	Name	R.A., Decl., 2000.0 h m s o ' "	Type
V0660 Lyr	18 35 42.4 +32 58 46	BY	V0714 Lyr	19 21 14.6 +37 48 04	BY:
V0661 Lyr	18 35 44.6 +30 08 15	BY	V0715 Lyr	19 21 16.1 +37 46 46	SR
V0662 Lyr	18 36 08.4 +26 45 15	SRB	V0716 Lyr	19 21 17.3 +37 45 05	EA/RS
V0663 Lyr	18 37 07.3 +45 07 41	BY	V0717 Lyr	19 21 18.2 +37 51 07	ELL:+UV
V0664 Lyr	18 38 24.5 +42 36 32	EW	V0718 Lyr	19 21 18.7 +37 43 36	BY:
V0665 Lyr	18 38 25.3 +34 06 44	RS	V0719 Lyr	19 21 19.0 +37 47 56	BY
V0666 Lyr	18 39 23.9 +31 00 02	EW	V0720 Lyr	19 21 20.9 +37 46 19	BY:
V0667 Lyr	18 42 32.2 +37 55 34	EA	V0721 Lyr	19 21 22.4 +37 50 30	BY:
V0668 Lyr	18 44 21.5 +28 06 05	DSCTC	V0722 Lyr	19 21 55.3 +35 02 55	*
V0669 Lyr	18 47 06.3 +43 40 35	RS	V0723 Lyr	19 23 57.4 +38 06 52	DSCTC
V0670 Lyr	18 55 43.9 +28 13 07	BY	V0724 Lyr	19 27 30.7 +42 24 40	SR
V0671 Lyr	19 03 23.6 +36 45 35	EW	DH Mic	20 36 08.3 -36 07 11	BY
V0672 Lyr	19 04 09.8 +36 37 58	EP	DI Mic	21 02 39.1 -35 43 33	EW
V0673 Lyr	19 04 20.5 +36 30 57	EW	DK Mic	21 23 36.5 -39 49 34	RRAB
V0674 Lyr	19 04 29.2 +36 39 49	EW	V0959 Mon	06 39 38.6 +05 53 53	NB
V0675 Lyr	19 06 46.6 +44 01 46	E/RS	V0453 Nor	16 00 47.4 -48 46 08	UG
V0676 Lyr	19 13 02.6 +44 36 16	RS	V0454 Nor	16 05 28.3 -42 34 55	M
V0677 Lyr	19 15 12.1 +39 42 51	SRD:	V0455 Nor	16 06 33.8 -54 44 42	LB
V0678 Lyr	19 19 37.1 +37 41 41	BY	V0456 Nor	16 06 36.8 -57 56 01	M
V0679 Lyr	19 19 39.1 +37 37 01	BY	V0457 Nor	16 06 52.5 -52 36 52	M
V0680 Lyr	19 19 39.1 +37 32 10	BY	V0458 Nor	16 11 33.9 -48 19 51	M
V0681 Lyr	19 19 40.0 +37 29 45	L:	V0459 Nor	16 12 06.2 -59 42 49	RRC
V0682 Lyr	19 19 42.3 +37 42 48	EW	V0460 Nor	16 12 22.1 -54 28 02	M
V0683 Lyr	19 19 42.9 +37 29 07	EA	V0461 Nor	16 12 30.9 -54 11 24	EB
V0684 Lyr	19 19 43.0 +37 30 07	EB	V0462 Nor	16 12 33.5 -54 23 16	M
V0685 Lyr	19 19 43.8 +37 35 30	EW	V0463 Nor	16 13 23.3 -59 22 44	M
V0686 Lyr	19 19 56.4 +37 34 12	ELL	V0464 Nor	16 13 38.9 -54 08 18	M
V0687 Lyr	19 19 58.5 +37 35 44	EW	V0465 Nor	16 13 52.4 -54 01 54	M
V0688 Lyr	19 20 09.1 +37 44 10	ELL:	V0466 Nor	16 14 00.9 -54 06 03	M
V0689 Lyr	19 20 10.6 +37 38 56	EW	V0467 Nor	16 14 03.6 -53 54 04	M
V0690 Lyr	19 20 18.7 +37 30 29	EW	V0468 Nor	16 14 31.2 -53 36 59	M
V0691 Lyr	19 20 19.1 +37 47 16	EW	V0469 Nor	16 15 43.0 -53 34 49	M
V0692 Lyr	19 20 21.5 +37 48 22	BY:	V0470 Nor	16 15 48.8 -53 33 05	M
V0693 Lyr	19 20 27.6 +37 47 15	EA	V0471 Nor	16 16 06.4 -53 54 43	M
V0694 Lyr	19 20 30.8 +37 50 55	RV:	V0472 Nor	16 16 41.9 -54 15 30	M
V0695 Lyr	19 20 30.9 +37 36 51	RS:	V0473 Nor	16 16 49.1 -53 26 13	M
V0696 Lyr	19 20 32.2 +37 44 21	LB	V0474 Nor	16 16 51.0 -53 56 52	M
V0697 Lyr	19 20 35.2 +37 31 04	RS:	V0475 Nor	16 17 13.5 -53 33 55	M
V0698 Lyr	19 20 39.6 +37 38 30	BY	V0476 Nor	16 17 29.1 -53 41 32	M
V0699 Lyr	19 20 44.1 +37 30 42	EA	V0477 Nor	16 17 47.1 -53 35 34	RRAB
V0700 Lyr	19 20 44.9 +37 33 42	EW	V0478 Nor	16 17 48.2 -54 12 25	M
V0701 Lyr	19 20 46.0 +37 42 06	BY:	V0479 Nor	16 18 57.9 -51 03 30	BCEP
V0702 Lyr	19 20 47.9 +37 45 58	BY:	V0480 Nor	16 20 50.4 -48 06 53	M
V0703 Lyr	19 20 57.9 +37 31 07	BY:	V0481 Nor	16 23 54.5 -52 30 21	EA
V0704 Lyr	19 21 00.2 +37 42 53	BY	V0482 Nor	16 24 18.1 -52 20 13	M
V0705 Lyr	19 21 00.5 +37 38 23	EA:	V0483 Nor	16 25 01.3 -52 27 27	M
V0706 Lyr	19 21 06.1 +37 41 40	L	V0484 Nor	16 25 41.6 -51 53 06	M
V0707 Lyr	19 21 07.2 +37 44 35	L	V0485 Nor	16 25 55.2 -52 15 19	M
V0708 Lyr	19 21 07.5 +37 43 06	BY:	V0486 Nor	16 26 08.7 -51 51 42	M
V0709 Lyr	19 21 08.4 +37 44 55	SR	V0487 Nor	16 27 10.1 -52 02 39	M
V0710 Lyr	19 21 10.5 +37 43 25	L	V0488 Nor	16 27 14.8 -51 59 06	RRAB
V0711 Lyr	19 21 11.4 +37 29 55	L	V0489 Nor	16 27 54.7 -52 06 36	M
V0712 Lyr	19 21 12.2 +37 44 55	BY	V0490 Nor	16 28 14.5 -52 04 14	M
V0713 Lyr	19 21 12.9 +37 45 52	ELL	FG Oct	18 56 39.0 -77 10 31	RRAB

Table 1 (continued)

Name	R.A., Decl., 2000.0	Type	Name	R.A., Decl., 2000.0	Type
	h m s o ' "			h m s o ' "	
FH Oct	19 05 25.0 -78 26 44	RS	V2725 Oph	17 23 13.4 +01 51 51	RRAB
FI Oct	19 14 04.5 -86 01 25	RRAB	V2726 Oph	17 23 36.1 -01 11 27	RRAB
FK Oct	20 38 37.7 -80 00 27	SRB	V2727 Oph	17 25 18.2 -23 30 46	M
FL Oct	21 26 58.2 -85 42 06	RS	V2728 Oph	17 27 26.1 +08 43 14	EW
FM Oct	22 18 46.7 -84 38 30	BY	V2729 Oph	17 28 49.8 +12 22 30	EA
V2676 Oph	17 26 07.0 -25 51 43	NA	V2730 Oph	17 30 02.6 +10 03 22	EB
V2677 Oph	17 39 57.0 -24 47 07	NA	V2731 Oph	17 30 21.9 -05 59 32	XM
V2678 Oph	16 22 26.3 +00 07 23	RS	V2732 Oph	17 30 23.4 +08 50 07	RRAB
V2679 Oph	16 22 26.9 -00 10 08	RRAB	V2733 Oph	17 31 21.9 -17 43 40	CWB
V2680 Oph	16 23 33.2 -00 05 49	RRAB	V2734 Oph	17 34 56.5 -00 23 07	RRAB
V2681 Oph	16 23 34.9 +00 24 30	SR	V2735 Oph	17 35 02.1 -27 14 51	CWB
V2682 Oph	16 26 14.2 -00 50 27	RRAB	V2736 Oph	17 35 08.1 -27 31 26	CWB
V2683 Oph	16 28 10.8 +03 04 13	RRAB	V2737 Oph	17 35 08.4 -29 23 28	EA
V2684 Oph	16 28 59.2 -00 15 53	RRAB	V2738 Oph	17 35 13.8 -27 03 17	CWB
V2685 Oph	16 31 11.9 -01 25 14	RRAB	V2739 Oph	17 35 29.1 -26 55 53	CWB
V2686 Oph	16 31 21.7 -00 06 12	RRAB	V2740 Oph	17 37 00.8 +12 58 30	SRB
V2687 Oph	16 32 08.7 -00 38 34	RRAB	V2741 Oph	17 37 21.7 -09 40 36	SRB
V2688 Oph	16 35 12.1 -00 59 03	RRC	V2742 Oph	17 39 04.5 +02 03 15	GDOR
V2689 Oph	16 36 19.1 -00 10 22	RRAB	V2743 Oph	17 40 50.3 +07 42 19	RRAB
V2690 Oph	16 37 22.2 -00 19 57	UGSU	V2744 Oph	17 41 08.3 -23 28 28	DCEPS
V2691 Oph	16 39 19.9 -02 08 08	RRAB	V2745 Oph	17 42 39.0 +02 58 51	EA
V2692 Oph	16 39 28.5 -01 27 18	RRAB	V2746 Oph	17 42 44.4 -17 28 53	SRA
V2693 Oph	16 39 40.3 -01 27 55	RRAB	V2747 Oph	17 43 25.3 +11 06 04	RRAB
V2694 Oph	16 40 28.3 -00 42 39	RRC	V2748 Oph	17 44 31.6 +13 12 57	BY
V2695 Oph	16 41 24.4 -01 59 51	RRAB	V2749 Oph	17 45 26.3 +08 22 02	RRAB
V2696 Oph	16 43 27.3 -14 12 00	LB	V2750 Oph	17 46 32.6 +01 25 20	LB
V2697 Oph	16 44 44.2 +03 09 34	RRAB	V2751 Oph	17 48 44.7 -05 07 15	BY
V2698 Oph	16 47 17.3 +02 38 48	EA	V2752 Oph	17 49 43.5 +04 13 24	EA
V2699 Oph	16 48 43.4 -01 54 21	RRAB	V2753 Oph	17 51 30.6 -00 51 51	SRB
V2700 Oph	16 51 22.1 -00 50 01	BY	V2754 Oph	17 51 37.9 +08 44 02	DSCT
V2701 Oph	16 53 08.3 +11 23 43	EW	V2755 Oph	17 51 52.9 +09 37 52	BY
V2702 Oph	16 53 57.7 +07 34 50	RS	V2756 Oph	17 52 15.6 -00 38 46	SRA
V2703 Oph	16 55 36.8 +12 25 51	RRAB	V2757 Oph	17 52 16.4 +09 37 58	BY
V2704 Oph	16 57 36.1 -29 55 06	SRA	V2758 Oph	17 53 02.6 +04 05 41	EW
V2705 Oph	16 59 20.5 -08 07 04	M	V2759 Oph	17 53 03.7 +03 42 45	LB
V2706 Oph	16 59 22.2 -21 22 49	SRA:	V2760 Oph	17 53 14.9 -01 28 54	SRB
V2707 Oph	16 59 25.4 -28 23 17	SRA	V2761 Oph	17 53 44.7 +11 30 48	EA
V2708 Oph	16 59 50.2 -24 21 20	SRA	V2762 Oph	17 58 09.4 +09 22 41	BY
V2709 Oph	17 02 23.2 -24 21 59	RRAB	V2763 Oph	17 59 54.4 +10 44 19	BY
V2710 Oph	17 05 09.8 +04 13 39	RRAB	V2764 Oph	18 02 55.6 +04 00 10	RRAB
V2711 Oph	17 05 23.4 +03 26 19	DSCTC	V2765 Oph	18 03 28.5 +01 16 31	SRB
V2712 Oph	17 05 25.3 -16 05 46	EB	V2766 Oph	18 03 31.3 +08 08 36	EA/RS
V2713 Oph	17 06 53.1 +06 35 01	EB	V2767 Oph	18 05 00.4 +11 10 14	BY
V2714 Oph	17 07 55.7 -28 52 06	M	V2768 Oph	18 05 11.5 +01 29 56	EW
V2715 Oph	17 09 30.3 -26 39 20	XB	V2769 Oph	18 05 14.4 +11 31 49	BY
V2716 Oph	17 15 36.8 -10 06 42	EW	V2770 Oph	18 06 37.2 +10 07 11	SXPHE
V2717 Oph	17 15 38.7 -08 05 30	EW	V2771 Oph	18 06 45.5 +10 28 18	EW
V2718 Oph	17 16 25.5 -28 14 03	RRAB	V2772 Oph	18 06 50.9 +10 05 36	EB
V2719 Oph	17 16 28.1 -28 03 18	EW:	V2773 Oph	18 07 09.4 +10 17 16	RRAB
V2720 Oph	17 16 43.9 -28 08 24	CEP:	V2774 Oph	18 07 15.7 +10 07 45	EW
V2721 Oph	17 16 55.7 -28 14 52	RRAB	V2775 Oph	18 07 46.6 +10 15 16	EW
V2722 Oph	17 17 00.8 -25 08 15	EA	V2776 Oph	18 07 59.5 +09 58 54	EB
V2723 Oph	17 17 11.5 +08 15 25	BY	V2777 Oph	18 08 03.3 +10 11 10	RRAB
V2724 Oph	17 21 56.9 +09 56 54	EB	V2778 Oph	18 08 14.2 +10 04 53	EW

Table 1 (continued)

Name	R.A., Decl., 2000.0 h m s o ' "	Type	Name	R.A., Decl., 2000.0 h m s o ' "	Type
V2779 Oph	18 08 35.8 +10 10 30	E+NL	V0418 Pav	20 53 42.9 -66 09 22	RRAB
V2780 Oph	18 08 38.7 +09 56 08	EA	V0419 Pav	21 05 26.4 -60 46 04	RRAB
V2781 Oph	18 08 45.6 +10 08 45	RRC	V0420 Pav	21 09 17.4 -74 08 56	RRAB
V2782 Oph	18 09 05.4 +09 57 11	EW	V0423 Peg	21 10 24.9 +14 48 46	EW
V2783 Oph	18 09 07.0 +10 15 23	EW	V0424 Peg	21 10 36.8 +12 23 52	SR
V2784 Oph	18 09 10.0 +10 18 24	RRAB	V0425 Peg	21 10 44.8 +16 23 24	BY
V2785 Oph	18 09 15.9 +10 18 57	RRC	V0426 Peg	21 10 44.9 +15 35 42	EW
V2786 Oph	18 09 16.5 +13 13 24	SRB	V0427 Peg	21 14 36.7 +19 52 56	BY
V2787 Oph	18 09 33.7 +10 21 04	EA	V0428 Peg	21 16 32.7 +19 42 13	RS
V2788 Oph	18 09 41.6 +11 09 03	LB	V0429 Peg	21 20 34.2 +18 37 17	RRAB
V2789 Oph	18 09 43.4 +10 25 48	RRAB	V0430 Peg	21 23 41.7 +15 21 48	BY
V2790 Oph	18 09 45.0 +10 24 57	EW	V0431 Peg	21 28 12.9 +07 52 27	BY
V2791 Oph	18 10 04.2 +09 06 21	BY	V0432 Peg	21 28 13.7 +11 57 45	EA
V2792 Oph	18 13 50.5 +13 49 37	BY	V0433 Peg	21 28 46.9 +23 20 13	BY
V2793 Oph	18 20 53.5 +11 27 55	RRAB	V0434 Peg	21 29 34.8 +09 35 30	BY
V2794 Oph	18 22 08.3 +06 42 41	EW	V0435 Peg	21 29 48.0 +15 28 33	EW
V2795 Oph	18 22 10.2 +06 23 20	DSCTC:	V0436 Peg	21 30 01.5 +15 26 45	EW
V2796 Oph	18 23 06.9 +06 42 13	DSCTC:	V0437 Peg	21 30 04.1 +12 04 29	BY
V2797 Oph	18 23 09.1 +06 51 34	DSCTC:	V0438 Peg	21 30 17.5 +18 43 57	RRAB
V2798 Oph	18 23 42.5 +06 24 09	DSCTC:	V0439 Peg	21 30 40.6 +22 01 43	BY
V2799 Oph	18 23 47.9 +07 28 06	EA	V0440 Peg	21 30 48.1 +17 38 48	RRAB
V2800 Oph	18 24 26.8 +06 45 41	DSCTC:	V0441 Peg	21 31 16.7 +22 53 57	BY
V2801 Oph	18 24 32.6 +07 30 46	DSCTC:	V0442 Peg	21 32 22.0 +24 33 42	BY
V2802 Oph	18 24 40.7 +07 04 06	DSCTC:	V0443 Peg	21 35 36.0 +03 34 36	RRAB
V2803 Oph	18 25 04.2 +06 25 55	DSCTC:	V0444 Peg	21 37 01.8 +07 14 46	UGSU
V2804 Oph	18 25 14.8 +06 33 53	DSCTC:	V0445 Peg	21 37 50.2 +26 46 46	EB:
V2805 Oph	18 26 19.7 +07 27 58	DSCTC:	V0446 Peg	21 38 22.3 +26 37 39	EW
V2806 Oph	18 26 54.1 +06 58 05	DSCTC:	V0447 Peg	21 38 30.9 +27 22 09	SRB
V2807 Oph	18 27 33.4 +06 56 00	DSCTC:	V0448 Peg	21 39 27.6 +27 15 57	LB
V2808 Oph	18 27 40.9 +07 08 33	DSCTC:	V0449 Peg	21 39 43.1 +28 22 39	EW
V2809 Oph	18 27 49.5 +11 51 49	EA	V0450 Peg	21 39 43.4 +26 34 46	EA
V2810 Oph	18 28 33.9 +06 53 15	DSCTC:	V0451 Peg	21 41 12.7 +11 21 20	RRAB
V2811 Oph	18 28 42.9 +06 51 25	DSCTC:	V0452 Peg	21 43 06.4 +08 03 32	RRAB
V2812 Oph	18 28 58.0 +07 28 32	DSCT	V0453 Peg	21 44 53.2 +04 21 43	RRAB
V2813 Oph	18 29 04.4 +06 26 54	EA	V0454 Peg	21 45 37.4 +27 11 11	BY
V2814 Oph	18 29 10.2 +06 43 51	DSCTC:	V0455 Peg	21 47 44.3 +19 29 08	DSCTC
V2815 Oph	18 30 15.3 +07 02 19	LB	V0456 Peg	21 48 09.4 +19 10 13	BY
V2816 Oph	18 30 41.9 +06 47 50	BCEP:	V0457 Peg	21 48 27.4 +22 37 02	DSCT
V2817 Oph	18 30 52.3 +07 09 27	EA	V0458 Peg	21 49 00.2 +12 16 00	EA
V2818 Oph	18 30 59.8 +07 11 50	DSCTC:	V0459 Peg	21 49 56.1 +20 58 43	EW
V2819 Oph	18 31 00.8 +07 08 26	EA	V0460 Peg	21 50 08.2 +19 25 26	ELL+DSCTC
V2820 Oph	18 31 18.7 +07 05 24	DSCTC:	V0461 Peg	21 50 23.7 +17 46 22	EA:
V2821 Oph	18 32 05.6 +07 14 56	DSCTC:	V0462 Peg	21 50 25.4 +14 51 06	EB
V2822 Oph	18 32 22.4 +06 37 12	EA	V0463 Peg	21 50 25.6 +17 43 43	EW
V2823 Oph	18 32 52.0 +06 49 01	EW	V0464 Peg	21 51 03.1 +35 10 46	EW
V2824 Oph	18 33 16.5 +06 29 09	DSCTC:	V0465 Peg	21 51 52.3 +17 44 43	DSCT
V0410 Pav	17 46 36.6 -58 38 51	EW	V0466 Peg	21 52 43.7 +21 44 53	EA:
V0411 Pav	17 50 17.3 -58 45 37	RRAB	V0467 Peg	21 52 47.7 +18 17 33	EW
V0412 Pav	18 37 40.7 -57 27 39	RRC	V0468 Peg	21 53 12.0 +22 23 38	EA
V0413 Pav	18 41 10.0 -72 29 42	EB	V0469 Peg	21 53 21.2 +22 37 11	SR
V0414 Pav	18 46 52.6 -62 10 36	BY	V0470 Peg	21 53 23.7 +17 30 20	BY
V0415 Pav	18 58 39.6 -68 58 35	RRAB	V0471 Peg	21 53 45.3 +18 31 59	EA
V0416 Pav	19 39 33.5 -65 28 51	RR(B)	V0472 Peg	21 54 06.8 +34 28 37	BY
V0417 Pav	20 28 44.2 -64 43 06	RRAB	V0473 Peg	21 54 29.9 +19 03 52	EW

Table 1 (continued)

Name	R.A., Decl., 2000.0 h m s o ' "	Type	Name	R.A., Decl., 2000.0 h m s o ' "	Type
V0474 Peg	21 54 30.1 +35 51 46	EW	V0528 Peg	22 26 04.5 +34 59 06	EW
V0475 Peg	21 54 33.5 +14 32 05	DSCTC	V0529 Peg	22 26 14.5 +21 32 10	BY
V0476 Peg	21 54 33.7 +35 50 18	UGSU:	V0530 Peg	22 26 19.3 +26 03 38	SR
V0477 Peg	21 55 01.2 +20 20 26	EW	V0531 Peg	22 26 26.6 +35 00 25	EW
V0478 Peg	21 55 25.4 +19 37 17	EA	V0532 Peg	22 28 04.0 +18 36 07	BY:
V0479 Peg	21 56 26.5 +15 34 41	RRAB	V0533 Peg	22 28 20.7 +17 39 59	BY
V0480 Peg	21 56 42.1 +22 03 12	EW	V0534 Peg	22 33 28.4 +16 39 01	EA
V0481 Peg	21 57 11.2 +22 40 11	EW	V0535 Peg	22 36 16.8 +33 18 57	EW
V0482 Peg	21 58 32.7 +21 49 25	DSCT	V0536 Peg	22 39 54.2 +13 26 14	DSCT
V0483 Peg	21 59 05.4 +17 44 32	EW	V0537 Peg	22 43 40.7 +30 55 20	UG
V0484 Peg	21 59 29.0 +14 58 17	EW	V0538 Peg	22 43 55.2 +29 36 48	EA:
V0485 Peg	22 00 14.2 +23 05 01	EW	V0539 Peg	22 44 10.0 +14 46 39	EA
V0486 Peg	22 00 36.1 +16 15 01	EW	V0540 Peg	22 44 46.1 +30 29 34	BY
V0487 Peg	22 00 41.6 +27 15 14	BY	V0541 Peg	22 46 31.9 +35 11 36	BY
V0488 Peg	22 01 42.5 +17 28 45	EB	V0542 Peg	22 47 05.5 +26 52 55	RS
V0489 Peg	22 01 49.3 +17 59 42	EW	V0543 Peg	22 47 22.7 +23 13 17	BY
V0490 Peg	22 02 14.0 +15 20 14	BY	V0544 Peg	22 47 39.5 +15 17 43	RRAB
V0491 Peg	22 02 37.1 +03 42 16	RRAB	V0545 Peg	22 49 27.5 +30 54 43	EB
V0492 Peg	22 02 37.7 +18 54 03	GDOR+DSCTC	V0546 Peg	22 49 52.1 +30 50 57	EB
V0493 Peg	22 03 04.0 +16 44 19	RRAB	V0547 Peg	22 50 15.5 +04 28 42	RRC
V0494 Peg	22 03 10.9 +22 32 07	EA	V0548 Peg	22 51 34.2 +34 57 53	EW
V0495 Peg	22 03 28.0 +18 19 23	EB	V0549 Peg	22 51 55.5 +35 39 15	BY
V0496 Peg	22 03 30.2 +19 39 13	EA	V0550 Peg	22 53 23.1 +08 46 07	RRAB
V0497 Peg	22 03 39.8 +03 57 07	RRAB	V0551 Peg	22 53 38.1 +29 13 05	BY
V0498 Peg	22 04 51.5 +14 46 18	EB	V0552 Peg	22 54 55.0 +24 14 45	BY
V0499 Peg	22 05 42.0 +19 55 08	EW	V0553 Peg	22 55 19.2 +17 45 00	RRAB
V0500 Peg	22 06 00.1 +19 35 50	EB	V0554 Peg	22 55 38.9 +28 10 35	BY
V0501 Peg	22 06 01.0 +17 10 38	BY	V0555 Peg	22 56 17.6 +20 52 36	BY
V0502 Peg	22 07 53.8 +22 43 59	EW	V0556 Peg	22 57 20.1 +34 24 31	EA
V0503 Peg	22 08 25.9 +18 34 57	EW	V0557 Peg	22 59 23.5 +32 51 33	EA/RS
V0504 Peg	22 08 27.1 +18 35 25	EW:	V0558 Peg	22 59 56.8 +35 09 48	M
V0505 Peg	22 09 19.1 +19 43 58	RRAB	V0559 Peg	22 59 57.0 +29 15 29	EW
V0506 Peg	22 12 17.2 +15 11 46	EW	V0560 Peg	23 01 31.5 +30 44 27	EA:
V0507 Peg	22 12 47.5 +18 24 10	EW	V0561 Peg	23 01 46.8 +13 05 14	M
V0508 Peg	22 12 51.8 +17 20 16	EW	V0562 Peg	23 01 58.5 +35 04 19	EW
V0509 Peg	22 13 36.6 +26 46 46	RRAB	V0563 Peg	23 02 00.2 +31 02 18	EW
V0510 Peg	22 13 38.6 +18 54 10	DSCTC	V0564 Peg	23 03 10.3 +34 25 07	RRC
V0511 Peg	22 13 46.9 +18 21 03	EW	V0565 Peg	23 05 07.9 +34 17 23	DSCT:
V0512 Peg	22 15 38.7 +22 19 34	EW	V0566 Peg	23 06 23.7 +34 09 33	SR:
V0513 Peg	22 16 31.2 +29 00 20	UG	V0567 Peg	23 07 24.9 +31 50 14	BY
V0514 Peg	22 16 52.2 +22 29 34	EB	V0568 Peg	23 08 13.0 +33 03 04	EW
V0515 Peg	22 17 34.8 +15 31 33	DSCTC	V0569 Peg	23 08 43.0 +21 37 18	BY
V0516 Peg	22 17 40.0 +17 10 17	EB	V0570 Peg	23 09 04.2 +31 53 20	EW
V0517 Peg	22 18 22.5 +22 08 10	RRAB	V0571 Peg	23 09 15.9 +34 19 24	LB
V0518 Peg	22 18 44.1 +14 21 30	BY	V0572 Peg	23 10 25.7 +34 08 43	EW
V0519 Peg	22 19 23.7 +03 34 04	BY	V0573 Peg	23 10 34.2 +31 42 54	EW
V0520 Peg	22 20 54.4 +16 18 35	EW	V0574 Peg	23 10 34.3 +09 29 51	BY
V0521 Peg	22 21 44.8 +18 40 08	UGSU	V0575 Peg	23 10 36.9 +20 55 26	BY
V0522 Peg	22 22 02.8 +08 49 24	RRAB	V0576 Peg	23 10 59.5 +21 42 43	EW
V0523 Peg	22 22 28.8 +29 22 12	EW	V0577 Peg	23 11 24.7 +34 31 17	EA
V0524 Peg	22 23 41.4 +04 06 14	RRAB	V0578 Peg	23 11 38.6 +32 10 27	EA
V0525 Peg	22 25 28.1 +20 09 11	RRAB	V0579 Peg	23 11 59.6 +19 44 30	RRAB
V0526 Peg	22 25 36.8 +35 07 45	RRAB	V0580 Peg	23 12 29.0 +17 09 22	BY
V0527 Peg	22 25 58.2 +21 08 42	BY	V0581 Peg	23 13 21.7 +34 20 25	EB

Table 1 (continued)

Name	R.A., Decl., 2000.0	Type	Name	R.A., Decl., 2000.0	Type
	h m s o ' "			h m s o ' "	
V0582 Peg	23 13 59.3 +32 17 07	EW	AD PsA	22 03 23.6 -29 28 52	RRAB
V0583 Peg	23 14 55.8 +27 39 59	BY	AE PsA	22 15 55.8 -25 22 38	RRAB
V0584 Peg	23 15 06.8 +32 14 24	EW	AF PsA	22 42 26.5 -34 04 29	BY:
V0585 Peg	23 15 21.5 +29 05 01	RPHS	AG PsA	23 04 49.1 -33 45 14	RR(B)
V0586 Peg	23 17 08.2 +11 37 00	BY	V0375 Sge	19 07 58.6 +20 18 21	EA
V0587 Peg	23 17 13.2 +32 29 17	EW	V0376 Sge	19 19 49.5 +20 32 36	LB
V0588 Peg	23 18 06.6 +15 52 59	RRAB	V0377 Sge	19 29 25.0 +19 09 23	DCEP
V0589 Peg	23 20 48.1 +29 21 56	BY	V0378 Sge	19 45 34.5 +18 40 30	DSCTC:
V0590 Peg	23 21 38.8 +34 42 52	EA/RS	V0379 Sge	19 45 47.3 +18 39 38	EB
V0591 Peg	23 21 51.0 +12 47 24	RRAB	V0380 Sge	19 54 15.1 +17 12 53	EB
V0592 Peg	23 21 53.1 +23 16 56	BY	V0381 Sge	20 01 48.7 +16 30 45	DSCTC
V0593 Peg	23 22 58.5 +32 43 49	EW	V0382 Sge	20 13 52.0 +21 33 31	EA
V0594 Peg	23 23 58.5 +31 39 34	SR	V0383 Sge	20 15 14.4 +18 53 26	SR
V0595 Peg	23 26 17.1 +27 52 03	BY	V0384 Sge	20 20 18.6 +21 18 45	EA:
V0596 Peg	23 26 29.3 +31 20 41	EW	V5589 Sgr	17 45 28.0 -23 05 23	NA
V0597 Peg	23 32 04.6 +32 27 56	RS	V5590 Sgr	18 11 03.7 -27 17 29	ZAND:
V0598 Peg	23 33 26.0 +15 22 22	AM	V5591 Sgr	17 52 25.8 -21 26 22	NA
V0599 Peg	23 34 09.0 +34 18 55	EA	V5592 Sgr	18 20 27.3 -27 44 26	NA
V0600 Peg	23 34 58.9 +13 44 06	RRAB	V5593 Sgr	18 19 36.9 -19 07 41	NA
V0601 Peg	23 37 09.7 +30 37 14	EW	V5594 Sgr	17 46 56.8 -23 10 05	CWB
V0602 Peg	23 37 10.7 +31 36 11	EW	V5595 Sgr	17 47 01.9 -22 51 34	CWB
V0603 Peg	23 39 06.8 +22 04 12	BY	V5596 Sgr	17 47 16.2 -23 16 31	CWB
V0604 Peg	23 40 29.0 +29 59 12	BY	V5597 Sgr	17 49 30.9 -29 50 58	CWB
V0605 Peg	23 41 06.2 +27 06 43	BY	V5598 Sgr	17 49 51.3 -29 56 20	EP:
V0606 Peg	23 41 58.8 +18 13 01	RRAB	V5599 Sgr	17 50 21.5 -29 54 28	CWB
V0607 Peg	23 44 13.8 +32 05 23	EW	V5600 Sgr	17 50 54.0 -29 31 42	RRAB
V0608 Peg	23 44 16.2 +32 10 42	DSCT	V5601 Sgr	17 52 07.8 -29 57 01	CWB
V0609 Peg	23 45 21.0 +32 39 58	EW	V5602 Sgr	17 52 15.5 -30 00 16	CWB
V0610 Peg	23 45 50.8 +15 59 18	RRAB	V5603 Sgr	17 52 24.3 -29 39 22	EA
V0611 Peg	23 46 41.2 +17 38 03	RRAB	V5604 Sgr	17 52 26.0 -29 48 56	CWB:
V0612 Peg	23 46 43.5 +10 33 35	BY	V5605 Sgr	17 52 30.0 -29 33 02	EP:
V0613 Peg	23 47 10.9 +17 20 34	EA	V5606 Sgr	17 53 29.2 -29 48 52	CWB
V0614 Peg	23 47 20.8 +30 05 11	BY:	V5607 Sgr	17 54 06.6 -29 16 22	CWB
V0615 Peg	23 48 07.5 +32 04 48	EA	V5608 Sgr	17 54 09.1 -29 39 59	CWB
V0616 Peg	23 49 37.3 +20 25 42	RRAB	V5609 Sgr	17 54 55.6 -29 57 31	CWB
V0617 Peg	23 49 45.4 +31 26 27	BY	V5610 Sgr	17 54 59.2 -29 19 39	EA
V0618 Peg	23 56 00.8 +10 53 19	RRAB	V5611 Sgr	17 55 06.8 -29 18 08	CWB
V0619 Peg	23 56 57.8 +10 48 16	EW	V5612 Sgr	17 55 08.3 -29 48 51	EA
V0620 Peg	23 59 52.7 +29 49 47	BY	V5613 Sgr	17 55 23.1 -29 31 36	CWA
V0965 Per	03 11 16.2 +37 05 03	N	V5614 Sgr	17 55 43.8 -29 44 50	CWB
DH Phe	23 41 06.6 -42 08 49	RRC	V5615 Sgr	17 56 05.0 -29 54 52	CWB:
DI Phe	23 54 20.4 -47 00 21	EA+NL	V5616 Sgr	17 56 12.6 -29 45 02	EA
HW Psc	22 54 16.4 +03 04 48	RRAB	V5617 Sgr	17 58 01.5 -28 59 57	CWB
HX Psc	22 56 48.1 +05 22 09	RRAB	V5618 Sgr	17 58 03.4 -29 01 13	CWB
HY Psc	23 03 51.7 +01 06 51	UG	V5619 Sgr	17 58 14.6 -31 33 24	CWB
HZ Psc	23 15 26.1 +02 36 05	BY	V5620 Sgr	17 58 39.5 -33 20 34	EW
II Psc	23 15 56.7 +03 02 59	RRAB	V5621 Sgr	17 58 56.0 -28 43 20	CWB
IK Psc	23 20 09.4 +06 32 22	EW	V5622 Sgr	17 59 40.9 -33 39 11	LPB
IL Psc	23 22 01.4 +06 24 42	RRAB	V5623 Sgr	18 01 04.5 -28 41 21	CWB
IM Psc	23 22 06.5 +06 35 15	UV	V5624 Sgr	18 01 06.5 -17 44 23	M
IN Psc	23 36 37.4 -02 12 45	RRAB	V5625 Sgr	18 01 32.7 -29 49 12	CWB
IO Psc	23 50 51.1 -01 09 23	BY	V5626 Sgr	18 01 47.3 -29 07 39	CWB
IP Psc	23 57 57.3 -01 09 48	BY	V5627 Sgr	18 01 56.3 -27 22 56	UG:+E
AC PsA	21 40 03.9 -35 33 05	EW	V5628 Sgr	18 01 56.8 -28 55 12	CWB:

Table 1 (continued)

Name	R.A., Decl., 2000.0 h m s o ' "	Type	Name	R.A., Decl., 2000.0 h m s o ' "	Type
V5629 Sgr	18 02 56.0 -28 40 39	CWB	V1341 Sco	16 40 24.8 -44 24 53	RCB:
V5630 Sgr	18 04 19.9 -29 02 44	CWB	V1342 Sco	16 40 36.1 -44 24 27	EA
V5631 Sgr	18 06 04.7 -24 11 44	EA	V1343 Sco	16 40 46.8 -44 31 34	M
V5632 Sgr	18 06 42.0 -23 44 22	M	V1344 Sco	16 41 00.4 -44 28 23	M
V5633 Sgr	18 08 07.5 -34 34 32	BCEP	V1345 Sco	16 41 06.1 -44 32 46	M
V5634 Sgr	18 09 51.1 -19 43 52	XP	V1346 Sco	16 41 13.5 -45 06 14	M
V5635 Sgr	18 10 31.3 -26 04 56	CWB	V1347 Sco	16 41 13.9 -44 28 53	M
V5636 Sgr	18 10 34.2 -26 08 38	CEP:	V1348 Sco	16 41 21.5 -44 51 11	M
V5637 Sgr	18 13 12.2 -17 28 08	SRB	V1349 Sco	16 41 38.5 -44 26 06	M
V5638 Sgr	18 15 01.4 -22 43 58	M	V1350 Sco	16 41 46.8 -44 57 35	M
V5639 Sgr	18 16 39.2 -24 18 33	RCB	V1351 Sco	16 41 51.1 -44 36 06	M
V5640 Sgr	18 19 23.1 -28 28 57	DSCTC:	V1352 Sco	16 41 59.8 -45 06 09	M
V5641 Sgr	18 26 10.3 -17 04 21	BCEP	V1353 Sco	16 42 14.2 -44 15 51	M
V5642 Sgr	18 31 05.6 -25 11 37	M	V1354 Sco	16 42 14.6 -44 48 46	EB
V5643 Sgr	18 33 24.0 -19 30 20	EA	V1355 Sco	16 42 26.0 -44 37 28	M
V5644 Sgr	18 39 51.9 -32 00 55	RR(B)	V1356 Sco	16 42 37.7 -44 23 14	M
V5645 Sgr	18 41 16.7 -29 04 41	M	V1357 Sco	16 42 58.9 -44 10 59	M:
V5646 Sgr	18 42 50.9 -27 08 55	M	V1358 Sco	16 43 27.7 -44 16 13	M
V5647 Sgr	18 44 19.6 -20 33 07	M	V1359 Sco	16 43 36.6 -44 43 23	M
V5648 Sgr	18 52 43.6 -16 00 48	EA	V1360 Sco	16 43 47.5 -44 38 06	M
V5649 Sgr	19 02 55.8 -14 15 02	SRA:	V1361 Sco	16 44 25.3 -44 30 24	M
V5650 Sgr	19 07 26.6 -20 49 11	EB	V1362 Sco	16 44 46.9 -44 11 06	M
V5651 Sgr	19 11 34.7 -34 35 09	RS	V1363 Sco	16 49 38.6 -44 31 41	BCEP
V5652 Sgr	19 15 33.2 -24 10 46	BY	V1364 Sco	16 53 14.0 -43 44 58	BCEP
V5653 Sgr	19 30 08.7 -25 36 03	EA	V1365 Sco	16 54 29.5 -41 39 15	EA
V5654 Sgr	19 34 43.5 -24 22 14	EA	V1366 Sco	16 58 06.3 -42 19 24	M
V5655 Sgr	19 39 06.4 -25 44 06	RS	V1367 Sco	17 00 05.4 -44 44 14	EW
V5656 Sgr	19 42 17.1 -14 58 14	EA	V1368 Sco	17 00 06.2 -44 39 16	EW
V5657 Sgr	19 42 49.1 -41 19 52	EA:	V1369 Sco	17 00 08.2 -44 36 00	EW
V5658 Sgr	19 59 04.7 -37 50 28	EA	V1370 Sco	17 00 08.3 -44 43 43	EA
V5659 Sgr	19 59 26.7 -34 00 04	RRAB	V1371 Sco	17 00 09.1 -44 44 31	LB
V5660 Sgr	20 01 52.0 -17 52 01	BY	V1372 Sco	17 00 12.1 -44 39 53	EA
V5661 Sgr	20 02 27.9 -37 00 17	RRAB	V1373 Sco	17 00 18.7 -44 38 02	EA
V5662 Sgr	20 05 51.1 -29 35 00	NL	V1374 Sco	17 00 20.4 -44 44 02	EW
V5663 Sgr	20 05 56.4 -32 16 59	RS	V1375 Sco	17 00 21.3 -44 45 43	SR:
V5664 Sgr	20 07 49.4 -42 43 47	RRC:	V1376 Sco	17 00 25.0 -44 46 49	EW
V5665 Sgr	20 13 49.1 -37 49 27	RRAB	V1377 Sco	17 00 26.2 -44 39 55	EW
V1324 Sco	17 50 53.9 -32 37 21	NA	V1378 Sco	17 00 27.3 -44 42 27	EW
V1325 Sco	16 00 28.9 -29 11 53	EA	V1379 Sco	17 00 28.9 -44 39 35	M
V1326 Sco	16 02 42.7 -26 54 38	M	V1380 Sco	17 00 30.6 -44 35 57	EA
V1327 Sco	16 02 54.0 -20 22 48	RS	V1381 Sco	17 00 34.7 -44 39 13	EA
V1328 Sco	16 03 31.9 -28 12 08	SRB	V1382 Sco	17 00 37.1 -44 36 34	EA
V1329 Sco	16 09 36.2 -21 53 52	RRAB	V1383 Sco	17 00 37.9 -44 35 15	EW
V1330 Sco	16 23 07.8 -23 01 00	INT:	V1384 Sco	17 00 43.1 -44 42 58	EW
V1331 Sco	16 23 53.2 -26 22 24	GDOR	V1385 Sco	17 00 44.1 -44 22 05	M
V1332 Sco	16 24 02.0 -29 10 45	IT:	V1386 Sco	17 00 44.4 -44 43 03	EW
V1333 Sco	16 26 20.4 -34 17 13	SRD	V1387 Sco	17 00 45.0 -44 23 18	M
V1334 Sco	16 28 59.6 -32 06 59	EA	V1388 Sco	17 00 46.3 -44 41 57	M
V1335 Sco	16 39 56.6 -45 16 28	M	V1389 Sco	17 00 46.5 -44 29 21	M
V1336 Sco	16 40 12.1 -44 33 20	M	V1390 Sco	17 00 46.6 -44 39 56	EW
V1337 Sco	16 40 13.0 -45 06 06	M	V1391 Sco	17 00 47.1 -44 37 18	EA
V1338 Sco	16 40 22.4 -45 13 43	M	V1392 Sco	17 00 47.7 -44 34 17	LB
V1339 Sco	16 40 23.0 -44 41 48	M	V1393 Sco	17 00 50.8 -44 38 47	EW
V1340 Sco	16 40 23.4 -45 11 14	M	V1394 Sco	17 00 51.0 -44 44 11	EW

Table 1 (continued)

Name	R.A., Decl., 2000.0 h m s o ' "	Type	Name	R.A., Decl., 2000.0 h m s o ' "	Type
V1395 Sco	17 00 53.8 -44 45 17	EW	V1449 Sco	17 12 06.0 -32 17 05	M
V1396 Sco	17 00 59.3 -44 37 26	SR	V1450 Sco	17 12 13.8 -32 18 49	M
V1397 Sco	17 00 59.3 -44 34 32	EW	V1451 Sco	17 12 15.1 -33 15 18	M
V1398 Sco	17 01 00.8 -44 40 37	EA	V1452 Sco	17 12 18.4 -33 06 03	BCEP
V1399 Sco	17 01 00.9 -44 13 27	M	V1453 Sco	17 12 23.2 -34 06 46	M
V1400 Sco	17 01 05.5 -44 36 31	SR	V1454 Sco	17 12 31.8 -32 48 46	M
V1401 Sco	17 01 06.2 -44 35 24	EA	V1455 Sco	17 12 41.3 -32 04 52	M
V1402 Sco	17 01 06.3 -44 42 52	M:	V1456 Sco	17 12 54.0 -32 14 24	M
V1403 Sco	17 01 07.0 -44 39 56	EB	V1457 Sco	17 13 01.1 -33 41 36	M
V1404 Sco	17 01 09.3 -44 45 24	EW	V1458 Sco	17 13 02.9 -33 36 12	M
V1405 Sco	17 01 10.0 -44 36 31	SR	V1459 Sco	17 13 10.4 -32 39 20	M
V1406 Sco	17 01 10.1 -44 42 55	EW	V1460 Sco	17 13 11.1 -32 49 16	M
V1407 Sco	17 01 11.0 -44 55 00	M	V1461 Sco	17 13 13.1 -37 44 07	EA
V1408 Sco	17 01 12.0 -44 42 36	EW	V1462 Sco	17 13 15.2 -32 07 25	M
V1409 Sco	17 01 12.4 -44 36 20	EW	V1463 Sco	17 13 24.1 -32 11 59	M
V1410 Sco	17 01 13.8 -44 34 05	EB	V1464 Sco	17 13 33.1 -32 56 52	M
V1411 Sco	17 01 16.6 -44 41 28	EW	V1465 Sco	17 13 37.4 -33 08 31	M
V1412 Sco	17 01 19.8 -44 37 48	EA	V1466 Sco	17 13 54.4 -32 54 02	M
V1413 Sco	17 01 34.8 -44 26 44	M	V1467 Sco	17 13 56.7 -34 01 57	M
V1414 Sco	17 01 38.0 -44 28 56	M	V1468 Sco	17 13 59.5 -32 26 55	M
V1415 Sco	17 01 50.8 -44 15 16	M	V1469 Sco	17 13 59.9 -37 50 14	M
V1416 Sco	17 01 52.4 -44 45 28	M	V1470 Sco	17 14 00.2 -32 03 14	M
V1417 Sco	17 02 14.2 -44 24 09	M	V1471 Sco	17 14 00.3 -32 51 58	M
V1418 Sco	17 02 26.2 -44 17 17	M	V1472 Sco	17 14 03.3 -32 00 31	M
V1419 Sco	17 02 42.4 -44 27 28	M	V1473 Sco	17 14 04.3 -32 21 49	M
V1420 Sco	17 03 09.7 -44 27 03	M	V1474 Sco	17 14 06.1 -32 04 32	M
V1421 Sco	17 04 02.2 -44 32 19	M	V1475 Sco	17 14 06.3 -32 03 19	M
V1422 Sco	17 04 14.6 -44 10 53	M	V1476 Sco	17 14 09.8 -33 07 56	M
V1423 Sco	17 04 32.0 -44 50 19	M	V1477 Sco	17 14 23.3 -32 27 20	M
V1424 Sco	17 04 35.6 -44 30 43	M	V1478 Sco	17 14 35.6 -33 40 34	M
V1425 Sco	17 04 43.5 -44 27 30	M	V1479 Sco	17 14 39.7 -32 24 53	M
V1426 Sco	17 04 56.4 -44 33 54	M	V1480 Sco	17 14 40.4 -32 25 59	M
V1427 Sco	17 04 57.3 -44 37 07	M	V1481 Sco	17 14 42.0 -32 09 10	M
V1428 Sco	17 05 06.1 -44 26 26	RRAB	V1482 Sco	17 14 43.5 -32 10 22	M
V1429 Sco	17 05 14.5 -44 23 16	M	V1483 Sco	17 14 48.7 -32 41 20	M
V1430 Sco	17 07 58.0 -34 26 12	DSCT	V1484 Sco	17 14 53.7 -32 06 22	M
V1431 Sco	17 11 02.7 -34 02 47	M	V1485 Sco	17 15 15.0 -33 25 21	M
V1432 Sco	17 11 15.5 -32 38 05	M	V1486 Sco	17 15 22.1 -32 20 41	M
V1433 Sco	17 11 16.7 -33 58 59	M	V1487 Sco	17 15 22.9 -32 36 18	M
V1434 Sco	17 11 20.3 -32 26 28	M	V1488 Sco	17 15 24.5 -32 28 17	M
V1435 Sco	17 11 27.4 -32 56 23	M	V1489 Sco	17 15 26.4 -32 26 46	M
V1436 Sco	17 11 32.3 -32 24 57	M	V1490 Sco	17 15 29.1 -32 14 29	M
V1437 Sco	17 11 32.5 -32 29 11	M	V1491 Sco	17 15 33.7 -32 46 25	M
V1438 Sco	17 11 34.4 -32 12 27	M	V1492 Sco	17 16 30.1 -33 36 23	M
V1439 Sco	17 11 41.8 -33 27 40	M	V1493 Sco	17 16 32.7 -39 10 46	M
V1440 Sco	17 11 43.1 -33 28 03	M	V1494 Sco	17 16 34.6 -32 38 52	M
V1441 Sco	17 11 43.2 -33 17 27	M	V1495 Sco	17 16 39.0 -32 40 00	M
V1442 Sco	17 11 50.2 -32 34 53	M	V1496 Sco	17 16 52.4 -33 00 28	M
V1443 Sco	17 11 51.7 -32 51 49	M	V1497 Sco	17 17 09.8 -34 15 48	M
V1444 Sco	17 11 53.0 -33 00 52	M	V1498 Sco	17 17 19.7 -32 46 12	M
V1445 Sco	17 11 53.1 -33 19 49	M	V1499 Sco	17 17 22.1 -32 17 29	M
V1446 Sco	17 11 53.7 -32 59 48	M	V1500 Sco	17 17 58.7 -34 13 15	M
V1447 Sco	17 11 55.9 -32 57 54	M	V1501 Sco	17 18 06.9 -32 47 30	M
V1448 Sco	17 12 05.3 -32 13 38	M	V1502 Sco	17 18 34.2 -32 07 36	M

Table 1 (continued)

Name	R.A., Decl., 2000.0 h m s o ' "	Type	Name	R.A., Decl., 2000.0 h m s o ' "	Type
V1503 Sco	17 25 13.1 -39 19 22	M	V0510 Ser	16 07 04.3 +02 38 24	RS
V1504 Sco	17 26 58.7 -43 33 13	RVB	V0511 Ser	16 07 12.1 -01 45 22	RRAB
V1505 Sco	17 27 24.1 -39 51 31	CWB	V0512 Ser	16 07 39.1 -00 47 13	RRAB
V1506 Sco	17 27 38.2 -38 08 36	EW	V0513 Ser	16 08 07.2 +11 22 28	RRAB
V1507 Sco	17 32 28.2 -34 03 14	LB	V0514 Ser	16 08 55.0 -00 15 45	RRAB
V1508 Sco	17 34 18.5 -34 06 51	EA	V0515 Ser	16 08 59.9 -01 21 45	RRAB
V1509 Sco	17 34 20.6 -32 29 19	IT	V0516 Ser	16 09 15.8 -02 00 40	RRAB
V1510 Sco	17 34 47.9 -32 31 51	BY:	V0517 Ser	16 09 20.3 -01 00 16	RRAB
V1511 Sco	17 34 48.5 -32 37 21	DSCTC	V0518 Ser	16 09 59.7 -01 54 04	RRAB
V1512 Sco	17 35 10.2 -32 29 04	DSCTC	V0519 Ser	16 10 07.5 +03 52 33	XM
V1513 Sco	17 47 23.2 -37 12 36	CWB	V0520 Ser	16 11 32.5 +00 31 11	SRB
V1514 Sco	17 47 48.5 -35 16 06	CWA	V0521 Ser	16 11 59.4 -00 41 38	RRAB
V1515 Sco	17 48 12.2 -40 49 36	M	V0522 Ser	16 12 44.5 -00 21 44	RRAB
V1516 Sco	17 49 50.0 -40 07 58	M	V0523 Ser	16 15 09.8 -01 49 36	RRC
V1517 Sco	17 50 08.5 -37 04 14	DSCT	V0524 Ser	16 15 41.2 -00 05 24	RRAB
V1518 Sco	17 50 13.1 -30 20 56	CWB	V0525 Ser	16 17 48.2 +00 03 00	RRAB
V1519 Sco	17 50 38.6 -30 03 49	CWB	V0526 Ser	16 21 28.1 -01 00 42	RRAB
V1520 Sco	17 50 58.6 -37 02 19	RRAB	V0527 Ser	17 35 13.1 -10 15 12	CWA:
V1521 Sco	17 50 59.0 -33 08 53	CWB	V0528 Ser	17 43 14.6 -14 58 04	RRAB
V1522 Sco	17 51 42.5 -32 41 41	CWB	V0529 Ser	17 47 03.6 -12 37 15	SRA
V1523 Sco	17 52 36.2 -30 08 33	CWB	V0530 Ser	17 57 33.1 -03 36 12	LB
V1524 Sco	17 53 27.8 -30 19 55	CWB	V0531 Ser	17 59 36.1 -01 25 03	SRB
V1525 Sco	17 53 34.8 -30 12 40	CWB	V0532 Ser	17 59 59.2 -00 41 13	SRA
V1526 Sco	17 53 44.4 -32 57 14	RRAB	V0533 Ser	18 06 57.5 -00 24 56	SRB
V1527 Sco	17 54 00.1 -33 08 23	CWB	V0534 Ser	18 08 41.9 -14 18 59	DSCTC
V1528 Sco	17 54 24.3 -33 06 51	CWB	V0535 Ser	18 09 24.3 -07 22 14	M
V1529 Sco	17 54 38.3 -30 10 42	CWB	V0536 Ser	18 11 30.6 -15 55 34	DCEP:
V1530 Sco	17 55 12.4 -30 07 24	CWB	V0537 Ser	18 11 35.6 -02 19 46	LB
V1531 Sco	17 56 33.0 -30 36 34	CWB:	V0538 Ser	18 14 17.7 -01 05 00	SR:
V1532 Sco	17 56 46.5 -31 07 08	CWB	V0539 Ser	18 17 16.1 -15 27 06	BCEP
CV Scl	23 09 30.5 -35 47 17	RRAB	V0540 Ser	18 23 27.6 +06 12 05	DSCTC:
CW Scl	23 28 01.1 -33 59 52	EW	V0541 Ser	18 24 40.2 +06 10 04	DSCTC:
CX Scl	23 45 20.2 -31 00 25	E+DSCTC	V0542 Ser	18 24 45.3 +06 05 31	RRC:
V0497 Sct	18 24 09.7 -10 37 38	SRB	V0543 Ser	18 24 55.0 -00 57 14	LB
V0498 Sct	18 26 16.9 -15 15 43	BCEP	V0544 Ser	18 25 22.0 -00 00 43	X
V0499 Sct	18 26 39.5 -06 54 04	M	V0545 Ser	18 27 53.3 +06 08 51	BCEP:
V0500 Sct	18 27 25.9 -14 42 08	BCEP	V0546 Ser	18 28 04.1 +05 58 13	DSCTC:
V0501 Sct	18 27 34.2 -08 37 23	M	V0547 Ser	18 28 24.4 +06 13 36	E
V0502 Sct	18 34 14.6 -05 59 51	SRB	V0548 Ser	18 28 39.0 +04 54 48	EA
V0503 Sct	18 36 30.6 -13 09 11	SRB	V0549 Ser	18 29 17.7 +05 39 19	DSCTC:
V0504 Sct	18 38 14.1 -05 31 15	M	V0550 Ser	18 29 34.1 +03 02 35	EA
V0505 Sct	18 56 14.8 -04 12 49	M:	V0551 Ser	18 30 29.0 +05 48 38	DSCTC:
V0506 Sct	18 57 18.2 -10 01 50	SRA	V0552 Ser	18 31 59.1 +05 40 20	BY
V0499 Ser	16 00 43.6 +07 48 03	RPHS	V0553 Ser	18 33 17.4 +05 59 31	RRC:
V0500 Ser	16 00 46.7 +24 15 39	EW	V0554 Ser	18 40 10.1 -00 47 42	EA
V0501 Ser	16 01 04.6 -00 57 20	RRC	V0555 Ser	18 42 56.0 +04 35 00	EA
V0502 Ser	16 01 05.6 -00 13 07	LB	V0370 Tel	18 21 05.1 -54 07 45	EA
V0503 Ser	16 01 35.5 -01 13 59	RRAB	V0371 Tel	18 26 08.3 -56 02 09	RRAB
V0504 Ser	16 01 52.3 +22 22 48	RRAB	V0372 Tel	18 27 40.8 -51 53 04	RRAB
V0505 Ser	16 02 48.2 +25 20 38	EA+RS	V0373 Tel	18 30 16.5 -52 12 30	RRAB
V0506 Ser	16 02 58.6 -00 14 03	RRC	V0374 Tel	18 40 35.3 -53 50 32	RR(B)
V0507 Ser	16 03 08.7 -00 18 57	RRAB	V0375 Tel	18 41 41.1 -55 03 33	RRAB
V0508 Ser	16 05 25.6 +01 30 46	EW	V0376 Tel	18 47 40.4 -48 36 03	CWA
V0509 Ser	16 05 29.2 -01 19 53	RRAB	V0377 Tel	19 08 58.7 -47 14 09	RRAB

Table 1 (continued)

Name	R.A., Decl., 2000.0 h m s o ' "	Type	Name	R.A., Decl., 2000.0 h m s o ' "	Type
V0378 Tel	19 22 39.0 -45 40 23	RRAB	V0477 Vul	19 43 06.8 +23 16 37	DSCTC
V0379 Tel	19 28 32.5 -50 01 34	E+AM	V0478 Vul	19 43 09.0 +23 17 07	INB:
V0380 Tel	19 47 22.4 -54 31 29	RRAB	V0479 Vul	19 43 09.1 +23 17 49	DSCTC
V0381 Tel	19 56 12.0 -50 43 46	RR(B)	V0480 Vul	19 43 09.3 +23 16 12	INB:
V0382 Tel	20 09 55.2 -45 59 47	RS	V0481 Vul	19 43 10.5 +23 17 25	ELL
V0337 TrA	16 00 07.0 -68 35 17	M	V0482 Vul	19 43 11.6 +23 18 20	LB
V0338 TrA	16 02 28.7 -67 29 10	SR	V0483 Vul	19 43 11.6 +23 18 26	INB:
V0339 TrA	16 03 22.4 -67 47 51	M	V0484 Vul	19 43 11.7 +23 16 00	LB:
V0340 TrA	16 03 46.9 -64 11 03	M	V0485 Vul	19 43 12.2 +23 17 17	LPB:
V0341 TrA	16 04 12.0 -69 10 02	RRAB	V0486 Vul	19 43 12.9 +23 18 19	INB:
V0342 TrA	16 06 04.8 -64 53 19	SRA	V0487 Vul	19 43 14.6 +23 16 01	EA
V0343 TrA	16 16 45.9 -60 44 20	LB	V0488 Vul	19 43 20.3 +23 19 20	INB:
V0344 TrA	16 48 01.2 -67 15 10	EW	V0489 Vul	19 43 21.0 +23 19 02	LB
V0345 TrA	16 48 03.1 -67 15 18	EA	V0490 Vul	19 43 52.7 +23 11 41	SRB
EO Tuc	22 24 17.8 -65 41 03	RRAB	V0491 Vul	19 46 22.7 +24 37 48	EA
EP Tuc	22 34 26.7 -56 35 25	RRAB	V0492 Vul	19 47 55.4 +27 22 56	SRB
EQ Tuc	22 38 35.7 -63 34 21	BY	V0493 Vul	19 51 52.8 +27 25 03	EB
ER Tuc	22 49 15.8 -66 30 41	RRAB	V0494 Vul	19 53 16.6 +20 33 43	DSCT
ES Tuc	22 57 26.0 -56 45 41	BY	V0495 Vul	19 53 45.3 +20 30 33	EA
ET Tuc	23 30 01.0 -66 47 23	RRAB	V0496 Vul	19 53 49.7 +23 30 40	EW
EU Tuc	23 35 31.1 -64 00 52	RRAB	V0497 Vul	19 55 11.6 +24 57 10	EW
EV Tuc	23 39 00.9 -64 45 31	RRAB	V0498 Vul	19 59 51.3 +22 42 32	UGSU
AB UMi	16 03 31.0 +77 11 12	RRC	V0499 Vul	20 17 50.7 +28 58 07	EA
AC UMi	16 13 19.9 +81 23 35	EA	V0500 Vul	20 20 56.2 +21 00 45	EA
AD UMi	16 19 47.5 +83 08 53	LB	V0501 Vul	20 21 14.4 +21 51 29	EW
AE UMi	16 46 08.9 +83 15 33	EA	V0502 Vul	20 31 01.0 +24 02 00	EA
AF UMi	17 00 24.5 +80 36 39	RRAB	V0503 Vul	20 35 29.5 +26 07 25	EW
AG UMi	17 10 22.5 +78 14 59	RRAB	V0504 Vul	20 39 04.7 +23 38 47	BY
AH UMi	17 22 27.4 +80 13 59	EA	V0505 Vul	20 40 09.1 +25 03 30	SR
AI UMi	19 36 53.6 +88 27 23	EW	V0506 Vul	20 42 32.1 +20 36 45	SR
AK UMi	19 40 42.5 +86 21 09	RRC:	V0507 Vul	20 49 45.8 +24 12 45	RRC
AL UMi	19 57 12.2 +86 45 26	EW	V0508 Vul	20 50 59.2 +26 28 14	LB
V0468 Vul	19 11 45.8 +22 31 05	SR	V0509 Vul	20 52 05.9 +21 49 22	RRAB
V0469 Vul	19 28 52.2 +27 10 01	LB:	V0510 Vul	20 56 59.6 +23 44 30	BY
V0470 Vul	19 28 54.0 +22 21 36	LB	V0511 Vul	20 58 18.8 +25 28 14	EW
V0471 Vul	19 34 15.8 +19 34 15	DCEP	V0512 Vul	21 03 38.2 +21 28 08	EA
V0472 Vul	19 37 09.2 +19 53 52	EA	V0513 Vul	21 04 55.7 +24 56 15	EW
V0473 Vul	19 37 51.9 +21 35 26	EB	V0514 Vul	21 07 04.6 +24 45 41	EB
V0474 Vul	19 41 51.1 +22 24 13	DCEP	V0515 Vul	21 25 19.6 +26 56 54	BY
V0475 Vul	19 42 59.1 +23 17 48	LB	V0516 Vul	21 30 09.2 +25 10 42	EW:
V0476 Vul	19 43 06.0 +23 16 49	INB:			

Remarks for unusual variable stars (type *).

V1801 Aql. A post-asymptotic-branch star. Spectroscopic binary, $P_{\rm orb} = 119\overset{\rm d}{.}5$, $e = 0.37$. $P_{\rm orb}$ is not detected in photometry.

V1815 Aql. A magnetic white dwarf, varies presumably due to starspots and axial rotation.

V0354 Dra. A magnetic white dwarf with unusual properties. Variations are probably related to spots and axial rotation.

V0722 Lyr. A post-asymptotic-branch star with non-periodic, sometimes rapid, brightness variations.

Table 2. Novae

GCVS	Nova name	GCVS	Nova name
V1724 Aql	Nova Aql 2012	V0965 Per	Nova Per 2011
V0834 Car	Nova Car 2012	V5589 Sgr	Nova Sgr 2012 No. 1
V1368 Cen	Nova Cen 2012	V5590 Sgr	Nova Sgr 2012 No. 2
V0809 Cep	Nova Cep 2013	V5591 Sgr	Nova Sgr 2012 No. 3
V0959 Mon	Nova Mon 2012	V5592 Sgr	Nova Sgr 2012 No. 4
V2676 Oph	Nova Oph 2012 No. 1	V5593 Sgr	Nova Sgr 2012 No. 5
V2677 Oph	Nova Oph 2012 No. 2	V1324 Sco	Nova Sco 2012

COMMISSIONS 27 AND 42 OF THE IAU
INFORMATION BULLETIN ON VARIABLE STARS

Number 6053

Konkoly Observatory
Budapest
11 April 2013

HU ISSN 0374 – 0676

CONFIRMING THE DELTA SCUTI NATURE OF GSC 02696-02622

ZHANG, LIYUN; PI, QINGFENG; ZHANG, GUOYIN

College of Science/Department of Physics & NAOC-GZU-Sponsored Center for Astronomy Research, Guizhou University, Guiyang 550025, P.R. China; e-mail: liy_zhang@hotmail.com

GSC 02696-02622 (α_{2000}=$20^{\rm h}58^{\rm m}02\overset{\rm s}{.}6$, δ_{2000}=+35°09′19″.4; 2MASS J20580154+3509196) is a bright star ($B = 10\overset{\rm m}{.}77$, $V = 10\overset{\rm m}{.}39$; Høg et al. 2000). GSC 02696-02622 has been chosen several times as a comparison star by Yu (1923) and Dapergolas et al. (1988). Since 1991, this star has been suspected to be a variable star (Heckert & Zeilik 1991). In 2008, the observations of Hambalek (2008) showed very small variations ($\Delta B \cong 0.07$ mag, $\Delta V \cong 0.05$ mag, $\Delta R \cong \Delta I \cong 0.04$ mag). Recently, Nanouris & Antonopoulou (2010) found the star to be variable by 0.04 mag and 0.08 mag in B and V filters, respectively. In this paper, we present our new higher time-resolution light curves and SuperWASP data of GSC 02696-02622, and discuss its properties.

Our new photometric observations were carried out on three consecutive nights (Oct. 1, 2 and 3, 2009) with the 85-cm telescope of Xinglong station of the National Astronomical Observatories of China (NAOC). The photometer was equipped with a 1024×1024 pixel CCD and the standard Johnson-Cousins-Bessell $BVRI$ filters (Zhou et al. 2009). Each pixel of the CCD camera covers about 0.96″ on the sky, leading to a field of view of 16.5′× 16.5′. Exposure times were 7, 4, 3 and 2 s in B, V, R, and I bands, respectively. All observed CCD images were reduced by means of the IRAF* package in the standard fashion. The star GSC 02696-02207 and the star (α_{2000}= $20^{\rm h}57^{\rm m}50\overset{\rm s}{.}5$; δ_{2000}= +35°15′11″.4) served as comparison and check stars, respectively. Figure 1 shows the light curves of GSC 02696-02622. The errors of individual points are about 0.007 mag in all bands. The photometric observations are made available online at the IBVS website (*6053-t2.txt*), as Heliocentric Julian Date (HJD) and the delta magnitude (Variable minus Comparison star) in $BVRI$ bands.

Our light curves show that GSC 02696-02622 is obviously an oscillating variable. To search for periodicity of the light variation, a Fourier analysis was performed by using the software package Period04 (Lenz & Breger 2005). The $BVRI$ amplitude spectra of GSC 02696-02622 for our data are given in Figure 2, and the spectral window of GSC 02696-02622 in B band is plotted in Figure 3. At the same time, we also collected published data (`http://www.wasp.le.ac.uk/public/lc/index.php`) of GSC 02696-02622 (see Figure 4, *6053-t3.txt*) from the SuperWASP photometric survey (Pollacco et al. 2006). The amplitude spectra and spectral window of the SuperWASP

* IRAF is distributed by the National Optical Astronomy Observatories, which are operated by the Association of Universities for Research in Astronomy, Inc., under cooperative agreement with the National Science Foundation.

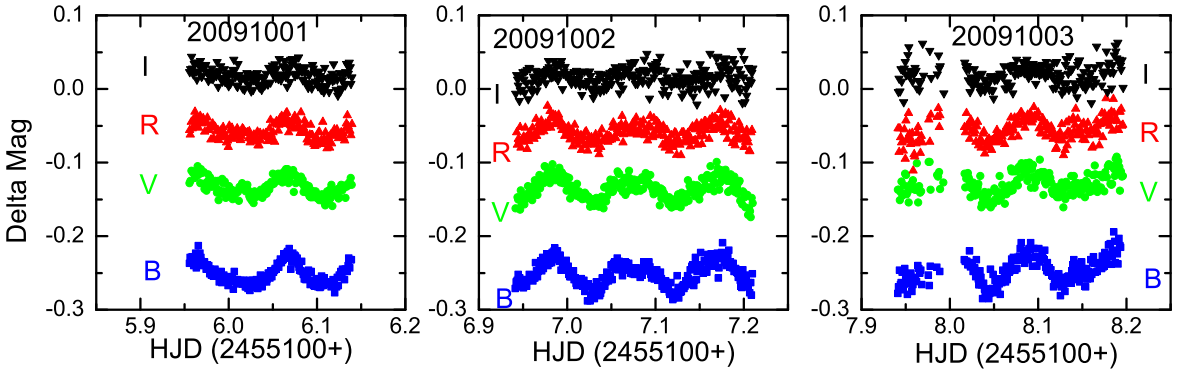

Figure 1. New Light curves for GSC 02696-02622 at Xinglong station, NAOC, in Oct. 2009.

data for GSC 02696-02622 are plotted in Figures 5 and 6, respectively. The results of the frequency analysis for GSC 02696-02622 are given in Table 1. The errors of the amplitudes were determined by using the formal least-squares method, which tend to be smaller than the real errors (Montgomery & O'Donoghue 1999). For our data, maximum amplitudes are 0.0185 mag, 0.0144 mag, 0.0118 mag, and 0.0077 mag in $BVRI$ band, respectively . For the SuperWASP data, maximum amplitude is 0.0135 mag in V band, which is similar to the result from our data of V band. Our obtained amplitudes are smaller than the previous results (Hambalek 2008; Nanouris & Antonopoulou 2010). This is an indication that the amplitude might vary. This phenomenon was also found in other delta Scuti stars, such as BR Cancri (Zhou et al. 2001). The dominant oscillation period of GSC 02696-02622 is about 2.21 hours for BVR bands. Other potential frequencies are weak, as can be seen from the frequency spectra (Figures 2 and 5). Because the data in the I band show larger scatter, we used the frequency of the other bands to calculate the amplitude value of the I band. Our results of oscillation period are similar to the previous results (Hambalek 2008; Nanouris & Antonopoulou 2010).The star's colour index $J-H=0.126$ mag (Cutri et al. 2003) corresponds to effective temperature of 6638 $\pm$ 92 K (Collier Cameron et al. 2007), which suggests the spectral type to be about F5. The main period and amplitude are wholly consistent with delta Scuti pulsation. Therefore, we confirmed that it is a δ Scuti variable star with an amplitude smaller than 0.02 mag. More time-series photometric data and spectroscopic observations are needed to determine a more accurate spectral type and study the multi-periodic nature of the pulsation.

Table 1. The pulsation properties of GSC 02696-02622.

Band	Peak Amplitude	Uncertainty	Frequency	Source
	mag	mag	d^{-1}	
B	0.0185	0.0005	10.86	Our observation
V	0.0144	0.0006	10.85	Our observation
R	0.0118	0.0006	10.85	Our observation
I	0.0077	0.0007	10.85	Our observation
V	0.0135	0.0003	10.86	SuperWASP

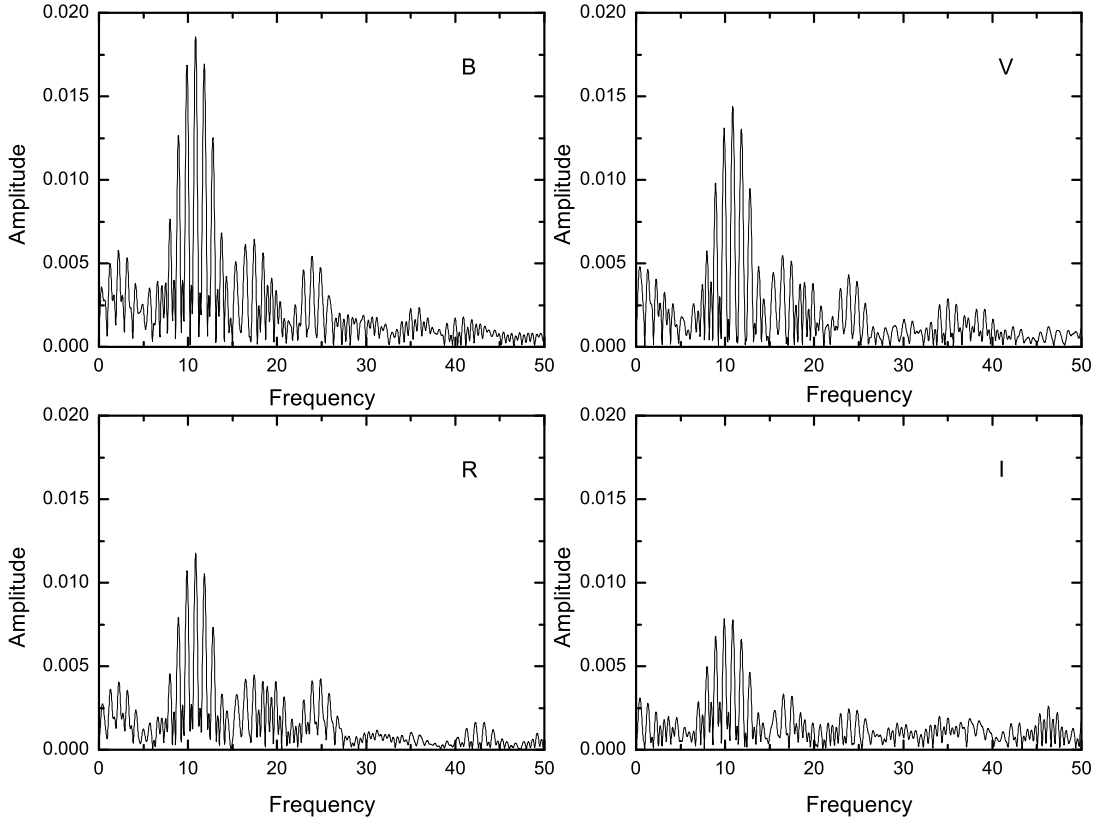

Figure 2. Amplitude spectrum of GSC 02696-02622 for our observational data in $BVRI$ bands.

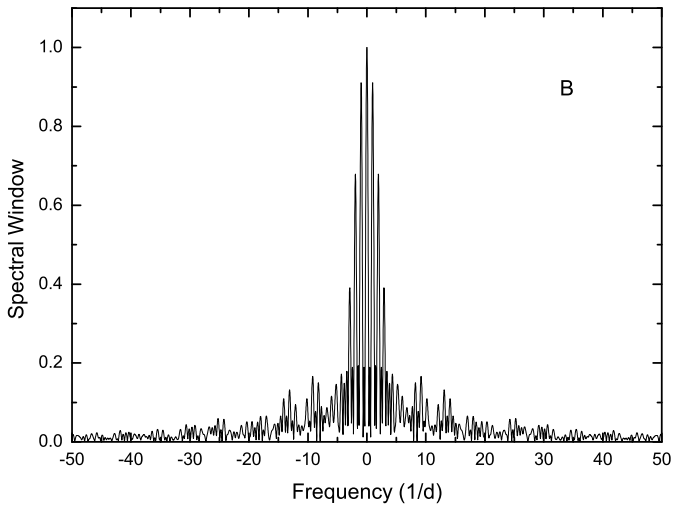

Figure 3. Spectral window of GSC 02696-02622 for our observational data in B band.

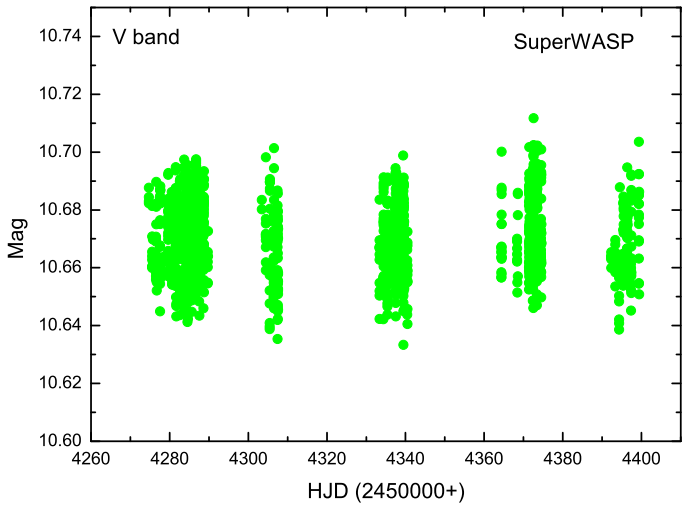

Figure 4. Light curve for GSC 02696-02622 from SuperWASP survey.

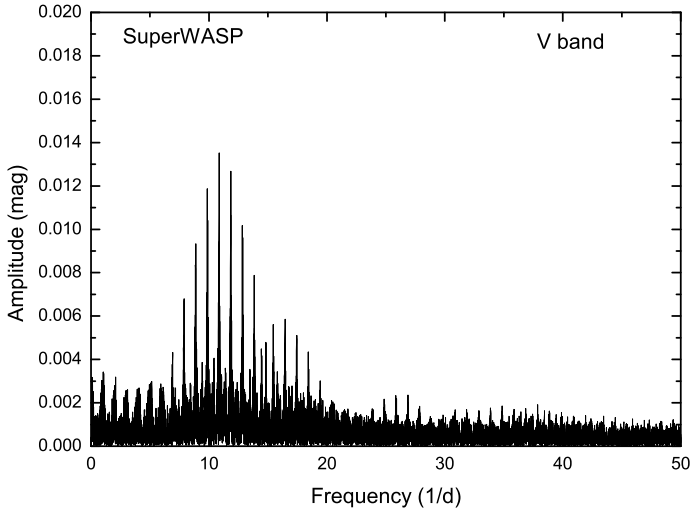

Figure 5. Amplitude spectrum of SuperWASP data for GSC 02696-02622.

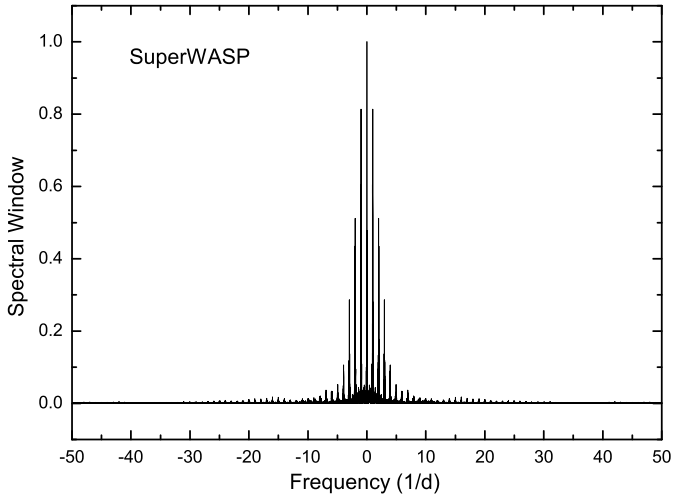

Figure 6. Spectral window of SuperWASP data for GSC 02696-02622.

ACKNOWLEDGMENTS: The authors would like to thank the observing assists of 85 cm telescope of Xinglong station for their help during our observations. This work is partly supported by by the Joint Fund of Astronomy of the National Natural Science Foundation of China (NSFC) and the Chinese Academy of Sciences (CAS) grant No. 10978010 and No. 11263001.

References:

Collier Cameron A., Wilson D. M., West R. G., et al., 2007, *MNRAS*, **380**, 1230
Cutri R. M., Skrutskie M. F., van Dyk S., et al. 2003, 2MASS All-Sky Catalog of Point Sources
Dapergolas A., Kontizas E. & Kontizas M. 1988, *IBVS*, No. 3249
Hambalek L., 2008, *OEJV*, **95**, 42
Heckert P. A. & Zeilik M., 1991, *IBVS*, No. 3688
Høg E., Fabricius C., Makarov V. V., et al. 2000, *A&A*, **355**, L27
Lenz P., & Breger M., 2005, *Commun. Asteroseismol.*, **146**, 53
Montgomery, M. H.; O'Donoghue, D., 1999, *Delta Scuti Star Newsl.*, **13**, 28
Nanouris N., & Antonopoulou E., 2010, *ASPC*, **424**, 212
Pollacco D. L., Skillen I., Cameron A. C., et al., 2006, *PASP*, **118**, 1407
Yu C. L., 1923, *ApJ*, **58**, 75
Zhou A. Y., Rodriguez E., Rolland, A., et al., 2001, *MNRAS*, **323**, 923
Zhou A. Y., Jiang X. J., Zhang Y. P., et al., 2009, *RAA*, **9**, 349

COMMISSIONS 27 AND 42 OF THE IAU
INFORMATION BULLETIN ON VARIABLE STARS

Number 6054

Konkoly Observatory
Budapest
19 April 2013

HU ISSN 0374 – 0676

PHOTOMETRIC ANALYSIS OF VARIABLE STARS IN NGC 299

SANDERS, R.J.[1]; SARRAJ, I.[1]; SCHMIDTKE, P.C.[1]; UDALSKI, A.[2]

[1] School of Earth and Space Exploration, Arizona State University, Box 871404, Tempe, Arizona 85287 USA
E-mail: Raymond.J.Sanders@asu.edu, Ibrahim.Sarraj@asu.edu, Paul.Schmidtke@asu.edu

[2] Warsaw University Observatory, Aleje Ujazdowskie 4, 00-478 Warsaw, Poland
E-mail: Udalski@astrouw.edu.pl

NGC 299 (RA $00^{\rm h}53^{\rm m}24.74^{\rm s}$, DEC $-72°11'47.6''$, J2000) is a young and relatively small star cluster in the Small Magellanic Cloud (SMC). It is classified as a Type I cluster on the SWB scale (Searle, Wilkinson, & Bagnuolo 1980). Matteucci et al. (2002) analyzed a color-magnitude diagram (CMD) from B and V observations and, based on the brightness of the upper main-sequence termination point, estimated the cluster's age to be 15-20 Myr. They commented on the three brightest stars in the field and suggested these might be He-burning giants. We further discuss the nature of these stars later in this paper. Rafelski & Zaritsky (2005), using data from the Magellanic Clouds Photometric Survey (MCPS; Zaritsky et al. 2002), calculated integrated colors for a sample of SMC clusters. From a comparison of these colors with simple stellar-population models, they derived an extinction-corrected age of 28-100 Myr for NGC 299. Fitting an isochrone model to a MCPS CMD, Glatt, Grebel, & Koch (2010) found a cluster age of ∼25 Myr. Piatti et al. (2008) fitted a CMD on the Washington photometric system with an isochrone model to obtain an age of 25^{+6}_{-5} Myr. They also examined the stellar density profile (stars per unit area, unweighted by luminosity) and determined the cluster's full width at half maximum ($r_{\rm FWHM}$) and outer radius ($r_{\rm cls}$) that we adopt below. Hill & Zaritsky (2006) showed the brightness profile of NGC 299 is well modeled by a King model.

A significant percentage of hot stars in the SMC are photometrically variable. This behavior is most pronounced for Be stars. Diago et al. (2008) analyzed MACHO observations for a large sample of spectroscopically selected stars and found that 4.9% (9 out of 183) of B stars and 25.3% (32 out of 126) of Be stars were low-amplitude, short-period pulsating variables. Similarly, in a study of OGLE-II data for NGC 330 (a SMC cluster notable for its large population of Be stars), Schmidtke, Chobanian, & Cowley (2008) found that pulsations were present in >20% of their entire sample. The percentage was even greater for known Be stars. Although no comprehensive spectroscopic study of NGC 299 has been undertaken, Martayan et al. (2007), in a survey of SMC B and Be stars, investigated four stars that might be cluster members. The three brightest of these (i.e., #11617, #11998, and #14323 on the numbering system discussed below) were found to be evolved B-type stars, while the faintest one (#11979) was classified as type B3 IVe.

We present here an analysis of 8 seasons of OGLE-III photometry (Udalski 2003; Udalski et al. 2008) for NGC 299, which lies in field SMC102.1. An I-band finding chart

is shown in Fig. 1. The two inner circles mark radii corresponding to $r_{\rm FWHM}$ (=12.6″) and $r_{\rm cls}$ (=29.4″), respectively. All stars within the outer circle ($r_{\rm lim}$=45″) were examined. The central portion of the cluster is dominated by light from a very bright star that lies ∼1″ from the center. Hence, the central region is not well resolved, and the OGLE-III star closest to the center position is at r=5″.

A CMD from V and I data in the OGLE-III photometry maps is shown in Fig. 2. A box is drawn around hot stars on or near the upper main sequence. Stars in this region of the diagram are likely to show short-period, low-amplitude pulsations (e.g. see Balona 2010; Kołaczkowski et al. 2006; Moffat 2013). The faint limit of the box is set at I=18.2, which corresponds to the expected brightness of a B5 V star at the distance of and with an extinction appropriate for the SMC. Within the box there are 27 stars, of which 6 have $r>r_{\rm cls}$. These outliers are unlikely to be cluster members. When scaled by area on the sky, we estimate that ∼1 (out of 12) of the hot stars with $r<r_{\rm FWHM}$ is not a cluster member. Similarly, about 4 stars (out of 9) with $r_{\rm FWHM}<r<r_{\rm cls}$ are not members. Based on the young age for NGC 299, none of the red giants lying to the right side of the box can be a cluster member.

A plot of σ_I vs. I from OGLE-III data is shown in Fig. 3. Many stars fainter than I∼18.5 have larger than expected photometric dispersion for their mean brightness. However, almost all faint stars with usually high σ_I lie close to the cluster's center ($r<r_{\rm FWHM}$), while very few are found outside $r_{\rm cls}$. Hence, we conclude that it is the lack of consistent spatial resolution of stars near the cluster's core, rather than photometric variability, that leads to most of the scatter for faint stars in the diagram.

All stars within the box shown in Fig. 2 were selected for further study. There were ∼710 I-band observations per star. The time-series data were analyzed for periodic signals using the Period04 analysis package (Lenz & Breger 2005). The search covered frequencies in the range 0-20 day^{-1}, which is appropriate for the identification of orbital systems as well as pulsating B/Be stars. For one star with a decidedly non-sinusoidal light curve (very narrow eclipses), the phase-dispersion minimization technique of Stellingwerf (1978) was used to determine the best photometric period.

As noted by Diago et al. (2008), the period analysis of a synoptic data set often shows significant 1-day aliasing. Many stars in the present sample show this effect, having fictitious periods comparable to the duration of OGLE-III observing or at high-frequency aliases near f=1, 2, 3, ... day^{-1}. The analysis can be further complicated by inadequate spatial resolution. Only three hot stars in the direction of NGC 299 show a meaningful photometric signal. Two stars are eclipsing binaries, while a third star shows large, intrinsic variations that are not periodic. There is no evidence for variability in the four hot stars with known spectral types. The results are summarized in Table 1 and shown in Fig. 4. We note that no short-period pulsating variables are present in NGC 299. This may be related to age, as other SMC clusters with a large population of pulsating variables (i.e., NGC 330) are thought to be slightly older.

Comments on individual sources.

SMC102.1 #11727: Based on its brightness (the third brightest of all stars enclosed by the box in Fig. 2) and its proximity to the cluster's center (well within $r_{\rm FWHM}$), this star is likely to be a cluster member. The photometric variability is typical of a Be star, although no spectrum is available. The large amplitude (ΔI=0.35 mag) and long duration (>3 yr) of the outburst are consistent with that of a Be star with a Type-1 (hump-like) light curve (Mennickent et al. 2002). We searched for low-amplitude pulsations in the

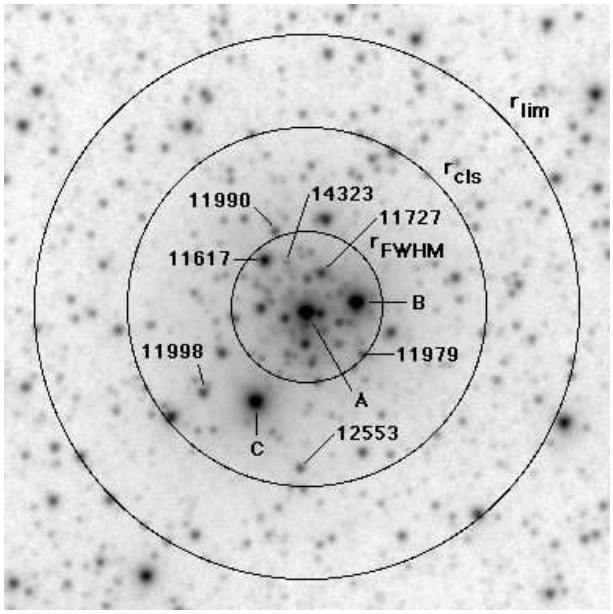

Figure 1. An I-band finding chart for NGC 299. The field of view is $100''\times100''$, with north up and east to the left. Stars with numerical identifications refer to their sequence number in OGLE-III field SMC102.1, while the stars labeled A, B, and C are too bright to be in the OGLE data base.

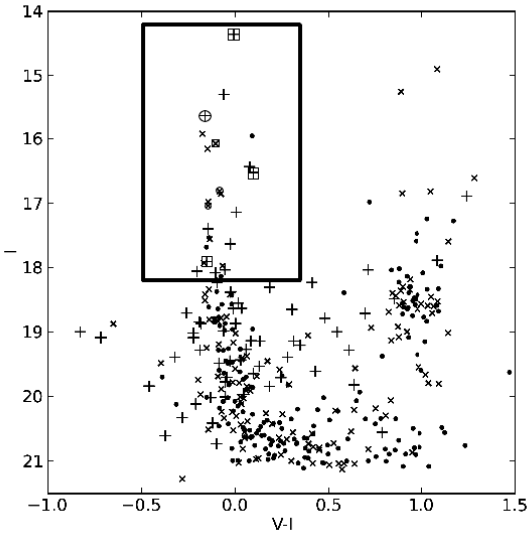

Figure 2. I vs. $V-I$ CMD from OGLE-III data for NGC 299. The box outlines that portion of the diagram in which hot, pulsating variables are likely to be found. Different symbols indicate relative distances from the cluster's center: plusses (+) for $r<r_{\rm FWHM}$, crosses (×) for $r_{\rm FWHM}<r<r_{\rm cls}$, and filled circles (•) for $r_{\rm cls}<r<r_{\rm lim}$. Open circles (◯) are drawn around variable stars, while open squares (□) mark those stars with known spectral types (either B or Be).

Table 1. Variable Stars in the Field of NGC 299

OGLE-III ID	RA (J2000)	DEC (J2000)	I (mag)	$V-I$ (mag)	T_0 (JD 2453000+)	GCVS Type	P (days)	r ($\prime\prime$)
SMC102.1 #11727	0:53:24.14	−72:11:42.3	15.638	−0.160	...	BE?	...	6.0
SMC102.1 #11990	0:53:25.77	−72:11:35.3	16.812	−0.084	1.022	EB	1.59362	13.2
SMC102.1 #12553	0:53:24.98	−72:12:14.4	17.032	−0.144	1.25	EA	14.74086	26.9

OGLE-III ID refers to the sequence number in field SMC102.1. I and $V-I$ are the mean magnitude and color in the OGLE-III photometry map. T_0 represents the time of phase zero, GCVS Type is the variability type, P denotes the period, and r is the distance from the cluster's center.

first 4 seasons of OGLE-III data (when the light curve was nearly flat), but found none. An additional search was made of the entire data set, after subtracting second-order polynomial fits from individual seasons of data. Again, no low-amplitude pulsations were found.

SMC102.1 #11990: This star lies just outside $r_{\rm FWHM}$ and is likely to be a cluster member. An orbital period of 1.59 days was found in this β Lyrae-type eclipsing binary system. The primary eclipse has a depth of ΔI=0.12 mag, with the depth of secondary eclipse being 0.09 mag.

SMC102.1 #12553: The cluster membership of this star is questionable, as it lies close to $r_{\rm cls}$. An orbital period of 14.74 days was found in this Algol-type eclipsing binary system. The light curve shows two very narrow eclipses, neither of which is fully resolved in OGLE-III data. We tentatively identify the broader eclipse (with a duration of ∼0.04P) as the primary and the narrower eclipse (∼0.02P) as the secondary. Further observations are needed to confirm these assignments. The depths and durations of the eclipses are consistent with two nearly identical mid-B main-sequence stars in a 14-day orbit and viewed at an inclination close to 90°. Secondary eclipse falls at phase 0.533, implying an eccentric orbit.

The brightest stars in the direction of NGC 299 (labeled A, B, and C in Fig. 1) have been observed by the Two Micron All Sky Survey (2MASS; Cutri et al. 2003). The K_s magnitudes and $J-K_s$ colors for these stars are consistent with those of red supergiants in the SMC (Boyer et al. 2011). All three stars are likely to be cluster members. Stars A and B are well within $r_{\rm FWHM}$, while star C lies just outside of it. No OGLE-III photometry is available for these stars. Therefore, we could not examine their long-term variability.

Acknowledgments: The OGLE project has received funding from the European Research Council under the European Community's Seventh Framework Programme (FP7/2007-2013) / ERC grant agreement no. 246678 to AU.

References:

Balona, L. A. 2010, Challenges in Stellar Pulsation, Bentham Science Publishers, p. 25
Boyer, M. L., et al. 2011, AJ, 142, 103
Cutri, R. M., et al. 2003, VizieR On-line Data Catalog, II/246
Diago, P. D., Gutiérrez-Soto, J., Fabregat, J., & Martayan, C. 2008, A&A, 480, 179
Glatt, K., Grebel, E. K., & Koch A. 2010, A&A, 517, A50
Hill, A., & Zaritsky, S. 2006, AJ, 131, 414
Kołaczkowski, Z., et al. 2006, Mem. Soc. Astron. Ital., 77, 336
Lenz, P., Breger, M. 2005, CoAst, 146, 53

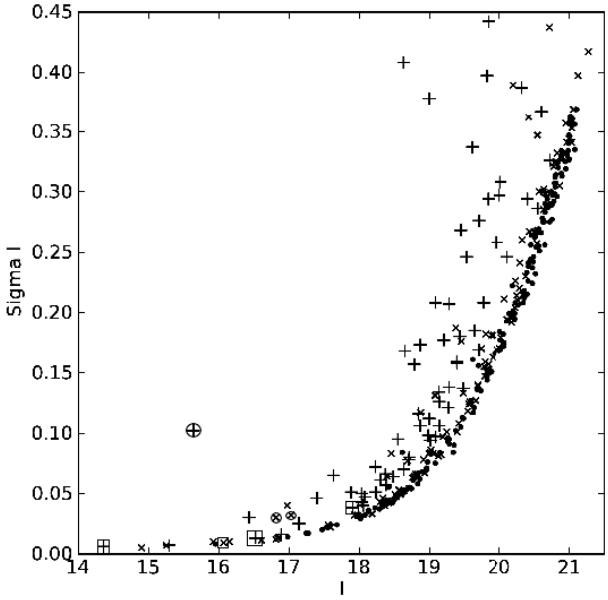

Figure 3. σ_I vs. I from OGLE-III data for NGC 299. Different symbols indicate relative distances from the cluster's center: plusses (+) for $r<r_{\rm FWHM}$, crosses (×) for $r_{\rm FWHM}<r<r_{\rm cls}$, and filled circles (•) for $r_{\rm cls}<r<r_{\rm lim}$. Open circles (◯) are drawn around variable stars, while open squares (□) mark those stars with known spectral types (either B or Be).

Martayan, C., Frémat, Y., Hubert, A.-M., Floquet, M., Zorec, J., & Neiner, C. 2007, A&A, 462, 683
Matteucci, A., Ripepi, V., Brocato, E., & Castellani, V. 2002, A&A, 387, 861
Mennickent, R.E., Pietrzyński, G., Gieren, W., & Szewczyk, O. 2002, A&A, 393, 887
Moffat, A. F. J. 2013, ASP Conf. Ser., 465, 3
Piatti, A. E., Geisler, D., Sarajedini, A., Gallart, C., & Wischnjewsky, M. 2008, MNRAS, 389, 429
Rafelski, M., & Zaritsky, D. 2005, AJ, 129, 2701
Schmidtke, P. C., Cobanian, J. B., & Cowley, A. P. 2008, AJ, 135, 1350
Searle, L., Wilkinson, A., & Bagnuolo, W. G. 1980, ApJ, 239, 803
Stellingwerf, R.F. 1978, ApJ, 224, 953
Udalski, A. 2003, Acta Astron., 53, 291
Udalski, A., et al. 2008, Acta Astron., 58, 329
Zaritsky, D., Harris, J, Thompson, I. B., Grebel, E. K., & Massey, P. 2002, AJ, 123, 855

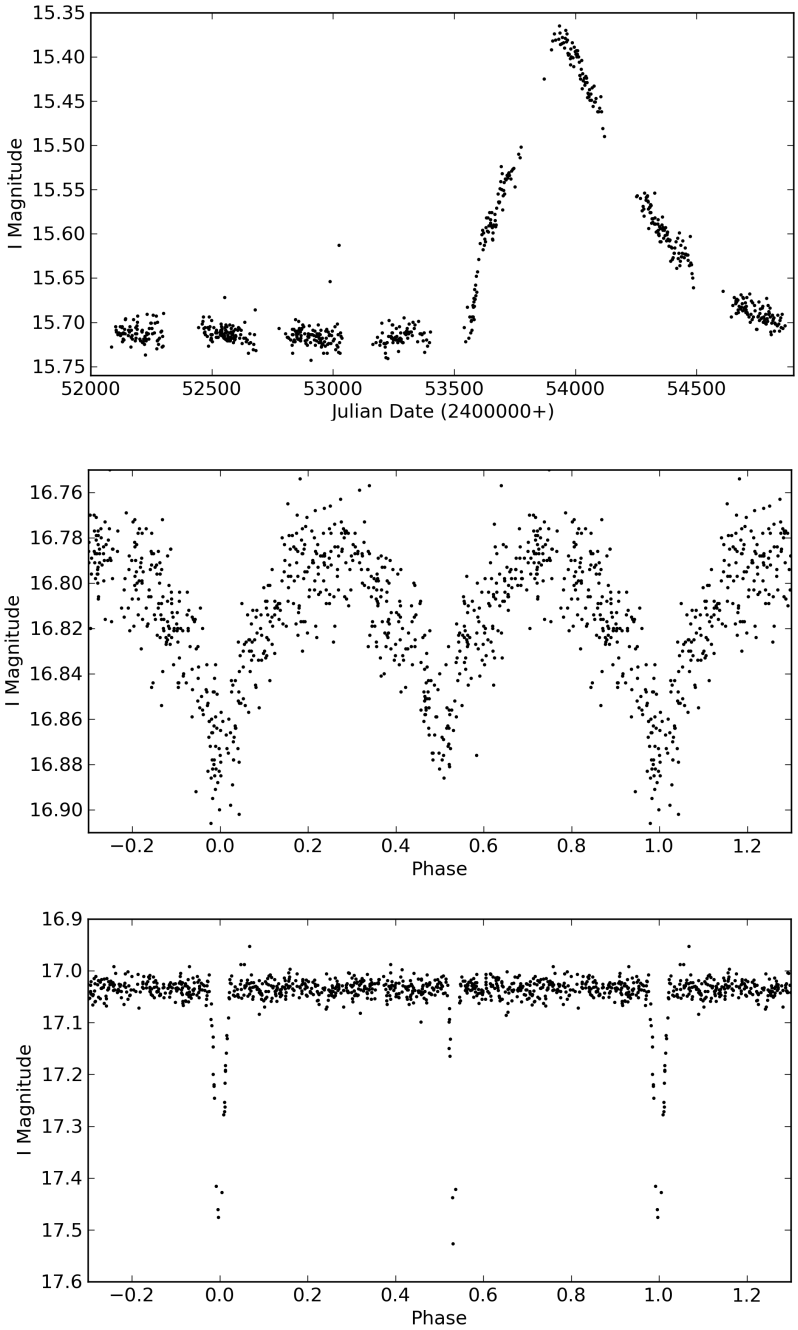

Figure 4. OGLE-III *I*-band light curves for variable stars in the field of NGC 299: SMC102.1 #11727 (top), SMC102.1 #11990 (middle), and SMC102.1 #12553 (bottom). See the text and Table 1 for additional information and comments on individual sources.

COMMISSIONS 27 AND 42 OF THE IAU
INFORMATION BULLETIN ON VARIABLE STARS

Number 6055

Konkoly Observatory
Budapest
25 April 2013

HU ISSN 0374 – 0676

BIPOLAR EJECTION FROM THE SYMBIOTIC BINARY Hen 3-1341 DURING ITS 2012 OUTBURST

TOMOV, N.; TOMOVA, M.

Institute of Astronomy and National Astronomical Observatory, Bulgarian Academy of Sciences, POBox 136, 4700 Smolyan, Bulgaria, e-mail: tomov@astro.bas.bg, mtomova@astro.bas.bg

The binary star Hen 3-1341 consists of a cool primary of spectral type M4 (Mürset & Schmid 1999) and a hot luminous compact object with an effective temperature of 1.2 $\times$ 10^5 K as a secondary component (Munari et al. 2005). The stellar components are embedded in a dense, radiation bounded circumbinary nebula (Munari et al. 2005). The system underwent a large optical outburst lasting from 1998 to 2004 with a V amplitude of about 2 magnitudes (Tomov et al. 2000, Munari et al. 2005). The data of Tomov et al. (2000) show that the line Hα had an intensive central component and additional weaker emissions symmetrically displaced to the central component at a velocity of about 800 km s^{-1} indicating bipolar jets. The profile of the line He I λ 5876 contained the same components, but it had one P Cyg absorption in addition. The system Hen 3-1341 underwent second outburst in 2012 (Munari et al. 2012a). Munari et al. (2012b) established the appearance of satellite emissions with a velocity of 1100 km s^{-1}, symmetrically displaced to the center of the line Hα, indicating bipolar collimated outflow. They noted that the helium lines acquired P Cyg signatures of stellar wind. Because of the uniqueness of the event we organized spectral observations of this star with the aim to take high resolution data in the region of its lines where indication of mass outflow was detected.

Spectroscopic data were obtained on June 6 and August 4, 2012 with the Photometrics CCD camera mounted on the Coudé spectrograph of the 2m Ritchey-Chrétien-Coudé (RCC) telescope of the Rozhen National Astronomical Observatory. Because of the weakness of the star and its small height above the horizon we were able to take frames covering only Hα and He I λ 5876 lines. The resolving power in their ranges was 32000 and 29000. Two exposures with duration of 20 minutes were taken in each range and the spectra were added with the aim to improve the signal-to-noise ratio. The IRAF package[1] was used for the data reduction as well as for obtaining the dispersion curve, calculating the radial velocities and equivalent widths.

On June 6 the profile of the line Hα was multicomponent one consisting of a central emission located around the reference wavelength, broad wings with low intensity extended to not less than $\pm$ 2000 km s^{-1} from the center of the line, and additional satellite emission components with a velocity of 1160 km s^{-1} on both sides of the central emission, indicating

[1]The IRAF package is distributed by the National Optical Astronomy Observatories, which is operated by the Association of Universities for Research in Astronomy, Inc., under contract with the National Science Foundation.

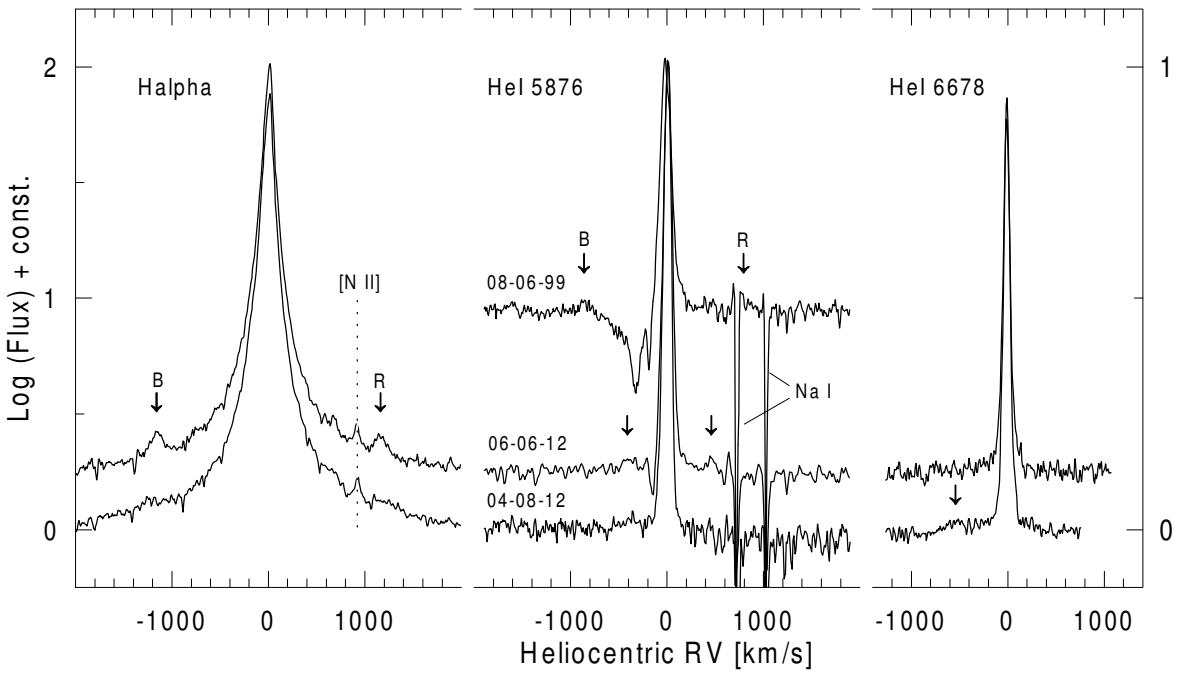

Figure 1. The profile of the Hα, He I λ 5876 and He I λ 6678 lines. The spectra are in units of the continuum and a logarithmic scale is used for better visibility of the profile. The right y-scale is related to the intensity of the helium lines only. The profile of the He I λ 5876 line on June 08, 1999 from the paper of Tomov et al. (2000) is shown for comparison.

Table 1: The radial velocities RV (km s^{-1}), widths FWHM (km s^{-1}) and equivalent widths W$_\lambda$(Å) of the satellite emissions in the Hα line. The third column compares the total Hα equivalent width.

Date	HJD(245...)	W$_\lambda$(Å)	Blue			Red		
			RV	FWHM	W$_\lambda$	RV	FWHM	W$_\lambda$
June 6, 2012	6085.335	221.53	−1160	141	0.90	1164	144	0.74
Aug. 4, 2012	6144.312	282.02						

bipolar collimated ejection from the system (Fig. 1). The satellite components were fitted with Gaussian, and the rest of the line (the core plus the wings) – with Lorentzians to determine their radial velocity position and equivalent width. Resulting parameters are presented in Table 1. The uncertainties in the equivalent width of the whole line and the satellite emissions are 3 and 15-20 per cent. The uncertainty in the radial velocity of the satellite emissions is about 3 km s^{-1}. The ratio of the equivalent widths of the satellite components and the rest of the line is 1:134 which is equal to the ratio of the Hα fluxes of the area of bipolar ejection and the other part of the circumbinary nebula. On August 4 the profile of the line Hα was similar, the satellite emissions disappeared and only weak remnants were visible at their radial velocity position. Having in mind they emerged in the beginning of March 2012 (Munari et al. 2012b) it can be concluded that they have been presented in the spectrum of the star for about five-six months.

The profile of the He I λ 5876 line (Fig. 1) on June 6 consisted of emission component of nebular origin and a P Cyg absorption indicating mass outflow from the system with a velocity of about 150 km s^{-1}. On both sides of the nebular component, however, two

Table 2: The radial velocities RV ($km\,s^{-1}$), widths FWHM ($km\,s^{-1}$) and equivalent widths W_λ(Å) of the He I lines.

Date	HJD(245...)	He I λ 5876			He I λ 6678		
		RV	FWHM	W_λ	RV	FWHM	W_λ
June 6, 2012	6085.335	10	80	11.6	−11	66	7.8
Aug. 4, 2012	6144.312	6	71	13.8	−9	57	10.6

very weak emission details were visible pointed with arrows in the figure. Their velocity was much lower than the velocity of the Hα satellite components. The velocity of the blueshifted one was 410 $km\,s^{-1}$ and the velocity of the redshifted was 460 $km\,s^{-1}$. On August 4 only the blueshifted emission was visible together with the central nebular component.

The emission line He I λ 6678 had nebular profile (Fig. 1). Possible blueshifted emission component with a velocity of about 500 $km\,s^{-1}$ in the August 4 spectrum was very faint.

The emission components of the helium lines were fitted with Gaussian. Resulting parameters are presented in Table 2. The uncertainties in the equivalent width is 5 per cent and the uncertainty in the radial velocity is not more than 3 $km\,s^{-1}$.

Our observations confirmed the emergence of high-velocity satellite emission Hα components indicating bipolar collimated ejection and P Cyg He I absorption with intermediate velocity indicating stellar wind from the compact object in the system Hen 3-1341 (Munari et al. 2012b) and demonstrated their transient nature being observed for five-six months.

Acknowledgements: This work has been partly supported by the Bulgarian Scientific Research Fund (Grant 01/14 from Bilateral scientific-technical collaboration between R. Bulgaria and Slovak Republic), and the Russian and Bulgarian Academies of Sciences through a collaborative program in basic space research. The authors thank Dr. T. Tomov for the kindly given opportunity to use the spectrum of Hen 3-1341 in the region of the He I λ 5876 line, taken on Jun 08, 1999. The authors thank also the anonymous referee whose suggestions contributed to the improvement of the paper.

References:

Munari U., Siviero A., Henden A. 2005, *MNRAS*, **360**, 1257
Munari U., Milani A., Siviero A. et al. 2012a, *ATel*, **3946**
Munari U., Valisa P., Dallaporta S., Siviero A. 2012b, *ATel*, **3952**
Mürset U., Schmid H. M. 1999, *A&AS*, **137**, 473
Tomov T., Munari U., Marrese P. M. 2000, *A&A*, **354**, L25

COMMISSIONS 27 AND 42 OF THE IAU
INFORMATION BULLETIN ON VARIABLE STARS

Number 6056

Konkoly Observatory
Budapest
11 May 2013

HU ISSN 0374 – 0676

NEW OUTBURST OF AX PERSEI IN 2012

KONDRATYEVA, L.; RSPAEV, F.

Fessenkov Astrophysical Institute, Almaty, Kazakhstan. e-mail: kondr.lud@gmail.com; lu_kondr@mail.ru

The well-known eclipsing binary AX Per consists of the a giant M4.5 (T_{eff}=3400 ± 150 K) and a white dwarf with the orbital inclination i ≈ 90° and mass ratio of 2.4 (Skopal et al. 2011; Mürset & Schmid 1999; Mikolajewska & Kenyon 1992). During its history this object underwent some active stages. The major outburst (1988-1992) has led AX Per to the optical brightening about 3^m (Skopal et al. 2001). The next active stage has begun in 2007 (Skopal et al. 2011). Some flashes were registered in 2009-2010 (Munari & Siviero 2009, 2010). Later on, instead of the expected quiescence phase a new brightening began in 2012 July (Munari et al. 2012). We observed the continuation and the development of this event at the end of 2012.

Our photometric observations have been made using two reflectors: the 1-meter Carl Zeiss Jena and the 70 cm telescope AZT-8, equipped with ST-7 and ST-8 CCD cameras, respectively and samples of B, V, R Johnson filters. All frames were dark subtracted and flat fielded. The stars: HD10465, HD10546 and HD10054 were adopted as standards. The results of photometry: B, V, R magnitudes are compiled in Table 1. Photometric phases were computed according to the ephemeris: JD_{min}=2447551.26+E×680.83 day (Skopal et al. 2011). Figure 1 shows the photometric data of AX Per, obtained in 2009-2013 by Skopal et al. (2011, 2012) and Munari et al. (2012) together with our results. There is a good agreement between our results for 2009-2011 and the data of other authors. The flash, registered in 2012, lasted about 200 days. The B and V values, measured in the maximum, are comparable and even a little bit above the values measured in the maximum phase, 2007-2010, but below the magnitudes ($V \approx 9.3^m$), achieved in 1990 (see Fig. 1). However, most likely the true maximum happened between July and October, 2012.

Spectral observations have been carried out with the same telescopes of the Fessenkov Astrophysical Institute. The slit spectrographs were equipped with the CCD cameras ST-8. Wavelength calibration was done using laboratory sources of HeI, NeI and ArI emission lines. Spectra of standard stars HD 12279, HD 12303, obtained just before or after the target were used for the flux calibration. All spectrograms were corrected for atmospheric extinction. Spectrograms with dispersions of 0.75 and 0.49 Å pixel^{-1} were obtained in the ranges 4340-5200 and 6100-7000 Å with the 70-cm and 1-meter telescopes, respectively. Exposure time was 20-30 minutes for the object and 1-2 minutes for the standard. The fluxes of emission lines are compiled in Table 2.

It is seen that increase of the fluxes of all presented lines were registered in 2009 October, and it was a residual phenomenon of the object brightening, which was observed in 2009 April by Munari & Siviero (2009). The very last active stage was followed by an even larger strengthening of emission lines.

Table 1: Photometric results

Date	HJD	Phase	B	V	R
	2400000+		mag	mag	mag
23.10.2009	55127.288	0.128	12.11±0.01	11.39±0.01	9.56±0.01
12.11.2009	55148.257	0.158	11.99±0.05	11.27±0.05	9.38±0.05
16.11.2009	55152.179	0.164	11.87±0.05	11.42±0.05	9.37±0.04
12.10.2010	55482.229	0.649	12.69±0.05	11.82±0.05	9.53±0.01
08.11.2010	55509.158	0.689	12.52±0.04	11.55±0.03	9.63±0.02
26.09.2011	55831.292	0.162	12.52±0.01	11.65±0.01	9.70±0.01
23.12.2011	55919.146	0.291	12.72±0.02	11.50±0.01	9.51±0.05
11.10.2012	56212.263	0.721	11.04±0.01	10.23±0.01	9.96±0.01
20.11.2012	56252.149	0.780	11.18±0.05	10.44±0.01	9.09±0.01
04.12.2012	56266.127	0.800	11.52±0.02	10.57±0.01	8.90±0.04
09.01.2013	56302.046	0.853	12.08±0.01	11.01±0.02	9.14±0.03
11.02.2013	56335.050	0.902	12.35±0.02	11.08±0.02	9.26±0.01

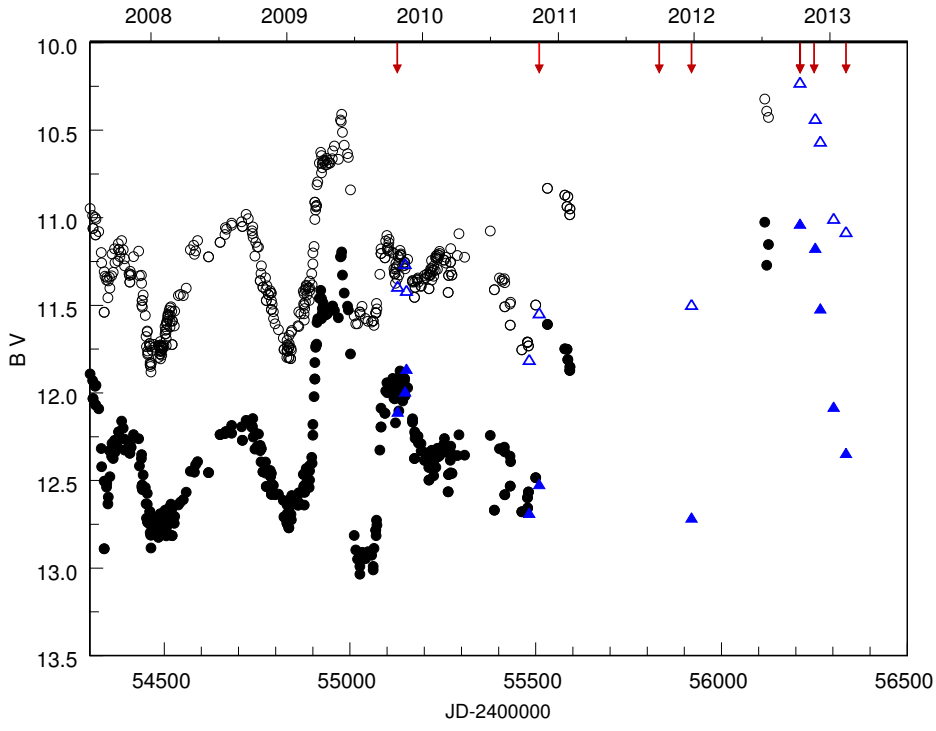

Figure 1. The B and V magnitudes of AX Per in 2008-2013. Data of Skopal et al. (2011, 2012) and Munari et al. (2012) are denoted by circles (empty for V and solid for B), our results are denoted by blue triangles, empty for V and solid for B. Arrows at the top denote dates of our spectral observations.

Table 2: Observed fluxes of selected emission lines in the AX Per spectrum

Date		22.10 2009	08.11 2010	27.09 2011	23.12 2011	10.10 2012	11.10 2012	17.11 2012	11.02 2013
HJD2450000+		5127.23	5509.19	5832.21	5919.09	6211.32	6212.00	6249.15	6335.09
Phase		0.128	0.689	0.163	0.291	0.720	0.721	0.775	0.902
Telescope		0.7 m	1 m	1 m	1 m	1 m	1 m	1 m	0.7 m
λ	ion	Flux in 10^{-12}erg cm^{-2}sec^{-1}							
4363	[OIII]	1.41	0.26	0.12		1.06	1.06	0.74	0.59
4471	HeI	0.39	0.11	0.23		0.88	0.90	0.82	0.13
4634	NIII	0.40	0.20			0.22	0.30	0.08	0.07
4641	NIII	0.68	0.16	0.28	0.29	0.61	0.52	0.56	0.09
4647	CIII	0.52	0.17	0.34		0.50	0.43	0.46	0.03
4686	HeII	2.57	1.32	2.34	1.57	2.50	2.54	1.40	1.22
4713	HeI	0.12	0.07	0.19		0.32	0.34	0.26	0.06
4861	Hβ	4.60	3.09	2.84	3.39	11.5	11.4	9.73	2.30
4922	HeI	0.74	0.28	0.29	0.14	0.90	0.93	0.84	0.43
4959	[OIII]	0.67	0.12	0.16	0.11	0.79	0.76	0.53	0.29
5007	[OIII]	2.15	0.38	0.49	0.33	2.44	2.40	2.18	0.99
5015	HeI		0.04	0.05		0.98	0.94	0.68	0.59
6563	Hα	33.5	48.2		31.5	65.0		60.6	19.2
6678	HeI	1.42	1.71		0.85	1.63		1.43	0.53

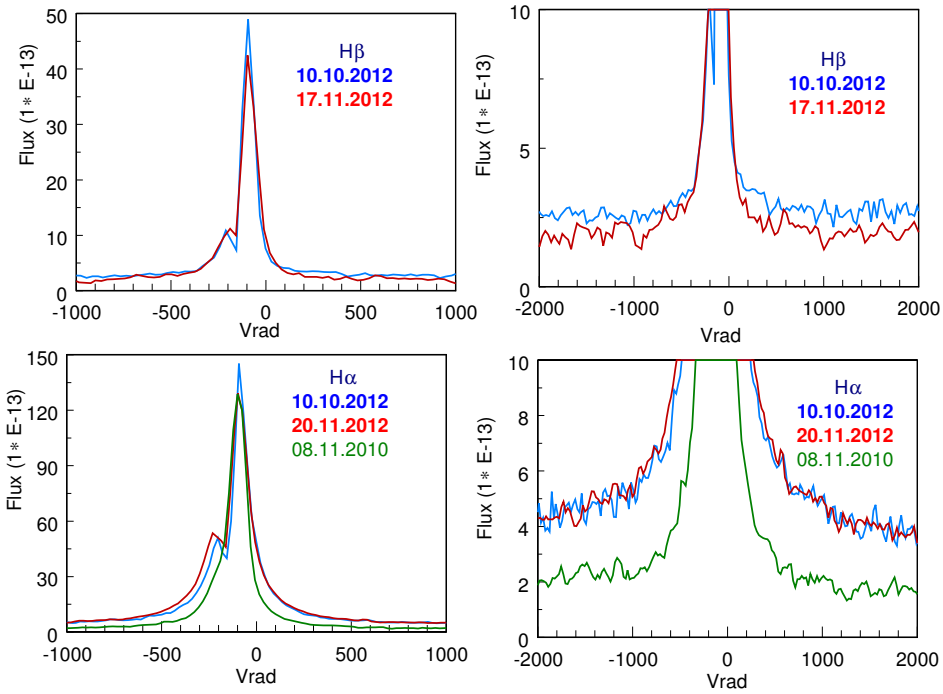

Figure 2. Left panels: the Hβ and Hα profiles, obtained with 0.49 Å dispersion pixel^{-1}. The horizontal axis corresponds to radial velocities in (km sec^{-1}). The vertical axis shows the fluxes on the scale (10^{-13} erg cm^{-2}sec^{-1}Å^{-1}). Dates of observations are presented on the panels. The right panels are the same, but with expanded vertical range and with the broader interval of radial velocities.

Munari et al. (2012) reported that on 2012 July 18 the line profiles were sharp Gaussian-like, with no P Cyg absorption components. However in October and in November the profiles of Hβ and Hα were distorted by absorption components. Spectrograms taken on December 4 with 0.75 Å dispersion pixel^{-1} (without an absolute calibration) show the single profiles, probably due to the lower dispersion. It is seen from Figure 2 that the profiles, obtained on different dates during the maximum are broader and have more extended wings than the single profile obtained on 2010 November 8, when the object was in quiescence.

References:

Mikolajewska J. & Kenyon S. 1992, AJ, **103**, 579
Munari U., Ochner P., Dallaporta S., et al. 2012, ATel, No. 4265
Munari U. & Siviero A. 2009, CBET, No. 1757
Munari U., Siviero A., et al. 2010, CBET, No. 2555
Mürset U. & Schmid H. M. 1999, A&AS, **137**, 473
Skopal A., Teodorani M., Errico L., et al. 2001, A&A, **367**, 199
Skopal A., Tarasova T., Cariková Z., et a1. 2011, A&A, **536**, A27
Skopal A., Shugarov S., Vaňko M., et al. 2012, AN, **333**, 242

COMMISSIONS 27 AND 42 OF THE IAU
INFORMATION BULLETIN ON VARIABLE STARS

Number 6057

Konkoly Observatory
Budapest
14 May 2013

HU ISSN 0374 – 0676

GSC 02996-00858: A NEW ALGOL-TYPE ECLIPSING BINARY IN LEO

AYIOMAMITIS, ANTHONY[1,2]

[1] Perseus Observatory, Athens, Greece; e-mail: anthony@perseus.gr

[2] Helliniki Astronomiki Enosi, Greece

The previously unknown variable GSC 02996-00858 (α_{2000}: $09^{\rm h}53^{\rm m}35^{\rm s}$, δ_{2000}: $+40°33'20''$, $V = 14.48$) was followed over six nights and confirmed to be an eclipsing binary with a deep primary minimum and a shallow secondary minimum. Perhaps of greater interest is the unexpected flare-like event associated with GSC 02996-00858 which was identified during one of the follow-up sessions. Single filter light elements with light curve and period analysis are presented.

A supplementary analysis of the sparse field of view centered on the exoplanet host star KELT-3 (SAO 43097, α_{2000}: $09^{\rm h}54^{\rm m}34\overset{\rm s}{.}39$, δ_{2000}: $+40°23'17\overset{''}{.}0$) and measuring $46' \times 31'$ revealed the presence of two potential new variable stars. Further analysis of one of these candidates suggested the presence of an eclipsing binary with a deep minimum (approximately 0.50 mag) owing to the single minimum captured during the initial session. Five further nights immediately thereafter were dedicated for follow-up observations and additional data so as to constrain the parameters of interest further.

An Astro-Physics AP 305/f3.8 Riccardi-Honders astrograph with AP 1200/CP3 German equatorial mount and SBIG ST-10XME CCD camera (KAF 3200ME NABG sensor, 2184×1472 pixel array, 6.8 μm per pixel) with clear filter (UV/IR blocked) were used in both the initial discovery and follow-up monitoring. Image capture was accomplished using CCDSoft V5.00.201 (Software Bisque, 2012) using 1×1 binning mode, thus yielding an image scale of $1\overset{''}{.}21$ per pixel. The CCD camera was cooled to approximately 30 degrees below ambient temperature (operating temperature at −15.0°C). Image acquisition exploited the availability of the TC-237H guide chip (657×495 pixel array, 7.4 μm per pixel) in the ST-10XME CCD camera for autoguiding purposes and where four-second guide exposures were consistently employed during the 39.2 hours of observation.

All data were analysed using AIP4Win V2.4.0 (Berry and Burnell 2011). The differential photometry analysis involved full calibration comprised of a master bias (30 individual frames, min-max average combine with n=2) and a master sky flat (15 individual flat frames, min-max median combine with n=2) obtained during each session whereas the master dark (15 individual dark frames, min-max average combine with n=2) was produced at the end of the first session and reused for the follow-up sessions immediately thereafter.

The dim magnitude for the new eclipsing binary, mag 14.48 (v), allowed for the use of a brighter comparison and check star, thus allowing for greater confidence in the differential photometry. To this end, GSC 2996-0819 (α_{2000}: $09^{\rm h}53^{\rm m}50^{\rm s}$, δ_{2000}: $+40°31'23''$, mag

Table 1: Observation log for GSC 2996-0858

Session	Time (UT)	Duration (hrs)	N	Exposure (sec)	Filter	Notes
2013-03-09	18:50-00:50	6.0	293	60	Clear	(1)
2013-03-12	18:00-00:50	6.8	331	60	Clear	(2)
2013-03-22	17:50-01:17	7.5	363	60	Clear	
2013-03-23	17:46-00:33	6.8	330	60	Clear	
2013-04-04	17:50-23:51	6.0	293	60	Clear	(3)
2013-04-05	18:45-00:50	6.1	294	60	Clear	

Notes: (1) Discovery light curve (primary minimum)
(2) Discovery light curve (secondary minimum)
(3) Discovery light curve (unexpected flare-like event)

12.30) served as the comparison star whereas GSC 2996-0651 (α_{2000}: $09^{\rm h}53^{\rm m}24^{\rm s}$, δ_{2000}: $+40°27'31''$, mag 12.45) was used as the check star. The standard errors associated with each measurement (var-comp and comp-check) during the six sessions and as reported by AIP4Win varied from 0.010 to 0.025 mag but were slightly higher during moments of heavy humidity.

Table 1 presents a breakdown of the 1904 data points using 60-sec exposures collected during six sessions and representing a total observation time of 39.2 hours (JD 2456361.2864 to 2456388.5348). Heliocentric corrections were computed using the online facility by Bruton. The data are available electronically via the IBVS database (see `6057-t4.txt`).

Figure 1 provides the field of view as per one of the 60-sec exposures including KELT-3, GSC 2996-0858 as well as the comparison and check stars.

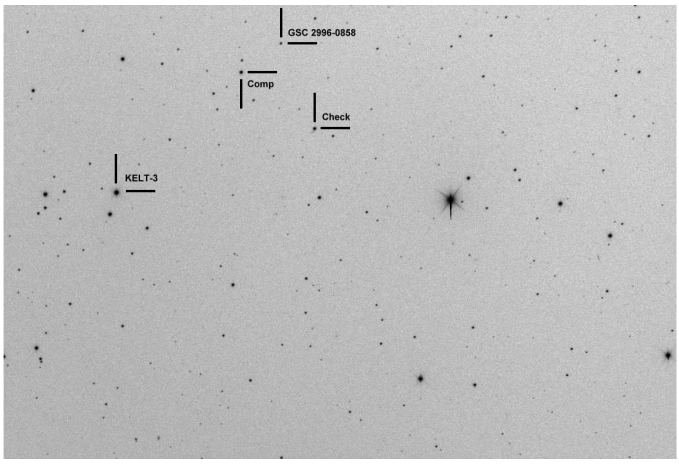

Figure 1. Finder chart for GSC 2996-0858 including KELT-3, GSC 2996-0858 and comp/check stars

Figures 2 and 3 provide the discovery light curves for the primary and secondary minima, respectively, whereas Figure 4 provides the light curve involving the unexpected flare-like event of GSC 2996-0858 approximately 90 minutes before the primary minimum observed during the evening of 4 April 2013.

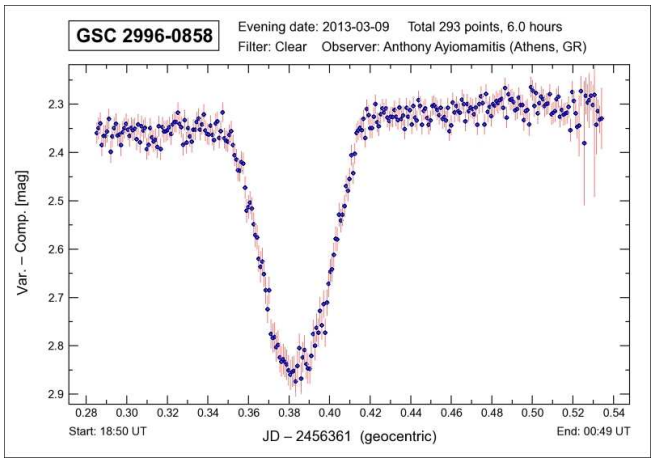

Figure 2. Discovery light curve involving the primary eclipse of GSC 2996-0858

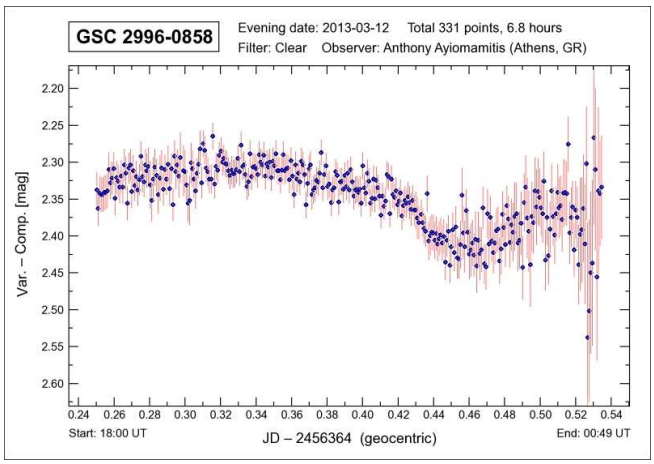

Figure 3. Discovery light curve involving the secondary eclipse of GSC 2996-0858

Determination of extrema and period analysis was accomplished using the Kwee-van Woerden (1956) method (with linear interpolation) and two iterations of a Phase-Binned ANOVA as implemented in the Peranso V2.50 software package (Vanmunster).

Figure 5 provides the prominent periods identified by the initial Phase-Binned ANOVA. The dominating spike at 0.6906 days (1.44800 c/d) with $\theta = 1894.49$ proved to be erroneous on the basis of the ensuing phase plot. In contrast, a visually perfect phase plot was produced when using the next most prominent period, namely 0.4727 days (2.11533 c/d, $\theta = 401.31$) and which served the basis for a second Phase-Binned ANOVA with a greater resolution step-size (1000 units) so as to further finetune the period to 0.4726 days (2.11578 c/d, $\theta = 443.41$). The third most prominent period from the initial Phase-Binned ANOVA at 0.4769 days (2.09667 c/d, $\theta = 276.66$) also proved to be unsatisfactory.

This period of 0.4726 days documents the difficulty encountered during the 39.2 hours of data collection and where there was an inability to acquire both a primary and secondary minimum together during the approximately 6 to 7.5 hours per session and where a single minimum only – primary or secondary – was always observed.

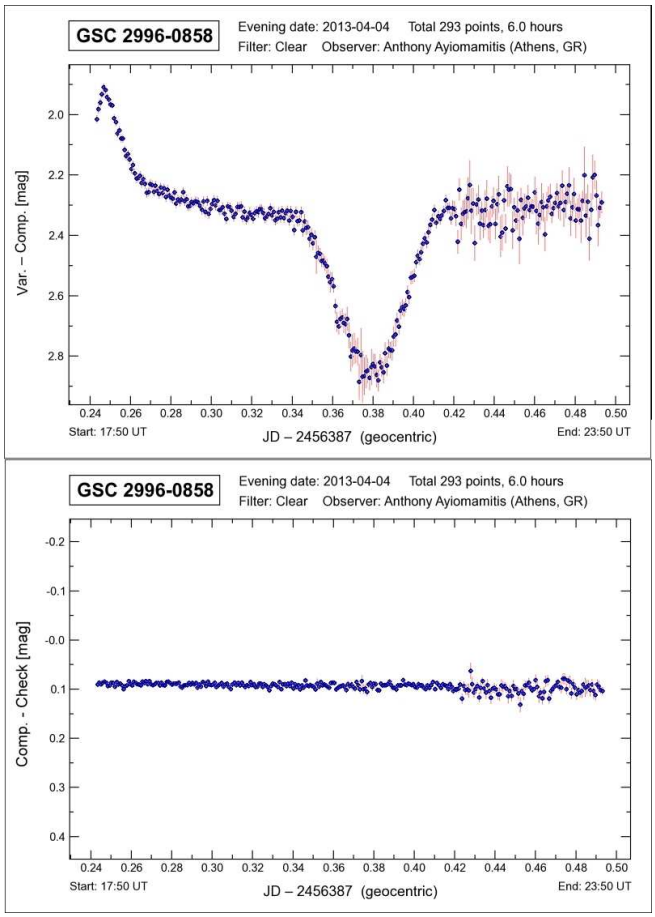

Figure 4. Light curve for GSC 2996-0858 with flare-like event during one session

Table 2: Computed minima and maxima for GSC 2996-0858

Minima (JD−2456000)	Error	Type	Filter	HJD Correction
361.3836	0.0001	I	Clear	+0.0043
364.4682	0.0003	II	Clear	+0.0044
374.3854	0.0002	II	Clear	+0.0036
375.3379	0.0002	II	Clear	+0.0035
387.3791	0.0001	I	Clear	+0.0027
388.3237	0.0001	I	Clear	+0.0026
Maxima (JD−2456000)	**Error**	**Type**	**Filter**	**HJD Correction**
387.2472	0.0002	N/A	Clear	+0.0027

Table 3: O−C results for the observed minima of GSC 2996-0858

Minima (HJD−2456000)	Type	Epoch	O−C
361.3879	I	0	0.0000
387.3818	I	55	0.0009
388.3263	I	57	0.0002
364.4726	II	−23	0.0010
374.3890	II	−2	−0.0072
375.3414	II	0	0.0000

Table 2 provides the six computed extrema observed and comprised of three primary and three secondary minima. The Kwee-van Woerden method with linear interpolation was preferred over spline interpolation and no interpolation at all since a lower standard error was reported for the estimate of each computed extremum.

Figure 6 provides a phase plot for GSC 2996-0858 using the aforementioned period of 0.4726 days (2.11578 cycles/day) whereas Table 3 provides the O−C results using the initial light elements above.

Initial light elements using the primary and secondary epochs with the lowest standard error (Table 2):

$$\text{HJD} = 2456361.3879 \pm 0.0001 + (0.4726 \pm 0.0001) \times \text{E (Primary)}$$
$$\text{HJD} = 2456375.3414 \pm 0.0002 + (0.4726 \pm 0.0001) \times \text{E (Secondary)}$$

The phase plot suggests this eclipsing binary to be an Algol-type system with a relatively bright primary and dim(mer) secondary which are detached while orbiting around a common center of mass. Careful inspection of Figure 6 suggests that star spotting is most probably present, for the secondary maximum is lower than primary maximum and the light curve seems to be distorted post secondary minimum. The flare-like event observed during one of the sessions and the spotting which is implied in Figure 6 suggests that GSC 2996-0858 may be an RS CVn-type Algol.

The phase diagram in Figure 6 suggests a circular orbit is most probable given the location of the secondary minimum at mid-phase. Furthermore, eccentric orbits for such short-period variables are generally highly unlikely phenomena.

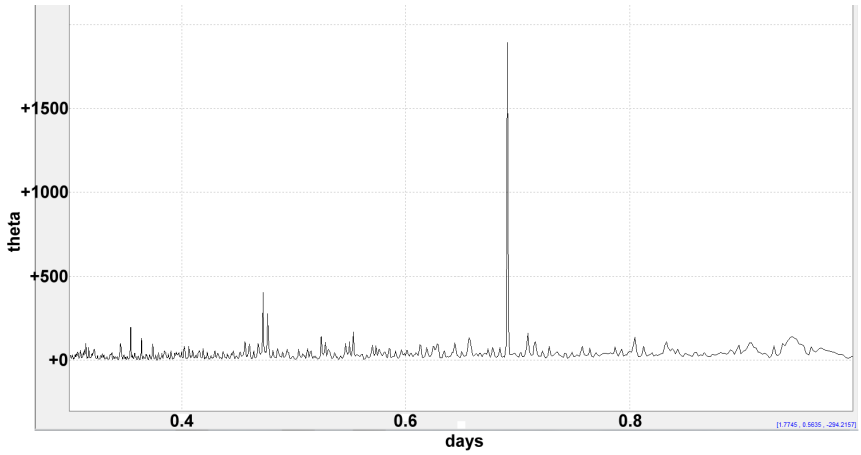

Figure 5. Prominent periods for GSC 2996-0858 using a Phase-Binned ANOVA

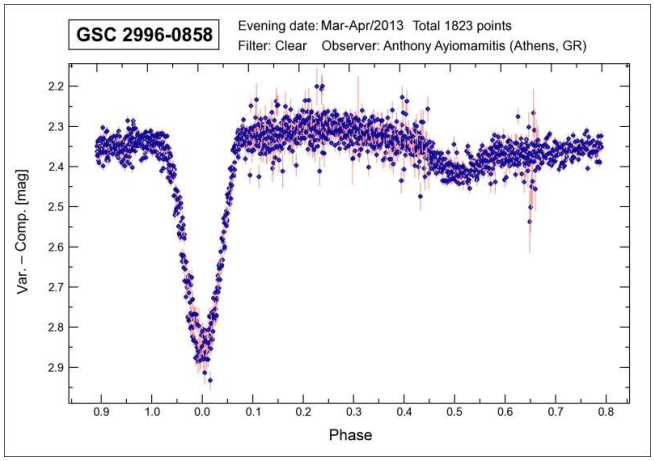

Figure 6. Phase plot for GSC 2996-0858 using a period of 0.4726 days (Maximum in Figure 4 excluded)

The primary eclipse is characterized with a depth of about 0.52 magnitudes and a duration of approximately 95 minutes. In contrast, the secondary eclipse is much shallower with a depth of about 0.10 magnitudes and a duration of approximately 105 minutes. Similarly, the single maximum observed during one of the sessions (Figure 4) and suspected to be a flare-type event is characterized with an amplitude of approximately 0.40 magnitudes and with an implied duration of about 90 minutes.

A Fisher randomization test with 200 iterations revealed a very low False Alarm Probability Level, namely < 0.001, thus reinforcing the integrity of the computed period of 0.4726 days. A Schwarzenberg-Czerny (1991) analysis yields an error for the dominant period of ± 0.0001 ($\pm$ 1 sigma).

Although the 39.2 hours of data captured for this analysis was sufficient to finally acquire a complete phase curve and in spite of the single minimum observed during each session, an effort involving multiple observers across more than one time zone would be welcome so as to obtain a complete phase cure within a single night. The chance flare-type event observed (Figure 4) and which was totally unexpected will be the focus of further study immediately so as to further document its behaviour in relation to magnitude and frequency.

Follow-up analysis involving spectroscopy and photometry is also encouraged so as to further assess various characteristics of this newly discovered eclipsing binary system.

Acknowledgements:

The author acknowledges the use of the Guide Star Catalog II (GSC 2.3.3) from the Catalogs and Surveys Group (CASG), Space Telescope Science Institute (STScI) for the J2000 coordinates and magnitudes reported above for the variable, comparison and check stars. The author is also grateful to the anonymous reviewer for constructive criticism and feedback.

References:

Software Bisque, CCDSoft software package, http://www.bisque.com/sc/

Berry, R. and Burnell, J., 2011, The Handbook of Astronomical Image Processing With AIP for Windows Software, Willmann-Bell, http://www.willbell.com/aip4win/aip.htm

Bruton, D., HJD computing facility, http://www.physics.sfasu.edu/astro/javascript/hjd.html

Kwee, K.K., & van Woerden, H., 1956, B.A.N. 12, (464), 327-330

Schwarzenberg-Czerny, A., 1991, *MNRAS*, **253**, 198-206

Vanmunster, T., Peranso software package, http://www.peranso.com

COMMISSIONS 27 AND 42 OF THE IAU
INFORMATION BULLETIN ON VARIABLE STARS

Number 6058

Konkoly Observatory
Budapest
3 June 2013

HU ISSN 0374 – 0676

SEARCH FOR RAPID OSCILLATIONS AMONG SEVEN NORTHERN CP STARS

PAUNZEN, E.[1,2]; HANDLER, G.[3]; NETOPIL, M.[4]; FOSSATI, L.[5]; ILIEV, I. KH.[2]; RODE-PAUNZEN, M.[4]; LÜFTINGER, T.[4]; RYABCHIKOVA, T.[6]; BOŽIĆ, H.[7]

[1] Department of Theoretical Physics and Astrophysics, Masaryk University, Kotlarska 2, CZ-611 37 Brno, Czech Republic; e-mail: epaunzen@physics.muni.cz

[2] Rozhen National Astronomical Observatory, Institute of Astronomy of the Bulgarian Academy of Sciences, P.O. Box 136, BG-4700 Smolyan, Bulgaria

[3] Copernicus Astronomical Center, Bartycka 18, 00-716, Warsaw, Poland

[4] Institut für Astrophysik der Universität Wien, Türkenschanzstr. 17, A-1180 Wien, Austria

[5] Argelander Institut für Astronomie, Auf dem Hügel 71, Bonn, 53121, Germany

[6] Institute of Astronomy, Russian Academy of Sciences, Pyatnitskaya 48, 119017 Moscow, Russia

[7] Hvar Observatory, Faculty of Geodesy, University of Zagreb, Kačićeva 26, HR-10000 Zagreb, Croatia

Up to now, there are only about 45 rapidly oscillating Ap (roAp) stars known. They are located within an area of pulsational instability in the Hertzsprung-Russell diagram, at the main sequence, ranging in effective temperature from about 6600 K to 8500 K.

Photometric investigations for these stars show a period range of five to twenty five minutes, which is consistent with acoustic (p-mode) pulsations of low degree and high radial overtone (Kurtz et al. 2011).

The driving mechanism of their oscillation modes is still a matter of debate. But the most probable explanation seems to be the "classical" κ-mechanism operating in the hydrogen ionisation zone. Many physical processes could play a role in this context: for example the coupling with the magnetic field, the ability of the latter to freeze convection and allow the stratification of chemical elements (Balmforth et al. 2001).

Paunzen et al. (2012) published a list of roAp candidates based on their location in the Hertzsprung-Russell diagram which served us as a primary source. In addition, we selected targets from the catalogue of Ap, HgMn and Am stars by Renson & Manfroid (2009). Since most of the known roAp stars are classified as SrCrEu, we searched for such objects in the aforementioned reference. The fundamental parameters of our targets listed in Table 1 were calibrated as described in Paunzen et al. (2012). Luminosities are only derived if Hipparcos parallaxes were available.

The observations were done at the 0.75m APT at Fairborn Observatory (Arizona) either in Strömgren v or Johnson B depending on the brightness of the target. The integration time was set to 20 seconds with apertures of 30 and 45 arcseconds, respectively. No comparison stars were used because a good sampling of the possible periods are needed. A polynomial function was fitted to the sky subtracted data to account for the extinction and atmospheric variations. In Table 2 the observation log is given. Because all data have

an arbitrary zero point, the measurements for each individual star were scaled and then merged.

The final light curves were examined in more detail using the Period04 program (Lenz & Breger 2005), which performs a discrete Fourier transformation. Significant peaks with periods of more than one hour were subtracted. In Figure 1, the Fourier spectra of all light curves are shown. There is no peak, which exceeds 1.3 mmag. For BD +35 3616, we notice a quite prominent peak at about 5 mHz which corresponds to about 200 seconds. Such a high frequency was never detected in any roAp star, so far. However, we are not able find to a possible explanation for this peak.

Table 1: Fundamental data of our target stars.

Star ID	V	Spec	$T_{\rm eff}$ [K]	$\log(L/L_\odot)$
BD +25 4371	9.45	F0 Sr Cr Eu	8040(160)	–
BD +35 3616	9.47	F0 Sr Eu	6830(410)	–
HD 62140	6.47	A8 Sr Eu	7800(140)	1.30(7)
HD 94427	7.36	A5 Sr Eu Cr	7500(250)	1.29(10)
HD 96707	6.08	A8 Sr	7820(230)	1.55(6)
HD 98088	6.11	A8 Sr Cr Eu	8030(120)	1.66(12)
HD 115606	8.55	A2 Sr	7880(250)	1.20(21)

Table 2: Observation log.

Star ID (BD ...)	HJD(start) 2456200+	HJD(end) 2456200+	N	Star ID (HD ...)	HJD(start) 2456200+	HJD(end) 2456200+	N
+25 4371	61.5687	61.6422	254	62140	64.0183	64.0465	103
	62.5603	62.6340	256		66.0085	66.0244	62
	64.5695	64.5695	224		86.9491	86.9840	69
+35 3616	21.6505	21.6682	48	94427	73.9817	74.0476	224
	23.5663	23.6548	242		74.9755	75.0449	235
	25.6500	25.6570	260	96707	69.9945	70.0507	189
	27.5633	27.6461	232		71.9850	72.0516	224
	28.5686	28.6459	216		90.9760	90.9946	66
	29.5620	29.6451	232	98088	82.0011	82.0535	138
	30.5615	30.6446	234		82.9552	83.0515	309
	31.5763	31.6405	175	115606	86.9870	87.0141	93
	32.5628	32.6338	138				
	33.5605	33.6331	205				
	34.5589	34.6325	204				

Acknowledgements: This work was supported by grant GA ČR P209/12/0217, DO 02-85 of Bulgarian NSF, the Austrian Research Fund via the project FWF P22691-N16 and the financial contributions of the Austrian Agency for International Cooperation in Education and Research (CZ-10/2012).

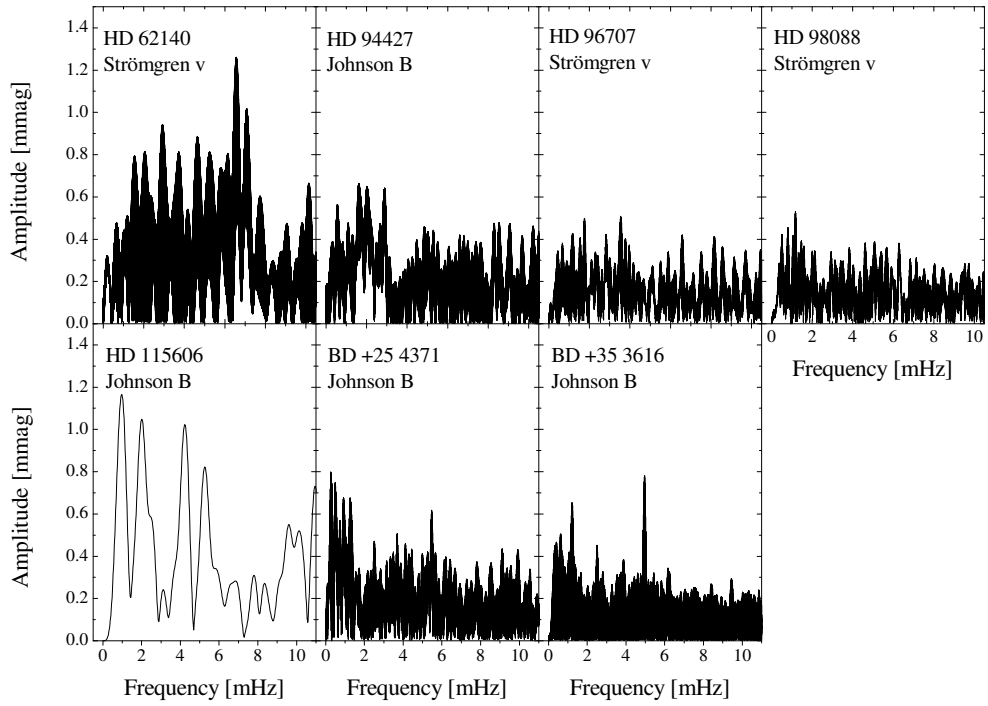

Figure 1. Fourier spectra of the target star light curves.

References:

Balmforth, N.J., Cunha, M.S., Dolez, N., Gough, D.O., Vauclair, S. 2001, *MNRAS*, **323**, 362

Kurtz, D.W., Cunha, M.S., Saio, H., et al. 2011, *MNRAS*, **414**, 2550

Lenz, P., Breger, M. 2005, *CoAst*, **146**, 53

Paunzen, E., Netopil, M., Rode-Paunzen, M., et al. 2012, *A&A*, **542**, A89

Renson, P., Manfroid, J. 2009, *A&A*, **498**, 961

COMMISSIONS 27 AND 42 OF THE IAU
INFORMATION BULLETIN ON VARIABLE STARS

Number 6059

Konkoly Observatory
Budapest
11 June 2013

HU ISSN 0374 – 0676

THE 2013 FLARE OF ASASSN-13AE

NESCI, R.[1]; CARAVANO, A.[2]; FALASCA, V.[2]; VILLANI, L.[2]

[1] INAF/IAPS, via Fosso del Cavaliere 100, 00133, Roma, Italy, e-mail: roberto.nesci@iaps.inaf.it

[2] Osservatorio Cittadino, via Bolletta 18, 06034, Foligno, Italy

We followed the optical transient ASASSN-13ae (Prieto et al. 2013, ATel #4999) with the 0.30 m Schmidt-Cassegrain telescope of the Foligno Observatory, equipped with a Nikon D50 camera, from 2013-04-23 until 2013-06-05. A minimum of three images with 450 s exposure were taken each night. The effective bandwidth of the camera is similar to that of the V filter. Aperture photometry was performed with IRAF/apphot, with 3 arcsec radius: a comparison sequence of 15 stars, within 7 arcmin from the source, was derived from the APASS catalogue. The mean value for each night is reported in Table 1.

Table 1. Average magnitude of ASASSN-13ae from our photometry.

J.D.	V	rms
2456406.41	13.03	0.03
2456411.40	13.40	0.06
2456417.43	13.96	0.09
2456421.34	14.30	0.03
2456427.39	15.60	0.04
2456431.41	14.78	0.08
2456437.40	15.13	0.09
2456449.40	18.50	0.07

The star showed a monotonic decreasing trend of approximately 0.08 mag/day for about 20 days. After that, the light curve became more irregular and then much steeper, finally falling below our photometric limit. On May 8 we also looked for short-term periodic oscillations, possibly induced by the orbital period of a binary system, following the star for three hours, without finding any definite trend at our sensitivity limit (0.03 mag).

We plot in Fig. 1 our points as crosses: the discovery photometric value of ATel 4999 is reported as an asterisk, it is well aligned with our fitting line of the decreasing trend. Three points from the Catalina Sky Survey (CSS) are reported as filled circles: the first of these points seems to be somewhat before the flare peak.

The overall behaviour of the light curve is similar to that observed in the only known previous flare of this source, recorded by the CSS in 2007 (CSS 130418). The 2007 light curve is reported for comparison in the same Figure (open squares) shifted in time by

2167 days to approximately match the peak position: it shows a slope in the bright phase similar to ours. From this CSS light curve it appears that at the epoch of the GALEX observation in a bright state (MJD 54248), reported in ATel 4999, the source was at V=13.8 near the flare peak.

Our observations confirm that the source is a cataclysmic variable star, as suggested by Prieto et al. (2013), likely of the WZ Sge type with a recurrence of about 5.9 years. A search in historical plate archives would be useful to confirm the flare time scale. We have checked that no useful plates are available in the Asiago plate archive (Barbieri et al. 2003) and the star is not visible in a plate of the Digitized First Byurakan Survey (Mickaelian et al. 2007) taken in 1973, when it was expected to be in quiescent state (V ∼20 from CSS) if the recurrence period is true.

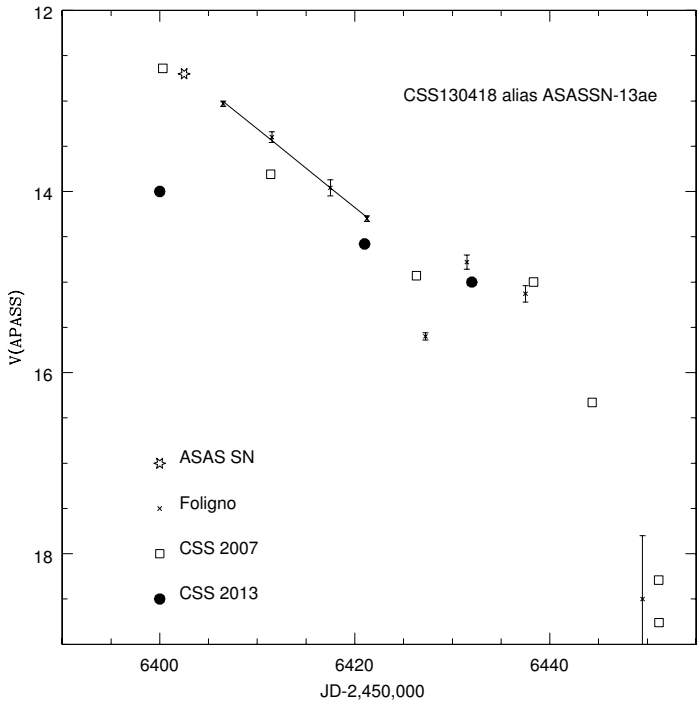

Figure 1.

Figure 1: Light curve of ASASSN-13ae in the year 2013 from our data (crosses with error bars) and data from the CSS (filled circles). The linear fit to the bright part of the light curve is shown. Data from CSS relative to the flare of 2007 are reported as open squares.

References:

AAVSO Photometric Sky Atlas, `http://www.aavso.org/apass`
Barbieri et al. 2003, *Experimental Astronomy*, **15**, 29
Catalina Sky Survey, `http://www.lpl.arizona.edu/css/`
Mickaelian et al. 2007, *A&A*, **464**, 1177
Prieto J.L., Hainline K., Hickox R., et al., 2013, *ATel*, 4999

COMMISSIONS 27 AND 42 OF THE IAU
INFORMATION BULLETIN ON VARIABLE STARS

Number 6060

Konkoly Observatory
Budapest
14 June 2013

HU ISSN 0374 – 0676

PHOTOMETRIC AND SPECTROSCOPIC VARIATIONS OF THE Be STAR HD 112999†

CORTI, M. A. [1,2]; GAMEN, R. C. [2,3]; AIDELMAN, Y. J.[2,3]; FERRERO, G. A.[2,3]; WEIDMANN, W. A.[4]

[1] Instituto Argentino de Radioastronomía (CCT-La Plata, CONICET),Villa Elisa, Argentina

[2] Facultad de Ciencias Astronómicas y Geofísicas, Universidad Nacional de La Plata, Argentina
e-mail: mariela@fcaglp.unlp.edu.ar

[3] Instituto de Astrofísica de La Plata (CCT-La Plata, CONICET), Argentina

[4] Observatorio Astronómico Córdoba, Universidad Nacional de Córdoba, Argentina

1 Introduction

Be stars were defined as "non-supergiant B-type stars whose spectrum have or had at a time, one or more Balmer lines in emission" by Jaschek et al. (1981). This class of stars has circumstellar disks that originate emission in hydrogen, helium, and/or metal lines. These disks seem to be mainly generated by rapid rotation and/or binarity, combined with non-radial pulsations (Huat et al., 2009; Neiner et al., 2012). These phenomena occur as an episode during the evolution of hot B-type stars.

One of the most intriguing properties of Be stars is their long-term variability, which seems to be related to disk growth or loss events (Hubert & Floquet, 1998). These events produce spectroscopic and photometric effects, i.e. changes from emission to absorption lines (and vice versa), and also flux and color variations. Given the great variety of observed events, many open questions remain unanswered (see the review by Porter & Rivinius, 2003, and references therein), which raises the importance of studying these objects. As the same authors state "Be stars are in a unique position to make contributions to several important branches of stellar physics, e.g., asymmetric mass loss processes, stellar angular momentum distribution evolution, asteroseismology, and magnetic field evolution".

The primary goal of this paper is to present the analysis carried out on a new possible transient Be star, labelled HD 112999 (α_{J2000} =13:01:35, δ_{J2000} = −60:40:16). This star was observed by one of us (MAC) while trying to identify possible members of the Centaurus OB1 (CenOB1) stellar association (Corti & Orellana, 2013). The spectral classification of this star varies depending on the bibliography available. It was first reported as a Be star by Bidelman & MacConnell (1973). Other authors reported different spectral types, i.e. Cannon & Pickering (B8; 1920), Houk & Cowley (B6 III (N); 1975), and

†Visiting Astronomer, Complejo Astronómico El Leoncito operated under agreement between the Consejo Nacional de Investigaciones Científicas y Técnicas de la República Argentina and the National Universities of La Plata, Córdoba and San Juan.

Table 1: Instrumental configurations used

run	Observat.	Epoch(s)	HJD 2400000+	Telesc. [m]	Spectrograph	Rec. disp. [Å px^{-1}]	$\Delta\lambda$ [Å]	exp. time [sec]	S/N
A	La Silla/ESO	2008 May	54603.68	2.2	FEROS	0.03	3700-8600	600	70-120
B	CASLEO	2009 Apr.	54941.70	2.1	REOSC CD	0.2	3700-6000	1200	20-50
C	CASLEO	2012 Jan.	55930.86	2.1	REOSC CD	0.2	3700-6000	1200	20-50
D	CASLEO	2012 Apr.	56047.66	2.1	REOSC SD	1.6	5900-7400	700	150-200
E	CASLEO	2012 June	56086.00	2.1	Boller&Chivens	2.7	3500-5000	150	160-250

Garrison et al. (B6 V; 1977). Nowadays, HD 112999 is listed in the BeSS catalogue[1] as B6 III ne (Neiner et al., 2011). This star prompted further attention because our optical spectrum, taken on 2009, was very different from those classified before. We consulted spectral and photometric databases and found that HD 112999 is a variable Be star which seems to have experimented disk − loss and growth − events over the last decades. In the following sections, we describe these facts.

2 Observational Data

2.1 Spectroscopic data

The observational material belongs to different program runs obtained at the Complejo Astronómico El Leoncito (CASLEO), Argentina and La Silla Observatory, Chile. Different instrumental configurations, detailed in Table 1, were used in these runs.

For CASLEO observations, comparison arc images were observed in the same sky position where the stellar images were located immediately after or before the stellar exposures, being Th−Ar for the echelle mode of the REOSC spectrograph, Cu−Ar for the simple mode, and He−Ne−Ar if the B&C was used. Moreover, bias frames, standard stars of radial velocity, and spectral type were observed every night, the latter only during run B. We also took the spectrum of the standard of rotational velocity, τ Sco (Slettebak et al., 1975), during run C. These spectra were processed and analysed with IRAF[2] routines.

The spectrum retrieved from the ESO database was obtained with the FEROS spectrograph and processed with the MIDAS pipeline. The radial velocities were obtained by simple cross-correlation of the echelle orders of the HD 112999 star and of the simultaneous calibration fiber with regard to the pertinent reference spectrum.

2.2 Photometric data

The photometric data were taken from two sources: the Epoch Photometry Annex of Hipparcos Astrometry Mission (Perryman & ESA, 1997) and The All Sky Automated Survey (ASAS) (Pojmanski, 1997).

The Hipparcos data consist of 214 observations made between December 1989 and January 1993. The measurements are in the interval $7.31 < H_p < 7.48$; the errors of the individual measurements range from 0.007 to 0.020 mag. According to the criteria adopted when Hipparcos data were analysed, this star was classified as an "unsolved variable"[3]. Following the Hipparcos calibration for a star with colour index $V - I = 0.070$, as in this case, the relation $H_p - V_J = 0.025$ should hold, where V_J is the magnitude in the V filter of the Johnson photometric system.

[1] http://basebe.obspm.fr

[2] IRAF is distributed by the National Optical Astronomy Observatories, which are operated by the Association of Universities for Research in Astronomy, Inc., under cooperative agreement with the National Science Foundation.

[3] cf. The Hipparcos and Tycho Catalogues, Vol. 1, Introduction and Guide to the Data, Sec. 1.3 App. 2.

The ASAS data include 1030 magnitude determinations obtained between November 2000 and December 2009. ASAS provides aperture photometry with several apertures. For this study, the aperture labeled as MAG 1 in the dataset was selected because larger apertures could be contaminated by a neighbor star. The errors of individual measurements are up to 0.120 mag, with a typical value $\mathrm{err}_{ASAS} = 0.040$ mag. Since $\mathrm{err}_{ASAS} > (H_p - V_J)$, no zero-point correction was applied to compare the two datasets.

3 Results

3.1 Spectral Analysis

The FEROS spectrum (labelled A in Table 1) shows typical Be features such as the Balmer lines Hγ, Hβ and Hα in emission (see Fig 2). There, at least one additional emission line, Fe I λ4328 bluer than Hγ, and two additional emission lines, Fe I λ4849 and Fe I λ4875 of Hβ, can be observed. The spectrum also presents other metallic lines, i.e. O II, Fe II, Cr II, Ti III, C III, etc, as weak emissions, some of them shown in Fig 1. All of these emission lines could be originated in a disk. A Be star with mid inclination angle might cause the double structure observed in Hα emission lines. The rotation of the disk plus a possible absorption ("reversal" of the emission) against the edge of the star or disk cause such profiles of double structure. Other features as He I, λ4009, 4026, 4144, 4387, 4471, 4921, 5875, 6678 and 7065, Si II $\lambda\lambda$4128-30 and Mg II λ4481 can be observed in absorption. These lines are thought to be originated in the stellar photosphere. This composite spectrum indicates that the HD 112999's disk was thick and extended during 2008 May.

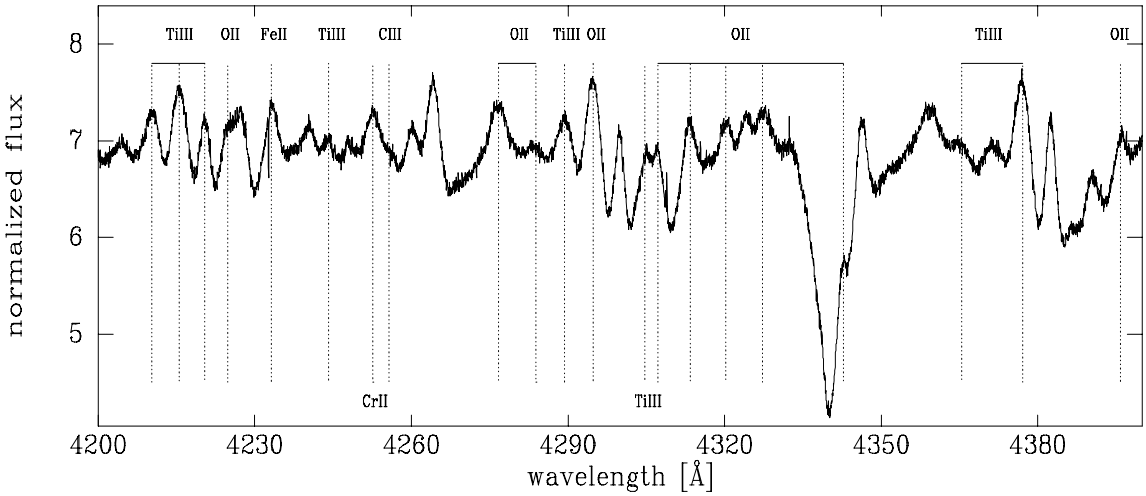

Figure 1. Some metallic emission lines in the FEROS spectrum.

Our B spectrum, obtained about one year later than A, shows a very weak emission contribution in the Hβ profile and an almost marginal one in the Hγ line. The metallic lines (seen as weak emissions in A) have not been detected in this spectrum. We think that this is not due to the fact that the B spectrum has a poorer S/N ratio than A. The absorption lines, which would result from the stellar photosphere in the A spectrum, can also be observed here.

Three years later, the C spectrum presented the Balmer lines Hγ and Hβ as pure absorption, i.e. there were no traces of emission contribution in these lines (see Fig. 2).

The D spectrum was obtained by one of us (WAW) to see the profile of the Hα line, as neither B nor C spectra included it in their spectral ranges. Thus, we proved that Hα is a conspicuous absorption line in the spectrum taken in April 2012 (see Fig. 2).

The E spectrum is the one we have been able to obtain more recently (Fig. 3). It shows the same absorption spectral lines than the other spectra, plus a very narrow absorption line at 4233 Å, which we have identified as Fe II. We argue that this line seems to have originated in a shell because its FWHM is

Table 2: Radial velocities measured in the high resolution spectra

Line	run A [km s^{-1}]	run B [km s^{-1}]	run C [km s^{-1}]
He I 4026	−20	5	7
He I 4471	−35	−15	−31
Mg II 4481	−92	−5	−2
He I 5876	−20	36	−19
Na I 5890-96	4.5	5.5	2.5

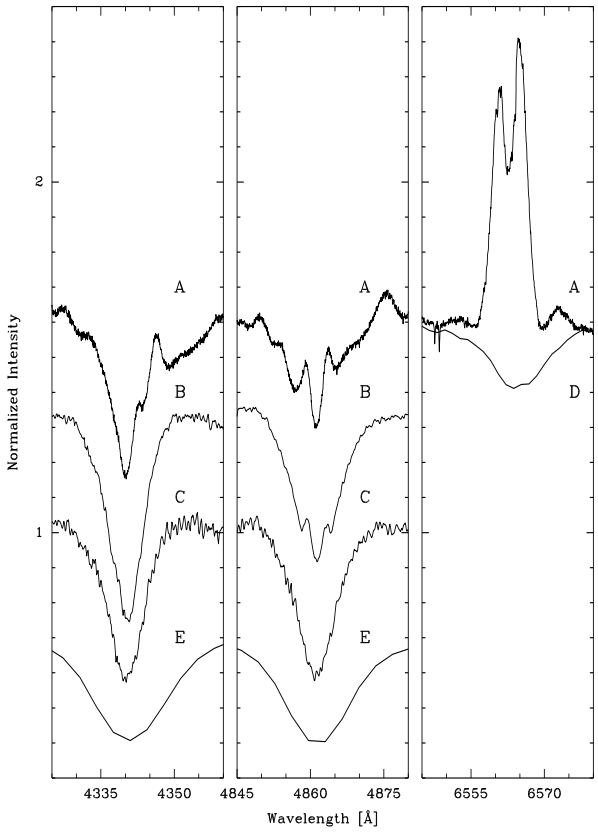

Figure 2. Variations of the Hγ, Hβ and Hα lines from spectra obtained in different runs (see Table 1). Other emission lines identified as Fe I λ 4328 (in the Hγ region), Fe I λ 4849 and λ 4875 (Hβ region), and Fe I λ 6574 (Hα region) can also be observed.

$\sim$ 2.5 Å compared to the FWHM $\sim$ 8 Å of the photospheric He I absorption lines. This assumption is in good agreement with the fact that the forming region of Fe II lines is located close to the central star (Arias et al. 2006).

We classified the Be-type spectra A, B, and E as B2−3 V, following the criteria of Walborn & Fitzpatrick (1990), i.e. the ratio between Si III λ4552 and Si IV λ4089, the declining strengths of the C III+O II blends at $\lambda\lambda$4070 and 4650, and the weakness of all the Si II-III features. From the spectral type B2 to B3, Si II $\lambda\lambda$4128-30, C II λ4267 and Mg II λ4481 increase in prominence. The very large He I $\lambda\lambda$4144/4121 ratio is a characteristic of the B2 V spectra and the principal luminosity criterion is Si III λ4552/ He I λ4387.

The projected rotational velocity ($v \sin i$) in this class of stars is an important parameter. To estimate it, we used the spectrum of the star τ Sco, which was convolved with rotation line profiles calculated for different projected rotational velocities, and the *FWHM* of the absorption line He I λ5015 was measured for each velocity. Then, a linear relation between *FWHM* and the $v \sin i$ was fitted. This empirical relation was used to translate the *FWHM* of the line in the spectrum of HD 112999 into a $v \sin i$ estimation. In this way we obtained $v \sin i = 170 \pm 40$ km s^{-1}, the error being so large because of the low S/N ratio of the spectrum and the weakness of the line.

The B star becomes a Be star exhibiting rapid rotation probably as the result of disk instabilities caused by the spun up by binary mass transfer (McSwain et al., 2009). In order to know if this is the case for HD 112999 star, we measured the radial velocities in its three high-resolution spectra (A, B, and C). For this, we fitted Gaussian profiles to the selected spectral lines, i.e. He I $\lambda\lambda$4026, 4471 and 5876, and Mg II λ4481, as well as the interstellar lines of Na I. A comparison of the values of Na I showed no systematic differences between the spectrographs used (within an error of 3 km s^{-1}), nevertheless, the He I and Mg II λ4481 absorption lines present discrepancies within one spectrum which are much larger than for any of these lines between different spectra. The observed differences between spectra cannot be exploited to speculate a possible binarity, because the different values are expected from one spectrum to another in the case of a binary star and all the lines should vary in the same way within one spectrum. We provide the radial velocity measurements in Table 2 for future reference.

3.1.1 BCD fundamental parameters

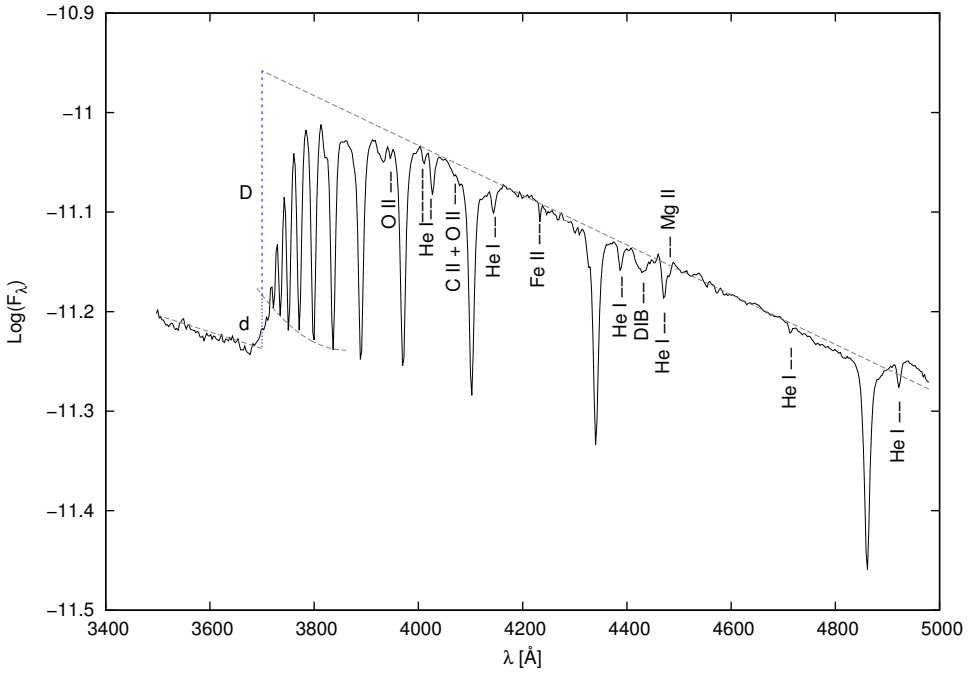

Figure 3. Balmer discontinuity: D is the first Balmer jump for normal B star, d is the second discontinuity in absorption, indicating the presence of the circumstellar envelope.

Some physical properties from the E spectrum of HD 112999 were derived by using the BCD (Barbier-Chalonge-Divan) spectrophotometric system (Chalonge & Divan, 1973, 1977). A detailed description of this method is presented in Zorec et al. (2009, Appendix A) and further applications to Be stars were made by Zorec et al. (2005) and Aidelman et al. (2012). This method is ideal for studying peculiar stars, and in particular Be stars, due to the fact that the parameters defined by the method are not affected by interstellar extinction and absorption/emission from the circumstellar envelope (Zorec & Briot, 1991). Then, we determined a B3 spectral type (with one subtype error) of luminosity class III, an effective temperature $T_{\rm eff} = 17\,500 \pm 1\,000$ K, a surface gravity $log\ g = 3.3 \pm 0.5$, an absolute magnitude $M_V = -2.5 \pm 0.5$ mag, and a color excess $E_{B-V} = 0.11 \pm 0.07$ mag.

The presence of the second Balmer discontinuity in the E spectrum indicates that a circumstellar envelope can still be observed (Divan, 1979). Figure 3 shows this spectrum in the Balmer discontinuity region, where the first jump, D, corresponds to a normal B star while the second one, d, is originated by the envelope.

Later on, we estimated the distance from HD 112999 to the Sun, using its extreme V magnitudes, i.e. $7.3 \leq V \leq 7.5$ (see Fig. 4), corrected by colour excess $E_{B-V} = 0.11 \pm 0.07$ mag and considering the standard selective absorption coefficient, $R_v = 3.1$ (Schultz & Wiemer, 1975). We obtained a distance modulus of 9.5 ± 0.5 mag (790 ± 180 pc) and 9.7 ± 0.5 mag (870 ± 200 pc), respectively. These estimated distance values with their respective errors are slightly larger than the Hipparcos distance (654 pc). Then, HD 112999 is closer than the Cen OB1 association, $V_0 - M_v = 12$ mag (2500 pc) (Corti et al., 2012).

3.2 Light curve analysis

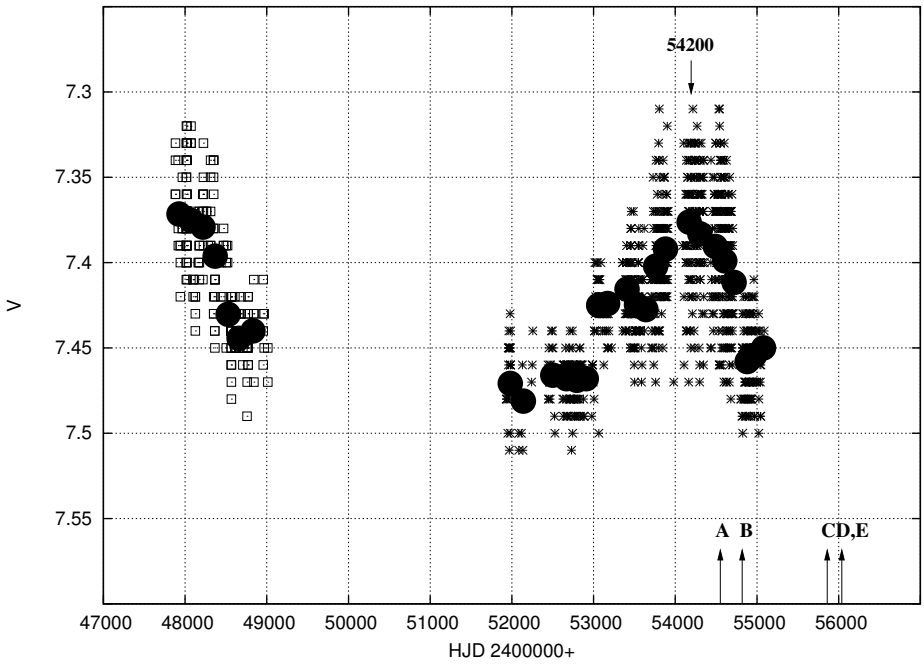

Figure 4. Light curve of HD 112999. Boxes and asterisks correspond to Hipparcos and ASAS data, respectively. Filled circles depict the average magnitude in about 114 days. The capital letters (see Table 1) show the almost temporal coincidence between the photometric and spectroscopic data explained in section 3.2.

The collected photometric data were analysed together and the resulting light curve is shown in Fig. 4. HD 112999 presents two kinds of variabilities: short-term one (1.302 days; Hubert & Floquet, 1998) and long-term one ($\sim$ years). The formerone with an amplitude smaller than 0.1 mag, is included in the Hipparcos data (see Fig. 5), and it is the reason why this star has been included in the General Catalogue

of Variable Stars (Samus et al., 2009) and classified as BE[4].

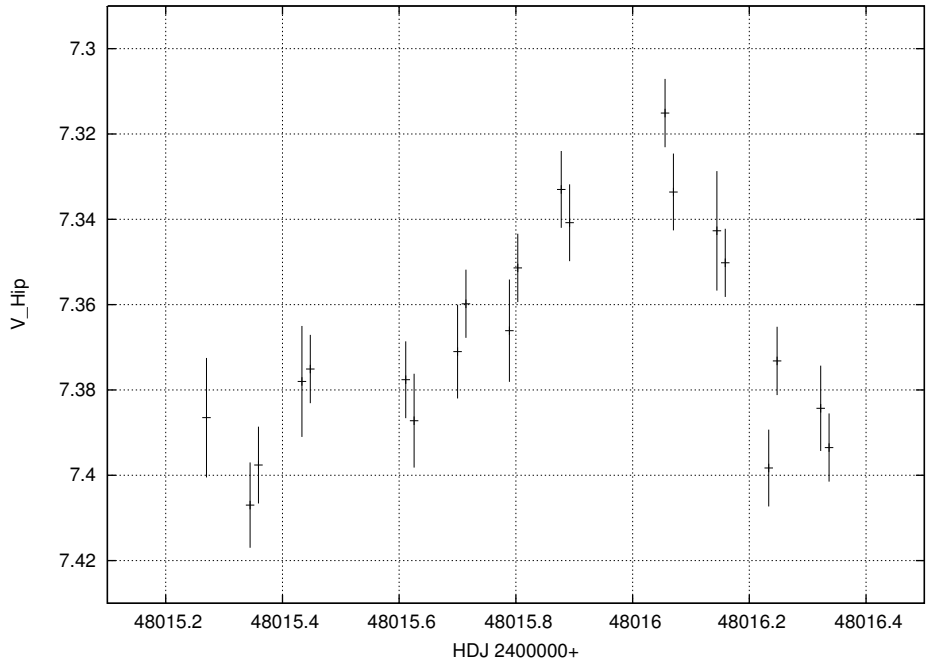

Figure 5. Hipparcos data showing variability smaller than 0.1 mag with a period $\sim$ 1 day.

The long-term variation can be better observed in the ASAS data. To enhance and show it more clearly, we represent unweighted averages (calculated within intervals of $\sim$114 days) with filled circles. In Fig. 4 we identified the light maximum reached around HJD 2 454 200 (ASAS data).

4 Discussion

The collected spectra show important variations, especially noticeable in the Balmer lines, i.e. their emission profiles decrease in intensity from May 2008 to June 2012 (A to E). Similar variability was already detected in other Be stars like MG 31 and MG 119 in NGC 3766 (McSwain et al., 2008); Pleione and κ Dra (Hubert & Floquet, 1998) and 66 Ophiuchi (Floquet et al., 2002).

The relation between the photometric and spectroscopic data is shown in Fig. 4. The capital letters are the same defined in Table 1. The light curve and the spectra obtained in A and B runs, are well correlated in the sense that as the star fades, the Balmer emissions decrease their intensities (Fig. 2). This behavior is related to disk dissipation. The lack of photometric data after 2009 August prevents us to determine if the star reached the minimum between B and C runs or it will be reached later.

The behavior observed in HD 112999 led us to search in the existing literature for more information about this star. Thus, we learned that the only Be spectrum of HD 112999 was obtained in the period 1967−1969 by Bidelman & MacConnell (1973)[5]. Unfortunately, they did not provide a precise date of observation. As already mentioned in Section 1, other authors have reported different spectral classifications for HD 112999. We adopted the B2−3 V spectral type for HD 112999, which was determined following the criteria of Walborn & Fitzpatrick (1990).

[4]Due to the type of variability, BE is used when a Be variable cannot be readily described as a Gamma Cassiopeiae variable (GCAS) star, (Samus et al. 2009)

[5]This observation was the reason to be included in the Catalogue of Be Stars (Jaschek & Egret, 1982)

5 Summary

The analysis of the spectroscopic and photometric data of HD 112999 allowed us to identify a long-term variability in its V light curve and the change of the Balmer line profiles from emission to absorption. The decline in V magnitudes between 2007 and 2009 is related to the disappearance of emission lines, very noticeable in some Balmer lines. We propose that the reported changes are induced by the loss of the disk. Photometric data were not sufficient to search for long-term periodicities; therefore, we encourage other researchers to monitor this star in the future. We classified our spectra as B2−3, the luminosity class should be clarified with further observations.

We used the observations obtained in different observing programs to measure some important parameters such as the projected rotational velocity and the distance modulus. Also, our last spectrum E, obtained in June 2012, was analysed with the BCD method, from which we noted that a circumstellar envelope is still present. Hence, further spectra should be obtained to determine if HD 112999 will reach a normal B-type.

ACKNOWLEDGMENTS: This research used of the SIMBAD database, operated at CDS, Strasbourg, France, and also the WEBDA database, operated at the Institute of Astronomy of the University of Vienna. This paper was partially supported by Consejo Nacional de Investigaciones Científicas y Técnicas CONICET under projects PIP 01299 and 0523 and by Universidad Nacional de La Plata (UNLP) under project G091. We are very grateful to Dra. Granada Anahí and Dra. Cidale Lydia for their interesting and valuable comments. We thank Mrs Roxana Kotton and the English Department of FCAyG (UNLP) for a careful reading of the manuscript.

References:

Aidelman, Y., Cidale, L. S., Zorec, J., Arias, M. L., 2012, *A&A*, **544**, A64
Arias, M. L., Zorec, J., Cidale, L. S. et al., 2006, *A&A*, **460**, 821
Bidelman, W. P., MacConnell, D. J., 1973, *AJ*, **78**, 687
Cannon, A. J., Pickering, E. C., 1920, *Annals of Harvard College Observatory*, **95**, 1
Chalonge, D., Divan, L., 1973, *A&A*, **23**, 69
Chalonge, D., Divan, L., 1977, *A&A*, **55**, 117
Corti, M. A., Arnal, E. M., Orellana, R. B., 2012, *A&A*, **546**, A62
Corti, M. A., Orellana, R. B., 2013, *A&A*, **553**, A108
Divan, L., 1979, *Ricerche Astronomiche*, **9**, 247
Floquet, M., Neiner, C., Janot-Pacheco, E., Hubert, A. M., et al., 2002, *A&A*, **394**, 137
Garrison, R. F., Hiltner, W. A., Schild, R. E., 1977, *ApJS*, **35**, 111
Houk, N., Cowley, A. P., 1975, *University of Michigan Catalogue of two-dimensional spectral types for the HD stars.* Volume **I**. Declinations -90 to -53
Huat, A. L., Hubert, A. M., Baudin, F., Floquet, M., Neiner, C., et al., 2009, *A&A*, **506**, 95
Hubert, A. M., Floquet, M., 1998, *A&A*, **335**, 565
Jaschek, M., Slettebak, A., Jaschek, C., 1981, *BeSN*, **4**, 9
Jaschek, M., Egret, D., 1982, *IAU Symposium*, **98**, 261
McSwain, M. V., Huang, W., Gies, D. R., 2009, *ApJ*, **700**, 1216
McSwain, M. V., Huang, W., Gies, D. R., Grundstrom, E. D., Townsend, R. H. D., 2008, *ApJ*, **672**, 590
Neiner, C., de Batz, B., Cochard, F., Floquet, M., Mekkas, A., Desnoux, V., 2011, *AJ*, **142**, 149
Neiner, C., Grunhut, J. H., Petit, V., ud-Doula, A., Wade, G. A., et al., 2012, *MNRAS*, **426**, 2738
Perryman, M. A. C., ESA, eds. 1997, *ESA Special Publication*, Vol. **1200**, The HIPPARCOS and TYCHO catalogues.
Pojmanski, G., 1997, *Acta Astron.* **47**, 467
Porter, J. M., Rivinius, T., 2003, *PASP*, **115**, 1153
Samus, N. N., Durlevich, O. V., et al., 2009, VizieR On-line Data Catalog B/gcvs
Schultz, G. V., Wiemer, W., 1975, *A&A*, **43**, 133
Slettebak, A., Collins, II, G. W., Parkinson, T. D., Boyce, P. B., White, N. M., 1975, *ApJSS*, **29**, 137
Walborn, N., Fitzpatrick, E., 1990, *PASP*, **102**, 379
Zorec, J., Briot, D., 1991, *A&A*, **245**, 150
Zorec, J., Cidale, L., Arias, M. L. et al., 2009, *A&A*, **501**, 297
Zorec, J., Frémat, Y., Cidale, L., 2005, *A&A*, **441**, 235

COMMISSIONS 27 AND 42 OF THE IAU
INFORMATION BULLETIN ON VARIABLE STARS

Number 6061

Konkoly Observatory
Budapest
3 July 2013

HU ISSN 0374 – 0676

DISCOVERY OF IRREGULAR VARIABILITY OF FIVE STARS IN THE VICINITY OF THE YOUNG STELLAR OBJECT V645 CYGNI

SOBOLEV, A. M.; GORDA, S. YU.; DAVYDOVA, O. A.

Astronomical Observatory, Ural Federal University, Russia
E-mail: Andrej.Sobolev@usu.ru, Stanislav.Gorda@usu.ru

We carried out a search for irregular variable stars in the vicinity of the young massive star V645 Cyg. The search was performed on the basis of a set of CCD frames obtained at the Astronomical Observatory of the Ural Federal University. The data was collected in the course of the 1.5-year photometric monitoring of the young variable star V645 Cyg in filters V and R_c. All frames were obtained with the AZT-3 reflector ($D = 0.45$ m, $F_{\rm Newton} = 2.0$ m) equipped with Alta-U6 CCD camera (Kodak KAF-1001E, 1048×1048, 24-micron chip). The frames contain information on sources within about $40' \times 40'$ fields centered approximately at V645 Cyg. These sources include several suspected young stellar objects (YSOs), e.g. IRAS 21377+4955 and IRAS 21389+5003, which are poorly studied at optical wavelengths.

Search for the YSOs in the V645 Cyg vicinity is necessary to find other young stars which could be born together with this massive star which recently emerged from its cocoon. At present there are no firmly established YSOs in the vicinity of V645 Cyg. This is enigmatic because the current paradigma implies that "massive stars are seldomly (if at all) formed in isolation" (Zinnecker and Yorke 2007).

In this study we considered objects in $15'$ vicinity of V645 Cyg. YSOs are characterized by being brighter in infrared than expected for the main sequence stars. In order to identify YSO candidates in the obtained frames we carried out photometry of a number of selected stars which show infrared colour indices $H - K_s > 0\overset{\rm m}{.}3$ in 2MASS catalog. The area is rich in the sources that are surely more distant than V645 Cyg. In order to avoid them we introduced the following criterion: $K_s < 11^{\rm m}$. One object (2MASS 21385638+5012061) violates this criterion and was included in the list because of its high red colour index $V - R = 1\overset{\rm m}{.}98$ in the NOMAD1 catalogue. We did not introduce any stringent criterion on the infrared colour indices in order to avoid possible elimination of Orion variables of IN type, etc. Some young variable stars of this type have 2MASS colours close to the main sequence stars and have good chances to be associated with the massive young variable V645 Cyg. Another selection criterion was the optical brightness of objects $R < 14^{\rm m}$. The latter criterion is necessary to achieve the photometric accuracy of the order of $0\overset{\rm m}{.}01$ for the frames obtained with exposure times adjusted for the V645 Cyg photometry. The list includes three fainter objects which allowed sufficiently high photometric accuracy.

Table 1. List of target stars and comparison stars. Stellar magnitudes are taken from the NOMAD1 catalogue

Objects				Comparison stars (2MASS)		
#	2MASS	m_V	m_R	C_1	C_2	C_3
1	21395825+5014209 (V645 Cyg)	∼13	∼12	21401743+5013545	21395248+5015526	21393905+5012016
2	21392977+5009286 (IRAS 21377+4955)	14.31	12.36	21393905+5012016	21394305+5010491	21393643+5008273
3	21404646+5016489 (IRAS 21389+5003)	12.61	10.72	21403765+5016258	21405102+5017094	21394758+5017008
4	21385638+5012061	15.53	13.55	21391128+5011193	21385214+5011225	21384244+5012131
5	21390639+5004544	13.01	11.15	21384996+5007368	21391834+5003325	21390691+5003206
6	21393188+5006596	16.00	14.75	21394160+5009340	21393870+5006470	21391935+5008547
7	21402043+5020007	15.04	13.84	21403180+5019153	21403029+5017160	21401798+5022063
8	21403143+5021300	15.73	14.51	21401858+5022036	21403180+5019153	21405252+5022075
9	21403966+5010088	16.04	14.29	21404627+5010344	21404549+5007301	21403186+5009173
10	21404091+5013584	13.24	11.33	21410979+5012361	21403765+5016258	21404271+5010334
11	21410408+5010083	12.90	11.60	21410979+5012361	21410818+5008461	21404271+5010334
12	21410428+5014152	14.41	12.88	21411409+5016534	21405102+5017094	21410979+5012361
13	21410943+5018008	11.38	10.51	21411409+5016534	21410645+5017483	21412779+5018164
14	21411121+5010380	13.91	12.83	21410818+5008461	21410979+5012361	21412626+5009326

In total, 14 stars were selected for analysis. We included V645 Cyg in the analysis because it satisfies our selection criteria. Except for V645 Cyg the list includes 2 other members of the IRAS point source catalogue, the rest of the target stars have considerable red colour indices.

One of the IRAS sources (IRAS 21377+4955, 2MASS 21392977+5009286) was previously identified as a carbon star (Alksnis and Alksne, 1988) and suspected to be variable (NSV 25721). The list of IRAS sources and other target stars is given in Table 1 in order of increasing right ascension. Designations of the stars are given according to the 2MASS catalog. For each target star we selected three stars of comparison in its near vicinity ($r < 5'$), see Table 1.

The reduction of the CCD frames was carried out using *Muniwin* software (`http://c-munipack.sourceforge.net`). After that we calculated values of the night-average differences of the brightness for each star with respect to the three comparison stars. Before averaging all the values were reduced to a particular comparison star (C1 stars in Table 1).

In order to determine the degree of brightness variability for the investigated stars we used a simple criterion similar to the Stetson index (Stetson, 1996). Namely, we considered ratio of the root mean square (rms) brightness differences for the target stars to rms brightness differences for the comparison stars calculated for the whole period of observations. In this case the dispersion of the brightness differences for the stars of comparison characterizes accuracy of the brightness measurements for the target stars.

As a criterion for the existence of variability we adopted 3σ criterion. This means that the star was considered to be variable if the rms difference of the brightness of a target star in both filters exceeds the corresponding rms difference for the comparison stars more than three times. Tables 2 and 3 contain values of the rms brightness difference for the target stars ($\sigma_{\rm var}$) and the comparison stars ($\sigma_{\rm comp}$), correspondingly. It is seen that $\sigma_{\rm comp}$ in filter R_c is of the order of $0\overset{\rm m}{.}01$ and less. The accuracy of measurements in filter V in a few cases is about twice worse because the target stars are fainter in this passband.

Analysis of the data from Tables 2 and 3 shows that the 3σ criterion of variability is satisfied for 6 target stars including V645 Cyg. The other target stars with one exception did

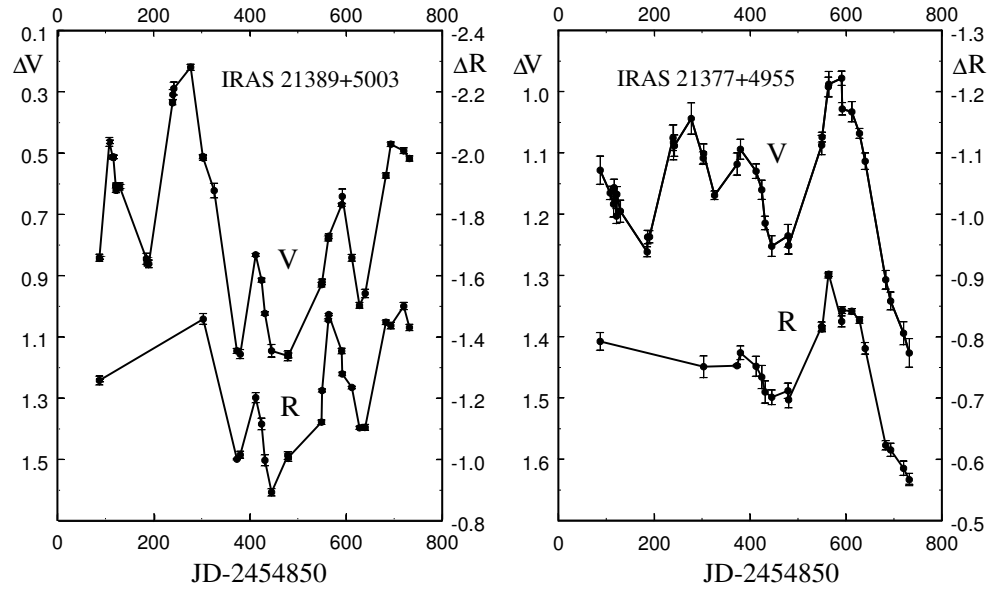

Figure 1. The light curves of the IRAS point sources. The bars correspond to the rms scatter of brightness during one night.

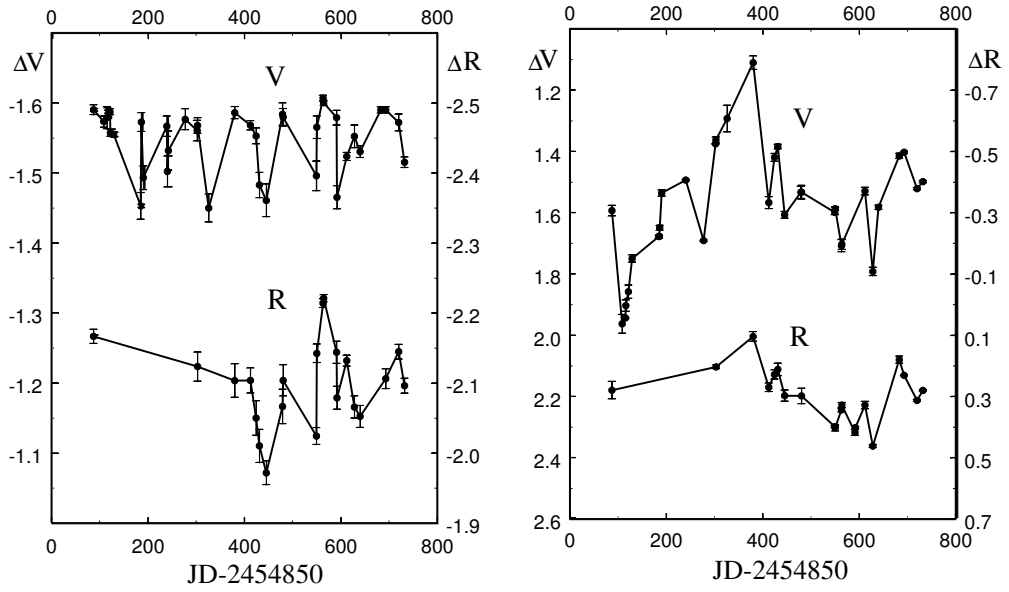

Figure 2. The light curves of 2MASS 21410943+5018008 (#13, left) and 2MASS 21403966+5010088 (#9, right). The bars correspond to the rms scatter of brightness during one night.

Table 2. Target stars with detected variability

				V		R		V	R
#	2MASS	IRAS	NSV	$\sigma_{\rm var}$	$\sigma_{\rm comp}$	$\sigma_{\rm var}$	$\sigma_{\rm comp}$	$\sigma_{\rm var}/\sigma_{\rm comp}$	$\sigma_{\rm var}/\sigma_{\rm comp}$
1	21395825+5014209	(V645 Cyg)		0.097	0.011	0.077	0.009	8.8	8.6
2	21392977+5009286	21377+4955	25721	0.104	0.009	0.093	0.006	11.2	16.0
3	21404646+5016489	21389+5003		0.265	0.015	0.190	0.008	17.5	23.8
5	21390639+5004544			0.217	0.013	0.237	0.010	16.5	23.7
9	21403966+5010088			0.187	0.007	0.090	0.006	25.9	15.6
13	21410943+5018008			0.047	0.008	0.063	0.004	5.8	15.2

Table 3. Target stars without detected variability

		V		R		V	R
#	2MASS	$\sigma_{\rm var}$	$\sigma_{\rm comp}$	$\sigma_{\rm var}$	$\sigma_{\rm comp}$	$\sigma_{\rm var}/\sigma_{\rm comp}$	$\sigma_{\rm var}/\sigma_{\rm comp}$
4	21385638+5012061	0.042	0.022	0.013	0.010	1.9	1.3
6	21393188+5006596	0.028	0.017	0.023	0.011	1.7	2.1
7	21402043+5020007	0.039	0.013	0.056	0.011	3.0	5.1
8	21403143+5021300	0.028	0.010	0.014	0.008	2.7	1.8
10	21404091+5013584	0.008	0.009	0.015	0.006	0.9	2.4
11	21410408+5010083	0.016	0.010	0.013	0.007	1.5	1.9
12	21410428+5014152	0.018	0.011	0.016	0.008	1.6	2.0
14	21411121+5010380	0.016	0.012	0.014	0.009	1.3	1.6

not show significant variability of brightness. This exception is 2MASS 21402043+5020007 (#7) for which the 3σ criterion is satisfied only in filter R_c. We consider the detection of variability of this star uncertain.

We analysed the changes of brightness of newly found variable stars and V645 Cyg during particular nights. In several cases observations during one night lasted for up to 6 hours. In most cases variability had a character of monotonic brightness changes. In a few cases one brightness extremum was registered during a single night.

We examined the brightness data of the six variable stars for possible periodicity. For this purpose we implemented the Lafler-Kinman method realized in the package winefk3 written by Goranskij V.P. (the program with comments in English can be downloaded from http://variablestars.ru/FILES/winefk.rar). Brightness changes for all newly found variable stars and V645 Cyg were found to be non-periodic.

We found that the bright infrared point sources IRAS 21377+4955 and IRAS 21389+5003 show brightness variability of irregular type with amplitudes up to $0\overset{\rm m}{.}8$. For IRAS 21389+5003 the variability of brightness is registered for the first time. For another bright infrared source IRAS 21377+4955 only photographic estimates of the optical brightness were reported (Alksnis and Alksne, 1988). In this study we present results of much more accurate CCD measurements of the brightness in filters V and R_c for a period of 1.5 years.

Far infrared colour indices of IRAS 21377+4955 and IRAS 21389+5003 are characteristic of the YSOs. Brightness of these stars as point sources of the WISE (Wide-Field Infrared Survey Explorer) survey increases with wavelength (the longest wavelength of the survey is 22 microns). However, combination of the colour indices and irregular type of variability cannot be used as a strict proof of the YSO nature of the sources. For example, IRAS 21377+4955 was identified as a carbon star on the basis of its photographic spectrum in the red part of the optical range (Alksnis and Alksne, 1988). However, no other carbon stars were reported in our field though it was inspected by Alksnis and Alksne (1988). Additional spectroscopy is necessary to establish the nature of the sources.

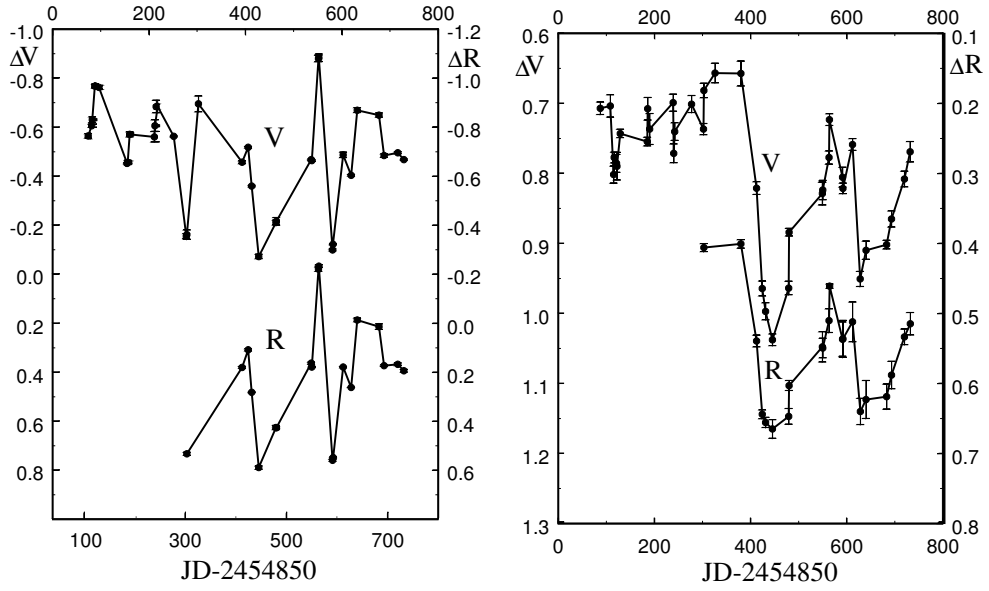

Figure 3. The light curves of 2MASS 21390639+5004544 (#5, left) and V645 Cyg (right). The bars correspond to the rms scatter of brightness during one night.

In this study we have registered the irregular type of optical variability of the mentioned IRAS sources by means of CCD photometery.

Brightness changes of similar character were detected for 3 other target stars and V645 Cyg. Variability of brightness had considerable amplitudes $\Delta m = |m_{max} - m_{min}|$:

- $\Delta m \sim 1\overset{\text{m}}{.}0$ – 2MASS 21390639+5004544 (#5),
- $\Delta m \sim 0\overset{\text{m}}{.}9$ – 2MASS 21403966+5010088 (#9),
- $\Delta m \sim 0\overset{\text{m}}{.}3$ – 2MASS 21410943+5018008 (#13),
- $\Delta m \sim 0\overset{\text{m}}{.}4$ – 2MASS 21395825+5014209 (V645 Cyg).

The light curves of the 5 target stars and V645 Cyg with variability detected in filters V and R_c are shown in Figures 1-3. Measured values of the brightness changes for the 5 newly found variable stars and V645 Cyg are presented in Table 4 (online only).

Thus, in the course of the current study we have found 4 new variable stars in 15′ vicinity of the young massive variable star V645 Cyg and confirmed variability of one suspected variable. All of these stars show variability of irregular type and have considerable infrared colour indices characteristic of the young stellar objects. Amplitudes of variability of the newly detected variables are similar to those of some Orion variables of IN type. According to the General Catalogue of Variable Stars (GCVS) the amplitudes of the IN type variables have values in the range from 0.5 to 1-2 magnitudes on the time scale of several tens to hundreds of days. The nature of these sources and their association with V645 Cyg will be discussed in a forthcoming paper.

The study was partly supported by the Russian federal task program “Research and operations on priority directions of development of the science and technology complex

of Russia for 2007-2013" (state contract No. 14.518.11.7064). The authors are grateful to the anonymous referee who helped to improve the quality of our paper.

References:

Alksnis, A. and Alksne, Z., 1988, Carbon stars in a field in Cygnus, Riga: Zinatne, 12.
Stetson, P. B., 1996, *PASP*, **108**, 851.
Zinnecker, H. and Yorke, H.W., 2007, *Ann. Rev. Astron. Astrophys.*, **45**, 481.

COMMISSIONS 27 AND 42 OF THE IAU
INFORMATION BULLETIN ON VARIABLE STARS

Number 6062

Konkoly Observatory
Budapest
4 July 2013

HU ISSN 0374 – 0676

NEW LIGHT ELEMENTS FOR 63 LONG PERIOD VARIABLE STARS FROM ASAS-3 DATABASE

MINA, FEDERICO D.

Grupo de Astrometría y Fotometría, Observatorio Astronómico Córdoba, Argentina
Facultad de Filosofía y Humanidades, Universidad Nacional de Córdoba, Argentina
email: fede_mina@hotmail.com

We present new light elements of 63 long period variable stars in the southern hemisphere ($-83° < \mathrm{DEC} < -15°$). All observations were obtained from the ASAS-3 database. The observations were made between 2001 and 2009. An average of 400 data points was available for each star, and never less than 100. All observations were made in the V-band (Pojmanski 2002, 2003).

The names, alternative names and positions of Table 1 were obtained from the VSX catalog (Watson et al. 2006). Almost all the stars studied were classified as Mira-type variables in VSX. In some particular cases, we refine the periods already in VSX.

When enough data points were available, we also calculated 287 times of maxima of these variable stars. The method used for these calculations was to adjust the best bi-gaussian profile for each period (see Buys and De Clerk 1972 for a complete description of bi-gaussian profiles), which showed better results than the method of bisected chords (Knott et al. 1863), especially when there were few or none observations near maximum. This was performed by Origin 8.6.0 software (OriginLab, Northampton, MA). These times of extrema were used both to determine the epoch and to build an O−C diagram for the stars. Potentially interesting O−C diagrams are presented in Figures 1 to 4, and were made with a spreadsheet made by the author.

The periods were determined using Scargle Periodogram in the AVE software (Barberá, 1999). In some cases, the period was refined using the O−C diagrams for each star.

Table 1. New elements for 63 variables.

Star Variable	Name Other ID	Position RA J2000	Position DEC J2000	Epoch (HJD2450000+)	Period (days)	Spectral type
OV Pup		07 33 51.50	−28 23 45.8	2912.3	138.0	M8:e (1)
V0470 Pup		07 40 42.81	−22 10 35.6	1959.8	108.9	M8-M9 (2)
NR Pup		07 59 42.63	−50 08 34.1	4261.9	174.9	Me (1)
II Pup		08 03 25.75	−27 55 26.0	2605.1	153.1	M8-M9 (4)
OY Pup		08 06 08.18	−37 17 46.6	3405.6	217.3	Me (1)
DP Pup	NSVS J0810431-151944	08 10 43.09	−15 19 46.9	2755.0	322.0	M8e (5)
LZ Pup		08 12 10.82	−23 43 48.5	2974.2	132.1	M8 (4)
FT Pup	ASAS J082543-2337.3	08 25 42.70	−23 37 14.1	2925.7	266.0	S (1)

Table 1. New elements for 63 variables (cont).

Star Variable	Name Other ID	Position RA J2000	Position DEC J2000	Epoch (HJD2450000+)	Period (days)	Spectral type
WY Pyx	ASAS J083649-3627.7	08 36 48.98	−36 27 36.4	2515.6	362.6	Me (2)
UU Pyx		08 43 12.06	−33 05 45.1	2690.5	162.3	Me (1)
RU Cha		10 14 29.93	−81 19 44.0	2010.4	104.2	
XZ Cha	ASAS J111209-7854.7	11 12 08.82	−78 54 39.8	1949.5	231.0	
CK Cha	ASAS J113324-7727.4	11 33 23.75	−77 27 21.7	2082.2	203.0	Me (1)
AK Cha	ASAS J120841-8235.3	12 08 43.65	−82 35 16.4	2964.6	186.1	
OS Mus	ASAS J120846-6545.5	12 08 46.00	−65 45 30.0	2954.0	611.4	M4 (1)
AM Cha		12 12 02.18	−77 00 34.9	2463.0	106.6	
AO Cha	ASAS J121611-8045.0	12 16 10.63	−80 45 01.2	3068.1	214.0	
CH Mus	ASAS J122046-7532.9	12 20 45.75	−75 32 52.8	2067.1	343.4	Me (1)
AV Cha		12 37 09.07	−77 18 17.7	1894.8	86.3	
CO Cha	ASAS J124007-8031.9	12 40 08.14	−80 31 55.2	2014.7	209.8	
CS Mus		13 02 59.73	−74 12 00.6	3410.3	191.0	
BU Cha	ASAS J134300-7947.7	13 43 00.02	−79 47 41.6	2076.7	185.0	Me (1)
VZ Cir	ASAS J142402-6605.9	14 24 02.00	−66 05 54.	2082.5	81.8	M6 (2)
TBR V0151		14 44 30.90	−59 51 57.0	3555.6	143.0	
TBR V0200		14 48 59.20	−68 36 20.0	1970.0	429.5	
CT Cir		14 58 41.16	−57 51 04.0	1958.6	40.0	M4III (6)
FF Lup	ASAS J151138-4354.7	15 11 37.80	−43 54 41.9	3152.8	218.2	Me (1)
AS Cir	ASAS J151339-6020.3	15 13 39.51	−60 20 18.3	2621.2	517.9	C (1)
FG Lup	ASAS J151508-3641.1	15 15 08.05	−36 40 57.2	2874.4	148.7	
FM Lup	ASAS J152022-3735.3	15 20 21.67	−37 35 15.7	1972.3	162.6	Me (1)
MW Aps		15 21 51.71	−74 33 49.9	2700.1	196.4	Me (2)
AQ Lup	ASAS J152218-4905.7	15 22 18.66	−49 05 39.2	2435.0	150.3	
GN Lup	ASAS J152409-3302.7	15 24 08.39	−33 02 41.5	2792.1	324.0	S3,8 (1)
TBR V0116		15 26 06.20	−60 49 47.0	1939.2	282.3	
GP Lup		15 28 35.61	−37 34 02.1	3843.3	70.4	Me (1)
V0344 Nor		15 40 30.64	−51 12 55.6	2064.5	91.2	M2/5e (2)
AW Aps		15 48 32.17	−73 28 16.3	2125.8	158.6	
IR TrA	ASAS J155247-6441.8	15 52 47.14	−64 41 52.6	2090.6	223.6	Me (1)
NU Lup		15 57 33.91	−30 08 27.9	1944.5	219.4	
BE Aps		16 06 07.10	−79 34 55.2	3778.9	389.0	Me (3)
BO Nor	ASAS J160648-5934.0	16 06 48.19	−59 34 04.3	2856.2	58.1	
NSV 7536		16 14 14.23	−53 34 47.3	2725.6	302.2	
CR Nor		16 14 17.50	−58 34 44.7	3482.8	271.5	
ER TrA	ASAS J161602-6312.4	16 16 01.78	−63 12 21.4	2054.3	352.	Me (1)
NSV 7610	ASAS J162058-6711.6	16 20 57.79	−67 11 33.2	1983.9	205.5	
PV Nor		16 21 02.08	−55 18 15.4	3451.6	208.3	
IX Nor	ASAS J162216-5528.6	16 22 14.62	−55 28 40.7	2165.1	254.8	
EX TrA	ASAS J162242-6124.7	16 22 42.65	−61 24 36.3	3572.4	212.7	Me (1)
X Nor	ASAS J162526-5155.6	16 25 25.76	−51 55 37.3	2715.2	520.2	C(Nb) (1)
NW Nor		16 29 47.32	−57 40 52.4	3147.5	251.9	
CC Aps		16 31 18.86	−79 51 28.8	2165.3	141.1	
LO Nor		16 33 21.13	−56 04 02.4	2118.4	281.6	
NSV 7825		16 36 36.89	−70 09 01.8	2066.9	289.4	
FV Aps		16 37 40.90	−75 08 24.6	2076.8	114.0	
V0356 Ara		16 40 10.47	−55 17 41.9	4201.1	222.9	
FW Aps		16 54 27.08	−75 11 12.9	2901.4	256.5	Me (3)
DH Aps	ASAS J170914-7338.8	17 09 13.50	−73 38 46.9	2107.4	188.8	
DX Aps		17 27 32.91	−76 38 47.2	1992.4	103.7	
EO Aps		17 38 24.01	−74 27 58.0	4741.9	79.2	Me (3)
DG Pav	ASAS J183627-6756.0	18 36 26.81	−67 56 01.4	2104.1	268.4	Me (1)
DI Pav	ASAS J193720-5657.9	19 37 20.09	−56 57 51.4	2696.1	256.0	Me (1)
NO Pav	ASAS J195905-6216.9	19 59 05.26	−62 16 51.2	3372.7	425.9	Me (1)
DM Pav		21 20 53.88	−61 34 27.7	2521.3	143.4	M8 (2)

Sources of spectral type:

(1) GCVS, Samus et al. (2013), (2) Skiff (2013), (3) Stock et al. (1972), (4) MacConnell (1993), (5) Vyssotsky (1943), (6) Kharchenko et al. (2009)

Notes on individual stars:
DP Pup = Period from the VSX
FT Pup = Period from the VSX
WY Pyx = Wrong period of 353 days in VSX
XZ Cha = Wrong period of 226 days in VSX
CK Cha = The period is from VSX
AK Cha = The period is from VSX
OS Mus = Wrong period of 734.56 days in VSX
AO Cha = Period of 212.83 days in VSX is not completely accurate
CH Mus = Period of 344.89 days in VSX is slightly inaccurate
CO Cha = Period of 209.09 days in VSX is slightly inaccurate
BU Cha = The period is from VSX
VZ Cir = The epoch is from VSX but the period of 78.864 in VSX is slightly inaccurate
FF Lup = Wrong period of 224.97 days in VSX
AS Cir = Wrong period of 532.14 days in VSX
FG Lup = Wrong period of 169.8 days in VSX
FM Lup = Period of 164.05 days in VSX is slightly inaccurate
AQ Lup = The epoch is from VSX but the period of 148.96 in VSX is slightly inaccurate
GN Lup = Period of 323.44 days in VSX is slightly inaccurate
IR TrA = Wrong period of 219.03 days in VSX
BO Nor = Period of 59.072 days in VSX is slightly inaccurate
ER TrA = The period is from VSX
NSV 7610 = Wrong period of 106.76 days in VSX
IX Nor = Period of 253.99 days in VSX is slightly inaccurate
EX TrA = Period of 209.61 days in VSX is slightly inaccurate
X Nor = Wrong period of 526.57 days in VSX
DH Aps= Wrong period of 184.66 days in VSX
DG Pav = Period of 266.01 days in VSX is slightly inaccurate
DI Pav = Period of 260.31 days in VSX is slightly inaccurate

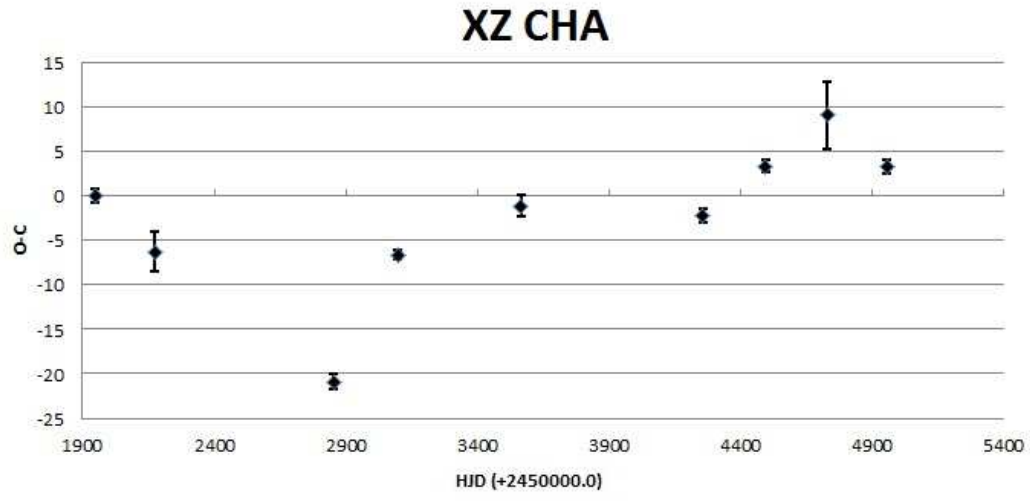

Figure 1. O−C diagram of XZ Cha.

Table 2. New Times of Maxima

Star Name	Time of Maxima HJD (+2450000)	Standard Error
OV Pup	2912.3	0.6
	3462.0	0.6
	3742.5	0.7
	4579.0	2.4
	4847.5	5.7
	5121.6	1.2
V470 Pup	1959.9	1.0
	2939.4	0.8
	4575.1	0.6
NR Pup	4262.0	1.6
II Pup	2605.2	2.4
	3066.5	1.1
	3517.7	1.8
	4447.6	1.4
OY Pup	2551.6	1.9
	2986.8	1.1
	3405.6	0.5
	3837.6	0.6
	4274.0	3.7
LZ Pup	2974.2	1.8
	3757.0	1.4
	4164.7	1.4
	4559.4	0.4
FT Pup	2925.7	3.8
	3158.6	2.4
	3486.7	3.3
	4543.4	4.7
	4798.4	7.4
WY Pyx	2145.9	6.0
	2515.6	7.7
	2879.2	4.8
	5054.5	8.7
UU Pyx	2690.5	0.3
	3030.5	0.6
	3669.9	1.3
	4969.3	1.9
RU Cha	2010.4	0.9
	2842.5	2.5
	3063.2	0.8
	3482.0	0.8
	3702.1	3.3
	4308.4	1.5
	4524.1	0.9
	4927.0	0.6
XZ Cha	1949.5	0.7
	2174.2	2.3
	2852.6	0.8
	3097.9	0.5
	3565.4	1.2
	4257.3	0.8
	4493.8	0.7
	4730.5	3.8
	4955.7	0.7
CK Cha	2082.2	0.8
	2494.7	2.0
	3127.0	2.8
	4307.9	1.6
	4511.3	0.9
AK Cha	2212.0	0.8
	2794.7	1.4
	2964.6	2.3
	3535.5	1.1

Table 2. New Times of Maxima (cont.)

Star Name	Time of Maxima HJD (+2450000)	Standard Error
AK Cha (cont.)	4284.1	0.9
	4457.0	0.6
	4632.7	0.4
AO Cha	2007.0	1.4
	2648.2	2.6
	2846.7	2.4
	3068.1	1.4
	3494.8	1.1
	4140.8	1.1
	4561.7	1.1
	4990.5	0.9
CH Mus	2067.1	0.5
	2758.6	1.4
	3098.5	0.6
	3443.4	0.5
	3786.4	0.8
	4123.3	1.9
	4468.4	0.8
	4814.8	1.6
AV Cha	1894.8	1.2
	3457.3	2.5
	4481.2	1.7
CO Cha	2014.7	1.2
	2643.3	1.3
	3062.1	2.5
	3471.2	0.8
	4326.1	1.0
	4529.0	0.5
	4952.6	0.8
CS Mus	3410.3	2.0
	3791.8	1.6
	4165.4	0.6
	4941.9	1.1
BU Cha	2076.7	1.5
	2465.1	4.0
	2822.5	1.3
	3556.1	1.4
	3746.2	4.5
	4304.5	2.8
	4484.9	4.2
	4665.4	2.7
	5039.1	4.2
VZ Cir	2473.6	1.1
	3819.8	2.8
	3883.8	2.3
	4532.7	4.7
	4693.2	1.5
TBR V0151	3555.6	1.4
	4842.3	1.6
TBR V0200	1970.0	0.8
	2818.4	1.4
	4975.9	1.6
CT Cir	1958.6	1.9
	3120.5	4.8
FF Lup	2057.5	1.1
	2502.9	2.0
	2709.9	0.9
	3152.8	1.3
	3589.5	1.4
	3806.9	1.2
	4250.4	1.5
	4895.9	1.2

Table 2. New Times of Maxima (cont.)

Star Name	Time of Maxima HJD (+2450000)	Standard Error
AS Cir	2621.2	3.9
	3154.5	1.2
	3671.6	8.6
	4168.3	2.5
	4716.4	5.7
FG Lup	1999.6	1.4
	2874.4	0.7
	3170.2	1.4
	3459.4	1.4
	4653.0	1.5
	4953.6	2.0
FM Lup	1972.3	1.5
	2786.3	1.6
	3432.7	1.0
	4244.4	1.9
	5050.0	4.7
	4872.7	0.8
MW Aps	2700.2	1.7
	3079.1	0.9
	3453.6	1.2
	4638.4	0.6
	5051.1	0.5
AQ Lup	2131.8	1.4
	2734.7	0.9
	3033.1	2.7
	3633.8	1.0
	4236.1	1.4
	4534.0	1.1
GN Lup	2455.0	0.9
	2792.1	1.0
	3117.4	1.9
	3435.4	1.2
	3764.7	1.5
	5061.2	1.3
TBR V0116	1939.2	2.0
	2502.7	2.6
	2777.2	2.8
	3068.9	4.1
GP Lup	2876.2	2.2
	3574.2	2.3
	3843.3	1.1
V0344 Nor	2064.5	3.8
	2894.0	1.6
	3433.5	1.2
	4527.0	1.9
	5075.4	1.9
AW Aps	2125.9	1.6
	3077.8	3.3
	3405.9	3.9
	4343.7	2.0
	4657.3	6.0
IR TrA	2090.6	1.4
	2536.2	1.6
	2753.1	0.5
	3419.8	0.7
	3642.0	0.9
	3864.5	1.1
	4317.0	0.9
	4547.4	0.9
	4995.5	1.6

Table 2. New Times of Maxima (cont.)

Star Name	Time of Maxima HJD (+2450000)	Standard Error
NU Lup	1944.5	2.1
	2836.1	1.6
	3055.4	4.6
	3479.4	1.6
	4562.9	1.0
	4998.5	1.2
BE Aps	3778.9	2.1
	4553.2	1.2
	4950.0	5.7
BO Nor	2856.2	2.2
	3153.5	6.6
	4364.1	10.5
	4543.8	15.4
CR Nor	3482.8	2.9
	4569.1	3.1
ER TrA	2054.3	5.5
	2753.7	1.5
	3099.0	1.4
	3819.6	5
	4174.2	2.6
	4858.1	6.5
NSV 7610	1983.9	1.4
	2081.7	2.4
	2819.5	1.3
	3829.0	3.5
	4241.6	3.4
	4655.5	2.9
PV Nor	3451.6	2.4
	4284.9	2.8
IX Nor	2165.1	4.8
	2674.7	2.0
	3436.8	3.5
	4213.1	3.6
	4712.6	1.4
EX TrA	2077.4	8.0
	2516.5	2.1
	2726.4	2.4
	3572.4	3.4
	4628.7	2.2
	5064.7	5.7
X Nor	2715.2	0.8
	4278.8	1.4
	4792.9	2.4
	5053.4	2.2
CC Aps	2165.3	0.8
	2727.6	1.2
	3578.2	1.3
	3854.6	1.3
	4706.5	1.7
	4988.4	6.7
LO Nor	2118.4	4.4
NSV 7825	2066.9	0.6
	3805.8	2.5
	4381.0	3.2
	4967.0	16.4
FV Aps	2076.9	0.7
	2528.6	0.7
	2764.3	0.9
	3443.7	0.7
	4126.9	1.1
	4358.5	0.9
	4596.1	4.4
V0356 Ara	4201.1	6.2

Table 2. New Times of Maxima (cont.)

Star Name	Time of Maxima HJD (+2450000)	Standard Error
FW Aps	2901.4	6.8
	3412.4	3.5
DH Aps	2107.5	1.1
	2520.6	2.0
	2920.1	6.0
	3059.5	2.8
	3477.5	1.7
	3842.3	1.4
	4237.3	2.4
	4374.9	1.7
	4566.7	1.2
	4972.4	2.9
DX Aps	1992.4	4.7
	2183.2	1.3
	3431.9	0.8
	3650.3	3.0
	3862.2	8.2
	4892.6	4.3
EO Aps	3545.0	2.7
	4255.6	4.7
	4741.9	2.6
DG Pav	2104.1	0.7
	2913.8	0.7
	3454.0	0.9
	4268.4	1.6
	5058.5	0.7
DI Pav	2185.4	0.4
	2945.1	0.5
	4242.1	0.7
	4750.7	0.6
	5009.1	0.9
NO Pav	2090.4	0.8
	2510.5	1.3
	2942.2	0.8
	4222.9	1.6
DM Pav	2521.3	1.8
	2796.7	1.0
	3114.1	7.3
	3663.3	1.1
	5102.4	3.9

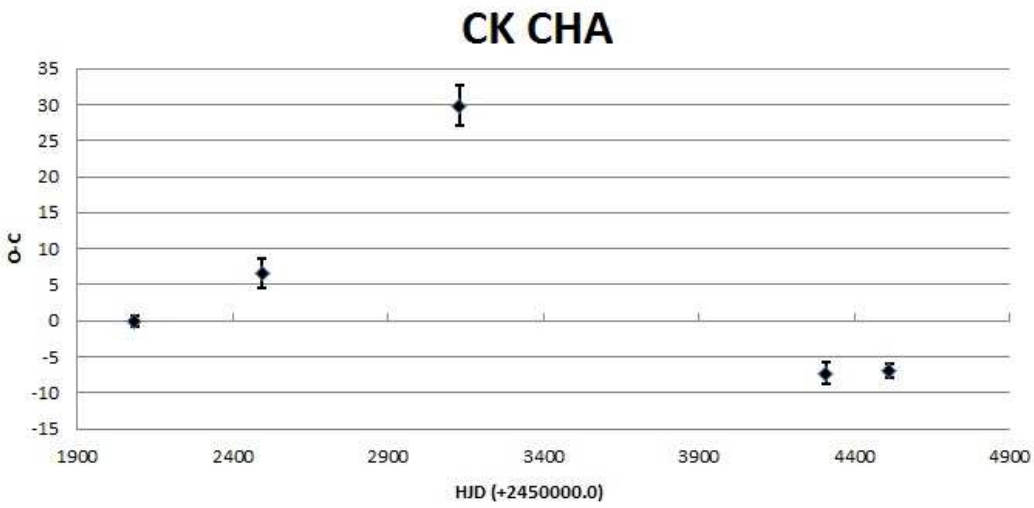

Figure 2. O−C diagram of CK Cha.

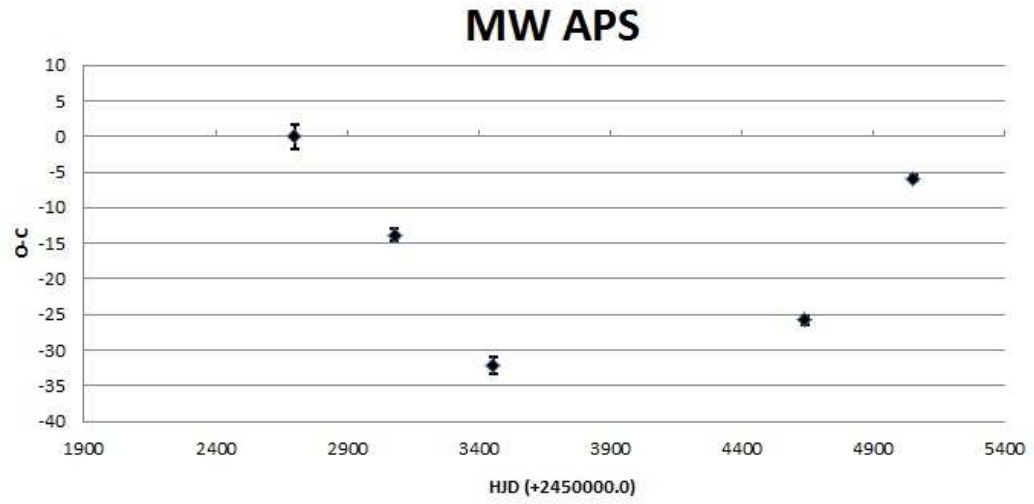

Figure 3. O−C diagram of MW Aps.

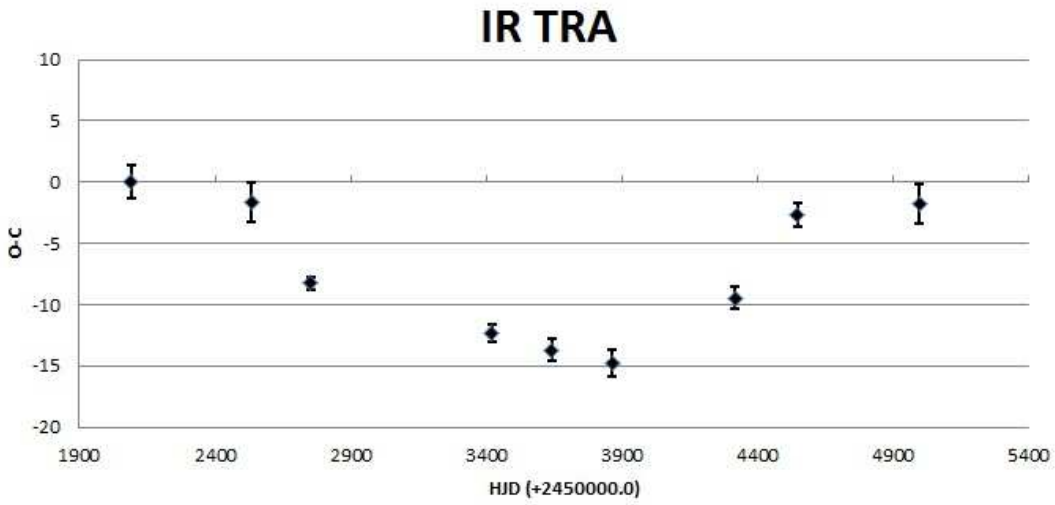

Figure 4. O−C diagram of IR TrA.

References:

Barberá, R., 1999, `http://www.astrogea.org/soft/ave/introave.htm`
Buys, T. S., De Clerk, K., 1972, *Anal. Chem.*, 44, (7), 1273
Kharchenko, N. V., Roeser, S., 2009 All-sky Compiled Catalogue of 2.5 million stars
Knott, G., Baxendell, J., 1863, *Astronomical Register*, **1**, A1-A16
MacConnell, D., 1993, IRAS Point Source Identifications
Pojmanski, G., 2002, *AcA*, **52**, 397
Pojmanski, G., 2003, *AcA*, **53**, 341
Samus, N. et al., 2013, General Catalog of Variable Stars (GCVS database)
Skiff, B. A., 2013, Catalogue of Stellar Spectral Classifications
Stock, J., Wroblewski, H., 1972, *Publ. Obs. Astron. Nacional, Cerro Calan*, **2**, 59
Vyssotsky, A. N., 1943, *PASP*, **55**, 325, 198
Watson C., Henden A. A., Price A., 2006, The AAVSO International Variable Star Index (VSX)

COMMISSIONS 27 AND 42 OF THE IAU
INFORMATION BULLETIN ON VARIABLE STARS

Number 6063

Konkoly Observatory
Budapest
18 July 2013

HU ISSN 0374 – 0676

TIMINGS OF MINIMA OF ECLIPSING BINARIES

DIETHELM, ROGER

Bahnhofstrasse 3, CH–4118 Rodersdorf, Switzerland

The following Table lists timings of minima of eclipsing binaries secured by CCD photometry, obtained in the first half of 2013. The given O-C values generally refer to the linear elements of the latest electronic version of the GCVS (Samus et al., 2013), except for the cases stated in the remarks, where the determination of current elements made use of the up-to-date ASAS data (`http://www.astrouw.edu.pl/asas/`) and the Lafler-Kinman algorithm of the PERANSO software (http://www.peranso.com/). In a two-step procedure, the period value is determined from the ASAS measurements, where obviously erroneous data are omitted. For most cases, the epoch is taken from a data point closest to the minimum of the light curve, while occasionally, all the data inside the minimum were used to find a time of minimum using the spline function tool of PERANSO. All times given are heliocentric UTC. All data were obtained at the R. Szafraniec Observatory operated at Astrokolkhoz Obs., Cloudcroft, N.M., USA. The support by T. Krajci at the site is acknowledged thankfully.

Table 1: Minima of eclipsing binaries

Variable	Type	HJD 24...	$O-C$	n	Remarks
V688 Aql	s	56447.9049(7)	+0.0104	94	V; eccentric
	s	56447.9116(6)	+0.0171	98	B
GSC 5117-2288 Aql	s	56443.92269(48)	+0.01557	57	V; el: 54753.556 + 1.202676 × E
	s	56443.93457(7)	+0.01745	57	B
	s	56443.93644(30)	+0.01932	56	R
CL Ari	p	56297.6529(14)	+0.0004	22	V; el: 52950.204 + 0.993603 × E
CG Aur	p	56311.7427(5)	−0.0032	50	V; el: Krakow Catalog; eccentric
CL Aur	p	56311.6973(1)	+0.0171	50	V
FR Aur	p	56313.6621(4)	+0.0003	47	V
GI Aur	p	56329.6945(17)	+0.0041	25	V
HP Aur	s	56313.6807(4)	−0.0004	48	V
	s	56323.6428(2)	+0.0020	38	V
IZ Aur	p	56314.6234(8)	+0.0041	35	V
MO Aur	p	56314.6265(13)	−0.0086	36	V
V555 Aur	s	56313.6381(7)	+0.0201	47	V; formerly ES Tau
V596 Aur	s	56309.6449(4)	+0.0100	31	V
V603 Aur	p	56313.6411(6)	−0.0002	47	V; el: 51403.8564 + 0.374564 × E
V609 Aur	p	56311.7048(1)	+0.0130	49	V
GSC 1477-516 Boo	p	56448.71995(13)	+0.00361	79	R; el: IBVS 5992
	p	56448.72049(12)	+0.00415	79	V
	p	56448.72070(8)	+0.00436	80	B
GSC 1999-404 Boo	p	56363.91335(10)	−0.00658	108	B; el: IBVS 5992
	p	56363.91368(9)	−0.00625	106	R
	p	56363.91409(12)	−0.00584	108	V
UU Cam	p	56297.6653(4)	−0.0060	41	V; el: CoSka 33, 38; d=0.05d

Table 1: Minima of eclipsing binaries (continued)

Variable	Type	HJD 24...	$O-C$	n	Remarks
AL Cam	p	56334.85394(9)	−0.03444	180	B
	p	56334.85419(18)	−0.03419	324	V
	p	56334.85490(11)	−0.03348	324	R
MT Cam	s	56310.6764(2)	+0.0035	36	V; el: IBVS 5871
V369 Cam	s	56315.6329(5)	−0.0042	16	V; el: 51609.63 + 0.345205 × E
V373 Cam	p	56312.6445(2)	+0.0014	38	V; el: 51553.706 + 0.370807 × E
V374 Cam	p	56312.616(3)	+0.000	14	V; el: 51489.326 + 0.8068401 × E; D=0.09d; d=0.022d
V381 Cam	p	56309.6378(6)	−0.0147	31	V
V385 Cam	s	56309.7391(7)	−0.0049	31	V; el: 51515.845 + 0.615272 × E
V396 Cam	p	56323.6067(30)	+0.0007	23	V; el: 51511.118 + 0.386297 × E
V470 Cam	p	56347.61128(23)	+0.00108	13	B
	p	56347.61342(20)	+0.00223	15	V
	p	56347.6143(8)	+0.0031	14	R
	s	56347.6596(6)	+0.0006	14	B
	s	56347.6607(4)	+0.0017	14	V
	s	56347.6616(10)	+0.0026	11	R
	p	56347.70892(26)	+0.00208	17	R
	p	56347.7099(8)	+0.0030	14	B
	p	56347.7104(13)	+0.0036	12	V
	s	56347.7554(14)	+0.0007	11	V
	s	56347.7562(5)	+0.0015	14	R
	s	56347.7573(9)	+0.0027	13	B
GSC 3715-43 Cam	s	56297.6594(6)	+0.0036	38	V; el: IBVS 6042
YY Cnc	p	56298.8633(3)	−0.0114	39	V; el: IBVS 5591
HN Cnc	p	56297.9303(5)	−0.0348	39	V
IM Cnc	p	56366.66334(17)	−0.03463	75	B; d=0.043d
	p	56366.66515(25)	−0.03282	57	V
	p	56366.66666(59)	−0.03131	57	R
IO Cnc	s	56309.8611(5)	+0.0041	43	V; el: IBVS 5992
KT Cnc	s	56298.9388(2)	−0.0099	39	V; d=0.024d
KY Cnc	s	56298.8604(4)	−0.0045	35	V; el: IBVS 6029; d=0.024d
LU Cnc	s	56377.71908(12)	−0.02445	99	B; d=0.021d
	s	56377.71980(12)	−0.02373	98	V
	s	56377.72042(17)	−0.02311	98	R
GSC 794-1208 Cnc	p	56297.9080(12)	−0.0043	39	V; el: IBVS 5992; d=0.021d
GSC 809-569 Cnc	p	56298.8357(4)	+0.0089	39	V; el: IBVS 5992
NSV 4158 Cnc	p	56298.9202(4)	+0.0007	38	V; el: IBVS 5992
RV CVn	p	56443.71255(18)	+0.02005	58	V
	p	56443.71339(6)	+0.02089	58	R
	p	56443.71443(21)	+0.02193	59	B
DI CVn	p	56352.91538(17)	−0.00134	81	V; el: Krakow Catalog
	p	56352.91622(12)	−0.00050	81	R
	p	56352.91720(12)	+0.00048	82	B
DY CVn	s	56447.69830(22)	−0.00279	57	B
	s	56447.69887(13)	−0.00222	58	R
	s	56447.70093(20)	−0.00016	58	V
AV CMi	s	56313.6462(6)	+0.1593	45	V; el: IBVS 5945; eccentric
	p	56314.6433(4)	+0.0174	35	V
MU Cas	p	56297.6249(12)	−0.0136	32	V; el: Krakow Catalog; eccentric
AQ Com	s	56338.87440(38)	−0.00799	61	R
	s	56338.87443(67)	−0.00796	62	B
	s	56338.87483(32)	−0.00756	60	V
CN Com	p	56353.90339(12)	+0.05931	81	B; d=0.094d
	p	56353.90442(10)	+0.06034	81	V; d=0.088d
	p	56353.90526(17)	+0.06118	81	R; d=0.088d
DG Com	p	56337.88816(17)	−0.05414	95	B; D=0.097d; d=0.012d
	p	56337.88890(12)	−0.05340	95	V
	p	56337.88952(13)	−0.05279	94	R

Table 1: Minima of eclipsing binaries (continued)

Variable	Type	HJD 24...	$O-C$	n	Remarks
GSC 1994-465 Com	p	56365.86602(16)	+0.01631	73	B; el: IBVS 5992
	p	56365.86635(14)	+0.01663	72	V
	p	56365.86720(14)	+0.01749	72	R
GSC 6077-1825 Crt	p	56401.71867(11)	−0.00800	90	R; el: IBVS 5992; D=0.22d
	p	56401.71892(11)	−0.00776	90	V
	p	56401.72029(15)	−0.00639	90	B
V2544 Cyg	p	56442.85523(19)	+0.01382	79	V; eccentric
	p	56442.85584(14)	+0.01442	78	R
	p	56442.85660(42)	+0.01518	79	B
NT Dra	p	56311.917(7)	+0.007	30	V
NV Dra	s	56405.68973(22)	+0.05571		R; D=0.103d
	s	56405.69049(28)	+0.05646	90	B
	s	56405.69123(18)	+0.05720	91	V
BQ Eri	p	56315.6410(9)	−0.0096	16	V; el: IBVS 6029
LW Eri	p	56312.7021(4)	−0.0173	38	V; el: IBVS 5960
GSC 5314-2102 Eri	s	56312.7190(7)	+0.0036	19	V
GSC 5321-819 Eri	s	56310.6749(4)	−0.0032	37	V; el: IBVS 5960; d=0.028d
HR Gem	p	56329.7097(18)	+0.0140	25	V
V383 Gem	p	56331.67181(12)	−0.00094	207	B
	p	56331.67158(8)	−0.00117	196	V
	p	56331.67234(29)	−0.00042	202	R
V1344 Her	s	56448.85970(17)	+0.29700	78	B; el: IBVS 5992; eccentric
	s	56448.86044(14)	+0.29774	78	V
	s	56448.86105(19)	+0.29835	78	R
GSC 950-560 Her	p	56404.88375(13)	−0.00892		V; el: IBVS 5894; D=0.168d
	p	56404.88435(8)	−0.00832	90	R
	p	56404.88511(9)	−0.00756	91	B
TY Hya	p	56310.8503(3)	−0.0060	50	V; el: IBVS 5992; d=0.074d
EZ Hya	s	56309.8763(2)	+0.0248	38	V; el: IBVS 5992
FG Hya	s	56298.8936(4)	+0.0170	39	V; el: IBVS 5992; d=0.043d
V474 Hya		56297.9823(20)		38	V
GSC 201-1119 Hya	p	56298.8900(3)	+0.0111	39	V; el: IBVS 5992
GSC 230-1627 Hya	p	56309.9228(4)	+0.0379	44	V; el: IBVS 5894; d=0.052d
GSC 238-2372 Hya	s	56312.9067(4)	+0.0019	43	V; el: IBVS 5992; d=0.024d
GSC 4853-30 Hya	s	56363.68263(11)	−0.00802	100	V; el: IBVS 5992
	s	56363.68324(10)	−0.00741	100	R
	s	56363.68399(12)	−0.00667	100	B
GSC 4881-888 Hya	p	56309.8869(4)	+0.0423	43	V; el: IBVS 5945; d=0.016d
GSC 4894-2310 Hya	s	56310.9166(2)	−0.0118	49	V; el: IBVS 5992
GSC 4897-1114 Hya	s	56310.9162(6)	+0.0055	50	V; el: IBVS 5992; d=0.054d; close double star
GSC 4897-1250 Hya	p	56310.8912(1)	+0.0155	50	V; el: IBVS 5992
GSC 5426-1920 Hya	s	56297.9444(6)	−0.0098	39	V; el: IBVS 5992; d=0.023d
GSC 5463-45 Hya	s	56309.9097(3)	−0.0347	42	V; el: IBVS 5945
GSC 5472-602 Hya	s	56311.8856(5)	+0.0283	30	V; el: IBVS 5992
GSC 5487-801 Hya	p	56313.8749(4)	−0.0219	35	V; el: IBVS 5992
GSC 5488-3 Hya	s	56313.8722(5)	−0.0076	42	V; el: IBVS 5992
GSC 6011-1986 Hya	p	56365.72001(7)	−0.00804	98	B; el: IBVS 5992
	p	56365.72285(24)	−0.00520	97	V
	p	56365.72346(26)	−0.00459	97	R
UU Leo	p	56310.9177(3)	+0.1851	49	V
UX Leo	p	56310.9295(3)	−0.0039	45	V; el: IBVS 5992
XY Leo	s	56312.8880(5)	+0.0444	39	V; el: IBVS 5945
GSC 234-960 Leo	s	56309.8690(5)	−0.0126	42	V; el: IBVS 5992; d=0.023d
GSC 263-585 Leo	p	56336.94854(8)	−0.01492	97	B; el: IBVS 5894
	p	56336.94934(14)	−0.01412	193	V
	p	56336.94929(16)	−0.01416	194	R; d=0.012d
GSC 267-162 Leo	p	56402.69976(27)	+0.02698	65	V; el: IBVS 5945
	p	56402.70019(26)	+0.02740	65	B
	p	56402.70060(19)	+0.02782	65	R

Table 1: Minima of eclipsing binaries (continued)

Variable	Type	HJD 24...	$O-C$	n	Remarks
GSC 270-777 Leo	p	56412.68837(14)	−0.03709	64	V; el: IBVS 5945
	p	56412.68922(8)	−0.03624	64	R
	p	56412.69026(29)	−0.03520	64	B
GSC 829-1040 Leo	p	56311.9101(6)	+0.0062	30	V; el: IBVS 5992
GSC 832-1401 Leo	p	56313.8388(2)	−0.0113	44	V; el: IBVS 5992
GSC 835-652 Leo	s	56313.8314(6)	+0.0038	20	V; el: 54193.647 + 0.295681 × E
	p	56313.9818	+0.0063	20	V
GSC 1417-401 Leo	s	56312.8560(3)	+0.0058	25	V; el: IBVS 5945
	p	56312.9747(11)	+0.0068	11	V
GSC 1434-1034 Leo	p	56311.9141(5)	+0.0004	25	V; el: IBVS 5945
GSC 1963-488 Leo	s	56310.8849(3)	−0.0013	49	V; el: IBVS 5992; d=0.037d
GSC 1971-916 Leo	p	56312.8819(2)	+0.0202	42	V; el: IBVS 5945
GSC 4936-907 Leo	s	56331.91931(12)	+0.02340	191	B; el: 53765.778 + 0.2771934 × E; d=0.013d
	s	56331.91966(11)	+0.02376	190	V
	s	56331.9220(6)	+0.260	197	R
RT LMi	p	56312.9315(2)	−0.0094	43	V; d=0.024d
XY LMi	p	56312.8488(2)	−0.0230	42	V; d=0.036d
SU Lep	p	56309.6946(6)	+0.0279	31	V; el: 52190.771 + 3.057829 × E
GSC 5345-815 Lep	s	56315.664(2)	+0.021	16	V; el: IBVS 5960
GSC 5351-457 Lep	p	56314.6763(3)	+0.0135	35	V; el: IBVS 6029
GSC 5352-540 Lep	p	56314.6800(5)	−0.0019	16	V; el: IBVS 5960; D=0.083d
FU Lib	p	56442.69073(17)	−0.00449	81	V; el: IBVS 5992; D=0.14p
	p	56442.69134(12)	−0.00388	81	R
	p	56442.69209(18)	−0.00313	81	B
V351 Lib	s	56401.86313(26)	−0.00550	66	V; el: IBVS 6029
	s	56401.86398(28)	−0.00465	65	R
	s	56401.86414(46)	−0.00449	64	B
DR Lyn	p	56354.69176(4)	+0.22376	105	B; el: IBVS 5599
FI Lyn	p	56297.9510(5)	+0.0128	39	V
FO Lyn	s	56298.8561(4)	+0.0216	38	V
CF Mon	p	56336.67331(32)	−0.00446	64	B; el: Krakow Catalog
	p	56336.67398(20)	−0.00380	122	R
	p	56336.67483(15)	−0.00295	122	V
V455 Mon	p	56338.70340(52)	+0.04140	66	V
	p	56338.7039(36)	+0.0419	65	R
	p	56338.70396(47)	+0.04197	66	B
V501 Mon	s	56339.65867(26)	−0.25909	70	B; eccentric
	s	56339.65954(38)	−0.25822	70	V
	s	56339.66015(22)	−0.25761	70	R
V521 Mon	s	56341.70741(20)	+0.30280	280	V; d=0.083d; el: Krakow Catalog; eccentric
	s	56341.71175(22)	+0.30714	204	I
	s	56341.71193(18)	+0.30731	209	R
	s	56341.71270(24)	+0.30809	111	B
V922 Mon	p	56337.70077(10)	−0.01494	330	V
	p	56337.70078(15)	−0.01494	329	R
	p	56337.70201(8)	−0.01371	166	B; D=0.21d
V953 Mon	s	56297.8443(6)	−0.0259	39	V; d=0.023d
GSC 4840-528 Mon	s	56351.68722(45)	−0.01060	92	R; el: IBVS 5945
	s	56351.68797(45)	−0.00984	93	B
	s	56351.68871(42)	−0.00910	93	V
GSC 4855-2438 Mon	p	56297.8655(3)	−0.0061	39	V; el: IBVS 6029
GSC 5640-366 Oph	p	56405.85396(71)	+0.00539	64	B; el: IBVS 5992; D=0.24d
	p	56405.85496(83)	+0.00638	64	R
	p	56405.85501(44)	+0.00643	64	V
GSC 6218-197 Oph	p	56412.85816(30)	−0.01784	62	R; el: IBVS 5992
	p	56412.86023(40)	−0.01577	62	B
	p	56412.86025(32)	−0.01575	62	V
DW Ori	p	56329.6732(4)	+0.0126	25	V
ET Ori	p	56310.6778(1)	−0.0038	36	V

Table 1: Minima of eclipsing binaries (continued)

Variable	Type	HJD 24...	$O-C$	n	Remarks
V648 Ori	p	56297.6637(2)	+0.0042	41	V; el: 54543.509 + 0.8132362 × E; d=0.021d
V1853 Ori	p	56311.7270(3)	+0.0202	50	V; d=0.028d
V2735 Ori	p	56323.7183(8)	+0.0501	32	V
V2783 Ori	p	56313.6238(12)	+0.2176	46	V; el: IBVS 5992; eccentric
	s	56334.70477(15)	+0.21758	125	R
	s	56334.70545(12)	+0.21826	124	V
	s	56334.70577(21)	+0.21858	125	B
GSC 104-1999 Ori	p	56311.7315(2)	−0.0116	50	V; el: IBVS 5871
GSC 108-1146 Ori	s	56309.6664(3)	+0.0111	31	V; el: IBVS 5992
GSC 127-719 Ori	p	56313.7054(4)	+0.0151	47	V; el: IBVS 5894
GSC 711-49 Ori	p	56311.7116(3)	−0.0156	50	V; el: IBVS 5992; d=0.03d
GSC 711-1701 Ori	p	56311.6453(5)	+0.0101	50	V; el: IBVS 5992; d=0.016d
GSC 4741-710 Ori	p	56309.6901(3)	−0.0057	31	V; el: 54868.595 + 0.751356 × E
GSC 4783-467 Ori	s	56329.6590(3)	+0.0150	24	v; el: IBVS 5960
GSC 5346-275 Ori	s	56323.7178(4)	+0.0069	37	V; el: IBVS 5960
IK Per	p	56310.7296(5)	−0.2066	37	V
NZ Per	p	56298.6703(2)	+0.0369	42	V
MS Per	p	56297.6625(7)	−0.0053	41	V; el: IBVS 5960
V432 Per	s	56297.6737(2)	−0.0201	42	V; el: BAV Rb. 43, 104
V947 Per	p	56298.7184(4)	−0.0002	42	V; el: 53756.342 + 0.2976673 × E
V951 Per	p	56298.6944(2)	−0.0233	42	V
V958 Per	p	56298.6668(3)	+0.0124	42	V
V959 Per	p	56310.6750(2)	+0.0221	37	V
V963 Per	p	56312.7041(5)	−0.0077	38	V; el: IBVS 6001
V964 Per	p	56310.6488(6)	−0.0726	22	V; el: IBVS 6011
GSC 5422-1430 Pup	s	56353.70197(21)	+0.01236	105	B; el: IBVS 5992
	s	56353.70270(15)	+0.01309	104	V
	s	56353.70332(16)	+0.01371	104	R
GSC 5439-620 Pup	s	56297.8951(2)	+0.0004	36	V; el: IBVS 5992
CL Sct	p	56444.87456(26)	+0.01106	57	V; el: 53819.9 + 1.638554 × E
	p	56444.87541(23)	+0.01190	56	R
	p	56444.87645(35)	+1.01200	57	B
GSC 361-795 Ser	p	56402.88486(7)	+0.00402	90	V; el: IBVS 5992; D=0.199d
	p	56402.88547(5)	+0.00464	90	R
	p	56402.88623(10)	+0.00540	91	B
GSC 242-2191 Sex	s	56312.9404(2)	+0.0350	43	V; el: IBVS 5992
GSC 243-397 Sex	p	56313.8946(3)	−0.0065	44	V; el: IBVS 5992
GSC 4896-33 Sex	p	56311.9262(4)	+0.0239	29	V; el: IBVS 5992
GSC 4906-447 Sex	s	56313.9050(2)	−0.0014	44	V; el: IBVS 5992
GSC 4909-1434 Sex	p	56313.9053(3)	+0.0007	44	V; el: IBVS 5992
GSC 4916-292 Sex	s	56313.8691(11)	+0.0085	44	V; el: IBVS 5894
GSC 5478-562 Sex	p	56310.8973(3)	+0.0043	49	V; el: IBVS 5992
AP Tau	s	56312.6966(5)	+0.0255	38	V
CT Tau	p	56329.6454(4)	−0.0612	25	V
CU Tau	s	56297.7466(6)	−0.0020	41	V; el: Krakow Catalog
EN Tau	p	56323.7043(3)	−0.0141	37	V; el: 53067.537 + 2.478068 × E; d=0.034d
GR Tau	p	56297.7178(5)	−0.0461	41	V
V1112 Tau	s	56310.6961(3)	−0.0428	37	V; el: IBVS 5871
V1352 Tau	p?	56309.7297(10)	−0.0225	31	V; el: IBVS 6011, eccentric; additional pulsation
V1367 Tau	p	56313.6167(4)	+0.0008	47	V; el: IBVS 5699
V1370 Tau	s	56323.6548(6)	−0.0647	38	V; probably pulsator
A054432+1305.7 Tau	p	56323.6591(2)	−0.0058	37	V; IBVS 5945
GSC 72-521 Tau	p	56298.6924(3)	+0.0158	42	V; el. IBVS 5945
GSC 681-692 Tau	p	56298.6758(2)	−0.0008	42	V; el: IBVS 5945
GSC 1274-564 Tau	p	56310.6687(3)	+0.0175	37	V; el: IBVS 5960
GSC 1831-687 Tau	s	56312.6565(1)	+0.0062	38	V; el: IBVS 5960
GSC 1852-1665 Tau	s	56309.7098(2)	+0.0123	31	V; el: IBVS 5960
NSV 1955 Tau	p	56311.6708(2)	+0.0152	49	V; el: IBVS 5871; d=0.022d

Table 1: Minima of eclipsing binaries (continued)

Variable	Type	HJD 24...	$O-C$	n	Remarks
XZ UMa	p	56309.8996(1)	−0.1155	40	V
AA UMa	s	56309.9250(3)	+0.0430	37	V
BE UMa	p	56341.85920(22)	+0.01295	65	B; D=0.044d
	p	56341.85726(21)	+0.01102	68	V
	p	56341.85691(27)	+0.01067	68	R
BM UMa	s	56404.67140(24)	+0.01141	67	B
	s	56404.67245(12)	+0.01246	66	V
	s	56404.67330(25)	+0.01330	66	R
ES UMa	p	56312.8695(4)	+0.0024	42	V; el: Krakow Catalog; d=0.030d
OQ UMa	p	56377.86967(19)	+0.00104	73	B; d=0.021d
	p	56377.86969(15)	+0.00106	74	V
	p	56377.87053(20)	+0.00190	73	R
QT UMa	s	56311.8814(2)	+0.0047	30	V; el: 51523.948 + 0.473538 × E
QV UMa	p	56311.9407(17)	−0.0009	30	V; el: 51354.68751 + 0.311444 × E
GSC 897-470 Vir	p	56339.91974(9)	+0.01622	69	B; d=0.012d
	p	56339.92060(9)	+0.01708	68	V
	p	56339.92122(18)	+0.01770	68	R
VZ UMi	p	56347.86449(28)	−0.00275	89	B; el: IBVS 6029; d=0.08d
	p	56347.86598(33)	−0.00126	89	R; d=0.087d
	p	56347.86617(33)	−0.00107	88	V; d=0.082d
GSC 4407-351 UMi	s	56351.8455(10)	+0.0386	65	B; el: PZP 10, 18
	s	56351.84576(20)	+0.03884	65	V
	s	56351.84661(41)	+0.03969	64	R
V391 Vir	p	56354.85170(15)	−0.00456	80	V; el: 54588.591 + 0.354316 × E; d= 0.013d
	p	56354.85255(10)	−0.00371	80	R; d=0.018d
	p	56354.85360(25)	−0.00266	81	B
GSC 898-3 Vir	p	56444.67736(18)	−0.00436	50	B; el: IBVS 5894
	p	56444.67737(27)	−0.00434	51	V
	p	56444.68083(26)	−0.00088	58	R
GSC 4969-725 Vir	p	56364.90391(13)	+0.01183	108	V; el: IBVS 5992
	p	56364.90417(14)	+0.01208	107	B
	p	56364.90453(9)	+0.01244	107	R

References:

Dahm, M., 1994, *BAV Rb.*, **43**, 104
Diethelm, R., 2009, *IBVS*, No. 5871
Diethelm, R., 2009, *IBVS*, No. 5894
Diethelm, R., 2010, *IBVS*, No. 5945
Diethelm, R., 2011, *IBVS*, No. 5960
Diethelm, R., 2011, *IBVS*, No. 5992
Diethelm, R., 2012, *IBVS*, No. 6011
Diethelm, R., 2012, *IBVS*, No. 6029
Diethelm, R., 2013, *IBVS*, No. 6042
Khruslov, A.V., 2005, *IBVS*, No. 5699
Khruslov, A.V., 2010, *PZP*, **10**, 18
Kreiner, J.M., 2004, *AcA*, **54**, 207 (Krakow Catalog)
Odell, A.P. et al., 2011, *IBVS*, No. 6001
Pribulla, T. et al., 2003, *Contrib. Astron. Obs. Skalnaté Pleso*, **33**, 38
Samus et al., 2013, GCVS http://www.sai.msu.su/gcvs/gcvs/
Zola, S. et al., 2005, *IBVS*, No. 5591

COMMISSIONS 27 AND 42 OF THE IAU
INFORMATION BULLETIN ON VARIABLE STARS

Number 6064

Konkoly Observatory
Budapest
2 August 2013

HU ISSN 0374 – 0676

VARIABLES FROM SDSS STRIPE 82 REGION

SESAR, B.[1]; BECKER, A.C.[2]; IVEZIĆ, Ž.[2,3]

[1] Division of Physics, Mathematics and Astronomy, Caltech, Pasadena, CA 91125, USA

[2] University of Washington, Department of Astronomy, P.O. Box 351580, Seattle, WA 98195-1580, USA

[3] Konkoly Observatory, Research Centre for Astronomy and Earth Sciences, Hungarian Academy of Sciences, Budapest, Hungary

We wish to draw attention of the variable star community to a catalog of 67,507 candidate variable point sources selected from SDSS stripe 82 ($|\mathrm{Dec}| < 1\overset{\circ}{.}266$ and R.A. in the range $20^{\mathrm{h}}34^{\mathrm{m}}$ to $4^{\mathrm{h}}00^{\mathrm{m}}$; about 300 sq.deg.). Details about the construction and testing of the catalog are described in Ivezić et al. (2007). Briefly, the selection criteria are:

1. unresolved source in imaging data, and at least one band with photometric error below $0\overset{\mathrm{m}}{.}05$,
2. SDSS processing flags BRIGHT, SATUR, BLENDED, or EDGE are not set,
3. at least 10 observations in the g and r bands are available,
4. the median g band magnitude brighter than 20.5,
5. "most likely variable": the root-mean-square scatter greater than $0\overset{\mathrm{m}}{.}05$, and $\chi^2_{dof} > 3$ in both g and r bands.

The distribution of selected objects in SDSS color-magnitude and color-color diagrams is shown in Fig. 1. This catalog and all light curves are publicly available[1]. The catalog lists SDSS positions, median *ugriz* photometry, number of observations, and some low-order statistics derived from light curves (including preliminary period estimates). The median number of observations per band is about 30. On average, the objects were most often re-observed every two days (the SDSS-II SN Survey cadence), followed by 5-day, 10-day, and yearly re-observations (see Fig. 1 in Sesar et al. 2010). Examples of light curves for objects at the faint end of the sample are shown in Fig. 2.

This dataset has not been fully explored yet. Initial analysis can be found in Sesar et al. (2007, 2010). As discussed there, this variable source catalog includes both stars and quasars (about 10,000; for detailed analysis, see MacLeod et al. 2010). Among the stellar sample, RR Lyrae stars (about 500) are an especially useful probe of the Galactic structure (Sesar et al. 2010). Except for the analysis of low-mass subsample by Becker et al. (2011), we are not aware of any other published detailed statistical analysis of eclipsing binary stars listed in this catalog. An M dwarf binary with extremely short period was analyzed in detail by Davenport et al. (2013).

[1] At the IBVS website and `http://www.astro.washington.edu/users/ivezic/sdss/catalogs/S82variables.html`

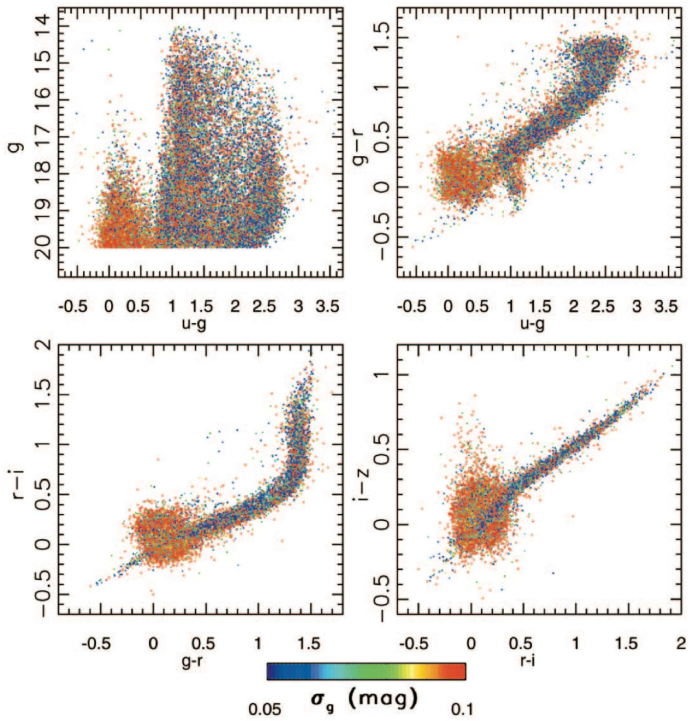

Figure 1. Color-magnitude and color-color distributions of candidate variables from SDSS Stripe 82. The dots are color-coded according to the observed rms scatter in the g band (see the legend). Objects with $u - g < 0.6$ are dominated by quasars. Adapted from Fig. 3 in Ivezić et al. (2007).

We note that, in addition to the catalog of variable sources from Stripe 82, a catalog of about million non-variable stars from the same sky region is also publicly available[2]. Thanks to averaging of multiple SDSS observations, the random photometric errors are below $0\overset{m}{.}01$ for stars brighter than 19.5, 20.5, 20.5, 20, 18.5 magnitudes in *ugriz*, respectively (about twice as good as for individual SDSS runs). The spatial variation of photometric zeropoints is not larger than $0\overset{m}{.}01$ (rms). For more details, please see Ivezić et al. (2007).

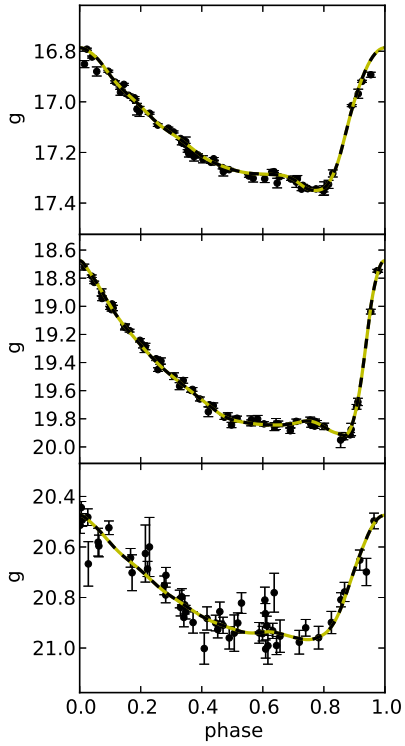

Figure 2. Examples of *g*-band light curves for three RR Lyrae stars (with catalog IDs equal to 4099, 74260, and 260984, from the top to the bottom panel, respectively) with brightness ranging from the bright to the faint end of the sample. The solid lines show the best-fit templates from Sesar et al. (2010).

Acknowledgements:
Ž.I. thanks the Hungarian Academy of Sciences for its support through the Distinguished Guest Professor grant No. E-1109/6/2012.

References:

Becker, A. C., Bochanski, J. J., Hawley, S. L., et al. 2011, ApJ, 731, 17
Davenport, J.R.A., Becker, A.C., West, A.A., et al. 2013, ApJ, 764, 62
Ivezić, Ž., Smith, J.A., Miknaitis, G., et al. 2007, AJ, 134, 973
MacLeod, C.L., Ivezić, Ž., Kochanek, C.S., et al. 2010, ApJ, 721, 1014
Sesar, B., Ivezić, Ž., Lupton, R.H., et al. 2007, AJ, 134, 2236
Sesar, B., Ivezić, Ž., Grammer, S., et al. 2010, ApJ, 708, 717

[2] `http://www.astro.washington.edu/users/ivezic/sdss/catalogs/stripe82.html`

COMMISSIONS 27 AND 42 OF THE IAU
INFORMATION BULLETIN ON VARIABLE STARS

Number 6065

Konkoly Observatory
Budapest
2 August 2013

HU ISSN 0374 – 0676

VARIABLE STARS FROM THE LINEAR SURVEY

PALAVERSA, L.[1]; SESAR, B.[2]; IVEZIĆ, Ž.[3,4]

[1] Observatoire astronomique de l'Université de Genève, 51 chemin des Maillettes, CH-1290 Sauverny, Switzerland

[2] Division of Physics, Mathematics and Astronomy, Caltech, Pasadena, CA 91125, USA

[3] University of Washington, Department of Astronomy, P.O. Box 351580, Seattle, WA 98195-1580, USA

[4] Konkoly Observatory, Research Centre for Astronomy and Earth Sciences, Hungarian Academy of Sciences, Budapest, Hungary

We announce publication of a catalog of 7,194 variable stars extracted from the LINEAR asteroid survey across 10,000 sq. deg. of northern sky (corresponding approximately to SDSS north Galactic cap; see Sesar et al. 2011 for details). The sample flux limit is several magnitudes fainter than for most other wide-angle surveys; the photometric errors range from about $0\overset{\mathrm{m}}{.}03$ at V=15 to $0\overset{\mathrm{m}}{.}20$ at V=18. Light curves include on average 250 data points (see Fig. 1), collected over about a decade with dense temporal sampling (see Fig. 2), and are visually confirmed and classified using phased light curves and additional attributes such as SDSS, 2MASS and WISE photometry and light curve statistics. The reliability and uniformity of visual classification across eight human classifiers was calibrated and tested using a catalog of variable stars from the SDSS Stripe 82 region, and verified using unsupervised machine learning approach. The resulting sample is dominated by 3,900 RR Lyrae stars and 2,700 eclipsing binary stars of all subtypes (see Fig. 3 for examples of light curves), and includes small fractions of relatively rare populations such as asymptotic giant branch stars and SX Phoenicis stars. The distribution of these mostly uncataloged variables in various diagrams constructed with optical-to-infrared SDSS, 2MASS and WISE photometry, and with LINEAR light curve features, is discussed in Palaversa et al. (2013). This large sample of robustly classified variable stars can enable detailed statistical studies of Galactic structure (see Sesar et al. 2013 for analysis of RR Lyrae stars) and physics of binary and other stars.

This catalog and all light curves are publicly available[1]. The catalog lists SDSS positions, variability type, median SDSS *ugriz* photometry, 2MASS and WISE photometry as well as the number of LINEAR observations, period and amplitude estimates, and some low-order statistics derived from light curves. We note that light curves for the full LINEAR sample of about 20 million objects are also publicly available through the SkyDOT Web site (https://astroweb.lanl.gov/lineardb/).

[1] At the IBVS website and `http://www.astro.washington.edu/users/ivezic/linear/PaperIII/PLV.html`

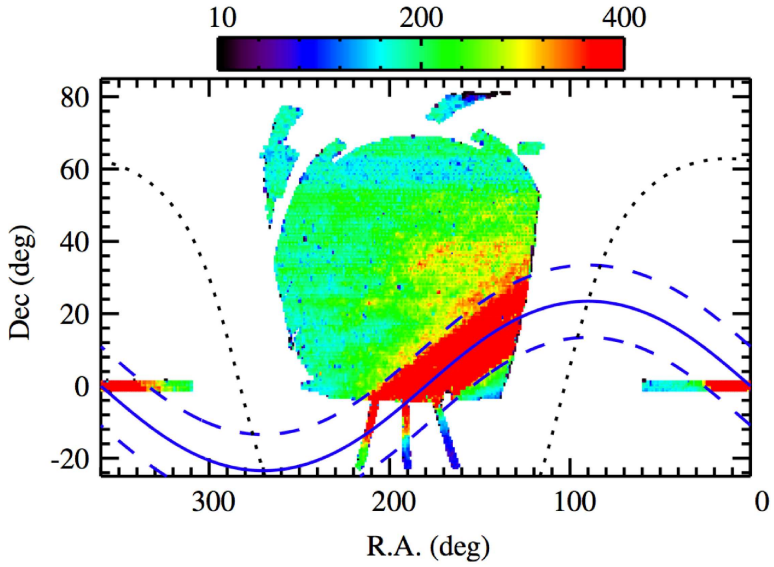

Figure 1. Median number of LINEAR observations per object as a function of equatorial coordinates. The values are color-coded according to the legend, with values outside the range saturating. The dashed lines show a 20 degree wide band around the Ecliptic plane (solid line) and the Galactic plane is shown as a dotted line. The average number of observations per object within 10 degrees from the Ecliptic plane is about 460, and about 200 elsewhere. Adapted from Fig. 10 in Sesar et al. (2011).

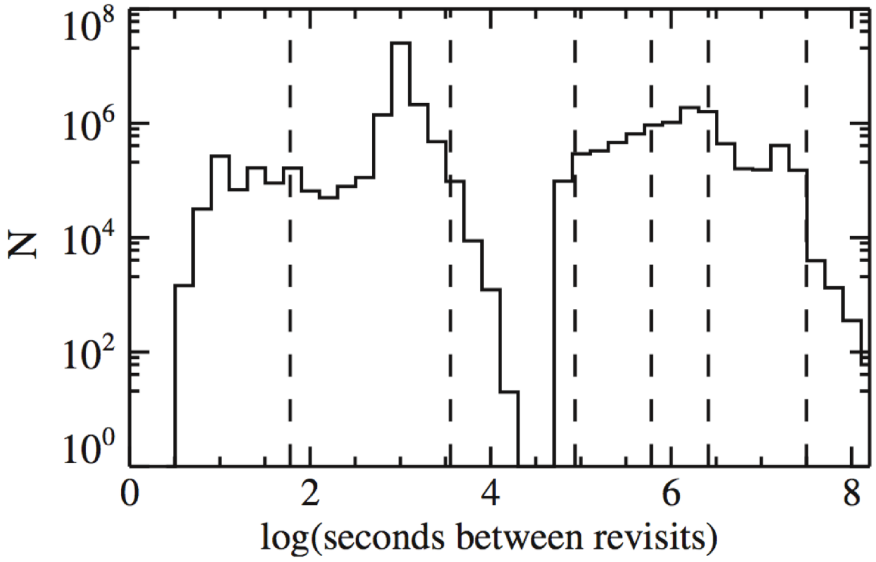

Figure 2. Cadence of LINEAR observations measured as the time between revisits of the same patch of sky. From left to right, the dashed lines show 1 minute, 1 hr, 1 day, 1 week, 1 month, and 1 year cadences. The LINEAR temporal coverage is fairly uniform, with a peak at ∼1000 sec corresponding to the main 15 minute cadence (optimized for asteroid observations). Adapted from Fig. 2 in Sesar et al. (2011).

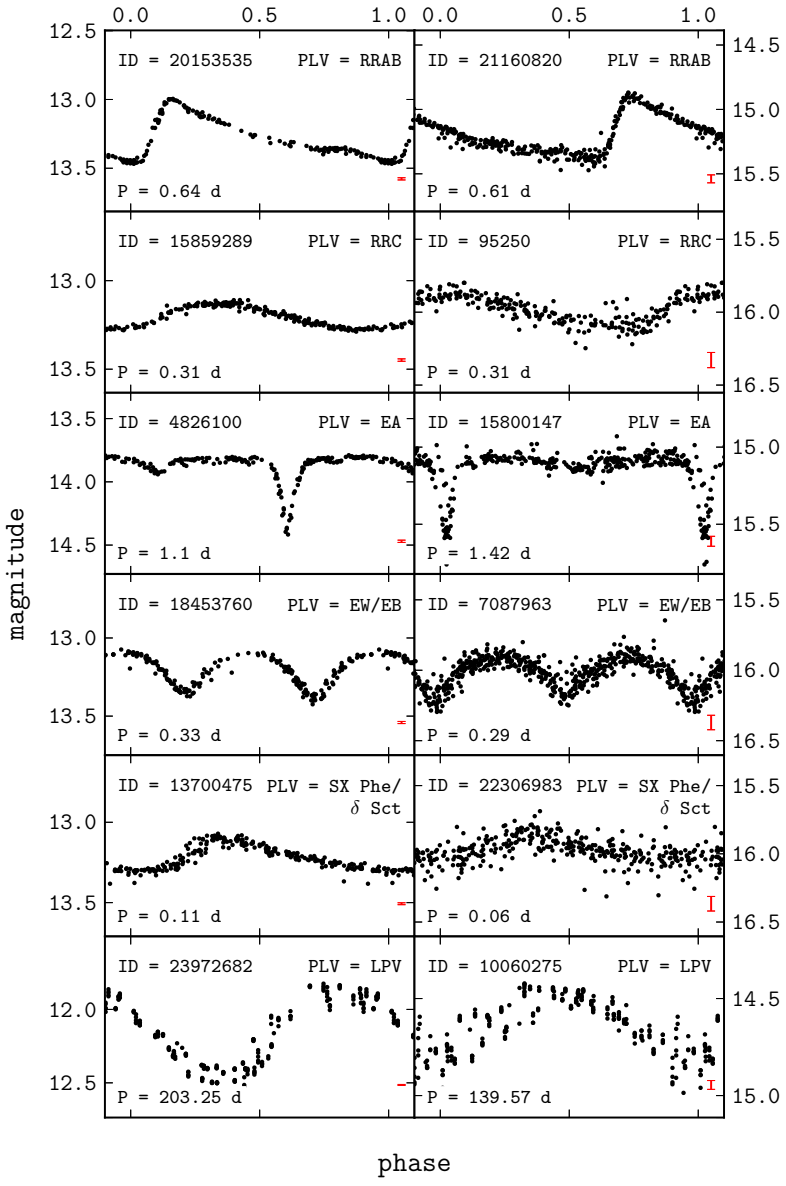

Figure 3. LINEAR light curve examples. Each row shows examples of light curves from most significant classes (bright examples on the left and faint examples on the right side of the figure

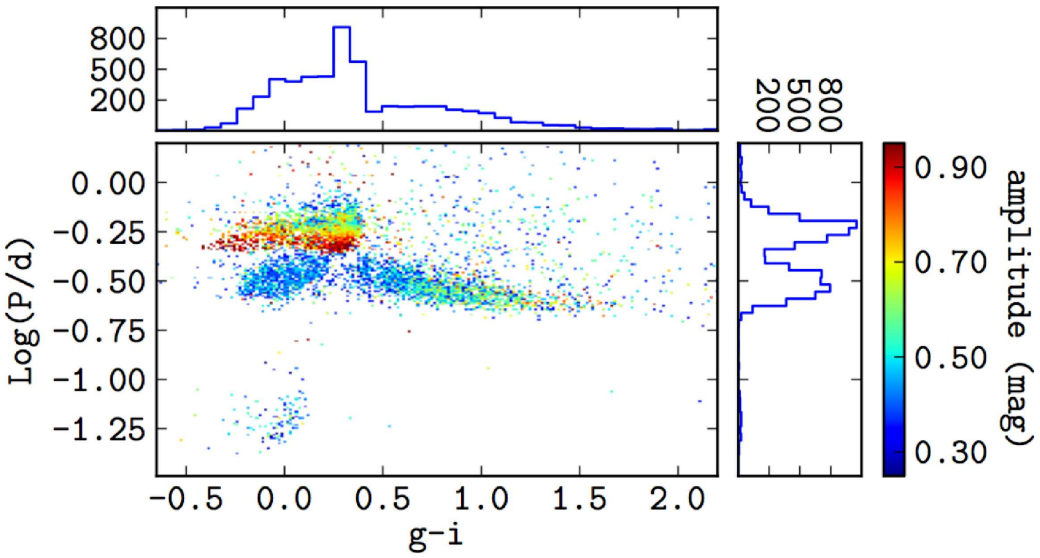

Figure 4. The distribution of periodic LINEAR variables in the period-color diagram. Bins are color coded by the median value of light curve amplitude according to the legend on the right. The two histograms show marginal distributions of the period and the $g - i$ color. Adapted from Fig. 8 in Palaversa et al. (2013).

Acknowledgements:

L.P. acknowledges support by the Gaia Research for European Astronomy Training (GREAT-ITN) Marie Curie network, funded through the European Union Seventh Framework Programme ([FP7/2007-2013] under grant agreement No. 264895.
Ž.I. acknowledges support by NSF grant AST-1008784 to the University of Washington and thanks the Hungarian Academy of Sciences for its support through the Distinguished Guest Professor grant No. E-1109/6/2012, and the Croatian National Science Foundation for its support through the grant O-1548-2009.

References:

Palaversa, L., Ivezić, Ž., Eyer, L., et al. 2013, accepted to AJ (July 2013), also arXiv:1308.0357
Sesar, B., Stuart, J. S., Ivezić, Ž., et al. 2011, AJ, 142, 190
Sesar, B., Ivezić, Ž., Stuart, J. S., et al. 2013, AJ, 146, 21

COMMISSIONS 27 AND 42 OF THE IAU
INFORMATION BULLETIN ON VARIABLE STARS

Number 6066

Konkoly Observatory
Budapest
3 August 2013

HU ISSN 0374 – 0676

PERIOD CHANGES IN THE ECLIPSING BINARY DX Vel

VOLKOV, I.M.[1,2]; CHOCHOL, D.[2]; GRYGAR, J.[3]; JELÍNEK, M.[4]; KUBÁNEK, P.[3]; MAŠEK, M.[3]; PROUZA, M.[3]; RIBEIRO, T.[5]; SEBASTIAN, D.[6]; VAN HOUTEN, C.J.[7]

[1] Sternberg Astronomical Institute, Moscow University,Universitetsky Ave. 13, Moscow 119992, Russia
E-mail: imv@sai.msu.ru

[2] Astronomical Institute of the Slovak Academy of Sciences, 059 60 Tatranská Lomnica, Slovakia
E-mail: chochol@ta3.sk

[3] Institute of Physics Czech Academy of Sciences, 182 21 Praha, The Czech Republic
E-mail: grygar@fzu.cz

[4] Instituto de Astrofísica de Andalucía (CSIC), Glorieta de la Astronomía, s/n, 18008 Granada, Spain

[5] Institution: SOAR Telescope, Colina El Pino s/n - Casilla 603 - La Serena, Chile
E-mail: tribeiro@ctio.noao.edu

[6] Thuringer Landessternwarte Tautenburg, Sternwarte 5,D-07778 Tautenburg, Germany
E-mail: sebastian@tls-tautenburg.de

[7] Sterrewacht, Huygens Laboratorium, 2300 RA Leiden, The Netherlands (passed away August 24, 2002)

The eclipsing binary DX Vel (HD 297655, $P = 1.12$ days, $V = 10.2$, A5, detached Algol binary) was discovered and studied photographically by van Houten (1950). In 1978 van Houten obtained the precise photoelectric light curve of the object in the Walraven system. The observations were published by van Houten et al. (2009).

Our CCD photometry of DX Vel was obtained between May 2012 and January 2013, using the FRAM (Photometric Robotic Atmospheric Monitor): 0.3 m Schmidt-Cassegrain telescope located in Argentina near the town of Malargue and operated by Institute of Physics, Czech Academy of Sciences (for more details see Prouza et al., 2010). The telescope FRAM works in fully automatic mode using RTS2 software system (Kubánek et al., 2004) as a part of the atmospheric monitoring program of the Pierre Auger Observatory (for the description of the Pierre Auger Observatory see e.g. Abraham et al., 2010). The telescope is equipped with the CCD camera G2-1600 of Moravian Instruments and Bessel set of filters. The observations were acquired in the standard $BVRcIc$ system.

The light curve analysis of our data with the PHOEBE software (Prsa & Zwitter 2005), assuming the sphere-sphere model with reflection effect subtracted, provides the parameters given in Table 1. The corresponding fit of the R light curve is shown in Fig. 1. The solution allows as much as 12 percent of third light in the system. We obtained the same results from van Houten's and ASAS light curves of DX Vel. As seen in Fig. 1, Van Houten's observations show small but significant anomalies in colour changes in the primary minimum. The source of the extra U-light in the bottom of the primary minimum could be an F star object, the third body in the system.

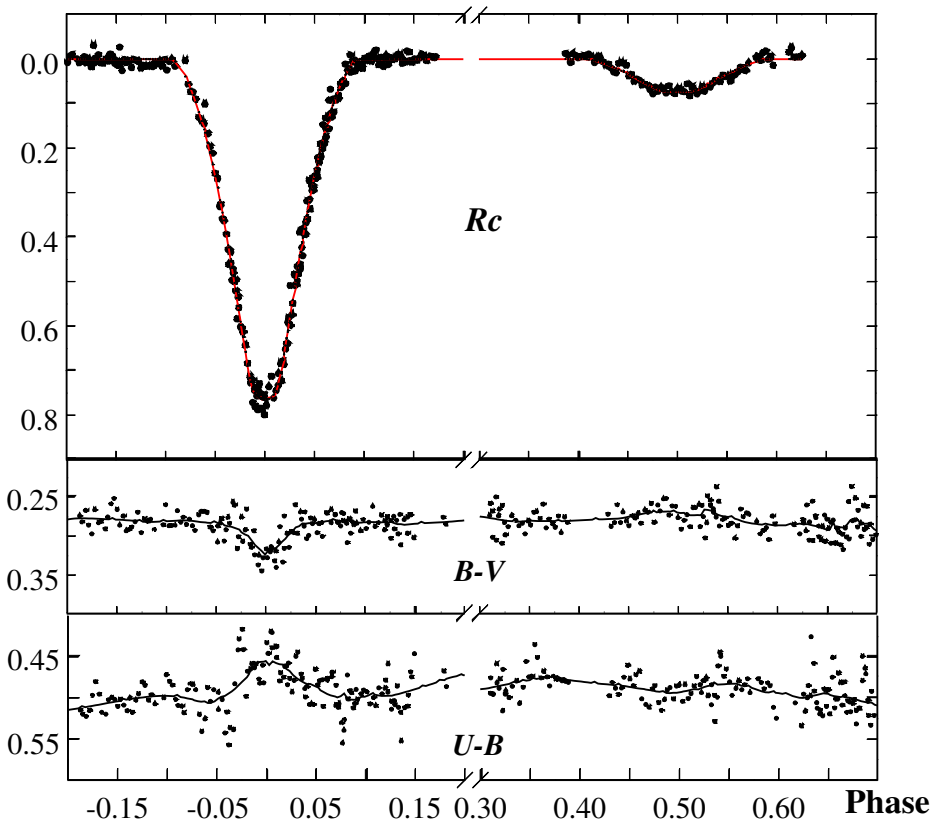

Figure 1. Part of our *Rc* light curve of DX Vel around both minima, taken by FRAM. Points denote the individual observations, solid red line stands for the theoretical fit, according to the parameters from Table 1 with L3=0.06. Van Houten's data transformed into $U-B$ and $B-V$ colours and phased with the same formula as *Rc* points are shown in two bottom panels.

In May 2012, Tiago Ribeiro obtained a spectrum of DX Vel during its primary minimum, with the 4-m SOAR telescope, using the GOODMAN spectrograph with the 1200 l/mm grating and the 0.46" slit allowing the spectral resolution of R=5900. The spectral classification was done by Daniel Sebastian, who classified the primary component of DX Vel as an A5 IV-III object. The classification was done by an automatic comparison of the spectrum with a catalog of template-spectra provided by Valdes et al. (2004). The used method is described in detail in Sebastian et al. (2012). The comparison of the part of our spectrum with the A5 III template is shown in Fig. 2. The size of the binary system with the orbital period 1.12 days is too small to contain an A5 subgiant or giant. The easiest explanation is to assume a third body in the DX Vel system, which affects the spectral classification.

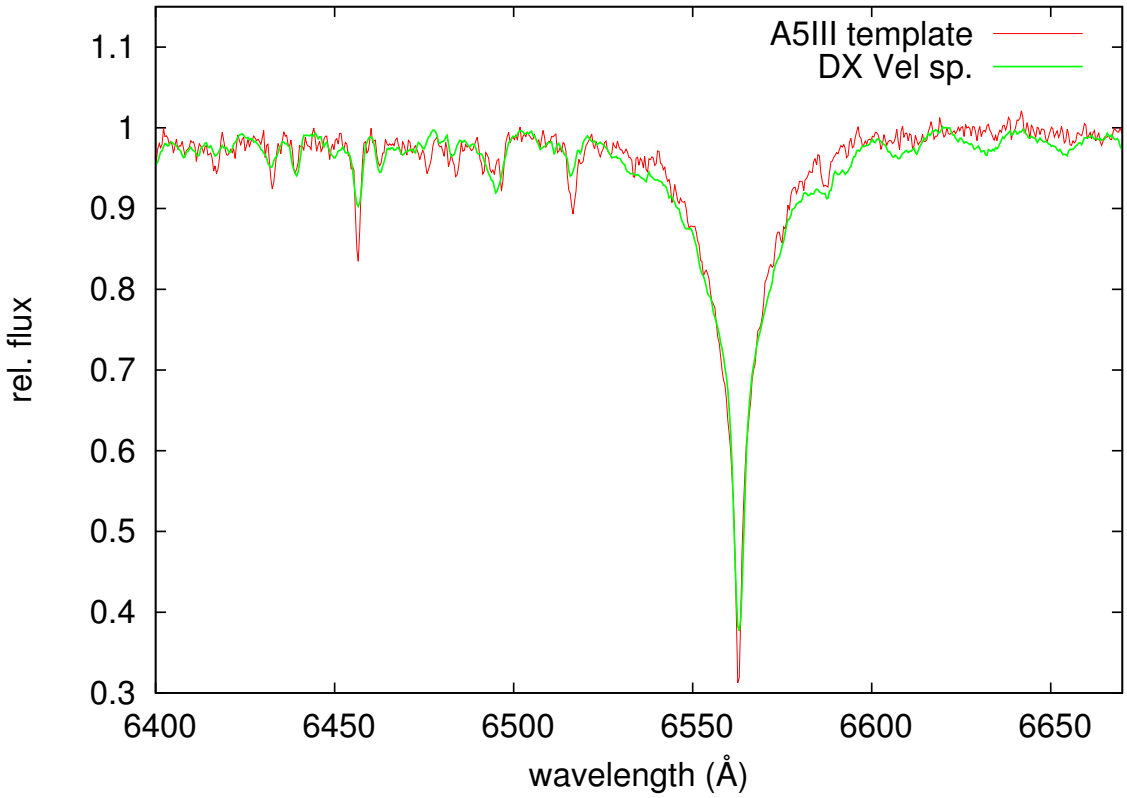

Figure 2. Comparison of the spectrum of DX Vel (green line) with the A5 III template (red line).

Table 1. Parameters of DX Vel

r_1	0.333 ± 0.002
T_1	$7400 \pm 300K$
r_2	0.236 ± 0.003
T_2	4400 ± 400
i	$85.4 - 89.9$ *

* depends on the value of the third light L3, varies from 0 to 0.12 in V and a little bit less in red and infrared.

All available primary minima times were used to construct the eclipse time variation (ETV) diagram. To derive the precise times of minima from photoelectric and CCD observations, we fitted the synthetic light curve through the individual observations by means of the least squares method. For simultaneous observations in several filters the timings of minima were weighted and mean values were calculated. To study the long-term period changes, we used 8 photographic minima times of DX Vel, published by van Houten (1950) and Hoffmeister (1951) to calculate one normal epoch of the primary minimum with a suitable precision. The ASAS data were divided into 6 intervals and normal minima for each interval were obtained. The times of minima are listed in Table 2. The $O-C$ residuals in the ETV diagram (Fig. 3) were calculated using the linear ephemeris: HJD Min I = 2443583.4618 + $1^{\rm d}.11730385\times$E, obtained by the least squares method.

Table 2. Times of minima for DX Vel

HJD − 2400000	Cycle	Residual (days)	Remarks
29037.280(8)	−13019	−0.0030	photographic
43583.4660(2)	0	+0.0042	van Houten
51985.5894(7)	7520	+0.0027	ASAS
52578.8771(7)	8051	+0.0020	ASAS
53165.4619(6)	8576	+0.0023	ASAS
53870.4778(8)	9207	−0.0006	ASAS
54482.7602(10)	9755	−0.0007	ASAS
54967.6704(12)	10189	−0.0003	ASAS
56053.6880(5)	11161	−0.0021	our observations
56080.5031(6)	11185	−0.0023	our observations
56292.7906(4)	11375	−0.0025	our observations

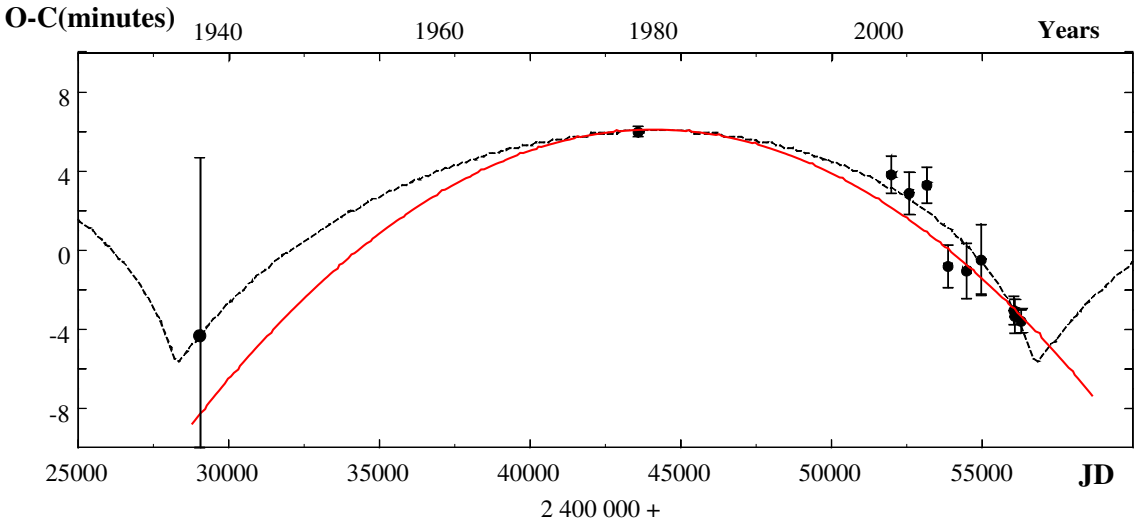

Figure 3. The ETV diagram for DX Vel. Solid red line - parabolic approximation, dashed line - the third body solution.

The minima times in ETV diagram can be fitted either by a parabola (continuous period change), represented by the following ephemeris:

$$\text{HJD Min I } = 2443583.4660(8) + 1^{\text{d}}.11730390(2) \times E - 5.51(4) \cdot 10^{-11} \times E^2$$

or by the third body orbit. Parameters of the formal third-body fit found by the least squares method are as follows:

$$P_3 \text{ (period)} = 28500 \pm 500 \text{ days, i.e. } 78.0 \text{ years}$$
$$T_0 \text{ (time of periastron)} = \text{J.D. } 2428200 \pm 500$$
$$A \text{ (semiamplitude)} = 0.00405 \pm 0.00020 \text{ day}$$
$$e = 0.9 \pm 0.1$$
$$\omega = 245^\circ \pm 15^\circ.$$

We would like to note that the similar situation in colour changes in minima had resulted in discovery of the third body in V577 Oph system (Volkov, 1991; Volkov & Volkova, 2010) and EQ Boo (Volkov et al., 2011, 2012).

We can conclude that the revealed orbital period change in DX Vel can be either real, caused by the mass transfer/mass loss effects or apparent, caused by the existence of the third body in the system.

Acknowledgements. This study was partly supported by the scholarship of the Slovak Academic Information Agency, RFBR grant 11-02-01213a and by the VEGA grant No. 2/0094/11. The operation of the robotic telescope FRAM is supported by the EU grant GLORIA (No. 283783 in FP7-Capacities program) and by the grant of the Ministry of Education of the Czech Republic (MSMT-CR LA08016). This work is partially based on observations obtained at the Southern Astrophysical Research (SOAR) telescope, which is a joint project of the Ministério da Ciência, Tecnologia, e Inovação (MCTI) da República Federativa do Brasil, the U.S. National Optical Astronomy Observatory (NOAO), the University of North Carolina at Chapel Hill (UNC), and Michigan State University (MSU).

References:

Abraham J. et al. (The Pierre Auger Collaboration), 2010, *Nucl. Instrum. Meth. A*, **620**, 227

Hoffmeister, C., 1951, *Mitt. Veränd. Sterne Sonneberg*, No. 138

van Houten, C.J., 1950, *Annalen Sterrewacht Leiden*, **20**, 223

van Houten, C.J., van Houten-Groeneveld, I., van Genderen, A.M. & Kwee, K.K., 2009, *The Journal of Astronomical Data*, **15**, 2

Kubánek, P. et al., 2004, *AIP Conference Proceedings*, **727**, 753

Prouza, M. et al., 2010, *Advances in Astronomy*, **2010**, article id. 849382

Prsa, A. & Zwitter, T., 2005, *ApJ*, **628**, 426

Sebastian, D., Guenther, E. W., Schaffenroth, V. et al., 2012, *Astron. Astrophys.*, **541**, A34

Valdes, F. et al. 2004, *ApJS*, **152**, 251

Volkov, I.M., 1991, *IBVS*, No. 3493

Volkov I.M. & Volkova N.S., 2010, *ASP Conf. Ser.*, **435**, 323

Volkov, I. M., Volkova, N. S., Nikolenko, I. V. & Chochol, D., 2011, *Astron. Reports*, **55**, 824

Volkov, I. M., Volkova, N. S., Nikolenko, I. V. & Chochol, D., 2012, *IAU Symp.*, **282**, 89

COMMISSIONS 27 AND 42 OF THE IAU
INFORMATION BULLETIN ON VARIABLE STARS

Number 6067

Konkoly Observatory
Budapest
8 August 2013

HU ISSN 0374 – 0676

VSX J075328.9+722424: A NEW SDB+M DWARF VARIABLE?

PRIBULLA, T.[1]; DIMITROV, D.[2]; KJURKCHIEVA, D.[3]; KOHL, S.[4]; KUNDRA, E.[1]; OHLERT, J.[5]; PERDELWITZ, V.[4]; SRDOC, G.[6]; VAŇKO, M.[1]

[1] Astronomical Institute of the Slovak Academy of Sciences, 059 60 Tatranská Lomnica, Slovakia
email: pribulla@ta3.sk

[2] Institute of Astronomy and National Astronomical Observatory, Bulgarian Academy of Sciences, 72 Tsarigradsko Shosse Blvd., 1784 Sofia, Bulgaria

[3] Department of Physics, Shumen University, 9700 Shumen, Bulgaria

[4] Hamburger Sternwarte, Gojenbergsweg 112, 21029 Hamburg, Germany

[5] Michael Adrian Observatory, Astronomie Stiftung Trebur, Fichtenstraße 7, 65468 Trebur, Germany

[6] Sarsoni 90, 51216 Viskovo, Croatia

VSX J075328.9+722424 (2MASS J07532886+7224246, FBS 0747+725) was identified as a blue object in the First Byurakan Survey of Northern blue stellar objects (Mickaelian, 2008). Based on low-dispersion spectra the object appeared to be a white dwarf of B1a spectral type.

The photometric observations of B. Stromar, K. Vardijan, and G. Srdoc implied that it is probably a new sdB+M dwarf eclipsing binary[1]. The extensive observations of G. Srdoc by a 30 cm telescope (Meade LX200 located at N 45°.38, E 14°.40) equipped with an SBIG ST-7XME CCD camera and the V filter clearly show a strong reflection effect amounting to about $0^{\rm m}.15$, deep primary and shallow secondary minima indicating a large difference between temperature of the components (Fig. 1). The orbital period of the system, $P \sim 5$ hours, and short duration of the minima precludes the primary component to be a main sequence star (see Połubek et al., 2007). The egress and ingress durations to the primary eclipse are longer than in the case the primary component would be a WD (this is confirmed by the fractional radius of the primary found by the light-curve analysis).

Fitting high-order symmetric trigonometric polynomials ($a_0 + \sum a_n \cos 2\pi n\varphi$, where φ is the orbital phase) to the discovery photometry led to the following preliminary ephemeris for the primary minimum:

$$\mathrm{MinI} = \mathrm{BJD\ (TDB)}2\,455\,868.74969(7) + 0^{\rm d}.2082535(6) \times E. \qquad (1)$$

The orbital period of the system is the second longest (after AA Dor) among the previously known sdB+M dwarf eclipsing binaries. Out of 13 known sdB + M eclipsing binaries (Barlow et al., 2013) the system shows deepest primary eclipses.

Follow-up observations of the object were obtained at several observatories in the framework of the *Dwarf* campaign (see Pribulla et al., 2012): 60 cm Cassegrain telescope

[1] see http://www.aavso.org/vsx/index.php?view=detail.top&oid=270274

Table 1: Preliminary light curve solution of VSX J075328.9+722424. r_1 and r_2 are dimensionless volume mean fractional radii of the components (with respect to the major axis of the system). The mass ratio was fixed to $q = m_2/m_1 = 0.55$.

Parameter		rms
i [deg]	88.215	0.048
r_1	0.1314	0.004
r_2	0.1774	0.0002
T_1 [K]	26200	–
T_2 [K]	3500	300
l_3(V)	0.0702	0.0004
l_3(R)	0.1113	0.0004

at the Stará Lesná Observatory (Slovak Academy of Sciences), 1.2 m Oskar-Lühning telescope of the Hamburger Sternwarte, 1.2 m telescope of the Michael Adrian Observatory at Trebur, and 2 m Zeiss telescope of the Rozhen Observatory. Exposure times were 60-120 seconds with the exception of the Rozhen Observatory measurements (30 seconds).

We used the high-precision Rozhen VR photometric data to derive preliminary system parameters. The CCD frames were reduced by standard IDL procedures (adapted from DAOPHOT) using seven comparison stars. The resulting light curves clearly show total eclipses in the system. The photometric elements were determined using program *PHOEBE* (Prša & Zwitter, 2005). For this aim we fixed: (a) the primary temperature to $T_1 = 26200$ K assuming its B1 spectral type (Mickaelian, 2008) and calibration of Popper (1980); (b) the gravity darkening coefficients to $g_1 = 1.00$, and $g_2 = 0.32$; (c) the bolometric albedo of the primary to $A_1 = 1.00$. The limb-darkening coefficients were adopted from the tables of van Hamme (1993). The mass ratio can reliably be determined from photometry only in the case of the totally eclipsing contact binaries and with lower precision in the case of semi-detached eclipsing systems (Terrell & Wilson, 2005). For known sdB+M binaries the mass ratio ranges between 0.145 and 0.340 (see Table 5 of Barlow et al., 2013). Thus we fixed it to several values between 0.1 and 1.0 with a step of 0.05 and ran the optimisation process from different starting parameters. As expected, the resulting quality of the fit depends only slightly on the mass ratio and it is formally best for $q = 0.55$ (see Fig. 2). In order to reproduce the VR light curves we were forced to set $A_2 = 1.00$ for the secondary component and to enable non-zero third light. The resulting parameters are given in Table 1. The relative radius of the primary component implies that it is a hot subdwarf star that contributes above 95% to the binary brightness in the visual wavelength range. The secondary component seems to be a cold K0-5 dwarf.

As suggested by an anonymous referee, we allowed bolometric albedos larger than unity to avoid non-zero third-light solutions. Because *PHOEBE* does not support $A > 1$, Binary Maker 3.0[2] was used. The quality of the resulting solution with $A_2 = 1.3$ is, however, inferior to the solution with $A_2 = 1.0$, and $l_3 > 0$.

The best fits to the VR observations (Fig. 3) were used to determine the times of minima (the fit to the V data was used as a template for the observations without a filter). The timing information is derived from the whole light curve (see Pribulla et al., 2012), i.e. there is one "minimum" even if the data cover several minima during the night. On the other hand, not all nightly light curves enabled us to determine a minimum. The weighted linear regression of the all available times of minima (Table 2) resulted in the

[2]http://www.binarymaker.com/

Table 2: Times of minimum light of VSX J075328.9+722424. Observatory abbreviations: VI - Viskovo, G1 - G1 pavilion of the Stará Lesná Observatory, RZ - Rozhen Observatory, TR - Michael Adrian Observatory, Trebur, HS - Hamburger Sternwarte

BJD (TDB)	σ	Epoch	Filter	Obs.	Exposure [sec]
2455805.649883	0.000062	−2741	*V*	VI	60
2455811.688940	0.000034	−2712	*V*	VI	60
2455814.812994	0.000086	−2697	*V*	VI	60
2455866.875644	0.000034	−2447	*V*	VI	60
2455875.830313	0.000048	−2404	*V*	VI	60
2455879.787107	0.000050	−2385	*V*	VI	60
2455880.828491	0.000042	−2380	*V*	VI	60
2455881.869827	0.000029	−2375	*V*	VI	60
2455882.702641	0.000036	−2371	*V*	VI	60
2455883.744146	0.000041	−2366	*V*	VI	60
2455884.577043	0.000031	−2362	*V*	VI	60
2455885.826512	0.000036	−2356	*V*	VI	60
2455886.659502	0.000038	−2352	*V*	VI	60
2456354.602198	0.000027	−105	-	G1	60
2456356.476378	0.000013	−96	*V*	RZ	30
2456357.517650	0.000013	−91	*R*	RZ	30
2456365.639405	0.000029	−52	-	TR	60
2456384.382176	0.000080	38	*V*	HS	90
2456397.293716	0.000044	100	-	G1	60
2456398.334954	0.000036	105	-	G1	60
2456429.364556	0.000043	254	-	G1	60

ephemeris:

$$\mathrm{MinI} = \mathrm{BJD\ (TDB)}2\,456\,376.46857(2) + 0\overset{\mathrm{d}}{.}208252121(16) \times E. \qquad (2)$$

It is well known that sdB stars often show non-radial pulsations (see e.g. 2M1938+4603, Østensen et al., 2010; NY Vir, Kilkenny et al., 1998). Hence, we performed a period analysis of the residuals from the best fits to the Rozhen photometry. The standard deviation of the light curve residuals from the best fits are $0\overset{\mathrm{m}}{.}008$ for the V passband and $0\overset{\mathrm{m}}{.}01$ for the R passband, which sets an upper limit for the pulsation amplitude. Unlike the case of NY Vir (Kilkenny et al., 1998), where the pulsations with semiamplitudes $0\overset{\mathrm{m}}{.}005$ (141 seconds) and $0\overset{\mathrm{m}}{.}01$ (184 seconds) are clearly visible, visual inspection of VSX J075328.9+722424 light curve does not reveal any periodic variability. The Fourier power spectra for the V and R passbands residuals are shown in Fig. 4. The power spectra differ for the V and R passband residuals and do not show any significant frequencies. The detection of the pulsations obviously requires observations of higher cadence and precision.

VSX J075328.9+722424 definitely deserves medium or high-resolution spectroscopy to find the spectroscopic orbit of the primary and to reliably estimate the absolute parameters of the components. The spectroscopy would also solve the issue of third light which might come from (i) an additional source (quite likely in the case of close binary stars, see Pribulla & Rucinski, 2006) or (ii) result from inadequate modelling of the reflection effect. For this $V = 16\overset{\mathrm{m}}{.}5$ short-period eclipsing binary an 8 m-class telescope is required.

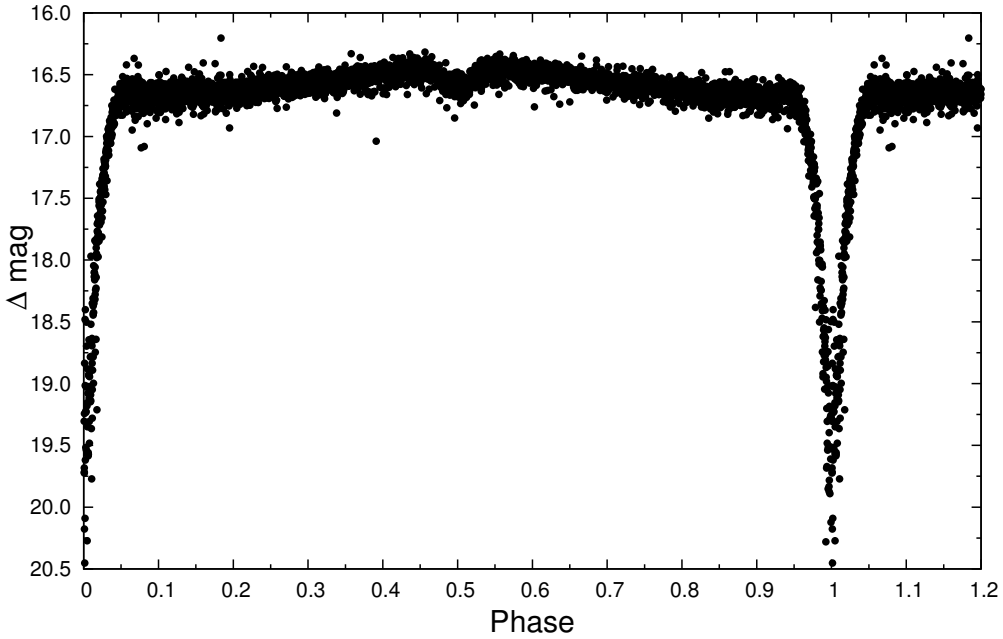

Figure 1. V light curve of VSX J075328.9+722424 obtained with 30 cm Schmidt-Cassegrain telescope at Viskovo, Croatia. The data were phased with ephemeris (1).

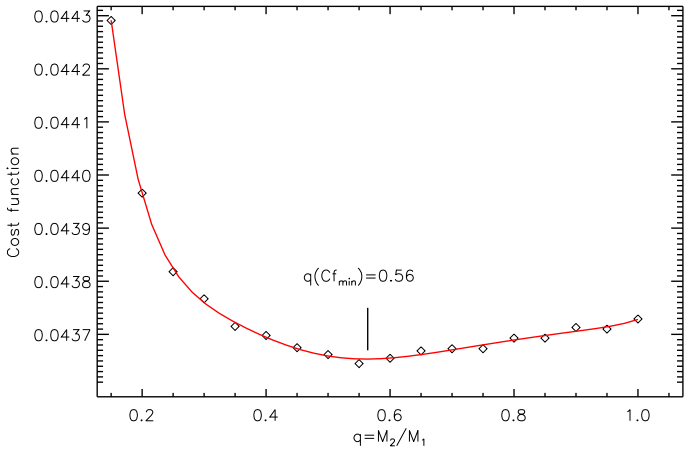

Figure 2. Goodness of the fit as the function of mass ratio

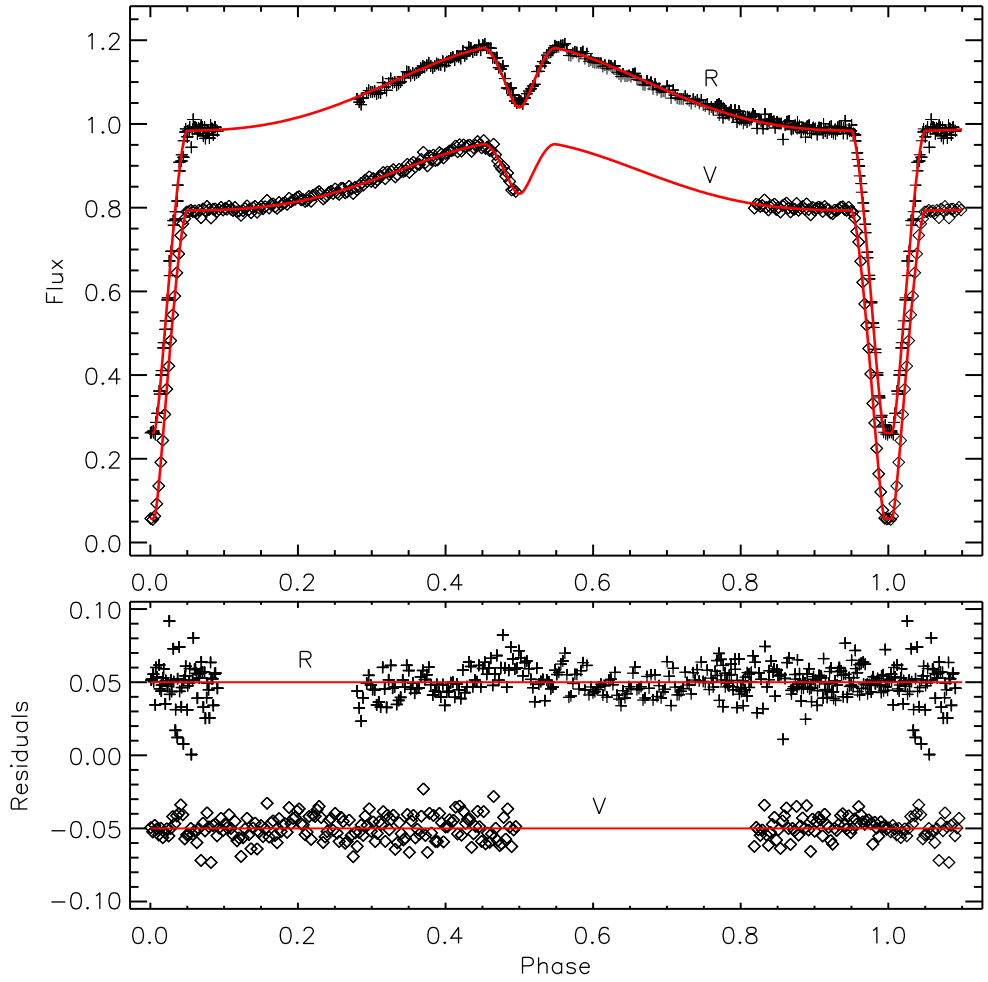

Figure 3. Rozhen VR photometric data and their fits corresponding to the parameters from Table 1.

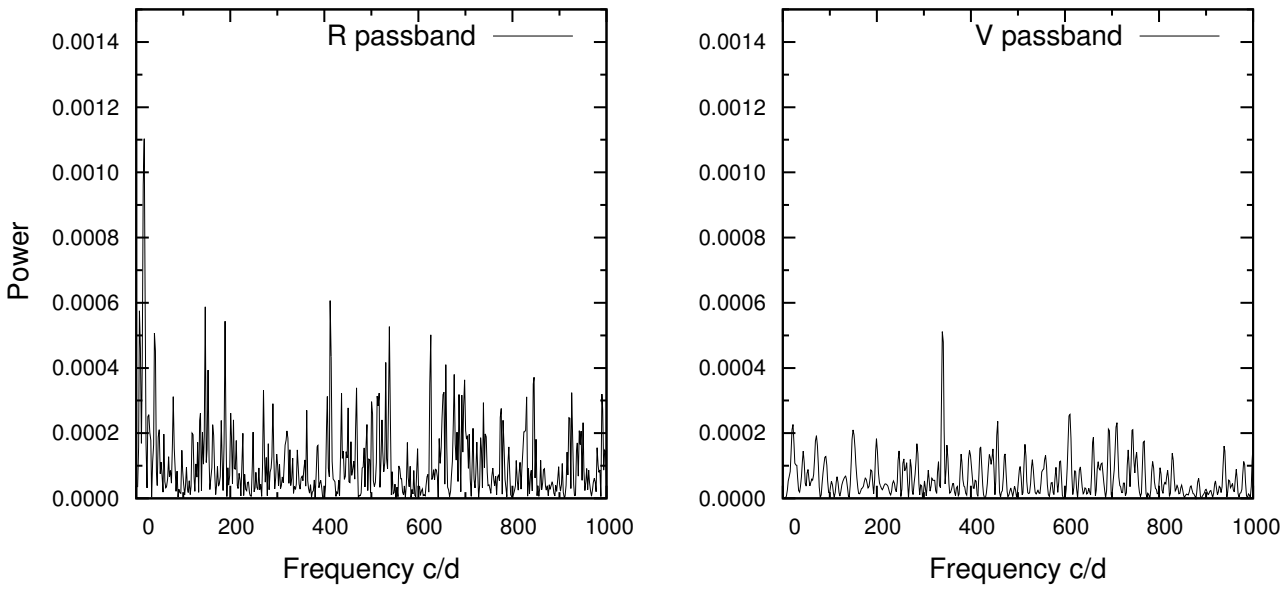

Figure 4. Power spectrum of the light-curve residual with respect to the best fit (Table 2) for the V and R passband data

Acknowledgements: The authors acknowledge support of grants: VEGA 2/0094/11 of Slovak Academy of Sciences; DDVU 02/40-2010 of the Bulgarian Scientific Foundation; RD 08-281 of Shumen University. This work was supported by the realization of the Project ITMS No. 26220120029, based on the supporting operational Research and development program financed from the European Regional Development Fund.

References:

Barlow, B.N., Kilkenny, D., Drechsel, H. et al., 2013, *MNRAS*, **430**, 22
Kilkenny, D., O'Donoghue, D., Koen, C. et al., 1998, *MNRAS*, **296**, 329
Mickaelian, A.M., 2008, *AJ*, **136**, 946
Østensen, R.H., Green, E.M., Bloemen, S. et al., 2010, *MNRAS*, **408**, L51
Połubek, G., Pigulski, A., Baran, A., Udalski, A., 2007, *ASP Conf. Series*, **372**, 487
Popper, D.M., 1980, *ARA&A*, **18**, 115
Pribulla, T., Rucinski, S.M., 2006, *AJ*, **131**, 2986
Pribulla, T., Vaňko, M., Ammler - von Eiff, M. et al., 2012, *AN*, 333, 754
Prša A., Zwitter T., 2005, *ApJ*, **628**, 426
Terrell, D., Wilson, R.E., 2005, *ApSS*, 296, 221
van Hamme, W., 1993, *AJ*, **106**, 2096

COMMISSIONS 27 AND 42 OF THE IAU
INFORMATION BULLETIN ON VARIABLE STARS

Number 6068

Konkoly Observatory
Budapest
14 August 2013

HU ISSN 0374 – 0676

CzeV283 AND CzeV397 – NEW RR LYRAE STARS SHOWING BLAZHKO EFFECT

SKARKA, M.[1]; CAGAŠ, P.[2]

[1] Department of Theoretical Physics and Astrophysics, Faculty of Science, Masaryk University, Kotlářská 2, Brno, Czech Republic, e-mail: maska@physics.muni.cz

[2] BSObservatory, Modrá 587, 760 01, Zlín, Czech Republic, e-mail: pavel.cagas@gmail.com

We present discovery of the Blazhko effect in two fundamental mode RR Lyrae variables CzeV283=USNO-A2.0 0975-17144916 (J2000 $\alpha = 19^{\rm h}55^{\rm m}38\overset{\rm s}{.}1$, $\delta = +13°43'22.4''$, Aql) and CzeV397=USNO-A2.0 0975-11853460 (J2000 $\alpha = 18^{\rm h}29^{\rm m}43\overset{\rm s}{.}3$, $\delta = +12°06'39\overset{''}{.}2$", Her), whose variabilities were unveiled recently (in 2011 and 2012) in the framework of private project dealing with searching for new variables in randomly chosen fields around known variables. This observation program resulted in discovery of more than a hundred new variable stars (see http://www.bsobservatory.org/results.html) among which some interesting cases occurred – e.g. a quadruple eclipsing binary system CzeV343 in Auriga constellation (Cagaš & Pejcha 2012).

The Blazhko effect, known for about century (firstly noted by S. N. Blazhko 1907), manifests itself as amplitude and phase modulations of the light curve. This phenomenon represents actual astrophysical challenge, because its nature remains unexplained. The most recent explanation, which is based on the data from *Kepler* space telescope, deals with the resonance 9:2 between the fundamental mode and the 9th radial overtone (Szabó et al. 2010). A brief overview of the Blazhko effect and proposed models can be found e.g. in Kolenberg (2011).

CzeV283 and CzeV397 join a group of about 270 known Blazhko stars from the Galactic field.[1] Except for results based on space missions, the most significant progresses in Blazhko variables research are *The Konkoly Blazhko survey* (Jurcsik et al. 2009) and works based on *GEOS* database (Le Borgne et al. 2007).

The surroundings of V729 Aql and V1134 Her were observed during three seasons between 2011 and 2013 (see Table 1 with a journal of observation) with a 10 inch f/5.4 Newtonian telescope equipped with a G4-16000 CCD camera[2] (field of view $71' \times 71'$) at the private observatory in Zlín, Czech Republic. As the aim of these measurements was searching for new variables, observations were carried out without filtering to gain the highest possible throughput.

Raw images, with exposure times of 240 and 180 seconds, were calibrated with appropriate dark frames and flat fields. Differential aperture photometry as well as the calibrations were performed using C-Munipack[3] software. USNO-A2.0 0975-17184388

[1] A list with Blazko variables is available at `http://physics.muni.cz/~blasgalf/` (Skarka 2013)
[2] Parameters of the detector can be found at `http://www.gxccd.com/`
[3] `http://c-munipack.sourceforge.net/`

(in CzeV283) and USNO-A2.0 0975-11774493 (in CzeV397) were chosen as comparison stars. In total we gained 910 measurements for CzeV283 in 19 nights with a time span of 413 d and 1255 points for CzeV397 in 22 nights (time span of 678 d). The relative precision of our photometry was about 0.05 mag.

We performed a frequency analysis of our time series with PERIOD04 (Lenz & Breger 2005) to get the basic pulsation periods. As we caught several maxima of both stars (Table 2), we were also able to determine their timings using polynomial fitting. On the basis of our investigations we give

$$\mathrm{HJD\ T_{max}} = 2456222.3286(6) + 0.558488(2)\mathrm{E_{puls}}, \quad (1)$$

for CzeV283 and

$$\mathrm{HJD\ T_{max}} = 2456132.3955(4) + 0.58664(3)\mathrm{E_{puls}}, \quad (2)$$

for CzeV397, respectively. Data of studied stars phased with respect to these elements are plotted in Fig. 1.

Table 1. Journal of observations. The meaning of t is the duration of observation, N is the number of points and TS corresponds to the time span.

CzeV283			CzeV397		
Night	t	N	Night	t	N
[HJD-2450000]	[hours]		[HJD-2450000]	[hours]	
5834	3.7	39	5830	1.6	27
5836	3.1	38	5835	3.1	43
5851	4.1	34	6095	3.0	26
5856	4.1	36	6101	1.1	19
5857	3.4	39	6102	2.7	47
5867	1.7	17	6121	3.6	64
5868	4.0	45	6131	4.3	69
5869	3.9	44	6132	3.8	66
5875	4.2	44	6145	1.5	22
5876	3.2	35	6152	3.6	64
6204	5.0	88	6153	2.4	41
6210	2.5	42	6155	4.2	68
6212	4.9	87	6157	3.1	56
6220	3.8	64	6158	4.5	75
6221	3.0	52	6159	4.3	75
6222	3.2	56	6180	4.7	79
6223	3.7	65	6181	2.8	40
6246	2.4	43	6483	4.2	66
6247	2.4	42	6494	5.1	89
			6495	4.8	85
			6507	4.1	72
			6508	4.0	62
		Total			
TS=413 d	66.3	910	TS=665 d	68.4	1121

After a few nights it was obvious that the light curves of both stars underwent changes (see Fig. 2), which is the sign of the Blazhko effect. Unfortunately our data were too sparse

to estimating the Blazhko period. In the case of CzeV397 we identified a suspicious side peak near f_0, which corresponds to 38 day modulation period. This period gives nice phased light curve, but it needs to be confirmed by further observations.

Table 2. Times of maximum light.

CzeV283	CzeV397
2455836.4148(8)	2456102.4842(4)
2455868.2524(9)	2456132.3955(4)
2456212.2797(5)	2456159.3754(3)
2456222.3286(6)	2456495.5320(14)
	2456508.4267(4)

To have at least a rough idea about the amplitude of the light changes of the stars we used PERIOD04 and fitted data with the sum of sines (the mean light curves in Fig. 1) in the form

$$A(t) = A_0 + \sum_{i=1}^{n} A_i \sin\left[2\pi\left(i\tau + \phi_i\right)\right], \tag{3}$$

where τ corresponds to the phase of the light curve (fractional part of $\left(\frac{t-T_0}{P}\right)$, where T_0 is the epoch and P is the basic pulsation period). The degree of the fit (n) was chosen according to visual inspection.

For CzeV283 we obtained min-to-max[4] range Δmag = 0.93 and Δmag = 0.67 for CzeV397, respectively.

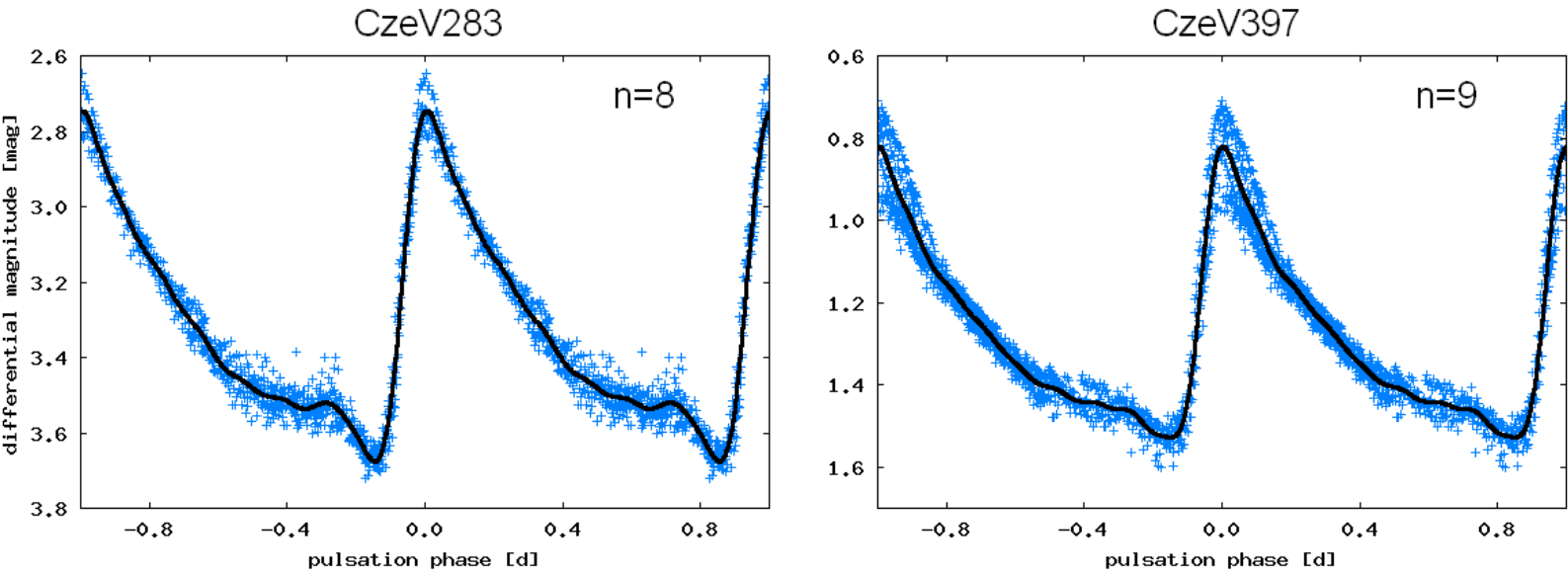

Figure 1. Data of CzeV283 and CzeV397 phased according to eq. 1 and 2, respectively. Solid line represents the fit with the sum of sines with respect to (3) of the degree n.

M. Skarka acknowledges the financial support of MU MUNI/A/0735/2012.

[4]We simply substracted minimum value of the fit from maximum.

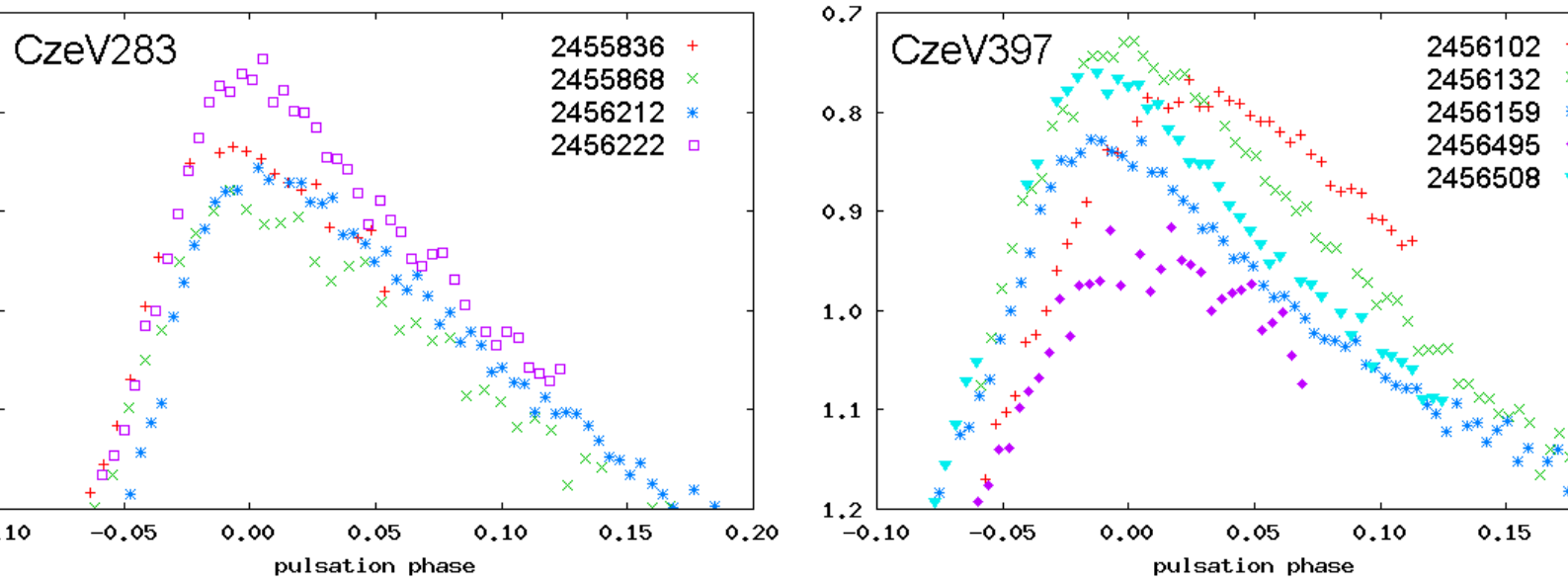

Figure 2. Close-up of the vicinities of the maxima of phased light curves. Change of the shape and amplitude in different nights is easily noticeable.

References:

Cagaš, P., & Pejcha, O. 2012, *A&A*, **544**, L3
Jurcsik, J., Sódor, Á., Szeidl, B., et al. 2009, *MNRAS*, **400**, 1006
Kolenberg, K. 2011, RR Lyrae Stars, Metal-Poor Stars, and the Galaxy, Carnegie Obs. Astrophys. Ser., vol. 5, ed. A. McWilliams, p. 100
Lenz P., Breger M., 2005, *Comm. Asteroseismology*, **146**, 53
Le Borgne, J. F., Paschke, A., Vandenbroere, J., et al. 2007, *A&A*, **476**, 307
Skarka, M. 2013, *A&A*, **549**, A101
Szabó, R., Kolláth, Z., Molnár, L., et al. 2010, *MNRAS*, **409**, 1244

COMMISSIONS 27 AND 42 OF THE IAU
INFORMATION BULLETIN ON VARIABLE STARS

Number 6069

Konkoly Observatory
Budapest
15 August 2013

HU ISSN 0374 – 0676

HIGH AND LOW RESOLUTION ABSOLUTE SPECTROPHOTOMETRY OF THE SYMBIOTIC NOVA VVV-NOV-003 = OGLE-2011-BLG-1444

MUNARI, U.[1]; VALISA, P.[2]; CETRULO, G.[2]; POLESKI, R.[3,4]

[1] INAF Osservatorio Astronomico di Padova, Sede di Asiago, I-36032 Asiago (VI), Italy

[2] ANS Collaboration, c/o Astronomical Observatory, 36012 Asiago (VI), Italy

[3] Warsaw University Observatory, Al. Ujazdowskie 4, 00-478 Warszawa, Poland

[4] Department of Astronomy, Ohio State University, 140 W. 18th Ave., Columbus, OH 43210, USA

VVV-NOV-003, at coordinates α=17:50:19.3, δ=−33:39:07 (J2000), has just been discovered by Beamin et al. (2013) as the third likely Galactic Nova in the VISTA Variables in The Via Lactea (VVV) survey data. The equatorial coordinates α=17:50:19.27, δ=−33:39:07.3 corresponds to Galactic values l=−3.523, b=−3.294, thus placing the object less than 5° from the Galactic center. The VVV survey (Minniti et al. 2010) first detected VVV-NOV-003 at K_s=15.80 mag on 6 October 2011, and measured it at K_s=10.70 on 7 March 2012. The progenitor was fainter than the limiting magnitude of K_s=17.13 in the field, setting the outburst amplitude to at least ΔK_s >6.4 mag. Beamin et al. (2013) estimated an extinction A_V=2.67 mag from VVV reddening maps (Gonzalez et al. 2012).

Poleski and Udalski (2013) noted the coincidence of VVV-NOV-003 with the transient OGLE-2011-BLG-1444, discovered by the OGLE-IV survey on 26 Sept 2011 and announced at that time as a candidate microlensing event. The OGLE light and color curves in V and I_C bands covering the period 2010-2013 are shown in Figure 1 (adapted from Poleski and Udalski 2013).

As noted already by Poleski and Udalski (2013), the light curve in Figure 1 is a close match to that of symbiotic novae, an exclusive group of ∼25 stars known in the Galaxy (Munari 1997), where a white dwarf accreting from a cool giant companion (frequently a Mira variable), suddenly begins to burn hydrogen at the surface and keep burning it for decades or centuries, with the consequence that the object remains close to maximum brightness for an equivalent long period. The total energy release is of the order of 10^{47}-10^{48} erg (Murset and Nussbaumer 1994), similar to that liberated by the outburst of a classical nova and corresponding to the hydrogen burning of $\sim 5\times10^{-5}$ $M_\odot$ of accreted material of solar composition. A light-curve closely similar to that of VVV-NOV-003 in Figure 1 has been exhibited by the symbiotic nova HM Sge (Yudin et al. 1994). During the 40 years elapsed since its 1973 eruption, HM Sge has declined by just 1.8 mag at optical wavelengths. HM Sge displayed large amplitude oscillation in brightness soon after optical maximum, similar to those visible in the light curve of VVV-NOV-003 in Figure 1. In HM Sge, their amplitude reduced with time and nulled after about four years.

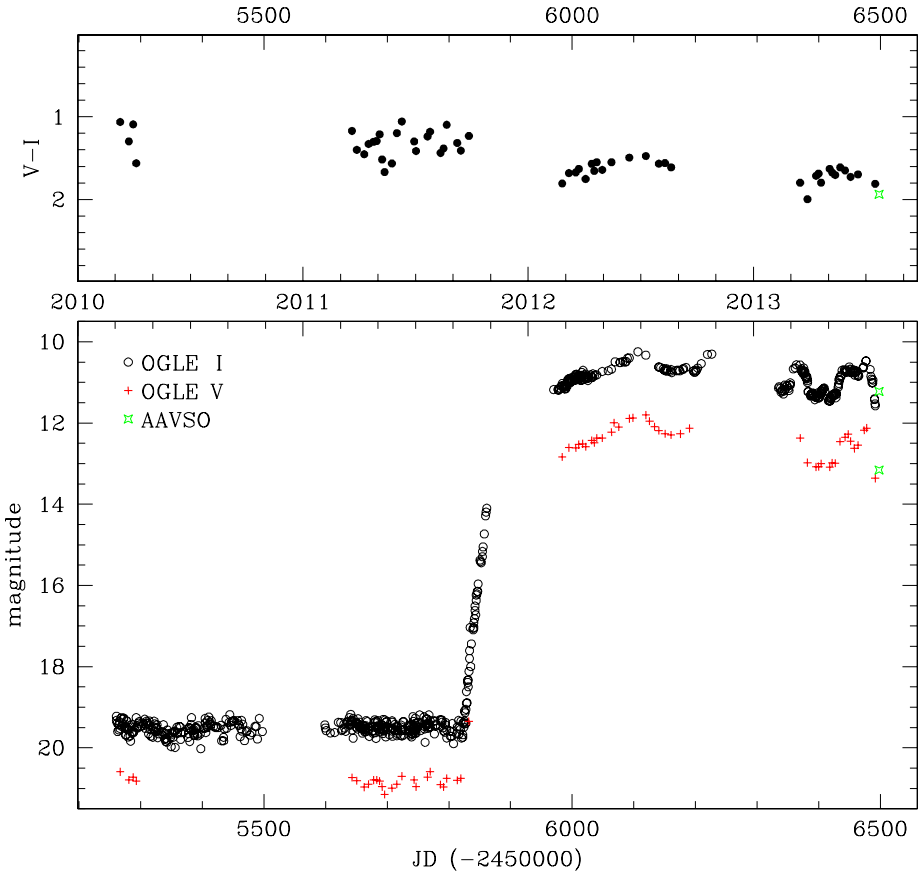

Figure 1. OGLE-IV light- and color-curves in V and I_C bands of the symbiotic nova VVV-NOV-003. The AAVSO data are the average of the few measurements collected since discovery announcement.

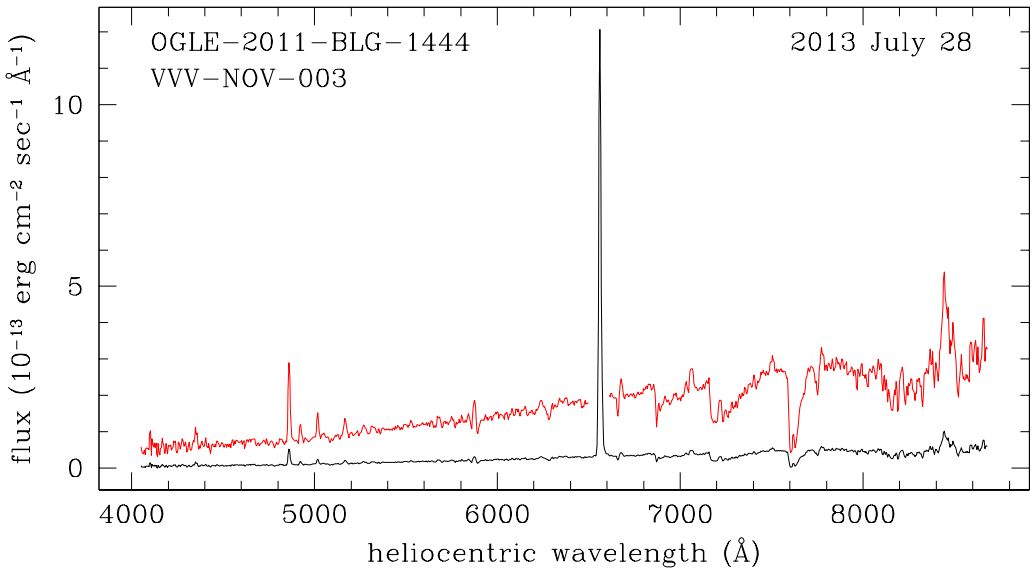

Figure 2. Low-resolution, fluxed spectrum of the symbiotic nova VVV-NOV-003 obtained on 2013 July 28 with the Multi-Mode Spectrograph on the Varese 0.61m telescope. A 5× stretched version is overplotted to enhance visibility of weak features.

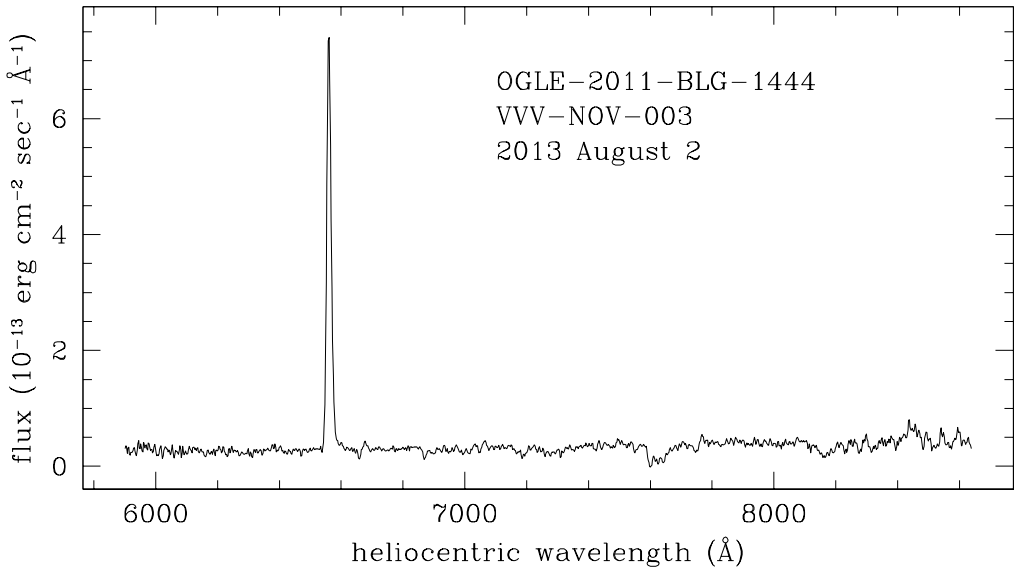

Figure 3. Low-resolution, fluxed spectrum of the symbiotic nova VVV-NOV-003 obtained on 2013 August 2 with the La Polse di Cougnes 0.70m telescope.

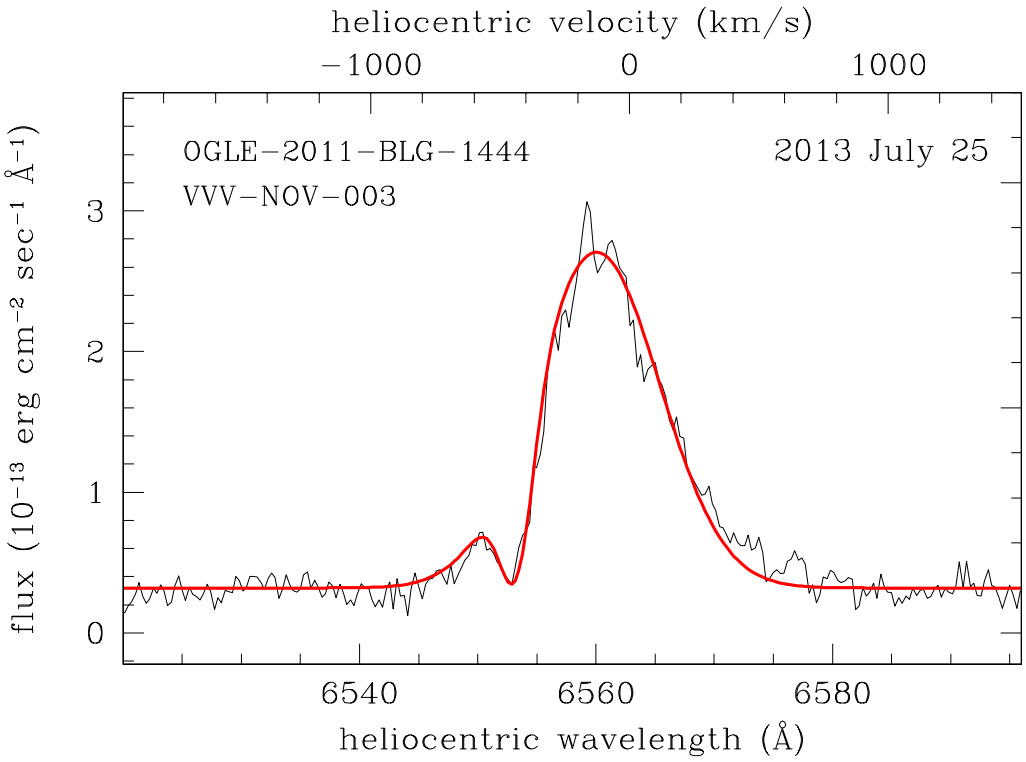

Figure 4. High-resolution Hα profile of VVV-NOV-003 obtained on 2013 July 25 with the Multi-Mode Spectrograph on the Varese 61cm telescope. The fit with two Guassians (one in emission and the other in absorption, as described in the text) is overplotted. The flux recorded on the continuum is too weak to show the second absorption which is well visible on the low resolution spectra −1100 km/s from the emission.

Table 1. Integrated fluxes of the emission line (in units of 10^{-13} erg cm^{-2} sec^{-1}) on the VVV-NOV-003 spectra of Figures 2 and 3.

$\lambda_\circ$	ion	flux	$\lambda_\circ$	ion	flux	$\lambda_\circ$	ion	flux
4101	Hδ	1.25	5876	HeI	1.86	8498	CaII	3.25
4340	Hγ	2.00	6563	Hα	184	8542	CaII	4.04
4861	Hβ	6.16	6678	HeI	2.12	8598	HI P14	4.80
4923	FeII #42	1.09	7065	HeI	1.67	8662	CaII	2.73
5018	FeII #42	1.98	7772	OI	1.90			
5169	FeII #42	2.07	8446	OI	15.2			

We obtained low dispersion fluxed spectra of VVV-NOV-003 with the Varese 0.61 m and La Polse di Cougnes 0.70 m telescopes, which are part of the ANS Collaboration network of telescopes (Munari et al. 2012). They are presented in Figures 2 and 3. The very low hight above the horizon reached by VVV-NOV-003 at culmination when observed from northern Italy, just $\sim$11°, prevented from reaching a higher S/N. A high resolution (resolving power 11 000) Hα profile of VVV-NOV-003 was obtained with the Multi Mode Spectrograph on the Varese 0.61m telescope operating in echelle mode. It is shown in Figure 4 where a fit with two Gaussians is superimposed (that in emission is centered at an heliocentric velocity of -126 km/s and has a FWHM=575 km/s, the one in absorption is centered at -432 km/s and has a FWHM=150 km/s).

The low resolution spectra in Figures 2 and 3 are very similar to those displayed by the symbiotic nova V4368 Sqr close to maximum (Grebel et al. 1994, Bragaglia et al. 1995, Munari et al. 2009). Table 1 lists the integrated flux of the principal emission lines we observed in VVV-NOV-003. There are two distinct P-Cyg absorption components simultaneously present: one, at a lower outflow velocity, is shifted by -300 km/s with respect to the emission component and is well visible in the high resolution Hα profile of Figure 4; the other, faster component is instead obvious in the low resolution spectra where it is shifted by -1100 km/s for Balmer lines and between -850 and -1050 km/s for HeI 5876, 6678, 7065 Å and OI at 7772 Å. The large inversion in the ratio of the emission lines of OI at 7772 and 8446 Å suggests fluorescent pumping by hydrogen Lyman-β.

References:

Beamin, J. C., Minniti, D., Saito, R. K., Kurtev, R. 2013, ATel, 5212
Bragaglia, A. et al. 1995, A&A, 297, 759
Gonzalez, O. A. et al. 2012, A&A, 543, 13
Grebel, E. K. et al. 1994, IBVS, 4019
Minniti, D. et al. 2010, New Astronomy, 15, 433
Munari, U. 1997, in: Physical Processes in Symbiotic Binaries and Related Systems, J. Mikolajewska ed., Copernicus Foundation for Polish Astronomy, 37
Munari, U. et al. 2009, Baltic Astron., 18, 75
Munari, U. et al. 2012, Baltic Astron., 21, 13
Murset, U., Nussbaumer, H. 1994, A&A, 282, 586
Poleski R., Udalski, A. 2013, ATel, 5215
Yudin, B. et al. 1994, A&AS, 105, 169

COMMISSIONS 27 AND 42 OF THE IAU
INFORMATION BULLETIN ON VARIABLE STARS

Number 6070

Konkoly Observatory
Budapest
17 August 2013

HU ISSN 0374 – 0676

BAV-RESULTS OF OBSERVATIONS - PHOTOELECTRIC MINIMA OF SELECTED ECLIPSING BINARIES AND MAXIMA OF PULSATING STARS

(BAV MITTEILUNGEN NO. 231)

HÜBSCHER, JOACHIM; LEHMANN, PETER B.

Bundesdeutsche Arbeitsgemeinschaft für Veränderliche Sterne e.V. (BAV), Munsterdamm 90, 12169 Berlin, Germany, `www.bav-astro.de`, `publikat@bav-astro.de`

In this 75th compilation of BAV results, photoelectric observations obtained mostly in the years 2012 and 2013 are presented on 523 variable stars giving 721 minima on eclipsing binaries and maxima on pulsating stars. All moments of minima and maxima are heliocentric UTC. The errors are tabulated in column '±'. The values in column '$O-C$' are determined without incorporating nonlinear terms. The references are given in the section 'Remarks'. All information about photometers and filters are specified in the column 'Rem'. The observations were made at private observatories. The photoelectric measurements and all the light curves with evaluations can be obtained from the office of the BAV for inspection.

Please use the following link for an easy access to all the publications of the BAV including the "Lichtenknecker Database of the BAV": `http://www.bav-astro.de/sfs` .

Table 1: Times of minima of eclipsing binaries

Variable	HJD 24.....	±	Obs	$O-C$		Ref	Fil	n	Rem
RT And	56188.3878	0.0011	AG	+0.0540		⟨21⟩	-I	40	12)
AA And	56219.6050	0.0026	AG	−0.0054		⟨21⟩	-I	40	12)
AD And	56219.4065	0.0012	AG	−0.0466		⟨21⟩	-I	40	12)
	56225.3235	0.0013	JU	−0.0469		⟨21⟩	o	53	5)
BD And	56188.3318	0.0040	AG	−0.0252		⟨21⟩	-I	39	12)
	56238.3256	0.0005	JU	−0.0252		⟨21⟩	o	83	5)
	56238.3317	0.0015	SCI	−0.0191		⟨21⟩	o	36	5)
	56245.2703	0.0050	SCI	−0.0241		⟨21⟩	o	156	5)
	56254.2933	0.0220	SCI	−0.0278	s	⟨21⟩	o	71	5)
BL And	56219.5390	0.0049	AG	+0.0054	s	⟨21⟩	-I	39	12)
CU And	56180.3669	0.0004	AG	−0.1051		⟨21⟩	-I	15	12)
CZ And	56219.3784	0.0038	AG	−0.4368		⟨21⟩	-I	41	12)
DK And	56219.5534	0.0011	AG	+0.0022		⟨62⟩	-I	40	12)
EX And	56159.5114	0.0048	AG	−0.0009	s	⟨21⟩	-I	37	12)
FK And	56220.3443	0.0020	AG				-I	31	12)
GZ And	56281.2622	0.0015	SCI	−0.0009	s	⟨21⟩	o	66	5)
	56281.4113	0.0021	SCI	−0.0043		⟨21⟩	o	100	5)
	56281.5630	0.0024	SCI	−0.0051	s	⟨21⟩	o	74	5)
KP And	56212.3487	0.0003	RAT RCR	+0.0519		⟨21⟩	R	157	13)
V404 And	56254.3358	0.0020	JU	+0.0094		⟨21⟩	o	80	5)
V406 And	55849.5713	0.0075	FR				o	32	15)
V425 And	56219.5655	0.0139	AG	−0.0334	s	⟨21⟩	-I	40	12)
V441 And	56220.4252	0.0010	AG	−0.0830		⟨21⟩	-I	31	12)
V504 And	56220.3410	0.0027	AG				-I	31	12)
V505 And	56220.3588	0.0017	AG				-I	31	12)

Table 1: (cont.)

Variable	HJD 24.....	±	Obs	$O-C$		Ref	Fil	n	Rem
V512 And	56220.4486	0.0024	AG				-I	31	12)
V514 And	56220.3004	0.0033	AG				-I	31	12)
V523 And	55952.2750	0.0002	RAT RCR				-U-I	86	13)
	56220.2863	0.0013	AG				-I	31	12)
DD Aqr	56210.3146	0.0002	RAT RCR	−0.0262		⟨21⟩	R	120	13)
HS Aqr	56177.3303	0.0002	RAT RCR	−0.0052		⟨21⟩	R	79	13)
HV Aqr	56156.4124	0.0005	RAT RCR	−0.0148		⟨21⟩	o	129	20)
LL Aqr	56174.4103	0.0047	NIC	−0.0716	s	⟨21⟩	V	150	6)
	56208.3539	0.0019	FR	−0.0277		⟨40⟩	-I	87	12)
V342 Aql	56096.4949	0.0002	RAT RCR	−0.1702		⟨21⟩	-U-I	196	13)
V609 Aql	56094.4037	0.0022	AG	−0.0599		⟨21⟩	-I	23	12)
V1096 Aql	56094.4667	0.0056	AG	−0.2477		⟨21⟩	-I	22	12)
V1426 Aql	55790.3766	0.0010	SIR				o	324	8)
	56179.3547	0.0003	WTR				o	100	4)
BN Ari	56251.2887	0.0001	RAT RCR				R	99	13)
CL Aur	56229.5678	0.0002	RAT RCR	+0.1558		⟨21⟩	R	182	13)
V364 Aur	56221.5148	0.0003	RAT RCR	−0.0019		⟨23⟩	R	194	13)
V591 Aur	56262.5284	0.0003	RAT RCR				R	246	13)
V599 Aur	56012.3489	0.0003	RAT RCR				-U-I	159	13)
V608 Aur	55993.3513	0.0003	RAT RCR				-U-I	137	13)
V640 Aur	55978.4578	0.0006	FR	−0.0166		⟨21⟩	V	42	15)
	55978.6096	0.0020	FR	−0.0288	s	⟨21⟩	V	42	15)
V648 Aur	56014.3970	0.0020	RAT RCR				-U-I	204	13)
TU Boo	56069.5493	0.0012	AG	+0.0233	s	⟨21⟩	-I	26	12)
TY Boo	56069.3859	0.0009	AG	−0.0423		⟨46⟩	V	28	12)
	56069.5470	0.0011	AG	−0.0398	s	⟨46⟩	V	28	12)
VW Boo	55969.5388	0.0002	RAT RCR	−0.0820	s	⟨50⟩	-U-I	113	13)
AC Boo	56065.4975	0.0003	AG	+0.0478	s	⟨21⟩	-I	36	12)
ET Boo	56065.4751	0.0016	AG	+0.0031		⟨23⟩	-I	36	12)
EW Boo	56069.4396	0.0035	AG	−0.0029		⟨23⟩	V	28	12)
GK Boo	56069.3923	0.0003	AG	+0.0027		⟨23⟩	V	26	12)
GS Boo	56069.3845	0.0032	AG	−0.0114		⟨23⟩	V	28	12)
HH Boo	56065.4166	0.0014	AG	+0.0245		⟨21⟩	-I	35	12)
IK Boo	56069.4604	0.0020	AG				-I	26	12)
IN Boo	56069.4460	0.0010	AG				-I	25	12)
IS Boo	56065.3791	0.0004	AG				-I	36	12)
	56065.5057	0.0008	AG				-I	36	12)
MN Boo	56065.4349	0.0038	AG	+0.0901		⟨21⟩	-I	36	12)
NT Boo	56065.3762	0.0005	AG				-I	36	12)
NX Boo	56069.3811	0.0009	AG				-I	29	12)
	56069.5051	0.0020	AG				-I	29	12)
NY Boo	56065.3823	0.0016	AG				-I	33	12)
PU Boo	56034.4755	0.0002	RAT RCR	−0.0171		⟨21⟩	-U-I	191	13)
PY Boo	56060.4449	0.0002	RAT RCR				-U-I	113	13)
Y Cam	56019.5478	0.0028	AG	+0.4038		⟨21⟩	-I	30	12)
SV Cam	56188.4276	0.0008	AG	+0.0561		⟨21⟩	-I	30	12)
AO Cam	56015.3781	0.0005	JU	+0.0396		⟨21⟩	o	62	5)
AS Cam	56321.2865	0.0012	AG	−0.2154	s	⟨21⟩	-I	19	12)
AY Cam	56019.5832	0.0043	AG	+0.0128		⟨21⟩	-I	28	12)
DN Cam	56167.4844	0.0038	AG	+0.0030		⟨23⟩	-I	29	12)
	56188.4104	0.0076	AG	+0.0000		⟨23⟩	-I	35	12)
FN Cam	56010.5265	0.0001	RAT RCR	+0.0061		⟨23⟩	-U-I	359	13)
NR Cam	55964.5026	0.0002	RAT RCR	+0.0077	s	⟨21⟩	-U-I	189	13)
	55964.6309	0.0002	RAT RCR	+0.0081		⟨21⟩	-U-I	189	13)
OQ Cam	56187.4611	0.0001	RAT RCR	−0.0166		⟨21⟩	R	230	13)
QU Cam	56178.5222	0.0002	RAT RCR				R	184	13)
V366 Cam	56188.5556	0.0047	AG				-I	34	12)
V379 Cam	56208.4995	0.0001	RAT RCR				C	136	13)

Table 1: (cont.)

Variable	HJD 24.....	±	Obs	$O-C$		Ref	Fil	n	Rem
V381 Cam	56224.4474	0.0004	RAT RCR				R	252	13)
V382 Cam	56167.4765	0.0019	AG	+0.0238	s	⟨21⟩	-I	29	12)
V389 Cam	56188.4582	0.0002	RAT RCR				R	280	13)
V419 Cam	55943.4910	0.0004	RAT RCR				-U-I	345	13)
V455 Cam	56222.4963	0.0004	RAT RCR				R	244	13)
V473 Cam	56015.3949	0.0001	RAT RCR	+0.0124		⟨21⟩	-U-I	177	13)
V479 Cam	56019.5063	0.0047	AG	+0.0254	s	⟨21⟩	-I	30	12)
V495 Cam	56019.5512	0.0050	AG				-I	30	12)
V514 Cam	56009.5745	0.0003	RAT RCR				-U-I	297	13)
	56055.4632	0.0002	RAT RCR				-U-I	261	13)
V518 Cam	55958.5286	0.0007	RAT RCR				-U-I	345	13)
EH Cnc	55969.3244	0.0002	RAT RCR	−0.0024	s	⟨23⟩	-U-I	108	13)
HN Cnc	55944.3595	0.0007	RAT RCR	−0.0281		⟨39⟩	-U-I	126	13)
EH CVn	56069.4340	0.0013	AG	−0.0571	s	⟨21⟩	-I	27	12)
FQ CVn	56069.5327	0.0038	AG				-I	27	12)
FV CVn	56031.3619	0.0004	RAT RCR	−0.0107		⟨21⟩	-U-I	108	13)
	56034.3584	0.0004	RAT RCR	−0.0102	s	⟨21⟩	-U-I	98	13)
	56069.5211	0.0036	AG	−0.0109		⟨21⟩	-I	25	12)
GG CVn	56069.4979	0.0038	AG				-I	29	12)
GM CVn	56069.4179	0.0053	AG				-I	24	12)
ZZ Cas	56219.5381	0.0083	AG	+0.0067	s	⟨21⟩	-I	49	12)
AB Cas	55463.3994	0.0035	PGL	+0.1048		⟨21⟩	V	154	14)
	56219.2932	0.0030	AG	+0.1174		⟨21⟩	-I	47	12)
AH Cas	56188.3529	0.0004	JU	−0.2154		⟨21⟩	o	66	5)
	56244.4429	0.0004	JU	−0.2160		⟨21⟩	o	65	5)
AX Cas	56179.3998	0.0010	JU	−0.0980		⟨21⟩	o	59	5)
DO Cas	56167.4913	0.0107	AG	−0.0019	s	⟨21⟩	-I	29	12)
EP Cas	56133.3979	0.0141	AG	−0.0358	s	⟨21⟩	-I	45	12)
	56219.6181	0.0012	AG	−0.0402	s	⟨21⟩	-I	47	12)
GT Cas	56133.4348	0.0057	AG	+0.1973		⟨21⟩	-I	43	12)
IL Cas	56167.4717	0.0112	AG	−0.0061		⟨60⟩	-I	29	12)
MU Cas	56133.5396	0.0059	AG	+0.1167		⟨21⟩	-I	43	12)
	56220.4110	0.0096	AG	+0.1123	s	⟨21⟩	-I	26	12)
OX Cas	56219.4201	0.0140	AG	+0.0071	s	⟨21⟩	-I	50	12)
PV Cas	56186.4025	0.0011	JU	−0.0356		⟨21⟩	o	55	5)
V336 Cas	56133.4108	0.0064	AG	−0.0145	s	⟨21⟩	-I	45	12)
V366 Cas	56158.434	0.011	AG	−0.006	s	⟨34⟩	-I	29	12)
V375 Cas	56219.4197	0.0094	AG	+0.2659	s	⟨49⟩	-I	48	12)
V380 Cas	56219.3689	0.0038	AG	−0.0677		⟨21⟩	-I	47	12)
V381 Cas	56159.4159	0.0024	AG	−0.0055	s	⟨49⟩	-I	37	12)
V459 Cas	56219.6407	0.0001	AG	−0.0202		⟨33⟩	-I	50	12)
V541 Cas	56220.3989	0.0020	AG	+0.0846	s	⟨21⟩	-I	27	12)
V651 Cas	56219.4857	0.0015	AG	+0.0027	s	⟨27⟩	-I	47	12)
V775 Cas	55879.2254:	0.0022	FR				o	86	15)
V776 Cas	56220.3713	0.0139	AG	−0.0135	s	⟨23⟩	-I	28	12)
V1001 Cas	56159.5296	0.0003	AG	+0.0121		⟨21⟩	-I	37	12)
V1007 Cas	56159.3903	0.0017	AG				-I	37	12)
	56159.5574	0.0012	AG				-I	37	12)
V1030 Cas	56159.4766	0.0016	AG				-I	36	12)
V1046 Cas	56133.5352	0.0005	AG				-I	45	12)
V1060 Cas	56219.5249	0.0116	AG				-I	50	12)
	56220.4324	0.0021	AG				-I	25	12)
V1061 Cas	55879.4237	0.0016	FR				o	19	15)
V1107 Cas	54390.2941	0.0006	JU	+0.0631	s	⟨48⟩	o	80	5)
	55835.4135	0.0004	JU	+0.0362		⟨48⟩	o	80	5)
	56179.3608	0.0009	JU	+0.0428	s	⟨48⟩	o	60	5)
	56220.3755	0.0013	JU	−0.0586	s	⟨48⟩	o	73	5)
	56222.2889	0.0006	JU	−0.0386	s	⟨48⟩	o	28	5)
	56222.4247	0.0006	JU	−0.0381		⟨48⟩	o	82	5)
SU Cep	56188.4410	0.0033	AG	+0.0083	s	⟨21⟩	-I	27	12)

Table 1: (cont.)

Variable	HJD 24.....	±	Obs	$O-C$		Ref	Fil	n	Rem
SU Cep	56203.3110	0.0007	AG	+0.0051		⟨21⟩	-I	17	12)
VW Cep	56180.3974	0.0019	AG	+0.0719		⟨21⟩	-I	24	12)
	56206.2799	0.0013	AG	+0.0711		⟨21⟩	-I	86	12)
	56206.4183	0.0006	AG	+0.0704	s	⟨21⟩	-I	86	12)
	56206.5587	0.0003	AG	+0.0716		⟨21⟩	-I	86	12)
VZ Cep	56220.2923	0.0001	AG	−0.0101		⟨21⟩	-I	27	12)
WX Cep	56180.4557	0.0006	AG	+0.0111		⟨21⟩	-I	56	12)
WY Cep	56058.4722	0.0048	AG	+0.0222		⟨21⟩	-I	48	12)
	56219.6036	0.0004	AG	+0.0254		⟨21⟩	-I	47	12)
XY Cep	55774.4484	0.0010	SIR	−0.0497		⟨21⟩	o	225	8)
ZZ Cep	56219.4748	0.0107	AG	−0.0124		⟨21⟩	-I	47	12)
AH Cep	56206.4429	0.0015	AG	−0.1019		⟨21⟩	-I	56	12)
CO Cep	56167.4411	0.0063	AG	−0.2023	s	⟨21⟩	-I	27	12)
CW Cep	56180.4323	0.0032	AG	+0.0193		⟨21⟩	-I	23	12)
GG Cep	56058.4664	0.0051	AG	−0.1068		⟨21⟩	-I	46	12)
GI Cep	56184.4764	0.0003	RAT RCR	−0.1225		⟨21⟩	R	246	13)
GK Cep	56180.3665	0.0027	AG	+0.1198		⟨21⟩	-I	21	12)
	56206.5821	0.0008	AG	+0.1230		⟨21⟩	-I	70	12)
GW Cep	56167.4793	0.0019	AG				-I	29	12)
IO Cep	56158.5076	0.0021	AG	+0.0208		⟨21⟩	-I	29	12)
IP Cep	56181.5041	0.0020	RAT RCR	−0.0275	s	⟨36⟩	R	231	13)
LM Cep	56072.4631	0.0049	AG	+0.1348		⟨21⟩	-I	46	12)
LP Cep	56072.4020	0.0031	AG	−0.0727	s	⟨21⟩	-I	46	12)
NW Cep	56167.4057	0.0088	AG	+0.9048		⟨21⟩	-I	33	12)
V397 Cep	56219.4431	0.0089	AG				-I	47	12)
	56220.3819	0.0060	AG				-I	28	12)
V711 Cep	56219.3518	0.0051	AG	+0.0013		⟨23⟩	-I	47	12)
V734 Cep	56167.5207	0.0037	AG				-I	29	12)
V737 Cep	56072.3892	0.0012	AG	+0.0184	s	⟨21⟩	-I	46	12)
	56072.5405	0.0010	AG	+0.0204		⟨21⟩	-I	46	12)
V834 Cep	56158.5441	0.0107	AG				-I	29	12)
RW Com	56061.4141	0.0015	AG	−0.0074	s	⟨21⟩	V	18	12)
RZ Com	56061.4568	0.0012	AG	+0.0468		⟨21⟩	V	18	12)
CC Com	55960.4593	0.0008	RAT RCR	−0.0173	s	⟨21⟩	-U-I	118	13)
	55960.5710	0.0001	RAT RCR	−0.0159		⟨21⟩	-U-I	118	13)
	56061.4250	0.0018	AG	−0.0156		⟨21⟩	V	19	12)
EK Com	56019.4518	0.0007	JU	+0.0047		⟨23⟩	o	79	5)
LL Com	55686.4759	0.0020	SIR	+0.0457		⟨31⟩	o	68	8)
LO Com	56061.4487	0.0020	AG	+0.0010		⟨23⟩	-I	18	12)
LP Com	56061.3935	0.0018	AG	+0.0088	s	⟨23⟩	-I	18	12)
NV Com	56035.3898	0.0005	RAT RCR				-U-I	87	13)
CV Cyg	56157.4752	0.0043	AG	+0.2005		⟨21⟩	-I	23	12)
DO Cyg	56132.5143	0.0001	RAT RCR	−0.0247		⟨21⟩	-U-I	241	13)
	56132.5145	0.0016	AG	−0.0245		⟨21⟩	-I	28	12)
DP Cyg	56167.3664	0.0055	AG	+0.5114	s	⟨21⟩	-I	33	12)
	56188.4894	0.0108	AG	+0.8894		⟨21⟩	-I	28	12)
GG Cyg	56074.5010	0.0027	AG	+0.1435		⟨21⟩	-I	25	12)
GM Cyg	56151.5575	0.0019	SCI	−0.2119		⟨21⟩	o	83	5)
GO Cyg	56158.5469	0.0036	AG	+0.0724	s	⟨21⟩	-I	29	12)
	56188.3273	0.0018	AG	+0.0656		⟨21⟩	-I	27	12)
GV Cyg	56167.5114	0.0103	AG	+0.1531		⟨21⟩	-I	33	12)
KR Cyg	56158.4718	0.0007	FR	+0.0206	s	⟨21⟩	-I	26	12)
	56186.3665	0.0023	FR	+0.0253	s	⟨21⟩	-I	105	12)
LO Cyg	56187.3732	0.0068	AG	−0.0252		⟨21⟩	-I	42	12)
MY Cyg	56158.5152	0.0027	AG	−1.9902		⟨21⟩	-I	29	12)
NU Cyg	56211.3273	0.0014	SCI	−0.0186		⟨21⟩	o	17	5)
	56211.4749	0.0018	SCI	−0.0115	s	⟨21⟩	o	25	5)
NZ Cyg	56191.3651	0.0018	SCI	+0.0636	s	⟨21⟩	o	40	5)
	56191.5661	0.0018	SCI	+0.0616		⟨21⟩	o	33	5)

Table 1: (cont.)

Variable	HJD 24.....	±	Obs	$O-C$		Ref	Fil	n	Rem
QU Cyg	56177.3882	0.0015	SCI	−0.0736		⟨21⟩	o	27	5)
	56177.5516	0.0014	SCI	−0.0836	s	⟨21⟩	o	26	5)
V345 Cyg	56167.5146	0.0003	RAT RCR	+0.0568		⟨36⟩	R	174	13)
V370 Cyg	56179.5632	0.0003	FR	−0.0332		⟨21⟩	V	94	15)
	56180.3417	0.0020	WTR	−0.0292		⟨21⟩	o	70	4)
V382 Cyg	56157.4331	0.0050	AG	+0.1110	s	⟨21⟩	-I	23	12)
V382 Cyg	56158.3765	0.0025	AG	+0.1116		⟨21⟩	-I	29	12)
V388 Cyg	56188.3457	0.0035	AG	−0.0970		⟨21⟩	-I	30	12)
V398 Cyg	56159.4365	0.0022	FR	−1.4926	s	⟨21⟩	-I	31	12)
V401 Cyg	56074.5313	0.0024	AG	+0.0708	s	⟨21⟩	-I	25	12)
	56093.4674	0.0002	RAT RCR	+0.0684		⟨21⟩	-U-I	217	13)
	56179.4258	0.0006	FR	+0.0753	s	⟨21⟩	V	47	15)
V442 Cyg	56188.3763	0.0030	AG	−0.0420		⟨21⟩	-I	25	12)
V448 Cyg	56157.4804	0.0037	FR	+0.0257		⟨21⟩	-I	47	12)
V454 Cyg	56229.3050	0.0004	RAT RCR	−0.0091		⟨21⟩	R	153	13)
V463 Cyg	56167.585 :	0.010	FR	+0.062	s	⟨21⟩	V	79	15)
V474 Cyg	56157.577	0.010	AG	+0.234		⟨21⟩	-I	23	12)
V478 Cyg	56158.4845	0.0113	AG	+0.0163	s	⟨21⟩	-I	29	12)
V490 Cyg	56186.5111	0.0004	FR	+0.1623		⟨21⟩	-I	54	12)
V501 Cyg	56132.4324	0.0035	SCI	−0.2958		⟨21⟩	o	76	5)
	56167.5068	0.0023	SCI	−0.2998	s	⟨21⟩	o	96	5)
V680 Cyg	56153.5525	0.0016	AG	+0.0215		⟨49⟩	-I	28	12)
V687 Cyg	56155.3870	0.0114	RAT RCR	−0.0065		⟨21⟩	o	45	20)
V725 Cyg	56158.6013	0.0021	FR	+0.2590	s	⟨21⟩	-I	55	12) 1)
	56186.3983	0.0030	FR	+0.2544	s	⟨21⟩	-I	33	12)
V796 Cyg	56158.4978	0.0019	SCI	+0.0001		⟨21⟩	o	246	5)
V841 Cyg	56074.4383	0.0028	AG	+0.0017		⟨21⟩	-I	25	12)
V859 Cyg	56074.4612	0.0030	AG	+0.0247	s	⟨21⟩	-I	25	12)
	56167.4200	0.0012	FR	+0.0357		⟨21⟩	V	36	15)
	56179.3497	0.0013	FR	+0.0179	s	⟨21⟩	V	68	15)
V869 Cyg	56167.5203	0.0008	FR	+0.1259	s	⟨21⟩	-I	46	12)
V874 Cyg	56074.4202	0.0024	AG	+0.0771		⟨21⟩	-I	25	12)
V887 Cyg	56179.4772	0.0030	FR	−0.0192	s	⟨21⟩	-I	47	12)
V902 Cyg	56179.5194	0.0009	FR	+0.0219		⟨21⟩	-I	31	12)
V907 Cyg	56179.3133	0.0011	FR	−0.1689		⟨21⟩	-I	32	12)
	56179.5848	0.0013	FR	+0.1104		⟨21⟩	-I	32	12)
V957 Cyg	56203.4017	0.0099	AG	+0.1403	s	⟨21⟩	-I	40	12)
V979 Cyg	56203.4550	0.0026	AG	+0.0174		⟨21⟩	-I	39	12)
V1009 Cyg	56203.4553	0.0029	AG	−0.0082		⟨21⟩	-I	41	12)
V1011 Cyg	56152.5860	0.0056	FR	+0.0723	s	⟨21⟩	-I	22	12)
V1013 Cyg	56074.4748	0.0120	AG	+0.1593	s	⟨21⟩	-I	25	12)
V1018 Cyg	56203.3988	0.0029	AG	−0.0915		⟨21⟩	-I	42	12)
V1019 Cyg	56203.3913	0.0062	AG	+0.1324		⟨21⟩	-I	42	12)
V1034 Cyg	56179.3224	0.0009	FR	+0.0291	s	⟨21⟩	V	94	15)
V1147 Cyg	56203.4515	0.0035	AG	+0.3934	s	⟨21⟩	-I	39	12)
V1171 Cyg	56152.4214	0.0002	FR	−0.0583		⟨21⟩	-I	69	12)
V1187 Cyg	56168.4943	0.0012	RAT RCR	−0.0161		⟨30⟩	R	109	13)
V1191 Cyg	56168.4723	0.0004	RAT RCR	+0.0120	s	⟨21⟩	R	107	13)
V1302 Cyg	56203.3205	0.0015	AG	−0.0982		⟨21⟩	-I	40	12)
V1401 Cyg	56158.4501	0.0057	AG	+0.2891	s	⟨21⟩	-I	40	12)
	56187.4192	0.0099	AG	+0.2750		⟨21⟩	-I	42	12)
V1411 Cyg	56167.3911	0.0023	AG	−0.1532	s	⟨21⟩	-I	33	12)
	56188.3630	0.0058	AG	−0.1533	s	⟨21⟩	-I	27	12)
V1417 Cyg	56133.4713	0.0019	AG	+0.1461	s	⟨21⟩	-I	32	12)
V1425 Cyg	56158.4896	0.0037	AG	+0.0124		⟨21⟩	-I	28	12)
V1437 Cyg	56167.3629	0.0019	FR	−0.0645		⟨21⟩	-I	44	12)
V1456 Cyg	56152.5202:	0.0077	FR				-I	33	12)
V1481 Cyg	56132.5384	0.0038	AG	+0.6502		⟨21⟩	-I	28	12)
V1877 Cyg	56159.4428	0.0008	FR	−0.0989	s	⟨23⟩	-I	50	12)
V2021 Cyg	56158.5087	0.0019	AG	+0.0006		⟨23⟩	-I	29	12)

Table 1: (cont.)

Variable	HJD 24.....	±	Obs	$O-C$		Ref	Fil	n	Rem
V2181 Cyg	56158.5607	0.0001	FR	+0.0113		⟨59⟩	-I	39	12)
	56186.3757	0.0008	FR	+0.0124	s	⟨59⟩	-I	74	12)
V2240 Cyg	56229.3920	0.0015	RAT RCR	−0.0095	s	⟨23⟩	R	153	13)
V2280 Cyg	56159.4129	0.0014	SCI	+0.0039	s	⟨23⟩	o	36	5)
	56159.5894	0.0010	SCI	+0.0037		⟨23⟩	o	31	5)
V2282 Cyg	56175.4500	0.0031	SCI	+0.0082	s	⟨23⟩	o	143	5)
	56188.3811	0.0024	SCI	+0.0053		⟨23⟩	o	83	5)
V2282 Cyg	56188.5532	0.0028	SCI	+0.0094	s	⟨23⟩	o	83	5)
V2284 Cyg	56178.3848	0.0011	SCI	−0.0015	s	⟨23⟩	o	50	5)
	56178.5374	0.0013	SCI	−0.0024		⟨23⟩	o	50	5)
V2291 Cyg	56169.3520	0.0015	RAT RCR				R	74	13)
V2294 Cyg	56186.4070	0.0015	SCI	−0.0428		⟨23⟩	o	61	5)
	56186.5874	0.0022	SCI	−0.0396	s	⟨23⟩	o	53	5)
V2364 Cyg	56157.4702	0.0057	AG	−0.0099	s	⟨21⟩	-I	23	12)
V2546 Cyg	56188.4792	0.0032	AG				-I	30	12)
BG Del	56094.4922	0.0057	AG	+0.0827	s	⟨21⟩	-I	21	12)
EX Del	56094.4248	0.0013	AG	−0.0599		⟨21⟩	-I	22	12)
FZ Del	56151.3493	0.0012	DIE	−0.0359		⟨21⟩	o	25	17)
GG Del	56094.5021	0.0016	AG	−0.0267		⟨21⟩	-I	22	12)
Z Dra	56014.6080	0.0004	RAT RCR	+0.4851		⟨21⟩	-U-I	274	13)
	56061.4393	0.0004	AG	−0.1945		⟨21⟩	-I	34	12)
TZ Dra	56157.4565	0.0074	AG	−0.0330	s	⟨21⟩	-I	24	12)
WX Dra	56157.4151	0.0012	SCI	+0.0190		⟨21⟩	o	46	5)
BE Dra	56187.3351	0.0002	RAT RCR	−0.1081	s	⟨21⟩	R	125	13)
BV Dra	56187.4049	0.0017	AG	+0.0078	s	⟨21⟩	-I	34	12)
EF Dra	56181.3378	0.0004	RAT RCR	+0.1003		⟨29⟩	R	121	13)
FX Dra	56062.4275	0.0079	AG				-I	57	12)
KZ Dra	56176.4959	0.0002	RAT RCR				R	221	13)
OO Dra	56061.3904	0.0023	AG				-I	34	12)
OQ Dra	56061.3651	0.0008	AG				-I	34	12)
	56061.5356	0.0008	AG				-I	34	12)
V338 Dra	56062.4120	0.0004	AG	−0.0279	s	⟨21⟩	-I	57	12)
	56062.5297	0.0006	AG	−0.0278		⟨21⟩	-I	57	12)
V344 Dra	56062.4105	0.0019	AG				-I	57	12)
RZ Equ	56133.4662	0.0002	RAT RCR	−0.8192		⟨21⟩	-U-I	221	13)
SV Equ	56116.4739	0.0006	RAT RCR	−0.1076	s	⟨21⟩	-U-I	200	13)
V404 Gem	56001.2949:		QU	+0.0015	s	⟨61⟩	Ic	36	6)
	56001.4694	0.0005	QU	+0.0016		⟨61⟩	Ic	36	6)
	56002.3453	0.0006	QU	+0.0057	s	⟨61⟩	V	36	6)
V405 Gem	56001.3938	0.0010	QU	−0.0131		⟨63⟩	Ic	74	6)
	56002.3288	0.0025	QU	−0.0023		⟨63⟩	V	79	6)
TU Her	56094.4830	0.0018	AG	−0.2177		⟨21⟩	-I	60	12)
CT Her	56031.5055	0.0002	RAT RCR	+0.0073		⟨21⟩	-U-I	265	13)
	56065.4463	0.0003	AG	+0.0069		⟨21⟩	V	15	12)
DH Her	56072.4392	0.0032	AG	+0.0015		⟨21⟩	-I	26	12)
GU Her	56058.5809	0.0014	AG	+0.9047	s	⟨21⟩	V	66	12)
IT Her	56072.4041	0.0016	AG	+0.0372		⟨21⟩	-I	26	12)
PW Her	56062.4496	0.0030	AG	−0.4132		⟨46⟩	V	33	12)
V502 Her	56074.4525	0.0014	AG	+0.0263		⟨21⟩	-I	42	12)
	56094.3927	0.0010	AG	+0.0255		⟨21⟩	-I	59	12)
V607 Her	56058.5117	0.0170	AG	+0.1531		⟨21⟩	-I	35	12)
V643 Her	56072.3993	0.0076	AG	+0.2724		⟨21⟩	-I	26	12)
V719 Her	56132.5200	0.0022	AG	−0.0284	s	⟨21⟩	-I	30	12)
V722 Her	56132.4195	0.0055	AG	−0.0776		⟨21⟩	-I	30	12)
V728 Her	56070.4969	0.0004	RAT RCR	+0.0821	s	⟨26⟩	-U-I	196	13)
	56132.4748	0.0042	AG	+0.0858		⟨26⟩	-I	31	12)
V865 Her	56132.4249	0.0125	AG	−0.0075		⟨23⟩	-I	30	12)
V1033 Her	56058.4969	0.0013	AG	+0.0013	s	⟨23⟩	V	35	12)
V1035 Her	56061.4775	0.0001	RAT RCR	+0.0000		⟨23⟩	-U-I	245	13)

Table 1: (cont.)

Variable	HJD 24.....	±	Obs	$O-C$		Ref	Fil	n	Rem
V1036 Her	56058.4953	0.0025	AG	+0.0066	s	⟨23⟩	V	33	12)
V1037 Her	56058.4713	0.0043	AG				V	35	12)
V1047 Her	56094.4373	0.0046	AG	−0.0027		⟨23⟩	-I	60	12)
V1055 Her	56071.5280	0.0003	RAT RCR	+0.0037		⟨23⟩	-U-I	204	13)
	56132.4028	0.0018	AG	+0.0049		⟨23⟩	-I	31	12)
	56132.5631	0.0010	AG	+0.0075	s	⟨23⟩	-I	31	12)
V1062 Her	56132.3965	0.0010	AG	+0.0060	s	⟨23⟩	-I	31	12)
	56132.5191	0.0003	AG	+0.0029		⟨23⟩	-I	31	12)
V1071 Her	56157.3949	0.0003	AG	+0.0033	s	⟨23⟩	-I	23	12)
V1073 Her	56062.4466	0.0003	AG	−0.0037		⟨23⟩	V	24	12)
	56074.5118	0.0009	AG	−0.0040		⟨23⟩	-I	42	12)
	56157.5004	0.0014	AG	−0.0031		⟨23⟩	-I	21	12)
	56201.3476	0.0002	RAT RCR	−0.0039		⟨23⟩	R	117	13)
V1095 Her	56132.3725	0.0003	AG	−0.0293		⟨21⟩	-I	31	12)
V1096 Her	56132.4826	0.0007	AG	+0.0274		⟨21⟩	-I	31	12)
V1100 Her	56157.4614	0.0015	AG	+0.0760	s	⟨21⟩	-I	20	12)
V1103 Her	56062.5170	0.0009	AG	−0.0048		⟨21⟩	V	24	12)
	56172.3554	0.0003	RAT RCR	−0.0064		⟨21⟩	V	143	13)
V1105 Her	56062.4532	0.0017	AG	+0.0243		⟨21⟩	-I	24	12)
	56074.5179	0.0029	AG	+0.0251	s	⟨21⟩	-I	42	12)
SW Lac	56155.3830	0.0005	DIE	+0.0598	s	⟨21⟩	o	25	17)
	56206.3792	0.0006	AG	+0.0614	s	⟨21⟩	-I	46	12)
VV Lac	56188.3625	0.0053	AG	+0.8474	s	⟨21⟩	-I	27	12)
AG Lac	56157.4896	0.0065	AG	−0.0217		⟨21⟩	-I	51	12)
	56180.4284	0.0020	AG	−0.0244	s	⟨21⟩	-I	17	12)
	56187.5725	0.0071	AG	−0.0260		⟨21⟩	-I	41	12)
AI Lac	56157.4981	0.0024	AG				-I	51	12)
	56188.3888	0.0007	AG				-I	27	12)
AU Lac	56158.3828	0.0009	AG	−0.0301		⟨21⟩	-I	40	12)
CY Lac	56188.4920	0.0042	AG	+0.6683	s	⟨21⟩	-I	28	12)
DG Lac	56157.4532	0.0034	AG	−0.2268		⟨21⟩	-I	51	12)
EL Lac	56158.4894	0.0001	RAT RCR	+0.1292		⟨21⟩	R	121	13)
ER Lac	56167.4408	0.0023	AG	−0.5648		⟨21⟩	-I	34	12)
ES Lac	56180.5555	0.0007	RAT RCR	+0.1424		⟨21⟩	R	334	13)
EX Lac	56133.4801	0.0113	AG	+0.2385	s	⟨21⟩	-I	31	12)
EY Lac	56188.4684	0.0011	AG	−0.3585	s	⟨21⟩	-I	27	12)
FL Lac	56219.6260	0.0015	AG	−0.0445		⟨21⟩	-I	41	12)
FP Lac	56180.4271	0.0006	AG	+0.1564		⟨21⟩	-I	15	12)
GH Lac	56219.3590	0.0101	AG	−0.0830		⟨21⟩	-I	40	12)
	56219.6215	0.0010	AG	−0.0868	s	⟨21⟩	-I	40	12)
HR Lac	56133.4422	0.0025	AG	+0.1114		⟨21⟩	-I	32	12)
	56167.5481	0.0006	AG	+0.1060	s	⟨21⟩	-I	33	12)
IL Lac	56158.5327	0.0054	AG	−0.4712	s	⟨23⟩	-I	40	12)
IM Lac	56158.5965	0.0012	AG	−0.1903		⟨21⟩	-I	40	12)
IU Lac	56187.4357	0.0027	AG	+0.0139		⟨21⟩	-I	41	12)
KU Lac	56158.4736	0.0047	AG	+0.5146		⟨21⟩	-I	40	12)
MZ Lac	56157.5826	0.0037	AG	+0.2693	s	⟨21⟩	-I	51	12)
NR Lac	56133.5079	0.0018	AG	+0.0660		⟨21⟩	-I	32	12)
NW Lac	56167.4908	0.0083	AG	−0.1513		⟨21⟩	-I	33	12)
OS Lac	56187.5344	0.0047	AG	+0.3079	s	⟨21⟩	-I	41	12)
PP Lac	56167.4313	0.0023	AG	−0.0558	s	⟨21⟩	-I	33	12)
V339 Lac	56132.4553	0.0031	AG	+0.1407		⟨21⟩	-I	28	12)
V342 Lac	56167.4722	0.0038	AG	−0.0732	s	⟨21⟩	-I	34	12)
V345 Lac	56187.4977	0.0106	AG	+0.0763		⟨21⟩	-I	41	12)
V441 Lac	56187.4619	0.0013	AG	−0.0110		⟨38⟩	-I	41	12)
	56187.6135	0.0042	AG	−0.0139	s	⟨38⟩	-I	41	12)
V450 Lac	56219.4436	0.0315	AG				-I	40	12)
V458 Lac	56219.3369	0.0018	AG				-I	40	12)
Y Leo	56013.3436	0.0002	JU	−0.0252		⟨21⟩	o	46	5)

Table 1: (cont.)

Variable	HJD 24.....	±	Obs	$O-C$		Ref	Fil	n	Rem
XX LMi	56006.3839	0.0007	RAT RCR	+0.0083		⟨21⟩	-U-I	177	13)
XY LMi	55959.4056	0.0020	RAT RCR	−0.0224		⟨21⟩	-U-I	80	13)
	56006.3721	0.0002	RAT RCR	−0.0215	s	⟨21⟩	-U-I	175	13)
RZ Lyn	55988.3375	0.0009	JU	−0.1289		⟨21⟩	o	44	5)
SW Lyn	56019.4305	0.0002	AG	+0.0549		⟨21⟩	V	48	12)
CD Lyn	56019.4824	0.0035	AG	−0.0264		⟨35⟩	V	58	12)
DE Lyn	56003.3706	0.0004	JU	−0.0107		⟨23⟩	o	80	5)
DZ Lyn	56019.5329	0.0027	AG	−0.0135		⟨21⟩	V	49	12)
FO Lyn	55963.5420	0.0003	RAT RCR	+0.0181		⟨21⟩	-U-I	338	13)
FS Lyn	55962.5303	0.0018	RAT RCR				-U-I	291	13)
TZ Lyr	56157.3669	0.0001	AG	+0.0063		⟨21⟩	-I	23	12)
DF Lyr	56072.4875	0.0014	AG	+0.0324		⟨21⟩	-I	26	12)
GZ Lyr	56072.3790	0.0033	AG	+0.0045		⟨21⟩	-I	27	12)
HY Lyr	56062.5070	0.0025	AG				-I	24	12)
IP Lyr	56062.3964		AG	−0.0117	s	⟨21⟩	-I	24	12)
MN Lyr	56062.4509	0.0022	AG	+0.0488	s	⟨21⟩	-I	24	12)
MZ Lyr	56072.5013	0.0024	AG	−0.0081	s	⟨21⟩	-I	26	12)
OT Lyr	56072.5023	0.0093	AG	−0.0070	s	⟨21⟩	-I	24	12)
	56153.4680	0.0006	RAT RCR	−0.0696	s	⟨21⟩	R	166	13)
PS Lyr	56167.3762	0.0010	FR	+0.0215		⟨21⟩	V	40	15)
QU Lyr	56074.5016	0.0017	AG	+0.0017	s	⟨21⟩	-I	24	12)
V574 Lyr	56062.4523	0.0017	AG	+0.0029	s	⟨23⟩	-I	24	12)
	56073.5127	0.0001	RAT RCR	+0.0017		⟨23⟩	-U-I	207	13)
V579 Lyr	56177.4256	0.0014	JU	−0.0114		⟨23⟩	o	63	5)
V591 Lyr	56062.4119	0.0008	AG				-I	24	12)
	56062.5623	0.0003	AG				-I	24	12)
V392 Ori	55602.2770	0.0001	RAT RCR	+0.0017		⟨21⟩	-U-I	160	13)
V648 Ori	55858.5149	0.0001	RAT RCR	+0.0657	s	⟨21⟩	-U-I	225	13)
V1799 Ori	55859.4981	0.0001	RAT RCR				-U-I	241	13)
V1823 Ori	55592.3535	0.0002	RAT RCR				-U-I	232	13)
V1853 Ori	55601.2630	0.0003	RAT RCR				-U-I	107	13)
	55857.4885	0.0003	RAT RCR				-U-I	238	13)
U Peg	55859.2433	0.0002	RAT RCR	−0.0197		⟨53⟩	-U-I	85	13)
BB Peg	56212.2869	0.0009	DIE	−0.0098		⟨21⟩	o	25	17)
BG Peg	56154.3744	0.0035	PGL	+0.3622	s	⟨52⟩	V	131	11)
	56154.4155	0.0035	PGL	+0.4033	s	⟨52⟩	V	131	11)
	56157.3897	0.0035	PGL	+0.4490		⟨52⟩	V	73	11)
BY Peg	55807.3671	0.0002	RAT RCR	−0.0249	s	⟨21⟩	-U-I	147	13)
CC Peg	55807.3703	0.0020	RAT RCR	−0.0233	s	⟨37⟩	-U-I	145	13)
DK Peg	55858.3132	0.0001	RAT RCR	+0.1110		⟨21⟩	-U-I	215	13)
V365 Peg	55794.4385	0.0002	RAT RCR				-U-I	182	13)
V404 Peg	55820.5145	0.0001	RAT RCR	−0.0942		⟨21⟩	-U-I	300	13)
RT Per	55625.3218	0.0001	RAT RCR	+0.0715		⟨21⟩	-U-I	105	13)
	55849.5662	0.0008	FR	+0.0742		⟨21⟩	o	54	15)
WY Per	55614.3396	0.0001	RAT RCR	−0.1900		⟨21⟩	-U-I	202	13)
IU Per	55849.4647	0.0012	FR	+0.0069		⟨21⟩	o	42	15)
LX Per	56151.4636	0.0035	FR	−0.0613	s	⟨21⟩	-I	22	12)
	56187.6478	0.0010	FR	−0.0490		⟨21⟩	-I	73	12) 1)
V432 Per	55849.3930	0.0022	FR	−0.0345		⟨28⟩	o	50	15)
	55849.5905	0.0054	FR	−0.0287	s	⟨28⟩	o	50	15)
	55887.5332	0.0001	RAT RCR	−0.0339	s	⟨28⟩	-U-I	307	13)
V570 Per	56151.4459	0.0011	FR	+0.0055		⟨23⟩	-I	33	12)
	56187.5617	0.0006	FR	+0.0034		⟨23⟩	-I	44	12)
V873 Per	55849.4248	0.0017	FR				o	26	15)
	55849.5695	0.0023	FR				o	26	15)
V881 Per	55622.3877	0.0004	RAT RCR				-U-I	156	13)
V887 Per	55849.3237	0.0038	FR				o	49	15)
V912 Per	55623.3501	0.0002	RAT RCR				-U-I	207	13)
DV Psc	55796.5269	0.0001	RAT RCR				-U-I	192	13)

Table 1: (cont.)

Variable	HJD 24.....	±	Obs	$O-C$		Ref	Fil	n	Rem
DZ Psc	55866.3053	0.0002	RAT RCR				-U-I	129	13)
EX Psc	55496.5171	0.0004	RAT RCR				-U-I	182	13)
GR Psc	55805.4800	0.0003	RAT RCR				-U-I	171	13)
	55859.3606	0.0001	RAT RCR				-U-I	144	13)
GY Psc	55894.3335	0.0007	RAT RCR				-U-I	204	13)
RW PsA	56153.3412	0.0008	WLH HUN				-U-I	139	19)
V365 Sge	56094.4591	0.0012	AG	−0.0602		⟨21⟩	-I	23	12)
AO Ser	55662.5137	0.0001	RAT RCR	−0.0139		⟨21⟩	-U-I	261	13)
AS Ser	55689.4029	0.0005	RAT RCR	−0.0162		⟨21⟩	-U-I	0	13)
AU Ser	55654.5464	0.0001	RAT RCR	+0.0883	s	⟨21⟩	-U-I	220	13)
	56065.3904	0.0004	AG	+0.0819	s	⟨21⟩	V	15	12)
CC Ser	55691.3653	0.0003	RAT RCR	−0.0635		⟨21⟩	-U-I	103	13)
V1094 Tau	56272.3318	0.0104	PGL	+0.0419		⟨32⟩	o	295	16)
BC Tri	55806.5640	0.0005	RAT RCR				-U-I	239	13)
BX Tri	55866.4883	0.0004	RAT RCR				-U-I	142	13)
	55866.5833	0.0004	RAT RCR				-U-I	142	13)
TY UMa	55687.5253	0.0001	RAT RCR	−0.0547	s	⟨21⟩	-U-I	325	13)
VV UMa	55623.5125	0.0001	RAT RCR	−0.0492		⟨21⟩	-U-I	335	13)
XY UMa	55643.5030	0.0004	RAT RCR	+0.0382	s	⟨21⟩	-U-I	215	13)
XZ UMa	55642.5212	0.0001	RAT RCR	−0.1071		⟨21⟩	-U-I	270	13)
	55669.4114	0.0002	RAT RCR	−0.1080		⟨21⟩	-U-I	123	13)
DW UMa	56002.3852	0.0004	JU	+0.0000		⟨23⟩	o	79	5)
EQ UMa	55671.3721	0.0004	RAT RCR				-U-I	130	13)
HN UMa	55649.5538	0.0002	RAT RCR				-U-I	238	13)
KM UMa	55671.5210	0.0001	RAT RCR	+0.0007		⟨23⟩	-U-I	264	13)
LP UMa	56002.4221	0.0025	JU	+0.0027		⟨23⟩	o	79	5)
MQ UMa	55644.5823	0.0003	RAT RCR	+0.0793		⟨21⟩	-U-I	253	13)
	55669.5757	0.0004	RAT RCR	+0.0796	s	⟨21⟩	-U-I	238	13)
NV UMa	55670.5200	0.0002	RAT RCR				-U-I	312	13)
VW UMi	55627.6671	0.0002	RAT RCR	−0.0796	s	⟨21⟩	-U-I	345	13)
CG Vir	55690.4350	0.0001	RAT RCR	+0.1395	s	⟨21⟩	-U-I	161	13)
PS Vir	55629.3898	0.0003	RAT RCR				-U-I	101	13)
BB Vul	56149.4346	0.0007	SIR	+0.0000		⟨23⟩	o	22	8)
BE Vul	56153.3926	0.0002	RAT RCR	+0.0848		⟨21⟩	o	151	20)
BU Vul	56132.3992	0.0017	DIE	+0.0212		⟨21⟩	o	22	17)
DR Vul	56178.3494	0.0004	JU	+0.0832		⟨21⟩	o	50	5)
	56178.3504	0.0020	WTR	+0.0842		⟨21⟩	o	75	4)
ER Vul	56206.3331	0.0030	AG	+0.0193		⟨21⟩	-I	25	12)
FR Vul	56167.5639	0.0005	FR	−0.0028		⟨21⟩	V	81	15)
GN Vul	56074.4725	0.0073	AG	+0.0404		⟨21⟩	-I	24	12)
GP Vul	56203.4317	0.0017	AG	−0.0642		⟨21⟩	-I	40	12)
HI Vul	56203.3441	0.0032	AG	−0.0609		⟨21⟩	-I	42	12)
GSC 00104-01058	55953.3642	0.0005	FR				-I	52	12)
GSC 00279-00695	56002.3441	0.0008	FR				-I	102	12)
	56002.5234	0.0006	FR				-I	102	12)
GSC 00861-00252	56001.4945	0.0024	FR				V	50	15)
GSC 00863-00753	56001.4576	0.0033	FR				V	48	15)
GSC 01127-01808	56188.4346	0.0005	QU				V	33	6)
GSC 01315-01104	55592.3246	0.0003	RAT RCR				-U-I	232	13)
GSC 01360-01778	55957.5113	0.0008	FR				-I	52	12)
GSC 01438-01514	56001.5049	0.0062	FR				V	27	15)
GSC 01643-01880	56094.4471	0.0018	AG				-I	22	12)
GSC 01920-01922	56013.4084	0.0039	FR				o	37	15)
GSC 01922-01415	56003.4179	0.0008	FR				V	44	15)
GSC 01939-00891	56013.4036	0.0013	FR				o	40	15)
GSC 02452-02005	56003.5199	0.0016	FR				V	44	15)
GSC 02454-00681	56003.3839	0.0021	FR				V	45	15)
	56003.5574	0.0022	FR				V	45	15)
	56013.3780	0.0022	FR				o	40	15)

Table 1: (cont.)

Variable	HJD 24.....	±	Obs	$O-C$		Ref	Fil	n	Rem
GSC 02454-01430	56003.4135	0.0040	FR				V	45	15)
GSC 02458-01669	56003.3964	0.0015	FR				V	46	15)
	56003.5461	0.0036	FR				V	46	15)
GSC 02461-00856	56003.3155	0.0003	FR				V	32	15)
GSC 02469-00087	56013.3030	0.0005	FR				o	40	15)
	56013.5081	0.0017	FR				o	40	15)
GSC 02474-00423	56013.4103	0.0023	FR				o	38	15)
GSC 02483-00686	56013.5012	0.0025	FR				o	44	15)
GSC 02610-00088	56074.4431	0.0149	AG	−0.0145		⟨45⟩	-I	42	12)
GSC 02677-00838	55833.3045	0.0005	FR				-I	41	12)
	55833.4788	0.0006	FR				-I	41	12)
	56152.4170	0.0003	FR				-I	34	12)
	56152.5854	0.0004	FR				-I	34	12)
GSC 02746-00463	56159.4324	0.0043	FR				o	33	15)
GSC 02757-01475	55820.5410	0.0007	RAT RCR				-U-I	290	13)
GSC 02797-01241	56220.3268	0.0038	AG				-I	31	12)
	56220.4660	0.0010	AG				-I	31	12)
GSC 02855-00949	55849.5118	0.0041	FR				o	24	15)
GSC 02869-00639	55849.3808	0.0016	FR				o	22	15)
	55849.5604	0.0026	FR				o	22	15)
GSC 02903-00067	55953.4948	0.0023	FR				V	34	15)
GSC 02933-01972	56001.3584	0.0012	JU				o	70	5)
GSC 03110-00482	56094.4678	0.0006	FR				o	17	15)
	56132.4125	0.0027	FR				o	30	15)
GSC 03111-00566	56094.4654	0.0010	FR				o	27	15)
GSC 03200-01298	56159.5928	0.0013	FR				o	75	15)
GSC 03205-01788	56159.3884	0.0010	FR				o	73	15)
GSC 03205-02277	56159.4888	0.0007	FR				o	36	15)
GSC 03223-01180	56159.4227	0.0010	FR				o	36	15)
	56159.5569	0.0008	FR				o	36	15)
GSC 03344-01247	55953.3260	0.0006	FR				V	34	15)
	55953.5057	0.0005	FR				V	34	15)
GSC 03373-01033	55978.4191	0.0016	FR				V	24	15)
GSC 03573-01677	55851.4772	0.0003	FR				o	43	15)
GSC 03578-00263	55874.3285	0.0062	FR				o	36	15)
GSC 03579-00488	55851.3906	0.0025	FR				o	46	15)
GSC 03581-01856	55874.3864	0.0010	FR				o	17	15)
GSC 03583-00309	55851.4049	0.0024	FR				o	46	15)
GSC 03590-01714	55857.4720	0.0029	FR				o	51	15)
GSC 03612-00014	56133.4876	0.0102	AG	+0.0012	s	⟨44⟩	-I	32	12)
	56187.3262	0.0017	AG	+0.0055		⟨44⟩	-I	42	12)
GSC 03618-00162	56167.4757	0.0034	AG	+0.0116		⟨44⟩	-I	34	12)
GSC 03619-00047	56132.5311	0.0025	AG	+0.0095		⟨44⟩	-I	28	12)
	56167.4438	0.0061	AG	+0.0095		⟨44⟩	-I	34	12)
GSC 03619-00715	56132.4100	0.0046	AG	+0.1023		⟨45⟩	-I	28	12)
GSC 03635-01628	56238.3097	0.0033	JU				o	53	5)
GSC 03748-00162	55978.5235	0.0013	FR				V	40	15)
GSC 03749-01263	55978.5995	0.0007	FR				V	36	15)
GSC 03983-00544	56180.3776	0.0009	RAT RCR				R	167	13)
	56180.5826	0.0011	RAT RCR				R	167	13)
GSC 04031-00546	56167.4749	0.0018	AG				-I	29	12)
GSC 04038-00816	55879.4187	0.0059	FR				o	43	15)
GSC 04043-01123	55878.5383	0.0026	FR				o	57	15)
	55879.3056	0.0030	FR				o	43	15)
GSC 04045-00231	55878.3464	0.0019	FR				o	63	15)
GSC 04045-00446	55878.3242	0.0019	FR				o	20	15)
	55878.4805	0.0027	FR				o	20	15)
	55878.6444	0.0023	FR				o	20	15)
	55879.2764	0.0004	FR				o	56	15)

Table 1: (cont.)

Variable	HJD 24.....	±	Obs	$O-C$		Ref	Fil	n	Rem
GSC 04297-01593	55878.3303	0.0015	FR				o	62	15)
	55878.5995	0.0069	FR				o	62	15)
	55879.3798	0.0024	FR				o	37	15)
GSC 04479-00391	55774.4788	0.0010	SIR				o	225	8)
GSC 04497-00283	56167.4994	0.0065	AG				-I	27	12)
GSC 04585-02642	56206.4432	0.0023	AG				-I	86	12)
GSC 04826-02102	55970.3528	0.0004	FR				-I	63	12)
GSC 04922-00133	56001.2957	0.0021	FR				-I	98	15)
NSVS 109935	56188.3577	0.0021	AG				-I	30	12)
NSVS 1541003	56219.5760	0.0025	AG				-I	47	12)
NSVS 1841163	56220.3268	0.0054	AG				-I	28	12)
NSVS 1929858	56167.5735	0.0059	AG				-I	29	12)
NSVS 2791123	56187.3397	0.0065	AG				-I	40	12)
NSVS 2871290	56062.3799	0.0022	AG				-I	57	12)
	56187.4093	0.0125	AG				-I	43	12)
NSVS 366701	56220.4445	0.0035	AG				-I	28	12)
NSVS 437746	56188.3462	0.0023	AG				-I	28	12)
U-A2 1125-18642389	55807.4245	0.0030	RAT RCR				-U-I	137	13)
U-B1 1398-0469064	56219.4224	0.0025	AG	−0.0493	s	⟨44⟩	-I	38	12)
	56219.5881	0.0015	AG	−0.0462		⟨44⟩	-I	38	12)
U-B1 1400-0455467	56187.4262	0.0044	AG	−0.0473		⟨45⟩	-I	41	12)
U-B1 1416-0454010	56132.4336	0.0038	AG				-I	28	12)
	56157.5049	0.0024	AG				-I	51	12)
	56158.4451	0.0017	AG				-I	40	12)
	56158.5980	0.0008	AG				-I	40	12)
	56167.3759	0.0014	AG				-I	34	12)
	56167.5348	0.0020	AG				-I	34	12)
	56180.3832	0.0020	AG				-I	15	12)
	56188.3758	0.0029	AG				-I	28	12)
U-B1 1440-0411990	56180.3780	0.0041	AG				-I	18	12)
U-B1 1500-0005759	56133.4956	0.0038	AG				-I	45	12)
U-B1 1503-0282065	56072.4190	0.0024	AG				-I	47	12)

Table 2: Times of maxima of pulsating stars

Variable	HJD 24.....	±	Obs	$O-C$	Ref	Fil	n	Rem
XX And	56220.414	0.001	AG	+0.029	⟨56⟩	-I	31	12)
GP And	56238.3748	0.0035	PGL	−0.0324	⟨21⟩	o	49	16)
	56239.2403	0.0035	PGL	−0.0324	⟨21⟩	o	91	16)
BS Aqr	56179.4267	0.0018	FLG	+0.0160	⟨21⟩	V	94	10)
CY Aqr	55451.3884	0.0001	NIC	−0.0024	⟨21⟩	C	50	6)
AA Aql	56181.4239	0.0011	FLG	+0.0050	⟨47⟩	V	119	10)
eta Aql	56007.00		VLM	−0.01	⟨21⟩	o	78	15)
UU Boo	56069.452	0.001	AG	+0.005	⟨22⟩	V	30	12)
YZ Boo	56069.441	0.001	AG	+0.008	⟨21⟩	V	29	12)
	56069.543	0.001	AG	+0.005	⟨21⟩	V	29	12)
	56119.4008	0.0008	WLH	+0.0034	⟨21⟩	o	68	18)
NT Cam	56019.445	0.002	AG	+0.024	⟨21⟩	-I	30	12)
	56019.523	0.002	AG	+0.020	⟨21⟩	-I	30	12)
	56019.602	0.002	AG	+0.016	⟨21⟩	-I	30	12)
EF Cnc	56001.4818	0.0030	MZ			-U-I	214	6)
	56010.3541	0.0030	MZ			-U-I	231	6)
ST CVn	56069.478	0.001	AG	−0.138	⟨58⟩	-I	26	12)
XY CVn	56069.409	0.002	AG	−0.046	⟨21⟩	-I	26	12)
AP CVn	56073.3997	0.0013	MZ	−0.2551	⟨21⟩	-U-I	98	6)
BR Cas	55083.3403	0.0013	MZ	−0.3022	⟨21⟩	-U-I	52	6)
	55828.4656	0.0010	MZ	+0.2774	⟨21⟩	-U-I	105	6)
	55881.3912	0.0013	MZ	+0.2818	⟨21⟩	-U-I	152	6)
	56201.3412	0.0013	MZ	+0.2718	⟨21⟩	-U-I	180	6)
	56210.4625	0.0013	MZ	+0.2688	⟨21⟩	-U-I	132	6)

Table 2: (cont.)

Variable	HJD 24.....	±	Obs	$O-C$	Ref	Fil	n	Rem
QY Cas	55837.4842	0.0020	MZ	−0.1398	⟨21⟩	-U-I	92	6)
	55856.4092	0.0010	MZ	−0.1148	⟨21⟩	-U-I	107	6) 3)
	55887.3512	0.0014	MZ	−0.1688	⟨21⟩	-U-I	65	6) 2)
	55887.3851	0.0040	MZ	−0.1349	⟨21⟩	-U-I	65	6) 3)
	55943.2712	0.0019	MZ	+0.1852	⟨21⟩	-U-I	59	6) 2)
	55943.3051	0.0016	MZ	−0.1589	⟨21⟩	-U-I	59	6) 3)
	55960.2687	0.0016	MZ	+0.1727	⟨21⟩	-U-I	63	6) 2)
	55960.2973	0.0035	MZ	−0.1767	⟨21⟩	-U-I	63	6) 3)
	55969.3178	0.0010	MZ	+0.1498	⟨21⟩	-U-I	73	6) 2)
	55969.3535	0.0016	MZ	+0.1855	⟨21⟩	-U-I	73	6) 3)
	56143.3894	0.0013	MZ	−0.0366	⟨21⟩	-U-I	57	6) 2)
	56143.4263	0.0013	MZ	+0.0003	⟨21⟩	-U-I	57	6)
	56152.4443	0.0016	MZ	−0.0537	⟨21⟩	-U-I	76	6) 2)
	56152.4673	0.0010	MZ	−0.0307	⟨21⟩	-U-I	76	6) 3)
V363 Cas	56133.394	0.001	AG	+0.108	⟨57⟩	-I	43	12)
V1041 Cas	56159.528	0.001	AG			-I	37	12)
V1057 Cas	55879.515	0.003	FR			o	39	15)
V1057 Cas	56219.450	0.001	AG			-I	49	12)
RZ Cep	56058.422	0.002	AG	−0.132	⟨21⟩	-I	48	12)
	56157.4871	0.0010	MZ	+0.1535	⟨21⟩	-U-I	60	6) 2)
	56157.5227	0.0011	MZ	−0.1196	⟨21⟩	-U-I	60	6) 3)
	56206.293	0.001	AG	−0.122	⟨21⟩	-I	55	12)
delta Cep	56027.24		VLM	−0.26	⟨21⟩	o	123	15)
TX Com	56074.4256	0.0013	MZ			-U-I	82	6)
RV CrB	56095.4319	0.0010	ALH	−0.0007	⟨21⟩	V	299	7) 2)
XX Cyg	56159.5321	0.0009	NIC	+0.0036	⟨21⟩	V	100	6)
NS Cyg	55830.5139	0.0010	MZ	+0.2111	⟨21⟩	-U-I	63	6)
	55834.3599	0.0016	MZ	+0.2050	⟨21⟩	-U-I	60	6)
	56168.4241	0.0013	MZ	+0.2371	⟨21⟩	-U-I	87	6)
	56211.3446	0.0014	MZ	+0.2342	⟨21⟩	-U-I	121	6)
V791 Cyg	56167.554	0.004	FR	−0.098	⟨21⟩	-I	88	12)
V881 Cyg	56179.465	0.002	FR	−0.083	⟨21⟩	-I	47	12)
V882 Cyg	56179.435	0.002	FR	−0.008	⟨21⟩	-I	47	12)
V1369 Cyg	56172.3921	0.0013	MZ	−0.1024	⟨21⟩	-U-I	119	6)
V1719 Cyg	55874.338	0.002	FR	−0.062	⟨21⟩	o	38	15)
	56158.477	0.001	AG	−0.062	⟨21⟩	-I	29	12)
	56206.324	0.001	AG	−0.062	⟨21⟩	-I	60	12)
V1962 Cyg	56180.3441	0.0014	MZ	−0.0336	⟨64⟩	-U-I	89	6)
V2470 Cyg	56101.4316	0.0011	MZ			-U-I	109	6)
CV Del	56179.4300	0.0010	MZ	−0.0506	⟨21⟩	-U-I	167	6)
VZ Dra	56062.408	0.002	AG	+0.069	⟨21⟩	-I	57	12)
NZ Dra	56061.401	0.001	AG			-I	34	12)
SX For	56155.5723	0.0002	WLH HUN	+0.0079	⟨21⟩	-U-I	142	9)
SZ Gem	56274.4078	0.0007	QU	+0.0114	⟨55⟩	V	90	6)
TW Her	56157.386	0.001	AG	−0.010	⟨21⟩	-I	20	12)
LS Her	56065.422	0.001	AG	+0.028	⟨21⟩	V	15	12)
V545 Her	56058.482	0.001	AG	+0.133	⟨21⟩	-I	35	12)
V686 Her	56065.453	0.002	AG			-I	15	12)
V718 Her	53849.458	0.001	AG	+0.025	⟨21⟩	-I	23	4)
	56132.478	0.001	AG	+0.123	⟨21⟩	-I	31	12)
V725 Her	56132.564	0.001	AG			-I	31	12)
V862 Her	56076.4792	0.0030	MZ			-U-I	119	6)
RV Leo	56009.4067	0.0010	MZ	−0.0556	⟨21⟩	-U-I	135	6)
DL Leo	56013.3645	0.0018	MZ	+0.0437	⟨25⟩	-U-I	119	6)
TV Lyn	56019.562	0.003	AG	+0.025	⟨21⟩	-I	49	12)
TW Lyn	56019.528	0.001	AG	+0.061	⟨21⟩	-I	46	12)
AN Lyn	56006.3442	0.0021	PGL			V	137	11)
	56046.4426	0.0014	PGL			V	149	11)
ZZ Lyr	56223.3472	0.0013	MZ	−0.0115	⟨21⟩	-U-I	59	6)

Table 2: (cont.)

Variable	HJD 24.....	±	Obs	$O-C$	Ref	Fil	n	Rem
DD Lyr	55848.2960	0.0016	MZ	−0.1388	⟨21⟩	-U-I	42	6)
	56096.4598	0.0018	MZ	−0.1381	⟨21⟩	-U-I	117	6)
	56162.4139	0.0013	MZ	−0.1373	⟨21⟩	-U-I	162	6)
	56228.3647	0.0018	MZ	−0.1397	⟨21⟩	-U-I	91	6)
EX Lyr	56158.4050	0.0013	MZ	−0.0623	⟨21⟩	-U-I	170	6)
QV Lyr	56157.4034	0.0008	MZ	+0.1152	⟨21⟩	-U-I	85	6)
BH Peg	56144.4031	0.0035	PGL	−0.0308	⟨54⟩	V	379	11)
	56151.4591	0.0035	PGL	−0.0257	⟨54⟩	V	311	11)
DH Peg	56251.3282	0.0104	PGL	+0.0404	⟨21⟩	o	84	16)
	56252.3297	0.0069	PGL	+0.0199	⟨21⟩	o	147	16)
DY Peg	56174.4245	0.0035	PGL	−0.0103	⟨21⟩	-I	49	16)
	56180.4024	0.0005	FLG	−0.0123	⟨21⟩	V	111	10)
	56180.4751	0.0004	FLG	−0.0126	⟨21⟩	V	111	10)
V398 Peg	56177.4990	0.0018	MZ	+0.0851	⟨21⟩	-U-I	144	6)
AN Per	56187.548	0.004	FR	+0.293	⟨21⟩	-I	45	12)
V378 Per	56223.4629	0.0008	MZ	+0.0977	⟨21⟩	-U-I	73	6)
BH Ser	56110.4547	0.0009	MZ	+0.1147	⟨21⟩	-U-I	129	6)
BT Ser	56134.4574	0.0020	MZ	−0.1080	⟨21⟩	-U-I	118	6)
	56150.3765	0.0015	MZ	−0.1449	⟨21⟩	-U-I	128	6)
V475 Ser	56065.453	0.001	AG			V	15	12)
AE UMa	55993.3036	0.0005	NIC	+0.0016	⟨56⟩	C	50	6)
	55993.3871	0.0005	NIC	−0.0010	⟨56⟩	C	50	6)
GSC 01935-01030	56013.3682	0.0042	FR			o	39	15)
GSC 01938-01628	56013.398	0.002	FR			o	39	15)
GSC 02670-04008	56158.557	0.002	FR	+0.011	⟨45⟩	-I	56	12)
	56186.386	0.002	FR	−0.046	⟨45⟩	-I	71	12)
GSC 02671-02149	56158.506	0.003	FR	−0.042	⟨45⟩	-I	47	12)
	56186.444	0.003	FR	+0.029	⟨45⟩	-I	54	12)
GSC 03092-01411	56157.460	0.002	AG			-I	20	12)
GSC 03577-02495	55851.503	0.003	FR			o	51	15)
GSC 03682-00018	55858.579	0.001	AG			-I	61	12)
	55859.380	0.001	AG			-I	54	12)
GSC 03755-00845	56319.3291	0.0069	PGL			V	158	16)
	56324.4261	0.0028	PGL			V	98	16)
GSC 03986-01266	56167.445	0.001	AG			-I	33	12)
GSC 04372-00436	55591.414	0.001	AG			-I	30	12)
	55591.595	0.001	AG			-I	32	12)
	55887.255	0.001	AG			-I	41	12)
	55887.530	0.001	AG			-I	32	12)
GSC 04433-00827	56181.3105	0.0030	RAT RCR			R	61	13)
	56181.3656	0.0030	RAT RCR			R	61	13)
TYC 1698-01052-1	56151.3888	0.0035	PGL			V	156	11)
	56151.4123	0.0035	PGL			V	156	11)
	56154.3891	0.0035	PGL			V	259	11)
U-B1 1422-0506537	56132.412	0.002	AG	+0.004	⟨45⟩	-I	28	12)
	56132.521	0.002	AG	+0.000	⟨45⟩	-I	28	12)
	56157.482	0.001	AG	+0.013	⟨45⟩	-I	51	12)
U-B1 1424-0504416	56132.501	0.002	AG	−0.049	⟨45⟩	-I	28	12)
	56157.489	0.001	AG	−0.006	⟨45⟩	-I	51	12)

Observers:

AG:	Agerer, F., Tiefenbach	PGL:	Pagel, Dr. L., Klockenhagen
ALH:	Alich, K., Schaffhausen	QU:	Quester, W., Esslingen
DIE:	Dietrich, M., Radebeul	RAT:	Rätz, M., Herges-Hallenberg
FLG:	Flechsig, Dr. G., Teterow	RCR:	Rätz, K., Herges-Hallenberg
FR:	Frank, P., Velden	SCI:	Schmidt, U., Karlsruhe
HUN:	Hunger, T., Warstein	SIR:	Schirmer, J., Willisau
JU:	Jungbluth, H., Karlsruhe	VLM:	Vollmann, W., Wien
MZ:	Maintz, Dr. G., Bonn	WLH:	Wollenhaupt, G., Oberwiesenthal
NIC:	Nickel, O., Mainz	WTR:	Walter, F., München

Remarks:

n	number of measurements
:	uncertain
s	secondary minimum
(1)	normal maximum
(2)	double maximum: time of the first maximum
(3)	double maximum: time of the second maximum
	Photometer
(4)	CCD camera ST-6: chip 375*242 uncoated
(5)	CCD camera ST-7
(6)	CCD camera ST-7E
(7)	CCD camera ST-8 XMEI
(8)	CCD camera ST-8 XME
(9)	CCD camera ST-7 XE
(10)	CCD camera Sigma 402: chip KAF0402ME
(11)	CCD camera Artemis 4021
(12)	CCD camera Sigma 1603
(13)	CCD camera Moravian G2-1600
(14)	CCD camera QHY8
(15)	CCD camera Canon EOS 450D
(16)	CCD camera Canon EOS1000D
(17)	CCD camera ATIK 314 L+
(18)	CCD camera SBIG STL-11000 M
(19)	CCD camera Nova 402
(20)	CCD camera ST-8
	Filter
o	without filter
V	V-filter
R	R-filter
Ic	I-filter cousins
-I	IR cut-off filter
-U-I	U and IR cut-off filter
C	Clearfilter

References:

Achterberg, H., Agerer, F., 2005, *BAV Rb.*, **54**, 105, http://www.bavdata-astro.de/rb/RB2005/seite105.html ⟨61⟩
Agerer, F., 1992, *IBVS*, No. 3797 (*BAV Mitt.*, **61**) ⟨28⟩
Agerer, F., 1994, *IBVS*, No. 4133 (*BAV Mitt.*, **73**) ⟨30⟩
Agerer, F., 2001, *IBVS*, No. 5024 (*BAV Mitt.*, **135**) ⟨38⟩
Agerer, F., 2010, *PZP*, **10**, 4. ⟨44⟩
Agerer, F., 2010, *PZP*, **10**, 13. ⟨45⟩
Agerer, F. et al., 1988, *IBVS*, No. 3234 (*BAV Mitt.*, **51**) ⟨26⟩
Agerer, F. et al., 1991, *IBVS*, No. 3554 (*BAV Mitt.*, **55**) ⟨27⟩
Agerer, F., et al., 1999, *IBVS*, No. 4798 (*BAV Mitt.*, **116**) ⟨34⟩
Agerer, F., et. al., 2001, *IBVS*, No. 5017 (*BAV Mitt.*, **133**) ⟨37⟩
Agerer, F., Hübscher, J., 2001, *IBVS*, No. 5016 (*BAV Mitt.*, **132**) ⟨36⟩
Agerer, F., Quester, W., 2008, *BAV Rb.*, **57**, 232. ⟨63⟩
Baldwin, M.E., 2000, *IBVS*, No. 4911 ⟨35⟩
BAV Services for Scientists, 2013, http://www.bav-astro.de/sfs/index.php?sprache=en&sprache_dial=de
Le Borgne, J. F., et. al., 2007, *A&A.*, **476**, 307. ⟨22⟩
Dahm, M., 1996, *BAV Rb.*, **45**, 3, http://www.bavdata-astro.de/rb/RB1996/seite3.html ⟨53⟩
Dahm, M., 2000, *BAV Rb.*, **49**, 41, http://www.bavdata-astro.de/rb/RB2000-2/seite41.html ⟨57⟩
Dahm, M., Kleikamp, W., 1998, *BAV Rb.*, **47**, 67, http://www.bavdata-astro.de/rb/RB1998/seite67.html ⟨54⟩
Dahm, M., Kleikamp, W., 1999, *BAV Rb.*, **48**, 189, http://www.bavdata-astro.de/rb/RB1999-4/seite189.html ⟨56⟩
Dahm, M., Paschke, A., 2000, *BAV Rb.*, **49**, 105, http://www.bavdata-astro.de/rb/RB2000-3/seite105.html ⟨58⟩
Frank, P., et. al., 1996, *IBVS*, No. 4386 (*BAV Mitt.*, **88**) ⟨31⟩
Hambsch, F., Husar, D., 2006, *BAV Rb.*, **55**, 106, http://www.bavdata-astro.de/rb/RB2006-3/106.html ⟨62⟩
Huisong, T., 1984, *IBVS*, No. 2533 ⟨25⟩
Hübscher, J., et al., 1992, *IBVS*, No. 3811 (*BAV Mitt.*, **63**) ⟨29⟩
Hübscher, J., et al., 1994, *BAV Mitt.*, **68**, http://www.bav-astro.de/sfs/mitteilungen/BAVM068.pdf ⟨46⟩
Hübscher, J., et al., 2006, *BAV Mitt.*, **178**, http://www.bav-astro.de/sfs/mitteilungen/BAVM178.pdf ⟨48⟩
Kaiser, D. H., et. al., 1998, *IBVS*, No. 4544 ⟨32⟩
Kämper, B., 1983, *BAV Rb.*, **32**, 122, http://www.bavdata-astro.de/rb/RB1983/seite122.html ⟨50⟩
Kreiner, J. M., 2004, *Acta Astr.*, **54**, 207. ⟨23⟩
Lichtenknecker, D., 1983, *BAV Rb.*, **32**, 36, http://www.bavdata-astro.de/rb/RB1983/seite36.html ⟨49⟩
Lichtenknecker, D., 1938 *BAV Rb.*, **37**, 24, http://www.bavdata-astro.de/rb/RB1988/seite24.html ⟨52⟩
Lichtenknecker Database of the BAV http://www.bav-astro.de/LkDB/index.php?lang=en&sprache_dial=de
Lloyd, C., et. al., 2002, *IBVS*, No. 5260 (*BAV Mitt.*, **150**) ⟨39⟩
Maintz, G., 2010, *BAV Rb.*, **59**, 236. http://www.bavdata-astro.de/rb/RB2010-4/236.html ⟨64⟩
Otero, S., et. al., 2004, *IBVS*, No. 5557 ⟨40⟩
Samus, N .N., et. al., 2011, http://www.sai.msu.su/gcvs/gcvs/index.htm ⟨21⟩
Sandberg, C., et. al., 1999, *IBVS*, No. 4737 ⟨33⟩
Wunder, E., 1995, *BAV Mitt.*, **78**, http://www.bav-astro.de/sfs/mitteilungen/BAVM078.pdf ⟨47⟩
Quester, W., 1999, *BAV Rb.*, **48**, 65, http://www.bavdata-astro.de/rb/RB1999/seite65.html ⟨55⟩
Quester, W., Frank, P., 2001, *BAV Rb.*, **50**, 45, http://www.bavdata-astro.de/rb/RB2001/seite45.html ⟨59⟩

Quester, W., Jungbluth, H, 2002, *BAV Rb.*, **51**, 1, http://www.bavdata-astro.de/rb/RB2002/seite1.html ⟨60⟩

ERRATUM FOR IBVS 6010 (BAVM 220)

AB Cas	55463.4821 PGL	has to be deleted
WZ Boo	55703.5169 MZ	has to be deleted
WZ Boo	55714.4861 MZ	has to be deleted

ERRATUM FOR IBVS 6070 (BAVM 231)

V366 Cas	56158.434 AG	has to be deleted

COMMISSIONS 27 AND 42 OF THE IAU
INFORMATION BULLETIN ON VARIABLE STARS

Number 6071

Konkoly Observatory
Budapest
19 August 2013

HU ISSN 0374 – 0676

TIME-SERIES PHOTOMETRY OF THE SYMBIOTIC NOVA NSV 11749 AND NEW VARIABLE STARS IN AQUILA

WEHRUNG, M.[1]; LAYDEN, A.[1]; ROGEL, A.[1]; REICHART, D.[2]; IVARSEN, K.[2]; HAISLIP, J.[2]; NYSEWANDER, M.[2]; LACLUYZE, A.[2]

[1] Physics & Astronomy Department, Bowling Green State University, Bowling Green, OH 43403, USA

[2] Department of Physics & Astronomy, University of North Carolina, Chapel Hill, NC, USA

The ChaMPlane project (Grindlay *et al.* 2005) is a survey to detect and optically identify low-luminosity X-ray point sources in the Galactic plane, with the goal of characterizing the Galactic distribution of accretion-powered sources such as X-ray binaries and cataclysmic variable (CV) stars. X-ray data were collected from archival deep (> 20 ks) Galactic plane ($|b| < 12^\circ$) fields, while photometric V, R, I, and $H\alpha$ data were obtained using CTIO and KPNO 4.0 m telescopes. Multi-fiber spectroscopy was obtained of stars with Hα excesses to separate CVs from other objects such as chromospherically active red dwarfs based on Doppler broadening of the Hα line (Rogel *et al.* 2006). A number of potential CV candidates were found, including a bright one with $R \approx 14$ mag which coincided with the emission object HBHA -0201-01 (Kohoutek & Wehmeyer 1997). Figure 1 shows the spectrum of this star taken with the WIYN 3.5 m telescope. The hydrogen and helium emission lines are overlaid on a very late-type stellar continuum, indicating a hot source in proximity to a cool star, suggestive of a CV or other accretion-powered system.

Meanwhile, Williams (2005) presented a significantly revised position of NSV 11749, a star discovered to be variable by Luyten (1937). This position corresponds to the CV candidate discussed above. Williams derived photometry from plates in the Harvard collection, showing an outburst *circa* 1903 reaching a photographic magnitude of 12.5, then slowly fading to go below the plate limit, $m_{pg} \approx 15$ mag, by 1912. It remained below this limit through 1988, the end of the plate sequence, though it was detected on a few deeper plates at $\sim$17 mag. Based on this outburst, Williams suggested that NSV 11749 is either a slow nova or a FU Orionis pre-main sequence star.

Miller Bertolami *et al.* (2011) compared the outburst light curve of NSV 11749 with the outbursts of V605 Aql and V4334 Sgr, two objects widely accepted as "born-again" asymptotic giant branch (AGB) stars. In these stars, a very late thermal pulse ignites helium burning in a star transitioning from the AGB to the top of the white dwarf sequence, causing the star to return temporarily to the tip of the AGB. Based on light curve similarities and fits of thermal pulse models to the observations, Miller Bertolami *et al.* (2011) suggested that NSV 11749 is also a born-again AGB star. Bond & Kasliwal (2012, hereafter "BK12") presented optical and infrared spectra of NSV 11749 showing Balmer and helium emission lines on a continuous spectrum of a late type star (they estimated M1-M2 III spectral type), much like our Figure 1. These spectra contrast

sharply with that of the born-again star V605 Aql by Clayton *et al.* (2006), which shows high excitation lines of helium, carbon and oxygen, indicative of a hot, compact, hydrogen-poor object. While both objects underwent outbursts about a century ago, these recent spectra show that the born-again AGB star has returned to its former state as a young white dwarf, albeit dust-enshrouded, while NSV 11749 has the spectral characteristics of an accreting compact binary. Thus, BK12 clearly showed that NSV 11749 is not a born-again AGB star.

BK12 argued that NSV 11749 is a symbiotic star, a compact object (likely a white dwarf) accreting matter from a giant star, rather than a dwarf star in a traditional cataclysmic variable.[1] They based this distinction on the presence of the broad emission feature at 6825 Å due to Raman scattering by neutral hydrogen, a feature only seen in symbiotic stars (hereafter "SSs"). Unfortunately, this feature is just off the red end of our spectrum, so we cannot confirm its presence. However, our spectrum has much higher signal-to-noise ratio than that of BK12, enabling us to see more clearly the bands of molecular titanium oxide in the stellar continuum. The lower panel of Figure 1 shows our spectrum divided by template spectra of M3, M4, and M5 III stars from Pickles (1998). A spectrum between M3 and M4 provides the best match, leaving little residual signature of the TiO bands. A smoothed version of the resulting curve is the inverse of the function needed to flux-calibrate our original spectrum, convolved with the interstellar reddening function.

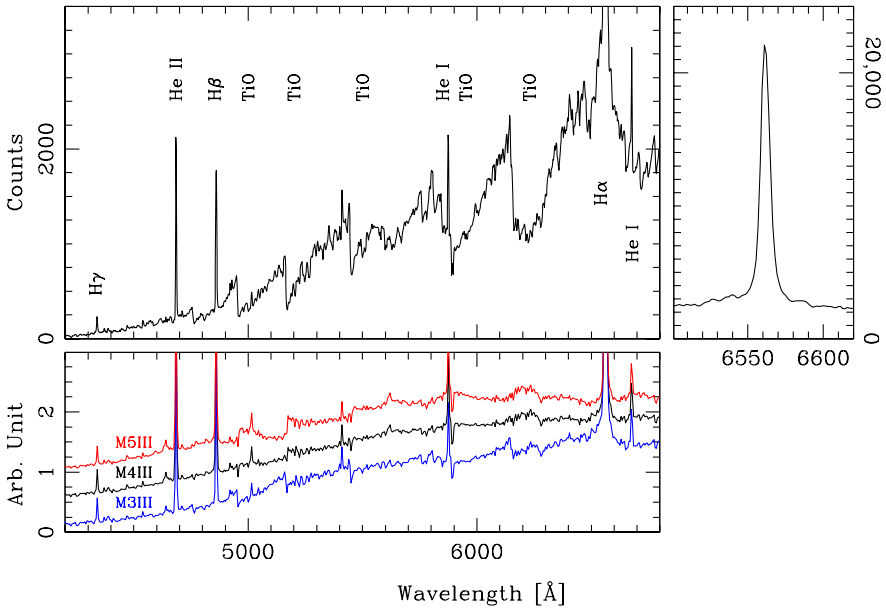

Figure 1. Top-left: the ChaMPlane spectrum of NSV 11749 (not flux calibrated). **Top-right:** a detail of the Hα line. **Bottom:** the NSV 11749 spectrum divided by template spectra of M3, M4, and M5 III stars (lower, middle, and upper curves, respectively).

BK12 matched their spectra with templates of M1 and M2 giants using a reddening function for $E(B-V) = 0.75$ mag. Had they used an M3 or M4 template, a lower reddening would be needed, trending toward the value of $E(B-V) = 0.67$ mag given by the dust maps of Schlegel, Finkbeiner & Davis (1998) at the location of NSV 11749,

[1]The powerful outburst of 1903 resembles the 1980 outburst of the symbiotic nova PU Vul shown in Figure 4 of Mikolajewska (2010), who provides a review of this rare subclass of symbiotic stars.

$(l, b) = (34.^{\circ}8313, -3.^{\circ}5974)$, or $E(B-V) = 0.57$ mag from the recalibration by Schlafly & Finkbeiner (2011). The spectral type difference may also reflect a change in the intrinsic color of the red giant if the star is a long period variable; our spectrum was taken on 2007 June 20 *versus* 2012 for BK12.

Reddenings from the dust maps are uncertain at low latitudes, so we compared the $R-I$ color of NSV 11749 (see below) with de-reddened $R-I$ colors of M3 and M4 giants in the Bright Star Catalog (Hoffleit & Jaschek 1991). This suggested an even lower reddening, $E(B-V) \approx 0.1$ mag, but the large range in intrinsic color at fixed spectral type and the effect of the hot companion star on the intrinsic $R-I$ of the red giant in NSV 11749 leave a very large uncertainty in this value. As usual, finding the reddening of a low latitude object is difficult.

The Williams (2005) photometry suggests NSV 11749 has been in a quiescent state since the nova outburst 110 years ago, but no time-series photometry is available since 1988, the last plate in Williams' sequence. We therefore undertook CCD photometry of NSV 11749 to provide a clearer understanding of its nature in quiescence, to confirm that its photometric behavior is consistent with its spectroscopic identification as a symbiotic nova, and to seek the orbital period as suggested by BK12. Here, we report the results of the first six months of photometric monitoring.

Images were acquired with the Bowling Green State University 0.5 m $f/8$ Cassegrain telescope and Apogee AP6e CCD camera from 2012 May 16 through July 11. The camera has a 21 × 21 arcmin field of view with 1.2 arcsec pixels. Images were taken in V (180 s) and I (120 s) and the star was visited at least twice each night, with each visit consisting of three images per filter, dithered to prevent stars from repeatedly landing on bad pixels. On one night, we visited the field ten times over an interval of 4.5 hours, and on two nights we visited continuously over 1-2 hours to search for short term variations. Preliminary photometry of the Bowling Green (BG) images indicated the star was variable, but exhibited a slow brightening over the 60 day interval with little short term variation.

We therefore initiated observations with the PROMPT #5 0.4 m telescope (P5; Reichart *et al.* 2005) located on Cerro Tololo in Chile, which we used from 2012 July 24 through November 17. We visited the field one night each week, taking three images each in V (60 s), R (30 s), and I (20 s). The darker skies in Chile yielded higher quality V images than we obtained from BG, though the camera field of view is smaller (10 × 10 arcmin). The images from BG and P5 were processed to remove the bias level and dark current, and to flatten sensitivity differences across the chip.

The images were analyzed using the DAOPHOT II point-spread function fitting photometry package (Stetson 1987). Combined use of DAOPHOT and ALLSTAR located all possible stars on each image. Because the seeing and sky background varied from one image to the next, the number of stars detected also varied. To create a more uniform object list, the best quality images in V, R and I were combined using MONTAGE to produce master images with high signal-to-noise. The DAOPHOT/ALLSTAR procedures were then applied to these master images, giving a master list of stars in the field. Stars were matched on each frame using DAOMASTER, and ALLFRAME (Stetson 1994) was run on all images using the master list from the respective MONTAGE images to produce both time-averaged and time series photometry for each star detected in the field.

Table 1. Photometric Calibration.

Date	Telescope	rms$_V$	rms$_R$	rms$_I$	$N_{\rm std}$	$N_{\rm fld}$	N_{SS}
2012 Jul 10	BG	0.027	...	0.031	76	13	12
2012 Jul 11	BG	0.043	...	0.041	41	6	12
2012 Nov 17	P5	0.022	0.021	0.023	60	8	3

On two photometric nights in BG and one at P5, images of standard stars (Landolt 1992) were taken over a range of airmass throughout the night. The instrumental aperture magnitudes of these standard stars, along with their $V - I$ color and airmass, X, were used to do least-squares fits,

$$m - M = c_0 + c_1 X + c_2 (V - I), \tag{1}$$

where m is the instrumental magnitude and M is the standard magnitude. For July 11, a linear time dependent term was added. Table 1 shows the dates of each night, the rms scatter of each fit, the number of standard stars observed, the number of independent visits to standard fields, and the number of observations made of the SS field. We then used the "c_i" coefficients to standardize the instrumental magnitudes of 15 uncrowded, non-variable stars in the SS field to serve as comparison stars for differential photometry of the variable stars. Given the details of our calibration, we estimate the final photometric zero-points on the comparison stars to be accurate to 0.01-0.02 mag in V and I and to ∼0.04 mag in R. The larger value for R reflects that data were taken on a single night at high airmass. The quality of our zero-points are demonstrated by comparing our V photometry to that in the APASS database.[2] We find a median difference of $V_{\rm BG} - V_{\rm APASS} = -0.012 \pm 0.011$ mag for 14 stars in common, with the uncertainties of the individual magnitudes being 3-5 times larger in APASS than in ours.

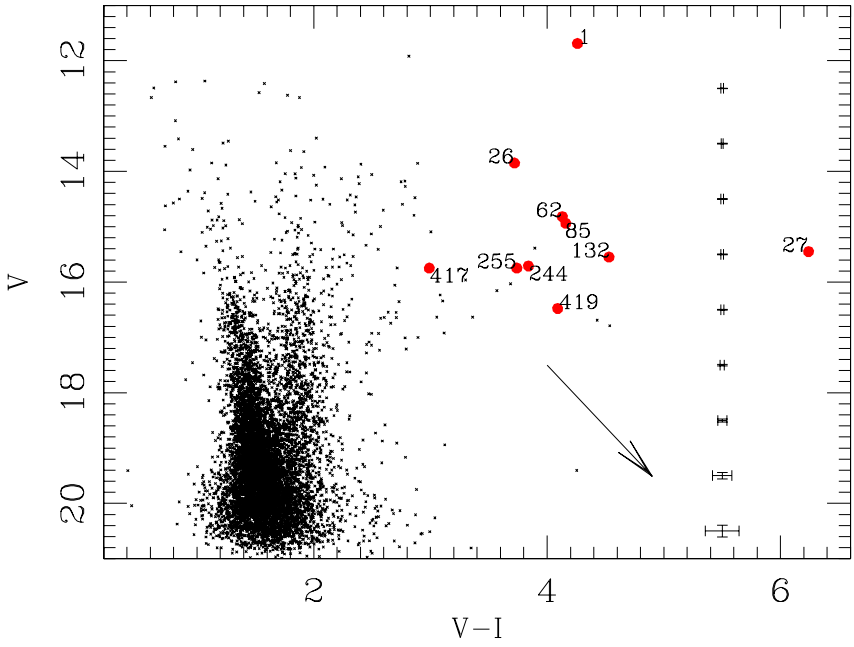

Figure 2. A color-magnitude diagram of the 10 × 10 arcmin P5 field around NSV 11749. The error bars and reddening vector are described in the text. The red circles and numbers mark the positions of the variable stars in Table 3; NSV 11749 is #417.

We also used these results to calibrate the time-averaged ALLFRAME photometry from P5 and produce a color-magnitude diagram of the field, which is shown in Figure 2. There are 7867 stars in total, of which 547 are brighter than $V = 17$ mag. The error bars along the right show mean errors in magnitude and color for stars binned by V

[2]Data Release 7, 2013 by the AAVSO, see `http://www.aavso.org/apass`.

magnitude. The pattern of bluer, main sequence disk stars and redder stars that include red giants is commonly seen in fields close to the Galactic plane (e.g., Ortolani, Bica & Barbuy 1993). The reddening vector is based on $E(B-V) = 0.67$ mag at the location of NSV 11749 (Schlegel, Finkbeiner & Davis 1998). There is no evidence for strong variations in reddening across our field, either from the dust maps, from inspection of our images, or from the the color-magnitude diagram.

When compiling photometry using DAOMASTER, each star is labeled with a variability index. Stars with the highest variability index were flagged in each of the five data sets (V and I from BG, and V, R, and I from P5), and these lists were compared to find stars in common. Through this method, we detected nine variable stars; NSV 11749 was below our initial detection threshold, but we extracted its photometry and found it to have low-level variations. Equatorial coordinates for each star were estimated from the Two-Micron All Sky Survey images (Skrutskie *et al.* 2006). These and the (x, y) coordinates on a master image[3] are shown in Table 2, along with a column indicating in which fields of view the star was visible. We searched the SIMBAD database at the equatorial coordinates of each star (see Table 2), and followed up named objects with the International Variable Star Index.[4] The results are discussed below, star by star.

Table 2. Variable Star Coordinates.

ID#	$X_{\rm pix}$	$Y_{\rm pix}$	RA (J2000)	Dec (J2000)	FOV	Name
417	485.1	547.1	19:07:42.4	+00:02:51	BG + P5	NSV 11749
1	460.8	331.4	19:07:44.3	+00:07:10	BG + P5	ASAS 190744+0007.1
26	325.9	414.7	19:07:55.1	+00:05:30	BG + P5	
27	546.4	381.8	19:07:37.5	+00:06:09	BG + P5	IRAS 19050+0001
62	485.0	571.2	19:07:42.4	+00:02:22	BG + P5	
85	637.9	832.3	19:07:30.2	–00:02:51	BG	
132	885.6	784.6	19:07:10.4	–00:01:55	BG	
244	700.9	640.0	19:07:25.1	+00:00:59	BG + P5	
255	407.9	412.6	19:07:48.5	+00:05:32	BG + P5	
419	800.6	655.5	19:07:17.2	+00:00:40	BG	

We paired each variable with as many of the comparison stars as possible ($N_{\rm comp}$), then calculated the differential photometry of each pair from the ALLFRAME time-series data, and transformed the result to the standard VRI system, taking the median magnitude of the $N_{\rm comp}$ measurements to represent the magnitude of that variable on that image. We adopted the standard error of the $N_{\rm comp}$ measurements as the random uncertainty in that magnitude. The calibrated time series photometry for each variable is available electronically. Figures 3–6 show the time series after multiple observations taken on a single night were medianed; the error bar on a given point shows the standard error of the $N_{\rm obs}$ magnitudes measured that night.

Table 3 shows the median, maximum (max) and minimum (min) brightness in V and I for each star, along with its median color. From Table 3 it is clear that all ten variables are extremely red, and the color-magnitude diagram shows that they are among the reddest stars in this field. As the bluest of the ten variables, NSV 11749, with its very late-type stellar continuum, sets a temperature upper limit on the other variables. Thus, they are likely to consist of, or contain, red giant or red dwarf stars. Unfortunately, only NSV 11749 was the target of a ChaMPlane spectrum, so no spectral information is available for the other variable stars.

[3]A FITS format image corresponding to these (x, y) coordinates is available at `http://physics.bgsu.edu/~layden/publ.htm` along with other data products from this research. The files are also available as 6071-d1.tar.gz from the IBVS website.

[4]The VSX is available at `http://www.aavso.org/vsx/`.

Inspection of the light curves provided approximate periods for most stars, and the ones with more regular periods were investigated using the phase dispersion minimization method. Also, for some stars we applied the template fitting program of Layden (1998) to fit ten standard light curve shapes to the data for each star to provide a best-fit amplitude and to provide an objective means for classifying the variability type based on light curve shape.

Table 3. Photometric Characteristics.

ID	$\langle V \rangle$	$V_{\max}$	$V_{\min}$	$\langle I \rangle$	$I_{\max}$	$I_{\min}$	$\langle V-I \rangle$	Period	Type
417	15.75	15.61	16.17	12.76	12.70	12.84	2.99	?	Z And
1	11.69	11.55	11.84	7.43	7.25	7.51	4.26	40-50	Lb
26	13.85	13.51	14.17	10.13	9.91	10.25	3.72	73 ± 2	SR
27	15.45	15.00	17.16	9.21	9.01	10.31	6.24	> 200	M
62	14.82	14.48	15.32	10.69	10.57	10.97	4.13	58/116	SRa/EW?
85	14.94	14.84	15.09	10.78	10.76	10.88	4.15	?	Lb?
132	15.55	15.38	15.76	11.02	10.95	11.11	4.54	?	Lb?
244	15.71	15.32	16.03	11.87	11.70	12.02	3.84	61 ± 5	Lb
255	15.75	15.48	15.94	12.01	11.92	12.06	3.74	47 ± 3	Lb
419	16.48	16.26	16.77	12.39	12.36	12.71	4.10	?	?

In Figure 3, the symbiotic star, NSV 11749 (ID #417), shows a gradual increase in V and I over the course of the BG observations, and a gentle decline in VRI during the P5 interval. The scatter in the BG V data is mostly observational, as the star was quite faint relative to the background sky. However, the slight variability seen in the P5 data seems to be correlated between VRI, so is probably real, with a time scale of roughly 40 days. The star showed no evidence of short-term variability ($\sigma < 0.015$ mag) over the three nights of high-cadence I-band observing from BG. Flickering due to variable accretion rates cannot be ruled out completely, however, since the cool red giant may dominate any flux variations due to accretion onto the hot companion. We intend to obtain high cadence observations in UBV to seek evidence for a variable accretion rate.

These limits on variability over the 1-5 hour time scale support the claim of BK12 that NSV 11749 is a rare symbiotic star, rather than a more common cataclysmic variable. Brightness modulations due to orbital effects should be evident if the star were a CV, which typically have orbital periods of hours (e.g., Warner 1995). Also, the lack of outbursts over the 184 days of observation is unusual for typical dwarf nova systems (Sterken & Jaschek 1996).

The slow variation seen in Fig. 3 is consistent with the behavior of symbiotic stars (Z Andromedae type; Sterken & Jaschek, 1996), in which the hot spot or accretion disk contributes the H and He emission lines seen in Fig. 1, while our I photometry is dominated by the light of a red giant companion. The orbital periods of SSs are typically hundreds to thousands of days, with the very rare subclass of symbiotic novae having periods greater than 800 days (Mikolajewska 2010). It is not clear from the small fraction of a light cycle seen in our photometry whether the behavior is sinusoidal, and indicative of the orbital period of an tidally-distorted red giant, or asymmetric and indicative of Mira-type pulsations seen in the secondaries of many symbiotic novae (Mikolajewska 2010). However, the colors and spectral type of NSV 11749 indicate a star hotter than the Mira variable #27, so as we gather more data in the coming years, we anticipate seeing an elliptical light curve with a period of $\sim$3 years.

Figure 4 shows the light curves of star #1. Despite being the brightest star in the field and saturated on some images, the star is clearly variable with a low amplitude ($\Delta V \sim 0.3$) mag and irregular cycle (40-50 days between peaks). The All Sky Automated Survey (ASAS; Pojmański & Maciejewski 2005) also detected this star, labeled ASAS

190744+0007.1, as variable with a mean V of 11.41 mag and a V amplitude of 0.35 mag. The period given by ASAS is 57.9 days, but they were unable to ascribe a variable type to the star; it is listed as "MISC." A time-magnitude plot of the ASAS data shows no regular periodicity, and the time and amplitude scales of the variability come in and out of coherence over months to years. Our photometry is consistent with the behavior seen in the ASAS photometry. Given the irregular behavior seen in both data sets, the lack of variation over hours, and the extremely red color of the star, we believe this star is a low-amplitude irregular pulsating giant star, type "Lb" in the GCVS notation (Samus *et al.* 2012).

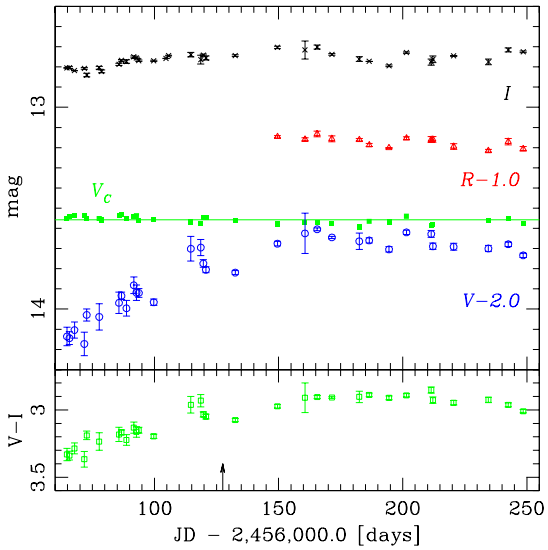

Figure 3. Light and color curves for NSV 11749 (ID#417) where the V and R data (◯ and △) have been shifted upward by 2.0 and 1.0 mag, respectively, for ease of display. The solid squares and line (V_C) show photometry of the non-variable star #127 for comparison. The arrow indicates the transition from BG to P5 data.

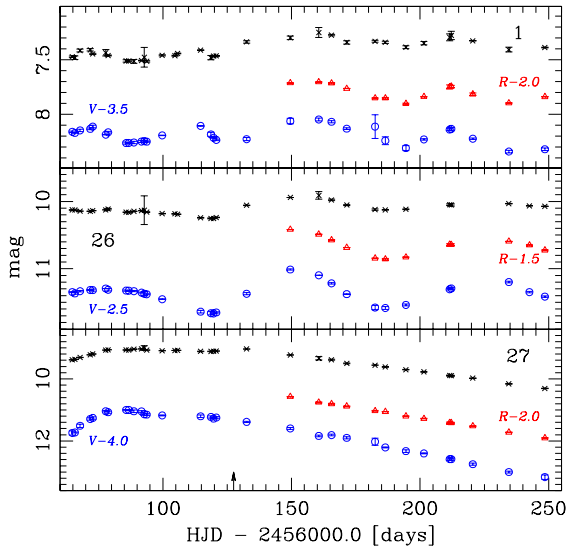

Figure 4. Light curves for stars #1, #26 and #27. Symbols are as in Fig. 3. Error bars in Figs. 3-6 are described in the text.

The light curves for star #26, shown in Fig. 4, indicate a more consistent periodicity of 73 ± 2 days over 2.5 light cycles, while the amplitude varies considerably from cycle to cycle. These and the star's red color suggest this star is a semi-regular (SR) long period variable. Our continuing observations will determine the level of periodicity and hence the sub-category SRa versus SRb.

The classification of star #27, also shown in Fig. 4, is clearer: it must be a Mira (M) type long period variable with a period longer than 200 days and an amplitude $\Delta V > 2.2$ mag. Continuing observations will refine these values. This very red star is 7.5 arcsec from the cataloged position of IRAS 19050+0001 and is almost certainly a match.

Star #62, shown in Fig. 5, has a regular periodicity superimposed on a linear decline over the 184 day observing interval. After fitting and removing the linear trend, we obtained a period of 58 ± 3 days. This could be interpreted as an SRa long period variable with a long secondary period (e.g., Kiss *et al.* 1999), or a contact binary (EW type) in which both components are giants and one has slow, low-level pulsation. Template fitting

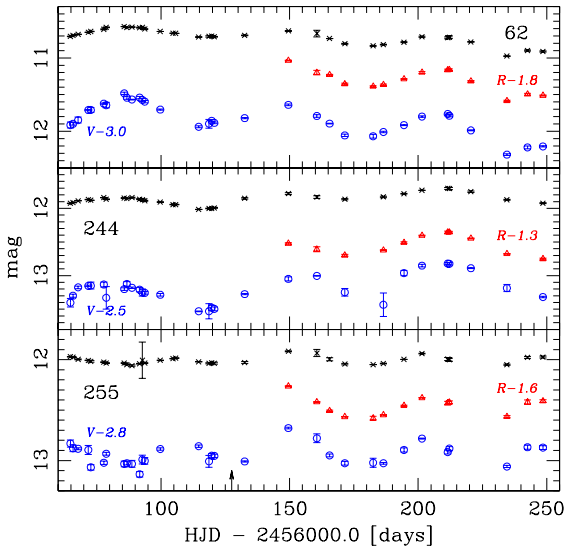

Figure 5. Light curves for stars #62, #244 and #255. Symbols are as in Fig. 3.

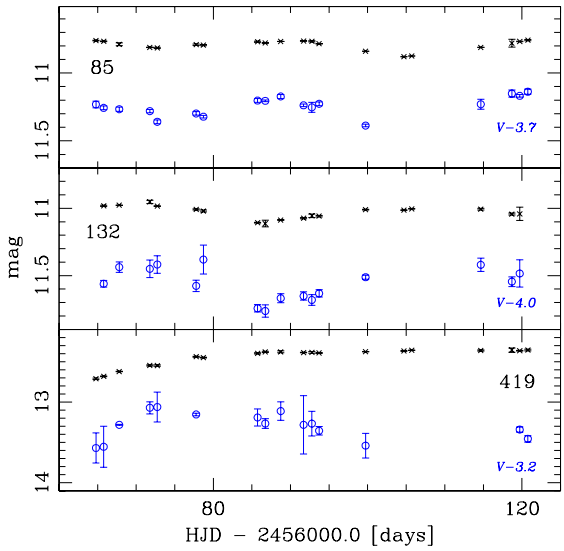

Figure 6. Light curves for the three stars viewed only from BG: #85, #132 and #419. Symbols are as in Fig. 3.

using the 58 day period resulted in a best fit using a sine curve template with an amplitude of 0.31 mag in V and 0.14 mag in I, while a 116 day period yielded an EW template with amplitudes of 0.34 and 0.14 mag, respectively. The rms scatter around the templates was comparable, giving us no reason to prefer one fit over the other. More photometric observations may clarify these two interpretations.

Stars #244 and #255 have similarly red colors and irregular light curves in terms of both period and amplitude (see Fig. 5). We classify them both as irregular long period variables of class Lb, with periods around 61 ± 5 days and 47 ± 3 days, respectively.

Stars #85, #132, and #419 were outside the P5 field of view, so we have only the 57 day time series obtained at BG to interpret their light curves (see Fig. 6). All three stars have $V - I \approx 4$ mag, and stars #85 and #132 have low amplitude variations. We tentatively classify these two stars as irregular long period variables of class Lb. Star #419 brightens and fades in V during our observations, while it remains bright in I. This deviation might indicate an epoch of dust formation, perhaps at maximum light of a Mira with a period much longer than 57 days. Longer time series data for all three of these stars is needed to clarify their behavior.

We note the similarities in the light curves of stars #1, 26, 62, 244, and 255. We reviewed our analysis and found no errors that could account for this behavior. Stars of similar brightness, color, and location (#417, 27, and a host of non-variable stars) behave differently, indicating that it cannot be due to systematic properties of the sky or CCD. These light curve similarities must be coincidental, and we expect to see them fall out of sync in future photometry.

In conclusion, we obtained six months of time series photometry on the emission line object NSV 11749 and confirmed its slow photometric variability, consistent with the determination of BK12 that this object is a symbiotic nova. We are continuing to monitor this field in $BVRI$ in order to find the orbital period of the binary. In the process of observing NSV 11749, we confirmed the variability of one known variable, and we detected eight new variable stars in the surrounding field. We classify the known variable, ASAS 190744+0007.1, as an irregular long period variable (Lb) and suspect the new variables are all red, long period variables (L). Our continuing observations of these stars will refine

their periods and sub-categories within the L type.

Acknowledgements: We thank an anonymous referee for his or her vigilance and helpful comments which greatly improved this study. This work partially fulfills the requirements for an undergraduate B.Sc. degree at Bowling Green State University (M.W.). This research has made use of the SIMBAD database, operated at CDS, Strasbourg, France; the International Variable Star Index (VSX) database, operated at AAVSO, Cambridge, Massachusetts, USA; and the AAVSO Photometric All-Sky Survey (APASS), funded by the Robert Martin Ayers Sciences Fund.

References:

Bond, H. E., Kasliwal, M. M., 2012, *PASP*, **124**, 1262 (BK12)
Clayton, G. C., Kerber, F., Pirzkal, N., et al., 2006, *ApJ*, **646**, L69
Grindlay, J. E., Hong, J., Zhao, P., et al., 2005, *ApJ*, **635**, 920
Hoffleit, D. & Jaschek, C., 1991, "The Bright Star Catalog," 5th ed., Yale University Observatory, New Haven
Kiss, L. L., Szatmáry, R. R., Cadmus, R. R. & Mattei, J. A., 1999, *A&A*, **346**, 542
Kohoutek, L. & Wehmeyer, R., 1997, *Astron. Abh. Hamburg. Sternw.*, **11**, 1
Landolt, A. U., 1992, *AJ*, **104**, 340
Layden, A. C., 1998, *AJ*, **115**, 193
Luyten, W. J., 1937, *Astron. Nachr.*, **261**, 451
Mikolajewska, J., 2010, arXiv:1011.5657
Miller Bertolami, M. M., Rohrmann, R. D., Granada, A., & Althaus, L. G., 2011, *ApJ*, **743**, L33
Ortolani, S., Bica, E. & Barbuy, B., 1993, *A&Ap*, **273**, 415
Pickles, A. J., 1998, *PASP*, **110**, 863
Pojmański, G. & Maciejewski, G., 2005, *Acta Astronomica*, **55**, 97
Reichart, D., Nysewander, M., Moran, J., et al., 2005, *Il Nuovo Cimento C*, **28**, 767
Rogel, A. B.. Lugger, P. M., Cohn, H. N., et al., 2006, *ApJS*, **163**, 160
Samus, N. N., Durlevich, O. V., Kazarovets, E. V., et al., 2012, "General Catalogue of Variable Stars," VizieR On-line Data Catalog B/gcvs
Schlafly, E. F. & Finkbeiner, D. P., 2011, *ApJ*, **737**, 103
Schlegel, D. J., Finkbeiner, D. P., & Davis, M., 1998, *ApJ*, **500**, 525
Skrutskie, M. F., Cutri, R. M., Stiening, R., et al., 2006, *AJ*, **131**, 1163
Sterken, C. & Jaschek, C., 1996, "Light Curves of Variable Stars: A Pictorial Atlas," Cambridge: Cambridge Univ. Press
Stetson, P. B., 1987, *PASP*, **99**, 191
Stetson, P. B., 1994, *PASP*, **106**, 250
Warner, B., 1995, "Cataclysmic Variable Stars," Cambridge: Cambridge Univ. Press
Williams, D. B., 2005, *JAAVSO*, **34**, 43

COMMISSIONS 27 AND 42 OF THE IAU
INFORMATION BULLETIN ON VARIABLE STARS

Number 6072

Konkoly Observatory
Budapest
24 August 2013

HU ISSN 0374 – 0676

A NEW W UMA-TYPE VARIABLE STAR NEAR R CMa

MKRTICHIAN, D.E.[1,2]; A-THANO, N.[3]; KOMONJINDA, S.[3]; RATTANASOON, S.[1]

[1] National Astronomical Research Institute of Thailand, 191 Siriphanich Bldg., Huay Kaew Rd., Suthep, Muang, 50200 Chiang Mai, Thailand

[2] Crimean Astrophysical Observatory, Nauchny, Crimea, 98409, Ukraine

[3] Department of Physics and Materials Science, Faculty of Science, Chiang Mai University, Muang, 50200 Chiang Mai, Thailand

TYC 5965-2398-1 (GSC 05965-02398) was discovered as a short period variable star during photometric observations of Algol-type eclipsing binary stars R CMa. It is situated about 4 arcmin from R CMa inside the field of view of the CCD camera. No information about the variability of this star has been found via ADS. The star has V=10.48, $B-V$=0.31 according to SIMBAD (Tycho-2) data base, the 2MASS catalogue gives J=9.758, H=9.615, K=9.551 magnitudes in the infrared bands.

The observations were performed in the B filter for five nights in December 2012 with an Apogee U9000 CCD camera attached to the 0.5 m telescope of the Thai National Observatory of the National Astronomical Research Institute of the Thailand (NARIT). We used HD 56971 and HD 56994 as comparison stars.

The standard procedures for the CCD data reduction and the aperture photometry have been applied to the images. Resulting instrumental magnitude differences ΔB (TYC 5965-2398-1−HD 56994) are shown in Figure 1. A well-defined short-period light curve with double minima is evident. The periodogram analysis was undertaken using the package PerSea written by G. Maciejewski, which is based on the optimal period search method of Schwarzenberg-Czerny (1996). The resulting periodogram is shown in Figure 2. The dominant peak is at frequency 3.3003 c/d. Another possible peak is located at twice the dominant frequency, at about 6.6006 c/d. The values of two possible periods were improved and the phased light curves are shown in Figures 3 and 4 respectively.

The phased light curve with a period of 0.15178±0.00002 days (f=6.58843±0.0018 c/d) may manifest Delta Scuti type variability with a mean amplitude of 0.036 mag and epoch of maximum of light curve on 2456280.7371.

The double wave phased curve better corresponds to W UMa type binary star variability with a period of 0.30349±0.0006 days (f=3.2950±0.007 c/d), epoch of minimum 2456281.25290 and primary minimum depth of 0.044 mag. The low amplitude of this eclipsing binary can be caused by low inclination or high third light which is common for W UMa stars.

The $B-V$=0.31 index of TYC 5965-2398-1 indicates about F0-F1 spectral class, thus we cannot rule out completely the Delta Scuti interpretation based on the spectral class alone. On the other hand, the shape of the phase curve for the half (0.15-day) period has a slow ascending branch and a rapid descending one. Such a shape does not correspond

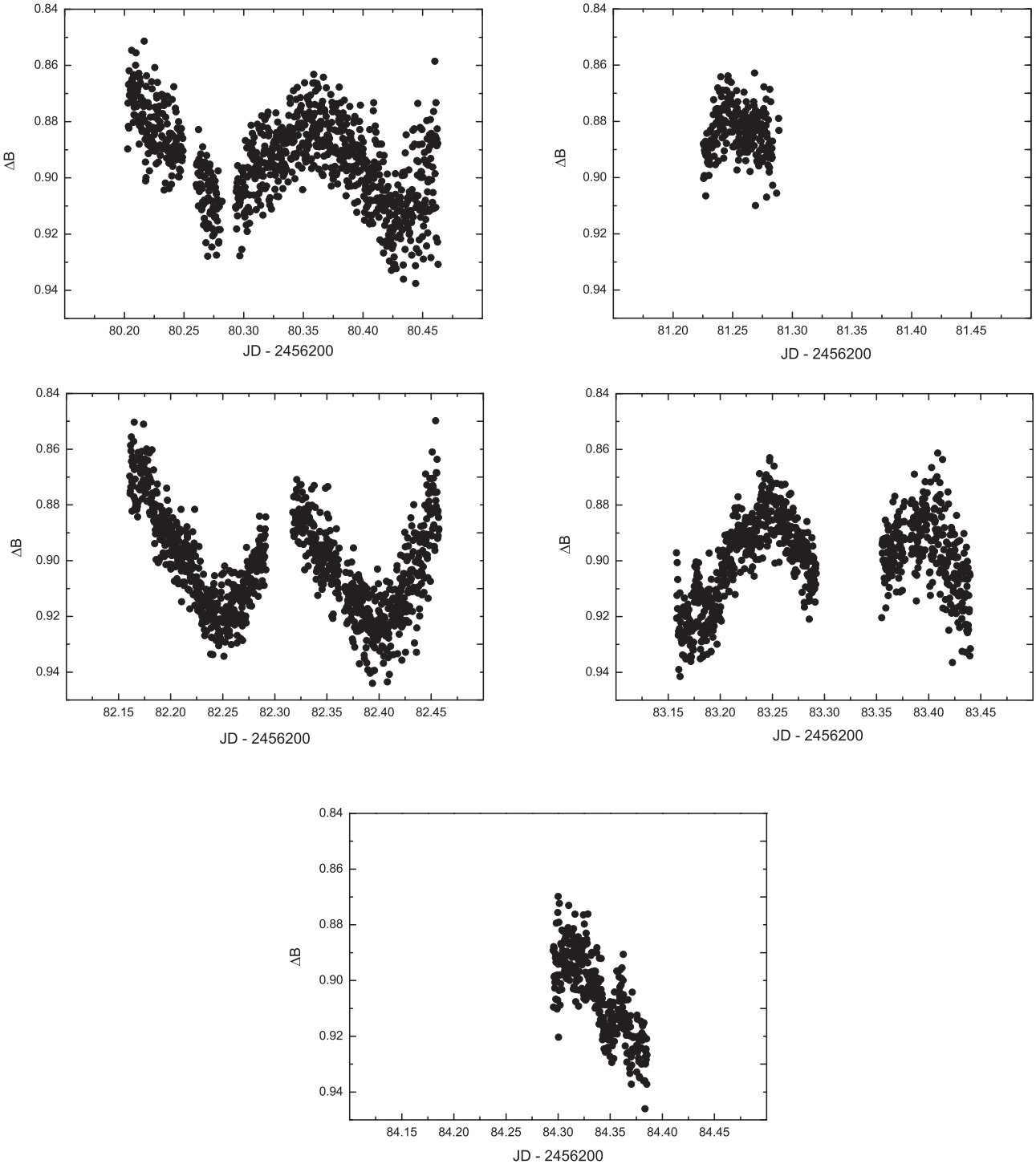

Figure 1. B-filter differential magnitudes (TYC 5965-2398-1−HD 56994).

to light curves of high amplitude Delta Scuti type stars that show a rapid ascending and a slow descending branch. Thus, the curve for 0.15 day is artificial.

The observations obtained at JD 2456280 and 2456282 clearly show two distinct minima, and two distinct maxima. These minima-maxima show the same depth. This is a characteristics of a W UMa-variable rather than a Delta Scuti type pulsators. We believe that the double-minima light curve better represents the found variability and corresponds to the binary nature of early F spectral-class components. We conclude that TYC 5965-2398-1 belongs to the class of short-period W UMa-type stars.

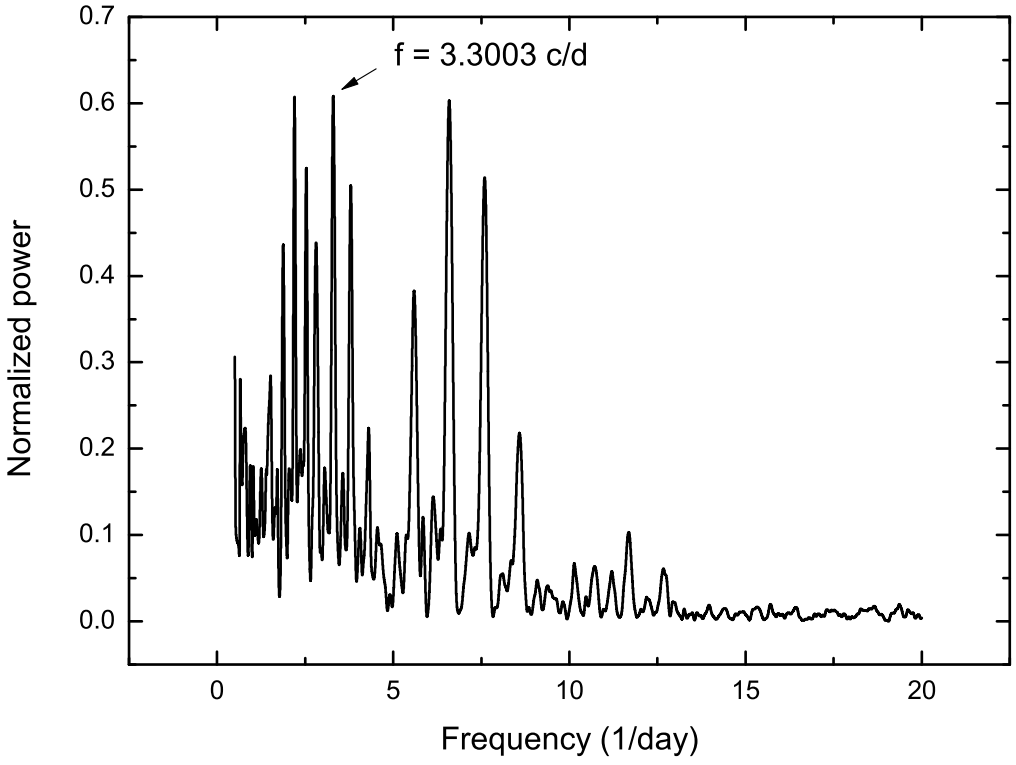

Figure 2. The periodogram of instrumental magnitudes (TYC 5965-2398-1−HD 56994). The dominant peak at 3.3003 c/d is marked by an arrow.

Acknowledgements: M.D.E. acknowledges his work as part of the research activity of the National Astronomical Research Institute of Thailand (NARIT, Public Organization), which is supported by the Ministry of Science and Technology of Thailand.

Reference:

Schwarzenberg-Czerny, A. 1996, *ApJ*, **460**, L107

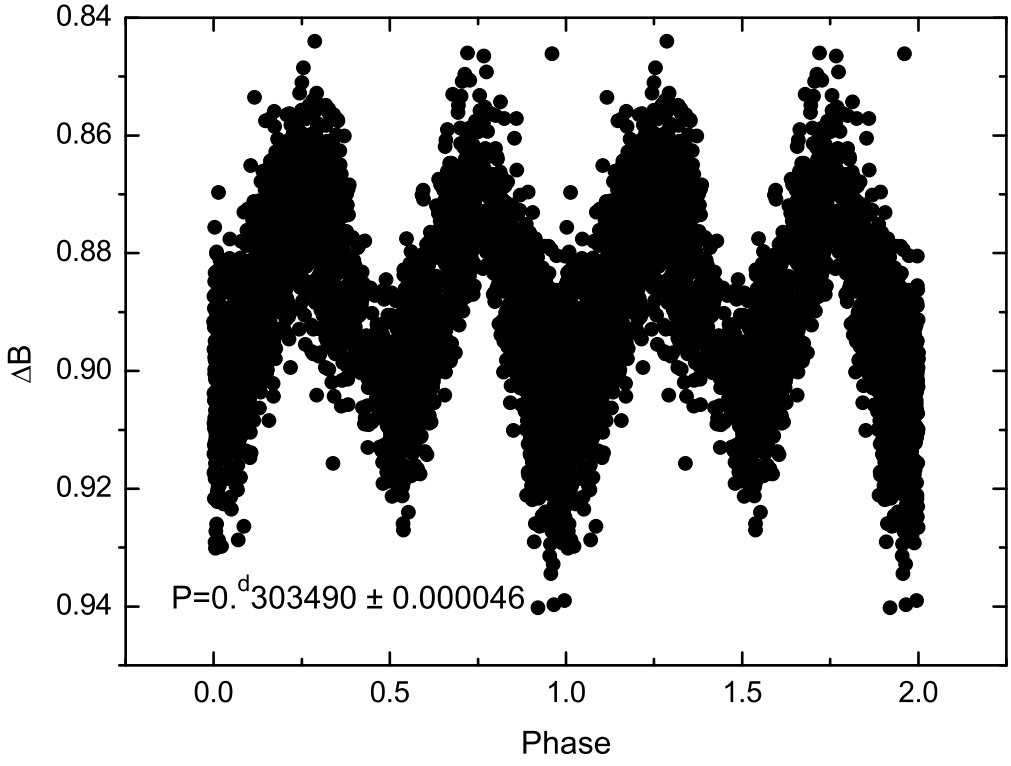

Figure 3. Light curve phased with the 0.303490 day period.

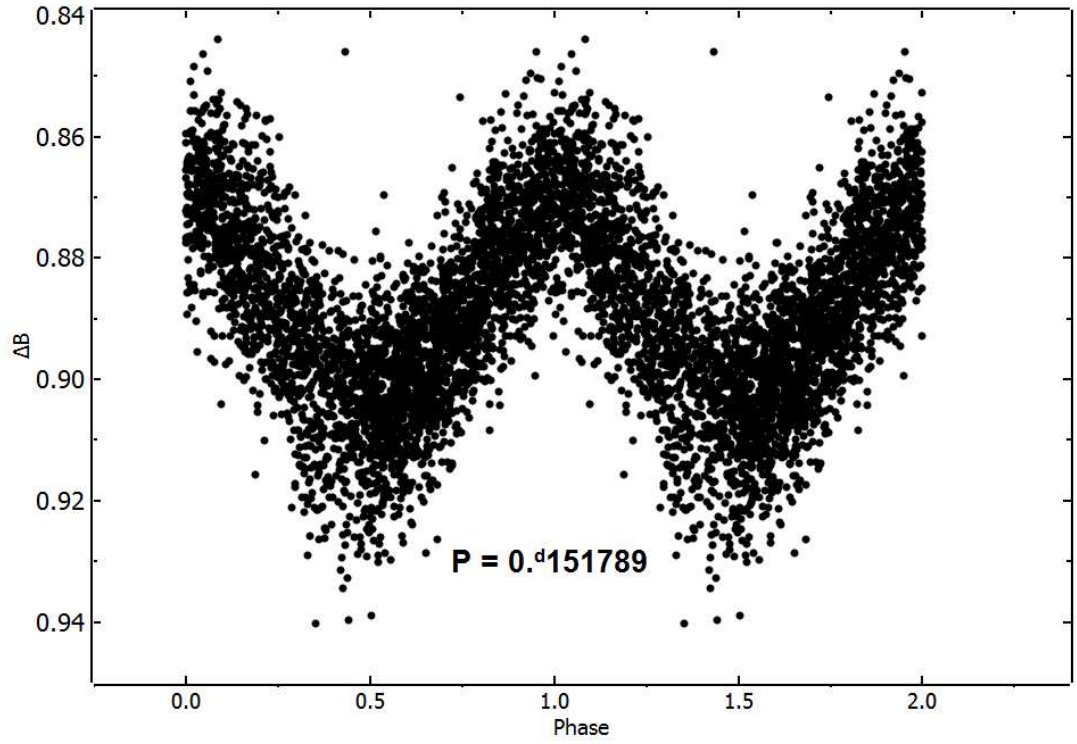

Figure 4. Light curve phased with the 0.151789 day period.

COMMISSIONS 27 AND 42 OF THE IAU
INFORMATION BULLETIN ON VARIABLE STARS

Number 6073

Konkoly Observatory
Budapest
26 August 2013

HU ISSN 0374 – 0676

FOLLOW-UP OF MASTER OTJ204200.48+041839.9

NESCI, R.[1]; CARAVANO, A.[2]; FALASCA, V.[2]; VILLANI, L.[2]

[1] INAF/IAPS, via Fosso del Cavaliere 100, 00133, Roma, Italy, e-mail: roberto.nesci@iaps.inaf.it

[2] Osservatorio Cittadino, via Bolletta 18, 06034, Foligno, Italia

Following the telegram by Denisenko et al. (2013) we observed the transient source MASTER OT J204200.48+041839.9 with the 30 cm telescope of the Foligno Observatory and a Nikon D90 camera. Images were taken in sequences of 15 with 30 s exposure each and then aligned and summed to achieve exposure times of 450 sec. Nearly all sequences were taken in monochrome mode, while one sequence was taken in color (RGB) mode to get the $B-V$ of the source. Aperture photometry was performed with IRAF/apphot, using a comparison sequence of about 35 nearby stars from the APASS (UCAC4, Zacharias et al. 2012) catalog down to V=15.0. The slope of the linear fit between instrumental (monochrome) and catalog V magnitudes was always nearly 1 with a rms deviation of 0.11 mag. We checked the presence of a color bias between our instrumental magnitudes and the UCAC4 ones: the comparison stars have $B-V$ colors ranging between 0.0 and 1.2 and are well distributed in V magnitude, so that this check was quite feasible. We actually found a slight trend of our V magnitudes derived from the monochrome images with the $B-V$ color. The correction is not large, C=$-0.285 \times (B-V) + 0.200$; it is smaller than our statistical error for intermediate spectral type stars ($B-V$ about 0.6) and appreciable only for very early or late spectral types.

Aperture photometry on the color image gave B=15.9 and V=15.7, again with slope very close to unity and rms deviations of 0.10 mag. A scatter plot of our $B-V$ colors for the reference stars against the UCAC4 values shows a systematic trend: the best fit line gives $(B-V)_{\rm ucac} = 1.33(B-V)_{\rm our} - 0.20$: for our variable the correction is therefore only +0.06 mag, smaller than the statistical error of our calibration regressions, both in B and in V. The astrophysical result is a clear indication of a rather blue color ($B-V$=0.26) for the source, as expected for a cataclysmic variable in outburst or a VY Scl type star.

The V magnitudes of the star, derived from the monochrome images, corrected by +0.13 mag for the color effect discussed above, are reported in Table 1: errors are always 0.10 mag. From this Table a flux decrease rate of at least 0.4 mag/day after 2 August 2013 is evident.

Table 1. Observed V magnitudes of MASTER OT J2042+0418.

date	JD	B	V
2013-08-01.88	2456506.32	16.09	15.83
2013-08-02.88	2456507.32		15.94
2013-08-06.90	2456511.33		>17.5
2013-08-09.90	2456514.33		>17.5

We searched for previous observations of this star in the Asiago direct plate archive (Barbieri et al. 2003), finding none and in the objective prism Digitized First Byurakan Survey (DFBS, Mickaelian et al. 2007) accessible on-line,[1] finding two plates. The star was clearly detected in the first plate, n.0907 (IIaF emulsion) taken on 19 October 1973 while it was undetected in the second one (n.1388, IIF emulsion) taken two years later on 6 November 1975, with magnitude limit R=16.3.

The star showed a quite blue continuum: unfortunately the low S/N level prevents a reliable identification of possible emission lines. Its magnitudes, retrieved from the DFBS archive, derived by integration of the spectrum on the proper wavelength bands, are B=15.55 and R=15.28 in the USNO-A2 scale.

Using the same set of reference stars used for our photometry, we derived a linear conversion from the USNO-A2 to the UCAC4 system for the B and r bands: the correlation coefficient was better than 0.98 and the results were B=16.09, r=15.70. The blue color found at the DFBS epoch, when the source was in a high state, is in fair agreement with that found by us in the flare of 1 August 2013 and with the $g-r$=0.18 color reported in the SDSS database, measured on 15 September 2004.

Denisenko et al. (2013) suggest a classification of this star as a VY Scl type: this kind of stars is characterized by long stays at high flux level, with short but deep faint phases (see e.g. the light curve of VY Scl on the AAVSO website). The sparse light curve of this variable, recorded by the CSS survey in the years 2006-2012, shows that the star oscillates between V=18.5 and V=15.8 without a preferred flux level, with only one recorded episode below the 19th magnitude. It is therefore rather different from the typical cataclysmic variable light curve and more similar to a VY Scl: also the fact that the SDSS, several POSS plates and the DFBS found the star in a high state favours this classification.

References:

AAVSO Photometric Sky Atlas, `http://www.aavso.org/apass`
Barbieri et al., 2003, *Experimental Astronomy*, **15**, 29.
Catalina Sky Survey, `http://www.lpl.arizona.edu/css/`
Denisenko et al., 2013, *ATel*, No. 5240
Mickaelian et al., 2007, *A&A*, **464**, 1177
Zacharias N., Finch C.T., Girard T.M., Henden A., Bartlet J.L., Monet D.G., Zacharias M.I., 2012, The fourth U.S. Naval Observatory CCD Astrograph Catalog (UCAC4).

[1] `http://byurakan.phys.uniroma1.it/`

COMMISSIONS 27 AND 42 OF THE IAU
INFORMATION BULLETIN ON VARIABLE STARS

Number 6074

Konkoly Observatory
Budapest
10 September 2013

HU ISSN 0374 – 0676

VARIABLE STARS IN THE SMC STAR CLUSTER BRÜCK 50

SCHMIDTKE, P.C.[1]; UDALSKI, A.[2]

[1] School of Earth and Space Exploration, Arizona State University, Box 871404, Tempe, Arizona 85287 USA
E-mail: Paul.Schmidtke@asu.edu

[2] Warsaw University Observatory, Aleje Ujazdowskie 4, 00-478 Warsaw, Poland
E-mail: Udalski@astrouw.edu.pl

Brück 50 (RA $00^{\rm h}49^{\rm m}02^{\rm s}$, DEC $-73°21'44''$, J2000) is a young, compact star cluster in the Small Magellanic Cloud (Brück 1976). The blue supergiant HD 4862 lies $5.2''$ from the cluster's center and is likely to be a cluster member. Lennon (1997) classified this star as B5 Ia, taking into account the low metallicity of the SMC. Bica & Schmitt (1995) determined the cluster's position and angular size ($r_{\rm cls}$=$16.5''$) that we adopt. This size, which corresponds to a radius of ∼5 pc at the SMC's distance, is comparable to many cluster candidates (e.g. Pietrzyński et al. 1998). Brück 50 is one of a close triplet of SMC clusters (de Oliveira et al. 2000), the other clusters being BS 41 (which lies $38''$ away) and L39 ($77''$ away). Some authors question whether Brück 50 should be considered an individual cluster or simply a portion of a more extensive grouping. For example, Oey, King, & Parker (2004), in a study of the clustering of OB stars, include several early-type stars associated with Brück 50 into a much larger structure (see their OB group #73). From a color-magnitude diagram (CMD) analysis of OGLE-II photometry, de Oliveira et al. (2000) estimated the age of Brück 50 to be <30 Myr. Using a low-resolution integrated spectrum, Talavera et al. (2007) derived a cluster age of 4±2 Myr, a result that is likely influenced by the brightness of HD 4862. Glatt, Grebel, & Koch (2010), fitting Padova and Geneva isochrone models to CMD data from the Magellanic Cloud Photometric Survey, determined an age of ∼10 Myr.

Young SMC star clusters like Brück 50 often contain a high proportion of hot stars that are photometrically variable. Schmidtke, Chobanian, & Cowley (2008) found low-amplitude short-period pulsations in OGLE-II photometry for >20% of hot stars in NGC 330, a cluster noted for its large population of Be stars. The percentage of pulsators in NGC 330 was even greater for previously known Be stars. Similarly, in a study of MACHO observations for a sample of spectroscopically selected stars in the SMC, Diago et al. (2008) found that 4.9% (9 out of 183) of B stars and 25.3% (32 out of 126) of Be stars were pulsating variables.

We present here an analysis of 12 seasons of OGLE photometry (Udalski, A., Kubiak, M., & Szymański 1997; Udalski et al. 2008a) for Brück 50, obtained between 1997 and 2009. The cluster is in field SMC_SC5 of Phase II and field SMC100.8 of Phase III. An I-band finding chart is shown in Fig. 1. The small change in background sky level for the bottom 1/3 of this reference image corresponds to a boundary between subframes of OGLE-III data processing. The inner circle marks the cluster radius from Bica & Schmitt

(1995), while the outer circle ($r_{\rm lim}$=30″) encloses all stars that we examined in detail. HD 4862 is too bright for inclusion in OGLE data bases, and its brightness masks other nearby stars. For example, the star that lies ∼2″ southeast of HD 4862 is not included, despite being resolved on the chart. In the OGLE-III photometric maps (Udalski et al. 2008b), data are available for 118 stars with $r<r_{\rm cls}$ and an additional 224 stars with $r_{\rm cls}<r<r_{\rm lim}$. The OGLE-II maps (Udalski et al. 1998) are not as deep and have poorer spatial resolution. Hence, the corresponding numbers are 72 and 194 stars, respectively.

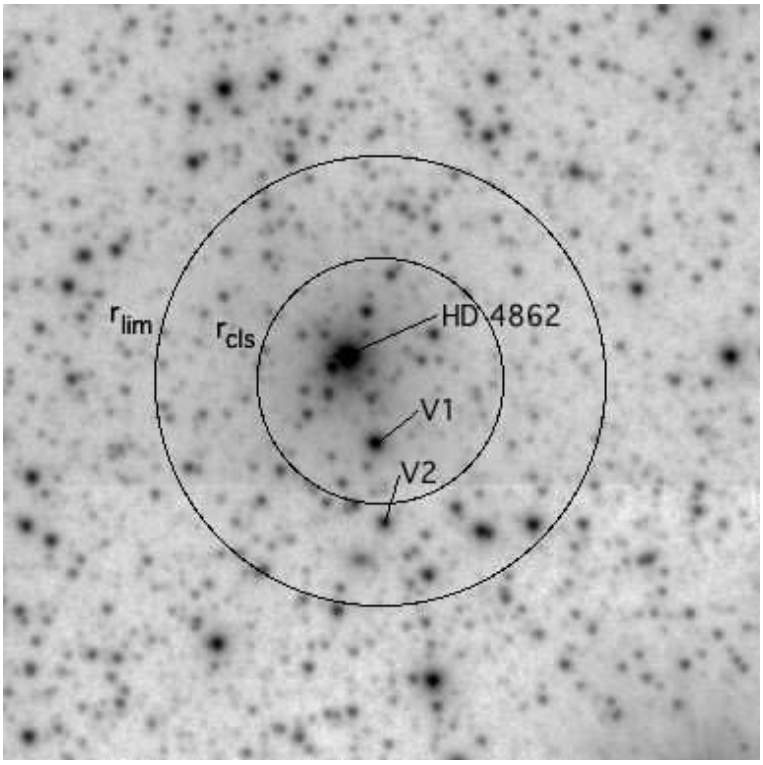

Figure 1. *I*-band finding chart for Brück 50. The field of view is 100″×100″, with north up and east to the left. The inner and outer circles identify $r_{\rm cls}$=16.5″ and $r_{\rm lim}$=30″, respectively. The blue supergiant HD 4862 and variable stars V1 and V2 are marked.

The stellar density (unweighted by brightness) of background stars in the direction of Brück 50 is high, complicating the assessment of membership for individual stars. Using a measurement of stellar density in an annulus surrounding $r_{\rm cls}$, we estimated the surplus of stars within the cluster radius. Only 17.8% (21 out of 118) of stars in the OGLE-III photometric maps with $r<r_{\rm cls}$ are expected to be true members of the cluster. Fitting a Gaussian profile to the spatial distribution of stars, we determined the FWHM to be 17.2″, which is consistent with the cluster size found by Bica and Schmitt (1995).

A CMD of *V* and *I* data for Brück 50 from the OGLE-III photometric maps is shown in Fig. 2. Stars in the upper left portion of the diagram often exhibit short-period, low-amplitude pulsations (e.g. see Balona 2010; Kołaczkowski et al. 2006; Moffat 2012). The dashed line at I=18.2 corresponds to the expected brightness of a B5 V star at the distance of and with an extinction appropriate for the SMC. None of the bright, cool stars in the figure can be a member of this young cluster.

A plot of σ_I vs. I from OGLE-III data for Brück 50 is shown in Fig. 3. At faint magnitudes there is an excess of stars with larger-than-expected photometric dispersion.

However, most stars with high σ_I lie within the cluster radius, while only a few are found outside $r_{\rm cls}$. This implies that a lack of consistent spatial resolution of stars near the cluster's core, rather than photometric variability, produces most of the scatter for faint stars in the diagram. Even among bright stars there are some with moderately large σ_I that turned out to be photometric blends.

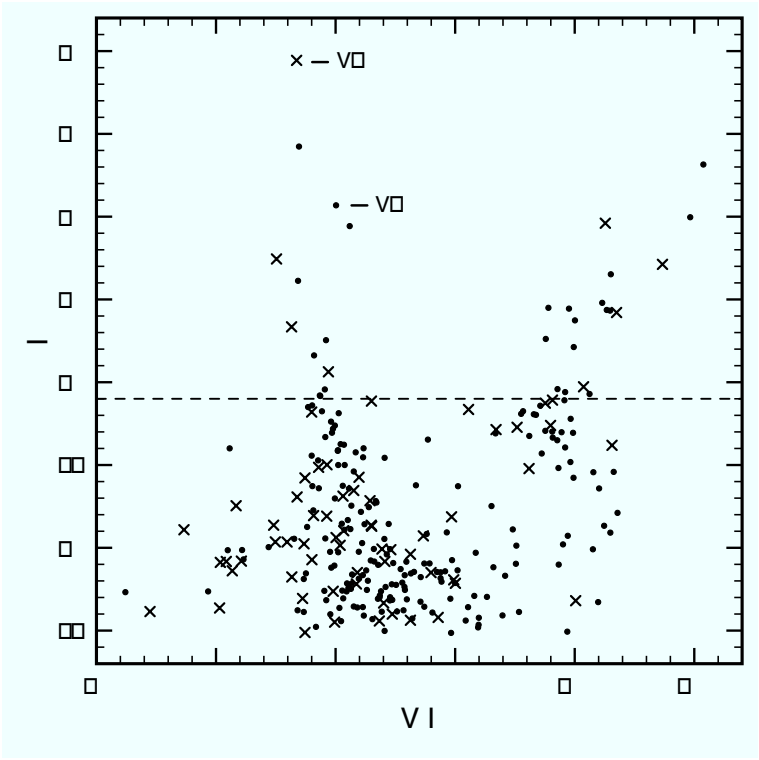

Figure 2. I vs. $V-I$ CMD from OGLE-III data for stars in Brück 50. Stars brighter than I=18.2 (the dashed line) were analyzed for photometric variability. Two variable stars were found. Crosses (×) represent stars within the cluster radius ($r_{\rm cls}$=16.5″), while filled circles (•) denote stars lying outside this boundary.

Table 1. Variable Stars in Brück 50

ID	RA[a] (J2000)	DEC[a] (J2000)	I^a (mag)	$V-I^a$ (mag)	GCVS Type	P (days)	Other IDs
V1	0:49:02.10	−73:21:52.3	14.112	−0.163	ELL	7.28417	SMC100.8 #45085 (OGLE-III) SMC_SC5 #16232 (OGLE-II)
V2	0:49:01.82	−73:22:02.8	15.863	0.002	BE	...	SMC100.8 #14736 (OGLE-III) SMC_SC5 #16286 (OGLE-II) [MA93] #277[b]

[a]From OGLE-III photometric maps of the SMC (Udalski et al. 2008)
[b]From Meyssonnier & Azzopardi (1993)

We selected all stars brighter than I=18.2 in the OGLE-III photometry maps, regardless of color, for further study. These stars were matched with their corresponding OGLE-II entries by position and magnitude. There are ∼340 and ∼720 I measurements for each star in the OGLE-II and -III data bases, respectively. After elimination of obviously discordant data points, spurious periodic signals were removed by subtracting

low-order polynomial fits from short segments of data, typically on a season by season basis. These pre-whitened observations are hereafter identified by the notation I^*.

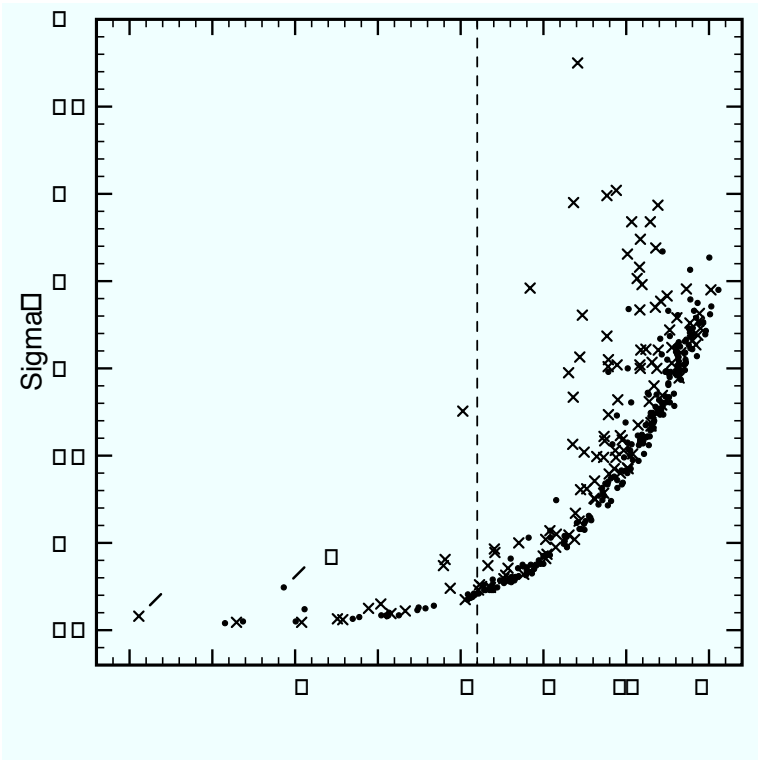

Figure 3. σ vs. I from OGLE-III data for stars in Brück 50. Stars brighter than I=18.2 (the dashed line) were analyzed for photometric variability. Two variable stars were found. Crosses (×) represent stars within the cluster radius ($r_{\rm cls}$=16.5″), while filled circles (•) denote stars lying outside this boundary.

The search for periodicities in I^* data used two techniques: periodogram analysis (Horne & Baliunas 1986) and, in the case of non-sinusoidal signals, phase dispersion minimization (Stellingwerf 1978). The period search covered frequencies in the range 0-20 day^{-1}, which is appropriate for the identification of orbital systems as well as pulsating B/Be stars. OGLE-II and -III data were analyzed separately and then combined if a common signal was present. An upper limit to a full-amplitude sine wave was estimated if no relevant signal could be identified. These limits depend on mean brightness, with typical values near 0.006, 0.012, and 0.018 mag for unblended OGLE-III stars with I ∼16, 17, and 18, respectively. The limits are slightly higher for OGLE-II data.

Only two stars in the direction of Brück 50 show meaningful photometric variations. The results are summarized in Table 1, and individual sources are discussed below. We note that no short-period pulsating variables are present in the cluster, a result that may be related to age. Other SMC clusters with a large population of pulsating variables (e.g. NGC 330) are thought to be slightly older.

Comments on individual sources.

V1: Except for HD 4862, for which no OGLE data are available, V1 is the brightest star in the sample. It lies well inside $r_{\rm cls}$ and is likely to be a member of the cluster. Periodogram analysis of OGLE-II and -III data revealed a very strong signal with P ∼3.64

days. However, when folded on this period, it was obvious that two minima with different depths were present. A revised period of 7.28417±0.00012 days, approximately double the original value, was determined using phase dispersion minimization. The folded I^* light curve, with an overall amplitude of ∼0.08 mag, is shown in Fig. 4. In addition to unequal depths of minima, the curve has two maxima of different heights and widths, which are not symmetrically spaced in phase. The adopted value of T_0 is HJD 2453000.97±0.07 and comes from the best-fit sine wave of the initial periodogram analysis. Hence, in the figure there is a small offset between phase zero and the phase of deepest minimum.

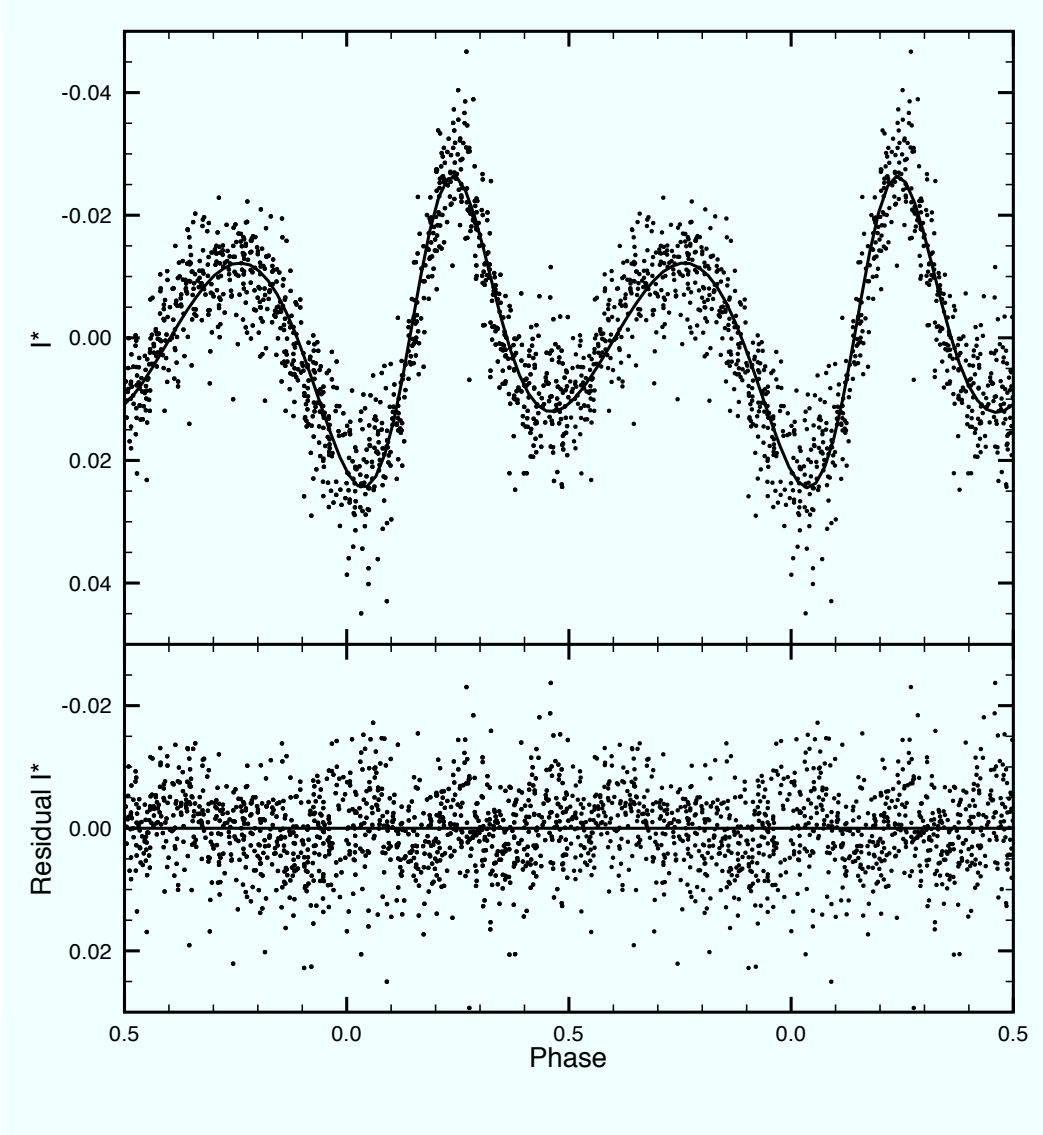

Figure 4. *I* light curve from OGLE-II and -III observations for star V1 of Brück 50. Top: Detrended data folded on the 7.28417-day photometric period, with the fitted model superimposed. Two cycles are shown for clarity. Bottom panel: Residuals between the observed light curve and fitted model. See text.

The light curve for V1 was modeled using version 0.31a of PHOEBE (Prša & Zwitter 2005), a convenient interface to the Wilson-Devinney code (Wilson & Devinney 1971). There are, however, only a few constraints from which to start the modeling process. Our working hypothesis is that of a detached binary system composed of a pair of early-

type (OB) stars, but little is known about the temperature of either component. The observed color is not a good discriminant for a combination of hot stars, and no spectrum is available to define the spectral type(s). The adopted temperature of the primary star was set at T_1=26000 K. The gravity darkening and albedo coefficients were fixed at values appropriate for radiative envelopes, i.e., g=1.0 and A=1.0. Limb darkening coefficients were estimated via interpolation of the van Hamme (1993) tables.

The orbital inclination must be great enough to reveal ellipsoidal variations of the tidally distorted components but not so large as to produce eclipses. In initial models, both i and the mass ratio q ($=M_2/M_1$) were adjusted until the depths of minimum matched the observed light curve. These parameters were then fixed at i=51.5° and q=1.175 for all subsequent calculations. Spectroscopic observations are needed to confirm the value for q. At this stage of the modeling process, fitted values were obtained for the semimajor axis (a), temperature of the secondary star (T_2), and surface potential of each component (ψ_1, ψ_2).

In the remaining step, the model was expanded to include the orbital eccentricity (e) and longitude of periastron (ω). These two parameters are needed to account for the observed heights, widths, and phasing of maxima. Because e and ω are highly correlated, one of them must be fixed in the final solution. We tested a set of models with a range of values for e. Satisfactory fits were produced for $0.07 \leq e \leq 0.10$. No stable solution was found for an eccentricity >0.10. We note that these values for e are consistent with those found in many short-period B-type spectroscopic binaries (see the summary by Abt 2005). Adopting e=0.10, a final solution with five fitting parameters was obtained. Our provisional results are listed in Table 2 and plotted in Fig. 4. The stellar sizes and gravities given in the table are calculated quantities that represent the equivalent values for spherical stars that have the same volume as the tidally distorted ones.

The modeled light curve is a good match to the observations at both minima and near the fainter maximum, but there are systematic errors at other phases. For example, neither the height of the narrow sharp peak of brighter maximum nor the rise to fainter maximum is well matched. These deficiencies likely occur due to changing shapes of the Roche potentials in an eccentric orbit. At periastron, the primary star must be close to filling its lobe, resulting in a temporary state of mass transfer and accounting for $M_2 > M_1$. Hence, there is a limiting value for e in stable solutions. The alternation between detached and semi-detached condition is a very difficult configuration to model, since lobe-filling binaries normally require the assumption of circular orbits. A series of spectra taken near periastron may help clarify our interpretation of this interesting binary system.

Table 2. Provisional Light Curve Parameters for Star V1

Fixed Parameters		Fitted Parameters		Calculated Parameters	
P	7.28417 d	a	48.34±0.03 $R_\odot$	M_1	13.17 $M_\odot$
T_1	26000 K	T_2	20040±120 K	M_2	15.48 $M_\odot$
$q=M_2/M_1$	1.175	ψ_1	5.13±0.04	R_1	12.84 $R_\odot$
i	51.5°	ψ_2	7.31±0.03	R_2	9.07 $R_\odot$
e	0.10	ω	2.80±0.01 rad	log g_1	3.34
				log g_2	3.71

V2: This is a known emission-line star, [MA93] #277 (Meyssonnier & Azzopardi 1993). Because it lies just outside of $r_{\rm cls}$, cluster membership is uncertain. The OGLE light curve, spanning 12 years of observations, is shown in Fig. 5. The erratic variations are consistent with those of Type-1 Be stars described by Mennickent et al. (2002). The smoothest data

segments were detrended and searched for periodicities. No coherent signal was found.

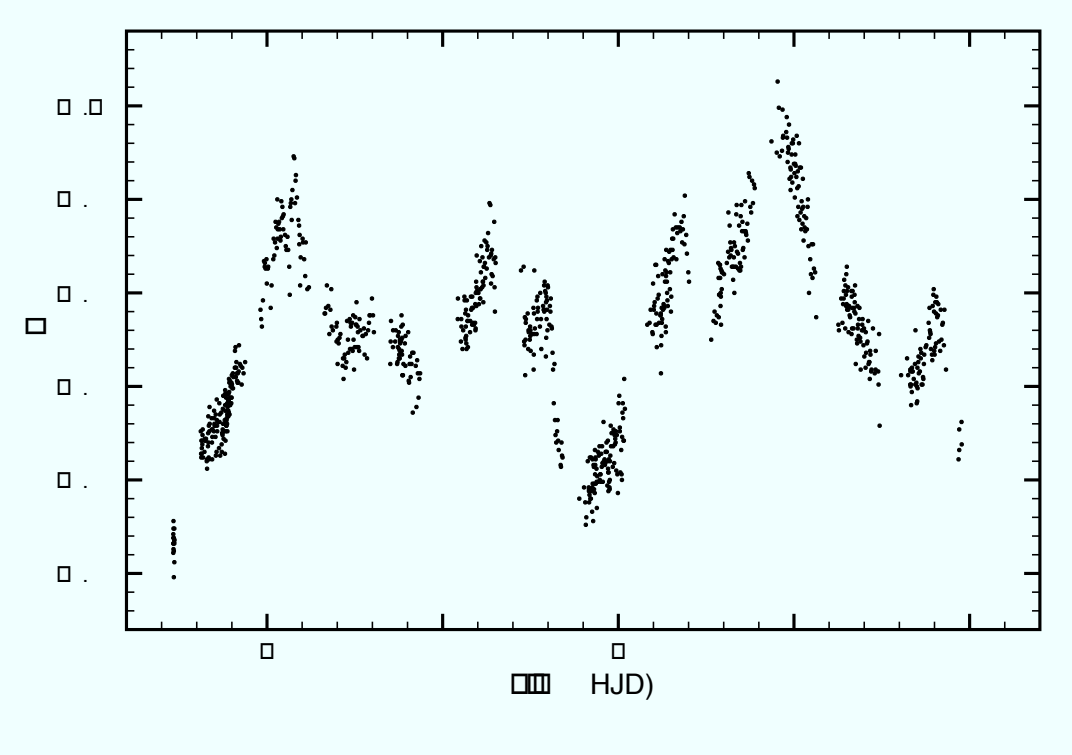

Figure . *I* light curve from OGLE-II and -III observations for star V2 of Brück 50.

Acknowledgments: The OGLE project has received funding from the European Research Council under the European Community's Seventh Framework Programme (FP7/2007-2013) / ERC grant agreement no. 246678 to AU.

References:

Abt, H. A., 2005, *ApJ*, **629**, 507
Balona, L. A., 2010, Challenges in Stellar Pulsation, Bentham Science Publishers, p. 25
Bica, E. L. D., & Schmitt, H. R., 1995, *ApJS*, **101**, 41
Brück, M. T., 1976, *Occas. Rep. R. Obs. Edinburgh*, No. **1**, 1
Diago, P. D., Gutiérrez-Soto, J., Fabregat, J., & Martayan, C., 2008, *A&A*, **480**, 179
de Oliveira, M., R., Dutra, C. M., Bica, E., & Dottori, H., 2000, *A&AS*, **146**, 57
Glatt, K., Grebel, E. K., & Koch A., 2010, *A&A*, **517**, A50
Horne, J. H., & Baliunas, S., L., 1986, *ApJ*, **302**, 757
Kołaczkowski, Z., et al., 2006, *Mem. Soc. Astron. Ital.*, **77**, 336
Lennon, D. J., 1997, *A&A*, **317**, 871
Mennickent, R.E., Pietrzyński, G., Gieren, W., & Szewczyk, O. 2002, *A&A*, **393**, 887
Meyssonnier, N., & Azzopardi, M. 1993, *A&AS*, **102**, 451
Moffat, A. F. J. 2012, *ASP Conf. Ser.*, **465**, 3
Pietrzyński, G., Udalski, A., Kubiak, M., Szymański, M., Woźniak, P., & Żebruń, K., 1998, *Acta Astron.*, **48**, 175
Prša, A., & Zwitter, T., 2005, *ApJ*, **628**, 426

Oey, M. S., King, N. L., & Parker, J., Wm., 2004, *AJ*, **127**, 1632
Schmidtke, P. C., Cobanian, J. B., & Cowley, A. P., 2008, *AJ*, **135**, 1350
Stellingwerf, R. F., 1978, *ApJ*, **224**, 953
Talavera, M. L., Ahumada, A. V., Clariá, J. J., Santos, J. F. C., Jr., Bica, E., Torres, M. C., 2007, *Boletín de la Asociación Argentina de Astronomía*, **50**, 157
Udalski, A., Kubiak, M., & Szymański, M., 1997, *Acta Astron.*, **47**, 319
Udalski, A., Szymański, M., Kubiak, M., Pietrzyński, G., Woźniak, P., & Żebruń, K., 1998, *Acta Astron.*, **48**, 147
Udalski, A., Szymański, M. K., Soszyński, I., & Poleski, R., 2008a, *Acta Astron.*, **58**, 69
Udalski, A., et al., 2008b, *Acta Astron.*, **58**, 329
van Hamme, W., 1993, *AJ*, **106**, 2096
Wilson, R. E., & Devinney, E. J., 1971, *ApJ*, **166**, 605

COMMISSIONS 27 AND 42 OF THE IAU
INFORMATION BULLETIN ON VARIABLE STARS

Number 6075

Konkoly Observatory
Budapest
12 September 2013

HU ISSN 0374 – 0676

NEW TIMES OF MINIMA FOR SOME ECLIPSING BINARY STARS

GÜRSOYTRAK, H.; DEMİRCAN, Y.; GÖKAY, G.; OKAN, A.; TERZİOĞLU, Z.; SARAL, G.; ŞEMUNİ, M.; KILIÇ Y.; CERİT, S.; ALPSOY, M.; YOLKOLU, A.; ŞAHİN, Ş.; GÜROL, B.

Ankara University Observatory, Faculty of Science, Astronomy and Space Sciences Department 06100, Tandoğan, Ankara, TÜRKİYE; e-mail: hande.gursoytrak@science.ankara.edu.tr

Observatory and telescope:
16″ Schmidt/Cassegrain telescope at Ankara University Observatory

Detector:	Apogee ALTA U47+ back illuminated CCD camera, Peltier cooling, E2V CCD47-10 chip, 1024 × 1024 pixels.

Method of data reduction:
Reduction of the CCD frames was made with the IRAF[1] CCDRED and DAOPHOT packages.

Method of minimum determination:
The minima times were computed with several methods in Minima25b (Nelson, 2006) (parabolic fit, tracing paper, bisectors of chords, Kwee and van Woerden method (Kwee & van Woerden, 1956), Fourier fit and sliding integration technique). We calculated the mean minimum-time value from all the filters for a given star and tabulated this value in the Table.

[1]IRAF is distributed by the National Optical Astronomical Observatories, operated by the Association of the Universities for Research in Astronomy, inc., under cooperative agreement with the National Science Foundation

Times of minima:					
Star name	Time of min. HJD 2400000+	Error	Type	Filter	Rem.
LO And	55825.5030	0.0001	II	VRI	TO-YK-MÖ
	55880.2883	0.0002	II	BVRI	AO-GG-MAk
V546 And	55854.3219	0.0000	I	BVRI	ZT
	55854.5136	0.0003	II	BVRI	ZT
GK Boo	56034.5133	0.0001	I	BVRI	AO-YŞ-DG
HH Boo	56046.2957	0.0001	II	BVI	YD
	56046.4537	0.0002	I	BVI	YD
AK Cam	55908.3271	0.0027	II	VRI	AO-GG-SC
V474 Cam	56034.3074	0.0000	I	BVRI	AO-YŞ-DG
EO CVn	56021.3562	0.0004	II	BVRI	ZT-AY
	56021.5340	0.0009	I	BVRI	ZT-AY
EY CVn	56010.5939	0.0017	II	RI	SC-YK
V1046 Cas	55836.4436	0.0001	I	BVRI	YD-TO-AK
	55865.3677	0.0007	II	BVRI	AY-MMK
	55866.3486	0.0008	II	BVRI	AO-GG-YŞ
EF Cep	55821.5536	0.0003	II	BVRI	CY-MA
	55829.4329	0.0004	II	BVRI	YD-TO-AK
	56008.2389	0.0007	II	BVRI	MBD-MNB
	56008.5420	0.0006	I	BVRI	MBD-MNB
V796 Cep	55874.5435	0.0002	I	VRI	MBD-MSH-MA
	55897.5311	0.0006	II	BVRI	GS-AY-MÖ
GSC 3996-0574	55873.4330	0.0008	I	BVRI	GG
ASAS J013630+0150.3	55855.2944	0.0002	I	BVRI	CY
	55855.4263	0.0002	II	BVRI	CY
	55855.5618	0.0002	I	BVRI	CY
TW CrB	56055.4373	0.0005	II	BVRI	AO-ŞŞŞ-YŞ
HI Dra	55825.2723	0.0047	I	BVRI	TO-YK-MÖ
TYC 3069-1654-1	56049.4065	0.0007	II	BVRI	ZT-OY-CY
	56082.4960	0.0007	II	BVRI	GG-MAk -EAy
GV Leo	56014.3221	0.0002	II	BVRI	AO-GG
TYC 1426-857-1	55970.5213	0.0002	II	BRI	GS
V2612 Oph	56081.4971	0.0003	II	BVRI	MNB-MBD
	56084.4990	0.0002	II	BVRI	ZT-OY
V407 Peg	55830.4822	0.0012	I	BVRI	AY-CY
	55832.3924	0.0017	I	BVRI	YK
	55833.3529	0.0006	II	BVRI	MBD-AY
	55834.3034	0.0009	I	BVRI	GS
GSC 2750-0854	55841.3555	0.0016	II	BVRI	GS-SC
ASAS J225956+1418.2	55855.2643	0.0002	II	BVRI	CY
V384 Ser	56080.3651	0.0001	I	BVRI	MSH
	56080.4991	0.0006	II	BVRI	MSH
V1367 Tau	55873.6325	0.0005	II	VRI	GG
	55901.4483	0.0008	II	BVRI	AO-YŞ-GG
	55901.6194	0.0007	I	VRI	AO-YŞ-GG
V354 UMa	56016.3144	0.0012	II	BVRI	CY-KG-EÇ
	56016.4583	0.0008	I	BVRI	CY-KG-EÇ
PS Vir	56011.3540	0.0002	II	BVRI	YD
	56011.5006	0.0003	I	BVRI	YD
ASAS J205847+2731.9	55829.3192	0.0002	I	BVRI	YD-TO-AK

Explanation of the remarks in the table:
Observers: AK: Altuğ KARADAĞ, AO: Abdullah OKAN, AY: Arzu YOLKOLU, CY: Ceren YILDIRIM, DG: Damla GÜMÜŞ, EAy : Ezgi AYDOĞDU, EÇ: Emine ÇÖLKUŞU, GG: Gökhan GÖKAY, GS: Gözde SARAL, KG: Kübra GÜLLÜ, MA: Mehmet ALPSOY, MAk : Mihriban AKI, MBD: Mustafa Burak DOĞRUEL, MMK: Metehan Metin KEKLİK, MNB: Mehmet Naim BAĞIRAN, MÖ: Maksude ÖZTÜRK, MSH: Muhammed ŞEMUNİ, OY: Onur YÖRÜKOĞLU, SC: Sonay CERİT, ŞŞŞ: Şakir Şenol ŞAHİN, TO: Tahsin OZUN, YD: Yahya DEMİRCAN, YK: Yücel KILIÇ, YŞ: Yunus ŞENDAĞ, ZT: Zahide TERZİOĞLU

Acknowledgements:
We are grateful to the Ankara University Observatory for the allocated telescope time and for the use of other facilities.

References:

Kwee, K. K., van Woerden, H., 1956, *Bull. Astron. Inst. Neth.*, **12**, 327.
Nelson, B., 2006, Minima v2.3, `http://www.members.shaw.ca/bob.nelson/software1.htm`

COMMISSIONS 27 AND 42 OF THE IAU
INFORMATION BULLETIN ON VARIABLE STARS

Number 6076

Konkoly Observatory
Budapest
17 September 2013

HU ISSN 0374 – 0676

SIMULTANEOUS MULTICOLOUR PHOTOMETRY OF LATE-TYPE GIANT STARS

KURATOV, K. S.[1]; MIROSHNICHENKO, A. S.[2]; ZAKHOZHAY, V. A.[3]; GORSHANOV, D.L.[4]

[1] Fesenkov Astrophysical Institute, Kamenskoe plato, Almaty 050020, Kazakhstan, e-mail: kenes_kuratov@mail.ru

[2] Department of Physics and Astronomy, University of North Carolina at Greensboro, Greensboro, NC 27402, USA, e-mail: a_mirosh@uncg.edu

[3] V. N. Karazin Kharkiv National University, 4 Svobody Sq., 310022 Kharkov, Ukraine, e-mail: zkhvladimir@mail.ru

[4] Central Astronomical Observatory of the Russian Academy of Sciences, Pulkovskoe chausse 65/1, Saint-Petersburg, 196140, Russia

Late-type giant stars are post-main-sequence objects undergoing a relatively fast evolution of their interior structure (e.g., dredge-ups, thermal pulses) that causes multi-wavelength variations of their brightness. Simultaneous photometric observations in wide wavelength ranges important to study the behaviour of the objects are still rare. Here we report the results of an observing programme that included 17 objects (7 carbon stars, 7 M–type giants, and 3 Mira variables) which have never been published, except for a short presentation at a carbon star conference (Miroshnichenko et al., 2000). The programme objects were selected from a list of IRAS sources studied by Ivezić & Elitzur (1995).

The $UBVRIJHK$ observations in the Johnson photometric system were obtained between August 1995 and March 1999 at a 1–meter telescope of the Tien-Shan Observatory of the Fesenkov Astrophysical Institute (Kazakhstan) with a two–channel photometer–polarimeter of the Pulkovo Observatory (Bergner et al., 1988). The results are presented in Table 1. The typical duration of an eight filter observation was ∼20 minutes. Each object was observed with one $UBVRI$ and one JHK standard star. The photometric data of standard stars shown in Table 2 was taken from Johnson et al. (1966) and Kornilov et al. (1991). A few missing colour-indices (e.g., $R-I$ and $J-H$) were derived by us. Observations of multiple standard stars every night ensured accurate atmospheric extinction determination and control of the detector's stability.

Transformations between the instrumental and standard photometric systems were derived by observing groups of standard stars every several months and found stable over long time (years). They depend on the spectral sensitivity of the detectors, that changed from time to time. The transformations for the detectors used in 1980's were published in Bergner et al. (1988). Those derived during the time of reported observations are as follows: $\Delta(U-B) = (0.958 \pm 0.008)\,\Delta(u-b)$, $\Delta(B-V) = (0.983 \pm 0.007)\,\Delta(b-v)$, $\Delta V = \Delta v + (0.077 \pm 0.012)\,\Delta(b-v)$, $\Delta R = \Delta r - (0.47 \pm 0.02)\,\Delta(r-i)$, $\Delta(R-I) = (0.90 \pm 0.02)\,\Delta(r-i)$, $\Delta(J-H) = (0.82 \pm 0.02)\,\Delta(j-h)$, $\Delta(H-K) = (0.99 \pm 0.02)\,\Delta(h-k)$, and $\Delta K = \Delta k + (0.02 \pm 0.02)\,\Delta(h-k)$. Capital letters refer to the standard system, and lower

case letters refer to the instrumental magnitudes and colour-indices free of atmospheric extinction. The Δ notation refers to the magnitude and colour-index differences between variables and comparison stars.

The photometer was designed to use two single-element detectors (a GaAs photomultiplier for the optical range and a PbS photoresistor for the near-IR range) simultaneously to collect the star light and subtract the sky background. It was ideal for observing objects with a very red continuum or strong IR excesses. Numerous results on a wide variety of objects ranging from pre-main-sequence stars to those at advanced evolutionary stages obtained with this device in 1984–2002 have been published in many papers. Some examples include multicolour photometry of VV Cep stars (Miroshnichenko & Ivanov, 1993), objects with the B[e] phenomenon (Bergner et al., 1995), the newly discovered Mira V1137 Aql (Miroshnichenko, 2001), the LBV candidate MWC 930 (Miroshnichenko et al., 2005), and the Be binary δ Scorpii (Carciofi et al., 2006).

The intent of this paper is to report the data which can be useful for constructing more detailed light curves of the objects, analyzing their spectral energy distributions, modeling their dusty envelopes, etc. These data may be important because all the objects are very bright in the near-IR region and therefore saturate most modern detectors, including those of actively used all-sky surveys (2MASS, DENIS, etc.).

Table 1. Photometric data

Star	JD−2400000	$U-B$	$B-V$	V	$V-R$	$R-I$	J	H	K
EP Aqr	49939.28	0.65	1.68	6.48	3.24	1.82	−0.28	−1.06	−1.44
EP Aqr	49943.34	0.59	1.76	6.53	3.07	1.99	−0.29	−1.05	−1.44
R Cnc	50093.35	−0.29	1.80	7.93	3.56	2.33	0.37	−0.49	−0.94
R Cnc	50105.32	−0.31	1.84	8.22	3.48	2.36	0.39	−0.44	−0.87
R Cnc	50415.48	−0.03	1.78	7.98	3.39	2.25	0.69	−0.04	−0.51
R Cnc	50416.48	0.00	1.74	8.03	3.37	2.34	0.68	−0.05	−0.47
R Cnc	50417.47	0.00	1.75	7.99	3.32	2.29	0.58	−0.15	−0.52
R Cnc	50419.45	0.01	1.74	8.04	3.36	2.18	0.68	−0.06	−0.51
R Cnc	50422.43	0.00	1.77	8.07	3.29	2.12	0.66	−0.10	−0.52
R Cnc	50423.44	−0.07	1.72	8.15	3.46	2.29	0.65	−0.08	−0.60
R Cnc	50424.44	−0.04	1.79	8.09	3.37	2.27	0.65	−0.15	−0.53
R Cnc	50429.43	−0.10	1.80	8.22	3.49	2.40	0.58	−0.21	−0.62
R Cnc	50433.40	−0.11	1.75	8.32	3.41	2.29	0.67	−0.01	−0.53
R Cnc	50439.39	−0.13	1.76	8.44	3.45	2.28	0.58	−0.18	−0.61
R Cnc	50538.16	−0.08	1.74	10.99	4.47	3.13	1.03	0.20	−0.47
R Cnc	51153.41	−0.11	1.64	7.74	3.56	2.24	–	–	–
Y CVn	50101.51	5.32	3.28	5.50	2.04	1.35	1.17	0.14	−0.61
Y CVn	50538.39	–	3.25	5.15	1.95	1.28	0.87	−0.05	−0.66
Y CVn	50540.34	–	3.20	5.30	1.95	1.27	0.90	−0.02	−0.70
V CVn	50540.38	1.13	1.81	7.97	2.64	1.86	2.21	1.41	1.10
S Cep	49940.44	–	6.17[a]	9.44[b]	3.16[b]	1.75	2.54	1.23	−0.01
S Cep	49944.36	–	5.71	9.34	3.10	1.68	2.51	1.24	−0.04
S Cep	50342.29	–	–	–	–	–	2.99	1.83	0.64
V CrB	50540.41	–	3.77	7.85	1.89	1.25	3.29	2.32	1.47
V CrB	51246.45	–	4.64	8.76	2.22	1.29	3.67	2.64	1.69

Table 1. Photometric data (continued)

Star	JD−2400000	$U-B$	$B-V$	V	$V-R$	$V-I$	J	H	K
U Cyg	50428.03	–	5.26	8.87	2.83	1.61	2.81	2.04	1.26
U Cyg	50433.03	–	5.29	8.58	2.66	1.69	2.75	1.94	1.20
RY Dra	50101.54	–	3.64	6.94	2.11	1.60	2.01	1.29	0.46
RY Dra	50107.46	4.42	3.72	6.92	2.17	1.43	2.00	1.28	0.44
RY Dra	50538.36	4.81	4.00	6.51	2.09	1.30	1.80	1.06	0.23
CS Dra	50093.49	0.49	2.02	10.73	3.80	2.77	2.09	1.18	0.72
CS Dra	50538.27	0.70	1.99	10.52	3.61	2.47	2.13	1.12	0.73
CS Dra	50540.31	0.28	1.75	10.75	3.46	2.47	2.36	1.45	0.92
RV Peg	50673.36	−0.03	1.97	11.72	4.19	2.58	3.03	2.30	1.86
RV Peg	50674.37	−0.09	1.92	11.71	4.15	2.54	3.06	2.32	1.82
RV Peg	50677.35	–	1.87	11.74	4.28	2.58	3.05	2.22	1.83
RZ Peg	50424.03	–	4.29	9.78	2.27	1.40	4.36	3.45	2.88
RZ Peg	50427.03	–	4.52[c]	9.63	2.13	1.39	4.40	3.44	2.82
RZ Peg	50429.04	–	–	–	–	–	4.40	3.47	2.89
RZ Peg	50439.03	–	4.17	9.34	2.16	1.28	4.36	3.53	2.83
TW Peg	49940.39	1.24	1.68	7.24	2.89	2.29	0.61	−0.13	−0.51
TW Peg	49942.39	1.23	1.76	7.16	2.85	2.41	0.63	−0.12	−0.52
TW Peg	49944.32	1.24	1.48	7.35	2.94	2.17	0.58	−0.12	–
S Per	50093.14	–	2.73	11.11	4.07	2.58	2.87	1.87	1.24
S Per	50353.45	–	2.68	11.90	3.99	2.17	3.46	2.42	1.65
R UMa	50093.43	0.74	1.29	7.99	2.58	2.19	2.50	1.79	1.30
R UMa	50097.39	0.69	1.32	7.93	2.62	2.10	2.43	1.69	1.27
R UMa	50107.44	0.58	1.27	8.19	2.74	2.27	2.34	1.62	1.15
R UMa	50538.25	0.46	1.92	11.97	4.13	2.71	2.70	1.89	1.44
R UMa	50540.27	0.26	2.08	11.86	4.03	2.71	2.62	1.94	1.45
R UMa	51246.29	0.61	1.57	10.74	3.74	2.52	3.06	2.34	1.76
RZ UMa	50419.48	0.76	1.80	9.46	3.36	2.16	2.09	1.42	1.09
RZ UMa	50422.48	0.68	1.98	9.38	3.08	1.98	2.07	1.35	1.03
RZ UMa	50423.48	0.76	1.78	9.54	3.45	2.24	2.11	1.32	1.00
RZ UMa	51160.43	0.88	1.82	8.89	3.15	2.12	–	–	–
VY UMa	50093.46	4.63	2.59	6.06	1.62	1.34	2.15	1.18	0.64
VY UMa	50097.41	4.56	2.61	6.03	1.66	1.25	2.11	1.19	0.66
VY UMa	50101.46	4.65	2.56	6.08	1.64	1.30	2.13	1.15	0.62
VY UMa	50107.42	4.83	2.58	6.11	1.64	1.32	2.12	1.17	0.64
VY UMa	50538.22	4.79	2.60	6.14	1.65	1.24	1.98	1.12	0.64
VY UMa	50540.29	4.96	2.69	6.08	1.67	1.25	1.92	1.04	0.52
VY UMa	51246.29	4.81	2.63	6.15	1.68	1.32	2.12	1.14	0.65
AZ UMa	50097.48	0.93	1.72	8.72	3.12	2.00	2.09	1.23	0.84
AZ UMa	50538.30	0.90	1.52	8.64	3.04	2.02	2.01	1.20	0.82

The typical uncertainties (including those of transformation from the instrumental to the standard photometric system) are as follows: $0\overset{\mathrm{m}}{.}02$ in V, $B-V$, J, H, and K; $0\overset{\mathrm{m}}{.}04$ in $V-R$ and $R-I$; $0\overset{\mathrm{m}}{.}02$ in $U-B$ for $U \leq 12\overset{\mathrm{m}}{.}5$; $0\overset{\mathrm{m}}{.}04$ in $U-B$ for fainter U–magnitudes.
Larger uncertainties for specific cases are marked with letters: [a] $0\overset{\mathrm{m}}{.}08$, [b] $0\overset{\mathrm{m}}{.}05$, [c] $0\overset{\mathrm{m}}{.}04$.

Table 2. Data on comparison stars

Var.	Vis. comp	$U-B$	$B-V$	V	$V-R$	$R-I$	IR comp	J	H	K
EP Aqr	HD 207435	0.83	1.01	6.67	0.75	0.32	BS 8414	1.47	1.09	0.97
R Cnc	HD 68425	1.75	1.55	7.65	1.02	0.90	BS 3249	1.08	0.28	0.15
V CVn	HD 116172	0.47	0.93	6.98	0.71	0.47	BS 4997	3.12	2.76	2.66
Y CVn	HD 110835	1.52	1.37	6.96	0.71	0.70	BS 4785	3.23	2.88	2.84
S Cep	HD 209111	1.57	1.54	6.53	1.83	1.60	BS 8347	2.62	1.90	1.70
V CrB	HD 140086	1.53	1.56	6.92	1.18	0.90	BS 5901	3.09	2.58	2.49
U Cyg	HD 194193	1.98	1.65	5.94	1.28	0.85	BS 7796	1.16	0.87	0.75
RY Dra	HD 112640	1.65	1.45	6.55	1.00	0.65	BS 4928	3.08	2.47	2.35
CS Dra	HD 97619	1.46	1.34	6.90	0.96	0.65	BS 4301	0.05	−0.55	−0.65
TW Peg	HD 212750	1.06	1.14	7.13	0.86	0.54	BS 8430	2.98	2.78	2.67
S Per	HD 13403	0.11	0.66	7.02	0.55	0.24	BS 799	3.34	3.07	2.98
RZ UMa	HD 66823	1.94	1.59	7.37	1.23	0.95	BS 3323	1.98	1.49	1.44
AZ UMa	HD 101853	0.73	0.97	6.73	1.02	0.90	BS 4518	1.72	1.08	0.95

Comparison stars for R UMa and VY UMa were the same as for CS Dra.
Comparison stars for RZ Peg and RV Peg were the same as for TW Peg .

References:

Bergner, Yu.K., Bondarenko, S.L., Miroshnichenko, A.S., et al., 1988, *Izv. Glavn. Astron. Obs. v Pulkove*, **205**, 142

Bergner, Yu.K., Miroshnichenko, A.S., Yudin, R.V., et al., 1995, *A&AS*, **112**, 221

Carciofi, A.C., Miroshnichenko, A.S., Kusakin, A.V., et al., 2006, *ApJ*, **652**, 1617

Ivezić, Ž., & Elitzur, M., 1995, *ApJ*, **445**, 415

Johnson, H.L., Mitchell, R.I., Iriarte, B., & Wisniewski, W.Z., 1966, *Comm. Lunar and Planetary Lab.*, **4**, 99

Kornilov, V.G., Volkov, I.M., Zakharov, A.I., et al., 1991, *Trudy Gos. Astron. Inst. Sternberga*, **63**, 4

Miroshnichenko, A.S., 2001, *IBVS*, **5183**, 1

Miroshnichenko, A.S., & Ivanov, A.S. 1993, *Astronomy Letters*, **19**, 372

Miroshnichenko, A.S., Kuratov, K.S., Ivezić, Ž., & Elitzur, M., 2000, IAU Symp. **177**, 566

Miroshnichenko, A.S., Bjorkman, K.S., Grosso, M., et al., 2005, *MNRAS*, **364**, 335

COMMISSIONS 27 AND 42 OF THE IAU
INFORMATION BULLETIN ON VARIABLE STARS

Number 6077

Konkoly Observatory
Budapest
8 October 2013

HU ISSN 0374 – 0676

DISCOVERY OF A NEW PERIODIC VARIABLE STAR CzeV503

LIŠKA, J.[1,2]; SKARKA, M.[1,2]

[1] Department of Theoretical Physics and Astrophysics, Masaryk University, Kotlářská 2, 611 37 Brno, Czech Republic, e-mails: jiriliska@post.cz, maska@physics.muni.cz

[2] Brno Observatory and Planetarium, Kraví hora 2, 616 00 Brno, Czech Republic

The field of the semi-regular variable KU Her (Hoffmeister 1935; Sipahi 2012) and the anomalous Cepheid in eclipsing binary system ASAS J182611+1212.6 (Pojmanski 2002; Antipin, Sokolovsky & Ignatieva 2007) was monitored during three months from June 2013 to September 2013 (see a journal of observations in Table 1). We performed Strömgren *vby* photometry at the Observatory and Planetarium in Brno using 14" Celestron CGE 1400 XLT telescope equipped with a G2-4000 CCD camera (2056×2062 KAI-4022 chip). As the observed stars are long-period variables, typically five frames in each passband with exposure times of 40 to 80 s were gathered per night. We combined the images collected in each night into one single frame (one frame for each passband) to achieve better signal-to-noise ratio. Subsequently, we searched for new long-term variables.

Our effort was rewarded by the identification of CzeV503[1] = USNO-A2 0975-11593384 as a new variable with an amplitude of light changes of about 0.2 mag in y. Although the variability of the star was also noticeable in other two passbands (v, b), these data were inappropriate for further analysis.

All frames were calibrated in the standard way (dark frames and flat fields). The aperture photometry, as well as the reduction, was done using C-Munipack software[2] (Motl 2009) which is based on DAOPHOT (Stetson 1987). USNO-A2 0975-11599404 and USNO-A2 0975-11604298 were used as comparison and check star, respectively.

Despite a three-month monitoring, our data[3] were insufficient for period determination. Fortunately, data of the variable were found in NSVS (Woźniak et al. 2004, unfiltered measurements) and in ASAS-3 (Pojmanski 2002, V band). ASAS data were unusable due to the low number of points (only 29 measurements) and high scatter (the star is too faint for ASAS, 14.7(6) mag). NSVS gathered 176 measurements with brightness 12.9(1) mag and the data showed periodic variations with similar amplitude as our y data. Therefore we stitched them together by simple linear fitting. Such combined dataset was used for period analysis.

We used the Period04 software (Lenz & Breger 2005) and found two probable periods of about 60 d and 120 d. Light variations $m(t)$ were fitted by non-linear least-squares

[1] star included in Czech catalogue of discovered variable stars http://var.astro.cz/newvar.php
[2] http://c-munipack.sourceforge.net/
[3] available online at the IBVS website.

Table 1: Journal of observations. N is the number of combined images.

Night	Start UTC	Exp. [s]	N	Night	Start UTC	Exp. [s]	N
20 June 2013	01:20	60	4	2 August 2013	20:51	80	8
1 July	01:07	40	5	3 August	19:51	80	6
2 July	01:31	40	7	5 August	19:53	80	6
4 July	01:02	40	6	6 August	19:56	80	5
6 July	22:45	40	11	7 August	19:53	80	4
9 July	23:56	40	10	8 August	21:49	80	5
15 July	01:19	40	7	11 August	19:49	80	4
16 July	01:24	40	8	12 August	19:46	80	3
17 July	21:05/1:46	80	5/8	30 August	20:58	80	5
18 July	20:25	80	2	6 September	20:24	80	10
19 July	01:18	40	6	17 September	21:16	80	4
21 July	23:43	80	6	30 September	19:37	80	6
30 July	20:16	80	5				

method, where the main function was selected as a second-order harmonic polynomial ($n = 2$)

$$m(t) = m_0 + \sum_{i=1}^{n} m_i \cos\left(2\,i\,\pi\,\frac{t - E_0}{P}\right), \tag{1}$$

without the often used phase terms (data accuracy is low for finding other free parameters). Time t is in HJD, E_0 is the zero epoch and P is period in days in equation (1). The uncertainty of parameters E_0, P was determined by bootstrap method. The shorter period probably corresponds to a pulsating variable (Fig. 1). The times of maximum light can be expressed as:

$$T_{\max} = 2451308.9(6) + 60.58(2)^{\mathrm{d}} \cdot E \tag{2}$$

According to measurements taken from Zacharias et al. (2004) $m_B = 15.890$ and $m_V = 14.330$ and infrared 2MASS magnitudes $m_J = 9.056(22)$, $m_H = 8.109(25)$ and $m_K = 7.714(23)$ (Cutri et al. 2003), the star is very cool. This can explain also the big difference between ASAS-3 and NSVS magnitudes. ASAS-3 contains measurements in the standard V-band (Pojmanski 2002) $\sim$ (500–600) nm and therefore CzeV503 is fainter than in NSVS that used unfiltered CCD cameras sensitive in range from 450 to 1000 nm (Woźniak et al. 2004) and thus also in infrared band where is CzeV503 brighter than in visual band. Assuming the cool nature of the object, together with the period close to 60 d and low light variations (0.2 mag), we excluded cepheids, which are bluer and of larger amplitudes, as a possible explanation for the variations. Therefore, if 60-day period is the right one, we guess that this star is either a pulsating red giant or a semi-regular giant star.

If the longer period is real (Fig. 2), we assume CzeV503 to be a rotating ellipsoidal variable (non-eclipsing binary; see e.g. Soszynski et al. 2004; Nicholls, Wood & Cioni 2010). The time of minimum can be calculated from the following ephemeris:

$$T_{\min} = 2451399.8(7) + 119.75(4)^{\mathrm{d}} \cdot E. \tag{3}$$

In any case, further observations are needed to solve the problem of the nature of variability of this object.

Acknowledgements: Authors are very grateful to Zdeněk Řehoř for technical support provided to our instruments. This work was supported by the Brno Observatory and Planetarium. We acknowledge the financial support of MUNI/A/0735/2012.

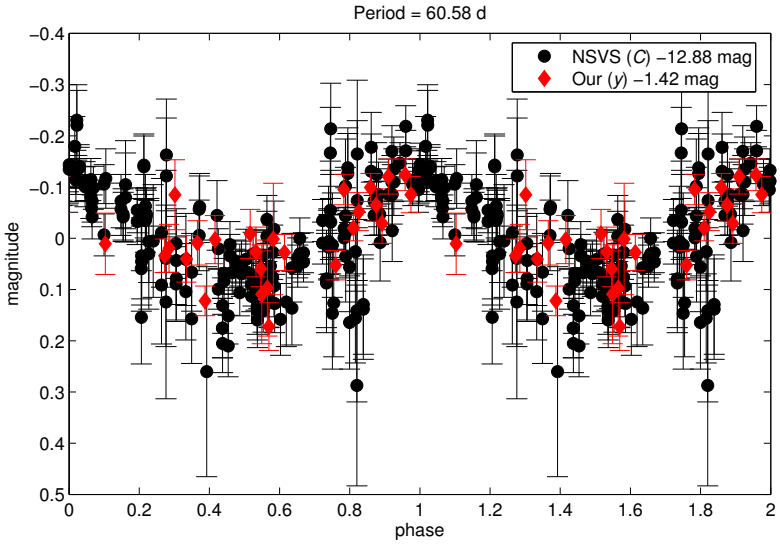

Figure 1. Our data together with data from NSVS database phased according to eq. (2).

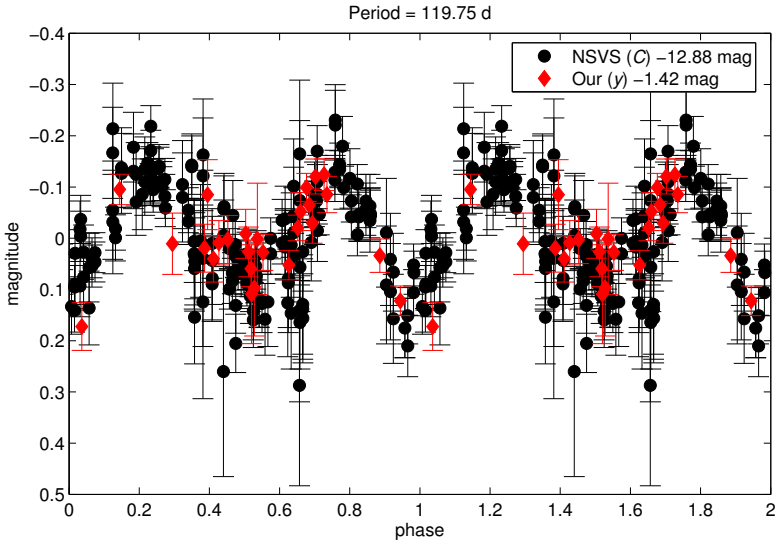

Figure 2. Data folded with the elements given in eq. (3).

References:

Antipin, S. V., Sokolovsky, K. V., Ignatieva, T. I, 2007, *MNRAS*, **379**, L60

Cutri, R. M., Skrutskie, M. F., van Dyk, S., Beichman, C. A., Carpenter, J. M., Chester, T., Cambresy, L., Evans, T., Fowler, J., Gizis, J., Howard, E., Huchra, J., Jarrett, T., Kopan, E. L., Kirkpatrick, J. D., Light, R. M., Marsh, K. A., McCallon, H., Schneider, S., Stiening, R., Sykes, M., Weinberg, M., Wheaton, W. A., Wheelock, S., Zacarias, N., 2003, *VizieR Online Data Catalog*, **2246**

Hoffmeister, C., 1935, *Astron. Nachr.*, **255**, 401

Lenz P., Breger M., 2005, *Comm. Asteroseismology*, **146**, 53

Motl, D., 2009, C-Munipack, http://c-munipack.sourceforge.net/

Nicholls, C. P., Wood, P. R., Cioni, M.-R. L., 2010, *MNRAS*, **405**, 1770

Pojmanski, G., 2002, *Acta Astronomica*, **52**, 397

Sipahi, E., 2012, *New Astronomy*, **17**, 377

Soszynski, I., Udalski, A., Kubiak, M., Szymanski, M. K., Pietrzynski, G., Zebrun, K., Szewczyk, O., Wyrzykowski, L., Dziembowski, W. A., 2004, *Acta Astronomica*, **54**, 347

Stetson, P.B., 1987, *PASP*, **99**, 191

Woźniak, P. R., Vestrand, W. T., Akerlof, C. W., Balsano, R., Bloch, J., Casperson, D., Fletcher, S., Gisler, G., Kehoe, R., Kinemuchi, K., Lee, B. C., Marshall, S., McGowan, K. E., McKay, T. A., Rykoff, E. S., Smith, D. A., Szymanski, J., Wren, J., 2004, *AJ*, **127**, 2436

Zacharias, N., Monet, D. G., Levine, S. E., Urban, S. E., Gaume, R., Wycoff, G. L., 2004, *BAAS*, **36**, 1418 (AAS 205.4815)

*This version of the paper contains corrections, and differs from the one appeared on-line originally. Date of last modification: Wed Nov 6 06:37:18 CET 2013

COMMISSIONS 27 AND 42 OF THE IAU
INFORMATION BULLETIN ON VARIABLE STARS

Number 6078

Konkoly Observatory
Budapest
17 October 2013

HU ISSN 0374 – 0676

A MISIDENTIFIED RR LYRAE VARIABLE STAR IN ω CENTAURI†

NAVARRETE, C.[1,2]; CATELAN, M.[1,2]; CONTRERAS RAMOS, R.[1,2]; ALONSO-GARCÍA, J.[1,2]; DÉKÁNY, I.[1,2]; GRAN, F.[1,2]; HEMPEL, M.[1,2]; ANGELONI, R.[1,2,3]

[1] Instituto de Astrofísica, Facultad de Física, Pontificia Universidad Católica de Chile, Av. Vicuña Mackenna 4860, 782-0436 Macul, Santiago, Chile; e-mail: (cnavarre;mcatelan)@astro.puc.cl

[2] The Milky Way Millennium Nucleus, Av. Vicuña Mackenna 4860, 782-0436 Macul, Santiago, Chile

[3] Departamento de Ingeniería Eléctrica, Pontificia Universidad Católica de Chile, Av. Vicuña Mackenna 4860, 782-0436 Macul, Santiago, Chile

With a total population of variable stars now approaching 500, including nearly 200 RR Lyrae (Clement et al. 2001; Kaluzny et al. 2004; Weldrake et al. 2007), ω Centauri = NGC 5139 (RA $13^{\rm h}26^{\rm m}47\overset{\rm s}{.}28$, DEC $-47\,^\circ28'46.1''$, J2000) represents an excellent laboratory for studies of stellar variability, and indeed is one of the best known such laboratories to study RR Lyrae-type variables in particular.

Kaluzny et al. (2004) performed a detailed variability search in ω Cen, finding 117 new variables, in addition to the 275 previously known ones (Clement et al. 2001). More recently, Weldrake et al. (2007) performed a new wide-field variability survey of the cluster, covering 0.75 deg^2 – i.e., 4 times the Kaluzny et al. field of view. They recovered 106 variables from the Kaluzny et al. catalogue, and reported the discovery of 81 additional variable stars.

In this note, we report the identification, from near-IR photometry, of an ω Cen RR Lyrae variable star previously misidentified by Weldrake et al. (2007). Accurate coordinates, light curves and periods are presented for both this star and the one with which it was erroneously associated.

Our work is based on time-series $J, K_{\rm s}$ observations, obtained with the 4-m VISTA telescope at ESO's Cerro Paranal Observatory, using the wide-field, near-IR VIRCAM camera (Dalton et al. 2006). The total (effective) FoV of the camera is 1.1×1.5 deg^2, which is larger than the field studied by Weldrake et al. (2007). We present the photometry for the so-called "pawprint" images (see, e.g., Minniti et al. 2010, for an explanation and additional references), hereafter referred to simply as images. The data set was obtained in service mode, between December 2011 and April 2012, comprising a total of 252 and 600 images in J and $K_{\rm s}$, respectively, covering a time span of 352 days. However, due to the way these images are taken (see Minniti et al. 2010), they effectively represent 42 and 100 independent epochs in J and $K_{\rm s}$, respectively. These observations were obtained mainly in an effort to obtain near-IR light curve templates, to assist in the automated classification of the light curves obtained in The Vista Variables in the Vía Láctea (VVV)

†Based on observations made with the ESO VISTA Telescope at Paranal Observatory under programme ID 087.D-0472(A).

ESO Public Survey (Minniti et al. 2010; Catelan et al. 2011, 2013). Nevertheless, a quick search for new variable stars was also carried out, using DAOPHOT II/ALLFRAME (Stetson 1987, 1994).

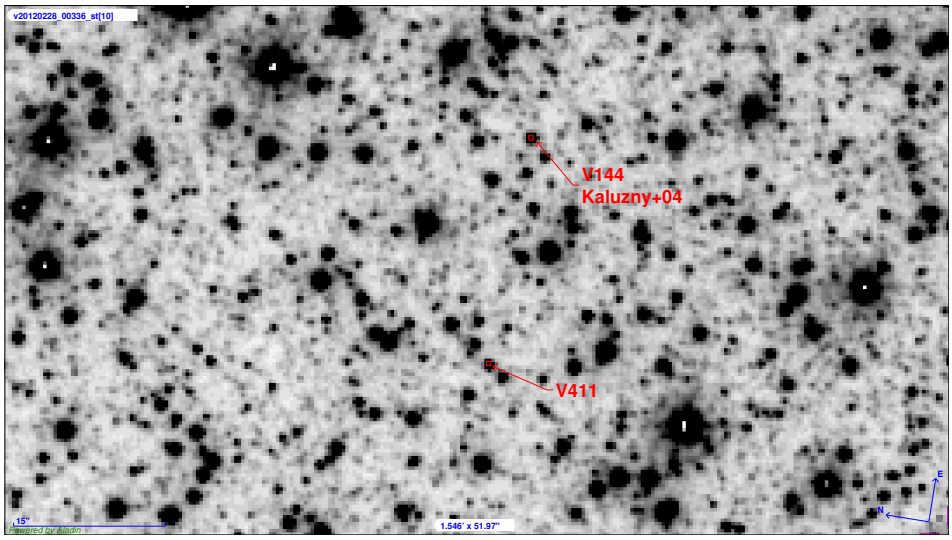

Figure 1. Finding chart for the two RR Lyrae variable stars, based on one of our K_s images. North is to the left and East is up. The scale is 0.34 arcsec/pixel. V411 is the new name proposed for ID-133 in Weldrake et al. (2007). The angular distance between V144 and V411 is 22.7 arcsec.

Thus, stars whose time series presented high standard deviation, compared to the non-variable stars, were selected as candidate variables. The analysis of variance (AoV) statistic (Schwarzenberg-Czerny 1989) was then used to determine the periods, if present, for these candidates. Periods were then refined using ANOVA (Schwarzenberg-Czerny 1996). Only stars brighter than 14th mag in K_s were considered, thus limiting our search mostly to RR Lyrae and type II Cepheids.

All the previously known variables in this magnitude range were recovered successfully. Among them, we recovered both V144 from Kaluzny et al. (2004) and ID-133 from Weldrake et al. (2007). This was initially surprising, since Weldrake et al. classified their ID-133 as being the same star as V144 in the Kaluzny et al. catalogue. Further analysis confirmed that these are indeed different stars. Figure 1 shows a finding chart, in one of our K_s images.

Coordinates, magnitude-weighted mean magnitudes, periods, and variability types are presented in Table 1. Despite the fact that the two variables have very similar periods and mean magnitudes, the differences are significant, and their respective light curve shapes present slight but noticeable differences as well (Fig. 2). For this reason, we propose to rename variable ID-133 in Weldrake et al. (2007) as V411, following the standard nomenclature and current entries in the latest edition of the Sawyer-Hogg/Clement catalogue of variable stars in globular clusters (Clement et al. 2001; Clement 2013, priv. comm.).

In order to check our results, we matched the positions of ID-133 (V411) and V144 with the Sollima et al. (2004) near-IR catalogue for stars in the ω Cen central region. Sollima et al. derived mean J and K_s magnitudes, in the 2MASS filter system, for 73,000 stars. Matching our coordinates with their catalogue, we find matches for both stars whose magnitudes are fully consistent with ours, to within the errors.

Table 1. Properties of V144 and V411, Based on VISTA Observations.

Name	Proposed ID[b]	LEID[c]	RA (J2000)	DEC (J2000)	$\langle J \rangle$	$\langle K_s \rangle$	Period (d)	Type
ID-133[a]	V411	42208	13:26:40.77	−47:28:17.00	13.236	12.878	0.84488	RRab
V144	V144	42231	13:26:43.02	−47:28:18.01	13.148	12.808	0.83352	RRab

Notes:
[a] As given in Weldrake et al. (2007).
[b] Following the Sawyer-Hogg scheme (Clement et al. 2001).
[c] LEID Identification number from van Leeuwen et al. (2000).

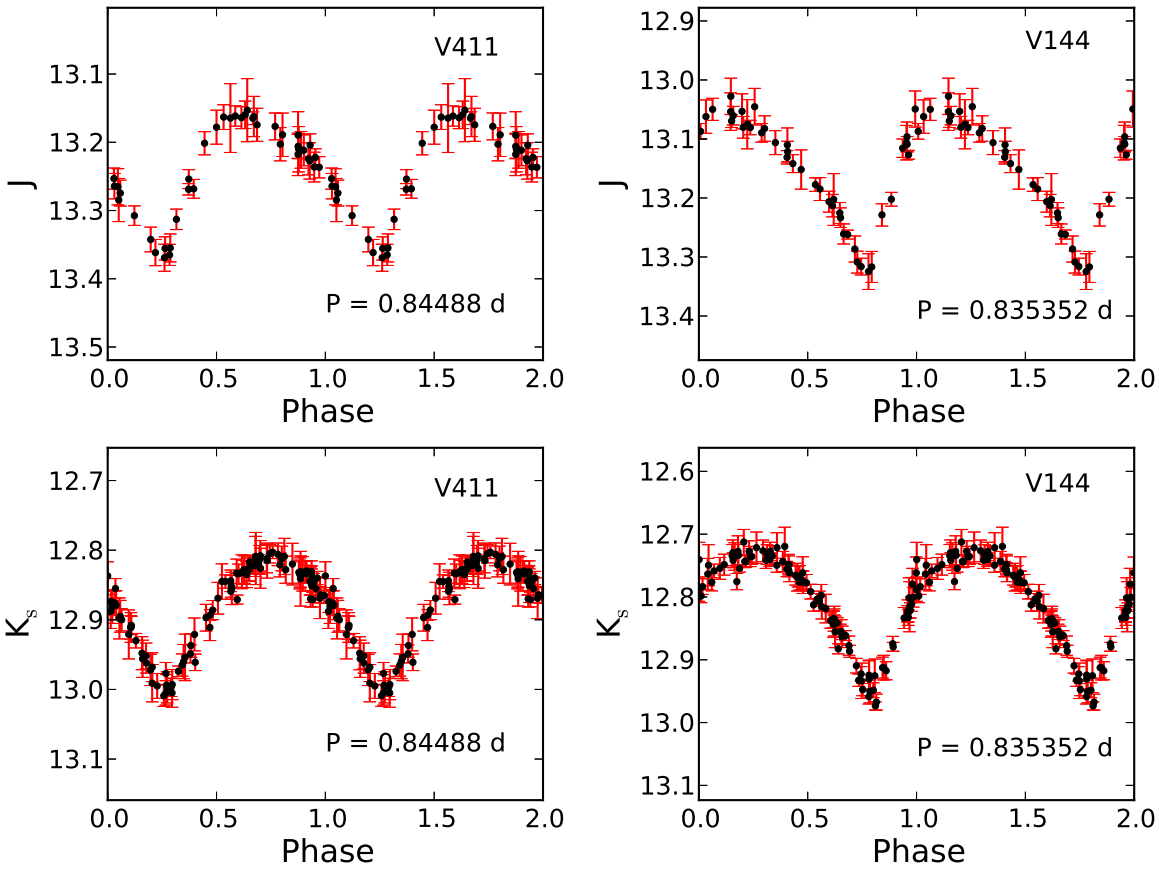

Figure 2. VISTA near-IR light curves for the two RR Lyrae stars, V411 = ID-133 in Weldrake et al. (2007, *left panels*) and V144 (*right panels*). The upper and lower panels show the light curves in J and K_s, respectively. All the light curves were folded considering MJD = 55693.965445 as zero point.

Based on this evidence, we conclude that ID-133 from Weldrake et al. (2007) is *not* the same star as V144 from Kaluzny et al. (2004), despite the fact that both variables have very similar magnitudes, colors, and periods. The total number of RR Lyrae stars known in ω Cen is accordingly revised to 198, including 192 from Kaluzny et al., 5 from Weldrake et al. (2007), and the misidentified one discussed in the present paper. We note, in closing, that the coordinates given by Weldrake et al. appear slightly offset (by 3.66 arcsec) from the ID-133 (V411) position in our images. However, no other misidentified star was found in our search.

Acknowledgments: We warmly thank C. M. Clement for useful discussions. Support for the authors is provided by the Ministry for the Economy, Development, and Tourism's Programa Iniciativa Científica Milenio through grant P07-021-F, awarded to The Milky Way Millennium Nucleus; by Proyecto Basal PFB-06/2007; and by FONDECYT grants #1110326 (C.N., M.C., I.D., J.A.-G.), 1130196 (F.G.), 3130320 (R.C.R.), and 3130552 (J.A.-G.). C.N. acknowledges additional support from CONICYT-PCHA/Magíster Nacional/2012-22121934.

References:

Catelan, M., et al. 2011, Carnegie Obs. Conf. Ser., 5, 145

Catelan, M., et al. 2013, in 40 Years of Variable Stars: A Celebration of Contributions by Horace A. Smith (ed. K. Kinemuchi, H. A. Smith, N. De Lee, & C. Kuehn), p. 141 arXiv:1310.1996

Clement, C. M., et al. 2001, *AJ*, **122**, 2587

Dalton, G. B., et al. 2006, *SPIE*, **6269**

Kaluzny, J., Olech, A., Thompson, I. B., Pych, W., Krzemiński, W., & Schwarzenberg-Czerny, A. 2004, *A&A*, **424**, 1101

Minniti, D., et al. 2010, *NewA*, **15**, 433

Schwarzenberg-Czerny, A. 1989, *MNRAS*, **241**, 153

Schwarzenberg-Czerny, A. 1996, *ApJ*, **460**, L107

Sollima, A., Ferraro, F. R., Origlia, L., Pancino, E., & Bellazzini, M. 2004, *A&A*, **420**, 173

Stetson, P. B. 1987, *PASP*, **99**, 191

Stetson, P. B. 1994, *PASP*, **106**, 250

van Leeuwen, F., Le Poole, R. S., Reijns, R. A., Freeman, K. C., & de Zeeuw, P. T. 2000, *A&A*, **360**, 472

Weldrake, D. T. F., Sackett, P. D., & Bridges, T. J. 2007, *AJ*, **133**, 1447

*This version of the paper contains corrections, and differs from the one appeared on-line originally. Date of last modification: Fri Dec 20 06:48:00 CET 2013

COMMISSIONS 27 AND 42 OF THE IAU
INFORMATION BULLETIN ON VARIABLE STARS

Number 6079

Konkoly Observatory
Budapest
8 November 2013

HU ISSN 0374 – 0676

AW UMa OBSERVED WITH MOST SATELLITE

RUCINSKI, S.M.[1]; MATTHEWS, J.M.[2]; CAMERON, C.[3]; GUENTHER, D.B.[4]; KUSCHNIG, R.[5]; MOFFAT, A.F.J.[6]; ROWE, J.F.[7]; SASSELOV, D.[8]; WEISS, W.W.[9]

[1] Department of Astronomy and Astrophysics, University of Toronto, 50 St. George Street, Toronto, Ontario M5S 3H4, Canada. E-mail: rucinski@astro.utoronto.ca

[2] Department of Physics and Astronomy, University of British Columbia, 6224 Agricultural Road, Vancouver, BC, V6T 1Z1, Canada. E-mail: matthews@astro.ubc.ca

[3] Department of Mathematics, Physics & Geology, Cape Breton University, 1250 Grand Lake Road, Sydney, NS, B1P 6L2, Canada. E-mail: ccamerongeneral@gmail.com

[4] Institute for Computational Astrophysics, Department of Astronomy and Physics, Saint Marys University, Halifax NS, B3H 3C3, Canada. E-mail: guenther@ap.stmarys.ca

[5] University of Vienna, Institute for Astronomy, Türkenschanzstrasse 17, A-1180 Vienna, Austria. E-mail: rainer.kuschnig@univie.ac.at

[6] Département de physique, Université de Montréal, C.P. 6128, Succ. Centre-Ville, Montréal, QC, H3C 3J7, Canada. E-mail: moffat@astro.umontreal.ca

[7] NASA Ames Research Center, Moffett Field, CA, 94035, USA. E-mail: jasonfrowe@gmail.com

[8] Harvard-Smithsonian Center for Astrophysics, 60 Garden Street, Cambridge, MA 02138, USA. E-mail: sasselov@cfa.harvard.edu

[9] University of Vienna, Institute for Astronomy, Türkenschanzstrasse 17, A-1180 Vienna, Austria. E-mail: werner.weiss@univie.ac.at

Since its discovery by Paczyński (1964), AW UMa (HD 99946) has played a special role in efforts to understand structure of W UMa-type binaries. This particular importance was realized after it had been shown by Mochnacki & Doughty (1972) that model light curves computed following the contact model of Lucy (1968a, 1968b) imply a very small mass-ratio of $q \simeq 0.080 \pm 0.005$. The agreement with the model for such a large disparity of masses has since been interpreted as a very strong support for the model. While the small mass ratio has been photometrically confirmed many times following the investigation of Mochnacki & Doughty, new spectroscopic observations of Pribulla & Rucinski (2008) revealed that AW UMa is a complex semi-detached binary with a significantly larger mass ratio ($q \geq 0.10$). These observations showed complicated flows in the system, with the undersized primary and a tiny secondary embedded in what may be interpreted as an accretion disk. One of the spectroscopically detectable features was the presence of inhomogeneities on the primary component which could possibly be non-radial oscillations. Such oscillations would not be excluded on an F2 main-sequence star which is located exactly in the middle of the δ Sct instability strip.

Continuous MOST observations with effective exposure times of one minute were obtained between 25 February and 9 March 2013 resulting in 14,020 individual observations

[†]Based on data from the MOST satellite, a Canadian Space Agency mission, jointly operated by Microsatellite Systems Canada Inc. (MSCI; formerly Dynacon Inc.), the University of Toronto Institute for Aerospace Studies and the University of British Columbia, with the assistance of the University of Vienna.

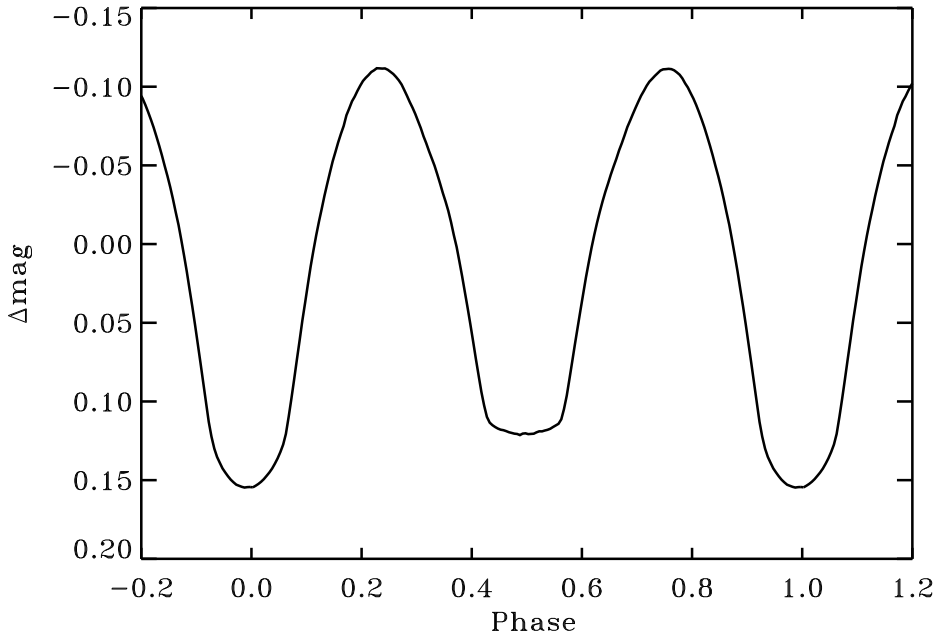

Figure 1. The mean light curve of AW UMa obtained from averaging all MOST observations in orbital phase is very well defined with errors smaller than the thickness of the line.

with a median error per point of 0.0005 mag. The mean, phased light curve obtained from averaging of 27 orbital cycles does not show any asymmetries which could be associated with spots or any other peculiarities (Figure 1). However, such a light curve is not convenient for modelling attempts because MOST uses one filter with a wide spectral band. Thus, we searched only for variability in the *deviations* from the mean light curve. A periodogram analysis for coherent oscillations and a wavelet analysis for localized oscillatory trains reveal no features which could not be explained as vestiges of the orbital binary (2.28 c/d, 4.56 c/d) and orbital satellite (1.0 c/d, 2.0 c/d and the explicitly removed 14.3 c/d) periodicities, their harmonics and combinations. Thus, no unexplained features larger than 0.0001 mag appear in the variability spectrum of the residuals from the average light curve (Figure 2).

The MOST observations gave the mean moments of eclipses:
Primary $HJD = 2,456,354.6668 \pm 0.0002$,
Secondary $HJD = 2,456,354.8866 \pm 0.0002$.
The $O - C$ diagram for AW UMa is shown in Figure 3. The eclipse timing data for the figure, covering the range $HJD\,2,438,045 - 2,455,669$, have been taken from the compilation in the Web page of the Czech Amateur Observers:
http://var.astro.cz/ocgate/ocgate.php?star=AW+UMa&submit=Submit&lang=en
where the assumed ephemeris was: $HJD = 2,452,311.81 + 0.438726 \times E$.

It has been known that AW UMa shortens its orbital period. However, the rate of the period change is not constant so that the eclipse moments cannot be fitted by a quadratic function. This is demonstrated in Figure 3 where the quadratic fit versus the epoch E is shown. The fit parameters are: $a_0 = +0.007 \pm 0.006$, $a_1 = (-8.6 \pm 1.7) \times 10^{-7}$, $a_2 = (-1.12 \pm 0.07) \times 10^{-10}$, where the quadratic term implies the e-folding time scale of

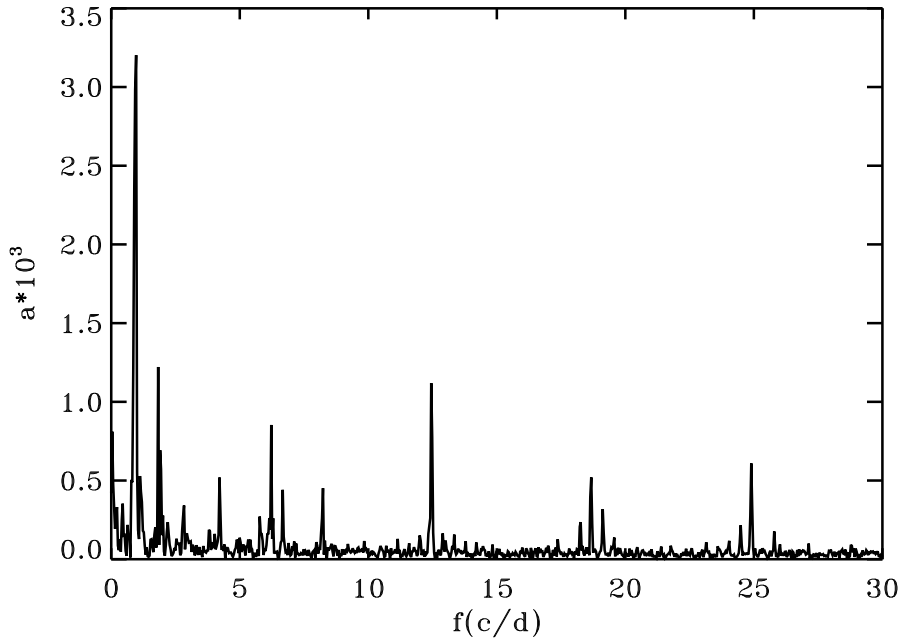

Figure 2. The periodogram of deviations from the average light curve of AW UMa. The frequencies are expressed in cycles per day while the vertical axis gives the amplitudes in units of 0.001 of the mean flux.

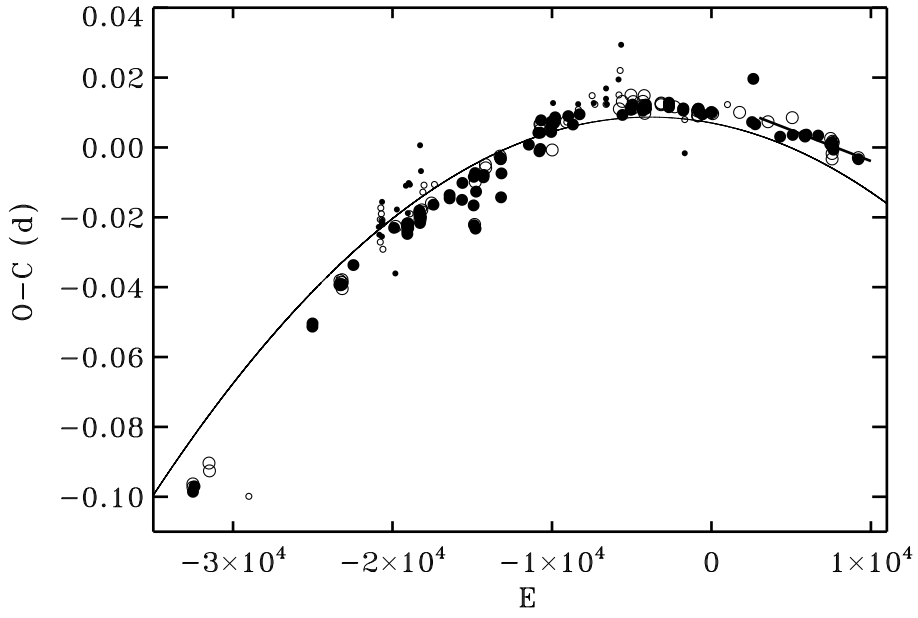

Figure 3. Deviations from the linear ephemeris of the Czech Amateur Observers for the primary (filled circles) and secondary eclipses (open circles) with visual observations marked by small symbols. The last symbol to the right is for the MOST observations. The short line for $E > 3000$ represents the current linear trend.

$\simeq 2.4 \times 10^8$ years. It appears that short segments better represent the observed $O-C$ curve. Because we needed a new linear ephemeris for the 2011 extensive spectroscopic observations of AW UMa at CFHT, we fitted a linear ephemeris for epochs $E > 3000$: $HJD = 2,455,632.9660(18) + 0.43872420(25) \times E$ where the mean errors, in parentheses are in units of the last decimal places.

Acknowledgements: D.B.G., J.M.M., A.F.J.M., and S.M.R. are supported by NSERC (Canada), R.K. and W.W.W. are supported by the Austrian Space Agency and the Austrian Science Fund. CC was supported by the Canadian Space Agency.

References:

Lucy L. B., 1968a, *ApJ*, **151**, 1123
Lucy L. B., 1968b, *ApJ*, **153**, 877
Mochnacki S. W., & Doughty N. A., 1972, *MNRAS*, **156**, 51
Paczyński, B., 1964, *AJ*, **69**, 124
Pribulla, T. & Rucinski, S.M., 2008, *MNRAS*, **386**, 377

ERRATUM FOR IBVS 6079

The last paragraph of the paper contains major errors which propagated into Fig.3. The corrected text and figure are given below.

It has been known that AW UMa shortens its orbital period. Figure 3 shows the quadratic fit versus the epoch E with the fit parameters: $a_0 = +0.0109(4)$, $a_1 = -4.5(6) \times 10^{-7}$, $a_2 = -1.16(4) \times 10^{-10}$, where the mean errors, in parentheses, are in units of the last decimal places. The quadratic term implies the e-folding time scale for the period change of 2.3×10^6 years. The rate of the period change may vary in time so that short segments may better represent the observed $O-C$ curve. Because we needed a new linear ephemeris for the 2011 extensive spectroscopic observations of AW UMa at CFHT, we fitted a linear ephemeris for epochs $E > 3000$: $HJD = 2,455,632.9660(18) + 0.43872420(25) * E$.

Acknowledgement: Thanks are due to Dr. Miloslav Zejda for pointing the substantial error in the paper.

The Author

*This version of the paper contains corrections, and differs from the one appeared on-line originally. Date of last modification: Mon Jan 27 10:03:55 CEST 2014

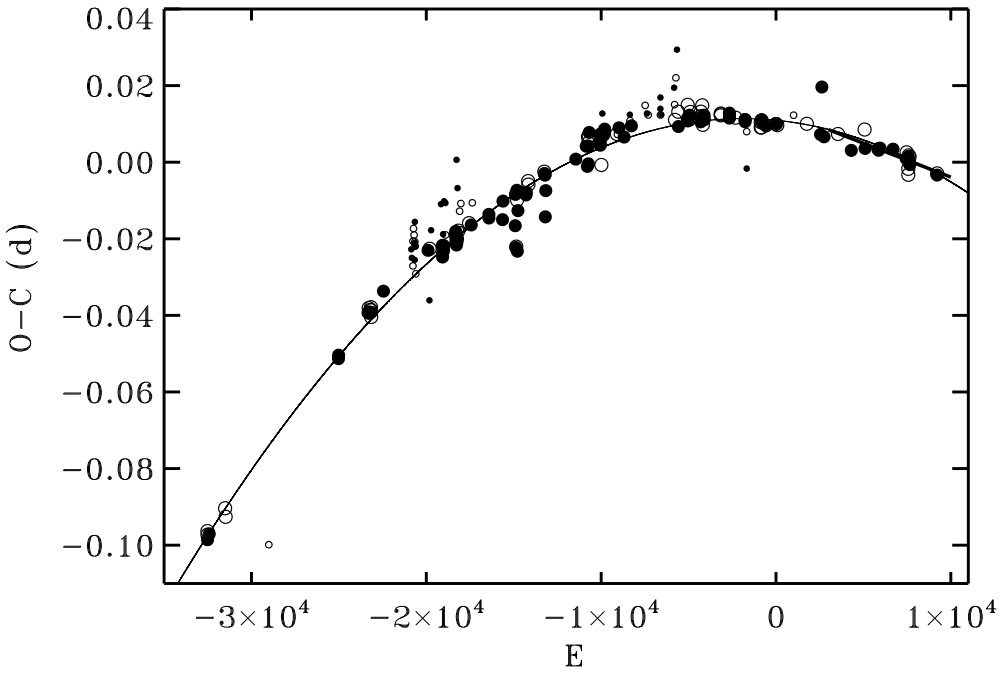

Figure 3a. Deviations from the linear ephemeris of the Czech Amateur Observers for the primary (filled circles) and secondary eclipses (open circles) with visual observations marked by small symbols. The last symbol to the right is for the MOST observations. The short thick line for $E > 3000$ represents the current linear trend.

COMMISSIONS 27 AND 42 OF THE IAU
INFORMATION BULLETIN ON VARIABLE STARS

Number 6080

Konkoly Observatory
Budapest
11 November 2013

HU ISSN 0374 – 0676

PHOTOMETRIC EVOLUTION OF NOVA Del 2013 (V339 Del) DURING THE OPTICALLY THICK PHASE

MUNARI, U.[1]; HENDEN, A.[2]; DALLAPORTA, S.[3]; CHERINI, G.[3]

[1] INAF Osservatorio Astronomico di Padova, Sede di Asiago, I-36032 Asiago (VI), Italy

[2] AAVSO, 49 Bay State Rd. Cambridge, MA 02138, USA

[3] ANS Collaboration, c/o Astronomical Observatory, 36012 Asiago (VI), Italy

The FeII-class Nova Del 2013 (=V339 Del) was discovered on 2013 Aug 14.584 UT by K. Itagaki when it was already visible at unfiltered 6.8 magnitude (cf. CBET 3628). The progenitor seems to be the blue star USNO B-1 1107-0509795 with $B\sim$17.2, $R_{\rm C}\sim$17.4. The observation by Denisenko et al. (cf. CBET 3628) reporting the nova still in quiescence at $\sim$17.1 mag on Aug 13.998 UT (14 hours before the discovery), would indicate a very fast rise to maximum. The very convenient placement in the evening sky and the naked-eye brightness attained by the nova favored a full suite of all-out observing efforts, which have produced a flurry of circulars and telegrams. Among others, descriptions of nova spectra have been provided by Shore et al. (2013a,b,c,d), Munari et al. (2013a,b,c,d), Tomov et al. (2013), Darnley & Bode (2013), Tarasova & Shakhovskoi (2013), Woodward et al. (2013); infrared observations have been reported by Gehrz et al. (2013), Cass et al. (2013a,b,c,d), Banerjee et al. (2013a,b), Shenavrin et al. (2013); development of X-ray emission has been monitored by Nelson et al. (2013) and Page et al. (2013a,b); and radio detections have been described by Dutta et al. (2013), Roy et al. (2013), Chomiuk et al. (2013), and Anderson et al. (2013). There also seems to be a 5σ detection of the nova in γ-rays (Hays et al. 2013).

No comprehensive description of the optical photometric evolution of Nova Del 2013 has been provided to date. In this paper we present our $BVR_{\rm C}I_{\rm C}$ light curve of Nova Del 2013 covering the evolution from discovery to day +77 past optical maximum, corresponding to the end of the optically thick phase of the ejecta and their transition to the nebular, optically thin regime. The light and color curves are presented in Figure 1, while Figure 2 highlights the phase of maximum brightness. The data are given in Table 1, available electronic only. To observe the nova we used eight different robotic or remotely controlled telescopes, equipped with photometric filters from various vendors (Schuler, Omega, Astrodon). Close to maximum brightness we used six small-diameter refractors: four 6-cm Bright Star Monitor instruments (part of AAVSOnet; located at AAVSO headquarters, Australia, California, New Mexico and identified in Figures 1 and 2 as BSM HQ, AU, CA and NM, respectively), and two operated by ANS Collaboration (a 6cm and a 15cm, with ANS identifiers 011 and 032. At the time of maximum nova brightness their aperture was reduced to 3 cm). At later times, when the nova had faded several magnitudes below maximum, two 30cm instruments joined the monitoring effort:

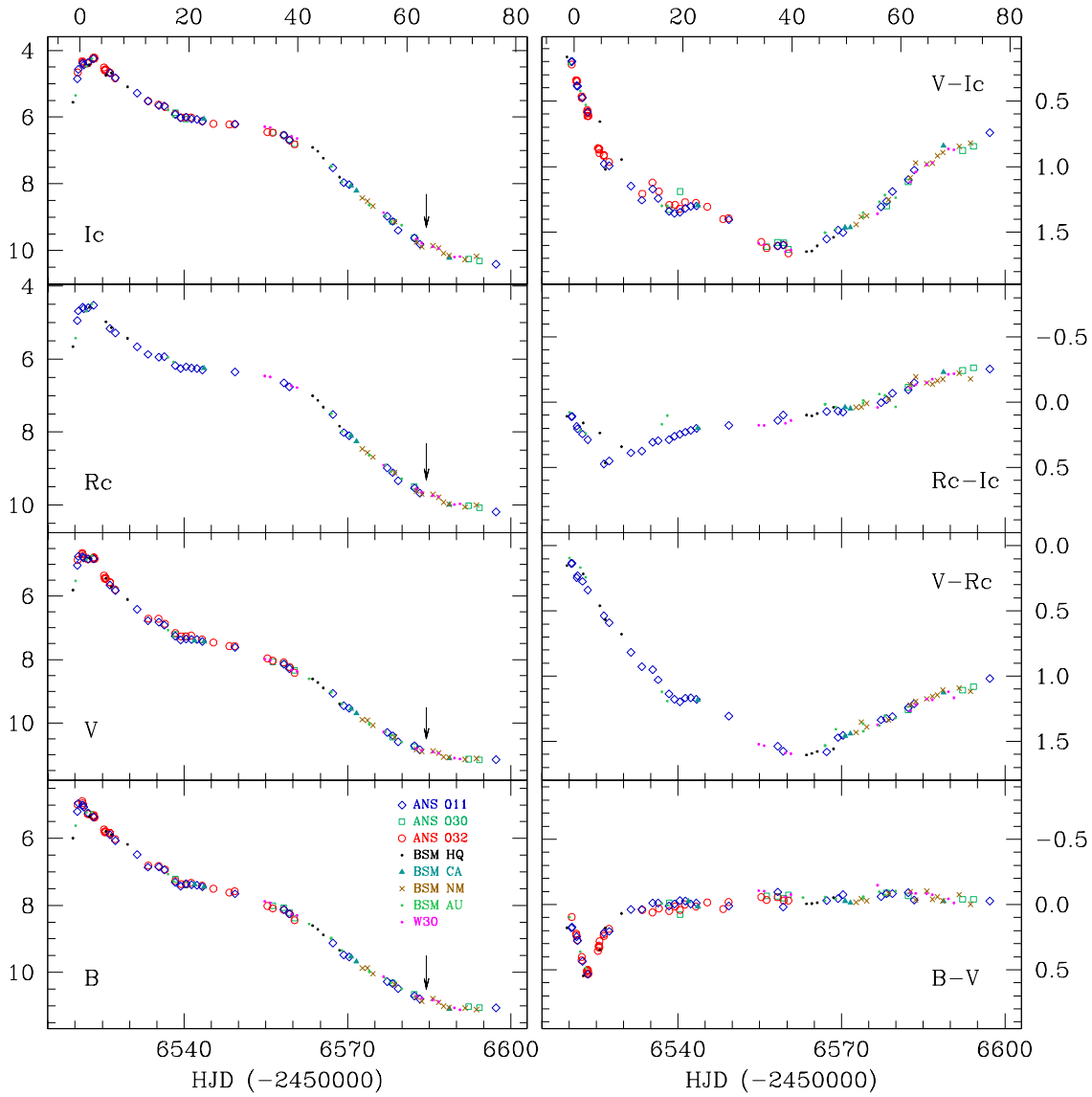

Figure 1. Our BVR_CI_C light and color curves of Nova Del 2013 extending to day +77 past maximum, covering the optically thick phase and the transition to nebular, optically thin conditions. The abscissae at the top of the graph are days counted from maximum brightness in V band. The arrows mark the time (Oct 17) when the flux of [OIII] 5007 Å emission lines equalled that of Hβ.

W30 from AAVSOnet and 030 from ANS Collaboration. The data collected at all these eight telescopes were reduced against the same local photometric sequence calibrated during photometric nights against Landolt (2009) equatorial standards. During data reduction, magnitude and colors were obtained separately and were not derived one from the other. The very strong emission lines displayed by Nova Del 2013 introduce some systematic deviation and offset (at the level of several hundredths of magnitude) between the light curves obtained with different instruments, which cannot be compensated for by the application of standard color equations. To rectify these small systematic offsets we have applied the light curve merging method (LMM) described by Munari et al. (2013e).

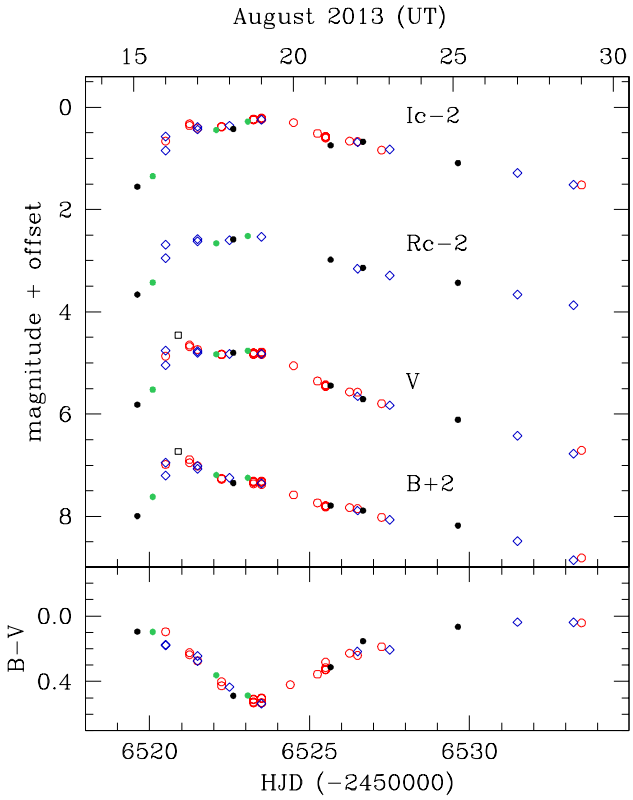

Figure 2. Zoomed view of Figure 1 around Nova Del 2013 maximum brightness.

The photometric evolution of Nova Del 2013 as illustrated in Figures 1 and 2 is characterized by: (1) a smooth behaviour, with short time scale variations – if any was actually present – not exceeding at any time a few hundredths of a magnitude; (2) a brief plateau appearing soon after maximum brightness and lasting ∼1.5 days; (3) a longer plateau extending from about day +20 to +37, that started when the nova had declined by ΔV=+2.8 mag from maximum brightness; (4) for both B and V bands, the rate of brightness decline before and after this long plateau remained the same: 0.125 mag/day. The R_C and I_C bands behaved similarly; (5) as typical of novae, a marked flattening of the decline rate occurred simultaneously with the transition of the ejecta from optically thick to nebular conditions. The time when the flux of [OIII] 5007 Å emission line equalled that of Hβ (October 17, from Munari et al. 2013e) is marked by an arrow in Figure 1. This transition to nebular conditions occurred when the nova had declined by ∼6 mag, much more than typically observed in other novae (where the transition occurs ∼3.5/4.0 mag below maximum brightness); and (6) a peculiar value and evolution for $B-V$ color, characterized by a nearly constant value apart from a brief excursion around the time of maximum brightness and the initial brief plateau. According to van den Bergh & Younger (1987), typical novae display $(B-V)_\circ = +0.23 \pm 0.06$ at B,V maximum brightness and $(B-V)_\circ = -0.02 \pm 0.04$ at t_2. The corresponding observed values for Nova Del 2013 were $B-V$=+0.14 and $B-V = +0.04$, that become $(B-V)_\circ = -0.04$ and $(B-V)_\circ = -0.14$ once corrected for the $E_{B-V} \simeq 0.18$ insterstellar reddening affecting the nova (cf. Tomov et al. 2013, Munari et al. 2013a).

Maximum light in B and V bands was attained by Nova Del 2013 during daytime in Italy on August 16, and during bad weather conditions at the AAVSOnet observing sites.

By interpolating data reported in CBET 3628, 3634 and by Burlak et al. (2013) it can be estimated that maximum brightness occurred around August 16.4 UT (JD 2456520.9), at $V \sim 4.46$ and $B \sim 4.70$. The outburst amplitude is therefore ΔB=12.5 mag, comparing with $B \sim 17.2$ for USNO B-1 1107-0509795 progenitor. This maximum is marked by an open black square in Figure 2. The evolution around maximum brightness looks different depending on the photometric band. In the B band, the maximum is sharp and the decline commenced immediately with characteristic times t_2^B=12 and t_3^B=30 days, that were t_2^V=10.5 and t_3^V=23.5 in V band, which place Nova Del 2013 in a borderline position between *fast* and *very fast* novae according to the Warner (1995) classification scheme. The brief plateau that the nova displayed in the V band soon after maximum and that lasted ∼1.5 days, corresponded to a prolonged flat maximum in the $R_{\rm C}$ band and to a delayed maximum in the $I_{\rm C}$ band, occurring ∼2.5 days after that in B.

References:

Banerjee D. P. K., et al., 2013a, ATel, 5337, 1
Banerjee D. P. K., et al., 2013b, ATel, 5404, 1
Burlak A. M., et al. 2013, ATel, 5294
Cass A. C., et al., 2013a, ATel, 5419
Cass A. C., et al., 2013b, ATel, 5434
Cass C. A., et al., 2013c, ATel, 5317
Cass C. A., et al., 2013d, ATel, 5340
Chomiuk L., et al., 2013, ATel, 5298
Darnley M. J., Bode M. F., 2013, ATel, 5300
Dutta P., et al., 2013, ATel, 5375
Gehrz R. D., et al., 2013, ATel, 5299
Hays E., et al., 2013, ATel, 5302
Landolt A. U., 2009, AJ, 137, 4186
Munari U., et al. 2013a, ATel, 5297
Munari U., et al. 2013b, ATel, 5304
Munari U., et al. 2013c, ATel, 5310
Munari U., et al. 2013d, ATel, 5533
Munari U., et al. 2013e, New Astronomy, 20, 30
Nelson T., et al., 2013, ATel, 5305
Page K. L., et al., 2013a, ATel, 5318
Page K. L., et al., 2013b, ATel, 5470
Roy N., et al., 2013, ATel, 5376
Shenavrin V. I., et al., 2013, ATel, 5431
Shore S. N., et al., 2013a, ATel, 5282
Shore S. N., et al., 2013b, ATel, 5312
Shore S. N., et al., 2013c, ATel, 5378
Shore S. N., et al., 2013d, ATel, 5409
Tarasova T. N., Shakhovskoi, D. N., 2013, ATel, 5291
Tomov T., et al., 2013, ATel, 5288
van der Bergh S., Younger P. F., 1987, A&AS, 70, 125
Warner B., 1995, Cataclysmic Variable Stars, Cambridge Univ. Press
Woodward C. E., et al., 2013, ATel, 5493

COMMISSIONS 27 AND 42 OF THE IAU
INFORMATION BULLETIN ON VARIABLE STARS

Number 6081

Konkoly Observatory
Budapest
17 November 2013

HU ISSN 0374 – 0676

CU TAU – A TYPE-A OVERCONTACT ECLIPSING BINARY

NELSON, R. H.[1,2]

[1] 1393 Garvin Street, Prince George, BC, Canada, V2M 3Z1 email: bob.nelson@shaw.ca

[2] Guest investigator, Dominion Astrophysical Observatory, Herzberg Institute of Astrophysics, National Research Council of Canada

CU Tau (= TYC 1804-2416-1, RA = $3^{\rm h}47^{\rm m}36\overset{\rm s}{.}914$, Dec = $+25°23'15\overset{''}{.}86$ (2000)) was discovered to be variable by Binnendijk (1950) during a photometric survey of AH Tau. He provided a light curve and eclipse elements, including a period of 0.4126022 days. As for type, he was unable to distinguish between "the cluster type [RR Lyrae] or of the W Ursae Majoris type". He also quoted a spectral type of G0, from a W.P. Bidelman [reference not available], who also noted "fairly broad lines" possibly caused by rotation. Therefore, Binnendijk favoured the identification as EW. Since then, numerous authors have found times of minima, showing the period to be decreasing at a constant rate. (See later discussion.)

Yang & Liu (2004) obtained CCD light curves in B and V. They presented four new times of minima, but unfortunately missed the true period of 0.412541(1) days at that epoch (obtainable with data presented in their paper) and were not able to detect the period decrease. (They instead used a period of 0.41341521(11) days for all their phasing, and attributed the large scatter in their eclipse timing (ET) plot [a.k.a. O-C diagram] scatter as due to irregular variations.) They used the 1994 version of the Wilson-Devinney (Wilson & Devinney, 1971; Wilson, 1990) code to reach a photometric solution, and pronounced the system to be type A. [In type A systems, the more massive – and hence larger – star has the higher surface temperature, making the primary eclipse a transit.] Lacking spectroscopic data, they estimated the mass ratio q [=M2/M1] by the so-called "q-search" method. Although this has since been shown to be very questionable or even invalid for EW-type systems undergoing partial eclipses [see Terrell & Wilson, 2005], this system makes a total eclipse, so the method is valid. They noted a small (0.017 magnitude) difference in the height of the maxima (V only) – this is the O'Connell effect (Davidge and Milone, 1984) – and applied a small cool spot to obtain a fit. Their results are presented in Table 5, along with those of the present study.

Qian et al. (2005) also determined a set of light curves in B and V. Obtaining four new times of minima and gathering together all times of minima available to them, they derived the correct period of 0.412538(5) days and displayed an ET diagram clearly showing a period decrease over time. (They derived a rate of period change $\mathrm{d}P/\mathrm{d}t = -1.81(2)\times10^{-6}$ days/year.) They then went on to perform a Wilson-Devinney (WD) analysis (ibid) using photometric data alone. Unlike Yang and Liu (2004), they did not detect an O'Connell effect. Also lacking spectroscopic data, the performed a q-search to obtain a starting

value for the mass ratio q. Their results are also presented in Table 5, along with those of the present study.

In view of the fact that the addition of radial velocity (RV) data (available to the author) allows the determination of fundamental parameters (such as mass, orbit size, stellar radii), it was decided to add this system to the author's programme.

The first task was to establish the proper elements (epoch, period) for phasing. All available elements were obtained (Nelson, 2013) and the ET plot of Fig. 1 obtained.

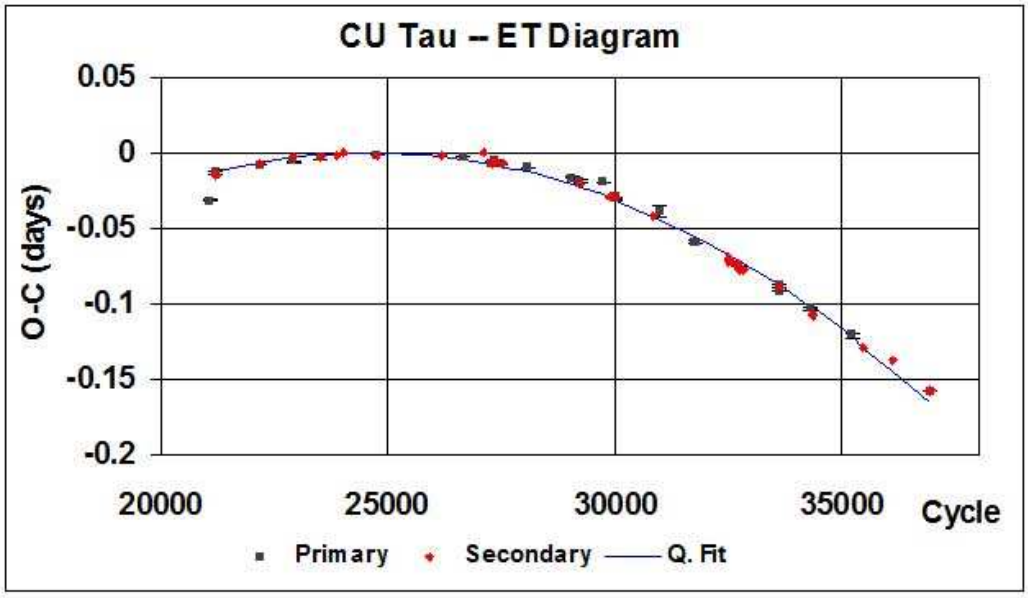

Figure 1. Eclipse timing diagram for CU Tau.

The least-squares best fit relation to fit the curve was found to be:

$$\text{HJD (min I)} = 2440970.031(15) + 0.412518(1)\ \text{E} - 1.09(2) \times 10^{-9}\ \text{E}^2 \qquad (1)$$

The quadratic coefficient yields a rate of period change $\mathrm{d}P/\mathrm{d}t = -1.94(3)\times10^{-6}$ days/year. Although the value of Qian et al. (2005) [$-1.81(2)\times10^{-}6$ days/year] lies outside the ranges predicted by the statistical errors, the discrepancy is not thought to be significant since experience shows that the addition of a few extra times of minima can easily change the value of $\mathrm{d}P/\mathrm{d}t$ by this difference.

At the suggestion of an anonymous referee, the author also plotted in Fig. 2 the residuals from the above plot (in the sense observed - calculated by quadratic fit). It seems that there is some sort of quasi-periodic variation, but its cause is unclear. As is so often the case, future data may tell the tale.

In September of 2006, 2007, and September-October of 2010, the author took 6 medium resolution spectra at the DAO. The grating (#21181) was 1800 lines/mm, blazed at 5000 angströms and used in first order, reciprocal linear dispersion = 10 Å/mm, resolving power = 10,000. The cameras used were the SITe-5 for the first two sessions, and the SITe-2 for the last. The spectral range covered was from 5000 to 5260 angströms, approximately.

Since the period was shown to be varying over the interval in which the data were taken,

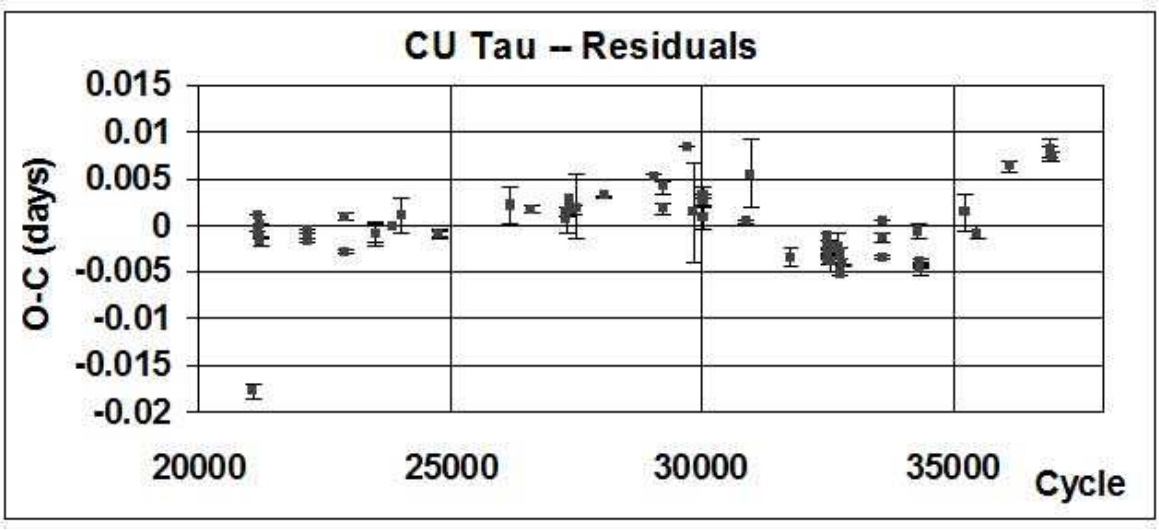

Figure 2. Residuals from quadratic best fit (Equation 1).

it was necessary to phase the data by using the current period, obtained by differentiating equation (1) getting:

$$P = \mathrm{d(HJD)}/\mathrm{d}t = 0.412518 - 2.18 \times 10^{-9}\ \mathrm{E} \tag{2}$$

The elements for each year were then:

Year	Epoch	Period (d)
2006	2454074.8901	0.412522
2007	2454406.5572	0.412520
2010	2455498.9036	0.412515

Table 1. Elements used for phasing RV data.

The author then used the Rucinski broadening functions (Rucinski, 2004) to obtain radial velocity (RV) curves (see Nelson, et al. (2006) and Nelson (2010) for details). A log of DAO observations and RV results is presented in Table 2. The results were corrected 7% up in this case to allow for the small phase smearing in the following way: the RVs were divided by the factor $f = (\sin X)/X$ [where $X = 2\pi t/P$ and t=exposure time, P=period]. For spherical stars, the correction is exact; in other cases, it can be shown to be close enough for any deviations to fall below observational errors. (This matter will be fully explored in a forthcoming paper.)

DAO Image #	Mid Time (HJD−2400000)	Exposure (sec)	Phase at Mid-exp	V1 (km/s)	V2 (km/s)
13090	53990.0188	3600	0.262	14.2	350.2
13227	54000.9571	3600	0.778	137.3	−191.1
11208	54367.0287	3600	0.178	43.8	318.2
17255	55468.9202	3600	0.316	25.9	320.3
17401	55474.8580	3600	0.709	114.4	−198.7
17492	55476.9685	3600	0.826	110.4	153.2

Table 2. Log of DAO observations.

In fitting two simple sine functions to the data, an overall rms deviation of 9.4 km/s was noted. These two best-fit functions yielded the following parameters:

$K_1 = 49.6 \pm 0.6$ km/s, $K_2 = 271.2 \pm 0.9$ km/s and $V_\gamma = 74.8 \pm 0.5$ km/s. Note that the latter high value is close to the threshold of 80 km/s that would classify the system as a high velocity star (Abell et al., 1991).

In October of 2012, the author took a total of 98 frames in V, 97 in R_c (Cousins) and 95 in the I_c (Cousins) band at his private observatory in Prince George, BC, Canada. (The telescope was a 33 cm f/4.5 Newtonian on a Paramount ME mount; the camera was an SBIG ST-10XME. Standard reductions were then applied. The comparison and check stars are listed in Table 3. The coordinates and magnitudes are from the Tycho Catalogue, Hog, et al., 2000.)

Type of target	GSC 1804-	R.A. J2000	Dec. J2000	V (Tycho) Mags	$B-V$ Mags
Variable	2416	03 47 36.911	+25 23 15.60	11.24	0.78
Comparison	2112	03 47 14.829	+25 22 17.94	11.22	1.22
Check	1922	03 47 46.731	+25 17 12.85	11.23	0.51

Table 3. Details of variable, comparison and check stars.

Here the elements for phasing, in accordance with equation (1), were:

$$\text{HJD (min I)} = 2456210.9102 + 0.412518\ \text{E} \tag{3}$$

The author used the 2004 version of the Wilson-Devinney (WD) light curve and radial velocity analysis program with Kurucz atmospheres (Wilson and Devinney, 1971, Wilson, 1990, Kallrath, et al., 1998) as implemented in the Windows front-end software WDwint (Nelson, 2009) to analyze the data. To get started, a spectral type G0 (Binnendijk, 1950) was used. Interpolated tables from Cox (2000) gave $T_1 = 5940 \pm 114$ K and $\log g = 4.375 \pm 0.012$; an interpolation program by Terrell (1994, available from Nelson 2009) gave the Van Hamme (1993) limb darkening values; and finally, a logarithmic (LD=2) law for the extinction coefficients was selected, appropriate for temperatures < 8500 K (ibid.). (The stated error in T_1 corresponds to one spectral sub-class.)

From the GCVS 4 designation and from the shape of the light curve mode 3 (overcontact binary) mode was used. Convergence by the method of multiple subsets was reached in a small number of iterations. Convective envelopes for both stars were used, appropriate for cooler stars (hence values gravity exponent, $g = 0.32$ and albedo, $A = 0.500$ were used for each). Detailed reflections were eventually used, with $n_{\text{ref}} = 3$, but with little or no change. The limb darkening coefficients are listed below in Table 4.

Band	x1	x2	y1	y2
Bol	0.647	0.647	0.216	0.216
V	0.752	0.752	0.246	0.246
Rc	0.681	0.681	0.262	0.262
Ic	0.597	0.597	0.255	0.255

Table 4. Limb darkening values from Van Hamme (1993).

The model is presented in Table 5. Note that the quoted error in T_2 listed here, outputted by the WD program, refers to the error relative to T_1. This error, when added statistically to the error in T_1 quoted, yields an absolute error of 115 K for T_2 (see Table 6).

The light curve data and the fitted curves are depicted in Figure 3. The presence of third light was tested for, but found not to be significant.

WD-	This work		Yang & Liu 2004*		Qian, et al. 2005		
Quantity	Value	error	Value	error	Value	error	Unit
$q = M_2/M_1$	0.190	0.002	0.179	0.001	0.1770	0.0017	—
Temperature T_1	5940	[fixed]	5900	[fixed]	5900	[fixed]	K
Temperature T_2	5800	17	5851	6	5938	10	K
Potential $\Omega_1 = \Omega_2$	2.153	0.005	2.1237	0.0026	2.1176	0.0036	—
Inclination, i	76.0	0.4	74.04	0.16	73.95	0.26	degrees
Semi-maj. axis a	2.75	0.01	—	—	—	—	solar
V_γ	74.2	0.7	—	—	—	—	km/s
Phase shift	-0.0022	0.0003	—	—	—	—	—
$L_1/(L_1 + L_2)$ (B)	—	—	0.8205	0.0010	0.8123	0.0004	—
$L_1/(L_1 + L_2)$ (V)	0.8248	0.0004	0.8219	0.0011	0.8104	0.0005	—
$L_1/(L_1 + L_2)$ (R_c)	0.8224	0.0004	—	—	—	—	—
$L_1/(L_1 + L_2)$ (I_c)	0.8206	0.0004	—	—	—	—	—
r_1 (pole)	0.5042	0.0013	0.5092	0.0004	0.5102	0.0010	orb. rad.
r_1 (side)	0.5542	0.0020	0.5613	0.0006	0.5628	0.0016	orb. rad
r_1 (back)	0.5806	0.0026	0.5877	0.0006	0.5890	0.0021	orb. rad
r_2 (pole)	0.2442	0.0032	0.2420	0.0007	0.2412	0.0031	orb. rad
r_2 (side)	0.2562	0.0040	0.2541	0.0009	0.2533	0.0038	orb. rad
r_2 (back)	0.3054	0.0099	0.3058	0.0014	0.3053	0.0100	orb. rad
Fill factor	0.44	0.05	0.49	—	0.501	0.032	—
$\sum \omega_{res}^2$	0.0215	—	0.007263	—	0.00042	—	—

*Unspotted solution only

Table 5. Wilson-Devinney parameters.

The RVs are shown in Fig. 4. A three dimensional representation from Binary Maker 3 (Bradstreet, 1993) is shown in Fig. 5.

The WD output fundamental parameters and errors are listed in Table 6. Most of the errors are output or derived estimates from the WD routines. The fill factor $f = (\Omega^{\rm I} - \Omega)/(\Omega^{\rm I} - \Omega^{\rm O})$, where Ω is the modified Kopal potential of the system, $\Omega^{\rm I}$ is that of the inner Lagrangian surface, and $\Omega^{\rm O}$, that of the outer Lagrangian surface, was also calculated.

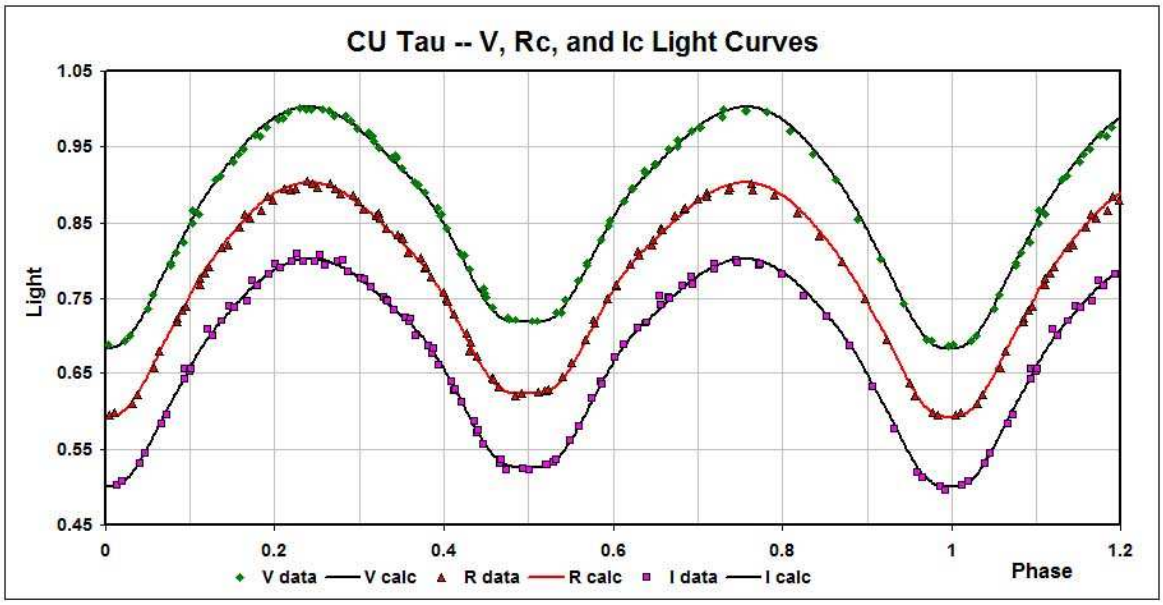

Figure 3. CU Tau: V, R_c, and I_c Light Curves – Data and WD fit.

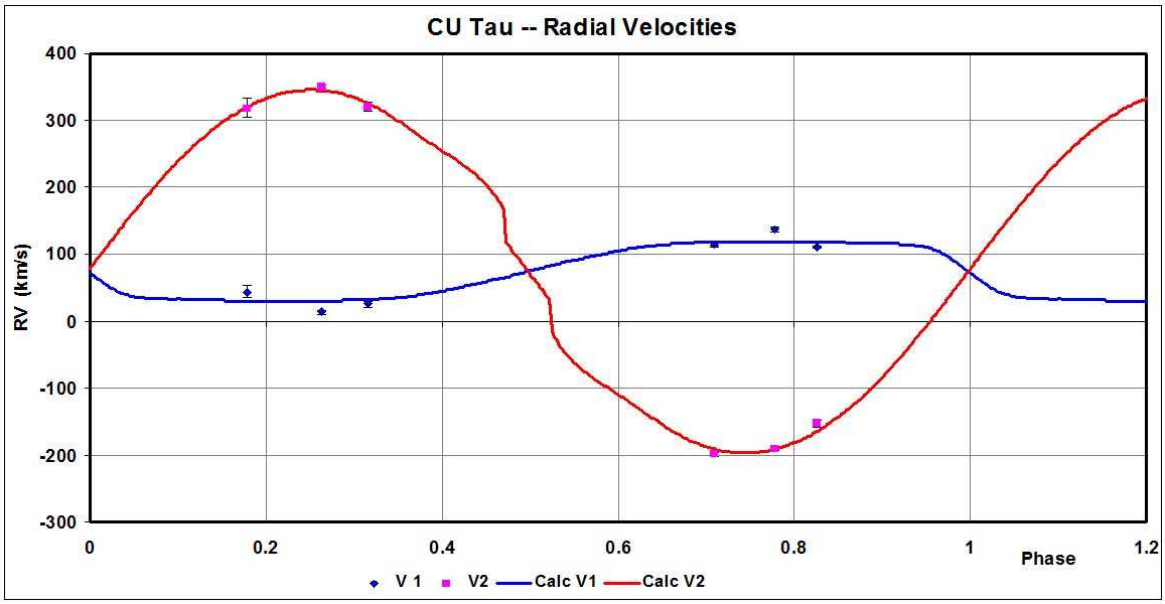

Figure 4. CU Tau: radial velocity curves – data and WD fit.

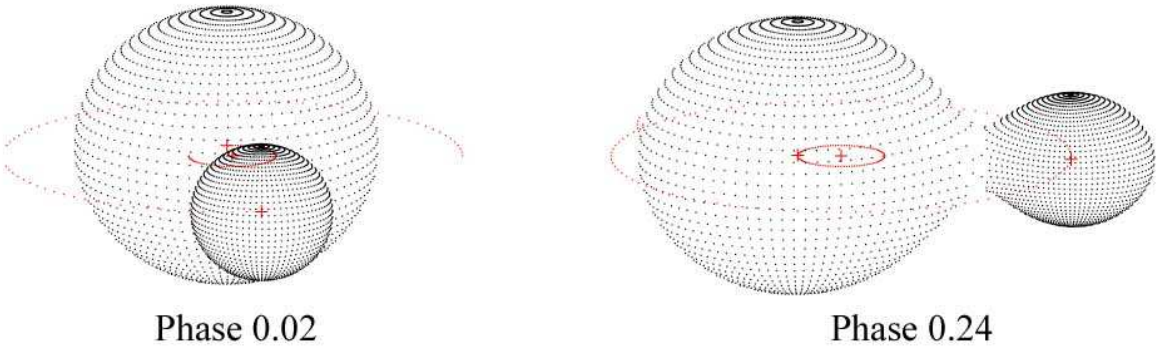

Figure 5. Binary Maker 3 representation of the system – at phases 0.02 and 0.74.

Quantity	Value	Error	unit
Temperature, T_1	5940	114	K
Temperature, T_2	5800	115	K
Mass, M_1	1.39	0.04	$M_\odot$
Mass, M_2	0.263	0.007	$M_\odot$
Radius, R_1	1.51	0.01	$R_\odot$
Radius, R_2	0.74	0.01	$R_\odot$
M_{bol}, 1	3.78	0.02	mag
M_{bol}, 2	5.42	0.02	mag
$\log g_1$	4.22	0.01	cgs
$\log g_2$	4.12	0.01	cgs
Luminosity, L_1	2.54	0.05	$L_\odot$
Luminosity, L_2	0.56	0.01	$L_\odot$
Distance, r	272	28	pc

Table 6. Fundamental parameters.

To determine the distance r, we proceeded as follows: first the WD routine gave the absolute bolometric magnitudes of each component, which were then converted to the absolute bolometric magnitude of both, getting $M_{bol} = 3.56$. The bolometric correction, BC $= -0.106$, was taken from interpolated tables from Cox (2000). The absolute magnitude in the V passband was then $M_V = M_{bol} + BC = 3.75$. The apparent magnitude in the V passband was $V = 11.37(4)$, taken from ensemble photometry of Tycho stars in the field (Hog et al., 2000). The colour excess, $E(B-V)$ was obtained from the $E(B-V)$ north galactic map (fits file) available from Schlegel et al. (2013). (The mapping formulas [galactic longitude, latitude > pixel column, row] were obtained from the original article by Schlegel et al. (1998), in Appendix C.) The images for the determination of the $E(B-V)$ values were obtained from Schlegel et al., 2013.) This gave $E(B-V) = 0.145$[1]. Galactic extinction was obtained from the usual relation $A_V = R \cdot E(B-V)$, using $R = 3.1$ for the reddening coefficient. Hence, distance $r = 272$ pc was calculated from the standard relation:

[1]Note: Since the $E(B-V)$ values were obtained from full-sky far-infrared measurements, this means that the former apply to a light path from the observer all the way through the Galaxy (in the specified direction), and therefore represent an upper limit for the appropriate value for a star lying somewhat closer than the far edge. The error estimate in this quantity has been set to 50% of this value, and is then the largest contributor to the overall error in r.

$$r = 10^{0.2(V - \mathrm{M}_V - A_V + 5)} \text{ parsecs} \quad (4)$$

The errors were assigned as follows: $\delta V = 0.04$, $\delta \mathrm{M_{bol,1}} = \mathrm{M_{bol,2}} = 0.02$, $\delta \mathrm{BC}_1 = \delta \mathrm{BC}_2 = 0.015$ (the variation of 1.5 spectral sub-classes), $\delta E(B-V) = 0.07$, all in magnitudes, and $\delta R = 0.1$. Combining the errors rigorously yielded an estimated error in r of 28 pc.

In conclusion, the fundamental parameters of this system have been determined. Our derived parameters in Table 5 are reasonably close to those of Qian et al. (2005). However, our values may be expected to be more accurate since our value of the mass ratio $q = M_2/M_1$ is more tightly constrained by the radial velocity values rather than by photometric data alone. A strange discrepancy is the fact that Qian et al. (2005) obtain a value for $T_2 > T_1$ even though they label the system as A-type.

Also, Qian et al. (2005), lacking RV data, estimated the mass of the primary by the relation

$$M_1 = 0.391(59) + 1.96(17)P \quad (5)$$

getting $M_1 = 1.20 \pm 0.09\ M_\odot$ and $M_2 = 0.21 \pm 0.02\ M_\odot$. These values lie outside the error range of values in the present study suggesting that the error estimates in equation (5) are perhaps too small.

Acknowledgements: It is a pleasure to thank the staff members at the DAO (especially Dmitry Monin and Les Saddlemyer) for their usual splendid help and assistance.

Reference:

Abell, G.O., Morrison, D., Wolff, S.C., 1991, "Exploration of the Universe", 6th ed., (Saunders, Philadelphia)

Binnendijk, L., 1950, *Bull. Astron. Inst. Netherlands*, **11**, 209

Bradstreet, D.H., 1993, "Binary Maker 2.0 - An Interactive Graphical Tool for Preliminary Light Curve Analysis", in Milone, E.F. (ed.) Light Curve Modelling of Eclipsing Binary Stars, pp 151-166 (Springer, New York)

Cox, A.N., ed., 2000, Allen's Astrophysical Quantities, 4th ed., (Springer-Verlag, New York, NY).

Davidge, T.J., and Milone, E.F., 1984, *Astrophys. J. Suppl. Ser.*, **55**, 571

Hog, E., Fabricius, C., Makarov, V. V., Urban, S., Corbin, T., Wycoff, G., Bastian, U., Schwekendiek, P., Wicenec, A., 2000, *Astronomy & Astrophysics*, **355**, L27

Kallrath, J., Milone, E.F., Terrell, D., and Young, A.T., 1998, *Astrophys. J.*, **508**, 308.

Nelson, R.H., Terrell, D., and Gross, J., 2006, *Inform. Bull. Var. Stars*, No. 5715

Nelson, R.H., 2009, Software, by Bob Nelson, `http://members.shaw.ca/bob.nelson/software1.htm`

Nelson, R.H., 2010, "Spectroscopy for Eclipsing Binary Analysis" in The Alt-Az Initiative, Telescope Mirror & Instrument Developments (Collins Foundation Press, Santa Margarita, CA), R.M. Genet, J.M. Johnson and V. Wallen (eds)

Nelson, R.H., 2013, Bob Nelson's O-C Files, `http://www.aavso.org/bob-nelsons-o-c-files`

Qian S.-B., Yang Y.-G., Soonthornthum B., Zhu L.-Y., He J.-J. and Yuan J.-Z., 2005, *AJ*, **130**, 224

Rucinski, S. M., 2004, *IAUS*, **215**, 17

Schlegel, D.J., Finkbeiner, D.P., Davis, M., 1998, *Astrophys. J.*, **500**, 525

Schlegel, D.J., Finkbeiner, D.P., Krigel, A., 2013,
`http://www.astro.princeton.edu/~schlegel/dust/data/data.html`
Terrell, D., 1994, Van Hamme Limb Darkening Tables, vers. 1.1.
Terrell, D. & Wilson, R.E., 2005, *Astrophys. Space Sci.*, **296**, 221
Van Hamme, W., 1993, *Astron. J.*, **106**, 2096
Wilson, R.E., 1990, *Astrophys. J.*, **356**, 613
Wilson, R.E., and Devinney, E.J., 1971, *Astrophys. J.*, **166**, 605
Yang, Y. and Liu, Q.-Y., 2004, *Astrophys. Space Sci*, **289**, 137

COMMISSIONS 27 AND 42 OF THE IAU
INFORMATION BULLETIN ON VARIABLE STARS

Number 6082

Konkoly Observatory
Budapest
20 November 2013

HU ISSN 0374 – 0676

NEW MID-TRANSIT TIMES FOR HAT-P-36b, TrES-3b, AND WASP-43b†

MACIEJEWSKI, G.[1]; PUCHALSKI, D.[1]; SARAL, G.[2,3]; DERMAN, E.[4]; KITZE, M.[5]; BUKOWIECKI, Ł.[1]; SEELIGER, M.[5]; NEUHAEUSER, R.[5]

[1] Centre for Astronomy, Faculty of Physics, Astronomy and Informatics, Nicolaus Copernicus University, Grudziadzka 5, 87-100 Torun, Poland, e-mail: gm@astri.umk.pl

[2] Harvard-Smithsonian Center for Astrophysics, 60 Garden Street, Cambridge, MA 02138, USA

[3] Astronomy and Space Sciences Department, Istanbul University, 34116 Fatih Istanbul, Turkey

[4] Astronomy and Space Sciences Department, Ankara University, 06100 Tandoğan, Ankara, Turkey

[5] Astrophysikalisches Institut und Universitäts-Sternwarte, Schillergässchen 2–3, D–07745 Jena, Germany

Photometric follow-up observations of exoplanetary transits allow one to refine transit ephemeris and to search for any deviations of mid-transit times from a strictly periodic case. Those so called transit timing variations (TTV) could result from gravitational interaction with unseen, even very low mass planetary companions (see e.g. Ballard et al. 2011). In 2009, we started observing campaigns for selected transiting planets to search for TTV signals (Maciejewski et al. 2011). A number of transit light curves have been acquired for backup targets as a by-product of our project.[1] In this research note, we report on new mid-transit times for transiting planets HAT-P-36 b, TrES-3 b, and WASP-43 b. Our new data extend the timespan covered by observations of these exoplanets, and allow us to refine their transit ephemerides.

Observations were gathered with the following instruments: a 0.4-m Schmidt-Cassegrain Meade LX200 GPS telescope coupled with an Apogee ALTA-U47 CCD camera (1024×1024 pixels, FoV: $11' \times 11'$) at the Ankara University Observatory (Turkey), the 0.6-m Cassegrain telescope and an SBIG STL-1001 CCD (1024×1024 pixels, FoV: $11\farcm8 \times 11\farcm8$) at the Centre for Astronomy of the Nicolaus Copernicus University (Toruń, Poland), and the 2.2-m telescope with the Calar Alto Faint Object Spectrograph (CAFOS) in its imaging mode (2048×2048 pixels, FoV windowed to $10\farcm4 \times 4\farcm8$) at the Calar Alto Observatory (Spain). Basic information on observations is summarized in Table 1. To increase effective efficiency of the 0.6-m telescope and to decrease timing errors, observations were performed in so-called clear filter, i.e. without any filter. We assumed that the instrumental response can be approximated by the quantum efficiency of the CCD matrix with a maximum between V and R bands.

Standard procedures including debiasing, dark correction, and flat-fielding using sky flats were employed in data reduction. Magnitudes were obtained with differential aperture photometry with respect to the comparison stars available in each field of view. The

†Partly based on observations made at the Centro Astronómico Hispano Alemán (CAHA), operated jointly by the Max-Planck-Institut für Astronomie and the Instituto de Astrofísica de Andalucía (CSIC).

[1] http://ttv.astri.umk.pl

`jktebop` code (Southworth et al. 2004a, 2004b) was used to detrend the light curves by fitting a second-order polynomial function of time along with a trial transit model, based on parameters taken from the literature. The best-fitting trend was subtracted from each light curve. Magnitudes were transformed into fluxes and normalised to unity outside of the transit. The timestamps were converted to barycentric Julian dates in barycentric dynamical time (BJD_{TDB}, Eastman et al. 2010). To quantify the quality of each light curve, we used the photometric noise rate (pnr) defined as

$$pnr = \frac{rms}{\sqrt{\Gamma}} \tag{1}$$

where the root mean square of the residuals, rms, is calculated from the light curve and a fitted model, and Γ is the median number of exposures per minute (Fulton et al. 2011). The individual light curves are plotted in Fig. 1.

Table 1. List of observed transits.

Date	Telescope	Filter	pnr (mmag)	Epoch	T_0 (BJD_{TDB}) +2450000	O–C (d)
			HAT-P-36b			
2013 Mar 14	0.6-m Toruń	clear	3.8	603	$6365.5280^{+0.0025}_{-0.0020}$	+0.0005
2013 Apr 14	0.6-m Toruń	clear	2.9	627	$6397.3817^{+0.0021}_{-0.0015}$	−0.0003
			TrES-3b			
2009 Aug 05	0.4-m Ankara	R	3.8	391	$5049.2985^{+0.0015}_{-0.0015}$	−0.0017
2010 Apr 10	0.4-m Ankara	R	4.9	581	$5297.4778^{+0.0008}_{-0.0008}$	+0.0022
2010 May 11	0.4-m Ankara	R	4.0	604	$5327.5172^{+0.0008}_{-0.0008}$	−0.0006
2010 Jun 17	0.4-m Ankara	R	5.3	633	$5365.3965^{+0.0012}_{-0.0011}$	−0.0008
2013 Mar 17	0.6-m Toruń	clear	2.5	1401	$6368.54705^{+0.00061}_{-0.00063}$	−0.00089
			WASP-43b			
2012 Feb 13	2.2-m Calar Alto	R	1.6	543	$5970.58532^{+0.00049}_{-0.00056}$	−0.00062
2013 Mar 16	0.6-m Toruń	clear	3.8	1032	$6368.3745^{+0.0009}_{-0.0010}$	−0.0013

The mid-transit times were determined by modelling the light curves with the `Transit Analysis Package`[2] (`TAP`, Gazak et al. 2012). The best-fitting parameters, based on the transit model of Mandel & Agol (2002), were determined with the Markov Chain Monte Carlo (MCMC) method, employing the Metropolis-Hastings algorithm and a Gibbs sampler. The conservative uncertainties were estimated including time-correlated noise which is characterised with the wavelet-based technique of Carter & Winn (2009). A quadratic law was used to characterise limb darkening of stellar disks. The theoretical coefficients were linearly interpolated from tables of Claret & Bloemen (2011) with the `EXOFAST` applet[3] (Eastman et al. 2013) for stellar parameters taken from the The Extrasolar Planets Encyclopaedia.[4] For data collected in clear filter, values of coefficients were calculated as an average of those for V and R bands.

In the fitting procedure, relative semi-major axis, relative planet radius, and mid-transit time allowed to vary for individual light curves. We also kept the flux slope and intercept free to account for their uncertainties in the total error budget of the fit. The orbital inclination and orbital period were fixed at the literature values. The limb darkening coefficients were fixed at the theoretical values. Ten chains of a length of 10^5 steps for each light curve were used in the MCMC procedure to obtain final posterior probability

[2] http://ifa.hawaii.edu/users/zgazak/IfA/TAP.html
[3] http://astroutils.astronomy.ohio-state.edu/exofast/limbdark.shtml
[4] http://exoplanet.eu

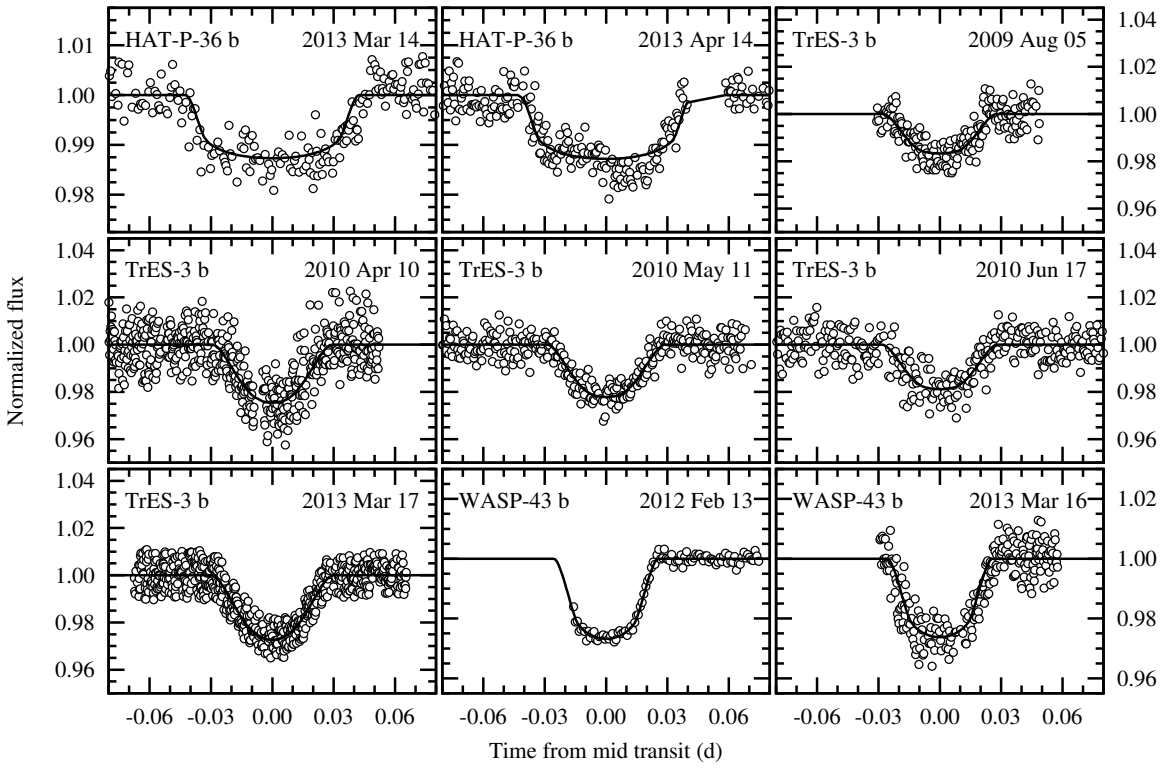

Figure 1. Transit light curves for HAT-P-36b, TrES-3b, and WASP-43b. The continuous lines show the best fitting transit models.

distributions. The first 10% of the links in each chain were discarded before calculating the best-fitting parameter values and their uncertainties. They were determined by taking the median value of marginalised posterior probability distributions. The upper and lower $1\,\sigma$ uncertainties were determined as 15.9 and 84.1 percentile values of the cumulative distributions. The new mid-transit times, which are listed in Table 1, were combined with the literature determinations, and transit ephemerides were redetermined by linear fits, weighted by individual timing errors. Figure 2 shows the O–C (observed minus calculated) diagrams for transit timing of investigated planets.

The transiting planet HAT-P-36 b was discovered by Bakos et al. (2012), and no follow-up observations have been carried out to date. The refined transit ephemeris is:

$$\begin{aligned} \mathrm{T_{mid}(BJD_{TDB})} = 2455565.18221 + 1\overset{\mathrm{d}}{.}3272729 \times E, \\ \pm 0.00006 \pm 0.0000008 \end{aligned} \tag{2}$$

where E is a transit number starting from the initial epoch given by Bakos et al. (2012). The precision of the time of the initial epoch has been improved by a factor of 3.3, and the precision of the orbital period has been increased by a factor of 3.8, as compared to values reported by Bakos et al. (2012).

The TrES-3 planetary system was discovered by O'Donovan et al. (2007), and has become a subject of numerous follow-up studies. We refer to a recent paper by Vaňko et al. (2013) for a detailed review. Those authors report new transit observations and reanalise all available transit light curves in a homogeneous way. We used their determinations

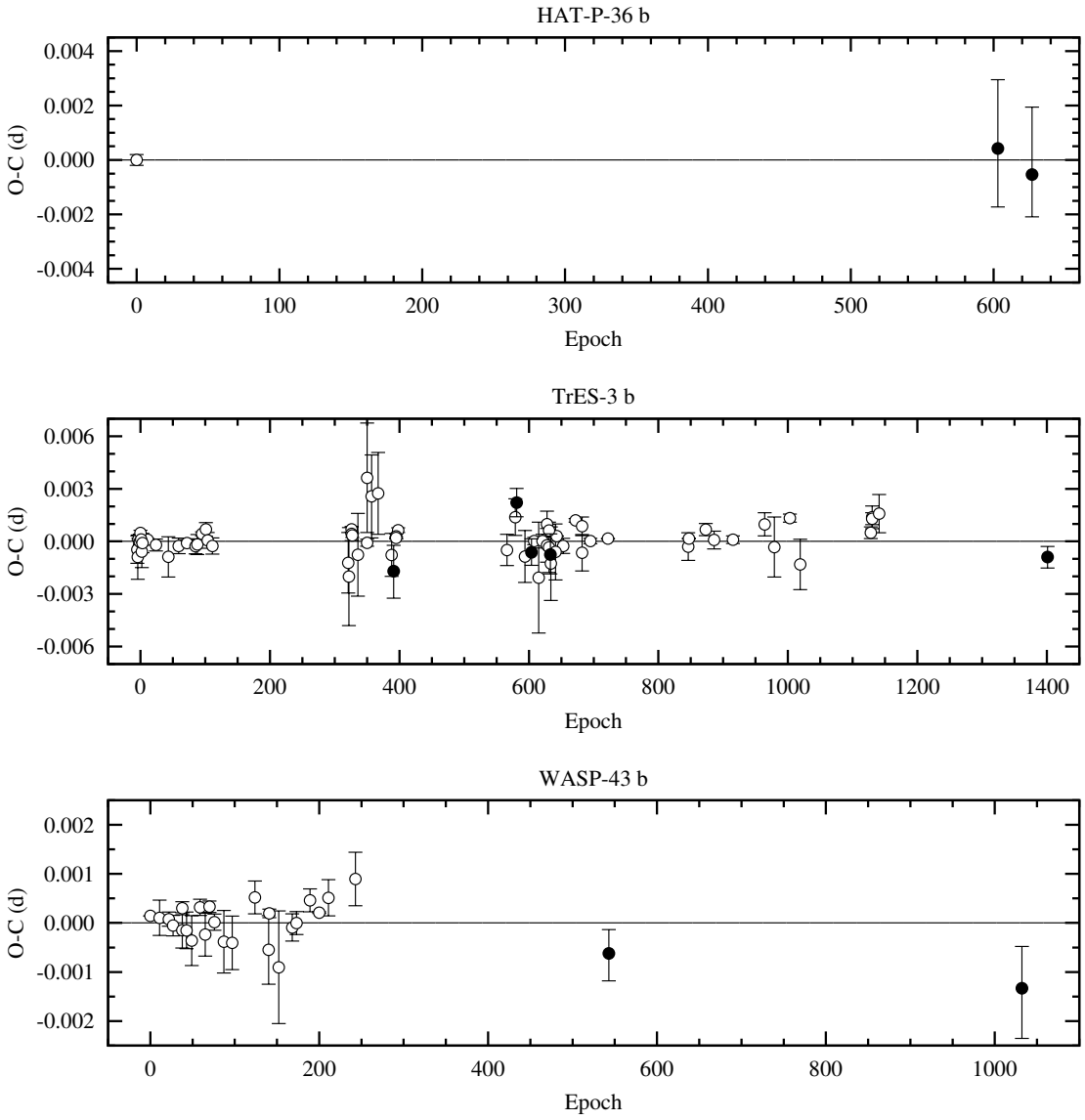

Figure 2. O–C diagram for transit timing of HAT-P-36b, TrES-3b, and WASP-43b. Open symbols denote literature data, and the filled circled mark mid-transit times reported in this work.

together with our new mid-transit times to refine the transit ephemeris:

$$\begin{aligned} \mathrm{T_{mid}(BJD_{TDB})} = 2454538.58158 + 1\overset{\mathrm{d}}{.}30618584 \times E. \\ \pm 0.00011 \pm 0.00000023 \end{aligned} \quad (3)$$

Transit numbering is from initial epoch given by Christiansen et al. (2011). Our new ephemeris agrees within error bars with values reported by Vaňko et al. (2013).

The WASP-43b planet belongs to a population of planetary companions on orbits with periods shorter than 1 day. It was discovered by Hellier et al. (2011). Gillon et al. (2012) redetermined system parameters, based on 23 high quality transit light curves. Our new mid-transit times extend the time span covered by observations by a factor of 4, and results in the refined ephemeris:

$$\begin{aligned} \mathrm{T_{mid}(BJD_{TDB})} = 2455528.86839 + 0\overset{\mathrm{d}}{.}8134762 \times E. \\ \pm 0.00012 \pm 0.0000009 \end{aligned} \quad (4)$$

The transit numbering starts from the epoch given by Hellier et al. (2011). Our new observations indicate that the orbital period is shorter than the value reported by Gillon et al. (2012) by 0.13 s.

New mid-transit times reported in this work were found to be consistent with linear ephemerides within 1–2σ, so there is no sign of TTVs for any planet.

Acknowledgements: GM, DP, and ŁB acknowledge the financial support from the Polish Ministry of Science and Higher Education through the Iuventus Plus grant IP2011 031971. MK would like to acknowledge the German National Science Foundation (Deutsche Forschungsgemeinschaft, DFG) for support in the Priority Programme SPP 1385 in projects NE 515/34-1 and -2.

References:

Bakos, G. Á., Hartman, J. D, Torres, G., et al., 2012, *AJ*, **144**, 19
Ballard, S., Fabrycky, D., Fressin, F., et al., 2011, *ApJ*, **743**, 200
Carter, J. A., & Winn, J. N., 2009, *ApJ*, **704**, 51
Christiansen, J. L., Ballard, S., Charbonneau, D., et al. 2011, *ApJ*, **726**, 94
Claret, A., & Bloemen, S., 2011, *A&A*, **529**, A75
Eastman, J., Siverd, R., & Gaudi, B. S., 2010, *PASP*, **122**, 935
Eastman, J., Gaudi, B. S., & Agol, E., 2013, *PASP*, **125**, 83
Fulton, B. J., Shporer, A., Winn, J. N., et al., 2011, *AJ*, **142**, 84
Gazak, J. Z., Johnson, J. A., Tonry, J., et al., 2012, *Advances in Astronomy*, 697967
Gillon, M., Triaud, A. H. M. J., Fortney, J. J., et al., 2012, *A&A*, **542**, A4
Hellier, C., Anderson, D. R., Collier Cameron, A., et al., 2011, *A&A*, **535**, L7
Maciejewski, G., Neuhaeuser, R., Raetz, St., et al., 2011, EPJ Web of Conferences, **11**, 05009
Mandel, K., & Agol, E., 2002, *ApJL*, **580**, L171
O'Donovan, F. T., Charbonneau, D., Bakos, G. Á., et al., 2007, *ApJ*, **663**, L37
Southworth, J., Maxted, P. F. L., & Smalley, B., 2004a, *MNRAS*, **349**, 547
Southworth, J., Maxted, P. F. L., & Smalley, B., 2004b, *MNRAS*, **351**, 1277
Vaňko, M., Maciejewski, G., Jakubík, M., et al., 2013, *MNRAS*, **432**, 944

COMMISSIONS 27 AND 42 OF THE IAU
INFORMATION BULLETIN ON VARIABLE STARS

Number 6083

Konkoly Observatory
Budapest
25 November 2013

HU ISSN 0374 – 0676

HISTORIC OUTBURSTS OF MASTER OT J023406.06+384142.4

NESCI, R.

INAF/IAPS, via Fosso del Cavaliere 100, 00133, Roma, Italy, e-mail: roberto.nesci@iaps.inaf.it

The robotic MASTER network reported on 2013-07-20 an optical transient at J023406.1 +384142 (Shurpakov et al. 2013). The source was detected at unfiltered magnitude 15.6, and a previous bright state at 17.5 mag was detected by NEAT on 2002-11-25. The authors suggested that the source is likely a cataclysmic variable of the SU UMa type from the 5 mag outburst amplitude. This kind of stars has frequent "normal" outbursts (about 3 mag amplitude) with rare superoutbursts (4 mag amplitude or more). I looked for historic outbursts of this star in the Schmidt plate collection of the Asiago Observatory, finding a large number of plates taken for the Asiago Supernova patrol. The logbook of the Asiago Plate Archive is downloadable from the Observatory web page.

Overall I checked 565 plates of the 50/40/100 cm Schmidt telescope (S50) and 86 plates of the 92/67/215 cm Schmidt telescope (S90), covering about 24 years. These exposures were taken on plates with blue sensitive emulsions: 103aO (351), TRI-X (188), PANCRO-ROYAL (24), mostly without filter in the case of the S50, 103aO with GG13 (blue) filter for the S90. In many cases two plates were taken each night with the S50 to compare different emulsions: the overall number of nights with useful observations is 384.

Stellar magnitudes were estimated by eye with a binocular microscope used for comparison a sequence of nearby stars taken from the GSC 2.3.2 catalog (Lasker et al. 2008), ranging from $B = 15\overset{m}{.}6$ to $19\overset{m}{.}5$. A histogram of the limiting magnitudes is shown in Fig. 1: for the S50 it was generally between $B = 17\overset{m}{.}0$ and $18\overset{m}{.}3$, while for the S90 it was nearly always better than $18\overset{m}{.}0$. A few plates were substantially less deep, due to weather conditions, moonlight or short exposure time. The star was clearly visible on 28 plates of the small Schmidt, grouped around 7 dates, and possibly detected on other 8 plates. It was also well detected on 3 plates of the S90, confirming detections of the S50.

In Table 1, for each brightening episode, the following data are reported: 1) the outburst date; 2) the corresponding MJD; 3) the peak magnitude; 4) the number of plates with the star detected; 5) the number of days the star was visible; 6) the number of days between the last plate without detection and the first detection; 7) the number of days between the last detection and the first plate without detection; 8) the time difference from the previous outburst; 9) a tentative recurrence time scale with an integer number of outbursts between the observed ones; 10) the telescope(s) used.

The maximum recorded brightness of the star was about 16 mag, similar to the MASTER outburst detection, with other high states at 16.5 or 17 mag. The number of plates with limiting magnitude $\leq$16 is 69, and $\leq$ 17 is 160. Besides that reason, several

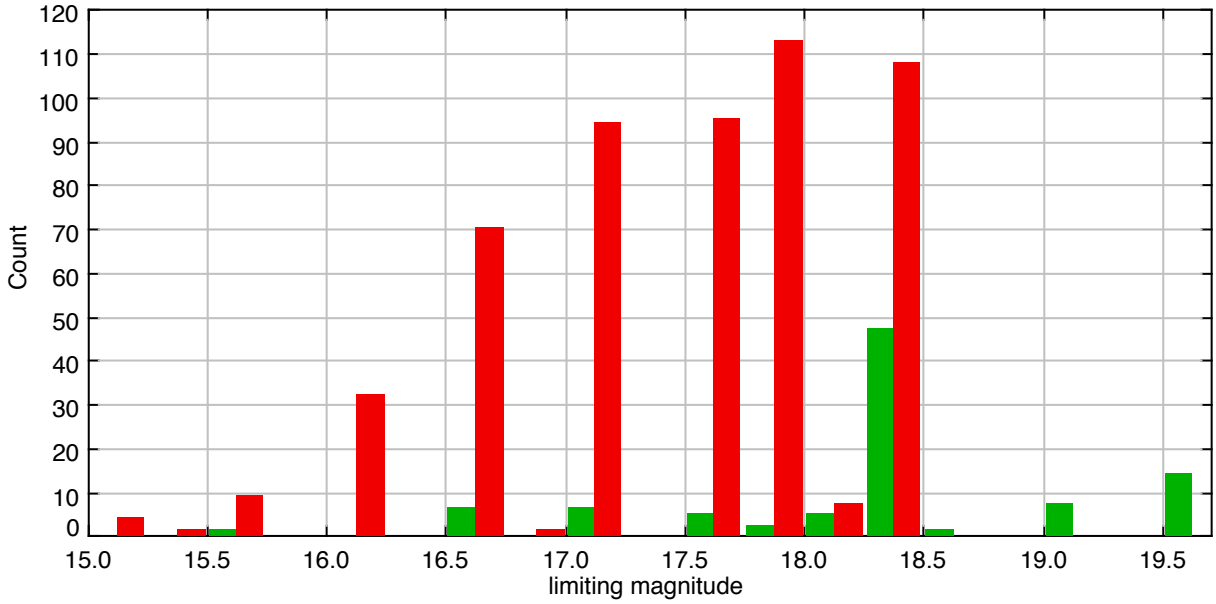

Figure 1. Histogram of the limiting magnitude of the Asiago plates. Green columns denote the S90 plates, while red columns show the S50 ones. Bins are 0.25 mag wide.

high states may have escaped detection due to time sampling, which was unavoidably not strictly regular, nor very dense. Following is a short description of the detected outbursts.

Table 1. Detected outbursts of J023406.1+384142.

1	2	3	4	5	6	7	8	9	10
YYYY-MM-DD	MJD	mag	np	days	before	after	delta	$N \times T$	comm
1961-27-12	37660.87	16.0	5	13	2	15	—	—	S50
1969-10-09	40503.99	16.0	9	8	1332	15	2838	9×315	S50
1971-02-25	41007.79	16.0	4	1	6	184	501	2×250	S50
1974-10-17	42337.01	17.0	5	6	242	4	1330	4×332	S50
1982-12-09	45312.88	16.5	3	2	27	52	2975	9×330	S90 and S50
1984-10-24	45997.01	16.5	3	1	28	7	683	2×341	S90 and S50
1985-09-10	46318.94	16.5	2	1	22	12	321	1×321	S50

- The first well recorded outburst was that on MJD 37660: the star was below 18.3 mag two days before, appeared at 16.0 mag and remained at this level for 10 days, began to drop at 16.5 mag two days after and was below 18 mag after further 15 days. The relevant light curve is shown in Fig. 2.
- The second well documented outburst was that on MJD 40503: the star appeared already at 16 mag, was bright for 8 days and was not detectable 15 days later.
- The third outburst was on MJD 41007: the star appeared at mag 16 in four plates taken the same day. The next plate was taken 6 months later, so we have no information on the outburst duration.
- The fourth outburst was definitely fainter, 17 mag, on MJD 42337. The star was possibly detected at the plate limit (18.3 mag) four days before, it was seen in two

pairs of plates on MJD 42337 and 42338 and was already below the plate limit (17.5 mag) four days after.

- The fifth outburst was caught by the small Schmidt at 17.5 mag on MJD 45312; it was confirmed two days later by the large Schmidt at 16.5 mag.
- The sixth outburst was on MJD 45997, recorded on two plates of the small Schmidt (17.0 mag) and one plate (16.5 mag) of the large Schmidt.
- The last outburst on MJD 46318 was recorded on two consecutive plates at 16.5 mag; the star was already below 18.3 mag in both Schmidt telescopes 12 days after.

From the best sampled outbursts we estimate that the star undergoes large brightenings with a duration of about 10 days. This is a typical time scale for several cataclysmic variables.

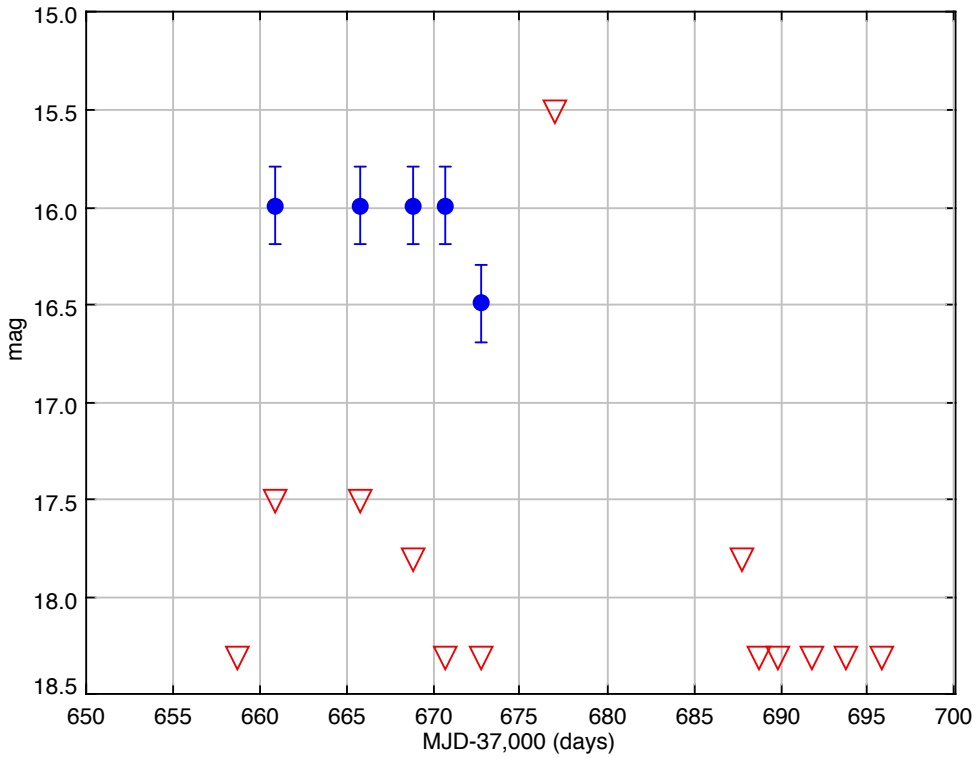

Figure 2. Light curve of the outburst on MJD 37660. Blue points are detections, red triangles the upper limit of the corresponding plate.

Trying to determine a recurrence time scale for the large outbursts is not easy due to the sparse sampling and to the very fact that these superoutbursts are not strictly periodic: an estimate can be obtained looking for the largest possible integer number of days T between two consecutive outbursts in Table 1: the results are listed in column 9 of Table 1, where the time interval T and the number of intervals N are reported. The results are fairly consistent, suggesting a recurrence time scale of the order of 300 days, which is nearly double of the typical superoutburst interval of SU UMa itself. I have checked if, assuming the recurrence time was true, the missed outbursts were lost for lack of plates at the proper date: this assumption often proved to be valid, but in some cases the outburst should be detected if it happened at the predicted date. However, given

the very short duration of the outbursts (about 10 days or less), the large gaps in the observations, and the large uncertainty of the outburst epochs due to the lack of a strict period in this kind of stars, this test cannot be conclusive.

Shurpakov et al. (2013) quoted also a previous bright state detected by the NEAT program on 2002-11-15 (MJD 52594). As a further check we computed the recurrence time scale using the last Asiago outburst, the NEAT outburst and the MASTER (MJD 56494) one in the same way. The results are: 20×330 d (Asiago-NEAT) and 12×325 d (NEAT-MASTER), therefore compatible with the recurrence time from the historical Asiago data.

All these finding support the classification of the star as a SU UMa cataclysmic variable.

From a statistical point of view, there are 384 dates with observations in the Asiago archive, spanning about 24 years (11061 days): assuming a high state of 10 days and an average recurrence of 320 days, one should expect about 34 outbursts and that the star was detectable on 340 days. Given our temporal fractional coverage of 0.0347 (384/11061) one should expect detection on 12 days, while we found 29. The "order of magnitude" agreement may be regarded as satisfactory, given the large uncertainties in the assumed recurrence time and outburst duration. A recurrence of 160 days instead of 320 would produce a very good statistical agreement and cannot be ruled out by the present data set.

The peak magnitude difference between an outburst and a superoutburst is about 1 mag in SU UMa stars: if superoutbursts in our star reach 16.0 mag then a brightening at 17.0 mag (like that on MJD 42337) might be considered as a normal outburst. The photometric accuracy of these plates is however rather low, especially near the plate limit, as is often the case for our star: due to the short (1 m) focal length of the telescope, the apparent diameter of a faint star is very similar to the emulsion grain size, and plate noise may be misinterpreted as a detection if located at the expected star position. Our estimate of 0.2 mag uncertainty is therefore rather optimistic in these cases.

The large majority of our plates are from the S50 telescope, with a limiting magnitude mostly in the magnitude range 17.0-17.5 (see Fig. 1): normal outbursts are therefore unlikely to have been recorded.

Further monitoring of this star may be easily performed even by amateurs with a small telescope and a CCD camera, for its position in the northern sky allows a good coverage during the year.

Acknowledgements: The author thanks the Asiago Observatory for access to the plate archive to perform this research.

References:

Asiago Plate Archive:
http://www.oapd.inaf.it/index.php/en/telescopes-and-instrumentations/archive-and-publication.html

Lasker B., Lattanzi M.G., McLean B.J. et al., 2008, *AJ*, **136**, 735, GSC 2.3.2 CDS catalog I/271

NEAT - SkyMorph GSFC: http://skyview.gsfc.nasa.gov/skymorph/skymorph.html

Shurpakov S., Denisenko, D., Lipunov V., et al., 2013, *ATel*, **5217**

COMMISSIONS 27 AND 42 OF THE IAU
INFORMATION BULLETIN ON VARIABLE STARS

Number 6084

Konkoly Observatory
Budapest
2 December 2013

HU ISSN 0374 – 0676

BAV-RESULTS OF OBSERVATIONS - PHOTOELECTRIC MINIMA OF SELECTED ECLIPSING BINARIES AND MAXIMA OF PULSATING STARS

(BAV MITTEILUNGEN NO. 232)

HÜBSCHER, JOACHIM

Bundesdeutsche Arbeitsgemeinschaft für Veränderliche Sterne e.V. (BAV), Munsterdamm 90, 12169 Berlin, Germany, www.bav-astro.de, publikat@bav-astro.de

In this 76^{th} compilation of BAV results, photoelectric observations obtained mostly in the years 2012 and 2013 are presented on 373 variable stars giving 524 minima on eclipsing binaries and maxima on pulsating stars. All moments of minima and maxima are heliocentric UTC. The errors are tabulated in column '±'. The values in column '$O-C$' are determined without incorporating nonlinear terms. The references are given in the section 'Remarks'. All information about photometers and filters are specified in the columns 'Fil' and 'Rem'. The observations were made at private observatories. The photoelectric measurements and all the light curves with evaluations can be obtained from the office of the BAV for inspection.

Please use the following link for an easy access to all the publications of the BAV including the "Lichtenknecker Database of the BAV": `http://www.bav-astro.de/sfs` .

Table 1: Times of minima of eclipsing binaries

Variable	HJD 24.....	±	Obs	$O-C$		Ref	Fil	n	Rem
CK Aqr	56516.4021	0.0002	RDL WLH	+0.0063	s	⟨6⟩	o	372	14)
OO Aql	56489.4831	0.0068	AG	+0.0575	s	⟨6⟩	-I	29	12)
OP Aql	56489.5506	0.0011	AG	−0.0081		⟨6⟩	-I	29	12)
V417 Aql	56489.5025	0.0019	AG	+0.0401		⟨6⟩	-I	29	12)
	56525.4214	0.0007	QU	+0.0565		⟨6⟩	V	53	5)
V640 Aql	56489.5217	0.0009	AG	−0.0373		⟨6⟩	-I	29	12)
V760 Aql	56489.4159	0.0008	AG	−0.0379		⟨6⟩	-I	29	12)
V997 Aql	56489.5151	0.0042	AG	+0.0055		⟨6⟩	-I	29	12)
V1168 Aql	56489.4199	0.0015	AG	+0.0030		⟨6⟩	-I	29	12)
V1692 Aql	56489.4842	0.0065	AG	−0.0690	s	⟨6⟩	-I	29	12)
V1714 Aql	56489.3899	0.0003	AG	−0.0105		⟨6⟩	-I	29	12)
CL Ari	56338.3736	0.0081	AG	−0.0629		⟨6⟩	-I	17	12)
RZ Aur	56356.4594	0.0053	AG	−0.0404		⟨6⟩	-I	43	12)
AH Aur	56334.3885	0.0030	AG	−0.0172	s	⟨6⟩	-I	36	12)
	56355.3859	0.0005	AG	−0.0194		⟨6⟩	-I	37	12)
AP Aur	56355.3323	0.0031	AG	+0.0968		⟨6⟩	-I	49	12)
	56355.6248	0.0035	AG	+0.1046	s	⟨6⟩	-I	49	12)
FP Aur	56356.4627	0.0028	AG	−0.0013		⟨6⟩	-I	48	12)
V410 Aur	56334.3411	0.0033	AG	+0.0165		⟨6⟩	-I	39	12)
V425 Aur	56334.3454	0.0113	AG	+0.0129		⟨6⟩	-I	39	12)
V455 Aur	56354.4583	0.0014	AG	−0.0676	s	⟨6⟩	-I	32	12)
V523 Aur	56355.4358	0.0007	AG	+0.0025	s	⟨6⟩	-I	48	12)
	56355.5990	0.0020	AG	+0.0005		⟨6⟩	-I	48	12)
V645 Aur	56354.4223	0.0038	AG	+0.0003		⟨6⟩	-I	17	12)
TX Boo	56408.3909	0.0089	AG	+0.0638		⟨6⟩	-I	35	12)

Table 1: (cont.)

Variable	HJD 24.....	±	Obs	$O-C$		Ref	Fil	n	Rem
TY Boo	56408.4154	0.0015	AG	−0.0066		⟨6⟩	-I	36	12)
	56408.5742	0.0006	AG	−0.0063	s	⟨6⟩	-I	36	12)
TZ Boo	56400.5676	0.0024	AG	−0.0076		⟨6⟩	-I	23	12)
XY Boo	56356.4703	0.0020	FR	−0.0241	s	⟨6⟩	V	70	18)
	56356.6574	0.0008	FR	−0.0223		⟨6⟩	V	70	18)
	56400.5695	0.0020	AG	−0.0234	s	⟨6⟩	-I	23	12)
	56418.3614	0.0038	AG	−0.0191	s	⟨6⟩	-I	30	12)
	56418.5387	0.0039	AG	−0.0271		⟨6⟩	-I	30	12)
AC Boo	56449.4926	0.0004	QU	+0.0052		⟨6⟩	V	65	5)
AQ Boo	56356.6148	0.0023	FR	−0.0088		⟨6⟩	V	33	18)
DU Boo	56418.4458	0.0092	AG	+0.0087		⟨6⟩	-I	32	12)
EQ Boo	56356.5959	0.0001	FR	−0.0061		⟨6⟩	-I	57	12)
FI Boo	56400.5157	0.0123	AG	−0.0263	s	⟨6⟩	-I	23	12)
FY Boo	56356.5307	0.0020	FR	+0.0088	s	⟨6⟩	V	35	18)
	56356.6520	0.0007	FR	+0.0095		⟨6⟩	V	35	18)
GK Boo	56400.4867	0.0024	AG	−0.0002		⟨6⟩	-I	23	12)
	56418.4035	0.0024	AG	+0.0002	s	⟨6⟩	-I	31	12)
GN Boo	56408.5605	0.0013	AG	+0.0265		⟨6⟩	-I	36	12)
GW Boo	56418.3519	0.0040	AG	+0.0342	s	⟨6⟩	-I	30	12)
KW Boo	56408.4645	0.0050	AG	+0.0071	s	⟨6⟩	-I	36	12)
NW Boo	56408.5712	0.0052	AG	+0.0038		⟨6⟩	-I	36	12)
NX Boo	56408.4112	0.0006	AG	+0.0352		⟨6⟩	-I	36	12)
	56408.5375	0.0014	AG	+0.0359	s	⟨6⟩	-I	36	12)
OQ Boo	56408.3769	0.0054	AG	−0.0452	s	⟨6⟩	-I	36	12)
	56408.5810	0.0037	AG	−0.0400		⟨6⟩	-I	36	12)
PY Boo	56400.4999	0.0048	AG	+0.0362		⟨6⟩	-I	23	12)
SV Cam	56356.2662	0.0007	AG	+0.0559		⟨6⟩	-I	33	12)
AW Cam	56356.3866	0.0095	AG	−0.0120	s	⟨6⟩	-I	22	12)
	56371.4304	0.0011	AG	−0.0094		⟨6⟩	-I	40	12)
AZ Cam	56408.3755	0.0031	AG	+0.0186		⟨6⟩	-I	34	12)
CV Cam	56187.4847	0.0038	FR				V	49	18)
FN Cam	56374.4861	0.0067	AG	+0.0050	s	⟨4⟩	-I	27	12)
HW Cam	56356.3366	0.0030	AG	+0.0021	s	⟨4⟩	-I	21	12)
	56371.6187	0.0009	AG	−0.0001	s	⟨4⟩	-I	30	12)
	56374.3521	0.0031	AG	+0.0040		⟨4⟩	-I	27	12)
V506 Cam	56371.5301	0.0027	AG	+0.0026	s	⟨6⟩	-I	30	12)
WY Cnc	56371.4447	0.0010	AG	−0.0361		⟨6⟩	-I	33	12)
VZ CVn	56408.4142	0.0035	AG	−0.0016	s	⟨6⟩	-I	33	12)
	56418.5254	0.0038	AG	+0.0000	s	⟨6⟩	-I	30	12)
BI CVn	56400.5747	0.0010	AG	−0.0236		⟨6⟩	-I	22	12)
	56407.4389	0.0071	AG	−0.0743		⟨6⟩	-I	36	12)
BO CVn	56408.4754	0.0048	AG	+0.0018		⟨4⟩	-I	34	12)
	56418.5698	0.0012	AG	+0.0057	s	⟨4⟩	-I	32	12)
EL CVn	56407.3910	0.0050	AG	−0.0214		⟨6⟩	-I	36	12)
	56418.5308	0.0096	AG	−0.0204		⟨6⟩	-I	31	12)
GG CVn	56418.3903	0.0092	AG	+0.0224		⟨6⟩	-I	32	12)
GM CVn	56408.5114	0.0051	AG	−0.0150	s	⟨6⟩	-I	34	12)
	56418.4159	0.0037	AG	−0.0192	s	⟨6⟩	-I	32	12)
RW CMi	56354.3940	0.0039	AG	−1.2470		⟨4⟩	-I	21	12)
TZ CMi	56354.4207	0.0012	AG	−0.6493		⟨6⟩	-I	21	12)
AK CMi	56354.4052	0.0004	AG	−0.0204		⟨6⟩	-I	18	12)
DW CMi	56354.4143	0.0003	AG	+0.0090	s	⟨6⟩	-I	17	12)
V523 Cas	56519.4294	0.0004	JU	−0.0188	s	⟨6⟩	o	47	4)
WY Cep	56489.3952	0.0038	AG	+0.0209		⟨6⟩	-I	25	12)
XX Cep	56533.4462	0.0011	JU	−0.0010		⟨6⟩	o	73	4)
XZ Cep	56219.3461	0.0020	AG	+0.0654		⟨6⟩	-I	54	12)
ZZ Cep	56491.4802	0.0042	AG	−0.0156		⟨6⟩	-I	20	12)
EG Cep	56485.5194	0.0033	AG	+0.0125		⟨6⟩	-I	23	12)
	56491.5105	0.0016	AG	+0.0128		⟨6⟩	-I	22	12)

Table 1: (cont.)

Variable	HJD 24.....	±	Obs	$O-C$		Ref	Fil	n	Rem
FK Cep	56490.3931	0.0036	AG				-I	32	12)
GG Cep	56490.4835	0.0009	AG	−0.1161		⟨6⟩	-I	32	12)
NS Cep	56490.4959	0.0007	AG	−0.1859		⟨6⟩	-I	32	12)
V711 Cep	56485.4484	0.0055	AG	+0.0092		⟨4⟩	-I	23	12)
V736 Cep	56480.5171	0.0082	AG	−0.0181		⟨6⟩	-I	16	12)
	56483.5213	0.0058	AG	−0.0164	s	⟨6⟩	-I	21	12)
V737 Cep	56490.5127	0.0003	AG	+0.0343		⟨6⟩	-I	32	12)
V738 Cep	56483.4535	0.0083	AG	−0.0197	s	⟨6⟩	-I	18	12)
	56485.4067	0.0010	AG	−0.0139		⟨6⟩	-I	21	12)
RZ Com	56397.4236	0.0015	AG	+0.0464	s	⟨6⟩	-I	24	12)
	56398.4405	0.0002	AG	+0.0477	s	⟨6⟩	-I	45	12)
	56407.4102	0.0059	AG	+0.0470		⟨6⟩	-I	36	12)
	56407.5825	0.0008	AG	+0.0501	s	⟨6⟩	-I	36	12)
Y Cyg	56491.4714	0.0057	AG	+0.1217	s	⟨6⟩	-I	19	12)
WZ Cyg	56521.3728	0.0002	WTR	+0.0661		⟨6⟩	o	71	3)
BR Cyg	56489.5030	0.0018	AG	+0.0004		⟨6⟩	-I	25	12)
CG Cyg	56480.5161	0.0015	AG	+0.0708		⟨6⟩	-I	16	12)
CV Cyg	55832.4561	0.0024	FR	+0.2053	s	⟨6⟩	o	47	18)
HK Cyg	56485.4406	0.0028	SCI	−0.2351		⟨6⟩	o	45	4)
KR Cyg	56483.4310	0.0006	AG	+0.0190		⟨6⟩	-I	19	12)
V382 Cyg	56157.4306	0.0011	FR	+0.1085	s	⟨6⟩	o	36	18)
V456 Cyg	56483.5319	0.0019	AG	+0.0482		⟨6⟩	-I	18	12)
V477 Cyg	56483.4699	0.0087	AG	+0.6692		⟨6⟩	-I	19	12)
V478 Cyg	56485.4697	0.0124	AG	+0.0194		⟨6⟩	-I	22	12)
V498 Cyg	55832.4415	0.0030	FR	+0.2210	s	⟨6⟩	o	47	18)
V526 Cyg	56491.4268	0.0011	AG	+0.0399		⟨6⟩	-I	33	12)
V548 Cyg	56515.4836	0.0010	ALH	+0.0314		⟨6⟩	V	480	7)
V680 Cyg	56490.5068	0.0067	AG	+0.0634		⟨6⟩	-I	31	12)
V687 Cyg	56167.3374	0.0008	FR	−0.0067		⟨6⟩	V	82	18)
V700 Cyg	56517.3914	0.0005	WTR	−0.0740	s	⟨6⟩	o	72	3)
V706 Cyg	56491.5098	0.0062	AG	−0.0602	s	⟨6⟩	-I	32	12)
V796 Cyg	56489.4434	0.0035	AG	−0.0287	s	⟨6⟩	-I	25	12)
V836 Cyg	56490.4547	0.0100	AG	+0.0198	s	⟨6⟩	-I	30	12)
V909 Cyg	56495.4328	0.0007	QU	−0.1706	s	⟨6⟩	V	80	5)
V936 Cyg	54023.3948	0.0050	FR	−0.0503		⟨6⟩	-I	23	11)
V1061 Cyg	56521.4847	0.0007	QU	−0.0112		⟨6⟩	V	106	5)
V1171 Cyg	56489.4409	0.0053	AG	−0.0584	s	⟨6⟩	-I	25	12)
V1191 Cyg	55832.3713	0.0015	FR	+0.0078		⟨6⟩	o	93	18)
	55832.5214	0.0027	FR	+0.0012	s	⟨6⟩	o	93	18)
V1193 Cyg	56489.5239	0.0025	SCI	−0.1541		⟨6⟩	o	36	4)
V1305 Cyg	55832.3918	0.0023	FR	+0.0057	s	⟨6⟩	o	42	18)
	56490.5012	0.0016	SCI	+0.0066		⟨6⟩	o	150	4)
V1425 Cyg	56483.4809	0.0083	AG	+0.0092	s	⟨6⟩	-I	21	12)
V1818 Cyg	56167.3842	0.0027	FR				V	62	18)
V1918 Cyg	56450.4430	0.0004	QU	+0.0071	s	⟨4⟩	V	90	5)
V2080 Cyg	56490.5049	0.0089	AG	−0.0133		⟨4⟩	-I	31	12)
V2278 Cyg	56218.5211	0.0021	SCI				o	107	4)
	56220.5145	0.0022	SCI				o	90	4)
	56221.3919	0.0025	SCI				o	70	4)
	56222.2764	0.0028	SCI				o	101	4)
	56225.3791	0.0028	SCI				o	58	4)
	56480.5020	0.0028	SCI				o	66	4)
	56486.4751	0.0025	SCI				o	66	4)
	56505.4823	0.0020	SCI				o	83	4)
V2364 Cyg	56490.5381	0.0043	AG	−0.0194		⟨6⟩	-I	31	12)
V2477 Cyg	56480.4606	0.0029	AG	+0.0000	s	⟨6⟩	-I	16	12)
V2520 Cyg	56179.5901	0.0033	FR	−0.0196	s	⟨6⟩	V	49	18)
TY Del	56489.5152	0.0008	AG	+0.0599		⟨6⟩	-I	25	12)
FZ Del	56490.4817	0.0008	AG	−0.0346		⟨6⟩	-I	30	12)

Table 1: (cont.)

Variable	HJD 24.....	±	Obs	$O-C$		Ref	Fil	n	Rem
RZ Dra	56485.5108	0.0029	AG	+0.0574	s	⟨6⟩	-I	23	12)
TZ Dra	56461.4294	0.0030	JU	−0.0383	s	⟨6⟩	o	31	4)
	56483.5157	0.0024	AG	−0.0359		⟨6⟩	-I	22	12)
	56490.4435	0.0019	AG	−0.0364		⟨6⟩	-I	31	12)
WW Dra	56400.5555	0.0059	AG	+0.5930		⟨6⟩	-I	23	12)
BH Dra	56489.4282	0.0018	AG	−0.0032		⟨6⟩	-I	25	12)
BS Dra	56483.4179	0.0045	AG	−0.0019	s	⟨6⟩	-I	20	12)
BV Dra	56408.4591	0.0014	AG	−0.0054		⟨6⟩	-I	34	12)
GM Dra	56483.4878	0.0024	AG	−0.0126	s	⟨4⟩	-I	22	12)
V341 Dra	56400.6049	0.0006	AG	+0.0041		⟨6⟩	-I	23	12)
AL Gem	56334.3053	0.0021	AG	+0.0785		⟨6⟩	-I	39	12)
	56338.4771	0.0014	AG	+0.0763		⟨6⟩	-I	25	12)
V345 Gem	56355.3776	0.0026	SCI	+0.0258		⟨4⟩	o	167	4)
V348 Gem	56355.4767	0.0020	FR				V	25	18)
V382 Gem	56354.3793	0.0024	AG	−0.0147	s	⟨6⟩	-I	19	12)
V389 Gem	56334.3476	0.0077	AG	−0.0113		⟨6⟩	-I	39	12)
V417 Gem	56355.4088	0.0063	AG	+0.0207	s	⟨6⟩	-I	40	12)
SZ Her	56491.475 :	0.006	AG	+0.391		⟨6⟩	-I	20	12)
UX Her	56460.4407	0.0006	QU	+0.0998		⟨6⟩	V	75	5)
BC Her	56487.4879	0.0024	SCI	−0.4204	s	⟨6⟩	o	97	4)
DH Her	56483.4550	0.0074	AG	+0.0095		⟨6⟩	-I	20	12)
DK Her	56493.4799	0.0024	SCI	−0.1480	s	⟨6⟩	o	71	4)
HS Her	56491.4564	0.0106	AG	−0.0278		⟨6⟩	-I	19	12)
V338 Her	56485.5277	0.0026	AG	+0.1182	s	⟨6⟩	-I	21	12)
	56487.4798	0.0006	JU	+0.1117		⟨6⟩	o	76	4)
V357 Her	56440.4917	0.0014	SCI	+0.0276	s	⟨6⟩	o	56	4)
	56448.5272	0.0028	SCI	+0.0290		⟨6⟩	o	55	4)
	56449.5107	0.0021	SCI	+0.0344		⟨6⟩	o	62	4)
	56451.4894	0.0019	SCI	−0.0129	s	⟨6⟩	o	38	4)
	56483.4955	0.0018	SCI	−0.0039	s	⟨6⟩	o	66	4)
V450 Her	56485.4293	0.0041	AG	+0.1060	s	⟨6⟩	-I	23	12)
	56495.4702	0.0017	JU	+0.1069	s	⟨6⟩	o	70	4)
V731 Her	56489.4190	0.0009	JU	+0.0990		⟨6⟩	o	65	4)
V732 Her	56450.4204	0.0090	JU	+0.0393	s	⟨6⟩	o	72	4)
	56451.4906	0.0050	JU	+0.0585	s	⟨6⟩	o	69	4)
V742 Her	56450.5170	0.0020	SCI	+0.0399	s	⟨6⟩	o	66	4)
V829 Her	56506.4867	0.0016	JU	+0.0138		⟨4⟩	o	81	4)
V842 Her	56480.4104	0.0002	WTR	+0.0064	s	⟨4⟩	o	61	3)
V857 Her	56480.4494	0.0007	JU	+0.0050		⟨4⟩	o	66	4)
V994 Her	56490.4522	0.0063	AG				-I	31	12)
V1047 Her	56505.4599	0.0015	JU	−0.0059	s	⟨4⟩	o	71	4)
V1055 Her	56462.4825	0.0012	JU	+0.0113	s	⟨4⟩	o	60	4)
RW Lac	56489.4428	0.0051	AG	−0.0134	s	⟨6⟩	-I	25	12)
V401 Lac	56491.4340	0.0044	AG				-I	21	12)
UV Leo	56371.5971	0.0005	AG	+0.0375	s	⟨6⟩	-I	23	12)
	56397.4002	0.0015	AG	+0.0370	s	⟨6⟩	-I	22	12)
UZ Leo	56371.5797	0.0021	AG	−0.0659	s	⟨6⟩	-I	23	12)
	56398.4630	0.0002	AG	−0.0674		⟨6⟩	-I	16	12)
XY Leo	56356.3607	0.0010	AG	−0.0439	s	⟨6⟩	-I	18	12)
	56371.5600	0.0037	AG	−0.0438		⟨6⟩	-I	23	12)
AL Leo	56356.3328	0.0025	AG	+0.8182	s	⟨6⟩	-I	18	12)
	56371.5835	0.0029	AG	−0.5087	s	⟨6⟩	-I	23	12)
AM Leo	56397.3619	0.0004	WTR	+0.0137		⟨6⟩	o	76	3)
	56397.3628	0.0015	AG	+0.0146		⟨6⟩	-I	22	12)
BW Leo	56356.4796	0.0017	SCI	+0.0456		⟨6⟩	o	29	4)
	56356.6491	0.0028	SCI	+0.0465	s	⟨6⟩	o	27	4)
EX Leo	56398.5324	0.0025	AG	+0.0123	s	⟨4⟩	-I	36	12)
VW LMi	56398.4076	0.0011	AG	+0.0116		⟨4⟩	-I	37	12)
SW Lyn	56356.2808	0.0001	AG	+0.0601		⟨6⟩	-I	21	12)

Table 1: (cont.)

Variable	HJD 24.....	±	Obs	$O-C$		Ref	Fil	n	Rem
SW Lyn	56371.4216	0.0025	AG	+0.0654	s	⟨6⟩	-I	29	12)
BG Lyn	56355.5344	0.0025	AG	−0.0001		⟨4⟩	-I	50	12)
CC Lyn	56355.4856	0.0021	AG	+0.0627	s	⟨4⟩	-I	43	12)
DY Lyn	56354.4512	0.0016	AG	−0.1878	s	⟨6⟩	-I	25	12)
	56356.4205	0.0005	AG	−0.1883		⟨6⟩	-I	21	12)
	56371.5211	0.0030	AG	−0.1900	s	⟨6⟩	-I	29	12)
DZ Lyn	56356.3443	0.0037	AG	−0.0161		⟨6⟩	-I	21	12)
	56371.4692	0.0011	AG	−0.0120		⟨6⟩	-I	20	12)
FI Lyn	56355.4371	0.0026	AG	+0.0169		⟨6⟩	-I	59	12)
	56355.6234	0.0018	AG	+0.0166	s	⟨6⟩	-I	59	12)
FN Lyn	56354.3422	0.0006	AG	+0.0641		⟨6⟩	-I	25	12)
AA Lyr	56500.4726	0.0005	FR	+0.2110		⟨6⟩	-I	53	12)
V574 Lyr	56490.4440	0.0008	JU	+0.0052	s	⟨4⟩	o	86	4)
V579 Lyr	56492.4709	0.0006	JU	−0.0157		⟨4⟩	o	64	4)
V580 Lyr	56478.4513	0.0008	JU	−0.0081		⟨4⟩	o	58	4)
V922 Mon	55968.2808	0.0002	RAT RCR	−0.0196		⟨6⟩	-U-I	116	15)
V451 Oph	56489.5001	0.0022	AG	−0.0041		⟨6⟩	-I	25	12)
V913 Oph	56046.5489	0.0002	RAT RCR	+0.3318		⟨6⟩	-U-I	232	15)
V2640 Oph	56072.4495	0.0003	RAT RCR	+0.0016		⟨6⟩	-U-I	188	15)
FK Ori	56220.4931	0.0005	RAT RCR	−0.0458		⟨6⟩	R	170	15)
V1848 Ori	55960.3064	0.0002	RAT RCR	−0.0026	s	⟨6⟩	-U-I	129	15)
V2735 Ori	56354.3222	0.0006	AG	−0.0130		⟨6⟩	-I	16	12)
V2790 Ori	55959.3466	0.0002	RAT RCR	−0.0085		⟨6⟩	-U-I	93	15)
TY Peg	56175.3641	0.0019	BHE	−0.3586		⟨6⟩	-I	329	16)
BB Peg	56148.4843	0.0003	RAT RCR	−0.0073	s	⟨6⟩	V	157	15)
BO Peg	56135.4829	0.0002	RAT RCR	−0.0378		⟨6⟩	-U-I	219	15)
BX Peg	56141.4758	0.0002	RAT RCR	+0.0324	s	⟨6⟩	V	138	15)
	56178.3510	0.0002	RAT RCR	+0.0323		⟨6⟩	R	83	15)
	56187.3246	0.0006	BHE	+0.0324		⟨6⟩	-I	328	16)
DK Peg	56181.4299	0.0013	BHE	+0.1289		⟨6⟩	-I	201	16)
V365 Peg	56131.4986	0.0002	RAT RCR				-U-I	231	15)
RT Per	56151.5264	0.0020	FR	+0.0726	s	⟨6⟩	o	38	18)
IT Per	56172.5130	0.0007	RAT RCR	−0.0210		⟨6⟩	V	180	15)
IU Per	55964.3132	0.0003	RAT RCR	+0.0140		⟨6⟩	-U-I	219	15)
KR Per	56334.3145	0.0042	AG	−0.0172		⟨6⟩	-I	37	12)
NZ Per	56334.3109	0.0035	AG	+0.0365		⟨6⟩	-I	36	12)
V432 Per	56210.4707	0.0001	RAT RCR	−0.0163	s	⟨6⟩	R	186	15)
V723 Per	56177.4666	0.0050	RAT RCR	−0.0537		⟨6⟩	R	191	15)
V732 Per	56151.4877	0.0018	FR	−0.1424		⟨6⟩	o	26	18)
	56187.5393	0.0013	FR	−0.1432		⟨6⟩	V	55	18)
V912 Per	55966.4410	0.0005	RAT RCR	+0.0874		⟨6⟩	-U-I	245	15)
V959 Per	56334.4515	0.0022	AG	+0.0214		⟨6⟩	-I	37	12)
	56338.4166	0.0041	AG	+0.0236		⟨6⟩	-I	25	12)
RV Psc	55962.2620	0.0002	RAT RCR	−0.0546		⟨6⟩	-U-I	130	15)
VZ Psc	56222.2724	0.0003	RAT RCR	+0.0318	s	⟨6⟩	R	117	15)
EX Psc	56221.3313	0.0020	RAT RCR	−0.0203	s	⟨6⟩	R	161	15)
GX Psc	55962.2678	0.0010	RAT RCR	−0.0600		⟨6⟩	-U-I	134	15)
MP Pup	56354.3792	0.0003	FR				-I	38	12)
CU Sge	56097.5072	0.0002	RAT RCR	+0.0192		⟨6⟩	-U-I	203	15)
DK Sge	56101.4595	0.0002	RAT RCR	−0.1481	s	⟨6⟩	-U-I	217	15)
GN Sge	56489.4109	0.0042	AG	+0.0041		⟨6⟩	-I	25	12)
V366 Sge	56060.5479	0.0004	RAT RCR	−0.0227		⟨6⟩	-U-I	174	15)
AO Ser	56450.4082	0.0002	WTR	−0.0147		⟨6⟩	o	60	3)
V384 Ser	56407.4080	0.0006	FR	−0.0024		⟨6⟩	-I	80	12)
	56407.5396	0.0002	FR	−0.0052	s	⟨6⟩	-I	80	12)
	56475.3965	0.0004	FR	−0.0023		⟨6⟩	-I	64	12)
	56475.5292	0.0003	FR	−0.0040	s	⟨6⟩	-I	64	12)
Y Sex	56009.394 :	0.002	RAT RCR	−0.012	s	⟨6⟩	-U-I	140	15)
WX Sex	55969.4027	0.0010	RAT RCR	+0.0000	s	⟨6⟩	-U-I	170	15)

Table 1: (cont.)

Variable	HJD 24.....	±	Obs	$O-C$		Ref	Fil	n	Rem
AI Sex	56009.3329	0.0009	RAT RCR	−0.0080		⟨6⟩	-U-I	138	15)
RZ Tau	55944.2889	0.0001	RAT RCR	+0.0659		⟨6⟩	-U-I	145	15)
CT Tau	56355.3208	0.0003	AG	−0.0588	s	⟨6⟩	-I	33	12)
	56356.3219	0.0007	AG	−0.0579		⟨6⟩	-I	17	12)
EQ Tau	56251.3860	0.0002	RAT RCR	−0.0267	s	⟨6⟩	R	106	15)
ET Tau	56354.3427	0.0089	AG	−0.0857		⟨6⟩	-I	20	12)
V1128 Tau	56218.5032	0.0001	RAT RCR	+0.0006	s	⟨4⟩	R	178	15)
V1370 Tau	55957.3634	0.0002	RAT RCR	−0.0554		⟨6⟩	-U-I	176	15)
V1374 Tau	56356.3020	0.0002	AG	−0.0310		⟨6⟩	-I	16	12)
BI Tri	55963.3692	0.0007	RAT RCR	+0.0896		⟨6⟩	-U-I	218	15)
CL Tri	56220.3922	0.0003	RAT RCR	+0.0098		⟨6⟩	R	125	15)
W UMa	56354.3130	0.0012	SCI	−0.0785		⟨6⟩	o	83	4)
	56354.4811	0.0012	SCI	−0.0772	s	⟨6⟩	o	116	4)
	56354.6496	0.0017	SCI	−0.0756		⟨6⟩	o	125	4)
	56397.3527	0.0016	AG	−0.0781		⟨6⟩	-I	21	12)
	56398.5202	0.0028	AG	−0.0783	s	⟨6⟩	-I	21	12)
	56408.3634	0.0010	AG	−0.0774		⟨6⟩	-I	28	12)
	56408.5303	0.0008	AG	−0.0773	s	⟨6⟩	-I	28	12)
VV UMa	56407.4646	0.0025	JU	−0.0540	s	⟨6⟩	o	106	4)
	56408.4964	0.0019	AG	−0.0533		⟨6⟩	-I	28	12)
XY UMa	56408.4636	0.0032	JU	+0.0445	s	⟨6⟩	o	69	4)
ZZ UMa	56012.5262	0.0001	RAT RCR	−0.0013		⟨6⟩	-U-I	302	15)
AF UMa	56407.5296	0.0061	AG	+0.5798		⟨6⟩	V	115	12)
	56407.5297	0.0063	AG	+0.5799		⟨6⟩	B	115	12)
DW UMa	56384.4728	0.0007	SCI	−0.0010		⟨4⟩	o	36	4)
GT UMa	56407.4222	0.0120	AG				B	115	12)
MQ UMa	56011.6263	0.0004	RAT RCR	+0.0825		⟨6⟩	-U-I	289	15)
MS UMa	56008.4486	0.0002	RAT RCR	+0.0397		⟨6⟩	-U-I	215	15)
	56008.6523	0.0003	RAT RCR	+0.0382	s	⟨6⟩	-U-I	215	15)
MW UMa	56408.4903	0.0017	AG	+0.1135	s	⟨6⟩	-I	34	12)
OX UMa	55966.6340	0.0020	RAT RCR	+0.0766		⟨6⟩	-U-I	262	15)
QT UMa	56002.6601	0.0010	RAT RCR	−0.0831		⟨6⟩	-U-I	299	15)
RU UMi	56400.5530	0.0058	AG	−0.0141	s	⟨6⟩	-I	23	12)
	56407.3791	0.0066	AG	−0.0120	s	⟨6⟩	-I	36	12)
TU UMi	55957.4887	0.0010	RAT RCR				-U-I	341	15)
TV UMi	56407.3595	0.0057	AG	+0.0016		⟨4⟩	-I	36	12)
WW UMi	55944.6236	0.0008	RAT RCR	+0.0658		⟨6⟩	-U-I	375	15)
AH Vir	56407.5369	0.0012	AG	+0.0510		⟨6⟩	-I	32	12)
BF Vir	56046.3823	0.0001	RAT RCR	+0.1017		⟨6⟩	-U-I	145	15)
V415 Vir	56407.4838	0.0043	AG	+0.0211	s	⟨6⟩	-I	33	12)
	56418.4981	0.0080	AG	+0.0111		⟨6⟩	-I	26	12)
BP Vul	56112.4526	0.0002	RAT RCR	−0.0142		⟨6⟩	-U-I	162	15)
HI Vul	56179.4133	0.0028	FR	−0.0578	s	⟨6⟩	-I	27	12)
ASAS J013711-3459.3	56153.5012	0.0002	WLH HUN				-U-I	88	4)
ASAS J062230+2734.7	56355.3751	0.0166	AG				-I	37	12)
ASAS J072000+2543.7	56334.3845	0.0080	AG				-I	39	12)
	56355.4056	0.0113	AG				-I	39	12)
ASAS J072125+2559.1	56355.3633	0.0057	AG				-I	39	12)
ASAS J140804+2303.6	56356.6268	0.0033	FR				V	63	18)
ASAS J191441+2747.7	56167.4720	0.0022	FR				V	43	18)
ASAS J191829+2608.7	56167.4926	0.0026	FR				V	75	18)
ASAS J192810+2542.0	56167.3917	0.0008	FR				V	87	18)
	56167.6026	0.0030	FR				V	87	18)
ASAS J193137+2635.7	56167.4651	0.0042	FR				V	40	18)
ASAS J193431+2548.2	56167.3634	0.0050	FR				V	37	18)
ASAS J194531+2821.4	56167.5412	0.0027	FR				V	27	18)
ASAS J194917+2824.0	56179.4786	0.0028	FR				V	41	18)
ASAS J195525+4326.1	55832.3014	0.0025	FR				V	85	18)
ASAS J200540+2805.2	56179.3799	0.0023	FR				V	47	18)
GSC 01935-00177	56013.4809	0.0025	FR				o	40	18)

Table 1: (cont.)

Variable	HJD 24.....	±	Obs	$O-C$		Ref	Fil	n	Rem
GSC 02038-00293	56407.3819	0.0012	FR	+0.0173	s	⟨3⟩	-I	166	12)
	56407.6131	0.0009	FR	+0.0008		⟨3⟩	-I	166	12)
	56475.4857	0.0005	FR	+0.0023		⟨3⟩	-I	32	12)
GSC 02111-00334	53282.2703	0.0006	FR				-I	40	10)
	53282.4096	0.0019	FR				-I	40	10)
	53284.3883	0.0008	FR				-I	49	10)
GSC 02134-00028	56500.4232	0.0035	FR				-I	30	12)
GSC 02134-00821	56500.5714	0.0010	FR				-I	70	12)
GSC 02150-01562	56179.3114	0.0018	FR				-I	186	12)
GSC 02151-04948	56167.3977	0.0039	FR				V	57	18)
GSC 02454-00681	56355.3813	0.0009	FR				V	51	18)
	56355.5670	0.0021	FR				V	51	18)
GSC 02454-01430	56355.4165	0.0048	FR				V	35	18)
GSC 02469-00087	56355.4217	0.0019	FR				V	46	18)
GSC 02675-00663	56179.5041	0.0042	FR				V	35	18)
GSC 02678-01769	55067.5285	0.0017	FR				-I	96	12)
GSC 02678-02360	55067.4677	0.0011	FR				-I	31	12)
GSC 02695-03163	54682.5165	0.0007	FR				-I	50	12)
	56158.4296	0.0066	AG				-I	29	12)
GSC 03098-00252	56418.5081	0.0022	JU				o	90	4)
GSC 03148-01402	55832.3914	0.0022	FR				V	43	18)
GSC 03179-00125	56152.4598	0.0020	FR				o	31	18)
GSC 03187-01564	56491.4309	0.0046	AG				-I	32	12)
GSC 03209-02182	56159.5725	0.0010	FR				o	21	18)
GSC 03578-00263	55857.3312	0.0016	FR				V	43	18)
	55857.5194	0.0056	FR				V	43	18)
GSC 03579-00488	55857.2513	0.0030	FR				V	23	18)
	55857.5159	0.0020	FR				V	23	18)
GSC 03581-01856	56152.4822	0.0015	FR				o	31	18)
GSC 03583-00309	55857.4000	0.0026	FR				V	48	18)
GSC 04009-00670	56133.4684	0.0154	AG	−0.0040		⟨2⟩	-I	44	12)
GSC 04552-01498	56456.4694	0.0013	ALH				V	128	7)
HAT 199-01628	55832.3120	0.0012	FR				V	45	18)
	55832.5084	0.0019	FR				V	45	18)
HAT 199-03655	55833.3808	0.0041	FR				-I	37	12)
	56152.3887	0.0054	FR				-I	50	12)
HAT 199-12172	55832.3328	0.0017	FR				V	42	18)
HAT 199-14347	55833.4801	0.0025	FR				-I	66	12)
HAT 199-15528	55832.4716	0.0046	FR				V	41	18)
HAT 199-27597	55832.4706	0.0025	FR				V	40	18)
HAT 199-34252	56179.5753	0.0070	FR				V	58	18)
HAT 199-36298	55832.3633	0.0035	FR				V	85	18)
	55832.5192	0.0032	FR				V	85	18)
NSVS 109935	56356.3859	0.0004	AG				-I	22	12)
	56371.6217	0.0018	AG				-I	30	12)
NSVS 1305379	56485.4861	0.0057	AG				-I	21	12)
NSVS 2465943	55966.6491	0.0006	RAT RCR				-U-I	203	15)
NSVS 2636345	56408.3715	0.0032	AG				-I	34	12)
	56408.5453	0.0026	AG				-I	34	12)
NSVS 2871290	56400.5771	0.0035	AG				-I	23	12)
NSVS 4073293	56151.5249	0.0017	FR				o	25	18)
NSVS 4116978	56151.5089	0.0010	FR				o	33	18)
NSVS 4323441	56334.4208	0.0073	AG				-I	36	12)
NSVS 4732433	56355.3782	0.0116	AG				-I	50	12)
	56371.4533	0.0028	AG				-I	29	12)
NSVS 4863977	55968.3943	0.0010	RAT RCR				-U-I	167	15)
	56006.5994	0.0004	RAT RCR				-U-I	234	15)
NSVS 6115851	56159.5430	0.0003	FR				o	29	18)
NSVS 6143186	56159.4492	0.0041	FR				o	46	18)
NSVS 7102202	56334.4073	0.0069	AG				-I	36	12)

Table 1: (cont.)

Variable	HJD 24.....	±	Obs	$O-C$	Ref	Fil	n	Rem
NSVS 7334235	56355.4202	0.0014	FR			V	54	18)
NSVS 7336417	56355.3507	0.0037	FR			V	44	18)
	56355.5325	0.0022	FR			V	44	18)
NSVS 7358116	56355.4536	0.0013	FR			V	18	18)
NSVS 7365626	56355.3283	0.0020	FR			V	25	18)
NSVS 7619496	56400.4473	0.0062	AG			-I	23	12)
NSVS 772055	55966.6138	0.0003	RAT RCR			-U-I	256	15)
NSVS 8385361	56167.3451	0.0022	FR			V	81	18)
NSVS 8744913	56408.4166	0.0067	AG			-I	34	12)
NSVS 8878981	56159.4132	0.0030	FR			o	53	18)
NSVS 958941	56408.4323	0.0049	AG			-I	34	12)
NSVS 99914	56356.3609	0.0054	AG			-I	21	12)
ROTSE1 J130705.50	56407.4192	0.0187	AG			-I	36	12)
ROTSE1 J175527.44	56485.4407	0.0014	AG			-I	20	12)
SAVS 025750+494214	56187.3920	0.0019	FR			V	42	18)
UCAC3 169-055676	54499.4475	0.0006	FR			V	46	8)
UCAC3 170-058819	55970.3894	0.0020	FR			-I	42	12)
UCAC3 213-102451	54942.538 :	0.003	FR			-I	31	12)
	55623.3942	0.0013	FR			-I	53	12)
	55623.5592	0.0014	FR			-I	53	12)
UCAC3 220-058696	50519.4101	0.0028	FR			o	37	10)
	50520.3910	0.0034	FR			o	35	10)
	53670.6286	0.0016	FR			-I	35	10)
	54080.3641	0.0029	FR			-I	24	10)
	54148.3856	0.0013	FR			-I	33	10)
	54148.5401	0.0006	FR			-I	33	10)
	54532.3841	0.0033	FR			-I	18	12)
UCAC3 231-243155	55830.5156	0.0012	FR			o	40	18)
UCAC3 240-187355	56179.3864	0.0009	FR			-I	46	12)
UCAC3 241-193174	50360.3944	0.0004	FR			o	46	10)
	50369.3966	0.0007	FR			o	58	10)
	50370.3803	0.0011	FR			o	31	10)
	50371.3599	0.0011	FR			o	23	10)
	50380.3595	0.0008	FR			o	33	10)
	50381.3417	0.0008	FR			o	29	10)
	50382.3204	0.0008	FR			o	18	10)
	50390.3427	0.0018	FR			o	29	10)
	50391.3223	0.0009	FR			o	28	10)
	50392.3054	0.0007	FR			o	30	10)
	54023.3390	0.0023	FR			o	20	10)
UCAC3 244-187342	53660.3246	0.0013	FR			-I	39	10)
	55084.3232	0.0036	FR			-I	204	12)
	55084.6018	0.0013	FR			-I	204	12)
	55837.2764	0.0010	FR			-I	93	12)
UCAC3 248-199991	55067.3589	0.0007	FR			-I	47	12)
UCAC3 248-200530	54712.4647	0.0032	FR			-I	14	12)
UCAC3 248-205306	55067.3821	0.0019	FR			-I	48	12)
UCAC3 249-240568	54682.5097	0.0008	FR			-I	78	12)
UCAC3 250-193174	56152.4839	0.0024	FR			-I	25	12)
UCAC3 250-197400	55067.5112	0.0020	FR			-I	23	12)
	56152.5504	0.0029	FR			-I	25	12)
UCAC3 323-013086	55944.4282	0.0014	JU			o	93	4)
	56188.3748	0.0019	JU			o	66	4)
	56199.3614	0.0014	JU			o	70	4)
U-A2 1275-15124020	56491.4084	0.0016	AG	+0.0202	s ⟨1⟩	-I	33	12)
U-B1 1503-0282065	56490.4745	0.0008	AG			-I	32	12)
VSX J034501.2+493659	56187.3440	0.0022	FR			V	47	18)
	56187.5329	0.0026	FR			V	47	18)
VSX J194336.7+322520	55837.2728	0.0020	FR			-I	68	12)
	55837.4570	0.0014	FR			-I	68	12)

Table 2: Times of maxima of pulsating stars

Variable	HJD 24.....	±	Obs	$O-C$	Ref	Fil	n	Rem
GP And	56516.3992	0.0006	FLG	+0.0058	⟨6⟩	V	77	13)
	56516.4780	0.0006	FLG	+0.0059	⟨6⟩	V	77	13)
V651 Aur	56355.359	0.002	AG	−0.062	⟨6⟩	-I	51	12)
SZ Boo	56408.402	0.001	AG	+0.000	⟨6⟩	-I	27	12)
TV Boo	56418.478	0.001	AG	+0.022	⟨6⟩	-I	32	12)
WZ Boo	55703.5811	0.0013	MZ	+0.0123	⟨6⟩	-I	82	5)
WZ Boo	55714.5506	0.0030	MZ	+0.0094	⟨6⟩	-I	67	5)
	56451.4574	0.0020	MZ	+0.0339	⟨6⟩	-I	93	5)
RR CVn	56407.4367	0.0013	MZ	+0.0127	⟨6⟩	-I	76	5)
RU CVn	56418.347	0.001	AG	+0.237	⟨6⟩	-I	32	12)
AP CVn	56408.4163	0.0015	MZ	−0.2594	⟨6⟩	-I	120	5)
	56431.3990	0.0015	MZ	−0.2627	⟨6⟩	-I	118	5)
	56458.4109	0.0020	MZ	−0.2594	⟨6⟩	-I	120	5)
FP Cep	56490.399	0.001	AG	−0.041	⟨6⟩	-I	32	12)
BT Com	56014.4676	0.0014	MZ	+0.1037	⟨6⟩	-I	58	5)
	56072.3922	0.0016	MZ	+0.1002	⟨6⟩	-I	104	5)
UY Cyg	56490.4375	0.0019	ALH	+0.0629	⟨6⟩	V	330	7)
XZ Cyg	56486.4212	0.0019	ALH	+0.0316	⟨6⟩	V	528	7)
DM Cyg	56507.5579	0.0009	ALH	+0.0751	⟨6⟩	o	365	7)
NS Cyg	56480.4573	0.0015	MZ	+0.2502	⟨6⟩	-I	108	5)
	56485.4151	0.0013	MZ	+0.2553	⟨6⟩	-I	114	5)
	56486.5150	0.0030	MZ	+0.2546	⟨6⟩	-I	107	5)
	56491.4609	0.0014	MZ	+0.2478	⟨6⟩	-I	139	5)
	56513.4711	0.0019	MZ	+0.2460	⟨6⟩	-I	126	5)
V833 Cyg	56105.4138	0.0011	MZ	−0.1707	⟨6⟩	-I	78	5)
	56493.4330	0.0011	MZ	−0.1741	⟨6⟩	-I	119	5)
	56500.4305	0.0013	MZ	−0.1728	⟨6⟩	-I	119	5)
	56528.4150	0.0010	MZ	−0.1733	⟨6⟩	-I	119	5)
DX Del	56504.4903	0.0011	ALH	+0.0676	⟨6⟩	o	588	7)
SU Dra	56408.483	0.001	AG	+0.063	⟨6⟩	-I	34	12)
	56480.4650	0.0017	ALH	+0.0587	⟨6⟩	V	403	7)
VZ Dra	56493.5450	0.0014	ALH	+0.0612	⟨6⟩	V	242	7)
XZ Dra	56489.5240	0.0008	ALH	−0.1218	⟨6⟩	V	409	7)
BK Dra	56498.4769	0.0018	ALH	−0.1639	⟨6⟩	V	547	7)
DD Dra	56485.4729	0.0016	ALH	−0.0471	⟨6⟩	V	159	7) 1)
	56485.5056	0.0016	ALH	−0.0144	⟨6⟩	V	159	7) 2)
OW Dra	56408.387	0.001	AG	+0.009	⟨6⟩	-I	34	12)
DT Gem	56295.483	0.001	QU	−0.261	⟨6⟩	V	60	5)
	56355.4134	0.0007	QU	−0.2366	⟨6⟩	V	85	5)
VZ Her	56450.4893	0.0013	ALH	+0.0704	⟨6⟩	V	464	7)
CK Her	56490.4686	0.0013	MZ	−0.0185	⟨6⟩	-I	113	5)
CM Her	56490.4639	0.0013	MZ	+0.1180	⟨6⟩	-I	113	5)
V633 Her	56487.4411	0.0013	MZ	−0.0009	⟨5⟩	-I	95	5)
V862 Her	56489.4368	0.0020	MZ			-I	107	5)
CZ Lac	56520.5527	0.0008	ALH	−0.1311	⟨6⟩	o	719	7)
RV Leo	56418.3672	0.0011	MZ	−0.0825	⟨6⟩	-I	83	5)
RW Lyn	56355.522	0.001	AG	−0.178	⟨6⟩	-I	50	12)
TW Lyn	56355.385	0.001	AG	+0.062	⟨6⟩	-I	50	12)
WZ Lyn	56355.470	0.001	AG			-I	47	12)
RZ Lyr	56487.4064	0.0010	ALH	−0.0579	⟨6⟩	V	341	7)
ZZ Lyr	56495.4829	0.0008	MZ	+0.0029	⟨6⟩	-I	71	5)
AQ Lyr	56460.4321	0.0010	WLH	+0.0035	⟨6⟩	-U-I	112	6)
CN Lyr	56474.4397	0.0014	ALH	+0.0138	⟨6⟩	V	322	7)
DD Lyr	56447.4723	0.0014	MZ	−0.1311	⟨6⟩	-I	111	5)
	56450.4527	0.0009	MZ	−0.1316	⟨6⟩	-I	124	5)
DI Lyr	56482.4144	0.0013	MZ	−0.0678	⟨6⟩	-I	114	5)
	56525.4095	0.0013	MZ	−0.0700	⟨6⟩	-I	120	5)

Table 2: (cont.)

Variable	HJD 24.....	±	Obs	$O-C$	Ref	Fil	n	Rem
EZ Lyr	56463.4066	0.0010	ALH	−0.1457	⟨6⟩	V	469	7)
IO Lyr	56475.4860	0.0012	ALH	−0.0477	⟨6⟩	V	314	7)
V462 Lyr	56521.4141	0.0023	WLH	−0.0215	⟨6⟩	-U-I	132	4)
AV Peg	56522.5384	0.0010	ALH	+0.1516	⟨6⟩	V	353	7)
BP Peg	56519.4246	0.0017	WLH	+0.0101	⟨6⟩	-U-I	104	4)
	56520.5192	0.0007	WLH	+0.0093	⟨6⟩	-U-I	140	4)
DY Peg	56510.3929	0.0008	FLG RDL	−0.0133	⟨6⟩	o	151	9)
	56510.4664	0.0007	FLG RDL	−0.0128	⟨6⟩	o	151	9)
BO Tau	56257.5028	0.0014	MZ	+0.1838	⟨6⟩	-I	60	5)
	56356.3249	0.0010	MZ	+0.1850	⟨6⟩	-I	119	5)
IY Tau	56337.4148	0.0013	MZ	+0.1541	⟨6⟩	-I	105	5)
	56354.3279	0.0030	MZ	+0.1252	⟨6⟩	-I	63	5)
AB UMa	56400.554	0.004	AG	+0.146	⟨6⟩	-I	20	12)
AE UMa	56342.3644	0.0003	SCI	+0.0026	⟨6⟩	o	66	4)
	56342.4461	0.0003	SCI	−0.0017	⟨6⟩	o	38	4)
	56342.5315	0.0009	SCI	−0.0024	⟨6⟩	o	32	4)
	56342.6268	0.0005	SCI	+0.0069	⟨6⟩	o	38	4)
GSC 02655-01364	56093.4626	0.0050	RAT RCR			-U-I	217	15)
GSC 02656-01095	53660.370	0.003	FR			-I	40	10)
	55084.424	0.002	FR			-I	68	12)
	55481.452	0.004	FR			-I	50	12)
GSC 03137-00318	55062.532	0.002	FR			-I	48	12)
GSC 08459-00201	56156.3409	0.0008	WLH			-U-I	84	4)
	56156.4516	0.0007	WLH			-U-I	84	4)
HAT 199-01886	55832.3680	0.0020	FR			V	90	18)
NSV 8701	56072.4778	0.0004	RAT RCR			-U-I	178	15)

Observers:

AG:	Agerer, F., Tiefenbach
ALH:	Alich, K., Schaffhausen
BHE:	Böhme, D., Nessa
FLG:	Flechsig, Dr. G., Teterow
FR:	Frank, P., Velden
HUN:	Hunger, T., Warstein
JU:	Jungbluth, H., Karlsruhe
MZ:	Maintz, Dr. G., Bonn
QU:	Quester, W., Esslingen
RAT:	Rätz, M., Herges-Hallenberg
RCR:	Rätz, K., Herges-Hallenberg
RDL:	Rudolph, E., Jena
SCI:	Schmidt, U., Karlsruhe
WLH:	Wollenhaupt, G., Oberwiesenthal
WTR:	Walter, F., München

Remarks:

n	number of measurements
:	uncertain
s	secondary minimum
(1)	double maximum: time of the first maximum
(2)	double maximum: time of the second maximum
	Photometer
(3)	CCD camera ST-6: chip 375*242 uncoated
(4)	CCD camera ST-7
(5)	CCD camera ST-7E
(6)	CCD camera ST-7 XE
(7)	CCD camera ST-8 XMEI
(8)	CCD camera ST-9: chip 512*512
(9)	CCD camera Sigma 402: chip KAF0402ME
(10)	CCD camera OES-LcCCD11
(11)	CCD camera OES-LcCCD12
(12)	CCD camera Sigma 1603
(13)	CCD camera Sigma 402
(14)	CCD camera Sigma 402ME
(15)	CCD camera Moravian G2-1600
(16)	CCD camera Mead DSI Pro 3
(17)	camera Canon powershot g3
(18)	camera Canon EOS 450D
	Filter
o	without filter
B	B-filter
V	V-filter
R	R-filter
-I	IR cut-off filter
-U-I	U and IR cut-off filter

References:

Agerer, F., 2006, *IBVS*, No. 5700, Obj. 93) ⟨1⟩
Agerer, F., 2010, *PZP*, **10**, 4. ⟨2⟩
BAV Services for Scientists, 2013,http://www.bav-astro.de/sfs/index.php?sprache=en&sprache_dial=de
Bernhard, K. Frank, P., 2006, *IBVS*, No. 5719 *BAV Mitt.*, **177** ⟨3⟩
Kreiner, J. M., 2004, *Acta Astr.*, **54**, 207. ⟨4⟩
Lichtenknecker Database of the BAV http://www.bav-astro.de/LkDB/index.php?lang=en&sprache_dial=de
Maintz, G., 2012, *BAV Rb.*, **61**, 83. ⟨5⟩
Samus, N .N., et. al., 2011, http://www.sai.msu.su/gcvs/gcvs/index.htm ⟨6⟩

ERRATUM FOR IBVS 6070 (BAVM 231)

V366 Cas 56158.434 AG has to be deleted

COMMISSIONS 27 AND 42 OF THE IAU
INFORMATION BULLETIN ON VARIABLE STARS

Number 6085

Konkoly Observatory
Budapest
2 December 2013

HU ISSN 0374 – 0676

V1100 Her – A W-TYPE OVERCONTACT ECLIPSING BINARY

NELSON, ROBERT H.[1,2]; ROBB, RUSSELL M.[2,3]

[1] 1393 Garvin Street, Prince George, BC, Canada, V2M 3Z1, email: bob.nelson@shaw.ca

[2] Guest investigator, Dominion Astrophysical Observatory, Herzberg Institute of Astrophysics, National Research Council of Canada

[3] Department of Physics and Astronomy, University of Victoria, Victoria, B.C., Canada, V8P 2W7

V1100 Her (= TYC 3092-1291-1= J174410.58+401650.7) was discovered to be variable by the ROTSE survey Akerlof et al. (2000). Sufficient data were available for them to classify it as an eclipsing binary of the EW type, and determine a period of 0.34694(4) days. Since then, numerous authors have reported times of minima (Nelson 2002, 2008, 2013a; Brát et al. 2008, 2011; Hübscher et al. 2010; Arena et al. 2011). Two early times of minima (Nelson 2002, 2008) led to equation (1):

$$\mathrm{JD_{hel}\,Min\,I} = 2452024.8148(18) + 0.3469283(1)\,E \qquad (1)$$

The resulting eclipse timing (ET) diagram (a.k.a. $O-C$ diagram) is displayed in Fig. 1.

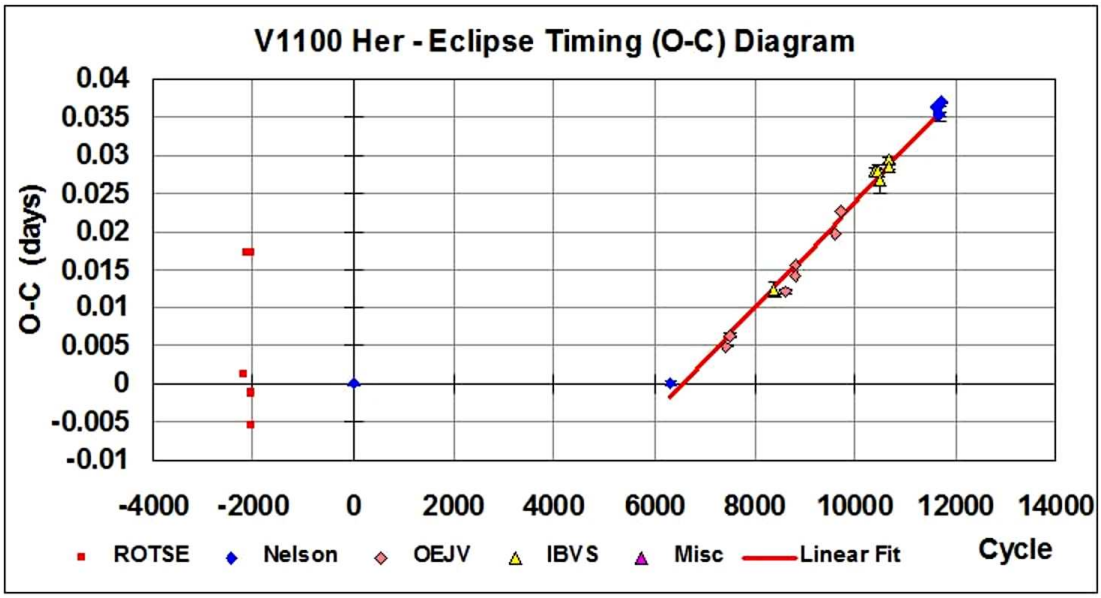

Figure 1. Eclipse timing diagram for V1100 Her using the elements of equation (1).

It seems to reveal a constant period from 1999 (cycle −2205) to 2007 (cycle 6327) but there are insufficient data points to make any realistic conclusions. After that there appears to be an episodic increase and a constant period until the last data points (in 2012). Least squares fitting of the 19 data points in the interval from 2007 to 2012 gives a period of 0.3469354(2) days; that and the last point in the plot (Nelson 2013a) were used in the elements of equation (2). The latter was used to phase all the data.

$$\mathrm{JD_{hel}\,Min\,I} = 2456089.8099(1) + 0.3469354(2)\,E \tag{2}$$

A further time of minimum, hitherto unpublished, is reported in Table 1 and plotted in Fig. 2.

Table 1. New time of minimum for V1100 Her.

HJD−2400000	Error (days)	Type	Filter
56569.6185	0.0003	I	R

An alternative fit, superimposing a sine function to the points since cycle 0, is plotted in Fig. 2 using the elements of equation (1).

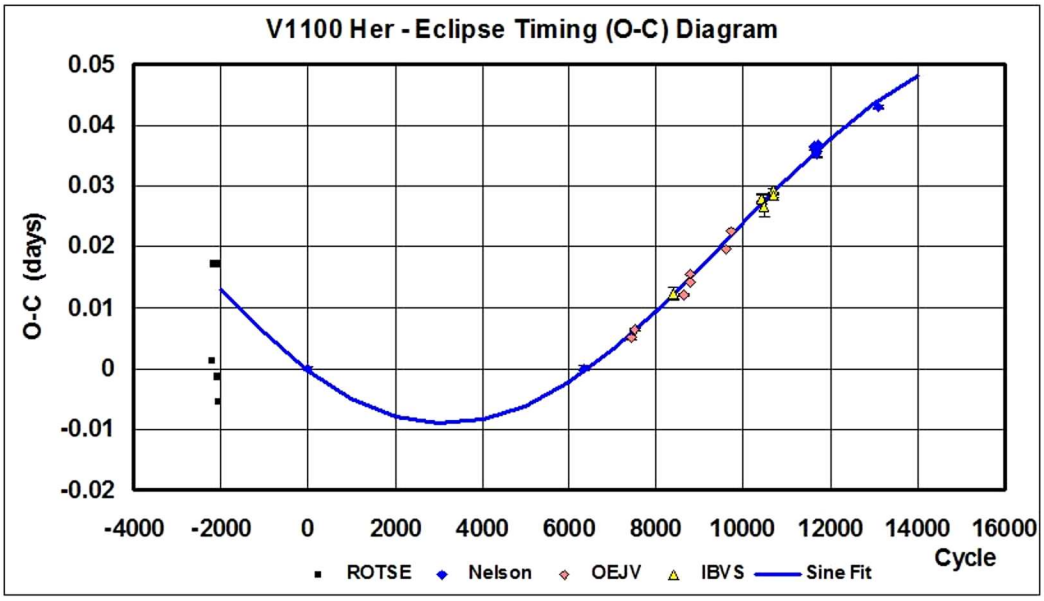

Figure 2. Eclipse Timing ($O - C$) diagram for V1100 Her (sine + linear fit).

The fit is in the form:

$$O - C = C_1 + C_2 n + C_3 \sin(C_4 n + C_5) \tag{3}$$

where $C_1 = 0.0255$ days, $C_2 = -3.8 \cdot 10^{-7}$ days/cycle, $C_3 = 0.0335$ days, $C_4 = 0.00023$ radians/cycle, $C_5 = 4.022$ radians, and n is the cycle number. Constant C_4 translates into a period $P_2 = 25.7$ years for the orbit of a possible third star. [Note that magnetic cycles may also cause cyclic variations in the periods of overcontact binaries – see, for example, Borkovits et al. (2005). However, this explanation is remote in this case, as the observational criteria have not yet been met (Applegate 1992, page 622, para 8).]

It must be admitted straight away that the sine fit is very speculative and liable to change with any new data. It may be completely false. On the other hand, it seems more physical than the scenario of a constant period followed by a sudden period change and then a new constant regime. Time will tell. This system is reminiscent of AC Boo (Nelson 2010a) where the period was constant from 1929 to 1982, followed by an episodic rise, followed by a period of increase at a constant rate since then.

See Nelson (2013b–updated annually) for the latest data and $O-C$ fit. Since V1100 Her has never had a full analysis, it was added to the author's observing programme.

A total of 153 frames in V, 145 in $R_{\rm C}$ (Cousins) and 143 in the $I_{\rm C}$ (Cousins) band were obtained by one of the authors (R.H.N.) at his private observatory in Prince George, BC, Canada in May and June of 2012. (The telescope was a 33 cm f/4.5 Newtonian on a Paramount ME mount; the camera was an SBIG ST-10XME. Standard reductions were then applied. The comparison and check stars are listed in Table 2 (coordinates, and $B-V$, V magnitudes are from SIMBAD). The V magnitude for V1100 Her was taken from our own ensemble photometry at phases 0.25 and 0.75 using Tycho stars in the field as standards.

Table 2. Details of variable, comparison and check stars.

Type of target	GSC 3092-	R.A. J2000	Dec. J2000	V Mags	$B-V$ Mags
Variable	1291	$17^{\rm h}44^{\rm m}10.588^{\rm s}$	$40°16'51''.15$	10.71	+0.61
Comparison	0934	$17^{\rm h}43^{\rm m}12.489^{\rm s}$	$40°08'58''.32$	10.94	+0.96
Check	1173	$17^{\rm h}43^{\rm m}14.686^{\rm s}$	$40°01'08''.01$	10.88	+0.34

For classification purposes, one of the authors (R.M.R.) took two low resolution spectra, on 2013 March 9 (HJD=2456360.4608) and 2013 June 22 (HJD=2456465.3077). He used the 1.85 m Plaskett telescope at the Dominion Astrophysical Observatory (DAO) in Victoria, British Columbia, Canada with the Cassegrain spectrograph in the 2131 configuration, resulting in a reciprocal dispersion of 60 Å/mm. The two spectra were very similar. The strength of the Calcium H&K lines, G-band, Hγ, Fe I 4384, Ca I 4227, and Hδ lines all indicated a F9 V$\pm$1 spectral classification for V1100 Her.

For radial velocity (RV) determination, the other author (R.H.N.) took 7 medium resolution spectra, also at the DAO, in April and September of 2011 using the same Plaskett telescope. In the 21181 configuration, the grating was 1800 lines/mm, blazed at 5000 Å and used in first order, with reciprocal dispersion = 10 Å/mm, and resolving power = 10,000. The camera was the SITe-2. The spectral range covered was from 5000 to 5260 Å, approximately.

R.H.N. then used the Rucinski broadening functions (Rucinski 2004) to obtain radial velocity curves (see Nelson et al. (2006) and Nelson (2010b) for details). A log of DAO observations and RV results is presented in Table 3. The results were corrected 9% up in this case to allow for the small phase smearing in the following way: the RVs were divided by the factor $f = (\sin X)/X$ (where $X = 2\pi t/P$ and t=exposure time, P=period). For spherical stars, the correction is exact; in other cases, it can be shown to be close enough for any deviations to fall below observational errors. (This matter will be fully explored in a forthcoming paper.)

Table 3. Log of DAO observations.

DAO Image #	Mid Time (HJD−2400000)	Exposure (sec)	Phase at Mid-exp	V_1 (km/s)	V_2 (km/s)
2537	55668.9002	3600	0.778	−58.7	277.60
2581	55670.9454	3600	0.673	−59.9	263.5
7954	55812.6763	3600	0.195	32.6	−281.9
7957	55812.7195	3600	0.320	40.9	−252.9
8011	55814.7589	3600	0.198	40.0	−295.5
8057	55815.8079	3600	0.222	24.6	−302.5
8181	55824.6473	3600	0.700	−48.2	285.7

A plot of two spectra of V1100 Her, #8057 (top) and #2537 (bottom), is given in Fig. 3.

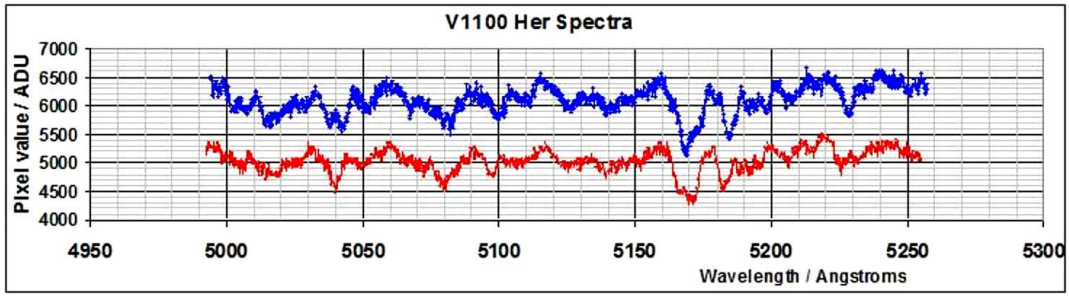

Figure 3. Two spectra of V1100 Her, at phases 0.222 (top) and 0.778 (bottom).

R.H.N. used the 2004 version of the Wilson-Devinney (WD) light curve and radial velocity analysis program with Kurucz atmospheres (Wilson & Devinney 1971; Wilson 1990; Kallrath et al. 1998) as implemented in the Windows front-end software WDwint (Nelson 2009) to analyze the data. To get started, a spectral type F9 V, mentioned above, and a temperature $T_2 = 6093 \pm 200$ K were used. (The temperature of the secondary, T_2, was fixed because the secondary star, being larger, might be expected to dominate the flux from the system, and hence the spectral classification. This assertion is borne out by the values of $L_1/(L_1 + L_2)$ given in Table 5.)

Interpolated tables from Cox (2000) gave $\log g = 4.367$; an interpolation program by Terrell (1994, available from Nelson 2009) gave the Van Hamme (1993) limb darkening values; and finally, a logarithmic (LD=2) law for the limb darkening coefficients was selected, appropriate for temperatures < 8500 K (ibid.). (The stated error in T_1 corresponds to one half spectral sub-class.)

From the GCVS 4 designation and from the shape of the light curve mode 3 (overcontact binary) mode was used. Early on, it was noted that the maxima between eclipses were unequal. This is the O'Connell effect (Davidge & Milone 1984, and references therein) and is usually explained by the presence of one or more star spots. Accordingly, one was added first to star 1, and this gave good results. (Moving the spot to star 2 gave poorer results and was abandoned.)

Convergence by the method of multiple subsets was reached in a small number of iterations. (The subsets were: (a, L_1), (T_1, Ω_1, q), and ($V_{\rm gam}$, i, q). The spots were

handled separately.) Convective envelopes for both stars were used, appropriate for cooler stars (hence values gravity exponent, $g = 0.32$ and albedo, $A = 0.500$ were used for each). Detailed reflections were used, with $n_{\rm ref} = 3$. The limb darkening coefficients are listed in Table 4. There are certain uncertainties in the process (see Csizmadia et al. 2013; Kurucz 2002). On the other hand, the solution is weakly dependent on the exact values used.

Table 4. Limb darkening values from Van Hamme (1993).

Band	x_1	x_2	y_1	y_2
Bol	0.644	0.641	0.226	0.235
V	0.739	0.721	0.259	0.271
$R_{\rm C}$	0.667	0.648	0.272	0.280
$I_{\rm C}$	0.583	0.565	0.264	0.271

The model is presented in Table 5. (Note that estimating the uncertainties in temperatures T_1 and T_2 is somewhat problematic. A common practice is to quote the temperature difference over half a spectral sub-class (assuming that the classification is good to one spectral sub-class, which precision might be rare). In addition, various different calibrations have been made (Cox 2000, page 388-390 and references therein; and Flower 1996), and the variations between the various calibrations can be significant. In our case the classification is ± 1 one sub-class. Therefore, we propose to assign an uncertainty of ± 200 K to the absolute temperatures of each, which would roughly span this range. The modelling error in temperature T_1, relative to T_2, is indicated by the WD output to be much smaller, around 4 K.)

Table 5. Wilson-Devinney parameters.

WD Quantity	Value	Error	Unit	W-D Quantity	Value	Error	Unit
Temperature T_1	6362	200	K	$L_1/(L_1+L_2)$ (V)	0.2011	0.0016	—
Temperature T_2	6093	[fixed]	K	$L_1/(L_1+L_2)$ $(R_{\rm C})$	0.1961	0.0014	—
$q = M_2/M_1$	6.227	0.010	—	$L_1/(L_1+L_2)$ $(I_{\rm C})$	0.1921	0.0011	—
Potential Ω_1=Ω_2	10.271	0.011	—	r_1 (pole)	0.2374	0.0008	orb. rad.
Inclination, i	68.3	0.3	deg	r_1 (side)	0.2497	0.0009	orb. rad
Semi-maj. axis a	2.56	0.01	sol.rad.	r_1 (back)	0.3075	0.0027	orb. rad
V_γ	−5.6	0.7	km/s	r_2 (pole)	0.5190	0.0005	orb. rad
Spot co-latitude	82	10	deg	r_2 (side)	0.5754	0.0007	orb. rad
Spot longitude	94	5	deg	r_2 (back)	0.6016	0.0009	orb. rad
Spot radius	47	2	deg	Phase shift	−0.0007	0.0004	—
Spot temp factor	0.958	0.005	—	$\omega^2_{\rm res}$	0.00387	—	—

The light curve data and the fitted curves are depicted in Fig. 4. The presence of third light was tested for, but found not to be significant.

The RVs are shown in Fig. 5. A three-dimensional representation from Binary Maker 3 (Bradstreet 1993) is shown in Fig. 6.

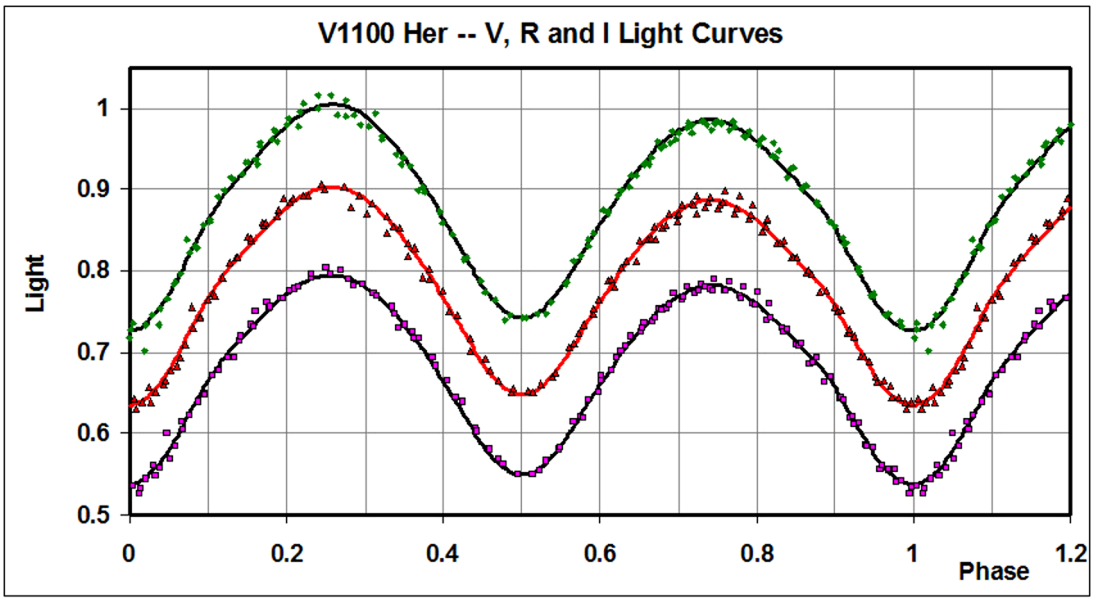

Figure 4. V1100 Her: V, R_C, and I_C light curves – data and WD fit.

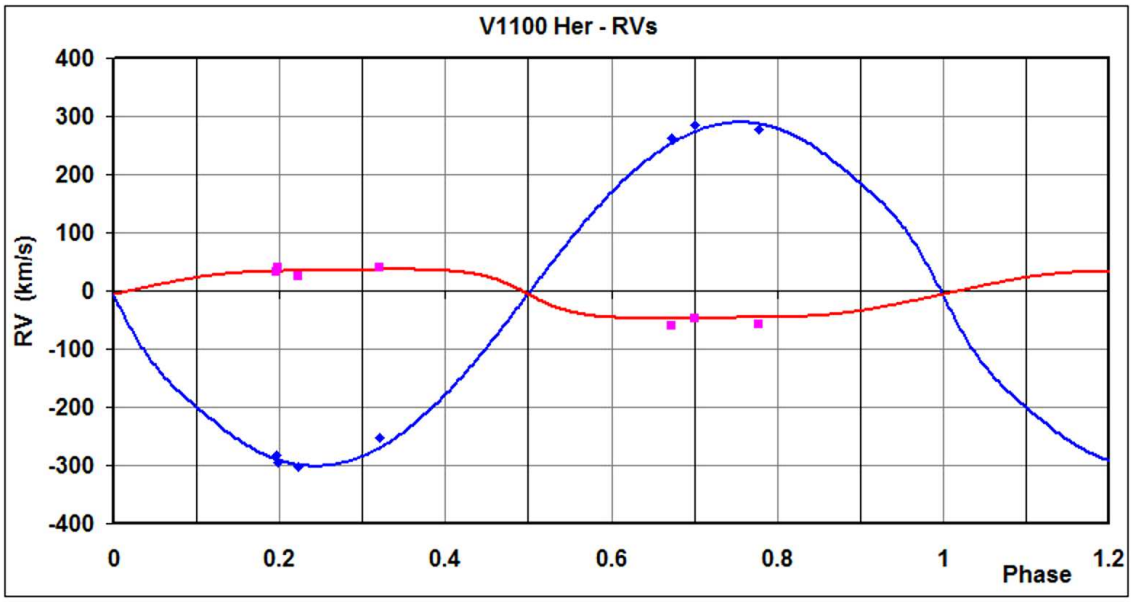

Figure 5. V1100 Her: radial velocity curves – data and WD fit.

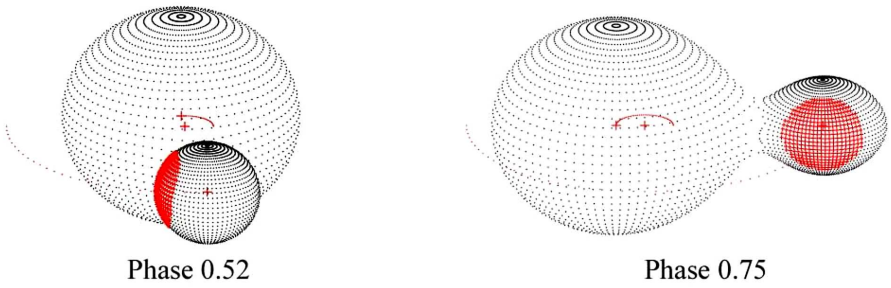

Figure 6. Binary Maker 3 representation of the system – at phases 0.52 and 0.75.

The WD output fundamental parameters and errors are listed in Table 6. Most of the errors are output or derived estimates from the WD routines. The fill-out factor $f = (\Omega^{\rm I} - \Omega)/(\Omega^{\rm I} - \Omega^{\rm O})$, where Ω is the modified Kopal potential of the system, $\Omega^{\rm I}$ is that of the inner Lagrangian surface, and $\Omega^{\rm O}$, that of the outer Lagrangian surface, was also calculated.

Table 6. Fundamental parameters.

Quantity	Value	Error	Unit
Temperature, T_1	6362	200	K
Temperature, T_2	6093	200	K
Mass, M_1	0.258	0.034	$M_\odot$
Mass, M_2	1.609	0.019	$M_\odot$
Radius, R_1	0.67	0.01	$R_\odot$
Radius, R_2	1.45	0.01	$R_\odot$
$M_{\rm bol,1}$	5.23	0.02	mag
$M_{\rm bol,2}$	3.76	0.02	mag
$\log g_1$	4.19	0.01	cgs
$\log g_2$	4.32	0.01	cgs
Luminosity, L_1	0.67	0.01	$L_\odot$
Luminosity, L_2	2.58	0.05	$L_\odot$
Fill-out factor	0.159	0.010	—
Distance, r	241	9	pc

To determine the distance r in column 2, we proceeded as follows: first the WD routine gave the absolute bolometric magnitudes of each component; these were then converted to the absolute visual (V) magnitudes of both, $M_{\rm V,1}$ and $M_{\rm V,2}$, using the bolometric corrections BC $= -0.160$ and -0.170, respectively. The latter were taken from interpolated tables in Cox (2000). The absolute V magnitude was then computed in the usual way, getting $M_{\rm V} = 3.68 \pm 0.03$ magnitudes. The apparent magnitude in the V passband was $V = 10.71 \pm 0.014$, taken from our ensemble photometry at phases 0.25 and 0.75 using Tycho stars in the field (Hog et al. 2000) as standards. The colour excess (in $B-V$) was obtained in the usual way, by subtracting the tabular value of $B-V$ (for that spectral class) from the observed (Tycho) value. This gave $E(B-V) = 0.06$ magnitudes. However, reference to the dust tables of Schlegel et al. (1998) revealed a value of $E(B-V) = 0.0395$ for those galactic coordinates. Since the $E(B-V)$ values have been derived from full-sky far-infrared measurements, they therefore apply to objects outside of the Galaxy;

this value of $E(B-V)$ so derived then represents an upper limit for closer objects within the Galaxy. Hence a lower value of $E(B-V) = 0.033$ was adopted. Galactic extinction was obtained from the usual relation $A_V = R \cdot E(B-V)$, using $R = 3.1$ for the reddening coefficient. Hence, distance $r = 241$ pc was calculated from the standard relation:

$$r = 10^{0.2(V-M_V-A_V+5)} \text{ parsecs.} \quad (4)$$

The errors were assigned as follows: $\delta M_{\rm bol,1} = \delta M_{\rm bol,2} = 0.02$, $\delta {\rm BC}_1 = \delta {\rm BC}_2 = 0.012$ (the variation of 1.5 spectral sub-classes), $\delta V = 0.04$, $\delta E(B-V) = 0.02$, all in magnitudes, and $\delta R = 0.1$. Combining the errors rigorously yielded an estimated error in r of 9 pc.

In conclusion, the fundamental parameters of this system have been determined. One of these is the mass ratio, defined by the WD routine as $q = {\rm m_2/m_1}$. Since, for W-type systems, the star eclipsed at primary minimum is the less massive one, here we have $q > 1$. However, many authors define q' to be less than 1 in both cases (and equal to ${\rm m_1/m_2}$ here). So therefore, for V1100 Her, $q' = 0.161$. This makes V1100 Her a low mass ratio system. All available W-type systems with $q < 0.2$ are listed in Table 7 for comparison.

Table 7. Some low mass ratio W-type overcontact eclipsing binaries.

Star	Spectral Type	T_1 (K)	T_2 (K)	q' (spectr.)	q' (photom.)	f	Spectr. Ref.	Photom. Ref.
V0902 Sgr	∼F6-7 V	6200	6256	—	0.132	0.39	—	1
UY UMa	G0?	5486	5900	—	0.133	0.05	—	2
TV Mus	G0-1 V	5980	6088	0.135	0.15	0.13	3	4
EF Dra	F9 V	6000	6054	0.16	0.16	0.455	5	6
V1100 Her	F9 V	6362	6093	0.161	0.161	0.159	7	7
AH Aur	F7 V	6215	6272	0.169	0.169	0.625	8	9
OU Ser	F9-G0 V	5960	6380	0.173	0.173	0.307	10	11
V0728 Her	F3 V	6622	6787	0.181	0.181	0.71	12	12

(1) Samec & Corbin (2002); (2) Yang et al. (2001); (3) Hilditch et al. (1989); (4) Pribulla et al. (2003); (5) Lu & Rucinski (1999); (6) Pribulla et al. (2001); (7) This paper; (8) Rucinski & Lu (1999); (9) Vaňko et al. (2001); (10) Rucinski et al. (2000); (11) Pribulla & Vaňko (2002); (12) Nelson et al. (1995)

It is seen from Table 7 that V1100 Her is most like TV Mus in terms of its mass ratio and fill-out factor. This is further borne out by the diagram of Fig. 7 in which we plot the fill-out factor f versus the mass ratio q using data taken from Csizmadia & Klagyivik (2004). The reader will note the clustering of points within the interval $q = 0.3$ to 0.7 and also for $f < 0.3$. This is typical of W-type overcontact binaries, which are known to display marginal contact (Lucy 1976). However, as mentioned, V1100 Her has a lower than normal mass ratio for a W-type (Binnendijk 1965). Therefore the newly derived results for V1100 Her can be added as 'grist for the mill' in efforts to understand the formation and evolution of this type of star.

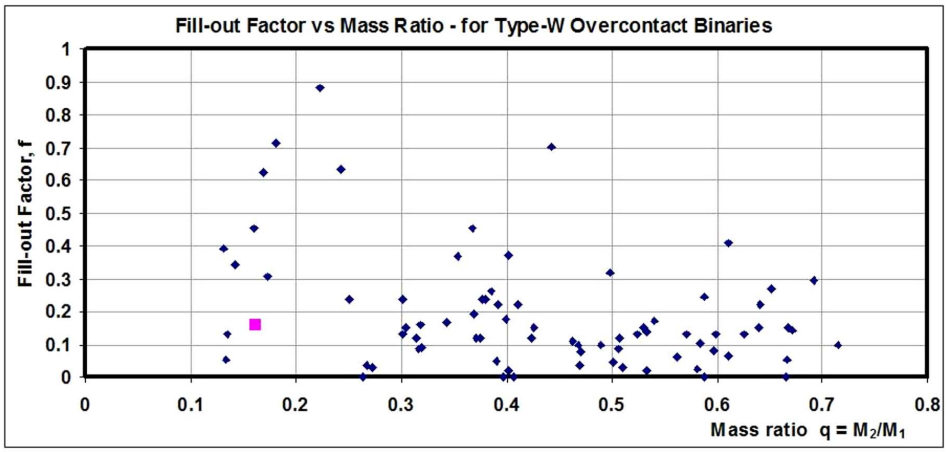

Figure 7. The values of the fill-out factor f are plotted versus mass ratio $q = M_2/M_1$ for W-type overcontact binaries using data from Csizmadia & Klagyivik (2004). The square denotes V1100 Her.

Acknowledgements: It is a pleasure to thank the staff members at the DAO (especially Dmitry Monin and Les Saddlemyer) for their usual splendid help and assistance.

References:

Akerlof, C., et al., 2000, *AJ*, **119**, 1901
Applegate, J. H., 1992, *ApJ*, **385**, 621
Arena, C., et al., 2011, *IBVS*, No. 5997
Binnendijk, L., 1965, *Kleine Veröff. Bamberg*, **4**, 36
Borkovits, T., et al., 2005, *A&A*, **441**, 1087
Bradstreet, D. H., 1993, "Binary Maker 2.0 - An Interactive Graphical Tool for Preliminary Light Curve Analysis", in Milone, E.F. (ed.) *Light Curve Modelling of Eclipsing Binary Stars*, pp 151-166 (Springer, New York, N.Y.)
Brát, L., et al., 2008, *OEJV*, **94**, 1
Brát, L., et al., 2011, *OEJV*, **137**, 1
Csizmadia, Sz. & Klagyivik, P., 2004, *A&A*, **426**, 1001
Csizmadia, Sz., Pasternacki, T., Dreyer, C., Cabrera, A., Erikson, A. & Rauer, H., 2013, *A&A*, **549**, A9
Cox, A. N., ed, 2000, *Allen's Astrophysical Quantities*, 4th ed., (Springer, New York, NY)
Davidge, T. J. & Milone, E.F., 1984, *ApJS*, **55**, 571
Flower, P. J., 1996, *ApJ*, **469**, 355
Høg, E., et al., 2000, *A&A*, **355**, L27
Hilditch, R. W., King, D. J. & McFarlane, T. M., 1989, *MNRAS*, **237**, 447
Hübscher, J., et al., 2010, *IBVS*, No. 5918
Kallrath, J., Milone, E. F., Terrell, D. & Young, A. T., 1998, *ApJ*, **508**, 308.
Kurucz, R. L., 2002, *Baltic Astron.*, **11**, 101
Lu, W. & Rucinski, S.M., 1999, *AJ*, **118**, 515
Lucy, L. B., 1976, *ApJ*, **205**, 208
Nelson, R. H., et al. 1995, *AJ*, **110**, 2400
Nelson, R. H., 2002, *IBVS*, No. 5224
Nelson, R. H., Terrell, D. & Gross, J., 2006, *IBVS*, No. 5715

Nelson, R. H., 2008, *IBVS*, No. 5820
Nelson, R. H., 2009, Software, by Bob Nelson, http://members.shaw.ca/bob.nelson/software1.htm
Nelson, R. H., 2010a, *IBVS*, No. 5951
Nelson, R. H., 2010b, "Spectroscopy for Eclipsing Binary Analysis" in *The Alt-Az Initiative, Telescope Mirror & Instrument Developments* (Collins Foundation Press, Santa Margarita, CA), R. M. Genet, J. M. Johnson & V. Wallen (eds)
Nelson, R. H., 2013a, *IBVS*, No. 6050
Nelson, R. H., 2013b, Bob Nelson's $O-C$ Files, http://www.aavso.org/bob-nelsons-o-c-files
Pribulla, T., Vaňko, M., Chochol, D. & Parimucha, Š., 2001, *CoSka*, **31**, 26
Pribulla, T. & Vaňko, M., 2002, *CoSka*, **32**, 79
Pribulla, T., Kreiner, J. M. & Tremko, J., 2003, *CoSka*, **33**, 38
Robb, R., 1992, *IBVS*, No. 3798
Rucinski, S. M. & Lu, W., 1999, *AJ*, **118**, 2451
Rucinski, S. M., Lu, W. & Mochnacki, S.W., 2000, *AJ*, **120**, 1133
Rucinski, S. M. 2004, *IAUS*, **215**, 17
Samec, R. & Corbin, S., 2002, *Obs.*, **122**, 22
Schlegel, D. J., Finkbeiner, D. P. & Davis, M., 1998, *ApJ*, **500**, 525
Terrell, D., 1994, *Van Hamme Limb Darkening Tables*, vers. 1.1.
Van Hamme, W., 1993, *AJ*, **106**, 2096
Vaňko, M., Pribulla, T., Chochol, D., Parimucha, Š., Kim, C., Lee, J. & Han, J. 2001, *CoSka*, **31**, 129
Wilson, R. E. & Devinney, E.J., 1971, *ApJ*, **166**, 605
Wilson, R. E., 1990, *ApJ*, **356**, 613
Yang, Y., Liu, Q. & Leung, K.-C., 2001, *A&A*, **370**, 507

COMMISSIONS 27 AND 42 OF THE IAU
INFORMATION BULLETIN ON VARIABLE STARS

Number 6086

Konkoly Observatory
Budapest
2 December 2013

HU ISSN 0374 – 0676

STANDARD UBV PHOTOMETRY AND IMPROVED PHYSICAL PROPERTIES OF TW Dra

BOŽIĆ, H.[1]; NEMRAVOVÁ, J.[2]; HARMANEC, P.[2]

[1] Hvar Observatory, Faculty of Geodesy, University of Zagreb, 10000 Zagreb, Croatia

[2] Astronomical Institute of the Charles University, Faculty of Mathematics and Physics, V Holešovičkách 2, CZ-180 00 Praha 8, Czech Republic

1 Introduction

The semi-detached eclipsing binary TW Dra (HD 139319, HIP 76196, SAO 16767, BD+64°1077A; $V = 7\overset{\mathrm{m}}{.}3$-$9\overset{\mathrm{m}}{.}2$) is the brighter member of the visual binary ADS 9706. The fainter component ADS 9706B has a Hipparcos H_{p} magnitude of $9\overset{\mathrm{m}}{.}887$ and is separated only 3″ from the eclipsing binary. Consequently, the light contribution from ADS 9706B affects any usual photoelectric observations of TW Dra and must be considered as a third light in the system.

The history of investigation of TW Dra was summarized by Zejda, Mikulášek and Wolf (2008) or Tkachenko, Lehmann and Mkrtichian (2010) and we shall restrict ourselves to only a few relevant citations.

The interest in the study of this system was renewed when rapid photometric variations with a period of $0\overset{\mathrm{d}}{.}0556$ and a full amplitude of only $0\overset{\mathrm{m}}{.}004$ were discovered (in addition to deep binary eclipses) by Kusakin (2001) and later confirmed by Zejda et al. (2006). Kim et al. (2003) found a period of $0\overset{\mathrm{d}}{.}0528$, which is a 1-d alias of the original period. Rapid multiperiodic line-profile changes were then reported by Lehmann et al. (2008) and Lehmann, Tkachenko and Mkrtichian (2009). They were unable to detect the periods reported from photometry but found three still shorter periods.

Table 1. Comparison and check stars of TW Dra.

	Name	V	$B-V$	$U-B$	Number of obs.	Comment
comp	HD 139549	$9\overset{\mathrm{m}}{.}131 \pm 0\overset{\mathrm{m}}{.}010$	$0\overset{\mathrm{m}}{.}413$	$-0\overset{\mathrm{m}}{.}042$	211	all–sky
check	HD 139703	$9\overset{\mathrm{m}}{.}292 \pm 0\overset{\mathrm{m}}{.}010$	$0\overset{\mathrm{m}}{.}939$	$0\overset{\mathrm{m}}{.}580$	174	all–sky
		$9\overset{\mathrm{m}}{.}292 \pm 0\overset{\mathrm{m}}{.}009$	$0\overset{\mathrm{m}}{.}938$	$0\overset{\mathrm{m}}{.}581$	542	differential

Rather complicated changes of the orbital period have been studied in detail by Zejda, Mikulášek and Wolf (2008), who also summarized previous studies on this topic.

A very detailed and careful study of a superb series of electronic spectra and determination of reliable orbital elements was carried out by Tkachenko, Lehmann and Mkrtichian (2010).

There are several complete light curves of TW Dra, but a multicolour light curve, transformed to a standard system in a reliable way, was still missing. This led us to obtain a complete UBV light curve at Hvar. Its solution, along with the spectroscopic elements by Tkachenko, Lehmann and Mkrtichian (2010), allowed us to improve the knowledge of the basic physical properties of the system, which might be helpful for the future studies of the nature of this binary, its rapid changes or period changes of the system.

2 Observations and their reduction

Differential photoelectric observations of TW Dra in the UBV filters were obtained with a single–channel photometer, equipped with an EMI9789QB tube attached to the 0.65 m Cassegrain reflector of the Hvar Observatory. The observations cover the time interval JD 2453517–2455804. HD 139549 = BD+64°1078 served as the comparison star while HD 139703 = BD+64°1079 was used as the check star and was observed as frequently as the variable. Altogether, 430 individual measurements were secured over 22 nights. The observations were reduced and transformed to the standard Johnson UBV system with the program HEC22 (Harmanec and Horn 1998). The transformation is based on nonlinear formulæ and on numerous observations of standard stars during the whole observing season (see Harmanec, Horn and Juza 1994 for the details). The latest rel. 18 of the program was used, which also allows modelling of variable extinction during individual observing nights. The mean Hvar all-sky UBV magnitudes of the comparison and check stars are listed in Table 1. For all observations the UBV magnitudes of the comparison listed in that Table were added to the magnitude differences var-comp and check-comp. To illustrate the quality of our transformation to the standard system, we also tabulate the mean differentially derived UBV magnitudes of the check star. The individual differential UBV observations of TW Dra with their heliocentric Julian dates are given in Tables 3, 4 & 5, published in electronic form only.

3 The light-curve solution and properties of the system

3.1 The initial ephemeris

Since Zejda, Mikulášek and Wolf (2008) found complicated period changes from their analysis of the orbital-period changes and minima timings of TW Dra over the past 150 years, it was necessary to decide, which ephemeris we should use to begin the solution in `PHOEBE`. The formulæ they derived permit the determination of the instantaneous values of the orbital period and the epoch of primary minimum and these were used by Tkachenko, Lehmann and Mkrtichian (2010). As the Hvar observations were secured during and shortly after the spectroscopic observations by Tkachenko et al., we first tried to adopt their linear ephemeris

$$T_{\mathrm{min.\,I}} = \mathrm{HJD}\,2\,454\,400.97997 + 2\overset{\mathrm{d}}{.}8068491 \times E, \qquad (1)$$

but we found that it leads to a small phase shift in the phase diagram. We therefore decided to allow also convergence of the epoch and local value of the period during the

light curve solution.

Table 2. The final light curve solutions obtained with PHOEBE. All epochs are in RJD = HJD − 2400000. Probable elements and their error estimates are provided. L_j ($j = 1, 2, 3$) are the relative luminosities of the components in individual photometric passbands, normalized in such a way that $L_1 + L_2 + L_3 = 1$. The magnitudes of the individual components refer to the orbital phase 0.25.

Element		Primary	System	Secondary
P	(d)		2.806791 ± 0.000003	
$T_{\rm min.I}$	(RJD)		55703.33053 ± 0.00008	
e			0 fixed	
a	$(R_\odot)$		12.2 fixed	
q			0.430 ± 0.002	
i	$(^\circ)$		87.08 ± 0.03	
r_{pole}	(a)	0.2152 ± 0.0006		0.2881 ± 0.0001
r_{side}	(a)	0.2168 ± 0.0006		0.3004 ± 0.0001
$T_{\rm eff}$	(K)	7815 ± 92		4442 ± 32
M	$(M_\odot)$	2.16 ± 0.11		0.93 ± 0.05
R	$(R_\odot)$	2.64 ± 0.04		3.66 ± 0.06
$M_{\rm bol}$	(mag.)	1.327 ± 0.062		3.163 ± 0.048
$\log g$	[cgs]	3.928 ± 0.026		3.314 ± 0.026
$L_{\rm V}$	V band	0.7924 ± 0.0004		0.0962 ± 0.0004
$L_{\rm B}$	B band	0.8639 ± 0.0004		0.044 ± 0.0004
$L_{\rm U}$	U band	0.8812 ± 0.0004		0.018 ± 0.0004
V	(mag.)	7.582 ± 0.001		9.870 ± 0.005
$(B-V)$	(mag.)	0.213 ± 0.001		1.148 ± 0.011
$(U-B)$	(mag.)	0.094 ± 0.001		1.076 ± 0.026
V_{1+2+3}	(mag.)		7.323	
B_{1+2+3}	(mag.)		7.630	
U_{1+2+3}	(mag.)		7.752	
			Third light	
L_3	V band		0.111 ± 0.002	
L_3	B band		0.092 ± 0.001	
L_3	U band		0.100 ± 0.001	
$^2V_3$	(mag.)		9.713 ± 0.006	
$^2(B-V)_3$	(mag.)		0.517 ± 0.009	
$^2(U-B)_3$	(mag.)		0.017 ± 0.010	

[1] The higher uncertainty bar of variables (a, $r_{\rm side}$, $T_{\rm eff}$, q) was used to propagate the uncertainty of the parameter.

[2] The errors of magnitudes and colours were derived from the formal errors of luminosities.

3.2 The light-curve solution

We derived the solution based on our new UBV light curves using the program PHOEBE (Prša and Zwitter, 2005, 2006). Our approach was the following: we first adopted the principal results from the spectroscopic study by Tkachenko, Lehmann and Mkrtichian (2010) as the input values for the PHOEBE iteration, adopting the circular orbit. These

authors, using spectra disentangling (Hadrava 1995, 1997, 2004) and the Shellspec07 inverse program (Budaj and Richards 2004), derived the semiamplitudes of the radial-velocity curves of 64.05±0.02 and 156±1 km s^{-1} (implying the mass ratio of 0.411±0.004), semimajor axis of (12.2 ± 0.2) $R_\odot$, and zero eccentricity. Note, however, that their result from the KOREL disentangling led to different values: semiamplitudes of 64.05 ± 0.34 and 150.0 ± 2.3 km s^{-1}, semimajor axis of (12.10 ± 0.47) $R_\odot$ and a mass ratio of 0.427 ± 0.011. Comparing the disentangled spectra to synthetic ones, they also derived the effective temperatures of 8160 ± 15 and 4538 ± 11 K for the primary and secondary, respectively.

As already mentioned, we could not exclude the close companion of TW Dra, ADS 9706B from our photoelectric observations and the third-light contribution had to be considered during the solution. To get some initial estimate how large the third light could be, we started with the only reliable photoelectric determination obtained by the Hipparcos satellite and published in the 2nd Tycho catalog, $H_\mathrm{p} = 9\overset{\mathrm{m}}{.}887 \pm 0\overset{\mathrm{m}}{.}047$. We adopted the F7 spectral class of the third body after Meisel (1968) and its colors $B-V = 0\overset{\mathrm{m}}{.}49$ and $U-B = 0\overset{\mathrm{m}}{.}00$ on the premise it is a main-sequence object from the compilation by Golay (1974). Then we could transform the observed H_p magnitude to the Johnson V using the transformation formula by Harmanec (1998). Having the Johnson UBV values for the third star in the system, it was then possible to calculate the relative luminosities L_j (j=1-3) in the units of the total luminosity of the system outside the eclipses ($L_1+L_2+L_3 = 1$) for all three components from the light curves. We took into account the fact that the primary eclipse is a total one. For the input values of the fractional luminosity of the third body we got $L_{3\mathrm{V}} = 0.095$, $L_{3\mathrm{B}} = 0.081$ and $L_{3\mathrm{U}} = 0.090$.

The bolometric albedos for both components of the close binary system were estimated from Claret (2001) and kept fixed during iterations at $A_1 = 0.94$ and $A_2 = 0.78$. The values for gravity–darkening coefficients were estimated from Claret (1998) as $g_1 = 0.95$ and $g_2 = 0.36$.

A linear limb–darkening law was adopted and the limb–darkening coefficients were interpolated every iteration from the 2010 pre-calculated tables, available with a recent *devel* version of the program `PHOEBE`, which we used. They were calculated by Dr. Prša on the basis of Castelli and Kurucz (2004) model atmospheres.

Using the scripter enviroment of `PHOEBE` (version 0.31), we explicitly assumed a semi-detached configuration and a circular orbit. The free parameters during iterations were: the orbital inclination i, the orbital period P, the epoch of the primary mid-eclipse, the mass ratio q, the effective temperatures of both components T_{eff1} and T_{eff2}, the surface potential of the primary Ω_1 and the luminosities of the components L_j, (j=1-3). We have chained five hundred minimizations of the cost function together, starting each minimization at the minimum found in the previous run. The solution converged to the surroundings of the final solution in less than ten iterations. The solution having the lowest cost function value was adopted as the final one.

We also carried out the calculations for the initial values of relative luminosities for the spectral class of the third body in the range from F4 to G0. The best fit, according to the cost function value, has been obtained for the spectral types F6 and F7, which makes the choice of Meisel's value legitimate.

The results of the solution are summarized in Table 2 and the light curves are plotted in Figure 1&2. Figure 1 shows a complete V-band light curve, residua from it and also the phase plot of individual differential observations of the check star to characterize the scatter of the data. Figure 2 is a zoomed part of the UBV light curves and their residua from the solution at the phases around both minima.

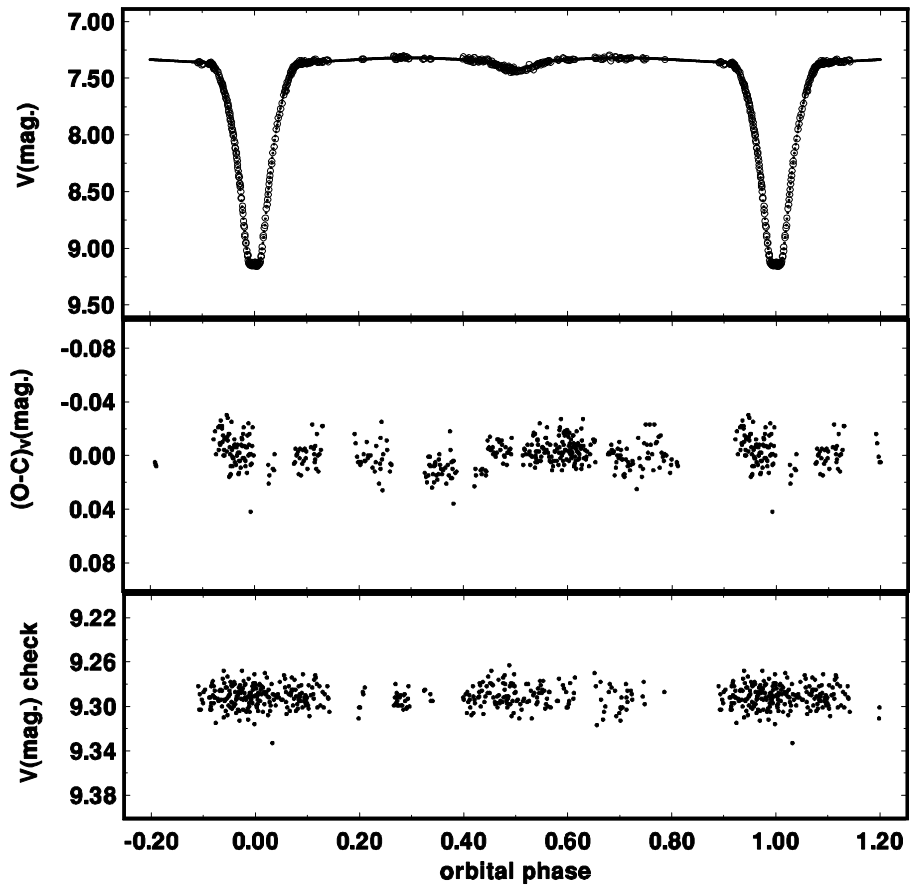

Figure 1. The V magnitude light curve of TW Dra and the final solution are shown in the upper panel. The residua from the solution are in the middle panel while the individual differential observations of the check star are shown in the bottom panel to illustrate the data accuracy.

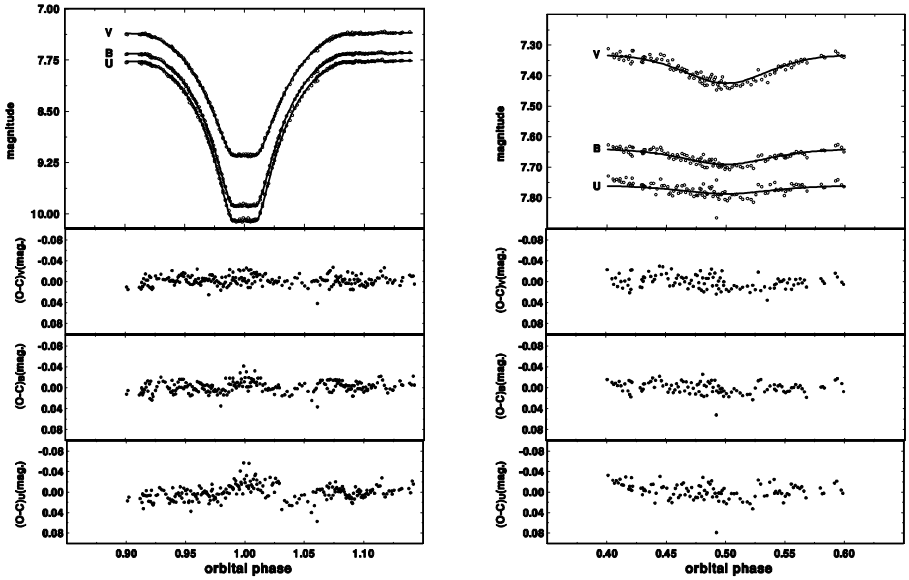

Figure 2. The UBV light curves of TW Dra and the final PHOEBE solution in the neighbourhood of the primary minimum (left) and the secondary minimum (right). The UBV residua from the solution are shown in the bottom panels.

The errors of all fitted parameters given in Table 2 are the formal errors derived in PHOEBE from a covariance matrix.

3.3 Basic properties of the system

There are several things worth mentioning in our new solution:

1. The $O-C$ residua in Fig. 2 show a slight central brightening around the primary mid-eclipse, with an amplitude increasing towards shorter wavelengths. The referee has pointed out that it might be caused by a poor theoretical spectral energy distribution over the Balmer jump region, where even small deviations can accumulate into a significant effect. Even though V light curve should not be affected, there seems to be similar brightening, hence it may also be related to the temperature distribution over the surface of the donor star.
2. Given a rather small distance to the system, the reddening is insignificant and the observed colours of all three components can be directly compared to the standard ones. Miner (1966) indeed found $E(B-V) = 0.0$ for TW Dra. Thanks to the fact that our observations are carefully transformed to the standard UBV system, the light-curve solution allows determination of colour indices of binary components and contains therefore information about photometric effective temperatures of both stars. We have used such an approach for a long time – cf, e.g., Mayer et al. (1991). The possibility to converge both effective temperatures using calibrated photometry was later realised by Prša, A. & Zwitter, T. (2005, 2006), who implemented it to the scripter environment of PHOEBE and the referee encouraged us to use this option in our light-curve solution. It is clear that this requires standardised photometry

of superb quality. In our case the situation is more favourable due to the fact that the temperatures of both components differ substantially from each other. We find the fact that it resulted in reasonable values notable. It represents one of the very first practical attempts along this line. Note that an even more elaborate attempt at the determination of both effective temperatures was carried out by Wilson & Raichur (2011). Referring again to the compilation by Golay (1974), we found the photometric spectral types of A6–A8V, K1–2III, and F8V for the primary, secondary, and tertiary, respectively. For comparison, deriving colour indices of the primary and secondary from the standard UBV values at maximum light and from relative luminosities in individual passbands correspond to $T_{\rm eff1} = 7700$ K and $T_{\rm eff2} = 4560$ K if Flower's (1996) calibration is used, and to 7600 and 4215 K if Popper's (1980) calibration is used.

3. The linear ephemeris, which follows from our solution and applies to the time interval JD 2455594-2455804 (the single night of observations secured in 2005 was obtained at maximum light and has little impact on the accurate determination of the orbital period; a solution without this night remains almost unaltered) is

$$T_{\rm min.\,I} = {\rm HJD}\,2\,455\,703.3305280(28) + 2\overset{\rm d}{.}806790(0) \times E, \qquad (2)$$

i.e. significantly shorter than the ephemeris used by Tkachenko et al. (2010). Zejda, Mikulášek and Wolf (2008) demonstrated the damping $O-C$ variations with a cycle of some 20 years which they attributed to the quadrupole moment variations in the system. One can speculate that the period decrease found by us could indicate an increase in the mass–transfer rate. The small–amplitude 6.5-year variation due to a hypothetical low–mass third body proposed by Wolf (1990) and Zejda, Mikulášek and Wolf (2008) is not sufficient to explain the large discrepancy between observed and expected value of the period.

4. Taken at face value, the mass of the primary of 2.2 $M_\odot$ would correspond to an A0-A1 main-sequence object (see Harmanec 1988), which strongly disagrees with the spectral class A5 found by Tkachenko, Lehmann and Mkrtichian (2010) or A6–A8 derived by us. One possibility is that the primary is somewhat evolved from the zero-age main sequence. However, we wish to offer an alternative possibility. TW Dra is an emission-line star seen edge-on (Richards and Albright 1999). In that case, we have a situation reminiscent of cases of the inverse correlation between the brightness and emission strength discussed by Harmanec (1983). The matter flowing from the contact secondary towards the primary may form *a pseudophotosphere*, which – seen equator-on – mimics a later spectral subclass than that, which one would get for the primary if it could be observed pole-on or totally without such a pseudophotosphere. In other words, we might not be observing an evolutionary effect but an effect of the densest parts of circumstellar matter projected against the disk of the primary.

   The idea might be worth testing via dedicated spectral observations. In passing we note that the continuing mass exchange in TW Dra seems to be supported by a recent study by Ibanoğlu et al. (2012), who found evidence of carbon deficiency, indicative of inflow of CNO reprocessed material into the atmosphere of the primary. Notably, these authors estimate the effective temperature of the primary from the Strömgren photometry to be 10800 K.

Acknowledgements: We acknowledge the use of the latest *devel* version of the `PHOEBE` program, written and freely distributed by Dr. A. Prša. A constructive criticism

of the previous version of this paper by the referee, Dr. A. Prša, helped to improve the paper. This research was supported from the grants P209/10/0715 of the Czech Science Foundation and 101-10/253289 of the Charles University in Prague and from the Research Program MSM0021620860 of the Ministry of Education, Youth and Sports of the Czech Republic. We profited from the use of the electronic database from CDS Strasbourg and electronic bibliography maintained by the NASA/ADS system.

References:

Budaj, J., Richards, M.T., 2004, *Contr. Astron. Obs. Skalnaté Pleso*, **34**, 167
Castelli, F., Kurucz, R.L., 2004, *New Grids of ATLAS9 model atmospheres arXiv:astro-ph/0405087*
Claret, A., 1998, *A&AS*, **131**, 395
Claret, A., 2001, *MNRAS*, **327**, 989
Flower, P.J., 1996, *ApJ*, **469**, 355
Golay, M., 1974, *ASSL*, **41**, 79
Hadrava, P., 1995, *A&AS*, **114**, 393
Hadrava, P., 1997, *A&AS*, **122**, 581
Hadrava, P., 2004, *Publications of the Astron. Inst. Acad. Sci. Czech Rep.*, **92**, 15
Harmanec, P., 1983, *Hvar Obs. Bull.*, **7**, 55
Harmanec, P., 1988, *BAICz*, **39**, 329
Harmanec, P., 1998, *A&A*, **334**, 558
Harmanec, P., Horn, J., 1998, *The Journal of Astronomical Data*, **4**, 5
Harmanec, P., Horn, J., Juza, K., 1994, *A&AS*, **104**, 121
Ibanoğlu, C., Dervişoğlu, A., Çakırlı, Ö, Sipahi, E., Yüce, K. 2012, *MNRAS*, **419**, 1472
Kim, S.-L., Lee, J.W., Kwon, S.-G. et al., 2003, *A&A*, **405**, 231
Kusakin, A.V., 2001, *IBVS*, 510
Lehmann, H., Tkachenko, A., Mkrtichian, D., 2009, *Comm. Asteroseismology*, **159**, 45
Lehmann, H., Tkachenko, A., Tsymbal, V., Mkrtichian, D.E., 2008, *Comm. Asteroseismology*, **157**, 332
Mayer, P., Hadrava, P., Harmanec, P., Chochol, D., 1991, *BAICz* **42**, 230
Meisel, D., 1968, *AJ*, **73**, 350
Miner, E.D., 1966, *ApJ*, **144**, 1101
Prša, A., Zwitter, T., 2005, *ApJ*, **628**, 426
Prša, A., Zwitter, T., 2006, *ApSS*, **304**, 347
Richards, M.T., Albright, G.E., 1999, *ApJS*, **123**, 537
Tkachenko, A., Lehmann, H., Mkrtichian, D., 2010, *AJ*, **139**, 1327
Wilson, R.E., Raichur, H., 2011, *MNRAS*, **415**, 596
Wolf, M., 1990, *JAAVSO*, **19**, 17
Zejda, M., Mikulášek, Z., Wolf, M., 2008, *A&A*, **489**, 321
Zejda, M., Mikulášek, Z., Wolf, M., Pejcha, O., 2006, *ApSS*, **304**, 161

*This version of the paper contains corrections, and differs from the one appeared on-line originally. Date of last modification: Dec 6 14:04:16 CET 2013

COMMISSIONS 27 AND 42 OF THE IAU
INFORMATION BULLETIN ON VARIABLE STARS

Number 6087

Konkoly Observatory
Budapest
19 December 2013

HU ISSN 0374 – 0676

PHOTOMETRY OF THE PROGENITOR OF NOVA Del 2013 (V339 Del) AND CALIBRATION OF A DEEP *BVRI* PHOTOMETRIC COMPARISON SEQUENCE

MUNARI, ULISSE[1,2]; HENDEN, ARNE[3]

[1] INAF Osservatorio Astronomico di Padova, Sede di Asiago, I-36032 Asiago (VI), Italy

[2] ANS Collaboration, c/o Astronomical Observatory, I-36012 Asiago (VI), Italy

[3] AAVSO, 49 Bay State Rd. Cambridge, MA 02138, USA

Nova Del 2013 (=V339 Del) was discovered on 2013 Aug 14.584 UT by K. Itagaki when it was already shining at unfiltered 6.8 magnitude (cf. CBET 3628). The observation by Denisenko et al. (cf. CBET 3628) reporting the nova still in quiescence at ∼17.1 mag on Aug 13.998 UT (14 hours before the discovery), would indicate a very fast rise to maximum. The photometric evolution of the nova during the optically thick phase has been presented by Munari et al. (2013a).

The nova appeared at a position coincident with the blue star USNO B-1 1107-0509795, reported at B ∼17.20, $R_{\rm C}$ ∼17.45 on the first Palomar Sky Survey plates (exposed on 7 July 1951), and at B ∼17.39, $R_{\rm C}$ ∼17.74 on the second Palomar Sky Survey plates (exposed on 18 July and 15 September 1990, respectively). The progenitor is bright enough to have been recorded on patrol plates taken with the Asiago Schmidt telescopes, in particular the 67/92 cm instrument. We searched the Asiago plate archive and found 25 plates imaging the area of the sky where the nova later appeared (16 in B band, 7 in V, and 2 in $I_{\rm C}$).

Prior to measuring these plates, it was necessary to establish an accurate and reliable photometric sequence around the nova. Given the huge interest this nova has received because of its peak brightness(V=4.46, B=4.70), it may be presumed that its remnant will be studied for long after the system has returned to quiescence. To ensure proper comparison of the pre-outburst photometric data with the post-outburst ones, a well calibrated and common photometric sequence must be adopted. To this aim we obtained deep exposures in $BVR_{\rm C}I_{\rm C}$ bands of the field surrounding the nova on three separate photometric nights with the TMO61 telescope (part of the AAVSOnet robotic network) in New Mexico (USA). The data for each night were independently calibrated against the equatorial Landolt (2009) standard stars, and the results were averaged.

From the common data set, we have extracted two sets of standards, presented in Tables 1 and 2. These standards are on the same photometric scale of the brighter ones used by Munari et al. (2013a) to derive the photometric evolution of the nova around maximum and early decline. The standards in Table 1 are optimized for CCD observations and are grouped within 5 arcmin of the nova. They were selected at three different

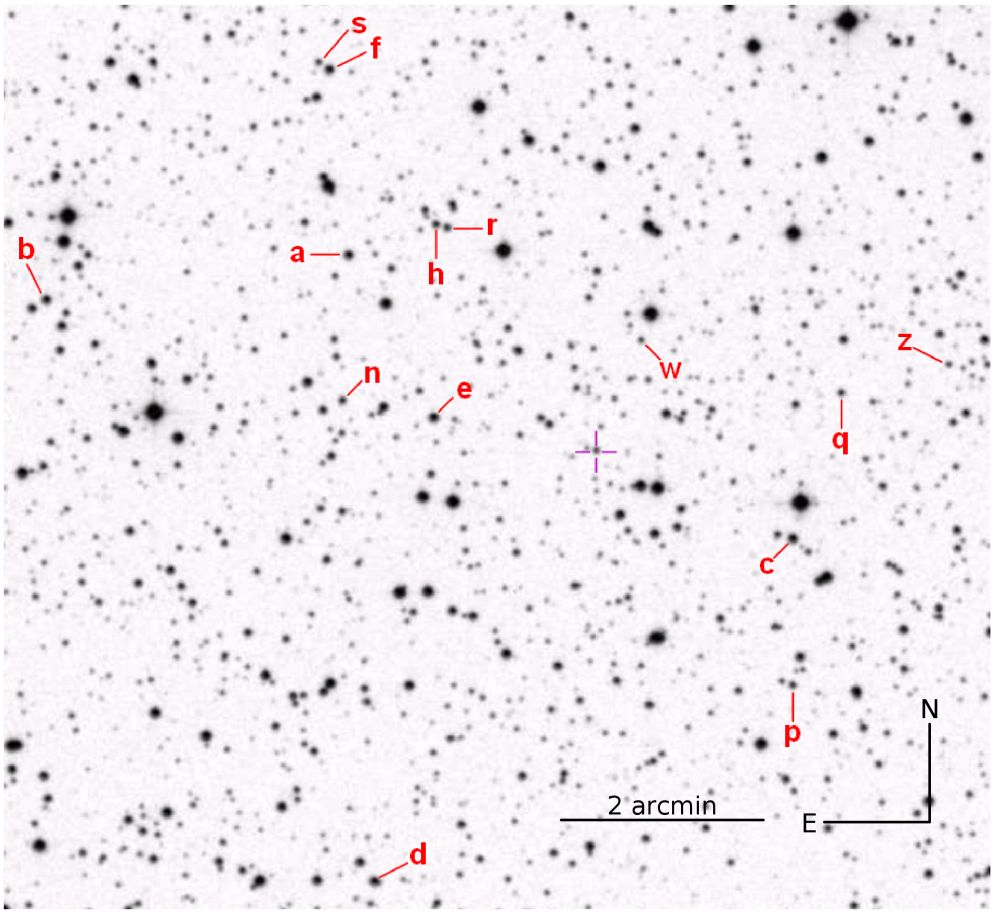

Figure 1. Finding chart for the BVR_CI_C photometric sequence in Table 1, optimized for CCD observations of Nova Del 2013 during the advanced decline and after its return to quiescence.

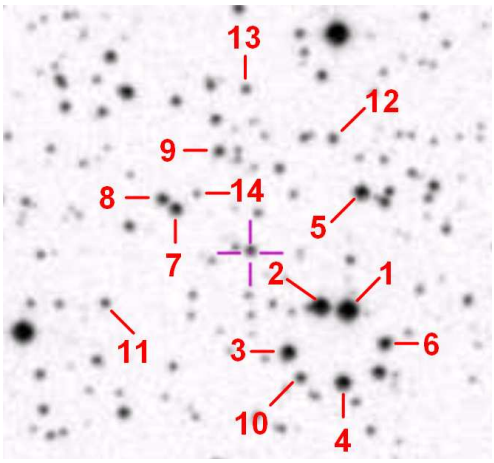

Figure 2. Finding chart for the BVR_CI_C photometric sequence in Table 2, optimized for measurement of the progenitor on archive photographic plates. The chart is 3.0 arcmin wide with North to the top and East to the left.

Table 1: BVR_CI_C photometric sequence (plotted in Figure 1), optimized for CCD observations of Nova Del 2013 during the advanced decline and after its return to quiescence.

	α (J2000.0)		δ (J2000.0)		N	V		$B-V$		$V-R_C$		R_C-I_C		$V-I_C$	
		±		±			±		±		±		±		±
a	305.923000	0.257	20.800496	0.245	3	14.628	0.017	1.075	0.031	0.578	0.031	0.525	0.019	1.106	0.038
b	305.977735	0.042	20.792703	0.033	3	14.431	0.017	1.267	0.013	0.718	0.033	0.611	0.014	1.329	0.028
c	305.842211	0.049	20.752941	0.007	3	14.751	0.019	0.643	0.014	0.370	0.018	0.363	0.015	0.734	0.033
d	305.917730	0.073	20.694474	0.031	3	14.777	0.022	0.788	0.019	0.461	0.023	0.420	0.009	0.881	0.031
e	305.907336	0.053	20.773056	0.008	3	14.821	0.011	0.533	0.029	0.325	0.002	0.339	0.033	0.667	0.039
	.														
f	305.926635	0.063	20.831951	0.022	3	15.171	0.045	0.457	0.017	0.273	0.033	0.286	0.017	0.559	0.045
g	305.812010	0.096	20.797778	0.037	3	15.638	0.025	0.515	0.013	0.340	0.013	0.344	0.019	0.686	0.027
h	305.907143	0.086	20.805805	0.018	3	15.685	0.017	1.217	0.031	0.617	0.021	0.586	0.011	1.211	0.032
m	305.810946	0.042	20.774322	0.022	3	15.789	0.022	0.625	0.021	0.394	0.018	0.393	0.007	0.791	0.022
n	305.923894	0.015	20.775920	0.049	3	15.854	0.029	1.063	0.007	0.602	0.047	0.594	0.004	1.205	0.041
r	305.905116	0.051	20.805268	0.039	3	15.983	0.021	0.784	0.038	0.443	0.036	0.395	0.026	0.837	0.010
	.														
s	305.928668	0.021	20.833250	0.031	3	16.335	0.019	1.239	0.028	0.774	0.040	0.734	0.013	1.519	0.023
p	305.842054	0.065	20.728134	0.045	3	16.350	0.013	0.653	0.041	0.364	0.043	0.366	0.034	0.733	0.036
q	305.833547	0.073	20.777642	0.006	3	16.414	0.014	0.746	0.049	0.348	0.034	0.396	0.032	0.753	0.011
z	305.814090	0.044	20.782587	0.027	3	16.832	0.024	0.915	0.048	0.497	0.015	0.486	0.014	0.989	0.011
w	305.869829	0.015	20.786390	0.015	3	16.892	0.035	0.596	0.041	0.424	0.020	0.364	0.042	0.786	0.037

Table 2: BVR_CI_C photometric sequence (plotted in Figure 2), optimized for measurement of the progenitor on archive photographic plates.

	α (J2000.0)		δ (J2000.0)		N	V		$B-V$		$V-R_C$		R_C-I_C		$V-I_C$	
		±		±			±		±		±		±		±
1	305.866822	0.000	20.761365	0.009	3	12.956	0.020	0.663	0.016	0.368	0.027	0.335	0.011	0.701	0.036
2	305.869855	0.021	20.761706	0.007	3	13.974	0.020	0.441	0.010	0.257	0.028	0.275	0.014	0.533	0.039
3	305.873531	0.021	20.756879	0.032	3	14.923	0.019	0.644	0.010	0.352	0.033	0.387	0.009	0.745	0.041
4	305.867263	0.047	20.753647	0.004	3	14.434	0.014	1.186	0.005	0.623	0.022	0.564	0.007	1.191	0.027
5	305.865298	0.049	20.773975	0.004	3	14.837	0.016	1.040	0.023	0.580	0.015	0.545	0.018	1.130	0.032
6	305.862514	0.036	20.757837	0.037	3	15.624	0.037	0.713	0.068	0.425	0.030	0.391	0.003	0.816	0.031
7	305.886392	0.053	20.772088	0.025	3	16.020	0.017	0.478	0.051	0.319	0.008	0.349	0.021	0.672	0.032
8	305.887957	0.033	20.773124	0.015	3	16.104	0.023	0.930	0.048	0.540	0.039	0.479	0.032	1.019	0.026
9	305.881489	0.057	20.778284	0.044	3	16.907	0.037	0.543	0.086	0.298	0.020	0.373	0.037	0.682	0.055
10	305.872048	0.044	20.754137	0.013	3	16.422	0.040	1.251	0.096	0.715	0.045	0.573	0.078	1.285	0.048
11	305.894345	0.026	20.762005	0.025	3	17.284	0.067	0.765	0.096	0.638	0.132	0.653	0.078	1.305	0.040
12	305.868499	0.101	20.779694	0.080	3	17.376	0.068	0.862	0.093	0.475	0.107	0.452	0.084	0.929	0.068
13	305.878491	0.244	20.784939	0.056	3	17.597	0.040	0.686	0.042	0.493	0.060	0.469	0.013	0.965	0.067
14	305.884012	0.276	20.773748	0.000	2	18.497	0.058	0.600	0.068	0.564	0.037	0.468	0.105	1.030	0.083

magnitude levels (V ∼14.6, 15.6, and 16.6 mag) to support photometric investigation of both the advanced decline and the following return to quiescence of the nova. At each of the three different magnitude levels, at least five standards are provided that cover a broad range of colors so to allow the calibration of color equations to transform the measurements from the local to the standard system. The standards in Table 2 are instead optimized to derive the magnitude of the progenitor on old photographic plates, most of which were exposed in blue light or in B band. They are grouped within 1 arcmin of the nova.

Table 3: The brightness of the progenitor of Nova Del 2013 as measured on Asiago photographic plates.

plate	tel.	date	UT	exp. time min	emulsion	filter	band	mag
10005	67/92	1979 04 23	00:06	5	103 a-O	GG 13	B	>13.6
10033	67/92	1979 05 20	00:03	15	103 a-O	GG 13	B	>14.5
10034	67/92	1979 05 20	00:31	20	I-N Sen.	RG 5	I	>15.3
10055	67/92	1979 05 23	00:09	20	103 a-O	GG 13	B	17.2
10056	67/92	1979 05 23	00:42	30	I-N Sen.	RG 5	I	>15.3
10240	67/92	1979 10 24	21:21	20	103 a-D	GG 14	V	>17.3
10262	67/92	1979 11 20	20:20	20	103 a-O	GG 13	B	>17.5
10303	67/92	1979 12 11	19:57	15	103 a-O	GG 13	B	>16.5
10484	67/92	1980 05 12	23:26	15	103 a-D	GG 14	V	>16.1
10530	67/92	1980 07 09	20:50	15	103 a-O	GG 13	B	>17.5
10531	67/92	1980 07 09	21:16	15	103 a-D	GG 14	V	>16.4
10546	67/92	1980 07 16	00:03	15	103 a-O	GG 13	B	17.2
10547	67/92	1980 07 16	00:25	15	103 a-D	GG 14	V	>16.9
10624	67/92	1980 09 30	20:01	15	103 a-D	GG 14	V	>16.4
10646	67/92	1980 10 13	21:34	15	103 a-O	GG 13	B	17.8
11035	67/92	1981 07 26	22:55	20	103 a-D	GG 14	V	17.4
11076	67/92	1981 08 23	23:47	30	103 a-O	GG 13	B	17.2
11100	67/92	1981 09 06	22:20	20	103 a-O	GG 13	B	17.2
11122	67/92	1981 10 23	21:10	20	103 a-O	GG 13	B	17.2
11178	67/92	1981 11 16	18:11	20	103 a-O	GG 13	B	17.1
11231	67/92	1981 11 22	19:35	30	103 a-O	GG 13	B	17.4
11568	67/92	1982 06 28	01:18	20	103 a-O	GG 13	B	17.5
11578	67/92	1982 07 16	01:00	20	103 a-O	GG 13	B	16.9
11716	67/92	1982 10 20	20:45	30	103 a-D	GG 14	V	17.8
15355	40/50	1983 04 09	21:43	15	103 a-O	GG 13	B	>17.5

The magnitude of the progenitor of Nova Del 2013 on Asiago photographic plates was estimated by eye through a high quality Zeiss microscope. The plates were independently re-measured a few days later and the results were found to be the same within 0.1 mag, which is therefore taken as the error associated to the measurements. The results are presented in Table 3. The mean brightness of the progenitor on these plates is $\langle B\rangle$=17.27 and $\langle V\rangle$=17.6, for a mean color $B-V=-0.33$. The recorded total amplitude of variation in B band is 0.9 mag. Color and variability are in agreement with a progenitor dominated by the emission from an accretion disc. The reddening toward Nova Del 2013 is low (E_{B-V}=0.18, e.g. Munari et al. 2013b) given its high galactic latitude ($b = -9\overset{\circ}{.}4$). Brightness level and color are in excellent agreement with the USNO-B1 values from Palomar surveys 1 and 2, arguing for a long term stability before the 2013 eruption.

The progenitor was marginally detected also by the APASS all sky survey, when it visited the field on 2012 April 21, 24 and 25, thus about 18 months before the nova eruption. We have stacked the CCD images from these three visits and measured the progenitor at $B = 17.33 \pm 0.09$ and $V = 17.06 \pm 0.10$.

References:

Landolt, A. U. 2009, *AJ*, **137**, 4186
Munari, U. et al. 2013a, *IBVS*, **6080**
Munari, U. et al. 2013b, *ATel*, **5297**

COMMISSIONS 27 AND 42 OF THE IAU
INFORMATION BULLETIN ON VARIABLE STARS

Number 6088

Konkoly Observatory
Budapest
22 December 2013

HU ISSN 0374 – 0676

IDENTIFICATION OF Be AND CARBON STARS IN THE MAGELLANIC CLOUDS AS A BY-PRODUCT OF A SYMBIOTIC STAR SEARCH†

CIESLINSKI, DEONISIO[1]; DIAZ, MARCOS P.[2]; MENNICKENT, RONALD E.[3]; KOŁACZKOWSKI, ZBIGNIEW[4]; PEREIRA, CLÁUDIO B.[5]

[1] Instituto Nacional de Pesquisas Espaciais, Divisão de Astrofísica, Brazil

[2] Instituto de Astronomia, Geofísica e Ciências Atmosféricas, Universidade de São Paulo, Brazil

[3] Depto. de Astronomía, Universidad de Concepción, Chile

[4] Astronomical Institute, University of Wrocław, Poland

[5] Observatório Nacional, Rio de Janeiro, Brazil

Symbiotic stars are a sub-group of interacting binaries consisting of a cool giant which transfers material via stellar wind or Roche-lobe overflow to a hot and compact object which is thought to be a white dwarf or even, in a few cases, a neutron star. The optical spectra show the presence of a continuum with TiO and/or VO absorption bands, eventually Swan bands, absorption lines of neutral and singly ionized metals (from the cool star) and emission lines of the Balmer series, HeI, [OIII] as well as emission lines of high ionization species such as HeII and [FeVII], which are associated with the surrounding nebula and/or an accretion disc. Photometrically they present variability on several time scales, from minutes to several decades with amplitudes from a few thousandths to several magnitudes. The orbital periods are ranging from ∼200 days to several years or even decades. Reviews on symbiotic stars can be found in Friedjung & Viotti (1982), Kenyon (1986), Mikołajewska et al. (1988), Mikołajewska (1997), Corradi, Mikołajewska & Mahoney (2003) and Mikołajewska & Szczerba (2007).

Nowadays, about 200 symbiotic stars are known, see e.g., the catalog of Belczyński et al. (2000). This catalog contains 188 objects confirmed as true symbiotics and 30 as suspected. Surprisingly, however, among the confirmed symbiotics only 8 are in Large Magellanic Cloud and 6 in the Small Magellanic Cloud, with half of them harboring carbon stars. It is a known fact that the physical condition driving the symbiotic phenomenon depends on several factors, the surface metallicity of the cool star being one of them (see, e.g., the discussion of Jorissen 2003). In this sense, one may expect qualitative differences between the population of symbiotics in our Galaxy and those in the Magellanic Clouds. Unfortunately, the sample of symbiotics in the LMC and SMC is far too small to enable any statistical comparison with the population of symbiotics in our Galaxy. In addition, the proposed evolutionary link between Super-Soft X-Ray Sources (SSS) and symbiotic systems in the Clouds still depends on a better knowledge of the symbiotic population in

†This paper includes data gathered with the 6.5 meter Magellan Telescopes located at Las Campanas Observatory, Chile and with the Southern Astrophysical Research (SOAR) telescope, which is a joint project of the Ministério da Ciência, Tecnologia, e Inovação (MCTI) da República Federativa do Brasil, the U.S. National Optical Astronomy Observatory (NOAO), the University of North Carolina at Chapel Hill (UNC), and Michigan State University (MSU).

this environment, where the population of SSS is much better defined than in our Galaxy (e.g., Kahabka 1997). Such a comparison may help us to understand the evolutionary links between symbiotics, supersoft X-ray sources, type Ia supernovae, and the metallicity-dependent mechanisms of mass loss in those binaries. This fact motivated us to design and conduct a search program aiming at discovering and confirming new symbiotic binaries in these nearby galaxies.

The fact that symbiotic stars present spectral and photometric peculiarities provides us with several ways of discovering them, i.e., we can find candidates to this class using published photometric and/or spectroscopic data. Consequently, targets can be selected among objects with peculiar colors (e.g., presence of UV excess with red colors with respect to normal stars), light curve peculiarities (e.g., eruptions or large-amplitude irregular variations) and among catalogues of objects with emission lines. In fact, we have discovered some new symbiotic stars during a photometric and spectroscopic survey on L-, I- and IS-type irregular variables (Cieslinski et al. 1994, 1997).

In this work the targets were selected using combined criteria comprising their color, photometric variability and the presence of emission lines. Our first step was to define the intrinsic color region for known symbiotics with M-type giants in our Galaxy using data from the literature (Munari et al. 1992 and Munari & Jurdana-Sepic 2002; see also Henden & Munari 2008) (Fig. 1). Such a wide region reflects the presence of a red continuum with an enhanced UV/blue emission. A large number (10^5) of potential targets, corrected for extinction towards the LMC and SMC, were selected, above the three dashed segments of Fig. 1, from the photometric *UBVI* surveys of Zaritsky et al. (2002, 2004). The long lists were further constrained by the typical absolute magnitude range of symbiotics with giant primaries (usually brighter than a G5 giant) based on the LMC/SMC distance moduli. Those are still numerous samples with contamination from binaries and normal stars with similar color indices. These lists were then cross-correlated with the OGLE and MACHO variable stars database, yielding a few hundred targets. Known variables were removed from our lists. Finally, the light curves of the LMC candidates were visually inspected, searching for photometric variability that would be consistent with those of a photometrically active symbiotic stars. The observation priority for the LMC targets was defined by the morphology of their MACHO light curves. A different strategy was adopted for the SMC for which three emission line object catalogs are publicly available (Meyssonnier & Azzopardi 1993, Murphy & Bessell 2000 and Evans et al. 2004). The cross-correlation of the photometrically selected sample with the emission line sources yields a list with 90 candidates.

The observations reported in this contribution were performed from 2004 to 2009 with the Magellan Clay 6-m LDSS-31 and the SOAR 4.1-m GOODMAN spectrograph (Clemens et al. 2004). The spectral resolution obtained is ∼0.7 nm and ∼0.2 nm for the SOAR and Magellan spectra, respectively. The spectral coverage of the individual spectra is indicated in column 7 of Tables 1 and 2. Relative flux calibration was performed in arbitrary units on all Magellan spectra. In this case, the relative flux calibration was attempted by applying an average extinction curve and a sensitivity function estimated by comparing the spectra of observed B stars with literature SEDs having the same spectral type (Jacoby et al. 1984). An approximate absolute flux calibration was performed on the SOAR data by using an average extinction curve and the observations of one or two tertiary spectrophotometric standard stars from Hamuy et al. (1994) per night. Absolute calibration errors are estimated to be smaller than 0.2 mag for the SOAR data. Thin cirrus clouds were present during the Magellan observations while photometric conditions

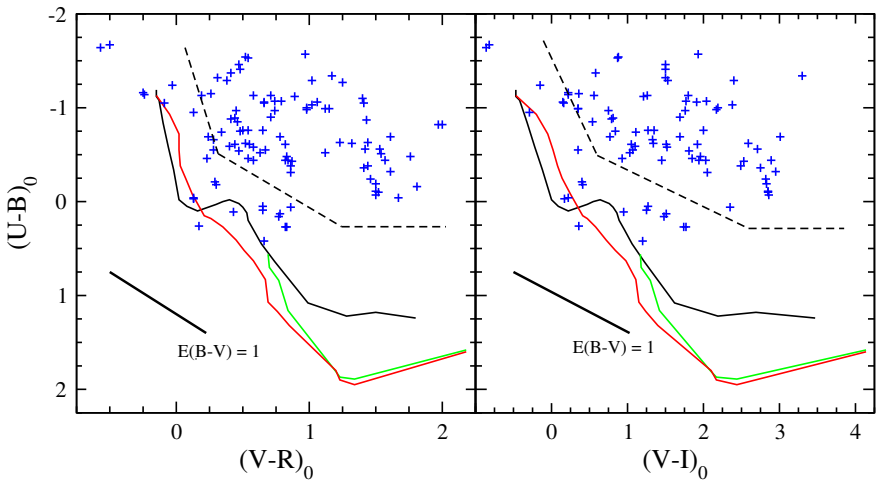

Figure 1. Color diagrams for known symbiotic stars in the Galaxy, corrected for interstellar extinction (blue pluses). Approximante reddening corrections were computed using the galactic extinction model by Amôres & Lépine (2005) and a few values from literature, when available. The black, red and green curves show the main-sequence, supergiant and giant colors, respectively. Reddening vectors are plotted in the lower left corners. The straight dashed lines represent our initial selection criteria and were used to select objects from the photometric *UBVI* surveys of Zaritsky et al. (2002, 2004). Additional photometric and/or spectroscopic criteria were applied to this subsample to finally obtain our candidate lists for the LMC and the SMC.

prevailed for most of the SOAR science exposures. The wavelength-calibration exposures were taken before or after the target exposures. However, the SOAR spectra may include small (few times the FWHM resolution) wavelength shifts and should not be used for deriving radial velocities. All the reduction of the spectroscopic data was done with the IRAF package[1].

The log of the observations is listed in Table 1 (Be stars) and Table 2 (carbon stars). In these tables, column 1 gives the file name of the spectrum, columns 2 and 3 are the coordinates of the object, column 4 indicates the Heliocentric Julian Day of the middle of the exposure, column 5 is the exposure time in seconds, column 6 gives the signal to noise ratio of the spectrum, column 7 shows the spectral coverage in nm, column 8 gives the OGLE and/or MACHO identification (if any), while the numbers in column 9 indicate the comments on individual objects, cited in the footnotes of these tables.

Several Be and carbon stars were found in our sample. The applied selection criteria plus the presence of emission lines in the SMC targets proved to be effective in selecting carbon and Be stars. This small but homogeneously selected sample comprises both types of objects in the LMC and SMC. Carbon stars were identified by the presence of a red continuum with Swan bands in the optical region (e.g., in 438.2, 473.7, 516.5, 563.6 and 619.1 nm). We classified the target as a carbon star if one or more of these bands were present. The identification of the Be stars was performed by considering the presence of a blue continuum with at least one emission line of the Balmer series (generally, Hα). Some objects also show other emission lines such as HeI, FeII, CaII triplet at 849.8, 854.2 and

[1]IRAF is distributed by the National Optical Astronomy Observatories, which are operated by the Association of Universities for Research in Astronomy, Inc., under cooperative agreement with the National Science Foundation.

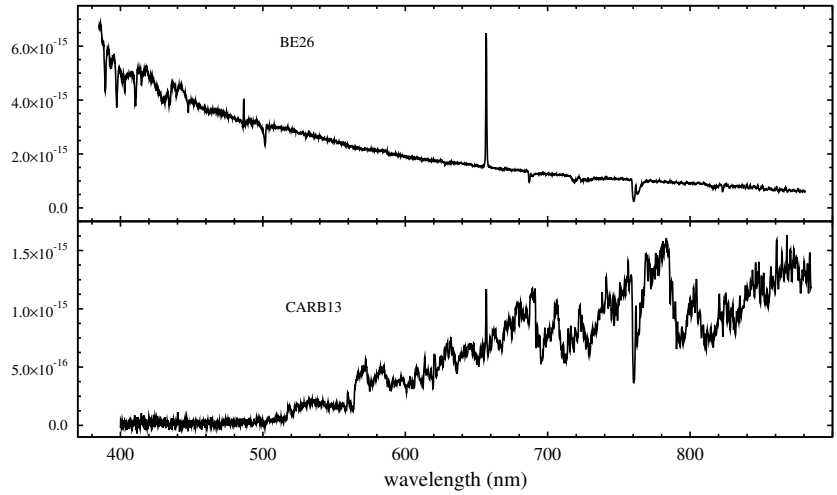

Figure 2. Sample spectra of Be stars (top) and carbon stars (bottom). Flux units are erg cm^{-2} s^{-1} Å^{-1}.

866.2 nm, OI in 777.2 and 844.6 nm and some lines of Paschen series. Six objects with 'flat' continuum and/or objects in which the flux calibration is more uncertain (mainly the ones observed with Magellan Clay telescopes) were classified as Be or Ce candidates.

A brief description of the main spectroscopic characteristics of each individual object is given in the notes of Tables 1 and 2. Sample spectra for both classes can be seen in Fig. 2. All the spectra (in ASCII format) are accessible in the auxiliary files 6088-d1.tar.gz and 6088-d2.tar.gz.

Some objects, however, appear to be more interesting and deserve more detailed investigation. Among them, we mention the carbon stars with indications of a blue continuum that might indicate binarity, and the objects with a 'flat' continuum. From the data at hand we conclude that most of the carbon stars we found are cool. Nevertheless, a precise classification of the sample of carbon stars may require additional observations. Among the Be stars some objects present HeI and FeII emission lines. Absorption line reversals are also seen in some objects. Metallicity effects are important in the evolution of carbon stars and also for the mass loss mechanism feeding the circumstellar disks of Be stars. Statistical comparison of controlled samples in our Galaxy and in the Clouds may help to improve our knowledge on these objects.

Acknowledgements. MPD thanks CNPq grant #305175. We also thank the anonymous referee for his/her comments and suggestions.

References:

Amôres, E. B., Lépine, J. R. D., 2005, *AJ*, **130**, 659
Belczyński, K., Mikołajewska, J., Munari, U., Ivison, R. J., Friedjung, M., 2000, *A&AS*, **146**, 407
Cieslinski, D., Elizalde, F., Steiner, J. E., 1994, *A&AS*, **106**, 243
Cieslinski, D., Steiner, J. E., Elizalde, F., Pereira, M. G., 1997, *A&AS*, **124**, 57
Clemens, J. C., Crain, J. A., Anderson, R., 2004, *Proc. SPIE*, **5492**, 331

Corradi, R. L. M., Mikołajewska, J., Mahoney, T. J., eds., 2003, *ASP Conference Series*, Vol. **303**
Evans, C. J., Howarth, I. D., Irwin, M. J., Burnley, A. W., Harries, T. J., 2004, *MNRAS*, **353**, 601
Friedjung, M., Viotti, R., eds., 1982, *IAU Coll.*, **70**, 45
Hamuy, M., Suntzeff, N. B., Heathcote, S. R., Walker, A. R., Gigoux, P., Phillips, M. M., 1994, *PASP*, **106**, 566
Henden, A., Munari, U., 2008, *Baltic Astronomy*, **17**, 293
Jacoby, G. H., Hunter, D. A., Christian, C. A., 1984, *ApJS*, **56**, 257
Jorissen, A., 2003, *ASP Conference Series*, **303**, 25
Kahabka, P., 1997, *ARA&A*, **35**, 69
Kenyon, S. J., 1986, *The Symbiotic Stars*, Cambridge University Press, Cambridge
Meyssonnier, N., Azzopardi, M., 1993, *A&AS*, **102**, 451
Mikołajewska, J., Friedjung, M., Kenyon, S. J., Viotti, R., eds., 1988, *IAU Coll.*, **103**
Mikołajewska, J., ed., 1997, *Physical Processes in Symbiotic Binaries and Related Systems*, Copernicus Foundation for Polish Astronomy, Warsaw
Mikołajewska, J., Szczerba R., eds., 2007, *Evolution and Chemistry of Symbiotic Stars, Binary Post-AGB and Related Objects*, *Baltic Astronomy*, **16**, No.1, 1-164
Munari, U., Yudin, B. F., Taranova, O. G., Massone, G., Marang, F., Roberts, G., Winkler, H., Whitelock, P. A., 1992, *A&AS*, **93**, 383
Munari, U., Jurdana-Sepic, R., 2002, *VizieR Online Data Catalog*, 338
Murphy, M. T., Bessell, M. S., 2000, *MNRAS*, **311**, 741
Zaritsky, D., Harris, J., Thompson, I. B., Grebel, E. K., Massey, P., 2002, *AJ*, **123**, 855
Zaritsky, D., Harris, J., Thompson, I. B., Grebel, E. K., 2004, *AJ*, **128**, 1606

Table 1: Be stars and candidates

File name	α_{2000}	δ_{2000}	HJD (2450000+)[a]	Exp. Time (s)	S/N[b]	Sp. coverage (nm)	Other names[c]	Notes
be01.txt	00:43:05.3	−72:35:48.8	4710.8560	51	24.78	385−880		1
be02.txt	00:46:41.7	−73:22:53.8	4683.8808	60	44.79	460−890		2
be03.txt	00:47:01.4	−73:26:46.0	4792.6039	600	44.37	385−880		3
be04a.txt	00:48:23.7	−73:15:29.1	4710.7503	50	29.48	385−880	OGLE004823.67−731528.9	4
be04b.txt	”	”	4301.7712	360	73.50	530−815	”	”
be04c.txt	”	”	4301.7712	360	72.39	375−528	”	”
be05.txt	00:48:34.9	−73:17:53.6	4710.6959	38	21.49	385−880		5
be06a.txt	00:48:43.0	−73:03:10.9	4301.7818	420	70.35	530−815		6
be06b.txt	”	”	4301.7818	420	24.52	375−528		”
be07.txt	00:49:29.8	−72:56:01.2	3339.6529	200	19.64	380−704	OGLE004929.80−725550.0/208.15910.39	7
be08.txt	00:49:38.0	−73:06:10.0	4710.6166	30	17.79	385−880		8
be09.txt	00:49:55.7	−73:07:35.0	4709.8495	34	14.71	385−880		9
be10a.txt	00:50:14.8	−73:05:55.8	4301.7016	360	69.13	530−815	OGLE005014.80−730555.8	10
be10b.txt	”	”	4301.7016	360	38.67	375−528	”	”
be11a.txt	00:52:06.5	−73:18:18.9	4301.7380	360	109.27	530−815	OGLE005206.37−731818.7	11
be11b.txt	”	”	4301.7380	360	37.81	375−528	”	”
be11c.txt	”	”	4734.7926	120	25.66	385−880	”	”
be12.txt	00:52:13.0	−72:31:46.4	4708.8664	30	22.63	385−880		12
be13.txt	00:52:31.0	−73:13:38.7	4710.6674	34	17.42	385−880		13
be14a.txt	00:52:52.6	−73:18:33.7	4301.7129	360	76.85	530−815	OGLE005252.49−731833.5	14
be14b.txt	”	”	4301.7129	360	173.38	375−528	”	”
be15a.txt	00:54:21.2	−73:16:31.5	4301.7610	420	100.60	530−815	OGLE005421.16−731631.5	15
be15b.txt	”	”	4301.7610	420	27.73	530−815	”	”
be15c.txt	”	”	4734.8167	180	34.57	375−528	”	”
be16a.txt	00:54:41.2	−72:27:54.4	4301.7512	420	46.50	530−815	OGLE005441.15−722754.5	16
be16b.txt	”	”	4301.7512	420	98.19	375−528	”	”
be16c.txt	”	”	4734.8341	240	3.12	385−880	”	”
be17.txt	00:54:42.0	−73:45:50.3	4734.8642	240	31.05	385−880		17
be18a.txt	00:56:40.0	−72:45:23.7	4301.6853	300	120.50	530−815	OGLE005639.94−724523.9	18
be18b.txt	”	”	4301.6853	300	133.91	375−528	”	”
be18c.txt	”	”	4709.8898	30	32.09	385−880	”	”
be19.txt	00:57:24.5	−71:44:52.2	4708.9020	36	43.55	385−880		19
be20.txt	00:58:45.2	−72:36:51.8	4709.7735	200	7.91	385−880		20
be21.txt	00:58:58.3	−72:28:53.1	4710.6398	30	8.78	385−880		21
be22.txt	01:05:42.7	−72:27:46.7	4709.8071	34	30.85	385−880		22
be23.txt	01:15:45.9	−73:20:39.8	4734.8037	180	32.70	385−880		23
be24.txt	01:17:09.0	−73:17:09.0	4710.7226	50	34.40	385−880		24
be25.txt	05:04:52.3	−69:54:43.6	4803.7147	600	35.22	385−880		25
be26.txt	05:15:27.2	−68:54:03.3	4836.7415	550	74.75	385−880		26
be27.txt	05:22:02.7	−69:46:14.6	4803.6572	450	49.92	405−880	OGLE052202.89−694614.6	27
be28.txt	05:25:35.8	−69:47:26.4	4795.7735	600	85.76	385−880	OGLE052536.74−694726.4	28
be29.txt	05:27:21.4	−69:22:57.0	4834.7113	300	62.77	385−880	OGLE052721.71−692257.1	29
be30.txt	05:28:45.0	−69:21:18.0	4795.7515	600	105.25	385−880	OGLE052845.28−692117.9	30
be31.txt	05:35:43.6	−69:09:30.9	4835.6047	400	38.29	385−880		31

a) HJD of the middle of the exposition
b) S/N was measured redward of Hα (or Hβ for data in the blue)
c) OGLE/MACHO name
1) Blue continuum + Hα and Hβ in emission (FeII 523.5 and HeI 587.6 nm in emission?)
2) Flat continuum + Hα in emission; CaII triplet (849.8, 854.2 and 866.2 nm) in absorption → Be or Ge?
3) Flat continuum + Hα and Hβ in emission (HeI 587.6 nm in emission?); CaII triplet in absorption (HeI 501.6 nm in absorption?, G Band in 430.0 nm?) → Be or Ge?
4) Blue continuum + Hα, Hβ and Hγ in emission
5) Blue continuum + Hα and Hβ in emission (HeI 587.6 nm and HeI 706.5 nm in emission?)
6) Blue continuum(?) + Hα and Hβ in emission (HeI 587.6 nm in emission?) → Be?
7) Blue continuum + Hα in emission; the other Balmer lines are in absorption
8) Blue continuum + Hα in emission; Hδ and Hϵ in absorption
9) Blue continuum + Hα in emission (Hβ and HeI 587.6 nm in emission?); Hγ and Hδ in absorption
10) Blue continuum(?) + Hα in emission; the other Balmer lines are in absorption → Be?
11) Flat continuum + Hα and Hβ in emission → Be or Ge?
12) Blue continuum + Hα in emission; the other Balmer lines are in absorption
13) Blue continuum + Hα, Hβ, HeI 587.6, HeI 667.8 and HeI 706.5 nm in emission
14) Blue continuum(?) + Hα and Hβ in emission → Be?
15) Weak blue continuum + Hα and Hβ in emission (Hβ with P Cygni profile in JD 2454301.5)
16) Blue continuum + Hα and Hβ in emission (Hβ with emission core in JD 2454301.5); the other Balmer lines and HeI in 402.6 and 447.1 nm are in absorption
17) Blue continuum + Hα and Hβ in emission (Hβ with P Cygni profile?); Hδ and Hγ in absorption (with emission core?)
18) Blue continuum + Hα, Hβ, HeI 587.6, HeI 667.8 and HeI 706.5 nm in emission (Hβ with P Cygni profile in JD 2454301.5); the other Balmer lines are in absorption; emission in ∼393.8 nm (CIII/FeII or artifact?), ∼464.5 nm (CIII/NIII or arfifact?) and ∼674.5 nm (CIII or artifact?)
19) Blue continuum + Hα in emission; the other Balmer lines and CaII triplet are in absorption
20) Blue continuum + Hα and Hβ in emission
21) Blue continuum + Hα, Hβ, HeI 587.6, HeI 667.8(?) and HeI 706.5 nm in emission
22) Blue continuum + Hα, Hβ, HeI 587.6, HeI 667.8 and HeI 706.5 nm in emission; Hϵ, Hδ and Hγ in absorption
23) Blue continuum + Hα, Hβ, Hγ, FeII (417.3, 417.8, 435.2, 516.9, 531.7 and 553.5 nm), CaII triplet and OI 844.6 nm in emission
24) Blue continuum + Hα in emission; the other Balmer lines are in absorption (emission core in Hγ?); CaII triplet in absorption
25) Blue continuum + Hα and Hβ in emission (OI 844.6 nm in emission?); the other Balmer lines are in absorption (CaII triplet in absorption?)
26) Blue continuum + Hα, Hβ (with emission core) and FeII (516.9, 519.8 and 531.7 nm) in emission (CaII triplet and some lines of Paschen series in emission?); H8+HeI 388.9, Hϵ, Hγ, HeI(402.6, 414.5, 438.7, 447.1, 492.2 and 501.6 nm) in absorption
27) Blue continuum + Hα and Hβ in emission; Hδ and Hγ in absorption (CaII triplet and some lines of Paschen series in emission?)
28) Blue continuum + Hα in emission (Hβ with emission core?; HeI in 587.6 and 706.5 nm, CaII triplet and some lines of Paschen series in emission?); Hϵ, Hδ, Hγ and HeI 501.6 nm in absorption
29) Blue continuum + Hα, Hβ, Hγ (with emission core), HeI 587.6, HeI 667.8, HeI 706.5, OI 777.2, OI 844.6 nm and some lines of Paschen series in emission
30) Blue continuum + Hα, Hβ, Hγ (with emission core), HeI 587.6 and HeI 706.5 nm in emission (CaII triplet and some lines of Paschen series in emission?); Hϵ, Hδ (emission core?) and HeI 501.6 nm in absorption
31) Blue continuum + Hα and Hβ in emission (OI 844.6 nm in emission?); Hγ in absorption

Table 2: Carbon stars

File name	α_{2000}	δ_{2000}	HJD (2450000+)[a]	Exp. Time (s)	S/N[b]	Sp. coverage (nm)	Other names[c]	Notes
carb01.txt	00:37:22.2	−73:22:25.0	3339.5371	200	7.38	379−704	OGLE003722.15−732222.8/213.15162.5	1
carb02.txt	00:40:14.2	−72:49:59.2	4792.5573	600	4.50	400−886		2
carb03.txt	00:42:15.3	−72:57:29.6	3340.5535	200	8.92	383−704	OGLE004216.08−725731.9/213.15453.10	3
carb04.txt	00:44:56.5	−73:12:25.7	3339.5865	200	7.10	379−704	OGLE004456.46−731224.2/212.15621.153	4
carb05.txt	00:50:58.5	−73:00:03.4	3340.5802	200	17.09	383−704	OGLE005058.90−730006.6/212.16023.42	5
carb06.txt	00:51:06.6	−73:05:09.2	3339.6705	200	9.34	379−704	OGLE005106.53−730502.8/212.16021.35	6
carb07.txt	00:55:17.4	−72:57:37.2	3339.7391	200	2.28	379−704	OGLE005516.51−725733.4/211.16308.19	7
carb08.txt	00:58:35.1	−72:59:31.9	3340.6092	300	21.03	383−704	OGLE005835.16−725935.4/211.16479.2	8
carb09.txt	00:59:29.1	−72:39:24.7	3340.6245	300	8.90	383−704	OGLE005929.08−723926.7/207.16541.11	9
carb10.txt	01:08:47.3	−72:40:16.6	3340.6585	200	1.90	383−704	OGLE010846.90−724019.4/206.17168.79	10
carb11.txt	05:05:16.5	−68:44:44.3	3339.7479	100	5.77	379−704	OGLE050515.90−684446.6/1.4056.1146	11
carb12a.txt	05:06:49.1	−69:51:41.7	4302.9302	300	22.04	530−815		12
carb12b.txt	”	”	4302.9302	300	19.36	375−528		”
carb13.txt	05:11:25.1	−69:47:03.7	4836.6489	500	12.91	400−884		13
carb14.txt	05:11:40.7	−68:48:15.3	3339.7555	100	15.78	379−704	OGLE051139.99−684816.8/79.5023.40	14
carb15a.txt	05:11:59.0	−68:43:01.7	4301.9438	300	18.34	530−815		15
carb15b.txt	”	”	4301.9438	300	11.05	375−528		”
carb16.txt	05:16:10.3	−69:35:19.1	3339.8446	200	8.77	379−704	OGLE051609.74−693517.9/78.5737.19	16
carb17a.txt	05:16:44.7	−69:27:47.3	4302.8806	300	25.77	530−815		17
carb17b.txt	”	”	4302.8806	300	30.92	375−528		”
carb18.txt	05:18:10.5	−69:26:20.7	3340.7342	300	20.21	383−704	OGLE051810.88−692626.5/78.6102.490	18
carb19.txt	05:19:53.9	−69:27:55.8	3340.7680	300	4.40	383−704	OGLE051954.02−692802.8/78.6465.85	19
carb20.txt	05:19:58.3	−69:14:09.4	3340.7808	300	2.58	383−704	OGLE051958.26−691416.7/80.6468.77	20
carb21.txt	05:20:47.3	−69:50:38.8	3340.7982	300	2.68	383−704	OGLE052047.00−605046.2/78.6580.62	21
carb22.txt	05:21:54.6	−70:56:49.0	3340.8095	200	9.28	383−704	OGLE052154.24−705657.0/13.6685.29	22
carb23.txt	05:25:55.8	−69:43:52.9	3339.7669	200	3.18	379−704	OGLE052555.11−6945354.1/77.7429.64	23
carb24.txt	05:28:18.8	−70:05:23.1	4795.7236	600	1.46	400−886	OGLE052818.82−700523.1	24
carb25.txt	05:36:09.3	−70:22:19.6	3339.7761	100	3.67	379−704	OGLE053608.58−702220.5/11.8992.23	25
carb26.txt	05:39:00.6	−69:52:24.5	3339.7876	200	7.56	379−704	OGLE053900.00−695225.1/81.9484.20	26
carb27.txt	05:42:23.7	−70:18:01.6	3340.8424	300	10.52	383−704	OGLE054223.01−701810.3/12.100821.100	27
carb28.txt	05:44:34.5	−70:39:48.2	3339.8070	200	15.05	379−704	OGLE054433.79−703949.1/12.10440.10	28
carb29.txt	05:46:58.9	−70:25:04.9	3339.8168	200	9.44	379−704	OGLE054658.32−702505.6/12.10807.15	29

a) HJD of the middle of the exposition
b) S/N was measured in the continuum between 450 and 540 nm
c) OGLE/MACHO name
1) Swan bands in 438.2, 473.7, 516.5 and 563.6 nm
2) Weak Swan bands in 563.6 and 619.1 nm
3) Swan bands in 473.7, 516.5 and 563.6 nm + weak Hα in emission
4) Swan bands in 438.2, 473.7, 516.5 and 563.6 nm
5) Swan bands in 473.7, 516.5 and 563.6 nm
6) Swan bands in 438.2, 473.7, 516.5 and 563.6 nm
7) Swan bands in 473.7, 516.5 and 563.6 nm (the bumps below 450.0 nm is artifact?)
8) Swan bands in 516.5 and 563.6 nm + presence of a blue continuum below of 465 nm → binary star?
9) Swan bands in 438.2, 473.7, 516.5 and 563.6 nm
10) Swan bands in 516.5 and 563.6 nm + Hα in emission
11) Swan bands in 473.7, 516.5 and 563.6 nm
12) Swan bands in 516.5, 563.6 and 619.1 nm
13) Swan bands in 516.5 and 563.6 nm + Hα in emission
14) Swan bands in 473.7, 516.5 and 563.6 nm + Hα and Hβ in emission
15) Swan bands in 516.5, 563.6 and 619.1 nm
16) Swan bands in 516.5 and 563.6 nm + Hα in emission, weak blue continuum below of 500 nm? → binary star?
17) Swan bands in 473.7, 516.5 and 563.6 nm
18) Swan bands in 516.5 and 563.6 nm + Hα in emission + weak blue continuum with the other Balmer lines in absorption → binary star?
19) Swan bands in 473.7, 516.5 and 563.6 nm + weak Hα in emission
20) Swan bands in 516.5 and 563.6 nm + weak Hα in emission
21) Swan bands in 516.5 and 563.6 nm
22) Swan bands in 473.7, 516.5 and 563.6 nm
23) Swan bands in 473.7, 516.5 and 563.6 nm
24) Swan bands in 516.5 and 563.6 nm
25) Swan bands in 438.2, 473.7, 516.5 and 563.6 nm
26) Swan bands in 516.5 and 563.6 nm
27) Swan bands in 516.5 and 563.6 nm + weak Hα in emission
28) Swan bands in 473.7, 516.5 and 563.6 nm + weak Hα in emission
29) Swan bands in 473.7, 516.5 and 563.6 nm + weak Hα in emission

COMMISSIONS 27 AND 42 OF THE IAU
INFORMATION BULLETIN ON VARIABLE STARS

Number 6089

Konkoly Observatory
Budapest
4 January 2014

HU ISSN 0374 – 0676

V1117 Her: A HERBIG Ae STAR AT HIGH GALACTIC LATITUDE?

KUN, M.; RÁCZ, M.; SZABADOS, L.

Konkoly Observatory, H-1121 Budapest, Konkoly Thege út 15–17, Hungary, e-mail: kun@konkoly.hu

1 Introduction

The variations of the star located at RA(2000) = $16^{\rm h}39^{\rm m}06.42^{\rm s}$, D(2000)=+09°47′55.3″ were discovered by Blazhko (1929), but the nature of the variability has remained unexplored until recently. Thanks to the massive photometric monitoring projects *ROTSE* (Akerlof et al. 2000) and *ASAS* (Pojmanski 2002), and the observers of the *AAVSO* now decade-long V-band light curve is available for this star. The Northern Sky Variability Survey (*NSVS*, Woźniak et al. 2004a), conducted in the course of the Robotic Optical Transient Search Experiment (ROTSE-I), catalogued NSVS 1639065+094755 as a long period variable having an (unfiltered) average magnitude of 13.080, amplitude of 1.938 mag, and period of 114 days (Woźniak et al. 2004b). The *support vector machines* method, applied during the construction of the *NSVS* catalogue, classified the star as a Mira variable, combining its light curve characteristics with colour indices formed from the median *ROTSE* and *2MASS* magnitudes. However, no spectroscopic observation, required for the confirmation of this classification is available in the literature. The name V1117 Her was given in 2008 (Kazarovets et al. 2008). The GCVS (Samus et al. 2007–2012) classification of this star is *IS*, i.e. "rapid irregular variables having no apparent connection with diffuse nebulae and showing light changes of about 0.5–1.0 mag within several hours or days". The long-term light curve of V1117 Her exhibits steep fadings resembling those of the young UX Ori-type stars. This may be a reason that this star has been included in the young stellar object (YSO) monitoring programme of the *AAVSO* since 2006. The data are available upon request at the *AAVSO* Web site.[1] UX Ori-type variables belong to the class of Herbig Ae stars, i.e. intermediate-mass pre-main sequence stars surrounded by circumstellar dust disks and/or envelopes. Their recurrent dimmings most probably originate from the variations of circumstellar extinction due to non-axisymmetric and changeable, orbiting dust structures (e.g. Bibo & Thé 1990, Herbst et al. 1994). The high infrared brightness of V1117 Her at the *2MASS* and *WISE* wavelengths indeed suggests the presence of circumstellar dust. This star, however, lies at a high Galactic latitude (b=+33.80), far from known star forming regions. The interstellar extinction toward its direction, read from the SFD (Schlegel et al. 1998) Galactic dust map, is $A_{\rm V} \sim 0.07$ mag. To test the hypothesis that V1117 Her is a pre-main sequence star, in this paper we examine its brightness and colour variations, optical spectrum, spectral energy distribution and the possible birthplace.

[1] http://www.aavso.org/

2 Data

2.1 Light curves

The V-band light curve, containing the 179 *NSVS* and 151 *ASAS* data points, as well as 303 *AAVSO* CCD and 271 *AAVSO* visual measurements, is shown in Fig. 1. In all, the 633 V-band CCD and 271 visual measurements cover a time span of 5231 days (14.33 years). Since the *NSVS* photometry is tied to the Johnson V magnitude scale (Woźniak et al. 2004a), we plotted the *NSVS* magnitudes together with the V-band data. The average of the 633 CCD measurements is $\langle V \rangle = 13.223$ mag. The peak-to-peak V-band amplitude is 2.775 mag.

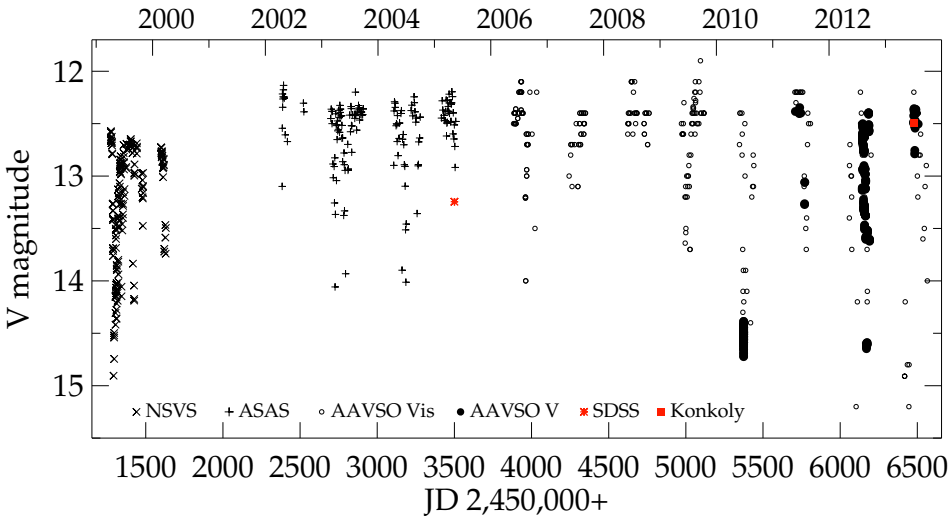

Figure 1. V-band light curve of V1117 Her, based on all of the available data.

The light curve in Figure 1 clearly indicates the presence of cyclic fading events. The visual inspection of the temporal brightness variations implies a cycle length of about 400 days. To determine a more accurate value of the cycle length, a period search was performed, using the program package MUFRAN (Kolláth 1990). This software calculates the Fourier transform of the photometric time series. The visual observations have not been taken into account during the period analysis. The *ASAS*, *NSVS*, and *AAVSO* V-band CCD data were merged into one data file containing also our single-epoch photometric V observation, as well as the single-epoch *SDSS* magnitude transformed to the V band (see Sect. 2.2).

Because the light curve itself is neither strictly repetitive, nor sinusoidal, no high peak is expected in the noisy periodogram. Nevertheless, a clear periodicity appears at 408.247 days in accordance with the value expected from the visual inspection of the light curve in Fig. 1.

The selected frequency peak in the periodogram (which is not the highest one) is physically meaningful because it appears in the power spectra of both *AAVSO* and *ASAS* photometric observational series when studied separately. The uncertainty of the period is estimated to be ± 11.5 days from the width of the selected peak in the periodogram.

The V data folded with the best period value of 408.247 days are plotted in Fig. 2 (left panel). The symbols are the same as in Fig. 1, and the data based on visual observations

(disregarded during the period search) are also plotted here. The phase curve implies an eclipsing-like behaviour. This phase curve is similar to that of UX Ori, the archetype of UXor variables (Fig. 4 in Rostopchina et al. 1999), implying eclipses. The eclipsing-like phase curve in Fig. 2 shows a secondary minimum but this feature is outlined by a few visual data only thus it may not be a real phenomenon. If it exists, it may indicate an asymmetric distribution of the circumstellar matter. The histograms of the V magnitudes for each data series are plotted in the right panel of Fig. 2.

Both the *NSVS* and *ASAS* histograms suggest that the light curve is shaped by short dips, superimposed on a higher flux level. The mean brightness apparently increased between the *NSVS* and *ASAS* surveys, although it cannot be excluded that the differences originate from some inconsistency between the *NSVS* and Johnson V magnitude scale. The histogram of the *AAVSO* data is biased by the great density of measurements near the deep minimum in 2010. Both the amplitude and data distribution support the hypothesis that V1117 Her is a UX Ori type star (cf. Herbst et al. 1994, Xiao et al. 2010).

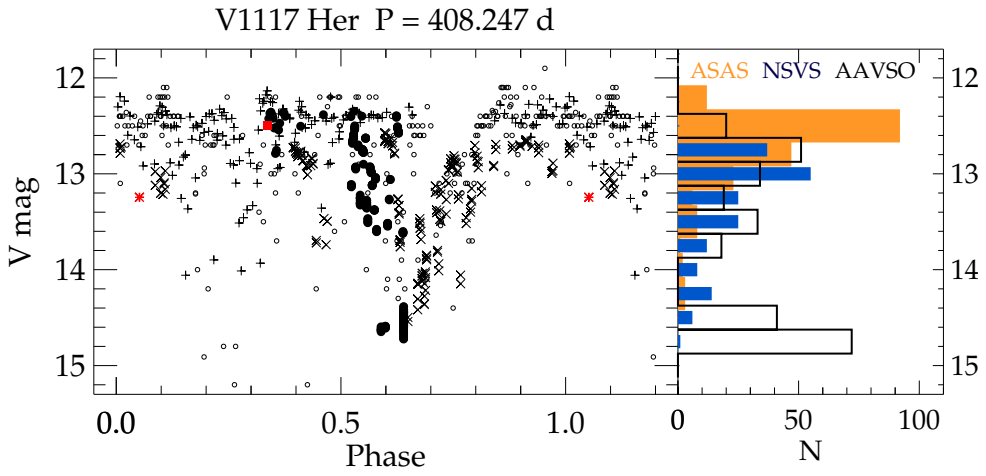

Figure 2. Left: The V data folded on the best period value of 408.247 days. Symbols are same as in Fig. 1. Right: Histograms of the V magnitudes in the *NSVS*, *ASAS*, and *AAVSO* data bases.

2.2 Colour behaviour

The first multiband optical data of V1117 Her can be found in the *SDSS* data base (Ahn et al. 2012), and were obtained on 2005 May 10. We transformed the *griz* magnitudes into the $BVR_{\rm C}I_{\rm C}$ system using the formulae published by Ivezić et al. (2007). The V data point obtained in this manner is also plotted on the light curve (red asterisk).

We observed V1117 Her on 2013 July 1 in the $BVR_{\rm C}I_{\rm C}$ bands using the 1-m RCC telescope of the Konkoly Observatory, equipped with a Princeton Instruments VersArray:1300B camera. After bias subtraction and flat-field correction we performed aperture photometry on each star found in the images. Nineteen of these star had high-quality *SDSS gri* data. We calculated their $BVR_{\rm C}I_{\rm C}$ magnitudes as above, and used these data to establish the transformation between the instrumental and the standard $BVR_{\rm C}I_{\rm C}$ system. The resulting magnitudes of V1117 Her are listed in Table 1, and the V magnitude is plotted in Fig. 1 (red filled square).

Table 1: BVR_CI_C magnitudes of V1117 Her on July 1 2013

JD	$B\,(\Delta B)$	$V\,(\Delta V)$	$R_C\,(\Delta R_C)$	$I_C\,(\Delta I_C)$
2456475.4083	12.792 (0.054)	12.493 (0.015)	12.260 (0.050)	12.032 (0.051)

The *AAVSO* data base contains three B-band measurements. Together with the *SDSS* and our own data we plotted a V vs. $B-V$ colour–magnitude diagram in Fig. 3 (left panel). The slope of the interstellar extinction, assuming $R_V = 3.1$ is also indicated. The few available data points suggest that the star is reddening when fading in accordance with the interstellar extinction law, suggesting that dust structures, moving into the line of sight, may cause the light variations.

The middle panel of Fig. 3 shows the position of V1117 Her in the *2MASS* colour-colour diagram. We plotted for comparison three well-known UXor variables. All of them are found to the right of the reddened main sequence, around the locus of unreddened pre-main sequence stars surrounded by circumstellar disks (Meyer, Calvet & Hillenbrand 1997).

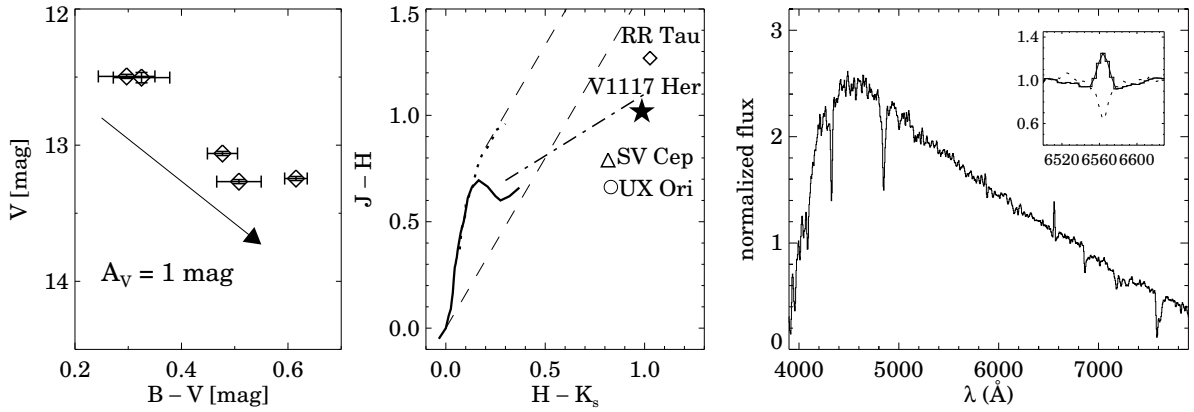

Figure 3. Left: V vs. $B-V$ colour–magnitude diagram of V1117 Her. The arrow indicates the displacement resulting from an interstellar extinction of $A_V = 1$ mag. Middle: Position of V1117 Her and three well-known UX Ori type stars in the *2MASS* $J-H$ vs. $H-K_s$ colour-colour diagram. Solid line indicates the colours of the main sequence stars, and dotted line the giants (Bessell & Brett 1988). Dashed lines border the band of the reddened main sequence and giant stars, and the dash-dotted line is the locus of T Tauri stars (Meyer et al. 1997). Right: Optical spectrum of V1117 Her, obtained with the low-resolution spectrograph installed on the 1-m RCC telescope of the Konkoly Observatory on 2013 July 1. The inset shows the Hα line, together with that of the A9 type star HD 23733 (dotted line).

3 Spectral type of V1117 Her

An optical spectrum of V1117 Her, centred on 5500 Å and covering a 4500 Å-wide region was obtained on 2013 July 1 with the low-resolution spectrograph installed on the 1-m RCC telescope of the Konkoly Observatory. The exposure time was 1800 s. Using the 300 lines/mm grating and 3″ slit width, the spectral resolution was $R = 7.3$ Å. Spectrum

of a halogen incandescent lamp was detected for flatfield correction, and a Hg–Ne lamp was observed for wavelength calibration. Neither telluric correction, nor flux calibration was applied. The spectrum was reduced in IRAF, and is shown in the right panel of Fig. 3. The strong Balmer absorption lines and weak G-band indicate a late A-type star, and the Hα emission suggests that V1117 Her may be a pre-main sequence star. We measured the equivalent widths of the Hβ and Hγ lines using the IRAF *sbands* task, and compared them with those in a number of standard stars both observed with the same instrument setup and found in the spectrum library of Jacoby, Hunter, & Christian (1984). This procedure resulted in a spectral type of A8–A9. The equivalent width of the Hα emission line is EW(Hα)=-5.25 ± 0.5 Å. This emission is superimposed on the photospheric absorption. We measured EW(Hα)=4.87 ± 0.5 Å in the A9-type star HD 23733, thus the total EW of the emission in V1117 Her is about -10.1 ± 0.7 Å. Chromospheric emission in a late A-type star is negligible, therefore the Hα emission probably originates from accretion and wind in V1117 Her.

4 Spectral energy distribution

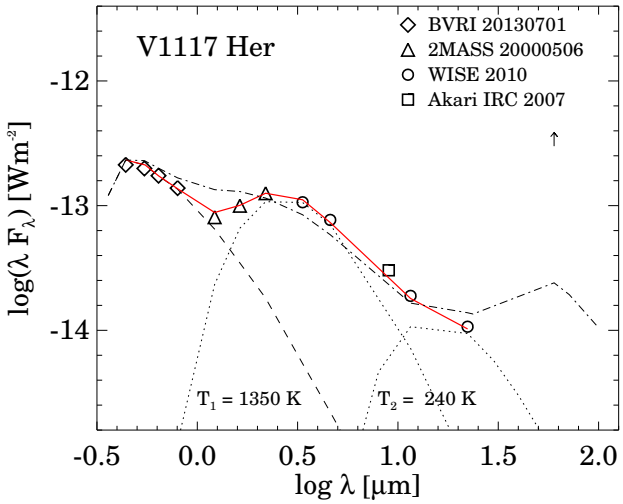

Figure 4. Spectral energy distribution of V1117 Her, based on our $BVR_{\rm C}I_{\rm C}$ data, *2MASS JHK$_s$*, *Akari IRC* 9.0 μm, and *WISE* 3.4, 4.6, 12, and 22 μm data. Dashed line shows the photosphere of an A9 type star behind a foreground extinction of $A_{\rm V} = 0.07$ mag. Dotted lines show the blackbody curves fitted to the IR excess fluxes, and the solid line indicates the sum of the photosphere and the two blackbodies. The dash-dotted line indicates the YSO model No. 3015085 from the model grid of Robitaille et al. (2007), viewed from a distance of 300 pc, at an inclination of 87.13°, and through a foreground interstellar extinction $A_{\rm V} = 0.07$ mag. Upward arrow indicates the *IRAS* lower flux limit at 60 μm.

The spectral energy distribution (SED) of V1117 Her, based on our $BVR_{\rm C}I_{\rm C}$ data, *2MASS JHK$_s$* (Cutri et al. 2003), *Akari IRC* 9.0 μm (Ishihara et al. 2010), and *WISE* 3.4, 4.6, 12, and 22 μm (Wright et al. 2010) data is plotted in Fig. 4. The dashed line indicates the photospheric flux of an A9 type star, fitted to our V-band data, using the colour indices of Pecaut & Mamajek (2013), and assuming a foreground extinction $A_{\rm V} = 0.07$ mag. The *near-infrared bump*, observed in several Herbig Ae stars (e.g. Natta

et al. 2001), is conspicuous in the SED. It can be fitted with a 1350 K blackbody (dotted curve in Fig. 4). This temperature is close to the sublimation temperature of ~ 1500 K of silicate grains, suggesting that a large amount of dust is found near the sublimation radius, located at 0.3–0.5 AU from the star (Dullemond & Monnier 2010). The 9–22 μm fluxes suggest the presence of colder dust, located farther from the star.

5 Discussion

The absolute visual magnitude of an A9 type star ($T_{\rm eff} = 7390$ K, Kenyon & Hartmann 1995) on the zero-age main sequence (ZAMS) is $M_{\rm V} \approx +2.4$ (e.g. Siess et al. 2000). The mass of such a star is about 2 $M_\odot$. The optical colour indices in Table 1 suggest negligible reddening. With the assumptions that V1117 Her is on the ZAMS and its light suffers an extinction of $A_{\rm V} = 0.07$ mag at the maximum brightness of V=12.135, we find that its distance from us is 860 pc. It corresponds to a distance of $z \approx 430$ pc from the Galactic plane, well outside the disk of the interstellar medium. If V1117 Her is above the ZAMS, even larger distances are obtained. A young star so far from the Galactic disk is fairly unlikely. This Galactic position suggests that V1117 Her is either not a young star and its Herbig Ae-like emission spectrum, infrared excess, and UXor-like light curve need another explanation, or it is much closer to us and to the Galactic plane. Dust-enshrouded stars in the Galactic halo are the R Coronae Borealis stars, a few of them exhibiting early type spectra. These stars, however, are hydrogen-deficient, thus the spectrum of V1117 Her excludes this possibility. The disk around an evolved star might have originated from a disrupted close companion like in the case of BP Psc (Zuckerman et al. 2008).

V1117 Her may be closer to the star-forming disk of the Milky Way if its circumstellar disk is viewed edge-on. The UXor phenomenon requires high inclination. It was demonstrated by De Marchi et al. (2013), that a disk inclination larger than $\sim 85^{\rm o}$ would reduce the brightness at optical wavelengths by some 4.5 mag. In this case the star's photosphere is completely occulted by its outer disk, and the whole optical flux is due to scattered light from the outer disk atmosphere, similar in colour to the unreddened star. In this case the observed brightness would indicate a distance of ~ 300 pc and $z \approx 150$ pc for V1117 Her. To explore this possibility further, we examined the SED model grid of Robitaille et al. (2007). We looked for models that fulfil the following constraints, set by the observations. (1) The temperature of the central star is between 7300 and 7600 K; (2) the age of the central star exceeds 10^6 years (an assumption set by the absence of a star-forming environment); (3) the inner edge of the disk is located at the dust sublimation radius. We found that only one model, No. 3013085, viewed at an inclination of $87^{\rm o}$ and from a distance of 300 pc produced an SED close to the observed SED of V1117 Her over the wavelength interval covered by observational data. The model is plotted in Fig. 4 with dash-dotted line. At longer wavelengths the model predicts increasing fluxes, however lower than the threshold of the *IRAS* at 60 μm. The major parameters of the model are shown in Table 2. We conclude that a Herbig Ae star similar in brightness and colour indices to V1117 Her

Table 2: Major parameters of the SED model plotted in Fig. 4.

M_* ($M_\odot$)	$T_{\rm eff}$ (K)	Age (Myr)	$M_{\rm disk}$ ($M_\odot$)	$R_d^{\rm min}$ (AU)	$R_d^{\rm max}$ (AU)	Incl. ($^{\rm o}$)
1.95	7540	7.3	6.86E−3	0.3	8000	87

can be located as close as 300 pc to us. The age of the star, suggested by the modelling, is still higher than the typical lifetime of accretion disks, and at the hypothetical distance of 300 pc the star is farther away from the Galactic plane than typical star forming regions.

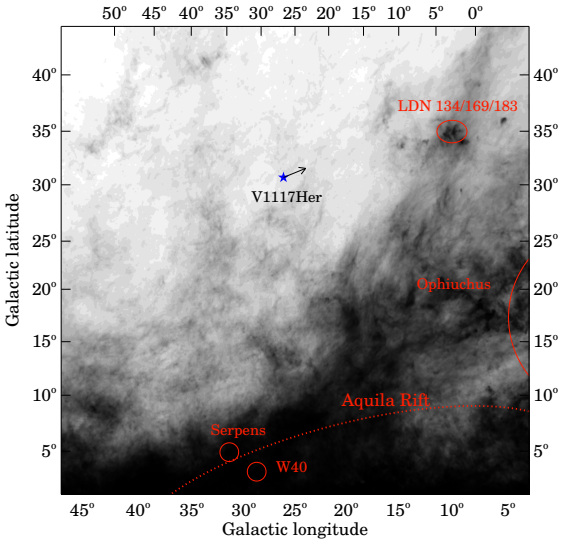

Figure 5. Galactic environment and proper motion of V1117 Her. The distribution of the interstellar extinction in a field of 50 × 50 deg, centred on $l = 25^{\circ}$, $b = +25^{\circ}$ is shown (Schlegel et al. 1998). The star forming regions found in the field are indicated.

Assuming a mass about 2 $M_{\odot}$ for V1117 Her, the 408 day period in its brightness variations is probably caused by obscuring dust clumps orbiting the star at $\sim$ 1.35 AU. The amplitude and duration of the dimming, estimated from the shape of folded light curve in Fig. 2, allow us to estimate the mass of the clump. To this end we assume that V1117 Her has a primordial disk, with interstellar dust to gas ratio. The amplitude of 2.4 mag then corresponds to $\Sigma \sim 0.007\,\mathrm{g\,cm^{-2}}$ gas+dust column density (Güver & Özel 2009). The duration of the dip is about 25 days, which implies a clump size of 0.5 AU at 1.35 AU from the star. The mass of such a clump is some $6 \times 10^{-9}\,M_{\odot}$. Since the period persisted during several years, the clump must be dynamically fairly stable, possibly a proto-planetesimal, similar to the structure found by Chen et al. (2012) in the circumstellar environment of GM Cep. Fig. 1 suggests that the dips are deeper in the latest years than earlier, suggesting the growth of the clump.

Figure 5 shows the distribution of the interstellar dust (Schlegel et al. 1998) in the wide-field Galactic environment of V1117 Her. The arrow indicates the displacement of the star during 1 million years, according to the proper motion given in the *NOMAD* Catalogue. At lower latitudes the Serpens, W40, and Aquila Rift star forming regions are located at 250–400 pc. V1117 Her might have escaped from a lower latitude nearby star forming region. A mean velocity of $20\,\mathrm{km\,s^{-1}}$ is sufficient for travelling 150 pc during 7 million years. At a distance of 300 pc, the catalogued proper motions correspond to a tangential velocity of $\sim$14 $\mathrm{km\,s^{-1}}$, compatible with this scenario. Reliable measurements of parallax, proper motion, and radial velocity, expected from Gaia, will certainly solve the contradictions in the observed properties of this star.

Acknowledgements This work was supported by the Hungarian OTKA grant K81966 and the ESTEC Contract No. 4000106398/12/NL/KML. The photometric contribution of

AAVSO observers Teofilo Arranz, Laurent Bichon, Thomas Grzybowski, James McMath, Kenneth Menzies, Gary Poyner, Michael Simonsen is gratefully acknowledged. This research has made use of the VizieR catalogue access tool, CDS, Strasbourg, France. The authors are grateful to the referee for the thorough and very helpful report.

References:

Ahn, C. P. et al. 2012, *ApJS*, **203**, 21
Akerlof, C. et al. 2000, *AJ*, **119**, 1901
Bessell, M. S., & Brett, J. M. 1988, *PASP*, **100**, 1134
Bibo, E. A., & Thé, P. S. 1990, *A&A*, **236**, 155
Blazhko, S. 1929, *Astron. Nachr.*, **236**, 279
Chen, W. P. et al. 2012, *ApJ*, **751**, 118
Cutri, R. M., et al. 2003, VizieR On-line Data Catalog: II/246
De Marchi, G., Panagia, N., Guarcello, M. G., & Bonito, R. 2013, *MNRAS*, **435**, 3058
Dullemond, C. P. & Monnier, J. D. 2010, *ARA&A*, **48**, 205
Güver, T., & Özel, F. 2009, *MNRAS*, **400**, 2050
Herbst, W., Herbst, D. K., Grossman, E. J., & Weinstein, D. 1994, *AJ*, **108**, 1906
Ishihara, D. et al. 2010, *A&A*, **514**, A1
Ivezić, Ž. et al. 2007, *ASPC*, **364**, 1651
Jacoby, G. H., Hunter, D. H., & Christian, C. A. 1984, *ApJS*, **56**, 257
Kazarovets, E. V., Samus, N. N., Durlevich, O. V., Kireeva, N. N., Pastukhova, E. N. 2008, *IBVS*, **5863**, 1
Kenyon, S. J., & Hartmann, L. 1995, *ApJS*, **101**, 117
Kolláth, Z. 1990, The Program Package MUFRAN, Occasional Technical Notes of the Konkoly Observatory, Budapest, No. 1;
`http://www.konkoly.hu/Mitteilungen/muf.tex`
Meyer, M. R., Calvet, N., & Hillenbrand, L. A. 1997, *AJ*, **114**, 288
Natta, A., Prusti, T., Neri, R., Wooden, D., Grinin, V. P. & Mannings, V. 2001, *A&A*, **371**, 186
Pecaut, M. J., & Mamajek, E. E. 2013, *ApJS*, **208**, 9
Pojmanski, G. 2002, *Acta Astronomica*, **52**, 397
Robitaille, T. P., Whitney, B. A., Indebetouw, R., & Wood, K. 2007, *ApJS*, **169**, 328
Rostopchina, A.N., Grinin, V.P., & Shakhovskoi, D.N. 1999, *Astr. Lett.*, **25**, 243
Samus, N. et al. 2007-2012, *General Catalogue of Variable Stars*, VizieR On-line Data Catalog: B/gcvs
Schlegel, D. J., Finkbeiner, D. P., & Davis, M. 1998, *ApJ*, **500**, 525
Siess, L., Dufour, E., Forestini, M. 2000, *A&A*, **358**, 593
Woźniak, P. R. et al. 2004a, *AJ*, **127**, 2436
Woźniak, P. R., Williams, S. J., Vestrand, W. T., Gupta, V. 2004b, *AJ*, **128**, 2965
Wright, E. L. et al. 2010, *AJ*, **140**, 1868
Xiao, L., Kroll, P., & Henden, A. A. 2010, *AJ*, **139**, 1527
Zuckerman, B. et al. 2008, *ApJ*, **683**, 1085

COMMISSIONS 27 AND 42 OF THE IAU
INFORMATION BULLETIN ON VARIABLE STARS

Number 6090

Konkoly Observatory
Budapest
13 January 2014

HU ISSN 0374 – 0676

SUPERWASP DATA RELEASE 1 PUBLIC AGAIN

PAUNZEN, E.[1]; KUBA, M.[2,3]; WEST, R. G.[4]; ZEJDA, M.[1]

[1] Institute of Theoretical Physics and Astrophysics, Masaryk University, Kotlářská 2, CZ - 611 37 Brno, Czech Republic. e-mail: epaunzen@physics.muni.cz

[2] Institute of Computer Science, Masaryk University, Šumavská 15, Brno, Czech Republic

[3] The national Center CERIT-SC (CERIT Scientific Cloud), Czech Republic

[4] Department of Physics, University of Warwick, Coventry, CV4 7AL, UK

The WASP (Wide Angle Search for Planets) project is an exoplanet transit survey established by a consortium of eight academic institutions which include Cambridge University, the Instituto de Astrofisica de Canarias, the Isaac Newton Group of telescopes, Keele University, Leicester University, the Open University, Queen's University Belfast and St. Andrew's University. Continual monitoring of the night sky, started with two instruments (at La Palma, Canary Islands and Sutherland, South Africa) in 2004 and resulted in photometric data and light curves of millions of unique objects (for more details see Butters et al., 2010). The first public data release (DR1) of the WASP archive makes available all these light curve data from 2004 up to 2008 in both the Northern and Southern hemispheres.

We are pleased to announce that the DR1 is publicly available again. The archive was copied to a new server at Masaryk University Brno, Czech Republic and using a new web interface, developed by the CERIT team, users can search for the data of selected objects (see `http://wasp.cerit-sc.cz/`). The data set contains 17 960 328 light curves, built from more than 110 billion data points available. The web interface will be supplemented by tools for data processing, time series analysis and imaging of light curves. Any recommendation and notes are welcome to support@cerit-sc.cz. We hope that the server will well serve to all scientific community.

Acknowledgement: The computing and storage facilities are provided by the project CERIT Scientific Cloud, reg. no. CZ.1.05/3.2.00/08.0144.

Reference:

Butters, O. W., West, R. G., Anderson, D. R., et al. 2010, *A&A*, **520**, L10

COMMISSIONS 27 AND 42 OF THE IAU
INFORMATION BULLETIN ON VARIABLE STARS

Number 6091

Konkoly Observatory
Budapest
15 January 2014

HU ISSN 0374 – 0676

CCD MAXIMA OF PULSATING STARS AND TIMES OF MINIMA OF AN ECLIPSING BINARY

MARTIGNONI, MASSIMILIANO

Stazione Astronomica Betelgeuse (SAB), Via Don Minzoni 26, I-20020 Magnago (Milano), Italy, e-mail: massimiliano.martignoni@alice.it

Observatory and telescope:
0.25 m Schmidt-Cassegrain Telescope (f/10)

Detector:	512×512 pixels Kodak KAF261E CCD cooled to (typ.) −20°C; 1.″6 per pixel (1×1 binning); 14′×14′ field of view; equipped with $BVR_{\rm C}I_{\rm C}$ photometric filters.

Method of data reduction:
Differential photometry on each CCD image using AIP4Win software. No reduction to standard photometric system was performed.

Method of minimum determination:
The times of maxima were calculated using parabolic fit; the minima times were calculated using Kwee & van Woerden's (1956) method.

Times of maxima of pulsating stars:

Star name	Time of max. HJD 2400000+	Error	Filter
ASAS J083947+1417.4	54565.3943	0.0011	$VR_{\rm C}I_{\rm C}$
	55975.4599	0.0001	$BVR_{\rm C}I_{\rm C}$
	55980.4260	0.0008	$BVR_{\rm C}I_{\rm C}$
ASAS J142511+1211.1	56064.4739	0.0007	$VR_{\rm C}$
	56076.4518	0.0017	$VR_{\rm C}$
ASAS J150509+1817.4	56077.5490	0.0022	$VR_{\rm C}$

Times of maxima of pulsating stars:			
Star name	Time of max. HJD 2400000+	Error	Filter
SW And	56609.3580	0.0025	V
XX And	56603.4739	0.0021	V
	56632.3854	0.0021	V
AT And	56629.3135	0.0030	V
DM And	56631.3006	0.0039	V
DR And	56603.3575	0.0026	V
OV And	56608.2966	0.0029	V
V569 And	56638.4332	0.0031	V
V1821 Aql	54684.4738	0.0010	$BVR_{\rm C}I_{\rm C}$
	54686.4465	0.0040	$BVR_{\rm C}I_{\rm C}$
	54687.4392	0.0006	$BVR_{\rm C}I_{\rm C}$
SY Ari	56268.3725	0.0001	V
CD Ari	56273.4585	0.0036	V
TZ Aur	55931.4204	0.0008	V
	55936.5107	0.0002	V
	56340.3295	0.0013	V
BH Aur	56609.4784	0.0013	V
	56630.4594	0.0018	V
NU Aur	56297.3497	0.0027	V
V377 Aur	56342.3150	0.0034	V
V575 Aur	56632.4821	0.0019	V
	56268.4964	0.0029	V
TY Cam	56322.3997	0.0034	V
AH Cam	56315.3553	0.0040	V
	56339.3554	0.0032	V
V354 Cam	56608.4646	0.0046	V
RW Cnc	56629.6847	0.0016	V
TT Cnc	56640.6061	0.0034	V
AS Cnc	56339.4557	0.0037	V
BN CVn	56339.5648	0.0036	V
HU Cas	56272.3328	0.0001	V
V363 Cas	56608.3850	0.0025	V
FP Cep	56185.3506	0.0001	V
KM Cep	56185.4240	0.0001	V
RR Cet	56630.3604	0.0022	V
U Com	56640.7223	0.0053	V
CK Del	56541.3424	0.0016	V
SU Dra	56332.5370	0.0042	V
XZ Dra	56479.5226	0.0028	V
AK Gem	56332.3224	0.0013	V
V397 Gem	56331.3838	0.0023	V
	56640.4367	0.0041	V
TW Her	56127.4122	0.0013	V
V392 Her	56483.4244	0.0021	V
RX Leo	56373.4319	0.0036	V
X LMi	56342.4560	0.0026	V
Y LMi	55985.4396	0.0021	V
	56340.4897	0.0010	V

Times of maxima of pulsating stars:			
Star name	Time of max. HJD 2400000+	Error	Filter
TV Lyn	55932.4471	0.0004	V
	55933.4141	0.0013	$VI_{\rm C}$
	55933.6554	0.0058	$VI_{\rm C}$
	55934.6106	0.0001	$VI_{\rm C}$
TW Lyn	56629.5619	0.0011	V
EZ Lyr	56485.4733	0.0016	V
FN Lyr	56478.5050	0.0041	V
V408 Oph	56483.5028	0.0021	V
V452 Oph	56485.4124	0.0020	V
V455 Oph	56479.4355	0.0032	V
V816 Oph	56479.3996	0.0018	V
CM Ori	56630.5311	0.0018	V
V1640 Ori	56640.5269	0.0038	V
VV Peg	56126.4835	0.0036	V
	56148.4633	0.0032	V
TU Per	56629.4621	0.0014	V
	56640.3911	0.0022	V
AR Per	56631.3488	0.0016	V
ET Per	56609.4156	0.0010	V
V375 Per	56300.3308	0.0021	V
SS Psc	56315.2938	0.0045	V
BR Tau	55937.3743	0.0005	V
	56272.5061	0.0001	V
	56631.4637	0.0017	V
	56638.4940	0.0015	V
U Tri	56266.4567	0.0001	V
MU UMa	56340.5875	0.0060	V
FK Vul	56184.4386	0.0007	V

Times of minima:					
Star name	Time of min. HJD 2400000+	Error	Type	Filter	Rem.
GN Boo	56057.4903	0.0020	Min.I	$VR_{\rm C}$	
	56058.3956	0.0015	Min.I	$VR_{\rm C}$	
	56062.4670	0.0018	Min.II	$VR_{\rm C}$	
	56066.3881	0.0020	Min.II	$VR_{\rm C}$	
	56066.5390	0.0022	Min.I	$VR_{\rm C}$	

Reference:

Kwee, K.K., van Woerden, H., 1956, *B.A.N.*, **12**, 327

*This version of the paper contains corrections, and differs from the one appeared on-line originally. Date of last modification: Wed Jan 22 09:28:12 CET 2014

COMMISSIONS 27 AND 42 OF THE IAU
INFORMATION BULLETIN ON VARIABLE STARS

Number 6092

Konkoly Observatory
Budapest
30 January 2014

HU ISSN 0374 – 0676

CCD MINIMA FOR SELECTED ECLIPSING BINARIES IN 2013

NELSON, ROBERT H.

1393 Garvin Street, Prince George, BC, Canada, V2M 3Z1, email: bob.nelson@shaw.ca

Observatory and Telescope: Sylvester Robotic Observatory (SyRO): 33 cm $f/4.5$ Newtonian on a Paramount ME.

Detector (CCD): SyRO: SBIG ST-10XME, 6.8″ pixels, 34.4′×23.2′ FOV, cooled to $-10 < \mathrm{T} < -30$°C.

Method of data reduction: Bias and dark subtraction, flat-fielding using light-box flats; aperture photometry – all using MIRA, by Mirametrics. Check stars were used throughout.

Method of minimum determination: Digital tracing paper method, bisection of chords, curve fitting, and (occasionally) Kwee and van Woerden (1956).

Table 1. Table of the times of minima.

Star name	Time of Minimum	Error	Type	Filter	O−C
V0523 And	56527.8946	0.0002	I	c	−0.0004
V0531 And	56593.7849	0.0003	I	c	0.0000
V0546 And	56594.695	0.0002	I	c	−0.0002
G2837-1343 And	56633.643	0.0003	II	c	−0.0002
G0471-0860 Aql	56422.9164	0.0001	II	c	0.0000
BO Ari	56514.9358	0.0002	I	VRI	0.0000
BO Ari	56526.8681	0.0003	I	VRI	0.0001
BO Ari	56535.9364	0.0001	I	VRI	−0.0001
BO Ari	56560.9145	0.0002	II	VRI	−0.0001
BO Ari	56579.6885	0.0001	II	VRI	0.0005
BO Ari	56579.8475	0.0001	I	VRI	0.0004
G1210-0442 Ari	56593.7849	0.0002	II	c	0.0000
V0364 Aur	56650.716	0.0002	I	c	−0.0001
V0410 Aur	56632.7425	0.0005	II	R	0.0028
V0569 Aur	56299.6838	0.0002	II	c	0.0000
XY Boo	56397.7891	0.0001	I	R	−0.0024

Star name	Time of Minimum	Error	Type	Filter	O−C
FI Boo	56303.022	0.0002	II	R	0.0026
GN Boo	56398.7575	0.0003	II	VRI	0.0012
GO Boo	56375.9018	0.0008	I	c	−0.0002
GR Boo	56356.912	0.0001	II	R	0.0006
PU Boo	56391.8136	0.0003	I	R	0.0021
V0339 Boo	56397.8729	0.0003	I	R	0.0000
AO Cam	56600.7874	0.0001	I	R	0.0011
FN Cam	56304.7418	0.0002	II	R	−0.0001
QU Cam	56629.622	0.0002	I	c	0.0002
V0337 Cam	56303.6375	0.0002	II	R	−0.0013
V0383 Cam	56629.744	0.0002	II	c	0.0008
V0474 Cam	56594.8821	0.0002	II	R	−0.0019
V0516 Cam	56294.843	0.002	I	c	0.0000
TW Cas	56550.867	0.005	II	VRI	0.0012
BS Cas	56525.9343	0.0001	II	c	0.0008
V1175 Cas	56594.7838	0.0002	I	V	−0.0025
V0699 Cep	56552.7083	0.0005	I	c	0.0001
V0736 Cep	56435.912	0.001	I	R	0.0021
V0737 Cep	56421.945	0.0002	II	c	−0.0005
G4475-0618 Cep	56429.9278	0.0002	I	c	0.0000
V0870 Cep	56488.846	0.0003	I	R	0.0007
AK CMi	56356.6684	0.0002	I	R	0.0002
DS Cmi	56349.78	0.001	II	c	0.000
GW Cnc	56359.7073	0.0004	I	c	0.0012
IL Cnc	56355.6678	0.0002	II	c	0.0012
IN Cnc	56374.6944	0.0005	II	c	0.0008
LR Com	56363.806	0.001	I	c	0.0005
TW CrB	56379.9098	0.0003	II	VRI	0.0013
AS CrB	56390.7656	0.0003	I	c	0.0038
AV CrB	56340.9119	0.0001	II	c	−0.0009
CX CVn	56370.8499	0.0002	I	R	−0.0002
DL CVn	56293.9353	0.0005	I	c	0.0008
G2530-1069 CVn	56360.8018	0.0002	I	V	0.0000
ZZ Cyg	56449.9125	0.0001	I	c	−0.0006
V0859 Cyg	56420.9437	0.0002	I	c	0.0007
V2278 Cyg	56417.9421	0.0003	II	c	0.0346
G2711-0645 Cyg	56493.8208	0.0004	II	c	0.0000
G2750-0054 Cyg	56506.913	0.001	I	R	−0.0001
G2750-0054 Cyg	56507.8561	0.001	I	c	−0.0008
G2750-0054 Cyg	56524.8448	0.0003	I	c	0.0000
G2750-0054 Cyg	56530.742	0.001	II	c	−0.0014
G2750-1476 Cyg	56507.833	0.002	I	c	0.003
G2750-1476 Cyg	56517.8543	0.0004	II	c	0.0042
G2750-1476 Cyg	56524.742	0.002	II	c	0.0125
G2750-1476 Cyg	56524.8791	0.0003	I	c	0.0000
G3581-1856 Cyg	56397.9885	0.0002	II	c	−0.0004
Z Dra	56601.0307	0.0006	II	VRI	0.0042
Z Dra	56632.9278	0.0001	I	R	0.0012
FX Dra	56421.7308	0.0002	I	VRI	0.0009

Star name	Time of Minimum	Error	Type	Filter	O−C
GQ Dra	56415.786	0.001	II	R	0.0006
G4424-1787 Dra	56356.0209	0.0001	I	c	0.0000
G4453-0432 Dra	56357.0639	0.0004	II	c	0.0000
G4436-1300 Dra	56358.8956	0.0002	I	R	0.0000
G4421-0400 Dra	56360.9707	0.0002	II	c	0.0000
G4552-1643 Dra	56362.7542	0.0002	I	c	0.0000
G4421-1217 Dra	56381.9344	0.0002	I	c	0.0005
G3897-1017 Dra	56417.7955	0.0003	I	c	0.0000
G4449-1278 Dra	56423.828	0.001	I	c	0.000
G4453-0432 Dra	56423.9161	0.0008	I	c	0.0000
G4448-1301 Dra	56438.8193	0.0002	II	c	0.0000
V0414 Gem	56293.7535	0.002	I	R	0.0027
V0829 Her	56374.8648	0.0002	II	R	0.0021
V0878 Her	56398.975	0.002	II	VRI	−0.0006
V0878 Her	56418.8298	0.0002	I	VRI	−0.0011
V0878 Her	56422.8038	0.0006	II	VRI	0.0019
V1092 Her	56378.9251	0.0002	I	c	−0.0006
V1101 Her	56413.9105	0.0001	I	c	−0.0006
V1098 Her	56415.9034	0.0001	II	c	0.0002
G0380-0247 Her	56435.8154	0.0006	II	R	−0.0057
AP Leo	56356.8352	0.0001	II	R	0.0016
G1965-0735 Leo	56302.8903	0.0002	I	V	−0.001
AG LMi	56369.7272	0.0002	I	c	0.0002
BG Lyn	56633.8954	0.0002	I	R	0.0008
V0448 Mon	56299.7712	0.0003	II	c	−0.0014
G0159-1018 Mon	56629.86115	0.0002	I	R	0.0000
G0410-2795 Oph	56358.9894	0.0001	I	c	0.0000
AT Peg	56509.8669	0.0007	I	BVRI	−0.0051
G2750-0854 Peg	56506.8331	0.0002	II	R	−0.0009
V0881 Per	56297.5893	0.0002	I	R	−0.002
CP Psc	56582.7085	0.0002	I	R	0.0000
EY Psc	56569.7125	0.0002	I	R	0.0000
HL Psc	56597.7048	0.0005	II	R	−0.0063
HN Psc	56632.62049	0.0002	II	R	0.0000
AI Sex	56375.7234	0.0003	I	R	0.0025
EQ Tau	56613.7242	0.0004	I	R	−0.0016
V1238 Tau	56305.8152	0.0005	I	R	0.0000
V1370 Tau	56593.9037	0.0002	I	c	−0.0002
CL Tri	56600.6447	0.0003	I	c	0.0002
XY UMa	56357.6878	0.0004	II	V	−0.0002
BS UMa	56359.8145	0.0002	I	c	0.001
FT UMa	56303.8347	0.0002	II	R	0.0000
HH UMa	56304.8716	0.0005	II	R	0.0006
HN UMa	56634.0231	0.0003	I	R	0.0084
G3011-1150 UMa	56355.8504	0.0002	I	c	0.0003
TV UMi	56362.891	0.0002	I	V	−0.0022
V0355 Vir	56357.907	0.02	I	c	0.005
DZ Vul	56554.6807	0.0003	I	c	−0.0004
V0467 Vul	56492.7984	0.0003	II	R	−0.0005

Remarks: Star name G denotes GSC.

Note: O−C values were computed using elements computed from the O−C database mentioned in the references (Nelson, 2013).

Acknowledgements: Thanks are due to Environment Canada for the website satellite views (see reference below) that were essential in predicting clear times for observing runs in this cloudy locale. Thanks are also due to Attilla Danko for his 'Clear Sky Charts', (see below). This research has made use of the SIMBAD database, operated at CDS, Strasbourg, France.

References:

Danko, A., Clear Sky Charts, http://cleardarksky.com/
Kwee, K. K., & van Woerden, H., 1956, *BAN*, **12**, 327
Nelson, R. H., 2013, Bob Nelson's O−C Files, http://www.aavso.org/bob-nelsons-o-c-files
Satellite Images for North America, http://weather.gc.ca/satellite/index_e.html

COMMISSIONS 27 AND 42 OF THE IAU
INFORMATION BULLETIN ON VARIABLE STARS

Number 6093

Konkoly Observatory
Budapest
31 January 2014

HU ISSN 0374 – 0676

TIMINGS OF MINIMA OF ECLIPSING BINARIES

DIETHELM, ROGER

Bahnhofstrasse 3, CH–4118 Rodersdorf, Switzerland

The following Table is my last list of timings of minima of eclipsing binaries secured by CCD photometry, obtained in the second half of 2013. To obtain these data, several telescopes operated by iTelescope.com in Spain, New Mexico (USA) and Australia were used. The given $O - C$ values generally refer to the linear elements of the newest electonic version of the GCVS (Samus et al., 2013), except for the cases stated in the remarks, where the determination of current elements made use of the up-to-date ASAS data (`http://www.astrouw.edu.pl/asas/`) and the Lafler-Kinman algorithm of the PERANSO software (`http://www.peranso.com/`). All times given are heliocentric UTC.

Table 1: Minima of eclipsing binaries

Variable	Type	HJD 24...	−	n	Remarks	
GSC 5248-1194 Aqr	p	56571.915(5)	−0 005	34	V; el: 54452.583 + 0.7896189	E
GSC 5821-87 Aqr	p	56575.9369(4)	+0 0009	34	V; el: IBVS 6011	
GSC 5822-1040 Aqr	p	56529.2181(2)	+0 0010	60	V; el: 54753.615 + 0.889580	E
GSC 5830-845 Aqr	p	56560.1184(2)	−0 0139	55	V; el: 54331.761 + 0.439868	E
GSC 6385-1045 Aqr	p	56530.1367(2)	+0 0014	59	V; el: 53166.916 + 0.548293	E
V871 Aql	p	56480.1838(2)	−0 1535	46	V; eccentric	
V889 Aql	p	56491.5058(3)	+0 0045	54	V; el: Krakow Catalog; eccentric	
GSC 497-590 Aql	p	56486.1895(2)	+0 0062	54	V; el: 54362.628 + 0.675861	E
OQ Cam	p	56585.8951(29)	−0 0349	42	V; el: IBVS 6011	
MM Cas	p	56602.7479(1)	+0 1054	60	V	
NU Cas	p	56582.6582(3)	−0 0015	60	V; el: Krakow Catalog	
NZ Cas	p	56587.824(9)	+0 007	55	V; el: Krakow Catalog	
OX Cas	s	56540.5429(20)	+0 0346	61	V; eccentric	
PV Cas	s	56477.8908(3)	−0 2426	64	V; eccentric	
V364 Cas	s	56558.8560(13)	−0 0219	30	V	
V381 Cas	p	56582.8282(1)	−0 0171	60	V; eccentric	
V821 Cas	s	56530.5196(5)	−0 2092	64	V; el: IBVS 5386; eccentric	
V1137 Cas	p	56526.7543(5)	−0 0293	49	V; eccentric	
EK Cep	p	56523.5101(2)	+0 0107	19	V; eccentric	
GS Cep	s	56559.8495(3)	+0 0009	53	V; el: IBVS 3596	
NR Cep	s	56569.8168(6)	−0 0596	60	V	
V796 Cep	s	56585.8106(4)	−0 0030	40	V; el: IBVS 6011	
V919 Cep	s	56513.7281(5)	−0 0344	47	V; eccentric	
GSC 4482-673 Cep	s	56557.8640(2)	+0 0053	70	V; el: OEJV 83	
VV Cet	s	56525.3093(2)	−0 0055	52	V; el: 54247.936 + 0.5223945	E
GSC 5278-346 Cet	p	56554.1228(1)	−0 0054	59	V; el: IBVS 6011	
Y Cyg	s	56488.480(3)	+0 127	16	V; eccentric	
MY Cyg	p	56448.872(5)	−0 007	71	V; eccentric	

Table 1: Minima of eclipsing binaries

Variable	Type	HJD 24...	−	n	Remarks
V498 Cyg	s	56494.517(3)	+0 178	35	V; eccentric
V974 Cyg	p	56466.5463(2)	−0 1695	97	V; eccentric
V1136 Cyg	s	56453.5311(6)	+0 3517	98	V; eccentric
V2281 Cyg	p	56490.4378(3)	+0 0082	28	V; el: 51460.801 + 1.07356 E
YY Eri	s	56575.1357(2)	−0 0051	23	V; el: IBVS 5960
Y Gru	p	56563.0309(1)	−0 0066	56	V; el: 54641.885 + 1.7168476 E
RX Gru	p	56546.0967(3)	+0 0064	37	V; el: 53732.563 + 0.7431398 E
FN Her	p	56494.9519(6)	+0 0919	79	V
LV Her	p	56454.4575(1)	+0 0355	134	V; el: IBVS 5201; eccentric
V1059 Her	p	56456.7861(2)	+0 0153	90	V; el: 53477.795 + 0.749051 E
RV Hyi	s	56586.0217(3)	+0 8464	50	V; el: Krakow Catalog; eccentric
CO Lac	p	56524.4899(3)	−0 0012	57	V; el: Krakow Catalog; eccentric
IL Lac	p	56495.5011(5)	+0 0042	48	V; el: IBVS 5621; eccentric
MZ Lac	s	56514.5166(3)	+0 0865	56	V; el: JAAVSO 19, 12; eccentric
OO Lac	p	56519.5008(4)	+0 1586	42	V
V364 Lac	s	56545.5051(28)	+0 1495	60	V; eccentric
RZ Mic	p	56520.0693(2)	−0 0104	80	V; el: 54759.575 + 3.9830423 E
AH Mic	p	56523.0043(4)	−0 0440	77	V; el: 53656.53 +0.387315 E
CY Mic	p	56526.018(5)	−0 010	52	V; el: 52908.598 + 1.6287393 E
GV Nor	s	56465.9450(2)	−0 1786	90	V; el: Krakow Catalog; eccentric
WZ Oph	p	56491.0050(2)	+0 0031	72	V
V509 Oph	p	56470.799(3)	+0 051	60	V
V752 Oph	p	56455.8065(3)	−0 1406	63	V
EQ Per	p	56597.8500(3)	+0 6261	40	V
LS Per	p	56588.7932(9)	+0 0133	54	V; el: Krakow Catalog
V449 Per	p	56600.8248(3)	+0 0559	52	V
FY Psc	p	56604.7329(3)	+0 0001	38	V; el: 51486.775 + 0.3562053 E
GSC 5254-59 Psc	s	56510.2397(2)	−0 0164	36	V; el: IBVS 6011
YY PsA	p	56555.1424(2)	+0 0077	50	V; el: 54437.558 + 1.8624245 E
YY Sgr	s	56477.2091(3)	−0 2484	100	V; eccentric
V5565 Sgr	s	56466.043(3)	−0 469	82	V; el: Krakow Catalog; eccentric
GSC 5720-943 Sgr	s	56475.0578(7)	−0 0206	40	V; el: 54432.762 + 0.401596 E
GSC 5700-639 Sct	s	56477.034(5)	0 009	100	V; el: 54550.871 + 2.403187 E
V351 Tel	p	56501.9718(7)	+0 0350	76	V; el: 53490.874 + 6.4476719 E; eccentric
CU Tuc	p	56589.9292(4)	−0 0034	58	V; el: 53175.927 + 0.8658396 E
ZZ UMi	p	56470.7323(2)	+0 0041	76	V
FQ Vul	p	56482.8309(12)	+0 2862	43	V; eccentric
V495 Vul	p	56469.7300(2)	−0 0004	73	V

References:

Dahm, M., 1994, *B V RB*, **43**, 104
Degirmenci, O.L. et al., 2003, *IBV* , No. 5386
Diethelm, R., 2009a, *IBV* , No. 5871
Diethelm, R., 2009b, *IBV* , No. 5894
Diethelm, R., 2010, *IBV* , No. 5945
Diethelm, R., 2011a, *IBV* , No. 5960
Diethelm, R., 2011b, *IBV* , No. 5992
Diethelm, R., 2012a, *IBV* , No. 6011
Diethelm, R., 2012b, *IBV* , No. 6029
Diethelm, R., 2013, *IBV* , No. 6063
Hanzl, D. et al., 1991, *IBV* , No. 3596
Khruslov, A.V., 2005, *IBV* , No. 5699
Khruslov, A.V., 2010, , **10**, No. 18
Kreiner, J.M., 2004, , **54**, 207; Krakow Catalog
Odell, A.P. et al., 2011, *IBV* , No. 6001
Otero, S.A., 2006, *IBV* , No. 5699
Otero, S.A., 2008, *V*, No. 83
Pribulla, T. et al., 2003, *R* , **33**, 38

Silhan, J., 1990, V , 19, 12
Torres, G. et al., 2001, *IBV* , No. 5201
Zola, S. et al., 2005, *IBV* , No. 5591

COMMISSIONS 27 AND 42 OF THE IAU
INFORMATION BULLETIN ON VARIABLE STARS

Number 6094

Konkoly Observatory
Budapest
17 February 2014

HU ISSN 0374 – 0676

MINIMA OF ECLIPSING BINARY STARS

CORFINI, G.[1]; ACETI, P.[1]; ARENA, C.[1,2,3]; BANFI, M.[1]; BARBIERI, L.[1,4]; BIANCIARDI, G.[1,5]; BONAVENTURA, G.[1,2]; CERVONI, M.[1,6]; FOSSEY, S.[3]; LOPRESTI, C.[1,7]; MARCHINI, A.[1,8]; MARINO, G.[1,2]; MARTINENGO, M.[1]; PAPINI, R.[1]; RUOCCO, N.[1,9]; SALVAGGIO, F.[1,2]; ZAMBELLI, R.[1]

[1] Sezione Stelle Variabili – Unione Astrofili Italiani (UAI), e-mail: `stellevariabili@uai.it`

[2] Gruppo Astrofili Catanesi - Catania, Italy

[3] University of London Observatory, UCL - London, UK

[4] Associazione Astrofili Bolognesi - Bologna, Italy

[5] Telescopio remoto UAI/Skylive/University of Siena - Italy

[6] Associazione Tuscolana di Astronomia - Roma - Italy

[7] Istituto Spezzino Ricerche Astronomiche - La Spezia, Italy

[8] University of Siena Astronomical Observatory - Siena, Italy

[9] Astrocampania, Sez. Stabia – Penisola Sorrentina, - Italy

The list below contains 98 times of minima for 59 eclipsing binary stars calculated from CCD observations made by participants in the SSV-UAI Eclipsing Binaries Program. Except for two (Univ. College London Obs. and Univ. Siena Obs.) all the observatories are privately operated. Some light curves were remotely obtained (via Internet) using the UAI Remote Telescope, that is publicly available on the web site `www.skylive.it`.
The observations were reduced following standard procedures (see next section) and the light curves were analyzed using the Kwee−van Woerden algorithm (Kwee & van Woerden, 1956) to determine the times of minima. All the times of minima listed in this paper are heliocentric.
It is worth noting that most of the observed stars are neglected objects.

Observatory and telescope:
36-cm Schmidt–Cassegrain (SC36)
30-cm Schmidt–Cassegrain (SC30)
25-cm Schmidt–Cassegrain (SC25)
25-cm Newton (N25)
23-cm Schmidt–Cassegrain (SC23)
20-cm Schmidt–Cassegrain (SC20)
20-cm Newton (N20)
13-cm Maksutov–Cassegrain (MC13)

Detector:	Meade DSI Pro II Monochromatic CCD camera (DSI) QSI 516wsg CCD camera (QSI) SBIG ST-7 CCD camera (ST7) SBIG ST-8XME CCD camera (ST8) SBIG ST-9 CCD camera (ST9) SBIG STL-6303 CCD camera (STL) Sony ICX429ALL based CCD camera (UAI) Canon Eos 1100D DSLR (Eos)

Method of data reduction:

Frame calibration (dark subtraction and flat field correction) and photometric analysis (differential photometry on each image) were performed using MaxIm DL or Mira Pro software packages.

Method of minimum determination:

Times of minima, expressed as Heliocentric Julian Day (see the attached Table), were computed adopting the KW method (Kwee & van Woerden, 1956) using AVE (Barberá, 1996). This algorithm also provides an error estimate, that is the formal internal error of the KW method, which can be considered as a lower limit of the actual uncertainty on times of minima. Together with that error we provide, as upper limit of the uncertainty, an alternative estimate error according to the Arlot's (modified) method (Arlot et al., 2009) by adopting the formula $\sigma_{ToM} = \frac{1}{\sqrt{2}}\frac{\sigma_m}{\Delta m}\Delta t$, where σ_m is the average error in magnitude and Δm is the magnitude drop during a time range Δt delimiting the part of the light curve where the speed of decrease in magnitude is the highest.

Times of minima:

Star name	Time of min. HJD 2400000+	Error	Type	Filter	Rem.
V473 And	56185.5181	0.0004[a] 0.0001[b]	I	c	Banfi/SC25/ST7
V473 And	56186.3198	0.0007 0.0004	I	*V*	Corfini/N20/UAI
V473 And	56553.3065	0.0010 0.0002	II	c	Cervoni/SC36/ST8
V473 And	56644.4018	0.0015 0.0003	II	*V*	Barbieri/SC30/ST9
V608 Aur	56280.3285	0.0001 0.0001	i	c	Ruocco/SC25/ST7
V609 Aur	56280.3732	0.0003 0.0002	I	c	Ruocco/SC25/ST7
V609 Aur	56280.6120	0.0015 0.0005	II	c	Ruocco/SC25/ST7
V618 Aur	56290.3306	0.0006 0.0004	i	c	Ruocco/SC25/ST7
AQ Boo	56474.3809	0.0004 0.0004	ii	c	Salvaggio/SC23/ST8
IW Boo	56416.4280	0.0022 0.0005	I	*V*	Banfi/SC25/ST7
IW Boo	56416.5582	0.0009 0.0003	II	*V*	Banfi/SC25/ST7
LY Boo	56426.4597	0.0010 0.0007	i	c	Ruocco/SC25/ST7
MT Boo	56433.3348	0.0013 0.0010	ii	c	Ruocco/SC25/ST7
OQ Cam	56371.3541	0.0005 0.0001	i	c	Salvaggio/SC23/ST8
GO Cnc	56348.3574	0.0011 0.0002	i	*V*	Marino/N25/ST7
EX CVn	56395.4009	0.0012 0.0004	ii	c	Ruocco/SC25/ST7
SU Cep	56633.2807	0.0002 0.0001	I	*R*	Marino et al./N25/ST7
VW Cep	56451.4689	0.0033 0.0002	i	c	Bonaventura/MC13/Eos
V737 Cep	56141.4078	0.0010 0.0006	ii	*V*	Aceti et al./SC20/ST8
UCAC4 737-078030	56633.2715	0.0036 0.0006	I	*R*	Marino/N25/ST7
UCAC4 737-078030	56637.3727	0.0067 0.0005	II	*R*	Marino/N25/ST7
UCAC4 737-078030	56639.3136	0.0076 0.0003	I	*R*	Marino/N25/ST7
UCAC4 737-078030	56644.2780	0.0060 0.0006	II	*R*	Marino/N25/ST7
AS CrB	56446.3428	0.0004 0.0006	i	c	Ruocco/SC25/ST7
LN Cyg	56521.3706	0.0004 0.0003	I	c	Ruocco/SC25/ST7

Times of minima:					
Star name	Time of min. HJD 2400000+	Error	Type	Filter	Rem.
PY Cyg	56498.4447	0.0027 0.0004	i	c	Ruocco/SC25/ST7
V447 Cyg	56136.4345	0.0007 0.0002	i	c	Ruocco/SC25/ST7
V456 Cyg	56153.3446	0.0004 0.0007	ii	*V*	Salvaggio/SC23/ST7
V869 Cyg	56471.4078	0.0014 0.0004	i	c	Ruocco/SC25/ST7
V884 Cyg	56455.3963	0.0006 0.0004	ii	c	Salvaggio/SC23/ST8
V931 Cyg	56456.4112	0.0002 0.0001	i	c	Salvaggio/SC23/ST8
V979 Cyg	56454.4075	0.0003 0.0003	ii	c	Salvaggio/SC23/ST8
V1044 Cyg	56185.3528	0.0012 0.0006	i	*V*	Martinengo/SC20/QSI
V1045 Cyg	56185.4878	0.0005 0.0005	ii	*V*	Martinengo/SC20/QSI
V1187 Cyg	56138.3541	0.0010 0.0003	i	c	Corfini/N20/UAI
V1187 Cyg	56523.3895	0.0017 0.0005	ii	*V*	Marino/N25/ST7
V1191 Cyg	56523.3831	0.0009 0.0003	ii	*V*	Marino/N25/ST7
V1457 Cyg	56137.4737	0.0004 0.0003	i	c	Ruocco/SC25/ST7
V1665 Cyg	56189.3146	0.0013 0.0002	i	c	Ruocco/SC25/ST7
V1870 Cyg	56508.5757	0.0014 0.0004	II	c	Ruocco/SC25/ST7
V1870 Cyg	56509.3678	0.0010 0.0008	II	c	Ruocco/SC25/ST7
V1870 Cyg	56512.5247	0.0015 0.0007	II	c	Ruocco/SC25/ST7
V1870 Cyg	56516.4742	0.0023 0.0006	II	c	Ruocco/SC25/ST7
V1870 Cyg	56518.4483	0.0002 0.0002	I	c	Ruocco/SC25/ST7
KIC 1061825	56451.5009	0.0004 0.0003	ii	c	Marino/N20/ST7
GSC 03089-01273	56129.5241	0.0002 0.0003	ii	c	Marino/N20/ST7
GSC 03089-01273	56129.5258	0.0013 0.0003	ii	c	Arena/N20/DSI
V1072 Her	56522.4967	0.0005 0.0001	I	*V*	Cervoni/SC36/ST8
V1072 Her	56533.3736	0.0025 0.0003	II	*V*	Cervoni/SC36/ST8
V1092 Her	56461.4064	0.0005 0.0003	i	*V*	Marino/N25/ST7
V1106 Her	56119.4252	0.0004 0.0002	ii	c	Corfini/N20/UAI
V1106 Her	56124.3921	0.0004 0.0003	i	c	Corfini/N20/UAI
V1106 Her	56126.4282	0.0014 0.0012	i	c	Banfi/SC25/ST7
V1106 Her	56126.5551	0.0006 0.0002	ii	c	Banfi/SC25/ST7
V1106 Her	56127.4476	0.0002 0.0002	i	c	Corfini/N20/UAI
V1106 Her	56157.3617	0.0005 0.0003	ii	c	Corfini/N20/UAI
V1106 Her	56180.4048	0.0005 0.0002	i	c	Banfi/SC25/ST7
V1106 Her	56185.3682	0.0000 0.0001	ii	*V*	Corfini/N20/UAI
V1106 Her	56191.3523	0.0010 0.0003	i	*V*	Corfini/N20/UAI
V1106 Her	56203.3183	0.0005 0.0002	i	c	Corfini/N20/UAI
V1106 Her	56224.3210	0.0001 0.0003	ii	c	Zambelli/RC40/STL
V1106 Her	56459.4460	0.0005 0.0001	i	c	Marino/N25/ST7
V1106 Her	56499.4151	0.0028 0.0003	i	c	Barbieri/SC30/ST9
V1106 Her	56499.5518	0.0038 0.0005	ii	c	Barbieri/SC30/ST9
V1106 Her	56516.3489	0.0009 0.0001	ii	c	Barbieri/SC30/ST9
V1106 Her	56516.4762	0.0019 0.0003	i	c	Barbieri/SC30/ST9
V1106 Her	56528.4420	0.0015 0.0007	i	*V*	Cervoni/SC36/ST8
V1175 Her	56135.4275	0.0009 0.0002	I	*V*	Aceti et al./SC20/ST8
V1175 Her	56158.3929	0.0006 0.0002	II	c	Corfini/N20/UAI
UCAC4 638-056476	56129.5617	0.0013 0.0003	i	c	Marino/N20/ST7
VX Lac	56584.2572	0.0031 0.0011	ii	c	Ruocco/SC25/ST7
VY Lac	56269.2665	0.0004 0.0001	i	c	Salvaggio/SC23/ST8
UCAC4 708-102815	56598.4890	0.0037 0.0010	i	*V*	Marino/N25/ST7
UCAC4 708-102876	56598.5124	0.0048 0.0013	ii	*V*	Marino/N25/ST7
UCAC4 708-102942	56598.4101	0.0059 0.0016	i	*V*	Marino/N25/ST7
IW Lyr	56446.4314	0.0009 0.0007	II	c	Ruocco/SC25/ST7
IW Lyr	56448.4215	0.0003 0.0001	I	c	Ruocco/SC25/ST7
NS Lyr	56092.5440	0.0008 0.0005	i	c	Ruocco/SC25/ST7

Times of minima:					
Star name	Time of min. HJD 2400000+	Error	Type	Filter	Rem.
QQ Lyr	56184.4009	0.0054 0.0017	II	c	Banfi/SC25/ST7
QQ Lyr	56550.3634	0.0048 0.0003	I	c	Cervoni/SC36/ST8
V417 Lyr	56459.4393	0.0003 0.0003	ii	c	Ruocco/SC25/ST7
V417 Lyr	56459.5887	0.0003 0.0005	i	c	Ruocco/SC25/ST7
V431 Lyr	56450.4307	0.0018 0.0005	ii	c	Ruocco/SC25/ST7
V556 Lyr	56452.4622	0.0079 0.0003	i	c	Bonaventura/MC13/Eos
V556 Lyr	56593.3241	0.0242 0.0002	ii	*V*	Marino/N25/ST7
V864 Mon	56354.3415	0.0004 0.0000	ii	*V*	Marino/N25/ST7
KN Per	56293.2412	0.0011 0.0008	ii	c	Ruocco/SC25/ST7
V880 Per	56274.2808	0.0009 0.0003	i	c	Ruocco/SC25/ST7
V912 Per	56265.3465	0.0005 0.0003	i	c	Ruocco/SC25/ST7
AH Tau	56322.4137	0.0006 0.0002	i	c	Salvaggio/SC23/ST8
EQ Tau	56290.4697	0.0004 0.0001	i	*V*	Marino/N20/ST7
IV Tau	56291.3029	0.0020 0.0004	i	c	Ruocco/SC25/ST7
V423 Tau	56281.4846	0.0021 0.0009	i	*V*	Corfini/N20/UAI
V423 Tau	56290.3501	0.0029 0.0002	i	c	Marino/N20/ST7
ES UMa	56342.4839	0.0007 0.0002	i	*V*	Arena, Fossey/SC36/STL
HW Vir	56417.3374	0.0003 0.0001	II	*V*	Banfi/SC25/ST7
HW Vir	56417.3957	0.0001 0.0000	I	*V*	Banfi/SC25/ST7
HW Vir	56417.4538	0.0004 0.0002	II	*V*	Banfi/SC25/ST7

Explanation of the remarks in the table:

Error:
[a] Arlot's modified method, [b] as given by KW method

Type:
I [II] the deeper [shallower] minimum
i [ii] the type of minimum simply assumed at 0 [0.5] phase according to the ephemeris provided by Kreiner's (2004) web site or by B.R.N.O. – *O−C Gateway* web site (`http://var.astro.cz/ocgate`), because:
– the two minima observed during one night had the same depth (for V1106 Her)
– only one minimum was observed or
– the minima were not covered enough to allow to deduce the relative depth.

Remark:
Observer[s]/Telescope/Detector

References:

Arlot, J.-E. et al., 2009, *A&A*, **493**, 1171
Barberá, R., 1996, AVE home page, `http://www.astrogea.org/soft/ave/introave.htm`
Kreiner, J. M., 2004, *AcA*, **54**, 207, `http://www.as.up.krakow.pl/ephem`
Kwee, K. K., van Woerden, H., 1956, *Bull. Astr. Inst. Neth.*, **12**, 327, (No. 464)

COMMISSIONS 27 AND 42 OF THE IAU
INFORMATION BULLETIN ON VARIABLE STARS

Number 6095

Konkoly Observatory
Budapest
18 February 2014

HU ISSN 0374 – 0676

105 MINIMA TIMINGS OF ECLIPSING BINARIES

LIAKOS, A.[1]; GAZEAS, K.[2]; NANOURIS, N.[2,3]

[1]Institute for Astronomy & Astrophysics, Space Applications & Remote Sensing, National Observatory of Athens, Penteli, Athens, Greece; e-mail: alliakos@noa.gr

[2]Department of Astrophysics, Astronomy and Mechanics, National & Kapodistrian University of Athens, Zografos, Athens, Greece; e-mail: kgaze@phys.uoa.gr; nanouris@phys.uoa.gr

[3]Department of Environment Technologists, School of Technological Applications, Technological and Educational Institute of the Ionian Islands, Panagoula, Zakynthos Is., Greece

Observatory and telescope:
T1: 40 cm Cassegrain telescope (f/8), and **T2**: 25 cm Newtonian reflector telescope (f/4.7) located at the Gerostathopoulion Observatory of the University of Athens **T3**: 1.2 m Cassegrain telescope (f/13) located at the Kryonerion Observatory (Mt. Killini, Corinthia, Hellas) of the National Observatory of Athens.

Detector:	**C1**: ST-10XME CCD camera, KAF-3200ME chip, $16' \times 11'$ and $25' \times 17'$ (using a focal reducer) field of view (FoV) with T1, 2184 × 1472 pixels, **C2**: ST-8XMEI CCD camera, KAF-1603ME chip, $15' \times 10'$ FoV with T1 and $40' \times 27'$ FoV with T2, **C3**: AP47p CCD camera, Marconi 47-10 chip, $2.5' \times 2.5'$ FoV with T3. All CCDs have a Peltier-type cooling system and are equipped with Bessell $UBVRI$ filters.

Method of data reduction:
Differential photometry

Method of minimum determination:
Kwee & van Woerden (1956).

Times of minima:					
Star name	Time of min. HJD 2400000+	Error	Type	Filter	Rem.
QX And	55882.3077	0.0005	II	$BVRI$	T1+C1
	55882.5141	0.0006	I	$BVRI$	T1+C1
	55884.3688	0.0004	II	$BVRI$	T1+C1
	55887.2533	0.0003	II	$BVRI$	T1+C1
	55887.4600	0.0003	I	$BVRI$	T1+C1

Times of minima:					
Star name	Time of min. HJD 2400000+	Error	Type	Filter	Rem.
V1464 Aql	56174.3242	0.0003	I	*BVRI*	T1+C1
	56181.3019	0.0004	I	*BVRI*	T1+C1
FN Cam	55929.6065	0.0011	II	*BVRI*	T1+C1
	55930.2817	0.0015	II	*BVRI*	T1+C1
	55930.6240	0.0007	I	*BVRI*	T1+C1
	55935.3642	0.0002	I	*BVRI*	T1+C1
IO Cep	56530.4827	0.0003	I	*BVRI*	T3+C3
TW CrB	56049.5494	0.0003	II	*BVRI*	T1+C1
	56057.4995	0.0005	I	*BVRI*	T1+C1
	56067.5098	0.0001	I	*BVRI*	T1+C1
	56078.4038	0.0002	II	*BVRI*	T1+C1
AE Cyg	56528.5496	0.0005	I	*BVRI*	T3+C3
V366 Cyg	56529.4209	0.0010	I	*BVRI*	T3+C3
V1187 Cyg	56168.4935	0.0003	I	*BVRI*	T1+C1
	56171.5095	0.0005	I	*BVRI*	T1+C1
V1191 Cyg	56166.4343	0.0002	I	*BVRI*	T1+C1
	56167.3749	0.0002	I	*BVRI*	T1+C1
	56168.3145	0.0002	I	*BVRI*	T1+C1
	56168.4719	0.0002	II	*BVRI*	T1+C1
	56169.2539	0.0007	I	*BVRI*	T1+C1
	56169.4123	0.0002	II	*BVRI*	T1+C1
	56170.3528	0.0003	II	*BVRI*	T1+C1
	56170.5089	0.0002	I	*BVRI*	T1+C1
	56171.2930	0.0002	II	*BVRI*	T1+C1
	56171.4489	0.0002	I	*BVRI*	T1+C1
YY Eri	55891.4726	0.0001	I	*BVRI*	T1+C1
	55894.5262	0.0001	II	*BVRI*	T1+C1
GSC 0163-1415	55632.3604	0.0037	I	*I*	T1+C1
GSC 0389-0120	56463.4435	0.0004	II	*BVRI*	T1+C1
	56464.3844	0.0004	I	*BVRI*	T1+C1
	56465.5142	0.0003	I	*BVRI*	T1+C1
	56470.4135	0.0002	I	*BVRI*	T1+C1
	56472.4858	0.0004	II	*BVRI*	T1+C1
GSC 1137-0293	56146.3836	0.0005	I	*B*	T1+C1
	56146.5701	0.0010	II	*BVRI*	T1+C1
	56148.4673	0.0009	II	*BVRI*	T1+C1
	56153.3782	0.0010	II	*BVRI*	T1+C1
	56153.5674	0.0009	I	*BVRI*	T1+C1
	56155.4612	0.0010	I	*BVRI*	T1+C1
	56157.5350	0.0010	II	*BVRI*	T1+C1
	56159.4258	0.0008	II	*BVRI*	T1+C1
GSC 2816-0743	55887.4764	0.0012	I	*BVRI*	T1+C1
GSC 3332-0638	55847.4869	0.0075	I	*VRI*	T1+C1
	55848.5258	0.0076	II	*VRI*	T1+C1
	55852.6150	0.0094	II	*I*	T1+C1
	55854.4571	0.0018	I	*I*	T1+C1
	55855.4815	0.0024	II	*RI*	T1+C1
	55856.5096	0.0068	I	*BVRI*	T1+C1

Times of minima:					
Star name	Time of min. HJD 2400000+	Error	Type	Filter	Rem.
	55866.3433	0.0050	I	*RI*	T1+C1
	55867.3691	0.0019	II	*I*	T1+C1
	55867.5653	0.0041	I	*I*	T1+C1
	55868.3816	0.0050	I	*RI*	T1+C1
	55869.4026	0.0024	II	*I*	T1+C1
	55874.3295	0.0030	II	*I*	T1+C1
TT Her	56079.4869	0.0001	I	*BVRI*	T1+C1
	56084.5003	0.0004	II	*BVRI*	T1+C1
UX Her	56089.4797	0.0003	II	*BVRI*	T1+C1
	56093.3568	0.0001	II	*BVRI*	T1+C1
LT Her	56050.4343	0.0002	I	*BV*	T1+C1
	56070.4840	0.0007	II	*BV*	T1+C1
V878 Her	56077.3202	0.0002	I	*BVRI*	T1+C1
	56082.3525	0.0004	II	*BVRI*	T1+C1
V1097 Her	56111.3994	0.0002	II	*BVRI*	T1+C1
	56112.3004	0.0003	I	*BVRI*	T1+C1
	56112.4819	0.0002	II	*BVRI*	T1+C1
	56113.3827	0.0001	I	*BVRI*	T1+C1
	56114.4646	0.0002	I	*BVRI*	T1+C1
AU Lac	56531.5572	0.0003	I	*BVRI*	T3+C3
AL Leo	56014.3571	0.0001	I	*BVRI*	T1+C1
	56047.2698	0.0003	II	*BVRI*	T1+C1
RR Lep	55953.2674	0.0004	I	*BV*	T1+C1
V868 Mon	55939.4617	0.0002	I	*BVRI*	T1+C1
	55940.4192	0.0002	II	*BVRI*	T1+C1
	55953.4923	0.0002	I	*BVRI*	T1+C1
V1387 Ori	55898.3965	0.0006	II	*BVI*	T1+C1
	55904.5730	0.0009	I	*BVRI*	T1+C1
V407 Peg	56156.5656	0.0003	I	*BVRI*	T2+C2
	56175.3593	0.0002	II	*BVRI*	T2+C2
	56176.3065	0.0008	I	*BVRI*	T2+C2
UV Psc	54369.3737	0.0002	I	*VR*	T1+C2
EX Psc	56243.3327	0.0006	II	*BVRI*	T1+C1
	56245.2136	0.0009	I	*BVRI*	T1+C1
	56245.3587	0.0008	II	*BVRI*	T1+C1
	56246.2260	0.0007	II	*BVRI*	T1+C1
	56246.3705	0.0008	I	*BVRI*	T1+C1
XX Sex	55982.4356	0.0007	II	*BVRI*	T1+C1
	56006.4612	0.0003	I	*BVRI*	T1+C1
	56008.3536	0.0002	II	*BVRI*	T1+C1
HX UMa	55975.4313	0.0002	I	*BVRI*	T1+C1
	55975.6226	0.0003	II	*BVRI*	T1+C1
USNO-A2.0 1125-08352535	56111.3690	0.0004	II	*I*	T1+C1
	56112.4105	0.0005	II	*BVRI*	T1+C1
	56113.4523	0.0008	II	*BVRI*	T1+C1
	56114.3180	0.0024	I	*BVRI*	T1+C1
	56114.4945	0.0008	II	*VRI*	T1+C1

Times of minima:					
Star name	Time of min. HJD 2400000+	Error	Type	Filter	Rem.
USNO-A2.0 1275-01929590	55818.5318	0.0019	II	*BVRI*	T1+C1
	55819.5033	0.0017	I	*BVRI*	T1+C1
	55833.4731	0.0035	I	*BVRI*	T1+C1
	55835.6033	0.0076	II	*BVRI*	T1+C1
ER Vul	54330.5464	0.0003	I	*R*	T1+C2

Explanation of the remarks in the table:

T1, T2, T3, C1, C2, and C3 refer to the instrumentation (telescope and CCD camera) used for each case.

Remarks:

The systems GSC 0163-1415, GSC 1137-0293, GSC 3332-0638, and USNO-A2.0 1275-01929590 were recently discovered by Liakos & Niarchos (2011, 2012). GSC 0389-0120, GSC 2816-0743, and USNO-A2.0 1125-08352535 are also new eclipsing binaries discovered by Pojmanski (2002), Zhang et al. (2009), and Mondal et al. (2010), respectively.

Acknowledgements:

This work was performed in the framework of PROTEAS project within GSRT's KRIPIS action for A.L., funded by Hellas and the European Regional Development Fund of the European Union under the O.P. Competitiveness and Entrepreneurship, NSRF 2007-2013.

References:

Kwee, K., van Woerden, H., 1956, *Bulletin of the Astronomical Institutes of the Netherlands*, **12**, 327

Liakos, A., Niarchos, P., 2011, *Peremennye Zvezdy Prilozhenie*, **11**, 2

Liakos, A., Niarchos, P., 2012, *Peremennye Zvezdy Prilozhenie*, **12**, 2

Mondal, S., Lin, C. C., Chen, W. P., Zhang, Z.-W., Alcock, C., et al., 2010, *AJ*, **139**, 2026

Pojmanski, G., 2002, *AcA*, **52**, 397

Zhang, X. B., Luo, C. Q., Luo, Y. P., Deng, L. C., 2009, *IBVS*, **5900**, 3

*This version of the paper contains corrections, and differs from the one appeared on-line originally. Date of last modification: Sun Feb 23 17:31:38 CET 2014

COMMISSIONS 27 AND 42 OF THE IAU
INFORMATION BULLETIN ON VARIABLE STARS

Number 6096

Konkoly Observatory
Budapest
24 February 2014

HU ISSN 0374 – 0676

RADIAL VELOCITY SOLUTION OF THE SYSTEM IP Dra

KJURKCHIEVA, D.; MARCHEV, D.

Department of Physics, Shumen University, 9700 Shumen, Bulgaria

e-mail: d.kyurkchieva@shu-bg.net, d.marchev@shu-bg.net

The light variability of IP Dra with an amplitude of $0\overset{m}{.}06$ and a period of 1.7184 days was detected by *Hipparcos* (ESA 1997) and the star was classified as EB of β Lyr type. The available data for this star are: $V=7\overset{m}{.}76$, $B-V=0\overset{m}{.}535$, $V-I=0\overset{m}{.}61$, parallax 8.27 mas (distance 121 pc), spectral type F5, age 2.7 Gyr (ESA 1997; Kazarovets et al. 1999; Nordström et al. 2004; Malkov et al. 2006).

In order to obtain radial velocity solution of IP Dra we acquired few tens of spectra with the 2-m telescope of the National Astronomical Observatory at Rozhen (Table 1). We used a CCD Photometrics AT200 camera with the SITe SI003AB 1024×1024 pixels chip mounted on the coudé spectrograph (grating B&L632/14.7°). The exposure time was 15 min and the mean S/N ratio was around 60-70.

Table 1. Journal of observations.

Year	Month, date	number of spectra	Phase range
2004	Aug 25	4	0.545-0.685
2005	Jul 29	2	0.675
2006	Feb 03	2	0.295
2006	Feb 04	4	0.805-0.825
2006	Feb 07	11	0.594-0.755
2006	Jun 21	8	0.524-0.60
2006	Jun 22	6	0.101-0.186
2006	Jul 18	3	0.31, 0.365
2006	Jul 19	14	0.792-0.956
2007	Feb 09	1	0.175
2007	Mar 24	5	0.282-0.322
2007	Aug 07	7	0.295-0.435
2007	Aug 08	4	0.006-0.030
2007	Dec 21	1	0.491
2010	May 03	2	0.96
2013	Aug 25	1	0.52

Most of the spectra were in the spectral range around the Hα line (6470-6670 Å) with 0.19 Å/pixel resolution and they covered well the orbital cycle. Moreover, several spectra around the CaII H & K and NaD lines were obtained.

The spectral data were reduced in a standard way using the PCIPS software packages (Smirnov et al. 1992) by bias subtraction, flat-field division and wavelength calibration (with Th-Ar comparison source exposures). β Vir was used as a radial velocity standard.

Our data were phased according to the ephemeris of *Hipparcos* (ESA 1997):

$$\mathrm{MinI} = 2448501.317 + 1.7184 \times \mathrm{E} \; .$$

Normalized H_α spectra around characteristic orbital phases are shown in Fig. 1.

The profiles of the Hα line of IP Dra are single-shaped at all phases and their strength is appropriate to the spectral type F5 of the primary. The profiles of the CaII H & K and NaD lines (Fig. 2) also correspond to the F5 primary and do not reveal contribution of the secondary. These facts allowed us to classify the target as a single-lined spectroscopic binary with a low-luminosity secondary.

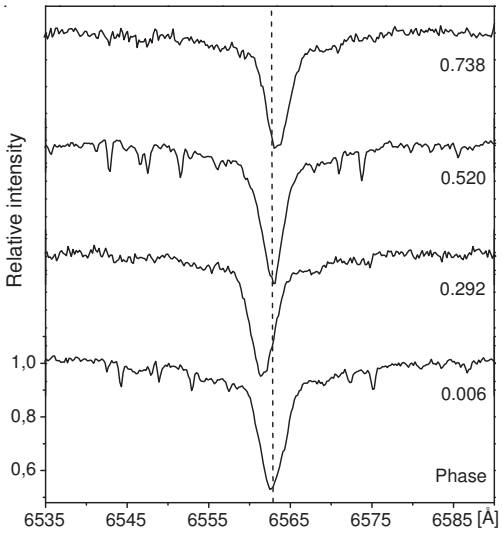

Figure 1. The Hα lines of IP Dra around the eclipses and quadratures.

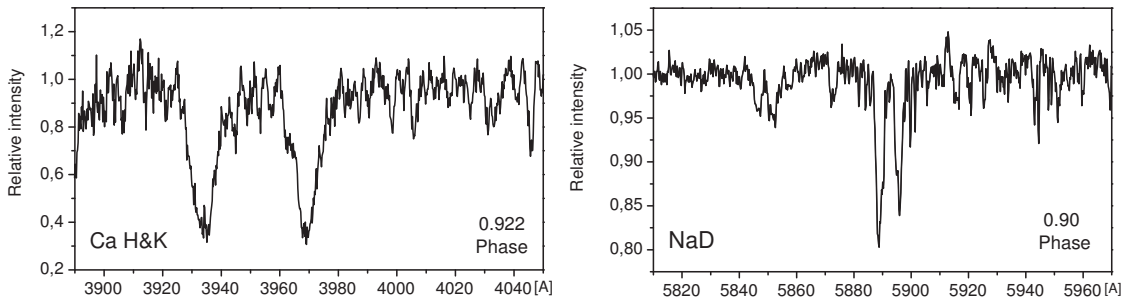

Figure 2. The spectra of IP Dra around the CaII H & K lines (left) and NaD line (right) from July 19 2006.

The FWHM, EW and depth of the Hα line change during the cycle correspondingly in the ranges 3.2-3.9 Å, 2.1-3 Å and 0.48-0.63. Their variability do not reveal any considerable trends with phase.

The Doppler shifts of the Hα line (Fig. 1) confirm that IP Dra is a binary system. The measured radial velocities were fitted by a sinusoid with a semi-amplitude $K_1 \sin i$=65.7±1.6 km/s and a systemic velocity V_0=3.6±2.1 km/s (Fig. 3).

In order to obtain estimations of the fundamental parameters of IP Dra we made some speculations based on its photometric and spectral observations.

The small-amplitude quasi-sinusoidal light curve of IP Dra (ESA 1997) implies ellipsoidal variations rather than eclipses because even grazing eclipses would cause some sharp dips in the light curve. The absence of spectral features from the secondary means that its luminosity should be less than 10% of that of the primary.

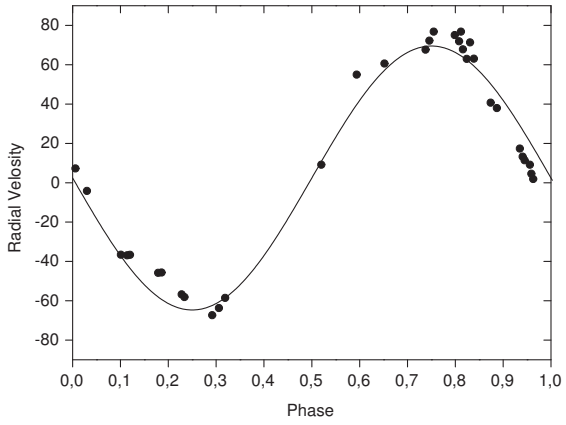

Figure 3. Radial velocity data of IP Dra and their fit.

The solution of the available low-precision, quasi-sinusoidal (*Hipparcos*) light curve is quite ambiguous, i.e. it may be reproduced with a great number of combinations of parameters whose values are within large ranges. The number of solutions can be reduced if one assumes that the two components are MS stars and uses the known empirical relations.

Thus the upper limit L_2=0.1L_1 allowed us to fix mass ratio q=0.56, secondary temperature T_2=0.708T_1=4600 K and relative radius of the secondary r_2=0.65r_1. As a result we obtained solutions within narrow ranges of the fitted parameters r_1 (relative radius of the primary) and i (orbital inclination), namely 0.39–0.43 and 50.5–37.5°. For the reasonable low limit L_2=0.01L_1 we fixed q=0.316, T_2=0.5T_1=3250 K, r_2=0.422r_1, and obtained even narrower ranges of the fitted parameters r_1 and i: 0.48–0.482 and correspondingly 50–40°.

The presented considerations led us to the conclusion that IP Dra is (or almost is) a semidetached binary with a low-luminosity secondary component.

The mean rotational broadening of the spectral lines of IP Dra corresponds to $V_1^{eq} \sin i$=73 km/s. This means $V_1^{eq} \geq$ 95 km/s (equality for i = 50°). If IP Dra is a synchronized binary (P_{orb}=P_{rot}) this result leads to an absolute radius $R_1 \geq$ 3.24 $R_\odot$. Thus the primary is oversized for an F5 MS star. This conclusion from our spectroscopy supports the big relative radius of the primary derived from the light curve solution.

Acknowledgement: Based on spectral observations collected at the National Astronomical Observatory at Rozhen. The research was supported partly by funds of a project of

Scientific Foundation of Shumen University. We are grateful to the anonymous referee, and the editor, László Molnár, for the useful notes.

References:

ESA, 1997, *The Hipparcos and Tycho Catalogues*, vol. 11, Hipparcos Variability Annex, ESA SP-1200
Kazarovets A. et al., 1999, *IBVS*, No 4659
Malkov O., Oblak E., Snegireva E., Torra J., 2006, *A&A*, **446**, 785
Nordström, B. et al., 2004, *A&A*, **418**, 989
Smirnov O., Piskunov N., Afanasyev V., Morozov A., 1992, *ASP Conf. Ser.*, **25**, 344

COMMISSIONS 27 AND 42 OF THE IAU
INFORMATION BULLETIN ON VARIABLE STARS

Number 6097

Konkoly Observatory
Budapest
11 March 2014

HU ISSN 0374 – 0676

DISCOVERY OF AN SU UMa-TYPE ECLIPSING CATACLYSMIC VARIABLE STAR INSIDE THE CV "PERIOD GAP"

CAGAŠ, PAVEL; CAGAŠ, PETR

BSObservatory, Modrá 587, 760 01 Zlín, Czech Republic

e-mail: pavel.cagas@bsobservatory.org, p.cagas@gmail.com

Introduction

SU UMa-type cataclysmic variable (CV) stars consists of close pair of a white dwarf (primary) and a main sequence (secondary) star. The secondary star fills its Roche-lobe, which causes a mass transfer to the primary star, creating an accretion disc (provided the magnetic field of the primary star is not strong enough to prohibit building up of the accretion disc). A hot spot is formed on the accretion disc, where the stream of mass from the secondary star intersects the disc's outer edge. Thermal instability in the accretion disc causes semi-periodic brightenings (outbursts).

The orbital periods of SU UMa-type CVs span a range from approx. 80 minutes up to tens of hours, with a distinct gap between 2 and 3 hours. Orbital period decreases through the CV evolution due to angular momentum loses (e.g. by magnetic braking). When the orbital period reaches approx. 3 hours, the secondary star becomes fully convective through the mass loss, shrinks inside its Roche-lobe and the mass transfer to the primary star is significantly reduced. Outbursts stop to occur and the particular CV becomes undetectable. Mass transfer is restored again when the orbital period decreases to approx. 2 hours by gravitational radiation and the secondary star fills its Roche-lobe again (e.g. Howell et al., 2001).

Observations

CzeV404 (USNO-A2.0 0975-11872373, $\alpha_{2000} = 18^{\rm h}30^{\rm m}1\overset{\rm s}{.}833$, $\delta_{2000} = +12°33'47\overset{''}{.}43$) was found on a series of wide-field CCD exposures of a field in Hercules acquired on 22 July, 2012. The light curve showed two eclipses approx. 2.35 hours apart and prominent brightness peaks preceding each eclipse, indicating an accretion disc hot spot. All these light curve features suggest previously unknown eclipsing CV star.

CzeV404 was discovered and observed using G4-16000 CCD camera on 0.25 m f/5.4 Newtonian telescope. Each image has $71' \times 71'$ field of view with sampling $1\overset{''}{.}39$/pixel. Individual unfiltered exposures were 240 s or 180 s long, depending on seeing and transparency on the particular observing night.

Another star within the field of view (GSC 01031-01228) with similar brightness and color index was chosen as a comparison star to correct for atmospheric extinction. Beside

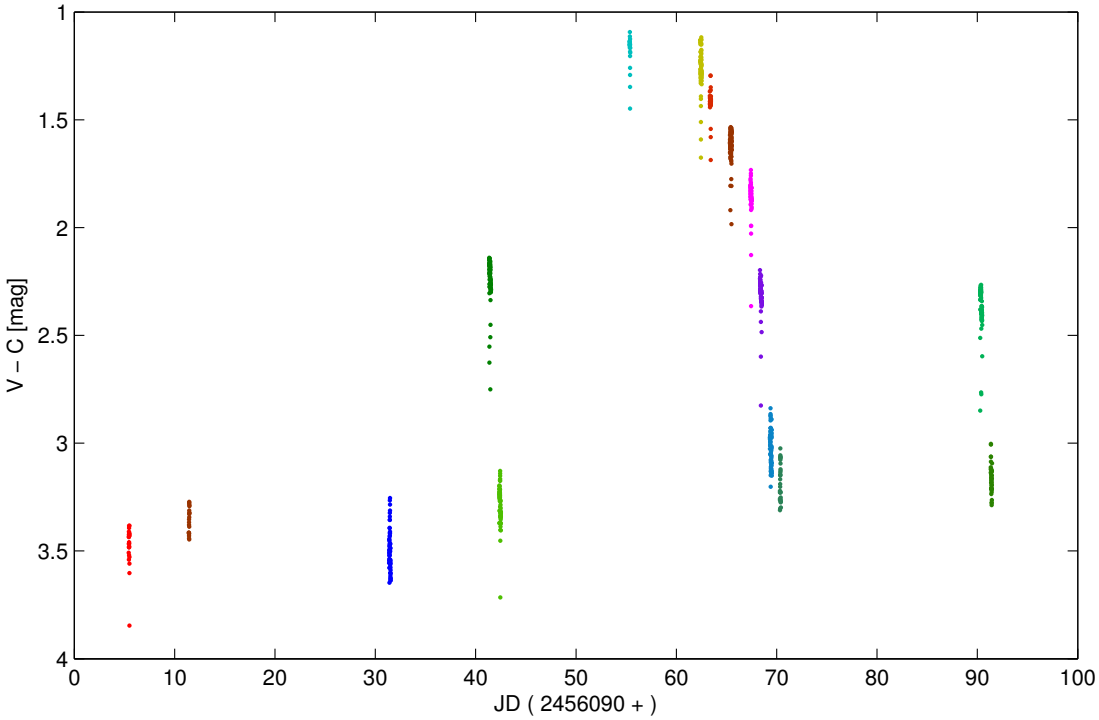

Figure 1. Observations of CzeV404 spanning June to September 2012.

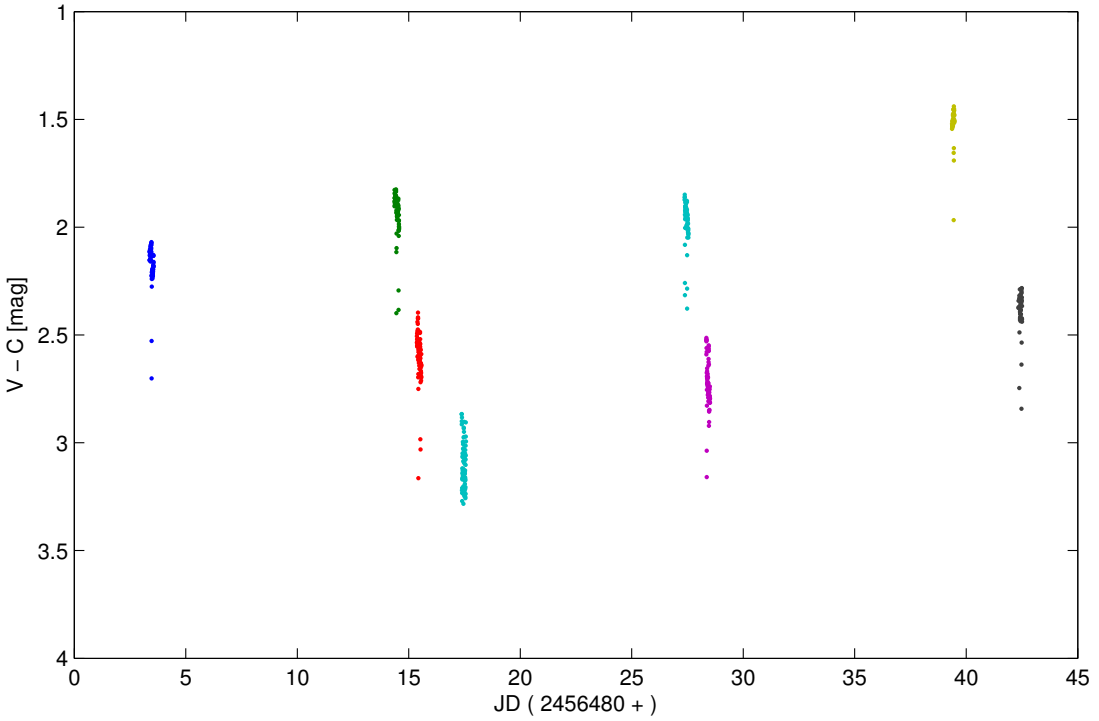

Figure 2. Observations of CzeV404 spanning June to August 2013.

CzeV404, 55 other variable stars and variable star suspects were observed within the field of view. The selected comparison star is one of the eight carefully chosen comparison stars in the field of view, selected according to $B-V$ index to correspond to the $B-V$ indices of individual observed stars. Six observed variable stars out of total 56 stars were compared with the above mentioned comparison stars.

Images were acquired using the SIPS software package. All exposures were calibrated with appropriate dark frames and flat fields, that were created as a median of five individual dark and flat exposures. Photometry was processed using the C-munipack software package (Motl, 2004).

Our light curve shows that CzeV404 exhibits outbursts from the quiescent magnitude of about 16.7 mag (Figures 1 and 2). We observed two types of outbursts: short ones lasting several days (on JD 2456132 and JD 2456181) and one longer and brighter outburst lasting about 15 days with peak brightness of 14.4 mag, which occurred between JD 2456145 and JD 2456160 (Figure 1). This light curve is compatible with an SU UMa-type CV, which exhibits normal outbursts and superoutbursts.

We observed significant changes in the light curve shape in phases that we identified as outburst and superoutburst (Figure 3).

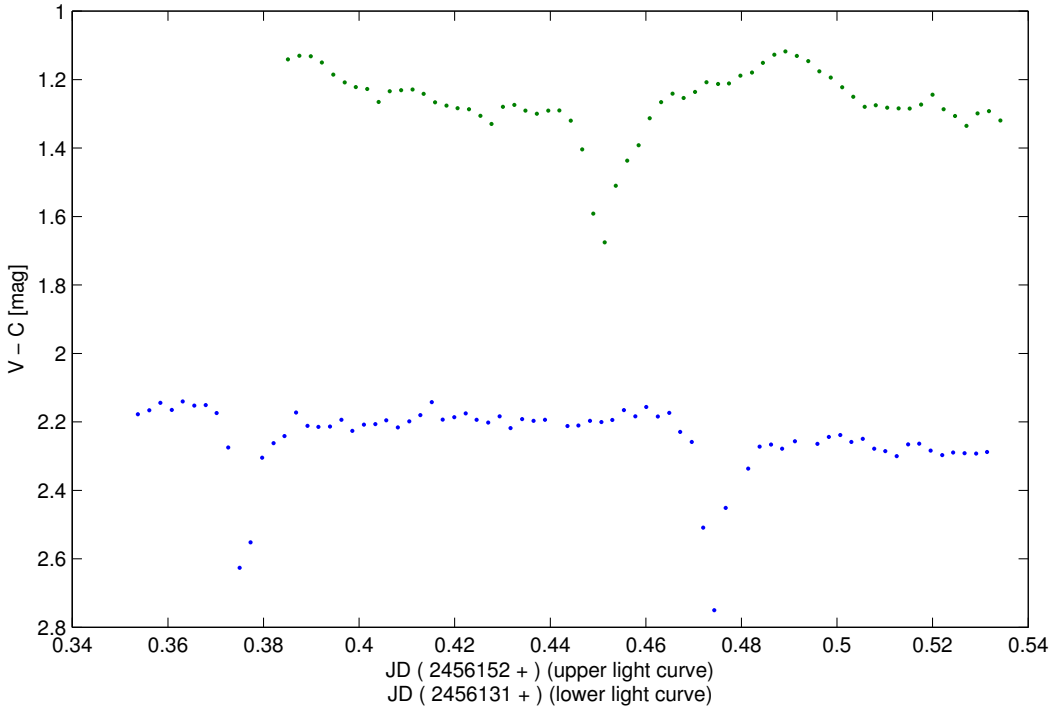

Figure 3. Light curves of CzeV404 during outburst on 22 July 2012 (lower light curve) and during superoutburst on 12 August 2012 (upper light curve).

In the outburst phase the CzeV404 light curve showed brightenings just before eclipse, caused by an accretion disc hot spot. This brightening disappeared during superoutburst phase, but we observed periodic oscillations with a period close to but not identical with the orbital period. We have identified these oscillations as superhumps with the period ~ 0.1 days. This further strengthens the classification of CzeV404 as an SU UMa-type

CV[1]. More details about superhumps are given in Section Results.

The photometric measurements are affected by a nearby star, just around 3.6 pixels ($\sim$ 5 arc seconds) apart (see the left panel in Figures 4 and 5). The brightness of the nearby star was not measured due to close proximity of both stars, but it is somewhat fainter than CzeV404 in the quiescence state. The aperture used to determine CzeV404 brightness is 5 pixels in diameter, so the nearby star slightly affects the measured CzeV404 flux. We carefully checked that the variable star is indeed the object marked (1) on the left panel of Figure 4.

Image from DSS2 Red survey and especially high-resolution image acquired with the 0.65 m telescope of the Ondřejov Observatory (Astronomical Institute of the Czech Academy of Sciences) with 0.″5/pixel sampling show three faint stars in close angular proximity to CzeC404 (see the right panel in Figure 5). However, the faint star to the north of CzeV404 is outside of the photometric aperture and while the faint star to the west of CzeV404 is projected to the aperture, its brightness is so low that it cannot be traced on individual frames from the photometric telescope, so we consider its effect to photometry negligible.

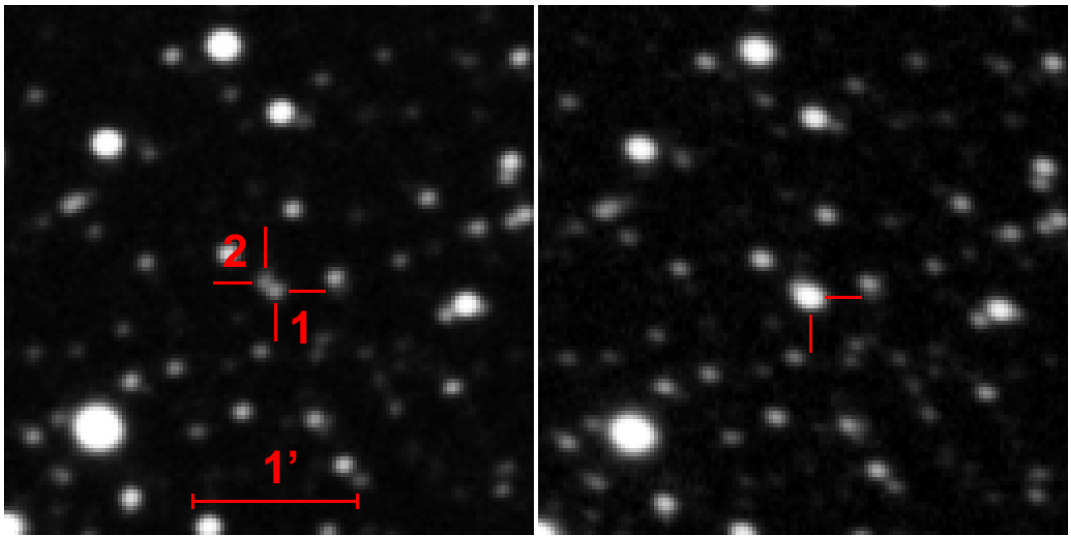

Figure 4. Left panel: CzeV404 (1) in quiescence state and a nearby star approx. 5″ apart to the north-east (2) on 12 July 2012. Right panel: The same field with CzeV404 captured during superoutburst on 5 August 2012. Star shapes are slightly distorted due to aberrations of used wide-field optics. Both panels are cropped from the original photometry telescope field of view, the image scale is 1.″39/pixel.

[1] http://www.sai.msu.su/gcvs/gcvs/iii/vartype.txt

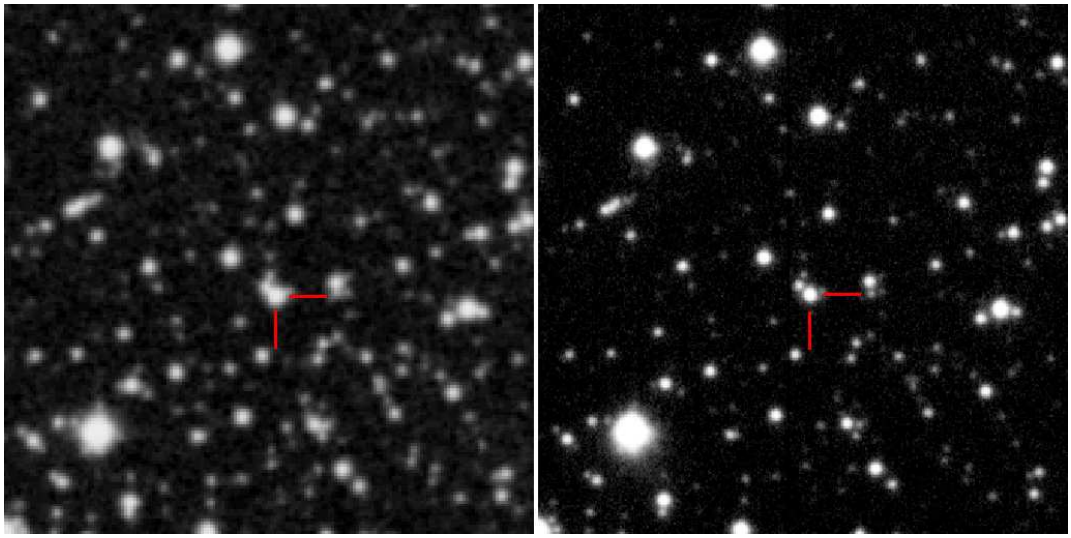

Figure 5. Left panel: Corresponding field from DSS2 Red survey, obviously capturing CzeV404 during an outburst phase. Right panel: The same field imaged with the 0.65 m telescope of the Ondřejov Observatory. This image shows 4 stars within or close to the photometric aperture used to measure CzeV404. Sampling is 0.″5/pixel.

Series start (JD)	Length [h]	Data points	Max. mag	Supposed state
2456095.4311	1:42	30	16.7	quiescence
2456101.4244	1:11	22	16.6	quiescence
2456121.3822	3:39	65	16.6	quiescence
2456131.3493	4:16	76	15.5	outburst
2456132.3568	3:49	67	16.4	quiescence
2456145.3486	1:18	24	14.4	superoutburst
2456152.3816	3:35	64	14.4	superoutburst
2456153.3428	2:27	44	14.5	superoutburst
2456155.3432	4:22	79	14.9	superoutburst
2456157.3776	3:08	56	15.1	superoutburst
2456158.3410	4:32	77	15.5	superoutburst
2456159.3311	4:40	80	16.2	quiescence
2456160.3266	1:59	36	16.3	quiescence
2456180.2841	4:42	81	15.6	outburst
2456181.3362	2:48	45	16.4	quiescence

Table 1. A summary of CzeV404 observations in 2012.

Note: Maximum magnitudes of each series were calculated as comparison star V magnitude (13.3 mag, derived from the USNO A-2.0 catalog) plus the instrumental magnitude of the data set in the clear filter.

Supposed state was determined from the light curve in Figure 1.

Minima during the quiescence phase often dropped below the minimal detectable brightness (around $V \sim 17$ mag, the actual limit slightly varies among individual datasets, because it depends on observing conditions like seeing, sky transparency, lunar phase etc.), thus they are missing from the data sets.

In addition to 15 observing nights in 2012, we acquired another 8 observations of CzeV404 from July to August 2013. Unfortunately, the weather in 2013 did not allow to acquire data as frequent as needed and therefore the estimation of outburst length and possible distinction between outbursts and superoutbursts was not possible. However, we were able to identify 10 more eclipses in 2013, which significantly increased precision of determination of the orbital period.

Series start (JD)	Length [h]	Data points	Max. mag
2456483.3718	4:24	77	15.4
2456494.3551	5:04	89	15.1
2456495.3611	4:48	86	15.7
2456497.3687	4:33	75	16.1
2456507.3681	4:06	72	15.1
2456508.3395	3:58	71	15.8
2456519.3627	2:32	45	14.7
2456522.3395	3:54	53	15.6

Table 2. A summary of CzeV404 observations in 2013.

Results

There were 12 minima observed in 2012 and 11 more minima observed in 2013. Each minimum is very deep ($\sim$ 0.5 mag) and distinct. The orbital period is well constrained, because we observed two consecutive minima in five different nights.

We used the online tool[2] to fit light curves around each minimum with an empirical function (Brát, Pejcha, Mikulášek, 2014) and to determine the center of the eclipse together with uncertainties in 16 cases (see Table 3).

BJD	σ (bootstrap)
2456145.38776	+0.00085/−0.00010
2456152.44554	+0.00072/−0.00035
2456155.38005	+0.00003/−0.00057
2456155.48286	+0.00018/−0.00022
2456157.44426	+0.00153/−0.00010
2456158.42416	+0.00010/−0.00013
2456483.46431	+0.00067/−0.00004
2456494.44191	+0.00119/−0.00004
2456494.54025	+0.00059/−0.00152
2456495.42247	+0.00124/−0.00016
2456495.52077	+0.00017/−0.00010
2456507.38021	+0.00099/−0.00011
2456507.47783	+0.00013/−0.00103
2456508.36069	+0.00077/−0.00036
2456519.43606	+0.00077/−0.00034
2456522.47506	+0.00011/−0.00039

Table 3. A summary of CzeV404 minima used to determine orbital period.

We used four cases, in which two subsequent eclipses occurred in single uninterrupted run, to estimate orbital period. This estimate was used to determine epoch of each

[2] `http://var2.astro.cz`

minimum and then we used linear regression to fit times of eclipses against epoch number to determine the precise period.

$$BJD_{\rm min} = 2456145.3895(9) + 0.098021(1) \times {\rm E}$$

Figure 6 shows observations from 2012 folded with the determined orbital period. It is worth noting that the period $\sim$ 2.35 hours is within the "period gap" of cataclysmic variables.

Brightenings caused by the accretion disc hot spot, observable immediately before each eclipse during the quiescence and outburst phases, disappeared during the superoutburst phase from 12 August to 17 August 2012. Instead, a clearly visible superhump appeared in the light curve.

We only slightly modified the method, used for determination of the orbital period, to determine the period of superhump maxima. We inverted the magnitude scale on particular nights, so the peaks appeared as minima, and utilized the same tool to fit light curves around each minimum with an empirical function (Brát, Pejcha, Mikulášek, 2014) and to determine the center of each peak together with uncertainties in 7 cases (see Table 4).

We observed two subsequent maxima in single uninterrupted run in three cases. These three cases were used to estimate period of superhump brightening. This estimate was used to determine epoch of each maximum and then we used linear regression to fit times of peak brightness against the epoch number to determine the superhump period.

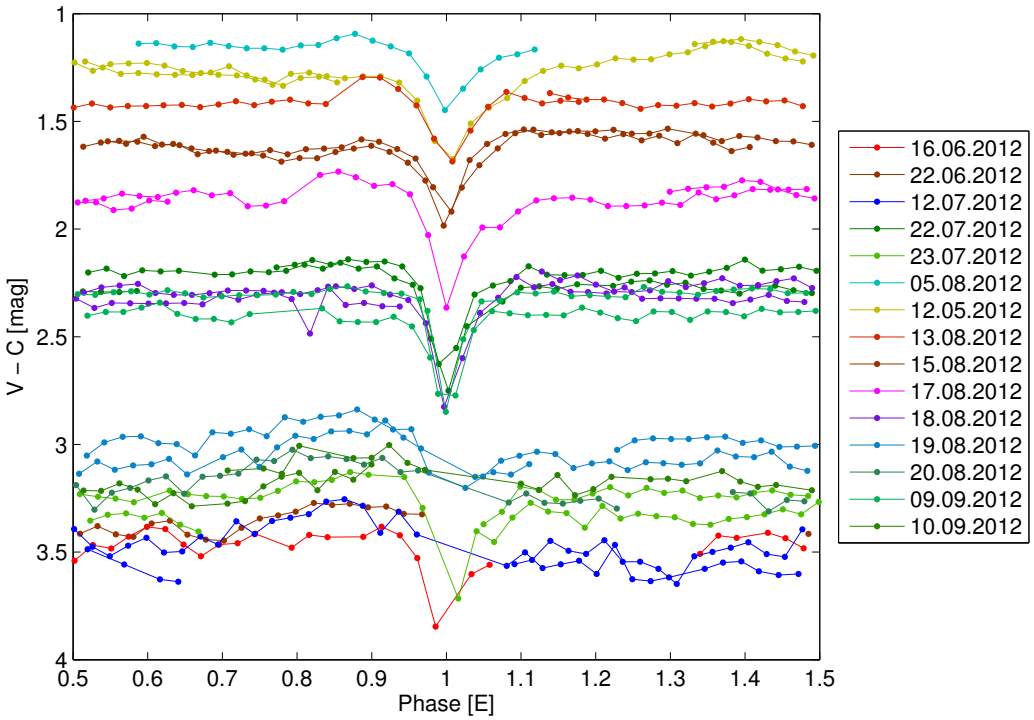

Figure 6. All CzeV404 observations folded with the 0.098021 days orbital period.

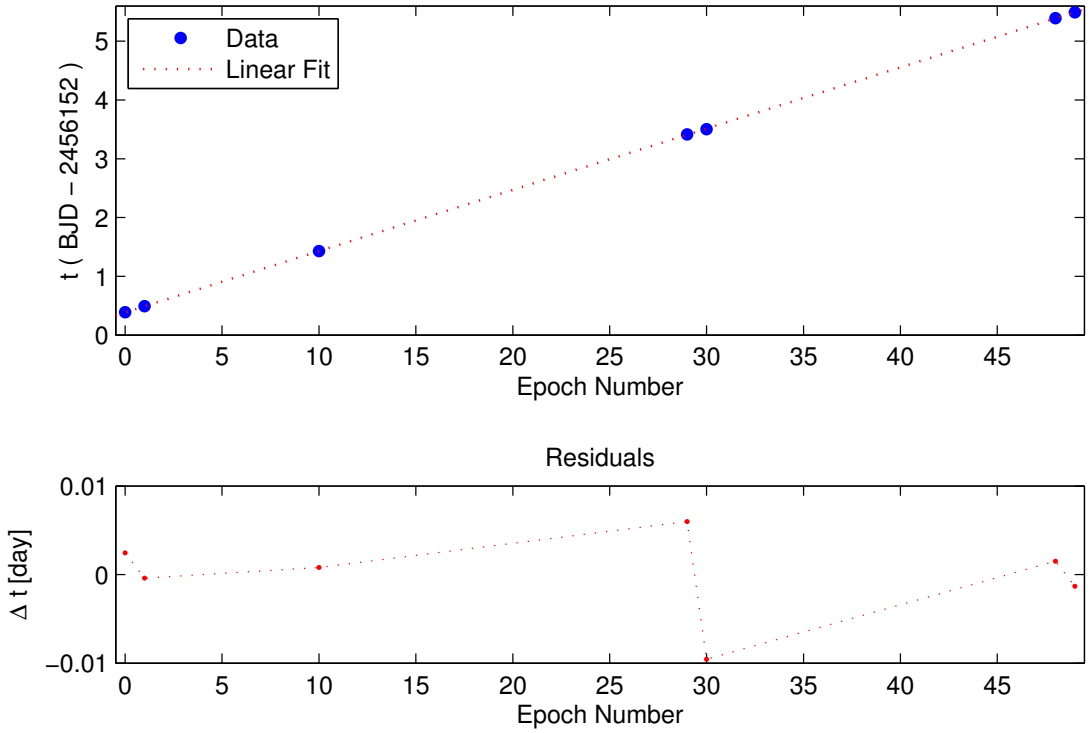

Figure 7. Fit of the CzeV404 superhump period.

BJD	σ (bootstrap)
2456152.38888	+0.00064/−0.00119
2456152.49025	+0.00009/−0.00014
2456153.42948	+0.00023/−0.00036
2456155.41488	+0.00124/−0.00088
2456155.50354	+0.00131/−0.00099
2456157.39060	+0.00042/−0.00071
2456157.49200	+0.00106/−0.00133

Table 4. A summary of CzeV404 superhump maxima used to determine the superhump period.

With the exception on 13 August 2012, stellar eclipses did not overlap with superhump maxima, so they did not affect measurements of the maxima instances. The superhump on 13 August 2012 occurred at the same time as the stellar eclipse, but lasted longer than the eclipse itself. We did not use the data points acquired during the eclipse and calculated the instant of the superhump maximum from the portions of light curve not affected by the eclipse. The resulting superhump period is:

$$BJD_{\rm max} = 2456155.410(5) + 0.1042(1) \times {\rm E}$$

Measurement of both orbital and superhump periods enables calculation of a period excess $\epsilon = P_{\rm sh}/P_{\rm orb} - 1$ (Stolz & Schoembs, 1984), where $P_{\rm sh}$ is the superhump period and $P_{\rm orb}$ is the orbital period.

$$\epsilon = 0.063 \pm 0.001$$

The determined period excess roughly corresponds to the empirical relation between the period excess and the orbital period, given by Olech et al. (2011). However, this relation predicts period excess around 0.05 for the orbital period ∼0.1 days.

Patterson (1998) published an empirical relation between a CV period excess and a system mass ratio $q = M_2/M_1$:

$$\epsilon = \frac{0.23q}{1 + 0.27q}. \quad (1)$$

The resulting mass ratio of CzeV404 is

$$q = 0.30 \pm 0.01.$$

However, according to Olech et al. (2011), that high mass ratio can cause significant problems for establishing regions in 3:1 resonance in the accretion disk, considered to be the source of superhump brightenings. Obviously CzeV404 deserves more observations to gather more data from subsequent superoutbursts, especially periods of superhumps.

Acknowledgments

We thank Ondřej Pejcha for valuable input and advices. We also thank Václav Přibík and Luboš Brát for comments and discussions and Kamil Hornoch for acquiring the high-resolution image of CzeV404.

References:

Brát, L., Pejcha, O., Mikulášek, Z., 2014, in preparation, available at
`http://var2.astro.cz/library/1350745528_ebfit.pdf`
Howell, S. B., Nelson, L. A., & Rappaport, S., 2001, *ApJ*, **550**, 897
Motl, D., 2004, C-MUNIPACK, `http://c-munipack.sourceforge.net/`
Olech, A. et al., 2011, *A&A*, **532**, A64
Patterson, J., 1998, *PASP*, **110**, 1132
Stolz, B., & Schoembs, R., 1984, *A&A*, **132**, 187

COMMISSIONS 27 AND 42 OF THE IAU
INFORMATION BULLETIN ON VARIABLE STARS

Number 6098

Konkoly Observatory
Budapest
13 March 2014

HU ISSN 0374 – 0676

NEW TIMES OF MINIMA OF SOME ECLIPSING VARIABLES

LACY, C. H. S.

Department of Physics, University of Arkansas, Fayetteville, Arkansas 72701, USA; e-mail: clacy@uark.edu

Observatory and telescope:
NFO: NFO WebScope near Silver City, NM, USA (www.nfo.edu); 24-inch classical Cassegrain.

Detector:	**NFO:** 2102×2092 pixels Kodak KAF 4300E CCD cooled to (typ.) –20 °C; 0.78″ square pixels; 27′ square field of view.

Method of data reduction:
Virtual measuring engine (Multi-Measure 2.2) written by C.H.S. Lacy (2013).

Method of minimum determination:
Kwee & van Woerden (1956).

Times of minima:

Star name	Time of min. HJD 2400000+	Error	Type	Filter	Rem.
AP And	56566.8518	0.0001	1	V	NFO
	56567.6454	0.0002	2	V	NFO
	56586.6927	0.0003	2	V	NFO
	56593.8361	0.0003	1	V	NFO
	56597.8046	0.0002	2	V	NFO
	56598.5976	0.0002	1	V	NFO
	56628.7560	0.0005	1	V	NFO
V651 Cas	56638.6427	0.0002	1	V	NFO
V1136 Cyg	56366.9813	0.0019	2	V	NFO
V501 Her	56460.8970	0.0005	2	V	NFO
V501 Mon	56676.6771	0.0009	2	V	NFO

Times of minima:					
Star name	Time of min. HJD 2400000+	Error	Type	Filter	Rem.
V506 Oph	56448.7532	0.0004	2	V	NFO
	56449.8140	0.0002	2	V	NFO
	56450.8728	0.0003	2	V	NFO
V536 Ori	56575.9147	0.0002	1	V	NFO
	56670.6709	0.0004	1	V	NFO
IM Per	56563.8022	0.0005	1	V	NFO
	56572.8197	0.0004	1	V	NFO
	56582.9487	0.0005	2	V	NFO
	56589.7089	0.0004	2	V	NFO
	56600.9805	0.0005	2	V	NFO
	56606.6337	0.0005	1	V	NFO
	56608.8869	0.0003	1	V	NFO
	56668.6047	0.0006	2	V	NFO
	56678.7672	0.0004	1	V	NFO
NP Per	56575.8011	0.0003	1	V	NFO
	56576.9207	0.0010	2	V	NFO
	56586.9412	0.0010	1	V	NFO
	56633.7454	0.0005	1	V	NFO
	56652.6908	0.0016	2	V	NFO
	56661.6048	0.0010	2	V	NFO
	56671.6305	0.0003	1	V	NFO
V482 Per	56588.9787	0.0005	2	V	NFO
	56610.9964	0.0008	2	V	NFO
V514 Per	56646.6443	0.0006	2	V	NFO
BP Vul	56557.7224	0.0002	2	V	NFO

Explanation of the remarks in the table:

NFO refers to the instrumentation (telescope and CCD camera) used.

Remarks:

A sample of the observations has been published by Lacy, Hood & Straughn (2001).

Acknowledgements:

Construction and operation of the NFO telescope were partially funded by the National Science Foundation, the Arkansas Center for Space and Planetary Sciences, the NASA Arkansas Space Grant Consortium, the University of Arkansas, Fayetteville, the University of Arkansas at Little Rock, and the Harvard-Smithsonian Center for Astrophysics. We are grateful to Bill Neely for initial processing of the images and construction, maintenance, and operation of the NFO equipment and software.

References:

Kwee, K., van Woerden, H., 1956, *Bulletin of the Astronomical Institutes of the Netherlands*, **12**, 327

Lacy, C. H. S., Hood, B. & Straughn, A., 2001, *IBVS*, No. 5067

COMMISSIONS 27 AND 42 OF THE IAU
INFORMATION BULLETIN ON VARIABLE STARS

Number 6099

Konkoly Observatory
Budapest
13 March 2014

HU ISSN 0374 – 0676

Previous reports can be found in IBVS 5999.

Date: 10 November 2011

Reported by:
Liakos, A. - Department of Astrophysics, Astronomy and Mechanics, Faculty of Physics, National and Kapodistrian University of Athens, GR 157 84, Panepistimiopolis, Zografos, Athens, Greece, alliakos@phys.uoa.gr
Niarchos, P. - Department of Astrophysics, Astronomy and Mechanics, Faculty of Physics, National and Kapodistrian University of Athens, GR 157 84, Panepistimiopolis, Zografos, Athens, Greece, pniarcho@phys.uoa.gr

Name of the object:

TU UMa

Remarks:

New UBVRI observations of TU UMa are presented. A normal maximum time is derived:

$$\text{Max} = \text{HJD } 2455664.2930\ (4)$$

Date: 5 December 2011

Reported by:
Monninger, G. - Bundesdeutsche Arbeitsgemeinschaft für Veränderliche Sterne e.V. (BAV), Munsterdamm 90, DE-12169 Berlin, Germany, gerold.monninger@online.de
Hoffman, D.I. - Infrared Processing and Analysis Center, California Institute of Technology, Pasadena, CA 91125, USA, dhoffman@ipac.caltech.edu

Name of the object:

GSC 01924-01134

Remarks:

GSC 01924-01134 was identified as a variable object and classified into the variable star class 'Short Period Delta Scuti Candidates' (Hoffman et al., 2009). Our observation confirmed the classification for the first time. GSC 01924-01134 is a high amplitude delta scuti variable (HADS), with a modulation in its light curve. The main period is 0.088535 d.

Date: 7 December 2011

Reported by:
Hojjatpanah, S. - Department of Physics, Biruni Observatory, Shiraz University, P.O.Box 71454, Shiraz, Iran, saeedm31@gmail.com
Zangi, P. - Department of Physics, Biruni Observatory, Shiraz University, P.O.Box 71454, Shiraz, Iran
Khazraei, M. - Astronomical society of Mehr, Shiraz, P.O. Box 71878-35691
Riazi, N. - Department of Physics, Biruni Observatory, Shiraz University, P.O.Box 71454, Shiraz, Iran

Name of the object:

DY Peg

Remarks:

We observed DY Peg during August 2011 at Biruni Observatory of Shiraz University. We used an 11 inch Schmidt-Cassegrain robotic telescope with focal reducer and monochrome DSI pro II as the detector with a cooling system. The observations were carried out in the standard Johnson V band. We had 7 uninterrupted clear nights and ∼7000 FITS images with 30 seconds exposure times were taken. We reduced the data by using dark, bias and flat-field frames. The differential photometry was obtained and HD 218587 ($V = 9\overset{m}{.}80$) was observed as the comparison star. The times of maxima were listed in `6099-t3.txt` calculated by fitting a parabolic curve to the data around the maxima.

Name of the object:

CY Aqr

Remarks:

Observations of CY Aqr were carried out in Johnson's V band during August 2011 at Biruni Observatory. We observed CY Aqr with the same instruments that were mentioned for DY Peg, also the same data reduction and analysis were done on the data for obtaining maximum times. However, the moments of maxima were obtained by third degree polynomial fitting. The star GSC 00567-01826 ($V=12\overset{m}{.}1$) was used as the comparison star. The times of maxima are presented in `6099-t5.txt` which are obtained for 2 nights of observations and ∼2100 good FITS images.

Date: 10 January 2012

Reported by:
Martignoni, Massimiliano - Stazione Astronomica Betelgeuse, Magnago, Milano, Italy, massimiliano.martignoni@alice.it

Name of the object:

KM And

Remarks:

KM And, a possibly RR type variable star, was observed between JD 2455838 and JD 2455890 with a 0.25m Schmidt-Cassegrain Telescope (f/10) of the ,,Stazione Astronomica Betelgeuse" in Magnago, Italy equipped with a 512×512 pixels Kodak KAF261E CCD cooled to (typ.) −20°C; 1.6 arcsec per pixel (1×1 binning); 14'×14' field of view, with BVR_CI_C photometric filters. As comparison and check stars Tycho2 02831-01169-1 and Tycho2 02831-02445-1 were used. A total of 119 measures in (V) and 90 in (R_C) band were collected; reduction to standard photometric system was performed. No evidence of variation has been detected beyond the standard deviation of our measures.

Name of the object:
CI Com
Remarks:
CI Com, type RRC, was observed between JD2455644 and JD2455664 with a 0.25m Schmidt-Cassegrain Telescope (f/10) of the ,,Stazione Astronomica Betelgeuse" in Magnago, Italy equipped with a 512×512 pixels Kodak KAF261E CCD cooled to (typ.) −20°C; 1.6 arcsec per pixel (1×1 binning); 14'×14' field of view, with BVR_CI_C photometric filters. As comparison and check stars Tycho2 00872-00598-1 and 2MASS J12140380+1403031 were used. A total of 251 measures in (V) and 267 in (I_C) band were collected; reduction to standard photometric system was performed. The following new elements have been determined: Max = JD2450925.4670 + $0^d.3599876$ × E.

Name of the object:
V2369 Cyg
Remarks:
V2369 Cyg, type RRC, was observed between JD2453573 and JD2454718 with a 0.2 m Schmidt-Cassegrain Telescope (f/10) of the ,,Stazione Astronomica Betelgeuse" in Magnago, Italy equipped with a 765×510 pixels Kodak KAF401E CCD cooled to (typ.) −20°C; 1.9 arcsec per pixel (2×2 binning); 12'×8' field of view, with BVR_CI_C photometric filters. As comparison and check stars Tycho2 03136-00628-1 and Tycho2 03135-00976-1 were used. A total of 169 measures in (B), 208 in (V), 165 in (R_C) and 132 in (I_C) band were collected; reduction to standard photometric system was performed. The following new elements have been determined: Max = JD2452907.3292 + $0^d.2972438$ × E.

Name of the object:
AV Peg
Remarks:
AV Peg, type RRAB, was observed between JD2453613 and JD2454417 with a 0.2 m Schmidt-Cassegrain Telescope (f/10) of the ,,Stazione Astronomica Betelgeuse" in Magnago, Italy equipped with a 765×510 pixels Kodak KAF401E CCD cooled to (typ.) −20°C; 1.9 arcsec per pixel (2×2 binning); 12'×8' field of view; with BVR_CI_C photometric filters. As comparison and check stars Tycho2 02202-01658-1 and Tycho2 02202-01459-1 were used. A total of 267 measures in (B) and 401 in (V) band were collected; reduction to standard photometric system was performed. The following new elements have been determined: Max = JD2443790.3160 + $0^d.3903788$ × E.

Name of the object:
EV Psc
Remarks:
EV Psc, type RRC, was observed between JD2453350 and JD2455498 with a 0.2 m Schmidt-Cassegrain Telescope (f/10) of the ,,Stazione Astronomica Betelgeuse" in Magnago, Italy equipped with a 765×510 pixels Kodak KAF401E CCD cooled to (typ.) −20°C; 1.9 arcsec per pixel (2×2 binning); 12'×8' field of view; with BVR_CI_C photometric filters. As comparison and check stars Tycho2 00587-00360-1 and Tycho2 00587-00477-1 were used. A total of 246 measures in (V) band were collected; no reduction to standard photometric system was performed. The following new elements have been determined: Max = JD2451463.6800 + $0^d.3062573$ × E.

Date: 27 February 2012

Reported by:
Pollmann, E. - Spektroskopische Arbeitsgemeinschaft ASPA, 51375 Leverkusen, Germany
Mauclaire, B. - Observatoire du Val de l'Arc, Bouches de Rhône 13, France
Bücke, R. - Spektroskopische Arbeitsgemeinschaft ASPA, 21035 Hamburg, Germany

Name of the object:

ζ Tau

Remarks:

The binary Be star ζ Tau shows periodic behaviour in the radial velocity of the HeI 6678 absorption line. We observed zeta Tau from February 2008 until March 2009 at different locations with 20 cm Newton- and 40 cm SC-telescopes, 0.1 and 0.3 Å/pix spectrographs. The spectra have been reduced with standard professional procedures (instr. response, normalisation, wavelength calibration) by using of the program VSPEC.
We started our long-term observing campaign of the HeI 6678 line at the time, when the investigations of Ruzdjak et al. (2009) ended, approximately at JD 2454500. Our findings on the long-term variability of the radial velocity of HeI 6678 is shown in Fig. 1 (113 measurements). We present the results of our period analysis (after subtracting the long-term component fitted by a 3rd order polynomial).

Table 1:

Element	Sol. 3	Sol. 4	Sol. 5	Our result
P (d)	132.92±0.013	133.0±0.034	132.901±0.044	132.2±0.8 AVE 131.3±0.9 SPS
T_{RV} (HJD, 24...)	47016.4±3.6	47027.2±3.5	47027.9±1.3	54608.9
K ($km\,s^{-1}$)	9.74±0.41	7.6±1.2	8.29±0.61	9.1±0.8
rms ($km\,s^{-1}$)	8.09	16.25	4.44	5.94
No. of RVs	801	509	178	113

Columns 2-4: from Ruzdjak et al. (2009), column 5: our results, using the programs AVE and SPS.

As can be seen in Figure 2 and Table 1, our findings are very close to those of Ruzdjak et al. (2009) for the most important parameters. Sometimes significant intensity variations of the continuum in the area of the blue and/or red side, as well within the wings of the HeI 6678 absorption line, are seen. So-called "co-rotating circumstellar clouds and/or matter" in the outer photosphere of the primary could be the cause (Balona & Kaye, 1999). Because of this phenomenon we cannot expect a smooth continuum within this area all the time.

Date: 10 October 2012

Reported by:
Monninger, G. - Bundesdeutsche Arbeitsgemeinschaft für Veränderliche Sterne e.V. (BAV), Munsterdamm 90, DE-12169 Berlin, Germany, gerold.monninger@online.de
Hoffman, D.I. - Infrared Processing and Analysis Center, California Institute of Technology, Pasadena, CA 91125, USA, dhoffman@ipac.caltech.edu

Name of the object:

GSC 01750-01237

Remarks:

The variability of GSC 01750-01237 was discovered by Pojmanski (2002). GSC 01750-01237 was also identified as a variable object and classified into the variable star class 'Short Period/Delta Scuti Candidates' (Hoffman et al., 2009).
GSC 01750-01237 is a high amplitude delta Scuti variable (HADS).
The photometric observations of the variable star were carried out with a SBIG ST10XME CCD camera and V filter attached at a 14 inch cassegrain telescope at f/6 in Gemmingen (Germany).
The revised ephemeris is based on our follow-up observations in 2011 and 6 maxima published in the literature (Wils et al., 2011, 2012). A linear fit to the 16 times of maxima provides the following ephemeris:
HJDmax = 2455824.4952(1) + 0.08697753(6) d * E

Date: 8 January 2013

Reported by:

Nesci, R. - INAF/IAPS, Roma, Italia; e-mail: roberto.nesci@inaf.iaps.it
Falasca, V. - Osservatorio Cittadino, via Bolletta 18, 06034, Foligno, Italia
Villani, L. - Osservatorio Cittadino, via Bolletta 18, 06034, Foligno, Italia
Caravano, A. - Osservatorio Cittadino, via Bolletta 18, 06034, Foligno, Italia
Fantaulli, S. - Osservatorio Cittadino, via Bolletta 18, 06034, Foligno, Italia

Name of the object:

MASTER OT J211322.9+260647.4

Remarks:

We observed the optical transient OT 211322.9+260647.4 (Shurpakov et al. 2012, ATel No. 4675) with the 0.30 m Schmidt-Cassegrain telescope of the Foligno Observatory, equipped with a Nikon D50 camera. Exposure times of 900 s were obtained stacking 30 consecutive frames of 30 seconds each.
Aperture photometry was performed with IRAF/apphot, using a sequence of 32 comparison stars, within 5 arcmin from the source, taken from the UCAC4 catalogue.
The star showed a monotonic decreasing trend of approximately 0.1 mag/day, similar to that observed in the large flare by WZ Sge in 2001 (Patterson et al. 2002). Our observations therefore support the suggestion by Shurpakov et al. (2012) that the source OT 211322.9+260647 is likely a star of the WZ Sge type.

Date: 22 May 2013

Reported by:

Hasanzadeh, A. - The Internatilonal Occultation Timing Association-Middle East section (IOTA-ME); Institute of Geophysics, University of Tehran, Tehran, Iran, iotamiddleeast@yahoo.com
Bay, M. - IOTA-ME
Khaleghi, K. - IOTA-ME
Poro, A. - IOTA-ME

Name of the object:

V873 Per

Remarks:

V873 Per (TYC 2853-18-1, GSC 2853-0018) was discovered by TYCHO-2 as an eclipsing binary (Nicholson and Varley 2006). The V magnitude range is 10.8-11.5 and the variable was identified as an EW type (Samec et al. 2009). The B,V,R light curves were taken at Iranian Space Agency (ISA) observatory in Iran. The phases of the observations were calculated from ephemeris

$$\text{Min I (HJD)} = 2451370.875 + 0.2949039 \times \text{E}(1)$$

given by Samec et al. (2009).

The light curve in filter B shows that transit depths are about the same for primary and secondary transits, even transit depths for secondary (in filter V and R) are deeper than the primary. It can imply starspot activity. The high quality observations can be investigated for this effect.

We determined two times of minimum light from our observations using Kwee & van Woerden method (1956) and are the mean values from B, V and R observations. The derived times of minima in HJD and O−C residuals calculated from Equation 1 are given in the data file.

To improve the ephemeris of V873 Per, we collected all available times of minimum light and listed them in Table 1). The (O−C)1 and (O−C)2 values computed with the old (Equation 1) and new ephemerides, respectively. We calculated the following ephemeris form times of minimum light (except the first one):

Min I (HJD) = 2451370.8993 ($\pm$0.0017) + 0.29490155 ($\pm$0.00000012) $\times$ E (2) The corresponding O−C values were calculated with the new ephemeris (equation 2). The resultant O−C diagrams from times of minima is shown in figures 20 and 21 (available electronically). As displayed in fig. 21, the scatter of new residuals is less, so it can be used for predicting minimum times for V873 Per.

Thanks to: Iranian Space Agency for help and disposal of the ISA observatory in Mahdasht, Iran.

Date: 30 August 2013

Reported by:

Saad, M.S. - National Research Institute of Astronomy and Geophysics (NRIAG), Helwan, Cairo, Egypt, saadmhsaad@gmail.com ; Kottamia Center of Scientific Excellence for Astronomy and Space Sciences

Elkhateeb, M.M. - NRIAG, Helwan, Cairo, Egypt ; Physics Dept., College of Science, Northern Border University, Arar, Saudi Arabia

Shokry, A.A. - NRIAG, Helwan, Cairo, Egypt ; Kottamia Center of Scientific Excellence for Astronomy and Space Sciences

Name of the object:

1SWASP J133105.91+121538.0

Remarks:

We have obtained new light curves with the 1.8m Kottamia optical telescope using a 2Kx2K CCD camera in BVRI filters for the short period eclipsing binary 1SWASP J133105.91+121538.0.

New timings of one primary and one secondary minimum were obtained for each filter using the Kwee & Van Woerden (1956) method. A new ephemeris was determined from the present time of minimum.

HJD $T_{\rm Min}$I=2456417.31329+$0^{\rm d}$.21801× E.

HJD	Error	Filter	Min
2456417.31311	0.00008	B	I
2456417.31329	0.00004	V	I
2456417.31337	0.00007	R	I
2456417.31337	0.00011	I	I
2456417.42178	0.00001	B	II
2456417.42190	0.00008	V	II
2456417.42211	0.00006	R	II
2456417.42235	0.00010	I	II

This research has made use of Science and Technology Development Fund (STDF) N5217, Academy of Scientific Research and Technology (ASRT), Cairo, Egypt. and Kottamia Center of Scientific Excellence for Astronomy and Space Sciences (KCSE_ASSc), National Research Institute of Astronomy and Geophysics (NRIAG).

Date: 16 October 2013

Reported by:

Nilforoushan, M. - Mahdasht Observatory of Iranian Space Agency (ISA), Alborz, Iran; Department of Physics, Zanjan University, Zanjan, Iran, nilforoushan@znu.ac.ir

Asadishad, T. - Mahdasht Observatory of Iranian Space Agency (ISA), Alborz, Iran; Faculty of Physics, Shahid Beheshti University, Evin, Tehran, Iran, asadishad@sbu.ac.ir

Name of the object:

EG Cep

Remarks:

Observation of EG Cep was carried out at the Iranian Space Agency (ISA) Observatory, with a Meade 16″ 0.4-m f/10 Schmidt-Cassegrain telescope on Paramount GT-1100 mount at Mahdasht, Alborz province. The used detector was a 2745×4008 pixels CCD SBIG STL-11000M ($9\times9\mu m$), with a $20\farcm9\times30\farcm5$ FOV, cooled to -10° Celsius.
Reduction of the CCD images was done with the IRAF package. The Sky 6.0, SBIG CCDOps v5.51 and IRIS v5.59 were used for aperture photometry.
The minimum times were computed by parabolic fit with the Kwee - van Woerden algorithm (1956) and TableCurve v5.01 for parallel activity around minimum times.

Star name	**Time of min.** HJD 2400000+	**Error**	**Type**	**Filter**	$O-C$ [day]	**Rem.**
EG Cep	56167.459013	0.00014	I	BVR	0.011518	NM/AT
	56191.422608	0.00024	I	BVR	0.011336	NM/AT
	56192.252530	0.00051	II	BVR	0.025789	NM/AT
	56193.352083	0.00170	II	BVR	0.034799	NM/AT

Observers: NM ∼ Mohammad Nilforoushan; AT ∼ Tannaz Asadishad.

More than 1630 observations in standard Morgan-Johnson BVR filters were made at the Iranian Space Agency (ISA) Observatory to characterize the light curve.
The amplitude of the star was found to be $0\overset{\mathrm{m}}{.}92$ in the R filter, $0\overset{\mathrm{m}}{.}96$ in the V filter and $1\overset{\mathrm{m}}{.}00$ in the B filter. Comparison/check stars were HD 194400 (F8, $V = 9.72$) and HD 194130 (F2, $V = 8.87$), respectively. The exposure time was 4 seconds. Standard deviations of the comparison/check star magnitudes were less than $0\overset{\mathrm{m}}{.}04$.
We used O-C data from Mallama (1980) and Nelson (2012) along with our new measurements to derive an updated ephemeris and period for this system:

$$\text{Min. I} = \text{HJD } 2440050.4551(\pm10^{-4}) + 0\overset{\mathrm{d}}{.}54462168(\pm4\times10^{-8})\times E$$

The epoch and period above was adopted from the latest and best times of minima that reported in last years.

Acknowledgements: We would like to thank the contributions of Mr. Hasanzadeh. We also acknowledge the partial support by the Iranian Space Agency and the Alborz - Mahdasht Space Center Observatory Branch.

Date: 16 October 2013

Reported by:
Behre, Otto Peter - Hamburger Sternwarte, Univ. Hamburg, Germany, opbehre@t-online.de
Hünsch, Matthias - Hamburger Sternwarte, Univ. Hamburg, Germany, matthias@huensch.de

Name of the object:

RZ CrB

Remarks:
The star has been identified by Shapley (1923) as variable, by Bond (1978) as an F0-star and by Drake et al. (2013) as an RRab Lyrae-star. From 2010-06-17 to 2013-07-01 we performed 424 observations in V, 151 observations in B, and 173 observations in R. Corrected for atmospheric and interstellar extinction we obtained maximum magnitudes of $B = 14.177$, $V = 13.891$ and $R = 13.930$ and minimum values of $B = 15.699$, $V = 15.105$ and $R = 14.935$. Accordingly, T_{eff} changes between $\approx$ 6150 K at minimum and $\approx$ 7500 K at maximum. Combining our observations with those of Drake et al. for $\mathrm{MJD_{Peak}} = 53479.90060$ we derive a period of 0.49637155d. The difference to the period given by Drake et al. from observations in 2005-2011 is smaller than -0.3 s and to our observations from 2010-2013 is smaller than $+0.1$ s. The period of RZ CrB seems to be rather constant. The lightcurves and these values support the classification as an RRab-Lyrae-star with a minimum at JD = 2456474.951 + 0.49637155×E at a distance of 6.15 kpc ± 0.44 kpc.

Date: 11 March 2011
Reported by:
Liakos, A. - National Observatory of Athens, Palaia Penteli, Athens, Greece, alliakos@noa.gr Niarchos, P. - National and Kapodistrian University of Athens, Zografos, Athens, Greece, pniarcho@phys.uoa.gr

Name of the object:
GSC 3159-1188
Remarks:
Detected in the FoV of V1187 Cyg and V1191 Cyg

References:

Balona, L. A., Kaye, A. B., 1999, *ApJ*, **521**, 407
Bond, H.E., 1978, *PASP*, **90**, 526
B.R.N.O. Project – Variable Star and Exoplanet Section of Czech Astronomical Society : `http://var2.astro.cz/EN/brno/index.php`
Diethelm, R., 2010, IBVS, No. 5920
Diethelm, R., 2011, IBVS, No. 5960
Diethelm, R., 2012, IBVS, No. 6011
Diethelm, R., 2013, IBVS, No. 6042
Drake, A.J., Catelan, M., Djorgovski, S.G., et al., 2013, *ApJ*, **763**, 32
Hoffman, D.I. et al., 2009, *AJ*, **138**, 466
Kwee, K. K., Van Woerden, H., 1956, *BAN*, **12**, 327
Mallama, A. D., 1980, *ApJS*, **44**, 241
Nagai, K., 2013, *VSOLJ*, No. **55**
Nelson, R. H., 2012, *Bob Nelson's O-C Files*, `http://binaries.boulder.swri.edu/binaries/omc/`
Nicholson, M., Varley, H., 2006, IBVS, No. 5700
Patterson, J., Masi, G., Richmond, M.W., et al. 2002, *PASP*, **114**, 721
Pojmanski, G. 2002, *Acta Astronomica*, **52**, 397
Ruzdjak, D. et al., 2009, *A&A*, **506**, 1319
Samec, R.G. et al., 2009, IBVS, No. 5901
Shapley, H., 1923, *Harvard Bulletin*, **791**
Shurpakov, S., Desinenko, D., Balanutsa, P., et al. 2012, *ATel*, 4675
Wils, P. et al. 2011, IBVS No. 5977
Wils, P. et al. 2012, IBVS No. 6015

Zacharias N., Finch C.T., Girard T.M., Henden A., Bartlet J.L., Monet D.G., Zacharias M.I. 2012, The fourth U.S. Naval Observatory CCD Astrograph Catalog (UCAC4).

ERRATUM FOR IBVS 6099

Report No. 10., 2013 October 16., by Nilforoushan et al.

Editor's notice: The president of the IOTA/ME reported that these observations were already published in the local IOTA/ME paper Journal on Occultation and Eclipse (JOE, 2013, No. 29, pp. 20-21.) but the derived O-C values differ from the ones listed in this report.

COMMISSIONS 27 AND 42 OF THE IAU
INFORMATION BULLETIN ON VARIABLE STARS

Number 6100

Konkoly Observatory
Budapest
13 March 2014

HU ISSN 0374 – 0676

Previous reports can be found in

Date: 27 September 2011

Observer(s) and affiliation(s):
Monninger, G. - Bundesdeutsche Arbeitsgemeinschaft für Veränderliche Sterne e.V. (BAV), Munsterdamm 90, DE-12169 Berlin, Germany, gerold.monninger@online.de

RA(J2000)	**Dec(J2000)**	**type**	**Mag.**
22 07 15.50	+41 11 56.9	DSCT	11.93 (Vmag - GSC2.3)

Period	**Epoch**
0.07855(1) d	2455805.4193(7)

Cross-identification(s):
GSC 3202-0370 = USNO-A2.0 1275-17055482 = USNO-B1.0 1311-0458390 = Tycho-2 3202-00370-1 = 2MASS 22071548+4111573 = GSC2.3 N2XB000049

Date: 8 December 2011

Observer(s) and affiliation(s):
Liakos, A. - Department of Astrophysics, Astronomy and Mechanics, National and Kapodistrian University of Athens, Panepistimioupolis, GR-157 84, Zografos, Athens, Hellas, alliakos@phys.uoa.gr
Niarchos, P. - Department of Astrophysics, Astronomy and Mechanics, National and Kapodistrian University of Athens, Panepistimioupolis, GR-157 84, Zografos, Athens, Hellas, pniarcho@phys.uoa.gr

Remark: Detected in the FoV of V482 Per.

RA(J2000)	**Dec(J2000)**	**type**	**Mag.**
04 15 44.8	+47 29 18.2	DSCT	B=10.677 mag (The Hipparcos and Tycho Catalogues)

Period	**Epoch**
1.08095 h	-

Cross-identification(s):
GSC 3332-0388 = TYC 3332-0388-1 = USNO-A2.0 1350-04385880

Remark: Detected in the FoV of TW Lac and V413 Lac

RA(J2000)	**Dec(J2000)**	**type**	**Mag.**
22 30 02.3	+54 46 57.9	DSCT	B=13.9 mag (The USNO-A2.0 Catalogue)

Period	**Epoch**
1.27973 h	-

Cross-identification(s):
GSC 3987-1298 = USNO-A2.0 1425-13529111

Remark: Detected in the FoV of QX And

RA(J2000)	**Dec(J2000)**	**type**	**Mag.**
01 57 12.04	+37 54 35.9	DSCT	R=15.5 mag (The USNO-A2.0 Catalogue)

Period	**Epoch**
2.792904 h	-

Cross-identification(s):
USNO-A2.0 1275-01165814

Date: 13 January 2012

Observer(s) and affiliation(s):
Martignoni, Massimiliano - Stazione Astronomica Betelgeuse, Magnago, Milano, Italy, massimiliano.martignoni@alice.it

Remark: UCAC3 276-106147 is an EW type eclipsing binary in the field of view of TV Lyn.

RA(J2000)	**Dec(J2000)**	**type**	**Mag.**
07 34 16.6	47 54 02.4	EW	14.15-14.75 (V)

Period	**Epoch**
0.3150905d	2455933.5083

Cross-identification(s):
UCAC3 276-106147

Date: 20 February 2012

Observer(s) and affiliation(s):
Monninger, G. - Bundesdeutsche Arbeitsgemeinschaft für Veränderliche Sterne e.V. (BAV), Munsterdamm 90, DE-12169 Berlin, Germany, gerold.monninger@online.de

Remark: In the field of the high amplitude delta scuti variable (HADS) GSC 01924-01134 (this IBVS issue, Monninger, 2011). USNO-B1.0 1191-0155860 is listed in the Catalogue of SDSS BHB candidates (Smith et al., 2010). A modulation in the light curve was observed.

RA(J2000)	**Dec(J2000)**	**type**	**Mag.**
07 44 07.84	+29 08 20.12	RRab	15.92 (Vmag - GSC2.3)

Period	**Epoch**
0.45283(1) d	2455887.611(1)

Cross-identification(s):
USNO-B1.0 1191-0155860 = USNO-A2.0 1125-05322478 = 2MASS 07440785+2908199 = GSC2.3 N8R3014149

Date: 4 June 2012

Observer(s) and affiliation(s):
Hümmerich, Stefan - Bundesdeutsche Arbeitsgemeinschaft für Veränderliche Sterne e.V. (BAV), Munsterdamm 90, DE-12169 Berlin, Germany, ernham@rz-online.de
Bernhard, Klaus - Bundesdeutsche Arbeitsgemeinschaft für Veränderliche Sterne e.V. (BAV), Munsterdamm 90, DE-12169 Berlin, Germany, klaus.bernhard@liwest.at

Remark: GSC 02504-01101 (2MASS J-K = 0.264) has been identified as a double-mode RR Lyrae (RRd) star by analysis of CRTS data (Drake et al., 2009) with Period04 (Lenz et al., 2005):

	frequency (c/d)	semi-amplitude (mag)	
F1	2.9274089	0.1759	(first overtone)
F2	2.1747158	0.1423	(fundamental)
F3	5.1021296	0.0564	(F1+F2)
F4	4.3494536	0.0419	(2F2)

With a fundamental period of 0.4598 d, the star is near the lower edge of known RRd stars in the Petersen diagram; the ratio F2/F1=0.743 is in agreement with other RRd variables. GSC 02504-01101 is listed in the Catalogue of SDSS BHB candidates (Smith et al., 2010).

RA(J2000)	**Dec(J2000)**	**type**	**Mag.**
09 40 51.026	+34 52 05.32	RRd	14.69 (Vmag - GSC)

Period	**Epoch**
0.4598 d	-

Cross-identification(s):
GSC 02504-01101 = USNO-B1.0 1248-0174773 = 2MASS J09405102+3452053 = WISE J094051.03+345205.3 = CSS_J094051.0+345205

Date: 12 June 2012

Observer(s) and affiliation(s):
Bernhard, Klaus - Bundesdeutsche Arbeitsgemeinschaft für Veränderliche Sterne e.V. (BAV), Munsterdamm 90, DE-12169 Berlin, Germany, klaus.bernhard@liwest.at
Hümmerich, Stefan - Bundesdeutsche Arbeitsgemeinschaft für Veränderliche Sterne e.V. (BAV), Munsterdamm 90, DE-12169 Berlin, Germany, ernham@rz-online.de

Remark: USNO-B1.0 1221-0206959 (2MASS J-K = 0.119) has been identified as a double-mode RR Lyrae (RRd) star by analysis of CRTS data (Drake et al., 2009) with Period04 (Lenz et al., 2005):

	frequency (c/d)	semi-amplitude (mag)	
F1	2.66122	0.1944	(first overtone)
F2	1.98192	0.1006	(fundamental)
F3	5.32245	0.0424	(2F1)
F4	4.64316	0.0443	(F1+F2)

Analysis and folded lightcurves were based on CRTS data from HJD 2453481 to 2455358 as the period is possibly variable. With a fundamental period of 0.50456 d, the star is situated in the middle of the Petersen diagram; the ratio F1/F2=0.745 is in agreement with other RRd variables. USNO-B1.0 1221-0206959 is listed in the Catalogue of SDSS BHB candidates (Smith et al., 2010).

RA(J2000)	**Dec(J2000)**	**type**	**Mag.**
09 30 44.097	+32 09 16.83	RRd	15.27 (Vmag - NOMAD)

Period	**Epoch**
0.50456 d	-

Cross-identification(s):
USNO-B1.0 1221-0206959 = UCAC3 245-100368 = 2MASS J09304409+3209168 = WISE J093044.10+320917.1 = CSS_J093044.1+320916

Date: 23 July 2012

Observer(s) and affiliation(s):
Nelson, R.H. - Sylvester Robotic Observatory, Prince George, BC, Canada, bob.nelson@shaw.ca
Lubcke, G. - 1400 E Washington Ave, Madison, WI 53703, lubcke@tds.net

Remark: In the vicinity of V471 Cas.

RA(J2000)	**Dec(J2000)**	**type**	**Mag.**
01 32 32.8	+55 15 26.23	EW	13.43 (R mag = GSC2.3)

Period	**Epoch**
0.2409532(2)	2455937.5483(12)

Cross-identification(s):
GSC 3674-1587

Date: 15 August 2012

Observer(s) and affiliation(s):
Bernhard, Klaus - Bundesdeutsche Arbeitsgemeinschaft für Veränderliche Sterne e.V. (BAV), Munsterdamm 90, DE-12169 Berlin, Germany, klaus.bernhard@liwest.at
Hümmerich, Stefan - Bundesdeutsche Arbeitsgemeinschaft für Veränderliche Sterne e.V. (BAV), Munsterdamm 90, DE-12169 Berlin, Germany, ernham@rz-online.de

Remark: USNO-B1.0 1220-0275842 (2MASS J-K = 0.193) has been identified as a double-mode RR Lyrae (RRd) star by analysis of CRTS data (Drake et al., 2009) with Period04 (Lenz et al., 2005):

	frequency (c/d)	period (d)	semi-amplitude (mag)	epoch (max)	
F1	2.857841	0.349914	0.196	2456018.599	(first overtone)
F2	2.124844	0.470622	0.170	2456018.684	(fundamental)

With a fundamental period of 0.470622 d, the star is near the lower edge of known RRd stars in the Petersen diagram; the ratio F2/F1=0.7435 is in agreement with other RRd variables. No linear combination modes could be found in the data. USNO-B1.0 1220-0275842 is listed in the Catalogue of SDSS BHB candidates (Smith et al., 2010).

RA(J2000)	**Dec(J2000)**	**type**	**Mag.**
15 16 09.239	+32 00 07.27	RRd	15.77 - 16.45 (CV - CRTS)

Period	**Epoch**
0.470622 d	-

Cross-identification(s):
USNO-B1.0 1220-0275842 = UCAC4 611-051459 = 2MASS J15160921+3200073 = WISE J151609.21+320007.3 = CSS_J151609.2+320007

Date: 15 August 2012

Observer(s) and affiliation(s):
Hümmerich, Stefan - Bundesdeutsche Arbeitsgemeinschaft für Veränderliche Sterne e.V. (BAV), Munsterdamm 90, DE-12169 Berlin, Germany, ernham@rz-online.de
Bernhard, Klaus - Bundesdeutsche Arbeitsgemeinschaft für Veränderliche Sterne e.V. (BAV), Munsterdamm 90, DE-12169 Berlin, Germany, klaus.bernhard@liwest.at

Remark: GSC 02015-00233 (2MASS J-K = 0.225) has been identified as a double-mode RR Lyrae (RRd) star by analysis of CRTS data (Drake et al., 2009) with Period04 (Lenz et al., 2005):

	frequency (c/d)	period (d)	semi-amplitude (mag)	epoch (max)	
F1	2.709041	0.369134	0.187	2456042.399	(first overtone)
F2	2.01935	0.495208	0.062	2456042.233	(fundamental)

With a fundamental period of 0.495208 d, the star is situated in the middle of known RRd stars in the Petersen diagram; the ratio F2/F1=0.745 is in agreement with other RRd variables. No linear combination modes could be found in the data. GSC 02015-00233 is listed in the Catalogue of SDSS BHB candidates (Smith et al., 2010).

RA(J2000)	**Dec(J2000)**	**type**	**Mag.**
14 31 30.858	+22 50 23.37	RRd	15.34 - 15.87 (CV - CRTS)

Period	**Epoch**
0.495208 d	-

Cross-identification(s):
GSC 02015-00233 = USNO-B1.0 1128-0282033 = UCAC4 565-051392 = 2MASS J14313085+2250234 = WISE J143130.85+225023.3 = CSS_J143130.9+225023

Date: 15 August 2012

Observer(s) and affiliation(s):
Hümmerich, Stefan - Bundesdeutsche Arbeitsgemeinschaft für Veränderliche Sterne e.V. (BAV), Munsterdamm 90, DE-12169 Berlin, Germany, ernham@rz-online.de
Drake, A.J. - Catalina Real-Time Transient Survey

Remark: UCAC4 position. J-K=0.216 (2MASS). Rise duration: 39%. USNO-B1.0 1185-0218778 is listed in the Catalogue of SDSS BHB candidates (Smith et al., 2010).

RA(J2000)	**Dec(J2000)**	**type**	**Mag.**
14 20 31.084	+28 31 25.59	RRc	14.98 - 15.50 (CV)

Period	**Epoch**
0.291608 d	2453479.80

Cross-identification(s):
USNO-B1.0 1185-0218778 = UCAC4 593-052447 = 2MASS J14203110+2831255 = WISE J142031.08+283125.6 = CSS_J142031.1+283125

Remark: UCAC4 position. J-K=0.339 (2MASS). Rise duration: 11%. USNO-B1.0 1047-0235244 is listed in the Catalogue of SDSS BHB candidates (Smith et al., 2010).

RA(J2000)	**Dec(J2000)**	**type**	**Mag.**
14 36 37.890	+14 47 49.16	RRab	15.17 - 16.13 (CV)

Period	**Epoch**
0.523764 d	2455365.745

Cross-identification(s):
USNO-B1.0 1047-0235244 = UCAC4 524-056277 = 2MASS J14363788+1447491 = WISE J143637.88+144749.1 = CSS_J143637.9+144749

Remark: UCAC4 position. J-K=0.556 (2MASS). Rise duration: 13%. USNO-B1.0 1014-0232010 is listed in the Catalogue of SDSS BHB candidates (Smith et al., 2010).

RA(J2000)	**Dec(J2000)**	**type**	**Mag.**
14 45 59.525	+11 28 07.26	RRab	15.52 - 16.60 (CV)

Period	**Epoch**
0.499028 d	2454515.932

Cross-identification(s):
USNO-B1.0 1014-0232010 = UCAC4 508-058222 = 2MASS J14455953+1128071 = WISE J144559.53+112807.1 = CSS_J144559.5+112807

Remark: 2MASS position. J-H=0.084 (2MASS; J-H value given as Kmag is flagged as being of bad quality.) Rise duration: 15%. USNO-B1.0 1138-0226755 is listed in the Catalogue of SDSS BHB candidates (Smith et al., 2010).

RA(J2000)	**Dec(J2000)**	**type**	**Mag.**
15 35 21.609	+23 53 50.07	RRab	15.60 - 16.62 (CV)

Period	**Epoch**
0.526759 d	2453560.740

Cross-identification(s):
USNO-B1.0 1138-0226755 = 2MASS J15352160+2353500 = WISE J153521.60+235350.1 = CSS_J153521.6+235350

Remark: UCAC4 position. J-K=0.277 (2MASS). Rise duration: 14%. USNO-B1.0 1060-0220956 is listed in the Catalogue of SDSS BHB candidates (Smith et al., 2010).

RA(J2000)	**Dec(J2000)**	**type**	**Mag.**
14 26 44.107	+16 04 57.82	RRab	15.00 - 16.14 (CV)

Period	**Epoch**
0.457791 d	2455351.779

Cross-identification(s):
USNO-B1.0 1060-0220956 = UCAC4 531-055289 = 2MASS J14264411+1604579 = WISE J142644.11+160457.8 = CSS_J142644.1+160457

Remark: UCAC4 position. J-K=0.291 (2MASS). Rise duration: 13%. USNO-B1.0 1360-0241542 is listed in the Catalogue of SDSS BHB candidates (Smith et al., 2010).

RA(J2000)	**Dec(J2000)**	**type**	**Mag.**
14 47 06.527	+46 02 13.79	RRab	14.49 - 15.66 (CV)

Period	**Epoch**
0.481240 d	2454905.952

Cross-identification(s):
USNO-B1.0 1360-0241542 = UCAC4 681-055635 = 2MASS J14470651+4602136 = WISE J144706.53+460213.7 = CSS_J144706.6+460213

Date: 14 January 2013

Observer(s) and affiliation(s):
Hümmerich, S. - Bundesdeutsche Arbeitsgemeinschaft für Veränderliche Sterne e.V. (BAV), Munsterdamm 90, DE-12169 Berlin, Germany, ernham@rz-online.de

Remark: GSC 00330-01491 has been identified as an RRc star by analysis of CRTS data (Drake et al., 2009). UCAC4 position. $J - K = 0.073$ (2MASS; Skrutskie et al., 2006). Rise duration: 47GSC 00330-01491 is listed in the Catalogue of SDSS BHB candidates (Smith et al., 2010).

RA(J2000)	**Dec(J2000)**	**type**	**Mag.**
14 59 54.942	+04 44 26.04	RRc	14.26 - 14.67 (CV)

Period	**Epoch**
0.352039 d	2453904.783

Cross-identification(s):
GSC 00330-01491 = USNO-B1.0 0947-0233808 = UCAC4 474-052391 = 2MASS J14595492+0444259 = WISE J145954.93+044425.9 = CSS_J145954.9+044426

Remark: USNO-B1.0 0994-0247663 has been identified as an RRc star by analysis of CRTS data (Drake et al., 2009). UCAC4 position. $J - K$=0.265 (2MASS; Skrutskie et al., 2006). Rise duration: 39USNO-B1.0 0994-0247663 is listed in the Catalogue of SDSS BHB candidates (Smith et al., 2010).

RA(J2000)	**Dec(J2000)**	**type**	**Mag.**
15 47 24.001	+08 44 34.63	RRab	14.72 - 15.83 (CV)

Period	**Epoch**
0.501280 d	2453818.922

Cross-identification(s):
USNO-B1.0 0994-0247663 = UCAC4 498-063752 = 2MASS J15060750+0926369 = WISE J150607.50+092636.9 = CSS_J150607.5+092636

Remark: USNO-B1.0 1049-0245939 has been identified as an RRc star by analysis of CRTS data (Drake et al., 2009). UCAC4 position. $J - K$=0.183 (2MASS; Skrutskie et al., 2006). Rise duration: 40USNO-B1.0 1049-0245939 is listed in the Catalogue of SDSS BHB candidates (Smith et al., 2010).

RA(J2000)	**Dec(J2000)**	**type**	**Mag.**
15 37 26.810	+14 56 58.31	RRc	15.18 - 15.64 (CV)

Period	**Epoch**
0.362629 d	2454346.644

Cross-identification(s):
USNO-B1.0 1049-0245939 = UCAC4 525-059342 = 2MASS J15372680+1456583 = WISE J153726.79+145658.2 = CSS_J153726.8+145658

Date: 7 February 2013

Observer(s) and affiliation(s):
Martignoni, Massimiliano - "Stazione Astronomica Betelgeuse", Magnago, Milano, Italy, massimiliano.martignoni@alice.it

Remark: TYC 5378-1590-1 is an EA type eclipsing binary in the field of view of DV Mon. It was observed with a 0.25m Schmidt-Cassegrain Telescope (f/10) of the "Stazione Astronomica Betelgeuse" in Magnago, Italy equipped with a 512x512 pixels Kodak KAF261E CCD cooled to (typ.) -20C; 1.6 arcsec per pixel (1x1 binning); 14'x14' field of view, with a V photometric filter. Reduction to standard photometric system was performed. As comparison and check stars were used UCAC4 406-017649 (V=11.47) and UCAC4 406-017634 (V=12.79). Using also V magnitude data coming from the All Sky Automated Survey (ASAS), a total of 916 measures were collected. The star shows a secondary minimum approximately at phase 0.70.

RA(J2000)	**Dec(J2000)**	**type**	**Mag.**
06 45 43.95	-08 50 35.6	EA	10.85-11.50 (V)

Period	**Epoch**
3.73235d	2456263.980

Cross-identification(s):
TYC 5378-1590-1 = UCAC4 406-017746

Date: 25 March 2013

Observer(s) and affiliation(s):
Nelson, R.H. - 1393 Garvin St., Prince George, BC, V2M 3Z1 Canada, bob.nelson@shaw.ca
Lubcke, Gil - 6816 South Avenue, Middleton, Wisconsin, 53562. USA, lubcke@tds.net
Molnar, Larry - Calvin College, Grand Rapids, MI, 49546-4403, lmolnar@calvin.edlu

Remark: Star was discovered to be variable by R.H. Nelson on 2012-10-10 while observing GSC 4267-0682. He obtained a light curve around a primary minimum in R (Cousins). Follow-up data was acquired by G. Lubcke and L. Molnar. The latter discovered the period and obtained a largely full light curve in R (Cousins) with some additional data in V.

RA(J2000)	**Dec(J2000)**	**type**	**Mag.**
22 05 43.480	+61 55 18.835	EA	B mag = 11.06, V mag = 10.81 (SIMBAD)

Period	**Epoch**
2.6334576 d	2456297.54746

Cross-identification(s):
GSC 4267-0588 = TYC 4267-588-1 = 2MASS J22054347+6155189

Date: 23 August 2013
Observer(s) and affiliation(s): Srdoc, Gregor - Sarsoni 90 Viskovo, Croatia, gregor@vip.hr Frank, Peter - Bundesdeutsche Arbeitsgemeinschaft für Veränderliche Sterne e.V. (BAV), Munsterdamm 90, DE-12169 Berlin, Germany, frank.velden@t-online.de Hümmerich, Stefan - Bundesdeutsche Arbeitsgemeinschaft für Veränderliche Sterne e.V. (BAV), Munsterdamm 90, DE-12169 Berlin, Germany, ernham@rz-online.de Bernhard, Klaus - Bundesdeutsche Arbeitsgemeinschaft für Veränderliche Sterne e.V. (BAV), Munsterdamm 90, DE-12169 Berlin, Germany, Klaus.Bernhard@liwest.at

Remark: GSC 02075-01605 has been discovered as a candidate variable star by investigation of light curves from the SuperWASP public archive (Butters et al., 2010). Follow-up observations by G. Srdoc (V filter; 19 nights; black circles in folded light curve) and P. Frank ($-IR$ filter; 2 nights; grey circles) indicate that GSC 02075-01605 is a DSCT variable. $J-K$=0.101 (2MASS; Skrutskie et al., 2006). Positional information was drawn from the UCAC4 catalogue (Zacharias et al., 2013). The difference in mean magnitude between the two datasets results from the use of different filters and telescope systems. The given magnitude range has been derived from G. Srdoc's observations because of the use of a V-filter.

RA(J2000)	**Dec(J2000)**	**type**	**Mag.**
17 28 31.533	+22 34 18.93	RRab	13.15 - 13.45 (CV)

Period	**Epoch**
0.049113 d	2456462.4354

Cross-identification(s):
GSC 02075-01605 = UCAC4 563-061083 = 2MASS 17283152+2234189

Date: 9 September 2013
Observer(s) and affiliation(s): Nelson, Robert H. - Sylvester Robotic Observatory, Prince George, BC, Canada bob.nelson@shaw.ca Buchheim, Robert - Altimira Observatory (minor planet center observatory code G76) Bob@kbuchheim.org

Remark: Minima Determination: Fourier 5-term fit (Nelson), Kwee & van Woerden (both).

RA(J2000)	**Dec(J2000)**	**type**	**Mag.**
23 00 07.0183	+30 39 17.709	EA	14.07 (USNO A2.0: B=15.2, R=13.8)

Period	**Epoch**
0.47187 (2) d	2456530.5060(6)

Cross-identification(s):
GSC 2750-0054 = USNO A2.0 1200-19628029

Date: 25 September 2013
Observer(s) and affiliation(s): Nelson, Robert H. - Sylvester Robotic Observatory, Prince George, BC, Canada bob.nelson@shaw.ca Buchheim, Robert - Altimira Observatory (minor planet center observatory code G76) Bob@kbuchheim.org

RA(J2000)	**Dec(J2000)**	**type**	**Mag.**
23 00 00.8628	+30 39 00.458	EB?	13.58 (USNO A2.0: B=14.5, R=13.1)

Period	**Epoch**
0.2991 (1) d	56529.9697 (36)

Cross-identification(s):
GSC 2750-1476 = USNO A2.0 1200-19626931

Date: 17 January 2014
Observer(s) and affiliation(s): Martignoni, Massimiliano - Stazione Astronomica Betelgeuse, Magnago, Milano, Italy, massimiliano.martignoni@alice.it

RA(J2000)	**Dec(J2000)**	**type**	**Mag.**
22 10 27.06	+55 09 29.7	EB	13.17 (0.04) ± 0.02 (V)

Period	**Epoch**
0.181378 d	2 456 185.220

Cross-identification(s):
UCAC4 726-082768

Remark: UCAC4 726-082768 is an EB type eclipsing binary type variable star in the field of view of KM Cep. It was observed with a 0.25 m Schmidt-Cassegrain telescope (f/10) of the Stazione Astronomica Betelgeuse in Magnago, Italy equipped with a 512×512 pixels Kodak KAF261E CCD cooled to (typ.) −20°C; 1.6 arcsec per pixel (1×1 binning); 14′×14′ field of view, with V photometric filter. As comparison and check stars were used UCAC4 726-082801 and UCAC4 726-082806. A total of 380 measures in V band were collected; reduction to the standard photometric system was not performed.

Date: 29 January 2014
Observer(s) and affiliation(s): Martignoni, Massimiliano - Stazione Astronomica Betelgeuse, Magnago, Milano, Italy, massimiliano.martignoni@alice.it

RA(J2000)	**Dec(J2000)**	**type**	**Mag.**
22 10 29.04	+55 09 01.2	L:	14.5: (0.5:) (V)

Period	**Epoch**

Cross-identification(s):
UCAC4 726-082786

Remark: UCAC4 726-082786 is an L: type variable star in the field of view of KM Cep. It was observed with a 0.25 m Schmidt-Cassegrain telescope (f/10) of the Stazione Astronomica Betelgeuse in Magnago, Italy equipped with a 512×512 pixels Kodak KAF261E CCD cooled to (typ.) −20°C; 1.6 arcsec per pixel (1×1 binning); 14′×14′, with V photometric filter. As comparison and check stars were used UCAC4 726-082801 and UCAC4 726-082806. A total of 396 measures in V band were collected; reduction to the standard photometric system was not performed.

Date: 27 February 2014
Observer(s) and affiliation(s): Liakos, A. - National Observatory of Athens, Institute for Astronomy & Astrophysics, Space Applications & Remote Sensing, I. Metaxa & Vas. Pavlou St., GR-152 36, Palaia Penteli, Athens, Greece, alliakos@noa.gr Niarchos, P. - Department of Astrophysics, Astronomy and Mechanics, National and Kapodistrian University of Athens, Panepistimioupolis, GR-157 84, Zografos, Athens, Greece, pniarcho@phys.uoa.gr

RA(J2000)	**Dec(J2000)**	**type**	**Mag.**
18 42 29	+08 58 35	CV or SR	11.2 (V)

Period	**Epoch**
	Multiperiodic

Cross-identification(s):
GSC 1025-0798 = TYC 1025-798-1 = 2MASS J18422913+0858346

Remark: Detected in the FoV of V456 Oph.

RA(J2000)	**Dec(J2000)**	**type**	**Mag.**
07 38 20.2	−02 48 04.8	EW	13.6 (V)

Period	**Epoch**
0.4245(1)	2455939.383(9)

Cross-identification(s):
GSC 4835-1716 = USNO A2.0 0825-05281746 = 2MASS 07382020-0248044 = NOMAD1 0871-0207620

Remark: Detected in the FoV of V868 Mon.

Date: 5 March 2014

Observer(s) and affiliation(s):
Liakos, A. - National Observatory of Athens, Institute for Astronomy & Astrophysics, Space Applications & Remote Sensing, I. Metaxa & Vas. Pavlou St., GR-152 36, Palaia Penteli, Athens, Greece, alliakos@noa.gr
Niarchos, P. - Department of Astrophysics, Astronomy and Mechanics, National and Kapodistrian University of Athens, Panepistimioupolis, GR-157 84, Zografos, Athens, Greece, pniarcho@phys.uoa.gr

RA(J2000)	**Dec(J2000)**	**type**	**Mag.**
01 57 54.9	+37 47 53.4	EC	14.0 (B)

Period	**Epoch**

Cross-identification(s):
GSC 2816-2000 = USNO 1275-01172833 = 2MASS 01575487+3747534 = NOMAD1 1277-0038470

Remark: Detected in the FoV of QX And and GSC 2816-0743 (= NGC 752 170; discovered by Zhang et al. (2009)). The C-K light curve is given for direct comparison with the V-C one.

RA(J2000)	**Dec(J2000)**	**type**	**Mag.**
18 28 39.6	+06 46 00.9	EC	12.3 (V_T)

Period	**Epoch**

Cross-identification(s):
GSC 0445-0903 = TYC 445-903-1 = 2MASS 18283962+0645598

Remark: Detected in the FoV of V2612 Oph. The minimum in I-filter is deeper than the one in V-filter. Therefore, it corresponds to the secondary minimum of the binary's light curve. This suggests Algol-type variability. The C-K light curves are given for direct comparison with the V-C ones.

RA(J2000)	**Dec(J2000)**	**type**	**Mag.**
20 19 35.2	+33 47 26.5	EC	12.2 (B)

Period	**Epoch**

Cross-identification(s):
GSC 2680-1387 = USNO 1200-14916877 = 2MASS 20193521+3347262 = NOMAD1 1237-0465366

Remark: Detected in the FoV of MY Cyg. The C-K light curve is given for direct comparison with the V-C one.

RA(J2000)	**Dec(J2000)**	**type**	**Mag.**
08 10 54.2	+57 40 01.3	EC	11.6 (V)

Period	**Epoch**

Cross-identification(s):
GSC 3802-1680 = TYC 3802-1680-1 = USNO-A2.0 1425-07102186 = NOMAD1 1476-0238610

Remark: Detected in the FoV of SX Lyn and GSC 3802-1986 (discovered by Liakos & Niarchos (2011)).

RA(J2000)	**Dec(J2000)**	**type**	**Mag.**
02 34 46.6	+71 31 21.4	EA	9.7 (B)
Period		**Epoch**	
Cross-identification(s): GSC 4320-1033 = TYC 4320-1033-1 = USNO-A2.0 1575-01428060 = 2MASS 02344652+7131209			

Remark: Detected in the FoV of AB Cas and V663 Cas.

RA(J2000)	**Dec(J2000)**	**type**	**Mag.**
07 09 34.9	+12 10 37.2	EA	13.8 (I)
Period		**Epoch** 2455537.4735(5)	
Cross-identification(s): USNO-A2.0 0975-04711370 = NOMAD1 1021-0151694 = 2MASS 07093486 +1210369 = UCAC4 511-036297			

Remark: Detected in the FoV of AV CMi, 2MASS J07083972+1214429 (discovered by Liakos & Niarchos 2010), GSC 0770-0523 (discovered by Liakos & Niarchos 2010), and USNO-A2.0 0975-04721840 (discovered by Liakos & Niarchos 2011).

RA(J2000)	**Dec(J2000)**	**type**	**Mag.**
20 20 56.8	+18 26 12.4	EA	14.1 (B)
Period 8.935		**Epoch** 2455856.289	
Cross-identification(s): USNO A2.0 1050-17346460 = 2MASS 20205676+1826120 = NOMAD1 1084-0573113			

Remark: Detected in the FoV of BX Del and BW Del. The reference time of minimum as given in the ephemeris (2455856.289) was assumed and it is not a true minimum time. The period is also uncertain, but the value given describes the data in the most sufficient way. The system may have eccentric orbit.

RA(J2000)	**Dec(J2000)**	**type**	**Mag.**
04 16 10.6	+47 38 14.9	EC	15.1 (R)
Period		**Epoch**	
Cross-identification(s): USNO A2.0 1350-04394387 = 2MASS 04161058+4738146 = NOMAD1 1376-0126986			

Remark: Detected in the FoV of V482 Per. The period is probably between 4.66 and 13.99 days, but more times of minima are needed for its determination.

References:

Butters, O.W. et al., 2010, *A&A*, **520L**, 10
Drake, A.J. et al., 2009, *ApJ*, **696**, 870
Kwee, K. K., Van Woerden, H., 1956, *BAN*, **12**, 327
Lenz, P. et al., 2005, *CoAst*, **146**, 53
Liakos, A., Niarchos, P., 2010, *Peremennye Zvezdy Prilozhenie*, **10**, 9
Liakos, A., Niarchos, P., 2011, *IBVS*, **5998**, 8
Liakos, A., Niarchos, P., 2011, *IBVS*, **5999**, 5
Monninger, G., 2011, *IBVS*, **6100**, 1
Skrutskie, M.F. et al., 2006, *AJ*, **131**, 1163
Smith, K.W., Bailer-Jones, C.A.L., Klement, R.J., Xue, X.X., 2010, *A&A*, **522**, A88
Zhang, X. B., Luo, C. Q., Luo, Y. P., Deng, L. C., 2009, *IBVS*, **5900**, 3